Metal Ions in Life Sciences 11

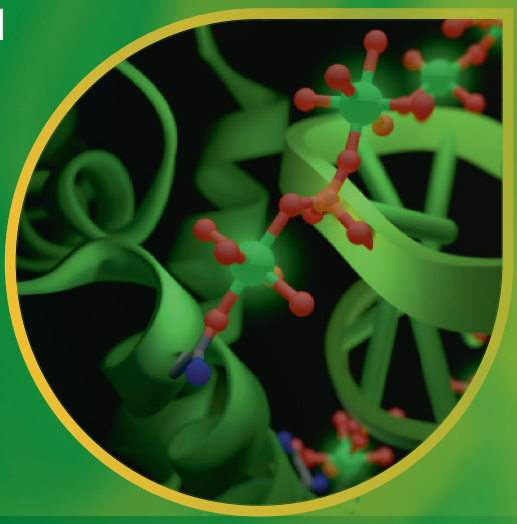

Astrid Sigel
Helmut Sigel
Roland K.O. Sigel
Editors

Cadmium: From Toxicity to Essentiality

Springer

Cadmium: From Toxicity to Essentiality

Metal Ions in Life Sciences

Volume 11

Series Editors:

Astrid Sigel, Helmut Sigel, and Roland K.O. Sigel

For further volumes:
http://www.springer.com/series/8385 and http://www.mils-series.com

Astrid Sigel • Helmut Sigel • Roland K.O. Sigel
Editors

Cadmium: From Toxicity to Essentiality

Springer

Editors
Astrid Sigel
Department of Chemistry
Inorganic Chemistry
University of Basel
Spitalstrasse 51
CH-4056 Basel
Switzerland
astrid.sigel@unibas.ch

Helmut Sigel
Department of Chemistry
Inorganic Chemistry
University of Basel
Spitalstrasse 51
CH-4056 Basel
Switzerland
helmut.sigel@unibas.ch

Roland K.O. Sigel
Institute of Inorganic Chemistry
University of Zürich
Winterthurerstrasse 190
CH-8057 Zürich
Switzerland
roland.sigel@aci.uzh.ch

ISSN 1559-0836 ISSN 1868-0402 (electronic)
ISBN 978-94-007-5178-1 ISBN 978-94-007-5179-8 (eBook)
DOI 10.1007/978-94-007-5179-8
Springer Dordrecht Heidelberg New York London

Library of Congress Control Number: 2012956184

Cover illustration: Cover figure of the MILS series since Volume 11: RNA-protein interface of the Ile-tRNA synthetase complex held together by a string of Mg^{2+} ions, illustrating the importance of metal ions in both the protein and the nucleic acid world as well as connecting the two; hence, representing the role of Metal Ions in Life Sciences. tRNA synthetases are not only essential to life, but also serve as a target for novel classes of drugs making such RNA-protein complexes crucial also for the health sciences. The figure was prepared by Joachim Schnabl and Roland K.O. Sigel using the PDB coordinates 1FFY.

Printed on acid-free paper

Springer is part of Springer Science+Business Media (www.springer.com)

Historical Development and Perspectives of the Series

Metal Ions in Life Sciences*

It is an old wisdom that metals are indispensable for life. Indeed, several of them, like sodium, potassium, and calcium, are easily discovered in living matter. However, the role of metals and their impact on life remained largely hidden until inorganic chemistry and coordination chemistry experienced a pronounced revival in the 1950s. The experimental and theoretical tools created in this period and their application to biochemical problems led to the development of the field or discipline now known as *Bioinorganic Chemistry*, *Inorganic Biochemistry*, or more recently also often addressed as *Biological Inorganic Chemistry*.

By 1970 *Bioinorganic Chemistry* was established and further promoted by the book series *Metal Ions in Biological Systems* founded in 1973 (edited by H.S., who was soon joined by A.S.) and published by Marcel Dekker, Inc., New York, for more than 30 years. After this company ceased to be a family endeavor and its acquisition by another company, we decided, after having edited 44 volumes of the *MIBS* series (the last two together with R.K.O.S.) to launch a new and broader minded series to cover today's needs in the *Life Sciences*. Therefore, the Sigels new series is entitled

Metal Ions in Life Sciences

After publication of the first four volumes (2006–2008) with John Wiley & Sons, Ltd., Chichester, UK, and the next five volumes (2009–2011) with the Royal Society of Chemistry, Cambridge, UK, we are happy to join forces now in this still new endeavor with Springer Science+Business Media B.V., Dordrecht, The Netherlands; a most experienced Publisher in the *Sciences*.

---

*Reproduced with some alterations by permission of John Wiley & Sons, Ltd., Chichester, UK (copyright 2006) from pages v and vi of Volume 1 of the series *Metal Ions in Life Sciences* (MILS-1).

The development of *Biological Inorganic Chemistry* during the past 40 years was and still is driven by several factors; among these are (i) the attempts to reveal the interplay between metal ions and peptides, nucleotides, hormones or vitamins, etc., (ii) the efforts regarding the understanding of accumulation, transport, metabolism and toxicity of metal ions, (iii) the development and application of metal-based drugs, (iv) biomimetic syntheses with the aim to understand biological processes as well as to create efficient catalysts, (v) the determination of high-resolution structures of proteins, nucleic acids, and other biomolecules, (vi) the utilization of powerful spectroscopic tools allowing studies of structures and dynamics, and (vii), more recently, the widespread use of macromolecular engineering to create new biologically relevant structures at will. All this and more is and will be reflected in the volumes of the series *Metal Ions in Life Sciences*.

The importance of metal ions to the vital functions of living organisms, hence, to their health and well-being, is nowadays well accepted. However, in spite of all the progress made, we are still only at the brink of understanding these processes. Therefore, the series *Metal Ions in Life Sciences* will endeavor to link coordination chemistry and biochemistry in their widest sense. Despite the evident expectation that a great deal of future outstanding discoveries will be made in the interdisciplinary areas of science, there are still "language" barriers between the historically separate spheres of chemistry, biology, medicine, and physics. Thus, it is one of the aims of this series to catalyze mutual "understanding".

It is our hope that *Metal Ions in Life Sciences* proves a stimulus for new activities in the fascinating "field" of *Biological Inorganic Chemistry*. If so, it will well serve its purpose and be a rewarding result for the efforts spent by the authors.

Astrid Sigel and Helmut Sigel
Department of Chemistry, Inorganic Chemistry,
University of Basel, CH-4056 Basel, Switzerland

Roland K.O. Sigel
Institute of Inorganic Chemistry,
Unversity of Zürich, CH-8057 Zürich, Switzerland

October 2005,
October 2008,
and August 2011

Preface to Volume 11

Cadmium: From Toxicity to Essentiality

Chapter 1, devoted to the bioinorganic chemistry of cadmium(II), sets the scene for Volume 11, which covers the whole range from toxicity to essentiality of this element. Cadmium, discovered in 1817, is technically used for many purposes, e.g., as a yellow-orange pigment when combined with chalcogenides, as an anticorrosion agent in steel, as a stabilizer for plastic or in NiCd batteries. Of biological relevance is its high affinity for sulfur sites, which means, e.g., that in metallothionein with ZnS_4 units, Cd^{2+} concentrations need to be only one thousandth of those of Zn^{2+} for an effective competition. Indeed, Cd^{2+} is toxic to almost all forms of life and therefore the understanding of its biogeochemical cycling and release into the environment is of high relevance as is pointed out in Chapter 2. Cadmium is released to the environment through natural and anthropogenic sources. Already at the end of the 1980's the total industrial and natural weathering cycle has been estimated as 24'000 t/yr and 4.5 t/yr, respectively, demonstrating the dominance of anthropogenic discharges. The cadmium content of zinc ores ranges from about 0.2 to 0.7% by weight, making this by-product extraction the major source of cadmium. From about 20 t/yr at the beginning of the 20th century, the global production rose to 21'500 t in 2011 with the bulk production occurring in China (7'500 t), the Republic of Korea (2'500 t), and Japan (2'000 t). In Chapter 3 an effort is made to quantify the speciation of cadmium in the atmosphere, in marine and fresh waters as well as in soils and sediments. The behavior of cadmium is assessed by modeling its reactivity towards the main classes of ligands usually present in natural systems, like chloride, carbonate, sulfate, carboxylates, amines, amino acids, phosph(on)ates or thiols.

It is evident that the precise determination of cadmium in biological samples, including blood, plasma, serum, and urine as well as hair, saliva, and various tissues is an important issue. Chapter 4 describes the relevant analytical tools like inductively coupled plasma mass spectrometry (ICP-MS), atomic absorption spectrometry (AAS), electrochemical methods, neutron activation analysis (NAA), and X- ray

fluorescence spectrometry (XRF). The very modern approach of direct imaging and sensing of Cd^{2+} in cells is in the focus of Chapter 5, where the application of fluorescence imaging in a variety of cell types is described. The use of ^{113}Cd NMR to probe the zinc binding sites in metallothioneins as well as those in Ca^{2+} binding proteins is reviewed in Chapter 6. It is not surprising that Cd^{2+} is a good surrogate for Zn^{2+} as both are in the same group of the periodic table with a d^{10} valence electron configuration and similar ligand and coordination number preferences, although the ionic radius of Cd^{2+} is larger than the one of Zn^{2+}. It is probably more surprising that Cd^{2+} is also a good substitute for Ca^{2+} even though their coordination chemistry is quite different, Cd^{2+} having a preference for N/S and Ca^{2+} for O ligation, but the ionic radii are quite similar.

Crystal structures of Cd^{2+} complexes as determined by X-ray diffractometry are the topic of Chapter 7. The authors consider three broad classes of ligands of potential biological interest: (i) N donors (purines, pyrimidines), (ii) carboxylates (amino acids, water soluble vitamins), and (iii) S donors (thiols/thiolates, dithiocarbamates). In Chapter 8 complex formation of Cd^{2+} in aqueous solution with sugar residues, nucleobases, phosphates, nucleotides, and nucleic acids is evaluated in comparison with mainly that of Zn^{2+}, Co^{2+}, Ca^{2+}, and Mg^{2+}. Among many aspects including mixed ligand complex and intramolecular aromatic-ring stack formation it is shown that the phosphodiester bridge is only a weak binding site but that it still allows (possibly in part outersphere) macrochelate formation when N7 of a purine base is primarily coordinated. The effect of a non-bridging sulfur atom in a thiophosphate group (*versus* a normal phosphate group) is considered and it is emphasized that Cd^{2+} is regularly used in so-called thiorescue experiments which help to provide insights into ribozyme catalysis. Complexes of Cd^{2+} with amino acids and peptides, including glutathione as well as peptides with multiple cysteinyl sites and phytochelatins are dealt with in Chapter 9. Natural and artificial proteins containing Cd^{2+} are described in Chapter 10. It focuses on designed proteins with the aim to understand the structure, spectroscopy, and dynamics of proteins that bind Cd^{2+} in general. Metallothioneins are low-molecular-mass and cysteine-rich proteins with the ability to bind mono- and divalent metal ions with a d^{10} electron configuration, especially Cu(I) and Zn(II), in the form of metal-thiolate clusters (Chapter 11). However, Cd^{2+} can be bound to certain metallothioneins *in vivo* as well, giving rise to the perception that one of the physiological roles of metallothioneins is the detoxification of heavy metal ions. Methods applied in the studies of structural and chemical properties of Cd(II)-MTs are also presented in Chapter 11.

Plants are categorized in three groups concerning their uptake of heavy metals: indicators, excluders, and hyperaccumulators as is summarized in Chapter 12. Hyperaccumulators are presently not without reason a vibrant research area; they can be used biotechnologically for (i) phytoremediation, i.e., cleaning of anthropogenically Cd^{2+}-contaminated soils, and (ii) phytomining, i.e., using plants for commercial metal extraction. The toxicity of Cd^{2+} for plants (Chapter 13) includes oxidative stress, inhibition of the photosynthetic apparatus, a genotoxicity, and inhibition of root metabolism.

The detrimental health effects of cadmium were first mentioned in the mid-19th century. The real challenge in the 21st century is now to cope with the chronic low exposure that occurs in a global setting mainly from dietary sources. The ubiquity of cadmium constitutes a serious environmental health problem and therefore the cellular and molecular mechanisms for chronic (and acute) Cd^{2+} toxicity need to be revealed. Chapter 14 details with great care the Cd^{2+} effects on the target organs including kidney, liver, bone, endocrine glands, hematopoiesis and hemostasis, as well as on the respiratory, cardiovascular, nervous, and reproductive systems. Furthermore, cadmium is an established animal and human carcinogen as reviewed in Chapter 15. Cadmium leads to an elevated risk for lung cancer after occupational exposure, but associations between such exposures and tumors at other locations including kidney, breast, and prostate may be relevant as well. As far as its mechanisms of action are concerned, it appears that direct Cd^{2+} interactions with DNA are of minor importance; important are elevated levels of reactive oxygen species (ROS) which have been detected in diverse experimental systems, presumably due to an inactivation of detoxifying enzymes. Cd^{2+} interference with proteins participating in the cellular response to DNA damage, the deregulation of cell growth as well as resistance to apoptosis appears to be involved in Cd^{2+}-induced carcinogenicity. Moreover, Cd^{2+} has been shown to disturb nucleotide excision repair, base excision repair, and mismatch repair.

The volume terminates with Chapter 16 in which also the essentiality of Cd^{2+} for certain diatoms is pointed out. The distribution of Cd^{2+} in the ocean is very similar to that of major nutrients suggesting that it may be taken up by marine phytoplankton at the surface and remineralized at depth. At high concentration, Cd^{2+} is toxic to phytoplankton as it is for many organisms. However, at relatively low concentrations, Cd^{2+} can enhance the growth of a number of phytoplankton species under Zn^{2+} limitation; possibly Cd^{2+} is taken up either by the Mn^{2+} or the Zn^{2+} transport system. The only known biological function of Cd^{2+} is to serve as a metal ion cofactor in cadmium-carbonic anhydrase (CDCA) in diatoms. The expression of CDCA is regulated by the availabilities of Cd^{2+} and Zn^{2+}; both Zn^{2+} and Cd^{2+} can be used as the metal ion cofactor and be exchanged for each other in certain marine phytoplankton species.

Astrid Sigel
Helmut Sigel
Roland K.O. Sigel

Contents

Historical Development and Perspectives of the Series v

Preface to Volume 11 vii

Contributors to Volume 11 xvii

Titles of Volumes 1-44 in the *Metal Ions in Biological Systems* Series xxi

Contents of Volumes in the *Metal Ions in Life Sciences* Series xxiii

1 The Bioinorganic Chemistry of Cadmium in the Context of Its Toxicity 1
Wolfgang Maret and Jean-Marc Moulis

Abstract 2
1 Introduction 2
2 Cadmium Coordination Chemistry of Biological Relevance . . . 3
3 Cadmium Biochemistry 6
4 Cadmium Toxicity 14
5 Concluding Remarks and Future Directions 23
References 26

2 Biogeochemistry of Cadmium and Its Release to the Environment 31
Jay T. Cullen and Maria T. Maldonado

Abstract 32
1 Introduction 32
2 Geochemistry of Cadmium 33
3 Mobilization of Cadmium 35
4 Cadmium in the Atmosphere 37

5 Cadmium in the Terrestrial and Freshwater Environment 40
6 Cadmium in Ocean Waters 44
7 Summary and Conclusions 56
References 58

3 Speciation of Cadmium in the Environment 63
Francesco Crea, Claudia Foti, Demetrio Milea, and Silvio Sammartano

Abstract 63
1 Introduction 64
2 Presence in the Environment 64
3 Speciation in the Atmosphere 65
4 Speciation in Natural Waters 66
5 Speciation in Soils and Sediments 69
6 Chemical Reactivity towards Different Ligand Classes 71
7 Conclusions 78
References 80

4 Determination of Cadmium in Biological Samples 85
Katrin Klotz, Wobbeke Weistenhöfer, and Hans Drexler

Abstract 85
1 Introduction 86
2 Biomarkers of Exposure 86
3 Biomarkers of Effect 92
4 Conclusions 95
References 96

5 Imaging and Sensing of Cadmium in Cells 99
Masayasu Taki

Abstract 99
1 Introduction 100
2 Cadmium Toxicity in Cells 101
3 Detection of Intracellular Cadmium 103
4 Cadmium-Selective Fluorescent Probes 106
5 Concluding Remarks 112
References 114

6 Use of ^{113}Cd NMR to Probe the Native Metal Binding Sites in Metalloproteins: An Overview 117
Ian M. Armitage, Torbjörn Drakenberg, and Brian Reilly

Abstract 117
1 Introduction 118
2 General Considerations and Basic Principles 119

3 ^{113}Cd NMR Chemical Shifts from ^{113}Cd-Substituted Metalloproteins 123
4 Specific Highlights of Studies on Alkaline Phosphatase, Calcium Binding Proteins, and Metallothioneins 126
5 Conclusions and Outlook 137
References 138

7 Solid State Structures of Cadmium Complexes with Relevance for Biological Systems 145
Rosa Carballo, Alfonso Castiñeiras, Alicia Domínguez-Martín, Isabel García-Santos, and Juan Niclós-Gutiérrez

Abstract 146
1 Introduction 146
2 Cadmium Complexes with Nucleobases and Related Ligands . . 147
3 Cadmium(II) Complexes with α-Amino Acids 155
4 Complexes of Cadmium with Vitamins and Derivatives 160
5 Other Cadmium Complexes 170
6 General Conclusions 182
References 185

8 Complex Formation of Cadmium with Sugar Residues, Nucleobases, Phosphates, Nucleotides, and Nucleic Acids 191
Roland K.O. Sigel, Miriam Skilandat, Astrid Sigel, Bert P. Operschall, and Helmut Sigel

Abstract 192
1 Introduction 193
2 Comparisons of the Properties of Cadmium(II) with Those of Zinc(II), Calcium(II), Magnesium(II), and Other Related Metal Ions 195
3 Cadmium(II)-Sugar Interactions 198
4 Interactions of Cadmium(II) with Nucleobase Residues 204
5 Complexes of Cadmium(II) with Phosphates 218
6 Cadmium(II) Complexes of Nucleotides 222
7 Cadmium(II) Complexes of Nucleotide Analogues 239
8 A Short Appraisal of Mixed Ligand Complexes Containing a Nucleotide 247
9 Cadmium(II) Binding in Dinucleotides and Dinucleoside Monophosphates 253
10 Cadmium(II) Binding to Nucleic Acids 258
11 Concluding Remarks 262
References 266

9 Cadmium(II) Complexes of Amino Acids and Peptides 275
Imre Sóvágó and Katalin Várnagy

Abstract 276
1 Introduction 276
2 Complexes of Amino Acids and Derivatives 278
3 Complexes of Peptides and Related Ligands 286
4 Comparison of Cadmium(II) Complexes with Other Transition Elements 295
References 299

10 Natural and Artificial Proteins Containing Cadmium 303
Anna F.A. Peacock and Vincent L. Pecoraro

Abstract 304
1 Introduction 304
2 Function and Coordination Chemistry of Cd(II) in Metalloregulatory Proteins 305
3 Strategies for Designing Peptides for Complexation of Cd(II) . . 309
4 Physical Properties of Cd(II) in Thiolate Proteins 325
5 General Conclusions: Lessons for Understanding the Biological Chemistry of Cd(II) 333
References 335

11 Cadmium in Metallothioneins 339
Eva Freisinger and Milan Vašák

Abstract 339
1 Introduction 340
2 Spectroscopic Characterization 342
3 Binding Affinity and Reactivity 358
4 Three-Dimensional Structures 361
5 Concluding Remarks 365
References 367

12 Cadmium-Accumulating Plants 373
Hendrik Küpper and Barbara Leitenmaier

Abstract 373
1 Introduction: Importance of Cadmium Accumulation in Plants . 374
2 Ecological Role of Cadmium Hyperaccumulation 377
3 Mechanisms of Cadmium Hyperaccumulation 378
4 Biotechnological Use of Cadmium Hyperaccumulators 383
5 Outlook 386
References 388

13 Cadmium Toxicity in Plants 395
Elisa Andresen and Hendrik Küpper

Abstract 395
1 Introduction: Environmental Relevance of Cadmium Toxicity in Plants 396
2 Cadmium Toxicity to Roots 397
3 Cadmium-Induced Inhibition of the Photosynthetic Apparatus 399
4 Cadmium-Induced Oxidative Stress 402
5 Genotoxicity of Cadmium in Plants 405
6 Outlook 407
References 409

14 Toxicology of Cadmium and Its Damage to Mammalian Organs 415
Frank Thévenod and Wing-Kee Lee

Abstract 416
1 Introduction 417
2 Sources and Exposures 418
3 Entry Pathways, Transport, and Trafficking 421
4 Health Effects 426
5 Cellular and Molecular Mechanisms of Toxicity 446
6 Endogenous Detoxification 466
7 Concluding Remarks and Future Directions 468
References 472

15 Cadmium and Cancer 491
Andrea Hartwig

Abstract 491
1 Introduction 492
2 Epidemiology and Animal Carcinogenicity 493
3 Direct and Indirect Genotoxicity 494
4 Interactions with the DNA Damage Response System 496
5 Impact on Gene Expression and Deregulation of Cell Proliferation 500
6 Interactions on the Molecular Level: Mechanistic Considerations and the Role of Adaptation 500
7 Concluding Remarks 502
References 504

16 Cadmium in Marine Phytoplankton 509
Yan Xu and François M.M. Morel

Abstract 510
1 Introduction 510
2 Cadmium Distribution in the Ocean 511
3 Effects of Cadmium on Phytoplankton Growth 513
4 Cadmium Uptake by Phytoplankton 515
5 Cadmium and Thiol Production 517
6 Cadmium Carbonic Anhydrase 520
7 Concluding Remarks and Future Directions 525
References 526

Erratum E1

Index 529

Contributors to Volume 11

Numbers in parentheses indicate the pages on which the authors' contributions begin.

Elisa Andresen Fachbereich Biologie, Universität Konstanz, D-78457 Konstanz, Germany (395)

Ian M. Armitage Department of Biochemistry, Molecular Biology and Biophysics, University of Minnesota, 6-555 Jackson Hall, 321 Church Street S. E., Minneapolis, MN 55455, USA, armit001@umn.edu (117)

Rosa Carballo Departamento de Química Inorgánica, Facultad de Química, Universidad de Vigo, E-36310 Vigo, Spain (145)

Alfonso Castiñeiras Departamento de Química Inorganica, Facultad de Farmacia, Universidad de Santiago de Compostela, E-15782 Santiago de Compostela, Spain, alfonso.castineiras@usc.es (145)

Francesco Crea Department of Inorganic, Analytical, and Physical Chemistry, University of Messina, Viale S. Stagno D'Alcontres 31, I-98166 Messina, Italy, fcrea@unime.it (63)

Jay T. Cullen School of Earth and Ocean Sciences, Bob Wright Centre A405, University of Victoria, P.O. Box 3065 STN CsC, Victoria, BC V8W 3V6, Canada, jcullen@uvic.ca (31)

Alicia Domínguez-Martín Departamento de Química Inorgánica, Facultad de Farmacia, Universidad de Granada, E-18071 Granada, Spain (145)

Torbjörn Drakenberg Department of Biophysical Chemistry, Lund University, P. O. Box 124, SE-22100 Lund, Sweden, torbjorn.drakenberg@bpc.lu.se (117)

Hans Drexler Institute and Outpatient Clinic of Occupational, Social and Environmental Medicine, Friedrich-Alexander University (FAU) Erlangen-Nuremberg, Schillerstrasse 25/29, D-91052 Erlangen, Germany, hans.drexler@ipasum.uni-erlangen.de (85)

Claudia Foti Department of Inorganic, Analytical, and Physical Chemistry, University of Messina, Viale S. Stagno D'Alcontres 31, I-98166 Messina, Italy, cfoti@unime.it (63)

Eva Freisinger Institute of Inorganic Chemistry, University of Zürich, Winterthurerstrasse 190, CH-8057 Zürich, Switzerland, freisinger@aci.uzh.ch (339)

Isabel García-Santos Departamento de Química Inorganica, Facultad de Farmacia, Universidad de Santiago de Compostela, E-15782 Santiago de Compostela, Spain (145)

Andrea Hartwig Karlsruher Institut für Technologie (KIT), Institut für Angewandte Biowissenschaften, Abteilung Lebensmittelchemie und Toxikologie, Kaiserstrasse 12, D-76131 Karlsruhe, Germany, andrea.hartwig@kit.edu (491)

Katrin Klotz Institute and Outpatient Clinic of Occupational Social and Environmental Medicine, Friedrich-Alexander University (FAU) Erlangen-Nuremberg, Schillerstrasse 25/29, D-91052 Erlangen, Germany, katrin.klotz@ipasum.med.uni-erlangen.de (85)

Hendrik Küpper Fachbereich Biologie, Universität Konstanz, D-78457 Konstanz, Germany, hendrik.kuepper@uni-konstanz.de (375, 395)

Wing-Kee Lee Centre for Biomedical Training and Research (ZBAF) Institute of Physiology and Pathophysiology, Faculty of Health, Private University of Witten/ Herdecke GmbH, Alfred-Herrhausen-Strasse 50, D-58448 Witten, Germany, wing-kee.lee@uni-wh.de (415)

Barbara Leitenmaier Institute of Inorganic Chemistry, University of Zürich, Winterthurerstrasse 190, CH-8057 Zürich, Switzerland (373)

Maria T. Maldonado Department of Earth and Ocean Sciences, University of British Columbia, Vancouver, BC, Canada, mmaldonado@eos.ubc.ca (31)

Wolfgang Maret Diabetes and Nutritional Sciences Division, Metal Metabolism Group, King's College London, School of Medicine, London SE1 9NH, UK, wolfgang.maret@kcl.ac.uk (1)

Demetrio Milea Department of Inorganic, Analytical, and Physical Chemistry, University of Messina, Viale S. Stagno D'Alcontres 31, I-98166 Messina, Italy, dmilea@unime.it (63)

François M.M. Morel Department of Geosciences, Princeton University Princeton, NJ 08544, USA, morel@princeton.edu (509)

Jean-Marc Moulis CEA, DSV, IRTSV, Laboratoire de Chimie et Biologie des Métaux, 17 ave des Martyrs, F-38054 Grenoble, France and CNRS UMR5249, Université Joseph Fourier, Grenoble 1, France, jean-marc.moulis@cea.fr (1)

Juan Niclós-Gutierrez Departamento de Química Inorgánica, Facultad de Farmacia, Universidad de Granada, E-18071 Granada, Spain (145)

Bert P. Operschall Department of Chemistry, Inorganic Chemistry, University of Basel, Spitalstrasse 51, CH-4056 Basel, Switzerland (191)

Anna F.A. Peacock School of Chemistry, University of Birmingham, Edgbaston, B15 2TT, UK, a.f.a.peacock@bham.ac.uk (303)

Vincent L. Pecoraro Department of Chemistry, University of Michigan, 930 N. University, Ann Arbor, MI 48105-1055, USA, vlpec@umich.edu (303)

Brian Reilly Department of Biochemistry, Molecular Biology and Biophysics, University of Minnesota, 6-555 Jackson Hall, 321 Church Street S. E., Minneapolis MN 55455, USA, reil0080@umn.edu (117)

Silvio Sammartano Department of Inorganic, Analytical, and Physical Chemistry, University of Messina, Viale S. Stagno D'Alcontres 31, I-98166 Messina, Italy, ssammartano@unime.it (63)

Astrid Sigel Department of Chemistry, Inorganic Chemistry, University of Basel, Spitalstrasse 51, CH-4056 Basel, Switzerland, astrid.sigel@unibas.ch (191)

Helmut Sigel Department of Chemistry, Inorganic Chemistry, University of Basel, Spitalstrasse 51, CH-4056 Basel, Switzerland, helmut.sigel@unibas.ch (191)

Roland K.O. Sigel Institute of Inorganic Chemistry, University of Zürich, Winterthurerstrasse 190, CH-8057 Zürich, Switzerland, roland.sigel@aci.unizh.ch (191)

Miriam Skilandat Institute of Inorganic Chemistry, University of Zürich, Winterthurerstrasse 190, CH-8057 Zürich, Switzerland (191)

Imre Sóvágó Department of Inorganic and Analytical Chemistry, University of Debrecen, P.O. Box 21, H-4010 Debrecen, Hungary, sovago@science.unideb.hu (275)

Masayasu Taki Graduate School of Human and Environmental Studies and Graduate School of Global Environmental Studies, Kyoto University Yoshida, Sakyo-ku, Kyoto 606-8501, Japan, taki.masayasu.4c@kyoto-u.ac.jp (99)

Frank Thévenod Centre for Biomedical Training and Research (ZBAF), Institute of Physiology and Pathophysiology, Faculty of Health, Private University of Witten/Herdecke GmbH, Alfred-Herrhausen-Strasse 50, D-58448 Witten, Germany, frank.thevenod@uni-wh.de (415)

Katalin Várnagy Department of Inorganic and Analytical Chemistry, University of Debrecen, P.O. Box 21, H-4010 Debrecen, Hungary, varnagy.katalin@science.unideb.hu (275)

Milan Vašák Institute of Inorganic Chemistry, University of Zürich, Winterthurerstrasse 190, CH-8057 Zürich, Switzerland, mvasak@bioc.uzh.ch (339)

Wobbeke Weistenhöfer Institute and Outpatient Clinic of Occupational Social and Environmental Medicine, Friedrich-Alexander University (FAU), Erlangen-Nuremberg, Schillerstrasse 25/29, D-91052 Erlangen, Germany (85)

Yan Xu Department of Geosciences, Princeton University, Princeton, NJ 08544, USA. Present address: Department of Molecular and Cellular Physiology, School of Medicine, Stanford University, Stanford, CA 94305, USA, yanxu12@stanford.edu (509)

Titles of Volumes 1-44 in the *Metal Ions in Biological Systems* Series

edited by the SIGELs
and published by Dekker/Taylor & Francis (1973–2005)

Volume 1:	**Simple Complexes**
Volume 2:	**Mixed-Ligand Complexes**
Volume 3:	**High Molecular Complexes**
Volume 4:	**Metal Ions as Probes**
Volume 5:	**Reactivity of Coordination Compounds**
Volume 6:	**Biological Action of Metal Ions**
Volume 7:	**Iron in Model and Natural Compounds**
Volume 8:	**Nucleotides and Derivatives: Their Ligating Ambivalency**
Volume 9:	**Amino Acids and Derivatives as Ambivalent Ligands**
Volume 10:	**Carcinogenicity and Metal Ions**
Volume 11:	**Metal Complexes as Anticancer Agents**
Volume 12:	**Properties of Copper**
Volume 13:	**Copper Proteins**
Volume 14:	**Inorganic Drugs in Deficiency and Disease**
Volume 15:	**Zinc and Its Role in Biology and Nutrition**
Volume 16:	**Methods Involving Metal Ions and Complexes in Clinical Chemistry**
Volume 17:	**Calcium and Its Role in Biology**
Volume 18:	**Circulation of Metals in the Environment**
Volume 19:	**Antibiotics and Their Complexes**
Volume 20:	**Concepts on Metal Ion Toxicity**
Volume 21:	**Applications of Nuclear Magnetic Resonance to Paramagnetic Species**
Volume 22:	**ENDOR, EPR, and Electron Spin Echo for Probing Coordination Spheres**
Volume 23:	**Nickel and Its Role in Biology**
Volume 24:	**Aluminum and Its Role in Biology**
Volume 25:	**Interrelations Among Metal Ions, Enzymes, and Gene Expression**
Volume 26:	**Compendium on Magnesium and Its Role in Biology, Nutrition, and Physiology**

Volume 27: **Electron Transfer Reactions in Metalloproteins**
Volume 28: **Degradation of Environmental Pollutants by Microorganisms and Their Metalloenzymes**
Volume 29: **Biological Properties of Metal Alkyl Derivatives**
Volume 30: **Metalloenzymes Involving Amino Acid-Residue and Related Radicals**
Volume 31: **Vanadium and Its Role for Life**
Volume 32: **Interactions of Metal Ions with Nucleotides, Nucleic Acids, and Their Constituents**
Volume 33: **Probing Nucleic Acids by Metal Ion Complexes of Small Molecules**
Volume 34: **Mercury and Its Effects on Environment and Biology**
Volume 35: **Iron Transport and Storage in Microorganisms, Plants, and Animals**
Volume 36: **Interrelations Between Free Radicals and Metal Ions in Life Processes**
Volume 37: **Manganese and Its Role in Biological Processes**
Volume 38: **Probing of Proteins by Metal Ions and Their Low-Molecular-Weight Complexes**
Volume 39: **Molybdenum and Tungsten. Their Roles in Biological Processes**
Volume 40: **The Lanthanides and Their Interrelations with Biosystems**
Volume 41: **Metal Ions and Their Complexes in Medication**
Volume 42: **Metal Complexes in Tumor Diagnosis and as Anticancer Agents**
Volume 43: **Biogeochemical Cycles of Elements**
Volume 44: **Biogeochemistry, Availability, and Transport of Metals in the Environment**

Contents of Volumes in the *Metal Ions in Life Sciences* Series

edited by the SIGELs

Volumes 1–4
published by John Wiley & Sons, Ltd., Chichester, UK (2006–2008)
<http://www.Wiley.com/go/mils>

Volume 5–9
published by the Royal Society of Chemistry, Cambridge, UK (2009–2011)
<http://www.rsc.org/shop/metalionsinlifesciences>

and from Volume 10 on
published by Springer Science+Business Media BV, Dordrecht, The Netherlands (since 2012)
<http://www.mils-series.com>

Volume 1 Neurodegenerative Diseases and Metal Ions

1 **The Role of Metal Ions in Neurology. An Introduction**
Dorothea Strozyk and Ashley I. Bush

2 **Protein Folding, Misfolding, and Disease**
Jennifer C. Lee, Judy E. Kim, Ekaterina V. Pletneva, Jasmin Faraone-Mennella, Harry B. Gray, and Jay R. Winkler

3 **Metal Ion Binding Properties of Proteins Related to Neurodegeneration**
Henryk Kozlowski, Marek Luczkowski, Daniela Valensin, and Gianni Valensin

4 **Metallic Prions: Mining the Core of Transmissible Spongiform Encephalopathies**
David R. Brown

5 **The Role of Metal Ions in the Amyloid Precursor Protein and in Alzheimer's Disease**
Thomas A. Bayer and Gerd Multhaup

6 The Role of Iron in the Pathogenesis of Parkinson's Disease
Manfred Gerlach, Kay L. Double, Mario E. Götz, Moussa B.H. Youdim, and Peter Riederer

7 *In Vivo* Assessment of Iron in Huntington's Disease and Other Age-Related Neurodegenerative Brain Diseases
George Bartzokis, Po H. Lu, Todd A. Tishler, and Susan Perlman

8 Copper-Zinc Superoxide Dismutase and Familial Amyotrophic Lateral Sclerosis
Lisa J. Whitson and P. John Hart

9 The Malfunctioning of Copper Transport in Wilson and Menkes Diseases
Bibudhendra Sarkar

10 Iron and Its Role in Neurodegenerative Diseases
Roberta J. Ward and Robert R. Crichton

11 The Chemical Interplay between Catecholamines and Metal Ions in Neurological Diseases
Wolfgang Linert, Guy N. L. Jameson, Reginald F. Jameson, and Kurt A. Jellinger

12 Zinc Metalloneurochemistry: Physiology, Pathology, and Probes
Christopher J. Chang and Stephen J. Lippard

13 The Role of Aluminum in Neurotoxic and Neurodegenerative Processes
Tamás Kiss, Krisztina Gajda-Schrantz, and Paolo F. Zatta

14 Neurotoxicity of Cadmium, Lead, and Mercury
Hana R. Pohl, Henry G. Abadin, and John F. Risher

15 Neurodegerative Diseases and Metal Ions. A Concluding Overview
Dorothea Strozyk and Ashley I. Bush

Subject Index

Volume 2 Nickel and Its Surprising Impact in Nature

1 Biogeochemistry of Nickel and Its Release into the Environment
Tiina M. Nieminen, Liisa Ukonmaanaho, Nicole Rausch, and William Shotyk

2 Nickel in the Environment and Its Role in the Metabolism of Plants and Cyanobacteria
Hendrik Küpper and Peter M.H. Kroneck

3 Nickel Ion Complexes of Amino Acids and Peptides
Teresa Kowalik-Jankowska, Henryk Kozlowski, Etelka Farkas, and Imre Sóvágó

4 Complex Formation of Nickel(II) and Related Metal Ions with Sugar Residues, Nucleobases, Phosphates, Nucleotides, and Nucleic Acids
Roland K.O. Sigel and Helmut Sigel

5 Synthetic Models for the Active Sites of Nickel-Containing Enzymes
Jarl Ivar van der Vlugt and Franc Meyer

6 Urease: Recent Insights in the Role of Nickel
Stefano Ciurli

7 Nickel Iron Hydrogenases
Wolfgang Lubitz, Maurice van Gastel, and Wolfgang Gärtner

8 Methyl-Coenzyme M Reductase and Its Nickel Corphin Coenzyme F_{430} in Methanogenic Archaea
Bernhard Jaun and Rudolf K. Thauer

9 Acetyl-Coenzyme A Synthases and Nickel-Containing Carbon Monoxide Dehydrogenases
Paul A. Lindahl and David E. Graham

10 Nickel Superoxide Dismutase
Peter A. Bryngelson and Michael J. Maroney

11 Biochemistry of the Nickel-Dependent Glyoxylase I Enzymes
Nicole Sukdeo, Elisabeth Daub, and John F. Honek

12 Nickel in Acireductone Dioxygenase
Thomas C. Pochapsky, Tingting Ju, Marina Dang, Rachel Beaulieu, Gina Pagani, and Bo OuYang

13 The Nickel-Regulated Peptidyl-Prolyl *cis*/*trans* Isomerase SlyD
Frank Erdmann and Gunter Fischer

14 Chaperones of Nickel Metabolism
Soledad Quiroz, Jong K. Kim, Scott B. Mulrooney, and Robert P. Hausinger

15 The Role of Nickel in Environmental Adaptation of the Gastric Pathogen *Helicobacter pylori*
Florian D. Ernst, Arnoud H. M. van Vliet, Manfred Kist, Johannes G. Kusters, and Stefan Bereswill

16 Nickel-Dependent Gene Expression
Konstantin Salnikow and Kazimierz S. Kasprzak

17 Nickel Toxicity and Carcinogenesis
Kazimierz S. Kasprzak and Konstantin Salnikow

Subject Index

Volume 3 The Ubiquitous Roles of Cytochrome P450 Proteins

1 Diversities and Similarities of P450 Systems: An Introduction
Mary A. Schuler and Stephen G. Sligar

2 Structural and Functional Mimics of Cytochromes P450
Wolf-D. Woggon

3 Structures of P450 Proteins and Their Molecular Phylogeny
Thomas L. Poulos and Yergalem T. Meharenna

4 Aquatic P450 Species
Mark J. Snyder

5 The Electrochemistry of Cytochrome P450
Alan M. Bond, Barry D. Fleming, and Lisandra L. Martin

6 P450 Electron Transfer Reactions
Andrew K. Udit, Stephen M. Contakes, and Harry B. Gray

7 Leakage in Cytochrome P450 Reactions in Relation to Protein Structural Properties
Christiane Jung

8 Cytochromes P450. Structural Basis for Binding and Catalysis
Konstanze von König and Ilme Schlichting

9 Beyond Heme-Thiolate Interactions: Roles of the Secondary Coordination Sphere in P450 Systems
Yi Lu and Thomas D. Pfister

10 Interactions of Cytochrome P450 with Nitric Oxide and Related Ligands
Andrew W. Munro, Kirsty J. McLean, and Hazel M. Girvan

11 Cytochrome P450-Catalyzed Hydroxylations and Epoxidations
Roshan Perera, Shengxi Jin, Masanori Sono, and John H. Dawson

12 Cytochrome P450 and Steroid Hormone Biosynthesis
Rita Bernhardt and Michael R. Waterman

13 Carbon-Carbon Bond Cleavage by P450 Systems
James J. De Voss and Max J. Cryle

14 Design and Engineering of Cytochrome P450 Systems
Stephen G. Bell, Nicola Hoskins, Christopher J. C. Whitehouse, and Luet L. Wong

15 Chemical Defense and Exploitation. Biotransformation of Xenobiotics by Cytochrome P450 Enzymes
Elizabeth M. J. Gillam and Dominic J. B. Hunter

16 Drug Metabolism as Catalyzed by Human Cytochrome P450 Systems
F. Peter Guengerich

17 Cytochrome P450 Enzymes: Observations from the Clinic
Peggy L. Carver

Subject Index

Volume 4 Biomineralization. From Nature to Application

1 Crystals and Life: An Introduction
Arthur Veis

2 What Genes and Genomes Tell Us about Calcium Carbonate Biomineralization
Fred H. Wilt and Christopher E. Killian

3 The Role of Enzymes in Biomineralization Processes
Ingrid M. Weiss and Frédéric Marin

4 Metal–Bacteria Interactions at Both the Planktonic Cell and Biofilm Levels
Ryan C. Hunter and Terry J. Beveridge

5 Biomineralization of Calcium Carbonate. The Interplay with Biosubstrates
Amir Berman

6 Sulfate-Containing Biominerals
Fabienne Bosselmann and Matthias Epple

7 Oxalate Biominerals
Enrique J. Baran and Paula V. Monje

8 Molecular Processes of Biosilicification in Diatoms
Aubrey K. Davis and Mark Hildebrand

9 Heavy Metals in the Jaws of Invertebrates
Helga C. Lichtenegger, Henrik Birkedal, and J. Herbert Waite

10 Ferritin. Biomineralization of Iron
Elizabeth C. Theil, Xiaofeng S. Liu, and Manolis Matzapetakis

11 Magnetism and Molecular Biology of Magnetic Iron Minerals in Bacteria
Richard B. Frankel, Sabrina Schübbe, and Dennis A. Bazylinski

12 Biominerals. Recorders of the Past?
Danielle Fortin, Sean R. Langley, and Susan Glasauer

13 Dynamics of Biomineralization and Biodemineralization
Lijun Wang and George H. Nancollas

14 Mechanism of Mineralization of Collagen-Based Connective Tissues
Adele L. Boskey

15 Mammalian Enamel Formation
Janet Moradian-Oldak and Michael L. Paine

16 Mechanical Design of Biomineralized Tissues. Bone and Other Hierarchical Materials
Peter Fratzl

17 Bioinspired Growth of Mineralized Tissue
Darilis Suárez-González and William L. Murphy

18 Polymer-Controlled Biomimetic Mineralization of Novel Inorganic Materials
Helmut Cölfen and Markus Antonietti

Subject Index

Volume 5 Metallothioneins and Related Chelators

1 Metallothioneins. Historical Development and Overview
Monica Nordberg and Gunnar F. Nordberg

2 Regulation of Metallothionein Gene Expression
Kuppusamy Balamurugan and Walter Schaffner

3 Bacterial Metallothioneins
Claudia A. Blindauer

4 Metallothioneins in Yeast and Fungi
Benedikt Dolderer, Hans-Jürgen Hartmann, and Ulrich Weser

5 Metallothioneins in Plants
Eva Freisinger

6 Metallothioneins in Diptera
Silvia Atrian

7 Earthworm and Nematode Metallothioneins
Stephen R. Stürzenbaum

8 Metallothioneins in Aquatic Organisms: Fish, Crustaceans, Molluscs, and Echinoderms
Laura Vergani

9 Metal Detoxification in Freshwater Animals. Roles of Metallothioneins
Peter G. C. Campbell and Landis Hare

10 Structure and Function of Vertebrate Metallothioneins
Juan Hidalgo, Roger Chung, Milena Penkowa, and Milan Vašák

11 Metallothionein-3, Zinc, and Copper in the Central Nervous System
Milan Vašák and Gabriele Meloni

12 Metallothionein Toxicology: Metal Ion Trafficking and Cellular Protection
David H. Petering, Susan Krezoski, and Niloofar M. Tabatabai

13 Metallothionein in Inorganic Carcinogenesis
Michael P. Waalkes and Jie Liu

14 Thioredoxins and Glutaredoxins. Functions and Metal Ion Interactions
Christopher Horst Lillig and Carsten Berndt

15 Metal Ion-Binding Properties of Phytochelatins and Related Ligands
Aurélie Devez, Eric Achterberg, and Martha Gledhill

Subject Index

Volume 6 Metal-Carbon Bonds in Enzymes and Cofactors

1 Organometallic Chemistry of B_{12} Coenzymes
Bernhard Kräutler

2 Cobalamin- and Corrinoid-Dependent Enzymes
Rowena G. Matthews

3 Nickel-Alkyl Bond Formation in the Active Site of Methyl-Coenzyme M Reductase
Bernhard Jaun and Rudolf K. Thauer

4 Nickel-Carbon Bonds in Acetyl-Coenzyme A Synthases/ Carbon Monoxide Dehydrogenases
Paul A. Lindahl

5 Structure and Function of [NiFe]-Hydrogenases
Juan C. Fontecilla-Camps

6 Carbon Monoxide and Cyanide Ligands in the Active Site of [FeFe]-Hydrogenases
John W. Peters

7 Carbon Monoxide as Intrinsic Ligand to Iron in the Active Site of [Fe]-Hydrogenase
Seigo Shima, Rudolf K. Thauer, and Ulrich Ermler

8 The Dual Role of Heme as Cofactor and Substrate in the Biosynthesis of Carbon Monoxide
Mario Rivera and Juan C. Rodriguez

9 Copper-Carbon Bonds in Mechanistic and Structural Probing of Proteins as well as in Situations where Copper Is a Catalytic or Receptor Site
Heather R. Lucas and Kenneth D. Karlin

10 Interaction of Cyanide with Enzymes Containing Vanadium and Manganese, Non-Heme Iron, and Zinc
Martha E. Sosa-Torres and Peter M. H. Kroneck

11 The Reaction Mechanism of the Molybdenum Hydroxylase Xanthine Oxidoreductase: Evidence against the Formation of Intermediates Having Metal-Carbon Bonds
Russ Hille

12 Computational Studies of Bioorganometallic Enzymes and Cofactors
Matthew D. Liptak, Katherine M. Van Heuvelen, and Thomas C. Brunold

Subject Index

Author Index of *MIBS*-1 to *MIBS*-44 and *MILS*-1 to *MILS*-6

Volume 7 Organometallics in Environment and Toxicology

1 Roles of Organometal(loid) Compounds in Environmental Cycles
John S. Thayer

2 Analysis of Organometal(loid) Compounds in Environmental and Biological Samples
Christopher F. Harrington, Daniel S. Vidler, and Richard O. Jenkins

3 Evidence for Organometallic Intermediates in Bacterial Methane Formation Involving the Nickel Coenzyme F_{430}
Mishtu Dey, Xianghui Li, Yuzhen Zhou, and Stephen W. Ragsdale

4 Organotins. Formation, Use, Speciation, and Toxicology
Tamas Gajda and Attila Jancsó

5 Alkyllead Compounds and Their Environmental Toxicology
Henry G. Abadin and Hana R. Pohl

6 Organoarsenicals: Distribution and Transformation in the Environment
Kenneth J. Reimer, Iris Koch, and William R. Cullen

7 Organoarsenicals. Uptake, Metabolism, and Toxicity
Elke Dopp, Andrew D. Kligerman, and Roland A. Diaz-Bone

8 Alkyl Derivatives of Antimony in the Environment
Montserrat Filella

9 Alkyl Derivatives of Bismuth in Environmental and Biological Media
Montserrat Filella

10 Formation, Occurrence and Significance of Organoselenium and Organotellurium Compounds in the Environment
Dirk Wallschläger and Jörg Feldmann

11 Organomercurials. Their Formation and Pathways in the Environment
Holger Hintelmann

12 Toxicology of Alkylmercury Compounds
Michael Aschner, Natalia Onishchenko, and Sandra Ceccatelli

13 Environmental Bioindication, Biomonitoring, and Bioremediation of Organometal(loid)s
John S. Thayer

14 Methylated Metal(loid) Species in Humans
Alfred V. Hirner and Albert W. Rettenmeier

Subject Index

Volume 8 Metal Ions in Toxicology: Effects, Interactions, Interdependencies

1 Understanding Combined Effects for Metal Co-exposure in Ecotoxicology
Rolf Altenburger

2 Human Risk Assessment of Heavy Metals: Principles and Applications
Jean-Lou C. M. Dorne, George E. N. Kass, Luisa R. Bordajandi, Billy Amzal, Ulla Bertelsen, Anna F. Castoldi, Claudia Heppner, Mari Eskola, Stefan Fabiansson, Pietro Ferrari, Elena Scaravelli, Eugenia Dogliotti, Peter Fuerst, Alan R. Boobis, and Philippe Verger

3 Mixtures and Their Risk Assessment in Toxicology
Moiz M. Mumtaz, Hugh Hansen, and Hana R. Pohl

4 Metal Ions Affecting the Pulmonary and Cardiovascular Systems
Massimo Corradi and Antonio Mutti

5 Metal Ions Affecting the Gastrointestinal System Including the Liver
Declan P. Naughton, Tamás Nepusz, and Andrea Petroczi

6 Metal Ions Affecting the Kidney
Bruce A. Fowler

7 Metal Ions Affecting the Hematological System
Nickolette Roney, Henry G. Abadin, Bruce Fowler, and Hana R. Pohl

8 Metal Ions Affecting the Immune System
Irina Lehmann, Ulrich Sack, and Jörg Lehmann

9 Metal Ions Affecting the Skin and Eyes
Alan B. G. Lansdown

10 Metal Ions Affecting the Neurological System
Hana R. Pohl, Nickolette Roney, and Henry G. Abadin

11 Metal Ions Affecting Reproduction and Development
Pietro Apostoli and Simona Catalani

12 Are Cadmium and Other Heavy Metal Compounds Acting as Endocrine Disrupters?
Andreas Kortenkamp

13 Genotoxicity of Metal Ions: Chemical Insights
Woijciech Bal, Anna Maria Protas, and Kazimierz S. Kasprzak

14 Metal Ions in Human Cancer Development
Erik J. Tokar, Lamia Benbrahim-Tallaa, and Michael P. Waalkes

Subject Index

Volume 9 Structural and Catalytic Roles of Metal Ions in RNA

1 Metal Ion Binding to RNA
Pascal Auffinger, Neena Grover, and Eric Westhof

2 Methods to Detect and Characterize Metal Ion Binding Sites in RNA
Michèle C. Erat and Roland K.O. Sigel

3 Importance of Diffuse Metal Ion Binding to RNA
Zhi-Jie Tan and Shi-Jie Chen

4 RNA Quadruplexes
Kangkan Halder and Jörg S. Hartig

5 The Roles of Metal Ions in Regulation by Riboswitches
Adrian Ferré-D'Amaré and Wade C. Winkler

6 Metal Ions: Supporting Actors in the Playbook of Small Ribozymes
Alexander E. Johnson-Buck, Sarah E. McDowell, and Nils G. Walter

7 Multiple Roles of Metal Ions in Large Ribozymes
Daniela Donghi and Joachim Schnabl

8 The Spliceosome and Its Metal Ions
Samuel E. Butcher

9 The Ribosome: A Molecular Machine Powered by RNA
Krista Trappl and Norbert Polacek

10 Metal Ion Requirements in Artificial Ribozymes that Catalyze Aminoacylations and Redox Reactions
Hiroaki Suga, Kazuki Futai, and Koichiro Jin

11 Metal Ion Binding and Function in Natural and Artificial Small RNA Enzymes from a Structural Perspective
Joseph E. Wedekind

12 Binding of Kinetically Inert Metal Ions to RNA: The Case of Platinum(II)
Erich G. Chapman, Alethia A. Hostetter, Maire F. Osborn, Amanda L. Miller, and Victoria J. DeRose

Subject Index

Volume 10 Interplay between Metal Ions and Nucleic Acids

1 Characterization of Metal Ion-Nucleic Acid Interactions in Solution
Maria Pechlaner and Roland K.O. Sigel

2 Nucleic Acid-Metal Ion Interactions in the Solid State
Katsuyuki Aoki and Kazutaka Murayama

3 Metal Ion-Promoted Conformational Changes of Oligonucleotides
Bernhard Spingler

4 G-Quadruplexes and Metal Ions
Nancy H. Campbell and Stephen Neidle

5 Metal Ion-Mediated DNA-Protein Interactions
Barbara Zambelli, Francesco Musiani, and Stefano Ciurli

6 Spectroscopic Investigations of Lanthanide Ion Binding to Nucleic Acids
Janet R. Morrow and Christopher M. Andolina

7 Oxidative DNA Damage Mediated by Transition Metal Ions and Their Complexes
Geneviève Pratviel

8 Metal Ion-Dependent DNAzymes and Their Applications as Biosensors
Tian Lan and Yi Lu

9 Enantioselective Catalysis at the DNA Scaffold
Almudena García-Fernández and Gerard Roelfes

10 Alternative DNA Base Pairing through Metal Coordination
Guido H. Clever and Mitsuhiko Shionoya

11 Metal-Mediated Base Pairs in Nucleic Acids with Purine- and Pyrimidine-Derived Nucleosides
Dominik A. Megger, Nicole Megger, and Jens Müller

12 Metal Complex Derivatives of Peptide Nucleic Acids
Roland Krämer and Andrij Mokhir

Subject Index

Volume 11 Cadmium: From Toxicity to Essentiality (this book)

Volume 12 Metallomics and the Cell
Guest Editor: Lucia Banci

Obituary to Ivano Bertini

1 Metallomics and the Cell: Some Definitions and General Comments
Lucia Banci and Ivano Bertini

2 Technologies for Detecting Metals in Single Cells
James E. Penner-Hahn

3 Sodium/Potassium Homeostasis in the Cell
Michael J.V. Clausen and Hanne Poulsen

4 Cellular Magnesium Homeostasis in Mammalian Cells
Andrea M.P. Romani

5 Intracellular Calcium Homeostasis and Signaling
Marisa Brini, Tito Calì, Denis Ottolini, and Ernesto Carafoli

6 Manganese Homeostasis and Transport
Jerome Roth, Silvia Ponzoni, and Michael Aschner

7 Control of Iron Metabolism in Bacteria
Ian Norton, Arvindkumar S. Salunkhe, Helen Goodluck, Wafaa S.M. Aly, Hanna Mourad-Agha, Pierre Cornelis, and Simon C. Andrews

8 The Iron Metallome in Eukaryotic Organisms
Adrienne C. Dlouhy and Caryn E. Outten

9 Heme Uptake and Metabolism in Bacteria
David R. Benson and Mario Rivera

10 Cobalt and Corrinoid Transport and Biochemistry
Valentin Cracan and Ruma Banerjee

11 Nickel Metallomics: General Themes Guiding Nickel Homeostasis
Andrew M. Sydor and Deborah B. Zamble

12 The Copper Metallome in Prokaryotic Cells
Christopher Rensing and Sylvia Franke McDevitt

13 The Copper Metallome in Eukaryotic Cells
Katherine E. Vest, Hayaa F. Hashemi, and Paul A. Cobine

14 Zinc and the Zinc Proteome
Wolfgang Maret

15 Metabolism of Molybdenum
Ralf R. Mendel

16 Comparative Genomics Analysis of the Metallomes
Vadim N. Gladyshev and Yan Zhang

Subject Index

Volume 13 Interrelations between Essential Metal Ions and Human Diseases
(in preparation)

1 Metal Ions and Infectious Diseases. An Overview from the Clinic
Peggy L. Carver

2 Sodium and Potassium in Health and Disease
Hana R. Pohl

3 Magnesium in Health and Disease
Andrea M. P. Romani

4 Calcium in Health and Disease
Marisa Brini and Ernesto Carafoli

5 Chromium. Is It Essential, Pharmacologically Relevant or Toxic?
John B. Vincent

6 Vanadium. Its Role for Humans
Dieter Rehder

7 Manganese in Health and Disease
Michael Aschner

8 Iron: Effects of Deficiency and Overload
Xiaole Kong and Robert C. Hider

9 Cobalt: Its Role in Health and Disease
Kazuhiro Yamada

10 Nickel and Human Health
Barbara Zambelli and Stefano Ciurli

11 Copper: Effects of Deficiency and Overload
Julian F. B. Mercer and Roxana Llanos

12 Zinc and Human Disease
Wolfgang Maret

13 Molybdenum in Human Health and Disease
Guenter Schwarz

14 Silicon. The Health Benefits of a Metalloid
Keith R. Martin

15 Arsenic. Can this Toxic Metalloid Sustain Life?
Dean E. Wilcox and Brian P. Jackson

16 Selenium. Role of the Essential Metalloid in Health
Suguru Kurokawa and Marla J. Berry

Subject Index

Volume 14 The Metal-Driven Biogeochemistry of Gaseous Compounds in the Environment (in preparation)
Guest Editors: Peter M.H. Kroneck and Martha E. Sosa-Torres

Comments and suggestions with regard to contents, topics, and the like for future volumes of the series are welcome.

Chapter 1
The Bioinorganic Chemistry of Cadmium in the Context of Its Toxicity

Wolfgang Maret and Jean-Marc Moulis

Contents

ABSTRACT 2
1 INTRODUCTION 2
2 CADMIUM COORDINATION CHEMISTRY OF BIOLOGICAL RELEVANCE 3
2.1 Cadmium Complexes, Stabilities, and Properties 3
2.2 Cadmium Protein Complexes 4
2.3 Cadmium Interactions with Other Biomolecules 6
3 CADMIUM BIOCHEMISTRY 6
3.1 Tissue Concentrations, Distribution, and Speciation in Humans and Animals 8
3.2 Transport and Trafficking: General Principles and Main Actors in Animal Cells 9
3.2.1 Cadmium Trafficking 10
3.2.2 Transport of Cadmium Salts via Transporters for Other Cations 10
3.2.3 Transport of Complexed Forms of Cd^{2+} 13
3.2.4 Other Ways to Cross Membranes 13
4 CADMIUM TOXICITY 14
4.1 Exposure of Humans to Cadmium and Patho-Physiological Consequences 14
4.2 Mechanisms of Molecular Toxicity 16
4.2.1 Interference with Redox Homeostasis 16
4.2.2 Interference with Homeostasis of Essential Metal Ions 17
4.2.3 Interactions with Metalloproteins 19
4.2.4 Interaction with Other Proteins 20
4.2.5 Other Mechanisms 21
4.3 Toxicology with Reference to Specific Organs 22

W. Maret (✉)
King's College London, School of Medicine, Diabetes and Nutritional Sciences Division, Metal Metabolism Group, London, SE1 9NH, UK
e-mail: wolfgang.maret@kcl.ac.uk

J.-M. Moulis
CEA, DSV, IRTSV, Laboratoire de Chimie et Biologie des Métaux,
17 ave des Martyrs, F-38054 Grenoble, France

CNRS UMR5249, Grenoble, France

Université Joseph Fourier, Grenoble 1, France
e-mail: jean-marc.moulis@cea.fr

A. Sigel, H. Sigel, and R.K.O. Sigel (eds.), *Cadmium: From Toxicity to Essentiality*,
Metal Ions in Life Sciences 11, DOI 10.1007/978-94-007-5179-8_1,

5 CONCLUDING REMARKS AND FUTURE DIRECTIONS 23
5.1 Reference Dose and Recommendations about Cadmium in Water, Soil, and Food 23
5.2 Where Is the Problem? Do We Know What We Need to Know? Problem Solved? 24
ABBREVIATIONS 25
REFERENCES 26

Abstract Cadmium is known for its toxicity in animals and man as it is not used in these species. Its only role in biology is as a zinc replacement at the catalytic site of a particular class of carbonic anhydrases in some marine diatoms. The toxicity of cadmium continues to be a significant public health concern as cadmium enters the food chain and it is taken up by tobacco smokers. The biochemical basis for its toxicity has been the objective of research for over 50 years. Cadmium damages the kidneys, the lungs upon inhalation, and interferes with bone metabolism. Evidence is accumulating that it affects the cardiovascular system. Cadmium is classified as a human carcinogen. It generates oxidative stress. This chapter discusses the chemistry and biochemistry of cadmium(II) ions, the only important state of cadmium in biology. This background is needed to interpret the countless effects of cadmium in laboratory experiments with cultured cells or with animals with regard to their significance for human health. Evaluation of the risks of cadmium exposure and the risk factors that affect cadmium's biological effects in tissues is an on-going process. It appears that the more we learn about the biochemistry of cadmium and the more sensitive assays we develop for determining exposure, the lower we need to set the upper limits for exposure to protect those at risk. But proper control of cadmium's presence and interactions with living species and the environment still needs to be based on improved knowledge about the mechanisms of cadmium toxicity; the gaps in our knowledge in this area are discussed herein.

Keywords buffering of metals • cadmium • metal homeostasis • metal signaling • toxicity

1 Introduction

According to Greek Mythology, Cadmus, son of a Phoenician king, founded Thebes, and gave the Greeks the letters of their alphabet. But he and his wife Harmonia ended their lives as serpents. It is this dichotomy of achievement and fatality that are reminiscent of cadmium's role in industrial chemistry and biology.

In group 12 of the Periodic System of the Chemical Elements, cadmium is between zinc and mercury. It shares some properties with the essential element zinc, its lower atomic weight neighbor, and with the toxic element mercury, its higher atomic weight neighbor.

Two chemists discovered cadmium independently as an impurity of calamine (zinc carbonate) in 1817. There is 0.1–0.5 ppm of cadmium in the earth's crust. Cadmium is used as a yellow/orange pigment when combined with chalcogenides,

as an anticorrosion agent in steel, as a plastic stabilizer, as an electrode material in NiCd batteries, and as a semi-conductor in Cd-chalcogenide solar cells. Its mining, smelting, and industrial usage increased the availability in the environment and anthropogenic sources are the most significant threat to human health. The main route of exposure is through nutrition and smoking. Some plants, e.g., rice, tobacco, and mushrooms accumulate cadmium several fold from the soil on which they grow and they are a source of contamination to wildlife, livestock, and humans. Use of phosphate fertilizers and sewage sludge, and improper maintenance of soils contributes to cadmium mobilization in the environment and accumulation in crops.

2 Cadmium Coordination Chemistry of Biological Relevance

2.1 Cadmium Complexes, Stabilities, and Properties

With a filled *d*-shell of electrons, cadmium(II) biology resembles zinc(II) biology regarding the flexibility in coordination and the lack of redox chemistry. Thus, the only valence state important for biology is cadmium(II). The crystal ionic radius (109 pm) of Cd^{2+} is larger than that of Zn^{2+} (88 pm), increasing the potential of cadmium to adopt higher coordination numbers. This leads to slightly longer bond lengths in its coordination compounds. Cadmium(II) is a softer Lewis acid than zinc(II). Hence, it has slightly lower stabilities in complexes with oxygen and nitrogen ligands. For example, the log *K* values of citrate, aspartate, histidine, and EDTA are 4.8, 5.7, 6.5, and 16.5 for Zn^{2+} and 3.7, 4.5, 5.4, and 16.5 for Cd^{2+} [1]. However, relative affinities of the two ions are reversed for sulfur ligands as cadmium is considerably more thiophilic than zinc, e.g., the log *K* values of cysteine are 9.2 for Zn^{2+} and 11.0 for Cd^{2+}. This fact has been expressed as a stability ruler [2]. It is not widely documented in the biological cadmium literature, but it is perhaps the single most important characteristic of cadmium for the interpretation of its biological intracellular effects as sulfur coordination chemistry is typical for intracellular but not extracellular coordination. Outside cells, the reduction potential is higher than inside, and most thiols are oxidized to disulfides. With a relative large number of sulfur donors available intracellularly, on average, cadmium is bound more strongly than zinc in the cell. In biological coordination spheres with multiple cysteine ligands, the increase in affinity is compounded. For example in metallothionein (MT), cadmium is in a tetrathiolate coordination environment and its binding is three orders of magnitude higher than that of zinc. From these thermodynamic considerations one predicts that cadmium binds with decreasing affinity in the series of tetrahedral zinc sites in proteins: $ZnS_4 > ZnNS_3 > ZnN_2S_2$ as verified experimentally [3]. Thus, cadmium binds more strongly to ZnS_4 than to ZnN_2S_2 sites of classic zinc finger transcription factors [4]. The relative affinities mean that cadmium(II) ion concentrations must be higher than zinc concentrations to displace zinc from coordination sites with oxygen and nitrogen donors. However, to bind in ZnS_4 sites, cadmium(II) ion concentrations

need to be only one thousandth of those of zinc for effective competition. For zinc, such large differential affinities between different biological coordination environments are less pronounced [5].

In a biological application of the Irving-Williams series, which was founded on nitrogen and oxygen donor atoms in similar coordination environments, cadmium is bound relatively tightly compared to the alkaline earth cations of calcium and magnesium. Its binding is about 6 orders higher than that of calcium and about 9 orders higher than that of magnesium [6]. Therefore, cadmium could compete with calcium, the cellular concentrations of which are a few millimolar, when its cellular concentrations reach a few nanomolar. However, because of the relatively high buffering capacity of high affinity thiolate coordination sites, where calcium does not bind, competition is not readily realized. Still cadmium(II) ions bind in calcium-binding sites of proteins *in vitro* because the ionic radius of Ca^{2+} (114 pm) is quite similar to that of Cd^{2+} (109 pm). On the above theoretical grounds, cadmium would compete effectively with sulfur-bound Cu^{+}, or iron in iron-sulfur proteins, although experimental evidence *in vivo* is lacking [7]. The prediction on first principles of metal/Cd substitution is borne out by the fact that cadmium will be found in proteins with sulfur donors, such as MT.

An analysis of the cadmium proteome under different conditions of exposure has not been performed, in part because coordination compounds do not readily sustain the harsh conditions implemented for efficient proteomic analysis. Hence, we do not know which proteins other than MT contain cadmium. These considerations have yet other important consequences. Essential transition metal ions are homeostatically controlled. Cadmium, which is not essential for animals and man, is not under such homeostatic control. Both essential and non-essential metal ions are buffered at concentrations that are governed by the Irving-Williams series [8]. A non-essential metal ion, such as cadmium, is not buffered by any specific system but may interact with molecules involved in the control of essential transition metal ions. For biological cadmium coordination, there is very tight binding of cadmium to proteins, in the range of picomolar or even less. Because intracellular zinc buffering involves sulfur donors from thiols [9], free cytosolic cadmium(II) ion concentrations are expected to be lower than those of zinc. With estimates of free zinc(II) ion concentrations in the range of tens or hundreds of picomolar, free cadmium(II) ion concentrations at cellular loads that do not surpass the zinc buffering capacity can be estimated to be subpicomolar. The biochemistry of cadmium is based on its strong complexation with proteins and other molecules such as glutathione (GSH). Any cellular mechanisms that invoke free cadmium(II) ions as the cytotoxic species would need to postulate the absence of any cellular binding sites for cadmium, which is an unrealistic assumption.

2.2 Cadmium Protein Complexes

Some characteristics of cadmium are favorable for biophysical investigations of metalloproteins. Consequently, cadmium is often used as probe for the native metal

ions. Though it is diamagnetic as zinc is, it has some physical properties that zinc does not have. ^{111}Cd and ^{113}Cd isotopes are NMR-active and they have been employed to investigate the metal coordination chemistry in cadmium-substituted zinc proteins (see also Chapter 6). An excited, metastable state of ^{111m}Cd is used for perturbed angular correlation (PAC) spectroscopy of γ rays, another method that probes the coordination environment of cadmium in solution. Cadmium-substituted metalloproteins are also used in X-ray crystallography as the heavy metal atom helps solving the phase problem. Accordingly, the protein database contains the structure of about 600 proteins with bound cadmium (www.rcsb.org). This relatively large number of proteins and the relative ease of substituting metals in metalloproteins by cadmium should not be perceived as a biological role of cadmium in these proteins.

Cadmium often has a very similar coordination sphere as zinc in proteins, though bonds are longer, and there is a tendency for binding of an additional ligand and thus an increase in coordination number. Substitution of zinc by cadmium in structural sites has little influence on protein structure. However, small as these structural effects are, they may have some consequences on metal selectivity. Thus the volumes of the cadmium/thiolate clusters in cadmium-MT are about 20% higher than the volumes of the zinc/thiolate clusters in zinc-MT [10]. If the metal-binding site has other than purely structural functions, the situation is different. For example, some zinc/thiolate sites are redox switches, in which the redox chemistry of the thiolate ligands determines zinc association and dissociation [11]. A cadmium-sulfur bond does not have the same reactivity as a zinc-sulfur bond. Whether or not cadmium blocks or reduces significantly the activity of such redox switches is not known. Also, cadmium(II) is a weaker Lewis acid than zinc(II): therefore any acid/base chemistry in a catalytic site of a zinc enzyme will be different from the corresponding cadmium-substituted enzyme. For example, if a zinc-bound hydroxide is the nucleophile in the enzymatic reaction, then the cadmium-bound water of the cadmium-substituted enzyme, which has a higher pK_a than the zinc-bound water, would lower the activity at physiological pH. Though cadmium-substituted enzymes are often active, their kinetic properties are different. The biological consequences may be more drastic when cadmium binds to a protein and blocks its activity if it is an essential one. Similarly, cadmium binding to MT could well interfere with the function of this protein in zinc homeostasis. Due to the higher affinity of cadmium in the tetrathiolate site, its dissociation rates are slower than those of zinc. Thus, any metal function based on metal transfer rates will be affected.

Though cadmium exchanges rather fast in intramolecular ligand-exchange reactions in sulfur sites, e.g., in the order of seconds in the two domains of MT, its biological half life in the body is several years. The reason is that cadmium enters cells with relative ease, e.g., through some zinc transporters of the ZIP (Zrt- and Irt-related proteins) family, but the human ZnT exporters seem to be rather selective for zinc and do not seem to transport cadmium out of cells [11b]. Thus, in addition to cadmium becoming trapped intracellularly in proteins such as MT, there seems to be no mechanism for export of the cadmium(II) ion. Only complexed forms of cadmium can leave cells and can diffuse throughout the body, from the liver to the kidneys for cadmium-MT, for instance (see Section 3).

One major hypothesis is that most of cadmium toxicology occurs through interference with the control of cellular zinc homeostasis. A discussion of the biological effects of cadmium in relation to its closest chemical congener zinc needs to be based on important recent developments in understanding cellular zinc metabolism. The zinc proteome comprises about 3000 human proteins [12]. The total cellular zinc ion concentrations are rather high, in the range of a few hundred micromolar. Cellular zinc ions are highly compartmentalized. Two dozen zinc transporters orchestrate the inter- and intra-compartmental zinc traffic. Thus the cellular biology of cadmium needs to consider the subcellular distribution of zinc, in particular which of the zinc transporters carry cadmium through biological membranes. One recent development is the realization that intracellularly stored zinc(II) ions are released in a controlled way, e.g., from the endoplasmic reticulum, and serve regulatory functions in the cell ("zinc signaling") [13]. Here, the issue whether or not cadmium(II) ions are stored and released in a similar way, and if so, whether they bias normal physiological zinc signaling or stores provide an intracellular source of cadmium(II) ions, needs experimental scrutiny.

2.3 Cadmium Interactions with Other Biomolecules

Cadmium(II) ions bind to many biomolecules other than proteins. However, any biological data invoking such interactions must account for competition between binding to the biomolecule and binding to abundant protein sites, unoccupied or occupied with other metal ions. In order to compete effectively non-protein binding sites need to have higher affinities than protein sites. Given the high affinity of some proteins such as MTs for cadmium, cadmium complexes not being kinetically inert, and the thiophilic nature of cadmium, it appears that binding to biomolecules other than proteins is not readily realized in the cell under steady state conditions. The zinc buffering capacity must be completely exhausted before the free cadmium(II) ion concentration becomes higher than the free zinc(II) concentration. Furthermore, once cadmium competed effectively with zinc sites for which it has higher affinity, the total cadmium concentration still would have to be about as high as the total cellular zinc concentration, which is a few hundred micromolar, for efficient competition with the other sites.

3 Cadmium Biochemistry

The biochemistry of cadmium is intimately linked to that of MT. The discovery of MT was the result of a search for a biological function of cadmium [14]. The name metallothionein was chosen for this cadmium-binding protein isolated from horse kidneys to indicate the occurrence of several types of metal ions in the isolated

material (*metallo-*) and the high sulfur (cysteine) content of the protein (*-thionein*). Under normal physiological conditions MTs bind zinc or copper. The binding of cadmium is a result of the accumulation of this metal ion in the kidney cortex with age or under conditions of environmental and nutritional exposures. Cadmium also accumulates as a result of perturbations of metal homeostasis in certain diseases that constitute a cumulative risk for cadmium toxicology and co-morbidity. The field of cadmium biology started with the discovery of MT, but it never fulfilled the original expectation that cadmium may have an essential function in mammalian biology. In 2000 it was reported that *Thalassiosira weissflogii*, a marine diatom, employs cadmium in a carbonic anhydrase, which otherwise is a zinc enzyme [15]. It demonstrates the flexibility and sometimes promiscuity of some unicellular organisms in switching from one metal to another depending on metal availability in ecological niches [16].

A characteristic feature of mammalian MTs is the binding of seven divalent transition metal ions in two metal/thiolate clusters, a $M(II)_3S_9$ cluster in the N-terminal β-domain and a $M(II)_4S_{11}$ cluster in the C-terminal α-domain. In mammalian MTs, the metals determine the tertiary structure of the protein, and they are buried in the interior of the two domains. The peptide chain wraps around the two clusters, and binds up to seven divalent transition metal ions with tetrahedral geometry and exclusively with the sulfur donors of the twenty cysteines. In humans, MTs belong to a family of at least a dozen proteins [17].

Cadmium induces MT. However, this induction was postulated to occur through a mechanism where cadmium displaces zinc in the extant MT and then the released zinc activates metal response element (MRE)-binding transcription factor-1 (MTF1), the transcription factor involved in zinc-dependent MT expression [18]. Under conditions of sublethal cadmium exposure, the maximum number of cadmium ions accumulating in rat MT is five. A species with seven cadmium ions can be prepared by removing all metals from isolated MTs and then reconstituting the protein with cadmium. The crystal structure of cadmium-induced rat MT shows four of the cadmium ions in the α-domain and one cadmium ion and two zinc ions at defined positions in the β-domain [19]. This distribution likely reflects differential affinities of the individual metal binding sites in MT [20], but the cadmium affinity for MT is on average three orders of magnitude higher than that of zinc.

While thermodynamically a sink for cadmium, MT is not a safe storage for cadmium. MT is a reactive molecule that is involved in the intracellular re-distribution of metal ions. MT exchanges cadmium with other thiol-containing proteins by ligand exchange. The cysteine thiols in MT react with electrophiles and concomitant metal dissociation. The metal load of MT is a major factor in determining this reactivity. The thiolate ligands in MT confer redox activity on the metal/thiolate clusters, and therefore MTs are redox proteins [21]. In contrast to other redox-active metalloproteins, the ligands, and not the central cadmium or zinc ions, which are redox-inert in biology, are redox-active in MT. A host of thiol-reactive electrophiles release metal ions from either isolated or cellular MT. Nitrogen monoxide reacts with MT and releases cadmium from MT [22]. Because of the higher thermodynamic stability of Cd_7- *versus* Zn_7-MT, the reactivity with electrophiles is considerably quenched in the former. However, since

the species *in vivo* is not Cd_7-MT but a species with a maximum of five cadmium ions, as demonstrated by rat Cd_5Zn_2MT prepared for the determination of the crystal structure of MT, cellular cadmium MT retains zinc/thiolate bonds that are expected to remain reactive like in Zn_7-MT. Detoxification of cadmium is certainly not the primary function of MT, which is in zinc traffic and transient zinc storage. Hence, cadmium toxicology with regard to MT needs to be discussed with regard to cadmium's effect on zinc and, possibly, copper homeostasis. MT-1/-2 knock-out mice are more sensitive to cadmium toxicity [23,24] but they are also more sensitive to zinc toxicity [25].

Cells take up MT from the circulation through a megalin/cubilin scavenger receptor pathway [26,27]. The internalized MT then releases cadmium in an endosomal/lysosomal compartment and divalent metal transporter 1 (DMT1) transports cadmium into the cytosol where it binds to extant MT and/or induces additional MT through the release of zinc from extant MT [28]. MT also is secreted from cells [29]. However, the pathway and mechanism of MT secretion remains elusive as in animals and man no pre-protein with an amino acid signature for export has been identified. Cd-MT may cross the plasma membrane of liver and other cells by fluid-phase exocytosis [30]. Extracellular MT is found under a variety of conditions including increasing cadmium loads [31].

3.1 Tissue Concentrations, Distribution, and Speciation in Humans and Animals

Cadmium in blood is bound to red blood cells. Cadmium analysis of whole blood is a measure of recent exposure. The main target organs of cadmium are the liver and the kidneys, accounting together for about 50–75% of body cadmium [32]. The highest tissue concentration and accumulation is in the kidneys. Relatively higher concentrations when compared to muscle and bone are found in testes, pancreas, and spleen. Cadmium distributes to most but not all organs since some tissues are protected. Cadmium has a very long biological half-life in tissues, which has been estimated to be more than ten years for most of them [33,34]. The uptake of cadmium is 40-60% from inhaled particles in the respiratory tract *versus* 5–10% from ingested forms in the gastrointestinal tract. These percentages reflect the efficiency of uptake rather than the role of these tissues in the absolute amount of cadmium taken up. The relatively high proportion of cadmium taken up by lungs poses a considerable and high risk for damage to this organ through inhaled cadmium, as is the case for smokers. From the blood, cadmium reaches the liver, where it induces MT. MT then is distributed to other organs. In the kidney, cadmium is filtered by the glomeruli and re-absorbed by the epithelial cells of the proximal tubules, where it accumulates.

MT scavenges cadmium in most cells and also contributes to carrying it in the circulation. Proximal tubules internalize Cd-MT by receptor-mediated endocytosis

and they seem to efficiently release toxic forms of cadmium from their endosomes. At threshold levels, cadmium damages the proximal tubules with ensuing proteinuria and "cadmiumuria", followed by a renal Fanconi syndrome, and eventually kidney failure. The critical cadmium burden for the kidney is about 200 μg/g. This figure must be compared with the range of 15–40 μg/g estimated in the general population of 40–60 years of age in Europe [35], and with values of 70-85 μg/g reported for older people in Japan [36]. The urinary concentration of cadmium in otherwise healthy individuals is <1μg per g of creatine and is proportional to the cadmium content of the kidney, yet the excretion is too insignificant to rid the body of cadmium as the total excretion daily through all pathways (urine, intestine, sweat) is only $<0.01\%$ of the total body cadmium. Reabsorptive dysfunction can be measured by a range of biomarkers that are secreted into urine.

Damage is generally considered significant for urinary cadmium concentrations above 2 μg/g creatinine as they correlate with increased β_2-microglobulin excretion (see for instance [37]). Also, patients with cadmium-induced kidney damage lose calcium with ensuing skeletal changes resulting in osteomalacia and osteoporosis. In addition, the damaged kidneys may decrease the conversion rate of vitamin D into the active hormone calcitriol leading to less bone mineralization [38]. However, even low doses of cadmium exposure affect bone mineral density [39,40]. The other two important factors in tissue accumulation and distribution of cadmium are that uptake is higher in children and that it accumulates steadily throughout life [32], thus calling attention to the adverse health effects of cadmium in the elderly. Cadmium transport from the placenta to the fetus and into the mother's milk is restricted, protecting the fetus and the newborn, although urinary cadmium levels of infants follow those of their mothers [41]. The blood-brain barrier seems to be an efficient protection of the brain against cadmium, but more data in humans and animals are needed to support this conclusion.

Cadmium uptake is also dependent on gender, the nutritional status, in particular the status of other metal ions, and calcium and fiber in the diet. Under iron and zinc deficiency, cadmium uptake is higher (see Section 3.2.2 below). Vegetarian diets are of concern due to cadmium accumulation in crops and nutritionally induced mineral deficiencies. The damage to the kidney is dependent on these factors with contribution from co-morbidities, such as diabetic nephropathies.

3.2 Transport and Trafficking: General Principles and Main Actors in Animal Cells

Throughout evolution, living species have been exposed to cadmium in proportion to the occurrence of the element in different and varying ecological settings. However, no evidence shows that Life has ever developed any specialized system to deal with cadmium. Consequently, transport and trafficking of cadmium, in higher eukaryotes in particular, relies on molecular components, which are

invariably present for other purposes than cadmium handling. This hitch-hiker behavior of cadmium involves a surprisingly wide array of biological molecules. This is a consequence of the peculiar properties of Cd^{2+} presented above (Sections 1 and 2), and the abundance and variety of potential ligands in biological systems.

3.2.1 Cadmium Trafficking

Entry of cadmium into the body is mainly via inhalation of particulate material or via ingestion from the diet and water. Biochemical processing of the chemical forms of cadmium found in these media is likely, for example when transporters help Cd^{2+} to permeate the intestinal and lung barriers. However, some other complexed forms of cadmium also appear to be absorbed. For instance, cadmium-bound phytochelatins, polymers of the γ-glutamate-cysteine dipeptide bound to a terminal glycine as in glutathione, found in contaminated crops are efficient vectors for cadmium absorption [42]. Also, Cd-MT present in meat, offal-containing diets in particular, seems to be absorbed intact by enterocytes and to be degraded only when it reaches the kidneys [43].

Once in the circulation, cadmium mainly associates with proteins, such as albumin [44], transferrin [45], and MT [46]. But attempts to measure the chemical environment of cadmium ions in animal tissues and fluids refuted the idea that cadmium is bound in a unique compound such as a universal chelating agent. The data indicate instead that a dynamic exchange of cadmium occurs among many different molecules, both in the circulation and within cells, and many molecules interact with Cd^{2+} and move it over large distances in multi-cellular organisms. Yet, some intracellular components play prominent roles in cadmium traffic. GSH is an abundant cellular compound, present at mM concentrations. It binds cadmium and undoubtedly participates in its traffic. Also, as much as zinc and copper, but by different mechanisms, cadmium is a strong inducer of MTs, which are major actors in cadmium trafficking (see above).

Throughout the process of cadmium distribution within the body, membrane systems are necessarily involved in helping cadmium to cross ion-tight biological barriers and to permeate cells. A survey of such systems in animals follows.

3.2.2 Transport of Cadmium Salts via Transporters for Other Cations

The early period of research into the toxicity of cadmium for animals did not lead to conclusive evidence for a single, ubiquitous, high affinity, and dedicated component that would allow Cd^{2+} to cross biological membranes and to obtain indiscriminate access to any location. However, it was soon realized that many ionic channels do interact with Cd^{2+}. Numerous electrophysiological studies described the inhibition of potassium, sodium, magnesium, or calcium fluxes by high concentrations of cadmium salts (reviewed in [47]), in neuronal cells in particular. Of note, such inhibitory effects induced by Cd^{2+} may not result from simple competition between the physiological cations and cadmium at the sites of transport. Indeed, many

channels and transporters are gated by various molecules and ions via readily accessible regulatory sites and Cd^{2+} can bind to many of these sites, following the 'rules' presented in the Introduction and in Section 2. Some of the proteins involved in the transport of alkali and alkaline earth metal ions have been suggested as cadmium transporters. Yet, such suggestions have not reached a level of certainty that would leave no doubt about the physiological involvement of ion channels in actual cadmium transport [48]. The most likely candidates are the ones supported by several independent studies. They include some members of the rather diverse TRP (transient receptor potential) family, such as TRPM(melastatin)7 [49,50] and TRPV(vanilloid)6 [51]. Although supposedly selective channels for calcium, all of them may participate in Cd^{2+} uptake in epithelial cells.

Genetic ablation of MTs I and II in fibroblasts and adaptation to a moderate (10 μM) but lethal concentration of Cd^{2+} [52] showed that one member of the T-type calcium channel was a likely mediator of Cd^{2+} uptake in these transformed cells. The involvement of such molecules in cadmium traffic cannot be excluded in cells that synthesize such channels. The search for specificity for Cd^{2+} is futile, considering that gradients of sodium, calcium, or potassium are in the range of mM and cadmium concentrations are unlikely to be that high under any condition of contamination/exposure. Thus, some Cd^{2+} ions may follow the massive fluxes of other cations that can be triggered by changing conditions, especially for excitable cells, via channels with leaky selectivity filters. But conclusive evidence for this mechanism is lacking. And the actual mechanism of cadmium transport by calcium channels may even be more sophisticated: ZnT-1 (see below) ablation in cortical neurons increased the uptake of Ca^{2+}, Zn^{2+}, and Cd^{2+}, a finding that was attributed to L-type calcium channels [53] cooperating with the zinc transporter in calcium and cadmium influx and zinc efflux.

Membrane proteins involved in the active transport of abundant ions such as calcium and potassium do not seem to be capable of carrying Cd^{2+} across membranes. Convincing data exist only in the case of some transporters of essential transition metal cations.

Divalent metal transporter 1 was identified in the enterocytes of the small intestine and in other cells as a proton symporter, favoring the transport from more acidic media, and it was assigned a major role in the assimilation of iron from the animal diet [54]. But its lack of selectivity in reconstituted systems soon became apparent, showing that Cd^{2+} is efficiently transported by DMT1 *in vitro* [54,55]. This observation was extended to include a correlation of DMT1 expression and Cd^{2+} transport, both in cellular models [56–58] and in animals with iron-manipulated diets [59,60]. Furthermore, animal [61], and human [62] studies comparing iron status and cadmium burden fully corroborated the association of Cd^{2+} transport with the plasma membrane form(s) of DMT1. Hence, there is no doubt that DMT1 transports Cd^{2+} in cells that produce this transporter. This conclusion is relevant to an individual's susceptibility to cadmium toxicity since DMT1 is strongly iron-regulated and cadmium transport thus depends on the nutritional and (patho)physiological iron status, in particular for intestinal absorption.

Likewise, some zinc transporters of the ZIP family transport cadmium. The most clear-cut evidence is for ZIP8, which was first associated with sensitivity to cadmium-induced testicular necrosis in mice [63], and later characterized as an efficient *in vitro* Cd^{2+} co-transporter with bicarbonate anions [64]. It is thus very likely that ZIP8 prominently participates in Cd^{2+} import into vascular endothelial cells of the lung, testes, and kidney. ZIP8 is induced by TNFα. Thus lung inflammation, e.g., caused by tobacco smoking, increases the uptake of cadmium and ensuing cadmium-induced cell death [65]. Given the properties of DMT1 and ZIP8, the former is more efficient at low pH, whereas the latter has an optimum at neutral pH. Therefore, these transporters handle cadmium under different cellular conditions. Interestingly, studies aimed at characterizing Cd^{2+} transport suggested that the physiological substrate of ZIP8 is the manganous ion [64,66].

Another ZIP transporter, ZIP14, allows Cd^{2+} to permeate the plasma membrane of ZIP14-transfected mouse fibroblasts and canine kidney epithelial cells [67]. ZIP14 also transports non-transferrin bound ferrous iron [68,69], but the impact of ZIP14 regulation on permeation of different metal ions may be indirect, involving distant signaling events [70], such as crosstalk with other transporters.

The above and other transporters involved in the uptake of essential metal cations for animals are subject to extensive regulation [71]. The regulatory mechanisms can be sophisticated and they can involve networks of essential and toxic metals as recently demonstrated and reviewed [7,70,72]. Since increased hepatic accumulation of ingested cadmium is associated with upregulation of several intestinal transporters in mice fed diets deficient in essential metals, it follows that Cd^{2+} entry into cells, and its intestinal absorption in particular, strongly depends on the status of the animal or human with respect to these essential metals.

Another family of transporters, also preferentially associated with zinc transport, namely the group of ZnT proteins, is involved in movement of ions in the opposite direction, namely removing zinc from the cytoplasm [73]. Although the role of ZnT-1 in zinc export from cells, for instance, is now beyond doubt, transport of cadmium by any of the mammalian ZnT members has not been supported experimentally. Also, the only well-characterized iron cellular exporter, ferroportin, does not assist cadmium crossing biological membranes. However, common features of genes encoding ZnT1 and ferroportin are metal-responsive elements in their promoter regions. Hence, cadmium induces these genes strongly via MTF-1 [74,75]. Even though ZnTs and ferroportin may not transport cadmium, this toxic element potentially impacts the function of these transporters in homeostasis of their physiological substrates, namely iron, zinc, and manganese ions.

The fact that metal cation importers mediate cadmium entry into cells whereas Cd^{2+} does not appear to be a substrate for exporters of essential transition metals points at an important issue of cadmium speciation in biological systems. Upon exposure of cells, particularly those protecting the body from its environment, such as epithelial cells, Cd^{2+} is presented in relatively weak complexes allowing Cd^{2+} to easily dissociate and bind to cadmium transporters, and it may cross membranes as a free ion. In contrast, once inside cells, strong ligands of Cd^{2+} are generally

available, and transport may either involve transporters for complexed cadmium forms or other mechanisms of metal ion delivery to the transporter, such as hijacking metallochaperones, though experimental evidence has not been adduced.

3.2.3 Transport of Complexed Forms of Cd^{2+}

Thus it does not come as a surprise that most membrane proteins proposed to exclude cadmium from the cytosol transport organic compounds to which Cd^{2+} binds. GSH is an abundant intracellular reductant with good chelating properties for Cd^{2+} [76,77]. Thus cells capable of producing pumps exporting GSH compounds are more likely to remove chelated forms of cadmium. This is the case of one of the major detoxification transporters, MRP1 (ABCC1), and potentially other members of this large family of ABC proteins with broad substrate specificity, which accommodate xeno- as well as endobiotics [78]. Among ABC proteins, the MRP1-related and cadmium-regulated CFTR (cystic fibrosis trans-membrane conductance regulator) is a candidate for expelling Cd^{2+}-GSH complexes from epithelial cells for instance [79]. But not all ABC transporters located at the plasma membrane and involved in detoxification, such as the multidrug resistance P-glycoprotein, have the capacity to transport Cd^{2+}-GSH complexes [80].

Other thiols, including cysteine, bind Cd^{2+}, but experimental evidence remains scarce for transport of cadmium cysteine complexes. A similar argument can be made for Cd^{2+}-complexes with nitrogen or oxygen ligands, which are even less stable than sulfur-based chelates under mildly reducing conditions such as found within cells. In contrast to the scarcity of data on cellular cadmium complexes, intracellular Cd^{2+}-MT complexes have been clearly identified, in hepatocytes in particular. No exporters of Cd-MT have been identified (see Section 3), but Cd-MT is found in the blood plasma and urine and taken up by renal tubular cells. The discovery of this process marked an important milestone in cadmium trafficking by demonstrating that cadmium employs other biochemical pathways for exit from and entry into cells.

3.2.4 Other Ways to Cross Membranes

The presentation of MT-bound cadmium to the luminal membrane of renal tubular cells in several models is associated with cubilin-megalin internalization and with cell death (see [48] for review). Hence, MT gains entry into these cells by receptor-mediated endocytosis. Indeed, the elevated residence time of cadmium in the body after intoxication is due to its trapping in the kidneys, and renal MT hydrolysis may release a form of cadmium that cannot be mobilized further and detoxified. In a similar way, another membrane receptor, 24p3R, internalizes metal-binding proteins, including MT, thus mediating cadmium toxicity [81]. 24p3R was initially

described as the tight binding receptor for lipocalin-2, a siderophore-binding protein involved in iron handling, as part of the inflammatory response [82]. Given the widespread occurrence of 24p3R, receptor-mediated endocytosis of metalloproteins by this pathway may occur more frequently than currently acknowledged, but this process remains to be fully assessed.

To conclude, the diversity of transport mechanisms described for cadmium may be due in part to the laboratory use of improper chemical forms of cadmium, physiologically irrelevant concentrations, and animal cells that cadmium may never reach *in vivo* because they are protected by efficient biological barriers. Furthermore, cadmium has numerous effects on membrane traffic ranging from plain inhibition through conformational quenching of transporters, for instance, to impact on distant targets mediated by signaling cascades or by interference with the maturation of some proteins. Despite these potential pitfalls, cadmium traffic and transport actually relies on many different pathways, including some involved in the homeostasis of essential metals and contributing to the extensive distribution of the toxicant throughout the body. Yet cadmium has a high residence time inside cells, renal ones in particular, which is due to cadmium's tight binding to proteins and the inability of cells to mobilize it. The accumulation of cadmium in specific organs, such as the kidney, indicates that the chain of events and alternative pathways fail to detoxify cadmium in a reasonably short period of time.

4 Cadmium Toxicity

4.1 Exposure of Humans to Cadmium and Patho-Physiological Consequences

Human exposure mainly arises from combustion of fuels, plants, and waste, and consumption of adventitious cadmium present in food and water [83]. Humans and animals breathe cadmium-containing particles (mainly the oxide) and ingest cadmium complexes with their food and drinks. Cigarette smoking is a major route of uptake, whereas skin contact is not widespread owing to the natural dilution of cadmium, except for occupational settings. Dietary cadmium is more concentrated in some food items such as shellfish, offal, grains, and seeds. Some crops, such as rice, soybeans, or wheat, are more likely to accumulate cadmium from polluted soils than others.

Cases of accidental acute intake of cadmium are rare. The symptoms include nausea, vomiting, choking, headache, and pulmonary irritation upon inhalation.

In cases of chronic and moderate exposure and in the absence of obvious cadmium nephrotoxicity health effects are less easy to identify. The efficiency of cadmium intake seems to be higher from inhaled particles than from ingested forms (see Section 3.1), but this parameter depends on many others, including the

individual health status, and contributes to the relatively large variability of the individual health impacts of cadmium, at least after relatively short periods of exposure.

Manufacturing of cadmium compounds resulted in occupational exposure in the twentieth century. Workers contaminated by inhalation are likely to suffer from lung cancer as are smokers [84]. Other types of cancers have been linked to cadmium exposure including those of the prostate, kidney, bladder, pancreas, and breast [85]. But data may not always be conclusive enough to demonstrate the significance for larger populations and hence to receive widespread acceptance. The available evidence led several regulatory agencies to classify cadmium as a carcinogen. In any case, the role of cadmium as a co-carcinogen should be acknowledged as it is supported by convincing biochemical data (see below). Any remaining uncertainty concerns only the concentrations at which a significant health effect is noticed. Another area that is receiving considerable attention is the role of cadmium in epigenetic mechanisms of carcinogenesis based on initial observations that some toxic effects of cadmium resemble those seen in abnormal methyl metabolism [86].

Beyond neoplasms, other cadmium-induced health effects have been reported. It is beyond doubt that humans and animals with a high cadmium burden suffer from renal diseases. Tubular and glomerular damage may lead to nephritis, nephrosis, and features resembling the Toni-Debré-Fanconi's syndrome. It is usual practice to measure cadmium in urine as a marker of cadmium's effect (see Section 3.1). There are no specific biomarkers for the other human health conditions associated with cadmium exposure. About 50 years ago, it was demonstrated that rats receiving 5 ppm cadmium in their drinking water from the time of weaning until death developed chronic arterial hypertension [87]. Peripheral arterial disease has been associated with high cadmium burden via cadmium-triggered atherosclerosis [88]. The latter is likely to underlie hypertension, and other mostly fatal cardiac problems and vascular diseases, such as stroke, cardiac arrest, and heart failure. Also, some epidemiological evidence points to cadmium exposure as a risk factor for type II diabetes and diabetic complication, in particular nephropathy.

An increased risk of osteoporosis correlates with the cadmium burden in different populations, especially for post-menopausal women. Cadmium exposure decreases bone mineral density and thus increases the risk for fractures. These effects on the bones are related to kidney malfunction and poor calcium reabsorption in the nephron, as witnessed by (hyper)calciuria. The consequences of cadmium exposure on the human skeleton were particularly obvious for Japanese living along the Jinzu river basin in the 20th century. Water and rice contaminated by cadmium as a result of zinc-mining activities upstream afflicted the local people with the *Itai-Itai* disease, a particularly acute and painful form of osteomalacia [44].

Other health consequences of cadmium exposure, such as anemia, liver disease, nerve or brain damage, have been suggested, but the causation is less straightforward in these cases, probably because these conditions may depend on a variety of other confounding factors.

4.2 Mechanisms of Molecular Toxicity

4.2.1 Interference with Redox Homeostasis

A major concept that emerged from biochemical research is that cells maintain proper oxido-reduction (redox) equilibria to grow or fulfill their tasks. On the one hand, the presence of oxidative species, under so-called oxidative stress conditions, can modify and jeopardize the functioning of a range of bio-molecules such as proteins, sugars, and lipids. On the other hand, subtle shifts to more oxidizing or reducing conditions activate or inhibit 'signaling' molecules that trigger or stop processes that determine the cellular fate, such as proliferation, differentiation, and regulated death. This concept defines the field of redox signaling. Examples of redox-sensitive signaling molecules include transcription factors and signal transduction cascades, such as HIF (hypoxia inducible factor)1, Nrf2, or MAPK (mitogen-activated protein kinases). To counteract an excess of oxidative species, animal cells implement small molecules, such as glutathione, lipoic acid, or some vitamins, and enzymatic systems, such as superoxide dismutases, peroxiredoxins and catalases.

On the basis of the biochemical properties of cadmium outlined in the preceding sections, its cation reacts very efficiently with thiol-containing and other nucleophilic compounds. Many molecules involved in antioxidant defense mechanisms are additional candidates for binding cadmium because they rely on electron-donating reactive groups like thiolates for their function. Cd-GSH complexes are prominent participants in intracellular cadmium handling, and they are thought to be involved in the dynamic exchange of cadmium with other molecules within cells, as well as in some transport mechanisms. Proteins such as thioredoxins and peroxiredoxins, which regulate redox-dependent cellular mechanisms, have the potential to bind cadmium with their reactive cysteines. These examples, and many others, indicate that cadmium can recruit and deplete major actors defending cells from oxidative insults. In addition, cadmium appears to interfere with proper mitochondrial function, probably by crossing the mitochondrial membrane(s) and acting inside the organelle [48,89]. Cadmium affects the mitochondrial respiratory chain, which is one of the major producers of partially reduced oxygen species, and enhances this production and contributes to redox imbalance [89]. In isolated mitochondria, cadmium enters mitochondria through the Ca^{2+} uniporter and inhibits the respiratory chain mainly at complex III [90]. This action is similar to that of zinc, which inhibits the respiratory chain with concomitant production of reactive oxygen species [91,92]. Defective mitochondria are also involved in the induction of cell death, which is the outcome of cadmium exposure in many different conditions.

In the case of redox-sensitive signaling reactions, blocking of reactive nucleophiles by cadmium may enhance cell death, but it may also induce survival or even proliferation. Bad- and Bax-triggered caspase activation is an example of the pro-apoptotic action of cadmium, while growth responses are sometimes

activated after exposure to low doses of cadmium. The actual effects of cadmium depend on a wide range of parameters including the cell type, the developmental stage, and the presence of additional chemicals, to name but a few. It is very likely that such interference with redox homeostasis is part of the different steps of cadmium-induced carcinogenesis. For instance, DNA repair makes use of apurinic/apyrimidinic endonucleases, which, like Apex1 (Ref-1), are activated by redox-based mechanisms and inhibited by cadmium.

4.2.2 Interference with Homeostasis of Essential Metal Ions

As a cation, Cd^{2+} hijacks molecular systems involved in the handling of other essential metal cations. High concentrations of divalent alkaline earth cations (magnesium, calcium) and, less often, monovalent alkali ones (sodium, potassium) have to be considered in cadmium traffic. Less abundant cations from the transition series, mainly iron, copper, zinc, and manganese, are also affected. Cadmium may target proteins transporting, storing, using, or regulating metal cations that are crucial for proper cellular functions.

Although the chemical properties of calcium differ from those of cadmium, both divalent cations have the same overall charge and very close ionic radii (see Section 2.1). Consequently, Cd^{2+} is a steric mimic for calcium (see also Chapter 6). For instance, Cd^{2+} readily replaces Ca^{2+} in hydroxyapatite, a mineral form of phosphate that is widely used as a fertilizer. Spreading of calcium phosphate on farmland contributes significantly to cadmium mobilization into the environment. In a somewhat similar way, bones contain hydroxyapatite microcrystals: osteoblasts may thus incorporate cadmium ions upon remodeling, thereby changing the mechanical properties of the skeleton. A major role of calcium in biology is that of a secondary messenger. The cellular capacity to move large amounts of cations through the cytoplasmic and organellar membranes, and to generate large gradients, is based on a wide range of calcium channels and transporters with different molecular mechanisms. As indicated above (Section 3.2), cadmium ions may be transported by calcium carriers or they may inhibit them. Yet, efficient cadmium inhibition of calcium fluxes *in vivo* by channel or transporter blockade has not been clearly established. More sensitive ways of amplifying the toxic effects of cadmium ions may occur when cadmium targets the sensory systems for calcium. A calcium receptor has been identified on the surface of cells in the intestine, brain, kidney, bone, thyroid, and other cells [93]. This G-protein coupled receptor senses calcium availability and triggers intracellular calcium mobilization. Similarly, a G-coupled zinc receptor has been identified [94]. Cadmium, at concentrations of a few micromolar, binds to a surface receptor and elicits intracellular calcium release [95,96]. An alternative or additional mechanism of cadmium's effect on calcium functions is its influence on redox homeostasis (Section 4.1.2). Calcium signaling and other calcium-dependent activities are sensitive to redox changes and they may be affected by cadmium [97].

Clearly, cadmium traffic is often mediated by zinc transporters, mainly those belonging to the ZIP family (Section 3.2). Although these transporters allow cadmium to reach the cell cytoplasm, it is not established that cadmium transport interferes with zinc traffic. However, once inside cells, cadmium interacts with and induces MTs (Section 2.2). The Cd-MT complexes participate in cadmium distribution (Section 3.2), but their formation may also impact zinc homeostasis. Indeed, MT is the main intracellular zinc buffering molecule so far identified, and hijacking MT by cadmium binding, or over-expressing MT by cadmium-induced transcription, may perturb zinc exchange within cells. Furthermore, MT translocation to the nucleus, and possibly other sub-cellular locations, may change depending on its metal load (cadmium *versus* zinc or copper) with potential differences in zinc re-distribution and zinc- or copper-dependent processes. Last but not least, the redox reactivity of Zn-MT is changed upon cadmium binding (Section 2.2), possibly impacting the cellular pro- or antioxidant potential of zinc and MT. In addition, part of the antioxidant defense mechanism afforded by zinc is due to MTF1 inducing transcription of genes involved in protection against stress. Examples include genes encoding MT, heme oxygenase 1, and γ-glutamylcysteine synthetase. Overexpression of some of these genes in cells displaying resistance to cadmium toxicity strongly suggests that cellular zinc handling, response to stress, and cadmium exposure are functionally linked via this pathway.

The homeostasis of redox-active transition metal ions depends on the cell's capacity to control the ambient redox potential. In this way, control of redox homeostasis is linked to proper homeostasis of transition metal ions. Cadmium is expected to interfere with the redox-buffering properties of the cell, in a similar way as presented above for zinc. Indirect mechanisms of this kind are likely to be more effective in terms of cadmium toxicity than direct impairment of transport or regulation of transition metals. Indeed, transport of cadmium by membrane proteins involved in zinc, iron, and manganese traffic has been demonstrated (Section 3.2), but the evidence linking cadmium to the control of homeostasis of these metals is weak. Examples for interference with iron include cadmium-induced changes of the kinetic properties of ferrochelatase [98] and δ-aminolevulinic acid dehydratase [99], two enzymes involved in critical steps of heme biosynthesis, cadmium binding to ferritin [100], and cadmium-induced decreased solubility of iron regulatory protein 1 [101]. However, the circumstances of cadmium poisoning being actually involved in these molecular effects *in vivo* remain to be delineated. For instance, cases of anemia after cadmium intoxication have been reported, but it is not clear whether the sequence of events impacting erythropoiesis is an immediate consequence of impaired heme synthesis or iron deregulation [102]. Similar considerations hold for copper and manganese homeostases for which gaps in knowledge persist and where cadmium interference in mammals is poorly documented.

Available evidence more convincingly indicates that homeostasis of essential transition metals is sensitive to cadmium poisoning by indirect mechanisms. All demonstrated and suggested pathways cannot be presented here, but the

mechanisms follow the principles outlined elsewhere in this chapter, including the cellular redox balance (Section 4.2.1) and the effect on proteins that are not metalloproteins (Sections 4.2.4 and 4.2.5).

4.2.3 Interactions with Metalloproteins

The binding of cadmium ions to thioneins has been presented above (Section 2) and it is a major mediator of cadmium's toxicity. Similarly, the interaction with GSH in mammalian systems is important in the distribution, reactivity, and toxicity of cadmium. But it is worth repeating that these complexes do not hide cadmium from other biological reactions including those in which cadmium replaces other cations at the active sites of metalloproteins. In fact, these complexes may actively redistribute cellular cadmium.

Two separate situations can be distinguished for the binding of Cd^{2+} to the cation-binding sites of metalloproteins, namely (i) incorporation into nascent polypeptides during folding and (ii) exchange of cations in the fully folded proteins. The latter situation is likely relevant for MT in view of its higher affinity for Cd^{2+}, although the former situation may also be realized. The possibility of cadmium being incorporated into newly synthesized metalloproteins must be considered for proteins binding complex prosthetic groups. For heme, cadmium inhibits ferrochelatase, but it does not seem to be efficiently processed as Cd-protoporphyrin IX [98], although the occurrence of this product cannot be dismissed altogether [103]. In the case of iron-sulfur clusters, exposure of microorganisms to cadmium impacts the expression of genes involved in the biosynthesis of these prosthetic groups and of some other genes encoding iron-sulfur proteins [104], but similar observations are not documented in mammals. For simple metal cation sites, evidence for cadmium incorporation during protein translation has not been adduced. It may be a critical missing piece of information for understanding cadmium toxicity.

In contrast, cadmium binding to fully folded metalloproteins has been reported widely, but mainly and if not exclusively from data obtained with pure proteins. A case in point is that of the large family of 'zinc finger' proteins that are involved in a variety of biological interactions and thought to represent around 3% of the coding human genome. Investigations of zinc replacement by cadmium *in vitro* abound. They include domains belonging to transcription factors, such as Sp1, MTF-1, or GATA1, regulatory proteins such as p53, and DNA repair enzymes like XPA (xeroderma pigmentosum, complementation group A) and PARP1 (poly (ADP-ribose) polymerase 1) [104]. Yet, it is not clear what the functional consequences of cadmium substitution in zinc finger proteins are, and, more importantly, whether such replacements are widespread *in vivo*. Another area of cadmium's possible targets is the role of zinc binding between protein subunits of the same or different proteins. These sites often use thiol ligands to bind the metal. Cadmium substituting for zinc in the tetrathiolate binding sites bridging the subunits in nitrogen monoxide synthase or bridging the CD4/CD8 T-cell receptor and the kinase lck intracellularly [105] may well change the functions of these interactions.

Other metalloproteins bind cadmium as well. Ferritin accommodates a variable number of cadmium ions in crystals prepared in the presence of cadmium salts. The Cd^{2+} ions bind to residues with different side chains (His, Cys, Glu, and others), which were assigned different roles in the storage of iron, such as shuttling iron in and out of the ferritin envelope or as nucleation sites. Cadmium binding also occurs to proteins such as transferrin, a protein involved in iron distribution and lacking cation selectivity *in vitro*, albumin, which has several but separate binding sites for zinc and copper, and possibly ceruloplasmin, a copper-containing ferrooxidase. All these proteins occur in the circulation and they may contribute to cadmium distribution to tissues. But cadmium binding may (transferrin) or may not (albumin) occur at the sites where the native metal ions bind.

Also, as indicated above for calcium-cadmium exchange in hydroxyapatite, cadmium replacement of calcium in calcium-binding domains has been demonstrated *in vitro* and cadmium may replace calcium in calcium proteins *in vivo*. Examples are proteins with E-F hand motifs such as troponin, calmodulin, or cadherin. Exposure of cells to cadmium perturbs the organization of cellular junctions, affects the distribution and integrity of cadherins [106] and downstream signaling by β-catenin. Similarly, cadmium activates Ca^{2+}/calmodulin dependent kinases with subsequent effects on calcium signaling [107]. More generally, exposing cells to cadmium activates survival or apoptotic programs depending on conditions. Many of these effects are calcium-dependent, and it is not always clear whether calcium substitution by cadmium at specific calcium-binding sites, such as in calmodulin, is the underlying mechanism. Cadmium interaction with calcium-proteins may involve cation-binding sites in addition to those used by Ca^{2+}; for instance, the regulatory domain of the calcium-gated potassium channels binds more cadmium ions than calcium ions which enhances activation [108].

4.2.4 Interaction with Other Proteins

Proteins do not need to be metalloproteins to interact with cadmium, and the proteins with reactive cysteines described in Section 4.2.1 are examples of non-metalloproteins interacting with cadmium. In addition, some proteins that are not recognized as metalloproteins bind zinc extremely tightly. For example, the cytoplasmic domain of receptor protein tyrosine phosphatase β binds zinc with a K_i value of 27 pM [109]. Cadmium is expected to bind tightly to these sites. Significantly, the widespread use of $CdCl_2$ in crystallization studies, to prepare heavy metal derivatives and to phase the diffraction data, provides hundreds of protein structures in which Cd^{2+} interacts with amino-acid residues, often in positions that are not known to bind cations.

A well-publicized example of cadmium binding to a specific protein was discovered following the observation that cadmium behaves like a hormone [110]. The hormonal effect was assigned to cadmium binding to a site containing cysteine residues in the ligand (estrogen) binding domain of the estrogen receptor (ER). The subsequent downstream effects triggered by ER activation may be part of

cadmium's toxicity in the environment, toward animal life in particular [111]. Beyond this example, it is not feasible to comprehensively cover all aspects of cadmium binding to proteins and potential consequences, but some general mechanisms can be outlined. In a way reminiscent of some roles of zinc ions, Cd^{2+} may bind to sites belonging to mobile parts of proteins: such binding may cross-link parts that otherwise would have to move to support activity. This 'freezing effect' of cadmium on conformational changes that are needed for switching activities may trap the protein in either a fully inactive or a fully activated form; either effect could impair function. Other more local molecular consequences like shielding of reactive amino-acid residues or steric hindrance for substrates may apply. Hence, the molecular mechanisms of cadmium toxicity cannot be restricted to the mere competition with other metal cations.

4.2.5 Other Mechanisms

It is unclear whether the basis of cadmium toxicity is sufficiently well presented by the already diverse interactions of cadmium with proteins described above. Many complex mechanisms of cadmium toxicity can be explained with some of the already outlined principles. Hence, interference with the antioxidant response and generation of reactive species (Section 4.2.1) and perturbation of zinc-dependent activities and calcium signaling (Section 4.2.3) explain the toxic effects in considerable depth. As a result, but also due to additional molecular interactions of the kind just presented (Section 4.2.4), exposure of cells to cadmium impacts a range of signaling systems [97]. These effects depend on the type of cell, and therefore the range of genes they express, and on the cadmium-cell interaction in terms of concentration and length of exposure, i.e., the acute or chronic doses of cadmium.

The pathways that respond to cadmium include those triggered by receptor activation. The relevant receptors may normally recognize growth factors or hormones, and they may activate signaling pathways like those implementing mitogen-activated protein kinases. Cadmium can interfere with some (de)phosphorylations at various levels. The members of the MAPK signaling cascades function along parallel successive molecular events, but with cross interference and with variable outcomes, such as triggering cell death or survival and proliferation. Other signaling systems have also been shown to be sensitive to the presence of cadmium, those responding to hypoxia via HIF1α and others depending on cyclic nucleotides and NF-κB. Most of these pathways contribute to large changes in gene expression and the effects of cadmium are observed at different levels: transcription, translation, post-translation. Consequently, it is difficult to determine whether the apparent diversity of cadmium targets is due to the interaction of the metal with a multitude of proteins or just a few selected ones in central pathways that are initially sensitive but impact scores of downstream components. In view of the variety of regulatory pathways responding to cadmium, it is not surprising to see high level functions such as proteasomal activity or autophagy being affected by cadmium. Overall the biological implications of cadmium exposure are so

many that explaining cadmium toxicology resembles separating the wheat from the chaff, but it is beyond doubt that the competition of cadmium with other metal cations cannot explain all observations and that cadmium interactions with non-metalloproteins play an important role.

4.3 Toxicology with Reference to Specific Organs

Liver and kidney are the main organs targeted by cadmium, with lungs affected when exposure occurs by inhalation. In rare cases of acute human ingestion, rapid intestinal symptoms aim at expelling cadmium by vomiting and diarrhea, whereas inhalation irritates the upper respiratory tract and may develop into, sometimes fatal, pulmonary diseases. More frequent chronic exposure is associated with more diverse symptoms, and the main target organs are lungs after inhalation, and kidneys and bones irrespective of the absorption route. Cadmium-triggered kidney damage is monitored by the release in urine of a variety of biomarkers for decreased reabsorption and protein release from cells of the proximal tubule [37]. Paradoxically, although the liver is an organ to which absorbed cadmium easily gains access to, few specific hepatic symptoms have been directly and unambiguously assigned to cadmium poisoning.

Since MT is efficiently induced by cadmium in the liver, this organ may not be harmed by the Cd-MT complex. Cadmium is mainly deleterious for the kidneys after having been processed by the liver. Many studies have reported osteomalacia and osteoporosis for subjects exposed to cadmium, one of the most prominent example being the victims of the infamous *Itai-Itai* disease in Japan [40]. The actual mechanism of cadmium toxicity to the bones remains debated, probably because it is multifactorial. It includes direct and indirect interactions with osteoclasts and osteoblasts, while showing limited incorporation of cadmium into the organ. For instance, cadmium measurements in selected populations of Japanese people failed to provide values above the detection limit of the implemented method for bones, whereas values were largely significant for liver and kidneys [36]. The testicular necrosis observed in laboratory animals exposed to cadmium led to the discovery of ZIP8 as an efficient cadmium transporter [63], which suggests a potential impact of cadmium on male fertility. Effects on female fertility, successful pregnancy and fetus development also need to be considered, because of the interaction of cadmium with the ER (see Section 4.2.4), but they have been difficult to demonstrate in human populations exposed to relatively low levels of cadmium. For preventing injury, it may be prudent to consider the adage “absence of evidence is not evidence for absence.”

The occupational risk of lung carcinogenesis upon cadmium exposure has been recognized by regulatory authorities (see Section 5.1), despite the warnings from some scientists for confounding parameters [112] in the studies on which the decision was based. Similar reflections apply to cadmium-triggered carcinogenesis of other tissues, including the endometrium, bladder, pancreas, testes, prostate, and breast (see also Chapter 15).

Three decades ago, it was observed that 10–20 μg cadmium per kg per day changes systolic blood pressure in rats [113]. The authors suggested that exposure to cadmium may contribute to the development of essential hypertension in humans. This issue has received renewed interest regarding the effects of cadmium on cardiovascular disease [88]. Both epidemiological and experimental investigations provide support for a role of cadmium in atherogenesis.

5 Concluding Remarks and Future Directions

5.1 Reference Dose and Recommendations about Cadmium in Water, Soil, and Food

Cadmium has been classified as a human carcinogen [114] or as a probable carcinogen (EPA group B1) by inhalation. The European Food Safety Authority [115] also acknowledges that cadmium triggers renal injuries.

The guideline for upper levels of cadmium in drinking water are 3 μg/L [83]. LD_{50} values for mice and rats range from 100–300 mg/kg body weight. The maximum level of cadmium is set at 10 mg/kg dry weight in animal feed [116] and at 5 ng/m^3 in ambient air [83].

The normal intake of cadmium from cereals and other vegetables is about 2–25 μg per day for children and 10–50 μg for adults, with the higher values corresponding to areas with industrial activities involving cadmium. On average, the cadmium concentration in food is less than 0.15 μg/g dry weight, but can be higher than 1 μg/g for shellfish or 0.5 μg/g for kidneys. The Provisional Tolerable Weekly Intake (PTWI) was set at 65 μg/day for a 65 kg human male, i.e., 1 μg/kg per day or 7 μg/kg per week [115]. In 2010, this figure was decreased to 5.8 μg/kg body weight by the Joint FAO/WHO Expert Committee on Food Additives that issued the first recommendation more than 20 years ago.

A panel of scientists has received a mandate from the European Commission to evaluate the risks of cadmium to human health [115]. The exposure range from the diet was estimated in the range from 1.9 to 3.0 μg/kg body weight per week (mean 2.3 μg/kg) in the general population, i.e., the mean intake is very close to the PTWI. Using urinary β_2-microglobulin as a marker of tubular effects in relation with cadmium burden and applying modeling of the data from a non-smoking population of elderly women, a tolerable weekly intake of 2.5 μg/kg body weight for 50 years was derived and proposed. Thus, the general European population receives a cadmium dose close to the set tolerable value, and some sub-populations, such as children, smokers, or people with unbalanced diets and micronutrient deficiencies, are likely to absorb more cadmium. It should be emphasized that these figures are solely based on renal damage assessed with one particular, and perhaps not most sensitive, assay, and that they may not be relevant to other cadmium-induced health effects, for which suitable biomarkers do not exist.

Mainly based on studies with animals, ATSDR has determined minimal risk levels of 0.03 μg Cd/m^3 and 0.01 μg Cd/m^3 for acute and chronic inhalation, respectively. A value of 0.1 μg Cd/kg/day for chronic oral intake was also indicated with a reference dose of 5×10^{-4} mg/kg/day in water and 1×10^{-3} mg/(kg.day) in food to avoid reaching 200 μg/g in kidneys [117].

5.2 *Where Is the Problem? Do We Know What We Need to Know? Problem Solved?*

The scientific literature on cadmium has been prolific for many decades. With cadmium having strong affinities to proteins, the numerous reported interactions do not surprise. The physiological relevance of many experiments that employ cultured cells or cadmium injections into animals is not immediate because many barriers involved in the uptake of cadmium in organisms are bypassed in these experiments. There is a surprising scarcity of measurements of cadmium in human tissues at various ages and various levels of documented exposures. This is in part due to a lack of efficient and non-invasive methods for measuring cadmium in humans. Such analytical data would seem critical in evaluating the significance of the plethora of biochemical findings. Another critical issue in interpreting observations is the buffering capacity of cells for cadmium(II) ions, which is obviously quite different from buffering of metal ions in *in vitro* investigations.

The well established coordination chemistry of cadmium should support the evaluation of the biological effects of this cation. Starting with the discovery of MT, the number of biological processes being potentially impacted by the presence of cadmium has increased enormously. A similar trend has been followed by the variety of mechanisms that have been proposed to underlie cadmium's toxicity. Cadmium in some sites of metalloproteins, such as zinc proteins, may have very subtle effects on their structure and function, possibly with cumulative effects on the organism over time, whereas in other proteins cadmium may affect function drastically. Redox-inert cadmium bound in sites that require redox-active metal ions does not support function. Mammals have no apparent use of this metal, even at very low concentrations. The main organs functionally affected by cadmium (kidneys, bones, lungs) have been identified, although they do not exactly match those (liver, kidney, pancreas, thyroid gland) that display the highest concentration of metal per mass unit.

Therefore, risk assessment for human health is limited by (i) the scarcity of analytical data and poor predictive power of cadmium distribution in the body in relation to health outcome, (ii) the lack of information about chronic effects of cadmium accumulating over decades in tissues, and (iii) the lack of suitable biomarkers other than for irreversible kidney damage. Thus, the epidemiological studies linking health effects and cadmium exposure suffer from a relative lack of consensus knowledge about the modes of action of cadmium in multi-cellular

systems as complex and as highly regulated as mammals. Hence, quantitative data aiming at setting limiting values heavily rely on the quality of experimental data, which are not always easy to obtain and often inconclusive due to the inherent limitations of experimental systems and the short timeframe of the experiments in relation to long-term effects of cadmium accumulation. Modeling efforts aim at compensating these drawbacks by considering the complex and still incomplete toxico-kinetics of cadmium.

The missing link in cadmium toxicology thus lies between molecular data and health effects. Progress in filling this gap may come from a better appreciation of the biochemical speciation of cadmium in cells. A comprehensive list of binding molecules in animals, with their exchange rates, the (sub)-cellular locations accumulating cadmium, and the half-lives of cadmium within cells and in the circulation should precisely track the fate of cadmium once taken up. Refined models will have an improved capacity for deriving damaging concentrations to organs at particular doses. Such improvements would depend on significant progress in the analytical biochemistry of cadmium. It likely will profit from the combination of complementary approaches, implementing selective sensors [118,119], methods identifying molecules interacting with metals [120], preferably under non-destructive experimental conditions, and real-time measurements of the cadmium distribution throughout the body, even at minimal levels.

Once this ambitious program has been fulfilled, data comparing health effects with exposure will reveal the pathways followed by cadmium. Along the way, investigations will identify unambiguous biomarkers of exposure and of effect. They will be instrumental in reaching consensus values for monitoring cadmium concentrations in the environment and for protecting populations. It may still be a long quest for this Holy Grail, despite recent progress in mostly technical aspects referred to in this chapter.

Abbreviations

ATDSR	Agency for Toxic Substances and Disease Registry
CFTR	cystic fibrosis transmembrane conductance regulator
DMT1	divalent metal transporter 1
EDTA	ethylenediamine-N,N,N',N'-tetraacetate
ER	estrogen receptor
GSH	glutathione
HIF	hypoxia inducible factor
LD	lethal dose
MAPK	mitogen activated protein kinase
MRE	metal response element
MRP1	multiple drug resistance protein
MT	metallothionein
MTF-1	metal transcription factor 1

NF-κB	necrosis factor κB
PAC	perturbed angular correlation
PARP1	poly (ADP-ribose) polymerase 1
PTWI	provisional tolerable weekly intake
TNFα	tumor necrosis factor α
TRP	transient receptor potential
XPA	xeroderma pigmentosum complementation group A
ZIP	Zrt- and Irt-related proteins
ZnT	zinc transporter

References

1. C. A. Blindauer, R. Schmid, *Metallomics* **2010**, *2*, 510–529.
2. R. B. Martin, *J. Chem. Ed.* **1987**, *64*, 402.
3. B. A. Krizek, D. L. Merkle, J. M. Berg, *Inorg. Chem.* **1993**, *32*, 937–940.
4. J. M. Berg, H. A. Godwin, *Annu. Rev. Biophys. Biomol. Struct.* **1997**, *26*, 357–371.
5. W. Maret, Y. Li, *Chem. Rev.* **2009**, *109*, 4682–4707.
6. R. J. Williams, *J. Inorg. Biochem.* **2002**, *88*, 241–250.
7. J. M. Moulis, *Biometals* **2010**, *23*, 877–896.
8. H. Irving, R. J. P. Williams, *Nature* **1948**, *162*, 746–747.
9. A. Krezel, Q. Hao, W. Maret, *Arch. Biochem. Biophys.* **2007**, *463*, 188–200.
10. W. Braun, M. Vašák, A. H. Robbins, C. D. Stout, G. Wagner, J. H. Kägi, K. Wüthrich, *Proc. Natl. Acad. Sci. USA* **1992**, *89*, 10124–10128.
11. (a) W. Maret, *Antioxid. Redox Signal.* **2006**, *8*, 1419–1441. (b) E. Hoch, W. Lin, J. Chai, M. Hershfinkel, D. Fu, I. Sekler, *Proc. Natl. Acad. Sci. USA* **2012**, *109*, 7202–7207.
12. C. Andreini, L. Banci, I. Bertini, A. Rosato, *J. Proteome Res.* **2006**, *5*, 3173–3178.
13. K. M. Taylor, S. Hiscox, R. I. Nicholson, C. Hogstrand, P. Kille, *Sci. Signal* **2012**, *5*, ra11.
14. M. Margoshes, B. L. Vallee, *J. Am. Chem. Soc.* **1957**, *79*, 4813–4814.
15. T. W. Lane, F. M. M. Morel, *Proc. Natl. Acad. Sci. USA* **2000**, *97*, 4627–4631.
16. F. M. M. Morel, *Geobiology* **2008**, *6*, 318–324.
17. Y. Li, W. Maret, *J. Anal. At. Spectrom.* **2008**, *23*, 1055–1062.
18. B. Zhang, O. Georgiev, M. Hagmann, C. Gunes, M. Cramer, P. Faller, M. Vašák, W. Schaffner, *Mol. Cell Biol.* **2003**, *23*, 8471–8485.
19. A. H. Robbins, D. E. McRee, M. Williamson, S. A. Collett, N. H. Xuong, W. F. Furey, B. C. Wang, C. D. Stout, *J. Mol. Biol.* **1991**, *221*, 1269–1293.
20. A. Krezel, W. Maret, *J. Am. Chem. Soc.* **2007**, *129*, 10911–10921.
21. W. Maret, B. L. Vallee, *Proc. Natl. Acad. Sci. USA* **1998**, *95*, 3478–3482.
22. R. R. Misra, J. F. Hochadel, G. T. Smith, J. C. Cook, M. P. Waalkes, D. A. Wink, *Chem. Res. Toxicol.* **1996**, *9*, 326–332.
23. A. E. Michalska, K. H. Choo, *Proc. Natl. Acad. Sci. USA* **1993**, *90*, 8088–8092.
24. B. A. Masters, E. J. Kelly, C. J. Quaife, R. L. Brinster, R. D. Palmiter, *Proc. Natl. Acad. Sci. USA* **1994**, *91*, 584–588.
25. E. J. Kelly, C. J. Quaife, G. J. Froelick, R. D. Palmiter, *J. Nutr.* **1996**, *126*, 1782–1790.
26. R. B. Klassen, K. Crenshaw, R. Kozyraki, P. J. Verroust, L. Tio, S. Atrian, P. L. Allen, T. G. Hammond, *Am. J. Physiol. Renal Physiol.* **2004**, *287*, F393–403.
27. N. A. Wolff, M. Abouhamed, P. J. Verroust, F. Thevenod, *J. Pharmacol. Exp. Ther.* **2006**, *318*, 782–791.
28. M. Abouhamed, N. A. Wolff, W. K. Lee, C. P. Smith, F. Thevenod, *Am. J. Physiol. Renal Physiol.* **2007**, *293*, F705–712.
29. O. Moltedo, C. Verde, A. Capasso, E. Parisi, P. Remondelli, S. Bonatti, X. Alvarez-Hernandez, J. Glass, C. G. Alvino, A. Leone, *J. Biol. Chem.* **2000**, *275*, 31819–31825.

30. N. Ballatori, *Drug Metab. Rev.* **1991**, *23*, 83–132.
31. I. Bremner, R. K. Mehra, *Methods Enzymol.* **1991**, *205*, 60–70.
32. T. Kjellstrom, *Environ. Health Perspect.* **1979**, *28*, 169–197.
33. G. F. Nordberg, T. Kjellstrom, *Environ. Health Perspect.* **1979**, *28*, 211–217.
34. K. Tsuchiya, M. Sugita, Y. Seki, *Keio J. Med.* **1976**, *25*, 73–82.
35. WHO, Cadmium. in: *Air quality guidelines for Europe,* 2nd ed. Copenhagen, Denmark, 2000.
36. M. Uetani, E. Kobayashi, Y. Suwazono, R. Honda, M. Nishijo, H. Nakagawa, T. Kido, K. Nogawa, *Biometals* **2006**, *19*, 521–525.
37. W. C. Prozialeck, J. R. Edwards, *Biometals* **2010**, *23*, 793–809.
38. K. Nogawa, R. Honda, T. Kido, I. Tsuritani, Y. Yamada, M. Ishizaki, H. Yamaya, *Environ. Res.* **1989**, *48*, 7–16.
39. J. A. Staessen, H. A. Roels, D. Emelianov, T. Kuznetsova, L. Thijs, J. Vangronsveld, R. Fagard, *Lancet* **1999**, *353*, 1140–1144.
40. M. H. Bhattacharyya, *Toxicol. Appl. Pharmacol.* **2009**, *238*, 258–265.
41. M. Kippler, B. Nermell, J. Hamadani, F. Tofail, S. Moore, M. Vahter, *Toxicol. Lett.* **2010**, *198*, 20–25.
42. Y. Fujita, H. I. el Belbasi, K. S. Min, S. Onosaka, Y. Okada, Y. Matsumoto, N. Mutoh, K. Tanaka, *Res. Commun. Chem. Pathol. Pharmacol.* **1993**, *82*, 357–365.
43. M. G. Cherian, *Environ. Health Perspect.* **1979**, *28*, 127–130.
44. G. F. Nordberg, *Toxicol. Appl. Pharmacol.* **2009**, *238*, 192–200.
45. B. J. Scott, A. R. Bradwell, *Clin. Chem.* **1983**, *29*, 629–633.
46. M. A. Lynes, K. Zaffuto, D. W. Unfricht, G. Marusov, J. S. Samson, X. Yin, *Exp. Biol. Med.* **2006**, *231*, 1548–1554.
47. E. Van Kerkhove, V. Pennemans, Q. Swennen, *Biometals* **2010**, *23*, 823–855.
48. F. Thevenod, *Biometals* **2010**, *23*, 857–875.
49. M. K. Monteilh-Zoller, M. C. Hermosura, M. J. Nadler, A. M. Scharenberg, R. Penner, A. Fleig, *J. Gen. Physiol.* **2003**, *121*, 49–60.
50. C. Martineau, E. Abed, G. Medina, L. A. Jomphe, M. Mantha, C. Jumarie, R. Moreau, *Toxicol. Lett.* **2010**, *199*, 357–363.
51. G. Kovacs, T. Danko, M. J. Bergeron, B. Balazs, Y. Suzuki, A. Zsembery, M. A. Hediger, *Cell Calcium* **2011**, *49*, 43–55.
52. E. M. Leslie, J. Liu, C. D. Klaassen, M. P. Waalkes, *Mol. Pharmacol.* **2006**, *69*, 629–639.
53. E. Ohana, I. Sekler, T. Kaisman, N. Kahn, J. Cove, W. F. Silverman, A. Amsterdam, M. Hershfinkel, *J. Mol. Med.* **2006**, *84*, 753–763.
54. H. Gunshin, B. Mackenzie, U. V. Berger, Y. Gunshin, M. F. Romero, W. F. Boron, S. Nussberger, J. L. Gollan, M. A. Hediger, *Nature* **1997**, *388*, 482–488.
55. B. Mackenzie, H. Takanaga, N. Hubert, A. Rolfs, M. A. Hediger, *Biochem. J.* **2007**, *403*, 59–69.
56. J. Tallkvist, C. L. Bowlus, B. Lonnerdal, *Toxicol. Lett.* **2001**, *122*, 171–177.
57. L. Olivi, J. Sisk, J. Bressler, *Am. J. Physiol. Cell Physiol.* **2001**, *281*, C793–800.
58. F. Elisma, C. Jumarie, *Biochem. Biophys. Res. Commun.* **2001**, *285*, 662–668.
59. J. D. Park, N. J. Cherrington, C. D. Klaassen, *Toxicol. Sci.* **2002**, *68*, 288–294.
60. D. Y. Ryu, S. J. Lee, D. W. Park, B. S. Choi, C. D. Klaassen, J. D. Park, *Toxicol. Lett.* **2004**, *152*, 19–25.
61. T. M. Leazer, Y. Liu, C. D. Klaassen, *Toxicol. Appl. Pharmacol.* **2002**, *185*, 18–24.
62. A. Åkesson, M. Berglund, A. Schütz, P. Bjellerup, K. Bremme, M. Vahter, *Am. J. Public Health* **2002**, *92*, 284–287.
63. T. P. Dalton, L. He, B. Wang, M. L. Miller, L. Jin, K. F. Stringer, X. Chang, C. S. Baxter, D. W. Nebert, *Proc. Natl. Acad. Sci. USA* **2005**, *102*, 3401–3406.
64. L. He, K. Girijashanker, T. P. Dalton, J. Reed, H. Li, M. Soleimani, D. W. Nebert, *Mol. Pharmacol.* **2006**, *70*, 171–180.
65. J. R. Napolitano, M. J. Liu, S. Bao, M. Crawford, P. Nana-Sinkam, E. Cormet-Boyaka, D. L. Knoell, *Am. J. Physiol. Lung Cell. Mol. Physiol.* **2012**, *302*, L909–918.

66. H. Fujishiro, K. Kubota, D. Inoue, A. Inoue, T. Yanagiya, S. Enomoto, S. Himeno, *Toxicology* **2011**, *280*, 118–125.
67. K. Girijashanker, L. He, M. Soleimani, J. M. Reed, H. Li, Z. Liu, B. Wang, T. P. Dalton, D. W. Nebert, *Mol. Pharmacol.* **2008**, *73*, 1413–1423.
68. J. P. Liuzzi, F. Aydemir, H. Nam, M. D. Knutson, R. J. Cousins, *Proc. Natl. Acad. Sci. USA* **2006**, *103*, 13612–13617.
69. J. J. Pinilla-Tenas, B. K. Sparkman, A. Shawki, A. C. Illing, C. J. Mitchell, N. Zhao, J. P. Liuzzi, R. J. Cousins, M. D. Knutson, B. Mackenzie, *Am. J. Physiol. Cell Physiol.* **2011**, *301*, C862–871.
70. S. Hojyo, T. Fukada, S. Shimoda, W. Ohashi, B. H. Bin, H. Koseki, T. Hirano, *PLoS One* **2011**, *6*, e18059.
71. K. S. Min, H. Ueda, T. Kihara, K. Tanaka, *Toxicol. Sci.* **2008**, *106*, 284–289.
72. E. Rousselet, P. Richaud, T. Douki, J. Garcia-Chantegrel, A. Favier, A. Bouron, J. M. Moulis, *Toxicol. Appl. Pharmacol.* **2008**, *230*, 312–319.
73. L. A. Lichten, R. J. Cousins, *Annu. Rev. Nutr.* **2009**, *29*, 153–176.
74. S. J. Langmade, R. Ravindra, P. J. Daniels, G. K. Andrews, *J. Biol. Chem.* **2000**, *275*, 34803–34809.
75. M. B. Troadec, D. M. Ward, E. Lo, J. Kaplan, I. De Domenico, *Blood* **2010**, *116*, 4657–4664.
76. D. D. Perrin, A. E. Watt, *Biochim. Biophys. Acta* **1971**, *230*, 96–104.
77. O. Delalande, H. Desvaux, E. Godat, A. Valleix, C. Junot, J. Labarre, Y. Boulard, *FEBS J.* **2010**, *277*, 5086–5096.
78. R. G. Deeley, C. Westlake, S. P. Cole, *Physiol. Rev.* **2006**, *86*, 849–899.
79. S. L'Hoste, A. Chargui, R. Belfodil, C. Duranton, I. Rubera, B. Mograbi, C. Poujeol, M. Tauc, P. Poujeol, *Free Radic. Biol. Med.* **2009**, *46*, 1017–1031.
80. W. K. Lee, B. Torchalski, N. Kohistani, F. Thevenod, *Toxicol. Sci.* **2011**, *121*, 343–356.
81. C. Langelueddecke, E. Roussa, R. A. Fenton, N. A. Wolff, W. K. Lee, F. Thevenod, *J. Biol. Chem.* **2012**, *287*, 159–169.
82. N. Borregaard, J. B. Cowland, *Biometals* **2006**, *19*, 211–215.
83. WHO, *Exposure to Cadmium: a major public health concern*, Geneva, 2010.
84. T. Nawrot, M. Plusquin, J. Hogervorst, H. A. Roels, H. Celis, L. Thijs, J. Vangronsveld, E. Van Hecke, J. A. Staessen, *Lancet Oncol.* **2006**, *7*, 119–126.
85. T. S. Nawrot, J. A. Staessen, H. A. Roels, E. Munters, A. Cuypers, T. Richart, A. Ruttens, K. Smeets, H. Clijsters, J. Vangronsveld, *Biometals* **2010**, *23*, 769–782.
86. L. A. Poirier, T. I. Vlasova, *Environ. Health Perspect.* **2002**, *110 Suppl 5*, 793–795.
87. H. A. Schroeder, *Am. J. Physiol.* **1964**, *207*, 62–66.
88. B. Messner, D. Bernhard, *Biometals* **2010**, *23*, 811–822.
89. A. Cuypers, M. Plusquin, T. Remans, M. Jozefczak, E. Keunen, H. Gielen, K. Opdenakker, A. R. Nair, E. Munters, T. J. Artois, T. Nawrot, J. Vangronsveld, K. Smeets, *Biometals* **2010**, *23*, 927–940.
90. Y. Wang, J. Fang, S. S. Leonard, K. M. Rao, *Free Radic. Biol. Med.* **2004**, *36*, 1434–1443.
91. B. Ye, W. Maret, B. L. Vallee, *Proc. Natl. Acad. Sci. USA* **2001**, *98*, 2317–2322.
92. S. L. Sensi, D. Ton-That, P. G. Sullivan, E. A. Jonas, K. R. Gee, L. K. Kaczmarek, J. H. Weiss, *Proc. Natl. Acad. Sci. USA* **2003**, *100*, 6157–6162.
93. W. Chang, D. Shoback, *Cell Calcium* **2004**, *35*, 183–196.
94. M. Hershfinkel, A. Moran, N. Grossman, I. Sekler, *Proc. Natl. Acad. Sci. USA* **2001**, *98*, 11749–11754.
95. L. Smith, V. Pijuan, Y. Zhuang, J. B. Smith, *Exp. Cell Res.* **1992**, *202*, 174–182.
96. B. Faurskov, H. F. Bjerregaard, *Pflugers Arch.* **2002**, *445*, 40–50.
97. F. Thévenod, *Toxicol. Appl. Pharmacol.* **2009**, *238*, 221–239.
98. A. E. Medlock, M. Carter, T. A. Dailey, H. A. Dailey, W. N. Lanzilotta, *J. Mol. Biol.* **2009**, *393*, 308–319.
99. R. Sommer, D. Beyersmann, *J. Inorg. Biochem.* **1984**, *20*, 131–145.
100. J. Hegenauer, P. Saltman, L. Hatlen, *Biochem. J.* **1979**, *177*, 693–695.

101. A. Martelli, J. M. Moulis, *J. Inorg. Biochem.* **2004**, *98*, 1413–1420.
102. E. Rousselet, J. M. Moulis, *Biochem. Cell Biol.* **2008**, *86*, 416–424.
103. J. A. Staessen, J. P. Buchet, G. Ginucchio, R. R. Lauwerys, P. Lijnen, H. Roels, R. Fagard, *J. Cardiovasc. Risk* **1996**, *3*, 26–41.
104. K. Helbig, C. Grosse, D. H. Nies, *J. Bacteriol.* **2008**, *190*, 5439–5454.
105. H. Haase, L. Rink, *Annu. Rev. Nutr.* **2009**, *29*, 133–152.
106. W. C. Prozialeck, J. R. Edwards, *Pharmacol. Ther.* **2007**, *114*, 74–93.
107. W. Xiao, Y. Liu, D. M. Templeton, *Toxicol. Appl. Pharmacol.* **2009**, *238*, 315–326.
108. H. Dvir, E. Valera, S. Choe, *J. Struct. Biol.* **2010**, *171*, 231–237.
109. M. Wilson, C. Hogstrand, W. Maret, *J. Biol. Chem.* **2012**, *287*, 9322–9326.
110. A. Stoica, B. S. Katzenellenbogen, M. B. Martin, *Mol. Endocrinol.* **2000**, *14*, 545–553.
111. C. Byrne, S. D. Divekar, G. B. Storchan, D. A. Parodi, M. B. Martin, *Toxicol. Appl. Pharmacol.* **2009**, *238*, 266–271.
112. G. F. Nordberg, *Lancet Oncol.* **2006**, *7*, 99–101.
113. S. J. Kopp, T. Glonek, H. M. Perry, Jr., M. Erlanger, E. F. Perry, *Science* **1982**, *217*, 837–839.
114. IARC (International Agency for Research on Cancer), *Summaries & evaluations: Cadmium and cadmium compounds (Group 1)*. Lyon, 1993.
115. J. Alexander, D. Benford, A. Cockburn, J.-P. Cravedi, E. Dogliotti, A. Di Domenico, M. L. Férnandez-Cruz, P. Fürst, J. Fink-Gremmels, C. L. Galli, P. Grandjean, J. Gzyl, G. Heinemeyer, N. Johansson, A. Mutti, J. Schlatter, R. van Leeuwen, C. Van Peteghem, P. Verger, *The EFSA Journal* **2009**, *980*, 1–139.
116. NRC (Nuclear Regulatory Commission), *Recommended Dietary Allowances*, Washington, D. C., 1980.
117. ATSDR, *Agency for Toxic Substances and Disease Registry. Toxicological Profile for Cadmium*, Atlanta, GA, USA, 2008, pp. 517.
118. Q. Zhao, R. F. Li, S. K. Xing, X. M. Liu, T. L. Hu, X. H. Bu, *Inorg. Chem.* **2011**, *50*, 10041–10046.
119. J. L. Vinkenborg, S. M. van Duijnhoven, M. Merkx, *Chem. Commun.* **2011**, *47*, 11879–11881.
120. S. Mounicou, J. Szpunar, R. Lobinski, *Chem. Soc. Rev.* **2009**, *38*, 1119–1138.

Chapter 2
Biogeochemistry of Cadmium and Its Release to the Environment

Jay T. Cullen and Maria T. Maldonado

Contents

ABSTRACT 32
1 INTRODUCTION 32
2 GEOCHEMISTRY OF CADMIUM 33
2.1 Chemical Properties 33
2.2 Abundance in the Continental Crust 34
3 MOBILIZATION OF CADMIUM 35
3.1 Natural Sources 35
3.2 Anthropogenic Sources 36
4 CADMIUM IN THE ATMOSPHERE 37
4.1 Sources 37
4.2 Deposition and Fate 38
5 CADMIUM IN THE TERRESTRIAL AND FRESHWATER ENVIRONMENT 40
5.1 Behavior in Soils 40
5.2 Speciation and Fate in Lakes and Rivers 42
6 CADMIUM IN OCEAN WATERS 44
6.1 Distribution 44
6.2 Speciation 46
6.3 Biogeochemical Cycling 47
7 SUMMARY AND CONCLUSIONS 56
ABBREVIATIONS AND DEFINITIONS 57
ACKNOWLEDGMENT 58
REFERENCES 58

J.T. Cullen (✉)
School of Earth and Ocean Sciences, University of Victoria, Victoria, BC, Canada
e-mail: jcullen@uvic.ca

M.T. Maldonado
Department of Earth and Ocean Sciences, University of British Columbia, Vancouver, BC, Canada
e-mail: mmaldonado@eos.ubc.ca

A. Sigel, H. Sigel, and R.K.O. Sigel (eds.), *Cadmium: From Toxicity to Essentiality*, Metal Ions in Life Sciences 11, DOI 10.1007/978-94-007-5179-8_2,

Abstract Cadmium is at the end of the 4d-transition series, it is relatively mobile and acutely toxic to almost all forms of life. In this review we present a summary of information describing cadmium's physical and chemical properties, its distribtion in crustal materials, and the processes, both natural and anthropogenic, that contribute to the metal's mobilization in the biosphere. The relatively high volatility of Cd metal, its large ionic radius, and its chemical speciation in aquatic systems makes Cd particularly susceptible to mobilization by anthropogenic and natural processes. The biogeochemical cycle of Cd is observed to be significantly altered by anthropogenic inputs, especially since the beginning of the industrial revolution drove increases in fossil fuel burning and non-ferrous metal extraction. Estimates of the flux of Cd to the atmosphere, its deposition and processing in soils and freshwater systems are presented. Finally, the basin scale distribution of dissolved Cd in the ocean, the ultimate receptacle of Cd, is interpreted in light of the chemical speciation and biogeochemical cycling of Cd in seawater. Paradoxically, Cd behaves as a nutrient in the ocean and its cycling and fate is intimately tied to uptake by photosynthetic microbes, their death, sinking and remineralization in the ocean interior. Proximate controls on the incorporation of Cd into biomass are discussed to explain the regional specificity of the relationship between dissolved Cd and the algal nutrient phosphate (PO_4^{3-}) in oceanic surface waters and nutriclines. Understanding variability in the Cd/PO_4^{3-} is of primary interest to paleoceanographers developing a proxy to probe the links between nutrient utilization in oceanic surface waters and atmospheric CO_2 levels. An ongoing international survey of trace elements and their isotopes in seawater will undoubtedly increase our understanding of the deposition, biogeochemical cycling and fate of this enigmatic, sometimes toxic, sometimes beneficial heavy metal.

Keywords anthropogenic emissions • biogeochemistry • cadmium • cadmium/phosphorus ratio • marine biogeochemistry • pollution • trace metal

1 Introduction

Cadmium is released to the environment through natural and anthropogenic sources. Because of its acute toxicity toward all forms of life and its relative abundance, there is strong motivation to understand the sources and mobility of Cd in the environment. Measurements of Cd in the atmosphere, natural waters, snow, and ice indicate that anthropogenic sources now dominate the biogeochemical cycle for the element with contamination being evident in even the most remote reaches of the globe. Total industrial and natural weathering cycle mobilizations of Cd in the biosphere by the end of the 1980's are estimated to have been 24,000 t/yr and 4.5 t/yr respectively, demonstrating the dominance of anthropogenic discharges [1]. Global anthropogenic Cd emissions to the atmosphere are reasonably well constrained and were 7,570 t/yr in 1983 with more recent estimates for the mid-1990's dropping to 2,983 t/yr compared to natural emissions of 1,440 t/yr [2,3].

Thus the major anthropogenic sources to the atmosphere from non-ferrous metal production (2,171 t/y) and fossil fuel combustion (691 t/yr) exceed major natural sources like volcanic outgassing (0.82 t/yr), and wind borne dust (0.21 t/yr), by a factor of ~2 [1–3]. The declining trend in anthropogenic emissions reflects more stringent regulations on Cd use, capture of Cd at point sources, and more efficient recycling of Cd from consumer goods despite increasing Cd production trends during the same period.

Compared to other metals, Cd is relatively mobile in soils and freshwater systems and Cd concentrations are enriched relatively to crustal concentrations in oceanic surface waters [4]. The biogeochemistry of Cd in the ocean is a matter of much interest for marine chemists and oceanographers given the nutrient-like behavior of the element and its close correlation with the major algal nutrients nitrate (NO_3^-) and phosphate (PO_4^{3-}). Factors governing the uptake of Cd by marine phytoplankton and the ocean basin scale distribution of the metal will be discussed in detail.

2 Geochemistry of Cadmium

2.1 Chemical Properties

As member of Group 12 of the periodic table, cadmium (Z = 48, atomic weight 112.41) is similar to zinc and mercury in its chemical and physical properties (Table 1) [5,6]. Indeed, Cd was first isolated and identified as an impurity in

Table 1 Relevant physical and chemical properties of cadmium[a].

Property	
Atomic number	48
Atomic weight (g mol^{-1})[b]	112.411
Atomic radius (pm)[c]	155
Ionic radius of Cd^{2+} (pm)[d]	95
Electron configuration	$[Kr]4d^{10}5s^2$
Melting point (°C)	320.9
Boiling point (°C)	767.3
Density at 25°C (g cm^{-3})	8.642
Oxidation states	+2, +1 (not common)
Reduction potential (E^0) for $Cd^{2+} + 2e^- = Cd$ (V)	−4.02
First ionization energy (kJ mol^{-1})	867
Second ionization energy (kJ mol^{-1})	1,625

[a] Adapted with kind permission from Springer Science+Business Media from [6]; copyright 2011.
[b] [123].
[c] [124].
[d] [125].

Zn-containing carbonates (e.g., smithsonite; $ZnCO_{3(s)}$). Cadmium presents as a bluish-white divalent metal that is soft and malleable. This heavy metal has a stable d^{10} electron configuration ($[Kr]4d^{10}5s^2$) and can exist in the +I oxidation state but is found almost exclusively in a +II valence in the natural environment. Cadmium has relatively low melting (321.07°C), and boiling (767°C) points and a density equal to 8.65 g cm^{-3} at 20°C. The atomic weight of Cd results from a mixture of eight stable isotopes with naturally occurring as well as artificial radioisotopes (Table 2) [6,7]. The metal will readily oxidize in moist air, forming a brown CdO oxide coating that resists further corrosion unless exposed to more extreme pH solutions.

Table 2 Stable and radioactive isotopes of cadmium along with their natural abundance[a].

Mass Number	Half-Life	Decay Mode	Natural Abundance (%)[b]
103	10 min	β^+, γ	
104	57 min	β^+, γ	
105	55 min	β^+, γ	
106	stable		1.25
107	6.5 h	β^+, γ	
108	stable		0.89
109	450 days	γ	
110	stable		12.49
111	stable		12.80
112	stable		24.13
113	stable		12.22
114	stable		28.73
115	53.5 h	β^-	
116	stable		7.49
117	2.4 h	β^-	
118	49 min	β^-	
119	2.7 min	β^-	

[a] Adapted with kind permission from Springer Science+Business Media from [6]; copyright 2011.
[b] Natural abundance from mole fractions reported in [126].

2.2 Abundance in the Continental Crust

Cadmium is a rare element in the crust with a concentration in the lithosphere of 0.08–0.1 ppm that is roughly 650 fold lower than its Group 12 neighbor Zn [8,9]. As a chalcophilic element, Cd tends to be concentrated in sulfide minerals. While there are no commercially exploitable Cd mineral deposits, the most common minerals are forms of CdS (greenockite and hawleyite), cadmoselite (CdSe), monteponite (CdO), otavite ($CdCO_3$), and cadmian metacinnabar ((Hg,Cd)S). The most significant concentrations (~1%) of Cd are present as surface coatings associated with the zinc sulfides (spharelite and wurtzite) with more modest levels

Table 3 The concentration of cadmium in crustal materials and soils[a].

Type of Material	Cadmium Content (μg g^{-1})
Crust[b,c]	0.08, 0.10
Upper Crust	*0.09*
Middle Crust	*0.06*
Lower Crust	*0.1*
Granite[d,e]	0.15, 0.13
Basalt[d,e]	0.2, 0.2
Shale[d,e]	1.4, 0.3
Sandstone[d]	<0.03
Limestone[d,e]	0.05, 0.03
Soils (general) [d]	0.35
Soils (world)[f]	0.06
Soils (UK)[g]	0.8
Soils (USA)[g]	0.27

[a] Adapted from [12] with permission from Elsevier; copyright 2003.
[b] Composition of the average crust and upper, middle and lower units from [8].
[c] Average continental crust Cd composition from [9].
[d] Values from [127].
[e] Values from [128].
[f] Value from [129].
[g] Value from [130].

(~500 ppb) in metal sulfides like galena (PbS), metacinnabar (HgS), and chalcopyrite ($CuFeS_2$). Certain Zn silicates and carbonates can contain up to 1.2% concentrations of Cd [5,10,11]. A summary of Cd in crustal materials and soils is presented in Table 3 [5,9,12,13]. The Cd composition of the mantle is relevant given the importance of natural volcanic emissions to the atmosphere and has been estimated to be 64 ppb [14].

3 Mobilization of Cadmium

3.1 Natural Sources

Natural mobilization of the trace Cd concentrations contained in the continental crust and mantle can occur through volcanic eruptions, physical and chemical weathering of the parent rock material or derived soils, burning of vegetation, sea salt spray, and the production of marine biogenic aerosols [1–3,15]. Global estimates of natural Cd fluxes must be interpreted with caution whenever they are based on contemporary measurements as the potential for anthropogenic impact is high and estimates therefore likely represent maximum natural emissions.

Worldwide estimates of natural Cd emissions to the atmosphere suggest that of the ~1,400 t/yr released, a full 60% can be attributed to volcanic emissions with much of the remaining flux coming from wind-borne particles, aerosols, and

terrestrial biomass burning [1]. Quantification of the global volcanic source of Cd is challenging given the remote locations of some sources, the variability in Cd content of erupted material and that the eruptions are stochastic and ephemeral in nature [16,17]. Analysis of Antarctic ice core records of atmospheric inputs of Cd over the last two full glacial-inter glacial cycles indicate that natural sources show considerable temporal variability. The majority of Cd in the ice record can be accounted for by long-range transport of the metal released by quiescent volcanic degassing with terrestrial dust, sea salt spray, and other natural sources playing relatively minor roles [18,19].

Estimates of the natural input of Cd to the oceans from continental runoff, based on the weathering cycle, are roughly 500 t/yr, representing approximately one third of the natural atmospheric flux [12,20]. Global compilations of the Cd abundance in river water allows for an estimate of the mobility of Cd during chemical and physical weathering by comparing the concentration of Cd in river waters to its crustal concentration (C_w/C_c). The C_w/C_c of Cd is of the same order as sodium and boron and suggests that Cd is highly mobile [4], but this analysis does not account for anthropogenic inputs to the watershed and should be interpreted with caution. Based on available estimates discussed below, natural sources of Cd to the biosphere have been eclipsed by anthropogenic mobilization of the metal through industrialization over the last ~130 years.

3.2 Anthropogenic Sources

The best available observations suggest that the human perturbation to the natural biogeochemical cycle of Cd is pronounced [2,12,15]. Mobilization of Cd occurs indirectly through the processing of non-ferrous ores, combustion of fossil fuels, and incineration of refuse and directly through the manufacture, use, and disposal of Cd-containing products. World production of Cd is tied to the processing of primary ores rich in Cu, Pb, and principally Zn such that production levels are largely independent of demand for Cd. For example, Zn ore bodies (e.g., sphalerite, ZnS) range in Cd content from 0.2–0.7% by weight [5,21], making by-product extraction of Cd the major source of production rather than mining of Cd specific minerals. With the exception of years characterized by widespread economic depression in 1930's and 1940's there has been a general increase in global Cd production rising from ~20 t at the beginning of the 20th century and stabilizing at ~20,000 t by 1990 (Figure 1). Most recent figures available for 2011 put global production at 21,500 t with the bulk of production occurring in China (7,500 t), Republic of Korea (2,500 t), and Japan (2,000 t) [22].

Rechargeable battery manufacture (nickel-cadmium; NiCd) continues to the major industrial application for Cd. This battery enjoys widespread use because, in comparison to other rechargeable technologies, the NiCd can (i) withstand deep discharge without damage, (ii) tolerate many recharge-discharge cycles over their lifetimes, (iii) have significantly higher energy densities than other acid-metal batteries (e.g., acid-lead), and (iv) does not produce gas when properly charged

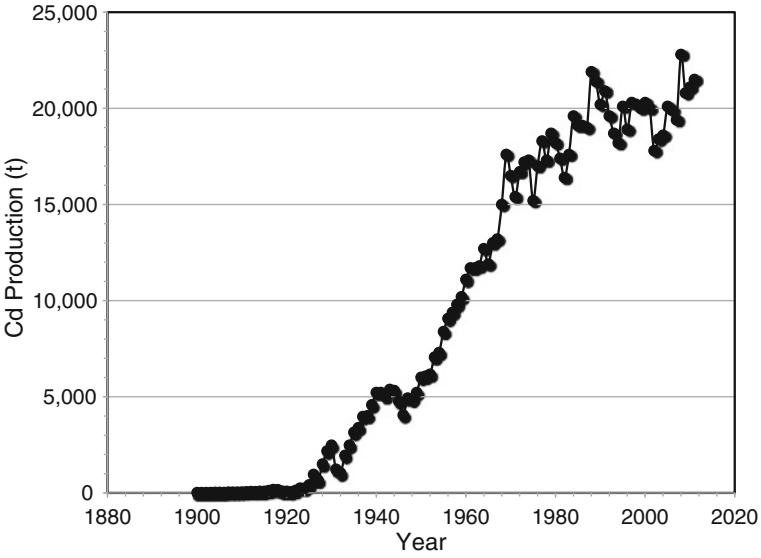

Figure 1 World refinery production of cadmium with time as reported by the U.S. Geological Survey [160]. Data before 1937 represent only a subset of countries.

and discharged. The major disadvantage of the NiCd technology is the cost of the raw materials and environmental impact and potential toxicity of Cd in the biosphere. The next most significant application of Cd is for the production of pigments to color plastics, inks, paints, rubber, and other consumer goods [5,23]. Despite the potential for toxic effects and the relative cost, Cd pigments are still produced because of a number of desirous properties including, (i) deep and rich color from high indices of refraction, (ii) high heat stability, and, (iii) good resistance to light and weathering attack in typical environmental conditions and in the presence of strong base and hydrogen sulfide. Indeed, for many applications there exist few equally effective alternate agents [23]. Other quantitatively important industrial applications include the use of Cd in the stabilization of plastics and protective electroplating of metal surfaces. Concerns about the toxicity of Cd have lead to regulation and declining industrial use of the metal and lowered emissions from developed countries over the last 30–40 years.

4 Cadmium in the Atmosphere

4.1 Sources

As outlined above, anthropogenic emissions of Cd have significantly altered the global biogeochemical cycle and now dominate the natural fluxes of the metal to the

atmosphere [1,2,15,17]. Identification of the major sources of Cd to the atmosphere has been the subject of ongoing efforts and these fluxes are relatively well characterized compared to other heavy metal contaminants [3]. The most important sources estimated for the mid-1990's include non-ferrous metal production (2,171 t/yr), fossil fuel combustion (691 t/yr), iron and steel production (64 t/yr), waste disposal (40 t/yr), and cement production (17 t/yr) [2,3]. The most recent estimates of the flux of anthropogenic Cd to the atmosphere range up to 3,000–7,570 t/yr compared to natural fluxes totaling 1,440 t/yr (Table 4) [3,24]. This pollution can be detected in precipitation over urban, rural, and remote regions [17,25,26]. Indeed, the most remote locations of the globe including the snow pack and glaciers of the high Himalaya, the Arctic and Antarctic record increasing atmospheric transport and deposition of Cd in response to industrial emissions [18,27–29].

Table 4 Global anthropogenic and natural emissions of cadmium in mid-1990s[a].

Anthropogenic		Natural[b]	
Source	Cd Emission (t yr^{-1})	Source	Cd Emission (t yr^{-1})
Fossil fuel combustion	691	Volcanoes	820
Non-ferrous metal production	2,171	Biogenic	240
Iron and steel production	64	Wind-borne dust	210
Cement production	17	Terrestrial biomass burning	110
Waste disposal	40	Sea-salt spray	60
Total	2,983	Total	1,440
1983 emission[c]	7,570		

[a] Adapted using data from [3].
[b] Estimates from [24].
[c] Estimate from [2].

4.2 Deposition and Fate

Cadmium emissions to the atmosphere are predominantly anthropogenic and occur mainly in the form of aerosol and small particulate matter (with a mean mass size distribution centered ~1 μm diameter) that can be easily dispersed by the wind and ultimately deposited by wet and dry deposition [17,30]. Indeed, these small size particles can disperse Cd-enriched material thousands of kilometers through the atmosphere and pollute even remote and otherwise pristine environments. Dry deposition of particles can be significant in areas downwind of point sources and account for up to 90% of bulk deposition but typically will comprise 30–70% of deposition over land, depending on land use and proximity to anthropogenic sources [16,17,31]. Solubility of Cd aerosols are typically high with 80–100% of Cd dissolving within 6 h of exposure to seawater [16,32]. Therefore, in more remote areas of the globe wet deposition is most important as precipitation leads to washout of the small particulates and aerosols that have been transported great distances via

the atmosphere. Over the world ocean, for example, wet deposition can account for 80–90% of the depositional flux of Cd [16,32].

Measurement of Cd in the atmosphere and in rain and snow at various locations on the globe indicate that the primary source of Cd to the atmosphere is anthropogenic and show a pronounced latitudinal gradient in deposition [27,28,33–35]. The deposition of Cd in precipitation and bulk aerosol samples is observed to occur at significant crustal enrichment factors (EF_C) where

$$EF_C = \frac{(Cd/Al)_x}{(Cd/Al)_{crust}} \quad (1)$$

and the Cd concentration ratio to aluminum (Al) in phase x (where x represents an aerosol, rain or snow sample), is compared to the ratio expected in average continental crust. An EF_C significantly larger than 10 is accepted as an indication that a significant component of the Cd in the sample is of anthropogenic origin. EF_C for Cd in atmospheric aerosol samples measured in remote locations tend to be elevated with a range from ~700 at mid-latitudes in the North Atlantic to greater than 70,000 at high latitudes in the Arctic Ocean [17,31,36,37]. Precipitation samples are also characterized by high EF_C for Cd. Rain samples collected in the North Atlantic Ocean had a range of Cd EF_C from 820–26,000 [38]. Precipitation samples over the North Pacific were not as extreme with an average value of 200 $\pm$ 110 but indicate largely non-crustal sources of Cd in rainwater [32]. In Antarctic snow (~77°S) EF_C values have increased since the beginning of the industrial revolution from 80 to mean values of 133 for the period 1959–1990 [28]. Similarly high modern EF_C values are found in snows collected from the northeastern flank of Mt. Everest (~28°N) with an average of ~50 and as high as ~180 [27]. Snow records from 1991–1995 in central Greenland have Cd EF_C's of 200–300 with a tendency to extreme values (10^4) in some samples [33]. The range in EF_C for Cd in the atmosphere reflects varying mixtures of high EF_C anthropogenic point source emissions – and to a lesser degree naturally high EF_C volcanic outgassing material – with crustal material transported as wind blown dust from more arid terrestrial regions. These high EF_C values for Cd in atmospheric aerosol samples and in precipitation, combined with increasing EF_C with time in snow and ice, suggest that the dominant source of atmospherically transported Cd is from anthropogenic point sources.

Rain and snow remove a significant fraction of Cd from the atmosphere either through the solubilization of Cd aerosols in water droplets or the washout of particles associated with precipitation events [17,39]. Concentrations of Cd in rainwater show a considerable range that is related to air mass history and proximity to anthropogenic point sources. Rainwater Cd concentrations over Europe tend to track emissions and have declined from maximum values of 0.7 μg L^{-1} in the mid-1980's to ~0.1 μg L^{-1} in 2004 [40]. Similar Cd concentrations exist in rainwater over the North Atlantic spanning a wide range from 0.07 to 0.95 μg L^{-1} [38]. In the North Pacific (37°–47°N) much lower concentrations were measured in

rainwater collected at longitudes near to the Hawaiian Islands with an average of 4.8 ± 2.6 ng L^{-1} [32]. Rainwater collected on the Hawaiian island of Oahu had higher and more variable rainwater Cd of 48 ± 45 ng L^{-1} reflecting the impact of local anthropogenic aerosol scavenging on the wet deposition of Cd from the atmosphere [32].

The deposition flux of Cd includes both wet and dry fluxes and has been monitored through programs (e.g., AMAP, ADIOS, EMEP) and studies aimed at understanding the temporal and spatial variability in the deposition of key pollutants. Most recent estimates in Europe and for the Mediterranean Sea indicate that fluxes of Cd from the atmosphere over the period 1986–2002 have dropped from 17500 pg cm^{-2} yr^{-1} in 1986 to 2500 pg cm^{-2} yr^{-1} in 2002 as the emissions of Cd for the same period have diminished from ~1000 t yr^{-1} to ~400 t yr^{-1} for the region [41]. The flux of Cd from the atmosphere is also recorded in snow pits that have been sampled in remote locations [27,28,33–35]. These fluxes appear to vary as a function of latitude with the lowest fluxes in Antarctica and the highest values found at mid-latitudes of the northern hemisphere where point sources to the atmosphere are concentrated. Snows on Mt. Blanc (45.5°N) support an atmospheric Cd flux estimate of 1750 pg cm^{-2} yr^{-1} for the period 1990-1991 [35], while deposition was lower during 2004–2005 at 151 pg cm^{-2} yr^{-1} on Mt. Everest (28°N) [27]. As one heads to higher latitudes the flux is much diminished falling to 28 pg cm^{-2} yr^{-1} in Greenland during the time 1991–1995 [33], and to extremely low values in Antarctica of 6 pg cm^{-2} yr^{-1} (from 1983–1986) [34]. Despite the likelihood that atmospheric emissions have decreased in response to regulation over the time periods sampled above, contemporaneous measurements support the conclusion that there exists a latitudinal gradient in deposition with diminishing Cd flux with distance from mid-latitude, atmospheric point sources.

5 Cadmium in the Terrestrial and Freshwater Environment

5.1 Behavior in Soils

The soils produced from the chemical and physical weathering should, to a first approximation, represent the Cd content of the parent rocks (see Table 3). However, a dominant fraction of Cd in soils, like other heavy metals, is the result of the anthropogenically mobilized Cd deposited from the atmosphere or directly applied to soils in the form of background contamination in fertilizers or biosolids [5,42]. Soils, sediments, and freshwater systems represent a complicated environment where heterogeneous reactions can act to modulate the flux of natural and anthropogenic Cd from the land, via rivers and groundwater, to the ocean. The mobility and bioavailability of Cd in freshwater and soil systems depends ultimately on its chemical speciation which in turn is a function of the reduction-oxidation potential, pH, and the presence of inorganic and organic cations and anions in soil porewater.

The introduction of Cd to the soil and its initial solubilization is followed by a cascade of reactions with soil components which normally leads to the formation of progressively less soluble forms [43]. For example, Cd can be incorporated into minerals or bound to soil surfaces through absorption, co-precipitation, ion exchange, and complexation reactions. Most importantly, and particularly for Cd, is the fact that mobility decreases only very slowly with decades of time required for complete equilibration of deposited Cd with the soil solid phases [43–46].

Given the inherent complexity of natural soils much of the information to follow is derived from experimental work with soil components like metal oxyhydroxides, clays, and calcium carbonates in isolation or in mixture [43]. Experiments with iron oxyhydroxides (e.g., goethite; FeO(OH)) indicate that Cd remained rather soluble after an initial fast adsorption period with the proportion of adsorbed Cd increasing with time, pH, and experimental temperature and decreasing with the initial concentration of soluble metal [47]. Experiments with gibbsite ($Al(OH)_3$) and montmorillonite (e.g., $Na_2.7Al_2O_3.22SiO_2.nH_2O$) indicate that Cd is sorbed to the mineral surface rather than being incorporated into the crystal lattice and can be remobilized by acid treatment or the addition of competing cations before substantial Al is released [48]. The sorption of Cd to calcite ($CaCO_{3(s)}$) in model systems is observed to occur in two steps. Over the first 24 hrs a rapid association of the Cd with the calcite surface is observed followed by a second, slow, and nearly constant process where Cd is incorporated during recrystallization of the calcite requiring a minimum of 7 d [49]. While useful for understanding the short term processes that govern Cd behavior in soil-aqueous solution systems, it is likely that experiments with fresh and aged model sediments are not fully representative of Cd mobility in natural soils.

Experiments with natural soils demonstrate that Cd is relatively slow to react within the system compared to other metals of biogeochemical importance, like Cu and Zn. The addition of Cd associated with sewage sludge to various soil types indicates that the adsorption of Cd increased with increasing temperature, as determined by the fraction of Cd leached with a H_2O_2-NH_4OAc mixture [50]. Similar to the model systems, the addition of Cd was followed by a short (<1 h) period of rapid removal and then by a slow and extended period of equilibration, which was attributed to the large ionic radius of Cd and its incompatibility with mineral lattices compared to the other metals [51].

In experiments where low concentrations of Cd were introduced to loamy and sandy soils, equilibrium between the dissolved and particulate phase was reached in 1 hr and no change in this partitioning was observed over 67 subsequent weeks [52,53]. Only in cases where Cd was introduced to soils in a predominantly organic matrix (e.g., sewage sludge) was there an appreciable increase in the mobility of Cd with time, presumably because complexing organics were degraded [54]. Consequently, the forms and availability of Cd in soils are strongly determined by the origin and history of the metal since emission to the atmosphere and/or deposition on land. The bulk of evidence suggests that Cd is largely bound in soils by reversible adsorption to mineral surfaces and should be easily mobilized, especially under the low pH conditions that predominate in most interstitial waters or in environments where anthropogenic acidification is significant [55].

5.2 Speciation and Fate in Lakes and Rivers

Mobilization of anthropogenic Cd deposited to the terrestrial environment has led to higher concentrations in freshwater systems. Cadmium in streams, rivers, and lakes has increased from pre-industrial background concentrations of ~0.0001–0.002 μg L^{-1} to an average concentration in world rivers of 0.08 μg L^{-1} [4,56]. As with atmospheric aerosols, rain, and snow, the Cd in the suspended particulate phase carried in world rivers is typified by high EF_C, on average ~15 and sometimes greater than 100 [56]. While some of this among river variability is related to differences in the Cd content of geological units drained by world rivers, the ~250% difference in the suspended particulate Cd concentrations is more likely related to point source input of anthropogenic, Cd-rich materials. A compilation of dissolved and particulate Cd in some world rivers is presented in Table 5 [4,56].

Table 5 Dissolved concentration for some major world rivers and estimates of the average concentration and particulate transport[a].

River[b]	Dissolved Cd concentration (μg L^{-1})
Europe	
Harz Mountains, Germany	0.42
Idel River[c]	0.02
North America	
St. Lawrence	0.0114
Ottawa	0.0207
Mistassini	0.0873
Mackenzie	0.1838
Peel	0.0347
Beatton	0.1206
Upper Yukon	0.0906
Skeena	0.0194
South America	
Amazon	0.1781
Rio Beni at Riberalta	0.0081
Rio Beni at Rurrenabaque	0.0011
Mamore	0.0091
Asia	
Ob	0.0006–0.0008
Yenisei	0.0012–0.0018
Lena	0.0089
Changjiang	0.0033
Huanghe	0.0011–0.0055
World Average Dissolved Cd Concentration	0.08
Dissolved Riverine Flux (t yr^{-1})	3,000
Particulate Riverine Flux (t yr^{-1})[c]	23,000

[a] Adapted from Table 1 in [4] with permission from Elsevier; copyright 2003.
[b] Consult [4] for detailed information on primary source material for dissolved Cd concentrations.
[c] Particulate Cd flux associated with suspended material carried by world rivers from [56].

The fate of Cd in freshwater systems is controlled by its chemical speciation. For example, the availability and toxicity of Cd to freshwater organisms is strongly dependent on metal speciation [57,58]. Cadmium tends to be largely complexed by natural organic matter under normal conditions in oxygenated freshwaters. The degree of complexation with naturally occurring organic ligands depends upon the concentrations and binding characteristics of dissolved organic carbon (DOC), pH, and competition with other major and trace cations [59,60]. Binding of Cd with various natural organic ligands from river, lake, and soil solution has been examined [58,60–65]. This complexation decreases free [Cd^{2+}] so that typically dissolved [Cd^{2+}]/[Cd]$_{Tot}$ range from 0.01–0.03 in eutrophic lakes to higher values of 0.05–0.09 in rivers [59,60]. The ligands typically have conditional stability constants in the range log $K = 9.4$–10.3 [58,60]. Organic complexation was observed to be lower in more oligotrophic or acidic lakes (pH < 7.3) with some characterized by dissolved [Cd^{2+}]/[Cd]$_{Tot}$ as high as 0.8 [58].

Sorption of Cd to particle surfaces suspended in solution or in sediments is recognized as a significant factor controlling its fate in freshwater systems [12,66]. The propensity of Cd to adsorb to suspended particles or aquatic sediments will be governed by pH, ionic strength, and the concentration of competing cations, as well as organic and inorganic ligands. The partitioning of Cd between the dissolved phase and suspended solids, in aquatic sediments and in soil-solution systems can be described by the distribution coefficient (K_d) where:

$$K_d = \frac{\text{amount sorbed per unit mass}}{\text{equilibrium dissolved concentration}} \tag{2}$$

giving the parameter units of L kg^{-1}. Although somewhat simplistic, using K_d allows for a prediction of the mobility of Cd in freshwater and freshwater-soil systems and can easily be incorporated in models of Cd transport, fate, and bioavailability [67]. There is a wide range of literature K_d values for Cd in soil-solution systems ranging from 0.44–192,000 L kg^{-1}, with a median value of 390 L kg^{-1}. In rivers, and lakes lower values of K_d tend to be found for clays like kaolinite (380 $\pm$ 50 L kg^{-1}) while higher values for humic acid rich particles (18,000 $\pm$ 3,000 L kg^{-1}) and river muds (6,000-40,000 L kg^{-1}) are common [66,68]. The greatest predictors of K_d for Cd in freshwater systems are solution pH and the concentration of organic matter, with the adsorption of Cd to solid phases increasing with each property [4,66,67,69].

Before ultimately being delivered to the oceans, the flux of Cd from world rivers is modified by transit through estuaries and by mixing and entrainment of saline marine waters [70]. The net effect of this mixing is to dramatically alter the speciation of Cd through the formation of soluble and stable chloro complexes [71–73]. For example, mobilization and increases in the dissolved load of Cd are observed in the Gironde and Rhone river estuaries [71,72], the Amazon plume – although the increase in dissolved Cd through the estuary was less convincing – [74], the Orinoco, the Chanjiang, and the Huanghe estuaries [71,75]. The increase of Cd in

the dissolved phase can be substantial, with ~90% of particulate Cd being mobilized in some cases, resulting in an 2 to 30-fold increase in the dissolved flux between the river upstream and the lower estuary [71]. Recent compilations calculate global dissolved and particulate Cd riverine fluxes to the ocean of 3,000 t/yr and 23,000 t/yr, respectively (Table 5) [4,56]. Seasonal variability in river flow, dissolved and particulate Cd concentrations, as well as the non-conservative behavior of Cd and the undersampling of world rivers require that these estimates remain semi-quantitative [70].

6 Cadmium in Ocean Waters

6.1 Distribution

The ocean receives Cd mobilized from the crust through riverine and atmospheric input. These fluxes are poorly constrained at present but given an ocean Cd inventory of ~10^{10} g, the residence time of Cd is similar to biologically utilized elements and approaches 10^4 years [70]. The predominant form of Cd in the ocean is in the dissolved phase with concentrations ranging from 1 to 1000 pmol kg^{-1} [76–78]. The vertical distribution of Cd in the oceanic water column resembles profiles of phytoplankton nutrients, with minimum concentrations at the surface that increase to maximum values in the main thermocline and remain relatively constant from there to the ocean bottom (Figure 2) [76–78]. Particulate Cd concentrations are significantly lower and fall between 0.04 and 4 pmol kg^{-1} and are, conversely, maximal in surface waters [79]. This distribution reflects the uptake of Cd by photosynthetic plankton at the surface and the sinking and subsequent decomposition of particulate matter in the water column.

These vertical processes and major source terms of Cd to the sea overlay the general thermohaline and wind driven circulation of the ocean to control the horizontal distribution patterns for this element. The concentration of dissolved Cd in coastal surface waters is higher than oceanic waters and in the range of 0.2–0.9 nmol kg^{-1}. These high values represent terrestrial inputs of the metal from riverine and atmospheric sources, as well as wind driven upwelling of high nutrient and high Cd subsurface waters along the coast [80,81]. Similar to plant nutrients, the concentration of dissolved Cd is relatively low in the deep Atlantic Ocean (~0.3 nmol kg^{-1}) compared to the deep Indian (~0.6–0.7 nmol kg^{-1}), Southern (depending on sector but ~0.6–0.7 nmol kg^{-1} to higher values) and Pacific Oceans (0.8–1.0 nmol kg^{-1}) (Figure 2). This pattern reflects the accumulation of remineralized Cd from sinking particles as deepwater ages after forming in the north Atlantic and flowing through the Southern, Indian and ultimately the Pacific Ocean basin before returning to the Atlantic in surface currents [82].

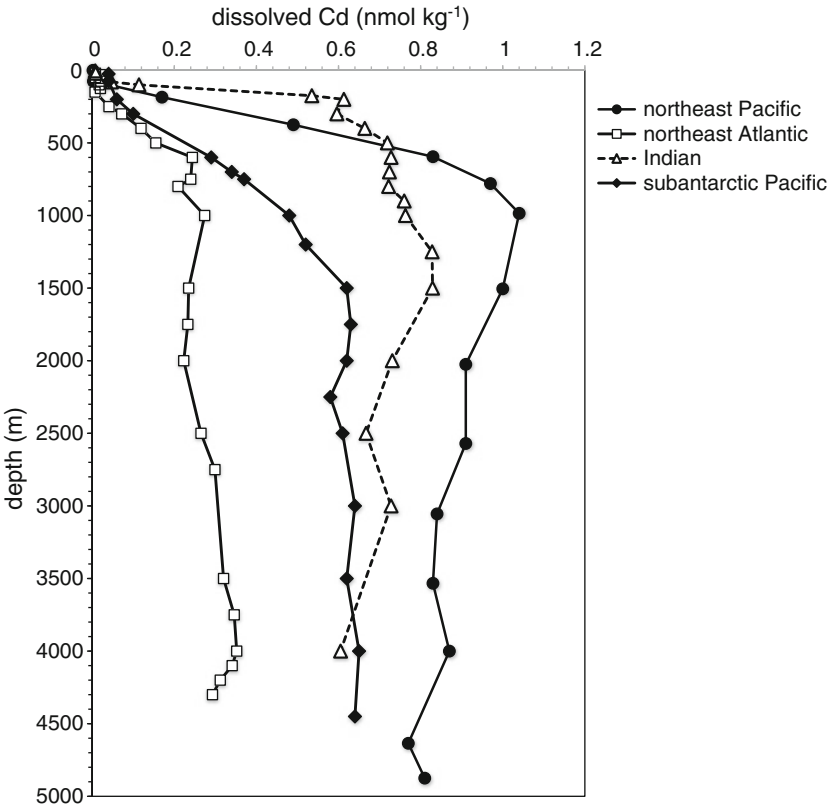

Figure 2 The concentration of dissolved Cd versus depth in the northeast Atlantic [155], subantarctic Pacific [142,143], the Indian Ocean [154], and the northeast Pacific [135].

The strength of the correlation between dissolved Cd and PO_4^{3-} (Figure 3), combined with faithful records of ancient seawater Cd concentrations in fossil foraminiferal calcite ($CaCO_{3(s)}$) tests, has been exploited to infer past nutrient distributions in the paleoocean interior [83–86]. More recent efforts have focused on the potential of planktonic foraminiferal records of dissolved Cd in order to determine past surface nutrient distributions [87,88]. The goal is to constrain temporal variability in the strength of the biological pump and the effect on the partitioning of inorganic carbon between the atmosphere and ocean in relation to past climate change [87,88]. However, there exists significant variability and regional specificity of the dissolved Cd/PO_4^{3-} in surface seawater [78] and within the nutricline [89], confounding the accurate determination of past surface nutrient concentrations. Understanding the biogeochemical cycling of Cd, and more specifically, the factors controlling the regional variability in the relative export and recycling of Cd and P in the upper ocean, are prerequisite for verifying the application of this emerging paleoproxy.

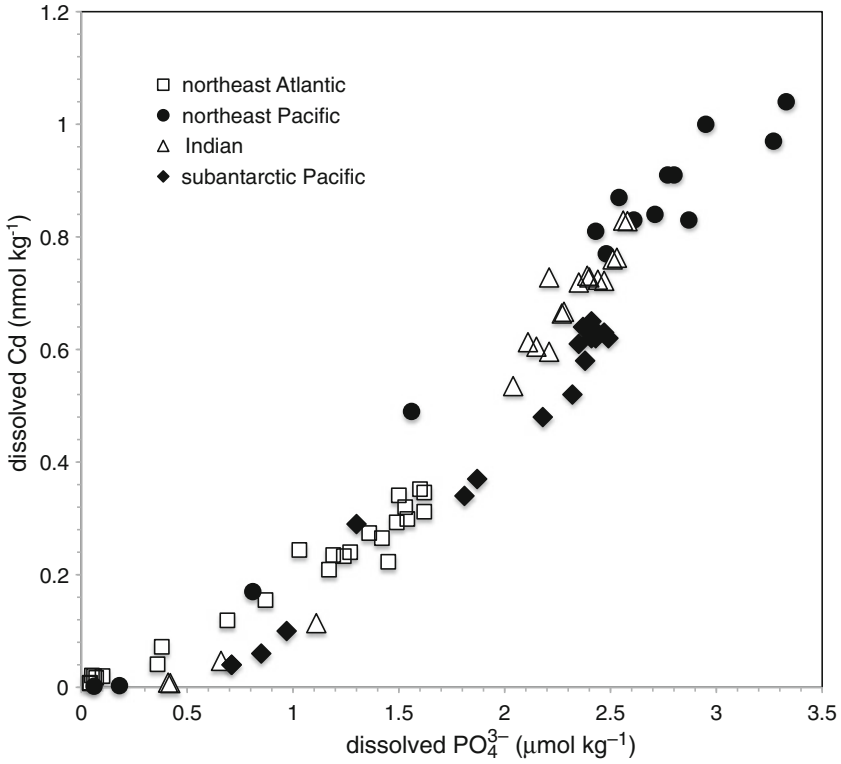

Figure 3 Concentrations of dissolved Cd versus PO_4^{3-} measured in seawater from a subset of the global dataset representing the major ocean basins. Data are from the same references in Figure 2 and demonstrate the correlation between dissolved Cd and PO_4^{3-} in the world ocean.

6.2 Speciation

The chemical speciation of Cd in seawater is largely controlled by complexation with the inorganic ligand chloride and association with strong organic ligands whose structure and provenance are poorly characterized [90]. There is a limited number of anodic stripping voltammetry (ASV) studies, primarily from the north and subantarctic Pacific Ocean, investigating the speciation of dissolved Cd in seawater. A study in the north Pacific found that 67% of dissolved Cd in surface waters (<175 m) was complexed by strong organic ligands, presenting an average concentration of 0.1 nM and possessing conditional stability constants $K'_{cond,Cd'} = 10^{9.9-10.7}\ M^{-1}$ [91]. Similarly strong ligands ($K'_{cond,Cd'} = 10^{9.82-10.93}\ M^{-1}$) were also detected in the subantarctic waters off the coast of New Zealand but at significantly higher concentrations (1–2.5 nmol kg^{-1}) [92]. These strong ligands are only detected in the near surface waters, such that the equilibrium speciation of Cd in the subsurface and deep ocean is predicted to be dominated by the formation of

chlorocomplexes, primarily $CdCl^+$ and $CdCl_2$ [90,91]. The impact of organic complexation in surface waters is to reduce the concentration of inorganic Cd ([Cd']) to extremely low values, ranging from 0.6–1.8 pM in the north Pacific and 0.2–23 pmol kg^{-1} in subantarctic water. Free ionic Cd ($[Cd^{2+}]$) concentrations may be as low as 25 fM ($10^{-13.6}$ M) in surface waters under these conditions. Models of the availability of Cd to marine phytoplankton indicate that algal uptake depends directly, but not solely, upon [Cd'] [93,94]. Thus organic complexation and the resulting speciation will influence the incorporation of Cd into biomass and the degree to which biological processes influence the marine geochemistry of Cd.

6.3 Biogeochemical Cycling

The distribution of cadmium in the ocean follows that of the macronutrient phosphate, suggesting a potential physiological role of Cd in marine phytoplankton [76,77]. This observation remained enigmatic for years, as Cd was not known to have any cellular or physiological function. In 1990, however, Price and Morel [95] provided the first evidence of a biological role for Cd, showing that Cd additions enhanced the growth of Zn-limited *Thalassiosira weissflogii*, a centric marine diatom. These authors speculated that Cd was able to replace the Zn cofactor in the enzyme carbonic anhydrase (CA), which catalyzes HCO_3^--CO_2 interconversion as part of the cellular carbon concentrating mechanism (CCM). Indeed, follow up studies over the next decade [96–98] demonstrated the presence of a catalytically active Cd-containing CA (Cd-CA) in *T. weissflogii* whose activity was enhanced under low Zn culture conditions. When diatoms are Zn-limited, the Cd-CA replaces the most common Zn-containing CA, and as expected, its activity is enhanced at low pCO_2 [96] where the diffusive flux of CO_2 to the photosynthetic algae could theoretically limit growth [99–102]. Most recently, CA has been shown to be a cambialistic enzyme, using either Zn or Cd for catalysis [103], nevertheless the catalysis is slower for the Cd- than the Zn-loaded enzyme.

While we now have a better understanding of the biological function of Cd, at least in diatoms, the intracellular Cd content of marine phytoplankton (both in culture and in field populations) varies widely. Some of the key environmental controls on the biomass normalized Cd (normally reported as particulate Cd:P) in phytoplankton include trace metal availability (Cd, Zn and Mn), aqueous CO_2 concentrations, irradiance and phytoplankton species composition. Lab studies have shown that the uptake of Cd by phytoplankton is directly proportional to dissolved Cd concentrations and indirectly proportional to dissolved Zn and Mn concentrations [94]. The antagonistic interaction between Cd and Mn is due to the upregulation of a high affinity Mn transporter under low Mn, which also transports Cd. In contrast, the antagonistic interaction between Cd and Zn is mediated by the upregulation of a high affinity Cd/Co transport system under low Zn. The assimilation of Cd allows Zn-limited phytoplankton to use the Cd-CA, enhancing their ability to acquire inorganic C and partly alleviating Zn limitation [95,97,98].

Given the role of Cd in CA and the diatom CCM, cellular Cd levels are expected to vary in response to CO_2 availability. Indeed, aqueous CO_2 concentrations in cultures have also been shown to affect Cd-specific CA in the centric diatom *T. weissflogii*, increasing its abundance under low CO_2 [96]. These findings have been supported by shipboard incubations in productive waters off Monterey Bay, California, where significantly higher (2 to 5 fold) Cd:P ratios were observed for indigenous phytoplankton exposed to low CO_2 (100 ppm), relative to high CO_2 (800 ppm) [104]. Additions of Zn or Mn to these incubations decreased phytoplankton Cd uptake by 20- or 2–4-fold, respectively, highlighting the interaction between Zn/Mn and CO_2 in controlling Cd ratios. Furthermore, the Cd content of natural phytoplankton assemblages in highly productive, upwelled waters off California were also shown to increase (from 0.05 to 0.8 mmol Cd: mol P) along decreasing *in situ* surface water pCO_2 gradients (~800 to 250 ppm) [105].

In addition to Cd, Zn and Mn concentrations, most recently, Fe availability has been shown to affect Cd:P ratios in phytoplankton. The first link between Fe limitation and high Cd:P ratios was based on field observations in the northeast Subarctic Pacific in the late 1980s. Low dissolved Cd:P ratios in surface waters at an Fe-limited station in this region suggested preferential removal of Cd relative to P by Fe-limited phytoplankton [106]. This field observation was then supported by higher Cd content in Fe limited cultures of the centric diatom *Thalassiosira oceanica*, under low Zn [94]. The interaction between Fe and Zn nutrition in controlling Cd quotas in *T. oceanica* was linked to faster rates of silica uptake for Fe-limited diatoms [107,108], and the Zn dependency of Si transport. However, evidence supporting a role for Zn in Si uptake remains elusive. In contrast, the inadvertent incorporation of Zn into the diatoms' frustules is well documented and reflects bioavailability of Zn in the cultures [109]. However, independent of Zn availability, a link between Fe limitation and high phytoplankton Cd:P ratios, was observed by shipboard incubations in a high nitrate, low chlorophyll region in the Southern Ocean, where a 3-fold decreased in phytoplankton Cd:P was observed after an Fe addition, at high Zn concentrations (~pZn = 8.2 [110]). Until recently, the accumulation of Cd by Fe-limited phytoplankton was attributed to growth rate biodilution, where growth rate decreases due to Fe limitation while Cd uptake remains constant. The resulting effect is an increase in phytoplankton Cd content. However, a more recent study [111], has presented strong evidence for Cd uptake via a putative, divalent metal transporter that is upregulated under Fe deficiency, providing a physiological mechanism underlining higher Cd quotas by Fe limited phytoplankton, independent of Zn levels. A follow up study also demonstrated that growth biodilution and faster Cd uptake rates were equally important in explaining the higher Cd content of Fe-limited cells, both accounting for ~ 50% of the observed increase [89].

These laboratory and field studies have provided important insights into how Fe, Mn, Zn, and Cd availability controls Cd uptake in phytoplankton, and have highlighted the complex interaction between trace metals in controlling Cd:P ratios. However, our understanding of how trace element availability affects phytoplankton Cd transport in surface waters has been hindered by a limited data set on

dissolved Zn, Fe, Mn, and Cd concentrations in the global ocean. The GEOTRACES international program [112], is poised to provide the required trace metal data to validate these laboratory observations, and thus will contribute significantly toward our understanding of how Fe, Zn, Mn, and Cd availabilities control uptake of Cd by phytoplankton and ultimately the distribution of Cd in the ocean.

Beyond trace metals and CO_2 concentrations, phytoplankton species composition might be one of the most important determinants of Cd:P ratios of phytoplankton field populations. Initial phytoplankton laboratory studies have demonstrated enormous variability in Cd:P ratios of phytoplankton even when grown under identical culturing conditions [89,113,114]. For example, Cd:P ratios differed by 105-fold (0.007 to 0.73 mmol Cd:mol P) among 15 eukaryotic phytoplankton species investigated by Ho et al. [114], (with chlorophytes and diatoms exhibiting the lowest Cd:P ratios and prymnesiophytes, prasinophytes, and dinoflagellates exhibiting the highest). Similarly, in a study investigating the effects of irradiance on Cd:P ratios in a wide variety of phytoplankton classes, Cd:P ratios were found to differ by 255-fold at a given irradiance (15 $\mu E\ m^{-2}\ s^{-1}$) (diatoms with the lowest Cd:P and prymnesiophytes the highest) and no systematic trends relating Cd:P to irradiance levels were established among classes [113]. A more recent investigation on the effect of Fe limitation on Cd:P ratios in 7 species of eukaryotic phytoplankton reported 66-fold difference under identical Fe levels (for example 0.013 to 0.84 mmol Cd:mol P for Fe sufficient cultures), with oceanic diatoms exhibiting the highest Cd:P ratios (0.87 mmol Cd:mol P) and naked prymnesiophytes the lowest (0.05 mmol Cd:mol P) [89]. These results suggest that phytoplankton species composition in surface waters might be the greatest determinant of Cd:P ratios in marine particles and of the drawdown of dissolved Cd and P in surface waters, in spite of the effects that other abiotic factors (such as Zn, Cd and/or Fe, as well as CO_2 concentrations, etc.) may also exert on these ratios.

Dissolved PO_4^{3-} is taken up by phytoplankton in surface waters, and is eventually transported as organic phosphate out of the euphotic zone, where it is remineralized back to dissolved PO_4^{3-} by heterotrophic bacterial activity. Bioactive metals such as Cd, follow a similar cycle of uptake, export, and regeneration. Assuming that the ocean is in steady-state, and that the remineralization efficiencies of Cd and PO_4^{3-} are similar at a given oceanic site, the change in dissolved Cd and PO_4^{3-} concentrations in the nutricline (ΔCd: ΔPO_4^{3-}slope) should represent the Cd:P ratios of the phytoplankton exported out of the euphotic zone. Based on this assumption and using published depth profiles of dissolved Cd and P concentrations one can estimate phytoplankton Cd:P ratios in the global ocean by calculating the regression slopes of dissolved Cd and PO_4^{3-} concentrations in nutriclines. Building on the global data set presented by Cullen [115] and Lane et al. [89], we estimated particulate Cd:P ratios for the global ocean ranging from 0.091 to 1.87 mmol Cd mol^{-1} P, showing a range of ~ 20-fold (Table 6; Figure 4). However, when these stations were classified as located in high nutrient-low chlorophyll (HNLC) or non-HNLC regions (based on yearly mean PO_4^{3-} concentrations in surface waters), and the average Cd:P ratios for these 2 regions were calculated, higher Cd:P ratios were observed for the HNLC stations (0.543 and 0.241 *versus* mmol Cd mol^{-1} P, [89]).

Table 6 Regression slopes of Cd:P (nmol μmol^{-1}) based on depth-dependent variations in dissolved Cd and PO_4^{3-} in oceanic nutriclines. The Cd:P ratios of HNLC stations are shown in bold. Stations were considered HNLC when surface PO_4^{3-} concentrations were >0.3 μmol L^{-1} [115], when surface PO_4^{3-} concentrations were not available classification was based on the predominant conditions in the area. n is the number of points in the nutricline analyzed using simple linear regression and r^2 is the correlation coefficient[a].

Reference	Latitude	Longitude	Surface Water PO_4^{3-} (μmol L^{-1})	Nutricline Depth Range (m)	Cd:P (nmol μmol^{-1})	n	r^2	Location
[131]	00°00 N	147°00 E	0.079	90–350	0.24	6	0.96	Equatorial Pacific
	00°00 N	178°00 E	0.539	99–399	**0.274**	5	0.979	Equatorial Pacific
	00°00 N	161°00 E	0.213	99–398	0.288	8	0.952	Equatorial Pacific
[132]	44°00 N	155°00 E	0.84	20–298	**0.365**	12	0.988	NW Pacific
	45°25 N	145°05 E		79–794	**0.441**	12	0.911	NW Pacific
[133]	25°40 N	125°15 E		350–900	**0.351**	8	0.987	NW Pacific
	23°00 N	126°20 E		350–700	**0.384**	10	0.988	NW Pacific
	25°12 N	123°41 E		250–700	**0.385**	12	0.983	NW Pacific
[76]	30°34 N	170°36 E	0.02	82–687	0.292	7	0.734	NW Pacific
	53°60 N	177°17 W	1.6	5–349	**0.406**	3	0.998	NW Pacific
	52°40 S	178°50 W	0.72	216–1290	**0.775**	6	0.901	SW Pacific
[134])	27°54 N	86°52 W	0.05	100–300	0.1	4	0.928	Gulf of Mexico
	26°54 N	91°24 W	0.02	90–200	0.167	5	0.945	Gulf of Mexico
	29°43 N	88°40 W	0.02	100–200	0.183	4	0.957	Gulf of Mexico
	25°59 N	86°22 W	0.02	100–400	0.187	4	0.976	Gulf of Mexico
	27°31 N	91°19 W	0.02	100–200	0.204	3	0.988	Gulf of Mexico
	24°10 N	84°49 W	0.07	100–750	0.257	6	0.991	Gulf of Mexico
[135]	32°41 N	144°60 W	0.06	75–595	0.314	4	0.99	NE Pacific
	36°52 N	122°53 W	0.6	130–500	**0.367**	3	0.975	NE Pacific
	37°00 N	124°12 W	0.47	75–490	**0.409**	4	0.994	NE Pacific
[136]	34°06 N	66°07 W	0.03	375–715	0.236	3	0.97	NW Atlantic
[137]	18°00 N	115°50 E		150–400	0.259	4	0.977	South China Sea
	15°70 N	116°70 E		150–800	0.352	6	0.935	South China Sea
	18°00 N	117°70 E	0.2	100–500	0.396	6	0.938	South China Sea

	22°50 N	119°67 E	0.02	100–600	0.421	4	0.991	South China Sea
	21°42 N	119°47 E	0.64	100–300	**0.462**	4	0.979	South China Sea
	20°25 N	118°58 E	0.44	100–500	**0.508**	5	0.959	South China Sea
[115]	56°33 N	171°60 W	0.42	15–50	0.273	4	0.978	Bering Sea
	55°00 N	178°99 W	1.31	70–300	**0.46**	4	0.929	Bering Sea
[138]	82°53 N	43°97 E	0.37	100–1000	**0.226**	4	0.931	Arctic Ocean
[139]	59°00	20°00 W		200–1000	0.138	3	0.81	NE Atlantic
	53°00 N	20°00 W		100–500	0.171	3	0.993	NE Atlantic
	40°30 N	15°00 W	0.1	100–1000	0.187	4	0.978	NE Atlantic
	48°30 N	20°00 W	0.08	100–1000	0.252	4	0.997	NE Atlantic
	64°10 N	05°40 W	0.53	100–500	**0.254**	3	0.885	NE Atlantic
	62°30 N	00°30 E	0.41	100–400	**0.295**	3	0.9	NE Atlantic
	60°47 N	14°00 W	0.68	100–500	**0.672**	3	0.998	NE Atlantic
[140]	72°30 S	174°00 W	1.83	100–275	**0.757**	3	0.99	Southern Ocean
[141]	62°10 S	83°20 E	1.49	54–155	**0.421**	2	0.999	Indian Ocean
[142]	48°05 S	164°30 E	0.71	100–1300	**0.35**	18	0.953	Southern Ocean
[143]	46°80 S	167°00 E	0.51	100–300	**0.161**	4	0.981	Doubtful Sound
	47°60 S	170°00 E		200–800	**0.33**	4	0.981	Foveaux Strait
	48°20 S	164°50 E	0.71	75–1590	**0.35**	22	0.964	Puyseger Trench
[144]	37°90 S	166°80 E		250–1250	0.162	7	0.907	Tasman Sea
	38°10 S	168°01 E	0.41	150–600	**0.258**	6	0.951	Tasman Sea
	34°30 S	171°42 E	0.26	22–520	0.272	8	0.795	Tasman Sea
	38°45 S	169°18 E	0.44	98–443	**0.276**	5	0.955	Tasman Sea
	34°47 S	170°30 E	0.28	191–1144	0.292	7	0.889	Tasman Sea
	35°50 S	162°40 E	0.16	100–1395	0.295	16	0.85	Tasman Sea
	34°38 S	171°26 E	0.42	100–897	**0.324**	6	0.965	Tasman Sea
	35°11 S	167°09 E	0.31	394–1280	**0.441**	7	0.889	Tasman Sea
	34°29 S	171°46 E	0.37	49–519	**0.441**	9	0.935	Tasman Sea
	39°14 S	170°59 E	0.26	200–600	**0.578**	5	0.985	Tasman Sea
	34°29 S	171°53 E	0.71	74–222	**0.718**	4	0.842	Tasman Sea

(continued)

Table 6 (continued)

Reference	Latitude	Longitude	Surface Water PO_4^{3-} ($\mu mol\ L^{-1}$)	Nutricline Depth Range (m)	Cd:P ($nmol\ \mu mol^{-1}$)	n	r^2	Location
	34°29 S	172°02 E	0.48	94–282	**0.974**	5	0.616	Tasman Sea
	34°24 S	172°18 E	0.53	50–100	**1.5**	3	0.923	Tasman Sea
[145]	47°00 N	131.50 W	0.67	50–900	**0.232**	4	0.983	NE Pacific
	47°00 N	128.00 W	0.46	50–300	**0.252**	4	0.96	NE Pacific
	47°00N	127.00 W	0.37	75–300	**0.57**	4	0.985	NE Pacific
	47°00N	125.50 W	0.31	50–200	**0.697**	3	0.96	NE Pacific
[146]	36°50 N	123°00 W	0.91	65–350	**0.444**	3	0.994	NE Pacific
[119]	55°01 S	06°00 W	1.79	150–300	**0.245**	3	0.984	Southern Ocean
	57°03 S	06°01 W	1.95	95–190	**0.324**	3	0.927	Southern Ocean
	55°00 S	06°01 W	1.89	100–300	**0.356**	4	0.997	Southern Ocean
	47°00 S	06°00 W	1.57	85–255	**0.376**	4	0.922	Southern Ocean
	49°00 S	06°00 W	1.15	100–300	**0.42**	3	0.966	Southern Ocean
	49°00 S	06°00 W	1.22	97–291	**0.429**	4	0.992	Southern Ocean
	56°01 S	06°00 W	1.88	100–200	**0.431**	3	0.995	Southern Ocean
	57°29 S	06°00 W	1.92	100–200	**0.441**	3	0.881	Southern Ocean
	55°59 S	06°04 W	1.84	95–284	**0.454**	4	0.999	Southern Ocean
	53°00 S	06°00 W	1.87	100–200	**0.458**	3	0.961	Southern Ocean
	48°41 S	05°59 W	1.32	97–194	**0.492**	3	0.998	Southern Ocean
	48°00 S	06°00 W	1.62	100–300	**0.519**	4	0.914	Southern Ocean
	48°00 S	06°00 W	1.65	74–277	**0.569**	3	0.999	Southern Ocean
	52°00 S	06°00 W	1.9	100–300	**0.615**	4	0.805	Southern Ocean
	58°00 S	06°00 W	1.95	100–300	**0.619**	3	0.865	Southern Ocean
	51°00 S	06°00 W	1.88	100–300	**0.622**	4	0.998	Southern Ocean
	56°09 S	15°26 W	1.91	100–300	**0.639**	4	0.883	Southern Ocean
	49°59 S	06°00 W	1.11	98–294	**0.784**	3	0.978	Southern Ocean
	50°00 S	06°00 W	1.71	100–300	**0.845**	4	0.947	Southern Ocean
	46°52 S	06°00 W		100–200	**0.88**	3	0.969	Southern Ocean

	54°00 S	06°00 W	1.9	98–197	**1.01**	3	0.955	Southern Ocean
	48°00 S	06°00 W	1.5	100–200	**1.13**	3	0.97	Southern Ocean
	57°00 S	23°19 W	1.87	100–300	**1.87**	4	0.833	Southern Ocean
[106]	39°60 N	140°77 W	0.2	100–690	0.343	9	0.952	NE Pacific
	45°00 N	142°87 W	0.63	20–580	**0.367**	10	0.934	NE Pacific
	50°00 N	145°00 W	0.72	20–290	**0.432**	7	0.974	NE Pacific
	55°50 N	147°50 W	0.39	20–150	**0.478**	4	0.996	NE Pacific
	58°68 N	147°95 W	0.73	20–150	**0.5**	4	0.999	NE Pacific
[147]	60°46 S	63°26 W	1.78	60–300	**0.694**	4	0.992	Drake Passage
[148]	47°00 N	20°00 W	0.05	75–600	0.238	8	0.961	N. Atlantic
[149]	08°27 S	52°43 E	0.24	180–957	0.091	4	0.862	SW Indian Ocean
	12°14 S	55°02 E	0.36	230–1000	**0.16**	7	0.816	SW Indian Ocean
	06°09 S	50°53 E	0.07	112–965	0.166	12	0.885	SW Indian Ocean
	18°36 S	55°36 E	0.17	115–1000	0.324	8	0.949	SW Indian Ocean
	27°00 S	56°58 E	0.27	298–1080	0.332	8	0.994	SW Indian Ocean
[150]	59°22 S	48°44 W	1.49	40–80	**0.59**	3	0.977	Southern Ocean
	61°60 S	48°60 W	2.01	100–300	**0.613**	3	0.648	Southern Ocean
	57°03 S	48°51 W	1.6	60–200	**0.772**	6	0.866	Southern Ocean
	58°00 S	48°59 W	1.76	80–120	**0.808**	3	0.916	Southern Ocean
	59°60 S	48°59 W	1.85	30–60	**0.934**	4	0.737	Southern Ocean
[151]	60°52 S	45°22 W	1.82	100–217	**0.535**	4	0.979	Antarctic Atlantic
	57°00 S	48°24 W	1.77	60–200	**0.705**	7	0.824	Antarctic Atlantic
	61°59 S	48°59 W	2.01	60–150	**1.19**	4	0.926	Antarctic Atlantic
[152]	51°40 S	32°00 E	2.81	184–720	**0.379**	3	0.965	Southern Ocean
[153]	21°45 N	124°00 E		254–1002	0.356	6	0.995	Philippine Sea
	21°45 N	124°00 E		301–801	0.364	6	0.99	Philippine Sea
	16°35 N	119°00 E		101–500	0.364	4	0.997	South China Sea
	21°45 N	127°00 E		252–798	0.365	5	0.995	Philippine Sea
	24°50 N	123°10 E		202–801	0.393	4	0.992	East China Sea
[154]	14°30 N	67°00 E	0.42	80–200	**0.398**	4	0.968	Indian Ocean

(continued)

Table 6 (continued)

Reference	Latitude	Longitude	Surface Water PO_4^{3-} ($\mu mol\ L^{-1}$)	Nutricline Depth Range (m)	Cd:P ($nmol\ \mu mol^{-1}$)	n	r^2	Location
	21°16 N	63°22 E	0.48	100–1200	**0.506**	7	0.93	Indian Ocean
	22°30 N	60°40 E	0.58	130–1200	**0.655**	8	0.967	Indian Ocean
[155]	40°33 N	20°08 W	0.2	20–150	0.094	5	0.999	NE Atlantic
	40°30 N	20°03 W	0.03	200–1500	0.125	6	0.866	NE Atlantic
	32°59 N	20°00 W	0.04	150–750	0.211	7	0.945	NE Atlantic
	58°30 N	20°30 W	0.52	75–900	**0.246**	10	0.721	NE Atlantic
	32°58 N	19°58 W	0.03	150–800	0.253	5	0.97	NE Atlantic
[156]	36°49 N	73°33 W	0.1	302–587	0.136	6	0.937	NW Atlantic
	37°38 N	73°38 W	0.05	245–490	0.156	3	0.721	NW Atlantic
	37°24 N	73°70 W	0.1	199–369	0.17	4	0.991	NW Atlantic
	37°33 N	73°20 W	0.1	83–398	0.179	4	0.969	NW Atlantic
	38°52 N	71°39 W	0.25	347–543	0.189	3	0.986	NW Atlantic
	39°24 N	71°90 W	0.1	66–269	0.19	8	0.845	NW Atlantic
	37°70 N	73°90 W	0.15	119–243	0.192	3	0.192	NW Atlantic
	37°19 N	72°44 W	0.1	106–242	0.203	5	0.988	NW Atlantic
	37°34 N	74°80 W		103–239	0.232	4	0.943	NW Atlantic
[157]	72°12 S	16°41 W	2.01	200–800	**0.322**	5	0.687	Weddell Sea
	73°55 S	39°39 W	2.11	100–400	**0.541**	3	0.999	Weddell Sea
	72°19 S	34°25 W		100–300	**0.542**	3	0.959	Weddell Sea
	72°01 S	16°50 W		100–600	**0.557**	4	0.932	Weddell Sea
	76°10 S	31°46 W		100–300	**0.72**	3	0.999	Weddell Sea
	64°00 S	59°39 W		200–400	**0.813**	3	0.912	Weddell Sea
[158]	32°00 N	64°50 W	0.06	95–1000	0.276	7	0.905	Sargasso Sea
	35°20 N	62°30 W	0.34	200–1200	**0.402**	4	0.965	Sargasso Sea
[159]	45°00 N	45°00 W	0.36	101–507	**0.293**	4	0.994	NW Atlantic
	53°00 N	41°00 W	0.86	47–191	**0.38**	3	0.997	NW Atlantic
	50°15 N	35°30 W	0.74	100–507	**0.415**	3	0.711	NW Atlantic

[a] Adapted from [89] with permission of Elsevier; copyright 2009.

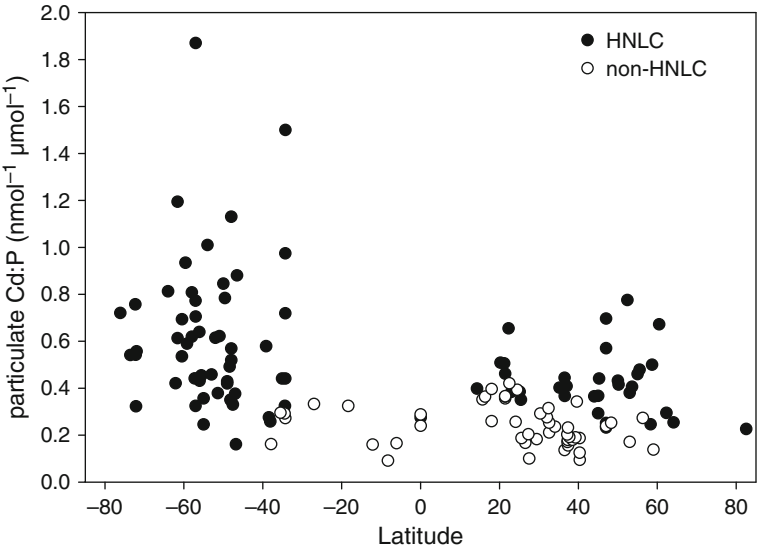

Figure 4 A compilation of calculated surface water particulate Cd:P (nmol µmol^{-1}) ratios estimated from the relative increase of dissolved Cd and PO_4^{3-} profiles in oceanic nutriclines plotted against latitude (Table 6). Solid symbols represent stations deemed to be from HNLC areas based on an average surface water [PO_4^{3-}] > 0.3 µmol kg^{-1} and open symbols from non-HNLC areas. Data from [89], used with permission from Elsevier; copyright 2009.

Iron limitation is widely recognized as the cause of HNLC conditions in the global ocean [116–118]. Coincidentally, these estimated values for Cd:P export in HNLC and non-HNLC waters are in close agreement with those measured for phytoplankton cultures grown under low and high Fe levels respectively (0.496 *versus* 0.261 mmol Cd mol^{-1} P, respectively [89]).

However, Cd:P ratios of phytoplankton in surface waters or derived from phytoplankton cultures are not directly comparable to those estimated from dissolved Cd and PO_4^{3-} concentrations in the nutricline, as only phytoplankton species that are exported out of the euphotic zone will leave an imprint of their Cd:P ratios in the nutricline. The relative recycling efficiency of P versus Cd in the nutricline may also affect these estimates. Yet, according to a study in the Antarctic Polar Front region [119], preferential Cd uptake by phytoplankton overrides the more efficient recycling of Cd (50–95%) compared to PO_4^{3-} (35%) in the upper ocean. Hence, phytoplankton Cd uptake at the surface and export out of the surface waters will greatly affect the dissolved Cd and PO_4^{3-} concentrations in nutriclines, and ultimately the estimated particulate Cd:P ratios.

Diatoms are considered to be the greatest players in carbon export out of surface waters [120]. Oceanic diatoms, such as *T. oceanica* and *Proboscia inermis*, also appear to have the highest Cd:P ratios (0.87 mmol:mol) relative to other ecologically important phytoplankton [89]. Hence, the growth of oceanic diatoms should result in the highest drawdown of dissolved Cd relative to P in surface waters. Interestingly,

during a Polar Front spring diatom bloom the dissolved Cd:P concentration in the surface waters was ~2-fold lower than that in surrounding waters, suggesting preferential uptake of Cd relative to P by the blooming diatoms [119].

A combination of the preferential export of diatoms and their physiological condition may therefore account for the higher estimates of particulate Cd:P ratios in HNLC regions [115]. Natural or simulated Fe additions in HNLC waters often promotes diatom blooms [121], which terminate following the onset of renewed Fe limitation [122]. At the end of the bloom, these diatoms will have faster uptake of Cd, due to both growth biodilution [94] and the upregulation of non-specific divalent transporters [111]. In addition, at the end of the bloom lower pCO_2 [121,122] and Zn concentrations in the euphotic zone might also be observed, further enhancing Cd uptake. The export of these oceanic diatoms with high intrinsic Cd:P ratios at the end of the bloom may explain the higher Cd:P ratios in the Fe limited regions of the global data set. This idea was first proposed by Cullen [115] and supported by field data for the Bering Sea. In this region lower surface-water dissolved Cd:PO_4^{3-} ratios (resulting from phytoplankton Cd uptake at the surface) were observed in the Fe-limited (0.31 mmol Cd:mol P) than in the Fe-sufficient station (0.21 mmol Cd:mol P). This study also presented a model relating Fe availability to phytoplankton Cd:P, the drawdown of surface-water dissolved Cd:PO_4^{3-} ratios and the nutricline slope of dissolved CdPO_4^{3-} in the nutricline, aiming to explain the non-linearity in the global dissolved Cd versus PO_4^{3-} relationship in the modern ocean.

7 Summary and Conclusions

The relative mobility of Cd and its inherent toxicity to organisms make it a heavy metal of concern and motivate the scientific community to understand its sources and fate in the environment. Humans have dramatically altered the biogeochemical cycle of Cd in the environment by mobilizing massive quantities of Cd in the biosphere. This mobilization occurs primarily through non-ferrous metal production and the burning of fossil fuels. As a consequence, material (both in the dissolved and particulate phase) in the atmosphere, as well as in rainwater, soils, sediments, and aquatic environments is significantly enriched in Cd relative to its average concentration in the continental crust.

The emissions of Cd to the environment appear to have been curbed since the 1980s in response to increased regulation of its use and the implementation of more efficient point source capture and recycling initiatives. Indeed, global Cd production reached a plateau in ~1990 at ~20,000 t/yr. Over the past 40 years, however, we have seen a shift in the regions of major Cd production from Europe and North America initially to countries in East Asia more recently. This production shift reflects growing demand for energy and increased industrialization in this area. One concern, going forward, is that emissions in Asia are roughly 3-fold higher than on the next nearest continent and appear to be increasing with time perhaps due to less

stringent emission controls. Whether or not global emissions of Cd will increase in response to the rapid industrialization of countries in Asia remains to be seen, but should be closely monitored.

Developments in the study of the marine biogeochemistry of Cd are particularly exciting and show significant progress since the first reliable measurements of dissolved Cd were made in the open ocean about 35 years ago. We now look upon Cd as a potentially ecologically significant nutrient involved in carbon acquisition by marine algae and have used sedimentary records of Cd preserved in biogenic calcium carbonates to infer past physical and chemical regimes in the ocean. Through the parallel efforts of algal physiologist and marine chemists we are unraveling the complex interplay between the chemical composition of seawater and the marine microbes that dominate Cd export from the surface. In so doing, we are gaining an improved understanding of the regional variability in the Cd versus PO_4^{3-} relationship in seawater and the processes that ultimately control the basin scale distribution of Cd in the ocean.

Pioneering studies investigating the stable isotope systematics of Cd in the environment will ultimately provide us with a way to track industrial emissions. Future measurements of Cd isotope fractionations in seawater will likely help to determine how micronutrient cycling affects modern ocean productivity and how past changes in ocean nutrient utilization are linked to global climate change. As the international GEOTRACES program is just beginning its large-scale effort to measure high resolution sections of trace elements and their isotopes in all the major ocean basins our understanding of Cd and its unique biogeochemistry is bound to expand.

Abbreviations and Definitions

ADIOS	Atmospheric Deposition and Impact on the Open Mediterranean Sea
AMAP	Arctic Monitoring and Assessment Program
ASV	anodic stripping voltammetry
CA	carbonic anhydrase
Cd-CA	cadmium containing carbonic anhydrase
$[Cd]_{tot}$	total dissolved Cd
CCM	carbon concentrating mechanism
Cd'	sum of inorganic cadmium complexes and free Cd ion
C_w/C_c	water concentration divided by crustal concentration for an element representing a global mobility index
DOC	dissolved organic carbon
EF_C	crustal enrichment factor
E^0	standard reduction-oxidation potential in volts
EMEP	Co-operative Programme for Monitoring and Evaluation of the Long-Range Transmission of Pollutants in Europe

GEOTRACES	an international program dedicated to studying trace elements and isotopes in the ocean
H_2O_2-NH_4OAc	hydrogen peroxide and ammonium acetate mixture
HNLC	high nutrient-low chlorophyll region of the ocean
$K'_{cond,Cd'}$	conditional stability or equilibrium constant for the binding of an organic ligand to inorganic Cd species
K_d	distribution coefficient
NiCd	nickel-cadmium battery
pCO_2	partial pressure of carbon dioxide
pH	$-\log\{H^+\}$
t	metric tonne = 1000 kg
Z	atomic number

Acknowledgment This work was supported in part by Canadian Natural Sciences and Engineering Research Council Discovery Grants to JTC and MM.

References

1. J. O. Nriagu, *Environment* **1990**, *32*, 7–33.
2. J. O. Nriagu, J. M. Pacyna, *Nature* **1988**, *333*, 134–139.
3. J. M. Pacyna, E. G. Pacyna, *Environ. Rev.* **2001**, *9*, 269–298.
4. J. Gaillardet, J. Viers, B. Dupré, in *Treatise on Geochemistry*, Eds H. D. Holland, K. K. Turekian, Elsevier Ltd., Amsterdam, 2003, Vol. 7, pp. 225–272.
5. J. O. Nriagu, in *Cadmium in the Environment, Part I: Ecological Cycling*, Ed J. O. Nriagu, John Wiley & Sons, New York, 1980, pp. 35–70.
6. M. Rehkamper, F. Wombacher, T. J. Horner, Z. Xue, *Handbook of Environmental Isotope Geochemistry*, Ed M. Baskaran, Springer Berlin Heidelberg, Berlin, Heidelberg, 2011.
7. W. Pritzkow, S. Wunderli, J. Vogl, G. Fortunato, *Int. J. Mass Spectrom.* **2007**, *261*, 74–85.
8. R. L. Rudnick, S. Gao, in *Treatise on Geochemistry*, Eds H. D. Holland, K. K. Turekian, Pergamon, Oxford, 2003, pp. 1–64.
9. K. H. Wedepohl, *Geochim. Cosmochim. Acta* **1995**, *59*, 1217–1232.
10. M. Fleischer, A. F. Sarofim, D. W. Fassett, P. Hammond, H. T. Shacklette, I. C. Nisbet, S. Epstein, *Environ. Health Persp.* **1974**, *7*, 253–232.
11. H. Gong, A. W. Rose, N. H. Suhr, *Geochim. Cosmochim. Acta* **1977**, *41*, 1687–1692.
12. E. Callender, in *Treatise on Geochemistry*, Eds H. D. Holland, K. K. Turekian, Pergamon, Oxford, 2003, Vol. 9, pp. 67–105.
13. S. R. Taylor, S. M. Mclennan, *Rev. Geophys.***1995**, *33*, 241–265.
14. H. Palme, H. S. C. O'Neill, in *Treatise on Geochemistry*, Eds H. D. Holland, K. K. Turekian, Pergamon, Oxford, 2007, pp. 1–38.
15. J. O. Nriagu, *Science* **1996**, *272*, 223–224.
16. R. Duce, P. Liss, J. Merrill, E. Atlas, P. Buat-Menard, B. Hicks, J. Miller, J. Prospero, R. Arimoto, T. M. Church, W. Ellis, J. N. Galloway, L. Hansen, T. D. Jickells, A. H. Knap, K. H. Reinhardt, B. Schneider, A. Soudine, J. Tokos, S. Tsunogai, R. Wollast, M. Zhou, *Global Biogeochem. Cycles* **1991**, *5*, 193–259.
17. J. O. Nriagu, in *Cadmium in the Envrionment, Part I: Ecological Cycling*, Ed J. O. Nriagu, John Wiley & Sons, New York, 1980, pp. 71–104.
18. S. Hong, *Geophys. Res. Lett.* **2004**, *31*, 5–8.
19. A. Matsumoto, T. K. Hinkley, *Earth Planet. Sci. Lett.* **2001**, *186*, 33–43.

20. K. Bertine, E. D. Goldberg, *Science* **1971**, *173*, 233–235.
21. D. M. Chizhikov, *Cadmium*, Pergamon, Oxford, 1966, pp. 263.
22. US Geological Survey, *Mineral Commodity Summaries: 2012*, US Geological Survey, 2012. 198 p.
23. P. Dunning, in *High Performance Pigments*, Wiley-VCH Verlag GmbH & Co. KGaA, Weinheim, 2003, pp. 13–26.
24. J. O. Nriagu, *Nature* **1989**, *338*, 47–49.
25. T. Berg, O. Røyset, E. Steinnes, *Atm. Environ.***1994**, *28*, 3519–3536.
26. T. Berg, E. Steinnes, *Met. Ions Biol. Syst.,* **2005**, *44*, 1–19.
27. K. Lee, S. D. Hur, S. Hou, S. Hong, X. Qin, J. Ren, Y. Liu, K. J. R. Rosman, C. Barbante, C. F. Boutron, *Sci. Total Environ.* **2008**, *404*, 171–181.
28. F. M. Planchon, C. E. Boutron, C. Barbante, G. Cozzi, V. Gaspari, E. W. Wolff, C. P. Ferrari, P. Cescon, *Sci. Total Environ.* **2002**, *300*, 129–142.
29. E. W. Wolff, E. D. Suttie, D. A. Peel, *Atmos. Environ.***1999**, *33*, 1535–1541.
30. C. I. Davidson, in *Cadmium in the Envrionment, Part I: Ecological Cycling*, Ed J. O. Nriagu, John Wiley & Sons, New York, 1980, pp. 115–138.
31. R. A. Duce, G. L. Hoffman, B. J. Ray, I. S. Fletcher, G. T. Wallace, J. L. Fasching, S. E. Piotrowctz, P. R. Walsh, E. J. Hoffman, J. M. Miller, J. L. Hefter, in *Marine Pollution Transfers*, Eds H. L. Windom, R. A. Duce, D.C. Heath, Lexington, 1976, pp. 77–119.
32. T. Patterson, R. Duce, *Tellus B* **1991**, *43B*, 12–29.
33. C. Barbante, C. Boutron, C. Morel, C. Ferrari, J. L. Jaffrezo, G. Cozzi, V. Gaspari, P. Cescon, *J. Environ. Monit.* **2003**, *5*, 328–335.
34. S. D. Hur, X. Cunde, S. Hong, C. Barbante, P. Gabrielli, K. Lee, C. F. Boutron, Y. Ming, *Atmos. Environ.* **2007**, *41*, 8567–8578.
35. K. Van de Velde, C. Boutron, C. P. Ferrari, A. Moreau, R. Delmas, C. Barbante, T. Bellomi, G. Capodaglio, P. Cescon, *Geophys. Res. Lett.* **2000**, *27*, 249–252.
36. R. A. Duce, G. L. Hoffman, W. H. Zoller, *Science* **1975**, *187*, 59–61.
37. V. V. Egorov, T. Zhigalov, S. G. Malakhov, *J. Geophys. Res.* **1970**, *75*, 3650–&.
38. T. Church, J. Tramontano, D. Whelpdale, M. O. Andreae, J. N. Galloway, W. Keene, A. H. Knap, J. Tokos, *J. Geophys. Res.* **1991**, *96*, 18705–18725.
39. J. O. Nriagu, G. S. Lawson, D. J. Gregor, *Bull. Environ. Contamin. Toxicol.***1994**, *52*, 756–759.
40. J. M. Pacyna, E. G. Pacyna, W. Aas, *Atmos. Environ.***2009**, *43*, 117–127.
41. C. Guieu, M.-D. Loÿe-Pilot, L. Benyahya, A. Dufour, *Marine Chemistry* **2010**, *120*, 164–178.
42. D. I. Orroño, R. S. Lavado, *Chem. Speciat. Bioavail.* **2009**, *21*, 193–198.
43. K. Lock, C. R. Janssen, *Rev. Environ. Contamin. Toxicol.* **2003**, *178*, 1–21.
44. N. J. Barrow, J. Gerth, G. W. Brummer, *J. Soil Sci.* **1989**, *40*, 437–450.
45. G. W. Bruemmer, J. Gerth, K. G. Tiller, *J. Soil Sci.***1988**, *39*, 37–52.
46. J. Gerth, G. Brummer, *Fresenius Zeitschr. Anal. Chemie* **1983**, *316*, 616–620.
47. C. E. Martinez, M. B. McBride, *Clays and Clay Minerals* **1998**, *46*, 537–545.
48. B. Lothenbach, G. Furrer, H. Scharli, R. Schulin, *Environ. Sci. Technol.***1999**, *33*, 2945–2952.
49. J. A. Davis, C. C. Fuller, A. D. Cook, *Geochim. Cosmochim. Acta* **1987**, *51*, 1477–1490.
50. P. S. Hooda, B. J. Alloway, *Int. J. Environ. Anal. Chem.* **1994**, *57*, 289–311.
51. N. J. Barrow, *Australian J. Soil Res.* **1998**, *36*, 941–950.
52. T. H. Christensen, *Water Air Soil Pollut.* **1984**, *21*, 105–114.
53. T. H. Christensen, *Water Air Soil Pollut.* **1984**, *21*, 115–125.
54. J. J. Street, W. L. Lindsay, B. R. Sabey, *J. Environ. Quality* **1977**, *6*, 72–77.
55. W. O. Nelson, P. G. Campbell, *Environmental Pollution (Barking, Essex: 1987)* **1991**, *71*, 91–130.
56. J. Viers, B. Dupré, J. Gaillardet, *Sci. Total Environ.***2009**, *407*, 853–868.
57. L. Hare, A. Tessier, *Nature* **1996**, *380*, 430–432.
58. L. Sigg, R. Behra, in *Metal Ions Biological Systems,* Vol 44, Eds A. Sigel, H. Sigel, R. K. O. Sigel, Taylor & Francis Ltd, Boca Raton, FL, 2005, pp. 47–73.

59. J. Cao, H. Xue, L. Sigg, *Aquat. Geochem.* **2006**, *12*, 375–387.
60. H. Xue, L. Sigg, *Anal. Chim. Acta* **1998**, *363*, 249–259.
61. G. Abate, J. C. Masini, *Organic Geochem.* **2002**, *33*, 1171–1182.
62. D. G. Kinniburgh, C. J. Milne, M. F. Benedetti, J. P. Pinheiro, J. Filius, L. K. Koopal, W. H. Van Riemsdijk, *Environ. Sci. Technol.* **1996**, *30*, 1687–1698.
63. D. G. Kinniburgh, W. H. van Riemsdijk, L. K. Koopal, M. Borkovec, M. F. Benedetti, M. J. Avena, *Colloids and Surfaces A-Physicochem. Engin. Aspects* **1999**, *151*, 147–166.
64. W. H. Otto, S. D. Burton, W. R. Carper, C. K. Larive, *Environ. Sci. Technol.* **2001**, *35*, 4900–4904.
65. W. H. Otto, W. R. Carper, C. K. Larive, *Environ. Sci. Technol.* **2001**, *35*, 1463–1468.
66. J. Gardiner, *Water Res.* **1974**, *8*, 157–164.
67. S. Sauve, W. Hendershot, H. Allen, *Environ. Sci. Technol.* **2000**, *34*, 1125–1131.
68. P. A. Yeats, J. Bewers, in *Cadmium in the Aquatic Environment*, Eds J. O. Nriagu, J. B. Sprague, John Wiley & Sons, New York, 1987, Vol. 19, pp. 19–34.
69. D. P. H. Laxen, *Water Res.* **1985**, *19*, 1229–1236.
70. K. Bruland, M. Lohan, in *Treatise on Geochemistry*, Eds H. D. Holland, K. K. Turekian, Elsevier, Ltd. Amsterdam, Vol. 6, 2003, pp. 23–47.
71. F. Elbaz-Poulichet, J. Martin, W. Huang, *Marine Chem.* **1987**, *22*, 125–136.
72. A. M. L. Kraepiel, J. F. Chiffoleau, J. M. Martin, F. M. M. Morel, *Geochim. Cosmochim. Acta* **1997**, *61*, 1421–1436.
73. A. M. Shiller, E. A. Boyle, *Geochim. Cosmochim. Acta* **1991**, *55*, 3241–3251.
74. E. A. Boyle, S. S. Huested, B. Grant, *Deep-Sea Res. Part A-Oceanogr. Res. Papers* **1982**, *29*, 1355–1364.
75. J. M. Edmond, A. Spivack, B. C. Grant, M. H. Hu, Z. X. Chen, S. Chen, X. S. Zeng, *Continental Shelf Research* **1985**, *4*, 17–36.
76. E. A. Boyle, F. Sclater, J. M. Edmond, *Nature* **1976**, *263*, 42–44.
77. K. W. Bruland, G. A. Knauer, J. H. Martin, *Limnol.Oceanogr.* **1978**, *23*, 618–625.
78. H. J. W. de Baar, P. M. Saager, R. F. Notling, J. van der Meer, *Marine Chem.* **1994**, *46*, 261–281.
79. R. M. Sherrell, E. A. Boyle, *Earth Planet. Sci. Lett.* **1992**, *111*, 155–174.
80. K. W. Bruland, R. P. Franks, in *Trace Metals in Seawater*, Eds C. S. Wong, E. Boyle, K. W. Bruland, D. Burton, E. D. Goldberg, Plenum, New York, 1983, Vol. 9, pp. 395–414.
81. R. K. Takesue, A. van Geen, *Limnol. Oceanogr.* **2002**, *47*, 176–185.
82. W. S. Broecker, T.-H. Peng, *Tracers in the Sea*, Eldigio Press, Palisades, 1982.
83. E. A. Boyle, *Paleoceanography* **1988**, *3*, 471–489.
84. E. A. Boyle, *Annu. Rev. Earth Planet. Sci.* **1992**, *20*, 245–287.
85. K. Hester, E. A. Boyle, *Nature* **1982**, *298*, 260–262.
86. Y. Rosenthal, E. A. Boyle, L. Labeyrie, *Paleoceanography* **1997**, *12*, 787–796.
87. H. Elderfield, R. E. M. Rickaby, *Nature* **2000**, *405*, 305–310.
88. R. E. M. Rickaby, H. Elderfield, *Paleoceanography* **1999**, *14*, 293–303.
89. E. S. Lane, D. M. Semeniuk, R. F. Strzepek, J. T. Cullen, M. T. Maldonado, *Marine Chem.* **2009**, *115*, 155–162.
90. F. M. M. Morel, J. Hering, *Principles and Applications of Aquatic Chemistry*, John Wiley & Sons, New York, 1993.
91. K. W. Bruland, *Limnol. Oceanogr.* **1992**, *37*, 1008–1017.
92. M. J. Ellwood, *Marine Chem.***2004**, *87*, 37–58.
93. W. G. Sunda, S. A. Huntsman, *Environ. Sci. Technol.***1998**, *32*, 2961–2968.
94. W. G. Sunda, S. A. Huntsman, *Limnol. Oceanogr.***2000**, *45*, 1501–1516.
95. N. M. Price, F. M. M. Morel, *Nature* **1990**, *344*, 658–660.
96. T. W. Lane, F. M. M. Morel, *Proc. Nat. Acad. Sci. USA* **2000**, *97*, 4627–4631.
97. J. G. Lee, F. M. M. Morel, *Marine Ecol. Progr. Series* **1995**, *127*, 305–309.
98. J. G. Lee, S. B. Roberts, F. M. M. Morel, *Limnol. Oceanogr.* **1995**, *40*, 1056–1063.
99. U. Riebesell, D. A. Wolf–Gladrow, V. Smetacek, *Nature* **1993**, *361*, 249–251.

100. P. D. Tortell, G. R. DiTullio, D. M. Sigman, F. M. M. Morel, *Marine Ecol. Progr. Series* **2002**, *236*, 37–43.
101. P. D. Tortell, G. H. Rau, F. M. M. Morel, *Limnol. Oceanogr.* **2000**, *45*, 1485–1500.
102. P. D. Tortell, J. R. Reinfelder, F. M. M. Morel, *Nature* **1997**, *390*, 243–244.
103. Y. Xu, L. Feng, P. D. Jeffrey, Y. G. Shi, F. M. M. Morel, *Nature* **2008**, *452*, 56–U53.
104. J. T. Cullen, R. M. Sherrell, *Limnol. Oceanogr.* **2005**, *50*, 1193–1204.
105. J. T. Cullen, T. W. Lane, F. M. M. Morel, R. M. Sherrell, *Nature* **1999**, *402*, 165–167.
106. J. H. Martin, R. M. Gordon, S. Fitzwater, W. W. Broenkow, *Deep-Sea Res.* **1989**, *36*, 649–680.
107. D. A. Hutchins, K. W. Bruland, *Nature* **1998**, *393*, 561–564.
108. S. Takeda, *Nature* **1998**, *393*, 774–777.
109. M. J. Ellwood, K. A. Hunter, *Limnol. Oceanogr.***2000**, *45*, 1517–1524.
110. J. T. Cullen, Z. Chase, K. H. Coale, S. Fitzwater, R. M. Sherrell, *Limnol. Oceanogr.* **2003**, *48*, 1079–1087.
111. E. S. Lane, K. Jang, J. T. Cullen, M. T. Maldonado, *Limnol. Oceanogr.* **2008**, *53*, 1784–1789.
112. G. M. Henderson, R. F. Anderson, J. Adkins, P. Andersson, E. A. Boyle, G. Cutter, H. de Baar, A. Eisenhauer, M. Frank, R. Francois, K. Orians, T. Gamo, C. German, W. Jenkins, J. Moffett, C. Jeandel, T. Jickells, S. Krishnaswami, D. Mackey, C. I. Measures, J. K. Moore, A. Oschlies, R. Pollard, M. R. D. van der Loeff, R. Schlitzer, M. Sharma, K. von Damm, J. Zhang, P. Masque, S. W. Grp, *Chemie der Erde-Geochemistry* **2007**, *67*, 85–131.
113. Z. V. Finkel, A. S. Quigg, R. K. Chiampi, O. E. Schofield, P. G. Falkowski, *Limnol. Oceanogr.* **2007**, *52*, 1131–1138.
114. T. Ho, A. Quigg, Z. V. Finkel, A. J. Milligan, K. Wyman, P. G. Falkowski, F. M. M. Morel, *J. Phycol.* **2003**, *39*, 1145–1159.
115. J. T. Cullen, *Limnol. Oceanogr.* **2006**, *51*, 1369–1380.
116. P. Boyd, A. J. Watson, C. S. Law, E. R. Abraham, T. Trull, R. Murdoch, D. C. E. Bakker, A. R. Bowie, K. O. Buesseler, H. Chang, M. Charette, P. L. Croot, K. Downing, R. D. Frew, M. Gall, M. Hadfield, J. Hall, M. Harvey, G. Jameson, J. LaRoche, M. L. Liddicoat, R. Ling, M. T. Maldonado, R. M. L. McKay, S. Nodder, S. Pickmere, R. Pridmore, S. Rintoul, K. Safi, P. Sutton, R. Strzepek, K. Tanneberger, S. Turner, A. Waite, J. Zeldis, *Nature* **2000**, *407*, 695–702.
117. K. H. Coale, K. S. Johnson, S. E. Fitzwater, R. M. Gordon, S. Tanner, F. P. Chavez, L. Ferioli, C. Sakamoto, P. Rogers, F. Millero, P. Steinberg, P. Nightingale, D. Cooper, W. P. Cochlan, M. R. Landry, J. Constantinou, G. Rollwagen, A. Trasvina, R. Kudela, *Nature* **1996**, *383*, 495–501.
118. J. H. Martin, K. H. Coale, K. S. Johnson, S. E. Fitzwater, R. M. Gordon, S. J. Tanner, C. N. Hunter, V. A. Elrod, J. L. Nowicki, T. L. Coley, R. T. Barber, S. Lindley, A. J. Watson, K. V. Scoy, C. S. Law, M. L. Liddicoat, R. Ling, T. Stanton, J. Stockel, C. Collins, A. Anderson, R. Bidigare, M. Ondrusek, M. Latasa, F. J. Millero, K. Lee, W. Yao, J. Z. Zhang, G. Friedrich, C. Sakamoto, F. Chavez, K. Buck, Z. Kolber, R. Greene, P. Falkowski, S. W. Chisholm, F. Hoge, R. Swift, J. Yungel, S. Turner, P. Nightingale, A. Hatton, P. Liss, N. W. Tindale, *Nature* **1994**, *371*, 123–129.
119. B. M. Löscher, J. T. M. d. Jong, H. J. W. d. Baar, *Marine Chem.* **1998**, *62*, 259–286.
120. X. Jin, N. Gruber, J. P. Dunne, J. L. Sarmiento, R. A. Armstrong, *Global Biogeochem. Cycles* **2006**, *20*.
121. P. W. Boyd, T. Jickells, C. S. Law, S. Blain, E. A. Boyle, K. O. Buesseler, K. H. Coale, J. J. Cullen, H. J. W. de Baar, M. Follows, M. Harvey, C. Lancelot, M. Levasseur, N. P. J. Owens, R. Pollard, R. B. Rivkin, J. Sarmiento, V. Schoemann, V. Smetacek, S. Takeda, A. Tsuda, S. Turner, A. J. Watson, *Science* **2007**, *315*, 612–617.
122. H. J. W. de Baar, P. W. Boyd, K. H. Coale, M. R. Landry, A. Tsuda, P. Assmy, D. C. E. Bakker, Y. Bozec, R. T. Barber, M. A. Brzezinski, K. O. Buesseler, M. Boye, P. L. Croot, F. Gervais, M. Y. Gorbunov, P. J. Harrison, W. T. Hiscock, P. Laan, C. Lancelot, C. S. Law, M. Levasseur, A. Marchetti, F. J. Millero, J. Nishioka, Y. Nojiri, T. van Oijen, U. Riebesell, M. J. A. Rijkenberg, H. Saito, S. Takeda, K. R. Timmermans, M. J. W. Veldhuis, A. M. Waite, C. S. Wong, *J. Geophys. Res. Oceans* **2005**, *110*.

123. M. E. Wieser, T. B. Coplen, *Pure Appl. Chem.* **2011**, *83*, 359–396.
124. J. C. Slater, *J. Chem. Phys.* **1964**, *41*, 3199–&.
125. R. D. Shannon, *Acta Crystallogr. Sect. A* **1976**, *32*, 751–767.
126. M. Berglund, M. E. Wieser, *Pure Appl. Chem.* **2011**, *83*, 397–410.
127. D. C. Adriano, *Trace Elements in the Terrestrial Environment*, Springer, New York, 1986.
128. J. I. Drever, *The Geochemistry of Natural Waters*, Prentice-Hall, New York, 1988.
129. A. Kabata-Pendias, *Trace Elements in Soils and Plants*, CRC Press, Boca Raton, 2000.
130. B. J. Alloway, *Heavy Metals in Soils*, Blackie Academic and Professional, London, 1995.
131. K. Abe, *Marine Chem.* **2001**, *74*, 197–211.
132. K. Abe, *Marine Chem.* **2002**, *79*, 27–36.
133. K. Abe, *J. Oceanogr.* **2002**, *58*, 577–588.
134. E. A. Boyle, D. F. Reid, S. S. Huested, J. Hering, *Earth Planet. Sci. Lett.* **1984**, *69*, 69–87.
135. K. W. Bruland, *Earth Planet. Sci. Lett.* **1980**, *47*, 176–198.
136. K. W. Bruland, R. P. Franks, in *Trace Metals in Seawater*, Eds C. S. Wong, E. A. Boyle, K. W. Bruland, J. D. Burton, E. D. Goldberg, Plenum, New York, 1983, pp. 394–414.
137. H. Y. Chen, T. H. Fang, L. S. Wen, *Continental Shelf Res.* **2005**, *25*, 297–310.
138. L. Danielsson, S. Westerlund, in *Trace Metals in Seawater*, Ed. C. S. Wong, E. A. Boyle, K. W. Bruland, J. D. Burton, E. D. Goldberg, Plenum Press, New York, 1983.
139. L. Danielsson, B. Magnusson, S. Westerlund, *Marine Chem.* **1985**, *17*, 23–41.
140. S. E. Fitzwater, K. S. Johnson, R. M. Gordon, K. H. Coale, W. O. Smith, Jr., *Deep Sea Research Part II: Topical Studies in Oceanography* **2000**, *47*, 3159–3179.
141. R. D. Frew, *Geophys. Res. Lett.* **1995**, *22*, 2349–2352.
142. R. D. Frew, K. A. Hunter, *Nature* **1992**, *360*, 144–146.
143. R. D. Frew, K. A. Hunter, *Marine Chem.* **1995**, *51*, 223–237.
144. K. A. Hunter, F. W. T. Ho, *Marine Chem.* **1991**, *33*, 279–298.
145. C. J. Jones, J. W. Murray, *Limnol. Oceanogr.* **1984**, *29*, 711–720.
146. G. A. Knauer, J. H. Martin, *J. Marine Res.* **1981**, *39*, 65–76.
147. J. H. Martin, R. M. Gordon, S. E. Fitzwater, *Nature* **1990**, *345*, 156–158.
148. J. H. Martin, S. E. Fitzwater, R. M. Gordon, C. N. Hunter, S. J. Tanner, *Deep-Sea Research Part II-Topical Studies in Oceanography* **1993**, *40*, 115–134.
149. N. H. Morley, P. J. Statham, J. D. Burton, *Deep Sea Res. I* **1993**, *40*, 1043–1062.
150. R. F. Nolting, H. J. W. d. Baar, *Marine Chem.* **1994**, *45*, 225–242.
151. R. F. Nolting, H. J. W. D. Baar, A. J. V. Bennekom, A. Masson, *Marine Chem.* **1991**, *35*, 219–243.
152. M. J. Orren, P. M. S. Monteiro, in *Antarctic Nutrient Cycles and Food Webs*, Eds W. R. Siegfried, P. R. Condy, R. M. Laws, Springer, New York, 1985, pp. 30–37.
153. S. Pai, H. Chen, *Marine Chem.* **1994**, *47*, 81–91.
154. P. M. Saager, H. J. W. Debaar, R. J. Howland, *Deep-Sea Research Part a-Oceanogr. Res. Papers* **1992**, *39*, 9–35.
155. P. M. Saager, H. J. W. de Baar, J. T. M. de Jong, R. F. Nolting, J. Schijf, *Marine Chem.* **1997**, *57*, 195–216.
156. C. M. Sakamoto-Arnold, A. K. Hanson, D. L. Huizenga, D. R. Kester, *J. Marine Res.* **1987**, *45*, 201–230.
157. S. Westerlund, P. Öhman, *Geochim. Cosmochim. Acta* **1991**, *55*, 2127–2146.
158. P. A. Yeats, *Sci. Total Envir.* **1988**, *72*, 131–149.
159. P. A. Yeats, J. A. Campbell, *Marine Chem.* **1983**, *12*, 43–58.
160. U. S. Geological Survey, in *Historical statistics for mineral and material commodities in the United States*, Eds T. D. Kelly, G. R. Matos, 2012, Vol. 140, pp. 36–37.

Chapter 3
Speciation of Cadmium in the Environment

Francesco Crea, Claudia Foti, Demetrio Milea, and Silvio Sammartano

Contents

ABSTRACT 63
1 INTRODUCTION 64
2 PRESENCE IN THE ENVIRONMENT 64
2.1 Anthropogenic Emissions 65
3 SPECIATION IN THE ATMOSPHERE 65
4 SPECIATION IN NATURAL WATERS 66
5 SPECIATION IN SOILS AND SEDIMENTS 69
5.1 The Soil Solution 70
6 CHEMICAL REACTIVITY TOWARDS DIFFERENT LIGAND CLASSES 71
6.1 Carboxylates, Amines, and Amino Acids 72
6.2 Complexones 73
6.3 Contributions of Other Functional Groups 74
6.4 General Considerations 75
6.4.1 Macrocycle/Chelate Effects and Enthalpic, Entropic Contributions 76
6.4.2 Other Empirical Correlations 77
7 CONCLUSIONS 78
ABBREVIATIONS 79
REFERENCES 80

Abstract This chapter reports an analysis of literature dedicated to the speciation of cadmium in various environmental compartments, i.e., atmosphere, natural waters, soils and sediments. The difficulty of the cadmium speciation studies, due to the variability of composition of different natural systems and to the low cadmium concentration in the environment, is highlighted. As an alternative approach, cadmium behavior is assessed by modelling its reactivity towards the main classes of ligands usually present in natural systems. The stability of cadmium complexes with

F. Crea • C. Foti • D. Milea • S. Sammartano (✉)
Department of Inorganic, Analytical and Physical Chemistry, University of Messina,
Viale F. Stagno d'Alcontres 31, I-98166 Messina, Italy
e-mail: fcrea@unime.it; cfoti@unime.it; dmilea@unime.it; ssammartano@unime.it

A. Sigel, H. Sigel, and R.K.O. Sigel (eds.), *Cadmium: From Toxicity to Essentiality*,
Metal Ions in Life Sciences 11, DOI 10.1007/978-94-007-5179-8_3,

various ligand classes is analyzed and modelled. Simple equations are proposed for the estimation of the stability of cadmium complexes with carboxylates, amines, amino acids, complexones, phosphates, phosphonates, and thiolates. The modelling ability of these equations is carefully analyzed. In addition, the sequestering ability of some ligands toward cadmium has been evaluated by the calculation of $pL_{0.5}$ (the total ligand concentration, as $-\log c_L$, able to bind 50% of a metal cation), an empirical parameter recently proposed for an objective "quantification" of this ability in defined conditions (pH, ionic strength, temperature, composition of solution).

Keywords aquatic environment • atmosphere • equilibrium constants • ligand classes • models • natural fluids • sediments • sequestering ability • soils • speciation analysis

1 Introduction

The environmental impact and the biological activity of cadmium, as well as other metals, organometals, and radionuclides, are strictly dependent on their speciation, unambiguously defined by IUPAC as the "distribution of an element amongst defined chemical species in a system" [1].

As already discussed in previous chapters, speciation plays an important role in cadmium toxicity and exposure to living organisms, influences its availability, accumulation, bio-modification, as well as its transport inside the organisms, and within and between environmental compartments too. That is why speciation studies are of fundamental importance to fully appreciate how this element behaves in the environment. Unfortunately, a careful analysis of literature dedicated to the speciation of cadmium reveals that this term is often abused and erroneously used, resulting in a consistent reduction of the papers really matching IUPAC recommendations and being effectively dedicated to cadmium speciation.

After a brief introduction on the presence and abundance of cadmium in various environmental compartments, this chapter will mainly focus on the distribution of cadmium species in the atmosphere, in aquatic environments and in soils and sediments. Owing to the different composition of these systems, in which a wide number of ligands and other metals is simultaneously present with cadmium, the stability of the species formed with different ligand classes will be carefully analyzed and modelled together with their sequestering ability.

2 Presence in the Environment

A detailed discussion on the presence of cadmium in the environment cannot be summarized in few words, and is outside the aims of this chapter. In fact, owing to the huge number of anthropogenic activities involving this element, its concentration in various systems is continuously monitored and, as a consequence, "available

literature on the exposure, pollution, and toxicology of cadmium is enormous and still growing" [2].

A comprehensive analysis of literature findings on these topics up to 2004 has been reported by Stoeppler [3] and Herber [2]. For this reason, more recent data will be mainly discussed in the next sections. For completeness, it must be mentioned here that natural cadmium occurrence is relatively low and variable, with concentrations ranging from few micrograms per kilogram in sea and river waters ($<0.01 - 0.1$ μg kg^{-1} [4]), to grams per kilogram ($1 - 12$ g kg^{-1} [2]) in zinc ores, the main cadmium sources. Its mean concentration in the continental and oceanic Earth's crust is 0.11 ± 0.02 (std. dev.) mg kg^{-1} [4]. Significant deviations from these values are observed in areas with intense anthropogenic activities.

2.1 Anthropogenic Emissions

Relatively high cadmium concentrations in the atmosphere, soils, and marine and fresh waters are observed close to urban or industrialized areas. Fortunately, though it is supposed that Cd emissions will increase in the near future in developing countries [2], they show a general decreasing annual trend. For example, Cd emissions have been reduced in the 27 member states of the European Community (EU-27) by 70% in the last 20 years (from 312 tons in 1990 to 94 tons in 2009) and by 10.8% from 2008 to 2009 [5]. The so called Key Categories [5] account for ~80% of total emissions (including 23.7% residential stationary plants, 14% stationary combustion in manufacturing industries and construction, 11% in public electricity and heat production), but the remaining 20% are mainly due to vehicular traffic (heavy and passenger transport), shipping, and/or combustion and incineration processes in various industrial fields [5].

Direct cadmium emissions to water arise from the chemical and metal industries, the transport sector, waste streams, and agriculture [6]. Of course, also the destiny of emissions to air is land and/or fresh and marine waters, where cadmium is washed from impervious surfaces, collected and directly or indirectly (via wastewater treatment plants) discharged to a receiving water [6].

3 Speciation in the Atmosphere

The atmospheric pollution by cadmium is a result both of natural and man-made activities, such as the combustion processes based on fossil fuels (in particular coal and oil) and the emission from processes in the pyro-metallurigical non-ferrous metal industries. The deposition, transport, and inhalation processes are controlled predominantly by the size of the atmospheric aerosols, so that the primary type of speciation of interest to atmospheric chemists is the metal size distribution. However, chemical speciation (in terms of the distribution of both the dissolved/particulate species and the inorganic/organic complexes) is important in governing

the catalytic behavior of metals in atmospheric reactions and their environmental impact.

From the data reported in the literature it generally appears that cadmium is predominantly contained in fine particles between 0.6 and 1.3 μm and in percentages up to ~60% [7,8], but there are cases where cadmium is contained in $PM_{2.5}$ (particulate matter, subscript refers to the dimension of the powder) and PM_{10} [9,10]. The concentration of cadmium in air was estimated ranging from 0.1 to 5 ng/m^3 in rural areas and from 2 to 15 ng/m^3 in urban areas, but in many cases it is up to 300 ng/m^3 in the major cities [11], and from 15 to 150 ng/m^3 in industrialized areas. There are cases [12] where the atmospheric cadmium concentration reached 5000 ng/m^3, one thousand times higher than admitted limits. Cadmium does not break down in the environment, but it may be affected by physical and chemical processes that change its mobility, bioavailability, and residence time in different environmental media. Atmospheric cadmium compounds, existing predominantly in fine particulate matter, are easily solubilized/removed from air by wet and dry deposition. Inorganic cadmium compounds, which primarily occur in particulate form in the atmosphere, have relatively short residence times (1 to 4 weeks) and low average concentrations (0.40 ng/m^3) and, since they do not absorb infrared radiation, they do not contribute to global climate change [13].

Cadmium produced during combustion processes or in the iron and steel manufacturing occurs in elemental [14] and oxide forms, often as mixed oxide with other metals; emissions from refuse incineration are dominantly as $CdCl_2$ [11]; CdS and $CdSO_4$ are present in dust emitted by lead smelter [8,15], or formed from coal combustion and non-ferrous metal production. In other cases, cadmium is present as Cd-aluminosilicates [16]. Recently, the speciation of cadmium was studied by using analytical tools such as XRD, EXAFS or ICP-AES and it resulted that, Cd often being associated with chloride, the formation of highly soluble compounds under the common environmental conditions is observed [17]. Organic complexation also plays an important role in the speciation of metal ions in the atmosphere [13], since the organic material (derived from anthropogenic combustion processes, biomass burning, biogenic emissions, marine emissions, and erosion of soil-based organic materials such as humic acids) represents about 20–50%, of aerosols [18–20], and rainwater [21], even if its composition is poorly known.

Since cadmium and many of its compounds are quite volatile, condensation on aerosols is common after the emission from high temperature processes. This leaves cadmium compounds condensed on the surface of particles which may increase the bioavailability [22].

4 Speciation in Natural Waters

Natural waters are multicomponent systems of highly variable composition. This section will be mainly focused on the interaction with inorganic and organic dissolved solutes. The soft character of Cd^{2+} implies a strong affinity towards soft

ligands (e.g., Cl^-), and a lower affinity towards hard (e.g., O-donor ligands, such as OH^-, CO_3^{2-} or some organic ligands). However, the relatively low concentration of cadmium in natural waters (from 0.01 to 0.1 μg kg^{-1} [4]) makes the direct determination of different chemical forms quite difficult. For this reason, a thermodynamic approach must be followed, since it proved very useful in predicting the metal distribution in different systems.

The interactions between Cd^{2+} and the main inorganic components of natural waters (OH^-, Cl^-, CO_3^{2-}, SO_4^{2-}, Br^- and F^-) are widely reported in the literature [23–25]. In two recent papers [26,27], literature data, together with new experimental ones, were analyzed and discussed in terms of Cd^{2+} speciation in natural waters. Powell et al. [26] provided a critical review of formation constants and related thermodynamic data and proposed recommended values at $I = 0$ mol kg^{-1} and $t = 25°C$, together with the empirical ion interaction parameters $\Delta\varepsilon$ for the dependence on ionic strength using the Brønsted–Guggenheim–Scatchard Specific ion Interaction Theory (SIT). According to the SIT equation [26], for the general reaction(1, 2) (charges omitted for simplicity) it holds:

$$pM + qL + rH_2O = M_pL_q(OH)_r + rH \tag{1}$$

$$\log\ \beta_{pqr} - \Delta z^2 D - r \log\ a_{(H_2O)} = \log\ \beta^0_{pqr} - \Delta\varepsilon I \tag{2}$$

where z is the charge and $\Delta z^2 = (pz_M + qz_L - r)^2 + r - p(z_M)^2 - q(z_L)^2$; D is the Debye-Hückel term; β_{pqr} and β^0_{pqr} are the stoichiometric formation constant and the formation constant at infinite dilution, respectively; $\Delta\varepsilon$ is the reaction specific ion interaction coefficient in a NX electrolyte, given by eq. (3):

$$\Delta\varepsilon = \varepsilon(\text{complex}, N^+ \text{ or } X^-) + r\ \varepsilon(H^+, X^-) - p\ \varepsilon(M^{n+}, X^-) - q\ \varepsilon(L^{m-}, N^+) \tag{3}$$

$\log \beta^0_{pqr}$ and $\Delta\varepsilon$ values for the major inorganic Cd^{2+} species are reported in Table 1 [26,27]. Other models can be also used for the modelling of the dependence of thermodynamic parameters on ionic strength. Some of them, like, e.g., the Pitzer model, have been widely used in speciation studies in natural fluids [28–30]. The application of these models to the equilibrium constants allows their calculation at the desired ionic strength values. As an example, in Table 1 the formation constants calculated at two different ionic strengths are reported, i.e., $I = 0.0015$ mol L^{-1} (typical of a fresh water) and $I = 0.67$ mol L^{-1} (typical of seawater). Knowing the equilibrium constants, one can examine the Cd^{2+} speciation in the different systems. (Figure 1a) shows the distribution of Cd^{2+} species at $I = 0.0015$ mol L^{-1}, considering the total concentrations of inorganic anions in a fresh water ($[Cl^-] = 0.23$, $[SO_4^{2-}] = 0.11$, $[CO_3^{2-}] = 0.9$ and $[F^-] = 0.005$ mmol L^{-1}) [31]. As an example, at pH = 9, 41.6% of Cd^{2+} is present as $CdCO_3$, 7% as $Cd(OH)^+$ and 49.3% is free ion Cd^{2+}. Other species (chloride, sulfate and fluoride complexes) are negligible with individually formation percentage <1%. At pH <7, almost all the

Table 1 Equilibrium constants for the formation of Cd^{2+} inorganic ligand complexes, at t = 25°C.

Reaction	log β^0_{pqr}	$\Delta\varepsilon$	log β_{pqr} $I = 0.0015^a$	log β_{pqr} $I = 0.67^a$	Ref.
$Cd^{2+} + H_2O = Cd(OH)^+ + H^+$	–9.80	–0.05	–9.85	–10.14	[26]
$Cd^{2+} + 2H_2O = Cd(OH)^0_2$	–20.19	–0.32	–20.23	–20.59	[26]
$Cd^{2+} + Cl^- = CdCl^+$	1.98	–0.14	1.90	1.33	[26]
$Cd^{2+} + 2Cl^- = CdCl^0_2$	2.63	–0.27	2.52	1.68	[26]
$Cd^{2+} + 3Cl^- = CdCl^-_3$	2.3	–0.40	2.19	1.45	[26]
$Cd^{2+} + Cl^- + H_2O = CdCl(OH)^0 + H^+$	–8.54	0.29[b]	–8.61	–9.09	[27]
$Cd^{2+} + CO^{2-}_3 = CdCO^0_3$	4.4	~0	4.25	2.72	[26]
$Cd^{2+} + SO^{2-}_4 = CdSO^0_4$	2.36	–0.09	2.21	0.93	[26]
$Cd^{2+} + Br^- = CdBr^+$	2.20	0.14	2.14	1.54	[c]
$Cd^{2+} + F^- = CdF^+$	1.37	0.12 [b]	1.29	0.72	[27]

[a] In mol L^{-1}.
[b] Calculated from ref. [27].
[c] Calculated from refs. [23,24].

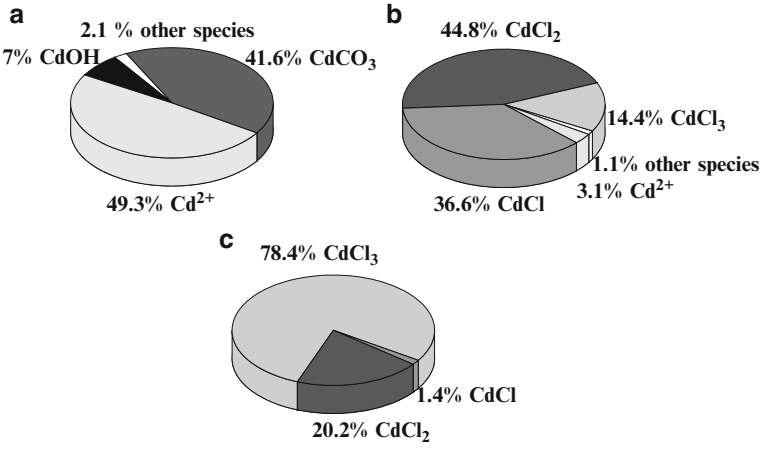

Figure 1 Distribution of inorganic Cd^{2+} species in different natural waters: (a) fresh water at pH = 9.0 and I = 0.0015 mol L^{-1}; (b) seawater at pH = 8.1 and I = 0.67 mol L^{-1}; (c) hypersaline water at pH = 6.4 and I = 6.3 mol L^{-1}.

cadmium is present as free cation Cd^{2+} with negligible amount (<1%) of $CdCl_i^{(2-i)}$ and $CdSO_4$ species. Considering the conditions of seawater (I = 0.67 mol L^{-1}, pH = 8.1, $[Cl^-]$ = 0.56 mol L^{-1}, $[SO^{2-}_4]$ = 0.029 mol L^{-1}, $[Br^-]$ = 0.0035 mol L^{-1}, $[HCO^-_3] + [CO^{2-}_3]$ = 0.2 mmol L^{-1} and $[F^-]$ = 0.07 mmol L^{-1} [32]), Cd^{2+} distribution is very different (Figure 1b), with a high formation percentage of chloride complexes and negligible amounts of other species. In particular, cadmium(II) is present for 44.8% as $CdCl_2$, 36.6% as $CdCl^+$, 14.4% as $CdCl^-_3$ and 3.1% as free Cd^{2+}. In hypersaline waters, such as that of the Dead Sea where the chloride concentration is very high (average $[Cl^-]$ = 6.58 mol kg^{-1} [33]), up to pH ~ 9 all the cadmium(II) is present as chloride complexes, with 78.4% of $CdCl^-_3$, 20.2% of $CdCl_2$, and 1.4 of $CdCl^+$ (Figure 1c).

To give a complete picture of Cd^{2+} speciation in natural waters, the complexing ability of dissolved organic matter (DOM) should be considered. The concentration of dissolved and particulate organic matter in natural water is less that 0.01% of the total amount of solids. DOM is a complex mixture of not well defined compounds: carbohydrates, amino acids, hydrocarbons, carboxylic acids, humic substances, and so on. The main percentage of DOM can be classified as dissolved organic carbon (DOC), which can bind trace metals and modify the speciation profile. The conditional formation constant for Cd(DOC) complex has been determined in different natural waters. Christensen and Christensen [34] report log K values ranging from 4.28 to 5.10 in ground water samples; Saar and Weber [35] derived for river water fulvic acid stability constants ranging from 3.13 to 4.08; Xue and Sigg [36] report in different fresh waters (lake, river and ground waters) for the Cd-natural organic ligand complex $8.2 \leq \log K \leq 10.2$; Ellwood [37] reports for subantartic water log K values ranging from 9.82 to 10.93. The variability of these data is probably due to the different nature of the organic matter involved in the complexation equilibria. In this light, it can be very useful to know the contribution of single functional groups to the overall stability of various species: this aspect will be better detailed in Section 6.

5 Speciation in Soils and Sediments

As is known, soil consists of a mixture of weathered minerals and varying amounts of organic matter. In soils and sediments, cadmium and other metals are present in a number of chemical forms dependent on the characteristic of the matrix. Typically, metals are relatively immobile in subsurface systems and are retained in the solid phase by different mechanisms (ion exchange, outer- and innersphere surface complexation/adsorption, precipitation or co-precipitation) [38].

Since reliable direct methods for the determination of cadmium speciation in the solid material do not exist, the methods based on the extraction of element species appears to be the more adequate, even if the metals' speciation often undergoes significant variation. Different sequential extraction methods were proposed [39–42], but the most used is that proposed by the European Standard, Measurements and Testing (SM&T) program, formerly the Community Bureau of Reference (BCR) [39,40,43–48]. Following the BCR procedure, the particulate-bound metal content was divided into several fractions. The *acid soluble fraction* includes exchangeable and carbonate phases and is the most variable because it is sensitive to pH changes. In the *reducible fraction*, the metals are bonded to Fe-Mn oxides. The percentage of this fraction is relatively high and represents a large portion of the non-residual metal. In the *oxidizable fraction* the metals are bound to organic matter and sulfur, and would be re-released under oxidative conditions. The organic fraction released in this step is hardly considered very mobile or available, since the metals associated with stable high-molecular-weight humic substances decompose slowly. The *residual fraction* contains chemically stable and biologically inactive metals. The greater

the percentage of metals in this fraction, the smaller the environmental risk is because this portion of the metals cannot be re-released to water under normal conditions [49–52].

Increasing the pH of soils rich in hydrous oxides and kaolinite, the total percentage of Cd ('% Cd') bound to hydrous oxides increases, whilst at lower pH values the exchangeable cadmium increases. In lateritic podzol (containing mainly kaolinite), pH increments from 4 to 5 result in an increase of % Cd in the exchangeable form, the major Cd form present. The quantity of exchangeable Cd decreases at higher pH values because the metal can be adsorbed onto sites that are less accessible and could be displaced only by acid extraction. Increasing the pH of a sandy soil increases exchangeable Cd *versus* soluble Cd. The higher the Cd amount in soil, the smaller is the decrease in soluble Cd because of a lack of cation exchange sites.

Speciation studies are important to assess the availability of the metal ions towards plants. For example, soils containing hydrous oxides at pH ~5.0 would have a low risk of contaminating waterways, but may not be able to supply cationic micronutrients for adequate plant growth [53]. In fact, at lower pH values, organic matter appears to be the only solid phase component capable of retaining trace metal ions, so that cadmium present in soluble and exchangeable form decreases drastically [11,54,55]. Speciation of trace elements may also vary with time, depending on the solid-phase components present, on pH, and on the number and accessibility of adsorption sites [55–57]. Both in the past and recently, a lot of papers on the speciation of cadmium in soils and sediments of different parts of the world have been published, and from the results reported it is evident that the distribution and speciation of cadmium changes significantly between the different sites, in dependence of the chemical and physical characteristics of the natural matrices, so that comparison between the different results are very difficult to make. A statistical data analysis showed that the two "exchangeable cadmium" and the "metal-fulvic acid-complex-bound cadmium" fractions represented the plant-available cadmium fractions to a great extent [51,58–65].

5.1 The Soil Solution

The soil solution acts as a link between solid soil phases and the other components of an ecosystem involved in biogeochemical cycling and is the medium through which the dissolved species are transported to the other environmental compartments [50,65–67]. Soil solutions contain both inorganic and organic (siderophores and carboxylic acids) low molecular weight ligands, as well as heterogeneous compounds of unknown structure with molecular weight ranging from 10^3–10^7 Da, whose amount in the speciation studies was determined by indirect methods including titratable acidity [68] or measuring dissolved organic carbon [69].

In soil solutions, the main speciation methods are based on dialysis and ion exchange [61,70]. Different chromatographic methods such as exclusion, reversed-phase HPLC and ion exchange chromatography were used to identify the

various species of cadmium [71]. From ion-exchange chromatographic analysis, cadmium was found to be present as inorganic cationic species including the free Cd^{2+}, though a significant cadmium amount is also present as organic and inorganic neutral species (e.g., $Cd(OH)_2$) [64], especially in soils with high pH [54,60,65,66,72,73]. Similar results were obtained by using other techniques such as the combination of the Donnan equilibrium and graphite furnace AAS methods [74] or DPASV [75], assuming that DPASV was sensitive to easily dissociated inorganic ion pairs and free Cd^{2+} ions, excluding organic complexes [76]. Some authors [63] found that Cd^{2+} ions were predominantly bound to the oxygen-containing functional groups of the fulvic acids investigated using ^{113}Cd NMR spectroscopy. These results are environmentally important because soil and aquatic fulvic acids affect the bioavailability and transport of metal ions [63].

Among the various sources of cadmium contamination are the plating operations and the disposal of cadmium-containing wastes. In these cases, the forms of cadmium also depend on the treatment of the waste prior to disposal. The most common forms include Cd^{2+}, cadmium-cyanide complexes, or $Cd(OH)_2$ solid sludge. Hydroxide ($Cd(OH)_2$) and carbonate ($CdCO_3$) solids dominate at high pH, whereas Cd^{2+} and aqueous sulfate species are the dominant cadmium forms at pH <8. Under reducing conditions, when sulfide is present, the stable solid $CdS_{(s)}$ is formed. Cadmium also precipitates in the presence of phosphate, arsenate, chromate, and other anions, although solubility will vary with pH and other chemical factors [77]. The free Cd^{2+} appears to be the form readily taken up by plants, whereas $CdCl^+$ is taken up more slowly, while Cd-humate is not adsorbed.

6 Chemical Reactivity towards Different Ligand Classes

Most of the properties of cadmium depend on its chemical reactivity in natural waters and biological fluids that, from a chemico-physical perspective, can be considered as multicomponent aqueous solutions, in which a wide number of organic and inorganic ligands, as well as other metal and organometal cations, are simultaneously present. Therefore, the knowledge of cadmium speciation in these systems is of fundamental importance, though their variability in composition makes speciation studies very difficult. From this point of view, owing to the objective impossibility of measuring all interactions of cadmium with all components of real systems, modelling studies are very useful. In this light, cadmium behavior in natural waters and biological fluids can be assessed by modelling its reactivity towards the main classes of ligands usually present in natural systems, of both natural origin or derived from anthropogenic activities.

The stability constants of cadmium complexes with various ligand classes available in the literature and in main databases (e.g., [23–25]) were analyzed and modelled here. In particular, the formation of $CdL_i^{(2+iz)}$ species was considered, according to equilibrium (4)

$$Cd^{2+} + iL^z = CdL_i^{(2+iz)} \qquad \beta_i \tag{4}$$

Due to their wide availability in the literature, the stability constant values analyzed here were those reported at $I = 0.1$ mol L^{-1} and t = 25°C or, where possible, those recalculated at these temperature and ionic strength values by common equations (see, e.g., Section 4 for the SIT model). Precision on fitted values is always reported as ± 95% confidence interval.

6.1 Carboxylates, Amines, and Amino Acids

For several different reasons, carboxylic acids, amines, and amino acids can be certainly rated among the most important organic ligand classes. Moreover, polyfunctional ligands (including organic matter) often contain in their structures carboxylic and/or amino groups in addition to others. As a consequence, it is useful to begin any modelling process from these three classes.

From the analysis of published stability constants of various cadmium complexes with low molecular weight carboxylates (excluding oxalate and carboxylates with linear alkyl chains longer than 7 methyl groups, which show peculiar properties), their values can be expressed by a simple function (eq. 5) that takes into account both the number of carboxylic groups of the ligand (n_{COOH}) and the number of ligands in the complex (i):

$$\log \beta_i = 1.40\ n_{COOH} - i(0.31\ n_{COOH} - 0.27) \tag{5}$$

with an estimated precision of log $\beta_i \pm 0.2$. The modelling ability of this equation is quite satisfactory: mean literature values for log β_i are 1.49 ± 0.09 and 2.45 ± 0.07 for mono- and dicarboxylates, respectively, while those calculated by eq. (5) resulted in 1.4 ± 0.1 and 2.46 ± 0.10. Another proof of the modelling ability of eq. (5) is represented by the estimation of log β_1 of some high-molecular-weight polycarboxylates (e.g., polyacrylic and polymethacrylic acids of different MW), on the basis of the "diprotic-like" model [78]: the mean literature [78] value for the CdL species is log $\beta_1 = 4.3 \pm 0.3$, that calculated by eq. (5) is log $\beta_1 = 4.6 \pm 0.3$.

The same kind of relationship of carboxylates was found for ammonia, amines, and low-molecular-weight polyamines (eq. 6).

$$\log \beta_i = 3.11\ n_N - i(0.33\ n_N + 0.26) \tag{6}$$

where n_N represents the number of amino groups. Also in this case, the estimated precision is log $\beta_i \pm 0.2$. For ammonia and linear amines of the series $C_{2i-2}N_iH_{5i-2}$ (with $1 \leq i \leq 5$), a simpler equation with higher precision (± 0.02) was found for the ML species, log $\beta_1 = 2.72\ n_N$. In this case, it is interesting to note that this value is, within the estimated precision, equivalent to the stability constant value estimated for cadmium complexes with N-alkylamino sugars, i.e., log $\beta = 2.78\ n_N$, which preferentially bind cadmium via the amino groups [79].

As expected, the best relationship for the modelling of the stability of various cadmium/amino acid complexes (not only α-amino acids) is a sort of combination of the equations used for the modelling of carboxylate and amine species, in which the contribution of both kinds of functional groups is taken into account (eq. 7):

$$\log\ \beta_i = 1.54\ n_{COOH} + 3.11\ n_N - i(0.23\ n_{COOH} + 0.34\ n_N + 0.13) \qquad (7)$$

with a precision of log $\beta_i \pm 0.4$. For the simplest amino acids with only one carboxylic and one amino group, the fact is worth mentioning that the stability of the CdL species is almost constant, i.e., log $\beta_1 = 3.85 \pm 0.09$. This value is in excellent agreement with that calculated by eq. (7), i.e., log $\beta_1 = 3.95$, as a confirmation of the good modelling ability of this kind of equations.

6.2 Complexones

As is well known, several ligands with very different functional groups are classified under this general name, and new ones are continuously synthesized and used as chelating agents. For simplicity, only the most common polyaminopolycarboxylates were considered here: NTA (nitrilotriacetate), EDTA (ethylenediamine-N,N,N',N'-tetraacetate), DTPA (diethylenetriamine-N,N,N',N",N"-pentaacetate), TTHA (triethylenetetraamine-N,N,N',N",N"',N"'-hexaacetate), EGTA (ethylene glycol-bis(2-aminoethylether)-N,N,N',N'-tetraacetate), EDDA (ethylenediamine-N,N'-diacetate). These ligands cannot be considered as simple polyaminoacids and, therefore, the stability of their complexes with cadmium cannot be modelled by eq. (7). The main reason of this behavior is the increased stability of their metal complexes, due to the macrocycle effect [80]. In this case, a satisfactory modelling ability (log $\beta_1 \pm 1$) of the stability of the CdL species of complexones was obtained by equation (8):

$$\log\ \beta_1 = 4.21\ n_{COOH} + 1.41\ n_N - 0.47\ n_{COOH}\ n_N \qquad (8)$$

In the case of the homologues of the series $(CH_2)_{2i-2}N_i(CH_2COOH)_{i+2}$ (i.e., NTA, EDTA, DTPA, TTHA with $1 \leq i \leq 4$), better results (with a precision log $\beta_1 \pm 0.4$) were obtained by equation (9):

$$\log\ \beta_1 = 1.31\ n_{COOH} + 8.19\ n_N - 1.35\ n^2{}_N \qquad (9)$$

Other important complexones, such as polyaminopolyphosphonic ligands, cannot be modelled alone in the same way, since available literature data on their cadmium complexes are not sufficient to propose a reliable model.

6.3 Contributions of Other Functional Groups

Several ligands may have other functional groups than carboxylic and/or amino groups. Modelling their behavior is not particularly difficult if one takes into account that, except for particular effects, the contribution of single functional groups to the overall stability are often additive [81,82]. In analogy with previous equations for carboxylic and amino groups, these contributions can be expressed in terms of $<\log \beta>$ of single functional groups. Only for ligands with one kind of functional groups $<\log \beta>$ would be equivalent to the real stability constant of the cadmium complex, otherwise the latter should be calculated as the summation of the contributions of all single groups of the ligand.

In the case of ligands containing phosphoric groups (n_P), including simple phosphates and nucleotides, their contribution to the stability of cadmium complexes, $<\log \beta>$, is given by equation (10):

$$<\log\ \beta> = 2.88\ n_P - 0.38\ n^2{}_P \tag{10}$$

with a precision of $<\log \beta> \pm 0.14$. Since it is known that nucleotides interact with cadmium also via the nitrogens of their nucleobases (e.g., via N7 for adenosine, see Chapter 8 of this book), the stability constants of cadmium/nucleotide complexes were modelled alone, in order to take also into account this contribution to the stability of the CdL species that, of course, cannot be assimilated to that of an amino group. Similar results were obtained by the same kind of relationship found for all phosphates together (eq 11):

$$<\log\ \beta> = 2.99\ n_P - 0.43\ n^2{}_P \tag{11}$$

Estimated precision is the same as of eq. (10), i.e., $<\log \beta> \pm 0.16$, but, as expected, the coefficients are slightly higher and reflect the extra-contribution of the nucleobase/cadmium interaction to the overall stability of CdL species.

Being often considered as a separate class, phosphonic ligands were analyzed alone. A satisfactory modelling ability has been obtained for the contribution of single phosphonic groups to the stability of cadmium/phosphonate complexes, by using the following equation (12) that, in analogy with some other classes, takes also into account the number of ligands (i) forming the complex:

$$<\log\ \beta_i> = 4.52\ n_P - i(1.95\ n_P - 1.43) \tag{12}$$

with a precision of $\log \beta_i \pm 0.9$.

Another class of ligands considered here was that of thiols and, in general, of ligands containing S-donor groups. Though their abundance in natural systems is generally lower than that of other simple O- and N-donor ligands, they could be of some importance if one takes into account the soft nature of cadmium and its affinity toward sulfur. The literature data analysis on Cd/thiol complexes evidenced

a great dispersion of available data, indicating that further and more accurate studies are necessary in this field. As a direct consequence of these discrepancies, estimated precision on the modelling of the contribution of S-donor groups to the stability of Cd/L species was only moderately satisfactory, i.e., $<\log \beta> \pm 1$, for equation (13):

$$<\log\ \beta_i> = 6.58\ n_{SH} - i(0.31\ n_S - 0.58) \tag{13}$$

Finally, worth mentioning is the contribution of hydroxo groups eventually present in the structure of some ligands such as, for example, hydroxocarboxylic acids. It is well known that these ligands very often form stable hydroxo complexes of the kind $M_pH_{-q}L_r$ (e.g., citrate forms the $Cd_2(OH)_2\ L_2$ species [83]). The stoichiometry of these complexes is due to the deprotonation of the hydroxo group of the ligand and not to the hydrolysis of the metal cation (though the two kind of complexes are stoichiometrically equivalent, see, e.g., ref. [83]). As a consequence, the deprotonated hydroxo group is able to give a strong contribution to the metal complexation (probably thanks to the formation of very stable chelate rings). In the case of cadmium hydroxocarboxylate species, this contribution is $<\log\ \beta_i> \sim 6n_{O^-}$, where n_{O^-} is the number of deprotonated hydroxo groups participating in the formation of the cadmium complex.

6.4 General Considerations

Relationships reported above for various ligand classes need some further comments of general validity. A very important factor to be considered in evaluating the reliability of these relationships concerns the precision (i.e., the confidence interval) of values calculated by the equations proposed. Errors associated range from $\log \beta \pm 0.14$ to $\log \beta \pm 1$ and may appear quite high. However, they are reasonable if (i) the origin of these relationships and (ii) the scope of their formulation are kept in mind. These equations were derived by the refinement of a huge number of stability constants of "different" ligands, determined by "different" groups, using "different" techniques, in "different" conditions, or adjusted to the desired ionic strength and temperature by "different" models. However, though the experimental determination of accurate stability constants is always highly encouraged, what is stated at the beginning of this Section is also clear: measuring all interactions of cadmium with all components of real systems is objectively impossible. That is why a rough but immediate estimation of these data is of key importance, especially for the modelling of the interactions of cadmium with organic matter in natural systems. The equations reported above can therefore be used for the estimation of the stability of cadmium complexes with most of the ligands containing one or more of the analyzed functional groups. Basically, this is possible thanks to the above cited additivity properties: contributions calculated by these equations for all the functional groups of the considered ligand should be simply summed to estimate the

value of the overall stability constant of the CdL_i complex. Of course, this estimation may be more or less accurate, and sometimes the structural complexity of a given ligand or other factors may lead to peculiar behaviors. This is the case, for example, for phytic acid [1,2,3,4,5,6-hexakis(dihydrogen phosphate) *myo*-inositol]: the stability of its cadmium complexes [84–86] cannot be estimated accurately by the simple sum of the contributions of six phosphoric functions, since the fact that these groups are forced to some particular conformations by the cyclohexane ring of inositol alters all phytate solution properties [87]. In other cases, however, these relationships may be fairly accurate. In fact, as a general rule, the chemico-physical properties of homogeneous series of ligands follow regular trends, resulting in both the formulations of simple empirical relationships and high modelling abilities. This is also the case of the stability of cadmium complexes where, for example, simpler equations and higher precisions were obtained for the amines of the series $C_{2i-2}N_iH_{5i-2}$ than for the modelling of all amines. Analogously, lower errors are associated with the estimation of the stability of CdL species of complexones of the series $(CH_2)_{2i-2}N_i(CH_2COOH)_{i+2}$ by the dedicated eq. (9) than by the general equation for all complexones (eq. 8).

6.4.1 Macrocycle/Chelate Effects and Enthalpic, Entropic Contributions

Concerning the above cited peculiarities of some ligands and the factors responsible for the deviations from the additivity, the macrocycle effect has already been mentioned in the case of complexones. An estimation of the contribution of this effect to the stability of cadmium/complexone species can be roughly obtained by the comparison of values calculated for these ligands alternatively by eq. (8) (specific for complexones) and eq. (7) for generic amino acids: for example, in the case of EDTA, this difference is ~5.3 log units in favor of log β by eq. (8). It is important to note that this value is only referred to the macrocycle effect. In fact, it does not include the contribution of the analogue chelate effect, which is already taken into account in eq. (7) (and in similar equations for other ligand classes), and may be approximately associated for cadmium complexes to the difference between the stability of the CdL species of any n-functional ligand and that of the CdL_i species (with $i = n$) of the monofunctional analogue. This "extra contribution" is quantified in the proposed relationships by the term in "i" of the kind (where a and b are empirical parameters and n is the number of functional groups):

$$i(a\ n + b) \tag{14}$$

In the case, for example, of carboxylates (eq. 5), the contribution of the chelate effect to the stability of a dicarboxylate/cadmium species is $(0.31 \times 2 - 0.27) = 0.35$. The same considerations hold for the chelate effect of amines (eq. 6), i.e., $(0.33 \times 2 + 0.26) = 0.92$.

It is also well known that both the chelate and macrocycle effects are entropic in nature. As an indirect demonstration, the analysis of available literature formation

enthalpy changes of CdL_i complexes showed that, at least for carboxylic, aminic, and phosphonic ligands, there is a constant and additive enthalpic contribution per kind and number of functional groups of the ligand, so that:

$$\Delta H \ (\text{kJ mol}^{-1}) = 2.7 \ n_{COOH} - 18.4 \ n_N - 3.3 \ n_P \tag{15}$$

Eq. (15) may be also exploited to derive the formation enthalpy changes of various CdL_i complexes and, therefore, to estimate with sufficient accuracy the stability of these species at other temperatures than t = 25°C by the van't Hoff equation.

6.4.2 Other Empirical Correlations

Finally, a last broad consideration: in our opinion, the approach of the "additivity factors" is very useful and has a lot of advantages. However, another interesting and successful procedure is represented by the formulation of empirical relationships between the stability of some CdL species and that of other metals, whose stability constants of analogue complexes are often more abundant in the literature. In fact, the ratio between the number of available stability constants of metal/ligand complexes of zinc and cadmium is approximately n_{ZnL}: $n_{CdL} = 1.2$, and is even high for copper (n_{CuL}: $n_{CdL} = 1.4$) and nickel (n_{NiL}: $n_{CdL} = 1.5$). Being in the same group of the periodic table, we made some attempts of correlating the stability of cadmium/ligand complexes with that of zinc. Considering the available data of Cd and Zn, we obtained an excellent linear correlation (±0.01) (eq. 16):

$$\log \ \beta_{CdL} = 0.98 \ \log \ \beta_{ZnL} \tag{16}$$

For the single ligand classes, in the case of carboxylates, amines, and amino acids, we found:

$$\log \ \beta_{CdL} = (0.899 \pm 0.008) \ \log \ \beta_{ZnL} \quad \text{for carboxylates}$$
$$\log \ \beta_{CdL} = (0.914 \pm 0.007) \ \log \ \beta_{ZnL} \quad \text{for amines}$$
$$\log \ \beta_{CdL} = (0.85 \pm 0.01) \ \log \ \beta_{ZnL} \quad \text{for amino acids}$$

For other ligands, in analogy with the previous approach, it is also possible to estimate the contribution (<log β>) of single functional groups to the overall stability of a given cadmium/ligand complex, by the following relationships:

$$<\log \ \beta_{CdL}> = (0.86 \pm 0.02) <\log \ \beta_{ZnL}> \quad \text{for phosphonates}$$
$$<\log \ \beta_{CdL}> = (1.04 \pm 0.01) <\log \ \beta_{ZnL}> \quad \text{for phosphates + nucleotides}$$
$$<\log \ \beta_{CdL}> = (1.000 \pm 0.004) <\log \ \beta_{ZnL}> \quad \text{for complexones}$$
$$<\log \ \beta_{CdL}> = (1.19 \pm 0.03) <\log \ \beta_{ZnL}> \quad \text{for thiols}$$

7 Conclusions

The speciation of cadmium in various environmental compartments, i.e., atmosphere, soils and sediments, and natural waters, has been summarized in this chapter.

In the atmosphere, cadmium is present as a result of both natural and man-made activities, mainly in finer particles. It mainly occurs in various inorganic forms, though organic complexation may play important roles in some cases. In the natural waters, cadmium is mainly present as chloride and/or carbonate species, though the presence of organic ligands may influence its speciation. In soils and sediments, including soil solutions, cadmium speciation is deeply affected by the characteristic of the matrix.

Considering the complexity of natural systems, it can be very useful to know the contribution of single functional groups. In this light, the reactivity of cadmium toward the main classes of ligands present in natural systems was modelled by some empirical equations. However, the simple analysis of single sets of stability constants of metal/ligand complexes is not always sufficient to assess the global binding (sequestering) ability of a ligand toward a given cation (cadmium in our case) in real conditions, owing to the difficulties regarding, for example, the different number and/or nature of complexes formed by single ligands. Moreover, other factors influence the formation yields of the species, such as the solution conditions, the acid–base properties of the ligand (since both the cadmium hydrolysis and the protonation reactions are competitive with respect to the formation reaction), the competition between other metals and ligands simultaneously present in natural systems. Because of this, two cadmium ligand systems may show the same formation percentages (in given conditions), even with different formation constants. This problem can be overcome by the calculation of $pL_{0.5}$ (also called pL_{50}) an empirical parameter that, once the experimental conditions (ionic strength, ionic medium, temperature, pH, and metal concentration) are fixed, can give an objective representation of the sequestering ability of a ligand (L) towards a metal ion (M). A detailed description of the method is given, e.g., in [88]. Briefly, the mole fraction (x) of a generic metal ion M (present in traces) complexed by a generic ligand L may be expressed as a function of pL, where $pL \equiv -\log c_L$ with c_L = total ligand concentration. This function is represented by a sigmoid curve (similar to a dose–response curve), with asymptotes of 1 for $pL \rightarrow -\infty$ and 0 for $pL \rightarrow +\infty$ (eq. 17):

$$x = \frac{1}{1 + 10^{(pL - pL_{0.5})}} \tag{17}$$

where the parameter $pL_{0.5}$ represents the total ligand concentration necessary to sequester 50% of the metal ion. Therefore, the higher the $pL_{0.5}$, the higher the sequestering ability is. The $pL_{0.5}$ is very useful because it gives a measure of the binding ability of a ligand towards a cation, in the conditions investigated. Worth mentioning is that in the calculation of $pL_{0.5}$, all the side interactions occurring in the system (metal hydrolysis, ligand protonation, interactions with other

components) are taken into account in the speciation model, but are excluded from estimation of $pL_{0.5}$ and do not make any contribution. In this way, the $pL_{0.5}$ value quantifies the sequestering power of a ligand, "cleaned" from all competitive reactions, simplifying comparisons. As an example, the total fraction x of cadmium complexed by HEDPA (1-hydroxyethane-1,1-diphosphonic acid), PSH (penicillamine), GSH (glutathione), and EDTA is shown in Figure 2 at pH = 8.1. The sequestering ability of the three ligands is very different, with $pL_{0.5}$ values varying (at $I = 0.1$ mol L^{-1} and t = 25°C) from 5.5 for HEDPA, to 8.5 for PSH and GSH, and to 12.5 for EDTA.

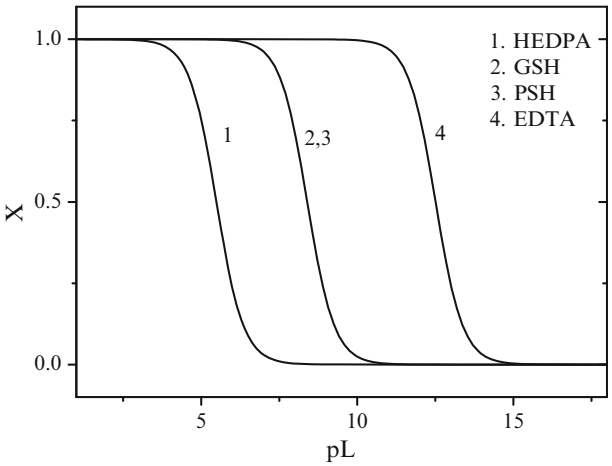

Figure 2 Sequestering ability of HEDTPA, PSH, GSH, and EDTA towards Cd^{2+}, at $I = 0.1$ mol L^{-1} and t = 25°C.

As reported elsewhere [89], "...for given experimental conditions, the $pL_{0.5}$ parameter allows one to compare the sequestering ability of different ligands towards one or more metal ions and to quantify the strength of the interaction of metal-ligand systems having quite different speciation models, independently of the type of complexes formed, so that this method was successfully used to analyze the binding ability of various ligands towards different metal ions, as well as towards polyammonium cations and anions...", and can be successfully applied to cadmium data too.

Abbreviations

BCR	Community Bureau of References
DOC	dissolved organic carbon
DOM	dissolved organic matter
DPASV	differential pulse anodic stripping voltammetry
DTPA	diethylenetriamine-N,N,N',N",N"-pentaacetate

EDDA	ethylenediamine-N,N'-diacetate
EDTA	ethylenediamine-N,N,N',N'-tetraacetate
EGTA	ethyleneglycol-bis(2-aminoethylether)-N,N,N',N'-tetraacetate
EXAFS	extended X-ray absorption fine structure
GSH	glutathione
HEDPA	1-hydroxyethane-1,1-diphosphonic acid
HPLC	high performance liquid chromatography
ICP-AES	inductively coupled plasma atomic emission spectroscopy
MW	molecular weight
NMR	nuclear magnetic resonance
NTA	nitrilotriacetate
$PM_{2.5/10}$	particulate matter (subscripts refer to the dimension of the powder, expressed in micrometer)
PSH	penicillamine
SIT	Specific ion Interaction Theory
SM&T	European Standard, Measurements and Testing program
std. dev.	standard deviation
TTHA	triethylenetetramine-N,N,N',N'',N''',N'''-hexaacetate
XRD	X-ray diffraction

References

1. D. M. Templeton, F. Ariese, R. Cornelis, L. G. Danielsson, H. Muntau, H. P. van Leeuwen, R. Lobinski, *Pure Appl. Chem.* **2000**, *72*, 1453-1470.
2. R. F. M. Herber, in *Elements and their Compounds in the Environment*, 2nd ed, Eds E. Merian, M. Anke, M. Ihnat, M. Stoeppler, Wiley-VCH Verlag GmbH & Co. KGaA, Weinheim, 2004, pp. 689–708.
3. M. Stoeppler, in *Metals and Their Compounds in the Environment*, Ed E. Merian, VCH, Weinheim, Germany, 1991, pp. 803–851.
4. K. H. Wedepohl, in *Elements and their Compounds in the Environment*, 2nd ed, Eds E. Merian, M. Anke, M. Ihnat, M. Stoeppler, Wiley-VCH Verlag GmbH & Co. KGaA, Weinheim, 2004, pp. 3–16.
5. "European Union emission inventory report 1990–2009 under the UNECE Convention on Long-range Transboundary Air Pollution (LRTAP) - Technical report No. 9/2011", European Environment Agency, Copenhagen, 2011.
6. "Hazardous substances in Europes's fresh and marine waters - Technical report No. 8/2011", European Environment Agency, Copenhagen, 2011.
7. F. Fernàndez Alvarez, M. Ternero Rodrìguez, A. J. Fernàndez Espinosa, A. Gutiérrez Dabàn, *Anal. Chim. Acta* **2004**, *524*, 33–40.
8. Y. Batonneau, C. Bremard, L. Gengembre, J. Laureyns, A. Le Maguer, D. Le Maguer, E. Perdrix, S. Sobanska, *Environ. Sci. Technol.* **2004**, *38*, 5281–5289.
9. B. Wojas, C. Almquist, *Atmos. Environ.* **2007**, *41*, 9064–9078.
10. A. Kuvarega, P. Taru, *Environ. Monit. Assess.* **2008**, *144*, 1–14.
11. J. Hlavay, K. Polyak, M. Weisz, *J. Environ. Monit.* **2001**, *3*, 74–80.
12. Y. Noack, M. Lefloch, D. Robin, "Environmental impact of a cadmium atmospheric pollution at Marseille (South France)", *Proceedings of the Journal de Physique IV: (XIIth International Conference on Heavy Mateals in the Environment)*, France, 2003, pp. 961–964.

13. L. J. Spokes, T. D. Jickells, in *Chemical Speciation in the Environment*, Blackwell Science Ltd, 2002, pp. 159–187.
14. L. Gandois, E. Tipping, C. Dumat, A. Probst, *Atmos. Environ.* **2010**, *44*, 824–833.
15. S. Sobanska, N. Ricq, A. Laboudigue, R. Guillermo, C. Brémard, J. Laureyns, J. C. Merlin, J. P. Wignacourt, *Environ. Sci. Technol.* **1999**, *33*, 1334–1339.
16. A. Profumo, G. Spini, L. Cucca, E. Zecca, *Talanta* **1998**, *47*, 605–612.
17. M. L. Sammut, Y. Noack, J. Rose, J. L. Hazemann, O. Proux, M. Depoux, A. Ziebel, E. Fiani, *Chemosphere* **2010**, *78*, 445–450.
18. P. S. Gill, T. E. Graedel, C. J. Weschler, *Rev. Geophys.* **1983**, *21*, 903–920.
19. P. Saxena, L. M. Hildemann, *J. Atmos. Chem.* **1996**, *24*, 57–109.
20. P. Saxena, L. M. Hildemann, P. H. McMurry, J. H. Seinfeld, *J. Geophys. Res.* **1995**, *100*, 18755–18770.
21. M. Nimmo, G. R. Fones, *Atmos. Environ.* **1997**, *31*, 693–702.
22. J. O. Nriagu, in *Cadmium in the Environment, Part 1, Ecological Cycling*, Ed. J. O. Nriagu, John Wiley and Sons, New York, 1980, pp. 71–114.
23. L. Pettit, K. J. Powell, in "The IUPAC Stability Constants Database", 2001.
24. A. E. Martell, R. M. Smith, R. J. Motekaitis, in "Critically Selected Stability Constants of Metal Complexes. National Institute of Standard and Technology, NIST", Gaithersburg, 2004.
25. P. M. May, D. Rowland, E. Königsberger, G. Hefter, *Talanta* **2010**, *81*, 142–148.
26. K. J. Powell, P. L. Brown, R. H. Byrne, T. Gajda, G. Hefter, A. Leuz, S. Sjöberg, H. Wanner, *Pure Appl. Chem.* **2011**, *83*, 1163–1214.
27. C. Foti, G. Lando, F. J. Millero, S. Sammartano, *Environ. Chem.* **2011**, *8*, 320–331.
28. K. S. Pitzer, *Activity Coefficients in Electrolyte Solutions,* 2nd ed, Ed K. S. Pitzer, CRC Press, Inc., Boca Raton, FL, 1991.
29. I. Grenthe, I. Puigdomenech, *Modelling in Aquatic Chemistry*, Eds I. Grenthe, I. Puigdomenech, OECD, Paris, 1997.
30. F. J. Millero, *Physical Chemistry of Natural Waters*, John Wiley & Sons, Inc., New York, 2001.
31. J. Buffle, *Complexation Reactions in Aquatic Systems: An Analytical Approach*, Ellis Horwood, Chichester, 1988.
32. F. J. Millero, in *Chemistry of Marine Waters and Sediments*, Eds A. Gianguzza, E. Pelizzetti, S. Sammartano, Springer-Verlag, Berlin, 2002, pp. 3–34.
33. B. S. Krumgalz, F. J. Millero, *Mar. Chem.* **1982**, *11*, 209–222.
34. J. B. Christensen, T. H. Christensen, *Water Res.* **2000**, *34*, 3743–3754.
35. R. A. Saar, J. H. Weber, *Can. J. Chem.* **1979**, *57*, 1263–1268.
36. H. Xue, L. Sigg, *Anal. Chim. Acta* **1998**, *363*, 249–259.
37. M. J. Ellwood, *Mar. Chem.* **2004**, *87*, 37–58.
38. G. S. P. Ritchie, G. Sposito, in *Chemical Speciation in the Environment*, Eds A. M. Ure, C. M. Davidson, Blackwell Science, Glasgow, 2002, pp. 237–264.
39. M. Kersten, U. Förstner, *Water Sci. Technol.* **1986**, *18*, 121–130.
40. K. Nemati, N. K. A. Bakar, M. R. Abas, E. Sobhanzadeh, *J. Hazard Mater.* **2011**, *192*, 402–410.
41. A. Tessier, P. G. C. Campbell, M. Bisson, *Anal. Chem.* **1979**, *51*, 844–851.
42. A. Alomary, S. Belhadj, *Environ. Monit. Assess.* **2007**, *135*, 265–280.
43. C. M. Davidson, R. P. Thomas, S. E. McVey, R. Perala, D. Littlejohn, A. M. Ure, *Anal. Chim. Acta* **1994**, *291*, 277–286.
44. A. V. Filgueiras, I. Lavilla, C. Bendicho, *J. Environ. Monit.* **2002**, *4*, 823–857.
45. R. Gemma, *Talanta* **1998**, *46*, 449–455.
46. C. Ianni, A. Bignasca, E. Magi, P. Rivaro, *Microchem. J.* **2010**, *96*, 308–316.
47. A. Naji, A. Ismail, A. R. Ismail, *Microchem. J.* **2010**, *95*, 285–292.
48. L. Wang, R. Yu, G. Hu, X. Tu, *Environ. Monit. Assess.* **2010**, *165*, 491–499.
49. A. S. Hursthouse, *J. Environ. Monit.* **2001**, *3*, 49–60.
50. A. Kabata-Pendias, H. Pendias, *Trace Elements in Soils and Plants*, CRC Press, Boca Raton, FL, 2001.

51. G. S. R. Krishnamurti, P. M. Huang, K. C. J. Van Rees, L. M. Kozak, H. P. W. Rostad, *Analyst* **1995**, *120*, 659–665.
52. R. J. G. Mortimer, J. E. Rae, *Mar. Pollut. Bull.* **2000**, *40*, 377–386.
53. F. Baraud, T. W. M. Fan, R. M. Higashi, in *Environmental Chemistry - Green Chemistry and Pollutants in Ecosystems*, Eds E. Lichtfouse, J. Schwarzbauer, D. Robert, Springer-Verlag, Berlin, Heidelberg (Germany), 2005, pp. 205–214.
54. R. G. Gerritse, W. van Driel, *J. Environ. Qual.* **1984**, *13*, 197–204.
55. S. S. Mann, G. S. P. Ritchie, *Soil Res.* **1993**, *31*, 255–270.
56. R. Aringhieri, P. Carrai, G. Petruzzelli, *Soil Sci.* **1985**, *139*, 197–204.
57. J. O. Onyatta, P. M. Huang, *Geoderma* **1999**, *91*, 87–101.
58. L. N. Benitez, J.-P. Dubois, *Int. J. Environ. Anal. Chem.* **1999**, *74*, 289–303.
59. M. D. Ho, G. J. Evans, *Anal. Comm.* **1997**, *34*, 363–364.
60. P. E. Holm, S. Andersen, T. H. Christensen, *Water Res.* **1995**, *29*, 803–809.
61. G. S. R. Krishnamurti, P. M. Huang, L. M. Kozak, H. P. W. Rostad, K. C. J. V. Rees, *Can. J. Soil Sci.* **1997**, *77*, 613–619.
62. G. S. R. Krishnamurti, R. Naidu, *Soil Res.* **2000**, *38*, 991–1004.
63. W. H. Otto, W. R. Carper, C. K. Larive, *Environ. Sci. Technol.* **2001**, *35*, 1463–1468.
64. Q. Wu, W. H. Hendershot, W. D. Marshall, Y. Ge, *Comm. Soil Sci. Plant Anal.* **2000**, *31*, 1129–1144.
65. S. Sauvé, W. A. Norvell, M. McBride, W. Hendershot, *Environ. Sci. Technol.* **2000**, *34*, 291–296.
66. F. Adams, in *In The Plant Root and Its Environment*, Ed E. W. Carson, University of Virginia Press, Charlottesville, VA, 1974, pp. 441–481.
67. J. Mulder, M. S. Cresser, in *Biogeochemistry of Small Catchments: A Tool for Environmental Research*, Eds J. V. Cerny, B. Moldan, John Wiley & Sons, Ltd, Chichester, UK, 1994, pp. 107–131.
68. M. H. B. Hayes, R. S. Swift, in *The Chemistry of Soil Constituents*, Eds D. J. Greenland, M. H. B. Hayes, John Wiley & Sons, Ltd., Chichester, UK, 1978, pp. 179–320.
69. M. Dalva, T. R. Moore, *Biogeochem.* **1991**, *15*, 1–19.
70. D. Berggren, *Int. J. Environ. Anal. Chem.* **1989**, *35*, 1–15.
71. A. R. Tills, B. J. Alloway, *J. Soil Sci.* **1983**, *34*, 769–781.
72. O. Krissanakriangkrai, W. Supanpaiboon, S. Juwa, S. Chaiwong, S. Swaddiwudhipong, K. A. Anderson, *Thammasat Int. J. Sci. Technol.* **2009**, *14*, 60–68.
73. D. Hirsch, A. Banin, *J. Environ. Qual.* **1988**, *19*, 366–372.
74. E. J. M. Temminghoff, A. C. C. Plette, R. Van Eck, W. H. Van Riemsdijk, *Anal. Chim. Acta* **2000**, *417*, 149–157.
75. J. Y. Cornu, C. Parat, A. Schneider, L. Authier, M. Dauthieu, V. Sappin-Didier, L. Denaix, *Chemosphere* **2009**, *76*, 502–508.
76. S. Sauvè, W. A. Norvell, M. McBride, W. Hendershot, *Environ. Sci. Technol.* **1999**, *34*, 291–296.
77. L. A. Smith, J. L. Means, A. Chen, B. Alleman, C. C. Chapman, J. S. J. Tixier, S. E. Brauning, A. R. Gavaskar, M. D. Royer, *Remedial Options for Metal-Contaminated Sites*, Lewis Publisher, Boca Raton, FL, 1995.
78. C. De Stefano, A. Gianguzza, A. Pettignano, S. Sammartano, S. Sciarrino, *J. Chem. Eng. Data* **2010**, *55*, 714–722.
79. B. L. Gyurcsik, L. S. Nagy, *Coord. Chem. Rev.* **2000**, *203*, 81–149.
80. D. K. Cabbiness, D. W. Margerum, *J. Am. Chem. Soc.* **1969**, *91*, 6540–6541.
81. A. De Robertis, C. De Stefano, D. Milea, S. Sammartano, *J. Solution Chem.* **2005**, *34*, 1211–1226.
82. A. Casale, C. De Stefano, G. Manfredi, D. Milea, S. Sammartano, *Bioinorg. Chem. Appl.* **2009**, *2009*, ID 219818. DOI 10.1155/2009/219818.
83. S. Capone, A. De Robertis, C. De Stefano, S. Sammartano, *Talanta* **1986**, *33*, 763–767.
84. C. De Stefano, D. Milea, N. Porcino, S. Sammartano, *Anal. Bioanal. Chem.* **2006**, *386*, 346–356.

85. C. De Stefano, G. Lando, D. Milea, A. Pettignano, S. Sammartano, *J. Solution Chem.* **2010**, *39*, 179–195.
86. R. M. Cigala, F. Crea, C. De Stefano, G. Lando, D. Milea, S. Sammartano, *J. Chem. Eng. Data* **2010**, *55*, 4757–4767.
87. F. Crea, C. De Stefano, D. Milea, S. Sammartano, *Coord. Chem. Rev.* **2008**, *252*, 1108–1120.
88. A. Gianguzza, O. Giuffrè, D. Piazzese, S. Sammartano, *Coord. Chem. Rev.* **2012**, *256*, 222–239.
89. C. Bazzicalupi, A. Bianchi, C. Giorgi, M. P. Clares, E. Garcia-Espana, *Coord. Chem. Rev.* **2012**, *256*, 13–27.

Chapter 4
Determination of Cadmium in Biological Samples

Katrin Klotz, Wobbeke Weistenhöfer, and Hans Drexler

Contents

ABSTRACT 85
1 INTRODUCTION 86
2 BIOMARKERS OF EXPOSURE 86
2.1 Overview 86
2.2 Pre-analytic Phase 87
2.3 Analytical Methods for the Determination of Cadmium 87
2.3.1 Inductively Coupled Plasma Mass Spectrometry 88
2.3.2 Atomic Absorption Spectrometry 88
2.3.3 Electrochemical Methods 90
2.3.4 Further Methods 91
2.4 Quality Control 92
2.5 Body Burden after Environmental and Occupational Exposure 92
3 BIOMARKERS OF EFFECT 92
3.1 Overview 92
3.2 Analytical Methods for β2-Microglobulin Quantification 93
3.3 Analytical Methods for the Quantification of the Retinol Binding Protein 94
3.4 Analytical Methods for the Quantification of Further Effect Markers 94
3.5 Effect Biomarkers after Exposure to Cadmium 94
4 CONCLUSIONS 95
ABBREVIATIONS 95
ACKNOWLEDGMENT 96
REFERENCES 96

Abstract Analyses of cadmium concentrations in biological material are performed using inductively coupled plasma mass spectrometry (ICP-MS) and atomic absorption spectrometry (AAS), but also electrochemical methods, neutron activation

K. Klotz (✉) • W. Weistenhöfer • H. Drexler
Institute and Outpatient Clinic of Occupational, Social and Environmental Medicine, Friedrich-Alexander University (FAU) of Erlangen-Nuremberg, Schillerstr. 25/29, D-91052 Erlangen, Germany
e-mail: katrin.klotz@ipasum.med.uni-erlangen.de

A. Sigel, H. Sigel, and R.K.O. Sigel (eds.), *Cadmium: From Toxicity to Essentiality*, Metal Ions in Life Sciences 11, DOI 10.1007/978-94-007-5179-8_4,

analysis (NAA), and X-ray fluorescence spectrometry (XRF). The predominant sample matrices include blood, plasma, serum, and urine, as well as hair, saliva, and tissue of kidney cortex, lung, and liver. While cadmium in blood reveals rather the recent exposure situation, cadmium in urine reflects the body burden and is an indicator for the cumulative long term exposure.

After chronic exposure, cadmium accumulates in the human body and causes kidney diseases, especially lesions of proximal tubular cells. A tubular proteinuria causes an increase in urinary excretion of microproteins. Excretions of retinol binding protein (RBP), β2-microglobulin (β2-M), and α1-microglobulin are validated biomarkers for analyzing cadmium effects. For this purpose, immunological procedures such as ELISA, and radio- and latex-immunoassays are used.

However, proteinuria is not specific to cadmium, but can also occur after exposure to other nephrotoxic agents or due to various kidney diseases. In summary, cadmium in urine and blood are the most specific biomarkers of cadmium exposure. A combination of parameters of exposure (cadmium in blood, cadmium in urine) and parameters of effect (e.g., β2-M, RBP) is required to reveal cadmium-induced nephrological effects.

Keywords AAS • analysis • biomonitoring • blood • cadmium • ICP-MS • immunoassay • urine

1 Introduction

This chapter presents different analytical procedures, which can be used to quantify the concentration of cadmium and its metabolites in biological material as well as biomarkers of effect after cadmium exposure.

Preferably, well-established standard methods of analysis are presented. In Germany, standard procedures for biological monitoring are published by the Working Group "Analyses of Hazardous Substances in Biological Materials" of the "Commission for the Investigation of Health Hazards of Chemical Compounds in the Work Area". Additionally, analytical methods are included, that modify former methods to improve accuracy and precision or obtain lower limits of detection.

2 Biomarkers of Exposure

2.1 Overview

For human biomonitoring, the following parameters are preferably used to analyze cadmium in biological material: cadmium in blood and cadmium in urine.

Additionally, analysis of cadmium can be performed in other matrices such as saliva, hair, nail, teeth and tissues. Overviews of analytical methods for determining cadmium in biological materials are given in Tables 1 to 3 (see below).

Cadmium in blood and in urine are used as parameters for assessing occupational and environmental exposure to cadmium. Cadmium in blood is a short term parameter, reflecting recent exposure to cadmium. Short time elevations of cadmium in blood may be caused by excessive exposure situations. After the end of exposure, there is a rapid decrease in the first stage, followed by a decrease that levels off, depending on accumulated body burden. After long term exposure, cadmium concentration in blood becomes more complex to interpret, as it reflects both the present and the long term exposure [1,2].

Cadmium in urine reflects the body burden of cadmium, especially the cadmium concentration in the main accumulation organ, the kidney (organ-specific accumulation). Therefore, it can be regarded as indicator of the cumulative long term exposure. As long as the renal function remains normal, the concentration of cadmium in urine is well correlated with the total cadmium body burden. After cadmium-induced irreversible tubular renal dysfunction with microproteinuria, the cadmium excretion in urine tends to increase, as cadmium is released from renal depots [2,3].

2.2 *Pre-analytic Phase*

Due to the ubiquitous presence of cadmium, there is a risk for contamination during the whole process of sampling and analysis, which has to be minimized by strict laboratory procedures.

As in any trace element analysis, reagents of the highest purity and contaminant-free tips of automatic pipettes, tubes, and glassware must be used (colored plastic tubes may contain cadmium). Plastic tubes used for specimen collection and treatment must be individually cleaned with 1 M nitric acid to avoid exogenous contamination. In practice, the tubes are filled with acid and allowed to stand for at least 2 hours. Afterwards, they are rinsed two to three times first with deionized water and then with ultrapure water before drying them. The cleaning can be made more effective by warming the nitric acid [4].

2.3 *Analytical Methods for the Determination of Cadmium*

The most common procedures for analyzing cadmium concentrations in blood and urine are inductively coupled plasma mass spectrometry (ICP-MS) and atomic absorption spectrometry (AAS). Furthermore, electrochemical methods, neutron activation analysis (NAA) and X-ray fluorescence spectrometry (XRF) can be applied. Several factors influence the choice of the analytical method, e.g. the matrix and the detection limit required.

2.3.1 Inductively Coupled Plasma Mass Spectrometry

In inductively coupled plasma mass spectrometry analysis, the sample is heated in an argon-plasma activated by a high-voltage field. Thereby, atoms are ionized. Using an electric field, the generated ions are accelerated to the analyser of the mass spectrometer, where they are separated according to the mass of the specific isotopes. In inductively coupled plasma optical emission spectroscopy (ICP-OES), also referred to as inductively coupled plasma atomic emission spectroscopy (ICP-AES), the sample is atomized in argon plasma and the excitation of an optical emission of cadmium is measured.

Using the ICP-MS and ICP-OES methods, cadmium present in **urine and blood** due to occupational or environmental exposure can be determined sensitively, specifically, and with little effort. Samples are usually prepared by digestion with acid [5–9] or dilution with acid [10–12]. An additional enrichment is achieved by extraction with organic solvents or by capillary micro-extraction [7,9,13]. Detection limits for ICP-MS analysis in blood or urine are predominantly reported in the lower range from 0.007 μg/L to 0.1 μg/L (for details see Table 1).

The Working Group "Analyses of Hazardous Substances in Biological Materials" of the "Commission for the Investigation of Health Hazards of Chemical Compounds in the Work Area" has published a standard procedure for the determination of cadmium in urine. Briefly, after UV digestion of the urine samples, an internal standard is added and the samples are introduced into the ICP-MS by means of a pneumatic nebulizer. Evaluation is carried out using the standard addition procedure. The limit of detection is specified with 0.02 μg/L urine. The method can be applied for samples from environmental as well as occupational-medical studies [5].

In addition to analysis in blood and urine, methods for other biological materials such as tissue of lung, liver, and kidney cortex as well as hair and nails have been published [11,14,15].

2.3.2 Atomic Absorption Spectrometry

In atomic absorption spectrometry the sample is heated by a flame or in a furnace, until the element atomizes. The atoms absorb light at the resonance line. The attenuation of intensity of the light beam can be measured.

Cadmium in **blood, urine, hair, saliva, and human milk** is predominantly analyzed with graphite furnace atomic absorption spectrometry (GF-AAS), also known as electrothermal AAS (ET-AAS). Samples are usually prepared by digestion with nitric acid [16–20]. Solubilizers (Triton® X-100) or matrix modifiers (e.g., diammonium hydrogen phosphate, Pd-components) are added [17,21–23].

At very low cadmium concentration, pre-concentration can be achieved by chelation and extraction with a mixture of organic solvents [4].

The limits of detection of AAS methods are with 0.02 µg/L to 0.5 µg/L higher than those of ICP-MS methods (see Tables 1 and 2).

Table 1 Analytical procedures using ICP for cadmium analysis in biological materials.

Analytical method	Sample matrix	Preparation method	LOD	Reference
ICP-SF-MS	blood	microwave digestion with nitric acid	0.1 µg/L	[6]
ICP-QMS	blood	wet-ashed	0.01 µg/L	[8]
ICP-MS	serum	dilution with acetic acid and Triton X-100	not specified	[10]
ICP-QMS	serum and urine	microwave digestion with nitric acid, online-capillary micro-extraction	0.007 µg/L	[9]
ICP-QMS	urine	UV digestion with HNO_3/H_2O_2	0.02 µg/L	[5]
ICP-QMS	urine	dilution with HNO_3/HCl	0.02 µg/L	[12]
LA-ICP-QMS	urine	drying	0.02 µg/g creatinine	[79]
ICP-MS	biological materials (whole blood, plasma, urine, hair)	dilution with nitric acid, Triton X-100 and butanol; hair: mineralization with nitric acid, dilution with nitric acid, Triton X-100 and butanol	0.011 µg/L (blood), 0.008 µg/L (plasma), 0.007 µg/L (urine), 0.0003 µg/g (hair)	[11]
ICP-MS	finger and toe nail	mineralization with nitric acid, dilution with nitric acid, Triton X-100 and butanol	0.0003 µg/g	[14]
ICP-MS	tissue (lung, liver, kidney cortex) and urine	digestion with nitric acid	not specified	[15]
FI-ICP-AES	biological materials	complexation with DPTH/ extraction with MIBK	23 µg/L	[13]
ICP-AES	biological materials	microwave digestion with HNO_3/HCl, followed by extraction with BPTH/MIBK	0.3 µg/L	[7]

AES = atomic emission spectroscopy; BPTH = 1,5-bis[phenyl-(2-pyridyl)-methylene]-thiocarbonohydrazide]; DPTH = 1,5-bis(di-2-pyridyl)methylene thiocarbohydrazide; FI = flow injection; ICP = inductively coupled plasma; LA = laser ablation; LOD = limit of detection; MIBK = methyl isobutyl ketone; MS = mass spectrometry; QMS = quadrupole mass spectrometry; SF-MS = sector field mass spectrometry

Table 2 Analytical procedures using AAS for cadmium analysis in biological materials.

Analytical method	Sample matrix	Preparation method	LOD	Reference
GF-AAS	blood	dilution with Triton X-100 and nitric acid	0.2 µg/L	[80]
GF-AAS	blood	digestion with HNO_3/H_2O_2	0.4 µg/L	[20]
GF-AAS	blood	dilution with Triton X-100, diammonium hydrogen phosphate and nitric acid	0.5 µg/L	[17]
GF-AAS (EC-THGA)	blood	dilution with Triton X-100, nitric acid and trichloroacetic acid; W, Rh and $NH_4H_2PO_4$ as modifiers	0.03 µg/L	[21]
GF-AAS	blood	dilution with diammonium hydrogen phosphate and Triton X-100	0.1 µg/L	[23]
GF-AAS	urine	chelation with HMA/HMDC, extraction with diisopropyl ketone/xylene	0.2 µg/L	[4]
GF-AAS	urine	acidification, microwave digestion with HNO_3/HCl	0.05 µg/L	[19]
GF-AAS	human milk	digestion with HNO_3/H_2O_2	0.5 µg/L	[18]
GF-AAS	biological samples (blood, urine, hair, saliva)	dilution with matrix $Mg(NO_3)_2$/$Pd(NO_3)_2$, Triton X-100 and nitric acid; for hair: dilution with HNO_3, HCl, H_2O_2 and microwave digestion	0.03 µg/L	[22,81]
GF-AAS	biological samples (blood, urine, scalp hair)	microwave digestion with HNO_3/H_2O_2	0.02 µg/L	[16]

AAS = atomic absorption spectrometry; EC-THGA = end-capped transversal heating graphite tubes; GF-AAS = graphite furnace atomic absorption spectrometry; HMA/HMDC = hexamethylene ammonium/hexamethylene dithiocarbamidate; LOD = limit of detection

2.3.3 Electrochemical Methods

In **differential pulse anodic stripping voltammetry (DPASV)**, cadmium ions are first reduced and amalgamated at the working electrode (a hanging mercury drop electrode or a mercury film electrode) during pre-electrolysis at a suitable applied potential. In the second step, the reduced amalgamated cadmium is re-oxidized by means of a potential ramp imposed between the working electrode and a platinum rod electrode [24]. The resulting peak is proportional to the cadmium concentration of the solution.

DPASV procedures have been applied to analyze cadmium in urine [24–26] and in human hair [27]. The samples were prepared by digestion with acids.

DPASV can be applied as an independent reference procedure for AAS and ICP-MS. It is suitable for analyzing cadmium concentrations in environmental as well as occupational-medical samples [25] (Table 3).

During **potentiometric stripping analysis (PSA)**, trace elements or ions are pre-concentrated by potentiostatic deposition on an electrode (e.g., mercury film on a glassy-carbon electrode). In contrast to DPASV, PSA is not subject to background

Table 3 Analytical procedures using electrochemical methods for cadmium analysis in biological materials.

Analytical method	Sample matrix	Preparation method	LOD	Reference
DPASV	urine	microwave digestion with nitric acid; acetate buffer for pH adjustment	0.06 µg/L	[24]
DPASV	urine	digestion with HNO_3/H_2SO_4; acetate buffer and citrate solution	0.2 µg/L	[25]
DPASV	urine	digestion with HNO_3, acetate buffer	not specified	[26]
DPASV	hair	microwave digestion with HNO_3/H_2O_2	0.02 µg/g	[27]
DPASV	blood	digestion with $HNO_3/HClO_4$, concentration step	0.1 µg/L	[29]
PSA	blood	HCl, $HgCl_2$ in HCl	for conc. < 0.1 µg/L: longer deposition time	[29]
PSA	blood	digestion with nitric acid	< 0.1 µg/L	[30]
PSA	blood	dissolve in tetramethylammonium hydroxide, dilution with Hg(II) in HCl	0.1 µg/L	[31]
PSA	urine	HCl	1 nM	[32]

DPASV = differential pulse anodic stripping voltammetry; PSA = potentiometric stripping analysis; LOD = limit of detection.

interferences from organic electroactive constituents in the sample or to the presence of dissolved oxygen [28]. It is used to analyze cadmium in whole blood [29–31] and urine [32] (Table 3).

2.3.4 Further Methods

Cadmium concentrations in biological materials can also be measured with **neutron activation analysis (NAA)** and **X-ray fluorescence spectroscopy (XRF)**. Both techniques depend on the detection of photons generated in cadmium by an externally incident beam of radiation. In NAA, the cadmium concentration in the sample is determined by studying the emission of γ-rays after the irradiation of the sample with neutrons [33,34]. In contrast, photon emission in XRF is produced by an incident beam of X-rays or γ-rays interacting with the atomic electrons of cadmium, resulting in the emission of characteristic X-rays [34].

The analyses of cadmium concentrations in human kidney and liver with **NAA** can be performed with direct *in vivo* [35–37] or *in vitro* measurements [38]. Additionally, NAA procedures for the quantification of cadmium in biological materials such as bovine liver and food samples [39], human hair [40], serum [41], and human central nervous system issue samples [42] have been described.

With **XRF**, cadmium in the kidney can be analyzed *in vivo* [43–45]. These procedures are used for clinical measurements in the kidney of persons occupationally exposed to cadmium. The detection limit of XRF is strongly dependent on the distance between skin and kidney, which has to be analyzed with ultrasound [45].

2.4 Quality Control

An internal quality control should be performed with each analytical run. Control materials for internal quality control of cadmium analytical procedures are commercially available, e.g., certified reference material for trace elements in urine, plasma, serum, and whole blood [46,47].

To assure the accuracy and comparability of the results with other laboratories, an appropriate external quality assessment is necessary. For external quality control, participation in a round robin test is recommended. There are various quality control programs containing cadmium in blood and urine, e.g., the international program of the German External Quality Assessment Scheme (E-QUAS), where cadmium analysis can be tested for the concentration range found in occupational and environmental medicine [48], or the external quality assessment schemes of the Centre of Toxicology in the National Institute of Public Health of Québec [49].

2.5 Body Burden after Environmental and Occupational Exposure

The German commission "Human-Biomonitoring" evaluated reference values (95th percentile of the cadmium background exposure) of 1.0 µg cadmium/L blood and 0.8 µg cadmium/L urine for non-smokers aged 18 to 69 [50,51]. Smokers showed higher 95th percentile values of 3.32 µg cadmium/L blood and 1.20 µg cadmium/L urine [52,53].

Occupational exposure to cadmium leads to higher levels in blood and urine. Workers exposed to cadmium in a non-ferrous smelter showed mean levels of 6.23 µg cadmium/g creatinine (range 0.87–165 µg/g creatinine) and 6.54 µg cadmium/L blood (range 1.6–51 µg/L) [54].

3 Biomarkers of Effect

3.1 Overview

Long term exposure to cadmium results in kidney diseases, especially tubular damage, as early and frequent health damage. The earliest sign of nephropathy induced by chronic cadmium exposure is an increased urinary excretion of low-molecular-weight proteins with a molecular weight of less than 40 kDa, such as β2-microglobulin (β2-M) and retinol-binding protein (RBP). In healthy persons, the reabsorption of those small proteins is almost complete. A decrease in the

tubular reabsorption capacity causes an increase in the urinary excretion of microproteins like β2-M and RBP [55].

There are sensitive methods available for the quantification of tubular proteinuria in populations exposed to cadmium occupationally or environmentally. RBP, β2-M, α1-microglobulin (α1-M, also called protein HC), metallothionein, and enzymes such as N-acetyl- β-D-glucosaminidase (NAG) in human urine are used as biomarkers of cadmium-induced effects [56–61]. However, the effects are not specific to cadmium exposure, but may also occur due to various renal diseases or nephrotoxic agents other than cadmium.

Urinary β2-M is a highly sensitive and widely used parameter [3,55]. Because of the instability of β2-M in acidic urine (pH $<$ 5.6), a strict pH-control of the urine is necessary. Even if patients are given bicarbonate before urine collection, a decomposition of β2-M in up to 30% of the urine samples is observed [55]. α1-M is very stable in urine, but less specific to tubular damage because of its larger size and slightly less sensitive than β2-M and RBP. RBP on the other hand is described as stable, specific, and as sensitive as β2-M [61].

3.2 Analytical Methods for β2-Microglobulin Quantification

The quantification of β2-M concentration in human urine and serum can be performed with immunoassays, e.g., enzyme-linked immunosorbent assay, radio immunoassay [62], latex immunoassay [63,64], immunoenzymatic assay with chemiluminescence detection, and immunoturbidimetric assay [65].

There are commercially available test kits for the quantitative determination of β2-M in plasma, serum, and urine with ELISA, e.g., from Immundiagnostik [66] or ORGENTEC Diagnostika GmbH [67]. In this method, immobilized antibodies against β2-M are fixed on the surface of a microtiter plate. During the immune reaction, the antibodies on the plate bind the β2-M in the sample. After the non-bonded components have been washed out, an enzyme (horseradish peroxidase) labeled anti-human β2-M-antibody is added, which binds to β2-M. The amount of bound enzyme is directly proportional to the β2-M-concentration of the sample. A chromogen (tetramethylbenzidine) is converted by the bound enzyme to a chromogenic compound, which is photometrically quantified [66].

Latex immunoassay was introduced by Bernard et al. [63,64]. In this method, the surface of polystyrene-latex particles is coated with specific antibodies sensitized to human β2-M. They agglutinate with β2-M molecules in the serum or urine sample. Unspecific agglutination of the particles carrying the antibodies is prevented by diluting the samples with a standardized albumin solution. The quantitative evaluation of the results is performed by counting the remaining non-agglutinated particles or by measuring the decrease of absorbance with a photometer at 360 nm. The limit of detection is 0.5 μg/L [63,64].

3.3 Analytical Methods for the Quantification of the Retinol Binding Protein

Retinol binding protein (RBP) in plasma, serum, and urine can be analyzed using different immunoassays, e.g., latex immunoassay [63], ELISA [59], monoclonal antibody-based fluorescence immunoassay [68] or immunonephelometry [69,70]. For principles of latex immunoassay and ELISA, see Section 3.2.

Immunonephelometry uses the effect of a diluted suspension of small particles to scatter a light-beam angular (Tyndall effect) to quantify aggregates formed in an antigen-antibody-reaction [71]. Test systems for RBP quantification are commercially available.

3.4 Analytical Methods for the Quantification of Further Effect Markers

The total protein concentration can be analyzed with commercially available kits based on Coomassie Brilliant Blue reaction. Albumin and α1-microglobulin (protein HC) are quantified by single radial immunodiffusion techniques [72,73] and immunonephelometry [60]. For N-acetyl-β-D-glucosaminidase determination, there are commercially available test kits based on spectrophotometric assay [74].

3.5 Effect Biomarkers after Exposure to Cadmium

Long-term or high exposure to cadmium causes tubular damage that may progress to glomerular damage with decreased glomerular filtration rate and the risk of renal failure. Taking a variety of early markers of kidney damage into account, a dose–response assessment identified early effects in the kidney at concentrations between 0.5 and 3 μg cadmium/g creatinine in the general population [75].

The reversibility of glomerular lesions induced by cadmium is still under discussion [61,76]. Tubular proteinuria (β2-M and RBP in urine) between 300 and 1000 μg/g creatinine might be reversible [61], but more severe tubular proteinuria (i.e., more than 1000 μg β2-M/g creatinine) seems to be irreversible [61,77]. A large study with 1699 subjects (aged 20–80 years) of the general population showed a 10% probability of values of urinary excretion of RBP, NAG, β2-M, amino acids, and calcium being abnormal when cadmium excretion exceeded 2–4 μg/24 h [78].

4 Conclusions

The analysis of cadmium concentrations in biological material is mainly performed with ICP-MS or AAS. ICP-MS attains lower limits of detection than AAS. In addition, electrochemical methods, NAA, and XRF can be applied. The predominant sample matrices include blood and urine, but also hair, saliva, and tissue are used. The application of neutron activation analysis and X-ray fluorescence enables *in vivo* measurements of cadmium.

Cadmium accumulates in the human body after chronic exposure and causes kidney diseases. A tubular proteinuria causes an increase in urinary excretion of microproteins. For routine screening, the excretion of β2-M, RBP, and α1-M have been validated as biomarkers for cadmium effects. Sensitive, particularly immunological analytical procedures have been published for these parameters. However, proteinuria is not specific to cadmium, but can also occur after exposure to other nephrotoxic agents or due to various kidney diseases. Thus, a combination of parameters of exposure (cadmium in blood, cadmium in urine) and parameters of effect (e.g., β2-M, RBP) is required to reveal cadmium-induced nephrological effects.

Abbreviations

α1-M	α1-microglobulin = protein HC
AAS	atomic absorption spectrometry
AES	atomic emission spectroscopy
β2-M	β2-microglobulin
BPTH	1,5-bis[phenyl-(2-pyridyl)-methylene]-thiocarbonohyrazide
DPASV	differential pulse anodic stripping voltammetry
DPTH	1,5-bis(di-2-pyridyl)methylene thiocarbohydrazide
EC-THGA	end-capped transversal heating graphite tubes
ELISA	enzyme-linked immunosorbent assay
E-QUAS	External Quality Assessment Scheme
ET-AAS	electrothermal atomic absorption spectrometry
ETV-ICP-MS	electrothermal vaporization inductively coupled plasma mass spectrometry
FI-ICP-AES	flow injection inductively coupled plasma atomic emission spectrometry
GF-AAS	graphite furnace atomic absorption spectrometry
HMA	hexamethylene ammonium
HMDC	hexamethylene dithiocarbamidate
ICP-AES	inductively coupled plasma atomic emission spectroscopy
ICP-MS	inductively coupled plasma mass spectrometry
ICP-OES	inductively coupled plasma optical emission spectroscopy

LA-ICP-MS	laser ablation inductively coupled plasma mass spectrometry
LOD	limit of detection
M	molar
MIBK	methyl isobutyl ketone
NAA	neutron activation analysis
NAG	N-acetyl-β-D-glucosaminidase
PSA	potentiometric stripping analysis
QMS	quadrupole mass spectrometry
RBP	retinol-binding protein
SF-MS	sector field mass spectrometry
XRF	X-ray fluorescence spectrometry

Acknowledgment We wish to thank Dr. Thomas Göen and Mrs Piia Lämmlein for their support in preparing this manuscript.

References

1. CDC, "Fourth National Report on Human Exposure to Environmental Chemicals. Department of Health and Human Services, Centers for Disease Control and Prevention", CDC, Atlanta, Georgia, USA, 2009.
2. EUROMETAUX, "Management of the risk related to chronic occupational exposure to cadmium and its compounds", 2005.
3. UBA, *Bundesgesundheitsblatt - Gesundheitsforschung - Gesundheitsschutz* **2011**, *54*, 981–996.
4. *Cadmium. Determination in Urine (Electrothermal atomic absorption spectrometry). Biomonitoring Methods*, *Analyses of Hazardous Substances in Biological Materials*, Wiley-VCH 1984 (http://onlinelibrary.wiley.com/book/10.1002/3527600418/topics).
5. *Antimony, Lead, Cadmium, Platinum, Mercury, Tellurium, Thallium, Bismuth, Tungsten, Tin. Determination in Urine (Inductively coupled plasma quadrupole mass spectrometry). Biomonitoring Methods*, *Analyses of Hazardous Substances in Biological Materials*, Wiley-VCH 1999 (http://onlinelibrary.wiley.com/book/10.1002/3527600418/topics).
6. M. Ikeda, F. Ohashi, Y. Fukui, S. Sakuragi, J. Moriguchi, *Int. Arch. Occup. Envir. Health* **2011**, *84*, 139–150.
7. M. T. Siles Cordero, A. Garcia de Torres, J. M. Cano Pavón, C. Bosch Ojeda, *Mikrochim. Acta* **1994**, *116*, 173–182.
8. Z. W. Zhang, S. Shimbo, N. Ochi, M. Eguchi, T. Watanabe, C. S. Moon, M. Ikeda, *Sci. Total Envir.* **1997**, *205*, 179–187.
9. F. Zheng, B. Hu, *Talanta* **2011**, *85*, 1166–1173.
10. R. Forrer, K. Gautschi, H. Lutz, *Biol. Trace Elem. Res.* **2001**, *80*, 77–93.
11. J. P. Goullé, L. Mahieu, J. Castermant, N. Neveu, L. Bonneau, G. Lainé, D. Bouige, C. Lacroix, *Forensic Sci. Int.* **2005**, *153*, 39–44.
12. P. Schramel, I. Wendler, J. Angerer, *Int. Arch. Occup. Envir. Health* **1997**, *69*, 219–223.
13. M. T. Siles Cordero, E. I. Vereda Alonso, A. Garcia De Torres, J. M. Cano Pavón, *J. Anal. At. Spectrometry* **1996**, *11*, 107–110.
14. J. P. Goullé, E. Saussereau, L. Mahieu, D. Bouige, S. Groenwont, M. Guerbet, C. Lacroix, *J. Anal. Toxicol.* **2009**, *33*, 92–98.
15. S. Satarug, J. R. Baker, P. E. B. Reilly, M. R. Moore, D. J. Williams, *Arch. Envir. Health* **2002**, *57*, 69–77.
16. H. I. Afridi, T. G. Kazi, M. K. Jamali, G. H. Kazi, M. B. Arain, N. Jalbani, G. Q. Shar, R. A. Sarfaraz, *Toxicol. Indust. Health* **2006**, *22*, 381–393.

17. Y. Fukui, F. Ohashi, S. Sakuragi, J. Moriguchi, M. Ikeda, *Indust. Health* **2011**, *49*, 338–343.
18. E. García-Esquinas, B. Pérez-Gómez, M. A. Fernández, A. M. Pérez-Meixeira, E. Gil, C. D. Paz, A. Iriso, J. C. Sanz, J. Astray, M. Cisneros, A. D. Santos, A. Asensio, J. M. García-Sagredo, J. F. García, J. Vioque, M. Pollán, G. López-Abente, M. J. González, M. Martínez, P. A. Bohigas, R. Pastor, N. Aragonés, *Chemosphere* **2011**, *85*, 268–276.
19. C. J. Horng, J. L. Tsai, P. H. Horng, S. C. Lin, S. R. Lin, C. C. Tzeng, *Talanta* **2002**, *56*, 1109–1115.
20. C. A. Roberts, J. M. Clark, *Bull. Envir. Contam. Toxicol.* **1986**, *36*, 496–499.
21. F. Kummrow, F. F. Silva, R. Kuno, A. L. Souza, P. V. Oliveira, *Talanta* **2008**, *75*, 246–252.
22. P. Olmedo, A. Pla, A. F. Hernández, O. López-Guarnido, L. Rodrigo, F. Gil, *Anal. Chim. Acta* **2010**, *659*, 60–67.
23. K. S. Subramanian, J. C. Meranger, *Clin. Chem.* **1981**, *27*, 1866–1871.
24. C. J. Horng, *Analyst* **1996**, *121*, 1511–1514.
25. *Cadmium. Inversvoltammetrie (DPP) in Harn*, *Analytische Methoden zur Prüfung gesundheitsschädlicher Arbeitsstoffe. Band 2: Analysen in biologischem Material*, Wiley-VCH 1983.
26. A. N. Onar, A. Temizer, *Analyst* **1987**, *112*, 227–229.
27. W. Wasiak, W. Ciszewska, A. Ciszewski, *Anal. Chim. Acta* **1996**, *335*, 201–207.
28. P. Ostapczuk, *Anal. Chim. Acta* **1993**, *273*, 35–40.
29. M. A. Moreno, C. Marin, F. Vinagre, P. Ostapczuk, *Sci. Total Envir.* **1999**, *229*, 209–215.
30. P. Ostapczuk, *Clin. Chem.* **1992**, *38*, 1995–2001.
31. A. Viksna, E. S. Lindgren, *Anal. Chim. Acta* **1997**, *353*, 307–311.
32. D. Jagner, M. Josefson, S. Westerlund, *Anal. Chim. Acta* **1981**, *Vol. 128*, 155–161.
33. D. R. Chettle, *J. Radioanal. Nucl. Chem.* **2006**, *268*, 653–661.
34. M. C. Scott, D. R. Chettle, *Scand. J. Work, Envir. Health* **1986**, *12*, 81–96.
35. D. R. Chettle, D. M. Franklin, C. J. G. Guthrie, M. C. Scott, L. J. Somervaille, *Biol. Trace Elem. Res.* **1987**, *13*, 191–208.
36. K. J. Ellis, S. H. Cohn, *J. Toxicol. Envir. Health* **1985**, *15*, 173–187.
37. F. E. McNeill, D. R. Chettle, *Appl. Radiat. Isotopes* **1998**, *49*, 699–700.
38. K. W. Lieberman, H. H. Kramer, *Anal. Chem.* **1970**, *42*, 266–267.
39. J. R. W. Woittiez, M. De La Cruz Tangonan, *J. Radioanal. Nucl. Chem.* **1992**, *158*, 313–321.
40. M. Saiki, M. B. A. Vasconcellos, L. J. De Arauz, R. Fulfaro, *J. Radioanal. Nucl. Chem.* **1998**, *236*, 25–28.
41. J. Kucera, L. Soukal, *J. Radioanal. Nucl. Chem.* **1993**, *168*, 185–199.
42. L. Tandon, B. F. Ni, X. X. Ding, W. D. Ehmann, E. J. Kasarskis, W. R. Markesbery, *J. Radioanal. Nucl. Chem.* **1994**, *179*, 331–339.
43. J. Börjesson, T. Bellander, L. Järup, C. G. Elinder, S. Mattsson, *Occupat. Environ. Med.* **1997**, *54*, 424–431.
44. J. O. Christoffersson, S. Mattsson, *Phys. Med. Biol.* **1983**, *28*, 1135–1144.
45. U. Nilsson, S. Skerfving, *Scand. J. Work, Environ. Health* **1993**, *19*, 54–58.
46. RECIPE Chemicals + Instruments GmbH, Munich, Germany.
47. SERO AS, Seronorm™ Trace Elements Urine, Serum, Whole Blood, Billingstad, Norway.
48. T. Göen, K. H. Schaller, H. Drexler, *Int. J. Hyg. Environ. Health* (in press) **2011**.
49. J. P. Weber, *Sci. Total Environ.* **1988**, *71*, 111–123.
50. UBA, *Bundesgesundheitsblatt - Gesundheitsforschung - Gesundheitsschutz* **2011**, *54*, 981–996.
51. M. Wilhelm, U. Ewers, C. Schulz, *Int. J. Hyg. Environ. Health* **2004**, *207*, 69–73.
52. K. Becker, S. Kaus, C. Krause, P. Lepom, C. Schulz, M. Seiwert, B. Seifert, *Int. J. Hyg. Environ.l Health* **2002**, *205*, 297–308.
53. K. Becker, C. Schulz, S. Kaus, M. Seiwert, B. Seifert, *Int. J. Hyg. Environ. Health* **2003**, *206*, 15–24.
54. A. Bernard, H. Roels, A. Cardenas, R. Lauwerys, *Brit. J. Industr. Med.* **1990**, *47*, 559–565.
55. A. Bernard, *BioMetals* **2004**, *17*, 519–523.

56. A. Chaumont, F. De Winter, X. Dumont, V. Haufroid, A. Bernard, *Occupat. Environ. Med.* **2011**, *68*, 257–264.
57. T. Kawada, C. Tohyama, S. Suzuki, *Int. Arch. Occupat. Environ. Health* **1990**, *62*, 95–100.
58. H. A. Roels, R. R. Lauwerys, J. P. Buchet, A. M. Bernard, A. Vos, M. Oversteyns, *Brit. J. Indust. Med.* **1989**, *46*, 755–764.
59. M. D. Topping, H. W. Forster, C. Dolman, *Clinical Chemistry* **1986**, *32*, 1863–1866.
60. F. Wolff, D. Willems, *Clin. Biochem.***2008**, *41*, 418–422.
61. A. Bernard, *Indian J. Med. Res.* **2008**, *128*, 557–564.
62. P. E. Evrin, P. A. Peterson, L. Wide, I. Berggård, *Scand. J. Clin. Lab. Invest.* **1971**, *28*, 439–443.
63. A. Bernard, R. R. Lauwerys, *Clin. Chem.***1983**, *29*, 1007–1011.
64. A. Bernard, A. Vyskocil, R. R. Lauwerys, *Clin. Chem.* **1981**, *27*, 832–837.
65. N. Terrier, A. Bonardet, B. Descomps, J. P. Cristol, A. M. Dupuy, *Clin. Lab.* **2004**, *50*, 675–683.
66. Immundiagnostik AG, ®2-Mikroglobulin ELISA-Kit zur in vitro Bestimmung des ®2-Mikroglobulin aus Plasma, Serum und Urin (http://www.labodia.com/Kit_Protocols/inserts_immundiagnostik/immuno/b2Microglobulin.pdf; http://www.immundiagnostik.com/home/unternehmen/unternehmen-und-schwerpunkte.html), Bensheim, 2010.
67. ORGENTEC Diagnostika GmbH, Beta-2-Microglobulin, ORG 5BM 96 Tests, 2011.
68. K. A. Burling, P. R. Cutillas, D. Church, M. Lapsley, A. G. W. Norden, *Clin. Chim. Acta* **2012**, *413*, 483–489.
69. H. Shimizu, M. Negishi, Y. Shimomura, M. Mori, *Diabetes Res. Clin. Practice* **1992**, *18*, 207–210.
70. S. J. Twyman, J. Overton, D. J. Rowe, *Clin. Chim. Acta* **2000**, *297*, 155–161.
71. J. T. Whicher, C. P. Price, K. Spencer, *Crit. Rev. Clin. Lab. Sci.* **1983**, *18*, 213–260.
72. K. Jung, M. Pergande, H. J. Graubaum, L. M. Fels, U. Endl, H. Stolte, *Clin. Chem.* **1993**, *39*, 757–765.
73. L. Järup, L. Hellström, T. Alfvén, M. D. Carlsson, A. Grubb, B. Persson, C. Pettersson, G. Spång, A. Schütz, C. G. Elinder, *Occupat. Environ. Med.* **2000**, *57*, 668–672.
74. A. Noto, Y. Ogawa, S. Mori, *Clin. Chem.* **1983**, *29*, 1713–1716.
75. L. Järup, A. Åkesson, *Toxicol. Appl. Pharmacol.* **2009**, *238*, 201–208.
76. P. Hotz, J. P. Buchet, A. Bernard, D. Lison, R. Lauwerys, *Lancet* **1999**, *354*, 1508–1513.
77. E. Kobayashi, Y. Suwazono, M. Dochi, R. Honda, M. Nishijo, T. Kido, H. Nakagawa, *Toxicol. Lett.* **2008**, *179*, 108–112.
78. J. P. Buchet, R. Lauwerys, H. Roels, A. Bernard, P. Bruaux, F. Claeys, G. Ducoffre, P. De Plaen, J. Staessen, A. Amery, P. Lijnen, L. Thijs, D. Rondia, F. Sartor, A. Saint Remy, L. Nick, *Lancet* **1990**, *336*, 699–702.
79. U. Kumtabtim, A. Siripinyanond, C. Auray-Blais, A. Ntwari, J. S. Becker, *Int. J. Mass Spectrom.* **2011**, *307*, 174–181.
80. *Cadmium. Determination in Blood (Flameless atomic absorption spectrometry). Biomonitoring Methods*, *Analyses of Hazardous Substances in Biological Materials*, Wiley-VCH 1981.
81. F. Gil, A. F. Hernández, C. Márquez, P. Femia, P. Olmedo, O. López-Guarnido, A. Pla, *Sci. Total Environ.* **2011**, *409*, 1172–1180.

Chapter 5
Imaging and Sensing of Cadmium in Cells

Masayasu Taki

Contents

ABSTRACT 99
1 INTRODUCTION 100
2 CADMIUM TOXICITY IN CELLS 101
3 DETECTION OF INTRACELLULAR CADMIUM 103
3.1 Overview of Cadmium Detection 103
3.2 Principles of the Development of Fluorescence Probes for Metal Ions 103
3.3 Fluorescence Imaging of Cadmium with Calcium or Zinc Fluorescence Probes ... 104
4 CADMIUM-SELECTIVE FLUORESCENT PROBES 106
4.1 Intensity-Based Fluorescent Probes 106
4.1.1 Ultraviolet Excitation 106
4.1.2 UV-Visible Excitation 107
4.2 Ratiometric Detection of Cadmium 110
5 CONCLUDING REMARKS 112
ABBREVIATIONS 113
ACKNOWLEDGMENT 113
REFERENCES 114

Abstract Cadmium is one of the highly toxic transition metals for human beings and is known as a human carcinogen. Once humans are exposed to Cd^{2+} on a chronic basis, Cd^{2+} primarily accumulates in the liver and kidney where it forms complexes with small peptides and proteins via sulfhydryl groups. Complexed Cd^{2+} or the ionic Cd^{2+} is then taken up by target cells and tissues and exerts the toxicity. However, the question of how non-essential Cd^{2+} crosses the cell membranes remains unanswered. Furthermore, the molecular mechanism of Cd^{2+}-induced physiological signaling disruption in cells is still not fully elucidated. Investigations

M. Taki (✉)
Graduate School of Human and Environmental Studies and Graduate School of Global Environmental Studies, Kyoto University, Yoshida, Sakyo-ku, Kyoto 606-8501, Japan
e-mail: taki.masayasu.4c@kyoto-u.ac.jp

A. Sigel, H. Sigel, and R.K.O. Sigel (eds.), *Cadmium: From Toxicity to Essentiality*, Metal Ions in Life Sciences 11, DOI 10.1007/978-94-007-5179-8_5,

of Cd^{2+} uptake kinetics, distributions, and concentrations in cells require chemical tools for its detection. Because of the easy use and high spatiotemporal resolution, optical imaging using fluorescence microscopy is a well-suited method for monitoring Cd^{2+} in biological samples. This chapter summarizes design principles of small molecule fluorescent sensors for Cd^{2+} detection in aqueous solution and their photophysical and metal-binding properties. Also the applications of probes for fluorescence imaging of Cd^{2+} in a variety of cell types are demonstrated.

Keywords cadmium ion • cellular uptake • fluorescent probe • fluorescence imaging • molecular design

1 Introduction

Cadmium is one of the most widely used metals, with applicability in many fields such as industry (e.g., Ni-Cd batteries and coloring agents) and agriculture (e.g., phosphate fertilizers) [1]. More recently, semiconductor cadmium chalcogenide (CdS, CdSe, and CdTe) nanocrystals have emerged as attractive materials for biological probes due to their unique photophysical characteristics [2,3]. Consequently, the number of sources of Cd^{2+} exposure continues to increase, and the high level of Cd^{2+} contamination in soil and crops has become a cause for concern. Exposure to Cd^{2+} may occur through the ingestion of contaminated food or water and the inhalation of cigarette smoke. Cd^{2+} accumulates in organs such as the kidney, liver, gastrointestinal tract, brain, and bones, giving rise to potentially serious health disorders and even certain cancers [4,5]. In addition, cadmium has been implicated as a possible etiological factor of neurodegenerative diseases such as Parkinson's disease [6], Alzheimer's disease [7], and amyotrophic lateral sclerosis (ALS) [8]. Cadmium is, therefore, ranked as high as seventh on the Top 20 Hazardous Substances Priority List by the Agency for Toxic Substances and Disease Registry (ATSDR) and the U. S. Environmental Protection Agency (EPA) [9,10].

Cadmium has multiple effects on cellular functions including cell-cycle progression, DNA replication and repair, differentiation, and apoptotic pathways [11]. It has been reported that low concentrations of Cd^{2+} (below 100 pM) significantly stimulate cell proliferation and DNA synthesis [12], whereas Cd^{2+} exposure at concentrations above 1 μM inhibits DNA synthesis and cell division [13]. However, little is understood about the molecular mechanisms of Cd^{2+} uptake by cells and the carcinogenesis due to Cd^{2+} in humans and other mammals [14]. Therefore, the development of non-invasive tools and techniques for detecting and monitoring traces of Cd^{2+} in biological samples is necessitated in the fields of cell biology, neurophysiology, and pathophysiology.

Compared with magnetic resonance imaging (MRI) and positron emission tomography, optical imaging with fluorescence probes offers the advantages of higher sensitivity and spatial resolution in the observation of biological processes at the single molecule level [15]. At present, fluorescence indicators have been developed for most biologically relevant alkali and alkaline earth metal ions (Ca^{2+}, Mg^{2+}, Na^{+}, and K^{+}) [16], as well as the first-row transition metal cations, including zinc, copper, and iron [17]. Despite the numerous reviews summarizing the principles and photophysics of these probe designs and their utilization for cell imaging which have been published to date [18,19], there is a dearth of literature focusing on Cd^{2+}-selective fluorescent probes based on synthetic small molecules and their cellular applications. Table 1 provides an overview of the molecular designs and the optical imaging techniques applicable for the detection of intracellular Cd^{2+}.

2 Cadmium Toxicity in Cells

Exposure of cells to cadmium may result in disruption of the physiological control of signaling dynamics with consequent cellular signaling dysfunctions [20]. For instance, the replacement of Ca^{2+} with Cd^{2+} in cellular signaling processes and replacement of Zn^{2+} in many enzymes and transcription factors may induce aberrant gene expression, resulting in the stimulation of cell proliferation or suppression of apoptosis [21,22]. Additionally, Cd^{2+} exerts inhibitory activity on antioxidative enzymes and the mitochondrial electron transport chain [23]. This inhibition leads to elevated intracellular levels of reactive oxygen species (ROS) with consequent damage to DNA strands (non-specific breakage), lipid peroxidation, and generation of oxidatively modified proteins, which may eventually lead to cellular dysfunction and necrotic cell death [24]. Furthermore, it has been reported that Cd^{2+} triggers the activation of other signaling cascades to induce pro-apoptotic and/or adaptive cell responses [25]; however, the contribution of ROS to Cd^{2+}-induced cellular events such as apoptotic and necrotic cell death remains controversial [26].

The mechanisms of cellular uptake and transport of Cd^{2+} are also unresolved issues pertaining to the biological effects of cadmium [27]. Currently, a number of hypotheses have been proposed for the uptake of Cd^{2+} by cells. One such hypothesis proposes that free Cd^{2+} ions are taken up through transporters for essential metals, including calcium, iron, and zinc transporters [28]. Cd^{2+} may then interact with the binding site(s) of membrane proteins specific to these ions due to ionic mimicry. An alternate hypothesized pathway for Cd^{2+}-uptake is the receptor-mediated endocytosis of metal complexes with low molecular weight thiols, such as glutathione (GSH) and cysteine (Cys) [5]. These complexes serve as molecular homologs or mimics for amino acids, oligopeptides, or organic cations at the sites of organic molecule transporters. However, the transporters that facilitate Cd^{2+} uptake to cytosol remain largely obscure.

Table 1 Binding affinities, fluorescence wavelengths, and biological applications of fluorescent cadmium sensors.

Probe[a]	K_d for Cd^{2+}	λ_{ex}, nm Free (Cd^{2+})	λ_{em}, nm Free (Cd^{2+})	Φ Free (Cd^{2+})	Applied Cell Type	refs.
1 (Fluo-3)		488	530	<0.005 (~0.1)	thymocyte, cerebellar neuron (rat)	[37,38]
2 (Fura-2)	0.7 pM	363 (337)	512 (490)	0.23 (0.69)	CHO	[40,43]
3 (BTC-5N)	1.4 μM	459 (417)	517 (532)		PC12	[42]
4 (Fura-5F)	~1 pM	367 (339)	511		HEK293	[44]
6	~1 μM	332	520	0.0001	HL-60, Cos-7, Saos-2	[56]
7	48 μM	600 (571)	656 (597)	0.12 (0.59)	PC12, DC, HUVEC	[59,60]
8	0.14 mM, 7.7 μM	550 (562)	500	0.003 (0.3)	HeLa	[61]
9 (CYP-1)	10 mM, 0.44 μM	766 (766)	791 (791)	0.0123 (0.0345)	HeLa	[62]
10 (CYP-2)	0.11 mM, 5.3 μM	771 (771)	793 (793)	0.0059 (0.0145)		[62]
11	0.12 μM	503	521 (521)	0.00638 (0.0172)	HK-2	[63]
12 (CadMQ)	0.16 nM	365 (333)	441 (445)	0.59 (0.70)	HeLa	[65]
13 (DBITA)	25 pM	340 (359)	534 (587)	0.18 (0.42)	HeLa, macrophage	[66]
14 (DQCd1)	41 pM	420 (370)	558 (495)	0.15 (0.11)	NIH3T3, HEK293	[57]
15	1.7 μM	460 (460)	531 (487)	0.27 (0.60)		[67]

[a] For the structures of the probes see Figures 1, 3, and 4.

3 Detection of Intracellular Cadmium

3.1 Overview of Cadmium Detection

In order to provide insight into the mechanistics of cadmium toxicity, investigations of the spatiotemporal dynamics of Cd^{2+}, which causes the disruption of the physiological signal controls in cells, have become an emergent field of research. Two techniques have primarily been applied to the experimental determination of intracellular Cd^{2+} concentration. The first is the radiotracer technique that involves the use of the radioactive isotope ^{109}Cd (half-life of 462.6 days) [29]. In this case, intracellular concentrations of Cd^{2+} can be measured with significantly high sensitivity (<0.5 nM) by using a radiometric detector. Radiotracer techniques have also been applied to the detection of other transition metals such as iron (^{59}Fe) [30], copper (^{64}Cu) [31], and zinc (^{65}Zn) [32], *in vitro* as well as *in vivo*. Although this technique offers the advantage of direct observation of the uptake kinetics of metal ions by cells without any artificial effects from organic and/or inorganic additives, the use of undesirable radioactive materials limits the utility of conventional and facile experiments. Furthermore, ionic and bound Cd^{2+} cannot be distinguished using radioactive tracing techniques.

Optical imaging with fluorescence probes, which provides a response to analyte binding due to the change in the rotational mobility of the fluorescent reporter, is an alternative technique that is advantageous in terms of the spatial and temporal resolution in live samples. Furthermore, fluorescence imaging is more easily handled relative to the radioactive counterparts [33]. This technique has been utilized for probing biologically important metal ions in living cells and in tissues, especially Ca^{2+} and Zn^{2+} [34,35]. For the detection of Cd^{2+} using fluorescence, the probe molecules must meet several requirements. The most important criterion is a selective fluorescence response to Cd^{2+} under physiological conditions. Because of the chemical similarities of Cd^{2+} to Ca^{2+} and Zn^{2+}, it has been a challenging objective to distinguish the response to Cd^{2+} from that to Ca^{2+} or Zn^{2+} in fluorescence. In addition, an excitation wavelength beyond the UV region is required to minimize cell damage and background signals from an excitation light source or endogenous autofluorescence.

3.2 Principles of the Development of Fluorescence Probes for Metal Ions

Photoinduced electron transfer (PET) is the most commonly employed method for the development of small molecule-based fluorescence probes, especially for metal ions. In PET sensors, the metal ion receptor (e.g., nitrogen atoms), which acts as an electron donor, is directly linked with the fluorophore that acts as an electron

acceptor. Photoexcitation of the unmetallated probe induces electron transfer from the donor to the acceptor fluorophore, which results in fluorescence quenching. When the analyte binds to the receptor, the energy level of the donor is lowered, and the PET quenching process is inhibited to restore the original fluorescence. As a result, intensity-based fluorescent metal ion indicators can be rationally designed.

Photoinduced charge transfer (PCT) is another mechanism commonly utilized for the molecular design of ratiometric probes, which, in principle, can provide accurate and quantitative determination of the target analytes by using ratiometric imaging techniques. Perturbation of the intramolecular charge transfer (ICT) state of a fluorophore by coordination to the target metal ion influences the energy gap between the ground and excited states, resulting in a shift in the wavelength of the excitation and/or emission maxima.

3.3 Fluorescence Imaging of Cadmium with Calcium or Zinc Fluorescence Probes

Several types of Ca^{2+}-selective fluorescence probes have been developed and applied to the investigation of calcium neurophysiology [36]. Generally, Ca^{2+}-chelators can be adopted for Zn^{2+} and Cd^{2+} as well. In fact, the BAPTA (bis(*o*-aminophenoxy)ethane-*N*,*N*,*N*′,*N*′-tetraacetic acid) chelator, which is designed for tightly binding with Ca^{2+} (K_d ~300 nM), displays much higher affinity for Zn^{2+} (K_d ~0.5 nM). Because the ionic radius of Cd^{2+} (0.97 Å) is closer to that of Ca^{2+} (0.99 Å) rather than Zn^{2+} (0.74 Å), the cavity size of the BAPTA chelator is more suitable for Cd^{2+} (K_d ~0.7 pM). As a result, BAPTA-based Ca^{2+} fluorescence probes, which include **1** through **4** (Figure 1), can form extremely stable Cd^{2+}-BAPTA complexes and these are potential tools for measuring intracellular free Cd^{2+}.

Fluo-3 (**1**) is a Ca^{2+}-responsive fluorescein sensor based on the PET mechanism. The fluorescence response of Fluo-3 to Cd^{2+} is the same as that observed with Ca^{2+} or Zn^{2+}; moreover, neither of these metals influences the Cd^{2+}-induced Fluo-3 fluorescence due to the large difference in their binding constants. In practical applications, the probe is loaded into rat thymocytes as the membrane-permeable acetoxymethyl (AM) ester form. Subsequent flow cytometric analysis is characterized by increased intensity of the Fluo-3 fluorescence when the cells are exposed to Cd^{2+}, corresponding to the formation of the Cd^{2+}-Fluo-3 complex in the cells [37,38].

Fura-2 (**2**) is one of the most widely used PCT-based Ca^{2+} indicator for ratiometric measurement [39]. Fura-2 exhibits a quite similar fluorescence response to Cd^{2+} as it exhibits to Ca^{2+}, where the fluorescence excitation maximum undergoes a blue shift from 363 to 337 nm upon Cd^{2+} binding. Because of the extremely high binding affinity of Fura-2 for Cd^{2+} ($K_d = 0.7$ pM), this can probe the exceedingly low concentration of free cytosolic Cd^{2+}. Cd^{2+} uptake by CHO

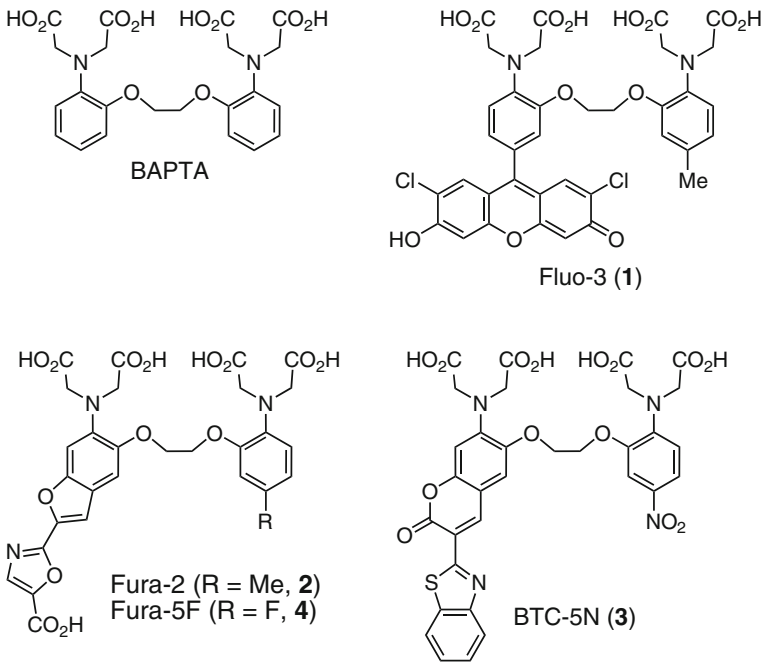

Figure 1 BAPTA-based fluorescent sensors.

cells expressing the bovine cardiac Na^+-Ca^{2+} exchanger has been detected by monitoring the change of Fura-2 ratio [40]. It has been found that the cytosolic free Cd^{2+} concentration of 0.5 ~ 2 pM stimulates the Na^+-Ca^{2+} exchange activity.

The mono-nitrated BAPTA chelator exhibits a much lower binding affinity for Ca^{2+} due to the strong electron withdrawing effect of the nitrate group, whereas the affinity for Cd^{2+} remains high enough to be exploited in the detection of intracellular Cd^{2+} (K_d = 4.4 mM for Ca^{2+} and 1.4 μM for Cd^{2+}, respectively) [41]. When PC12 cells are stained with BTC-5N (**3**), where the fluorophore is 5-nitrobenzothiazole coumarin, followed by treatment with Cd^{2+}, a considerable increase in the BTC-5N fluorescence is observed [42]. The increase in fluorescence is reduced by ~50% in the presence of Ca^{2+} channel blockers such as nifedipine and diltiazem. In contrast, treatment with Bay K 8644, which is a Ca^{2+} channel agonist, causes a significant enhancement in fluorescence. These results may indicate that Cd^{2+} enters neuronal cells through Ca^{2+} channels.

Another strategy for monitoring Cd^{2+} in cells using BAPTA-based fluorescence indicators involves the use of two types of dyes that exhibit different fluorescent responses to Ca^{2+} and Cd^{2+}, respectively. As opposed to Fura-2, no change in the fluorescence of Quin-2, which is a turn-on type Ca^{2+} indicator based on a quinoline scaffold, is induced by adding Cd^{2+} [43]. By taking advantage of the different photophysical properties of Cd^{2+} complexes of Fura-2 and Quin-2, Cd^{2+} uptake by GH3 or C6 cells can be monitored with discrimination from intracellular Ca^{2+} behavior. A similar strategy is adopted with Fura-5F (**4**) and the protein-based Ca^{2+}

sensor, Yellow Cameleon (YC) 3.60, the latter of which does not respond to changes in intracellular Cd^{2+} concentration [44]. In YC3.60-expressed HEK293 cells, Cd^{2+} exposure induces a significant change in the Fura-5F fluorescence ratios but does not induce any change in YC3.60 fluorescence.

Although BAPTA-based fluorescence probes have been used to measure intracellular Cd^{2+}, this type of probe is not appropriate when measuring the effect of Cd^{2+} on changes in the Ca^{2+} concentration.

4 Cadmium-Selective Fluorescent Probes

In order to avoid the influence of Ca^{2+} on the fluorescence imaging of target transition metal ions in cells, probes containing nitrogen and sulfur atoms in the chelator moiety rather than oxygen have been preferably employed. Among the numerous fluorescent probes developed for transition metals, Zn^{2+}-targeted probes are most commonly reported. However, most of these Zn^{2+} probes exhibit similar fluorescence responses to Cd^{2+} because of the comparable chemical properties (closed shell d^{10} configurations) of Zn^{2+} and Cd^{2+}. Thus, the design of molecules that can distinguish between Cd^{2+} and Zn^{2+} based on fluorescence is an important research objective for clarification of intracellular Cd^{2+} behavior.

4.1 Intensity-Based Fluorescent Probes

4.1.1 Ultraviolet Excitation

Several anthracene-based fluorescent sensors (compound **5** in Figure 2 is one example) that present different fluorescence responses to Cd^{2+} and Zn^{2+} in aqueous solutions have been synthesized [45–48]. In these molecules, the PET-quenched fluorescence is restored to the original anthracenic fluorescence in the presence of Zn^{2+} whereas addition of Cd^{2+} generates an anthracene-Cd^{2+} π-complex, and the resulting spectrum is red-shifted and broadened [47]. However, anthracene-based sensors for Cd^{2+} have not been utilized in cell imaging, possibly because of the instability of the d-π complex of Cd^{2+} in biological conditions.

Quinoline derivatives have been applied for monitoring labile Ca^{2+} and Zn^{2+} in cells and in the central nervous system [49,50]. Nevertheless, successful imaging of Cd^{2+} in cells using these derivatives has rarely been achieved although a number of quinoline-based Cd^{2+} sensors have been reported [51–57]. The quinoline sensor **6** (Figure 2) comprises an 8-hydroxyquinoline appended N_2S_2-donating 12-membered macrocycle [56]. The fluorescence is strongly quenched ($\Phi = 0.0001$) by an intramolecular photoinduced proton transfer (PPT) process between the hydroxyl group and the quinoline nitrogen atom. Upon addition of Cd^{2+} in a MOPS buffer solution (pH 7.4) containing liposomes, **6** may form the 1:1 Cd^{2+} complex with consequent

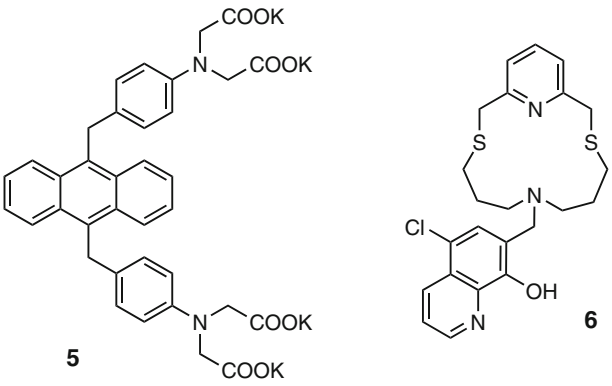

Figure 2 Ultra-violet excitable fluorescent Cd^{2+} sensors.

inhibition of the PPT process, which results in fluorescence enhancement with the maximum wavelength at 520 nm ($\lambda_{ex} = 332$ nm). The dissociation constant of the Cd^{2+} complex is ~1.0 μM in aqueous solution. Cellular Cd^{2+} imaging in HL-60, Cos-7, and Saos-2 cells has been performed using this probe. Fluorescence microscopy experiments of fixed Cos-7 cells or live cells of Saos-2 have demonstrated that this probe is cell-permeable and can respond specifically to changes in the intracellular Cd^{2+} levels. Furthermore, this probe can be applied to cytofluorimetric analyses of leukemic HL-60 cells. Co-incubation with propidium iodide (PI) allows discrimination of viable cells from damaged cells and the selective analysis of intracellular Cd^{2+} behavior.

Despite the capabilities of quinoline-based probes for selective detection of Cd^{2+}, these probes have limited applicability for optical imaging of biological samples due to the requirement for ultraviolet excitation ($\lambda_{ex} < 330$ nm), which is deleterious to biological samples and induces autofluorescence from endogenous cellular molecules such as NADH and FAD. Furthermore, the fluorescence properties of quinoline fluorophores generally depend on the solvent polarity, which may make them unsuitable for biological Cd^{2+} detection.

4.1.2 UV-Visible Excitation

Boradiazaindacene (BODIPY)-based fluorescence probes have been used for detecting Cd^{2+} in cells (Figure 3). The optical properties of BODIPY can be tuned by chemical modifications on the dye core. BODIPY dyes undergo an ICT process with a functional group at the 3'-position whereas the substituents at the *meso* position can alter the efficiency of the PET process [58].

Compound **7** is the first example of a BODIPY-based Cd^{2+}-selective probe that can be utilized for optical imaging [59]. This probe employs *N*,*N*-bis (pyridin-2-ylmethyl)benzenamine as the heavy metal ion receptor. In a mixture of aqueous acetone (1/9, v/v), the free probe exhibits a maximum emission at 656 nm

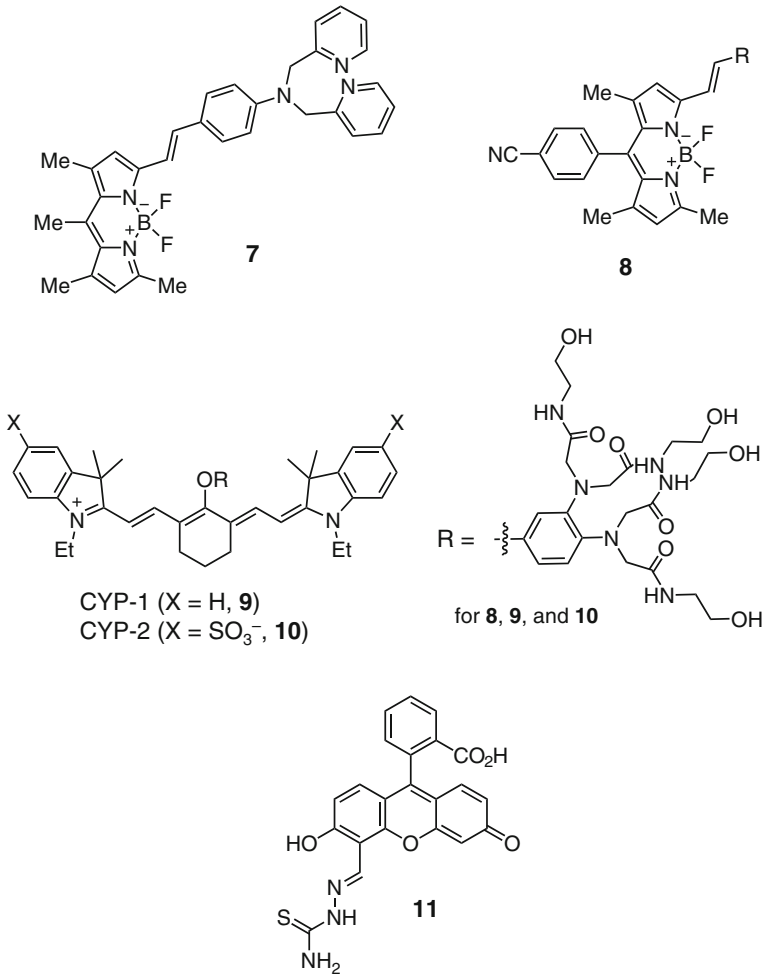

Figure 3 Intensity-based Cd^{2+} probes excitable with visible and NIR light.

with a quantum yield of 0.12. Upon addition of Cd^{2+}, the emission spectrum undergoes a blue shift to 597 nm with a quantum yield of 0.59. The emission intensity at 597 nm and the intensity ratio of two additional bands increase with gradual addition of Cd^{2+}, which allows the detection of Cd^{2+} by both normal fluorescence and ratiometric fluorescence as described in detail later in this chapter. Probe **7** forms a 1:1 Cd^{2+}-complex with a dissociation constant of 48 μM, and shows no fluorescence response to most heavy and transition metal ions including Zn^{2+}. This probe is cell-permeable and has been applied to the detection of changes in the Cd^{2+} concentrations in PC12 cells under visible light excitation. This probe can also be applied to the internalization of Cd^{2+} in Cd^{2+}-exposed human umbilical vein endothelial cells (HUVECs) [60]. In this case, the fluorescence intensity within the cells increases with increasing concentrations of Cd^{2+} in the media.

The background fluorescence of the free BODIPY probe can be minimized by introducing a strong electron-withdrawing group at the *meso* position of the BODIPY core, which results in an increase in the HOMO-LUMO gap. BODIPY **8** contains polyamide moieties as the Cd^{2+} receptor, which improves the water solubility [61]. Under physiological conditions, this probe displays very weak fluorescence ($\Phi = 0.003$) due to the efficient PET quenching of the BODIPY fluorophore by the polyamide appendage. Upon addition of Cd^{2+}, the probe undergoes a 195-fold increase in the emission intensity upon excitation at 550 nm. Probe **8** forms a Cd^{2+} complex with 1:2 stoichiometry. The enhancement of fluorescence intensity corresponds to the concentration of Cd^{2+} in a linear manner, which potentially allows for quantitative assay of the Cd^{2+} concentration. This polyamide chelator shows high Cd^{2+}-selectivity and can detect Cd^{2+} in the presence of various metal ions. Probe **8** can penetrate the cell membrane and has been used for imaging of Cd^{2+} in living cells. HeLa cells incubated with the probe followed by introduction of Cd^{2+} exhibit significantly enhanced fluorescence.

Fluorescent molecules that possess absorption and emission bands in the red/near-infrared (NIR) region are advantageous for *in vivo* imaging because of the deep penetration of this wavelength into tissues and the reduction in autofluorescence. NIR probes for Cd^{2+} include CYP-1 and CYP-2 (**9** and **10**, Figure 3), which are tricarbocyanine-based molecules [62]. These probes utilize a tetra-amide receptor for selective binding with Cd^{2+} in aqueous solutions. Cd^{2+} binding to CYP-2 triggers an increase of the fluorescence emission intensity at 793 nm in Tris-HCl buffer (pH 7.2). However, in general, the PET effect is not efficient in NIR fluorophores because of the low excitation energy. Therefore, the fluorescence quantum yield of the Cd^{2+}-bound form of CYP-2 is only twice as large as that of the metal-free form ($\Phi = 0.0059$ and 0.0145 for free and Cd^{2+} bound forms, respectively). The dissociation constants of the Cd^{2+} complexes are $K_d = 0.11$ mM and 5.3 μM corresponding to the 1:1 and 1:2 (probe : Cd^{2+}) complexes. Similar results are observed for CYP-1 in acetonitrile/water (9/1, v/v). The detection limits of Cd^{2+} are 3.1 μM with CYP-1 and 2.3 μM with CYP-2. CYP-1 is cell-permeable and has been used for imaging of Cd^{2+} in living cells. On the other hand, because of the anionic charges of the sulfonate groups, penetration of CYP-2 into the cell membrane is difficult. Incubation of HeLa cells with CYP-1 with subsequent exposure to Cd^{2+} results in fluorescence within the cells. However, in this case, it has not been confirmed whether the observed fluorescence enhancements are reversed by addition of a membrane-permeable chelator for transition metal ions such as *N*,*N*,*N*',*N*'-tetrakis(2-pyridylmethyl)ethylenediamine (TPEN).

Fluorescein and its derivatives are among the most widely employed fluorophores used as probes of metal ions, pH, enzyme, and biologically important small molecules. Although numerous fluorescence probes for Ca^{2+} and Zn^{2+} based on the fluorescein scaffold have been developed and applied to optical imaging of cells and tissues, analogs for Cd^{2+} are rare. The fluorescein-based sensor **11** (Figure 3) utilizes restriction of the C=N bond rotation upon complexation of cations to achieve on/off switching of the fluorescent system [63]. In the metal-free form, free rotation of the C=N bond elicits non-radiative quenching of the excited fluorophore and educes a relatively lower quantum yield ($\Phi = 0.00638$).

Cd^{2+} binding with probe **11** gives rise to a 1:1 complex with $K_d = 0.12$ μM; complexation occurs with a 2.7-fold fluorescence enhancement in HEPES buffer solution (pH 7.0). The fluorescence response is Cd^{2+}-selective; however, some transition metal cations such as Fe^{2+}, Co^{2+}, Ni^{2+}, Cu^{2+}, Hg^{2+}, and Zn^{2+} interfere with the Cd^{2+}-enhanced fluorescence due to the formation of stable complexes with these cations. Probe **11** is cell-permeable and has been applied to the detection of intracellular Cd^{2+} in HK-2 cells. No obvious fluorescence can be imaged in cells incubated in Cd^{2+}-free media, whereas strong fluorescence images are observed after incubation with Cd^{2+}. The intensity of the fluorescence within the cells increases with increasing concentration of Cd^{2+} in the media. Unfortunately, the quantum yield of the Cd^{2+}-bound probe is too low for optical imaging.

4.2 Ratiometric Detection of Cadmium

Fluorescent molecules that exhibit a large shift in the excitation and/or emission spectra upon analyte binding have been utilized as ratiometric probes. By monitoring the fluorescence intensity ratios at two different wavelengths before and after the reaction, the target concentrations can, in principle, be quantitatively determined without the influence of artifacts such as variations in the excitation source, emission collection efficiency, and sample thickness [64]. BODIPY **7** has been utilized not only as an intensity-based fluorescence probe but also as a tool for ratiometric imaging [59]. Upon complexation with Cd^{2+}, the ICT structure of **6** is destabilized and the emission maximum shifts from 656 to 597 nm under excitation at 580 nm. Consequently, the fluorescence intensity ratio of the peaks at 597 and 697 nm (F_{597}/F_{697}) increases. Ratiometric imaging of intracellular Cd^{2+} in dendritic cells (DCs) has been examined by utilizing probe **7**. Cd^{2+} uptake by the cells has been monitored ratiometrically by acquiring double-channel fluorescence images at 597 ± 15 and 697 ± 15 nm.

CadMQ (**12**, Figure 4) is another example of an ICT-based ratiometric fluorescence probe for Cd^{2+} [65]. This probe employs coumarin-120 (C120: 7-amino-4-methyl-coumarin) as the fluorophore. In higher polarity solvents such as water, C120 exists in the ICT configuration (planar structure), which has a relatively longer excitation wavelength than the non-planar conformation that is adopted in non-polar solvents. CadMQ exhibits an intense absorption band at 356 nm ($\varepsilon = 1.77 \times 10^5\ M^{-1}\ cm^{-1}$) in an HEPES buffer solution (pH 7.2), which is attributed to the ICT structure. Addition of Cd^{2+} triggers a decrease in the absorption band at 365 nm and a concomitant increase in the intensity of a new band at 333 nm ($\varepsilon = 1.42 \times 10^5\ M^{-1}\ cm^{-1}$) owing to the formation of a non-planar Cd^{2+} complex. The high quantum yields of both the free ligand and the Cd^{2+}-bound form ($\Phi = 0.59$ and 0.70, respectively) are suitable for the ratiometric detection of Cd^{2+} using the fluorescence intensities at two different wavelengths in the excitation spectrum. CadMQ undergoes strong complexation with Cd^{2+} ($K_d = 0.16$ nM) with a 1:1 stoichiometry, which makes this probe suitable for determining the

Cd^{2+} concentration in the detection range of 40 to 660 pM in aqueous solutions. Because of the TPEN-like receptor of CadMQ, high Cd^{2+} selectivity is exhibited by this probe even under conditions of high concentrations of Ca^{2+} and Mg^{2+}. More importantly, addition of Zn^{2+} does not affect the fluorescence ratio of the metallated/free probe. CadMQ is cell-permeable and localizes within the acidic sub-structures of cells. Addition of TPEN to Cd^{2+}-exposed HeLa cells results in a respective decrease and increase of the intensities at 340 and 387 nm. CadMQ is thus an effective probe for ratiometic monitoring of the changes in the intracellular Cd^{2+} levels.

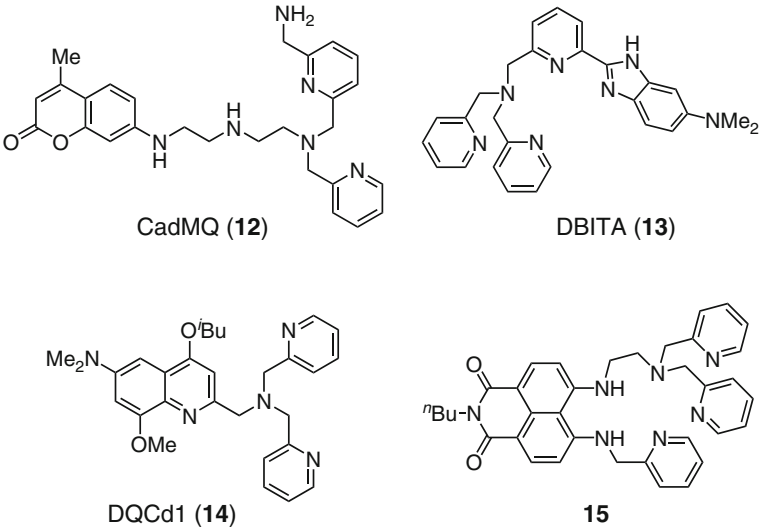

Figure 4 Ratiometric fluorescence sensors for Cd^{2+}.

The utilization of DBI (5-dimethylamino-2-(2-pyridinyl)-benzoimidazole) as a fluorophore is another approach for the development of Cd^{2+}-selective ICT probes [66]. Metal complexation with the DBI core occurs by chelation of the metal with the 2,2'-N atoms; this leads to co-planation of the pyridine and benzoimidazole moieties in DBI with consequent stabilization of the ICT structure. In this case, unlike CadMQ, red-shifted bands are observed in both the absorption and emission spectra. Free DBITA (**13**, Figure 4) exhibits an absorption band at 340 nm in an HEPES buffer solution (pH = 7.2), whereas this band is red-shifted to 359 nm upon addition of Cd^{2+} owing to the increased ICT effect in the Cd^{2+} complex. Addition of Cd^{2+} induces a distinct red shift of the emission band (λ_{ex} = 362 nm) of DBITA from 534 to 587 nm with a clear isoemissive point at 530 nm. The quantum yields are 0.18 and 0.42 for the metal free and Cd^{2+}-bound forms, respectively. Owing to the synergic coordination of the DBI and DPA chelators in DBITA to Cd^{2+}, DBITA coordinates strongly with Cd^{2+} (K_d ~ 25 pM) with a Cd^{2+}:DBITA stoichiometry of 1:1. Na^+, K^+, Ca^{2+}, and Mg^{2+} do not interfere with Cd^{2+} sensing using DBITA. Although Zn^{2+} addition triggers a red shift of the emission band

from 534 to 609 nm, there is little interference with the ratio of the fluorescence intensities at 587 and 493 nm (F_{587}/F_{493}). DBITA is membrane-permeable and has been used to track intracellular cadmium levels via dual-channel ratiometric imaging. When HeLa or macrophage cells are exposed to Cd^{2+}, changes in the intensity ratio of fluorescence within the cell, collected at 460–510 and 560–610 nm, are observed in response to the enhanced Cd^{2+} level. Treatment with TPEN distinctly reduces the emission ratio enhancement, implying that the change of the [Cd^{2+}] in cells can be reversibly monitored.

A quinoline-based ratiometric probe for Cd^{2+} has been prepared on the basis of a modified ICT mechanism [57]. In HEPES buffer solution (pH = 7.4), free DQCd1 (**14**) exhibits absorption and emission bands at 420 nm ($\varepsilon = 1.9 \times 10^3\ M^{-1}\ cm^{-1}$) and 558 nm ($\Phi = 0.15$), respectively. Under these conditions, this probe forms a resonance structure with protonation of the quinolinic nitrogen. In the presence of Cd^{2+}, DQCd1 can generate the corresponding Cd^{2+} complex ($\Phi = 0.11$) with concomitant blue shifts of the absorption and emission maxima to 370 and 495 nm, respectively. In this case, Cd^{2+} coordination to quinolinic nitrogen inhibits the formation of the resonance structure. Although Zn^{2+} partially quenches the emission of DQCd1 with a smaller hypsochromic shift ($\Delta\lambda = 48$ nm), addition of Cd^{2+} to the Zn^{2+} complex causes a rapid increase in both the fluorescence intensity and the ratio signals due to the much stronger binding affinity for Cd^{2+} ($K_d = 41$ pM). DQCd1 is cell-permeable and localizes within the acidic sub-structures of the cells. When NIH 3T3 or HEK293 cells are exposed to Cd^{2+} in the presence of this probe, a significant enhancement in the ratio of the corrected emission intensities at 430 to 490 nm and 530 to 590 nm is observed. Changes in the fluorescence can be reversed by the subsequent addition of TPEN, indicating that DQCd1 is suitable for visual observation of the changes in the intracellular [Cd^{2+}] using the ratio images.

Despite the fact that cellular application has not yet been executed, probe **15** exhibits ratiometric responses to Cd^{2+} [67]. This probe employs 4,5-diamino-1, 8-naphthalimide bearing a DPA chelator as the fluorophore. To distinguish between Zn^{2+} and Cd^{2+}, another pyridine moiety is substituted as the fifth ligand. Addition of Cd^{2+} to the free probe in a mixture of ethanol/water (1/9, v/v) induces an increase in the F_{487}/F_{531} intensity ratio. In contrast, Zn^{2+} coordination triggers a red shift of 27 nm with slight quenching of the fluorescence and does not affect the intensity ratio. Due to the use of the DPA chelator, this probe is not affected by the presence of Na^+, K^+, Ca^{2+}, and Mg^{2+}.

5 Concluding Remarks

Although many small molecule based fluorescent probes that respond to Cd^{2+} have been synthesized, only a few of these are suitable for detecting Cd^{2+} in cells with high selectivity and sensitivity. Because of the chemical similarity between Cd^{2+} and Zn^{2+}, the development of sensor molecules that are capable of distinguishing between Cd^{2+} and Zn^{2+} based on a fluorescence response remains challenging.

Establishment of strategies for rational design of the Cd^{2+} binding sites is still necessary for the efficient development of Cd^{2+}-selective fluorescent sensors. Optical imaging is a highly suitable method for monitoring cadmium uptake in cells and the toxic effects on cellular signaling processes and on mammalian tissues such as the kidney and liver. By taking advantage of multicolor imaging techniques with appropriate fluorescent indicators, changes in the intracellular Ca^{2+} and ROS concentrations can be simultaneously monitored with Cd^{2+}, and thereby, the mechanistic details of Cd^{2+} induced toxicity may be elucidated.

Abbreviations

ALS	amyotrophic lateral sclerosis
AM	acetoxymethyl
ATSDR	Agency for Toxic Substances and Disease Registry
BAPTA	bis(*o*-aminophenoxy)ethane-*N*,*N*,*N*',*N*'-tetraacetic acid
BODIPY	4,4-difluoro-4-bora-3a,4a-diaza-*s*-indacene
C120	7-amino-4-methyl-coumarin
CHO	Chinese hamster ovary
Cys	cysteine
DBI	5-dimethylamino-2-(2-pyridinyl)-benzoimidazole
DC	dendritic cell
DPA	di(2-picolyl)amine
EPA	Environmental Protection Agency
FAD	flavin adenine dinucleotide
GSH	glutathione
HEPES	4-(2-hydroxyethyl)-1-piperazineethanesulfonic acid
HUVEC	human umbilical vein endothelial cell
ICT	intramolecular charge transfer
MOPS	3-(*N*-morpholino)propanesulfonic acid
MRI	magnetic resonance imaging
NADH	reduced form of nicotinamide adenine dinucleotide
NIR	near-infrared
PCT	photoinduced charge transfer
PET	photoinduced electron transfer
PI	propidium iodide
PPT	photoinduced proton transfer
ROS	reactive oxygen species
TPEN	*N*,*N*,*N*',*N*'-tetrakis(2-pyridylmethyl)ethylenediamine
Tris	2-amino-2-hydroxymethyl-propane-1,3-diol
YC	Yellow Cameleon

Acknowledgment This work was financially supported by a Grant-in-Aid for Young Scientists (B) (No.17750155 to M.T.) from the Japan Society for the Promotion of Science (JSPS).

References

1. R. L. Chaney, J. A. Ryan, Y. M. Li, S. L. Brown, in *Cadmium in Soils and Plants*, Eds M. J. McLaughlin, B. R. Singh, Springer-Verlag, Berlin, 1999, Vol. 85, pp. 219–256.
2. A. M. Derfus, W. C. W. Chan, S. N. Bhatia, *Nano Lett.* **2004**, *4*, 11–18.
3. D. R. Larson, W. R. Zipfel, R. M. Williams, S. W. Clark, M. P. Bruchez, F. W. Wise, W. W. Webb, *Science* **2003**, *300*, 1434–1436.
4. J. D. Park, N. J. Cherrington, C. D. Klaassen, *Toxicol. Sci.* **2002**, *68*, 288–294.
5. C. C. Bridges, R. K. Zalups, *Toxicol. Appl. Pharmacol.* **2005**, *204*, 274–308.
6. B. Okuda, Y. Iwamoto, H. Tachibana, M. Sugita, *Clin. Neurol. Neurosurg.* **1997**, *99*, 263–265.
7. L. F. Jiang, T. M. Yao, Z. L. Zhu, C. Wang, L. N. Ji, *Biochim. Biophys. Acta* **2007**, *1774*, 1414–1421.
8. M. Bergomi, M. Vinceti, G. Nacci, V. Pietrini, P. Brätter, D. Alber, A. Ferrari, L. Vescovi, D. Guidetti, P. Sola, S. Malagu, C. Aramini, G. Vivoli, *Environ. Res.* **2002**, *89*, 116–123.
9. Agency for Toxic Substances and Disease Registry. Priority List of Hazardous Substances for 2011. http://www.atsdr.cdc.gov/spl/.
10. R. M. Ray, M. M. Mumtaz, *Food Chem. Toxicol.* **1996**, *34*, 1163–1165.
11. G. Bertin, D. Averbeck, *Biochimie* **2006**, *88*, 1549–1559.
12. T. von Zglinicki, C. Edwall, E. Östlund, B. Lind, M. Nordberg, N. R. Ringertz, J. Wroblewski, *J. Cell Sci.* **1992**, *103*, 1073–1081.
13. U. K. Misra, G. Gawdi, S. V. Pizzo, *Cell. Signal.* **2003**, *15*, 1059–1070.
14. M. P. Waalkes, *J. Inorg. Biochem.* **2000**, *79*, 241–244.
15. R. Y. Tsien, *Nat. Cell Biol.* **2003**, SS16–SS21.
16. I. Johnson, *Histochem. J.* **1998**, *30*, 123–140.
17. E. L. Que, D. W. Domaille, C. J. Chang, *Chem. Rev.* **2008**, *108*, 1517–1549.
18. P. J. Jiang, Z. J. Guo, *Coord. Chem. Rev.* **2004**, *248*, 205–229.
19. A. P. de Silva, H. Q. N. Gunaratne, T. Gunnlaugsson, A. J. M. Huxley, C. P. McCoy, J. T. Rademacher, T. E. Rice, *Chem. Rev.* **1997**, *97*, 1515–1566.
20. F. Thévenod, *Toxicol. Appl. Pharmacol.* **2009**, *238*, 221–239.
21. M. T. Antonio, L. Corredor, M. L. Leret, *Toxicol. Lett.* **2003**, *143*, 331–340.
22. E. López, C. Arce, M. J. Oset-Gasque, S. Cañadas, M. P. González, *Free Radic. Biol. Med.* **2006**, *40*, 940–951.
23. Y. D. Wang, J. Fang, S. S. Leonard, K. M. K. Rao, *Free Radic. Biol. Med.* **2004**, *36*, 1434–1443.
24. M. Waisberg, P. Joseph, B. Hale, D. Beyersmann, *Toxicology* **2003**, *192*, 95–117.
25. F. Thévenod, *Nephron Physiol.* **2003**, *93*, p87–93.
26. K. Nakamura, Y. Yasunaga, D. Ko, L. L. Xu, J. W. Moul, D. M. Peehl, S. Srivastava, J. S. Rhim, *Int. J. Oncol.* **2002**, *20*, 543–547.
27. R. K. Zalups, S. Ahmad, *Toxicol. Appl. Pharmacol.* **2003**, *186*, 163–188.
28. F. Thévenod, *Biometals* **2010**, *23*, 857–875.
29. C. Erfurt, E. Roussa, F. Thévenod, *Am. J. Physiol. Cell Physiol.* **2003**, *285*, C1367–C1376.
30. D. R. Richardson, A. C. G. Chua, E. Baker, *J. Lab. Clin. Med.* **1999**, *133*, 144–151.
31. N. Adonai, K. N. Nguyen, J. Walsh, M. Iyer, T. Toyokuni, M. E. Phelps, T. McCarthy, D. W. McCarthy, S. S. Gambhir, *Proc. Natl. Acad. Sci. USA* **2002**, *99*, 3030–3035.
32. A. Takeda, H. Tamano, S. Enomoto, N. Oku, *Cancer Res.* **2001**, *61*, 5065–5069.
33. R. McRae, P. Bagchi, S. Sumalekshmy, C. J. Fahrni, *Chem. Rev.* **2009**, *109*, 4780–4827.
34. J. W. Putney Jr., *Cell Calcium* **1990**, *11*, 611–624.
35. S. Ueno, M. Tsukamoto, T. Hirano, K. Kikuchi, M. K. Yamada, N. Nishiyama, T. Nagano, N. Matsuki, Y. Ikegaya, *J. Cell Biol.* **2002**, *158*, 215–220.
36. *Calcium Measurement Methods*, Vol. 43 of *Neuromethods*, Eds A. Verkhratsky, O. H. Petersen, Humana Press, New York, 2010, pp. 1–256.
37. T. Kawanai, M. Fujinaga, K. Koizumi, I. Kurotani, E. Hashimoto, M. Satoh, S. Imai, N. Miyoshi, Y. Oyama, *Biometals* **2011**, *24*, 903–914.

38. Y. Nishimura, J. Yamaguchi, A. Kanada, K. Horimoto, K. Kanemaru, M. Satoh, Y. Oyama, *Toxicol. Vitro* **2006**, *20*, 211–216.
39. G. Grynkiewicz, M. Poenie, R. Y. Tsien, *J. Biol. Chem.* **1985**, *260*, 3440–3450.
40. H. D. Le, A. Omelchenko, L. V. Hryshko, A. Uliyanova, M. Condrescu, J. P. Reeves, *J. Physiol.* **2005**, *563*, 105–117.
41. M. Soibinet, V. Souchon, I. Leray, B. Valeur, *J. Fluoresc.* **2008**, *18*, 1077–1082.
42. A. G. Kanthasamy, G. E. Isom, J. L. Borowitz, *Toxicol. Lett.* **1995**, *81*, 151–157.
43. P. M. Hinkle, E. D. Shanshala, E. J. Nelson, *J. Biol. Chem.* **1992**, *267*, 25553–25559.
44. B. E. Tvermoes, G. S. Bird, J. H. Freedman, *PLoS One* **2011**, *6*, e20542.
45. E. U. Akkaya, M. E. Huston, A. W. Czarnik, *J. Am. Chem. Soc.* **1990**, *112*, 3590–3593.
46. M. Choi, M. Kim, K. D. Lee, K. N. Han, I. A. Yoon, H. J. Chung, J. Yoon, *Org. Lett.* **2001**, *3*, 3455–3457.
47. T. Gunnlaugsson, T. C. Lee, R. Parkesh, *Org. Lett.* **2003**, *5*, 4065–4068.
48. T. Gunnlaugsson, T. C. Lee, R. Parkesh, *Tetrahedron* **2004**, *60*, 11239–11249.
49. R. Charest, P. F. Blackmore, B. Berthon, J. H. Exton, *J. Biol. Chem.* **1983**, *258*, 8769–8773.
50. C. J. Frederickson, *Int. Rev. Neurobiol.* **1989**, *31*, 145–238.
51. L. Xue, C. Liu, H. Jiang, *Org. Lett.* **2009**, *11*, 1655–1658.
52. L. Xue, Q. Liu, H. Jiang, *Org. Lett.* **2009**, *11*, 3454–3457.
53. L. Prodi, M. Montalti, N. Zaccheroni, J. S. Bradshaw, R. M. Izatt, P. B. Savage, *Tetrahedron Lett.* **2001**, *42*, 2941–2944.
54. X. L. Tang, X. H. Peng, W. Dou, J. Mao, J. R. Zheng, W. W. Qin, W. S. Liu, J. Chang, X. J. Yao, *Org. Lett.* **2008**, *10*, 3653–3656.
55. Y. M. Zhang, Y. Chen, Z. Q. Li, N. Li, Y. Liu, *Bioorg. Med. Chem.* **2010**, *18*, 1415–1420.
56. M. Mameli, M. C. Aragoni, M. Arca, C. Caltagirone, F. Demartin, G. Farruggia, G. De Filippo, F. A. Devillanova, A. Garau, F. Isaia, V. Lippolis, S. Murgia, L. Prodi, A. Pintus, N. Zaccheroni, *Chem. Eur. J.* **2010**, *16*, 919–930.
57. L. Xue, G. P. Li, Q. Liu, H. H. Wang, C. Liu, X. L. Ding, S. G. He, H. Jiang, *Inorg. Chem.* **2011**, *50*, 3680–3690.
58. T. Y. Cheng, T. Wang, W. P. Zhu, X. L. Chen, Y. J. Yang, Y. F. Xu, X. H. Qin, *Org. Lett.* **2011**, *13*, 3656–3659.
59. X. J. Peng, J. J. Du, J. L. Fan, J. Y. Wang, Y. K. Wu, J. Z. Zhao, S. G. Sun, T. Xu, *J. Am. Chem. Soc.* **2007**, *129*, 1500–1501.
60. Z. W. Dong, L. Wang, J. P. Xu, Y. L. Li, Y. Zhang, S. Zhang, J. Y. Miao, *Toxicol. Vitro* **2009**, *23*, 105–110.
61. T. Y. Cheng, Y. F. Xu, S. Y. Zhang, W. P. Zhu, X. H. Qian, L. P. Duan, *J. Am. Chem. Soc.* **2008**, *130*, 16160–16161.
62. Y. Y. Yang, T. Y. Cheng, W. P. Zhu, Y. F. Xu, X. H. Qian, *Org. Lett.* **2011**, *13*, 264–267.
63. W. M. Liu, L. W. Xu, R. L. Sheng, P. F. Wang, H. P. Li, S. K. Wu, *Org. Lett.* **2007**, *9*, 3829–3832.
64. R. Y. Tsien, M. Poenie, *Trends Biochem. Sci.* **1986**, *11*, 450–455.
65. M. Taki, M. Desaki, A. Ojida, S. Iyoshi, T. Hirayama, I. Hamachi, Y. Yamamoto, *J. Am. Chem. Soc.* **2008**, *130*, 12564–12565.
66. Z. P. Liu, C. L. Zhang, W. J. He, Z. H. Yang, X. A. Gao, Z. J. Guo, *Chem. Commun.* **2010**, *46*, 6138–6140.
67. C. L. Lu, Z. C. Xu, J. N. Cui, R. Zhang, X. H. Qian, *J. Org. Chem.* **2007**, *72*, 3554–3557.

Chapter 6
Use of ^{113}Cd NMR to Probe the Native Metal Binding Sites in Metalloproteins: An Overview

Ian M. Armitage, Torbjörn Drakenberg, and Brian Reilly

Contents

ABSTRACT 117
1 INTRODUCTION 118
2 GENERAL CONSIDERATIONS AND BASIC PRINCIPLES 119
3 ^{113}Cd NMR CHEMICAL SHIFTS FROM ^{113}Cd-SUBSTITUTED METALLOPROTEINS 123
4 SPECIFIC HIGHLIGHTS OF STUDIES ON ALKALINE PHOSPHATASE, CALCIUM BINDING PROTEINS, AND METALLOTHIONEINS 126
4.1 ^{113}Cd NMR and Alkaline Phosphatase 126
4.2 ^{113}Cd NMR and Calcium Binding Proteins 129
4.2.1 Calbindin D_{9k}, a Study of Mutants 129
4.2.2 Calmodulin, Target Peptide Binding 132
4.3 ^{113}Cd NMR and Metallothionein 134
5 CONCLUSIONS AND OUTLOOK 137
ABBREVIATIONS 138
ACKNOWLEDGMENTS 138
REFERENCES 138

Abstract Our laboratories have actively published in this area for several years and the objective of this chapter is to present as comprehensive an overview as possible. Following a brief review of the basic principles associated with ^{113}Cd NMR methods, we will present the results from a thorough literature search for ^{113}Cd chemical shifts from metalloproteins. The updated ^{113}Cd chemical shift

I.M. Armitage (✉) • B. Reilly
Department of Biochemistry, Molecular Biology, and Biophysics, University of Minnesota, 6-155 Jackson Hall, 321 Church Street S.E., Minneapolis, MN 55455, USA
e-mail: armit001@umn.edu; reil0080@umn.edu

T. Drakenberg
Department of Biophysical Chemistry, Lund University, P.O. Box 124, SE-22100 Lund, Sweden
e-mail: torbjorn.drakenberg@bpc.lu.se

A. Sigel, H. Sigel, and R.K.O. Sigel (eds.), *Cadmium: From Toxicity to Essentiality*, Metal Ions in Life Sciences 11, DOI 10.1007/978-94-007-5179-8_6,

figure in this chapter will further illustrate the excellent correlation of the ^{113}Cd chemical shift with the nature of the coordinating ligands (N, O, S) and coordination number/geometry, reaffirming how this method can be used not only to identify the nature of the protein ligands in uncharacterized cases but also the dynamics at the metal binding site. Specific examples will be drawn from studies on alkaline phosphatase, Ca^{2+} binding proteins, and metallothioneins.

In the case of *Escherichia coli* alkaline phosphatase, a dimeric zinc metalloenzyme where a total of six metal ions (three per monomer) are involved directly or indirectly in providing the enzyme with maximal catalytic activity and structural stability, ^{113}Cd NMR, in conjunction with ^{13}C and ^{31}P NMR methods, were instrumental in separating out the function of each class of metal binding sites. Perhaps most importantly, these studies revealed the chemical basis for negative cooperativity that had been reported for this enzyme under metal deficient conditions. Also noteworthy was the fact that these NMR studies preceeded the availability of the X-ray crystal structure.

In the case of the calcium binding proteins, we will focus on two proteins: calbindin D_{9k} and calmodulin. For calbindin D_{9k} and its mutants, ^{113}Cd NMR has been useful both to follow actual changes in the metal binding sites and the cooperativity in the metal binding. Ligand binding to calmodulin has been studied extensively with ^{113}Cd NMR showing that the metal binding sites are not directly involved in the ligand binding. The ^{113}Cd chemical shifts are, however, exquisitely sensitive to minute changes in the metal ion environment.

In the case of metallothionein, we will reflect upon how ^{113}Cd substitution and the establishment of specific Cd to Cys residue connectivity by proton-detected heteronuclear ^{1}H-^{113}Cd multiple-quantum coherence methods (HMQC) was essential for the initial establishment of the 3D structure of metallothioneins, a protein family deficient in the regular secondary structural elements of α-helix and β-sheet and the first native protein identified with bound Cd. The ^{113}Cd NMR studies also enabled the characterization of the affinity of the individual sites for ^{113}Cd and, in competition experiments, for other divalent metal ions: Zn, Cu, and Hg.

Keywords alkaline phosphatase • calbindin • calcium-binding proteins • calmodulin • metallothionein • ^{113}Cd NMR methods • ^{113}Cd NMR chemical shifts from metalloproteins

1 Introduction

Speaking on behalf of myself (IMA) and my co-authors, it was a delight to accept the invitation from the Editors to write a chapter for Volume 11 of this series. This provided us with the opportunity to do a thorough review of the use of ^{113}Cd NMR to probe the structure and dynamics at the metal binding sites in metalloproteins that we were actively involved in pioneering some 30 plus years ago [1–4] following up on the early study on the ligand dependence of the ^{113}Cd chemical shift in small molecules [5]. Several reviews devoted to ^{113}Cd NMR studies in

biological systems have appeared since in the literature [6–12]. In this chapter, we focus exclusively on solution ^{113}Cd NMR studies on biological systems. For solid state ^{113}Cd NMR studies we would refer the reader to the pioneering work of Ellis and co-workers [13] and the section on solid state ^{113}Cd NMR studies in the Summers review [9]. While the preponderance of these ^{113}Cd NMR studies report on Zn- or Ca-binding proteins, there are a handful of examples where ^{113}Cd has been used to probe the native Fe, Mn, Mg, and Cu sites in metalloproteins [14–17]. It is not surprising that Cd is a good surrogate for Zn as both are in the same group in the periodic table with a d^{10} valence electron configuration and similar ligand and coordination number preferences, although the ionic radius of Cd^{2+} is larger than Zn^{2+}, 0.98 Å *versus* 0.74 Å, respectively [18]. It may be somewhat more surprising that Cd is also a good substitute for Ca even though their coordination chemistry is quite different, as Cd strongly prefers nitrogen and sulfur over oxygen ligation, which is the preference for Ca. However, the ionic radius of Cd (0.98 Å) is very close to that of Ca (0.96 Å). The most unlikely metal ion, of the ones mentioned above, to be replaced by Cd is Mg which is much smaller than Cd and has a preference for oxygen ligands.

As will be discussed in Section 2, chemical exchange broadening may play a major role in the detection of the bound ^{113}Cd metal ion, which is a consequence of the extreme sensitivity of the Cd chemical shift to pertubations in its ligand environment. The simple illustration that we offer to explain ^{113}Cd sensitivity to chemical exchange broadening is the difference between ^{113}Cd NMR studies of a metalloprotein *versus* a metalloenzyme. In the former, the metal binding site is frequently there to establish the integrity of the protein, e.g., zinc finger proteins, metallothionein [12], or α-lactalbumin [19], where the metal coordination shell is usually filled with protein ligands, which helps suppress effects from chemical exchange. However, in the latter case there is frequently an open coordination site that is required for the binding of the substrate and catalysis. This situation can lead to the exchange of solvent counterions at the open coordination site that in many cases can result in an exchange-broadened and undetectable ^{113}Cd resonance, *vide infra* alkaline phosphatase. The four proteins that we have selected to highlight the biological applications of ^{113}Cd NMR provide a clear illustration of these fundamental differences (see Section 4).

2 General Considerations and Basic Principles

The preponderance of biological systems whose function depends on the binding of the native metal ions Zn, Mg, and Ca provided the impetus behind our efforts to develop and apply spin $I = 1/2$ ^{113}Cd NMR methods to characterize the structural and/or functional role of these native metal ions. While these native metal ions are not strictly spectroscopically silent, they all have isotopes with non-zero spin quantum number $I > 1$ which makes them difficult to use but not totally intractable for studies of macromolecules [7,20].

The foundation for developing the biological applications of ^{113}Cd NMR traces back to the early ^{113}Cd NMR studies on small molecules, which identified the extreme sensitivity of the chemical shift and relaxation properties to the ligand environment [5,21,22]. There are two spin ½ isotopes of Cd, ^{111}Cd and ^{113}Cd, with a natural abundance sensitivity about eight-fold that of natural abundance ^{13}C. Isotopic enrichment (96%) provides an additional eight-fold enhancement of sensitivity, which enables studies at a few tenths millimolar concentration of metalloprotein in most cases. An overwhelming majority of the Cd NMR studies have been on ^{113}Cd, which is slightly more sensitive than ^{111}Cd.

Chemical shifts/nuclear screening: Electrons around the nucleus shield it from the applied magnetic field giving rise to NMR's perhaps most ubiquitous parameter, the chemical shift. Electrons in s-orbitals have spherical symmetry and result in an upfield or diamagnetic shift while p- and d-orbitals result in a deshielding or paramagnetic shift. For protons, naturally the diamagnetic term dominates while for elements beyond the second row in the periodic table, the paramagnetic term usually dominates the screening. In this chapter, we have made our utmost effort to retrieve and list all the solution ^{113}Cd NMR studies of biological systems and present them with references in Section 3 and Figure 2. For the electron-rich ^{113}Cd ion complexed to a host of different metallo-proteins/enzymes, this translates into a chemical shift scale of ~950 ppm!

Coupling constants: The observation of through bond scalar coupling from/to ^{113}Cd provides, among other things, insight into the degree of covalency of the ^{113}Cd-ligand bond. For representative examples of ^{1}H, ^{13}C, ^{31}P, and ^{15}N scalar couplings to ^{113}Cd, which date back to the mid 70s and early 80s, the reader is referred to Table II in Armitage and Boulanger [8]. The significance of the observation of coupling from ^{113}Cd to the protein ligands will be clearly illustrated in the alkaline phosphatase and metallothionein studies presented in Section 4. Before leaving this section, we would be remiss by not mentioning the following. Many years ago, the dihedral angle dependence of three bond ^{1}H-^{1}H coupling was reported [23], which has subsequently been established for numerous three bond coupling constants and as such provided an important additional structural constraint in protein structure calculations. In 1994, the Vašák lab demonstrated the dihedral angle dependence of the three bond ^{113}Cd-^{1}H coupling [24].

Chemical Exchange: A phenomenon that is especially important in ^{113}Cd NMR is the effect of chemical exchange. The importance of this stems from the extreme sensitivity of the ^{113}Cd chemical shift (~950 ppm), which makes it sensitive to exchange rates that are faster by orders of magnitude compared to the conventional exchange rates affecting nuclei like ^{13}C and ^{1}H. In the Introduction, this has been alluded to with the analogy between metalloproteins and metalloenzymes.

There are at least three different kinds of exchange that can significantly affect the ^{113}Cd NMR spectrum: (i) Direct metal ion exchange between the free and protein bound states; (ii) Exchange of metal ion ligands and; (iii) Exchange between two or more protein conformations, which perturb the ^{113}Cd chemical shift with no direct change in metal coordination. The second type of exchange is not likely to appear in metalloproteins where the metal coordination shell is

usually filled with protein ligands. For metalloenzymes, on the other hand, an open coordination site is often essential for the function of the enzyme. The other two types of exchange could occur in any kind of metalloprotein and have been observed.

In view of the potential role of this exchange affecting the chemical shift, it is important to conduct the appropriate experiments (varying temperature, pH, solvent counterions, etc.) to rule in or out the presence of chemical exchange whenever the shift is being used to report on the nature of the protein ligands. Specific examples are: the shift of the A-site Cd in alkaline phosphatase (AP) from 122 ppm in Tris-acetate to 169 ppm in Tris-chloride and in human carbonic anhydrase B (HCAB) where the replacement of the Cd-bound H_2O or ^-OH with Cl^- results in a shift from ~145 ppm to ~ 240 ppm. Both of these examples illustrate the deshielding affect of the metal bound Cl^-.

Relaxation Properties: A knowledge of the spin relaxation properties is of interest for at least two reasons. The first is related to the use of acquisition parameters for optimum signal-to-noise acquisition times and the second is to use the relaxation data to provide important information concerning motional dynamics in and around the metal binding site. Unfortunately, to our knowledge there has been no comprehensive ^{113}Cd NMR relaxation study on macromolecular systems, which limits our discussion of this topic to early, preliminary investigative studies dating back to the mid to late 80s.

Our field-dependent ^{113}Cd NOE and T_1 measurements at 2.1 T and 4.7 T at that time revealed about an equal contribution from the chemical shift anisotropy (CSA) and dipolar relaxation mechanisms when analyzed by the standard isotropic rigid rotor expressions [6,25]. A strong contribution from CSA was not surprising but an almost equal dipolar contribution was, considering the relatively long distance ($\geq$ 3.5 Å) to the nearest ligand protons. However, the measured NOEs revealed a dipolar modulation process at a more effective relaxation frequency than overall protein reorientation was necessary to account for the experimental NOE. To explain the large dipolar contribution, we proposed a mechanism which involved the contribution from the facile exchange rate (10^8 to 10^9 s^{-1}) of ionizable protons on solvent molecules in the immediate vicinity of the metal ion. Support for this model comes from studies of the exchange rates of water molecules (10^8 to 10^9 s^{-1}) in the vicinity of the metal ion [26–28]. This model, and the supporting T_1 and NOE plots, was presented in a review on ^{113}Cd NMR by Armitage and Boulanger [8]. However, in the process of compiling the material for this chapter, IMA was made aware of an error that was made in the ^{1}H-^{113}Cd dipolar relaxation plots presented in this latter reference and in two earlier publications [6,25]. The error involved not properly taking into account both the sign of the gyromagnetic ratio and the opposite sense of the angular precession of the ^{113}Cd spins. This error was discovered after reading a paper by Kay et al. [29], which referred to two papers by Werbelow [30,31]. Subsequent communication with Lewis Kay and especially Larry Werbelow proved invaluable to the explanation and to our understanding of the miscalculation. Re-evaluating the interpretation of the relaxation rate and NOE values in the slow motion limit using the corrected plots provides a new

understanding of the data. For reference, Figure 1a shows the corrected NOE *versus* correlation time plot at three different field strengths with the incorrect plot at 4.7 T for comparison. Note the dramatic change in the slow motion limit NOE values, which was also reflected in this regime for the exchange NOE plot shown in Figure 1b.

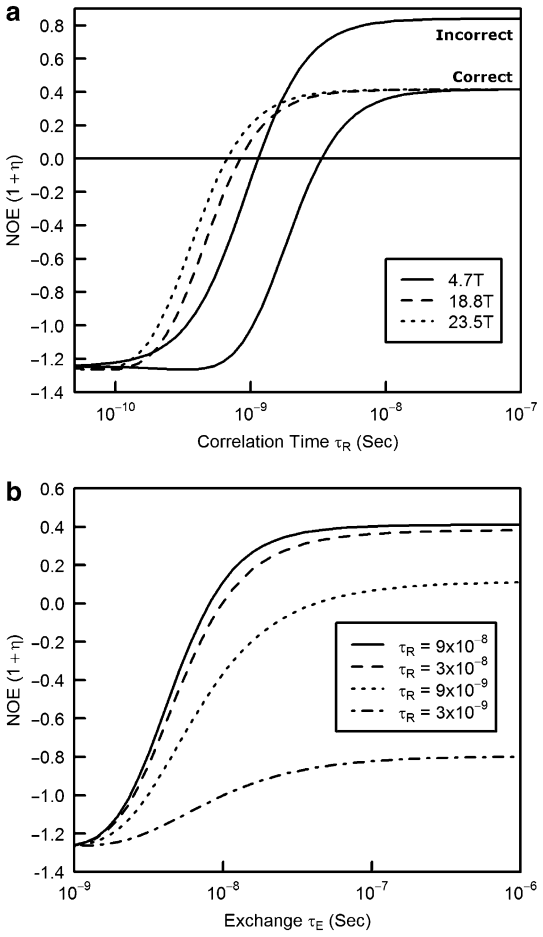

Figure 1 (**a**) Theoretical plots of the ^{1}H-^{113}Cd NOE *versus* correlation time, τ_R, in seconds at different field strengths. See [6,8,25] for the description of the model and parameters used. (**b**) Theoretical plots of the ^{113}Cd NOE *versus* exchange time, τ_e, at 2.1 T for a range of τ_R values. See [8] for a description of the model and parameters used.

3 ^{113}Cd NMR Chemical Shifts from ^{113}Cd-Substituted Metalloproteins

Figure 2 [1–4,13–17,19,24–26,32–187] illustrates that oxygen ligands provide the greatest shielding with a progressive deshielding upon substitution with nitrogen ligands to the most deshielded state containing all sulfur ligation from cysteines. In the case of mixed ligands (O, N, S), we would draw your attention to the excellent correlation in the deshielding with the number of N and S ligands. Starting from all oxygens, there is an approximate downfield shift of 100 ppm per N (from histidine) and 200 ppm per S (from cysteine). Also, in the case of all cysteine S ligation, there is a clear discrimination in the ^{113}Cd shift with the participation of terminal versus bridging cysteines with the former being the most deshielded, at about 700 ppm or lower field for 4S. There is also a clear difference between cysteine and methionine sulfur ligands with participation of the latter being more shielded by about 100 ppm. In addition to the shielding contributions originating from the identity of the ligands, there is a contribution from both the coordination number and geometry as is best seen for the all oxygen binding sites in the calcium binding proteins. More shielding results from increasing the coordination number and deshielding correlates well with the number of charged ligands.

All of the ^{113}Cd chemical shifts for cadmium bound to calcium sites are to high field of the 0.1 M $Cd(ClO_4)_2$ [$Cd(H_2O)_6^{2+}$] reference standard at 0 ppm and are, therefore, negative. The standard is in effect itself an all oxygen octahedral complex. They span almost 200 ppm with as yet no definitive consensus as to what causes the large spread. Contributing factors are definitely the number of charged ligands, the total number of ligands, and the symmetry of the site.

All Ca^{2+} binding sites for the proteins in Figure 2 are either hexa- or hepta-coordinated. The two hexa-coordinated structures, trypsin [188] and insulin [189], have ^{113}Cd shifts clearly downfield from the hepta-coordinated proteins in agreement with the notion that a higher coordination number will result in an upfield shift. The truly hepta-coordinated structures, α-lactalbumin [190], lysozyme [191], and peroxidase [192], differ by only one charge in the first coordination sphere, but the ^{113}Cd shift difference is more than 100 ppm between peroxidase and the other proteins. We have presently no explanation for this large shift difference unless the structure around the cadmium ion differs from that of calcium, for example, being octa-coordinated in peroxidase.

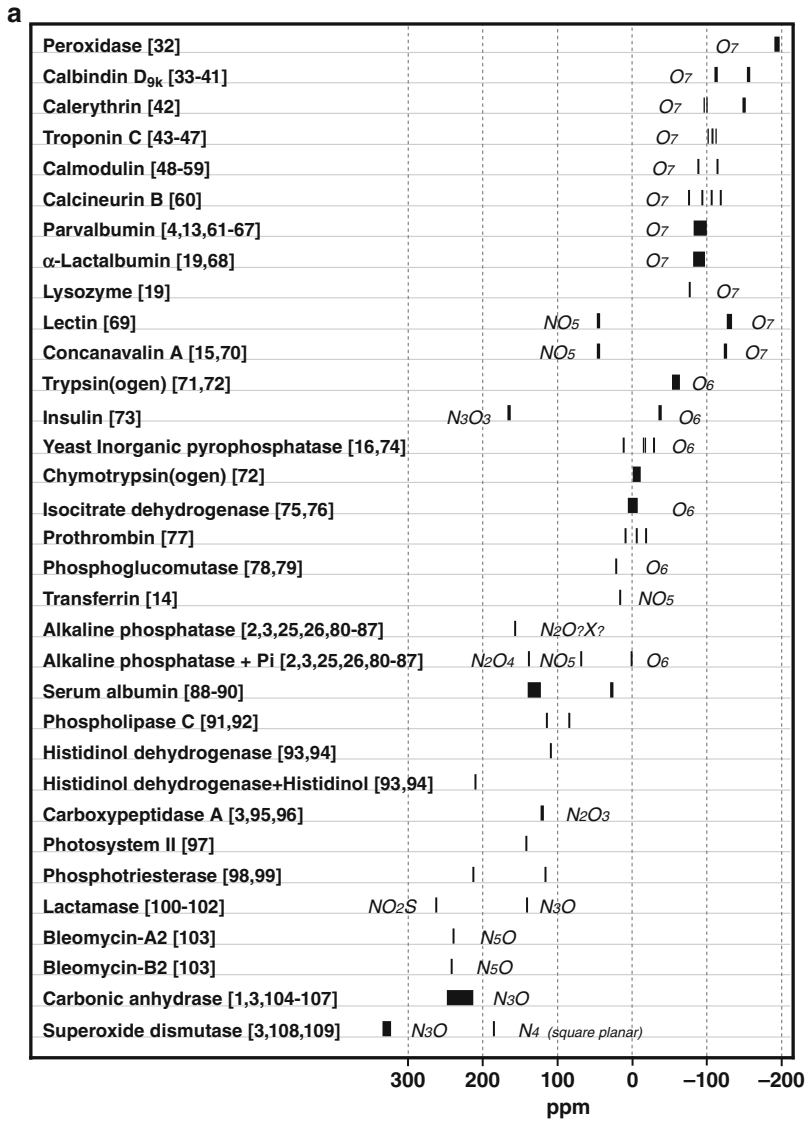

Figure 2 The ^{113}Cd NMR chemical shifts from ^{113}Cd-substituted metalloproteins. The chemical shifts are represented as bars. For proteins with representatives from different sources, like parvalbumin and metallothionein, the width of the bar indicate the spread in shift, including two for each parvalbumin and seven for each metallothionein. For most of the entries metal ligands are shown: S for cysteine, S* for methionine, N for histidine, and O for all types of oxygen ligands. Numbers within brackets refer to references in the list of references.

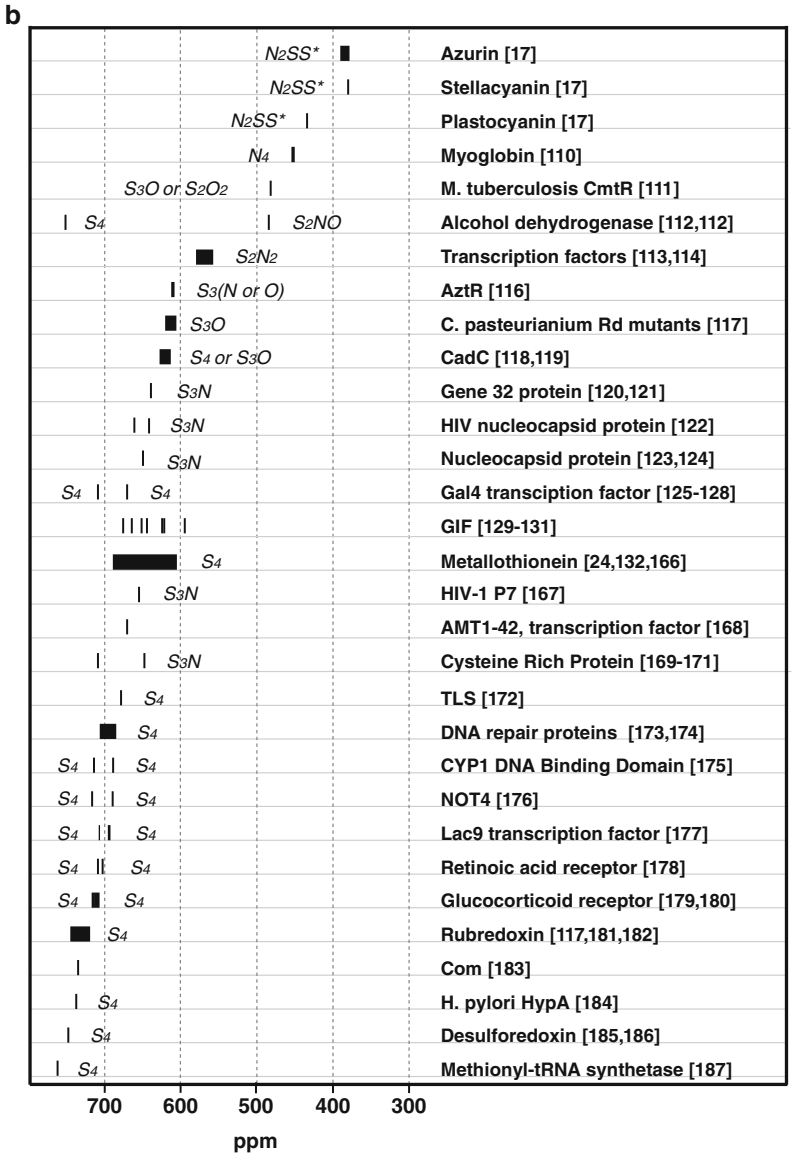

Figure 2 (continued)

The remainder of the calcium binding proteins in Figure 2 are formally hepta-coordinated but with bidentate cordination from a single carboxylate group which will make a distorted pentagonal bipyramidal structure that may more resemble octahedral symmetry with the bidentate group seen as a single ligand [193–200]. For this group of proteins, including almost forty ^{113}Cd shifts, a linear correlation is observed over 70 ppm for the ^{113}Cd chemical shift versus the number of charged ligands (Figure 3).

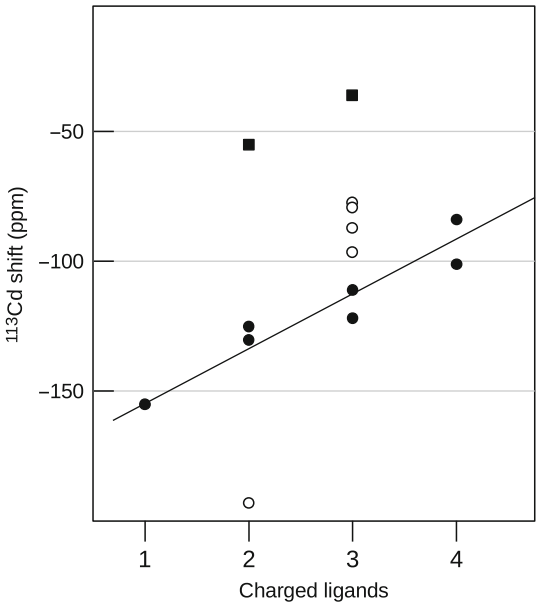

Figure 3 ^{113}Cd chemical shifts for calcium binding proteins with only oxygen ligands plotted *versus* the number of charged ligands. ■, hexa-coordinated, octahedral symmetry; ○, hepta-coordinated with only monodentate ligands; ●, hepta-coordinated with one bidentate and five monodentate ligands.

4 Specific Highlights of Studies on Alkaline Phosphatase, Calcium Binding Proteins, and Metallothioneins

Each of the examples discussed below in this section illustrate, in different ways, how ^{113}Cd NMR methods have been used to provide new insight into the structural, dynamics and functional role of the metal binding site.

4.1 ^{113}Cd NMR and Alkaline Phosphatase

Escherichia coli alkaline phosphatase, a dimeric zinc metalloenzyme (~95,500 Da), binds 2 Zn ions and 1 Mg ion per monomer and functions in the non-specific hydrolysis of phosphate monoester. ^{13}C NMR on ^{13}C labeled histidine biosynthetically incorporated into AP in conjunction with substrate ^{31}P NMR and ^{113}Cd NMR methods were used for the assignment of the three ^{113}Cd resonances to specific sites per monomer and their role in substrate binding. A full account of these studies can be found in the following references [6,25,80,82,201].

^{113}Cd titration of the apoenzyme showed that the first two equivalents of added ^{113}Cd gave a single sharp resonance at 169 ppm consistent with the selective binding to a pair of symmetrically disposed A sites on the dimer. Continued titration with ^{113}Cd to produce the saturated $^{113}Cd_6$ enzyme resulted in the progressive loss of the resonance at 169 ppm with no new ^{113}Cd resonances appearing. Chemical exchange broadening obliterates the ability to detect any ^{113}Cd resonance from the

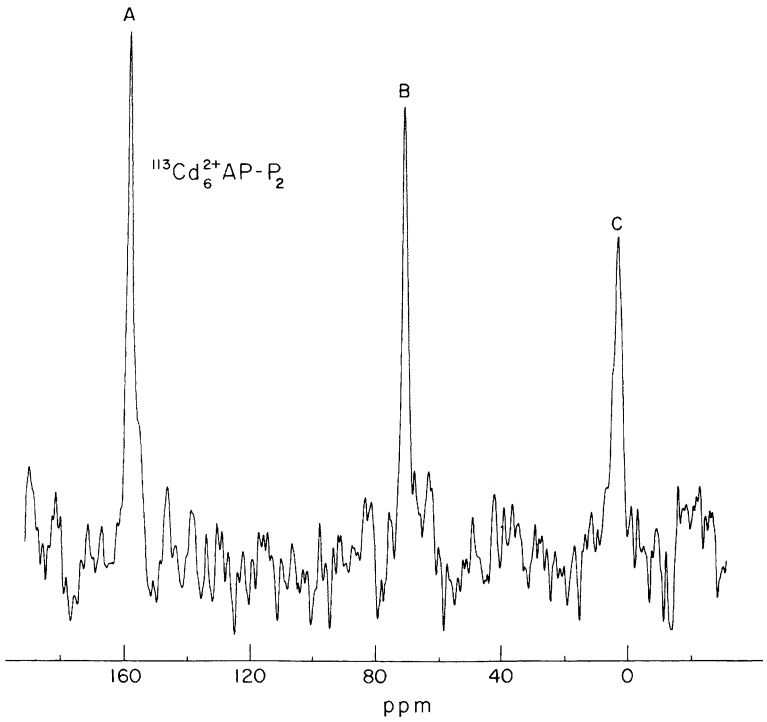

Figure 4 ^{113}Cd NMR spectrum at 44.4 MHz of 1.5 mM $^{113}Cd_6^{2+}$ diphosphoryl alkaline phosphatase, pH 6.2. Reproduced from [6] with kind permission from Springer Science + Business Media B.V.; copyright 1982.

six equivalents of bound ^{113}Cd. Phosphorylation of the active site serine residue, $Cd_6AP\text{-}P_2$, inhibits the exchange broadening with the appearance of three ^{113}Cd resonances at 160 ppm (A site), 70 ppm (B site), and 2 ppm (C site) (Figure 4). Concurrent ^{13}C NMR studies on the [γ-^{13}C]-histidine labeled $^{113}Cd_6AP\text{-}P_2$ and $^{112}Cd_6AP\text{-}P_2$ produced the spectra shown in Figure 5A and B [6,82].

Separate resonances are observed for each of the ten histidyl resonances per monomer in this symmetric dimer. The collapse of the doublet for resonances 7, 8, and 9 in Figure 5A, in Figure 5B with the spin I = 0 ^{112}Cd isotope provided unequivocal proof of three bond ^{113}Cd-^{13}C J coupling from Cd coordinated to $N_{\varepsilon 2}$ of three imidazole rings. Figure 5C shows the ^{13}C spectrum after the addition of eight equivalents of $^{112}Cd^{2+}$ to the sample in 5A and removal of the excess Cd^{2+} by ultrafiltration. The ^{113}Cd NMR spectrum of this sample, not shown, indicated a significant loss in the A and C site ^{113}Cd resonances through ^{112}Cd displacement, but none for ^{113}Cd at the B site. Histidyl resonance number 9 is therefore assigned to the B site metal and histidyl resonances number 7 and 8 to the A site metal. The assignment of the two low field histidyl resonances labeled 1 and 2 to ^{113}Cd ligands with coordination through the $N_{\delta 1}$ of the imidazole ring was based on the following: these resonances did not titrate, relaxation time measurement and, the absence of observable coupling, which would be consistent with a smaller 2 bond ^{113}Cd-^{13}C J

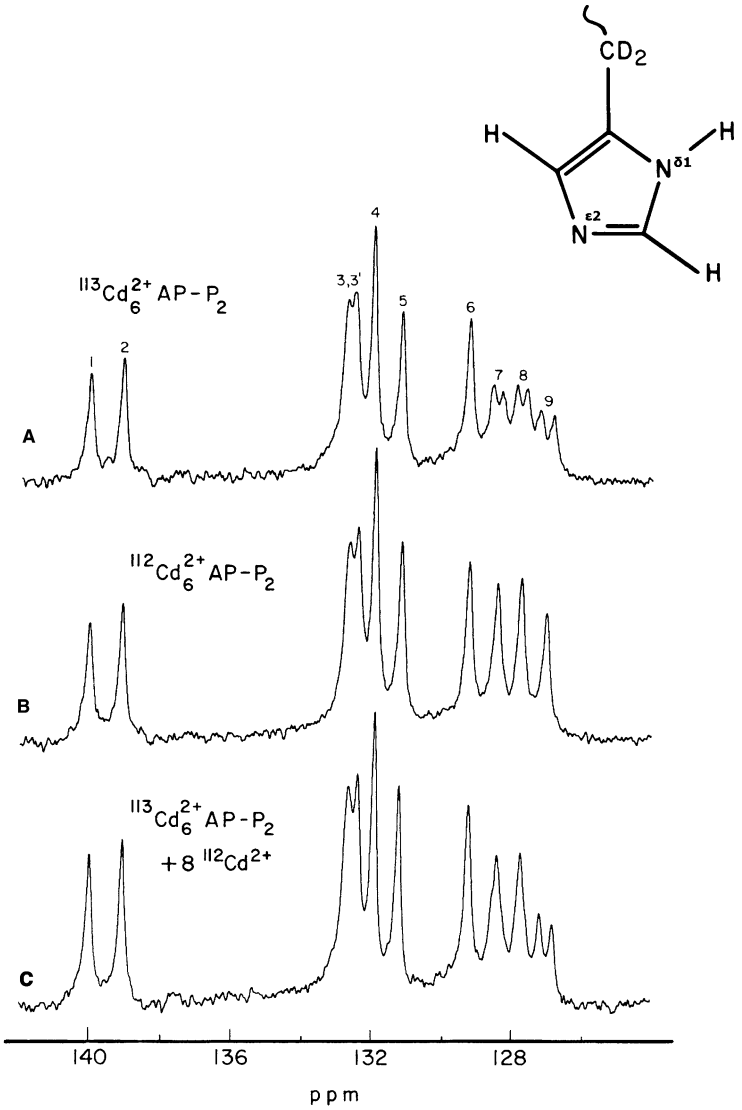

Figure 5 The effect of selective Cd^{2+} isotope exchange at the A and C sites on the 50.3 MHz ^{13}C NMR spectrum of the [γ-^{13}C]-histidine labeled Cd_6^{2+} diphosphoryl alkaline phosphatase. **(A)** $^{113}Cd_6^{2+}$ AP-P_2; **(B)** $^{112}Cd_6^{2+}$ AP-P_2 with spin I = 0 ^{112}Cd; **(C)** sample A after addition of 8 equivalents of $^{112}Cd^{2+}$ and removal of excess Cd^{2+} by ultrafiltration. The ^{113}Cd NMR spectrum of this sample, not shown, indicated an almost complete loss of the ^{113}Cd resonance at the A and C site through exchange with ^{112}Cd with no change of the ^{113}Cd resonance at the B site. On top at the right the imidazole ring is shown. Reproduced from [6] with kind permission from Springer Science+ Business Media B.V.; copyright 1982.

coupling [82]. However, these circumstantial pieces of evidence had to be retracted when the X-ray structure became available approximately 10 years later [202,203]. From the X-ray structure of AP (1ALK), the A site is a 6-coordinate octahedral with His412 $N_{\varepsilon 2}$, His331 $N_{\varepsilon 2}$, two O from Asp327 and two O from phosphate; the B site is a highly distorted octahedral with His370 $N_{\varepsilon 2}$, two O from Asp51, two O from Asp369 and Ser102. This is the serine that is phosphorylated, which is the form of the Cd enzyme being examined here which probably means the two oxygens from phosphate coordinated to the A site are replaced with waters and the B site Ser-OH is replaced with phosphate. The C site is the Mg site, which is a slightly distorted octahedron, with the ^{113}Cd resonance at 2 ppm arising from a bound Asp51 (1 bond), Thr155 OH, Glu322(1 bond), and three water molecules.

An unexpected bonus came from the above NMR studies using a combination of ^{113}Cd, ^{13}C, and ^{31}P NMR to monitor the disposition, occupancy, and role of the individual metal binding sites in substrate phosphate binding and serine phosphorylation. Specifically, these studies showed that substrate binding and phosphorylation requires a minimum occupancy of the A and B site on a monomer. Thus, while the first two equivalents of Cd added bind to the symmetric A sites on each monomer, addition of phosphate results in the relocation of the metal ions to give a distribution where 50% are apo monomers and 50% are di-metal monomers. This is the chemical explanation for the elusive half of the sites reactivity and negative cooperativity reported in some studies on this enzyme! Further addition of metal to saturate the 3 sites/monomer results in a symmetric diphosphorylated dimer giving rise to the spectra shown in Figures 4 and 5.

4.2 ^{113}Cd NMR and Calcium Binding Proteins

The most common Ca binding motif, the EF-hand or helix-loop-helix motif, consists of a 12 amino acid long loop with a helix of approximately 10 amino acids on each side. The loop contains all the metal ligands, in positions 1, 3, 5, 7, 9, and 12. Position 1 is always an Asp and position 12 always a bidentate Glu. There are two more side chain ligands that may or may not be charged. The remaining two ligands are either backbone C=O or water. It is, however, not a single calcium binding site that is the active unit but a pair of sites. The sites are connected via a short anti-parallel β-sheet, with amino acids 7 to 9 in each loop supplying one strand each.

4.2.1 Calbindin D_{9k}, a Study of Mutants

Calbindin D_{9k}, previously known as intestinal calcium binding protein, is the smallest (75 amino acids) in the calmodulin superfamily of proteins. A special characteristic of this EF-hand protein is that the first metal binding loop is modified compared to the typical EF-hand loop, a pseudo EF-hand, a common feature for

proteins belonging to the S100 family. The sites will be referred to as site I and site II for the pseudo site and the typical site, respectively. The pseudo loop is two residues longer than the typical EF-hand due to insertion of one residue after the first and one after the sixth residue in the loop. There is only one side chain group that coordinates the metal ion, the glutamate at position 14 which uses both carboxylic oxygens. The remaining ligands are backbone carbonyls and one water [195]. It looks like the site has turned itself inside out. Residues 9 to 11 are involved in the β-sheet connecting it to the other EF-hand. Despite these differences between the two calcium binding sites, the cooperativity in calcium binding is preserved.

The ^{113}Cd NMR spectrum for wild type bovine [34] and porcine [33] calbindin D_{9k} show the same feature when titrated with ^{113}Cd. First appears a resonance with a chemical shift of about –105 ppm that increases in intensity and stays with this shift up to one equivalent of added Cd. Thereafter, the resonance shifts towards higher field and broadens. A maximum broadening is observed at about 1.5 equivalents of added Cd. After addition of at least 2 equivalents of Cd, the shift has changed to about –110 ppm and the line width is back to what it was at low levels of added Cd. The first signal to appear has been assigned to site II, with a chemical shift in the same range as for other EF hands. A second signal observed only at lower temperatures has a shift of –155 ppm and is assigned to site I. This high field shift can, as seen in Figure 3, be explained as being due to the fact that there is only one negatively charged ligand. The broad signal not observed at room temperature is an example of exchange broadening due to direct metal ion exchange between free and protein bound ^{113}Cd. An off-rate for the bound metal ion of about 2000 s^{-1} would explain both the fact that no signal is observed at room temperature for site I ^{113}Cd and the broadening of site II ^{113}Cd at 1.5 equivalents of ^{113}Cd added.

The ^{113}Cd chemical shift is known to be very sensitive to even subtle changes in the immediate surrounding of the Cd ion. ^{113}Cd NMR has therefore shown itself to be an easy to use and sensitive monitor of structural changes due to mutations. It has been observed that mutations outside the metal binding loops have no effect on the ^{113}Cd shift. On the other hand, it has been found that charge mutants, where charges in loop residues whose side chains are not metal ligands have been removed, have diverse effects. Only the mutant Asp19Asn, and double and triple mutants containing Asp19Asn, show some effect on the ^{113}Cd shifts (Figure 6).

The ^{113}Cd shift of cadmium in site I has moved downfield by 20 ppm, as much as by adding a charged ligand according to Figure 3. Within this group of mutants there is no change in the ^{113}Cd shift of cadmium in site II with site I empty, however, the change in ^{113}Cd shift for site II cadmium upon cadmium binding to site I has diminished or totally disappeared for the triple mutant, Glu17Gln + Asp19Asn + Glu26Gln. This indicates that the interaction between the sites has decreased. This is also seen as a decreased cooperativity in the calcium binding. In fact there is a correlation, though weak, between the cooperativity in calcium binding and shift in site II ^{113}Cd caused by binding of Cd to site I [38,40,41].

A more pronounced effect on the ^{113}Cd spectrum was seen for mutants directly affecting the metal binding. Changing loop I into a normal EF-hand loop, either by

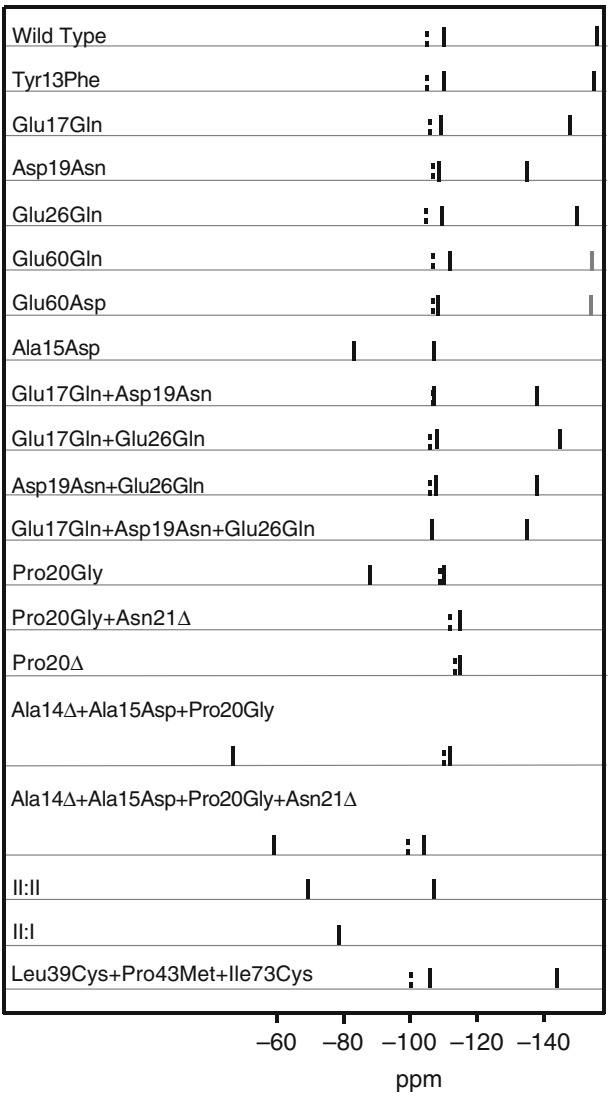

Figure 6 Bars indicating the chemical shifts for the two ^{113}Cd resonances in calbindin D_{9k} and for a set of mutants. Note that the typical EF-hand ^{113}Cd signal has an almost constant shift, –105 to –110 ppm. The dashed bars refer to proteins with only one bound $^{113}Cd^{2+}$ ion and the solid bars refer to proteins with two bound $^{113}Cd^{2+}$ ions. The entry II:II denotes the mutant with site two loop sequence also in site one, and II:I the mutant with interchanged loop sequences. Δ denotes a deletion. The mutant Leu39Cys + Pro43Met + Ile73Cys has been cleaved after Met43 and the S-S bond between Cys39 and Cys73 has been formed.

inserting the sequence of loop II or by the minimum number of replacements and deletions, did not result in a ^{113}Cd spectrum expected for two typical EF-hands, but a shift for site I ^{113}Cd of 20–30 ppm downfield from the expected value (Figure 6). This shows that the general structure around loop I does not easily adopt a typical EF-hand loop [34,37].

We hope that these examples show how useful ^{113}Cd NMR can be in studies of mutants to detect not only major changes but also very small changes in the structure of the studied protein.

4.2.2 Calmodulin, Target Peptide Binding

Calmodulin (CaM) is a small, 148 residue acidic protein that has four pair-wise oriented EF-hands. The amino acid sequence is strictly conserved among vertebrates, indicating that every amino acid is important for some function. CaM is a Ca^{2+} sensor protein that has no enzymatic activity by itself but has been shown to control the activity of hundreds of different functions in a Ca^{2+}-dependent manner [204]. Ca^{2+} binding studies have shown that there are two classes of metal binding sites with two metals each. Early ^{113}Cd NMR studies showed that when ^{113}Cd is titrated into a CaM solution two resonances, –88 and –115 ppm, appear and increase contemporaneously up to two added equivalents of Cd^{2+} [48]. Nothing more happened to the spectrum until more than four equivalents of Cd^{2+} had been added when a signal from free Cd^{2+} appeared. Two ^{113}Cd ions are evidently not seen by NMR due to some intermediate exchange process. By limited trypsin cleavage of CaM, two halves can be generated, TR_1C (residues 1-77) and TR_2C (residues 78-148). When ^{113}Cd is titrated into a solution of TR_2C a ^{113}Cd spectrum very similar to that of intact CaM is observed, showing that the two strong binding sites are in this half of CaM. When ^{113}Cd is titrated into a solution of TR_1C nothing happens until a signal from free ^{113}Cd appears when more than two equivalents have been added [51]. Evidently there is an exchange process, different from direct metal exchange, that broadens the ^{113}Cd signals beyond detection both for intact CaM and TR_1C.

The first crystal structure of Ca_4CaM, 5 years after our first ^{113}Cd NMR study [48], showed a dumbbell structure with two similar domains containing two EF-hands each and connected by a long helix [198,200]. SAXS data showed, however, that the solution structure deviates from the crystal structure in the distance between the two halves [205], interpreted as due to a flexibility in parts of the central helix. This was later confirmed in an NMR relaxation study [206]. NMR studies have shown that apo-CaM has a flexible dumbbell structure [207–209] similar to the structure of Ca_4CaM. The structures of the individual lobes differs, however, significantly between the apo- and Ca-forms of CaM. Ca^{2+} binding causes a rearrangement of the helices from a “closed conformation” in the apo-form to an “open conformation” in the Ca-form, where a hydrophobic patch has been exposed, similar for both lobes. Our present interpretation of the unseen ^{113}Cd signals from TR_1C is that Cd binding has not resulted in a dominating “open conformation” and that there is an intermediate exchange rate between the two conformations. It has more recently been shown for a mutant TR_2C fragment of CaM, Glu140Gln, that in the fully calcium-loaded form there is an exchange occurring between two conformers seemingly similar to the open and closed forms [210].

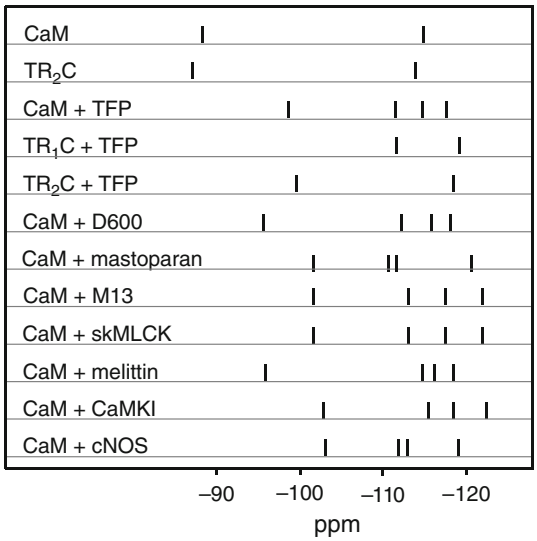

Figure 7 Bars indicating the ^{113}Cd chemical shifts of ^{113}Cd bound to calmodulin and fragments thereof as well as for CaM complexes with various natively occurring peptides or peptides derived from CaM-activated enzymes are shown. The resonance with a shift between –88 and –103 is from site IV, which has four negatively charged ligands, whereas the other three sites have three negative charged ligands. CaMKI, calcium-calmodulin-dependent protein kinase I; cNOS, constitutive nitric oxide synthase; D600, α[3-{[2-(3,4-dimethoxyphenyl)-ethyl]-methylamino}propyl]-3,4,5-trimethoxy-α-(1-methylethyl)-benzene-acetonitrile; M13, KRRWKKNFIAVSAANRFK-KISSSGAL; skMLCK, skeletal myosin light chain kinase.

Fortuitously, the two missing ^{113}Cd signals in CaM can be made visible by the addition of hydrophobic molecules, like trifluoperazine (TFP), that are thought to bind to the hydrophobic patches made solvent-exposed upon metal binding [198]. The binding of two molecules of, for example, TFP per CaM are needed to complete the change in the ^{113}Cd spectrum to show all four signals. For the TR_1C fragment one TFP molecule is sufficient [52,53].

As mentioned above, CaM interacts with a great number of different enzymes. The interaction is in most cases strictly calcium dependent. A few natively occurring small peptides that bind to CaM in a calcium-dependent manner have also been found. Before any crystal structure information was available it was possible to show by means of ^{113}Cd NMR that drug molecules like TFP bind to CaM and cause the same structural changes as the peptides, as judged from the ^{113}Cd shifts. However, one peptide molecule is able to cause the same, or at least very similar, effect as two TFP molecules (Figure 7) [54,55].

For one peptide to bind to both halves of CaM and affect all four metal binding sites as seen from the change in shifts for all four ^{113}Cd resonances, the distance between the two hydrophobic patches, one in each half of CaM, has to be much shorter than seen in the structure reported for Ca_4CaM [198]. A major structural change could therefore be postulated based on ^{113}Cd NMR alone and was later

confirmed when structures were determined in solution with NMR [211] and in crystals with X-ray crystallography [212,213]. These structures show CaM "grabbing" the peptide, however, with no detectable change in the structures of the individual halves of CaM. This compact structure was in fact first observed experimentally in SAXS studies [214]. We can thus see that even though the whole domain containing two EF-hands does not appear to change its structure there is a change in the ^{113}Cd shifts of up to 15 ppm upon peptide or drug binding. Thus again emphasizing the extreme sensitivity in the ^{113}Cd chemical shift to even very subtle changes in the structure surrounding the metal ion, structural changes so far not detected by other means.

4.3 ^{113}Cd NMR and Metallothionein

Metallothioneins (MTs) are small (6000–7000 Da), intracellular, cysteine-rich (~33% of the amino acids are cysteines) metal binding proteins that were first discovered in 1957 in equine kidney cortex. The subsequent purification of this protein identified it as the only known native cadmium-containing protein. Further studies showed this protein to bind both essential (e.g., Cu and Zn) and nonessential (e.g., Cd and Hg) metal ions and to be truly ubiquitously distributed in nature [215–218]. Additionally, MT biosynthesis is induced at the transcriptional level by a wide range of factors, which includes heavy metal ions that were subsequently found bound to the protein. All of the above factors suggest a role for this protein in heavy metal homeostasis, transport and detoxification [215–218]. Despite 55 years of extensive studies on MTs, which has included the high resolution characterization of the 3D structure and metal binding properties [134,136,138,151,154,218–222], the essential physiological functional role(s) of MT remains elusive. Of particular note in these studies was the determination of the NMR solution structure of a mammalian MT in a *tour de force* effort by the Wüthrich lab which resulted in the reinterpretation and correction of the only mammalian MT crystal structure currently available [223,224].

The objective in this section of this chapter is to illustrate how ^{113}Cd NMR methods were used to provide the first definitive evidence for the existence of polynuclear Cd clusters in MT, which was followed by the elucidation of the 3D solution structure of a variety of MTs and the establishment of the relative affinities of the multiple metal binding sites for Cd, Zn and Cu [132,136,138,143,154,219,220,225]. For a more in depth discussion on metallothioneins in general, the reader is referred to Chapter 11, "Cadmium in Metallothionein" by Freisinger and Vašák in this volume.

The existence of a naturally occurring cadmium binding protein with multiple, presumed isolated, metal mercaptide sites prior to our ^{113}Cd NMR studies, offered an irresistible challenge! From the very first ^{113}Cd NMR spectrum on the native ^{113}Cd MT obtained from the $^{113}CdCl_2$ induced protein isolated from rabbit liver (Figure 8) [132], we observed homonuclear ^{113}Cd scalar coupling in all of the ^{113}Cd resonances that could only arise from the existance of polynuclear Cd-thiolate

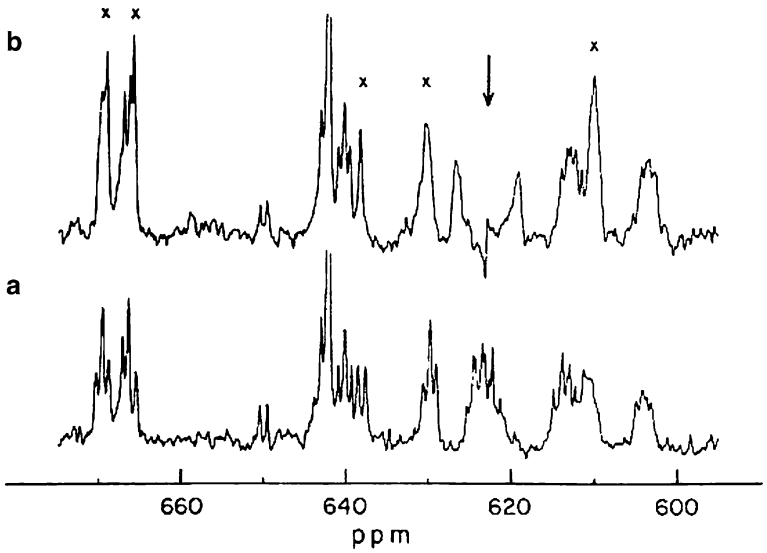

Figure 8 ^{113}Cd NMR spectra at 44.37 MHz of ^{113}Cd-induced native rabbit liver MT2 containing 4.4 g-atoms of ^{113}Cd and 2.6 g-atoms of Zn per mol protein. (**a**) Proton-decoupled. (**b**) Proton-decoupled with selective homonuclear decoupling at the position of the arrow with coupled resonances identified with an x. Reproduced from [132] by permission from the American Chemical Society; copyright 1979.

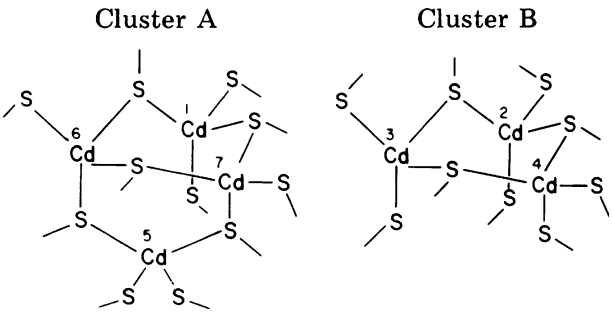

Figure 9 Structures of the 4-metal and 3-metal cluster located in the α- and β-domain respectively, of rabbit liver metallothionein deduced from spin coupling information. The numbers beside each Cd refers to the corresponding resonance position in the ^{113}Cd spectrum proceeding from low field to high field. Reproduced from [6] with kind permission from Springer Science + Business Media B.V.; copyright 1982.

metal cluster(s)! This feature immediately dispelled the prevailing model, which consisted of multiple, separate metal binding sites. Shortly thereafter the size and structures of the metal clusters in the mammalian protein were determined by selective homonuclear ^{113}Cd decoupling techniques (Figure 9) [133].

^{1}H-^{113}Cd HMQC experimental methods were then developed which enabled the establishment of the specific coordination of each of the ^{113}Cd resonances to the sequentially assigned cysteines in the 2D ^{1}H NMR spectrum [142,226]. As it turned

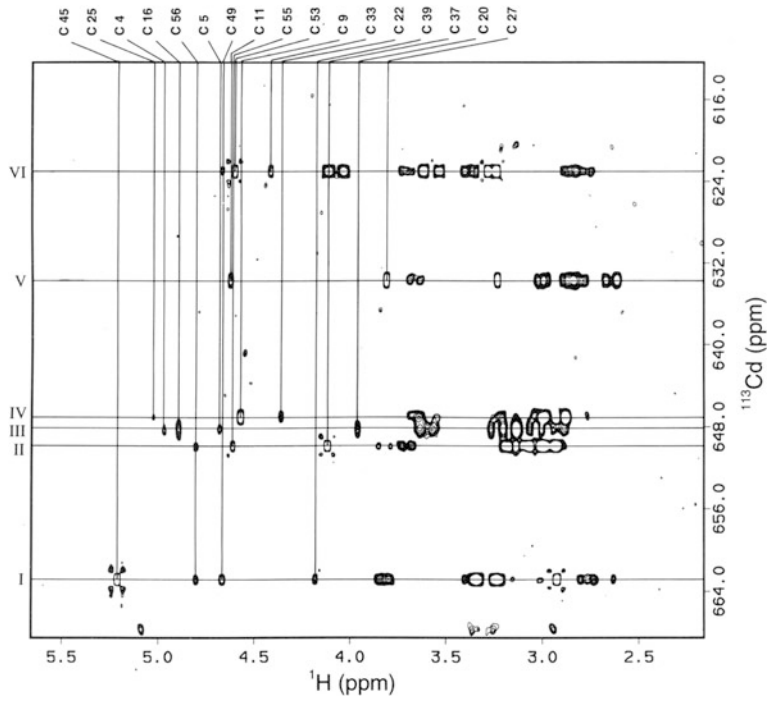

Figure 10 ^{1}H-^{113}Cd HMQC spectrum of $^{113}Cd_6$ blue crab MT1. The six ^{113}Cd resonances along the vertical axes are labeled by roman numerals according to their decreasing ^{113}Cd chemical shifts. Resonances on the horizontal axis are from the α and β protons of cysteine with the former assigned to specific cysteines in the primary sequence. Reproduced from [149] by permission from John Wiley & Sons Ltd., Chichester, UK; copyright 1993.

out, these latter structural constraints were absolutely essential for the determination of the 3D fold of MT where an insufficient number of ^{1}H-^{1}H dipolar constraints were observed in the early 2-dimensional ^{1}H NMR studies to calculate the 3D structure. This resulted from the lack of regular secondary structural elements, α-helix and β-sheet, in MT and their associated diagnostic dipolar constraints. A representative example of this experiment is shown for the $^{113}Cd_6$MT from blue crab *Callinectes sapidus* in Figure 10 with the 3D structure of both three-metal binding domains of this protein shown in Figure 11 [149,151].

As was the case with the solution structural studies on the mammalian proteins [154,219–222], there were no dipolar constraints between the two metal domains to permit their respective orientation. This was a limitation when working with MTs isolated from natural source at the time, which today could be overcome by the expression of recombinant MT with isotopic ^{15}N labeling and the use of residual dipolar coupling methods [227]. Another advancement in the 3D structural studies on this protein has arisen from the increased sensitivity of newer, higher field NMR instruments. NMR studies on MT at 800 MHz now provide a sufficient number of ^{1}H-^{1}H NOE dipolar constraints to permit the calculation of the tertiary fold of the protein backbone in MT *without* the need for ^{113}Cd substitution and the

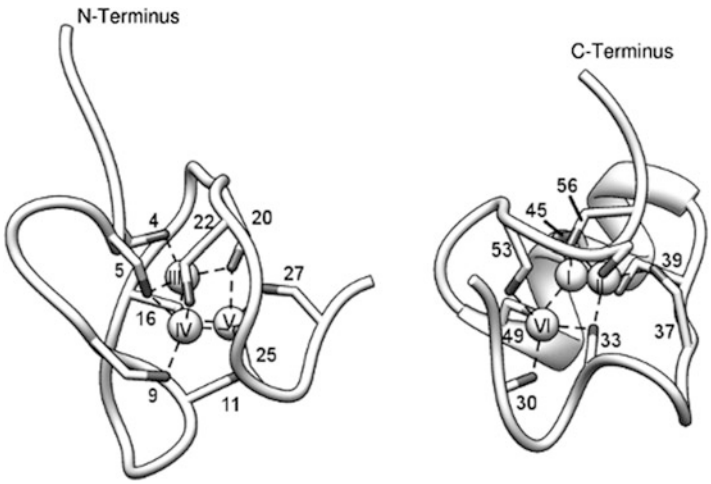

Figure 11 The 3D NMR structure of the two domains in blue crab MT1. The Cd ions are numbered according to their resonance position from low field to high field along with the sequence number of the liganding cysteines (PDB entries 1DMC and 1DME).

establishment of specific Cd to Cys residue number connectivities [228]. The reader is referred to this reference where the method is illustrated with the determination of the 3D fold of the protein backbone in Cu_6MT from the fungus *Neurospora crassa* with validation provided by the comparison of the calculated structure of the MT1 protein with and without ^{113}Cd-Cys restraints. The implication from this study is that with 800 MHz NMR data, accurate 3D protein backbone folds are readily obtainable for MTs from any species containing the bound native copper and/or zinc metal ions.

5 Conclusions and Outlook

While we don't foresee a resurgence in the use of ^{113}Cd NMR methods to the levels in the 80s, we sincerely hope that the material presented in this chapter provides a useful overview and guide for the use of ^{113}Cd NMR methods to potential new users. While we have attempted to be comprehensive in this overview, we hope that you will accept our apologies if your contribution in this area has not been highlighted. The excellent correlation in chemical shift *versus* ligand type and nature of coordination shown in Figure 2 provides information about the metal binding sites in metallo-proteins/enzymes that is not readily available by other methods. Additionally, the extreme sensitivity of the ^{113}Cd chemical shift provides one with a very sensitive monitor of dynamic changes around the metal binding site(s). Hopefully, illustration of the use of ^{113}Cd NMR with the select examples here will arouse new interest and applications.

Abbreviations

AP	alkaline phosphatase
AztR	*aztR* gene product
CadC	*cad* operon transcription regulating protein
CaM	calmodulin
CaMKI	calcium-calmodulin-dependent protein kinase I
cNOS	constitutive nitric oxide synthase
Com	bacteriophage MU *com* gene product
CSA	chemical shift anisotropy
D600	α[3-{[2-(3,4-dimethoxyphenyl)-ethyl]-methylamino}propyl]-3,4,5-trimethoxy-α-(1-methylethyl)-benzene-acetonitrile
GIF	neuronal growth inhibitory factor
HCAB	human carbonic anhydrase
HMQC	heteronuclear multiple quantum correlation
M13	KRRWKKNFIAVSAANRFKKISSSGAL
MT	metallothionein
NMR	nuclear magnetic resonance
NOE	nuclear Overhauser enhancement
p7	HIV-1 nucleic acid binding protein
R1	spin-lattice relaxation rate
Rd	rubredoxin
RDC	residual dipolar coupling
SAXS	small angle X-ray scattering
skMLCK	skeletal myosin light chain kinase
TFP	trifluoperazine
TR_1C	N-terminal half of calmodulin
TR_2C	C-terminal half of calmodulin

Acknowledgments IMA would like to express his sincere appreciation to all the students and postdocs who have conducted the ^{113}Cd NMR studies in his lab over the years and whose names can be found on the publications in the reference list. A special thanks is extended to his first postdoc, Dr. James D. Otvos, who embarked upon these studies at their outset in the mid 70s. A special thank you is also extended to Lewis Kay and Larry Werbelow for clarifying the correct treatment of relaxation rates and NOE for gyromagnetic ratios of opposite sign. We all thank Dr. Melanie Rogers for her assistance with both editing and formatting this chapter.

TD would like to dedicate this chapter to his long time colleague, Hans Lilja, who passed away last summer (2011). He was an electronics wizard and instumental to all our early NMR work. Hans you are dearly missed.

References

1. I. M. Armitage, R. T. Pajer, A. J. M. Schoot Uiterkamp, J. F. Chlebowski, J. E. Coleman, *J. Am. Chem. Soc*. **1976**, *98*, 5710–5712.
2. J. F. Chlebowski, I. M. Armitage, J. E. Coleman, *J. Biol. Chem*. **1977**, *252*, 7053–7061.

3. I. M. Armitage, A. J. M. Schoot Uiterkamp, J. F. Chlebowski, J. E. Coleman, *J. Magn. Reson.* **1978**, *29*, 375–392.
4. T. Drakenberg, B. Lindman, A. Cavé, J. Parello, *FEBS Lett.* **1978**, *92*, 346–350.
5. R. J. Kostelnik, A. A. Bothner-By, *J. Magn. Reson.* **1974**, *14*, 141–151.
6. I. M. Armitage, J. D. Otvos, *Biol. Magn. Res.* **1982**, *4*, 79–144.
7. H. J. Vogel, T. Drakenberg, S. Forsén, *NMR of Newly Accessible Nuclei,* Ed P. Laszlo, Vol. 1, Academic Press, New York, 1983, pp. 157–192.
8. I. M. Armitage, Y. Boulanger, *NMR of Newly Accessible Nuclei*, Ed P. Laszlo, Vol. 2, Academic Press, New York, 1983, pp. 337–365.
9. M. F. Summers, *Coord. Chem. Rev.* **1988**, *86*, 43–134.
10. C. Johansson, T. Drakenberg, *Annu. Rep. NMR Spectrosc.* **1990**, *22*, 1-59.
11. G. Öz, D. L. Pountney, I. M. Armitage, *Biochem. Cell Biol.* **1998**, *76*, 223–234.
12. K. Zangger, I. M. Armitage, *Handbook of Metalloproteins,* Eds A. Messerschmidt, M. Cygler, W. Bode, John Wiley & Sons Ltd., Chichester, UK, 2004.
13. P. S. Marchetti, P. D. Ellis, R. G. Bryant, *J. Am. Chem. Soc.* **1985**, *107*, 8191–8196.
14. M. Sola, *Inorg. Chem.* **1990**, *29*, 1113–1116.
15. A. R. Palmer, D. B. Bailey, W. D. Benhke, A. D. Cardin, P. P. Yang, P. D. Ellis, *Biochemistry* **1980**, *19*, 5063–5070.
16. K. M. Welsh, I. M. Armitage, B. S. Cooperman, *Biochemistry* **1983**, *22*, 1046–1054.
17. H. R. Engeseth, D. R. McMillin, J. D. Otvos, *J. Biol. Chem.* **1984**, *259*, 4822.
18. F. A. Cotton, G. Wilkinson, *Advanced Inorganic Chemistry*, Wiley, New York, 1988.
19. J. M. Aramini, T. Hiraoki, Y. Ke, K. Nitta, H. J. Vogel, *J. Biochem.* **1995**, *117*, 623–628.
20. T. Drakenberg, *The Biological Chemistry of Magnesium,* Ed J. A. Cowan, VCH Publishers Inc., New York, Weinheim, Cambridge, **1995**, *27–51*.
21. G. E. Maciel, M. Borzo, *J. Chem. Soc., Chem. Commun.* **1973**, 394a–394a.
22. A. D. Cardin, P. D. Ellis, J. D. Odom, J. W. Howard Jr, *J. Am. Chem. Soc.* **1975**, *97*, 1672–1679.
23. M. Karplus, *J. Chem. Phys.* **1959**, *30*, 11–15.
24. O. Zerbe, D. L. Pountney, W. von Philipsborn, M. Vašák, *J. Am. Chem. Soc.* **1994**, *116*, 377–378.
25. J. D. Otvos, I. M. Armitage, *Biochemistry* **1980**, *19*, 4031–4043.
26. J. E. Coleman, I. M. Armitage, J. F. Chlebowski, J. D. Otvos, A. J. M. Schoot Uiterkamp, *Biological Applications of Magnetic Resonance, Academic Press, London New York* **1979**, 345–395.
27. R. A. Dwek, *Nuclear Magnetic Resonance (NMR) in Biochemistry: Applications to Enzyme Systems*, Clarendon Press, Oxford, 1973.
28. E. Hsi, R. G. Bryant, *J. Phys. Chem.* **1977**, *81*, 462–465.
29. L. E. Kay, D. A. Torchia, A. Bax, *Biochemistry* **1989**, *28*, 8972–8979.
30. L. Werbelow, *J. Magn. Reson.* **1984**, *57*, 136–139.
31. L. G. Werbelow, *J. Chem. Soc., Faraday Trans. 2* **1987**, *83*, 897–904.
32. I. Morishima, M. Kurono, Y. Shiro, *J. Biol. Chem.* **1986**, *261*, 9391–9399.
33. H. J. Vogel, T. Drakenberg, S. Forsén, J. D. J. O'Neil, T. Hofmann, *Biochemistry* **1985**, *24*, 3870–3876.
34. S. Linse, P. Brodin, T. Drakenberg, E. Thulin, P. Sellers, K. Elmdén, T. Grundström, S. Forsén, *Biochemistry* **1987**, *26*, 6723–6735.
35. P. Brodin, C. Johansson, S. Forsén, T. Drakenberg, T. Grundström, *J. Biol. Chem.* **1990**, *265*, 11125–11130.
36. C. Johansson, P. Brodin, T. Grundström, E. Thulin, S. Forsén, T. Drakenberg, *Eur. J. Biochem.* **1990**, *187*, 455–460.
37. C. Johansson, P. Brodin, T. Grundström, S. Forsén, T. Drakenberg, *Eur. J. Biochem.* **1991**, *202*, 1283–1290.
38. S. Linse, C. Johansson, P. Brodin, T. Grundstroem, T. Drakenberg, S. Forsén, *Biochemistry* **1991**, *30*, 154–162.
39. J. Kördel, C. Johansson, T. Drakenberg, *J. Magn. Reson.* **1992**, *100*, 581–587.
40. S. Linse, E. Thulin, P. Sellers, *Protein Sci.* **1993**, *2*, 985–1000.

41. S. Linse, N. R. Bylsma, T. Drakenberg, P. Sellers, S. Forsén, E. Thulin, L. A. Svensson, I. Zajtzeva, V. Zajtsev, J. Marek, *Biochemistry* **1994**, *33*, 12478–12486.
42. N. Bylsma, T. Drakenberg, I. Andersson, P. F. Leadlay, S. Forsén, *FEBS Lett.* **1992**, *299*, 44–47.
43. S. Forsén, E. Thulin, H. Lilja, *FEBS Lett.* **1979**, *104*, 123–126.
44. O. Teleman, T. Drakenberg, S. Forsén, E. Thulin, *Eur. J. Biochem.* **1983**, *134*, 453–457.
45. P. D. Ellis, P. Strang, J. D. Potter, *J. Biol. Chem.* **1984**, *259*, 10348–10356.
46. T. Drakenberg, S. Forsén, E. Thulin, H. J. Vogel, *J. Biol. Chem.* **1987**, *262*, 672–678.
47. P. D. Ellis, P. S. Marchetti, P. Strang, J. D. Potter, *J. Biol. Chem.* **1988**, *263*, 10284–10288.
48. S. Forsén, E. Thulin, T. Drakenberg, J. Krebs, K. Seamon, *FEBS Lett.* **1980**, *117*, 189–194.
49. S. L. Boström, B. Ljung, S. Mårdh, S. Forsén, E. Thulin, *Nature* **1981**, *292*, 777–778.
50. T. Andersson, T. Drakenberg, S. Forsén, E. Thulin, *Eur. J. Biochem.* **1982**, *126*, 501–505.
51. A. Andersson, S. Forsén, E. Thulin, H. J. Vogel, *Biochemistry* **1983**, *22*, 2309–2313.
52. A. Andersson, T. Drakenberg, E. Thulin, S. Forsén, *Eur. J. Biochem.* **1983**, *134*, 459–465.
53. E. Thulin, A. Andersson, T. Drakenberg, S. Forsén, H. J. Vogel, *Biochemistry* **1984**, *23*, 1862–1870.
54. S. Linse, T. Drakenberg, S. Forsén, *FEBS Lett.* **1986**, *199*, 28–32.
55. M. Ikura, N. Hasegawa, S. Aimoto, M. Yazawa, K. Yagi, K. Hikichi, *Biochem. Biophys. Res. Commun.* **1989**, *161*, 1233–1238.
56. S. Ohki, U. Iwamoto, S. Aimoto, M. Yazawa, K. Hikichi, *J. Biol. Chem.* **1993**, *268*, 12388–12392.
57. M. Zhang, T. Yuan, J. M. Aramini, H. J. Vogel, *J. Biol. Chem.* **1995**, *270*, 20901–20907.
58. R. D. Brokx, H. J. Vogel, *Protein Sci.* **2000**, *9*, 964–975.
59. T. Yuan, A. V. Gomes, J. A. Barnes, H. N. Hunter, H. J. Vogel, *Arch. Biochem. Biophys.* **2004**, *421*, 192–206.
60. L. T. Kakalis, M. Kennedy, R. Sikkink, F. Rusnak, I. M. Armitage, *FEBS Lett.* **1995**, *362*, 55–58.
61. A. Cavé, J. Parello, T. Drakenberg, E. Thulin, B. Lindman, *FEBS Lett.* **1979**, *100*, 148–152.
62. A. Cavé, A. Saint-Yves, J. Parello, M. Swärd, E. Thulin, B. Lindman, *Mol. Cell. Biochem.* **1982**, *44*, 161–172.
63. L. Lee, B. D. Sykes, *Biochemistry* **1983**, *22*, 4366–4373.
64. T. Drakenberg, M. Swärd, A. Cavé, J. Parello, *Biochem. J.* **1985**, *227*, 711–717.
65. M. E. Bjornson, D. C. Corson, B. D. Sykes, *J. Inorg. Biochem.* **1985**, *25*, 141–149.
66. M. Svärd, T. Drakenberg, *Acta Chem. Scand. B: Org. Chem. Biochem.* **1986**, *40*, 689–693.
67. C. Zhang, D. J. Nelson, *J. Alloys Compd.* **1992**, *180*, 349–356.
68. L. J. Berliner, P. D. Ellis, K. Murakami, *Biochemistry* **1983**, *22*, 5061–5063.
69. L. Bhattacharyya, P. S. Marchetti, P. D. Ellis, C. F. Brewer, *J. Biol. Chem.* **1987**, *262*, 5616–5621.
70. D. B. Bailey, P. D. Ellis, A. D. Cardin, W. D. Behnke, *J. Am. Chem. Soc.* **1978**, *100*, 5236–5237.
71. E. Chiancone, T. Drakenberg, O. Teleman, S. Forsén, *J. Mol. Biol.* **1985**, *185*, 201–207.
72. F. Adebodun, F. Jordan, *Biochemistry* **1989**, *28*, 7524–7531.
73. J. L. Sudmeier, S. J. Bell, M. C. Storm, M. F. Dunn, *Science* **1981**, *212*, 560–562.
74. K. M. Welsh, B. S. Cooperman, *Biochemistry* **1984**, *23*, 4947–4955.
75. R. S. Ehrlich, R. F. Colman, *Biochemistry* **1989**, *28*, 2058–2065.
76. R. S. Ehrlich, R. F. Colman, *Biochim. Biophys. Acta-Protein Struct. Mol. Enzym.* **1995**, *1246*, 135–141.
77. P. B. Kingsley-Hickman, G. L. Nelsestuen, K. Ugurbil, *Biochemistry* **1986**, *25*, 3352–3355.
78. G. I. Rhyu, W. J. Ray Jr, J. L. Markley, *Biochemistry* **1985**, *24*, 2536–2541.
79. W. J. Ray Jr, C. B. Post, Y. Liu, G. I. Rhyu, *Biochemistry* **1993**, *32*, 48–57.
80. J. D. Otvos, J. R. Alger, J. E. Coleman, I. M. Armitage, *J. Biol. Chem.* **1979**, *254*, 1778–1780.
81. J. D. Otvos, I. M. Armitage, J. F. Chlebowski, J. E. Coleman, *J. Biol. Chem.* **1979**, *254*, 4707–4713.
82. J. D. Otvos, I. M. Armitage, *Biochemistry* **1980**, *19*, 4021–4030.
83. P. Gettins, J. E. Coleman, *J. Biol. Chem.* **1983**, *258*, 396–407.

84. P. Gettins, J. E. Coleman, *J. Biol. Chem.* **1984**, *259*, 4987–4990.
85. P. Gettins, J. E. Coleman, *J. Biol. Chem.* **1984**, *259*, 4991–4997.
86. P. Gettins, J. E. Coleman, *J. Biol. Chem.* **1984**, *259*, 11036–11040.
87. J. Afflitto, K. A. Smith, M. Patel, A. Esposito, E. Jensen, A. Gaffar, *Pharm. Res.* **1991**, *8*, 1384–1388.
88. E. O. Martins, T. Drakenberg, *Inorg. Chim. Acta* **1982**, *67*, 71–74.
89. W. Göumakos, J. P. Laussac, B. Sarkar, *Biochem. Cell Biol.* **1991**, *69*, 809–820.
90. P. J. Sadler, J. H. Viles, *Inorg. Chem.* **1996**, *35*, 4490–4496.
91. K. Aalmo, J. Krane, C. Little, C. S. Storm, *Biochem. Soc. Trans.* **1982**, *10*, 367–368.
92. K. Aalmo, L. Hansen, E. Hough, K. Jynge, J. Krane, C. Little, C. B. Storm, *Biochem. Int.* **1984**, *8*, 27–33.
93. K. Kanaori, N. Uodome, A. Nagai, D. Ohta, A. Ogawa, G. Iwasaki, A. Y. Nosaka, *Biochemistry* **1996**, *35*, 5949–5954.
94. K. Kanaori, D. Ohta, A. Y. Nosaka, *FEBS Lett.* **1997**, *412*, 301–304.
95. P. Gettins, *J. Biol. Chem.* **1986**, *261*, 15513–15518.
96. P. D. Ellis, *J. Biol. Chem.* **1989**, *264*, 3108–3110.
97. J. Matysik, G. Alia, G. Nachtegaal, H. J. van Gorkom, A. J. Hoff, H. J. M. de Groot, *Biochemistry* **2000**, *39*, 6751–6755.
98. G. A. Omburo, J. M. Kuo, L. S. Mullins, F. M. Raushel, *J. Biol. Chem.* **1992**, *267*, 13278–13283.
99. G. A. Omburo, L. S. Mullins, F. M. Raushel, *Biochemistry* **1993**, *32*, 9148–9155.
100. C. Damblon, C. Prosperi, L. Y. Lian, I. Barsukov, R. P. Soto, M. Galleni, J. M. Frère, G. C. K. Roberts, *J. Am. Chem. Soc.* **1999**, *121*, 11575–11576.
101. L. Hemmingsen, C. Damblon, J. Antony, M. Jensen, H. W. Adolph, S. Wommer, G. C. K. Roberts, R. Bauer, *J. Am. Chem. Soc.* **2001**, *123*, 10329–10335.
102. C. Damblon, M. Jensen, A. Ababou, I. Barsukov, C. Papamicael, C. J. Schofield, L. Olsen, R. Bauer, G. C. K. Roberts, *J. Biol. Chem.* **2003**, *278*, 29240–29251.
103. J. D. Otvos, W. E. Antholine, S. Wehrli, D. H. Petering, *Biochemistry* **1996**, *35*, 1458–1465.
104. J. L. Sudmeier, S. J. Bell, *J. Am. Chem. Soc.* **1977**, *99*, 4499–4500.
105. A. J. M. Schoot Uiterkamp, I. M. Armitage, J. E. Coleman, *J. Biol. Chem.* **1980**, *255*, 3911–3917.
106. N. B. Jonsson, L. A. Tibell, J. L. Evelhoch, S. J. Bell, J. L. Sudmeier, *Proc. Natl. Acad. Sci. USA* **1980**, *77*, 3269–3272.
107. J. L. Evelhoch, D. F. Bocian, J. L. Sudmeier, *Biochemistry* **1981**, *20*, 4951–4954.
108. D. B. Bailey, P. D. Ellis, J. A. Fee, *Biochemistry* **1980**, *19*, 591–596.
109. P. Kofod, R. Bauer, E. Danielsen, E. Larsen, M. J. Bjerrum, *Eur. J. Biochem.* **1991**, *198*, 607–611.
110. M. A. Kennedy, P. D. Ellis, *J. Am. Chem. Soc.* **1989**, *111*, 3195–3203.
111. Y. Wang, L. Hemmingsen, D. P. Giedroc, *Biochemistry* **2005**, *44*, 8976–8988.
112. B. R. Bobsein, R. J. Myers, *J. Am. Chem. Soc.* **1980**, *102*, 2454–2455.
113. B. R. Bobsein, R. J. Myers, *J. Biol. Chem.* **1981**, *256*, 5313–5316.
114. D. Krepkiy, F. H. Försterling, D. H. Petering, *Chem. Res. Toxicol.* **2004**, *17*, 863–870.
115. A. J. Bird, S. Swierczek, W. Qiao, D. J. Eide, D. R. Winge, *J. Biol. Chem.* **2006**, *281*, 25326–25335.
116. T. Liu, J. W. Golden, D. P. Giedroc, *Biochemistry* **2005**, *44*, 8673–8683.
117. Z. Xiao, M. J. Lavery, M. Ayhan, S. D. B. Scrofani, M. C. J. Wilce, J. M. Guss, P. A. Tregloan, G. N. George, A. G. Wedd, *J. Am. Chem. Soc.* **1998**, *120*, 4135–4150.
118. L. S. Busenlehner, N. J. Cosper, R. A. Scott, B. P. Rosen, M. D. Wong, D. P. Giedroc, *Biochemistry* **2001**, *40*, 4426–4436.
119. L. S. Busenlehner, T. C. Weng, J. E. Penner-Hahn, D. P. Giedroc, *J. Mol. Biol.* **2002**, *319*, 685–701.
120. D. P. Giedroc, B. A. Johnson, I. M. Armitage, J. E. Coleman, *Biochemistry* **1989**, *28*, 2410–2418.
121. D. P. Giedroc, H. Qiu, R. Khan, G. C. King, K. Chen, *Biochemistry* **1992**, *31*, 765–774.
122. D. W. Fitzgerald, J. E. Coleman, *Biochemistry* **1991**, *30*, 5195–5201.

123. W. J. Roberts, T. Pan, J. I. Elliott, J. E. Coleman, K. R. Williams, *Biochemistry* **1989**, *28*, 10043–10047.
124. X. Chen, M. Chu, D. P. Giedroc, *J. Biol. Inorg. Chem.* **2000**, *5*, 93–101.
125. T. Pan, J. E. Coleman, *Proc. Natl. Acad. Sci. USA* **1989**, *86*, 3145–3149.
126. T. Pan, J. E. Coleman, *Proc. Natl. Acad. Sci. USA* **1990**, *87*, 2077–2081.
127. T. Pan, J. E. Coleman, *Biochemistry* **1990**, *29*, 3023–3029.
128. K. H. Gardner, T. Pan, S. Narula, E. Rivera, J. E. Coleman, *Biochemistry* **1991**, *30*, 11292–11302.
129. D. W. Hasler, P. Faller, M. Vašák, *Biochemistry* **1998**, *37*, 14966–14973.
130. P. Faller, D. W. Hasler, O. Zerbe, S. Klauser, D. R. Winge, M. Vašák, *Biochemistry* **1999**, *38*, 10158–10167.
131. M. Vašák, D. W. Hasler, P. Faller, *J. Inorg. Biochem.* **2000**, *79*, 7–10.
132. J. D. Otvos, I. M. Armitage, *J. Am. Chem. Soc.* **1979**, *101*, 7734–7736.
133. J. D. Otvos, I. M. Armitage, *Proc. Natl. Acad. Sci. USA* **1980**, *77*, 7094–7098.
134. J. D. Otvos, I. M. Armitage, *Biochemical Structure Determination by NMR*, Marcel Dekker, New York, 1982, pp. 65.
135. I. M. Armitage, J. D. Otvos, R. W. Briggs, Y. Boulanger, *Fed. Proc.* **1982**, *41*, 68–74.
136. Y. Boulanger, I. M. Armitage, *J. Inorg. Biochem.* **1982**, *17*, 147–153.
137. Y. Boulanger, I. M. Armitage, K. A. Miklossy, D. R. Winge, *J. Biol. Chem.* **1982**, *257*, 13717–13719.
138. R. W. Briggs, I. M. Armitage, *J. Biol. Chem.* **1982**, *257*, 1259–1262.
139. J. D. Otvos, R. W. Olafson, I. M. Armitage, *J. Biol. Chem.* **1982**, *257*, 2427–2431.
140. D. Neuhaus, G. Wagner, M. Vašák, J. H. R. Kägi, K. Wüthrich, *Eur. J. Biochem.* **1984**, *143*, 659–667.
141. M. Vašák, G. E. Hawkes, J. K. Nicholson, P. J. Sadler, *Biochemistry* **1985**, *24*, 740–747.
142. D. Live, I. M. Armitage, D. C. Dalgarno, D. Cowburn, *J. Am. Chem. Soc.* **1985**, *107*, 1775–1777.
143. J. D. Otvos, H. R. Engeseth, S. Wehrli, *Biochemistry* **1985**, *24*, 6735–6740.
144. E. Wörgötter, G. Wagner, M. Vašák, J. H. R. Kägi, K. Wüthrich, *J. Am. Chem. Soc.* **1988**, *110*, 2388–2393.
145. M. Good, R. Hollenstein, P. J. Sadler, M. Vašák, *Biochemistry* **1988**, *27*, 7163–7166.
146. F. Vazquez, M. Vašák, *Biochem. J.* **1988**, *253*, 611–614.
147. M. J. Cismowski, S. S. Narula, I. M. Armitage, M. L. Chernaik, P. C. Huang, *J. Biol. Chem.* **1991**, *266*, 24390–24397.
148. P. Palumaa, O. Zerbe, M. Vašák, *Biochemistry* **1993**, *32*, 2874–2879.
149. S. S. Narula, I. M. Armitage, M. Brouwer, J. J. Enghild, *Magn. Reson. Chem.* **1993**, *31*, S96–S103.
150. P. K. Pan, F. Y. Hou, C. W. Cody, P. C. Huang, *Biochem. Biophys. Res. Commun.* **1994**, *202*, 621–628.
151. S. S. Narula, M. Brouwer, Y. Hua, I. M. Armitage, *Biochemistry* **1995**, *34*, 620–631.
152. Y. Wang, E. A. Mackay, O. Zerbe, D. Hess, P. E. Hunziker, M. Vašák, J. H. R. Kägi, *Biochemistry* **1995**, *34*, 7460–7467.
153. M. Vašák, *Biodegradation* **1998**, *9*, 501–512.
154. K. Zangger, G. Öz, I. M. Armitage, J. D. Otvos, *Protein Sci.* **1999**, *8*, 2630–2638.
155. C. You, E. A. Mackay, P. M. Gehrig, P. E. Hunziker, J. H. R. Kägi, *Arch. Biochem. Biophys.* **1999**, *372*, 44–52.
156. R. Riek, B. Prêcheur, Y. Wang, E. A. Mackay, G. Wider, P. Güntert, A. Liu, J. H. R. Kägi, K. Wüthrich, *J. Mol. Biol.* **1999**, *291*, 417–428.
157. J. Mendieta, M. S. Diaz–Cruz, A. Monjonell, R. Tauler, M. Esteban, *Anal. Chim. Acta* **1999**, *390*, 15–25.
158. D. W. Hasler, L. T. Jensen, O. Zerbe, D. R. Winge, M. Vašák, *Biochemistry* **2000**, *39*, 14567–14575.
159. K. Zangger, G. Shen, G. Öz, J. D. Otvos, I. M. Armitage, *Biochem. J.* **2001**, *359*, 353–360.
160. M. Vaher, N. Romero-Isart, M. Vašák, P. Palumaa, *J. Inorg. Biochem.* **2001**, *83*, 1–6.

161. A. Munoz, H. F. Försterling, F. C. Shaw, D. H. Petering, *J. Biol. Inorg. Chem.* **2002**, *7*, 713–724.
162. C. Capasso, V. Carginale, O. Crescenzi, D. Di Maro, E. Parisi, R. Spadaccini, P. A. Temussi, *Structure* **2003**, *11*, 435–443.
163. K. E. Rigby Duncan, C. W. Kirby, M. J. Stillman, *FEBS J.* **2008**, *275*, 2227–2239.
164. H. Wang, H. Li, B. Cai, Z. X. Huang, H. Sun, *J. Biol. Inorg. Chem.* **2008**, *13*, 411–419.
165. G. Digilio, C. Bracco, L. Vergani, M. Botta, D. Osella, A. Viarengo, *J. Biol. Inorg. Chem.* **2009**, *14*, 167–178.
166. D. E. K. Sutherland, M. J. Willans, M. J. Stillman, *Biochemistry*, *49*, 3593–3601.
167. T. L. South, B. Kim, M. F. Summers, *J. Am. Chem. Soc.* **1989**, *111*, 395–396.
168. R. A. Farrell, J. L. Thorvaldsen, D. R. Winge, *Biochemistry* **1996**, *35*, 1571–1580.
169. J. W. Michelsen, K. L. Schmeichel, M. C. Beckerle, D. R. Winge, *Proc. Natl. Acad. Sci. USA* **1993**, *90*, 4404–4408.
170. J. L. Kosa, J. W. Michelsen, H. A. Louis, J. I. Olsen, D. R. Davis, M. C. Beckerle, D. R. Winge, *Biochemistry* **1994**, *33*, 468–477.
171. J. W. Michelsen, A. K. Sewell, H. A. Louis, J. I. Olsen, D. R. Davis, D. R. Winge, M. C. Beckerle, *J. Biol. Chem.* **1994**, *269*, 11108–11113.
172. Y. Iko, T. S. Kodama, N. Kasai, T. Oyama, E. H. Morita, T. Muto, M. Okumura, R. Fujii, T. Takumi, S. Tate, *J. Biol. Chem.* **2004**, *279*, 44834–44840.
173. L. C. Myers, M. P. Terranova, A. E. Ferentz, G. Wagner, G. L. Verdine, *Science* **1993**, *261*, 1164–1167.
174. E. H. Morita, T. Ohkubo, I. Kuraoka, M. Shirakawa, K. Tanaka, K. Morikawa, *Genes Cells* **1996**, *1*, 437–442.
175. J. Timmerman, A. L. Vuidepot, F. Bontems, J. Y. Lallemand, M. Gervais, E. Shechter, B. Guiard, *J. Mol. Biol.* **1996**, *259*, 792–804.
176. H. Hanzawa, M. J. de Ruwe, T. K. Albert, P. C. van der Vliet, H. T. M. Timmers, R. Boelens, *J. Biol. Chem.* **2001**, *276*, 10185–10190.
177. T. Pan, Y. D. Halvorsen, R. C. Dickson, J. E. Coleman, *J. Biol. Chem.* **1990**, *265*, 21427–21429.
178. R. M. A. Knegtel, R. Boelens, M. L. Ganadu, A. V. E. George, P. T. Vandersaag, R. Kaptein, *Biochem. Biophys. Res. Commun.* **1993**, *192*, 492–498.
179. T. Pan, L. P. Freedman, J. E. Coleman, *Biochemistry* **1990**, *29*, 9218–9225.
180. E. Kellenbach, B. A. Maler, K. R. Yamamoto, R. Boelens, R. Kaptein, *FEBS Lett.* **1991**, *291*, 367–370.
181. C. J. Henehan, D. L. Pountney, M. Vašák, O. Zerbe, *Protein Sci.* **1993**, *2*, 1756–1764.
182. H. J. Lee, L. Y. Lian, N. S. Scrutton, *Biochem. J.* **1997**, *328*, 131–136.
183. R. T. Witkowski, S. Hattman, L. Newman, K. Clark, D. L. Tierney, J. Penner-Hahn, G. McLendon, *J. Mol. Biol.* **1995**, *247*, 753–764.
184. W. Xia, H. Li, K. H. Sze, H. Sun, *J. Am. Chem. Soc.* **2009**, *131*, 10031–10040.
185. F. Rusnak, C. Czaja, L. T. Kakalis, I. M. Armitage, *Inorg. Chem.* **1995**, *34*, 3833–3834.
186. B. J. Goodfellow, I. Moura, J. J. G. Moura, F. Rusnak, T. Domke, *Protein Sci.* **1998**, *7*, 928–937.
187. B. Xu, G. A. Krudy, P. R. Rosevear, *J. Biol. Chem.* **1993**, *268*, 16259–16264.
188. W. Bode, P. Schwager, *J. Mol. Biol.* **1975**, *98*, 693–717.
189. C. P. Hill, Z. Dauter, E. J. Dodson, G. G. Dodson, M. F. Dunn, *Biochemistry* **1991**, *30*, 917–924.
190. K. Ravi Acharya, J. Ren, D. I. Stuart, D. C. Phillips, R. E. Fenna, *J. Mol. Biol.* **1991**, *221*, 571–581.
191. K. Inaka, R. Kuroki, M. Kikuchi, M. Matsushima, *J. Biol. Chem.* **1991**, *266*, 20666–20671.
192. M. Gajhede, D. J. Schuller, A. Henriksen, A. T. Smith, T. L. Poulos, *Nat. Struct. Mol. Biol.* **1997**, *4*, 1032–1038.
193. P. C. Moews, R. H. Kretsinger, *J. Mol. Biol.* **1975**, *91*, 229–232.
194. A. L. Swain, R. H. Kretsinger, E. L. Amma, *J. Biol. Chem.* **1989**, *264*, 16620–16628.
195. D. M. Szebenyi, K. Moffat, *J. Biol. Chem.* **1986**, *261*, 8761–8777.

196. K. A. Satyshur, S. T. Rao, D. Pyzalska, W. Drendel, M. Greaser, M. Sundaralingam, *J. Biol. Chem.* **1988**, *263*, 1628–1647.
197. O. Herzberg, M. N. G. James, *Nature* **1985**, *313*, 653–659.
198. Y. S. Babu, J. S. Sack, T. J. Greenhough, C. E. Bugg, A. R. Means, W. J. Cook, *Nature* **1985**, *315*, 37–40.
199. R. H. Kretsinger, S. E. Rudnick, L. J. Weissman, *J. Inorg. Biochem.* **1986**, *28*, 289–302.
200. Y. S. Babu, C. E. Bugg, W. J. Cook, *J. Mol. Biol.* **1988**, *204*, 191–204.
201. J. D. Otvos, D. T. Browne, *Biochemistry* **1980**, *19*, 4011–4021.
202. E. E. Kim, H. W. Wyckoff, *Clin. Chim. Acta* **1990**, *186*, 175–187.
203. E. E. Kim, H. W. Wyckoff, *J. Mol. Biol.* **1991**, *218*, 449–464.
204. K. L. Yap, J. Kim, K. Truong, M. Sherman, T. Yuan, M. Ikura, *J. Struct. Funct. Genomics* **2000**, *1*, 8–14.
205. D. B. Heidorn, J. Trewhella, *Biochemistry* **1988**, *27*, 909–915.
206. G. Barbato, M. Ikura, L. E. Kay, R. W. Pastor, A. Bax, *Biochemistry* **1992**, *31*, 5269–5278.
207. M. Zhang, T. Tanaka, M. Ikura, *Nat. Struct. Mol. Biol.* **1995**, *2*, 758–767.
208. H. Kuboniwa, N. Tjandra, S. Grzesiek, H. Ren, C. B. Klee, A. Bax, *Nat. Struct. Mol. Biol.* **1995**, *2*, 768–776.
209. B. E. Finn, J. Evenäs, T. Drakenberg, J. P. Waltho, E. Thulin, S. Forsén, *Nat. Struct. Mol. Biol.* **1995**, *2*, 777–783.
210. J. Evenäs, A. Malmendal, M. Akke, *Structure* **2001**, *9*, 185–195.
211. M. Ikura, G. M. Clore, A. M. Gronenborn, G. Zhu, C. B. Klee, A. Bax, *Science* **1992**, *256*, 632–638.
212. W. E. Meador, A. R. Means, F. A. Quiocho, *Science* **1992**, *257*, 1251–1255.
213. W. E. Meador, A. R. Means, F. A. Quiocho, *Science* **1993**, *262*, 1718–1721.
214. N. Matsushima, Y. Izumi, T. Matsuo, H. Yoshino, T. Ueki, Y. Miyake, *J. Biochem.* **1989**, *105*, 883–887.
215. J. H. R. Kägi, M. Nordberg, *Metallothionein I*, Birkhäuser, Boston, 1979.
216. J. H. R. Kägi, Y. Kojima, *Metallothionein II: Proceedings of the Second International Meeting on Metallothionein and Other Low Molecular Weight Metal-binding Proteins: Zürich, August 21–24, 1985*, Birkhäuser Verlag, Boston, 1987.
217. K. T. Suzuki, N. Imura, M. Kimura, *Metallothionein III: Biological Roles and Medical Implications*, Birkhäuser Verlag Boston, 1993.
218. C. D. Klaassen, *Metallothionein IV*, Birkhäuser Verlag Boston, 1999.
219. G. Öz, K. Zangger, I. M. Armitage, *Biochemistry* **2001**, *40*, 11433–11441.
220. W. Braun, G. Wagner, E. Wörgötter, M. Vašák, J. H. R. Kägi, K. Wüthrich, *J. Mol. Biol.* **1986**, *187*, 125–129.
221. P. Schultze, E. Wörgötter, W. Braun, G. Wagner, M. Vašák, J. H. R. Kägi, K. Wüthrich, *J. Mol. Biol.* **1988**, *203*, 251–268.
222. B. A. Messerle, A. Schäffer, M. Vašák, J. H. R. Kägi, K. Wüthrich, *J. Mol. Biol.* **1990**, *214*, 765–779.
223. A. H. Robbins, D. E. McRee, M. Williamson, S. A. Collett, N. H. Xuong, W. F. Furey, B. C. Wang, C. D. Stout, *J. Mol. Biol.* **1991**, *221*, 1269–1293.
224. W. Braun, M. Vašák, A. H. Robbins, C. D. Stout, G. Wagner, J. H. R. Kägi, K. Wüthrich, *Proc. Natl. Acad. Sci. USA* **1992**, *89*, 10124–10128.
225. K. Zangger, I. M. Armitage, *J. Inorg. Biochem.* **2002**, *88*, 135–143.
226. K. Wüthrich, *NMR of Proteins and Nucleic Acids*, Wiley, New York, 1986.
227. J. R. Tolman, H. M. Al-Hashimi, L. E. Kay, J. H. Prestegard, *J. Am. Chem. Soc.* **2001**, *123*, 1416–1424.
228. P. A. Cobine, R. T. McKay, K. Zangger, C. T. Dameron, I. M. Armitage, *Eur. J. Biochem.* **2004**, *271*, 4213–4221.

Chapter 7
Solid State Structures of Cadmium Complexes with Relevance for Biological Systems

Rosa Carballo, Alfonso Castiñeiras, Alicia Domínguez-Martín, Isabel García-Santos, and Juan Niclós-Gutiérrez

Contents

ABSTRACT 146
1 INTRODUCTION 146
2 CADMIUM COMPLEXES WITH NUCLEOBASES AND RELATED LIGANDS 147
2.1 Adenine 147
2.2 N-Substituted Purines with Non-coordinating Pendant Arms 149
2.3 N-Substituted Purines with Potential Chelating Pendant Arms 150
2.4 6-Mercaptopurine 151
2.5 Oxopurines 153
2.6 Pyrimidines 154
3 CADMIUM(II) COMPLEXES WITH α-AMINO ACIDS 155
3.1 Complexes of α-Amino Acids as the Sole Ligand 155
3.2 α-Amino Acid Complexes with Water as Co-ligand 157
3.3 α-Amino Acid Complexes with a Halogen as Co-ligand 158
3.4 Complexes with α-Amino Acids and Other Co-ligands 158
4 COMPLEXES OF CADMIUM WITH VITAMINS AND DERIVATIVES 160
4.1 Thiamine (Vitamin B_1) 161
4.2 Nicotinic Acid (Vitamin B_3) 163
4.3 Vitamin B_6 168
5 OTHER CADMIUM COMPLEXES 170
5.1 Cadmium-Thiolate Complexes 170
5.1.1 Monothiolate Ligands 170
5.1.2 Dithiolate Ligands of the BAL Type 174

R. Carballo
Departamento de Química Inorgánica, Facultad de Química, Universidad de Vigo, E-36310 Vigo, Spain

A. Castiñeiras (✉) • I. García-Santos
Departamento de Química Inorgánica, Facultad de Farmacia, Universidad de Santiago de Compostela, E-15782 Santiago de Compostela, Spain
e-mail: alfonso.castineiras@usc.es

A. Domínguez-Martín • J. Niclós-Gutiérrez
Departamento de Química Inorgánica, Facultad de Farmacia, Universidad de Granada, E-18071 Granada, Spain

A. Sigel, H. Sigel, and R.K.O. Sigel (eds.), *Cadmium: From Toxicity to Essentiality*, Metal Ions in Life Sciences 11, DOI 10.1007/978-94-007-5179-8_7,

5.2 Dithiocarbamate Cadmium Complexes 176
5.3 Polycarboxylate Ligands of the EDTA Type 180
6 GENERAL CONCLUSIONS 182
ABBREVIATIONS AND DEFINITIONS 183
ACKNOWLEDGMENTS 185
REFERENCES 185

Abstract This chapter provides a review of the literature on structural information from crystal structures determined by X-ray diffractometry of cadmium(II) complexes containing ligands of potential biological interest. These ligands fall into three broad classes, (i) those containing N-donors such as purine or pyrimidine bases and derivatives of adenine, guanine or cytosine, (ii) those containing carboxylate groups such as α-amino acids, in particular the twenty essential ones, the water soluble vitamins (B-complex) or the polycarboxylates of EDTA type ligands, and (iii) S-donors such as thiols/thiolates or dithiocarbamates. A crystal and molecular structural analysis has been carried out for some representative complexes of these ligands, specifically addressing the coordination mode of ligands, the coordination environment of cadmium and, in some significant cases, the intermolecular interactions.

Keywords amino acids • cadmium complexes • crystal structures • nucleobases • thiolates • vitamins

1 Introduction

The biological interest in cadmium is based on the fact that its presence in a living being can seriously alter its metabolism, giving rise to acute or chronic intoxication, and therefore cadmium has been classified among the toxic elements [1]. Although the molecular mechanism for the toxicity of this metal is not known in detail, cadmium can be found in living beings as complexes with biochemical ligands and its toxic nature is a result of this coordination, disrupting the biological functions of these ligands. With this in mind, the therapeutic strategies developed to favor detoxification processes – for both chronic diseases and acute intoxications – are all based on the administration of external ligands that are able to successfully compete for the metal against the biological ligands, thus mobilizing the cadmium and favoring elimination via one of the available excretion channels [2].

The stability of cadmium complexes varies depending on the types of ligands and, as the Cd^{2+} ion is considered a *soft* Lewis acid, it prefers easily oxidizable *soft ligands* [3], not dismissing its affinity for other ligands, above all when the *chelate effect* comes into play.

The selection of the ligands of biological interest for a solid phase structural study of cadmium complexes that are relevant to biological systems took into account those compounds which can be applied as potential antidotes in the

treatment of cadmium toxicity. As a result, we considered several chelating agents such as adenosine 5'-triphosphate (ATP), as well as amino acids, nitrogenated bases, dithiocarbamates, thiolates, and vitamins.

In the following sections we describe the crystal structures, determined by single crystal X-ray diffraction, of those cadmium compounds that may be important with regard to understanding the metal-ligand interactions in a biological detoxification context for the aforementioned metal. Special attention is paid to compounds that illustrate the chemically (structurally) important species that may be formed by cadmium and those which are of biological relevance. All of the graphics were created using the ChemDraw Ultra [4], DIAMOND [5], and MERCURY [6] programs.

2 Cadmium Complexes with Nucleobases and Related Ligands

Given the stability of the +2 oxidation state of cadmium, broad and varied structural information is available regarding complexes of purine or pyrimidine bases and some related ligands (Scheme 1). In particular, attention should be paid to N-derivatives of adenine or guanine and cytosine. Likewise, a number of structures have been reported for cadmium complexes with nucleotides, although these structures are not discussed in detail here. However, the main characteristic of such compounds is that monophosphate nucleotides bind cadmium through the appropriate N7 donor atom of the nucleobases (Figure 1a) and an outersphere interaction with the phosphate group, whereas triphosphate nucleotides chelate cadmium through negatively charged O-phosphate donor atoms (Figure 1b).

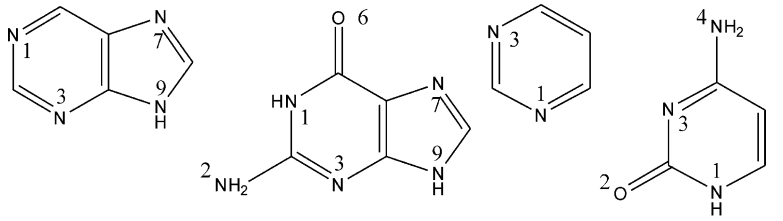

Scheme 1

2.1 Adenine

A number of structures of cadmium complexes have been described for purine-like bases such as adenine (Hade) and 2,6-diaminopurine (Hdap), either in neutral, cationic or anionic forms.

Neutral adenine has been reported in two polymeric compounds. The compound $\{[Cd(\mu_2\text{–ox})(H(N7)ade)(H_2O)]\cdot H_2O\}_n$ [7] consists of 1D zig-zag chains in which

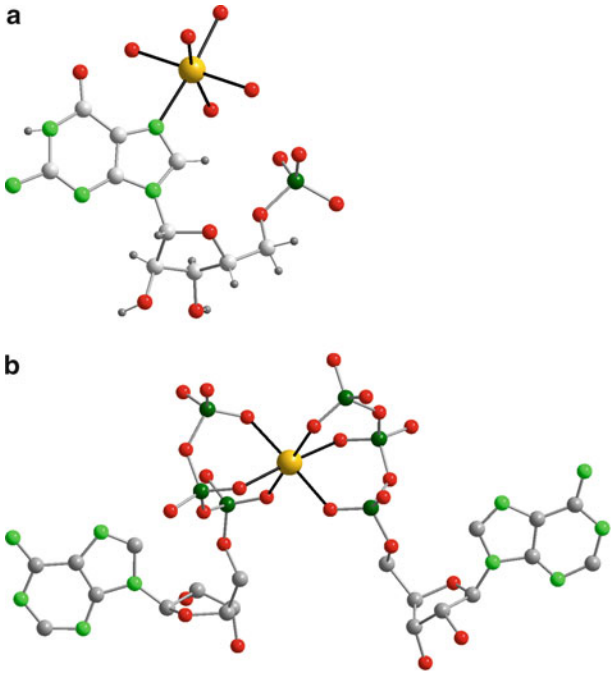

Figure 1 (**a**) Monophosphate nucleoside cadmium(II) complex; (**b**) triphosphate nucleoside cadmium(II) complex.

$Cd(H(N7)ade)(H_2O)^{2+}$ units are linked by μ_2-oxo bridges with tetradentate oxalate ligands. Curiously, Hade coordinates through the less basic heterocyclic donor atom, giving rise to the Cd–N3 bond (2.282 Å), which is assisted by an (aqua) O–H···N9 H-bond (2.766 Å, 147.7°). Thus, the tautomer H(N7)ade seems to be favored due to the involvement of the N7–H bond in the crystal packing. The compound $[Cd(\mu_3\text{–}SO_4)(\mu_2\text{–}N7,N9\text{-}H(N1)ade)]_n$ [8] contains the tautomer H(N1)ade, a situation consistent with the bidentate role of adenine and its basicity order (N9 > N1 > N7 > N3 > N6). The Cd–N9 bond (2.239 Å) does not cooperate with an interligand H-bonding interaction, whereas the Cd–N7 bond (2.204 Å) is reinforced by a N6–H···O(sulfate) interaction (2.940 Å, 164.7°). In these polymers the cadmium ion adopts a six-coordination mode.

The adeninium(1+) cation was reported in the binuclear compound $[Cd_2(\mu_2\text{–}N3,N9\text{-}H_2(N1,N7)ade)_2(\mu_2\text{–}H_2O)_2(O,O'\text{-}NO_3)_4](NO_3)_2$ [9] (Figure 2). In this compound the coordination number of the cadmium ion is eight. The two metal centers are separated by 3.6 Å and the Cd–N3 (2.467 Å) and Cd–N9 (2.414 Å) bonds are somewhat longer than the usually observed ones. The adeninate(1–) anion is known in two mixed-ligand metal complexes. In $[Cd(tren)(N9\text{-}ade)]ClO_4$ [10] the former ade^- anion coordinates the penta-coordinated metal ion through its most basic donor atom, giving rise to the Cd–N9 bond (2.193 Å) assisted by a very weak (electrostatic nature) (tren)N–H···N3 interaction (3.206 Å, 117.6°). The polymeric chain of $\{[Cd_3(\mu_3\text{–}ap)_2(\mu_3\text{–}N3,N7,N9\text{-}ade)_2(H_2O)_2]\cdot 1.5H_2O\}_n$ [11] is

based on the catenation of trinuclear motifs in which the central metal ion is six-coordinated, involving two Cd–N9 (2.195 Å) bonds. Alternatively, the other two metal centers have coordination number seven and show one Cd–N3 (2.326 Å) and a Cd–N7 (2.282 Å) bond.

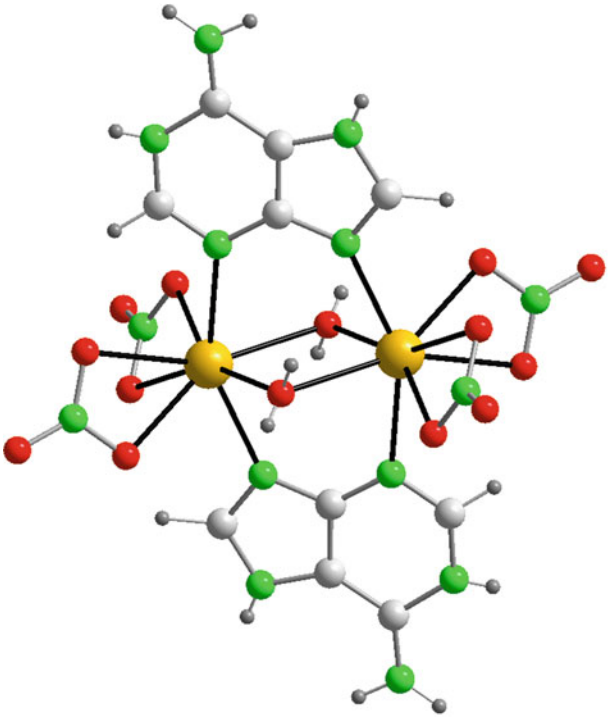

Figure 2 $[Cd_2(\mu_2\text{–}N3,N9\text{-}H_2(N1,N7)ade)_2(\mu_2\text{–}H_2O)_2(O,O'\text{-}NO_3)_4]^{2-}$.

Examples are known where the non-natural nucleobase 2,6-diaminopurine coordinates in cationic or anionic forms. In the compound $\{[Cd(H_2dap)\text{-}(H_2O)_2(tp)]_2(tp)\cdot 2H_2O\}_n$ [12], the diaminopurinium(1+) cation binds cadmium through the Cd–N7 bond (2.342 Å) in cooperation with the intramolecular interligand N6–H···O(coord., tp) interaction (2.923 Å, 146.6°). The anionic form dap^- builds the polymer $\{[Cd_3(\mu_3\text{–}ap)_2(\mu_3\text{–}N3,N7,N9\text{-}dap)_2(H_2O)_2]\cdot H_2O\}_n$ [12]. Note that this polymer is closely related to that described above for adeninate (Cd–N3 2.586 Å, Cd–N7 2.298 Å, Cd–N9 2.387 Å).

2.2 N-Substituted Purines with Non-coordinating Pendant Arms

The N-substitution of a heterocyclic N-donor of purines represents a significant restriction on the tautomeric possibilities associated with the H atom usually linked to N9(purines). Thus, alkylation at N9 on adenine or guanine increases the metal

binding possibilities of the N7 donor atom. This general consideration can be applied to the following compounds: $[Cd(9Meade)(O\text{-}dmso)(\mu_2\text{–}Cl)_2]_n$ [13], $[Cd(9Megua)_2(H_2O)_4](NO_3)_2$ [14] and $[Cd(9Etgua)_2(H_2O)_4](NO_3)_2$ [14]. The latter compounds have in common the Cd–N7 bond in cooperation with the intramolecular interligand N6–H···O(dmso) (2.877 Å) or (aqua)O–H···O6 (2.905 or 2.752 Å) interactions, respectively. The coordination number of cadmium in these compounds is six and the Cd–N7 bond distance is 2.358 Å (9Meade) or 2.283 Å (9Megua or 9Etgua).

A certain number of N6-substituted adenines display kinetin activity. In this context, cadmium derivatives have been reported with the N6-benzyl-adeninium-(1+) (BAD^+) and N6-furfuryl-adeninium(1+) (FAD^+) cations to yield the compounds $[Cd(\mu_2\text{–}Cl)_2Cl(H_2(N3,N7)BAD)]_n$ and $[Cd(\mu_2\text{–}Cl)_2Cl(H_2(N3,N7)FAD)]_n$ [15]. In these polymers the coordination number of cadmium is six. Both N6-adenine derivatives bind the metal via the Cd–N9 bond (2.348 or 2.361 Å, respectively) reinforced by an intramolecular interligand N3–H···(μ–Cl) interaction (3.188 Å, 159.3° or 3.154 Å, 165.1°, respectively). The protonation sites (N3, N7) of these N6-substituted adenines should be related to the aforementioned intramolecular N3–H···(μ–Cl) bond and the crystal packing. Indeed, the N7–H bond is involved in bifurcated H-bonding with two different chlorido ligands.

2.3 N-Substituted Purines with Potential Chelating Pendant Arms

The most relevant N-substituted purine-like ligand with a potential chelating pendant arm is the antiviral acyclovir [2-amino-9-(2-hydroxyethoxymethyl)-3*H*-purin-6-one]. It was reported in a recent paper [16] that this drug is able to bind metal ions by forming an M–N7 bond, which can cooperate with an appropriate intramolecular interligand H-bond involving the O6 atom as an H-acceptor. However, the available structural information indicates that the N9-pendant arm of acyclovir does not usually participate in metal binding. In fact, the unique exception to this rule is found in the compound $\{[Cd(\mu_2\text{–}Cl)_2(\mu_2\text{–}O,N7\text{-}acv)]\cdot H_2O\}_n$ [17] where the O-acv donor is the OH-alcoholic group in the pendant arm. In this compound the metal ion is six-coordinated and the bridging role of acv represents the Cd–N7 (2.402 Å) and the referred Cd–O (2.305 Å) bonds.

Several cadmium complexes are known with adenine, 2,6-diaminopurine, and guanine derivatives with the 2-(ethylenediamine)ethyl-N9-pendant arm (ede). In the compound $[Cd_3(Cl)_2(\mu_2\text{–}Cl)_4(\mu_2\text{–}N3,N7\text{-}[ede\text{-}ade])_2]_n$ [18], ede-ade acts both as a tridentate chelate and a bridging ligand. The chelating role involves the N3-ade donor atom (Cd–N3 2.418 Å) and two N atoms of the ethylenediamine moiety. Note that this chelating role involves the formation of one seven-membered and one five-membered chelate ring. Likewise, the bridging role also involves the Cd–N7 bond (2.389 Å). More recently, the structure of the compound $[Cd_3(Br)_2(\mu_2\text{–}Br)_4(\mu_2\text{–}N3,N7\text{-}[ede\text{-}ade])_2]_n$ has been described [19]. The aforementioned polymers give isotypic crystals.

Furthermore, two cadmium complexes with derivatives of such ligands have recently been reported. In the mononuclear compound $[Cd(ede\text{-}dap)_2(NO_3)_3]$ [20], the metal exhibits a trans-octahedral coordination involving two ethylenediamine moieties and two unidentate nitrate ligands. In contrast, the crystal of the polymer $[Cd_2(\mu_2\text{–}[edp\text{-}dap])(H_2O)(Cl)_2(NO_3)_2]_n$ [20] exhibits two non-equivalent cadmium coordination polyhedra and the edp-dap ligand plays a chelating and bridging role. The pentacoordinated cadmium center has two N7 donor atoms (Cd–N7 2.407 Å) from two edp-dap ligands plus two chlorido and one aqua ligand. Each Cd–N7 bond is reinforced by one N6–H···Cl interaction (3.260 Å, 174.4°). The other cadmium center has a trans-octahedral environment formed by two ethylenediamine moieties from the edp ligand and two nitrate ligands. The ligand ede-gua is found in the polymer $\{[Cd(ede\text{-}gua)(SO_4)(H_2O)]_4\cdot 7H_2O\}_n$ [18] (Figure 3). Herein, ede-gua plays both chelating and bridging roles using the ethylenediamine moiety and the N7 donor atom to give tetranuclear square-shaped motifs. The Cd–N7 bond (2.309 Å) is in cooperation with the N–H···O6 interaction (2.823 Å, 141.7°) and these link the terminal primary amino group from the ethylenediamine moiety of one ede-gua ligand and the O6 exocyclic atom of another one. In the crystal, four sulfate anions bridge metal centers in adjacent squares to build cylindrical polymers that interconnect to each other through π,π-stacking interactions between the six-membered ring of the guanine moieties.

A number of bis-adenine ligands with N,N'-spacers are also known. Their deprotonated cations (tm-N9,N9'-diade and tem-N9,N9'-diade) lead to outersphere complexes. In the compound $(H_2tm\text{-}N9,N9'\text{-}diade)_2[Cd(\mu_2\text{–}Cl)Cl_3(H_2O)]_2\cdot 4H_2O$ [21], the adenine moieties of the cation are protonated at N1 whereas in the related compound $\{(H_2tem\text{-}N9,N9'\text{-}diade)_2[Cd_4(\mu_3\text{–}Cl)_2(\mu_2\text{–}Cl)_6Cl_4(H_2O)_2]\cdot 4H_2O\}_n$ [22] there are two non-equivalent tautomeric cations in which the adenine moieties are protonated at N1 or N3. Regarding the asymmetric ligand tem-N3,N9'-diade, a mixed-ligand 1D polymer $\{[Cd_2(H_2tem\text{-}N3,N9'\text{-}diade)_2(\mu_2\text{–}Cl)_4Cl_4(H_2O)_2]\cdot 2H_2O\}_n$ [22] with two non-equivalent cadmium centers has been reported. One cadmium is surrounded by five chlorido ligands whilst the other is *trans* six-coordinated by four chlorido ligands and two $(H_2tem\text{-}N3,N9'\text{-}diade)^{2+}$ cations linked to the cadmium by the N7 donor atom of the N9-alkyl-substituted adenine moiety. Interestingly, the Cd–N7 bonds (2.375 Å) are reinforced by N6–H···Cl interaction (3.267 Å, 178.3°).

2.4 6-Mercaptopurine

The soft character and the oxidation state stability of the cadmium(II) ion mean that a good affinity to soft S donor atoms can be expected without the interference of redox chemistry. On this basis, interesting structural chemistry is documented for cadmium complexes with the non-natural nucleobase 6-mercaptopurine (H6MP). Five structures refer to compounds that contain the neutral H6MP. In $[Cd(H6MP)_2(Cl)_2]\cdot 2H6MP$ [23] the metal is six-coordinated and H6MP acts as a bidentate chelating ligand through the S6 and N7 donor atoms (Cd–S6 2.622 Å, Cd–N7 2.366 Å).

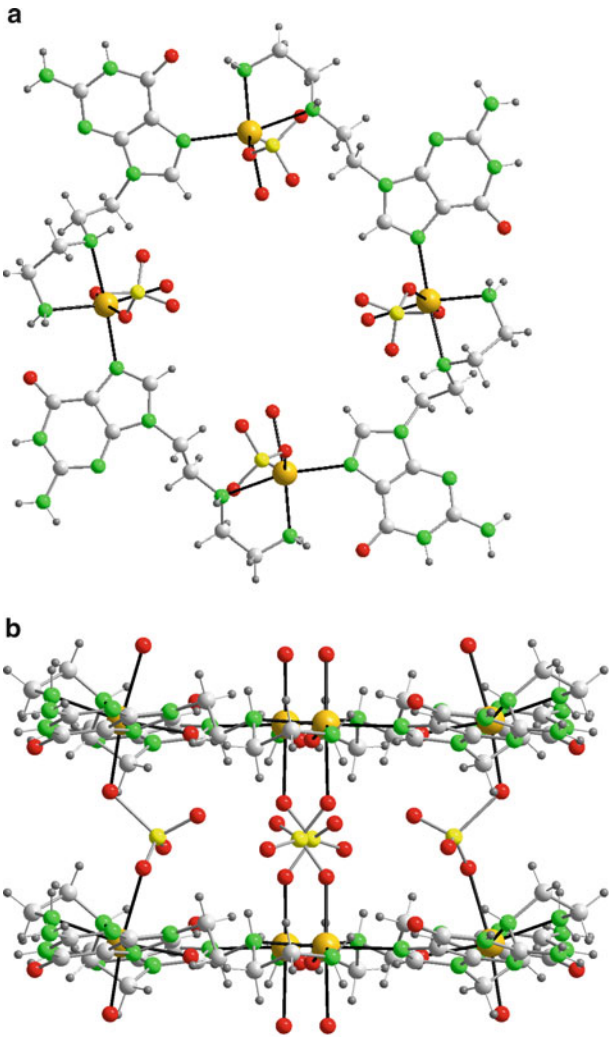

Figure 3 $\{[Cd(ede\text{-}gua)(SO_4)(H_2O)]_4 \cdot 7H_2O\}_n$.

The same chelating role of H6MP has been described in the binuclear complex molecule $[Cd(H6MP)(\mu_2\text{–}Cl)Cl(H_2O)]_2$ [24] (Cd–S6 2.790 Å, Cd–N7 2.324 Å). H6MP plays both chelating and bridging roles in the compounds $[Cd(\mu_2\text{–}H6MP)(H6MP)(H_2O)]_2(NO_3)_4 \cdot 2H_2O$ (Figure 4) and $[Cd(\mu_2\text{–}H6MP)(H6MP)(NO_3)]_2(NO_3)_2$ [25]. As shown in Figure 4, the binuclear compound has one chelating-S6,N7 ligand (Cd–S6 2.653 Å, Cd–N7 2.339 Å) and one chelating-S6,N7 (Cd–S6 2.763 Å, Cd–N7 2.287 Å) plus bridging-S6 (Cd–S6 2.914 Å) ligand per cadmium center. Within the cation of this compound, pairs of purine ligands are π,π-stacked through interactions involving the five-membered ring of the chelating H6MP

ligand and the six-membered ring of the chelating + bridging H6MP ligand. The centroid-centroid (Cg-Cg) distance for the stacked ring is 3.418 Å. The complex shown in Figure 4 has six coordination polyhedra whereas in the binuclear complex cation $[Cd(\mu_2 - H6MP)(H6MP)(NO_3)]_2^{2+}$ the bidentate role of nitrate ligands increase the coordination number of the metal ion to seven. The π,π-stacking interactions are not observed in the latter cation.

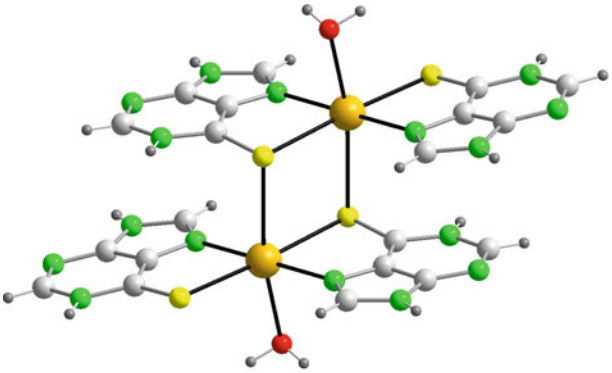

Figure 4 $[Cd(\mu_2–H6MP)(H6MP)(H_2O)]_2^{4+}$.

From a structural point of view, the compound $[Cd(\mu_2\text{-}Cl)Cl(H6MP)]_{2n}\cdot n[Cd(H6MP)_2(Cl)_2]$ consists of a 1D polymeric chain and discrete complex molecules, both of which have six-coordinated cadmium(II) centers. In the molecule $[Cd(H6MP)_2(Cl)_2]$, the H6MP ligand acts as a bidentate chelator (Cd–S6 2.632 Å, Cd–N7 2.392 Å). In the polymer, the H6MP ligands play a unique chelating-S6,N7 plus bridging-N3 role (Cd–S6 2.743 Å, Cd–N7 2.300 Å, Cd–N3 2.409 Å) [26].

The univalent anion 6MP plays a chelating-S6,N7 (Cd–S6 2.689 Å, Cd–N7 2.283 Å) plus a bridging-S6 (Cd–S6 2.868 Å) role in the polymer $\{[Cd(6MP)_2]\cdot 2H_2O\}_n$ [23]. The same chelating plus bridging role has been reported for the polymeric compound $\{[Ca(\mu_2–H_2O)_2(H_2O)_4][Cd(\mu_2–6MP\text{-}H)_2]\}_n$ [25], where 6MP-H is the divalent anion of H6MP (Cd–S6 2.741 Å, Cd–N7 2.266 Å, Cd–S6 2.888 Å).

2.5 *Oxopurines*

Very little structural information is available for cadmium(II) complexes with neutral oxopurines. Nevertheless, the basicity of the N-donors in this kind of oxopurine ligand, as well as the softness, increases after the dissociation of at least one of the protons. Consequently, most of the available crystal data concerning complexes of such ligands refer to the univalent anions of hypoxanthine (Hhyp), xanthine (Hxan) or theophylline (Htheo). Neutral hypoxanthine yields the compound $[Cd_2(\mu_2–N3,N9\text{-}H(N7)hyp)_2(\mu_2–H_2O)_2(SO_4)_2(H_2O)_2]$ [27], in which the

metal exhibits a six-coordination and the bridging μ_2–N3,N9-H(N7)hyp (Cd–N3 2.367 Å, Cd–N9 2.274 Å) and μ_2–H_2O ligands yield a binuclear complex molecule with a Cd···Cd separation of 3.452 Å. This bridging μ_2–N3,N9 coordination mode is reported for cationic, neutral, and anionic forms of adenine [28]. The hypoxanthinate (1–) anion yields the compound $[Cd_2(tren)_2(\mu_2\text{–N7,N9-hyp})](ClO_4)_3\cdot 0.5H_2O$ [7] in which the Cd–N7 (2.204 Å) and the Cd–N9 (2.197 Å) bonds are weakly assisted by H-bonding interactions [(tren)N–H···O6 3.061 Å, 128.9° or (tren)N–H···N3 3.171 Å, 135.3°, respectively]. Both metallic centers in this complex are five coordinated.

The cadmium(II) chelate of the tripodal tetradentate ligand 'tren' also yielded the mixed-ligand complex cation of the salt $[Cd(tren)(xan)]ClO_4\cdot H_2O$ [29], where the metal ion is only five-coordinated and the anionic xan^- ligand forms the Cd–N7 bond (2.224 Å) reinforced by the intramolecular interligand H-bond (tren)N–H···O6 (2.889 Å, 117.6°). In the compound *trans*-$[Cd(theo)_2(H_2O)_4]\cdot 2DMF$ [30], each theophilinate(1–) anion binds the cadmium(II) center by the Cd–N7 bond (2.300 Å) in cooperation with an intramolecular H-bond (aqua)O–H···O6 (2.689 Å, 158.5°).

2.6 Pyrimidines

The structural information concerning cadmium(II) complexes with pyrimidine nucleobases and closely related ligands is rather limited. However, the diversity of these systems is a good source of information. Most structures in this field concern cytosine and 1-substituted cytosine ligands. The compound $\{[Cd(\mu_2\text{–}Cl)_2(H_2O)_2]\cdot 2Hcyt\}_n$ [31] is a cytosine solvate of a polymeric complex in which the metal is six-coordinated. The crystal of this compound contains an H-bonded chain of Hcyt molecules built by two pairs of H-bonding interactions [N1–H···O2(exocyclic) and (exocyclic)N4–H···N3 with their symmetry related interactions]. A cytosinium(1+) salt of the formula $(H_2cyt)[CdBr_4]$ [32] has been reported and two different cytosinium(1+) cations are present in this compound. In this outersphere complex the cadmium(II) ion is tetrahedrally surrounded by the rather bulky bromido ligands and the cytosinium cations, which are involved in an extensive H-bonding network.

Closely related to the latter compounds is the complex $[Cd(Hcyt)_2(Br)_2]$ [33], in which the metal exhibits a rather distorted six-coordination due to the size of the bromido ligands and the chelating-O2,N3 role of Hcyt bases. The nature of the crystal packing (mainly the H-bonded network) means that both bromido and cytosine ligands are not strictly equivalent. The Hcyt ligands build a strained four-membered chelate ring (Cd–N3 2.243 or 2.281 Å, Cd–O2 2.825 or 2.780 Å, respectively). In the binuclear complex $[Cd(\mu_2\text{–hip})(hip)(Hcyt)(H_2O)]_2$ [34] the cadmium(II) is seven-coordinated and, in this centrosymmetric complex, the Hcyt ligand plays a bidentate-O2,N3 role (Cd–N3 2.240 Å, Cd–O2 2.2687 Å). All hippurate(1–) ligands play bidentate roles for one metal center or bridging between two cadmium(II) atoms. An interesting salt with a mixed-ligand cation and anion

has been reported. $[Cd(Hcyt)_3Cl][Cd(Hcyt)Cl_3]$ [31] is a nice example to show how a crystallographic study provides the best evidence for the mixed-ligand nature of the compounds. The five-coordinated anion has one chelating-O2,N3-Hcyt ligand (Cd–N3 2.253 Å, Cd–O2 2.751 Å) whereas the seven-coordinated cation has three non-equivalent chelating-O2,N3-Hcyt ligands (Cd–N3 2.266, 2.285 or 2.289 Å, Cd–O2 2.797, 2.680 or 2.982 Å, respectively).

Only one mixed-ligand cadmium(II) complex has been reported for the Hcyt isomer isocytosine (Hicyt). $[CdCl_2(Hicyt)_2]$ [35] exhibits a six-coordination for the metal with two non-equivalent chlorido and chelating-N3,O4-Hicyt ligands (Cd–N3 2.261 or 2.286 Å, Cd–O4 2.682 or 2.624 Å, respectively). Regarding uracil (Hura), in the structure of the molecular complex $[Cd(ura)_2(H_2O)_3]$ [36] the cadmium(II)···O4(ura) distance is 3.203 Å and this can not be considered as a coordination bond [the sum of van der Waals radii of cadmium(II) (1.60 Å) and oxygen (1.50) is 3.10 Å]. Therefore, this complex has five-coordinated cadmium(II) atoms in a bipyramidal-trigonal topology with two *trans*-apical aqua ligands (Cd–O 2.439 Å) and the remaining aqua ligand (Cd–O 2.269 Å) with the two uracilate(1–) ligands (Cd–N3 2.211 Å) in the equatorial plane.

In the molecular complex *cis*-$[Cd(1Mecyt)_2Cl_2]$ [37] the chlorido ligands fall in *cis*-coordination sites but are not equivalent for crystal packing reasons. Furthermore, the two 1Mecyt ligands are not equivalent and play a chelating-O2,N3 role (Cd–N3 2.282 or 2.297 Å, Cd–O2 2.780 or 2.676 Å). A closely related compound to the aforementioned complex is *cis*-$[Cd(1Toscyt)_2Cl_2]$ [38] where, once again, the chlorido and 1Toscyt ligands are non-equivalent and the 1Toscyt bases play a chelating-O2,N3 role (Cd–N3 2.260 or 2.278 Å, Cd–O2 2.839 or 2.846 Å, respectively).

3 Cadmium(II) Complexes with α-Amino Acids

Structural studies on cadmium(II) complexes with amino acids include a vast number of compounds. Therefore, hereafter, we will focus exclusively on those complexes that contain one or more of the twenty essential α-amino acids.

On reviewing the CSD we observed that, to date, only cadmium(II) complexes with 11 essential α-amino acids have been structurally studied in the solid state. Among them, there is only one known structure each for methionine (Hmet), phenylalanine (Hphe), tryptophan (Htrp), asparagine (Hasn), aspartic acid (H_2asp), and histidine (H_2his). However, the number of structures containing glycine (Hgly), alanine (Hala), proline (Hpro), cysteine (H_2cys) or glutamic acid (H_2glu) is relatively varied and includes a total of 28 examples.

3.1 Complexes of α-Amino Acids as the Sole Ligand

Complexes in which only the α-amino acid is coordinated to the cadmium can be monomeric, such as $[Cd(L\text{-}Hhis)_2]\cdot 2H_2O$, in which the cadmium is octahedrally

coordinated by two histidinate(1–) ligands via the amine [2.287(9) Å] and imidazole [2.290(8) Å] nitrogen atoms and via two carboxyl oxygen atoms [2.480(9) Å], with each histidinate ligand adopting a closed conformation with the imidazole ring folded back on top of the carboxylate group [39] (Figure 5). Nevertheless, the carboxylate group usually acts as an *anti-syn* bridging bidentate ligand, giving rise to chain structures such as $\{[Cd(gly)_2]\cdot H_2O\}_n$. In this compound the cadmium ions display a distorted octahedral coordination in which two glycinate(1–) ligands bind the metal through the nitrogen and oxygen atoms in a *trans* square planar configuration, whilst the axial positions are occupied by oxygen atoms of carboxylate groups from neighboring amino acids [40] (Figure 6). Similar behavior can be observed in complexes with methionine or asparagine [41], or in $[Cd(\text{L-trp})(\text{D-trp})]_n$ [42]. The novelty of the latter complex lies in the fact that, having used only L-trp as the starting material in the synthesis, in the complex both L-trp and a D-trp isomers are found binding the cadmium ion. In this polymer, the metal exhibits an

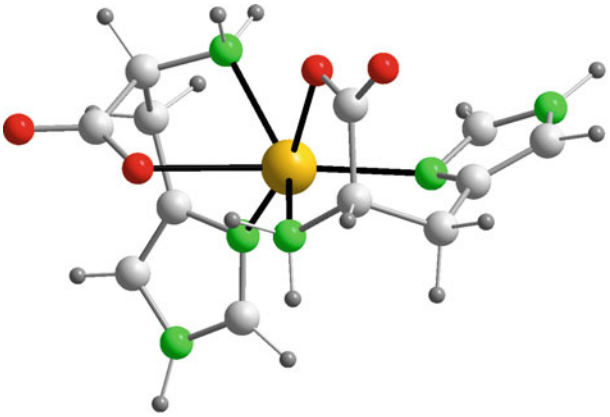

Figure 5 $[Cd(L\text{-}Hhis)_2]$.

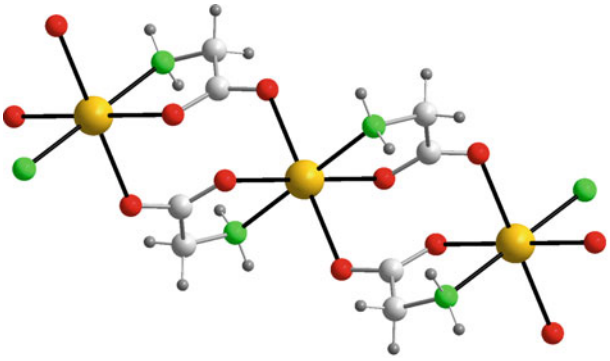

Figure 6 $\{[Cd(gly)_2]\}_n$.

octahedral coordination polyhedron. The L-trp and D-trp ligands display the same role acting as N,O-bidentate chelate for one metal center and as O,O'-bridging carboxylate ligand between two adjacent cadmium ions. The racemization of L-trp is not well understood and needs to be assessed.

$[Cd(L\text{-}cys)]_n$ is a different polymer based on a 1D ladder arrangement of Cd and S produced by thiolate bridges from the cysteine. These 1D units are linked in a regular manner by the carboxylate groups of the amino acid, which binds the metal centers from two neighboring ladders via their two oxygen atoms. The coordination sphere of each cadmium atom is octahedrally distorted, with an L-cysteinate dianion acting as a tridentate chelating ligand in an imposed *fac* manner via its amine, carboxylate, and thiolate groups. The aforementioned coordination sphere is completed by two new sulfur atoms from two cysteinate ligands, which chelate two neighboring cadmium ions in the chain itself and a carboxylate oxygen atom from a cysteinate from a neighbouring chain (Figure 7). As a result, the three sulfur atoms bonded to the same cadmium are in a *mer* arrangement and the two oxygen atoms are *cis* [43]. Interestingly, the L-cys^{2-} ligand plays an important role, with the S-thiolate atom binding three cadmium centers whilst the α-carboxylate groups bridge two Cd(II) in an *anti-syn* manner.

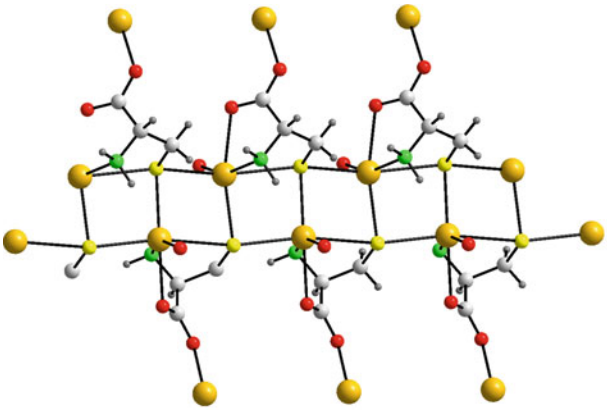

Figure 7 $[Cd(L\text{-}cys^{2-})]_n$.

3.2 α-Amino Acid Complexes with Water as Co-ligand

There are a number of known polymeric and monomeric cadmium complexes with α-amino acids that contain coordinated water. An example of a monomer is $[Cd(L\text{-}ala)_2(H_2O)]\cdot H_2O$ where the metal is octahedrally coordinated by two alaninate(1–) ligands that act as *cis*-O,O-*trans*-N,N chelating bidentate ligands [Cd–O, 2.326(5) Å, Cd–N, 2.334(5) Å] and by two water molecules that occupy *cis* positions [Cd–O, 2.296(4) Å] [44].

An example of a polymer is $\{[Cd(L\text{-}glu)(H_2O)]\cdot H_2O\}_n$, where the cadmium is octahedrally coordinated to L-glutamate(2–) ligands and a water molecule leading to a five-membered chelate ring. Indeed, each glutamate(2–) ligand binds three cadmium ions using its five donor atoms. The α-carboxylate group acts as chelating ligand – along with the amine group – for a cadmium center and as an *anti-syn* bidentate bridge, whereas the γ-carboxylate group acts as bidentate chelator [45]. Furthermore, another coordination polymer has been reported with glutamate and water and this has the formula $\{[Cd(L\text{-}glu)(H_2O)Cd(L\text{-}glu)(H_2O)_2]\cdot H_2O\}_n$, in which there are two crystallographically independent and hepta-coordinated cadmium atoms. One of these metal centers has a 'distorted square-based trigonal-capped' coordination polyhedron whereas the coordination geometry of the second is distorted trigonal bipyramidal [41].

3.3 α-Amino Acid Complexes with a Halogen as Co-ligand

There are several structures of cadmium chlorido complexes with α-amino acids. All of them are coordination polymers with the amino acid in its zwitterionic form. In $[CdCl_2(Hgly)_2]_n$, each cadmium atom has an octahedral Cl_3O_3 environment with one terminal chlorido ligand and the other two bridging to a neighbouring cadmium atom, to one oxygen atom from the carboxylate group of a glycine zwitterion and to two oxygen atoms from two glycines, which act as *anti-syn*-type bidentate bridging ligands to neighboring cadmiums, satisfy the coordination [46]. This structure contrasts with that of the complex $[Cd_3(\mu_2\text{–}Cl)_6(O,O'\text{-}Hgly)_2(O\text{-}Hgly)_2]_n$, that contains two symmetrically independent cadmium atoms with different coordination environments. One cadmium is surrounded by four chlorido ligands and two oxygen atoms in *trans* positions from two glycine zwitterions, which act as O-monodentate ligands. The other cadmium center is also bonded to four chlorido ligands and to two oxygen atoms from an asymmetric chelating bidentate glycine zwitterion [Cd–O, 2.318(5) and 2.534(5) Å]. The bridging chlorido ligands join the metal centers to form chains with the glycine zwitterions, which are connected in a hanging decorative fashion [47] (Figure 8). In $\{[Cd(\mu_2\text{–}Cl)_2(\mu_2\text{–}D,L\text{-}Hala)]\cdot xH_2O\}_n$ (x = 0 or 1) [48,49] and in {[$CdCl_2$(L-Hpro)]·H_2O}n [50], each cadmium ion is coordinated by four chlorido ligands and two carboxylate oxygen atoms to form a distorted octahedron. The four chlorido ligands that are coordinated to the metal center form square planes, which are linked to each other by means of *syn-syn*-type bidentate carboxylate bridges. This arrangement gives rise to 1D polymers in which the fragments of amino acid are hanging at the sides of the chain.

3.4 Complexes with α-Amino Acids and Other Co-ligands

A number of structures of cadmium complexes have been reported that contain, in addition to an α-amino acid and a halogen, a neutral ligand. One such example is

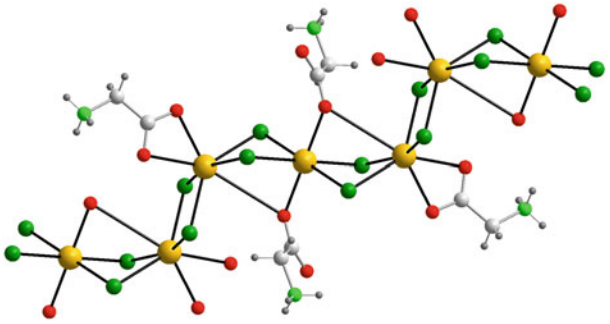

Figure 8 $[Cd_3Cl_6(Hgly)_4]_n$.

$[CdCl(\mu_2\text{–}N,O,O'\text{-gly})(DABT)]_n$ (DABT = 2,2'-diamino-4,4'-bis-1,3-thiazole). In this compound, each cadmium(II) is coordinated by a chlorido ion, a molecule from the diamine-bithiazole ligand and by two glycinate ions (one O-monodentate and the other N,O-bidentate). Consequently, the glycinate anions act as bridges between neighbouring cadmiums and form zig-zag chains [51].

In other structures an oxoanion is present instead of a halide. For example, in $[Cd(\mu_4\text{–Hasp})(\mu_2\text{–}NO_3)]_n$ the aspartate(1−) anion is in its zwitterionic form and the Cd^{2+} ion is hepta-coordinated, with a distorted environment in which the sixth position is doubly occupied by two oxygen atoms from the NO_3^-, which acts as a chelating bidentate ligand. The remaining coordination positions are occupied by an oxygen atom from a crystallographically equivalent nitrate ion (*trans* to the other nitrate) and by four oxygen atoms from four equivalent aspartate ligands, which are in *cis* positions to the nitrates. As a result, the nitrate and aspartate act as bridges between neighbouring metal centers, leading to a 2D structure [52] (Figure 9). This structure is in contrast to that found in $[Cd(L\text{-pro})(NO_3)(4,4'\text{-bipy})]_n$ (4,4'-bipy = 4,4'-bipyridine), where a prolinate(1–) ligand chelates a cadmium center in an N,O coordination mode. The structure extends in one dimension through the non-chelating carboxylate oxygen atom, which is bonded to an adjacent cadmium atom, which in turn is *trans* to the chelating oxygen. Furthermore, the bipy ligand coordinates orthogonally to link the cadmium-proline chains into 2D sheets. The coordination environment is completed with a monodentate NO_3^- anion bound in a *trans* position to the amine nitrogen of the proline [53].

There are also several cadmium cationic complexes with α-amino acids. In $[Cd_2(D,L\text{-ala})(tren)](ClO_4)_3$ [tren = tris-(2-aminoethyl)amine], the structural analysis indicates an ionic character, including two Cd^{2+} ions with different coordination environments in the cation $[Cd_2(D,L\text{-ala})(tren)]^{3+}$ (Figure 10). One cadmium is hexa-coordinated with a distorted octahedral geometry, whereas the other is penta-coordinated with a trigonal bipyramidal geometry. The alaninate anion acts as a bridging ligand between the two metal centers, coordinating to a cadmium in a bidentate N,O-chelate fashion and to the other cadmium in a monodentate fashion via the second oxygen atom of the carboxylate group [54].

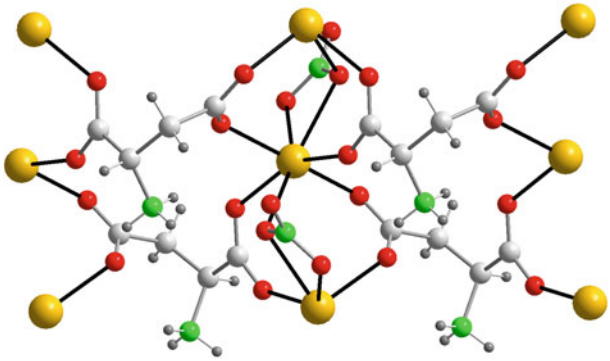

Figure 9 $[Cd(Hasp^{-})(NO_3)]_n$.

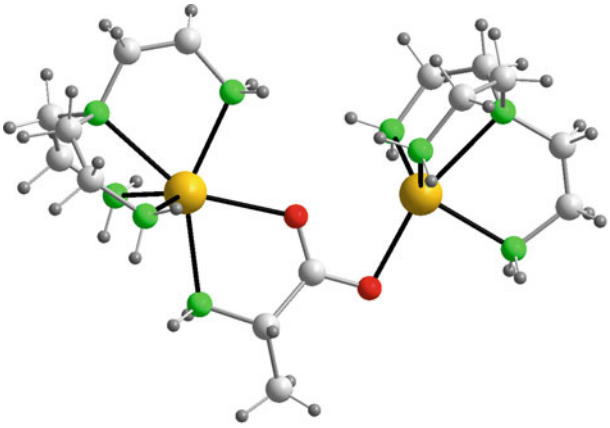

Figure 10 $[Cd_2(D,L\text{-ala})(tren)]^{3+}$.

4 Complexes of Cadmium with Vitamins and Derivatives

Although vitamins have different structures, sources, requirements, and mechanisms of action, they are classified according to their solubility in water or in fats. Vitamins A, D, E, and K are liposoluble, whereas the B-complex (B_1, B_2, B_6, B_{12}, niacin, pantothenic acid, biotin, and folic acid) and C vitamins are hydrosoluble. Moreover, there are some organic compounds related to vitamins that are usually classified with the B vitamins and are also hydrosoluble; i.e., *p*-aminobenzoic acid is included among these substances with similarities to vitamins.

To date, only some hydrosoluble vitamins are known to interact as ligands with metal ions and, with some exceptions, very few solid phase structures of these complexes have been obtained (Scheme 2). Indeed, only a few cadmium complex structures have been described.

In the following paragraphs, we will describe the most significant aspects of the known structures of cadmium complexes with vitamins, as obtained by X-ray diffraction analyses.

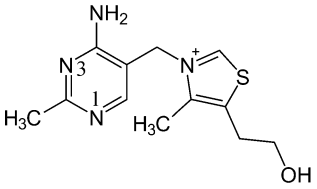

Thiamine (B1)

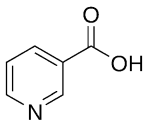

Nicotinic acid (B3)

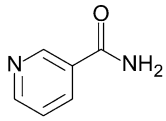

Nicotinamide (B3)

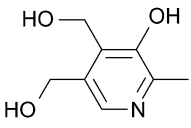

Pyridoxine (B6)

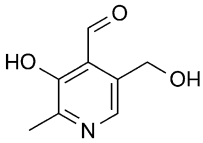

Pyridoxal (B6)

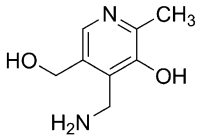

Pyridoxamine (B6)

Scheme 2

4.1 Thiamine (Vitamin B_1)

Thiamine is a monovalent cation with a structure that corresponds to a substituted pyrimidine bonded to a substituted thiazole. This structure leads to the presence of a quaternary N atom attached to the thiazole ring. Thus, thiamine – so-called vitamin B_1 – exists as salts of the physiological chloride anion or one of a wide variety of other counter anions. For solubility reasons, thiamine is commercially available as its hydrochloride salt, namely thiaminium(2+) dichloride. The structures of thiamine metal complexes correspond to two groups: those containing the divalent thiaminium cation and a cadmium complex as counterion, and those in which there is a direct cadmium-thiamine interaction.

There are two known structures with a thiaminium(2+) cation, one with the tetrahedrally coordinated cadmium ion in the anion $[CdCl_4]^{2-}$ [55] and the other with a 1D polymeric anion $[Cd_3Br_{4.4}Cl_{3.6}]^{2-}$, in which two of the three cadmium atoms are octahedrally coordinated and the third has a tetrahedral coordination geometry [55]. In both cases, as expected, the nitrogen atom in the pyrimidine ring *trans* to the exocyclic amine group is the protonation site for the thiamine cation. Thus, such a N-heterocyclic atom is considered to be the preferred protonation site of the thiamine cation and the selective metal binding donor atom in the metal complexes. In the crystal, the cations are linked to the anions by means of hydrogen bonds in which the O–H and N–H are donors and the halogen atoms of the anions are acceptors.

To date, there are only four reported cadmium complexes with thiamine and another three with derivatives in which there is a direct metal-ligand bond. The compound [Cd(thiamine)Cl_3]·0.6H_2O (Figure 11) contains a tetra-coordinated cadmium ion by three chloridos and the nitrogen atom from the pyrimidine *trans* to the amine group [Cd–N distance of 2.239(2) Å]. The relative orientations of the thiazolium and pyrimidine rings are quantitavely indicated by torsion angles ϕ_T and ϕ_P, respectively and, in this complex, the thiamine ion adopts the *S* conformation ($\phi_T = 113°$, $\phi_P = 130°$) [56]. A second compound of the formula [Cd(thiamine)-$(SCN)_3]_n$ has a polymeric structure with each cadmium octahedrally coordinated to a thiamine molecule through the oxygen atom of the hydroxyethyl side chain [Cd–O = 2.351(6) Å] and by five thiocyanate ligands. One thiocyanate is terminal and the remaining four are bridging, leading to the coordination $CdON_3S_2$. In this compound, the thiamine ligand adopts the *F* conformation ($\phi_T = 0°$, $\phi_P = –80°$) [57]. A third structure consists of centrosymmetric dimers [Cd(thiamine)$Cl_3]_2$, where two thiamine cations act as N,O bridges to two $CdCl_2$ units [Cd–N = 2.264 (5) Å, Cd–O = 2.697(5) Å] to give a $CdCl_3NO$ trigonal bipyramidal coordination environment (Figure 12). The vitamin adopts an *F* conformation ($\phi_T = 11°$, $\phi_P = 98°$) [58]. The fourth known cadmium complex with vitamin B_1 is the octahedral [Cd(thiamine)$_2Cl_4$]. This compound has a $CdCl_4N_2$ environment in which the metal is coordinated by two thiamine molecules in *trans* positions [Cd–N = 2.446(6) Å] and where the vitamin adopts an *S* conformation ($\phi_T = –92°$, $\phi_P = 176°$) [59].

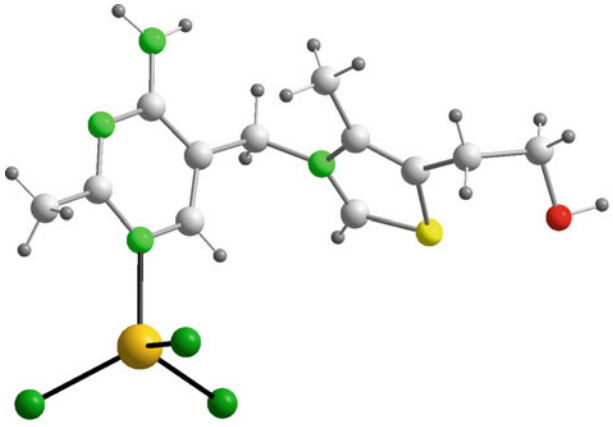

Figure 11 [Cd(thiamine)Cl_3].

There are also two known structures of cadmium complexes with 2-(α-hydroxybenzyl)thiamine (HBthiamine), an intermediate in thiamine catalysis with the α-hydroxybenzyl substituent in the C(2) position of the thiazolium ring. The complexes [Cd(HBthiamine)X_3] (X = Cl or Br) are isotypic, with a structure similar to that of [Cd(thiamine)Cl_3] [Cd–N = 2.251(3) Å and 2.257(9) Å]. In these structures the conformation of the thiamine skeleton is *S* ($\phi_T = 97$ and –97°,

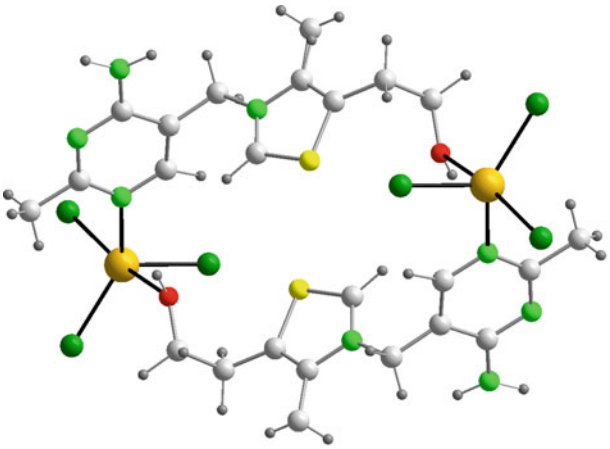

Figure 12 $[Cd(thiamine)Cl_3]_2$.

$\phi_P = 173°$) [60]. Furthermore, another structure of a cadmium complex with a thiamine derivative was studied by Casas et al. [61], namely $[Cd(\mu_2\text{–oxythiamine})(\mu_2\text{–Cl})Cl]_n$, where oxythiamine is an antagonist of thiamine that differs from it in that the exocyclic amine group within the pyrimidine ring is formally replaced by a hydroxyl group. In the structure polymer, each cadmium is coordinated by three chlorido ligands, two of which act as bridges between neighbouring cadmium atoms and by three donor atoms of two oxythiamine zwitterions. The N3(pyrimidine) and O4(exocyclic) donors build a four-membered chelate ring with one cadmium center [Cd–N, 2.317(4) Å; Cd–O, 2.561(4) Å; ∠N–C–O, 1170(5)°; ∠N–Cd–O, 54.5(1)°] whereas the N1(pyrimidine) donor bind a second metal center [Cd–N, 2.301(4) Å]. Consequently, the cadmium has a distorted octahedral $CdCl_3N_2O$ coordination (Figure 13). The conformation of the ligand seems to be closer to *V* rather than to the traditional *F* or *S* ($\phi_T = –115°$, $\phi_P = 61°$). In this structure it is worth noting the altered order of basicity for the nitrogen atoms of the pyrimidine ring on changing from thiamine to oxythiamine.

4.2 Nicotinic Acid (Vitamin B_3)

Niacin and niacinamide (also known as nicotinic acid and nicotinamide, respectively) or vitamin B_3, chemically 3-pyridinecarboxylic acid and 3-pyridinecarboxamide, are able to form various cadmium complexes with known crystal and molecular structures. In order to rationalize the analysis, hereafter the complexes have been differentiated according to the ligand and, within each case, we have only considered the most relevant structures.

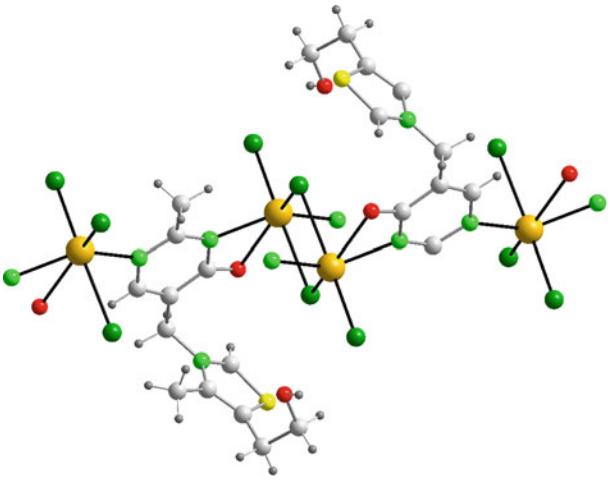

Figure 13 $[Cd(oxithiamine)Cl_2]_n$.

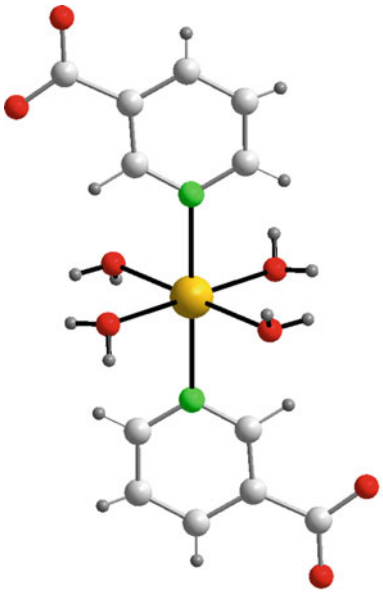

Figure 14 $[Cd(NA)_2(H_2O)_4]$.

In niacin, the existence of the pyridinic nitrogen atom and the variety of coordination possibilities of the carboxylic acid group lead to the formation of 1D, 2D, and 3D networks, albeit with some exceptions. One of these exceptions is $[Cd(NA)_2(H_2O)_4]$ (Figure 14), in which each metal atom is coordinated by two nitrogen atoms from the nicotinate groups and by four oxygen atoms from four water molecules in a slightly distorted octahedral geometry. Both nicotinate groups

occupy *trans* positions with Cd–N distances of 2.309(5) Å. The Cd–O distance is 2.321(4) Å [62].

A dinuclear complex has also been reported and, besides water, this compound contains ethylenediamine (en) as co-ligand (Figure 15). In $[Cd_2(NA)_4(en)_2(H_2O)_2]\cdot H_2O$ (NA = nicotinate), both Cd^{2+} ions display a distorted octahedral coordination geometry that includes two nitrogen atoms from two nicotinate anions, the nitrogen atoms from an ethylenediamine molecule, which forms a five-membered chelate ring, an oxygen atom from one of the nicotinate ions (which acts as an N,O bridge between the two cadmium ions) and an oxygen atom from a water molecule [63].

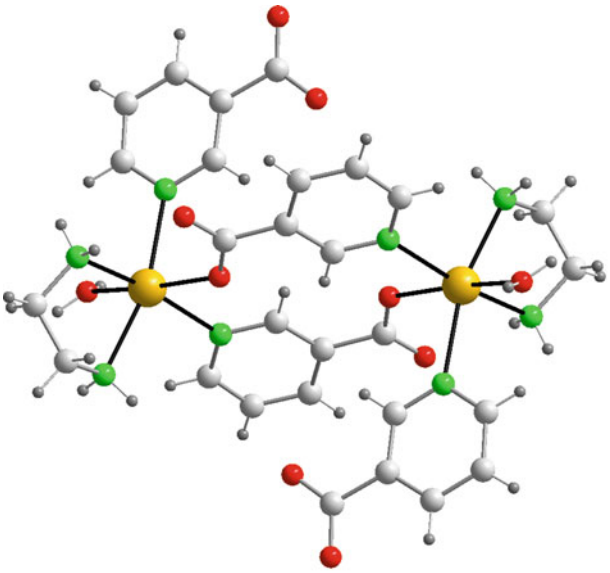

Figure 15 $[Cd_2(NA)_4(en)_2(H_2O)_2]$.

Two different groups of polymeric structures with nicotinate ions can be defined: those containing additional neutral ligands, such as H_2O, aromatic diamines, etc., and those with anionic ligands such as halides, thiocyanate, azide or nitrate.

$[Cd(NA)_2]_n$ is an example of the former group, with the cadmium ions coordinated by two nitrogen pyridyl atoms from two nicotinate molecules and by four carboxylate oxygen atoms from another two nicotinates, in an asymmetric chelating manner. As a result, two Cd–O bonds, one from each chelate, [2.397(3) Å and 2.247(3) Å] are much longer than the other two [2.271(3) Å and 2.317 (3) Å]. Each tridentate nicotinate ligand bridges two adjacent cadmium atoms to give rise to a 2D network [64]. Likewise, there is another structure with the same stoichiometry that is based on distorted square pyramidal cadmium centers coordinated by two independent nicotinate ligands. One of the ligands acts as an N,O_2-tridentate system and the other as N,O-bidentate. Each pair of cadmium atoms is bridged by two carboxylate groups from the tridentate nicotinate ligands, in an *anti-syn* bridging bidentate manner, to form a binuclear unit $Cd_2(NA)_4$. One of these oxygen

atoms occupies the axial site of the pyramid whilst the other occupies one of the basal positions, along with two nitrogen pyridyl atoms and an oxygen from three nicotinate ligands, two of which are bidentate, thus resulting in a 3D network [65].

Among the structures of polymeric complexes containing coordinated H_2O, $[Cd(NA)_2(H_2O)_2]_n$ (Figure 16) is a zig-zag chain with hepta-coordinated Cd^{2+} ions in a distorted pentagonal bipyramidal geometry. This unit involves one nitrogen donor atom and four oxygen donor atoms from two nicotinate ligands arranged in the equatorial plane, as well as the oxygen atoms from two coordinated water molecules at the axial sites. Therefore, one of the nicotinate ligands acts as a tridentate bridge whereas the other acts as a bidentate terminal ligand via the carboxylate group. In this structure, the Cd–O distance lies between 2.255(4) and 2.724(5) Å and the Cd–N distance is 2.278(4) Å [66].

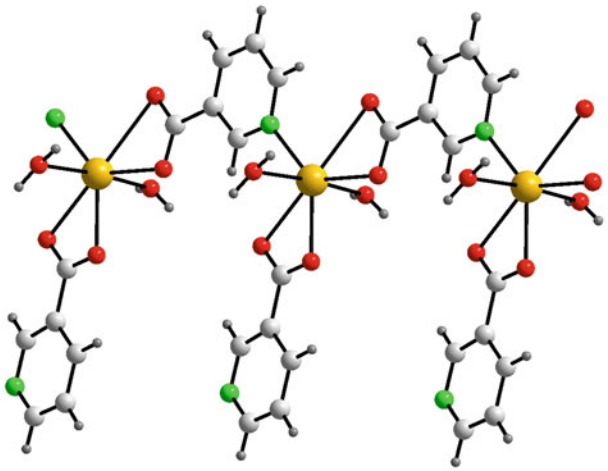

Figure 16 $[Cd(NA)_2(H_2O)_2]_n$.

There are also several complexes with 1D structures that incorporate an anion besides the nicotinate, such as the luminescent complexes $\{[Cd(NA)(phen)(NO_3)]\cdot 1/2H_2O\}_n$ and $\{[Cd(NA)(ptola)(H_2O)_2]\cdot(Hptola)\}_n$ (phen = 1,10 phenanthroline, Hptola = *p*-toluic acid) [67]. In both complexes, the nicotinate acts as an N,O_2-tridentate bridging ligand but in the first case the Cd^{2+} ion is hexa-coordinated with the nitrate as a monodentate ligand, and in the second case it is hepta-coordinated with the toluate acting as chelating bidentate ligand.

In other complexes, the characteristic polymeric coordination is achieved by a neutral auxiliary ligand, which acts as bridge, in addition to the nicotinate, or by an anionic ligand, such as halides [68, 69] or thiocyanate [70]. In the latter complex, $\{[Cd(SCN)_2(HNA)_2]\cdot HNA\}_n$, the Cd^{2+} ion is coordinated by two pyridyl nitrogen atoms from two molecules of nicotinic acid, by two nitrogen atoms from two thiocyanates and by two sulfur atoms from another two thiocyanates in a *trans* octahedral geometry, so that each pair of adjacent cadmium atoms is bridged by two μ_2–*N,S*-SCN ligands to form a 1D structure (Figure 17).

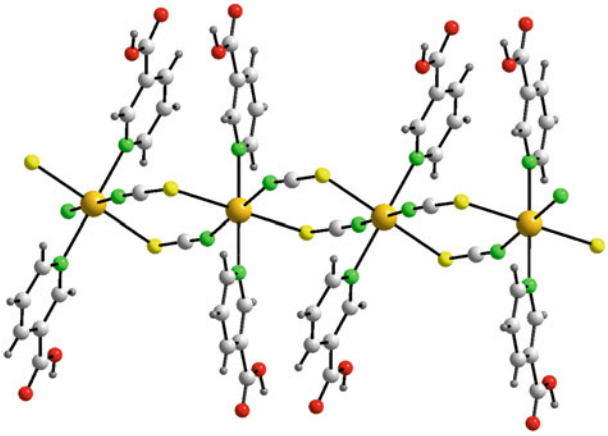

Figure 17 $[Cd(SCN)_2(HNA)_2]_n$.

In the few known structures of cadmium with nicotinamide (NADA), this ligand acts as a monodentate system via its pyridyl nitrogen atom and in every case the coordination environment of the metal is octahedral. Depending on the behavior of the anion, two types of mononuclear complexes can be distinguished. The first type is neutral, e.g., when the anion is coordinated as in $[Cd(H_2O)_2(NADA)_2(NO_3)_2]$ ·2NADA [71] (Figure 18) or $[Cd(H_2O)_2(NADA)_2(NBZ)_2]\cdot 2H_2O$ (NBZ = 2-nitrobenzoate) [72]. In cases where the anion is not coordinated, however, the complex is cationic with two molecules of nicotinamide in the axial positions and four coordinated water molecules at the equatorial sites, as in $[Cd(NADA)_2(H_2O)_4]$-X_2 (X = 4-formylbenzoate) [73,74].

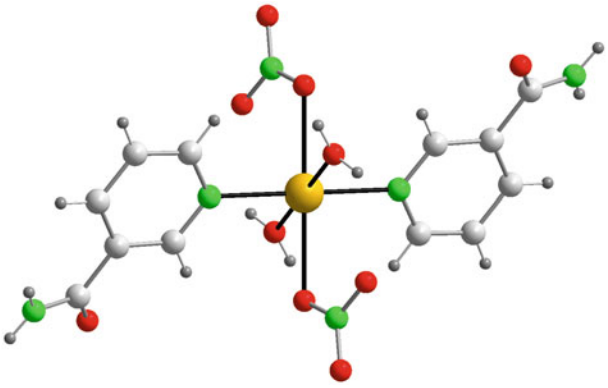

Figure 18 $[Cd(H_2O)_2(NADA)_2(NO_3)_2]$.

In some complexes, a carboxylate anion acts as a bidentate bridge to yield structures based on dinuclear complexes, as observed in $[Cd(PMAB)(NADA)(H_2O)]_2$ (Figure 19)

and $[Cd(DMAB)(NADA)(H_2O)]_2$ [PMAB = 4-(methylamino)benzoate, DMAB = 4-(dimethylamino)benzoate]. The cadmium ion is chelated by two carboxylate groups of aminobenzoate anions and coordinated by a nicotinamide molecule and a water molecule. An oxygen atom from a carboxylate group of an adjacent anion bridges the cadmium atom, thus completing an irregular hepta-coordinated geometry [75,76].

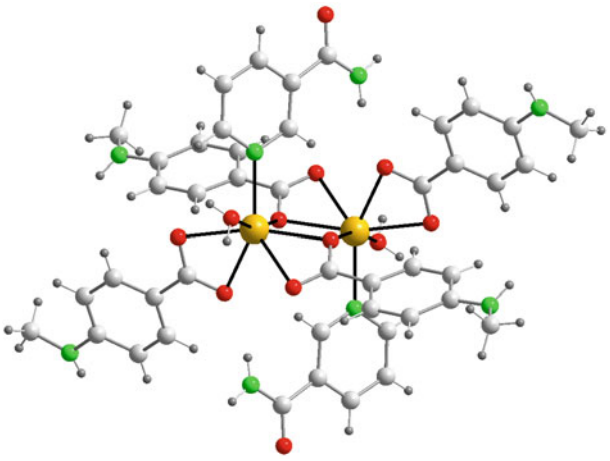

Figure 19 $[Cd(PMAB)(NADA)(H_2O)]_2$.

To date, only one example has been reported of a 2D cadmium coordination polymer constructed with thiocyanate and nicotinamide. In the referred polymer, each Cd^{2+} ion, located in a centrosymmetric octahedral environment, is coordinated by two nicotinamide molecules in *trans* positions and four thiocyanate ions, which act as N,S bridging ligands that link to four neighboring cadmium ions [70].

4.3 Vitamin B_6

Two crystal structures have been determined by X-ray diffraction for cadmium complexes with vitamin B_6. In both compounds the pyridoxine is found as a zwitterion, which is formed by migration of the phenolic hydrogen atom to the heterocyclic nitrogen atom. This process enables the chelating role of pyridoxine by the O-phenolate and the adjacent O-methanolic donor to build six-membered chelate rings. The coordination of Cd(II) is octahedral but the ligand:metal ratio is different in both compounds. The 1:1 compound $[Cd(\mu\text{–O-pyridoxine})(\mu\text{–Cl})Cl]_n$ [77] is a 1D-polymer, where a chlorido ligand and the O-phenolate donor of pyridoxine act as bridging atoms between two adjacent Cd(II) centers (Figure 20). In the salt *trans*-$[Cd(pyridoxine)_2(H_2O)_2]SO_4{\cdot}6H_2O$ [78] the Cd(II) atom is in the

centrosymmetric environment of the cationic complex (Figure 21). As expected, the bonds involved in bridging atoms are longer than similar bonds in unidentate roles. Hence, in $[Cd(\mu\text{–O–pyridoxine})(\mu\text{–Cl})Cl]_n$, the Cd–(μ–Cl) bonds (2.666 and 2.655 Å) are longer than the Cd–Cl bond (2.530 Å). Moreover, in this polymeric compound, the Cd–μ–O(phenolate) bonds (Cd–O, 2.316 and 2.307 Å) are longer than the single Cd–O(phenolate) bond (2.221 Å) in the complex cation *trans*-$[Cd(pyridoxine)_2(H_2O)_2]^{2+}$.

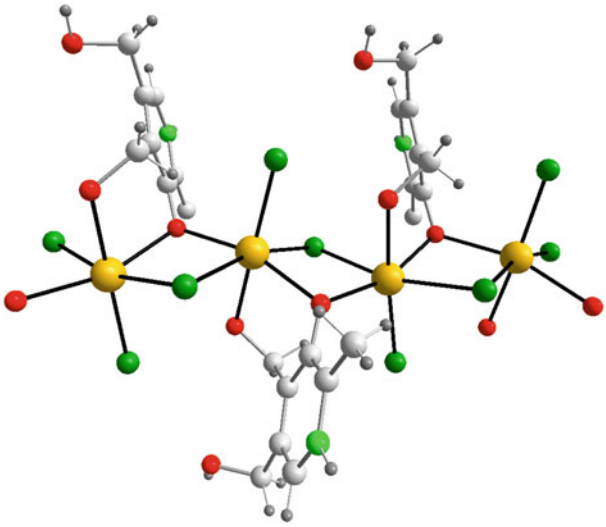

Figure 20 $[Cd(pyridoxine)Cl_2]_n$.

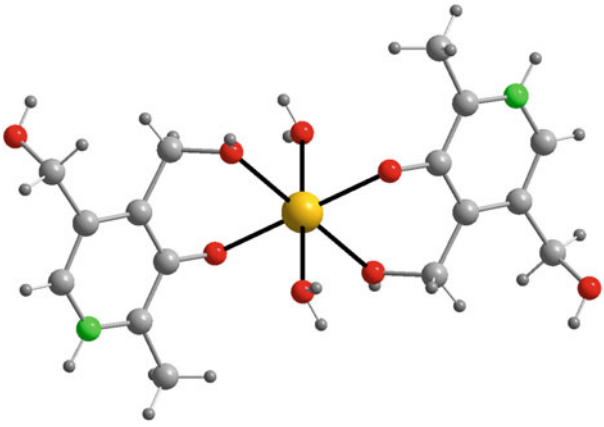

Figure 21 $[Cd(pyridoxine)_2(H_2O)_2]^{2+}$.

5 Other Cadmium Complexes

Given the d^{10} state of the Cd^{2+} ion, one would expect the coordination chemistry of this metal ion to be dominated by examples of coordination to four two-electron donors. In this sense, the ligands containing thiolate or carboxylate groups are interesting to mimic zinc-thiolate or zinc-carboxylate active sites, which play a relevant role in bioinorganic chemistry and in the field of cadmium detoxification by chelation.

5.1 Cadmium-Thiolate Complexes

At the molecular level, cadmium(II) ions bind to the thiolate (–S) groups of proteins, cysteine, and glutathione and inhibit the function of these biomolecules. Nevertheless, the CSD only refers to three crystal structures with thiols S-bonded to cadmium centers. Furthermore, cadmium ions are able to block the function of a number of cellular enzymes and they are also mimics of calcium(II) and zinc(II). For example, cadmium(II) can deposit in bones and bind calcium(II)-binding proteins. Not surprisingly, biological systems have responded to this toxicity with different strategies that share the same basic chemical principle: the strong affinity of cadmium(II) for thiol ligands. The strategy adopted by mammals mainly consists of cadmium(II) complexation and sequestration by metallothioneins, ubiquitous low-molecular-weight, cysteine-rich metalloproteins [79].

5.1.1 Monothiolate Ligands

Cadmium thiolates considered here include those compounds that, if mononuclear, only involve ligation by organothiolate anions (RS^-) and, if polynuclear, only contain these groups as skeletal bridging ligands. A nice review on the structural chemistry of metal thiolate complexes was published in 1986 by Dance [80].

5.1.1.1 Mononuclear and Dinuclear Complexes

The C_{3h} and Y-shaped isomers of $[Cd(S\text{-}2,4,6\text{-}iPr_3C_6H_2)_3]^-$ are examples of monomeric, three-coordinate complexes of cadmium with monothiolate ligands. The $[CdS_3]$ units in both isomers are planar and the sum of the three S–Cd–S angles in each compound is close to 360°. The C_{3h} isomer is characterized by S–Cd–S angles close to 120° and nearly equal Cd–S bond distances (between 2.417 and 2.427 Å) (Figure 22) [81]. The Y-shaped isomer is characterized by a wider range of S–Cd–S angles (between 100.71 and 135.33°) and Cd–S distances (between 2.422–2.453 Å) [82]. The distortions observed in the Y-shaped isomer can be thought of as an intermediate structure along the pathway toward the formation

of a linear two-coordinate complex by dissociation of the third thiolate ligand. The dinuclear complex $[Cd_2(S\text{-}2,4,6,^t\text{butyl}\ C_6H_2)_4]$, which in solution dissociates to monomers, also has trigonal-planar coordinate cadmium ions bridged by two thiolate ligands, with Cd–S_b distances close to 2.5 Å and a shorter Cd–S_t distance of 2.376 Å and angles in the Cd_2S_2 core of 83.24° (S–Cd–S) and 96.7° (Cd–S–Cd) (Figure 23) [83].

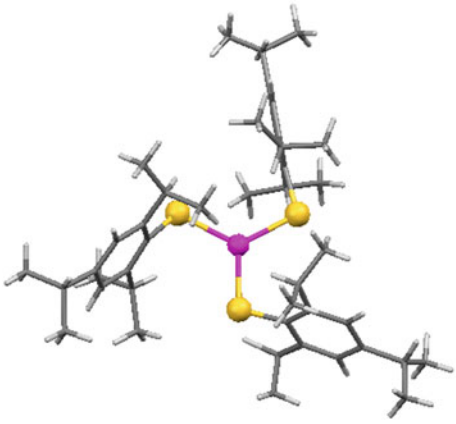

Figure 22 $[Cd(S\text{-}2,4,6\text{-}iPr_3C_6H_2)_3]$.

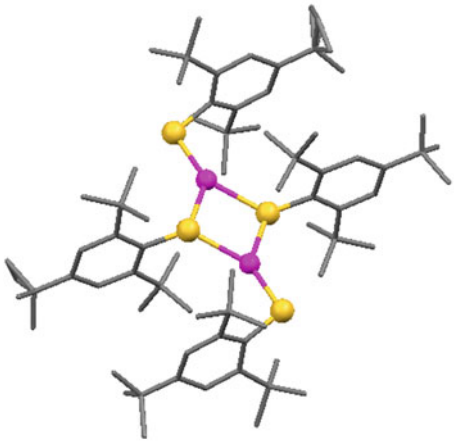

Figure 23 $[Cd_2(S\text{-}2,4,6,^t\text{butyl}\ C_6H_2)_4]$.

The structural principles for $[M^{II}(SPh)_4]^{2-}$ complexes were described in detail by Coucouvanis et al. [84]. The distortion of the tetrahedral MS_4 core can be caused by intermolecular interaction between the thiolate sulfur atom and an *ortho* proton of the RS^- group. There are two possible conformations for the $[M^{II}(SPh)_4]$ unit:

the D_{2d} and S_4 conformational isomers. The reduction in symmetry of the $[MS_4]$ core from T_d to D_{2d} symmetry converts the S–Cd–S tetrahedral angles (of 109.5°) into two sets of equivalent angles: the two S–Cd–S angles bisected by the S_4 axis are greater than 109.5° and the four remaining S–Cd–S angles are less than the tetrahedral angle. The D_{2d} isomer is predicted to have a tetragonally elongated $[MS_4]$ core, as observed in $[Et_4N]_2[Cd(S\text{-}2\text{-}Ph\text{-}C_6H_4)_4]$ [85]. The S_4 conformation is more difficult to discern but all the S_4 structures have $[MS_4]$ cores that are tetragonally compressed as in $[Me_4N]_2[Cd(SPh)_4]$ [86].

The dinuclear compound $(Ph_4P)_2[Cd_2(SPh)_6]$ crystallizes in two possible dimorphic forms, the monoclinic [87] (Figure 24) and the triclinic [88] forms. Both dimorphs contain the centrosymmetric $[(PhS)_2Cd(\mu\text{-}SPh)_2Cd(SPh)_2]^{2-}$ anion and this has an approximately tetrahedral coordination stereochemistry at the cadmium ion. The Cd–S_t distances are similar in the two dimorphs, but there are differences in the bridging region. The $[Cd_2S_2]$ core of the monoclinic dimorph is almost square and has equal Cd–S_b distances, whereas in the triclinic system the two independent Cd–S_b bond distances are different (2.583 and 2.651 Å) and the Cd···Cd distance is shorter (3.549 *versus* 3.692 Å). The overall crystal packing of the ions in the dimorphs is similar. A study by density functional methods shows that the intermolecular crystal packing energies are dominant as they are greater than the energies involved in the intramolecular conformational differences, while the energy differences associated with bond length variation of ± 0.04 Å are the smallest at only ca. 1 kcal mol^{-1} [88].

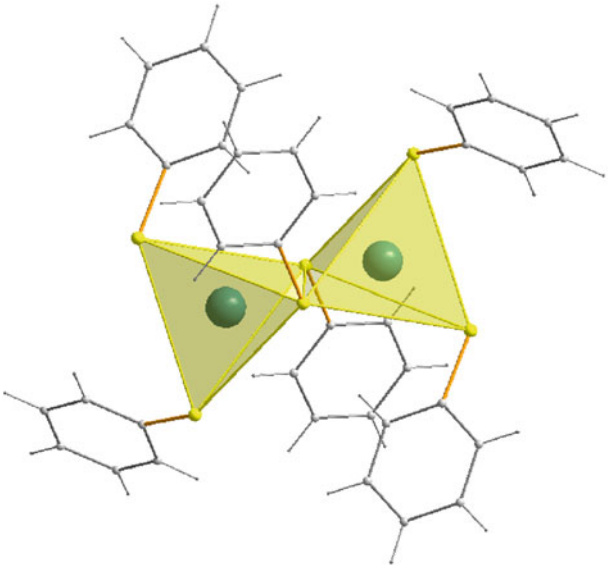

Figure 24 $[Cd_2(SC_6H_5)_6]^{2-}$.

5.1.1.2 Complexes with Higher Nuclearities

The core of the trinuclear cluster anion $[Cd_3(S\text{-}2,4,6\text{-}iPr_3C_6H_2)_7]^-$ is formed by a distorted cubane Cd_3S_4 cluster with three cadmium ions and four sulfur atoms at its vertices. The cluster closely approaches C_{3v} symmetry. Each cadmium atom has tetrahedral coordination and there are three types of coordination modes in the seven thiolate ligands: three terminal, three doubly bridging and one triply bridging thiolate [89] (Figure 25). In the uncharged trinuclear cadmium complex $[Cd_3(S\text{-}2,4,6\text{-}iPr_3C_6H_2)_6(HS\text{-}2,4,6\text{-}iPr_3C_6H_2)]$ the three cadmium atoms are coordinated by six thiolate (RS^-) and one thiol (RSH) ligand. Two of the three cadmium atoms have tetrahedral coordination and the third is trigonal planar [90].

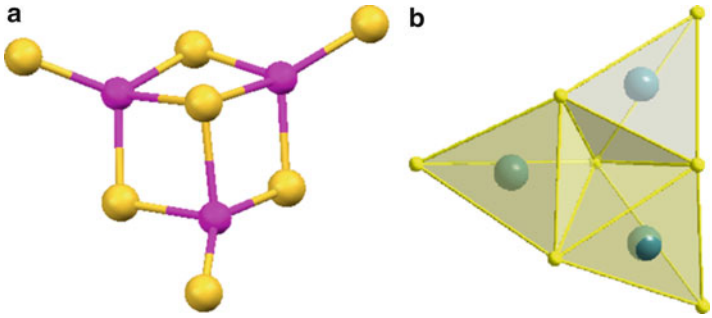

Figure 25 $[Cd_3(S\text{-}2,4,6\text{-}iPr_3C_6H_2)_7]^-$.

A review of the structural chemistry of $[M_x(SR)_y]^{2-}$ complexes with $x \geq 4$ reveals the existence of molecular cages in which bridging thiolate sulfur atoms and metal atoms each form recognizable polyhedra [91]. A frequently encountered structural unit is the adamantane-type tetranuclear cluster with an $[M_4(\mu\text{–}SR_6)]$ core containing a tetrahedrally disposed set of metal atoms and an octahedron of bridging thiolate atoms with overall (idealized) *Td* symmetry. This structural type has been established for the inorganic polymer $Cd(SPh)_2$, which consists of $Cd_4(SPh)_6$ cages, each of which is linked with four surrounding cages by four SPh bridges in the same helical conformation as the SiO_4 tetrahedra in cristobalite [92] (Figure 26). This $[Cd_4S_6]$ adamantane-like cage is also present in the tetranuclear anionic complexes $[Cd_4(SPh)_{10}]^{2-}$ [93] and $[Cd_4(ScHex)_{10}]^{2-}$ [94], with each Cd(II) ion bonded to one terminal (the outside of an adamantane-like cage) and three bridging thiolate ligands.

The terminal positions on the adamantane-like cage can be substituted by other ligands such as halido ions, leading to complexes such as $[Cd_4(SC_6H_4Bu^t\text{-}4)_7Cl_3]^{2-}$ [95] and $[Cd_4(SPh)_6I_4]^{2-}$ [96].

Several crystal structures of cadmium-thiolate complexes with nuclearity higher than 4 can be found in the literature. For example, the octanuclear molecule $[Cd_8(SPhF\text{-}3)_{14}(DMF)_6(NO_3)](NO_3)$ [97] (Figure 27) consists of a cubic cluster

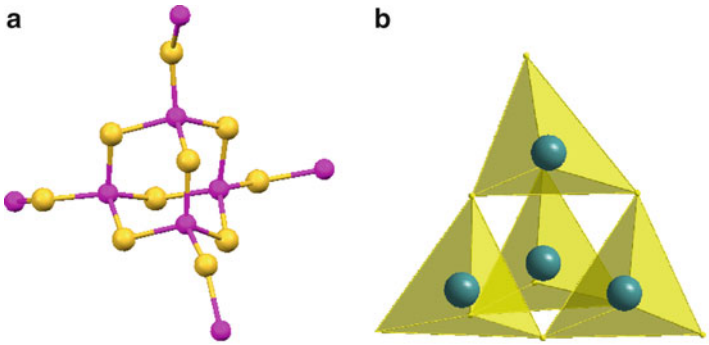

Figure 26 $[Cd_4S_6]$ core.

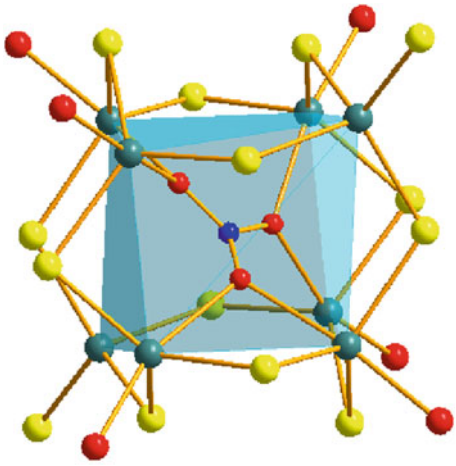

Figure 27 $[Cd_8(SPhF\text{-}3)_{14}(DMF)_6(NO_3)]^+$.

$[Cd_8(SPhF\text{-}3)_{14}(DMF)_6]^{2+}$ with eight cadmium ions arranged at the corners of a cube while twelve -SPhF-3 groups are distributed off the center of each cubic edge as bridging ligands. Six penta-coordinated cadmium sites are bonded to solvent DMF molecules and NO_3^- within the cage while the remaining two corners (tetrahedral cadmium sites) are occupied by -SPhF-3 groups.

5.1.2 Dithiolate Ligands of the BAL Type

The toxicity of cadmium is determined by chelation reactions: *in vivo*, Cd^{2+} exists exclusively in coordination complexes with biological ligands or with administered chelating agents. Generally, the stability of complexes increases with the number of

coordination groups contributed by the ligand. Consequently, complexes of Cd^{2+} with polydentate ligands containing SH groups are very stable. In chelation therapy, the requirement for induction of efficient detoxification of Cd^{2+} seems to be a relatively lipophilic chelating agent with two adjacent SH groups favouring tedrahedral coordination, as in the Cd-MT complex [98] (see also Chapter 11). Dithiolate ligands such as 2,3-dimercaptopropanol (dimercaprol, BAL = British Anti-Lewisite), dimercaptosuccinic acid (DMSA, Succimer) and 2,3-dimercapto-1-propanesulfonic acid (DMPS, Unithiol) have proven to be good chelating agents towards several toxic divalent metallic cations.

The coordination geometry in the ethanedithiolate compound $(Et_4N)_2[Cd(edt)_2]$ [99] approximates to tetrahedral (D_{2d}) symmetry (Figure 28) and the bond distances are comparable with those of other tetrahedral $M(SR)_4$ units and other mononuclear tetrahedral cadmium dithiolate complexes [100]. In the mononuclear tetrahedral benzenedithiolate compound $(PPh_4)_2[Cd\{bpvbd\}_2]$ [101] (Figure 29) the presence of intramolecular NH···S hydrogen bonds was established by X-ray crystallography and IR and NMR spectroscopy. The contribution of the NH···S hydrogen bond was

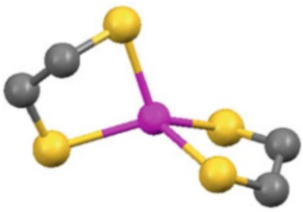

Figure 28 $[Cd(edt)_2]^{2-}$.

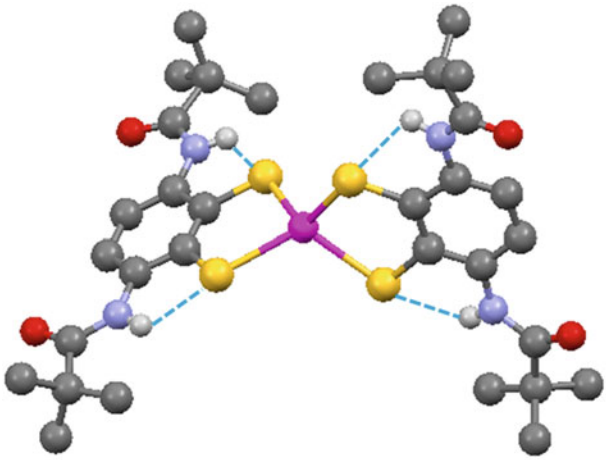

Figure 29 $[Cd\{bpvbd\}_2]^{2-}$.

analyzed using the NBO (Natural Bond Orbital) programme, which suggested stabilization of the complex by hydrogen bonding. The role of hydrogen bonds in metallothioneins has been discussed using model complexes [102] or a modified metallothionein [103]. In this sense, the X-ray crystal structure analysis of rat metallothionein-2 suggested that the coordinating sulfur atoms formed NH···S hydrogen bonds with the amide protons in the polypeptide backbone and with the ammonium protons in the lysine residues [104]. All the experimental and theoretical results suggest that the N···S hydrogen bond influences the efficient capture of toxic cadmium ions by metallothioneins.

5.2 Dithiocarbamate Cadmium Complexes

The importance of $[S_2CNR_2]^-$ dithiocarbamates in biological systems has emerged as result of the discovery by Gale et al. in 1981 of sodium diethyldithiocarbamate as an antidote for acute cadmium(II) chloride poisoning [105]. Since then, the coordination chemistry of cadmium(II) with dithiocarbamates has been steadily developed. The majority of studies were carried out in solution and it was not until recently that research focused on the solid state, due to the fact that dithio-/diselenocarbamates of cadmium are excellent precursors for the synthesis of CdS or CdSe nanoparticles, which have unique electronic and optical properties that make them suitable for optoelectronic applications [106–108].

In spite of this development, the number of known cadmium complex structures with dithiocarbamates is not very high and they fit within the motifs recently described for 1,1-dithiolates of group 13 metals [109]. These structures can be grouped into anionic and neutral categories. The former are monomeric with hexa-coordinated cadmium, which is in a distorted trigonal prismatic geometry. In these compounds three diethyldithiocarbamate ligands act as chelating S,S'-bidentate ligands in an anisobidentate manner, i.e., one Cd–S bond is somewhat shorter in comparison to the other, although the C–S distances are the same if the cation is tetra-*n*-butylammonium [110] (Figure 30). However, if the cation is $[M(en)_3]^{2+}$ (M = Ni, Zn or Cd) or PPh_4^+ the two aforementioned distances are different to a greater or lesser degree [111–113]. Nevertheless, there are two structures that have a penta-coordinated cadmium, one including isothiocyanate as an additional ligand [114] and the other with a coordinated molecule of tri-*tert*-butoxysilanethiolate and one iodido [115]. A third structure contains cadmium that is tetra-coordinated by one molecule of dithiocarbamate and two tri-*tert*-butoxysilanethiolate ligands [116].

There are two types of neutral complexes: homoleptic and heteroleptic. The former are generally dimers, with two cadmium atoms penta-coordinated by two molecules of dithiocarbamate, which acts as an anisobidentate ligand (Figure 31). One sulfur atom from one of the molecules coordinated to the cadmium ion acts as a bridge to the other cadmium atom, bringing about a distorted square pyramidal coordination geometry with the axial position occupied by the bridging sulfur atom [117].

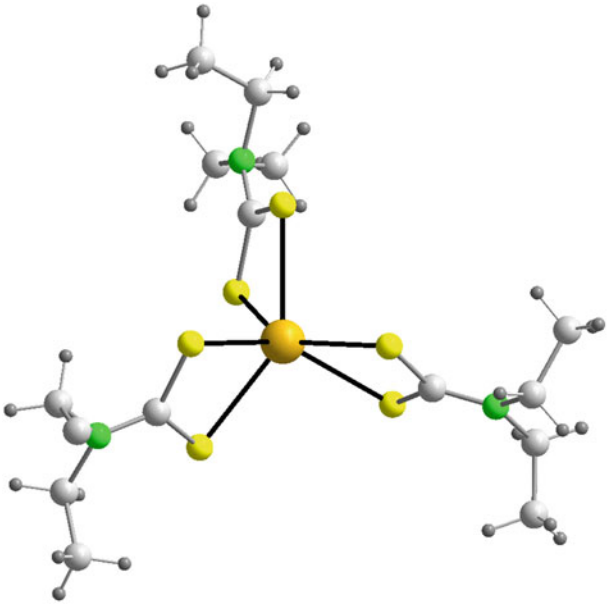

Figure 30 $[Cd(S_2CNEt_2)_3]^-$.

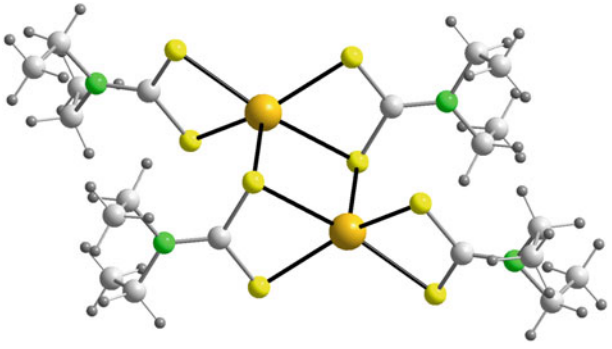

Figure 31 $[Cd(S_2CNEt_2)_2]_2$.

Some neutral homoleptic complexes with dithiocarbamates containing long alkyl substituents on the nitrogen atom, such as N-phenyldithiocarbamate or N-dodecyldithiocarbamate ligands, are 1D chains based on flat rectangular molecular units $[Cd(S_2CNHR)_2]$ connected by means of Cd···S intermolecular interactions (average 2.937 Å). This arrangement gives rise to a hexa-coordinated S_6 (4 + 2) environment around the cadmium ion in a rectangular bipyramidal geometry [118] (Figure 32). There is also a 1D methylcadmium polymer that has a coordination number of 4 (CNS_2) [119].

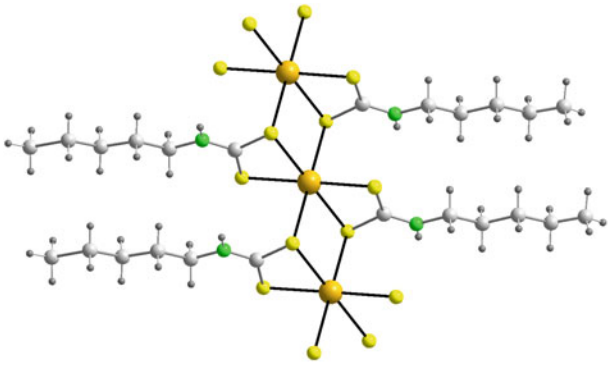

Figure 32 $[Cd\{S_2CNH(n\text{-}C_5H_{11})\}_2]_n$.

In the heteroleptic complexes the co-ligands are usually nitrogen donor ligands, although there are also some complexes with phosphine. The structure of these complexes and the coordination number of the cadmium ion depend on the type of co-ligand. If the ligand is monodentate, such as imidazole [120] (Figure 33) or pyridine [121,122], the coordination number is 5 (NS_4) and the complex is mononuclear, but if the ligand is an aromatic α,α'-diamine, such as 2,2'-bipy or 1,10-phen or derivatives, the metal ion coordination number is 6 (N_2S_4) [123–126]. However, some complexes are dinuclear because the auxiliary ligand acts like a bridge, as in $(\mu^2\text{–dppf})\{Cd(S_2CNEt_2)_2\}_2$ [127] or in $[Cd_2(\mu\text{–paa})(S_2CNPr_2)_4]$ [128]. In the former case, the cadmium coordination number is five and in the latter six. In $[Cd\{SSi(OBu^t)_3\}(S_2CNEt_2)]_2$ the coordination number of each metal center is four and the coordination geometry is tetrahedral [116]. There are also some penta-coordinated cadmium(II) dimers of S_2CNEt_2 with 1,4-diazabicyclo[2.2.2]octane as a bridging ligand and fullerene C_{60} of crystallisation [129]. To date, there are only four known coordination polymers based on heteroleptic cadmium complexes with dithiocarbamates in which the auxiliary ligand acts as a bridge. The structure of $[Cd(S_2CNEt_2)I]_n$ consists of dimeric units $[Cd_2(\mu\text{–}S_2CNEt_2)_2]^{2+}$ linked by two iodido bridges that link neighbouring *cis* cadmium ions, bringing about 1D chains in which each cadmium ion is penta-coordinated by an I_2S_3 group with an intermediate geometry between tetragonal pyramidal and trigonal pyramidal [130] (Figure 34). The structure of $[Cd(S_2CNEt_2)_2(dpe)]_n$ [dpe = 1,2-di(pyridin-4-yl)-ethane] is based on flat $Cd(S_2CNEt_2)_2$ units linked by *trans* dpe molecules, an arrangement that gives rise to a 1D chain in which each cadmium ion presents a distorted octahedral coordination geometry with a *trans*-N_2S_4 donor group [131]. Closely similar structures contain 4,4'-bipyridine or 1,2-bis(4-pyridyl)ethylene as spacers between rectangular $[Cd(S_2CNR_2)_2]$ units [132,133] (Figure 35).

An analysis of the most significant bonding parameters involved in the coordination of dithiocarbamates to the cadmium ion, in the 59 different structures reported to date, reveals that the Cd–S distances in each CdS_2C chelate, in general,

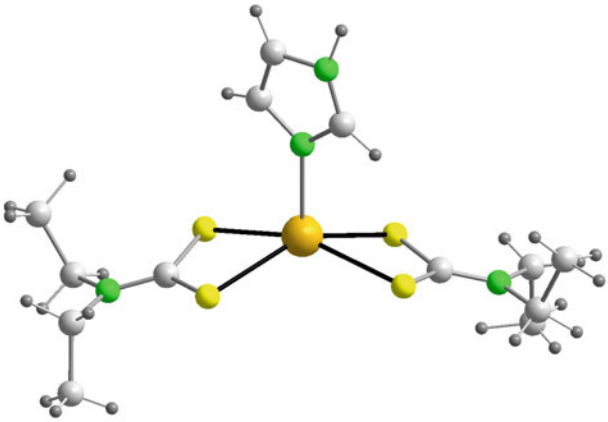

Figure 33 $[Cd(S_2CNEt_2)_2(HIm)]$.

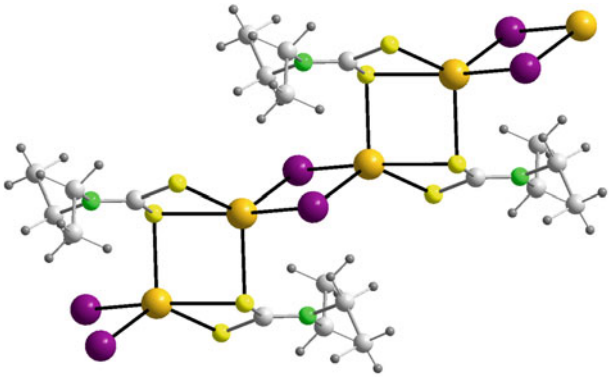

Figure 34 $[Cd(S_2CNEt_2)I]_n$.

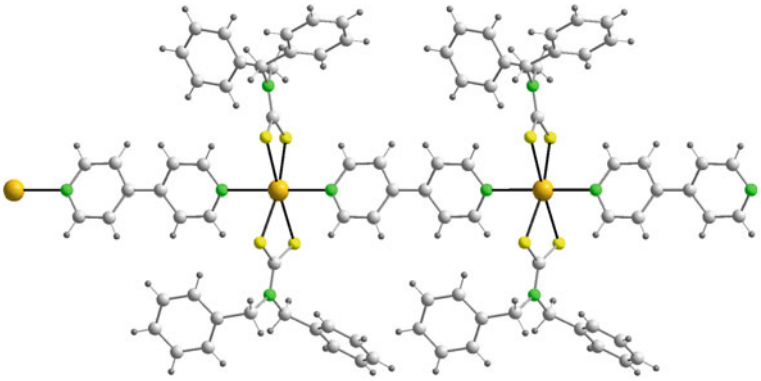

Figure 35 $[Cd(S_2CNBz_2)(4,4'\text{-bipy})]_n$.

differ by less than 0.1 Å, with average values of 2.610 and 2.716 Å. Nevertheless, in the dinuclear complexes in which one of the sulfur atoms acts as a bridge, the difference between the two Cd–S distances has an average value of 0.320 Å, with lower and upper limits of 2.768 and 2.975 Å, respectively. This range is in contrast with the average value of 2.604 Å for the distance from this sulfur atom to the second cadmium atom.

Likewise, the value of the S–Cd–S angle (*bite angle*) depends on the type of coordination and the geometry. Therefore, in anionic complexes with an S_6 coordination the average value is 65.62°, whereas in neutral complexes with N_2S_4 coordination it is 67.32°. In monomeric complexes with NS_4 coordination the average value is 68.97° and in the S_5 dimers the values are 66.71 and 70.07° for the two molecules of the ligand. Furthermore, the average value of the S–Cd–S angle in complexes with coordination number 4 is 69.11°.

Moreover, the coordination of the dithiocarbamates to the cadmium atom leads to a redistribution of the charge on the S_2CN group of the ligand, resulting in a partial positive charge located on the nitrogen atom whilst another negative charge is delocalized over the CdS_2C chelate ring; this is manifested in the values of the average C–S distances for each ligand of 1.712 and 1.728 Å, and also in the C–N bond length of 1.329 Å.

5.3 Polycarboxylate Ligands of the EDTA Type

Aminopolycarboxylate ligands such as the potentially hexadentate ethylenediamine-*N*,*N*,*N*′,*N*′-tetraacetate(4–) (EDTA) and related tetraacetate chelators, the potentially tetradentate nitrilotriacetate(3–) (NTA), and the potentially tridentate iminodiacetate (2–) (IDA) are useful chelating agents for metal chelation therapy. The degree of ionization of these aminopolycarboxylate chelating agents can be controlled by adjusting the pH value to give anionic [134] or neutral Cd(II) complexes.

In the neutral mononuclear complex $[Cd(H_2EDTA)(H_2O)]\cdot 2H_2O$ [135] (Figure 36), the diprotonated H_2EDTA acts as a hexadentate (2N + 4O) ligand and one water molecule increases the coordination number of the metal atom to seven. The tetravalent EDTA anion is found in the 2D polymer $\{[Cd_2(EDTA)(H_2O)]\cdot H_2O\}_n$ [136], which contains two crystallographically independent cadmium(II) cations. One of the cadmium ions, Cd1, is coordinated by five O atoms and two N atoms from two tetraanionic EDTA ligands in a distorted pentagonal-bipyramidal coordination geometry. The other cadmium ion, Cd2, is six-coordinated by five carboxylate O atoms from five EDTA ligands and one water molecule in a distorted octahedral geometry. Two neighbouring Cd1 ions are bridged by a pair of carboxylate oxygen atoms to form a centrosymmetric $[Cd_2(EDTA)_2]^{4-}$ unit, which is further extended into a two-dimensional structure through Cd2–O bonds.

The substitution of the ethylene group of EDTA with rigid aromatic rings such as phenylene (*o*-PhDTA) or toluene (3,4-TDTA) leads to ligands that are good complexing agents for Cd(II) over a wide pH range. These compounds also behave

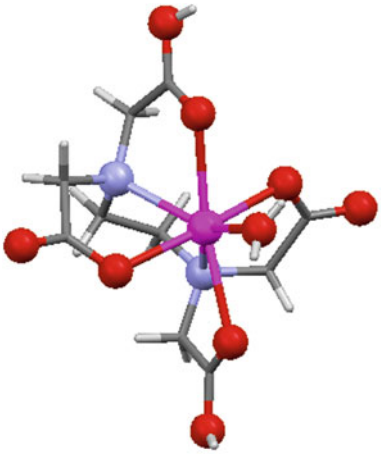

Figure 36 [Cd(H_2EDTA)(H_2O)].

as complexing groups towards several metal ions, inducing the formation of extended interlocked high dimensional structures. The 3D polymer [(H_2O)Cd-(μ–3,4-TDTA)Cd(H_2O)] has two types of cadmium environment [137]. The chelated Cd1 is coordinated to two N atoms and four carboxylate oxygen atoms from the ligand and a water molecule. This results in a roughly capped trigonal prismatic environment that forms a $[Cd1(3,4\text{-TDTA})]^{2-}$ unit, which is joined to four Cd2 atoms (Figure 37) in such a way that all the carboxylate oxygen atoms of the ligand are bound to cadmium(II) ions, thus making the ligand behave as a decadentate system. The Cd2 center is seven-coordinated with six oxygen atoms from four different $[Cd1(3,4\text{-TDTA})]^{2-}$ units and a water molecule in a very distorted capped trigonal prismatic coordination geometry.

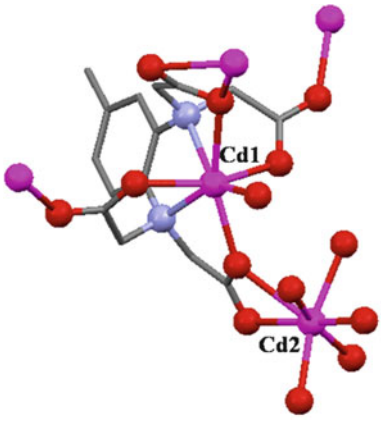

Figure 37 [(H_2O)Cd(μ–3,4-TDTA)Cd(H_2O)]$_n$.

In the 2D polymer {[Cd_3($IDA)_3$(H_2O)]·3H_2O}$_n$ [138] the iminodiacetate dianions behave as tridentate chelating ligands and show both facial and meridional

chelating configurations. One Cd(II) ion is surrounded by three IDA ligands: one N-monodentate, one O,O-bidentate and one N,O,O-tridentate in the *mer*-configuration. A second Cd(II) ion is coordinated by three IDA ligands (two O-monodentate and one N,O,O-tridentate in a *fac*-configuration) and one water molecule. The iminodiacetate dianion bridges neighbouring Cd(II) ions to form polymeric sheets.

6 General Conclusions

The electronic configuration ($4d^{10}$) and size of cadmium(II) clearly favor its affinity for soft donor atoms as well as a certain variability in coordination numbers and polyhedra. The structures discussed here reveal the ability of Cd(II) to exhibit coordination numbers from three to eight, with the six-coordination (octahedral or trigonal prism) polyhedra being the most common. Examples have been reported in which Cd(II) shows two different coordination numbers in the same crystal. Moreover, high coordination numbers favour the formation of polymers with various dimensionalities, whereas the tridentate ability of soft S-thiolate atoms build nice clusters.

Purine ligands coordinate to Cd(II) in monodentate (N3) or bridging modes (μ_2–N7,N9, μ_2–N3,N9, μ_3–N3,N7,N9). Purine derivatives with N9-non-coordinating groups bind Cd(II) through N7, usually assisted by an intra-molecular interligand H-bonding interaction. Likewise, related purines with N-donor atoms in the N9-pendant arm are able to coordinate to Cd(II) by N7, by N-donors from the pendant arm or through a combination of these two alternatives. N6-Substituted purines bind Cd(II) via N9 whilst 6-mercaptopurine promotes the S6,N7-bidentate mode in Cd(II) complexes due to the softness of the S atom and the chelate effect related to the five-membered chelating ring. Anionic forms of 6-mercaptopurine also play a μ_2–bridging role. In contrast, 6-oxopurines can bind Cd(II) through the N-heterocyclic donors but do not build O6,N7-chelate rings, in accordance with the hardness of the O6 atom. Nevertheless, some pyrimidine nucleobases can build constrained four-membered N(heterocyclic),O(exocyclic)-Cd(II) chelate rings.

Cd(II) complexes with amino acids are rich in examples where zwitterionic forms of these ligands act via the carboxylate groups. The presence of suitable side chains with donor atoms increases the denticity and the chelating ability of amino acidate ligands. Hence, L-histidinate(1–) acts as a chelating tridentate system in the bis-chelate $[Cd(L\text{-}Hhis)_2]\cdot 2H_2O$ but the dianion L-cysteinate(2–) is hexadentate in the polymer $[Cd(L\text{-}cys)]_n$ [N,O,S-chelating tridentate as well as S_3(thiolate)- and O,O'(carboxylate)-bridging roles].

Cd(II) complexes with various vitamins of the B group also reveal remarkable structural diversity. In particular, thiamine binds Cd(II) by its less hindered N heterocyclic donor, the O-alcoholic donor from its pendant arm or in a combined N,O-bidentate bridging mode. Interestingly, a closely related N,O-bridging role has been observed in the Cd(II)-acyclovir complex.

The affinity between soft Cd(II) ions and S donor atoms yields a rich structural pathway. Thiolate atoms act as mono-, bi- or tridentate donor groups. Dithiocarbamate ligands tend to build rather stable four-membered chelate rings, where the

S–Cd–S bite angle seems to depend on the coordination geometry. Curiously, structures of Cd(II) complexes with those dithiolate ligands proposed for Cd(II) detoxification have not yet been reported. Chelate ring constraints in EDTA-type Cd(II) complexes favor seven-coordination polyhedra.

Abbreviations and Definitions

acv	acyclovir[2-amine-9-(2-hydroxyethoxymethyl)-3*H*-purin-6-one
ap	adipate(2–)
ATP	adenosine 5'-triphosphate
BAL	British Anti-Lewisite (2,3-dimercaptopropanol)
2,2'-bipy	2,2'-bipyridine
4,4'-bipy	4,4'-bipyridine
bpvbd	3,6-bis(pivaloylamino)benzene-1,2-dithiolato-S,S'(2–)
CSD	Cambridge Structural Database
DABT	2,2'-diamino-4,4'-bis-1,3-thiazole
DMAB	4-(dimethylamino)benzoate(1–)
DMF	*N*,*N*-dimethylformamide
DMPS	2,3-dimercapto-1-propanesulfonate (1–)
DMSA	dimercaptosuccinate(2–)
dmso	dimethylsulfoxide
dpe	1,2-di(pyridin-4-yl)ethane
dppf	(diphenylphosphino)ferrocene
ede-ade	2-(ethylenediamine)ethyl-N9-adenine
ede-dap	2-(ethylenediamine)ethyl-N9-2,6-diaminopurine
ede-gua	2-(ethylenediamine)ethyl-N9-guanine
edp-dap	2-(ethylenediamine)propyl-N9-2,6-diaminopurine
edt	ethane-1,2-dithiolato
EDTA	ethylenediamine-N,N,N',N'-tetraacetate(4–)
en	1,2-ethylenediamine
9Etgua	9-ethylguanine
H6MP	6-mercaptopurine
Hade	adenine
Hala	alanine
Hasn	asparagine
Hasp	aspartate
HBthiamine	2-(α-hydroxybenzyl)thiamine
Hcyt	cytosine
Hdap	2,6-diaminopurine
Hgly	glycine
Hgua	guanine
Hhip	hippuric acid

Hhyp	hypoxanthine
Hhis	histidine
Hicyt	isocytosine
HIm	1*H*-imidazole
Hmet	methionine
Hphe	phenylalanine
Hpro	proline
Hptola	*p*-toluic acid
Hpur	purine
Hpym	pyrimidine
Htheo	theophiline
Htrp	tryptophan
Hura	uracil
Hxan	xanthine
H_2ap	adipic acid
H_2asp	aspartic acid glycine
H_2BAD^+	N^6-benzyladeninium cation
H_2cys	cysteine
H_2FAD^+	N^6-furfuryladeninium cation
H_2glu	glutamic acid
H_2tp	terephthalic acid
IDA	iminodiacetate(2–)
9Meade	9-methyladenine
1Mecyt	1-methylcytosine
9Megua	9-methylguanine
NA	nicotinate(1–)
NADA	nicotinamide
NBO	natural bond orbital programme
NBZ	2-nitrobenzoate(1–)
niacin	3-pyridinecarboxylic acid
niacinamide	3-pyridinecarboxamide
NTA	nitrilotriacetate(3–)
ox	oxalate(2–)
o-PhDTA	*ortho*-phenylenediamine-*N*,*N*,*N*',*N*'-tetraacetate(4–)
paa	2-pyridinealdazine
phen	1,10-phenanthroline
PMAB	4-(methylamino)benzoate(1–)
PPh_4^+	tetraphenylphosphonium
ptola	*p*-toluic acid
S-2,4,6-$iPr_3C_6H_2$	(2,4,6-tri-isopropyl)benzenethiolato(1–)
S-2,4,6,^{t}butyl C_6H_2	(2,4,6-tri-*tert*-butyl)benzenothiolato(1–)
$SC_6H_4Bu^t$-4	4-*tert*-butylbenzenothiolato(1–)
ScHex	cyclohexanethiolato(1–)
SCN	thiocyanate

SPh = SC_6H_5	benzenothiolato(1–)
SPhF-3	3-fluorobenzenethiolato(1–)
tem-N9,N9'-diade	N^9,N^9-tetramethylene-bis(adenine)
3,4-TDTA	3,4-toluenediamine-*N*,*N*,*N*',*N*'-tetraacetate(4–)
tm-N9,N9'-diade	N^9,$N^{9'}$-trimethylene-bis(adenine)
1Toscyt	1-(*p*-toluenesulfonyl)cytosine
tp	terephthalate(2–)
tren	tris-(2-aminoethyl)amine
trp	tryptophan

Acknowledgments Research in the authors' laboratories is funded by the Ministry of Science and Innovation and FEDER-EC (MAT2010-15594), Xunta de Galicia (INCITE08PXIB203128PR and 10TMT314002PR) and the University of Granada (Domestic Grant P18-2009). We also thank Professors Dr. J. M. González-Pérez and Dr. E. Vázquez-López for critically reading of the manuscript. ADM thanks the Ministry of Education for a FPU Ph.D. fellowship. The authors thank their current and former graduate students and post-doctoral fellows for their hard work and valuable discussion on this project.

References

1. 1. H. R. Pohl, H. G. Abadin, J. F. Risher, in *Neurotoxicity of Cadmium, Lead, and Mercury*, Vol. 1 of *Metal Ions in Life Sciences*, Eds A. Sigel, H. Sigel, R. K. O. Sigel, John Wiley & Sons, Chichester, UK, 2006, pp. 397-400.
2. J. S. Casas, V. Moreno, A. Sánchez, J. L. Sánchez, J. Sordo, *Química Bioinorgánica*, Síntesis, Madrid, 2002, pp. 276–285.
3. R. R. Crichton, *Biological Inorganic Chemistry. An Introduction*, Elsevier, Oxford, 2007, pp. 346–350.
4. ChemDraw Ultra, Cambridge Soft, ver. 12.0.2.1076, 2010.
5. K. Brandenburg, H. Putz, DIAMOND 3.x, Crystal Impact GbR, Bonn, Germany, 2004.
6. C. F. Macrae, I. J. Bruno, J. A. Chisholm, P. R. Edgington, P. McCabe, E. Pidcock, L. Rodríguez-Monge, R. Taylor, J. van de Streek, P. A. Wood, Mercury 2.0 CSD, *J. Appl. Cryst.*, **2008**, *41*, 466–470.
7. S. Péres-Yáñez, O. Castillo, J. Cepeda, J. P. García-Terán, A. Luque, P. Román, *Inorg. Chim. Acta*, **2011**, *365*, 211–219.
8. A. K. Paul, U. Sanyal, S. Natarajan, *Cryst. Growth Des.*, **2010**, *10*, 4161–4175.
9. C. H. Wei, K. B. Jacobson, *Inorg.Chem.*, **1981**, *20*, 356–363.
10. M. A. Salam, H. Q. Yuan, T. Kikuchi, N. A. Prasad, I. Fujisawa, K. Aoki, *Inorg. Chim. Acta*, **2009**, *362*, 1158–1168.
11. E.-C. Yang, H.-K. Zhao, B. Ding, X.-G. Wang, X.-J. Zhao, *New J. Chem.*, **2007**, *31*, 1887–1890.
12. E.-C. Yang, Y.-N. Chan, H. Liu, Z.-Ch. Wang, X.-J. Zhao, *Cryst. Growth Des.*, **2009**, *9*, 4933–4944.
13. E. A. H. Griffith, N. G. Charles, E. L. Amma, *Acta Crystallogr., Sect. B*, **1982**, *38*, 942–944.
14. P. A. Ochoa, M. I. Rodríguez-Tapiador, S. S. Alexandre, C. Pastor, F. Zamora, *J. Inorg. Biochem.*, **2005**, *99*, 1540–1547.
15. N. Stanley, P. T. Muthiah, P. Luger, M. Weber, S. J. Geib, *Inorg. Chem. Commun.*, **2005**, *8*, 1056–1059.
16. M. P. Brandi-Blanco, D. Choquesillo-Lazarte, A. Domíngez-Martín, J. M. González-Pérez, A. Castiñeiras, J. Niclós-Gutiérrez, *J. Inorg. Biochem.* **2011**, *105*, 616–623.

17. A. García-Raso, J. J. Fiol, F. Bádenas, R. Cons, A. Terrón, M. Quirós, *J. Chem. Soc., Dalton Trans*., **1999**, 167–174.
18. M. A. Shipman, C. Price, A. E. Gibson, M. R. J. Elsegood, W. Clegg, A. Houlton, *Chem. Eur. J*., **2000**, *6*, 4371–4378.
19. D. Amantia, M. A. Shipman, C. Price, M. R. J. Elsegood, W. Clegg, A. Houlton, *Inorg. Chim. Acta*, **2006**, *359*, 3515–3520.
20. M. A. Galindo, D. Amantia, A. Martínez, W. Clegg, R. W. Harrington, V. Moreno, A. Houlton, *Inorg. Chem*., **2009**, *48*, 10295–10303.
21. A. García-Raso, J. J. Fiol, F. Bádenas, X. Solans, M. Font-Bardía, *Polyhedron*, **1999**, *18*, 765–772.
22. A. García-Raso, J. J. Fiol, A. Tasada, F. M. Alberti, F. Bádenas, X. Solans, M. Font-Bardía, *Polyhedron*, **2007**, *26*, 949–957.
23. E. Dubler, E. Gyr, *Inorg. Chem*., **1988**, *27*, 1466–1473.
24. E. A. H. Griffith, E. L. Amma, *Chem. Commun*., **1979**, 1013–1014.
25. P. Amo-Ochoa, M. I. Rodríguez-Tapiador, O. Castillo, D. Olea, A. Guijarro, S. S. Alexandre, J. Gómez-Herrero, F. Zamora, *Inorg. Chem*., **2006**, *45*, 7642–7650.
26. E. Gyr, H.W. Schmalle, E. Dubler, 2008 (Private Communication), RAKSUS in CSD database.
27. E. Dubler, G. Hänggi, H. Schmalle, *Inorg. Chem*., **1990**, *29*, 2518–2523.
28. D. K. Patel, A. Domínguez-Martín, M. P. Brandi-Blanco, V. M. Nurchi, J. Niclós-Gutiérrez, *Coord. Chem. Rev*., **2012**, *256*, 193–211.
29. H. Q. Yuan, K. Aoki, I. Fujisawa, *Inorg. Chim. Acta*, **2009**, *362*, 975–984.
30. E. Buncel, R. Kumar, A. R. Norris, A. L. Beauchamp, *Can. J. Chem*., **1985**, *63*, 2575–2581.
31. G. D. Munno, S. Mauro, T. Pizzino, D. Viterbo, *J. Chem. Soc., Dalton Trans*., **1993**, 1113–1119.
32. L. Bancu, P. Bourosh, I. Jitaru, Yu. A. Siminov, J. Lipkowski, *Rev. Roum. Chim*., **2006**, *51*, 397–401.
33. P. T. Muthiah, J. J. Robert, S. B. Raj, G. Bocelli, R. Olla, *Acta Crystallogr., Sect.E*, **2001**, *57*, m558–m560.
34. M. C. Capllonch, A. García-Raso, A. Terrón, M. C. Apella, E. Espinosa, E. Molins, *J. Inorg. Biochem*., **2001**, *85*, 173–178.
35. K. Kaabi, M. El Glaoui, P. S. Pereira Silva, M. Ramos Silva, C. Ben Nasr, *Acta Crystallogr., Sect.E*, **2010**, *66*, m1225.
36. I. Mutikainen, P. Lumme, *Acta Crystallogr., Sect.B*, **1980**, *36*, 2237–2240.
37. C. Gagnon, A. L. Beauchamp, D. Tranqui, *Can. J. Chem*., **1979**, *57*, 1372–1376.
38. A. Visnjevac, N. Biliskov, B. Zinic, *Polyhedron*, **2009**, *28*, 3101–3109.
39. H. Fuess, H. Bartunik, *Acta Crystallogr., Sect. B*, **1976**, *32*, 2803–2806.
40. P. J. Barrie, A. Gyani, M. Motevalli, P. O'Brien, *Inorg. Chem*., **1993**, *32*, 3862–3867.
41. R. J. Flook, H. C. Freeman, C. J. Moore, M. L. Scudder, *Chem. Commun*., **1973**, 753–754.
42. J. Wang, X. Xu, W. Ma, F. Yin, T. Guo, L. Lu, X. Yang, X. Wang, *J. Inorg. Organomet. Polym. Mater*., **2009**, *19*, 401–405.
43. J.-N. Rebilly, P. W. Gardner, G. R. Darling, J. Bacsa, M. J. Rosseinsky, *Inorg. Chem*., **2008**, *47*, 9390–9399.
44. A. Demaret, F. Abraham, *Acta Crystallogr., Sect. C*, **1987**, *43*, 2067–2069.
45. D. W. Tomlin, T. M. Cooper, S. M. Cline, J. M. Hughes, W. W. Adams, *Acta Crystallogr., Sect. C*, **1997**, *53*, 1815–1816.
46. R. Thulasidhass, J. K. Mohanarao, *Curr. Sci*., **1980**, *49*, 349.
47. M. Dan, C. N. R. Rao, *Chem. Eur. J*., **2005**, *11*, 7102–7109.
48. K. I. Schaffers, D. A. Keszler, *Acta Crystallogr., Sect. C*, **1993**, *49*, 1156–1158.
49. M. S. Nandhini, R. V. Krishnakumar, S. Natarajan, *Acta Crystallogr., Sect. E*, **2003**, *59*, m756–m758.
50. A. Kandasamy, R. Siddeswaran, P. Murugakoothan, P. S. Kumar, R. Mohan, *Cryst. Growth Des*., **2007**, *7*, 183–186.

51. B.-X. Liu, J.-Y. Yu, D.-J. Xu, *Acta Crystallogr., Sect. E*, **2005**, *61*, m2291–m2293.
52. L. Gasque, S. Bernès, R. Ferrari, G. Mendoza-Díaz, *Polyhedron*, **2002**, *21*, 935–941.
53. M. J. Ingleson, J. Bacsa, M. J. Rosseinsky, *Chem.Commun*., **2007**, 3036–3038.
54. D. Deng, P. Liu, B. Ji, L. Wang, W. Fu, *Tetrahedron Lett*., **2010**, *51*, 5567–5570.
55. M. F. Richardson, K. Franklin, D. M. Thompson, *J. Am. Chem. Soc*., **1975**, *97*, 3204–3209.
56. R. E. Cramer, R. B. Maynard, J. A. Iber, *J. Am. Chem. Soc*., **1981**, *103*, 76–81.
57. K. Aoki, H. Yamazaki, A. Adeyemo, *Inorg. Chim. Acta*, **1991**, *180*, 117–124.
58. J. S. Casas, E. E. Castellano, M. D. Couce, A. Sánchez, J. Sordo, J. M. Varela, J. Zukerman-Schpector, *Inorg. Chem*., **1995**, *34*, 2430–2437.
59. J. S. Casas, A. Castiñeiras, M. D. Couce, A. Sánchez, J. Sordo, J. M. Varela, *Polyhedron*, **1995**, *14*, 1825–1829.
60. N.-H. Hu, T. Norifusa, K. Aoki, *Polyhedron*, **1999**, *18*, 2987–2994.
61. J. S. Casas, E. E. Castellano, M. D. Couce, J. Ellena, A. Sánchez, J. Sordo, C. Taboada, *J. Inorg. Biochem*., **2006**, *100*, 124–132.
62. Y. Zhou, W. Bi, X. Li, J. Chen, R. Cao, M. Hong, *Acta Crystallogr., Sect. E*, **2003**, *59*, m356–m358.
63. J. Moncol, D. Miklos, P. Segla, M. Koman, *Acta Crystallogr., Sect. E*, **2008**, *64*, m665–m666.
64. J. Y. Lu, M. A. Achten, A. Zhang, *Inorg. Chem. Commun*., **2007**, *10*, 114–116.
65. J. Y. Lu, E. E. Kohler, *Inorg. Chem. Commun*., **2002**, *5*, 196–198.
66. J. Zhang, Z.-J. Li, Y.-H. Wen, Y. Kang, Y.-Y. Qin, Y.-G. Yao, *Acta Crystallogr., Sect. C*, **2004**, *60*, m389–m391.
67. Y. X. Chi, Sh. Y. Niu, J. Jin, L. P. Sun, G. D. Yang, L. Ye, *Z. Anorg. Allg. Chem*., **2007**, *633*, 1274–1278.
68. C. Zhang, D. Xu, Y. Xu, X. Huang, *Acta Crystallogr., Sect.C*, **1996**, *52*, 591–593.
69. L. Yang, L. Liu, S. Li, *Z. Kristallogr.-New Cryst. Struct*., **2009**, *224*, 423–424.
70. G. Yang, H.-G. Zhu, B.-H. Liang, X.-M. Chen, *J. Chem. Soc., Dalton Trans*., **2001**, 580–585.
71. Z. Lian, N. Zhao, F. Yang, P. Liu, *Z. Kristallogr.-New Cryst. Struct*., **2011**, *226*, 289–290.
72. K.-L. Zhang, B. Yang, J.-G. Lin, S. W. Ng, *Acta Crystallogr., Sect. E*, **2009**, *65*, m292.
73. Z.-P. Deng, S. Gao, S. W. Ng, *Acta Crystallogr., Sect. E*, **2007**, *63*, m2323.
74. Ch. Li, M. Chen, Ch. Shao, *Acta Crystallogr., Sect. E*, **2008**, *64*, m424.
75. T. Hokelek, E. G. Saglam, B. Tercan, O. Aybirdi, H. Necefoglu, *Acta Crystallogr., Sect.E*, **2010**, *66*, m1559–m1560.
76. T. Hokelek, Y. Suzen, B. Tercan, O. Aybirdi, H. Necefoglu, *Acta Crystallogr., Sect.E*, **2010**, *66*, m782–m783.
77. A. Mosset, F. Nepveu-Juras, R. Harpin, J.-J. Bonnet, *J. Inorg. Nucl. Chem*., **1978**, *40*, 1259–1263.
78. N. G. Furmanova, Zh. I. Berdalieva, T. S. Chernaya, V. F. Resnyanskii, N. K. Shiitieva, K. S. Sulaimankulov, *Crystallogr. Rep*., **2009**, 54, 228–235.
79. A. Martelli, E. Rousselet, C. Dycke, A. Bouron, J.-M. Moulis, *Biochemie*, **2006**, *88*, 1807–1814.
80. I. G. Dance, *Polyhedron*, **1986**, *5*, 1037–1104.
81. E. S. Gruff, S. A. Koch, *J. Am. Chem. Soc*., **1990**, *112*, 1245–1247.
82. R. A. Santos, E. S. Gruff, S. A. Koch, G. S. Harbison, *J. Am. Chem. Soc*., **1991**, *113*, 469–475.
83. M. Bochmann, K. Webb, M. Harman, M. B. Hursthouse, *Angew. Chem., Int. Ed*., **1990**, *29*, 638–639.
84. D. Coucouvanis, D. Swenson, N.C. Baenziger, C. Murphy, D. G. Holah, N. Sfarnas, A. Simopoulos, A. Kostikas. *J. Am. Chem. Soc*., **1981**, *103*, 3350–3362.
85. A. Silver, S. A. Koch, M. Millar, *Inorg. Chim. Acta*, **1993**, *205*, 9–14.
86. N. Ueyama, T. Sugawara, K. Sasaki, A. Nakamura, S. Yamashita, Y. Wakatsuki, H. Yamazaki, N. Yasuoka, *Inorg. Chem*., **1988**, *27*, 741–747.
87. I. L. Abrahams, C. D. Garner, W. Clegg, *J. Chem. Soc., Dalton Trans*., **1987**, 1577–1579.
88. B. Ali, I. Dance, M. Scudder, D. Craig, *Cryst. Growth Des*., **2002**, *2*, 601–607.
89. K. Tang, A. Li, X. Jin, Y. Tang, *Chem. Commun*., **1991**, 1590–1591.

90. K. Tang, X. Jin, A. Li, S. Li, Z. Li, Y. Tang, *J. Coord. Chem.*, **1994**, *31*, 305–320.
91. K. S. Hagen, D. W. Stephan, R. H. Holm, *Inorg. Chem.*, **1982**, *21*, 3928–3936.
92. D. Craig, I. G. Dance, R. Garbutt, *Angew. Chem., Int. Ed.*, **1986**, *25*, 165–166.
93. K. S. Hagen, R. H. Holm. *Inorg. Chem.*, **1983**, *22*, 3171–3176.
94. Y. Matsunaga, K. Fujisawa, N. Ibi, M. Fujita, T. Ohashi, N. Amir, Y. Miyashita, K. Aika, Y. Izumi, K. Okamoto. *J. Inorg. Biochem.*, **2006**, *100*, 239–249.
95. K. Tang, T. Xia, X. Jin, Y. Tang, *Polyhedron*, **1994**, *13*, 3023–3026.
96. X. Zhang, Y. Tian, F. Jin, J. Wu, Y. Xie, X. Tao, M. Jiang, *Cryst. Growth Des.*, **2005**, *5*, 565–570.
97. Q. Zhang, Z. Lin, X. Bu, T. Wu, P. Feng, *Chem. Mater.*, **2008**, *20*, 3239–3241.
98. O. Andersen, *Environ. Health Persp.* **1984**, *54*, 249–266.
99. C. P. Rao, J. R. Dorfman, R. H. Holm, *Inorg. Chem.*, **1986**, *25*, 428–447.
100. L. Bustos, M. A. Khan, D. G. Tuck, *Can. J. Chem.*, **1983**, *61*, 1146–1152.
101. K. Baba, T. Okamura, H. Yamamoto, T. Yamamoto, N. Ueyama, *Inorg. Chem.*, **2008**, *47*, 2837–2848.
102. W. P. Chung, J. C. Dewan, M. A. Walters, *J. Am. Chem. Soc.*, **1991**, *113*, 525–530.
103. J. Pande, M. Vašák, J. H. R. Kägi, *Biochemistry*, **1985**, *24*, 6717–6722.
104. A. H. Robbins, D. E. McRee, M. Williamson, S. A. Collett, N. H. Xuong, W. F. Furey, B. C. Wang, C. D. Stout, *J. Mol. Biol.*, **1991**, *221*, 1269–1293.
105. R. G. Gale, A. B. Smith, E. M. Walker, Jr, *Ann. Clin. Lab. Sci.*, **1981**, *11*(6) 476–483.
106. T. Trindade, N. Pickett, P. O'Brien, *Chem. Mater.*, **2001**, *13*, 3843–3858.
107. N. Revaprasadu, S. N. Mlondo, *Pure Appl. Chem.*, **2006**, *78*, 1691–1702.
108. V. S. R. Rajasckhar Pullabhotta, M. Scriba, N. Revaprasadu, *J. Nanosci. Nanotechnol.*, **2011**, *11*(2), 1201–1204.
109. E. R. T. Tiekink, *CrystEngComm*, **2003**, *5*, 101–113.
110. J. A. McCleverty, S. Gill, R. S. Z. Kowalski, N. A. Bailey, H. Adams, K. W. Lumbard, M. A. Murphy, *J. Chem. Soc., Dalton Trans.*, **1982**, 493–503.
111. S. M. Zemskova, L. A. Glinskaya, R. F. Klevtsova, M. A. Fedotov, S. V. Larionov, *J. Struct. Chem.*, **1999**, 40, 284–292.
112. L. A. Glinskaya, S. M. Zemskova, R. F. Klevtsova, S. V. Larionov, S. A. Gromilov, *Polyhedron*, **1992**, *11*, 2951–2956.
113. R. Baggio, A. Frigerio, E. B. Halac, D. Vega, M. Perec, *J. Chem. Soc., Dalton Trans.*, **1992**, 1887–1892.
114. R. Baggio, A. Frigerio, E. B. Halac, D. Vega, M. Perec, *J. Chem. Soc., Dalton Trans.*, **1992**, 549–554.
115. A. Kropidlowska, J. Chojnacki, B. Becker, *Acta Crystallogr., Sect. E*, **2008**, m832.
116. A. Kropidlowska, J. Chojnacki, A. Fahmi, B. Becker, *Dalton Trans.*, **2008**, 6825–6831.
117. J. S. Casas, A. Sánchez, J. Bravo, S. García-Fontán, E. E. Castellano, M. M. Jones, *Inorg. Chim. Acta*, **1989**, *158*, 119–126.
118. L. H. van Poppel, T. L. Groy, M. T. Caudle, *Inorg. Chem.*, **2004**, *43*, 3180–3186.
119. M. A. Malik, M. Motevalli, T. Saeed, P. O'Brien, *Adv. Mater.*, **1993**, *5*, 653–654.
120. S. M. Zemskova, L. A. Glinskaya, R. F. Klevtsova, S. V. Larionov, *Zh. Neorg. Khim. (Russ. J. Inorg. Chem.),* **1993**, *38*, 466–471.
121. O. D. Fox, M. G. B. Drew, E. J. S. Wilkinson, P. D. Beer, *Chem. Commun.*, **2000**, 391–392.
122. F.-X. Wei, X. Yin, W.-G. Zhang, J. Fan, X.-H. Jiang, S.-L. Wang, *Z. Kristallogr.-New Cryst. Struct.*, **2005**, *220*, 417–419.
123. Ch. S. Lai, E. R. T. Tiekink, *Appl. Organomet. Chem.*, **2003**, *17*, 139–140.
124. M. Saravanan, R. Ramalingam, B. Arulprakasam, G. Bocelli, A. Cantoni, E. R. T. Tiekink, *Z. Kristallogr.-New Cryst. Struct.*, **2005**, *220*, 477–478.
125. Y.-H. Deng, J. Liu, N. Li, Y.-L. Yang, H.-W. Ma, *Huaxue Xuebao (Acta Chim. Sinica)*, **2007**, *65*, 2868–2874.
126. S. Thirumaran, K. Ramlingam, G. Bocelli, L. Righi, *Polyhedron*, **2009**, *28*, 263–268.
127. C. M. Dee, E. R. T. Tiekink, *Acta Crystallogr., Sect. E,* **2002**, *58*, m136–m138.

128. P. Poplaukhin, E. R. T. Tiekink, *Acta Crystallogr., Sect. E,* **2008**, *64*, m1176.
129. D. V. Konarev, S. S. Khasanov, D. V. Lopatin, V. V. Rodaev, R. N. Lyubovskaya, *Russ. Chem. Bull., Int. Ed.,* **2007**, *56*, 2145–2161.
130. A.-K. Duhme, S. Pohl, H. Strasdeit, *Inorg. Chim. Acta*, **1990**, *175*, 5–8.
131. V. Avila, R. E. Benson, G. A. Broker, L. M. Daniels, E. R. T. Tiekink, *Acta Crystallogr., Sect. E,* **2006**, *62*, m1425–m1427.
132. J. Fan, F.-X. Wei, W.-G. Zhang, X. Yin, Ch.-S. Lai, E. R. T. Tiekink, *Huaxue Xuebao*, **2007**, *65*, 2014–2018.
133. J. Chai, Ch. S. Lai, J. Yan, E. R. T. Tiekink, *Appl. Organomet. Chem.*, **2003**, *17*, 249–250.
134. X. F. Wang, Y. F. Wang, J. Wang, Zh. H. Zhang, J. Gao, B. Liu, Y. Ch. Jiang, X. D. Zhang, *Russ. J. Coord. Chem.*, **2008**, *34*, 555–563.
135. I. N. Polyakova, A. L. Poznyak, V. S. Sergienko, L. V. Stopolyanskaya, *Crystallogr. Rep.*, **2001**, *46,* 40–45.
136. E.-L. Yang, Y.-L. Jiang, Y.-L. Wang, Q.-Y. Liu, *Acta Crystalogr., Sect. C,* **2010**, *66*, m231–m234.
137. J. Sanchíz, P. Esparza, S. Domínguez, A. Mederos, D. Saysell, A. Sánchez, R. Ruano, J. M. Arrieta, *J. Chem. Soc., Dalton Trans.*, **2001**, 1559–1565.
138. B-X. Liu, D.-J. Xu, *Acta Crystallogr., Sect. E,* **2005**. *61*, m1218–m1220.

Chapter 8
Complex Formation of Cadmium with Sugar Residues, Nucleobases, Phosphates, Nucleotides, and Nucleic Acids

Roland K.O. Sigel, Miriam Skilandat, Astrid Sigel, Bert P. Operschall, and Helmut Sigel

Contents

ABSTRACT 192
1 INTRODUCTION 193
2 COMPARISONS OF THE PROPERTIES OF CADMIUM(II) WITH THOSE OF ZINC(II), CALCIUM(II), MAGNESIUM(II), AND OTHER RELATED METAL IONS 195
3 CADMIUM(II)-SUGAR INTERACTIONS 198
3.1 Hydroxyl Coordination in Carboxyhydrates Is Rare 198
3.2 The Metal Ion Affinity of Ribose-Hydroxyl Groups Is Small 199
3.3 A Favorable Steric Setting and a Reduced Solvent Polarity May Promote Metal Ion-Hydroxyl (or -Carbonyl) Group Binding 200
4 INTERACTIONS OF CADMIUM(II) WITH NUCLEOBASE RESIDUES 204
4.1 Cadmium(II) Complexes of Purine Derivatives 204
4.2 Cadmium(II) Complexes of Pyrimidine Derivatives 209
4.3 Cadmium(II) Complexes of Some Less Common Nucleobase Residues 214
4.3.1 Tubercidin 214
4.3.2 Orotidine 215
4.3.3 Xanthosine 215
4.3.4 Thiouridines 216
4.3.5 2-Thiocytidine 217
5 COMPLEXES OF CADMIUM(II) WITH PHOSPHATES 218
6 CADMIUM(II) COMPLEXES OF NUCLEOTIDES 222
6.1 Some General Considerations 222
6.2 Complexes of Nucleoside 5'-Monophosphates 224
6.2.1 Equilibrium Constants to Be Considered 224
6.2.2 Properties of Pyrimidine-Nucleoside 5'-Monophosphate Complexes 224

R.K.O. Sigel (✉) • M. Skilandat
Institute of Inorganic Chemistry, University of Zürich,
Winterthurerstrasse 190, CH-8057 Zürich, Switzerland
e-mail: roland.sigel@aci.uzh.ch

A. Sigel • B.P. Operschall • H. Sigel (✉)
Department of Chemistry, Inorganic Chemistry, University of Basel,
Spitalstrasse 51, CH-4056 Basel, Switzerland
e-mail: astrid.sigel@unibas.ch; bert.operschall@unibas.ch; helmut.sigel@unibas.ch

A. Sigel, H. Sigel, and R.K.O. Sigel (eds.), *Cadmium: From Toxicity to Essentiality*,
Metal Ions in Life Sciences 11, DOI 10.1007/978-94-007-5179-8_8,

6.2.3 Properties of Purine-Nucleoside 5'-Monophosphate Complexes 226
6.3 Complexes of Nucleoside 5'-Di- and -Triphosphates 229
6.4 Complexes of Less Common Nucleotides 232
6.4.1 Tubercidin 5'-Monophosphate 233
6.4.2 Nucleoside 2'- and 3'-Monophosphates 234
6.4.3 Orotidinate 5'-Monophosphate 235
6.4.4 Xanthosinate 5'-Monophosphate 236
6.4.5 Thiouracil Nucleotides 237
6.4.6 Flavin Mononucleotide 238
7 CADMIUM(II) COMPLEXES OF NUCLEOTIDE ANALOGUES 239
7.1 Properties of 1,N^6-Ethenoadenosine and of Its Phosphates 240
7.2 Complexes of Nucleoside 5'-*O*-Thiomonophosphates 241
7.3 Complexes of Acyclic Nucleotide Analogues 243
7.4 Cadmium(II) Binding to Nucleotides Containing a Platinum(II)-Coordinated Nucleobase Residue 245
8 A SHORT APPRAISAL OF MIXED LIGAND COMPLEXES CONTAINING A NUCLEOTIDE 247
8.1 Definitions and General Comments 247
8.2 Ternary Cadmium(II) Complexes Containing ATP^{4-} and a Buffer Molecule 248
8.3 Mixed Ligand Complexes Containing a Nucleotide and a Further Monodentate or Bidentate Ligand. Release of Purine-N7 and Formation of Stacks 251
9 CADMIUM(II) BINDING IN DINUCLEOTIDES AND DINUCLEOSIDE MONOPHOSPHATES 253
9.1 The Phosphodiester Link 254
9.2 The Guanine Residue in a Dinucleotide 255
9.3 The Non-bridging Sulfur of the Thiophosphodiester Link 256
9.4 Dinucleoside Monophosphates 257
10 CADMIUM(II) BINDING TO NUCLEIC ACIDS 258
10.1 Cadmium(II)-Rescue Experiments 258
10.2 Crystal Structures of RNA or DNA-Protein Complexes Containing Cd(II) 259
10.3 Cadmium(II) as Probe in EPR and NMR Spectroscopy 261
11 CONCLUDING REMARKS 262
ABBREVIATIONS AND DEFINITIONS 263
ACKNOWLEDGMENTS 266
REFERENCES 266

Abstract Cadmium(II), commonly classified as a relatively soft metal ion, prefers indeed aromatic-nitrogen sites (e.g., N7 of purines) over oxygen sites (like sugar-hydroxyl groups). However, matters are not that simple, though it is true that the affinity of Cd^{2+} towards ribose-hydroxyl groups is very small; yet, a correct orientation brought about by a suitable primary binding site and a reduced solvent polarity, as it is expected to occur in a folded nucleic acid, may facilitate metal ion-hydroxyl group binding very effectively. Cd^{2+} prefers the guanine(N7) over the adenine(N7), mainly because of the steric hindrance of the (C6)NH_2 group in the adenine residue. This Cd^{2+}-(N7) interaction in a guanine moiety leads to a significant acidification of the (N1)H meaning that the deprotonation reaction occurs now in the physiological pH range. N3 of the cytosine residue, together with the neighboring (C2)O, is also a remarkable Cd^{2+} binding site, though replacement of (C2)O by (C2)S enhances the affinity towards Cd^{2+} dramatically, giving in addition rise to

the deprotonation of the (C4)NH_2 group. The phosphodiester bridge is only a weak binding site but the affinity increases further from the mono- to the di- and the triphosphate. The same also holds for the corresponding nucleotides. Complex stability of the pyrimidine-nucleotides is solely determined by the coordination tendency of the phosphate group(s), whereas in the case of purine-nucleotides macrochelate formation takes place by the interaction of the phosphate-coordinated Cd^{2+} with N7. The extents of the formation degrees of these chelates are summarized and the effect of a non-bridging sulfur atom in a thiophosphate group (*versus* a normal phosphate group) is considered. Mixed ligand complexes containing a nucleotide and a further mono- or bidentate ligand are covered and it is concluded that in these species N7 is released from the coordination sphere of Cd^{2+}. In the case that the other ligand contains an aromatic residue (e.g., 2,2'-bipyridine or the indole ring of tryptophanate) intramolecular stack formation takes place. With buffers like Tris or Bistris mixed ligand complexes are formed. Cd^{2+} coordination to dinucleotides and to dinucleoside monophosphates provides some insights regarding the interaction between Cd^{2+} and nucleic acids. Cd^{2+} binding to oligonucleotides follows the principles of coordination to its units. The available crystal studies reveal that N7 of purines is the prominent binding site followed by phosphate oxygens and other heteroatoms in nucleic acids. Due to its high thiophilicity, Cd^{2+} is regularly used in so-called thiorescue experiments, which lead to the identification of a direct involvement of divalent metal ions in ribozyme catalysis.

Keywords cadmium • calcium • equilibrium constants • magnesium • metal ions • methods • ribozymes • RNA • zinc

1 Introduction

Cadmium is widely distributed in the environment at relatively low concentrations, except where it accumulated due to anthropogenic activities [1] (see also Chapters 2 and 3 of this book). Cadmium chemically resembles zinc and any differences are attributable to the larger size of Cd^{2+} compared with that of Zn^{2+} [2]. Indeed, cadmium occurs in the earth's crust and the upper lithosphere mainly together with zinc (zinc being present to ca. 0.02% [3]). The Cd/Zn ratio has been estimated to be about 1:250 [4], and cadmium is thus gained as by-product from zinc ores (Chapter 3).

Cadmium is a toxic element (see Chapters 1, 14, 15) that accumulates especially in kidney and liver [4] being bound preferably to metallothionein (Chapters 6, 11). On the other hand, the chemical similarity of Cd^{2+} to Zn^{2+} is confirmed by the fact that carbonic anhydrase of marine phytoplankton contains Cd^{2+} (Chapter 16), whereas the corresponding zinc enzymes are found in organisms from all kingdoms [5] catalyzing the reversible hydration of carbon dioxide. In marine diatoms cadmium, cobalt, and zinc can functionally substitute for one another to maintain optimal growth [6]. Cadmium-carbonic anhydrase is involved in the acquisition of inorganic carbon for photosynthesis [6].

Interestingly, already more than 50 years ago Wacker and Vallee detected cadmium as well as other metal ions in RNA from horse kidney cortex [7], but there is no indication for a "positive" role of any cadmium-nucleic acid interaction. However, nowadays Cd^{2+} is often applied as a probe to study the effects of metal ions on ribozymes [8,9] as well as the metal ion-binding properties of nucleic acids in general [10]. With this general analytical use in mind, this chapter has been written, concentrating on Cd^{2+} and several related metal ions (see Section 2) as well as on the nucleobases (NB) and their derivatives which are important for RNA and DNA (Figure 1) [11–14]. The four main nucleobases of RNA are adenine (Ade), guanine (Gua), cytosine (Cyt), and uracil (Ura); in DNA uracil is replaced by thymine (Thy). Hypoxanthine (Hyp) is included for comparisons with guanine. Below we will first consider some physicochemical properties of Cd^{2+} and related metal ions. Next, the interaction of these metal ions with sugar, phosphate, and nucleobase residues will be addressed, followed by nucleotides and nucleic acid complexes.

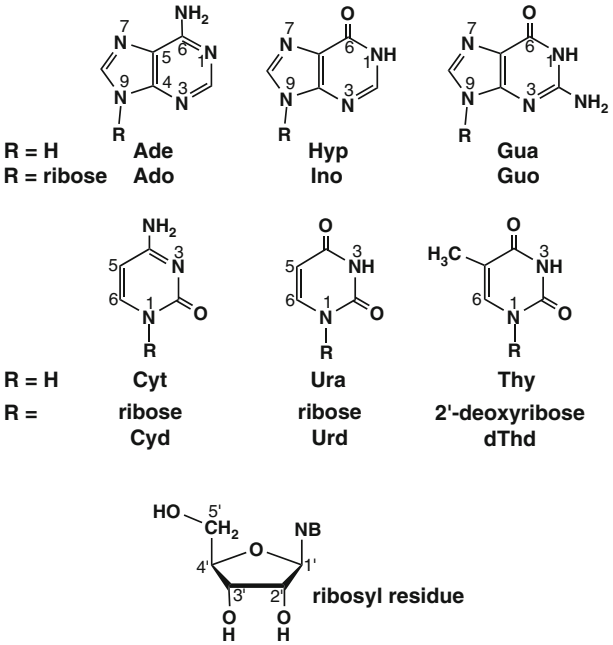

Figure 1 Chemical structures of the nucleobases (NB) (R = H) occurring in RNA: adenine (Ade), guanine (Gua), cytosine (Cyt), and uracil (Ura). Hypoxanthine (Hyp) is a rare nucleobase and shown for comparison with guanine. Thymine (Thy), which occurs in DNA, can also be addressed as 5-methyluracil. The corresponding nucleosides (Ns) (R = ribosyl residue) are adenosine (Ado), inosine (Ino), guanosine (Guo), cytidine (Cyd), uridine (Urd), and thymidine (dThd); in thymidine R is the 2'-deoxyribosyl residue. The dominating conformation of the nucleosides is the *anti* one [11–14]; this conformation is obtained if the substitution at C1' of the ribosyl residue is done in the way the bases are depicted within the plane.

2 Comparisons of the Properties of Cadmium(II) with Those of Zinc(II), Calcium(II), Magnesium(II), and Other Related Metal Ions

Despite its essentiality for marine diatoms [5,6], cadmium is best known for its toxicity to mammals [1,4,15,16] and in this context it is interesting to consider the interdependencies between Cd^{2+} and other elements. In Figure 2, which may not be complete, the most obvious interdependencies with Cd^{2+} are shown [17]. An arrow from element A to B, A→B, indicates that administration of element A may reduce toxicity due to element B. Hence, the toxicity of Cd^{2+} may be reduced by the ions of Ca, Zn, Cu, Fe, Co, and the metalloid Se. However, low levels of element A, e.g., of Ca^{2+}, Zn^{2+}, and Cu^{2+}, may increase the toxicity of element B (Cd^{2+}), or high levels of element B (Cd^{2+}) may inhibit salutary effects of element A (Zn^{2+}). Such interrelations are common, though not easy to reveal and to understand.

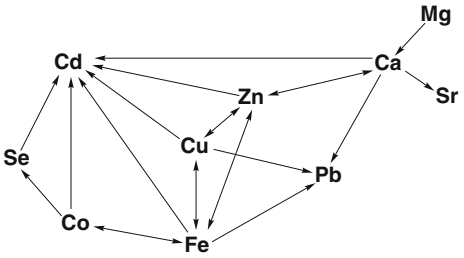

Figure 2 Interdependencies between several elements relevant for mammals. An arrow from element A → B indicates that administration of element A may reduce toxicity due to element B. Note, there may be further interdependencies which are not shown (see also text in Section 2). This figure is based on information provided by Martin in Figure 2 and the connected text of ref. [17].

Ignoring strontium and lead from the nine metals shown in Figure 2, we are left with the essential divalent metal ions Mg^{2+}, Ca^{2+}, Fe^{2+}, Co^{2+}, Zn^{2+}, and Cu^{2+}, and the toxic Cd^{2+}. Cd^{2+}, larger than Zn^{2+}, has nearly the size of Ca^{2+} (see below) and this has led to its use as Ca^{2+} probe [15,18] (see also Chapter 6). However, in its binding strength to ligands Cd^{2+} is more like Zn^{2+} (see below) and thus, it is employed as a Zn^{2+} probe as well [15] (Chapter 6). Although Cd^{2+} has a larger ionic radius than Mg^{2+}, it has recently been widely applied to mimic Mg^{2+} in ribozymes [8,19]. Like Mg^{2+}, Cd^{2+} preferentially forms non-distorted octahedral complexes, and it selectively replaces Mg^{2+} bound to purine-N7 sites via an innersphere coordination mode [19].

Based on the mentioned observations, we focus now on the properties of Cd^{2+} in comparison to those of Zn^{2+}, Ca^{2+}, and Mg^{2+} as well as their interactions with the bio-ligands relevant for nucleic acids as considered in this chapter. The properties and complexes of Fe^{2+}, Co^{2+}, and Cu^{2+} are to some extent taken into account as well, to allow, where needed, more systematic-type comparisons. With this in mind the content of Table 1 has been assembled [20–27].

Columns 2 to 4 of Table 1 list the coordination numbers of the divalent metal ions considered together with their corresponding ionic radii. Evidently, the radii of Zn^{2+} and Mg^{2+} are very similar, as are those of Cd^{2+} and Ca^{2+}. The alkaline earth

Table 1 Collection of some physicochemical properties of metal ions (M^{2+}), that is, preferred coordination numbers with the corresponding radii, preferred ligand atoms, $pK_{a/aq}$ values of bound water molecules (eq. 1), and stability constants (eq. 2) of 1:1 complexes formed with acetate, CH_3COO^- (Ac^-), and ammonia, NH_3, together with apparent stability constants (eq. 4) of the $M(NH_3)^{2+}$ complexes at pH 7.5.

Metal ion	Coordination number			Preferred ligand atoms[d]	$pK_{a/aq}$[e]	$\log K^{M}_{M(Ac)}$[f]	$\log K^{M}_{M(NH_3)}$[i]	$\log K^{M}_{M(NH_3)app}$[j]
	4[a]	6[a]	8[a]					
Mg^{2+}	57	*72*	89	O	11.44	0.51 ± 0.05	0.24 ± 0.01	–1.65
Ca^{2+}		100	*112*	O	12.85	0.55 ± 0.05	0.0 ± 0.1	–1.89
Fe^{2+}	63	*78*[b]	92	O, N	9.5	0.83[g]	1.68 ± 0.11	–0.21
Co^{2+}	58	*74*	90	N, O, S	9.65	0.86 ± 0.05	2.08 ± 0.03	0.19
Cu^{2+}	57	73		N, O	7.5	1.79 ± 0.06	4.18 ± 0.03	2.29
Zn^{2+}	60	*74*[c]	90	N, O, S	8.96	0.98 ± 0.13[h]	2.41 ± 0.09	0.52
Cd^{2+}	78	*95*	110	S, N, O	10.08	1.26 ± 0.07[h]	2.67 ± 0.03	0.78

[a] Effective ionic radii (pm); those with the more common coordination numbers are printed in *italics*. The values are taken from refs [15] and [20].

[b] High-spin value; the low-spin value is 61 pm.

[c] Zn^{2+} has a chameleon-type coordination sphere; coordination number 4 (tetrahedral) is common as well [21].

[d] According to refs [15,22] and our own intuition.

[e] From ref. [23] (see also [24]).

[f] From ref. [25]; 25°C; $I = 0.1$ M; $pK^{H}_{H(Ac)} = 4.56 \pm 0.03$ [25].

[g] Estimated value [26]; we estimate the error limit as ±0.06 log unit.

[h] For the $Zn(Ac)^+$ complex the listed stability constant (with an estimated error) is the average of those given for $I = 0.1$ and 0.5 M (25°C) in ref. [25]. The listed value for $Cd(Ac)^+$ refers to $I = 0.5$ M (25°C) [25].

[i] The values for $M(NH_3)^{2+}$, where $M^{2+} = Co^{2+}$, Cu^{2+}, Zn^{2+} or Cd^{2+}, are from Table 1 in ref. [27]; 25°C, $I = 0.1$ M; $pK^{H}_{H(NH_3)} = 9.38 \pm 0.01$ [27]. The value for $Fe(NH_3)^{2+}$ is an estimate based on $\log K^{Mn}_{Mn(NH_3)} = 1.27 \pm 0.10$ [27] and $\log K^{Co}_{Co(NH_3)} = 2.08 \pm 0.03$. The values for $Mg(NH_3)^{2+}$ ($I = 2.0$ M, NH_4NO_3) and $Ca(NH_3)^{2+}$ ($I = 1.0$ M, NH_4NO_3) are from ref. [25].

[j] The apparent stability constants valid for pH = 7.5 were calculated with eq. (4) and the stability constants listed in column 8 and the acidity constant given in footnote "*i*".

ions like to bind to oxygen donors (column 6) whereas the 3d metal ions as well as Zn^{2+} and Cd^{2+} have a preference for N sites, especially heteroaromatic amines, as we will see later. Among all these metal ions Cd^{2+} has the highest affinity for thiolate sites [15,17], which is of relevance for so-called rescue experiments [8,28] (see Sections 9.3 and 10.1).

Column 6 of Table 1 provides the acidity constants ($pK_{a/aq}$) for the hydrolysis reaction (1), charges being omitted:

$$M(H_2O)_n \rightleftharpoons M(OH)(H_2O)_{n-1} + H^+ \tag{1a}$$

$$K^{H}_{M(H_2O)_n} = \frac{[M(OH)(H_2O)_{n-1}][H^+]}{[M(H_2O)_n]} = K_{a/aq} \tag{1b}$$

This hydrolysis reaction leads to hydroxo complexes and the coordinated OH^- species can act as nucleophiles [24,29] or participate in general base catalysis [24], important for metal ion-containing catalytic cores of ribozymes, where also large pK_a shifts can occur [30]. The $pK_{a/aq}$ values of Table 1 show that in a simple aqueous solution at neutral pH all metal ions listed are present as M^{2+} ions, except Cu^{2+}, which forms a CuO precipitate [15]; of course, such a solid does not occur in plasma where Cu^{2+} is complexed by proteins [15].

Columns 7 and 8 of Table 1 provide the stability constants as defined by equation (2), of simple acetate, CH_3COO^-, and ammonia, NH_3, complexes (charges omitted):

$$M^{2+} + L \rightleftharpoons M(L) \tag{2a}$$

$$K^{M}_{M(L)} = [M(L)]/\left([M^{2+}][L]\right) \tag{2b}$$

At first sight the $M(NH_3)^{2+}$ complexes of the transition elements seem to be much more stable than those of the corresponding $M(CH_3COO)^+$ complexes. However, in the physiological pH range around 7.5 one needs to take into account the competition between M^{2+} and H^+ for binding at the ligand, that is, the size of the acidity constant of the protonated ligands is important. The acidity constants are defined by equation (3) (charges omitted):

$$H(L) \rightleftharpoons L + H^+ \tag{3a}$$

$$K^{H}_{H(L)} = [L][H^+]/[H(L)] = K_a \tag{3b}$$

Considering that the pK_a of acetic acid, CH_3COOH, is close to 4.6 and the one of the ammonium ion, NH_4^+, close to 9.4, it is evident that at pH ca. 7.5 the acetate ion is freely accessible for M^{2+} binding, whereas NH_3 exists overwhelmingly in the form of the NH_4^+ ion. The competition between M^{2+} and H^+ for binding at the ligand can be accounted for by defining so-called conditional or apparent (app) stability constants, which then hold only for a given pH. This constant, $K^{M}_{M(L)app}$, depends on the acidity constant of the ligand (eq. 3) and the stability constant of the complex (eq. 2) and is defined by equation (4) [15,22]:

$$K^{M}_{M(L)app} = K^{M}_{M(L)} \frac{1}{1 + [H^+]/K^{H}_{H(L)}} \tag{4a}$$

$$= K^{M}_{M(L)} \frac{K^{H}_{H(L)}}{[H^+]+K^{H}_{H(L)}} \tag{4b}$$

$$\log K^{M}_{M(L)app} = \log K^{M}_{M(L)} + \log [K^{H}_{H(L)}/([H^+] + K^{H}_{H(L)})] \tag{4c}$$

For pH $\gg$ p$K^{H}_{H(L)}$ the unbound ligand is predominantly in its basic form and log $K^{M}_{M(L)app} = \log K^{M}_{M(L)}$. Examples are neutral solutions of carboxylic acids with pK_a ca. 4 to 5. For pH $\ll$ p$K^{H}_{H(L)}$ the unbound ligand is predominantly protonated and equation (4c) reduces to $\log K^{M}_{M(L)app} = \log K^{M}_{M(L)} - pK^{H}_{H(L)} + pH$. An example for neutral solutions is the ammonium side chain of aliphatic amino acids with pK_a ca. 9.5 to 10. When the pH is within ± 2 log units of pK_a, the complete equation (4) should be employed.

With the above reasonings in mind, columns 7 to 9 of Table 1 should be compared: For acetate pH = 7.5 $\gg$ p$K^{H}_{H(Ac)}$ = 4.56 [25], that is, virtually all ligand is in its basic CH_3COO^- form and the apparent and conventional stability constants are equal. For ammonia this is different; at pH 7.5 only about 1.3% of the ligand is present in its free NH_3 form but 98.7% exist as NH_4^+. Consequently, $\log K^{M}_{M(NH_3)app} < \log K^{M}_{M(NH_3)}$; in fact, only for Cu^{2+} it holds $\log K^{M}_{M(Ac)} < \log K^{M}_{M(NH_3)app}$; for all other metal ions the $M(Ac)^+$ complexes are more stable than the $M(NH_3)^{2+}$ species.

The above lesson is of relevance for nucleic acids and their constituents. Considering that the monoprotonated phosphate groups of nucleotides have pK_a values of about 6.2 to 6.5 [31,32], the competition of the proton is not very pronounced at the physiological pH of about 7.5 and for RO–$P(O)_2^-$–OR' bridges of nucleic acids (pK_a ca. 1 [33,34]) no proton competition exists at all. This is also true for the $(N3)H^+$ sites of cytidine residues (pK_a ca. 4.3 [31,35]), the $(N1)H^+$ sides of adenosines (pK_a ca. 3.8 [31,36]) as well as the $(N7)H^+$ of guanosines (pK_a ca. 2.5 [31,37,38]), but *not* for the (N1)H units of guanosines with pK_a values of about 9.4 [31,37,38]. In these latter cases a strong competition for binding at $(N1)^-$ between the proton and metal ion exists. These general considerations will be reflected in the discussions to follow.

3 Cadmium(II)-Sugar Interactions

3.1 Hydroxyl Coordination in Carboxyhydrates Is Rare

Knowledge on binding of metal ions to carbohydrates is scarce [32,39,40] and little information exists on Cd^{2+}. Ca^{2+} binding to neutral monosaccharides is very weak unless they form a favorable tridentate disposition of three hydroxyl groups [18]. The same may be surmised for Cd^{2+}, though it has been concluded based on crystal structure studies that sugar-hydroxyl groups are good ligands for alkaline earth ions but not for transition and heavy metal ions [41]. The reason for this conclusion is most likely that it is based on solid-state studies of nucleosides (and derivatives) and there the N-sites become important for the latter type of metal ions (*vide infra*),

but still there is a polymeric Cd^{2+}/5'-IMP^{2-} complex with a M–O2'/3' chelation [11]: This polymer consists of $[Cd_2(IMP{\cdot}H)_2(IMP)(H_2O)_6]{\cdot}6H_2O$ units with two independent Cd^{2+} ions, one of which binds two ribose oxygen atoms, a purine-N7, and three water molecules [42]. There are also indications that in M(D-fructose)$X_2{\cdot}4H_2O$ (X = Cl^- or Br^-) species, where M^{2+} = Mg^{2+}, Zn^{2+} or Cd^{2+}, M^{2+} binds O2 and O3 of D-fructose [43].

Metal ion binding to sugars is strengthened when a suitable primary binding site is provided, e.g., a carboxylate group [18]. Similarly, potentiometric and spectroscopic studies in aqueous solution (25°C; I = 0.15 M, KNO_3) indicate that with 2-amino-2-deoxy-D-mannose metal ions bind not only to the primary amino site but also to the hydroxyl group (O3)H [44]: Cu^{2+}, Ni^{2+}, and Co^{2+} form 5-membered chelates and the same may be surmised for Cd^{2+}. With 2-amino-2-deoxy-D-glucose the complexes are less stable, which is in accord with the less favorable arrangements of the hydroxyl groups [44]. Similarly, metal ions coordinate initially via a 6-membered chelate to 1,3-diamino-2-propyl α-D-mannopyranoside and these coordinated metal ions should then, at least in theory, be able to interact with a hydroxyl group forming an 8-membered chelate, which, however, is not observed for the complexes of Cu^{2+}, Ni^{2+}, and Zn^{2+} [45].

3.2 The Metal Ion Affinity of Ribose-Hydroxyl Groups Is Small

How is the situation with the ribose and 2-deoxyribose residues, which are of significance for the nucleoside derivatives considered herein? The *cis* arrangement of the 2- and 3-hydroxyl groups as present in a ribose moiety favors deprotonation of one of the two OH groups because in the resulting anion intramolecular hydrogen bond formation occurs [34]. Yet, this favored deprotonation with pK_a = 12.5 is far above the physiological pH range, meaning that such a deprotonation can occur in a biological system only in a very special environment [30]. However, e.g., it can be facilitated by metal ions like Cu^{2+} which is apparently able to bind to the *cis*-glycol unit of a ribose moiety in aqueous solution at high pH values [43,46,47], as proven in experiments with adenosine. In contrast, 2'-deoxyadenosine shows no deprotonation of the 3'-hydroxyl group under the corresponding conditions. Since the acidifying power of Cd^{2+} is much smaller than the one of Cu^{2+} (cf. the p$K_{a/aq}$ values in Table 1, column 6), Cd^{2+} is not expected to achieve this type of binding.

In this context also a stability constant study in aqueous solution (25°C; I = 0.1 M, $NaNO_3$) of complexes formed with 2'AMP^{2-} and 3'AMP^{2-} is of relevance [48]. The complex stability of Cu(2'AMP) is enhanced by 0.25 log unit compared to the stability expected for a sole phosphate coordination; the stability of the Cu(3'AMP) complex is only very slightly enhanced, if at all. The different stability enhancements point to different structural properties of the two ligands. In case 7-membered chelates were formed by coordination of the phosphate-bound Cu^{2+} with the neighboring hydroxyl group, the situation in 2'AMP^{2-} and 3'AMP^{2-} would be equivalent and the same stability enhancement would be expected. Hence, a significant hydroxyl group interaction needs to be ruled out and this leaves as the only explanation of the observed results an interaction of Cu^{2+} in Cu(2'AMP) with N3 of the purine residue giving rise to an 8-membered macrochelate.

Indeed, space-filling molecular models indicate that 2'AMP^{2-} in its preferred *anti* conformation is perfectly suited for this type of macrochelate formation [48]. Furthermore, a crystal structure study [49] shows that Mg^{2+} is coordinated in Mg(2'AMP) to the phosphate group and that it interacts in addition in an outer-sphere manner, i.e., via a water molecule, with N3 of the adenine residue. Finally, among the 10 metal ions studied in solution, only Ni^{2+}, Zn^{2+}, and Cd^{2+} are likely to form small amounts of base-backbound species [50]; the stability enhancements for their M(2'AMP) complexes are just at the edge of significance [48]. No stability enhancement is observed for Cd(3'AMP) [48].

3.3 *A Favorable Steric Setting and a Reduced Solvent Polarity May Promote Metal Ion-Hydroxyl (or -Carbonyl) Group Binding*

More insight into Cd^{2+} binding to hydroxyl (and carbonyl) groups in solution encompassing the neutral pH range and having a phosphate group as a primary binding site, can be gained by considering the metal ion-binding properties of the keto-triose derivative dihydroxacetone phosphate (DHAP^{2-}) and the other three related compounds shown in Figure 3. The combination of coordinating groups

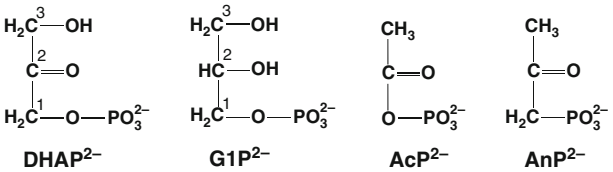

Figure 3 Chemical structures of dihydroxyacetone phosphate (DHAP^{2-}), glycerol 1-phosphate (G1P^{2-}), acetyl phosphate (AcP^{2-}), and acetonylphosphonate (AnP^{2-}).

seen at C1 and C2 for DHAP^{2-} and glycerol 1-phosphate (G1P^{2-}) is representative for many sugar moieties. From a steric point of view, an interaction of a phosphate-coordinated metal ion with the neighboring keto or hydroxyl group is very well possible in both instances. The questions are: Does such an interaction occur in aqueous solution? Are 7-membered chelates formed as expressed in a simplified manner (with charge neglection) in equilibrium (5)?

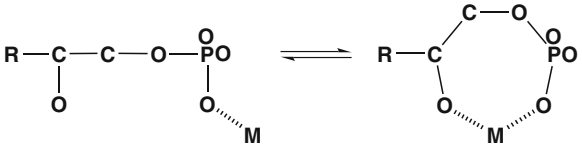

(5)

Any kind of chelate formation has to enhance complex stability [51]. Hence, a possibly increased stability, defined as log $\Delta_{M/L}$, of Cd(DHAP) or Cd(G1P), if compared with a pure phosphate coordination, could therefore be attributed to the participation of the oxygen at C2 in Cd^{2+} binding, i.e., equilibrium (5) would then

truly exist and at least in part be on its right side. However, the results log $\Delta_{Cd/DHAP} = 0.02 \pm 0.05$ and log $\Delta_{Cd/G1P} = -0.02 \pm 0.06$ (25°C; $I = 0.1$ M, $NaNO_3$) [52,53] are both zero within their error limits, and thus, no increased complex stability is observed and it must therefore be concluded that in aqueous solution equilibrium (5) is on its left side and that the (C2)=O and (C2)–OH groups do not participate in Cd^{2+} binding. Corresponding results have been obtained for the complexes of Co^{2+}, Cu^{2+}, and Zn^{2+} [52,53].

However, it needs to be added that a decreased solvent polarity is expected to increase the affinity in general, as has been shown to occur also in larger RNAs [54], and to favor weakly coordinating oxygen sites [30]. Indeed, for Cu(DHAP) and Cu(G1P) it has been shown that in water containing 50% 1,4-dioxane (v/v) the chelated species in equilibrium (5) reach a formation degree of about 45% [52,53]. A similar chelate formation must be anticipated for the corresponding Cd^{2+} complexes in solutions with a reduced dielectric constant or permittivity (ε). It is worthwhile to note that in the discussed examples the hydroxyl and carbonyl groups behave within the error limits quite alike.

A change in size of the potential 7-membered chelate ring (eq. 5) to a 6-membered one, demonstrates the importance of the steric orientation for weak interactions. Acetyl phosphate (AcP^{2-}) and acetonylphosphonate (AnP^{2-}) may form with metal ions 6-membered chelates as is show in equilibrium (6), where X = O (AcP^{2-}) or CH_2 (AnP^{2-}):

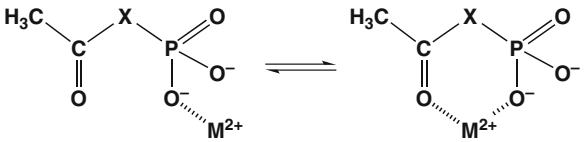

(6)

In fact, for Cd(AcP) and Cd(AnP) small, but significant, stability enhancements are observed, i.e., log $\Delta_{Cd/AcP} = 0.19 \pm 0.06$ and log $\Delta_{Cd/AnP} = 0.18 \pm 0.06$, respectively [52,55]. These stability enhancements correspond to a formation degree of about 35% for the chelate in the intramolecular equilibrium (6); the interrelation between log $\Delta_{M/L}$ and % $M(L)_{cl}$ will be presented in Section 4.2 [51]. For now it is enough to add that the formation degree of the chelated species is hardly affected in mixed ligand complexes as is evidenced from examples with $Cu(Arm)^{2+}$, where Arm = 2,2'-biypridine or 1,10-phenanthroline [52,56].

From the information presented above it follows that sugar hydroxyl (or carbonyl) groups are weak binding sites which will interact with Cd^{2+} (or other M^{2+}) in aqueous solution only under rather specific conditions. Indeed, from comparison of the results to be discussed in Section 6.2.3 for M(NMP) complexes, where NMP^{2-} = nucleoside 5'-monophosphate, with the above data it follows that N7 of purine-nucleobase residues have a more pronounced affinity for Cd^{2+} than a sugar hydroxyl group. On the other hand, the ligands shown in Figure 4, which contain different primary binding sites next to a hydroxyl group, allowing formation of 5-membered chelates, provide some further insights into hydroxyl group coordination as relevant for nucleic acids.

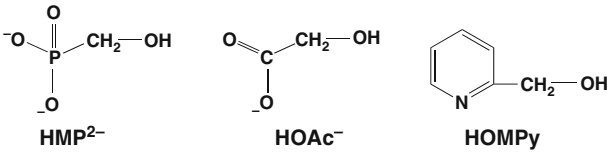

Figure 4 Chemical structures of hydroxymethylphosphonate (HMP^{2-}), hydroxyacetate ($HOAc^{-}$), and *o*-(hydroxymethyl)pyridine (HOMPy).

The experimentally measured stability constants (eq. 2), the stability enhancements, log $\Delta_{M/L}$, and the percentages of the closed isomers, % $M(L)_{cl}$ (in analogy to equilibria 5, 6) are listed in Table 2 [57] for the 1:1 complexes of several metal ions with the three ligands seen in Figure 4.

Unfortunately, not all desired data, especially for the Cd^{2+} complexes are available, but enough to draw a number of conclusions. Also, part of the data available for the complexes of hydroxyacetate refer to the rather high ionic strength of 2 M. Fortunately, the change in I from 0.1 to 2 M affects the overall stability constant (eq. 2), especially in the case of $Zn(HOAc)^{+}$, but has no remarkable influence on log $\Delta_{M/HOAc}$ and % $M(HOAc)^{+}_{cl}$, as is proven by the results for Cu^{2+} and Zn^{2+}. Consequently, all the listed values in Table 2 for the stability enhancements and the percentages of the chelated isomers can directly be compared with each other. Many comparisons are possible, a few follow below:

(i) The possibility to form 5-membered chelates is evidently a favorable setting; metal ion-hydroxyl group interactions occur in all instances. By taking also the preceding results into account, it follows that the stability of the chelates decreases with increasing ring size in the order 5-membered > 6-membered > 7-membered ring.

(ii) There is no correlation between the global stability of a complex (eq. 2) and the formation degree of the chelated isomer, which is the result of an intramolecular and thus concentration-independent equilibrium (see eqs 5, 6). For example, $Ca(HOAc)^{+}$ is less stable than $Cd(HOAc)^{+}$, yet the formation degree of the closed isomer is significantly larger in $Ca(HOAc)^{+}$.

(iii) However, there is a correlation between the charge of the primary binding site and the extent of chelate formation; the percentages of the closed forms increase in the order $M(HMP)_{cl} < M(HOAc)^{+}_{cl} < M(HOMPy)^{2+}_{cl}$. This is a reflection of charge neutralization at M^{2+} leading to a reduced affinity of the metal ion towards hydroxyl groups [57].

(iv) Point (iii) has an interesting bearing for nucleic acids: It allows the conclusion that a metal ion coordinated to the singly negatively charged phosphodiester bridge is better suited for a hydroxyl group interaction than a metal ion bound to a twofold negatively charged terminal phosphate group. Regarding ribozymes this result is revealing. It may be added that the acetate ion, CH_3COO^{-}, may be considered as a mimic of the phosphodiester unit, $RO–P(O)^{-}_{2}–OR'$ in the nucleic acid backbone as far as metal ion coordination is concerned [58] (see also Section 5).

Table 2 Comparison of the stability constants (eq. 2), the stability enhancements, log $\Delta_{M/L}$, and the percentage of the chelated or closed (cl) species, % $M(L)_{cl}$, for the 1:1 complexes formed by hydroxymethylphosphonate (HMP^{2-}), hydroxyacetate ($HOAc^{-}$) or *o*-(hydroxymethyl)pyridine ($HOMPy^{-}$) and several metal ions in aqueous solution (25°C)[a,b].

	HMP^{2-} ($I = 0.1$ M)			$HOAc^{-}$ ($I = 0.1$ M)[a]			$HOMPy^{-}$ ($I = 0.5$ M)		
M^{2+}	log $K^{M}_{M(HMP)}$	log $\Delta_{M/HMP}$	% $M(HMP)_{cl}$	log $K^{M}_{M(HOAc)}$	log $\Delta_{M/HOAc}$	% $M(HOAc)^{+}_{cl}$	log $K^{M}_{M(HOMPy)}$	log $\Delta_{M/HOMPy}$	% $M(HOMPy)^{2+}_{cl}$
Mg^{2+}	1.84 ± 0.10	0.12 ± 0.10	24 (5/40)[c]	0.92 ± 0.06	0.54 ± 0.07	71 ± 4			
Ca^{2+}	1.68 ± 0.06	0.13 ± 0.08	26 ± 13	1.11 ± 0.06	0.78 ± 0.08	83 ± 3			
Cu^{2+}	3.53 ± 0.06	0.30 ± 0.08	50 ± 10	2.40 ± 0.06	0.79 ± 0.08	84 ± 3	3.56 ± 0.02	2.48 ± 0.09	99.7 ± 0.1
				2.43 ± 0.03	*0.77 ± 0.05*	*83 ± 2*			
Zn^{2+}				1.98 ± 0.04	1.04 ± 0.06	91 ± 1	2.03 ± 0.15	1.92 ± 0.17	98.8 ± 0.5
				1.72 ± 0.06	*1.05 ± 0.09*	*91 ± 2*			
Cd^{2+}				*1.51 ± 0.02*	*0.50 ± 0.08*	*68 ± 6*	1.65 ± 0.10	1.03 ± 0.13	90.7 ± 2.9
Solvent: Water containing 50 % (v/v) 1,4-dioxane (25°C; $I = 0.1$ M, $NaClO_4$)[d]									
Cu^{2+}				3.96 ± 0.06	1.10 ± 0.06	92 ± 1			
Zn^{2+}				3.26 ± 0.06	1.24 ± 0.07	94 ± 1			

[a] Note, the values printed in *italics* refer to an ionic strength (I) of 2 M.

[b] All values are collected from various tables in ref. [57]. The acidity constants (25°C) of the ligands are $pK^{H}_{H(HMP)} = 6.97$, $pK^{H}_{H(HOAc)} = 3.62 \pm 0.03$ ($I = 0.1$ M) and *3.74 ± 0.03* ($I = 2$ M), and $pK^{H}_{H(HOMPy)} = 4.95$ [57].

[c] The values in parenthesis are the lower and upper limits of % $Mg(HMP)_{cl}$, respectively.

[d] Abstracted from Table 14 in ref. [57]; $pK^{H}_{H(HOAc)} = 4.88 \pm 0.03$.

(v) Similarly, the fact that pyridine-type nitrogens are ideal primary binding sites is in agreement with the suggested chelate formation in Cu(2'AMP) involving N3 of the adenine residue and the (C2)OH group (see Section 3.2). Note, the basicity, and thus the metal ion affinity, of N3 should not be underestimated: The micro acidity constant for the $(N3)H^+$ site in otherwise neutral adenosine was estimated as $pk_{a/(N3)H} = 1.5 \pm 0.3$ [36]; such a value is ideal for outersphere interactions [59–61], e.g., with Mg^{2+} (see the discussed solid-state structure of Mg(2'AMP) in Section 3.2).

(vi) The stability enhancements observed for the Cd(L) species are about half the size of those found for the corresponding Zn(L) complexes; consequently, it holds $\% Cd(L)_{cl} < \% Zn(L)_{cl}$. Yet, here a caveat is needed: If ligands are synthesized with a pocket that fits well the size of Cd^{2+} (but not of Zn^{2+}), then the situation towards hydroxyl group interactions may change dramatically [57]. Clearly, a nucleic acid cavity fitting the size of Ca^{2+} is expected to be also ideal for Cd^{2+}. Some ribozymes show a distinct specificity for Ca^{2+}, e.g., the antigenomic HDV ribozyme [62], group I introns [63–65], and group II introns, the latter being severely hampered in catalysis [66] and folding [67,68].

(vii) The results given in the lower part of Table 2 confirm the earlier conclusions (see the discussed Cu(DHAP) and Cu(G1P) complexes [52,53]) that a reduced solvent polarity favors M^{2+}-hydroxyl interactions.

(viii) A final point, which follows by taking the results of the whole section as well as further data [57] into account, is that, assuming a suitable primary binding site is present, the metal ion affinity to hydroxyl and carbonyl groups is quite alike, but the one towards ether oxygen atoms is much smaller, e.g., the stability enhancement for the Cu^{2+} complex of methoxyacetate, $CH_3OAc^- = CH_3OCH_2COO^-$, amounts only to $\log \Delta_{Cu/CH_3OAc} = 0.36 \pm 0.11$ [57] compared to $\log \Delta_{Cu/HOAc} = 0.79 \pm 0.08$ (Table 2).

4 Interactions of Cadmium(II) with Nucleobase Residues

The common purine and pyrimidine nucleobases are shown in Figure 1. We will concentrate in this section on (N9)-substituted purines and (N1)-substituted pyrimidines, the substituent being an alkyl group, and on the nucleosides which carry a (2'-deoxy)ribose residue at the corresponding position. Metal ion binding of the free nucleobases is not of relevance in the present context. It is evident from Figure 1 that these nucleobase residues possess quite a number of potential metal ion-binding sites [30,58], yet from a narrow point of view one may say that N7 is the crucial site for purines and N3/$(N3)^-$ for the pyrimidines. The details will be discussed below.

4.1 Cadmium(II) Complexes of Purine Derivatives

The dominance of the N7 site for the coordination chemistry of the purine nucleosides and related systems is even true under rather exceptional circumstances, that

is, even protonation at N1 does not necessarily prevent metal ion binding at N7 though it certainly diminishes it [69].

Considering the importance of N7, it seemed appropriate for us to evaluate its metal ion-binding properties somewhat more in detail. We are doing this by mimicking the N7 site of the purine nucleobases by the imidazole derivatives shown in the upper part of Figure 5. The N1 site of the adenine residue may be mimicked by pyridine and derivatives (Figure 5, lower part). The acidity constants of these ligands and the stability constants of their corresponding Cd^{2+} complexes are defined by equations (3) and (2), respectively. The corresponding results are listed in entries 1 to 6 of Table 3 [70–75].

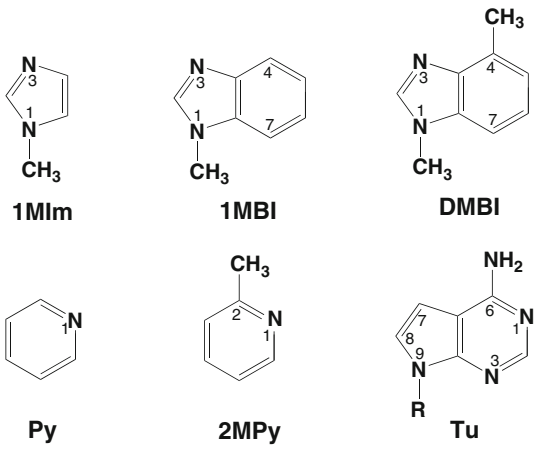

Figure 5 Chemical structures of 1-methylimidazole (1MIm) derivatives, i.e., 1-methylbenzimidazole (1MBI) and 1,4-dimethylbenzimidazole (DMBI = 6,9-dimethyl-1,3-dideazapurine), as mimics of the purine N7 site, and of pyridine (Py) derivatives, i.e., 2-methylpyridine and tubercidin for R = ribosyl residue (see Figure 1) (Tu = 7-deazaadenosine), as mimics of the purine N1 site. For tubercidin, like for adenosine (Figure 1), the *anti* conformation is dominant [13].

Annelation at imidazole giving benzimidazole reduces the basicity of N3 as is obvious from the first two entries of Table 3, but it also somewhat inhibits metal ion coordination. For Cd^{2+} the inhibition amounts to 0.25 ± 0.05 log unit if the basicity differences are taken into account [60]. However, a drastic inhibition occurs if at the neighboring C4 a methyl group is introduced (see Figure 5, top, right). Because the basicity of N3 in 1MBI is close to the one in DMBI (Table 3; entries 2, 3), the stability constants of the two Cd^{2+} complexes, $Cd(1MBI)^{2+}$ and $Cd(DMBI)^{2+}$, may directly be compared: The methyl substituent lowers complex stability by about 1.4 log units (= 2.10 – 0.72). Since the steric requests of a methyl and an amino substituent at an aromatic ring are comparable [59] (see also the straight-line plots in Figure 6; *vide infra*), that is, there is a shape complementarity between the 4-methylbenzimidazole and adenine residues [76], it follows that the steric inhibition of the $(C6)NH_2$ group on Cd^{2+} coordination at N7 is expected to be of a similar size: Indeed, this is in accord with results of other divalent metal ions [61]. Interestingly,

Table 3 Negative logarithms of the acidity constants (eq. 3) of some monoprotonated purine nucleobase (NB) derivatives and logarithms of the stability constants (eq. 2) of the corresponding $Cd(NB)^{2+}$ and $Cd(NB - H)^{+}$ complexes as determined by potentiometric pH titration in aqueous solution at 25°C and $I = 0.5$ M (entries 1 – 7) or 0.1 M (entries 8 – 10) ($NaNO_3$), together with data for 1-methylimidazole (1MIm) or pyridine (Py) derivatives (see Figure 5)[a].

		pK_a for				
	$H(NB)^+$	$(N7)H^+$	$(N1)H^{+/0}$	log $K^{Cd}_{Cd(NB)}$	log $K^{Cd}_{Cd(NB-H)}$	Ref.
1[b]	$H(1MIm)^+$	7.20 ± 0.02		2.76 ± 0.01		[70]
2[b]	$H(1MBI)^+$	5.67 ± 0.01		2.10 ± 0.06		[60]
3[b]	$H(DMBI)^+$	5.78 ± 0.02		0.72 ± 0.06		[71]
4[c]	$H(Py)^+$		5.34 ± 0.02	1.51 ± 0.05		[59]
5[c]	$H(2MPy)^+$		6.14 ± 0.02	0.68 ± 0.03		[59]
6[c]	$H(Tu)^+$		5.27 ± 0.02	0.71 ± 0.07		[59,72]
7[c]	$H(Ado)^+$	(2.15 ± 0.15)[d]	3.64 ± 0.02	0.64 ± 0.03		[32,73]
8	$H(Ino)^+$	1.06 ± 0.06	8.76 ± 0.03[e]	0.85 ± 0.2[f]	2.6 ± 0.25[f]	[74,75]
9	$H(Guo)^+$	2.11 ± 0.04	9.22 ± 0.02[e]			[74]
10	$H(dGuo)^+$	2.34 ± 0.03	9.25 ± 0.02[e]	1.53 ± 0.07	3.15 ± 0.03	[38]

[a] The errors given are three times the standard error of the mean value or the sum of the probable systematic errors, whichever is larger.
[b] In $H(1MIm)^+$, $H(1MBI)^+$, and $H(DMBI)^+$ the proton is at N3.
[c] The proton is released from the positively charged $(N1)H^+$ site.
[d] Micro acidity constant, $pk^{N7\text{-}N1}_{H\cdot N7\text{-}N1}$, for the $(N7)H^+$ site of Ado under conditions where N1 does not carry a proton [36].
[e] The proton is released from the neutral (N1)H site (see Figure 1).
[f] Estimated values (I ca. 0.5 – 1 M) [75].

the steric inhibition of the $(C6)NH_2$ group on N1 coordination is less severe; a comparison of the values given in entries 4 and 5, 6 of Table 3 (see also the structures in Figure 5) shows that it corresponds to about 0.8 log unit (see also refs [61,71]).

Considering that the pK_a values for both, the N7 and the N1 sites of monoprotonated adenosine are such that no competition between the proton and metal ions for binding at either site in the neutral pH range occurs, one expects that metal ions including Cd^{2+} actually may coordinate at either site. Indeed, for the $Cd(Ado)^{2+}$ complex a dichotomy exists and it was previously concluded that the N7 isomer occurs with 61 ± 10% [77]; a more recent evaluation [73] arrives at 35 ± 11%. The discrepancy between these results is no surprise as the evaluation methods differ significantly; in any case, the dichotomy is certain and occurs also, e.g., with Cu(9-methyladenine)$^{2+}$ where 59 ± 12% exist as the N7 isomer [61].

The N7 sites of inosine or (2'-deoxy)guanosine exist also deprotonated in the neutral pH range (Table 3, entries 8–10) and thus are easily accessible for metal ions. Such (N7)-bound metal ions form commonly a hydrogen bond from a ligated water molecule to (C6)O (cf. Figure 1) [11,78]; in contrast to an amino group a carbonyl or keto group at C6 does not exercise any steric hindrance (see also Section 4.2). Of course, at higher pH values the neutral (N1)H sites may be deprotonated. This reaction is expressed in eq. (7), where L represents a nucleobase residue. Naturally, the $(L - H)^-$ species formed in this way may also form complexes

according to eq. (8), and the $M(L)^{2+}$ complex may be deprotonated at (N1)H as well (eq. 9):

$$L \rightleftharpoons (L-H)^- + H^+ \tag{7a}$$

$$K_L^H = [(L-H)^-][H^+]/[L] \tag{7b}$$

$$M^{2+} + (L-H)^- \rightleftharpoons M(L-H)^+ \tag{8a}$$

$$K_{M(L-H)}^M = [M(L-H)^+]/([M^{2+}][(L-H)^-]) \tag{8b}$$

$$M(L)^{2+} \rightleftharpoons M(L-H)^+ + H^+ \tag{9a}$$

$$K_{M(L)}^H = [M(L-H)^+][H^+]/[M(L)^{2+}] \tag{9b}$$

Evidently, equilibria (2a) and (7a) to (9a) are connected with each other via the equilibrium scheme (10) [79]:

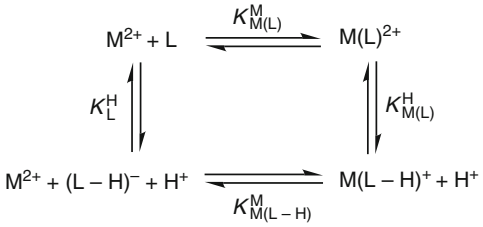

(10)

This scheme involves four equilibrium constants and because it is of a cyclic nature, only three constants are independent of each other; the fourth constant is automatically determined by the other three as follows from eq. (11):

$$\log K_{M(L)}^M - pK_{M(L)}^H = \log K_{M(L-H)}^M - pK_L^H \tag{11a}$$

$$pK_{M(L)}^H = pK_L^H + \log K_{M(L)}^M - \log K_{M(L-H)}^M \tag{11b}$$

The acidification of the (N1)H sites in $M(L)^{2+}$ complexes, as caused by the (N7)-coordinated metal ion, is defined by eq. (12):

$$\Delta\ pK_a = pK_L^H - pK_{M(L)}^H \tag{12}$$

The corresponding results for the Cd^{2+} systems with Ino and dGuo, based on the data in Table 3, are summarized in Table 4, where also some results obtained for related Ni^{2+} systems are listed [40,80]. It is remarkable that the (N7)-coordinated metal ion facilitates (N1)H deprotonation to such an extent that this reaction occurs now in or close to the physiological pH range (Table 4, column 5).

Table 4 Extent of the (N1)H acidification by (N7)-coordinated Cd^{2+} at inosine (Ino) and 2'-deoxyguanosine (dGuo) as defined by equation (12). The corresponding data of the Ni^{2+} complexes including those for 9-ethylguanine (9EtG) are given for comparison (aqueous solution; 25°C; $I = 0.1$ M, $NaNO_3$)[a].

$M(NB)^{2+}$	pK^{H}_{NB} (eq. 7)	$\log K^{M}_{M(NB)}$ (eq. 2)	$\log K^{M}_{M(NB-H)}$ (eq. 8)	$pK^{H}_{M(NB)}$ [b,c] (eqs 9,11)	ΔpK_a (eq. 12)
$Cd(Ino)^{2+}$	8.76 ± 0.03	0.85 ± 0.2	2.6 ± 0.25	7.01 ± 0.32[b]	1.75 ± 0.32
$Cd(dGuo)^{2+}$	9.25 ± 0.02	1.53 ± 0.07	3.15 ± 0.03	7.63 ± 0.08[b]	1.62 ± 0.08
$Ni(Ino)^{2+}$	8.76 ± 0.03	1.15 ± 0.13	2.8 ± 0.2	7.11 ± 0.24[c]	1.65 ± 0.24
$Ni(dGuo)^{2+}$	9.24 ± 0.03	1.53 ± 0.09	3.20 ± 0.18	7.57 ± 0.20[c]	1.67 ± 0.21
$Ni(9EtG)^{2+}$	9.57 ± 0.05	1.76 ± 0.10	3.48 ± 0.13	7.85 ± 0.17[c]	1.72 ± 0.18

[a] For the error limits see footnote "*a*" of Table 3; the error limits of the derived data were calculated according to the error propagation after Gauss.
[b] Values for $pK^{H}_{Cd(NB)}$ were calculated according to equation (11b) with the values listed above in columns 2–4 and which are taken from Table 3.
[c] The entries for the Ni^{2+} complexes are taken from Table 2 in ref. [40] (see also [80]).

The results of Table 4 are in accord with previous conclusions [80] and by taking into account the present insights for the Cd^{2+} systems, one may define the following series in which the acidifying effect of the (N7)-coordinated divalent metal ion decreases (the ΔpK_a values being inserted in parentheses): Cu^{2+} (2.2 ± 0.3) > Ni^{2+} (1.7 ± 0.15) ~ Cd^{2+} (~ Zn^{2+}) > Pt^{2+} (1.4 ± 0.1) ~ Pd^{2+}. Zn^{2+} is tentatively inserted into this series based on data given in ref. [80]. These results also indicate that in the (N1)H-deprotonated $M(NB - H)^{+}$ complexes the labile divalent metal ions are still largely at N7, though some dichotomy involving also $(N1)^{-}$ cannot be excluded. The reason why we favor mainly N7 coordination is the fact that the pK_a values for the kinetically inert and (N7)-bonded Pt^{2+} complexes fit perfectly into the given series [40]. Of course, in the complexes formed by purine-nucleotides and Cd^{2+} or other M^{2+}, even if (N1)H is deprotonated, the phosphate-coordinated metal ion interacts always with N7 [81] because $(N1)^{-}$ could only be reached in the *syn* conformation. However, this is not achieved because the *anti-syn* barrier is too high in energy [35].

Three more points may be added in the present context:

(i) The acidification (ΔpK_a) by Cd^{2+} and Ni^{2+} is identical within the error limits for all examples in Table 4, even though the acidity of the various (N1)H sites differs significantly.
(ii) The acidification of Cd^{2+} as observed in the $Cd(GpG)^{+}$ and $Cd[d(GpG)]^{+}$ complexes is with $\Delta pK_a = 1.8 \pm 0.4$ [38] within the error limits the same as given above in Table 4.
(iii) For the (Dien)Pt(9EtG-*N7*)$^{2+}$ complex it has been shown that the (N7)-coordinated Pt^{2+} not only acidifies (N1)H ($\Delta pK_a = 1.40 \pm 0.06$), but that the released proton can be replaced by another M^{2+}, such as Mg^{2+} or Cu^{2+}, giving complexes of the type (Dien)Pt(*N7*-9EtG-*N1*·M)$^{3+}$ [82]. The same may be surmised for Cd^{2+}. This shows that "clustering" of metal ions at a guanine residue is possible; an observation relevant for ribozymes [30].

4.2 Cadmium(II) Complexes of Pyrimidine Derivatives

Among the three pyrimidine-nucleobase residues shown in Figure 1 only the cytosine moiety is not protonated at N3 in the physiological pH range and hence, freely available for metal ion coordination. Therefore, this residue will be discussed first. The cytosine residue is an ambivalent ligating site as follows from crystal structure studies; e.g., Pt^{2+} coordinates to N3, Ba^{2+} to (C2)O, and Cu^{2+} binds to both sites [35,40]. Thus, in the latter instance chelate formation occurs and for aqueous solution then the intramolecular equilibrium (13) needs to be considered:

$$M(Cyd)_{op}^{2+} \rightleftharpoons M(Cyd)_{cl}^{2+} \tag{13}$$

Of course, a M^{2+} interaction may be innersphere or outersphere, but in any case a 'closed' (cl) species results. The 'open' (op) species may be N3- or (C2)O-bound, depending on the metal ion involved. Overall, one may imagine that 4-membered chelates exist, or if a water molecule participates, that a 6-membered so-called semichelate forms. In addition, a complete outersphere interaction with both sites can also not be excluded. As a consequence, the $M(Cyd)_{cl}^{2+}$ species are actually expected to be mixtures of chelated isomers [35].

Any kind of chelate formation must lead to a stability enhancement [51], which is defined in a general manner in equation (14), where for the present L = Cyd:

$$\log \Delta_{M/L} = \log K_{M(L)}^{M} - \log K_{M(L)op}^{M} \tag{14a}$$

$$= \log K_{M(L)exp}^{M} - \log K_{M(L)calc}^{M} = \log \Delta \tag{14b}$$

The first term in eq. (14) is experimentally accessible as it can be measured directly (eq. 2). To obtain a value for the open $M(L)_{op}$ complex is commonly more difficult. Most often plots of $\log K_{M(L)}^{M}$ *versus* $pK_{H(L)}^{H}$ are employed, which result for families of structurally related ligands in straight lines [51] as defined by equation (15),

$$\log K_{M(L)}^{M} = m \cdot pK_{H(L)}^{H} + b \tag{15}$$

where m represents the slope of the straight line and b the intercept with the y-axis. Clearly, if the parameters of eq. (15) are known, one may calculate with $pK_{H(L)}^{H}$ the stability of the M(L) complex.

The position of equilibrium (13) for Cyd = L is defined by the dimension-less intramolecular equilibrium constant K_I (eq. 16),

$$K_I = [M(L)_{cl}]/[M(L)_{op}] \tag{16}$$

which may be calculated according to equation (17) [51]:

$$K_{\mathrm{I}} = \frac{K^{\mathrm{M}}_{\mathrm{M(L)}}}{K^{\mathrm{M}}_{\mathrm{M(L)op}}} - 1 = 10^{\log \Delta} - 1 \tag{17}$$

Equation (14) defines log Δ, whereas $K^{\mathrm{M}}_{\mathrm{M(L)}}$ (eq. 2) and $K^{\mathrm{M}}_{\mathrm{M(L)op}}$ are defined by equations (18) and (19), respectively:

$$K^{\mathrm{M}}_{\mathrm{M(L)}} = \frac{[\mathrm{M(L)}]}{[\mathrm{M}][\mathrm{L}]} = \frac{([\mathrm{M(L)_{op}}] + [\mathrm{M(L)_{cl}}])}{[\mathrm{M}][\mathrm{L}]} \tag{18}$$

$$K^{\mathrm{M}}_{\mathrm{M(L)op}} = \frac{[\mathrm{M(L)_{op}}]}{[\mathrm{M}][\mathrm{L}]} \tag{19}$$

Of course, knowledge of K_{I} allows to calculate the formation degree of the closed or chelated species (eq. 13) according to equation (20):

$$\%\ \mathrm{M(L)_{cl}} = 100 \cdot K_{\mathrm{I}}/(1 + K_{\mathrm{I}}) \tag{20}$$

Some examples of log $K^{\mathrm{M}}_{\mathrm{M(L)}}$ *versus* p$K^{\mathrm{H}}_{\mathrm{H(L)}}$ straight-line plots for simple pyridine-type (PyN; open circles) as well as for *ortho*-aminopyridine-type (*o*PyN; crossed circles) ligands [59] are shown in Figure 6 [35,83]. Combination of these plots with the data points due to log $K^{\mathrm{M}}_{\mathrm{M(Cyd)}}$/p$K^{\mathrm{H}}_{\mathrm{H(Cyd)}}$ (full circles) [83] allows immediately several interesting conclusions:

(i) The M(*o*PyN)$^{2+}$ complexes of all studied metal ions [35,59] are less stable than the M(PyN)$^{2+}$ species. This proves the steric inhibition of an *ortho*-amino group next to the coordinating pyridine nitrogen.

(ii) The data point for the Co(Cyd)$^{2+}$ complex fits on the reference line defined by the M(*o*PyN)$^{2+}$ species, meaning that the neighboring carbonyl group does not participate in metal ion binding and that only the steric inhibition of the (C6)NH_2 group is in action.

(iii) This is different for the Cd(Cyd)$^{2+}$ complex which shows an increased complex stability, thus indicating the participation of the (C2)O group in metal ion binding. That is, the steric inhibition of the (C6)NH_2 group is partially offset by the (C2)O group.

(iv) The stabilities of the Ca(PyN)$^{2+}$ and the Ca(*o*PyN)$^{2+}$ complexes differ only little. The scatter of the data points originates in the low stability of these complexes [59], which is independent of the pK_a value of the pyridine derivative considered in the pH range 3–7. This indicates [59] that complex formation takes place in an outersphere manner [35].

(v) Furthermore, Ca(Cyd)$^{2+}$ is even more stable than the sterically unhindered Ca(PyN)$^{2+}$ species proving the importance of the (C2)O interaction in Ca(Cyd)$^{2+}$. The corresponding observations were made for the Mg^{2+} complexes [35,59].

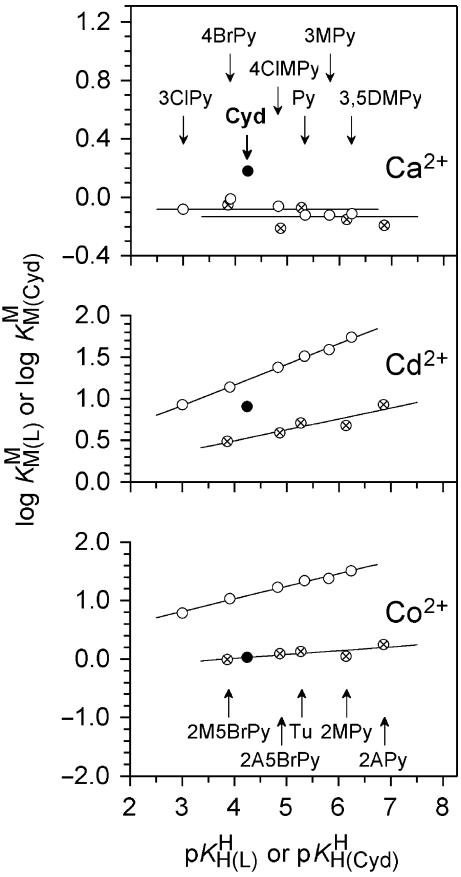

Figure 6 Evidence for the varying coordinating properties of cytidine (●) depending on the metal ion involved. This observation is based on the log $K^{M}_{M(L)}$ *versus* $pK^{H}_{H(L)}$ relationship for simple pyridine-type (○) as well as *ortho*-aminopyridine-type (⊗) ligands; the reduced stability of the complexes formed with the latter ligands reflects the steric inhibition due to an *ortho*-amino (or -methyl) group. The least-squares straight-reference lines for the simple pyridine-type ligands are defined by the equilibrium constants for the systems containing (○) (at the top from left to right) 3-chloropyridine (3ClPy), 4-bromopyridine (4BrPy), 4-(chloromethyl)pyridine (4ClMPy), pyridine (Py), β-picoline (= 3-methylpyridine, 3MPy), and 3,5-lutidine (= 3,5-dimethylpyridine, 3,5DMPy) and those for the *ortho*-aminopyridine-type ligands by the constants for the systems containing (⊗) (at the bottom from left to right) 2-methyl-5-bromopyridine (2M5BrPy), 2-amino-5-bromopyridine (2A5BrPy), tubercidin (= 7-deazaadenosine, Tu), α-picoline (= 2-methyl-pyridine, 2MPy) and 2-aminopyridine (2APy). All plotted equilibrium constants refer to aqueous solution at 25°C and $I = 0.5$ M ($NaNO_3$); the data for Cyd are from [83] and those for the pyridine derivatives from [59].

Of course, the data as summarized in Figure 6 can be evaluated in a quantitative manner by application of equations (14)–(20). Table 5 contains in column 2 the stability constants measured previously [83] for the $M(Cyd)^{2+}$ complexes. The stability constants for the open isomers (eqs 13, 19) were calculated based

on $pK^{H}_{H(Cyd)} = pK^{H}_{H(oPyN)} = 4.24 \pm 0.02$ [83] and the straight-line parameters as defined in equation (15) and listed in ref. [59]; these values for $M(Cyd)^{2+}_{op}$ are given in column 3. From the mentioned constants the log Δ values (eq. 14) (column 4) follow; they correspond to the vertical distances seen in Figure 6 between the experimentally determined points of a given $M(Cyd)^{2+}$ complex (solid circle) and its reference line (crossed circles); these values are listed in column 4 of Table 5. Application of equations (17) and (20) allows to calculate values for K_I (eqs 16, 17) and % $M(Cyd)^{2+}_{cl}$ (eq. 20), respectively; these results are listed in columns 5 and 6 of Table 5.

Table 5 Comparison of the measured stability constants, $K^{M}_{M(Cyd)}$ (eqs 2, 18), of the $M(Cyd)^{2+}$ complexes with the stability constants, $K^{M}_{M(Cyd)op}$ ($= K^{M}_{M(oPyN)}$; eq. 19), of the corresponding isomers with a sole N3 coordination of M^{2+}, and extent of the total chelate formation according to equilibrium (13) in the $M(Cyd)^{2+}$ complexes in aqueous solution at 25°C and $I = 0.5$ M ($NaNO_3$) as expressed by K_I (eqs 16, 17) and the percentages of $M(Cyd)^{2+}_{cl}$ (eq. 20)[a].

M^{2+}	log $K^{M}_{M(Cyd)}$	log $K^{M}_{M(Cyd)op}$	log $\Delta_{M/Cyd}$	K_I	% $M(Cyd)^{2+}_{cl}$
Mg^{2+}	0.12 ± 0.04	–0.06 ± 0.06	0.18 ± 0.07	0.51 ± 0.25	34 ± 11
Ca^{2+}	0.18 ± 0.06	–0.13 ± 0.13	0.31 ± 0.14	1.04 ± 0.67	51 ± 16
Co^{2+}	0.03 ± 0.08	0.03 ± 0.08	0.00 ± 0.11	0.00 ± 0.26	~0
Cu^{2+}	1.56 ± 0.06	0.79 ± 0.07	0.77 ± 0.09	4.89 ± 1.25	83 ± 4
Zn^{2+}	0.20 ± 0.11	0.04 ± 0.08	0.16 ± 0.14	0.45 (0.05/1.00)[b]	31(5/50)[b]
Cd^{2+}	0.91 ± 0.07	0.53 ± 0.09	0.38 ± 0.11	1.40 ± 0.63	58 ± 11

[a] For the error limits see footnotes "*a*" of Tables 3 and 4. The values of column 2 are from ref. [83], all the other values were calculated as described in the text based on the straight-line parameters (eq. 15) listed in ref. [59] and $pK^{H}_{H(Cyd)} = pK^{H}_{H(oPyN)} = 4.24 \pm 0.02$ [83] (for details see [35]).
[b] The values in parentheses correspond to the lower and upper limits.

From column 6 in Table 5 it follows that the closed species in the $M(Cyd)^{2+}$ systems reach remarkable formation degrees and that equilibrium (13) in many instances truly exists. Indeed, exceptions are only $Co(Cyd)^{2+}$ and $Ni(Cyd)^{2+}$ [35]. Furthermore, Table 5 allows some additional interesting conclusions:

(i) The closed complex, $Mg(Cyd)^{2+}_{cl}$, formed to about 35%, is most likely a semichelate which is mainly innersphere bound to (C2)O and outersphere to N3. This view is supported by the crystal structure of Ba(CMP)·8.5H_2O where the alkaline earth ion is bonded to (C2)O (and the sugar, but not to N3 or the phosphate) [11,84].

(ii) The same type of semichelate is also suggested for $Ca(Cyd)^{2+}_{cl}$. Interestingly, despite the significant stability difference between $Ca(Cyd)^{2+}$ and $Cd(Cyd)^{2+}$ (column 2; eq. 2) both complexes reach formation degrees of about 50% for the chelated isomer. Note, this is possible because K_I is a dimension-less constant which quantifies the position of an intramolecular equilibrium (eq. 13).

(iii) However, for $Cd(Cyd)^{2+}_{cl}$ one expects innersphere coordination of N3 and possibly outersphere binding to (C2)O. In this context it is revealing to note that in the polymeric Cd(dCMP) complex binding of the octahedral Cd^{2+} occurs to both N3 (2.30 Å) and (C2)O (2.64 Å) by formation of a 4-membered ring [85]. The same may be surmised for $Cd(Cyd)^{2+}_{cl}$, but in aqueous solution one expects it to be, at least, in equilibrium with the indicated semichelate.

(iv) In the polymeric Co(CMP) complex the metal ion coordinates to N3 (1.99 Å) and does not interact with (C2)O [86]; this agrees with the properties of $Co(Cyd)^{2+}$ for which equilibrium (13) is far to its left. However, considering the small slope of the $Co(o\text{PyN})^{2+}$ reference line seen in Figure 6 (compare with the Mg^{2+} situation) [59], it could well be that a significant amount of the metal ion in $Co(Cyd)^{2+}$ is also outersphere bound to N3.

The other two pyrimidine nucleobases, i.e., the uracil and thymine residues (Figure 1), bind strongly to metal ions only after deprotonation of their (N3)H site [87]. This means that carbonyl groups interact significantly with metal ions only if a suitable primary binding site is available (Section 3.3). To establish a sound basis for comparisons equilibria (7a) and (8a) were studied for several metal ion complexes of (N3)H-deprotonated uridine-type ligands (U), i.e., 5-fluorouridine, 5-chloro-2'-deoxyuridine, uridine, and thymidine (= 2'-deoxy-5-methyluridine). Plots of $\log K^{M}_{M(U-H)}$ *versus* pK^{H}_{U} result for the four ligand systems in straight lines [88] and these may be compared with the plots discussed above for pyridine- and *o*-aminopyridine-type ligands. Figure 7 shows the situation for the Cd^{2+} complexes together with the data for the corresponding Ca^{2+} and Co^{2+} complexes for comparison.

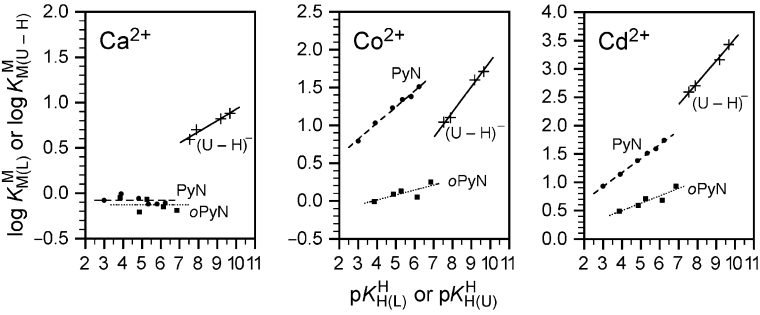

Figure 7 Comparison of the $\log K^{M}_{M(U-H)}$ *versus* pK^{H}_{U} relationships (+) for Ca^{2+}, Co^{2+}, and Cd^{2+} [88] with the corresponding $\log K^{M}_{M(L)}$ *versus* $pK^{H}_{H(L)}$ relationships [35] for simple pyridine-type (PyN) (●) and sterically inhibited *ortho*-amino(methyl)pyridine-type ligands (*o*PyN) (■). For the definition of the data points of the PyN and *o*PyN systems see legend of Figure 6 (compare from left to right) (25°C; $I = 0.5$ M, $NaNO_3$). The straight-reference line for the uridinate-type complexes (+) is defined (from left to right) by 5-fluorouridinate, 5-chloro-2'-deoxyuridinate, uridinate, and thymidinate (25°C; $I = 0.1$ M, $NaNO_3$; the corresponding equilibrium constants are listed in ref. [88]).

From the Ca^{2+} and Cd^{2+} parts of Figure 7 it follows that their $M(U-H)^{+}$ complexes are more stable than the $Ca(PyN)^{2+}$ and $Cd(PyN)^{2+}$ species, whereas the $Co(U-H)^{+}$ complexes are less stable than their $Co(PyN)^{2+}$ counterparts. Furthermore, the $Co(U-H)^{+}$ straight line is placed (although with a somewhat steeper slope) between the lines of the Co^{2+} complexes of the PyN- and *o*PyN-type ligands. This indicates that Co^{2+} (like Ni^{2+} [88]) suffers in its coordination to $(N3)^{-}$ of $(U-H)^{+}$ from a steric hindrance by the neighboring (C2)O/(C4)O groups. This hindrance, however, is less pronounced than that by an *o*-amino (or *o*-methyl) group. In contrast, in $Ca(U-H)^{+}$ and $Cd(U-H)^{+}$, (C2)O and (C4)O facilitate M^{2+} binding leading thus to an increased complex stability.

In a careful evaluation, taking into account the situation in $M(Cyd)^{2+}$ complexes [88], it was concluded that the 'lower limits' for the formation degrees of chelates can be assessed; 'lower limits' because in $(U - H)^-$ there is no steric hindrance by an *o*-NH_2 group, and two (C)O groups (not only one; see Figure 1) may participate in complex formation. Hence, the 'lower limits' for the formation degrees of chelates in $Ca(U - H)^+$ and $Cd(U - H)^+$ are about 50% and 60%, respectively. In $Cd(U - H)^+$ 4-membered chelates may form, but in aqueous solution it is highly likely that in addition semichelates occur via ligated water molecules to (C2)O and (C4)O. In contrast, no chelate formation is anticipated for the Co^{2+} (and Ni^{2+}) complex of $(U - H)^-$, i.e., the metal ion coordinates most likely in a monodentate fashion to $(N3)^-$ of the uridinates [88].

4.3 *Cadmium(II) Complexes of Some Less Common Nucleobase Residues*

In this section we will consider tubercidin (Figure 5; bottom, left) and the five nucleosides seen in Figure 8 [89].

4.3.1 Tubercidin

Tubercidin (Tu), also known as 7-deazaadenosine, is synthesized by molds and fungi [90] and has antibiotic properties. From its structure it follows that Tu is an *o*-aminopyridine-type ligand [59,72], and as we have already seen in Figure 6

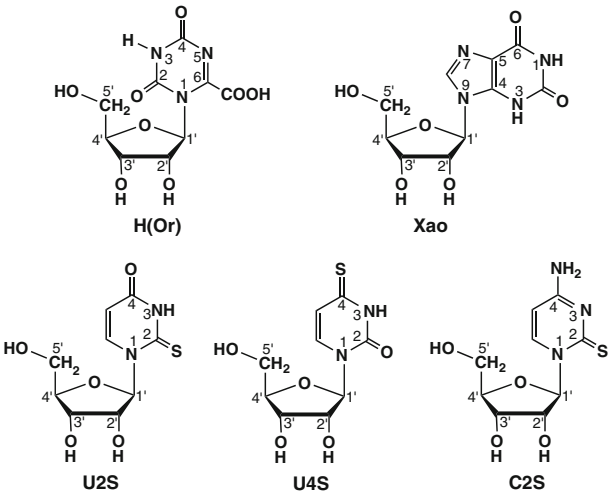

Figure 8 Chemical structures of some less common nucleosides, that is, orotidine [H(Or)], xanthosine (Xao), 2-thiouridine (U2S), 4-thiouridine (U4S), and 2-thiocytidine (C2S). US = U2S and/or U4S. Orotidine exists in solution mostly in the *syn* conformation [89]; for all the other nucleosides the *anti* conformation dominates.

(Section 4.2), it fits with its (C6)NH_2/N1 unit and the connected metal ion-binding properties, including for Cd^{2+}, perfectly into this picture [59] and no further discussion is therefore warranted.

4.3.2 Orotidine

Orotidine and its derivatives play an important role as intermediates in the metabolism of pyrimidine-nucleotides [91]. Its structure is shown in Figure 8 (top, left); it is closely related to uridine (see Figure 1), but due to the (C6)-carboxylate group it exists in solution mainly in the *syn* conformation [89]. The (C6)COOH group is very acidic; for aqueous solution it was estimated that $pK_a = 0.5 \pm 0.3$ [92]. Consequently, the stability constants of the orotidinate (Or^-) complexes of Mg^{2+}, Cu^{2+}, and Zn^{2+} (only these metal ions have been studied [92]) are somewhat below of those measured for the corresponding $M(Ac)^+$ complexes (see Table 1, column 7). There is no evidence for any significant chelate formation in aqueous solution [92]. Therefore, one may assume that all this also holds for the $Cd(Or)^+$ complex, which gives as an estimate for its stability $\log K^{Cd}_{Cd(Or)} = 1.0 \pm 0.3$.

The acidity constant of Or^- for the deprotonation of its (N3)H site in aqueous solution, $pK^H_{Or} = 9.12 \pm 0.02$ [92], is quite close to the corresponding one of its parent nucleoside, uridine, for which it holds $pK^H_{Urd} = 9.18 \pm 0.02$ [88]. Consequently, it is safe to assume that the stabilities of the M(Or – H) and $M(Urd - H)^+$ complexes, including Cd^{2+}, are also very similar (see also Figure 7). Hence, it is no surprise that the stabilities of the complexes formed with orotidinate 5'-monophosphate (OMP^{3-}) are determined by the basicity of the phosphate group [93]. No evidence was observed for macrochelate formation between the phosphate-coordinated metal ions and the carboxylate group, though there is a charge effect of about 0.4 log unit [93]. Hence, in $Cd(OMP)^-$ no interaction with the pyrimidine ring occurs, what corresponds to the situation in Cd(UMP).

4.3.3 Xanthosine

Xanthosine (Xao) and its derivatives are of relevance for the metabolism of purine-nucleosides/nucleotides [91,94]. Monoprotonated $H(Xao)^+$ carries a proton at N7, which is released with $pK^H_{H(Xao)} = 0.74 \pm 0.06$ [95]. The neutral Xao, as shown in Figure 8, loses a further proton already with $pK^H_{Xao} = 5.47 \pm 0.03$ [95] from the (N1)H/(N3)H sites and there is evidence for a tautomeric equilibrium between $(N3)^-$/(N1)H and (N3)H/$(N1)^-$ [96,97]. In any case, in the physiological pH range of about 7.5 this nucleoside is present in its anionic form, xanthosinate, and it differs therefore considerably from its relatives inosine and guanosine (Section 4.1; Table 3).

Stability constants of $M(Xao - H)^+$ complexes (including for Cd^{2+}) have been determined [95] and there is evidence that a dichotomy for M^{2+} binding between N1 and N7 occurs [95,98]; of course, the negative charge in the xanthine residue can be

delocalized over many atoms, that is, N3, (C2)O, N1, and (C6)O. There is no doubt that the indicated dichotomy exists, yet the percentages given for the isomers should be considered with some care, even though the agreement between the rather different evaluation methods is surprisingly good. For example, it is concluded that in $Cd(Xao - H)^+$ about 75% are N7-coordinated [95,98]; the value for $Co(Xao - H)^+$ is about 50% [95,98], whereas for $Zn(Xao - H)^+$ N7 binding is given as 58% in ref. [95] and as 38% in ref. [98]. Here more work is needed.

4.3.4 Thiouridines

Thiolation of uracil residues, especially in RNA wobble positions, affect the conformation of the nucleic acid in solution [99] and has implications for recognition processes. Furthermore, 4-thiouridine is found in bacterial and archaeal tRNA [100,101]. Therefore, we shall have a short look on 2-thiouridine (U2S) and 4-thiouridine (U4S) (see Figure 8, bottom part) and their complexes formed with Cd^{2+} and Cu^{2+} [102,103]. The exchange of an O atom by a S atom in uridine (see Figure 1) is expected, of course, to alter not only the acid-base but also the metal ion-binding properties [15,17,104]. Indeed, the acidity of (N3)H is increased by about one pK unit as follows from column 3 in Table 6 [105]. However, despite the reduced basicity of $(N3)^-$ in $(U2S - H)^-$ and $(U4S - H)^-$ the stabilities of their complexes with Cd^{2+} and Cu^{2+} are by about 1 and 1.8 log units higher than those of $Cd(Urd - H)^+$ and $Cu(Urd - H)^+$ (Table 6, column 5).

Table 6 Negative logarithms of the acidity constants (eq. 3) of uridine (Figure 1) and its thio derivatives (U) shown in Figure 8, together with the stability constant comparisons (log Δ; eq. 14) for several $M(U - H)^-$ complexes between the measured stability constants (eq. 2) and those calculated based on pK_U^H, equation (15) and the corresponding straight-line parameters given in ref. [88][a].

No.	U	pK_U^H	M^{2+}	log $K^M_{M(U-H)}$	log $K^M_{M(U-H)calc}$	log Δ
1a	Urd	9.18 ± 0.02	Cu^{2+}	4.13 ± 0.20	4.13 ± 0.21	0
b			Cd^{2+}	3.16 ± 0.04	3.21 ± 0.05	–0.05 ± 0.06
2a	U2S	8.05 ± 0.04	Cu^{2+}	5.91 ± 0.06	3.62 ± 0.21	2.29 ± 0.22
b			Cd^{2+}	4.11 ± 0.03	2.77 ± 0.05	1.34 ± 0.06
3b	U4S	8.01 ± 0.01	Cd^{2+}	4.34 ± 0.01	2.75 ± 0.05	1.59 ± 0.05

[a] The above data are abstracted from Table 1 in ref. [105]. The values in entries 1 are from ref. [88] (25°C; I = 0.1 M, $NaNO_3$) (3σ). The stability constant for $Cu(Urd - H)^+$ (entry 1a) is calculated from the log $K^{Cu}_{Cu(U-H)}$ *versus* pK_U^H plot [88]; this result agrees well with constants found in the literature (for details see [83]). Entry 2a is from ref. [102] and the values of entries 2b and 3b are from ref. [103] (25°C; I = 0.2 M, KCl) (1σ). The error limits listed above (σ = standard deviation) are those given in the various studies. The error limits of the derived data, in the present case for log Δ, were calculated according to the error propagation after Gauss.

A more careful evaluation of the data via log Δ (eq. 14) by taking the differences in acidity of the (N3)H sites into account, reveals that the true stability enhancement amounts for the Cd^{2+} complexes to more than 1.3 log units and for the Cu^{2+} species to about 2.3 log units (Table 6, column 7). Of course, the negative charge at $(N3)^-$ may be delocalized to the sulfur atoms at (C2)S or (C4)S and this makes these sulfur sites to excellent donors for Cd^{2+} (and Cu^{2+}) coordination [15,17,104]. Most likely the enhanced complex stability is not only due to monodentate (C)S–M^{2+} coordinations (next to a $(N3)^-$–M^{2+} one), but due to chelate formation involving both sites as well. From X-ray crystal structure studies it is known that Cd^{2+} [85] and Cu^{2+} [106] are able to form 4-membered chelates with the cytosine residue involving the N3 and (C2)O sites. For the present study this means that Cd^{2+} and Cu^{2+} most likely form 4-membered rings involving $[N3/(C)S]^-$, especially since such low-membered chelates are more easily formed if a (C)O is replaced by a (C)S site [107]. Of course, in aqueous solution there is the possibility that semichelates involving a ligated water molecule form [105].

In the terminating paragraph of Section 4.2 we have already concluded that the formation degree of chelates in the $M(Urd - H)^+$ species must be larger than it is in the $M(Cyd)^{2+}$ complexes. Considering the additional stability enhancement observed for the $M(U2S - H)^+$ and $M(U4S - H)^+$ complexes, these lower limits must be even more true for the complexes of the thiouridinates, that is, $Cd(US - H)^+_{cl} > Cd(Cyd)^{2+}_{cl}$ (= ca. 60%; see Table 5) and $Cu(U2S - H)^+_{cl} > Cu(Cyd)^{2+}_{cl}$ (= ca. 80%). In fact, we believe that the formation degree of the chelated species in the $Cd(US - H)^+$ and $Cu(U2S - H)^+$ systems is larger than 90% because this number corresponds to a stability enhancement of about 1 log unit being solely due to chelate formation (and attributing the remaining part of log Δ to the general participation of S in metal ion binding).

4.3.5 2-Thiocytidine

The thionucleoside 2-thiocytidine (C2S; Figure 8, lower part, right) occurs in Nature in tRNAs [108]. In addition, it also receives attention in diverse fields [109] like drug research [110] or nanotechnology [111]. The acidity constants of $H(C2S)^+$ and the stability constants of the $M(C2S)^{2+}$ and $M(C2S - H)^+$ complexes ($M^{2+} = Zn^{2+}, Cd^{2+}$) were determined by potentiometric pH titrations. These results [112] can be compared with those obtained for the parent nucleoside cytidine (Cyd; Figure 1; Section 4.2). Replacement of the (C2)=O unit by (C2)=S facilitates the release of the proton from $(N3)H^+$ in $H(C2S)^+$ ($pK_a = 3.44 \pm 0.01$ [112]; 25°C; $I = 0.5$ M, KNO_3) somewhat, compared with $H(Cyd)^+$ ($pK_a = 4.24 \pm 0.02$ [83]; 25°C; $I = 0.5$ M, $NaNO_3$). This moderate effect of about 0.8 pK unit contrasts with the strong acidification of about 4 pK units of the $(C4)NH_2$ group in C2S ($pK_a = 12.65 \pm 0.12$ [112]) compared with Cyd (pK_a ca. 16.7 [34,113]). The reason [112] for this result is that the amino-thione tautomer, which dominates for the neutral C2S molecule, is transformed upon deprotonation into the

imino-thioate form with the negative charge largely located on the sulfur; this is indicated in equilibrium (21):

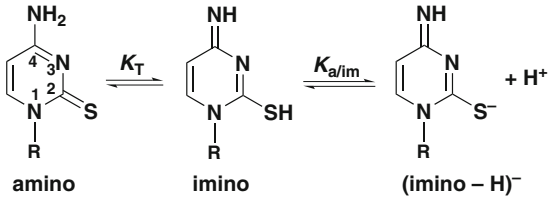

(21)

The intramolecular and dimensionless equilibrium constant K_T = [imino]/[amino] was estimated as being on the order of 10^{-4} to 10^{-6}, which leads to values for the acidity constant $K_{a/imino}$ of $10^{-8.65}$ to $10^{-6.65}$ [112].

In the $M(C2S)^{2+}$ complexes the (C2)S group is the primary binding site [112] rather than N3 as is the case in the $M(Cyd)^{2+}$ complexes (Section 4.2), though owing to chelate formation N3 is to some extent still involved in metal ion binding. Based on log $K^{M}_{M(L)}$ *versus* p$K^{H}_{H(L)}$ plots (eq. 15) for *o*PyN-type ligands [59] (see also Figure 6), the stability enhancements amount to log $\Delta_{Cd/C2S} = 3.3$ and log $\Delta_{Zn/C2S} = 2.6$ [112]. They are much larger than those observed for the corresponding $M(Cyd)^{2+}$ complexes (see Table 5) and lead to the conclusion that (C2)S–M^{2+} binding is important and dominates with more than 99%; a number which encompasses both, monodentate S coordination as well as chelate formation of an (C2S)-bound metal ion with N3. The structure of these chelates has been discussed [112]. Clearly, the monodentate (N3)–M^{2+} isomer occurs only in traces.

Similarly, in the $Zn(C2S - H)^{+}$ and $Cd(C2S - H)^{+}$ complexes the main metal ion binding site is the $(C2)S^{-}$ unit and the formation degree of its complex is above 99.9% (compared with that of N3). However, again a large degree of chelate formation with N3 must be surmised for the $M(C2S - H)^{+}$ species, and their structure was discussed [112]. It needs to be emphasized that upon metal ion binding the deprotonation of the $(C4)NH_2$ group (pK_a = 12.65) is dramatically acidified (pK_a ca. 3), confirming the very high stability of the $M(C2S - H)^{+}$ complexes and the importance of equilibrium (21). To conclude, the metal ion-binding capabilities of C2S differ strongly from those of its parent Cyd; this also holds for hydrogen-bond formation because (C)S is a much poorer H-acceptor than (C)O. Clearly, these differences must have consequences for the properties of those RNAs which contain this thionucleoside.

5 Complexes of Cadmium(II) with Phosphates

In Figure 9 the general structures for the monoesters of mono-, di-, and triphosphates, symbolized by R-MP^{2-}, R-DP^{3-}, and R-TP^{4-}, respectively, are shown together with the structure of a phosphodiester bridge, $(RO)_2PO_2^-$, as it occurs in the backbone of nucleic acids. This diester of a phosphate group may be

mimicked to some extent herein by acetate (Ac^-) as both ligands carry a charge of minus one. The most basic phosphate residue in the phosphomonoesters is always the terminal one, which carries a charge of two minus. In addition, the effect of the residue R on the basicity of such a phosphate group will be the more pronounced the closer they are. For example, the effect of a phenyl and a butyl residue in $R\text{-}MP^{2-}$ leads to the pK_a values of 5.81 ± 0.01 and 6.72 ± 0.02, respectively [114], whereas the effect of the same residues in $R\text{-}DP^{3-}$ leads to the much smaller pK_a span of 6.32 ± 0.02 to 6.65 ± 0.02 [115]. In the case of the triphosphates the residue R has practically no effect [37,116–118].

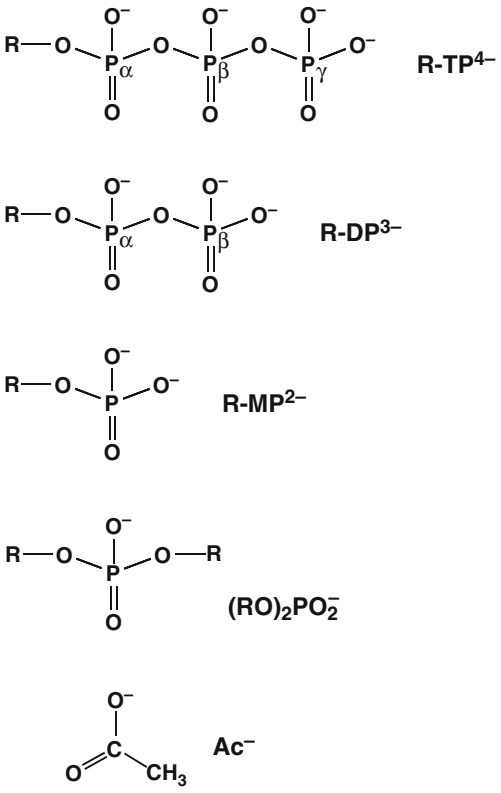

Figure 9 Chemical structures of simple monoesters of triphosphate ($R\text{-}TP^{4-}$), diphosphate ($R\text{-}DP^{3-}$), and monophosphate ($R\text{-}MP^{2-}$). R represents a residue which does not affect metal ion coordination at the phosphate, i.e., neither in a positive nor negative sense. $(RO)_2PO_2^-$ represents the phosphodiester bridge of a nucleic acid; acetate (Ac^-) is used as a primitive and simple mimic of such a singly negatively charged situation (see also [58]).

Pyrimidine-nucleoside phosphates furnish representative values for nucleotide comparisons because the pyrimidine residue does commonly not participate in metal ion binding with labile ions like Cd^{2+} [114–119]. The corresponding acidity constants for the terminal phosphate groups of pyrimidine-nucleotides are $pK^H_{H(R\text{-}MP)} = 6.20$ (eq. 3) for monophosphate monoesters [50,114], $pK^H_{H(R\text{-}DP)} = 6.40$ for diphosphate monoesters [115], and $pK^H_{H(R\text{-}TP)} = 6.50$ for triphosphate monoesters [37,116–118,120]. The stability constants (eq. 2), which correspond to these pK_a values [115,117], are listed in columns 3 to 5 of Table 7 (upper part) [121,122] for several M(R-MP), $M(R\text{-}DP)^-$, and $M(R\text{-}TP)^{2-}$ complexes.

Table 7 Comparison of the stability constants (eq. 2) of M^{2+} complexes formed with acetate (Ac^-), as a simple mimic of the phosphodiester bridge (Figure 9), mono- (R-MP^{2-}), di- (R-DP^{3-}), and triphosphate monoesters (R-TP^{4-}) in aqueous solution at 25°C and $I = 0.1$ M ($NaNO_3$), together with the corresponding stability differences as they follow from the data listed in neighboring columns[a,b,c].

	log $K^{M}_{M(L)}$ (eq. 2) for L =			
M^{2+}	Ac^-	R-MP^{2-}	R-DP^{3-}	R-TP^{4-}
H^+	(4.56 ± 0.03)[d,e]	6.20[d]	6.40[d]	6.50[d]
Mg^{2+}	0.51 ± 0.05	1.56 ± 0.03	3.30 ± 0.03	4.21 ± 0.04
Ca^{2+}	0.55 ± 0.05	1.45 ± 0.05	2.91 ± 0.03	3.84 ± 0.05
Fe^{2+}	0.83 ± 0.06	2.05 ± 0.10[f]	3.92 ± 0.10[f]	4.85 ± 0.10[f]
Co^{2+}	0.86 ± 0.05	1.94 ± 0.06	3.72 ± 0.05	4.76 ± 0.03
Cu^{2+}	1.46 ± 0.13[b]	2.87 ± 0.06	5.27 ± 0.04	5.86 ± 0.03
Zn^{2+}	0.98 ± 0.13	2.12 ± 0.06	4.12 ± 0.03	5.02 ± 0.02
Cd^{2+}	1.26 ± 0.07	2.44 ± 0.05	4.27 ± 0.03	5.07 ± 0.03

M^{2+}	log $\Delta_{R\text{-}MP/Ac}$	log $\Delta_{R\text{-}DP/R\text{-}MP}$	log $\Delta_{R\text{-}TP/R\text{-}DP}$
Mg^{2+}	1.05 ± 0.06	1.74 ± 0.04	0.91 ± 0.05
Ca^{2+}	0.90 ± 0.07	1.46 ± 0.06	0.93 ± 0.06
Fe^{2+}	1.22 ± 0.12	1.87 ± 0.14	0.93 ± 0.14
Co^{2+}	1.08 ± 0.08	1.78 ± 0.08	1.04 ± 0.06
Cu^{2+}	1.41 ± 0.14	2.40 ± 0.07	0.59 ± 0.05
Zn^{2+}	1.14 ± 0.14	2.00 ± 0.07	0.90 ± 0.04
Cd^{2+}	1.18 ± 0.09	1.83 ± 0.06	0.80 ± 0.04

[a] For the error limits see footnotes "*a*" of Tables 3 and 4.
[b] The constants for the $M(Ac)^+$ complexes are from column 7 of Table 1, with the exception of the value for the Cu^{2+} complex which corresponds to the Cu(chloroacetate)$^+$ complex because $pK^{H}_{H(ClAc)} = 2.7$ [25] is closer to $pK^{H}_{H[(RO)_2P(O)(OH)]}$ = ca. 1 [33,121]. The basicity effect in the other instances is small.[e]
[c] The values for the M(R-MP) complexes (column 3) were calculated with $pK^{H}_{H(R\text{-}MP)} = 6.20$ [114,115] and the straight-line equations given in refs [50,52,74,122]. The values for the $M(R\text{-}DP)^-$ complexes (column 4, including the acidity constant) are from Table 7 in ref. [115], and for the values of the $M(R\text{-}TP)^{2-}$ species it holds: Those for the alkaline earth ion complexes are from Table 2 in ref. [119] and all the others from Table IV of ref. [116] (see also [117]).
[d] These values are the acidity constants of the monoprotonated ligands and refer to $pK^{H}_{H(L)}$ (eq. 3).
[e] The pK_a value of $(RO)_2P(O)(OH)$ is ca. 1; despite the pK_a difference acetate mimics the complex stabilities of the $M[(RO)_2(PO_2]^+$ species relatively well [58] (see also text).
[f] The values for the Fe^{2+} complexes are estimates as are the error limits; they are taken from the terminating paragraph of ref. [115].

Unfortunately, no comprehensive set of stability constants of metal ion complexes formed with a phosphodiester has been measured [25]; the reason is the low basicity of $(RO)_2PO_2^-$, i.e., $pK^{H}_{H[(RO)_2PO_2]}$ = ca. 1 [33,34], which precludes potentiometric pH titrations which are based on the competition between H^+ and M^{2+} for binding at a given ligating site. Since in a first approximation the negative charge is distributed on two O atoms in $CH_3CO_2^-$ like in $(RO)_2PO_2^-$ (see Figure 9), the metal ion affinities of acetate (or chloroacetate or formate) may be assumed to reflect those of the phosphodiester bridge. Certainly, there is a difference in basicity between $R\text{-}CO_2^-$ and $(RO)_2PO_2^-$ (Table 7), but the slopes of log $K^{M}_{M(R\text{-}COO)}$ *versus* $pK^{H}_{H(R\text{-}COO)}$ plots are relatively small [57], which indicates that outersphere binding is important, and in

fact, this agrees with observations made at bridging phosphate groups in nucleic acids [30]. This conclusion agrees further with studies of poly(U) and Mg^{2+} or Ni^{2+} [123] where it was found that the apparent stability constants for the two metal ions are identical within the error limits: $\log K^{Mg}_{Mg(pU)app} = 1.80$ and $\log K^{Ni}_{Ni(pU)app} = 1.83$ (25°C; $I = 0.1$ M – 0.3 M). From these results, and for Cd^{2+} the analogous ones are expected, it was concluded "that innersphere coordination ... does not occur to a significant extent. Rather, the metal ions are bound in these systems mainly by electrostatic forces, forming a mobile cloud" [123].

The stability constants listed in column 2 of Table 7 (upper part) are reliable enough for the comparisons to be made herein with regard to the stability of $M[(RO)_2PO_2]^+$ complexes. Indeed, these values are only slightly larger than those proposed recently in another somewhat more comprehensive estimate [58]. That the listed values in Table 7 are on the correct order is further confirmed by the stability constant of the Ni^{2+} complex formed with monoprotonated D-ribose 5-monophosphate ($RibMP^{2-}$), i.e., $\log K^{Ni}_{Ni(H;RibMP)} = 0.7$ (15°C; $I = 0.1$ M, KNO_3) [124] and the Cd^{2+} complex of $H_2PO_4^-$, i.e., $\log K^{Cd}_{Cd(H_2PO_4)} = 1.2 \pm 0.2$ (25°C; $I \rightarrow 0$ M) [125]. These values are rather close to those given for $Fe(Ac)^+$, $Co(Ac)^+$, and $Cd(Ac)^+$ in Table 7. In this context one may note that with all types of phosphate complexes the Irving-Williams series [22,126] is not strictly followed [19,22,115–117,119], the complexes of Co^{2+} and especially Ni^{2+} are commonly somewhat lower in stability than those of Mn^{2+} and Zn^{2+}. In fact, this is also reflected to some extent by the data in columns 3 to 5 of Table 7 (upper part). One may note here that the strength of the metal ion-phosphate interaction is crucial for the activity of ribozymes: For example, the catalytic cleavage rate of hammerhead ribozymes shows a direct correlation to the above mentioned "irregular" phosphate affinities of the divalent metal ions [127].

To facilitate comparisons between the various types of complexes the log-stability differences listed in the lower part of Table 7 have been prepared. As one would expect, increase of the charge from minus one in $Ac^-/(RO)_2PO_2^-$ to minus two in $R\text{-}MP^{2-}$ (Figure 9) increases the stabilities of the complexes: The stability increases amount to about 0.9 (Ca^{2+}) to 1.2 (Cd^{2+}) log units; only for the Cu^{2+} complexes the effect is a bit more pronounced with $\log \Delta_{R\text{-}MP/Ac} = 1.4$ (lower part, column 2). In contrast, the stability increase of the complexes by going from M(R-MP) to $M(R\text{-}DP)^-$ varies significantly from metal ion to metal ion, i.e., within the relatively large span of about 1.45 to 2.4 log units. This changes again by going from $M(R\text{-}DP)^-$ to $M(R\text{-}TP)^{2-}$, then the stability increase is quite constant within the narrow range of about 0.8 to 1.0 log units, if the special case of Cu^{2+} with its distorted octahedral coordination sphere [128] is ignored. Overall this indicates in our view that outersphere species play a significant role in M(R-MP) complexes, which also include six-membered semichelates with one of the terminal oxygens innersphere and the other one outersphere [114]. Such outersphere interactions are hardly of relevance in the corresponding di- and triphosphate species where two neighboring phosphate units allow the formation of six-membered innersphere chelates. This is in accord with the $\log K^{M}_{M(R\text{-}MP)}$ *versus* $pK^{H}_{H(R\text{-}MP)}$ plots where the

slopes are much lower (Ca^{2+}: $m = 0.131 \pm 0.020$; Cd^{2+}: 0.329 ± 0.019 [122] (thus indicating partial outersphere binding) than for the log $K^{M}_{M(R\text{-}DP)}$ *versus* $pK^{H}_{H(R\text{-}DP)}$ plots (Ca^{2+}: 0.379 ± 0.097; Cd^{2+}: 0.945 ± 0.104 [115]). Clearly, for di- and triphosphates the formation of innersphere complexes is more pronounced compared with monophosphates, owing to the increased negative charge of these ligands. Overall, the situation may be summarized with the earlier statement [129], "the lower the charge, the more predominant are outersphere complexes".

6 Cadmium(II) Complexes of Nucleotides

6.1 Some General Considerations

The evaluations presented in this section are carried out in part in a manner analogous to our previous review on Ni^{2+}-nucleotide complexes [40]; of course, concentrating now on Cd^{2+} which was *not* a part of the previous account. As is well known, nucleotides exist in solution mainly in the so-called *anti* conformation. Two such examples are shown in Figure 10 [11–14,50]. It is the phosphate residue in nucleotides which determines to a very large part the stability of the complexes formed with labile metal ions including Cd^{2+} [74,117,119,130] independent of the kind of nucleobase involved or whether a nucleoside mono-, di-, or triphosphate is considered.

For purine-nucleoside 5'-phosphates the formation of macrochelates was proposed nearly 60 years ago [131] and more than 50 years ago it was concluded that they actually exist [132–135], i.e., a metal ion coordinated to the phosphate residue of a purine nucleotide may also interact in the dominating *anti* conformation with N7 of the purine moiety. Nowadays formation of macrochelates in complexes formed by purine nucleotides with various metal ions including Cd^{2+} is well established [117,120,136–138]. Clearly, the formation of such a macrochelate must give rise to the intramolecular equilibrium (22):

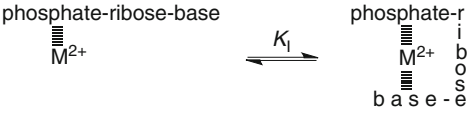

(22)

As already discussed in Section 4.2, any kind of equilibrium between an 'open' isomer, $M(L)_{op}$, and a chelated or 'closed' isomer, $M(L)_{cl}$, must be reflected in an increased complex stability compared to the situation where only the open complex can form [51]. This stability enhancement, log $\Delta_{M/L}$ (eq. 14), can be evaluated by equations (16) to (20) (Section 4.2), which furnish values for K_I (eqs 16, 17) and thus for the formation degree of the closed species, % $M(L)_{cl}$ (eq. 20).

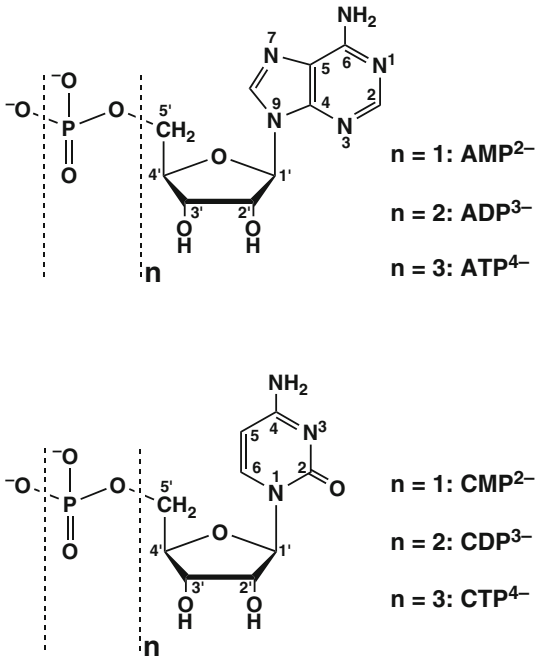

Figure 10 Chemical structures of adenosine 5'-monophosphate (n = 1: AMP^{2-}), adenosine 5'-diphosphate (n = 2: ADP^{3-}), and adenosine 5'-triphosphate (n = 3: ATP^{4-}) as well as of cytidine 5'-monophosphate (n = 1: CMP^{2-}), cytidine 5'-diphosphate (n = 2: CDP^{3-}), and cytidine 5'-triphosphate (n = 3: CTP^{4-}) in their dominating *anti* conformation [11–14,50]. Note, the triphosphate chain in nucleoside 5'-triphosphates (NTP^{4-}) is labeled α, β, and γ, where γ refers to the terminal phosphate group (see also Figure 9); for nucleoside 5'-diphosphates (NDP^{3-}) the situation is analogous with α and β (see Figure 9). The adenine and cytosine residues in the nucleotide structures shown above may be replaced by one of the other nucleobase residues shown in Figure 1; if this substitution is done in the way the bases are depicted within the plane (Figure 1), then the *anti* conformation will also result for the corresponding nucleoside 5'-phosphates. The abbreviations AMP^{2-}, ADP^{3-}, ATP^{4-}, IMP^{2-}, etc. in this text always represent the 5'-derivatives; 2'- and 3'-derivatives are defined by $2'AMP^{2-}$, $3'AMP^{2-}$, etc.; in a few instances where uncertainties might otherwise occur, the abbreviations $5'AMP^{2-}$, $5'ADP^{3-}$, etc. are also used.

One important aspect needs to be emphasized and kept in mind when dealing with purine derivatives: All of them show a pronounced tendency for self-association, which occurs via stacking of the purine rings [117,137,139,140]. Hence, experiments aimed at determining the properties of monomeric metal ion complexes of purine nucleosides or their phosphates should not be carried out in concentrations higher than 10^{-3} M. To be on the safe side, actually a maximum concentration of only 5×10^{-4} M is recommended (cf., e.g., [122,136]). The equilibrium constants discussed below were mostly obtained by potentiometric pH titrations and the corresponding experimental conditions adhere to the above request.

6.2 Complexes of Nucleoside 5'-Monophosphates

6.2.1 Equilibrium Constants to Be Considered

A combination of the information provided in Figures 1 and 10 reveals that there are nucleoside 5'-monophosphates (NMP^{2-}), which contain a nucleobase that may accept a proton, e.g., AMP^{2-}, whereas others contain a nucleobase that can only release one, e.g., UMP^{2-}. Therefore, if one neglects a twofold protonated phosphate group because this is not of relevance for a biological system due to its large acidity (e.g., for $H_2(UMP)$ $pK^{H}_{H_2(UMP)} = 0.7 \pm 0.3$ [114]), one has to consider eqs (3) and (7), next to equilibrium (23) (charges neglected):

$$H_2(L) \rightleftharpoons H(L) + H^+ \tag{23a}$$

$$K^{H}_{H_2(L)} = [H(L)][H^+]/[H_2(L)] \tag{23b}$$

Based on the structures of the various NMPs, it is clear that equilibria (23) and (3) hold for $H_2(CMP)^{\pm}$ and $H_2(AMP)^{\pm}$, and that equilibria (3) and (7) are of relevance for $H(UMP)^-$ and $H(dTMP)^-$, whereas all three equilibria (23), (3), and (7) are needed to describe the acid-base properties of $H_2(IMP)^{\pm}$ and $H_2(GMP)^{\pm}$. In all cases equilibrium (3) refers to the deprotonation of the $P(O)_2(OH)^-$ group in the $H(NMP)^-$ species.

Correspondingly, one has to consider the complexes $M(H;NMP)^+$ and M(NMP), the stabilities of which are defined in equilibria (24) and (2), respectively (charges neglected):

$$M^{2+} + H(L) \rightleftharpoons M(H;L) \tag{24a}$$

$$K^{M}_{M(H;L)} = [M(H;L)]/([M^{2+}][H(L)]) \tag{24b}$$

At high pH values also $Cd(NMP - H)^-$ species (eq. 8) might form but at present no information is available about these.

$M(H;NMP)^+$ [= M(H;L)] complexes form with CMP^{2-}, AMP^{2-}, IMP^{2-}, and GMP^{2-}. In these cases, M^{2+}, including Cd^{2+}, is mainly located at the nucleobase residue and the proton at the phosphate group [50,130,141]. However, because the proton is lost with a pK_a value of about 5 or below [50,130,141], these species are of relevance for biological systems only under very special conditions. At the common physiological pH of about 7.5 they are not important and therefore not considered further in the present context.

6.2.2 Properties of Pyrimidine-Nucleoside 5'-Monophosphate Complexes

The acidity constants of the pyrimidine-NMPs are listed in Table 8 together with the stability constants of their Cd(NMP) complexes (eq. 2), including the corresponding data for tubercidin 5'-monophosphate ($TuMP^{2-}$ = 7-deaza-AMP^{2-}).

This nucleotide has the structure of AMP^{2-} except that N7 is replaced by a CH unit (see Figures 5 and 10) and this exchange transforms this purine-type nucleotide into one with pyrimidine-type properties (*vide infra*).

Table 8 Acidity constants of protonated pyrimidine-NMPs (analogous to eqs 3, 7) and stability constants of their Cd(NMP) complexes (eq. 2). The corresponding data are also given for $H_2(TuMP)^{\pm}$ (aqueous solution; 25°C, $I = 0.1$ M, $NaNO_3$)[a].

Acid	$pK^{H}_{H_2(NMP)}$	$pK^{H}_{H(NMP)}$	pK^{H}_{NMP}	$\log K^{Cd}_{Cd(NMP)}$	Ref.
$H_2(CMP)^{\pm}$	4.33 ± 0.04[b]	6.19 ± 0.02		2.40 ± 0.08	[114][c]
$H(UMP)^{-}$		6.15 ± 0.01	9.45 ± 0.02[d]	2.38 ± 0.04	[114]
$H(dTMP)^{-}$		6.36 ± 0.01	9.90 ± 0.03[d]	2.42 ± 0.03	[114]
$H_2(TuMP)^{\pm}$	5.28 ± 0.02[e]	6.32 ± 0.01		2.42 ± 0.07	[136]

[a] For the error limits see footnotes "*a*" of Tables 3 and 4.
[b] This proton is released from the $(N3)H^+$ site (see Figure 10).
[c] See also ref. [141].
[d] The proton is released from the (N3)H site (see Figure 1).
[e] This proton is released from the $(N1)H^+$ site of the 7-deaza-purine residue (see Figures 1 and 5).

The α-phosphate group is close in distance to the nucleoside residue and its basicity properties are therefore somewhat affected by this residue (see also Section 5). Indeed, the acidity constants of $H(NMP)^{-}$ species as defined by equation (3) vary roughly between $pK^{H}_{H(NMP)} = 5.7$ and 6.3 [48,136]. As a consequence, a direct comparison of stability constants of M(NMP) complexes, like those given in Table 8, does not allow unequivocal conclusions regarding the solution structures of these species.

To overcome the indicated handicap, $\log K^{M}_{M(R\text{-}PO_3)}$ (eq. 2) *versus* $pK^{H}_{H(R\text{-}PO_3)}$ (eq. 3) plots were established for $R\text{-}PO_3^{2-}$ systems (R being a non-interacting residue), i.e., for simple phosphate monoesters, like phenyl phosphate or *n*-butyl phosphate, and phosphonate ligands, like methanephosphonate [122]. The resulting straight lines are defined by equation (15). The equilibrium data for the methyl phosphate and the hydrogen phosphate systems fit on these same reference lines, including those for $Cd(CH_3OPO_3)$ and $Cd(HOPO_3)$ [142], as do the data for $RibMP^{2-}$ and for the pyrimidine-NMPs, UMP^{2-} and dTMP, given in Table 8 (see also Figure 11 below) [114,122].

In the light of the results discussed in Sections 3.2 and 4.2, it is no surprise that the ribose residue and the uracil and thymine moieties do not participate in metal ion binding in M(RibMP), M(UMP), and M(dTMP) complexes [122]. How is the situation with Cd(CMP)? The mentioned straight-line parameters [122] are summarized for $Cd(R\text{-}PO_3)$ in equation (25) [the error limit (3σ) for a calculated $\log K^{Cd}_{Cd(R\text{-}PO_3)}$ value is ±0.05] (for details see ref. [122]):

$$\log K^{Cd}_{Cd(R\text{-}PO_3)} = (0.329 \pm 0.019) \cdot pK^{H}_{H(R\text{-}PO_3)} + (0.399 \pm 0.127) \qquad (25)$$

Application of $pK^{H}_{H(CMP)} = 6.19$ (Table 8) to eq. (25) allows to calculate the stability of the 'open' isomer $Cd(CMP)_{op}$ in equilibrium (22), i.e., $\log K^{Cd}_{Cd(R\text{-}PO_3)} = \log K^{Cd}_{Cd(CMP)op} = 2.44 \pm 0.05$. This calculated stability constant is within the

error limits identical with the measured one given in Table 8. Hence, there is no indication for an increased stability of the Cd(CMP) complex, which means that equilibrium (22) is far on its left side and that no remarkable amounts of macrochelates are formed. At first sight this result for Cd(CMP), which also holds for Cu(CMP) and other M(CMP) species [50], may seem surprising because the ability of the N3 site of the cytosine residue to interact with metal ions is well known (Section 4.2; Table 5). However, it should be recalled that CMP^{2-} exists predominately in the *anti* conformation (Figure 10) in which N3 is pointing away from the metal ion coordinated at the phosphate group. Evidently, for all divalent metal ions considered (Table 5) the *anti-syn* energy barrier, which has been estimated to be on the order of about 7 kJ/mol [35], is too large to be overcome by macrochelate formation.

6.2.3 Properties of Purine-Nucleoside 5'-Monophosphate Complexes

Purine-nucleotides represent a favored situation because not only N7 of the purine moiety is able to bind metal ions (Section 4.1; Table 3) but also a metal ion coordinated at the phosphate residue can reach N7 in the dominating *anti* conformation (Figure 10) as was already pointed out in Section 6.1. Such a possible N7 interaction, depending on the kind of metal ion involved, may give rise to macrochelate formation and if this occurs it must be reflected in an increased complex stability. Indeed, a very significant stability enhancement is observed for the Cd(NMP) complexes of AMP^{2-}, IMP^{2-}, and GMP^{2-} (Figure 11), whereas that for the corresponding Ca^{2+} complexes is much smaller. This confirms the well known high affinity of Cd^{2+} for N sites, the one of Ca^{2+} being much lower [22] (see also Section 2; Table 1).

The vertical distances between M(NMP) data points and their corresponding straight-reference line can easily be quantified. Application of the acidity constant $pK^{H}_{H(NMP)}$ to the straight-line equation (15), the parameters of which are listed in refs [50,52,122], provides the value of the intercept with the straight line and thus the stability constant of the 'open' species (eq. 19). In other words, with equation (14) one may now define the stability enhancement, if any, for the M^{2+} complexes of the purine-NMPs. Clearly, the calculated value for $\log K^{M}_{M(R\text{-}PO_3)}$ reflects the stability of the 'open' isomer in equilibrium (22), in which M^{2+} is only phosphate-coordinated. Now, with known values for $\log \Delta_{M/NMP}$ ($= \log \Delta$; eq. 14), the evaluation procedure defined in equations (16) through (20) (Section 4.2) can be applied and the formation degree of the macrochelate which appears in equilibrium (22) can be calculated (eq. 20). The corresponding results are summarized in Table 9 for the Cd(NMP) complexes of AMP^{2-}, IMP^{2-}, and GMP^{2-}, together with the analogous results of some other metal ions for comparisons.

The results of column 6 in Table 9 demonstrate that in all M^{2+} 1:1 complexes with purine-NMPs [with the possible exception of Ca(AMP)] at least some macrochelation occurs. Macrochelation by an interaction of the phosphate-coordinated M^{2+} with N7 is thereby proven with the Cd^{2+}/$TuMP^{2-}$ system (Table 8).

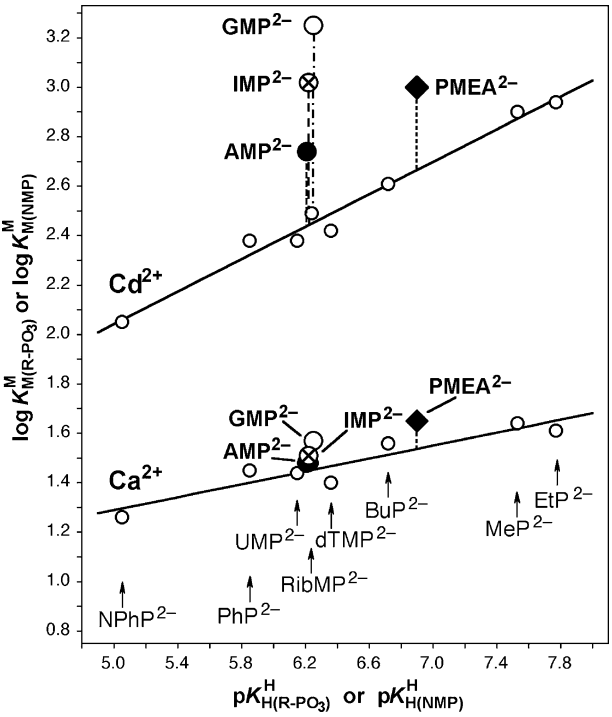

Figure 11 Evidence for an enhanced stability of the Cd^{2+} and Ca^{2+} 1:1 complexes (eq. 2) of AMP^{2-} (●), IMP^{2-} (⊗), and GMP^{2-} (○), based on the relationship between log $K^{M}_{M(R\text{-}PO_3)}$ and $pK^{H}_{H(R\text{-}PO_3)}$ for M(R-PO_3) complexes of some simple phosphate monoester and phosphonate ligands (R-PO_3^{2-}) (○): 4-nitrophenyl phosphate ($NPhP^{2-}$), phenyl phosphate (PhP^{2-}), uridine 5'-monophosphate (UMP^{2-}), D-ribose 5-monophosphate ($RibMP^{2-}$), thymidine [= 1-(2-deoxy-β-D-ribofuranosyl)thymine] 5'-monophosphate ($dTMP^{2-}$), *n*-butyl phosphate (BuP^{2-}), methanephosphonate (MeP^{2-}), and ethanephosphonate (EtP^{2-}) (from left to right). The least-squares lines (eq. 15) are drawn through the corresponding 8 data sets (○) taken from ref. [114] for the phosphate monoesters and from ref. [122] for the phosphonates. The points due to the equilibrium constants for the M^{2+}/NMP systems (○, ⊗, ●) are based on the values listed in Table 9. The equilibrium data for the M^{2+}/PMEA systems (◆) are from ref. [122]. These results are discussed in Section 7.3. The vertical (broken) lines emphasize the stability differences from the reference lines; they equal log $\Delta_{M/NMP}$ and log $\Delta_{M/PMEA}$, as defined in equation (14), for the M(NMP) complexes. All the plotted equilibrium constants refer to aqueous solutions at 25°C and $I = 0.1$ M ($NaNO_3$).

In $TuMP^{2-}$ a CH unit replaces the N7 of AMP^{2-} (Figures 5 and 10) which means that $TuMP^{2-}$ is no longer able to form the mentioned macrochelates. Indeed, the stability constants of its M(TuMP) complexes fit on the reference lines, thus proving that $TuMP^{2-}$ behaves like a simple phosphate monoester that binds metal ions only to its phosphate group [50,136]. Similar to the situation with pyrimidine NMPs and their N3 site, also with purines the N1 site cannot be reached in the *anti* conformation.

Table 9 Logarithms of the stability constants of several M(NMP) complexes as determined by potentiometric pH titration, together with the calculated stability constants of the 'open' forms, as well as with the enhanced complex stabilities, log $\Delta_{M/NMP}$ (eq. 14), and the extent of intramolecular macrochelate formation according to equilibrium (22) for aqueous solutions at 25°C and $I = 0.1$ M ($NaNO_3$)[a,b].

M(NMP)	log $K^{M}_{M(NMP)}$ (eqs 2, 18)	log $K^{M}_{M(NMP)op}$ (eq. 19)[c]	log $\Delta_{M/NMP}$ (eq. 14)	K_I (eqs 16, 17)	$\%M(NMP)_{cl}$ (eqs 20, 22)
Mg(AMP)	1.62 ± 0.04	1.56 ± 0.03	0.06 ± 0.05	0.15 ± 0.13	13 ± 10
Ca(AMP)	1.48 ± 0.03	1.45 ± 0.05	0.03 ± 0.06	0.07 ± 0.14	7 ± 13
Co(AMP)	2.30 ± 0.04	1.94 ± 0.06	0.36 ± 0.07	1.29 ± 0.38	56 ± 7
Zn(AMP)	2.38 ± 0.07	2.13 ± 0.06	0.25 ± 0.09	0.78 ± 0.38	44 ± 12
Cd(AMP)	2.74 ± 0.05	2.44 ± 0.05	0.30 ± 0.07	1.00 ± 0.32	50 ± 8
Mg(IMP)	1.68 ± 0.05	1.57 ± 0.03	0.11 ± 0.06	0.29 ± 0.17	22 ± 10
Ca(IMP)	1.51 ± 0.03	1.45 ± 0.05	0.06 ± 0.06	0.15 ± 0.15	13 ± 12
Co(IMP)	2.74 ± 0.03	1.94 ± 0.06	0.80 ± 0.07	5.31 ± 0.97	84 ± 2
Zn(IMP)	2.59 ± 0.04	2.13 ± 0.06	0.46 ± 0.07	1.88 ± 0.48	65 ± 6
Cd(IMP)	3.02 ± 0.05	2.45 ± 0.05	0.57 ± 0.07	2.72 ± 0.60	73 ± 4
Mg(GMP)	1.73 ± 0.03	1.57 ± 0.03	0.16 ± 0.04	0.45 ± 0.14	31 ± 7
Ca(GMP)	1.57 ± 0.03	1.45 ± 0.05	0.12 ± 0.06	0.32 ± 0.18	24 ± 10
Co(GMP)	2.99 ± 0.04	1.95 ± 0.06	1.04 ± 0.07	9.96 ± 1.82	91 ± 2
Zn(GMP)	2.83 ± 0.03	2.14 ± 0.06	0.69 ± 0.07	3.90 ± 0.76	80 ± 3
Cd(GMP)	3.25 ± 0.03	2.46 ± 0.05	0.79 ± 0.06	5.17 ± 0.83	84 ± 2

[a] For the error limits see footnotes "*a*" of Tables 3 and 4. The values for AMP are from ref. [130], those for IMP and GMP from ref. [50].

[b] The acidity constants are for $H_2(AMP)^{\pm}$ $pK^{H}_{H_2(AMP)} = 3.84 \pm 0.02$ (eq. 23) [$(N1)H^+$ site] and $pK^{H}_{H(AMP)} = 6.21 \pm 0.01$ (eq. 3), for $H_2(IMP)^{\pm}$ $pK^{H}_{H_2(IMP)} = 1.30 \pm 0.10$ (eq. 23) [mainly $(N7)H^+$; see Figure 2 in ref. [74] for the micro acidity constants], $pK^{H}_{H(IMP)} = 6.22 \pm 0.01$ (eq. 3) and $pK^{H}_{IMP} = 9.02 \pm 0.02$ (eq. 7), and for $H_2(GMP)^{\pm}$ $pK^{H}_{H_2(GMP)} = 2.48 \pm 0.04$ (eq. 23) [$(N7)H^+$ site], $pK^{H}_{H(GMP)} = 6.25 \pm 0.02$ (eq. 3) and $pK^{H}_{GMP} = 9.49 \pm 0.02$ (eq. 7) [74].

[c] The values in this column were calculated with $pK^{H}_{H(NMP)}$ and eq. (15) by using the straight-line parameters listed in refs [50,52,122].

The data assembled in Table 9 allow at least one more interesting conclusion: In all instances the formation degree of the macrochelates increases in the order $M(AMP)_{cl} < M(IMP)_{cl} < M(GMP)_{cl}$. This increase for $M(IMP)_{cl} < M(GMP)_{cl}$ is in accord with the increased basicity of N7 in GMP^{2-} compared with that of N7 in IMP^{2-} [74]. However, with AMP^{2-} the situation is more complicated: 9-methylguanine has a pK_a of 3.11 ± 0.06 [143,144] for its $(N7)H^+$ site and this value is rather close to the micro acidity constant for the same site in 9-methyladenine, $pk^{N7\text{-}N1}_{H\bullet N7\text{-}N1} = 2.96 \pm 0.10$ [143]. Hence, the N7 basicity cannot be responsible for the decreased complex stability. Similar to the situation with pyrimidine derivatives as discussed in Section 4.2, the reduced stability by about 0.5 log unit of Cd(AMP), compared to that of Cd(GMP), is to be attributed to the steric inhibition which $(C6)NH_2$ exercises on a metal ion coordinated at N7 [71]. The (C6)O group does not have such an effect. In contrast, it rather promotes the stability by forming outersphere bonds to a water molecule of the N7-bound metal ion [74].

Finally, a comment is needed about the effect of the ribose *versus* the 2'-deoxyribose residue on the metal ion-binding properties of purine nucleotides. Unfortunately no data for Cd^{2+} complexes are available, but for those of Mg^{2+}, Ni^{2+}, Cu^{2+}, and Zn^{2+} it was shown [121] that complex stability and extent of macrochelate formation (eq. 22) between the phosphate-coordinated metal ion and N7 of the purine residue is very similar (or even identical) for the AMP^{2-}/$dAMP^{2-}$ pair. This is different for the GMP^{2-}/$dGMP^{2-}$ pair: The stabilities of the M(dGMP) complexes are clearly higher, as are the formation degrees of the macrochelates compared to the M(GMP) complexes. This can be attributed to the enhanced basicity (Δ pK_a ca. 0.2 [31,121]) of N7 in the 2'-deoxy compound. It may be surmised that the complexes of Cd^{2+} also fit into the indicated picture. One may further add that the extent of macrochelation (eq. 22) is altered, if the permittivity (dielectric constant) of the solvent is changed, e.g., by adding 1,4-dioxane to an aqueous solution, as was shown for Cu^{2+} complexes of several purine-nucleotides [145–147].

6.3 Complexes of Nucleoside 5'-Di- and -Triphosphates

All the NDPs and NTPs considered here (Figures 1 and 10) form Cd(H;NDP) and $Cd(H;NTP)^-$ complexes [115,116,119,130,148], the proton being mainly at the terminal phosphate group. For the reasons already indicated in Section 6.2.1 for the $M(H;NMP)^+$ species, the corresponding Cd(H;NDP) and $Cd(H;NTP)^-$ complexes are also expected to play no or at best only a minor role at physiological pH and will therefore not be discussed here.

In the NDP^{3-} species the residue R (Figures 9 and 10) is still close enough to the terminal β-phosphate group to have a small influence on the basicity of this group. Therefore log $K^{M}_{M(R\text{-}DP)}$ *versus* p$K^{H}_{H(R\text{-}DP)}$ straight-line plots were constructed [115] to detect any possible stability enhancements for the complexes of purine-nucleoside 5'-diphosphates (*vide infra*). The important issue at this point is that in all instances the data points of the pyrimidine-nucleoside 5'-diphosphate complexes, including $Cd(UDP)^-$, $Cd(dTDP)^-$, and $Cd(CDP)^-$, fall within the error limits on the reference line constructed of ligands like phenyl diphosphate or *n*-butyl diphosphate as can be seen in Figure 12. Hence, in none of these cases does the pyrimidine-nucleobase interact with the metal ion coordinated at the phosphate residue. This corresponds to the observations discussed in Section 6.2.2 for the complexes of the pyrimidine-NMPs.

The situation for the complexes of the pyrimidine-nucleoside 5'-triphosphates is also quite similar: Here all the $H(NTP)^{3-}$ species have the same acidity constant, i.e., p$K^{H}_{H(NTP)}$ = 6.50 ± 0.05 [31,37,116–120] (see also Section 5 and footnote "b" of Table 11, *vide infra*). Indeed, for a given metal ion the stability constants of the $M(UTP)^{2-}$, $M(dTTP)^{2-}$, and $M(CTP)^{2-}$ complexes are identical within the error limits (with the single exception of $Cu(CTP)^{2-}$ [116]). Thus, these values can be averaged to obtain the stability of the 'open' complex in equilibrium (22), in which M^{2+} is only coordinated to the phosphate chain [116,119].

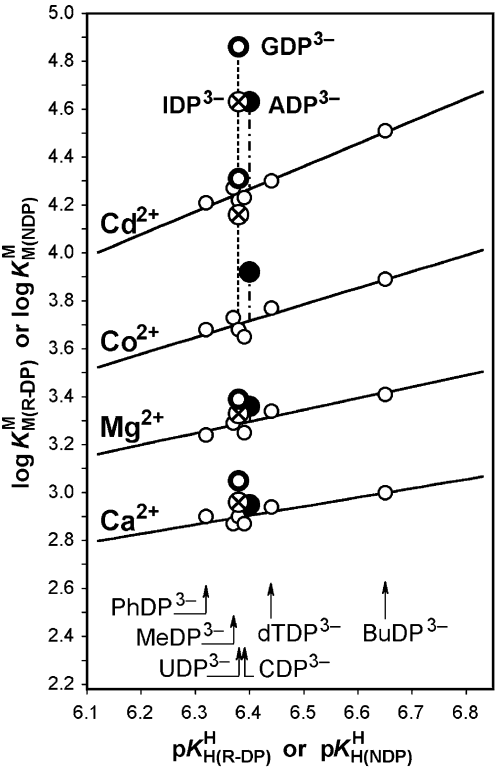

Figure 12 Evidence for an enhanced stability of the Cd^{2+} as well as the Ca^{2+}, Mg^{2+}, and Co^{2+} 1:1 complexes (eq. 2) of ADP^{3-} (●), IDP^{3-} (⊗), and GDP^{3-} (⊙), based on the relationship between log $K^{M}_{M(R\text{-}DP)}$ and $pK^{H}_{H(R\text{-}DP)}$ for simple $M(R\text{-}DP)^{-}$ complexes (○), where $R\text{-}DP^{3-}$ = phenyl diphosphate ($PhDP^{3-}$), methyl diphosphate ($MeDP^{3-}$), uridine 5'-diphosphate (UDP^{3-}), cytidine 5'-diphosphate (CDP^{3-}), thymidine [= 1-(2-deoxy-β-D-ribofuranosyl)thymine] 5'-diphosphate ($dTDP^{3-}$), and *n*-butyl diphosphate ($BuDP^{3-}$) (from left to right). The least-squares lines (eq. 15) are drawn through the indicated six data sets taken from ref. [115]. The points due to the M^{2+}/NDP systems are based on the values listed in Table 10. The vertical broken lines emphasize the stability differences from the reference lines; they equal log $\Delta_{M/NDP}$ as defined in analogy to equation (14) (see also Table 10, column 4). All the plotted equilibrium constants refer to aqueous solutions at 25°C and $I = 0.1$ M ($NaNO_3$).

With the above information at hand we are now in the position to investigate the situation for the complexes of purine-NDPs and purine-NTPs in analogy to the procedure discussed in Section 6.2.3 for M(NMP) complexes. Consequently, all the equations applied earlier, i.e., equations (16) to (20) as well as (2), (3), (7), (14), (23), and (24), are also valid here as long as L is replaced by NDP^{3-} or NTP^{4-}.

It follows from the enhanced stabilities of the purine-NDP complexes seen in Figure 12 that the formation degree of the macrochelated species according to equilibrium (22) increases within the series $Cd(ADP)^{-} \sim Cd(IDP)^{-} < Cd(GDP)^{-}$. Indeed, this is confirmed by % $M(NDP)^{-}_{cl}$ as listed in column 6 of Table 10. A similar observation is made for the $Cd(NTP)^{2-}$ complexes, that is, $Cd(ATP)^{2-}_{cl} < Cd(ITP)^{2-}_{cl} < Cd(GTP)^{2-}_{cl}$, the data of which are listed in Table 11.

At this point it is interesting to compare the results assembled in Tables 9 to 11. Of the many comparisons possible, only a few shall be indicated here. The extent of macrochelate formation in the Cd^{2+} complexes of the adenine-nucleotides is within the error limits identical, that is, $Cd(AMP)_{cl} \sim Cd(ADP)^{-}_{cl} \sim Cd(ATP)^{2-}_{cl}$. This means that the steric fit for a N7 interaction is about the same in all these complexes despite the fact that the overall stability spans a range from about 2.7 to 5.3 log units. Interestingly, for the Co^{2+} and Zn^{2+} complexes it holds $M(AMP)_{cl} > M(ADP)^{-}_{cl} \sim M(ADP)^{2-}_{cl}$; this is possibly the effect of the smaller radii of Co^{2+} and Zn^{2+} compared with the one of Cd^{2+} (Table 1). For situations with a lower formation degree of macrochelates, like with Mg^{2+} and Ca^{2+}, again $M(AMP)_{cl} \sim M(ADP)^{-}_{cl} \sim M(ATP)^{2-}_{cl}$ holds. For the $ADP^{3-}/dADP^{3-}$ pair (just as described for $AMP^{2-}/dAMP^{2-}$ in Section 6.2.3) complex stability and extent of macrochelate formation between the phosphate-coordinated metal ion and N7 of the adenine residue is very similar or even identical for the complexes of Mg^{2+}, Ni^{2+}, Cu^{2+}, Zn^{2+} [121]. In the case of $ATP^{4-}/dATP^{4-}$ the 2'-deoxy complexes are somewhat more stable and show also a slightly enhanced tendency for macrochelate formation. The same may be surmised for the corresponding Cd^{2+} complexes.

For all metal ion complexes, including those with Cd^{2+}, and for all ribose-purine nucleotides the extent of macrochelate formation increases in a first approximation for the nucleobase residues within the series adenine < hypoxanthine < guanine (Tables 9–11). This order is due to the steric influence of the $(C6)NH_2$ group in adenine, the likely partial (outersphere) participation of the (C6)O unit, and the higher basicity of N7 in guanine than in hypoxanthine as discussed already for the NMPs in Section 6.2.3. The significant formation degrees of the macrochelates involving N7 in the order of about 50 and 70% for $Zn(ITP)^{2-}_{cl}$ and $Zn(GTP)^{2-}_{cl}$, respectively (Table 11), lead to an acidification of the corresponding (N1)H sites, which amounts to $\Delta\ pK_a = 0.95$ and 1.40 for $Zn(ITP)^{2-}$ and $Zn(GTP)^{2-}$, respectively [81]. Consequently, a similar acidification is to be expected for the $Cd(ITP)^{2-}$ and $Cd(GTP)^{2-}$ complexes. Remarkably, the formation of ternary $M(Bpy)(NTP)^{2-}$ complexes with intramolecular stacks (Section 8.3) between the pyridyl and purine residues [81,140], diminishes the acidification considerably because of the removal of the metal ion from N7 [81].

There is one more point in the context of macrochelate formation. N7 may be innersphere but also outersphere bound to the already phosphate-coordinated metal ion. For example, based on several methods it was concluded for $Ni(ATP)^{2-}$ that about 30% are N7 innersphere, 25% are N7 outersphere, and 45% exist as $Ni(ATP)^{2-}_{op}$, i.e., the open form in equilibrium (22) [50,120]. In contrast, macrochelation occurs with Mg^{2+} only outersphere at N7 and with Cu^{2+} only innersphere [120]. For $Cd(ATP)^{2-}$ it was concluded that about 30% are N7 innersphere, 20% N7 outersphere, and ca. 50% exist as $Cd(ATP)^{2-}_{op}$ [116,120]. Similarly, based on ^1H NMR shift experiments it became evident that $Mg(ITP)^{2-}_{cl}$ and $Mg(GTP)^{2-}_{cl}$ are of an outersphere type [119,137], but that $Cd(ITP)^{2-}_{cl}$ and $Cd(GTP)^{2-}_{cl}$ are largely innersphere bound to N7. For the three $Mg(NDP)^{-}$ complexes with ADP^{3-}, IDP^{3-}, and GDP^{3-} again only outersphere binding to N7 is postulated, and for $Cd(IDP)^{-}_{cl}$ and $Cd(GDP)^{-}_{cl}$ it is concluded that they occur with

Table 10 Comparison of the measured stability constants, $K^{M}_{M(NDP)}$, of the $M(ADP)^{-}$, $M(IDP)^{-}$ and $M(GDP)^{-}$ complexes with the stability constants, $K^{M}_{M(NDP)op}$, of the corresponding isomers with a sole diphosphate coordination of M^{2+}, and extent of the intramolecular macrochelate formation according to equilibrium (22) in the mentioned $M(NDP)^{-}$ complexes in aqueous solution at 25°C and $I = 0.1$ M ($NaNO_3$)[a,b].

$M(NDP)^{-}$	$\log K^{M}_{M(NDP)}$ (eqs 2, 18)	$\log K^{M}_{M(NDP)op}$ (eq. 19)[c]	$\log \Delta_{M/NDP}$ (eq. 14)	K_I (eqs 16, 17)	$\%M(NDP)^{-}_{cl}$ (eqs 20, 22)
$Mg(ADP)^{-}$	3.36 ± 0.03	3.30 ± 0.03	0.06 ± 0.04	0.15 ± 0.11	13 ± 9
$Ca(ADP)^{-}$	2.95 ± 0.02	2.91 ± 0.03	0.04 ± 0.04	0.10 ± 0.09	9 ± 8
$Co(ADP)^{-}$	3.92 ± 0.02	3.72 ± 0.05	0.20 ± 0.05	0.58 ± 0.20	37 ± 8
$Zn(ADP)^{-}$	4.28 ± 0.05	4.12 ± 0.03	0.16 ± 0.06	0.44 ± 0.19	31 ± 9
$Cd(ADP)^{-}$	4.63 ± 0.04	4.27 ± 0.03	0.36 ± 0.05	1.29 ± 0.26	56 ± 5
$Mg(IDP)^{-}$	3.33 ± 0.03	3.29 ± 0.03	0.04 ± 0.04	0.10 ± 0.11	9 ± 9
$Ca(IDP)^{-}$	2.96 ± 0.06	2.90 ± 0.03	0.06 ± 0.07	0.15 ± 0.18	13 ± 13
$Co(IDP)^{-}$	4.16 ± 0.05	3.70 ± 0.05	0.46 ± 0.07	1.88 ± 0.47	65 ± 6
$Zn(IDP)^{-}$	4.34 ± 0.05	4.09 ± 0.03	0.25 ± 0.06	0.78 ± 0.24	44 ± 8
$Cd(IDP)^{-}$	4.63 ± 0.06	4.25 ± 0.03	0.38 ± 0.07	1.40 ± 0.37	58 ± 6
$Mg(GDP)^{-}$	3.39 ± 0.04	3.29 ± 0.03	0.10 ± 0.05	0.26 ± 0.14	21 ± 9
$Ca(GDP)^{-}$	3.05 ± 0.05	2.90 ± 0.03	0.15 ± 0.06	0.41 ± 0.19	29 ± 10
$Co(GDP)^{-}$	4.31 ± 0.05	3.70 ± 0.05	0.61 ± 0.07	3.07 ± 0.66	75 ± 4
$Zn(GDP)^{-}$	4.52 ± 0.03	4.09 ± 0.03	0.43 ± 0.04	1.69 ± 0.26	63 ± 4
$Cd(GDP)^{-}$	4.86 ± 0.03	4.25 ± 0.03	0.61 ± 0.04	3.07 ± 0.40	75 ± 2

[a] For the error limits see footnotes "*a*" of Tables 3 and 4. The values for ADP are from ref. [130], those for IDP and GDP from ref. [148].

[b] The acidity constants [130,148] are for $H_2(ADP)^{-}$ $pK^{H}_{H_2(ADP)} = 3.92 \pm 0.02$ (eq. 23) [$(N1)H^{+}$ site] and $pK^{H}_{H(ADP)} = 6.40 \pm 0.01$ (eq. 3), for $H_2(IDP)^{-}$ $pK^{H}_{H_2(IDP)} = 1.82 \pm 0.03$ (eq. 23) [mainly $(N7)H^{+}$], $pK^{H}_{H(IDP)} = 6.38 \pm 0.02$ (eq. 3) and $pK^{H}_{IDP} = 9.07 \pm 0.02$ (eq. 7), and for $H_2(GDP)^{-}$ $pK^{H}_{H_2(GDP)} = 2.67 \pm 0.02$ (eq. 23) [$(N7)H^{+}$ site], $pK^{H}_{H(GDP)} = 6.38 \pm 0.01$ (eq. 3) and $pK^{H}_{GDP} = 9.56 \pm 0.03$ (eq. 7).

[c] The values in this column were calculated with $pK^{H}_{H(NDP)}$ and eq. (15) by using the straight-line parameters listed in ref. [115].

nearly 100% innersphere coordination to N7 [149]. For $Cd(ADP)^{-}_{cl}$ also a significant N7 innersphere binding is surmised [149].

Finally, it is well known that metal ions promote the dephosphorylation of NTPs [117,150] and for the promoted hydrolysis of ATP at pH 7.5 the order $Cu^{2+} > Cd^{2+} > Zn^{2+} \gg Mn^{2+} \geq Ni^{2+} > Mg^{2+}$ was established [29,150]. It should be noted that $M_2(NTP)$ complexes are especially reactive in the hydrolysis reaction, which is actually a transphosphorylation to a water molecule; the reactive coordination mode is M(α,β)-M(γ) because this facilitates the break between the β- and γ-phosphate groups [29,117].

6.4 Complexes of Less Common Nucleotides

The structures of the nucleoside residues of the nucleotides considered in this section are shown in Figures 1 (Ado), 5 (Tu), and 8 (Or^{-}, Xao, U2S, U4S). The

Table 11 Comparison of the measured stability constants, $K^{M}_{M(NTP)}$, of the $M(ATP)^{2-}$, $M(ITP)^{2-}$ and $M(GTP)^{2-}$ complexes with the stability constants, $K^{M}_{M(NTP)op}$, of the corresponding isomers with a sole coordination of M^{2+} to the triphosphate chain, and extent of the intramolecular macrochelate formation according to equilibrium (22) in the mentioned $M(NTP)^{2-}$ complexes in aqueous solution at 25°C and $I = 0.1$ M ($NaNO_3$)[a,b].

$M(NTP)^{2-}$	log $K^{M}_{M(NTP)}$ (eqs 2, 18)	log $K^{M}_{M(NTP)op}$ (eq. 19)[c]	log $\Delta_{M/NTP}$ (eq. 14)	K_I (eqs 16, 17)	$\%M(NTP)^{-}_{cl}$ (eqs 20, 22)
$Mg(ATP)^{2-}$	4.29 ± 0.03	4.21 ± 0.04	0.08 ± 0.05	0.20 ± 0.14	17 ± 10
$Ca(ATP)^{2-}$	3.91 ± 0.03	3.84 ± 0.05	0.07 ± 0.06	0.17 ± 0.16	15 ± 12
$Co(ATP)^{2-}$	4.97 ± 0.09	4.76 ± 0.03	0.21 ± 0.09	0.62 ± 0.34	38 ± 13
$Zn(ATP)^{2-}$	5.16 ± 0.06	5.02 ± 0.02	0.14 ± 0.06	0.38 ± 0.19	28 ± 10
$Cd(ATP)^{2-}$	5.34 ± 0.03	5.07 ± 0.03	0.27 ± 0.04	0.86 ± 0.17	46 ± 5
$Mg(ITP)^{2-}$	4.29 ± 0.04	4.21 ± 0.04	0.08 ± 0.06	0.20 ± 0.17	17 ± 11
$Ca(ITP)^{2-}$	3.93 ± 0.05	3.84 ± 0.05	0.09 ± 0.07	0.23 ± 0.20	19 ± 13
$Co(ITP)^{2-}$	5.08 ± 0.07	4.76 ± 0.03	0.32 ± 0.08	1.09 ± 0.38	52 ± 9
$Zn(ITP)^{2-}$	5.32 ± 0.06	5.02 ± 0.02	0.30 ± 0.06	1.00 ± 0.28	50 ± 7
$Cd(ITP)^{2-}$	5.62 ± 0.05	5.07 ± 0.03	0.55 ± 0.06	2.55 ± 0.49	72 ± 4
$Mg(GTP)^{2-}$	4.31 ± 0.04	4.21 ± 0.04	0.10 ± 0.06	0.26 ± 0.17	21 ± 11
$Ca(GTP)^{2-}$	3.96 ± 0.03	3.84 ± 0.05	0.12 ± 0.06	0.32 ± 0.18	24 ± 10
$Co(GTP)^{2-}$	5.34 ± 0.05	4.76 ± 0.03	0.58 ± 0.06	2.80 ± 0.53	74 ± 4
$Zn(GTP)^{2-}$	5.52 ± 0.05	5.02 ± 0.02	0.50 ± 0.05	2.16 ± 0.36	68 ± 4
$Cd(GTP)^{2-}$	5.82 ± 0.05	5.07 ± 0.03	0.75 ± 0.06	4.62 ± 0.78	82 ± 2

[a] For the error limits see footnotes "*a*" of Tables 3 and 4. The values for ATP are from refs [116,119], those for ITP and GTP from ref. [119].

[b] The acidity constants [37] are for $H_2(ATP)^{2-}$ $pK^{H}_{H_2(ATP)} = 4.00 \pm 0.01$ (eq. 23) [$(N1)H^+$ site] and $pK^{H}_{H(ATP)} = 6.47 \pm 0.01$ (eq. 3), for $H_2(ITP)^{2-}$ $pK^{H}_{H_2(ITP)} = 2.19 \pm 0.05$ (eq. 23) [mainly $(N7)H^+$; see [33]], $pK^{H}_{H(ITP)} = 6.47 \pm 0.02$ (eq. 3) and $pK^{H}_{ITP} = 9.11 \pm 0.03$ (eq. 7), and for $H_2(GTP)^{2-}$ $pK^{H}_{H_2(GTP)} = 2.94 \pm 0.02$ (eq. 23) [$(N7)H^+$ site], $pK^{H}_{H(GTP)} = 6.50 \pm 0.02$ (eq. 3) and $pK^{H}_{GTP} = 9.57 \pm 0.02$ (eq. 7).

[c] log $K^{M}_{M(NTP)op} = K^{M}_{M(PyNTP)}$, where $PyNTP^{4-}$ = pyrimidine-nucleoside 5'-triphosphate; this means, for each metal ion the stability constants of the $M(UTP)^{2-}$, $M(dTTP)^{2-}$, and $M(CTP)^{2-}$ complexes have been averaged, with the exception for Cu^{2+}, where only the values for $Cu(UTP)^{2-}$ and $Cu(dTTP)^{2-}$ have been used [116] (see also [119]).

corresponding nucleoside monophosphates result if the (C5)OH group is phosphorylated (see also Figure 10) with the exception of 2'- and 3'AMP^{2-} where the phosphate group is located at C2 or C3, respectively.

6.4.1 Tubercidin 5'-Monophosphate

Tubercidin 5'-monophosphate, an analogue of AMP^{2-}, is synthesized by molds and fungi, as already indicated in Section 4.3.1. The corresponding nucleoside is identical in its structure with adenosine (Figures 1 and 5) except that N7 is substituted by CH [50,136]. As already indicated in Section 6.2.2, $TuMP^{2-}$ behaves in its binding properties towards Cd^{2+} like a pyrimidine-NMP, that is, like a simple phosphate monoester ligand. This conclusion is confirmed by calculating

the expected stability constant of the 'open' isomer (eqs 14, 19) for Cd(TuMP) by application of equation (25) and $pK^{H}_{H(TuMP)} = 6.32$ (Table 8): The result $\log K^{Cd}_{Cd(TuMP)calc} = 2.48 \pm 0.05$ is within the error limits identical with the measured stability constant $\log K^{Cd}_{Cd(TuMP)exp} = 2.42 \pm 0.07$ (Table 8), thus proving that equilibrium (22) is far to its left side. Because N7 is not present and the N1 site cannot be reached in $TuMP^{2-}$ by a phosphate-coordinated metal ion, the tubercidin moiety has no effect on the stability of M(TuMP) complexes [136]. The steric inhibition exercised by the $(C6)NH_2$ group on Cd^{2+} coordination to N1 has been quantified with *o*-amino(methyl)pyridine-type ligands [59] (see also Figure 6). This is mentioned here because this compound and derivatives thereof are often used as structural analogues of their corresponding parent adenine compounds.

6.4.2 Nucleoside 2'- and 3'-Monophosphates

Other adenine-nucleotides, which occur in nature and which are important for nucleic acids, are $2'AMP^{2-}$ and $3'AMP^{2-}$; several of their complexes have been studied [32,48]. What types of macrochelates are possible with these two AMPs? By considering their structures (cf. with Figure 10) it is evident that N7, though crucial for the properties of the M(5'AMP) complexes (Section 6.2.3; Table 9), is for steric reasons not accessible to a metal ion already bound to either the 2'- or 3'-phosphate group. Indeed, the stability enhancements observed for Cd(2'AMP) and Cd(3'AMP) are with $\log \Delta_{Cd/2'AMP} = 0.06 \pm 0.07$ and $\log \Delta_{Cd/3'AMP} = 0.02 \pm 0.06$ (3σ) (eq. 14) very small or even zero [48] (cf. with $\log \Delta_{Cd/5'AMP} = 0.30 \pm 0.07$; Table 9) and within the error limits also identical allowing no sophisticated conclusions. Nevertheless, one might be tempted to postulate some chelate formation with the neighboring OH groups of the ribose ring for both AMPs.

However, in the light of the discussions in Sections 3.2 and 3.3 the above indication appears as highly unlikely and based on the results obtained with Cu(2'AMP) and Cu(3'AMP) it can actually be excluded: The steric conditions for $2'AMP^{2-}$ and $3'AMP^{2-}$ to form such 7-membered chelates are identical and therefore equivalent properties for both complexes are expected, yet the results are $\log \Delta_{Cu/2'AMP} = 0.26 \pm 0.08$ and $\log \Delta_{Cu/3'AMP} = 0.08 \pm 0.08$ corresponding to formation degrees of $45 \pm 10\%$ and $17 \pm 16\%$ for $Cu(2'AMP)_{cl}$ and $Cu(3'AMP)_{cl}$, respectively [48]. Thus, different structural qualities of the two AMPs must be responsible for the different properties of the two complexes. The obvious conclusion is that in Cu(2'AMP) partial macrochelate formation occurs by an interaction of the 2'-phosphate-coordinated metal ion with N3 of the adenine residue. Actually, $2'AMP^{2-}$ in its preferred *anti* conformation is perfectly suited for this type of macrochelate formation [48], whereas in Cu(3'AMP) an N3 interaction can only be achieved if the nucleotide adopts the less favored *syn* conformation – and this costs energy and results thus in the observed lower formation degree of the macrochelate.

The following results obtained for the Cd^{2+} complexes of 2'GMP^{2-}, 3'GMP^{2-}, and 2'-deoxy-3'GMP^{2-} [151] corroborate at least to some extent with the above conclusions:

$$\log \Delta_{Cd/2'GMP} = 0.35 \pm 0.07 \quad \%Cd(2'GMP)_{cl} = 55 \pm 7$$
$$\log \Delta_{Cd/3'GMP} = 0.34 \pm 0.09 \quad \%Cd(3'GMP)_{cl} = 54 \pm 9$$
$$\log \Delta_{Cd/2'd3'GMP} = 0.29 \pm 0.09 \quad \%Cd(2'd3'GMP)_{cl} = 49 \pm 10$$

The stability enhancements for Cd(2'GMP) and Cd(3'GMP) are of about the same size, indicating that for the larger Cd^{2+} (compared with Cu^{2+}) the *anti*/*syn* transformation is apparently of lower relevance. The most important conclusion from this list, however, is the fact that removal of the 2'-hydroxy group from the ribose ring does not affect the stability enhancement and the degree of chelate formation. Hence, one may conclude that the 2'-OH group is not involved in metal ion binding and that an interaction with N3 is responsible for the stability enhancement. It should be added here that it is becoming increasingly clear from solution [152–154] as well as X-ray crystal structure studies that the N3 site of a purine may bind metal ions [155–160]. For example, Pt^{2+} [155] and Cd^{2+} [156] bind via N3 to adenine derivatives, Pd^{2+} to N6',N6',N9-trimethyladenine [157], Pt^{2+} to a guanine derivative [158], as well as Cu^{2+} [159] and Ni^{2+} [160] to neutral adenine.

6.4.3 Orotidinate 5'-Monophosphate

In Figure 8 (top, left) the structure of orotidine, the nucleoside of the above nucleotide, is shown; a stability constant of its Cd^{2+} complex has been measured [93]. Orotidinate 5'-monophosphate (OMP^{3-}) is involved in the biosynthesis of pyrimidine-nucleotides: OMP^{3-} is decarboxylated to UMP^{2-} (cf. Figures 1 and 8), which is then further transformed, e.g., to UTP^{4-} or CTP^{4-} (Figure 10). OMP^{3-} itself exists predominately in the *syn* conformation, which is depictured for H(Or) in Figure 8 (top, left) (i.e., the (C2)O group being above the ribose ring).

The carboxylic acid group at C6 of OMP is very acidic and is deprotonated with $pK_a = 1.46 \pm 0.10$ [93]. Due to the resulting negative charge the deprotonation of the $P(O)_2(OH)^-$ group of $H(OMP)^{2-}$ occurs at a slightly higher pH, i.e., $pK_a = 6.40 \pm 0.02$ [93], than that of the corresponding group of $H(UMP)^-$, i.e., $pK^H_{H(UMP)} = 6.15 \pm 0.01$ (Table 8). Consequently, at the physiological pH of 7.5 the species OMP^{3-} and UMP^{2-} dominate. For Cd(UMP) we have seen that the uracil moiety does not participate in metal ion binding (Section 6.2.2) and that its stability constant fits on the reference line (Figure 11). This is different for the stability of $Cd(OMP)^-$ which is by $\log \Delta_{Cd/OMP} = 0.49 \pm 0.07$ above this line and hence, this complex is more stable than expected on the basis of the basicity of the phosphate group. However, this enhanced complex stability is solely a charge effect of the non-coordinating (C6)COO^- group as follows from the average of the stability enhancements observed for 10 different M^{2+} ions in their $M(OMP)^-$ complexes, i.e., $\log \Delta_{M/OMP} = 0.40 \pm 0.06$ (3σ) (defined according to eq. 14) [93]. At higher

pH values when the (N3)H site is becoming deprotonated, the different metal ions behave differently due to their different affinity for an $(N3)^-$ site (Section 4.2; Figure 7): Now $Cd(OMP - H)^{2-}$ exists as a macrochelate with a formation degree of 93 ± 2% (see equilibrium 22); the phosphate-bound Cd^{2+} interacts with the $(N3)^-$ site [93], which is sterically easily reached (see Figure 8, top, left).

6.4.4 Xanthosinate 5'-Monophosphate

Like OMP being an intermediate in the metabolism of pyrimidines, XMP is one in the metabolism of purines (Section 4.3.3). It is most important to note that XMP exists at the physiological pH of 7.5 as a xanthine-deprotonated $(XMP - H)^{3-}$ species, more exactly written as $(X - H{\cdot}MP)^{3-}$ (see Figure 13) [96]. This fact has so far mostly been overlooked [96,161] and XMP is commonly written in textbooks in analogy to GMP^{2-} (see Figures 1 and 10), which is *not* correct. It must further be noted that in XMP the deprotonation of the xanthine moiety ($pK_a = 5.30 \pm 0.02$) takes place before that of the $P(O)_2(OH)^-$ group ($pK_a = 6.45 \pm 0.02$) [96]. Naturally, these acid-base properties affect the coordination chemistry of XMP [97,162,163].

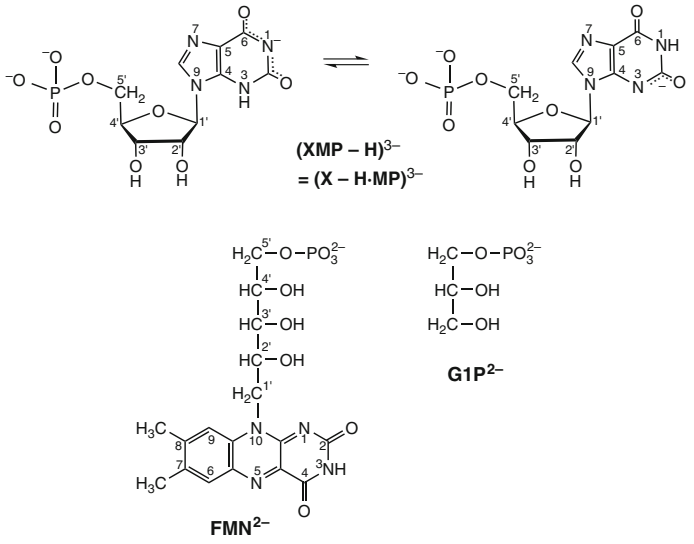

Figure 13 Chemical structures of xanthosinate 5'-monophosphate, which exists at the physiological pH of about 7.5 as $(XMP - H)^{3-}$, with a tautomeric equilibrium between $(N1)^-/(N3)H$ and $(N1)H/(N3)^-$ sites [96,97,162], and flavin mononucleotide (FMN^{2-} = riboflavin 5'-phosphate) as well as for comparison of glycerol 1-phosphate ($G1P^{2-}$). $(XMP - H)^{3-}$ is shown in its dominating *anti* conformation [11–13].

The M(XMP) complexes are quite special and they are better written as $(M{\cdot}X - H{\cdot}MP{\cdot}H)^{\pm}$ to indicate that the phosphate group carries a proton, and that the metal

ion is coordinated to N7 possibly also undergoing an (outersphere) interaction with (C6)O. With the nine metal ions Ba^{2+}, Sr^{2+}, Ca^{2+}, Mg^{2+}, Mn^{2+}, Co^{2+}, Cu^{2+}, Zn^{2+}, and Cd^{2+} the average stability enhancement for these complexes amounts to $\log \Delta_{M/XMP} = 0.46 \pm 0.11$ (3σ) [162]. These stability enhancements are based on the basicity- and charge-corrected stabilities of the M(xanthosinate)$^+$ complexes [162]. This equality indicates that the interaction of the N7-bound M^{2+} ions with the monoprotonated phosphate group occurs in an outersphere manner [97,162]. The stability enhancement for the $(Cd{\cdot}X - H{\cdot}MP{\cdot}H)^{\pm}$ complex is at the lower limit of the mentioned average, but with $\log \Delta_{Cd/XMP} = 0.30 \pm 0.16$ still within the error limits. From the given stability enhancements formation degrees of $64 \pm 9\%$ (3σ) follow on average for the $(M{\cdot}X - H{\cdot}MP{\cdot}H)^{\pm}_{cl}$ [$= M(XMP)_{cl}$] species (eq. 22), and $50 \pm 18\%$ if $(Cd{\cdot}X - H{\cdot}MP{\cdot}H)^{\pm}_{cl}$ is considered specifically, but again, the values overlap within the error limits [97,162].

Upon deprotonation of the phosphate group, which then becomes the primary binding site, the metal ions show, as expected (see, e.g., Figure 11), their common individual properties. Macrochelate formation according to equilibrium (22) involving N7 [and possibly also (C6)O] results for the $M(XMP - H)^-$ complexes, also written as $(X - H{\cdot}MP{\cdot}M)^-$ [162]. The stability enhancement $\log \Delta_{Cd(XMP-H)} = 1.05 \pm 0.17$ (eq. 14) corresponds to a formation degree of $91 \pm 3\%$ for $(X - H{\cdot}MP{\cdot}Cd)^-_{cl}$. The corresponding complexes with Cu^{2+} and Zn^{2+} form to $95 \pm 2\%$ ($\log \Delta_{Cu(XMP-H)} = 1.33 \pm 0.17$) and $88 \pm 5\%$ ($\log \Delta_{Zn(XMP-H)} = 0.92 \pm 0.17$), respectively, whereas for Mn^{2+} only $48 \pm 22\%$ form ($\log \Delta_{Mn(XMP-H)} = 0.28 \pm 0.18$) [162]. It may be added that by a different evaluation method [164], in which the various binding sites were considered independently [97], it was concluded that the total amount of $Cd(XMP - H)^-_{cl}$ [$= (X - H{\cdot}MP{\cdot}Cd)^-_{cl}$] (eq. 22) equals $87 \pm 4\%$ (which agrees within the error limits with the above result of $93 \pm 3\%$), but that there are two open isomers, one in which Cd^{2+} is coordinated to the phosphate group of $(XMP - H)^{3-}$ and one where it is at the xanthinate residue (Figure 13), the formation degrees being 9 and 4%, respectively [97].

6.4.5 Thiouracil Nucleotides

Though rare, thiouracil nucleotides occur in nature (see also Section 4.3.4), for example, 4-thiouridine 5'-monophosphate ($U4SMP^{2-}$) in bacterial and archaeal tRNA [100,101]. This nucleotide and its relative, 2-thiouridine 5'-monophosphate ($U2SMP^{2-}$), will be considered in this section. The structure of both nucleotides is evident if the formulas shown in Figure 8 are combined with the content of Figure 10.

It is revealing to compare first the acidity constants of the two thiouracil nucleotides with those of the parent compound, that is, uridine 5'-monophosphate (Figures 1 and 10): Deprotonation of the monoprotonated phosphate groups in $H(U2SMP)^-$ and $H(U4SMP)^-$ occurs with $pK^H_{H(U2SMP)} = 6.10 \pm 0.02$ and $pK^H_{H(U4SMP)} = 6.07 \pm 0.03$, respectively [105]; these values are very similar to that of the parent $H(UMP)^-$ species, $pK^H_{H(UMP)} = 6.15 \pm 0.01$ [114]. This is very different for the deprotonation

of the (N3)H sites in these compounds: For $U2SMP^{2-}$ and $U4SMP^{2-}$ $pK^{H}_{U2SMP} = 8.30 \pm 0.01$ and $pK^{H}_{U4SMP} = 8.23 \pm 0.02$, respectively [165], hold, showing that, if compared with UMP^{2-}, i.e., $pK^{H}_{UMP} = 9.45 \pm 0.02$ [114], the exchange of (C)O by a (C)S group has a very pronounced effect.

The problem is that M(USMP) complexes, where $USMP^{2-}$ = $U2SMP^{2-}$ or $U4SMP^{2-}$, form, at least in part [105,165], but that these species are better written as $[M{\cdot}(US - H)MP{\cdot}H]^{\pm}$, that is, the proton is at the phosphate group and the metal ion at the deprotonated uracil residue; of course, these species lose easily their proton from the $P(O)_2(OH)^-$ group (pK_a ca. 5.7 [165]). This result is not surprising if one compares, e.g., the stability of the $Cd(U - H)^+$ complexes in Figure 7 with that of Cu(UMP) in Figure 11; there is clearly the tendency visible that qualifies the (N3)-deprotonated thiouracil group as the primary binding site.

For the above reason the open species of the thiouracilate and phosphate groups were individually evaluated by considering also a potential chelate formation [105]. The result is that for $Cd[(U4S - H)MP]^-$ the complex is to 99% present as $[Cd{\cdot}(U4S - H)MP]^-$ (base-bound) and only 1% exists as $[(U4S - H)MP{\cdot}Cd]^-$ (phosphate-bound), hence, the Cd^{2+}-thiouracilate isomer dominates strongly; no indication for chelate formation was found. This is understandable because the structure of $[(U4S - H)MP]^{3-}$ is such that a metal ion bound at the $(C4)S/(N3)^-$ unit can hardly reach the phosphate group and *vice versa* (see Figure 8). Of course, the two open species are also in equilibrium with each other.

For $Cd[(U2S - H)MP]^-$ exactly the same isomer distribution may be surmised [105] because for the chelate effect [164] only 0.11 ± 0.15 log unit were derived [105]. Hence, within the error limits the chelate effect is zero, meaning that no chelate forms. However, based on the mentioned 0.11 log unit it could be that about 20% chelate, $M[(U2S - H)MP]^-_{cl}$, exist and that the remaining 80% of the open species are then present to ca. 79% with Cd^{2+} at the thiouracilate residue and about 1% bound at the phosphate group [105]. Of course, chelate formation of a metal ion coordinated at the $(C2)S/(N3)^-$ site with the phosphate group (or *vice versa*) is only possible if the nucleotide is transformed into the *syn* conformer (Figure 8). In any case, it is evident that replacement of (C)O by (C)S in the nucleobase residue enhances the stability of the Cd^{2+} complexes considerably.

6.4.6 Flavin Mononucleotide

Flavin mononucleotide (FMN^{2-}), also known as riboflavin 5'-phosphate, is a coenzyme of a large number of enzymes which catalyze redox reactions in biological systems [90,91]. It is composed of the 7,8-dimethyl isoalloxazine (i.e., the flavin) ring system, which is bound via N10 to the methylene group of the sugar-related ribit, giving 7,8-dimethyl-10-ribityl-isoalloxazine, also known as riboflavin or vitamin B_2 [90,91], which carries at its 5' position a phosphate monoester residue (see Figure 13, bottom). The corresponding $P(O)_2(OH)^-$ group has an acidity constant of the expected order, i.e., $pK_a = 6.18 \pm 0.01$ [166].

Surprisingly, the stability constants of the M(FMN) complexes, where M^{2+} = Mg^{2+}, Ca^{2+}, Sr^{2+}, Ba^{2+}, Mn^{2+}, Co^{2+}, Ni^{2+}, Cu^{2+}, Zn^{2+}, and Cd^{2+}, are throughout slightly more stable than is expected from the basicity of the phosphate group. This stability enhancement, as already summarized in the context of a Ni^{2+} review [40], amounts on average to log $\Delta_{M/FMN} = 0.16 \pm 0.04$ (3σ) (eq. 14) including also the value for the Cd(FMN) complex, log $\Delta_{Cd/FMN} = 0.17 \pm 0.06$ (3σ) [166]. This slight stability increase cannot be attributed to the formation of a 7-membered chelate according to equilibrium (5) (see Section 3.3) involving the ribit-hydroxyl group at C4'. This is demonstrated by the stabilities of the M(G1P) complexes which contain the same structural unit (Figure 13) but show no enhanced stability as already discussed in Section 3.3. Hence, in agreement with the results of a kinetic study [167] one has to conclude that the slight stability increase of the M(FMN) complexes has to be attributed to the isoalloxazine ring.

However, the equality of the stability increase of the complexes for all ten mentioned metal ions precludes its attributions to an interaction with a N site of the neutral isoalloxazine ring and makes a specific interaction with an O site also rather unlikely (note, deprotonation of (N3)H of FMN^{2-} occurs only with pK_a = 10.08 ± 0.05 [166]). Furthermore, carbonyl oxygens in aqueous solution are no favored binding sites in macrochelate formation (see Section 3.3). Maybe an outersphere interaction could be proposed – but to which site? The most likely explanation is the earlier proposal [166] that the small but overall significant stability increase originates from "bent" M(FMN) species in which the hydrophobic flavin residue [168,169] is getting close to the metal ion at the phosphate group, thereby lowering the intrinsic dielectric constant (permittivity) in the micro-environment of the metal ion and thus promoting indirectly the PO_3^{2-}/M^{2+} interaction [166].

The above mentioned average stability enhancement, log $\Delta_{M/FMN}$ = 0.16 ± 0.04, results in $K_I = 0.45 \pm 0.13$ (3σ) and a formation degree of the "bent" M(FMN) species of 31 ± 6% (3σ) [166]. It is amazing to note that this average formation degree is within the error limits identical with the one calculated [166] for $Ni(FMN)_{cl}$, i.e., 38 (±10)%, based on kinetic results [167]. Moreover, the stability data of Stuehr et al. [167], also for the Ni(FMN) complex, lead to log $\Delta_{Ni/FMN} = 0.17$ and yield 32% for $Ni(FMN)_{cl}$. To conclude, though the given explanation for the enhanced stability of the M(FMN) complexes remains somewhat uncertain, the occurrence of such a stability enhancement for the M(FMN) complexes including Cd^{2+} is definite.

7 Cadmium(II) Complexes of Nucleotide Analogues

The use of structurally altered nucleotides as probes is one way to study reactions of enzymes which involve nucleotides as substrates. Another goal for structural alterations is the hope to obtain compounds with useful pharmaceutical properties. In fact, over the years all three parts of nucleotides have been systematically

modified, i.e., the nucleobases, the ribose, and the phosphate residues [170,171]. In this section we shall discuss (at least) one example each by concentrating on such derivatives for which also the Cd^{2+} complexes have been studied. Therefore, the (N1)-oxides of the adenosine and inosine 5'-monophosphates will not be covered, though it needs to be pointed out that upon N-oxide formation the nucleobase residues become more acidic, e.g., $pK^{H}_{Ado} = 16.7$ [34,113] *versus* $pK^{H}_{Ado\cdot NO} = 12.86$ [172], and their metal ion-binding properties increase dramatically upon the loss of a proton. As a consequence, e.g., Zn^{2+} switches at pH 6.9 from the phosphate group to the deprotonated *o*-amino N-oxide unit [173]. The analogous properties are expected for Cd^{2+}. The properties of both (N1)-oxides have been reviewed [40,174]. Otherwise the organization of this section follows to a great deal one in which recently the properties of Ni^{2+} were summarized [40], but now, of course, the focus is on Cd^{2+}.

7.1 Properties of 1,N^6-Ethenoadenosine and of Its Phosphates

Formation of a 1,N^6-etheno bridge at the adenine residue leads to a 1,10-phenanthroline-like metal ion binding site in adenosine and gives so-called ε-adenosine (ε-Ado) [171]. It is thus no surprise that the stability of the Cd^{2+} complexes increases by a factor of more than 10 by going from adenosine (log $K^{Cd}_{Cd(Ado)} = 0.64$; Table 3) to ε-adenosine (log $K^{Cd}_{Cd(\varepsilon\text{-Ado})}$ = ca. 1.8 [175]). It may be added that N6 of ε-Ado can be protonated and that this proton is released with $pK^{H}_{H(\varepsilon\text{-Ado})} = 4.05 \pm 0.01$ [169]. For the most likely resonance structure of $H(\varepsilon\text{-Ado})^+$ ref. [175] should be consulted.

In accord with the above are the acid-base properties of $H_2(\varepsilon\text{-AMP})^{\pm}$ (for the structure see Figure 14, top [171,176,177]) which releases the proton from $(N6)H^+$ with $pK^{H}_{H_2(\varepsilon\text{-AMP})} = 4.23 \pm 0.02$ and the one from $P(O)_2(OH)^-$ with $pK^{H}_{H(\varepsilon\text{-AMP})} = 6.23 \pm 0.01$ [136,178]. Hence, in the neutral pH range complexes of the type M(ε-AMP) are expected and actually observed [136,178] though $M(H;\varepsilon\text{-AMP})^+$ species are also known [178]. The stability enhancement for the Zn(ε-AMP) complex, compared with a sole Zn^{2+}-phosphate binding (eq. 14), amounts to approximately 1 log unit meaning that the macrochelated species (equilibrium 22) dominate with a formation degree of about 90% [136]. Unfortunately, no data about the corresponding Cd^{2+} complex are known, but it is to be expected that the stability enhancement for Cd(ε-AMP) is at least as large as the one for Zn(ε-AMP).

In Section 6.3 we have seen that $Cd(ATP)^{2-}$ experiences a stability enhancement of log $\Delta_{Cd/ATP} = 0.27 \pm 0.04$ (Table 11) due to N7 binding of the phosphate-coordinated Cd^{2+} and that the macrochelate reaches a formation degree of about 45% (Table 11). There is no value known for $Cd(\varepsilon\text{-ATP})^{2-}$, but the extra stability enhancement for $Zn(\varepsilon\text{-ATP})^{2-}$ by going from $Zn(ATP)^{2-}$ (log $\Delta_{Zn/ATP} = 0.27$; Table 11) to $Zn(\varepsilon\text{-ATP})^{2-}$ (log $\Delta_{Zn/\varepsilon\text{-ATP}} = 0.62$ [179]) amounts to about 0.35 log unit; hence, one estimates for $Cd(\varepsilon\text{-ATP})^{2-}$ a stability enhancement of about 0.6 (= log $\Delta_{Cd/\varepsilon\text{-ATP}}$) meaning that the formation degree of $Cd(\varepsilon\text{-ATP})^{2-}_{cl}$ amounts

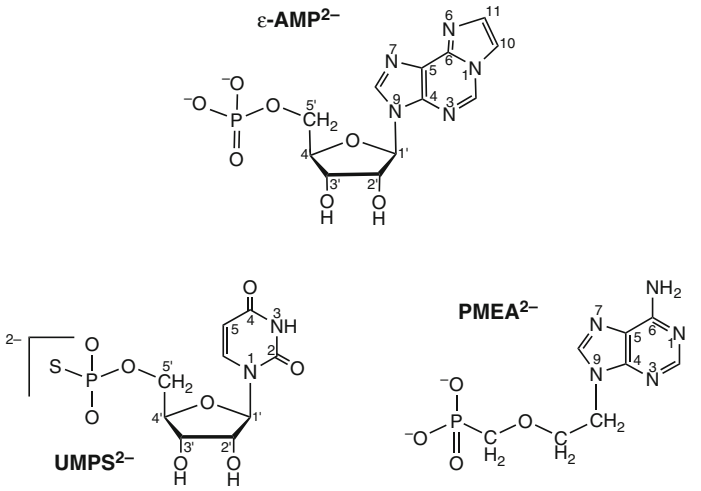

Figure 14 Chemical structures of 1,N^6-ethenoadenosine 5'-monophosphate (ε-AMP^{2-}) and of uridine 5'-*O*-thiomonophosphate ($UMPS^{2-}$), as well as of the dianion of the acyclic nucleotide analogue 9-[2-(phosphonomethoxy)ethyl]adenine ($PMEA^{2-}$). To facilitate comparisons between ε-AMP^{2-} and AMP^{2-} the conventional atom numbering for adenines is adapted, a procedure which is common [171]. The purine-nucleotide ε-AMP^{2-} [11–13] and the pyrimidine-nucleotide $UMPS^{2-}$ [11,14] are shown in their dominating *anti* conformation. ^{1}H-NMR shift measurements have shown [176] that in solution $PMEA^{2-}$ adopts an orientation which is similar to the *anti* conformation of AMP^{2-}; this conclusion is in accord with a crystal structure study [177] of the $H_2(PMEA)^{\pm}$ zwitterion.

to ca. 75% or more. The Cd^{2+}-promoted hydrolysis of ε-ATP has not been studied but from the results obtained with Cu^{2+} and Zn^{2+} [180] it is clear that the dephosphorylation reactions of ε-ATP differ significantly from those of ATP [150]. For example, the reaction in the Cu^{2+}/ATP system proceeds via a dimeric complex as the dependence of the reaction rate on the square of the concentration shows [150], whereas in the hydrolysis of the Cu^{2+}/ε-ATP system only a monomeric species is involved [180].

To conclude, it is evident that great care needs to be exercised if ε-adenosine phosphates are employed as probes for adenosine phosphates in the presence of Cd^{2+} or other divalent 3d-transition metal ions.

7.2 Complexes of Nucleoside 5'-O-Thiomonophosphates

The phosphate group of nucleotides has been altered in many ways [170]. The most popular alteration probably is the substitution of one of the oxygens by a sulfur atom. Such derivatives are then commonly employed as probes in ribozymes

[28,181]. Nevertheless, quantitative information on Cd^{2+} binding to $-OP(S)(O)_2^{2-}$ groups is scarce. There are only two studies, one involving adenosine 5'-*O*-thiomonophosphate ($AMPS^{2-}$) [170] and the other uridine 5'-*O*-thiomonophosphate ($UMPS^{2-}$) (see Figure 14; bottom, left) [182]. Into the latter study also methyl thiophosphate ($MeOPS^{2-}$) was included for reasons of comparison. Thereby it was proven, in accord with the discussion in Section 6.2.2, that the uracil residue is not involved in metal ion binding in M(UMPS) complexes. It may be added that thiophosphates are considerably less basic than phosphates with pK_a values of about 4.8 [182,183]. It was further concluded that one of the two negative charge units in a thiophosphate group is located on the sulfur atom whereas monoprotonation occurs at one of the two terminal oxygen atoms [183].

The stability constants of the Cd(PS) complexes, where $PS^{2-} = MeOPS^{2-}$, $UMPS^{2-}$ or $AMPS^{2-}$, are listed in column 2 of Table 12, together with the corresponding data for the Mg(PS) and Zn(PS) species. For the M(AMPS) complex it is assumed that macrochelate formation occurs to the same extent as in the M(AMP) complexes (see Section 6.2.3). In this way the stability enhancement due to macrochelation can be corrected for (Table 12, column 3) and one obtains

Table 12 Stability constant comparisons for the M(PS) complexes formed by Mg^{2+}, Cd^{2+}, or Zn^{2+} and methyl thiophosphate ($MeOPS^{2-}$), uridine 5'-*O*-thiomonophosphate ($UMPS^{2-}$) or adenosine 5'-*O*-thiomonophosphate ($AMPS^{2-}$) between the measured stability constants, $\log K^{M}_{M(PS)}$ (eq. 2), or the stability constants of M(AMPS) corrected for the macrochelate effect, $\log K^{M/cor}_{M(AMPS)}$, and the calculated stability constants, $\log K^{M}_{M(PS)calc}$, together with the stability difference (eq. 25) for aqueous solutions at 25°C and $I = 0.1$ M ($NaNO_3$)[a,b].

M(PS)	$\log K^{M}_{M(PS)}$	$\log \Delta_{M/AMP}$[c]	$\log K^{M/cor}_{M(AMPS)}$	$\log K^{M}_{M(PS)calc}$[d]	$\log \Delta_{M/PS}$
Mg(MeOPS)	1.33 ± 0.07			1.30 ± 0.03	0.03 ± 0.08
Mg(UMPS)	1.24 ± 0.05			1.27 ± 0.03	–0.03 ± 0.06
Mg(AMPS)	1.28 ± 0.04	0.06 ± 0.05	1.22 ± 0.06	1.25 ± 0.03	–0.03 ± 0.07
Cd(MeOPS)	4.50 ± 0.06			2.03 ± 0.05	2.47 ± 0.08
Cd(UMPS)	4.37 ± 0.08			1.97 ± 0.05	2.40 ± 0.09
Cd(AMPS)	4.62 ± 0.12	0.30 ± 0.07	4.32 ± 0.14	1.95 ± 0.05	2.37 ± 0.15
Zn(MeOPS)	2.34 ± 0.05			1.69 ± 0.06	0.65 ± 0.08
Zn(UMPS)	2.21 ± 0.06			1.63 ± 0.06	0.58 ± 0.08
Zn(AMPS)	2.52 ± 0.18	0.25 ± 0.09	2.27 ± 0.20	1.61 ± 0.06	0.66 ± 0.21

[a] For the error limits see footnotes "*a*" of Tables 3 and 4. The values for AMPS are from refs [170], those for MeOPS and UMPS from refs [182].

[b] The acidity constants are for $H(MeOPS)^-$ $pK^{H}_{H(MeOPS)} = 4.96 \pm 0.02$ (eq. 3), for $H(UMPS)^-$ $pK^{H}_{H(UMPS)} = 4.78 \pm 0.02$ (eq. 3) and $pK^{H}_{UMPS} = 9.47 \pm 0.02$ (eq. 7) [182], and for $H_2(AMPS)^{\pm}$ $pK^{H}_{H_2(AMPS)} = 3.72 \pm 0.03$ (eq. 23) and $pK^{H}_{H(AMPS)} = 4.83 \pm 0.02$ (eq. 3) [183]; the micro acidity constants for $H_2(AMPS)^{\pm}$, the second one being needed for the straight-line calculation,[d] are $pk^{AMPS\cdot H}_{H\cdot AMP\cdot H} = 3.84 \pm 0.02$ [(N1)H^+ deprotonation] and $pk^{AMPS}_{AMPS\cdot H} = 4.71 \pm 0.04$ (deprotonation of the thiophosphate group) [183].

[c] See Table 9 in Section 6.2.3 or refs [170].

[d] The values in this column were calculated with the $pK^{H}_{H(PS)}$ values given above[b] and eq. (15) by using the straight-line parameters listed in refs [50,52,122]

then stability values which reflect only the influence of the sulfur atom on metal ion binding in M(AMPS) species (column 4). Application of the previously defined straight-line plots (see Figure 11) allows then, together with the acidity constants of the $H(PS)^-$ species (see footnote "b" of Table 12), to calculate the stability of the complexes due to a (thio)phosphate-M^{2+} coordination (Table 12, column 5). Together with these values the stability difference according to equation (25) (which is analogous to eq. 14) can be calculated and in this way the effect of the sulfur substitution can be quantified:

$$\log \Delta_{M/PS} = \log K^{M}_{M(PS)} - \log K^{M}_{M(PS)calc} \tag{25}$$

From the results listed in column 6 of Table 12 it is evident that there is no difference in stability between the Mg^{2+} complexes of phosphate ($R\text{-}PO_3^{2-}$) or thiophosphate monoesters (PS^{2-}) if the different basicities of $R\text{-}PO_3^{2-}$ and PS^{2-} are taken into account. On the other hand, all three Zn(PS) complexes show within the error limits the same remarkable enhanced complex stability proving that the S atom of the thiophosphate group participates in Zn^{2+} binding. However, for the Cd(PS) complexes a very dramatic stability enhancement is observed, which is within the error limits also identical for the Cd(MeOPS), Cd(UMPS), and Cd(AMPS) species. Interestingly, if one applies the procedure described in refs [170] and [182], one calculates for the Zn(PS) complexes from the average value, $\log \Delta_{Zn/PS} = 0.63$, that about 77% of Zn^{2+} is S-coordinated and 23% is O-coordinated to the $-OP(S)(O)_2^{2-}$ residue. Yet, for the Cd(PS) species it follows from the average value, $\log \Delta_{Cd/PS} = 2.41$ (Table 12, column 6), that 99.6% of the complexes have a Cd^{2+}–S coordination and that only traces of Cd^{2+}–O coordination remain. Hence, it is clear that Cd^{2+} is considerably more thiophilic than Zn^{2+}, which is in accord with the solubility products of CdS and ZnS [170] and also the well known properties of metallothionein, which has an approximately 10000 times larger affinity for Cd^{2+} compared to that for Zn^{2+} [184]. Evidently Cd^{2+} is ideal for so-called "rescue" experiments, which are often applied in ribozyme chemistry [28,30] (see also Section 10.1).

7.3 *Complexes of Acyclic Nucleotide Analogues*

One way to alter the cyclic ribose residue of a nucleotide is to "delete" it. Indeed, acyclic nucleoside phosphonates, i.e., analogues of (2'-deoxy)nucleoside 5'-monophosphates, have been increasingly studied during the past 25 years. One of these compounds, 9-[2-(phosphonomethoxy)ethyl]adenine (PMEA; *Adefovir*; see Figure 14, bottom, right) was approved in 2002/2003 in the form of its bis-(pivaloyloxymethyl)ester for use in the therapy of hepatitis B, a disease evoked by a DNA virus. Diphosphorylated $PMEA^{2-}$, i.e., $PMEApp^{4-}$, is initially recognized by nucleic acid polymerases as an excellent substrate, but after insertion into the growing nucleic acid chain, transcription is terminated due to the lack of a

3'-hydroxyl group. Based on the metal ion-binding properties of $PMEApp^{4-}$ it can be explained why the ether oxygen in the aliphatic chain, $R–CH_2–O–CH_2–PO_3pp^{4-}$, is compulsory for a useful biological activity. The systematic progress made over the past 20 years [122] in understanding the coordination chemistry of these compounds can be followed in the reviews [153] (1995), [185] (1999), and [186] (2004) as well as in other recent works [187–189].

It can be seen from Figure 11 that the metal ion-binding properties of $PMEA^{2-}$ and AMP^{2-} differ, if one considers the stability of the Ca^{2+} complexes: Ca(PMEA) is evidently somewhat more stable than Ca(AMP)! By inclusion of the dianion of (phosphonylmethoxy)ethane (PME^{2-}) it could be shown that this increased stability is solely due to the formation of a 5-membered chelate involving the ether oxygen as expressed in equilibrium (26):

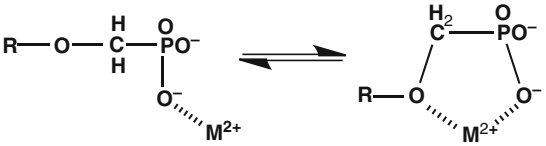

(26)

The percentage of the closed species amounts for Ca(PMEA) to 22 ± 13% (log $\Delta_{Ca/PMEA} = 0.11 \pm 0.07$) [122]. For Mn(PMEA) and Zn(PMEA) the situation is similar and the enhanced complex stabilities, log $\Delta_{Mn/PMEA} = 0.21 \pm 0.08$ and log $\Delta_{Zn/PMEA} = 0.30 \pm 0.10$ (eq. 14) [122,185], are solely explained with equilibrium (26). Exactly the same applies for the Cd(PMEA) complex with log $\Delta_{Cd/PMEA} = 0.33 \pm 0.06$ [122], which corresponds to a formation degree of the closed species of 53 ± 7% in equilibrium (26), with no hint for the coordination of any of the N sites of the adenine residue [185,186].

However, it ought to be mentioned that detailed studies over the years revealed that for Cu^{2+} [190] (and Ni^{2+} [191]) the situation is more complicated and that the four M(PMEA) isomers indicated in scheme (27) are in equilibrium with each other:

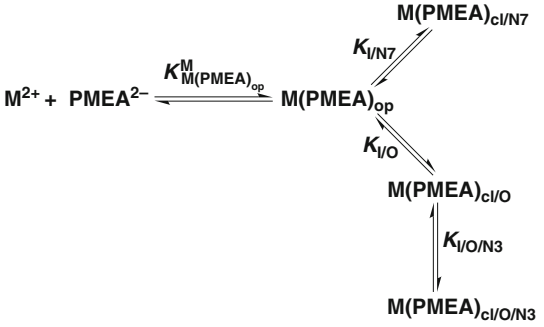

(27)

This means, there is an 'open' species in which M^{2+} is only phosphonate-coordinated, $M(PMEA)_{op}$, and which then interacts either with N7 or the ether O atom giving the chelated isomers, $M(PMEA)_{cl/N7}$ or $M(PMEA)_{cl/O}$, respectively.

Finally, the latter species may, in addition to the 5-membered chelate, also form a 7-membered ring by binding the coordinated M^{2+} also to N3, $M(PMEA)_{cl/O/N3}$. The formation degrees of the four isomers $M(PMEA)_{op}$, $M(PMEA)_{cl/N7}$, (eq. 22), $M(PMEA)_{cl/O}$ (eq. 26), and $M(PMEA)_{cl/O/N3}$ are about 17, 8, 34, and 41%, respectively, for the Cu^{2+} system [186,190–192].

Evidently, the dominating isomers in the case of Cu^{2+} are also those involving the ether O. In fact, $Cu(PMEA)_{cl/O}$ and $Cu(PMEA)_{cl/O/N3}$ amount together to 75%. This result confirms the rather high stability of the 5-membered chelates already indicated above in equilibrium (26). In contrast, the corresponding 6-membered chelate that could be formed with the dianion of 9-[2-(phosphonoethoxy)ethyl]-adenine ($PEEA^{2-}$) [one more CH_2 group is inserted between O and PO_3^{2-} (Figure 14)] is considerably less stable, what agrees with the observations described in Section 3.3. Indeed, $Cu(PEEA)_{cl/O}$ and $Cu(PEEA)_{cl/O/N3}$ amount together now to only 61%, but the formation degree of the macrochelate according to equilibrium (22), $Cu(PEEA)_{cl/N7}$, is now enhanced and amounts to about 18%. Even more revealing, with Ca^{2+} and Mg^{2+} the 6-membered chelate does not form at all, that is, $\log \Delta_{Ca/PEEA} = -0.05 \pm 0.06$ and $\log \Delta_{Mg/PEEA} = -0.01 \pm 0.07$ [193]. Also in the Cd^{2+} system $M(PEEA)_{cl/O}$ does not occur, only $Cd(PEEA)_{cl/N7}$ (eq. 22) occurs with $29 \pm 11\%$, next to the open species with a formation degree of $71 \pm 11\%$ [193].

Three lessons are to be learned here: (i) Five-membered chelates are more stable than 6-membered ones (see also Section 3.3), and this observation offers an explanation why PMEA is a nucleotide analogue with excellent antiviral properties and PEEA is not. In the latter case the second metal ion needed for the nucleotidyl transfer is not properly adjusted at the triphosphate residue [186,193] (see also the last paragraph in Section 6.3). (ii) From the Cu(PMEA) system it follows that if properly pre-orientated by another primary binding site, N3 of a purine is well able to coordinate metal ions (see also Section 6.4.2). (iii) The small structural difference as it occurs between $PMEA^{2-}$ (Figure 14) and $PEEA^{2-}$ changes the coordinating properties of Cd^{2+} towards these nucleotide analogues completely: With $PMEA^{2-}$ only the $Cd(PMEA)_{cl/O}$ isomer forms, whereas with $PEEA^{2-}$ only $Cd(PEEA)_{cl/N7}$ occurs.

7.4 *Cadmium(II) Binding to Nucleotides Containing a Platinum(II)-Coordinated Nucleobase Residue*

A further way to alter nucleotides via their nucleobases (cf. Section 7.1) is to "fix" a kinetically inert metal ion to the nucleobase. Several such examples have been studied with *cis*-$(NH_3)_2Pt^{2+}$ coordinated to N3 of $dCMP^{2-}$ [141] or to N7 of $dGMP^{2-}$ [194]. The main outcome of these studies is that the acid-base properties of the phosphate groups are only relatively little affected [195] and that this is also true for binding of divalent metal ions to the phosphate residues [141,194].

To give a specific example: Coordination of *cis*-$(NH_3)_2Pt(dGuo\text{-}N7)^{2+}$ to the N7 site of $dGMP^{2-}$ results in the complex *cis*-$(NH_3)_2Pt(dGuo\text{-}N7)(dGMP\text{-}N7)$ which may be protonated at its phosphate group. Comparison of the corresponding acidity constant, $pK^{H}_{H[Pt(dGuo)(dGMP)]} = 5.85 \pm 0.04$, with $pK^{H}_{H(dGMP)} = 6.29 \pm 0.01$ reveals an acidification of the $P(O)_2(OH)^-$ group due to charge repulsion by the N7-coordinated Pt(II) of $\Delta\ pK_a = 0.44 \pm 0.04$ [196]. The average acidification of *cis*-$(NH_3)_2Pt^{2+}$ in the same complex on the two (N1)H sites is somewhat more pronounced (as one would expect) and amounts to $\Delta\ pK_{a/av} = 0.78 \pm 0.11$ [196]. However, coordination of Mg^{2+}, Cu^{2+} or Zn^{2+} to the phosphate group of *cis*-$(NH_3)_2Pt(dGuo\text{-}N7)(dGMP\text{-}N7)$ is inhibited on average only by about 0.2 log unit [196]. The same may be surmised for Cd^{2+} binding. This moderate effect of –0.2 log unit suggests with regard to DNA or RNA that *cis*-$(NH_3)_2Pt^{2+}$, if coordinated to N7 of a guanine residue, affects metal ion binding to the nucleic acid phosphate backbone only little.

Another interesting case concerns the acyclic nucleotide analogue $PMEA^{2-}$ (Figure 12; bottom, left), already discussed in Section 7.3. Coordination of $(Dien)Pt^{2+}$ either to N1 [197] or to N7 [198] leads, if monoprotonated, to the complexes $H[(Dien)Pt(PMEA\text{-}N1)]^+$ and $H[(Dien)Pt(PMEA\text{-}N7)]^+$. Acidification of the $P(O)_2(OH)^-$ group by Pt^{2+} at N1 gives $\Delta\ pK_{a/N1} = 0.21 \pm 0.03$ (based on $pK^{H}_{H(PMEA)} = 6.90 \pm 0.01$) and by Pt^{2+} at N7 $\Delta\ pK_{a/N7} = 0.44 \pm 0.01$ [197]. The higher acidity of $H[(Dien)Pt(PMEA\text{-}N7)]^+$ provides evidence that in the (Dien)Pt(PMEA-*N7*) complex in aqueous solution an intramolecular, outersphere macrochelate is formed through hydrogen bonds between the PO_3^{2-} residue of $PMEA^{2-}$ and a Pt(II)-coordinated (Dien)-NH_2 group. This formation amounts to about 40% and is in accord with several other related observations [197].

Unfortunately, complex stability with Cd^{2+} has only been measured for (Dien)-Pt(PMEA-*N7*) as ligand: $\log K^{Cd}_{Cd[(Dien)Pt(PMEA\text{-}N7)]} = 2.13 \pm 0.09$ [198]. If this value is compared with the expected, i.e., calculated, stability constant based on the straight-line plot seen in Figure 11 and the acidity constant $pK^{H}_{H[(Dien)Pt(PMEA\text{-}N7)]} = 6.46 \pm 0.01$, that is, $\log K^{Cd}_{Cd[(Dien)Pt(PMEA\text{-}N7)]calc} = 2.52 \pm 0.05$, one obtains the stability reduction $\log \Delta_{Cd/(Dien)Pt(PMEA\text{-}N7)} = -0.39 \pm 0.10$ (in analogy to eq. 14), which is due to the repulsion between Pt^{2+} coordinated at N7 and Cd^{2+} bound at the PO_3^{2-} group (cf. Figure 14). This stability reduction is identical with the one observed for the corresponding complexes formed with Mg^{2+}, Ca^{2+}, Mn^{2+}, Co^{2+}, Ni^{2+} (and Cd^{2+}), which is on average $\log \Delta_{M/(Dien)Pt(PMEA\text{-}N7)/av} = -0.42 \pm 0.04$ [198]. This result indicates that in all these complexes the metal ion is only coordinated to the phosphonate group of the (Dien)Pt(PMEA-*N7*) ligand.

Overall, these results confirm the above conclusion that a purine-coordinated Pt^{2+} unit affects metal ion binding at the phosphate group of the same nucleotide only relatively little. This is of relevance for multiple metal ion binding to nucleotides and nucleic acids as is the already discussed result (Section 4.1) regarding $(Dien)Pt(9EtG\text{-}N7)^{2+}$ and its metal ion-binding properties, which are, despite the Pt^{2+} at N7 of the guanine residue, still quite remarkable at the $(N1)^-$ site [82] (see also ref. [69]).

8 A Short Appraisal of Mixed Ligand Complexes Containing a Nucleotide

8.1 Definitions and General Comments

In following previous considerations and pathways [40,117,139,189] we define that a mixed ligand or ternary complex of the kind to be considered here is composed of a metal ion and two different coordinated ligands. There are various ways to quantify the stability of such ternary complexes [199,200]. First we consider complexes in which a nucleotide (= NP = nucleoside phosphate) is bound in the coordination sphere of M^{2+} and to which a second ligand L binds, leading thus to the ternary $M(NP)(L)^{2+}$ complex and equilibrium (28) (charges deleted):

$$M(NP)^{2+} + L \rightleftharpoons M(NP)(L)^{2+} \tag{28a}$$

$$K^{M(NP)}_{M(NP)(L)} = [M(NP)(L)^{2+}]/([M(NP)^{2+}][L]) \tag{28b}$$

Evidently, this equilibrium is best compared with the following one (see also eq. 2):

$$M^{2+} + L \rightleftharpoons M(L)^{2+} \tag{29a}$$

$$K^{M}_{M(L)} = [M(L)^{2+}]/([M^{2+}][L]) \tag{29b}$$

The difference $\Delta \log K_{M/NP/L}$ (eq. 30),

$$\Delta \log K_{M/NP/L} = \log K^{M(NP)}_{M(NP)(L)} - \log K^{M}_{M(L)} \tag{30a}$$

$$= \log K^{M(L)}_{M(L)(NP)} - \log K^{M}_{M(NP)} \tag{30b}$$

characterizes the coordination tendency of L towards $M(NP)^{2+}$ (eq. 28) relative to $M(aq)^{2+}$ (eq. 29) and *vice versa* (eq. 30b) [199,200]. The latter point is important because it means that the difference $\Delta \log K_{M/NP/L}$ (eq. 30) also equals the one resulting from the following two equilibria:

$$M(L)^{2+} + NP \rightleftharpoons M(NP)(L)^{2+} \tag{31a}$$

$$K^{M(L)}_{M(L)(NP)} = [M(NP)(L)^{2+}]/([M(L)^{2+}][NP]) \tag{31b}$$

$$M^{2+} + NP \rightleftharpoons M(NP)^{2+} \tag{32a}$$

$$K^{M}_{M(NP)} = [M(NP)^{2+}]/([M^{2+}][NP]) \quad (32b)$$

Factors which arise through direct [139,189,201,202] or indirect (i.e., metal ion-mediated) [56,199,200,203,204] ligand-ligand interactions, being either favorable or unfavorable, will show up in this description.

One should note that $\Delta \log K_{M/NP/L}$ is the difference between two log stability constants and thus has to be a constant itself. Indeed, it quantifies the position of equilibrium (33):

$$M(NP)^{2+} + M(L)^{2+} \rightleftharpoons M(NP)(L)^{2+} + M^{2+} \quad (33a)$$

$$10^{\Delta \log K_{M/NP/L}} = \frac{[M(NP)(L)^{2+}][M^{2+}]}{[M(NP)^{2+}][M(L)^{2+}]} \quad (33b)$$

Since more coordination positions are available for binding of L to M^{2+} (eq. 29) than to $M(NP)^{2+}$ (eq. 28), one expects on statistical grounds [199,200] and in accord with the general rule [22] that $K^{M}_{M(L)} > K^{M(L)}_{M(L)_2}$ *negative* values for $\Delta \log K_{M/NP/L}$. For example, for the coordination of a bidentate ligand followed by a monodentate one in a regular octahedral (oh) coordination sphere like the one of Cd^{2+}, statistical considerations [205] provide the value $\Delta \log K_{2:1/stat/oh} = \log (4:1/6:1) = -0.18$. For two different bidentate ligands $\Delta \log K_{2:2/stat/oh} = \log (5/12) = -0.38$ [199] results. Correspondingly, for the Jahn-Teller distorted octahedral coordination sphere of Cu^{2+} a statistical value is more difficult to assess, but on the basis of previously advanced arguments [194] one obtains the values $\Delta \log K_{2:1/stat/Cu} = -0.5$ and $\Delta \log K_{2:2/stat/Cu} = -0.9$ [199,205].

The available information on mixed ligand complexes formed with Cd^{2+} and a nucleotide is rather limited. In addition, we shall concentrate below mainly on ternary complexes containing NTPs because in these instances the available equilibrium constants are relatively well defined.

8.2 *Ternary Cadmium(II) Complexes Containing ATP^{4-} and a Buffer Molecule*

Considering that many experiments in biochemistry are carried out in buffers to stabilize the pH of a solution, it is important to indicate possible drawbacks of this procedure (as was done, e.g., in refs [206–208]). In fact, the Zn^{2+}-promoted dephosphorylation of ATP is inhibited by acetate, Tris or borate buffers [150,209]. Similarly, buffers composed of imidazole [210] or phosphate [29,211] also inhibit the reactivity of M^{2+}/ATP systems. Corresponding effects must be anticipated for Cd^{2+}/NTP systems.

Tris is one of the most popular buffers used in biochemical studies probably because its buffer region encompasses the physiological to slightly alkaline pH range [212]. The same is true for Bistris which buffers in the pH range 6 to 7.5 [213]. Another widely employed buffer is Bicine [214,215] which is employed in the pH range 7.5 to 9. The structures of the three mentioned buffers are shown in Figure 15.

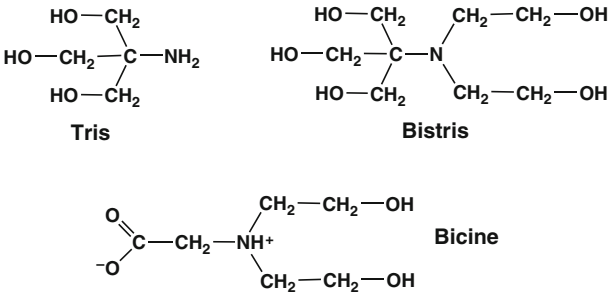

Figure 15 Chemical structures of 2-amino-2-(hydroxymethyl)-1,3-propanediol (Tris), 2-[bis(2-hydroxyethyl)amino]-2-(hydroxymethyl)-1,3-propanediol (Bistris), and *N*,*N*-bis(2-hydroxyethyl)-glycine (Bicine).

Because Bicine is derived from glycine, it was expected already nearly 50 years ago that this buffer forms complexes with metal ions [216]. For Tris and Bistris the awareness of metal ion interactions is much lower, and the fact that also mixed ligand complexes may form [212,213], has hardly been realized. Therefore, the stabilities of the ternary Cd^{2+} and some other metal ion complexes formed between these buffers and ATP^{4-} are briefly summarized. The stability constants according to equilibria (28) and (29) are listed in Table 13 together with the stability differences defined in equation (30).

The stabilities of the binary M^{2+} complexes of Tris and Bistris are quite large (Table 13, column 3) and this fact has been attributed to chelate formation with the hydroxyl groups [212,213]. The significant role of the hydroxyl group of these buffers is also confirmed by a comparison of the stability constants of the $M(Tris)^{2+}$ complexes with those of the corresponding $M(Bistris)^{2+}$ species (Table 13, column 3). The stability increase is between 0.05 and about 1.5 log units despite the fact that the basicity of the nitrogen in Bistris is about 1.5 p*K* units lower (see footnote "b" in Table 13). This confirms the earlier conclusion that most of the hydroxyl groups of Bistris participate in metal ion binding [213]. The rather high stability of the $Ca(Bistris)^{2+}$ complex is kind of a surprise but it has been verified [206]. The reason is probably that Ca^{2+} with its relatively large ionic radius fits well into the "pocket" provided by Bistris [57]. Moreover, it is known that Ca^{2+} has an exceptionally high affinity towards hydroxyl groups [57]. The stability of $Cd(Bistris)^{2+}$ is also relatively large, but again, it has been confirmed [208].

Table 13 Stability constants of some ternary M(ATP)(L) (eq. 28) and binary M(L) complexes (eq. 29), where L = Tris [212], Bistris [213], or Bicinate [214], as determined by potentiometric pH titrations [212,213] or spectrophotometric measurements [214] in aqueous solutions at 25°C, together with the stability differences according to eq. (30)[a,b].

L	M^{2+}	$\log K^{M}_{M(L)}$	$\log K^{M(ATP)}_{M(ATP)(L)}$	$\Delta \log K_{M/ATP/L}$
Tris	Ca^{2+}	≤0.7		
	Co^{2+}	1.73 ± 0.02	1.57 ± 0.05	–0.16 ± 0.05
	Cu^{2+}	4.05 ± 0.02	3.50 ± 0.05	–0.55 ± 0.05
	Cd^{2+}	1.94 ± 0.02	1.17 ± 0.05	–0.77 ± 0.05
Bistris	Ca^{2+}	2.25 ± 0.02	1.85 ± 0.09	–0.40 ± 0.09
	Co^{2+}	1.78 ± 0.03	1.33 ± 0.03	–0.45 ± 0.04
	Cu^{2+}	5.27 ± 0.01	3.62 ± 0.03	–1.65 ± 0.03
	Cd^{2+}	2.47 ± 0.02	1.14 ± 0.07	–1.33 ± 0.07
Bicinate	Co^{2+}	5.08 ± 0.13	4.53 ± 0.22	–0.55 ± 0.26
	Cu^{2+}	8.24 ± 0.09	6.57 ± 0.32	–1.67 ± 0.33

[a] For the error limits see footnotes "*a*" of Tables 3 and 4.

[b] The acidity constants and employed ionic strengths (*I*) are: (i) $pK^{H}_{H(Tris)}$ = 8.13 ± 0.01; *I* = 0.1 M, KNO_3 [212]. (ii) $pK^{H}_{H(Bistris)}$ = 6.72 ± 0.01; *I* = 1.0 M, KNO_3 [213]. For the acidity constant of $H(Bistris)^+$ at 25°C and *I* = 0.1 M (KNO_3) it holds $pK^{H}_{H(Bistris)}$ = 6.56 ± 0.04 [213]. (iii) The acidity constants of $H_2(Bicinate)^+$ as determined by potentiometric pH titration are $pK^{H}_{H_2(Bicinate)}$ = 2.13 ± 0.06 and $pK^{H}_{H(Bicinate)}$ = 8.33 ± 0.03; *I* = 1.0 M, KNO_3 [214].

The hydroxyl groups also play an important role in the ternary complexes containing ATP^{4-} as is evident from the in general small negative values observed for $\Delta \log K_{M/ATP/L}$ (Table 13, column 5). Indeed, the role of the hydroxyl groups for the stability of the $M(ATP)(Tris)^{2-}$ complexes follows, e.g., from a comparison with the stability constant of the $Cu(ATP)(NH_3)^{2-}$ complex ($\log K^{Cu(ATP)}_{Cu(ATP)(NH_3)}$ = 3.4 [27]). This constant is somewhat smaller than that of the corresponding Cu(ATP)-$(Tris)^{2-}$ complex, $\log K^{Cu(ATP)}_{Cu(ATP)(Tris)}$ = 3.5 (Table 13, column 4), despite the much lower basicity of Tris ($pK^{H}_{H(Tris)}$ = 8.13 [212]) compared to that of NH_3 ($pK^{H}_{NH_4}$ = 9.38 [27]). On the other hand, for the Cd^{2+} complexes the situation is less clear-cut ($\log K^{Cd(ATP)}_{Cd(ATP)(NH_3)} \leq 2.2$ [27] *versus* $\log K^{Cd(ATP)}_{Cd(ATP)(Tris)}$ = 1.17), but overall it follows that the OH groups play a role, though it is unclear to which extent they participate in different ternary complexes and if they do this via direct metal ion binding or *via* hydrogen bonding to the phosphate oxygens of the coordinated ATP^{4-}.

However, the values for $\Delta \log K_{M/ATP/Bistris}$ as observed for the Ca^{2+} and Co^{2+} complexes are relatively small (i.e., not strongly negative). Because the coordination spheres of these metal ions are already quite "saturated" by ATP^{4-} and the nitrogen of Bistris, the most plausible explanation for the relatively high complex stability is the additional formation of hydrogen bonds between some OH groups of the coordinated Bistris and phosphate oxygens of the also coordinated ATP^{4-}.

That $\Delta \log K_{Cu/ATP/Bistris}$ is with –1.65 log units rather low, is no surprise because of the Jahn-Teller distorted coordination sphere of Cu^{2+} [128]. The value of $\Delta \log K_{Cd/ATP/Bistris} = -1.33$ implies again that the $Cd(ATP)^{2-}$/OH interactions are not very pronounced as already indicated by the $Cd(ATP)(Tris)^{2-}$ data.

The stability constants of the two examples for binary $M(Bicinate)^{+}$ and ternary $M(ATP)(Bicinate)^{3-}$ complexes (no value for Cd^{2+} is known) provide an order and speak for themselves. These values are so large (Table 13) that Bicine, if used as buffer in the presence of metal ions, will certainly complex a very significant amount of metal ions present. It is further clear that the hydroxyl groups of Bicinate participate at least to some extent in metal ion binding. To put the observed negative values for $\Delta \log K_{M/ATP/L}$ overall into perspective, it may be helpful to recall that the expected statistical value for a regular octahedral coordination sphere of M^{2+} (e.g., Co^{2+}) and the coordination of two different but *simple* and *symmetrical* tridentate ligands amounts already to $\Delta \log K_{3:3/stat/oh} = -1.03$ [213].

8.3 *Mixed Ligand Complexes Containing a Nucleotide and a Further Monodentate or Bidentate Ligand. Release of Purine-N7 and Formation of Stacks*

About 40 years ago intramolecular aromatic-ring stacking was described for the first time [217,218] between heteroaromatic N bases (Arm), i.e., 2,2'-bipyridine or 1,10-phenanthroline, and AMP^{2-}, ADP^{3-} or ATP^{4-}, both ligands being bridged by a metal ion [200,219–221]. Originally the interactions had been proven by UV spectrophotometry [217–220] and ^{1}H NMR shift measurements [201,222,223]. Later, complexes of the type M(Arm)(adenine nucleotide) were also isolated in the solid state and the intramolecular stacking interaction was proven by X-ray crystal structure studies (e.g., refs [11,224–226]). The formation degrees of these intramolecular stacks in aqueous solution were largely determined by potentiometric pH titrations. A few results are summarized in Table 14 below.

From the results discussed in Section 6.3 it is evident that the "weak" point in macrochelate formation of $M(ATP)^{2-}$ complexes is the coordination of N7 of the adenine residue. Indeed, by ^{1}H NMR shift experiments it has been shown for Zn^{2+} and Cd^{2+} that already the formation of the ternary $M(ATP)(OH)^{3-}$ complexes releases N7 [227]. Similar observations have been made for $Cd(ATP)(NH_3)^{2-}$ [228]. For the ternary complexes of $M(ATP)(imidazole)^{2-}$, where $M^{2+} = Mn^{2+}$, Co^{2+}, Zn^{2+} or Cd^{2+}, it is shown, based on a careful analysis of stability data, that the adenine moiety is released from the coordination sphere [228]. However, there is also evidence that in these $M(ATP)(imidazole)^{2-}$ complexes intramolecular stacking between the purine moiety and the imidazole ring occurs to some extent (see Table 14 [229–232]).

Table 14 Extent of intramolecular aromatic-ring stacking or hydrophobic adduct formation in ternary M(N)(L) complexes, where N = nucleotide and L = another ligand, as depicted for example in equilibrium (34) and as calculated from stability constants determined via potentiometric (pot.) pH titrations: Stability enhancement log $\Delta_{M/N/L}$ (analogous to eq. 14), intramolecular and dimensionless equilibrium constant $K_{I/st}$ (eq. 34), and percentage of the "closed" $M(N)(L)_{cl}$ species in aqueous solution at 25°C and $I = 0.1$ M ($NaClO_4$ or KNO_3).[a,b] For comparison some results obtained from ^{1}H NMR shift experiments are also given.

No.	M(L)(N) or M(N)(L)	log $\Delta_{M/N/L}$	$K_{I/st}$	%M(N)(L)$_{st}$ pot.[b]	%M(N)(L)$_{st}$ NMR	Ref. [139,140]
1	Cu(Phen)(UMP)	0.33 ± 0.07	1.14 ± 0.34	53 ± 7		[231]
2	Cu(Phen)(AMP)	0.99 ± 0.08	8.77 ± 1.81	90 ± 2		[232]
3	Cu(Phen)(ATP)$^{2-}$	1.07	11	92 ± (2)		[233]
4	Zn(Phen)(ATP)$^{2-}$				≥95[c]	[222]
5	Zn(Bpy)(ATP)$^{2-}$	0.54	2.5	70	55[c]	[222,227]
6	Zn(Bpy)(UTP)$^{2-}$	0.45	1.8	65	40[c]	[222,227]
7	Cd(Bpy)(ATP)$^{2-}$	0.38	1.4	60		[227]
8	Cd(Bpy)(CTP)$^{2-}$	0.37	1.3	55		[227]
9	Zn(ATP)(Trp)$^{3-}$	0.59 ± 0.06	2.89 ± 0.51	74 ± 3	40 ± 15[c]	[179,230]
10	Zn(ATP)(Leu)$^{3-}$	0.02 ± 0.09	0.05 (0/0.29)[d]	5 (0/22)[d]	30 (20/75)[d,e]	[230]
11	Cd(ATP)(Leu)$^{3-}$				10 (5/25)[d,e]	[230]
12	Cd(ATP)(Im)$^{2-}$				35 (15/50)[c,d,f]	[229]

[a] For the error limits (where given) see footnotes "a" of Tables 3 and 4.
[b] The calculations were done in analogy to equations (14) and (16) to (20) given in Section 4.2 (see also refs, e.g., [51,221,230,231].
[c] These NMR experiments were carried out in D_2O at 27°C and $I = 0.1$ M ($NaNO_3$).
[d] In parentheses the lower and upper limits are given, respectively.
[e] Based on NMR experiments carried out in H_2O at 34°C and $I = 0.1 - 1.5$ M (KNO_3).
[f] The same result has been obtained for Zn(ATP)(imidazole)$^{2-}$ [229].

The first mixed ligand complex containing ATP and an amino acid was one with tryptophanate, i.e., Zn(ATP)(Trp)$^{3-}$. By ^{1}H NMR shift experiments it was shown that an indole-adenine interaction takes place [233], which may be promoted by Zn^{2+}. Later, the position of the intramolecular equilibrium (34) was determined:

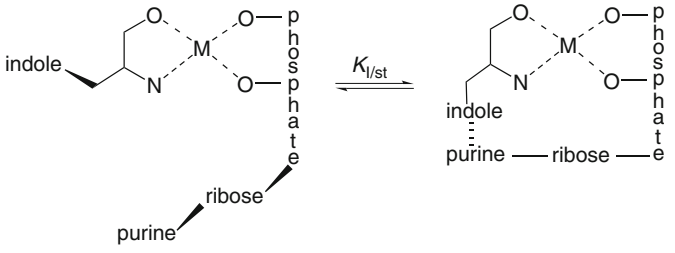

(34)

For Zn^{2+} as metal ion, it was concluded [230] that the stacked species occurs with a formation degree of approximately 75% (Table 14). Other metal ions were studied as well [179,230,234], and the occurrence of intramolecular stacks in M(ATP)(Trp)$^{3-}$ complexes was confirmed by several groups [235,236]. It was further shown that the isopropyl residue of leucinate is also able to undergo a hydrophobic interaction in M(ATP)(Leu)$^{3-}$ complexes [230]; e.g., the formation

degree of the "closed" species for the corresponding Cd^{2+} complex amounts from 5 to 25% [230]. The occurrence of such species with a hydrophobic interaction was again proven by ^1H NMR shift studies [230] and by comparisons of stability constants, mostly obtained via potentiometric pH titrations [230]. These stability data and their differences (stability enhancements) were evaluated in analogy to equations (14) and (16) – (20) in Section 4.2.

With Cd^{2+} only a few such complexes, allowing an intramolecular interaction, have been studied; the corresponding results, listed in entries 7, 8 and 11, 12 of Table 14, fit into the general picture: From entries 1 and 2 in Table 14 it is evident that the size of the aromatic-ring systems (uracil *versus* adenine) matters, whereas a replacement of AMP^{2-} by ATP^{4-} in the ternary complex (entry 3) does hardly affect the stacking intensity, even though the overall stability of the latter complex ($\log K^{Cu(Phen)}_{Cu(Phen)(ATP)} = 6.88 \pm 0.07$ [223]) is by a factor of about 1000 larger ($\log K^{Cu(Phen)}_{Cu(Phen)(AMP)} = 3.89 \pm 0.01$ [232]). As expected, replacement of the 3-ring Phen by Bpy reduces the formation degree of the intramolecular stack (entries 4, 5). It is also expected that the stacking interaction between the indole moiety of tryptophanate (Trp^-) and the adenine residue in $Zn(ATP)(Trp)^{3-}$ is more pronounced than the hydrophobic interaction between the isopropyl residue of leucinate (Leu^-) and adenine in $Zn(ATP)(Leu)^{3-}$ (entries 9, 10). The $Cd(ATP)(Leu)^{3-}$ complex fits into the picture. Maybe here it should be mentioned that the ^1H NMR experiments allow a direct proof of intramolecular adduct formation, but from potentiometric stability data usually the more exact formation degrees are obtained. The last entry (no. 12) in Table 14 refers to $Cd(ATP)(imidazole)^{2-}$ for which, just like for $Zn(ATP)(imidazole)^{2-}$ [229], stack formation between the adenine residue and the coordinated imidazole could be proven [229]. This result is in line with a suggestion [237] based on thermodynamic parameters that in $Zn(ATP)(histamine)^{2-}$ stacking occurs.

Finally, the above discussion should not distract from the fact that certain ligand combinations, as discovered nearly 50 years ago [238], can give rise to enhanced complex stabilities, i.e., the combination of a heteroaromatic N base (Arm) and an O donor ligand in combination with a transition metal ion leads to indirect effects being mediated by the metal ion [56,200,203,204]. For example, the combinations $Cu(Bpy/Phen)^{2+}/HPO_4^{2-}$ [239], $Mn(Bpy)^{2+}$/malonate [203] or $M(Arm)^{2+}$/pyrocatecholate [240] give rise to enhanced complex stabilities. Clearly, the direct (as discussed in this section) and indirect ligand-ligand interactions [200] that occur in mixed ligand complexes are of relevance regarding the discrimination and selectivity observed in nature.

9 Cadmium(II) Binding in Dinucleotides and Dinucleoside Monophosphates

One of the important questions in metal ion-nucleic acid coordination is to find out to what extent neighboring nucleotide units affect binding of a metal ion at a given site [58]. Some answers to this question can be found by studying ligands of the

kind shown in Figure 16. Unfortunately, the information regarding Cd^{2+} complexes and dinucleotides in general is limited to the nucleotide/nucleoside derivatives shown in Figure 16.

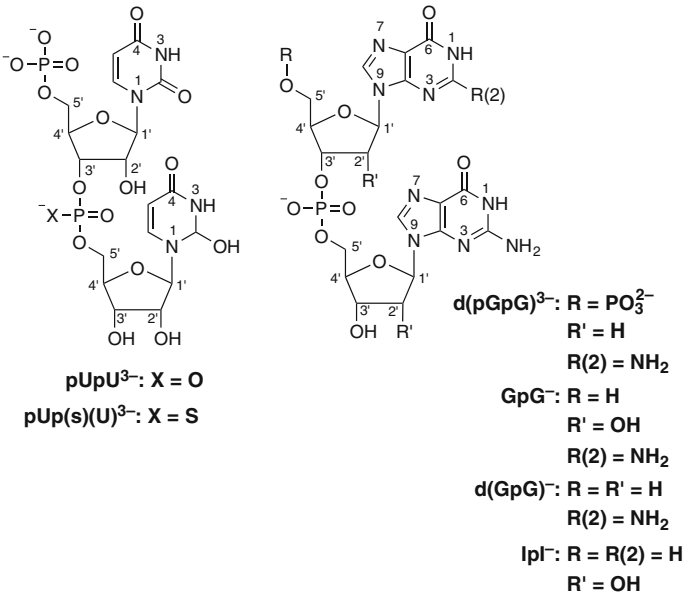

Figure 16 Chemical structures of three dinucleotides, i.e., uridylyl-(5'→3')-5'-uridylate ($pUpU^{3-}$), *p*-thiouridylyl-(5'→3')-5'-uridylate ($pUp(s)U^{3-}$), and 2'-deoxyguanylyl(5'→3')-2'-deoxy-5'-guanylate [$d(pGpG)^{3-}$], as well as of three dinucleoside monophosphates, i.e., guanylyl(3'→5')guanosine (GpG^{-}), 2'-deoxyguanylyl(3'→5')-2-deoxyguanosine [$d(GpG)^{-}$], and inosylyl(3'→5')inosine (IpI^{-}).

9.1 The Phosphodiester Link

If one recalls from Section 6.2.2 that the uracil moiety is not involved in metal ion binding, meaning that the log stability constants of the Cd(UMP) complex fits on the straight-reference line seen in Figure 11, one may expect that this "indifference" of the uracil residue also holds for the $pUpU^{3-}$ ligand. Indeed, if one applies the acidity constant $pK^{H}_{H(pUpU)} = 6.44$ (Table 15, footnote "b") to the straight-line equation (25), one obtains $\log K^{Cd}_{Cd(R\text{-}PO_3)} = 2.52 \pm 0.05$, which is 0.23 ± 0.05 log unit [33] lower than the measured stability constant $\log K^{Cd}_{Cd(pUpU)} = 2.75 \pm 0.03$ (Table 15 [241–243]).

Because a metal ion coordinated at the terminal phosphate group of $pUpU^{3-}$ will "feel" the negative charge of the phosphodiester bridge even if no 10-membered chelate is formed, some stability enhancement (eq. 14) is expected. Interestingly, for the complexes $M(pUpU)^{-}$ of Mg^{2+}, Mn^{2+}, and Cd^{2+} the stability enhancement

is within the error limits identical giving on average log $\Delta_{M/pUpU/charge} = 0.24 \pm 0.04$. This result for the three metal ions having rather different properties can only mean that the given value represents indeed the charge effect and that none of the three metal ions forms a 10-membered chelate with the diester bridge (a chelate occurs with Zn^{2+} and Pb^{2+} [33]) or interacts with the uracil moiety.

Table 15 Comparison of the stability constants for the $Cd(pUpU)^-$, $Cd[d(pGpG)]^-$, and $Cd(pUp(s)U)^-$ complexes (Figure 16) between the measured stability constants (eq. 2) and the calculated stability constants for $M(R\text{-}PO_3)$ species,[a] based on the basicity of the terminal phosphate group[b] of the corresponding dinucleotide and the reference-line equation (25) with its corresponding parameters [50,52,122], together with the stability differences log $\Delta_{M/L}$ as defined in equation (14) (aqueous solution; 25°C and $I = 0.1$ M, $NaNO_3$)[a,b].

Ligand (L)	log $K^{Cd}_{Cd(L)}$	log $K^{Cd}_{Cd(R\text{-}PO_3)}$	log $\Delta_{Cd/L}$
$pUpU^{3-}$	2.75 ± 0.03	2.52 ± 0.05	0.23 ± 0.05
$d(pGpG)^{3-}$	4.01 ± 0.06	2.56 ± 0.05	1.45 ± 0.08
$pUp(s)U^{3-}$	3.16 ± 0.07	2.48 ± 0.05	0.68 ± 0.09

[a] For the error limits see footnotes "*a*" of Tables 3 and 4. The values for the $M(pUpU)^-$, $M[d(pGpG)]^-$, and $M(pUp(s)U)^-$ systems are from refs [33], [241], and [242], respectively.
[b] Acidity constants (eq. 3) for the deprotonation of the monoprotonated terminal phosphate groups of the dinucleotides (Figure 16): $pK^H_{H(pUpU)} = 6.44 \pm 0.02$ [33,243], $pK^H_{H[d(pGpG)]} = 6.56 \pm 0.03$ [241,243], and $pK^H_{H(pUp(s)U)} = 6.32 \pm 0.03$ [242]. For the other acidity constants of the three dinucleotides see the given refs.

9.2 The Guanine Residue in a Dinucleotide

If one views the data for the $Cd[d(pGpG)]^-$ complex (second entry of Table 15) with the presented result for the Cd(pUpU) complex in mind, it is immediately evident that a new situation occurs: log $\Delta_{Cd/d(pGpG)} = 1.45 \pm 0.08$ [241] is far beyond the indicated charge effect (Section 9.1). In fact, the charge effect of the bridging phosphodiester unit is expected to be the same with $pUpU^{3-}$ and $d(pGpG)^{3-}$; furthermore, if coordinated to the terminal phosphate group Cd^{2+} does not interact with the diester bridge as seen from $Cd(pUpU)^-$, thus, it follows that in $Cd[d(pGpG)]^-$ a guanine-N7 interaction (eq. 22) must take place for which the charge-corrected stability enhancement log $\Delta_{Cd/d(pGpG)/charge,cor} = (1.45 \pm 0.08) - (0.24 \pm 0.04) = 1.21 \pm 0.09$ holds. Application of equations (14) and (16) – (20) leads to a formation degree for $Cd[d(pGpG)]^-_{cl/N7}$ of 94 ± 1.5% [241]. Are both guanine residues involved in this macrochelate formation or only one? A tentative answer may be obtained if one considers the stability enhancement for the Cd(dGMP) complex, which is unfortunately not known, but which may be estimated because the information for both Zn(GMP) [50] and Zn(dGMP) [244] exists. This estimate is justified because Zn(GMP) and Cd(GMP) reach within the error limits the same formation degree [50] for $M(GMP)_{cl/N7}$ (ca. 82%), despite

the different overall stability constants. Because of the somewhat higher basicity of N7 in dGMP, compared with that in GMP [31], one expects a somewhat larger formation degree of the chelate for the deoxy complex. Indeed, this follows from the given reasonings:

$$\begin{aligned}\log \Delta_{\mathrm{Cd/dGMP}} &= \log \Delta_{\mathrm{Cd/GMP}} + \log \Delta_{\mathrm{Zn/dGMP}} - \log \Delta_{\mathrm{Zn/GMP}} \\ &= (0.79 \pm 0.06) + (0.84 \pm 0.08) - (0.69 \pm 0.07) \\ &= 0.94 \pm 0.12\end{aligned}$$

This result corresponds to 88.5 ± 3.2% for $Cd(dGMP)_{cl/N7}$. This stability enhancement for the Cd(dGMP) complex is by 0.27 ± 0.15 log unit smaller than the one obtained for $Cd[d(pGpG)]^-$ indicating that in the dinucleotide complex both guanine residues (Figure 16) are involved to some extent.

It may be added that for the $Cd[d(pGpG)]^-$ system also the monoprotonated species, that is, Cd[H;d(pGpG)], was observed [241], where the proton is located at the terminal phosphate group and Cd^{2+} at guanine-N7. From other purine systems it is known that a metal ion bound to N7 in a nucleotide complex may form macrochelates by also interacting with the $P(O)_2(OH)^-$ residue [97,162]. Indeed, a detailed evaluation provided a stability enhancement of $\log \Delta_{\mathrm{Cd/H;d(pGpG)}} = 0.27 \pm 0.18$ for Cd[H;d(pGpG)] and this corresponds to a formation degree for the chelated species of 46 ± 22% [241]. Hence, taken together, all these results prove that metal ions are able to bridge the distance between a phosphate group and an N7 site in a d(GMP) unit. This is of relevance for the interaction of metal ions with nucleic acids.

9.3 The Non-bridging Sulfur of the Thiophosphodiester Link

Considering the already previously indicated importance of so-called "rescue" experiments in ribozyme chemistry (Sections 7.2 and 10.1), it is interesting to see that for $Cd(pUp(s)U)^-$ a stability enhancement of $\log \Delta_{\mathrm{Cd/pUp(s)U}} = 0.68 \pm 0.09$ is observed (Table 15 [242]) (Figure 16). If this value is charge-corrected in the way explained above, one obtains $\log \Delta_{\mathrm{Cd/pUp(s)U/charge,cor}} = (0.68 \pm 0.09) - (0.24 \pm 0.04) = 0.44 \pm 0.10$. Since no interaction with an oxygen in the diester bridge occurs in $Cd(pUpU)^-$, the whole charge-corrected stability enhancement needs to be attributed to a Cd^{2+}/S interaction with the non-bridging S of the thiophosphodiester link. The corresponding 10-membered chelate reaches a formation degree of 64 ± 8% [242].

It is worth to note that no stability enhancement is observed for the $Mg(pUp(s)U)^-$ and $Mn(pUp(s)U)^-$ complexes. Clearly, this observation has consequences for the "rescue" experiments in ribozyme chemistry [28].

9.4 Dinucleoside Monophosphates

Another interesting molecule in the present context is IpI^- (Figure 16) for which the Cd^{2+} complexes $Cd(IpI)^+$ and Cd(IpI – H) have been studied [75]. Since the stability constant of $Cd(IpI)^+$ could only be estimated, we will not consider this complex further, though it ought to be mentioned that it is transformed to Cd(IpI – H) with $pK^{H}_{Cd(IpI)} = 6.7 \pm 0.3$, meaning that the deprotonation reaction occurs close to the physiological pH range. By using the Cd^{2+} complexes of inosine as a basis a stability enhancement of $\log \Delta_{Cd/(IpI-H)} = 0.40 \pm 0.30$ was estimated for the Cd(IpI – H) complex and this corresponds to a formation degree of 60% (with lower and upper limits of 21 and 80%, respectively) [75] for the chelate.

Which is the structure of the closed or chelated species? Since N7 of a 5'-purine unit is in general somewhat more basic than the one of a 3' unit [38,48], one may assume that the initial complex formation in IpI^- occurs preferably at N7 of the 5'-inosine residue. This binding mode also allows an outersphere interaction with the (C6)O site, especially after deprotonation of (N1)H [74,119,162], as well as a maximal electrostatic interaction with the negatively charged phosphoryl bridge and possibly even macrochelate formation to a certain extent, as has been suggested before for an intermediate Pt(II) complex with a related dinucleoside monophosphate [245,246]. Such a structure is also well known for M(IMP) and related complexes (Section 6.2.3) [40,50,117]. Hence, one may conclude that two types of macrochelates are possible: (i) the one indicated above between N7 and the phosphodiester bridge or (ii) one that involves both N7 sites of $(IpI – H)^{2-}$. Of course, both types of macrochelates may occur in equilibrium with each other, and then the formation degree mentioned above encompasses both species.

Considering that Mg^{2+} does not form significant amounts of $Mg(IpI – H)_{cl}$ macrochelates [75] (whereas Co^{2+} and Zn^{2+} do), we favor N7/N7 macrochelates. However, in doing so, one has to answer the question why no significant amounts of macrochelates are observed with the Cd(GpG – H) and Cd[d(GpG – H)] systems (Figure 16) [38]. If one applies the indicated evaluation procedure [75] to the data of ref. [38], one notes that the $\log \Delta_{Cd/(GpG-H)}$ and $\log \Delta_{Cd/d(GpG-H)}$ values are zero within their error limits. This agrees with the earlier conclusion [38] that "no hint for the formation of significant amounts of intramolecular chelates involving both N7 sites" have been found, though low concentrations could still occur, of course. A possible explanation could be that the intramolecular stacking interaction in $(IpI – H)^{2-}$ is smaller than in $(GpG – H)^{2-}$, and in fact, this is expected [137,247,248]. Consequently, $(IpI – H)^{2-}$ is more flexible for adapting to the configuration needed in aqueous solution for an N7/N7 macrochelate which is known to form with the kinetically inert $cis\text{-}(NH_3)_2Pt^{2+}$ and both dinucleoside monophosphates [249,250]. One should emphasize here that the amount of free energy involved to shift the situation from one side to another is very small; for example, a formation degree of 20% of a macrochelate at 25°C corresponds only to a stability enhancement of $\log \Delta_{M/ligand} = 0.1$ (eq. 14) and a change in free energy of $\Delta G^0 = –0.57$ kJ/mol [52].

10 Cadmium(II) Binding to Nucleic Acids

Interest in the interaction of cadmium(II) with nucleic acids was triggered, at least in part, by the discovery of Wacker and Vallee [7] more than 50 years ago that RNA from the horse kidney cortex contained not only essential metal ions like those of Mg, Ca, Mn, Fe or Zn, but also Cd. The toxicity of cadmium(II) is well established for many years (see Chapters 1, 14, and 15) and it appears that it is primarily due to Cd(II)-protein interactions. However, due to its high affinity for R–S^- groups Cd^{2+} may affect thiolate-disulfide equilibria and thus the redox state of the cell. This in turn means that Cd^{2+} may stimulate the production of reactive oxygen species (ROS) and these may lead to DNA damage [251]. In addition, Cd^{2+} interferes with DNA repair pathways of the cell by directly inhibiting the relevant enzymes or by hampering their binding to aberrant DNA sites [251].

Despite the obvious toxic effects on living cells, Cd^{2+} is often used in *in vitro* studies as a probe of Mg^{2+} or Ca^{2+} (see Chapter 6) having the advantage of a higher affinity towards most ligands, including nucleotides and their constituents, as described in the previous sections. Below we consider now larger entities.

10.1 Cadmium(II)-Rescue Experiments

As indicated above in Section 7.2, Cd^{2+} binding to phosphorothioate nucleotides can be exploited in so-called rescue experiments where one takes advantage of the higher affinity of Cd^{2+} towards sulfur ligands compared to Mg^{2+} [170,252]. Such a rescue is also part of so-called nucleotide analogue interference mapping/suppression (NAIM/NAIS) experiments, which are used to identify catalytically crucial atoms within a RNA and/or tertiary contacts [253–255]. This technique has been widely applied to study metal ion binding sites and their influence on catalytic RNAs, i.e., ribozymes [256–262]. Major limitations of this method are the fact that (i) T7 RNA polymerase, which is generally used for the transcription of defined RNA sequences, inserts only S_p thionucleotides under inversion of their conformation to R_p. Consequently, in such T7-transcribed RNA molecules only the R_p configuration can be studied. (ii) Sulfur has a slightly larger radius compared to oxygen, which can lead to small perturbations in local geometry of a metal ion-binding pocket or a tertiary interaction within the global fold of the RNA. In such cases, the sulfur substitution cannot be rescued by the addition of Cd^{2+}.

The principle of cadmium(II) rescue experiments is as follows (see also refs [8,10]): Phosphorothioate nucleotides are inserted into a RNA at single, defined sites. In cases of significantly decreased or abolished enzymatic activity of the RNA and subsequent restoration of activity upon addition of soft metal ions like Cd^{2+}, one assumes that the respective phosphate moiety coordinates a metal ion which is relevant for the catalytic activity of the ribozymes.

The technique was first applied to the enzymes arginine kinase and creatinine kinase. Studies on ATPγS and on the stereospecificity for diastereomers of ATPαS

and ATPβS in the presence of Mg^{2+} and Cd^{2+} [263,264] proved that metal ions coordinate to the respective phosphate groups at certain steps of the catalytic cycle. Later, as the enzymatic nature of some RNA molecules was discovered, the technique proved powerful in shedding light on their catalytic mechanism as is exemplified with the following few examples.

The different metal ion-binding modes of the two classes of RNAse P, a ribonuclease and ribozyme, could be revealed [265,266]. For group II introns, it was shown that a metal ion is required to stabilize the leaving group in both steps of the splicing reaction [267]. In addition, the results of this study were consistent with the findings on the catalysis of the eukaryotic spliceosome [267,268], thus further corroborating a common ancestry of these two machineries. In the case of the group I intron, another large ribozyme, cadmium(II) rescue experiments helped to develop a very detailed understanding of the catalytic mechanism. It was found that three metal ions are required for the splicing mechanism, which bind in the active site and simultaneously contact the attacking nucleophile and the scissile phosphate [269,270].

Cadmium(II) binding was also intensively used to study metal ion requirements for the catalysis of the self-cleaving hammerhead ribozyme. Also here, phosphorothioate studies helped to prove the coordination of divalent metal ions during catalysis [271,272]. Cd^{2+} binds with a K_D of 25 μM in the ground state thereby increasing the activity 10^4-fold. The K_D of Cd^{2+} in the transition state was calculated to be 2.5 nM indicating that the metal ion recruits at least one more ligand in the transition state. Confusion was caused by the observation that this Cd^{2+} binding site was situated at a 20 Å distance from the scissile phosphate; this discrepancy originated in the fact that earlier studies were performed with a minimal ribozyme construct that lacked important tertiary contacts [273]. The Cd^{2+} interactions were also investigated using ^{31}P and ^{15}N NMR, with Cd^{2+} binding leading to an upfield shift of the thiophosphate-^{31}P or guanine-$^{15}N7$ resonance, respectively [274–277]. The catalytic activity of the hammerhead ribozyme was also shown to be in principle independent of divalent metal ions [278]: In the presence of unphysiologically high, i.e., molar, concentrations of monovalent cations, activity can be partly rescued, thus confirming that a direct M^{2+} binding to the active site is not mandatory but that also M^+ ions can be catalytically competent. Such an exchange of low concentration of divalent ions *versus* high concentrations of monovalent metal ions is well known and is explained by their differences in the binding affinities [127,279,280].

10.2 Crystal Structures of RNA or DNA-Protein Complexes Containing Cd(II)

More detailed information on cadmium(II) binding to nucleic acids is available from a small number of crystal structures of RNA as well as RNA- or DNA-protein complexes. There are only 23 entries in the Protein Data Base that contain Cd^{2+} ions

interacting with at least one atom of a DNA or RNA and of these 18 structures represent different parts of the 50s subunit of the prokaryotic ribosome; the other five are structures of a Diels-Alder ribozyme (1YKQ [281]), the product complex of the hammerhead ribozyme (488D [282]), a prokaryotic enzyme mediating DNA bending called "integration host factor" in complex with a DNA substrate (1IHF [283], 2HT0 [284]) and DNA polymerase β in complex with DNA and ATP (8ICE [285]).

Most of the binding sites identified in these structures confirm what is stated in the previous sections on Cd^{2+} binding to isolated nucleotides. Innersphere contacts are almost exclusively formed by guanine N7 or, to a lesser extent, by adenine N7 or one of the non-bridging phosphate oxygens (OP1 and OP2). Additional outersphere contacts are highly abundant. In case of innersphere binding the Cd^{2+}–ligand distance is about 2 Å. If guanine N7 is innersphere coordinated, then O6 of the same guanine is always in a distance to enable an outersphere interaction (usually at a distance of about 3 Å). One example of such a coordination pattern is found in the hammerhead ribozyme, where Cd^{2+} strongly influences catalytic activity (see Section 10.1). The sites G10.1 N7 and A9 OP2 constitute the innersphere contacs with the Cd^{2+} ion while numerous further atoms of five different nucleotides interact by outersphere coordination with the Cd^{2+} ion from distances between 2.9 and 5.6 Å (Figure 17) [282,286].

Apart from the above mentioned coordination pattern, Cd^{2+} contacts to nearly any nitrogen or oxygen atom in nucleotides can be observed. The total number of potential interactions to a single Cd^{2+} ion varies greatly depending on the binding site. The same is true for the number of involved residues that ranges from 2 to 6. In general, one nucleobase (mostly the one coordinated via N7) provides most further atoms to bind the Cd^{2+} ion while the residues at the n+1 and n–1 position and, if available, its base pairing partners provide few additional liganding atoms.

The only Cd^{2+}-containing RNA-protein complex deposited in the Protein Data Bank is the aforementioned 50s subunit of the ribosome. Surprisingly for such a giant molecular assembly, the maximum number is eight Cd^{2+} ions bound in one structure (1MMS [287]), seven of which make contacts to RNA. Two special Cd^{2+} coordination sites are detected in this 50s RNA. In the first case, uracil O4 is the only innersphere contact to Cd^{2+} with no N7 or phosphate oxygen being within 5 Å. In two further binding sites, one of which comprises numerous liganding atoms from six different nucleotides, rare innersphere contacts between Cd^{2+} and the ribose O2' are observed. These special cases illustrate how increasingly complex molecular assemblies open up coordination options by providing a complex and defined overall geometry. This allows for a summation of contributions of several weak interactions or facilitates weak interactions by a spatial pre-arrangement of strong interactions.

To the best of our knowledge there is no structure available of only DNA with bound Cd(II) ions. The structures of the prokaryotic DNA-bending protein IHF (integration host factor) with doubly nicked DNA (PDB 2HT0) or singly-nicked DNA (PDB 1IHF) mostly display conservative binding modes involving guanine and adenine N7 or phosphate oxygens. Often, a combination of amino acids, DNA nucleotides, and water molecules constitutes the binding sites for the single Cd^{2+} ions.

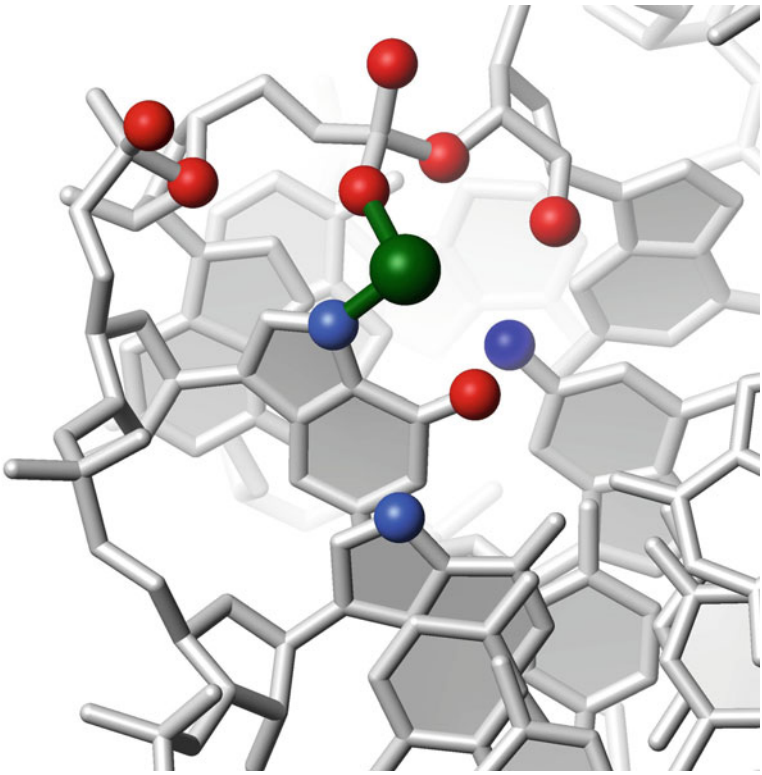

Figure 17 Cd^{2+} coordination within the hammerhead ribozyme. Two innersphere contacts of Cd^{2+} (green sphere) to N7 of G10.1 (blue) and OP2 of A9 (red) are shown. Further ligands for outersphere interactions at a distance less than 5 Å to Cd^{2+} are shown as blue (nitrogen) and red (oxygen) spheres. The figure was prepared with MOLMOL [286] using PDB entry 488D [282].

The PDB structure of DNA polymerase β with 7 base pairs of DNA and ATP bound (PDB 8ICE) contains just one binding site in which DNA is involved. The cadmium(II) has contacts to four different amino acids and two phosphate oxygens; it is also in coordination distance to O5' of adenine and O3' of a guanine. Additionally, four oxygen atoms of pyrophosphate coordinate the Cd^{2+}. This is a good example of how DNA-Cd^{2+} contacts can be facilitated by another main binding site. In this case, the pyrophosphate is required to bind a metal ion in this site as in its absence the site remains unoccupied [285].

10.3 Cadmium(II) as Probe in EPR and NMR Spectroscopy

Cadmium(II)-induced EPR silencing was applied to evaluate the affinity of Mn^{2+} to several distinct binding sites in the Diels-Alder ribozyme [288]. As Cd^{2+} is

EPR-silent, it was used to saturate four of five binding sites for divalent metal ions of the ribozyme to selectively study the affinity of Mn^{2+} for each binding site separately. This method relies on the fact that a Cd^{2+} ion once bound to the ribozyme cannot be substituted by Mn^{2+} since its affinity to all five binding sites is higher.

As mentioned above in Section 10.1, Cd^{2+} is readily applied in combination with thiophosphate derivatives using ^{31}P NMR making advantage of the chemical shift dispersion of the thiophosphate group as well as the higher affinity [274–277]. Similarly, Cd^{2+} can also be applied as mimic of Mg^{2+} in chemical shift titration experiments, its higher affinity being of advantage for better spectral quality [289]. In addition, ^{111}Cd or ^{113}Cd are NMR-active nuclei and regularly used in proteins to investigate Cd^{2+} binding [290,291] (see also Chapter 6). In larger nucleic acids, such studies are not as straightforward as with proteins due to the much lower affinity and faster exchange rates. Consequently, no distinct signal for $^{111/113}Cd$ is observed upon binding. We are aware of only one example where a change in chemical shift of the ^{113}Cd is observed upon addition to the central core of a group II intron ribozyme [292].

11 Concluding Remarks

Cadmium(II) is a metal ion that displays distinct coordinating properties with a mostly octahedral coordination sphere. It is commonly classified as a relatively soft ion and it prefers thus aromatic-nitrogen sites, especially N7 of purine residues. However, interactions with phosphate oxygens including those of the phosphodiester bridge are also not negligible and, provided a suitably located primary binding site is available, also hydroxyl and carbonyl groups may coordinate. Overall, one can conclude that the coordination chemistry of Cd^{2+} with nucleotides and the corresponding substituents is relatively well understood today; this includes the relations between the toxic Cd^{2+} and the essential Zn^{2+}, Ca^{2+}, and Mg^{2+} ions, for which it is often employed as a probe. However, with regard to less common nucleotides, which also occur in Nature, like thio-pyrimidine or -purine derivatives, our knowledge is very scarce and considerably more work is needed. This is of high relevance because Cd^{2+}-thio interactions are very stable, meaning that such an interaction can totally change the properties of a nucleic acid complex because commonly metal ion-nucleic acid interactions are weak compared to those of proteins.

Indeed, Cd^{2+} coordinates to nucleic acids often not only directly, like with purine-N7 sites, but also indirectly to oxygen and (other) nitrogen sites as is exemplified by many outersphere interactions found in nucleic acid structures. Most important in this respect is also the high affinity of Cd^{2+} towards sulfur ligands. These characteristics make Cd^{2+} on the one hand a toxic element that interferes especially with proteins in numerous metabolic pathways, but on the other hand it is also an interesting mimic

for other metal ions in *in vitro* studies. Especially as a replacement for Ca^{2+} and Mg^{2+} it is regularly applied in nucleic acid research.

The coordination chemistry of Cd^{2+} towards the building blocks of nucleic acids is well established and the intrinsic affinities to almost all possible coordinating atoms are known. This knowledge should provide a perfect basis to investigate in the future Cd^{2+} binding also to larger and more complex nucleic acid structures. The higher intrinsic affinity of Cd^{2+} compared to many other divalent metal ions, especially Mg^{2+} and Ca^{2+}, allows in many cases a more detailed investigation of the coordination pattern. In the case of ribozymes, a differing catalytic rate in the presence of Cd^{2+} *versus* that of Mg^{2+} should in principle allow to draw conclusions on Mg^{2+} binding. However, such investigations are in many instances severely hampered by the fact that even with Cd^{2+} it is often highly challenging to characterize a binding pocket down to the single coordinating atoms. This is due to the size of the RNA itself and the limited chemical diversity of its building blocks, which make it very difficult to distinguish individual nucleotides. Highly promising in this respect are combinations of ^{13}C, ^{15}N, and ^{113}Cd NMR, which allow to observe both the RNA liganding sites and the metal ion simultaneously. Although hampered by the fast exchange of the metal ion in nucleic acids, the increasing sensitivity of NMR probeheads, also for heteronuclei, will certainly lead to new developments and experiments in the future.

Abbreviations and Definitions

The abbreviations for the nucleobases and nucleosides are defined in Figure 1 and the labeling systems for the di- and triphosphate residues in Figure 9. Other abbreviations are defined below.

Species written in the text without a charge do not carry one or represent the species in general (i.e., independent of the protonation degree); which of the two possibilities applies is always clear from the context. In formulas such as $M(H;NMP)^+$ the H^+ and NMP^{2-} are separated by a semicolon to facilitate reading; yet they appear within the same parenthesis to indicate that the proton is at the ligand without defining its location. A formula like $(NB - H)^-$ means that the ligand, here a nucleobase residue, has lost a proton and it is to be read as NB *minus* H^+. The term (aq) is used to indicate that water is acting as a ligand.

Ac^-	acetate (Figure 9)
AcP^{2-}	acetyl phosphate (Figure 3)
Ade	adenine (Figure 1)
Ado	adenosine (Figure 1)
ADP^{3-}	adenosine 5'-diphosphate (Figure 10)
AMP^{2-}	adenosine 5'-monophosphate (Figure 3)
$AMPS^{2-}$	adenosine 5'-*O*-thiomonophosphate
AnP^{2-}	acetonylphosphonate (Figure 3)
ATP^{4-}	adenosine 5'-triphosphate (Figure 10)

Bicine	*N*,*N*-bis(2-hydroxyethyl)glycine (Figure 15)
Bistris	2-[bis(2-hydroxyethyl)amino]-2-(hydroxymethyl)-1,3-propanediol (Figure 15)
Bpy	2,2'-bipyridine
C2S	2-thiocytidine
CDP^{3-}	cytidine 5'-diphosphate (Figure 10)
CMP^{2-}	cytidine 5'-monophosphate (Figure 10)
CTP^{4-}	cytidine 5'-triphosphate (Figure 10)
Cyd	cytidine (Figure 1)
Cyt	cytosine (Figure 1)
$dCMP^{2-}$	2'-deoxycytidine 5'-monophosphate
$dGMP^{2-}$	2'-deoxyguanosine 5'-monophosphate
$d(GpG)^{-}$	2'-deoxyguanylyl(3'→5')-2'-deoxyguanosine (Figure 16)
dGuo	2'-deoxyguanosine
$DHAP^{2-}$	dihydroxyacetone phosphate (Figure 3)
Dien	diethylenetriamine (= 1,4,7-triazaheptane)
DMBI	1,4-dimethylbenzimidazole (= 6,9-dimethyl-1,3-dideazapurine) (Figure 5)
$d(pGpG)^{3-}$	2'-deoxyguanylyl(5'→3')-2'-deoxy-5'-guanylate (Figure 16)
$dTDP^{3-}$	thymidine [= 1-(2-deoxy-β-*D*-ribofuranosyl)thymine] 5'-diphosphate
dThd	thymidine [= 1-(2-deoxy-β-*D*-ribofuranosyl)thymine] (Figure 1)
$dTMP^{2-}$	thymidine [= 1-(2-deoxy-β-*D*-ribofuranosyl)thymine] 5'-monophosphate
$dTTP^{4-}$	thymidine [= 1-(2-deoxy-β-*D*-ribofuranosyl)thymine] 5'-triphosphate
ε	dielectric constant (or permittivity)
ε-Ado	ε-adenosine (= $1,N^6$-ethenoadenosine)
ε-AMP^{2-}	ε-adenosine 5'-monophosphate (= $1,N^6$-ethenoadenosine 5'-monophosphate) (Figure 14)
En	ethylenediamine (= 1,2-diaminoethane)
EPR	electron paramagnetic resonance
9EtG	9-ethylguanine
FMN^{2-}	flavin mononucleotide (= riboflavin 5'-phosphate) (Figure 13)
$G1P^{2-}$	glycerol 1-phosphate (Figures 3 and 13)
GDP^{3-}	guanosine 5'-diphosphate
GMP^{2-}	guanosine 5'-monophosphate
GpG^{-}	guanylyl(3'→5')guanosine (Figure 16)
GTP^{4-}	guanosine 5'-triphosphate
Gua	guanine (Figure 1)
Guo	guanosine (Figure 1)
HMP^{2-}	hydroxymethylphosphonate (Figure 4)
$HOAc^{-}$	hydroxyacetate (Figure 4)
HOMPy	*o*-(hydroxymethyl)pyridine (Figure 4)

H(Or)	orotidine (Figure 8)
Hyp	hypoxanthine (Figure 1)
I	ionic strength
IDP^{3-}	inosine 5'-diphosphate
IHF	integration host factor
Im	imidazole
IMP^{2-}	inosine 5'-monophosphate
Ino	inosine
IpI^{-}	inosylyl(3'→5')inosine (Figure 16)
ITP^{4-}	inosine 5'-triphosphate
K_a	general acidity constant
K_I	intramolecular equilibrium constant
L	general ligand
Leu	leucine
Leu^{-}	leucinate
M^{2+}	divalent metal ion
1MBI	1-methylbenzimidazole (Figure 5)
9MeA	9-methyladenine
9MeHyp	9-methylhypoxanthine
9MeG	9-methylguanine
$MeOPS^{2-}$	methyl thiophosphate
1MIm	1-methylimidazole (Figure 5)
2MPy	2-methylpyridine (Figure 5)
NAIM/NAIS	nucleotide analogue interference mapping/suppression
NB	nucleobase derivative
NDP^{3-}	nucleoside 5'-diphosphate
NMP^{2-}	nucleoside 5'-monophosphate
NP	nucleoside phosphate
NTP^{4-}	nucleoside 5'-triphosphate
oh	octahedral
OMP^{3-}	orotidinate 5'-monophosphate
*o*PyN	*ortho*-aminopyridine-type ligand (Figure 7)
Or^{-}	orotidinate (Figure 8)
PDB	Protein Data Bank
$PEEA^{2-}$	dianion of 9-[2-(phosphonoethoxy)ethyl]adenine
Phen	1,10-phenanthroline
PME^{2-}	(phosphonomethoxy)ethane = ethoxymethanephosphonate
$PMEA^{2-}$	dianion of 9-[2-(phosphonomethoxy)ethyl]adenine (= *Adefovir*) (Figure 14)
$PMEApp^{4-}$	diphosphorylated $PMEA^{2-}$
PS^{2-}	thiophosphate monoester
$pUpU^{3-}$	uridylyl-(5'→3')-5'-uridylate (Figure 16)
Py	pyridine
PyN	pyridine-type ligand (Figure 7)

R-DP^{3-}	diphosphate monoester (Figure 9)
RibMP^{2-}	D-ribose 5-monophosphate (cf. Figure 1)
R-MP^{2-}	monophosphate monoester (Figure 9)
$(RO)_2PO_2^-$	phosphodiester unit (Figure 9)
R-PO_3^{2-}	monophosphate monoester and/or phosphonate ligand
R-TP^{4-}	triphosphate monoester (Figure 9)
Thy	thymine (Figure 1)
Tris	2-amino-2-(hydroxymethyl)-1,3-propanediol (Figure 15)
Trp	tryptophan
Trp^-	tryptophanate
Tu	tubercidin (Figure 5)
TuMP^{2-}	tubercidin 5'-monophosphate (= 7-deaza-AMP^{2-})
U	uridine-type ligand
$(U - H)^-$	uridinate-type ligand
U2S	2-thiouridine (Figure 8)
U4S	4-thiouridine (Figure 8)
UDP^{3-}	uridine 5'-diphosphate
UMP^{2-}	uridine 5'-monophosphate
$UMPS^{2-}$	uridine 5'-*O*-thiomonophosphate (Figure 14)
Ura	uracil (Figure 1)
Urd	uridine (Figure 1)
UTP^{4-}	uridine 5'-triphosphate
Xao	xanthosine (Figure 8)
XMP^{3-}	xanthosinate 5'-monophosphate = $(XMP - H)^{3-}$ = $(X - H{\cdot}MP)^{3-}$ (Figure 13)

Acknowledgments Financial support from the Swiss National Science Foundation (R.K.O.S.), the European Research Council (ERC Starting Grant to R.K.O.S.), the Universities of Zürich (R.K.O.S.) and Basel (H.S.), and within the COST Action CM1105 (R.K.O.S.) are gratefully acknowledged.

References

1. J. K. Dunnick, B. A. Fowler, in *Handbook on Toxicity of Inorganic Compounds*, Eds H. G. Seiler, H. Sigel, A. Sigel, Marcel Dekker, New York, 1988, pp. 155–175.
2. C. E. Housecroft, A. G. Sharpe, *Inorganic Chemistry*, Pearson Education, Harlow, UK, 2001, p. 579.
3. L. Thunus, R. Lejeune, in Handbook on *Metals in Clinical and Analytical Chemistry*, Eds H. G. Seiler, A. Sigel, H. Sigel, Marcel Dekker, New York, 1994, p. 668.
4. R. F. M. Herber, in Handbook on *Metals in Clinical and Analytical Chemistry*, Eds H. G. Seiler, A. Sigel, H. Sigel, Marcel Dekker, New York, 1994, pp. 283–297.
5. Y. Xu, L. Feng, P. D. Jeffrey, Y. Shi, F. M. M. Morel, *Nature* **2008**, *452*, 56–61.
6. T. W. Lane, M. A. Saito, G. N. George, I. J. Pickering, R. C. Prince, F. M. M. Morel, *Nature* **2005**, *435*, 42.
7. W. E. C. Wacker, B. L. Vallee, *J. Biol. Chem.* **1959**, *234*, 3257–3262.

8. M. C. Erat, R. K. O. Sigel, *Met. Ions Life Sci.* **2011**, *9*, 37–100.
9. D. Donghi, J. Schnabl, *Met. Ions Life Sci.* **2011**, *9*, 197–234.
10. M. Pechlaner, R. K. O. Sigel, *Met. Ions Life Sci.* **2012**, *10*, 1–42.
11. K. Aoki, *Met. Ions Biol. Syst.* **1996**, *32*, 91–134.
12. R. B. Martin, Y. H. Mariam, *Met. Ions Biol. Syst.* **1979**, *8*, 57–124.
13. R. Tribolet, H. Sigel, *Eur. J. Biochem.* **1987**, *163*, 353–363.
14. D. B. Davies, P. Rajani, H. Sadikot, *J. Chem. Soc., Perkin Trans. 2*, **1985**, 279–285.
15. R. B. Martin, *Met. Ions Biol. Syst.* **1986**, *20*, 21–65.
16. P. B. Hammond, E. C. Foulkes, *Met. Ions Biol. Syst.* **1986**, *20*, 157–200.
17. R. B. Martin, in *Handbook on Toxicity of Inorganic Compounds*, Eds H. G. Seiler, H. Sigel, A. Sigel, Marcel Dekker, New York, **1988**, pp. 9–25.
18. R. B. Martin, *Met. Ions Biol. Syst.* **1984**, *17*, 1–49.
19. E. Freisinger, R. K. O. Sigel, *Coord. Chem. Rev.* **2007**, *251*, 1834–1851.
20. R. D. Shannon, *Acta Cryst.* **1976**, *A32*, 751–767.
21. H. Sigel, R. B. Martin, *Chem. Soc. Rev.* **1994**, *23*, 83–91.
22. H. Sigel, D. B. McCormick, *Acc. Chem. Res.* **1970**, *3*, 201–208.
23. C. F. Baes, Jr., R. E. Mesmer, *The Hydrolysis of Cations*, Krieger Publishing Co., Malabar, Florida, 1976, pp. 1–496.
24. A. M. Pyle, *Met. Ions Biol. Syst.* **1996**, *32*, 479–520.
25. *NIST Critically Selected Stability Contstants of Metal Complexes*, Reference Database 46, Version 8.0; data collected and selected by R. M. Smith, A. E. Martell; U. S. Department of Commerce, National Institute of Standards and Technology, Gaithersburg, MD, 2004.
26. R. K. O. Sigel, H. Sigel, in *Bioinorganic Fundamentals and Applications: Metals in Natural Living Systems and Metals in Toxicology and Medicine*, Eds V. L. Pecoraro, T. Hambley, in Volume 3 of *Comprehensive Inorganic Chemistry II*, Eds J. Reedijk, K. Poeppelmeier, Elsevier, Oxford, UK, 2013, in press.
27. N. Saha, H. Sigel, *J. Am. Chem. Soc.* **1982**, *104*, 4100–4105.
28. R. K. O. Sigel, *Eur. J. Inorg. Chem.* **2005**, 2281–2292.
29. H. Sigel, F. Hofstetter, R. B. Martin, R. M. Milburn, V. Scheller-Krattiger, K. H. Scheller, *J. Am. Chem. Soc.* **1984**, *106*, 7935–7946.
30. R. K. O. Sigel, A. M. Pyle, *Chem. Rev.* **2007**, *107*, 97–113.
31. A. Mucha, B. Knobloch, M. Jeżowska-Bojczuk, H. Kozłowski, R. K. O. Sigel, *Chem. Eur. J.* **2008**, *14*, 6663–6671.
32. H. Sigel, *Chem. Soc. Rev.* **1993**, *22*, 255–267.
33. B. Knobloch, D. Suliga, A. Okruszek, R. K. O. Sigel, *Chem. Eur. J.* **2005**, *11*, 4163–4170.
34. B. Lippert, *Prog. Inorg. Chem.* **2005**, *54*, 385–447.
35. B. Knobloch, H. Sigel, *J. Biol. Inorg. Chem.* **2004**, *9*, 365–373.
36. L. E. Kapinos, B. P. Operschall, E. Larsen, H. Sigel, *Chem. Eur. J.* **2011**, *17*, 8156–8164.
37. H. Sigel, E. M. Bianchi, N. A. Corfù, Y. Kinjo, R. Tribolet, R. B. Martin, *J. Chem. Soc., Perkin Trans. 2*, **2001**, 507–511.
38. C. P. Da Costa, H. Sigel, *Inorg. Chem.* **2003**, *42*, 3475–3482.
39. H. Pezzano, F. Podo, *Chem. Rev.* **1980**, *80*, 365–401.
40. R. K. O. Sigel, H. Sigel, *Met. Ions Life Sci.* **2007**, *2*, 109–180.
41. K. Aoki, K. Murayama, *Met. Ions Life Sci.* **2012**, *10*, 43–102.
42. D. M. L. Goodgame, I. Jeeves, C. D. Reynolds, A. C. Skapski, *Nucleic Acids Res.* **1975**, *2*, 1375–1379.
43. S. Yano, M. Otsuka, *Met. Ions Biol. Syst.* **1996**, *32*, 27–60.
44. H. Kozłowski, P. Decock, I. Olivier, G. Micera, A. Pusino, L. D. Pettit, *Carbohydrate Res.* **1990**, *197*, 109–117.
45. B. Song, P. Mehrkhodavandi, P. Buglyó, Y. Mikata, Y. Shinohara, K. Yoneda, S. Yano, C. Orvig, *J. Chem. Soc., Dalton Trans.* **2000**, 1325–1333.
46. H. Reinert, R. Weiss, *Hoppe-Seylers Z. Physiol. Chem.* **1969**, *350*, 1321–1326.
47. Y.-Y. H. Chao, D. R. Kearns, *J. Am. Chem. Soc.* **1977**, *99*, 6425–6434.

48. S. S. Massoud, H. Sigel, *Eur. J. Biochem.* **1989**, *179*, 451–458.
49. G. S. Padiyar, T. P. Seshadri, *J. Biomolecular Structure & Dynamics* **1998**, *15*, 803–821.
50. H. Sigel, B. Song, *Met. Ions Biol. Syst.* **1996**, *32*, 135–205.
51. R. B. Martin, H. Sigel, *Comments Inorg. Chem.* **1988**, *6*, 285–314.
52. H. Sigel, L. E. Kapinos, *Coord. Chem. Rev.* **2000**, *200–202*, 563–594.
53. G. Liang, D. Chen, M. Bastian, H. Sigel, *J. Am. Chem. Soc.* **1992**, *114*, 7780–7785.
54. M. Furler, B. Knobloch, R. K. O. Sigel, *Inorg. Chim. Acta* **2009**, *362*, 771–776.
55. H. Sigel, C. P. Da Costa, B. Song, P. Carloni, F. Gregáň, *J. Am. Chem. Soc.* **1999**, *121*, 6248–6257.
56. C. P. Da Costa, B. Song, F. Gregáň, H. Sigel, *J. Chem. Soc., Dalton Trans.* **2000**, 899–904.
57. F. M. Al-Sogair, B. P. Operschall, A. Sigel, H. Sigel, J. Schnabl, R. K. O. Sigel, *Chem. Rev.* **2011**, *111*, 4964–5003.
58. R. K. O. Sigel, H. Sigel, *Accounts Chem. Res.* **2010**, *43*, 974–984.
59. L. E. Kapinos, H. Sigel, *Inorg. Chim. Acta* **2002**, *337*, 131–142; ICA issue in honor of K. E. Wieghardt.
60. L. E. Kapinos, B. Song, H. Sigel, *Chem. Eur. J.* **1999**, *5*, 1794–1802.
61. A. Sigel, B. P. Operschall, H. Sigel, *Coord. Chem. Rev.* **2012**, *256*, 260–278.
62. A. T. Perrotta, M. D. Been, *Biochemistry* **2007**, *46*, 5124–5130.
63. A. S. Burton, N. Lehman, *Biochimie* **2006**, *88*, 819–825.
64. N. Lehman, G. F. Joyce, *Nature* **1993**, *361*, 182–185.
65. N. Lehman, G. F. Joyce, *Curr. Biol.* **1993**, *3*, 723–734.
66. M. C. Erat, R. K. O. Sigel, *J. Biol. Inorg. Chem.* **2008**, *13*, 1025–1036.
67. M. Steiner, K. S. Karunatilaka, R. K. O. Sigel, D. Rueda, *Proc. Natl. Acad. Sci. U.S.A.* **2008**, *105*, 13853–13858.
68. M. Steiner, D. Rueda, R. K. O. Sigel, *Angew. Chem. Int. Ed.* **2009**, *48*, 9739–9742.
69. R. Griesser, G. Kampf, L. E. Kapinos, S. Komeda, B. Lippert, J. Reedijk, H. Sigel, *Inorg. Chem.* **2003**, *42*, 32–41.
70. L. E. Kapinos, B. Song, H. Sigel, *Inorg. Chim. Acta* **1998**, *280*, 50–56; ICA issue in memory of Mark E. Vol'pin.
71. L. E. Kapinos, A. Holý, J. Günter, H. Sigel, *Inorg. Chem.* **2001**, *40*, 2500–2508.
72. L.-n. Ji, N. A. Corfù, H. Sigel, *J. Chem. Soc., Dalton Trans.* **1991**, 1367–1375.
73. L. E. Kapinos, H. Sigel, results to be published.
74. H. Sigel, S. S. Massoud, N. A. Corfù, *J. Am. Chem. Soc.* **1994**, *116*, 2958–2971.
75. B. Knobloch, A. Okruszek, H. Sigel, *Inorg. Chem.* **2008**, *47*, 2641–2648.
76. J. C. Morales, E. T. Kool, *Nat. Struct. Biol.* **1998**, *5*, 950–954.
77. H. Sigel, N. A. Corfù, L.-n. Ji, R. B. Martin, *Comments Inorg. Chem.* **1992**, *13*, 35–59.
78. M. A. Salam, K. Aoki, *Inorg. Chim. Acta* **2001**, *314*, 71–82.
79. H. Sigel, *Pure Appl. Chem.* **2004**, *76*, 1869–1886.
80. B. Song, J. Zhao, R. Griesser, C. Meiser, H. Sigel, B. Lippert, *Chem. Eur. J.* **1999**, *5*, 2374–2387.
81. H. Sigel, *J. Am. Chem. Soc.* **1975**, *97*, 3209–3214.
82. B. Knobloch, R. K. O. Sigel, B. Lippert, H. Sigel, *Angew. Chem. Int. Ed.* **2004**, *43*, 3793–3795.
83. Y. Kinjo, L.-n. Ji, N. A. Corfù, H. Sigel, *Inorg. Chem.* **1992**, *31*, 5588–5596.
84. J. Hogle, M. Sundaralingam, G. H. Y. Lin, *Acta Crystallogr., Sect. B* **1980**, *36*, 564–570.
85. K. Aoki, W. Saenger, *J. Inorg. Biochem.* **1984**, *20*, 225–245.
86. G. R. Clark, J. D. Orbell, *Acta Crystallogr., Sect. B.* **1978**, *34*, 1815–1822.
87. B. Knobloch, C. P. Da Costa, W. Linert, H. Sigel, *Inorg. Chem. Commun.* **2003**, *6*, 90–93.
88. B. Knobloch, W. Linert, H. Sigel, *Proc. Natl. Acad. Sci. U.S.A.* **2005**, *102*, 7459–7464.
89. H. Follmann, R. Pfeil, H. Witzel, *Eur. J. Biochem.* **1977**, *77*, 451–461.
90. H. R. Mahler, E. H. Cordes, *Biological Chemistry*, Harper & Row, New York, 1966.
91. J. D. Rawn, *Biochemistry*, Neil Patterson Publ., Burlington, North Carolina, USA, 1989.
92. M. Bastian, H. Sigel, *Inorg. Chim. Acta* **1990**, *178*, 249–259.

93. M. Bastian, H. Sigel, *J. Coord. Chem.* **1991**, *23*, 137–154.
94. R. Hille, *Met. Ions Life Sci.* **2009**, *6*, 395–416.
95. Y. Kinjo, R. Tribolet, N. A. Corfù, H. Sigel, *Inorg. Chem.* **1989**, *28*, 1480–1489.
96. S. S. Massoud, N. A. Corfù, R. Griesser, H. Sigel, *Chem. Eur. J.* **2004**, *10*, 5129–5137.
97. H. Sigel, B. P. Operschall, R. Griesser, *Chem. Soc. Rev.* **2009**, *38*, 2465–2494.
98. R. B. Martin, *Met. Ions Biol. Syst.* **1996**, *32*, 61–89.
99. H. Sierzputowska-Gracz, E. Sochacka, A. Malkiewicz, K. Kuo, C. W. Gehrke, P. F. Agris, *J. Am. Chem. Soc.* **1987**, *109*, 7171–7177.
100. L. Aravind, E. V. Koonin, *Trends Biochem. Sci.* **2001**, *26*, 215–217.
101. K. C. Rogers, A. T. Crescenzo, D. Söll, *Biochimie* **1995**, *77*, 66–74.
102. T. Kowalik-Jankowska, H. Kozlowski, I. Sóvágó, B. Nawrot, E. Sochacka, A. J. Malkiewicz, *J. Inorg. Biochem.* **1994**, *53*, 49–56.
103. T. Kowalik-Jankowska, K. Varnagy, J. Swiatek-Kozlowska, A. Jon, I. Sóvágó, E. Sochacka, A. Malkiewicz, J. Spychala, H. Kozlowski, *J. Inorg. Biochem.* **1997**, *65*, 257–262.
104. (a) R. B. Martin, in *Encyclopedia of Inorganic Chemistry*, Vol. 4, Ed R. B. King, Wiley, Chichester, UK, 1994, pp. 2185–2196. (b) R. B. Martin, in *Encyclopedia of Molecular Biology and Molecular Medicine*, Vol. 11, Ed R. A. Meyer, VCH, Weinheim, Germany, 1996, pp. 125–134.
105. A. Odani, H. Kozlowski, J. Swiatek-Kozlowska, J. Brasún, B. P. Operschall, H. Sigel, *J. Inorg. Biochem.* **2007**, *101*, 727–735.
106. P. T. Selvi, M. Murali, M. Palaniandavar, M. Köckerling, G. Henkel, *Inorg. Chim. Acta* **2002**, *340*, 139–146.
107. E. Dubler, *Met. Ions Biol. Syst.* **1996**, *32*, 301–338.
108. R. Leipuviene, Q. Qian, G. R. Björk, *J. Bacteriol.* **2004**, *186*, 758–766.
109. I. Lukovits, E. Kalman, F. Zucchi, *Corrosion* **2001**, *57*, 3–8.
110. A. R. Van Rompay, A. Norda, K. Lindén, M. Johansson, A. Karlsson, *Mol. Pharmacol.* **2001**, *59*, 1181–1186.
111. C. R. Raj, S. Behera, *Biosens. Bioelectron.* **2005**, *21*, 949–956.
112. J. Brasún, A. Matera, E. Sochacka, J. Swiatek-Kozlowska, H. Kozlowski, B. P. Operschall, H. Sigel, *J. Biol. Inorg. Chem.* **2008**, *13*, 663–674.
113. R. Stewart, M. G. Harris, *Can. J. Chem.* **1977**, *55*, 3807–3814.
114. S. S. Massoud, H. Sigel, *Inorg. Chem.* **1988**, *27*, 1447–1453.
115. S. A. A. Sajadi, B. Song, F. Gregáň, H. Sigel, *Inorg. Chem.* **1999**, *38*, 439–448.
116. H. Sigel, R. Tribolet, R. Malini-Balakrishnan, R. B. Martin, *Inorg. Chem.* **1987**, *26*, 2149–2157.
117. H. Sigel, R. Griesser, *Chem. Soc. Rev.* **2005**, *34*, 875–900.
118. H. Sigel, *Pure Appl. Chem.* **2004**, *76*, 375–388.
119. H. Sigel, E. M. Bianchi, N. A. Corfù, Y. Kinjo, R. Tribolet, R. B. Martin, *Chem. Eur. J.* **2001**, *7*, 3729–3737.
120. H. Sigel, *Eur. J. Biochem.* **1987**, *165*, 65–72.
121. A. Mucha, B. Knobloch, M. Jeżowska-Bojczuk, H. Kozłowski, R. K. O. Sigel, *Dalton Trans.* **2008**, 5368–5377.
122. H. Sigel, D. Chen, N. A. Corfù, F. Gregáň, A. Holý, M. Strašák, *Helv. Chim. Acta* **1992**, *75*, 2634–2656.
123. H. Diebler, F. Secco, M. Venturini, *Biophys. Chem.* **1987**, *26*, 193–205.
124. J. C. Thomas, C. M. Frey, J. E. Stuehr, *Inorg. Chem.* **1980**, *19*, 501–504.
125. K. J. Powell, P. L. Brown, R. H. Byrne, T. Gajda, G. Hefter, A.-K. Leuz, S. Sjöberg, H. Wanner, *Pure Appl. Chem.* **2011**, *83*, 1163–1214.
126. H. M. Irving, R. J. P. Williams, *J. Chem. Soc.* **1953**, 3192–3210.
127. J. Schnabl, R. K. O. Sigel, *Curr. Opin. Chem. Biol.* **2010**, *14*, 269–275.
128. H. Sigel, R. B. Martin, *Chem. Rev.* **1982**, *82*, 385–426.
129. H. Brintzinger, G. G. Hammes, *Inorg. Chem.* **1966**, *5*, 1286–1287.
130. E. M. Bianchi, S. A. A. Sajadi, B. Song, H. Sigel, *Chem. Eur. J.* **2003**, *9*, 881–892.

131. A. Szent-Györgyi, in *Enzymes; Units of Biological Structure and Function*, Ed O. H. Gaebler, Academic Press, New York, 1956, p. 393.
132. M. Cohn, T. R. Hughes, Jr., *J. Biol. Chem.* **1962**, *237*, 176–181.
133. P. W. Schneider, H. Brintzinger, H. Erlenmeyer, *Helv. Chim. Acta* **1964**, *47*, 992–1002.
134. (a) H. Sternlicht, R. G. Shulman, E. W. Anderson, *J. Chem. Phys.* **1965**, *43*, 3133–3143. (b) R. G. Shulman, H. Sternlicht, *J. Mol. Biol.* **1965**, *13*, 952–955.
135. (a) H. Sigel, *Experientia* **1966**, *22*, 497–499. (b) H. Sigel, H. Erlenmeyer, *Helv. Chim. Acta* **1966**, *49*, 1266–1274.
136. H. Sigel, S. S. Massoud, R. Tribolet, *J. Am. Chem. Soc.* **1988**, *110*, 6857–6865.
137. K. H. Scheller, F. Hofstetter, P. R. Mitchell, B. Prijs, H. Sigel, *J. Am. Chem. Soc.* **1981**, *103*, 247–260.
138. B. Knobloch, A. Mucha, B. P. Operschall, H. Sigel, M. Jeżowska-Bojczuk, H. Kozlowski, R. K. O. Sigel, *Chem. Eur. J.* **2011**, *17*, 5393–5403.
139. O. Yamauchi, A. Odani, H. Masuda, H. Sigel, *Met. Ions Biol. Syst.* **1996**, *32*, 207–270.
140. N. A. Corfù, A. Sigel, B. P. Operschall, H. Sigel, *J. Indian Chem. Soc.* **2011**, *88*, 1093–1115. JICS issue to commemorate Sir Prafulla Chandra Ray.
141. B. Song, G. Feldmann, M. Bastian, B. Lippert, H. Sigel, *Inorg. Chim. Acta* **1995**, *235*, 99–109.
142. A. Saha, N. Saha, L.-n. Ji, J. Zhao, F. Gregáň, S. A. A. Sajadi, B. Song, H. Sigel, *J. Biol. Inorg. Chem.* **1996**, *1*, 231–238.
143. G. Kampf, L. E. Kapinos, R. Griesser, B. Lippert, H. Sigel, *J. Chem. Soc., Perkin Trans. 2*, **2002**, 1320–1327.
144. R. K. O. Sigel, E. Freisinger, B. Lippert, *J. Biol. Inorg. Chem.* **2000**, *5*, 287–299.
145. G. Liang, H. Sigel, *Inorg. Chem.* **1990**, *29*, 3631–3632.
146. E. M. Bianchi, R. Griesser, H. Sigel, *Helv. Chim. Acta* **2005**, *88*, 406–425.
147. B. P. Operschall, E. M. Bianchi, R. Griesser, H. Sigel, *J. Coord. Chem.* **2009**, *62*, 23–39.
148. (a) E. M. Bianchi, *Comparison of the Stability and Solution Structures of Metal Ion Complexes Formed with 5'-Di- and 5'-Triphosphates of Purine Nucleotides* (Ph. D. Thesis, University of Basel), Logos Verlag, Berlin, 2003, pp. 1–216. (b) H. Sigel, E. M. Bianchi, et al. details to be published.
149. K. H. Scheller, H. Sigel, *J. Am. Chem. Soc.* **1983**, *105*, 5891–5900.
150. H. Sigel, *Coord. Chem. Rev.* **1990**, *100*, 453–539.
151. H. Sigel, M. C. F. Magalhães, J. Zhao, B. Song, results to be published.
152. W. Wirth, J. Blotevogel-Baltronat, U. Kleinkes, W. S. Sheldrick, *Inorg. Chim. Acta* **2002**, *339*, 14–26.
153. H. Sigel, *Coord. Chem. Rev.* **1995**, *144*, 287–319.
154. C. A. Blindauer, A. H. Emwas, A. Holý, H. Dvořáková, E. Sletten, H. Sigel, *Chem. Eur. J.* **1997**, *3*, 1526–1536.
155. C. Meiser, E. Freisinger, B. Lippert, *J. Chem. Soc., Dalton Trans.* **1998**, 2059–2064.
156. M. A. Shipman, C. Price, A. E. Gibson, M. R. J. Elsegood, W. Clegg, A. Houlton, *Chem. Eur. J.* **2000**, *6*, 4371–4378.
157. C. Meiser, B. Song, E. Freisinger, M. Peilert, H. Sigel, B. Lippert, *Chem. Eur. J.* **1997**, *3*, 388–398.
158. G. Raudaschl-Sieber, H. Schöllhorn, U. Thewalt, B. Lippert, *J. Am. Chem. Soc.* **1985**, *107*, 3591–3595.
159. E. Bugella-Altamirano, D. Choquesillo-Lazarte, J. M. González-Pérez, M. J. Sánchez-Moreno, R. Marín-Sanchez, J. D. Martín-Ramos, B. Covelo, R. Carballo, A. Castiñeiras, J. Niclós-Gutiérrez, *Inorg. Chim. Acta* **2002**, *339*, 160–170.
160. (a) A. Ciccarese, D. A. Clemente, A. Marzotto, M. Rosa, G. Valle, *J. Inorg. Biochem.* **1991**, *43*, 470. (b) A. Marzotto, D. A. Clemente, A. Ciccarese, G. Valle, *J. Cryst. Spectroscop. Res.* **1993**, *23*, 119–131.
161. E. Kulikowska, B. Kierdaszuk, D. Shugar, *Acta Biochim. Polonica* **2004**, *51*, 493–531.

162. H. Sigel, S. S. Massoud, B. Song, R. Griesser, B. Knobloch, B. P. Operschall, *Chem. Eur. J.* **2006**, *12*, 8106–8122.
163. H. Sigel, B. P. Operschall, S. S. Massoud, B. Song, R. Griesser, *Dalton Trans.* **2006**, 5521–5529.
164. M. J. Sánchez-Moreno, A. Fernández-Botello, R. B. Gómez-Coca, R. Griesser, J. Ochocki, A. Kotyński, J. Niclós-Gutiérrez, V. Moreno, H. Sigel, *Inorg. Chem.* **2004**, *43*, 1311–1322.
165. J. Swiatek-Kozlowska, J. Brasún, A. Dobosz, E. Sochacka, A. Glowacka, *J. Inorg. Biochem.* **2003**, *93*, 119–124.
166. H. Sigel, B. Song, G. Liang, R. Halbach, M. Felder, M. Bastian, *Inorg. Chim. Acta* **1995**, *240*, 313–322.
167. J. Bidwell, J. Thomas, J. Stuehr, *J. Am. Chem. Soc.* **1986**, *108*, 820–825.
168. M. Bastian, H. Sigel, *Inorg. Chem.* **1997**, *36*, 1619–1624.
169. M. Bastian, H. Sigel, *Biophys. Chem.* **1997**, *67*, 27–34.
170. R. K. O. Sigel, B. Song, H. Sigel, *J. Am. Chem. Soc.* **1997**, *119*, 744–755.
171. H. Sigel, *Chimia* **1987**, *41*, 11–26.
172. D. D. Perrin, *J. Am. Chem. Soc.* **1960**, *82*, 5642–5645.
173. H. Sigel, H. Brintzinger, *Helv. Chim. Acta* **1964**, *47*, 1701–1717; see also H. Sigel, B. Prijs, *Helv. Chim. Acta* **1967**, *50*, 2357–2362.
174. H. Sigel, *Met. Ions Biol. Syst.* **1979**, *8*, 125–158.
175. K. H. Scheller, H. Sigel, *J. Am. Chem. Soc.* **1983**, *105*, 3005–3014.
176. C. A. Blindauer, A. Holý, H. Dvořáková, H. Sigel, *J. Chem. Soc., Perkin Trans. 2*, **1997**, 2353–2363.
177. C. H. Schwalbe, W. Thomson, S. Freeman, *J. Chem. Soc., Perkin Trans. 1*, **1991**, 1348–1349.
178. H. Sigel, K. H. Scheller, *Eur. J. Biochem.* **1984**, *138*, 291–299.
179. H. Sigel, K. H. Scheller, V. Scheller-Krattiger, B. Prijs, *J. Am. Chem. Soc.* **1986**, *108*, 4171–4178.
180. V. Scheller-Krattiger, H. Sigel, *Inorg. Chem.* **1986**, *25*, 2628–2634.
181. L. Claus, S. Vortler, F. Eckstein, *Methods Enzymol.* **2000**, *317*, 74–91.
182. C. P. Da Costa, A. Okruszek, H. Sigel, *ChemBioChem* **2003**, *4*, 593–602.
183. B. Song, R. K. O. Sigel, H. Sigel, *Chem. Eur. J.* **1997**, *3*, 29–33.
184. M. Vasák, J. H. R. Kägi, *Met. Ions Biol. Syst.* **1983**, *15*, 213–273; cf. p. 261.
185. H. Sigel, *Pure Appl. Chem.* **1999**, *71*, 1727–1740.
186. H. Sigel, *Chem. Soc. Rev.* **2004**, *33*, 191–200.
187. E. De Clercq, A. Holý, *Nature Rev. Drug Discovery* **2005**, *4*, 928–940.
188. T. Tichý, G. Andrei, M. Dračínský, A. Holý, J. Balzarini, R. Snoeck, M. Krečmerová, *Bioinorg. Med. Chem.* **2011**, *19*, 3527–3539.
189. R. B. Gómez-Coca, C. A. Blindauer, A. Sigel, B. P. Operschall, H. Sigel, *Chem. Biodiversity* **2012**, *9*, 2008–2034.
190. R. B. Gómez-Coca, L. E. Kapinos, A. Holý, R. A. Vilaplana, F. González-Vilchez, H. Sigel, *J. Chem. Soc., Dalton Trans.* **2000**, 2077–2084.
191. R. B. Gómez-Coca, A. Holý, R. A. Vilaplana, F. González-Vilchez, H. Sigel, *Bioinorg. Chem. Appl.* **2004**, *2*, 331–352.
192. R. B. Gómez-Coca, L. E. Kapinos, A. Holý, R. A. Vilaplana, F. González-Vilchez, H. Sigel, *J. Biol. Inorg. Chem.* **2004**, *9*, 961–972.
193. A. Fernández-Botello, R. Griesser, A. Holý, V. Moreno, H. Sigel, *Inorg. Chem.* **2005**, *44*, 5104–5117.
194. B. Song, G. Oswald, J. Zhao, B. Lippert, H. Sigel, *Inorg. Chem.* **1998**, *37*, 4857–4864.
195. B. Song, G. Oswald, M. Bastian, H. Sigel, B. Lippert, *Metal-Based Drugs* **1996**, *3*, 131–141.
196. H. Sigel, B. Song, G. Oswald, B. Lippert, *Chem. Eur. J.* **1998**, *4*, 1053–1060.
197. G. Kampf, M. S. Lüth, L. E. Kapinos, J. Müller, A. Holý, B. Lippert, H. Sigel, *Chem. Eur. J.* **2001**, *7*, 1899–1908.
198. G. Kampf, M. S. Lüth, J. Müller, A. Holý, B. Lippert, H. Sigel, *Z. Naturforsch.* **2000**, *55b*, 1141–1152.

199. H. Sigel, *Angew. Chemie, Internat. Ed. Engl.* **1975**, *14*, 394–402.
200. H. Sigel, in *Coordination Chemistry-20*, Ed D. Banerjea, published by IUPAC through Pergamon Press, Oxford and New York, 1980, pp. 27–45.
201. B. E. Fischer, H. Sigel, *J. Am. Chem. Soc.* **1980**, *102*, 2998–3008.
202. A. Fernández-Botello, A. Holý, V. Moreno, H. Sigel, *J. Inorg. Biochem.* **2004**, *98*, 2114–2124.
203. H. Sigel, B. E. Fischer, B. Prijs, *J. Am. Chem. Soc.* **1977**, *99*, 4489–4496.
204. (a) H. Sigel, *Inorg. Chem.* **1980**, *19*, 1411–1413. (b) H. Sigel, D. B. McCormick, *J. Am. Chem. Soc.* **1971**, *93*, 2041–2044.
205. R. Malini-Balakrishnan, K. H. Scheller, U. K. Häring, R. Tribolet, H. Sigel, *Inorg. Chem.* **1985**, *24*, 2067–2076.
206. P. Champeil, T. Menguy, S. Soulié, B. Juul, A. Gomez de Gracia, F. Rusconi, P. Falson, L. Denoroy, F. Henao, M. le Maire, J. V. Møller, *J. Biol. Chem.* **1998**, *273*, 6619–6631.
207. C. Montigny, P. Champeil, *Analyt. Biochem.* **2007**, *366*, 96–98.
208. P. Leverrier, C. Montigny, M. Garrigos, P. Champeil, *Analyt. Biochem.* **2007**, *371*, 215–228.
209. P. E. Amsler, H. Sigel, *Eur. J. Biochem.* **1976**, *63*, 569–581.
210. D. H. Buisson, H. Sigel, *Biochim. Biophys. Acta* **1974**, *343*, 45–63.
211. H. Sigel, P. E. Amsler, *J. Am. Chem. Soc.* **1976**, *98*, 7390–7400.
212. B. E. Fischer, U. K. Häring, R. Tribolet, H. Sigel, *Eur. J. Biochem.* **1979**, *94*, 523–530.
213. K. H. Scheller, T. H. J. Abel, P. E. Polanyi, P. K. Wenk, B. E. Fischer, H. Sigel, *Eur. J. Biochem.* **1980**, *107*, 455–466.
214. N. A. Corfù, B. Song, L.-n. Ji, *Inorg. Chim. Acta* **1992**, *192*, 243–251.
215. H. Sigel, *Coord. Chem. Rev.* **1993**, *122*, 227–242.
216. N. E. Good, G. D. Winget, W. Winter, T. N. Connolly, S. Izawa, R. M. M. Singh, *Biochemistry* **1966**, *5*, 467–477.
217. C. F. Naumann, B. Prijs, H. Sigel, *Eur. J. Biochem.* **1974**, *41*, 209–216.
218. C. F. Naumann, H. Sigel, *J. Am. Chem. Soc.* **1974**, *96*, 2750–2756.
219. P. Chaudhuri, H. Sigel, *J. Am. Chem. Soc.* **1977**, *99*, 3142–3150.
220. P. R. Mitchell, H. Sigel, *J. Am. Chem. Soc.* **1978**, *100*, 1564–1570.
221. E. M. Bianchi, S. A. A. Sajadi, B. Song, H. Sigel, *Inorg. Chim. Acta* **2000**, *300–302*, 487–498.
222. P. R. Mitchell, B. Prijs, H. Sigel, *Helv. Chim. Acta* **1979**, *62*, 1723–1735.
223. R. Tribolet, R. Malini-Balakrishnan, H. Sigel, *J. Chem. Soc., Dalton Trans.* **1985**, 2291–2303.
224. K. Aoki, *J. Am. Chem. Soc.* **1978**, *100*, 7106–7108.
225. P. Orioli, R. Cini, D. Donati, S. Mangani, *J. Am. Chem. Soc.* **1981**, *103*, 4446–4452.
226. W. S. Sheldrick, *Z. Naturforsch.* **1982**, *37b*, 863–871.
227. H. Sigel, K. H. Scheller, R. M. Milburn, *Inorg. Chem.* **1984**, *23*, 1933–1938.
228. R. Tribolet, R. B. Martin, H. Sigel, *Inorg. Chem.* **1987**, *26*, 638–643.
229. H. Sigel, R. Tribolet, O. Yamauchi, *Comments Inorg. Chem.* **1990**, *9*, 305–330.
230. H. Sigel, B. E. Fischer, E. Farkas, *Inorg. Chem.* **1983**, *22*, 925–934.
231. S. S. Massoud, H. Sigel, *Inorg. Chim. Acta* **1989**, *159*, 243–252.
232. S. S. Massoud, R. Tribolet, H. Sigel, *Eur. J. Biochem.* **1990**, *187*, 387–393.
233. C. F. Naumann, H. Sigel, *FEBS Lett.* **1974**, *47*, 122–124.
234. H. Sigel, C. F. Naumann, *J. Am. Chem. Soc.* **1976**, *98*, 730–739.
235. J.-J. Toulmé, *Bioinorg. Chem.* **1978**, *8*, 319–329.
236. R. Basosi, E. Gaggelli, E. Tiezzi, *J. Chem. Res. (S')* **1977**, 278–279.
237. G. Arena, R. Calì, V. Cucinotta, S. Musumeci, E. Rizzarelli, S. Sammartano, *J. Chem. Soc., Dalton Trans.* **1984**, 1651–1658.
238. H. Sigel, *Chimia* **1967**, *21*, 489–500.
239. J. Zhao, B. Song, N. Saha, A. Saha, F. Gregáň, M. Bastian, H. Sigel, *Inorg. Chim. Acta* **1996**, *250*, 185–188.
240. B. E. Fischer, H. Sigel, *Inorg. Chem.* **1979**, *18*, 425–428.
241. B. Knobloch, H. Sigel, A. Okruszek, R. K. O. Sigel, *Chem. Eur. J.* **2007**, *13*, 1804–1814.
242. B. Knobloch, B. Nawrot, A. Okruszek, R. K. O. Sigel, *Chem. Eur. J.* **2008**, *14*, 3100–3109.

243. B. Knobloch, H. Sigel, A. Okruszek, R. K. O. Sigel, *Organic Biomol. Chem.* **2006**, *4*, 1085–1090.
244. B. Song, H. Sigel, *Inorg. Chem.* **1998**, *37*, 2066–2069.
245. J. Kozelka, G. Barre, *Chem. Eur. J.* **1997**, *3*, 1405–1409.
246. T. Weber, F. Legendre, V. Novozamsky, J. Kozelka, *Metal-Based Drugs* **1999**, *6*, 5–16.
247. N. A. Corfù, H. Sigel, *Eur. J. Biochem.* **1991**, *199*, 659–669.
248. H. Sigel, *Biol. Trace Elem. Res.* **1989**, *21*, 49–59.
249. J. C. Chottard, J. P. Girault, G. Chottard, J. Y. Lallemand, D. Mansuy, *J. Am. Chem. Soc.* **1980**, *102*, 5565–5572.
250. J. C. Chottard, J. P. Girault, G. Chottard, J. Y. Lallemand, D. Mansuy, *Nouv. J. Chim.* **1978**, *2*, 551–553.
251. G. Bertin, D. Averbeck, *Biochimie* **2006**, *88*, 1549–1559.
252. V. L. Pecoraro, J. D. Hermes, W. W. Cleland, *Biochemistry* **1984**, *23*, 5262–5271.
253. M. D. Erlacher, N. Polacek, *Methods Mol. Biol.* **2012**, *848*, 215–226.
254. S. Basu, M. J. Morris, C. Pazsint, *Methods Mol. Biol.* **2012**, *848*, 275–296.
255. O. Fedorova, A. M. Pyle, *EMBO J.* **2005**, *24*, 3906–3916.
256. P. M. Gordon, R. Fong, J. A. Piccirilli, *Chem. Biol.* **2007**, *14*, 607–612.
257. P. M. Gordon, J. A. Piccirilli, *Nat. Struct. Biol.* **2001**, *8*, 893–898.
258. P. M. Gordon, E. J. Sontheimer, J. A. Piccirilli, *Biochemistry* **2000**, *39*, 12939–12952.
259. S.-o. Shan, A. V. Kravchuk, J. A. Piccirilli, D. Herschlag, *Biochemistry* **2001**, *40*, 5161–5171.
260. S.-o. Shan, A. Yoshida, S. Sun, J. A. Piccirilli, D. Herschlag, *Proc. Natl. Acad. Sci. USA* **1999**, *96*, 12299–12304.
261. M. Boudvillain, A. de Lencastre, A. M. Pyle, *Nature* **2000**, *406*, 315–318.
262. M. Boudvillain, A. M. Pyle, *EMBO J.* **1998**, *17*, 7091–7104.
263. M. Cohn, N. Shih, J. Nick, *J. Biol. Chem.* **1982**, *257*, 7646–7649.
264. P. M. J. Burgers, F. Eckstein, *J. Biol. Chem.* **1980**, *255*, 8229–8233.
265. J. M. Warnecke, J. P. Fürste, W.-D. Hardt, V. A. Erdmann, R. K. Hartmann, *Proc. Natl. Acad. Sci. USA* **1996**, *93*, 8924–8928.
266. J. M. Warnecke, R. Held, S. Busch, R. K. Hartmann, *J. Mol. Biol.* **1999**, *290*, 433–445.
267. E. J. Sontheimer, P. M. Gordon, J. A. Piccirilli, *Genes Dev.* **1999**, *13*, 1729–1741.
268. S.-L. Yean, G. Wuenschell, J. Termini, R.-J. Lin, *Nature* **2000**, *408*, 881–884.
269. L. B. Weinstein, B. C. N. M. Jones, R. Cosstick, T. R. Cech, *Nature* **1997**, *388*, 805–808.
270. A. Yoshida, S. Sun, J. A. Piccirilli, *Nature Struct. Biol.* **1999**, *6*, 318–321.
271. E. C. Scott, O. C. Uhlenbeck, *Nucleic Acids Res.* **1999**, *27*, 479–484.
272. A. Peracchi, L. Beigelman, E. C. Scott, O. C. Uhlenbeck, D. Herschlag, *J. Biol. Chem.* **1997**, *272*, 26822–26826.
273. N. Kisseleva, A. Khvorova, E. Westhof, O. Schiemann, *RNA* **2005**, *11*, 1–6.
274. M. Maderia, L. M. Hunsicker, V. J. DeRose, *Biochemistry* **2000**, *39*, 12113–12120.
275. E. M. Osborne, W. L. Ward, M. Z. Ruehle, V. J. DeRose, *Biochemistry* **2009**, *48*, 10654–10664.
276. K.-i. Suzumura, K. Yoshinari, Y. Tanaka, Y. Takagi, Y. Kasai, M. Warashina, T. Kuwabara, M. Orita, K. Taira, *J. Am. Chem. Soc.* **2002**, *124*, 8230–8236.
277. Y. Tanaka, C. Kojima, E. H. Morita, Y. Kasai, K. Yamasaki, A. Ono, M. Kainosho, K. Taira, *J. Am. Chem. Soc.* **2002**, *124*, 4595–4601.
278. J. B. Murray, A. A. Seyhan, N. G. Walter, J. M. Burke, W. G. Scott, *Chem. Biol.* **1998**, *5*, 587–595.
279. H. Sigel, R. Tribolet, *J. Inorg. Biochem.* **1990**, *40*, 163–179.
280. H. Sigel, *Inorg. Chim. Acta* **1992**, *198–200*, 1–11.
281. A. Serganov, S. Keiper, L. Malinina, V. Tereshko, E. Skripkin, C. Höbartner, A. Polonskaia, A. T. Phan, R. Wombacher, R. Micura, Z. Dauter, A. Jäschke, D. J. Patel, *Nature Struct. Mol. Biol.* **2005**, *12*, 218–224.
282. J. B. Murray, H. Szöke, A. Szöke, W. G. Scott, *Mol. Cell* **2000**, *5*, 279–287.
283. P. A. Rice, S.-w. Yang, K. Mizuuchi, H. A. Nash, *Cell* **1996**, *87*, 1295–1306.
284. K. K. Swinger, P. A. Rice, *J. Mol. Biol.* **2007**, *365*, 1005–1016.

285. H. Pelletier, M. R. Sawaya, *Biochemistry* **1996**, *35*, 12778–12787.
286. R. Koradi, M. Billeter, K. Wüthrich, *J. Mol. Graphics* **1996**, *14*, 29–32, 51–55.
287. B. T. Wimberly, R. Guymon, J. P. McCutcheon, S. W. White, V. Ramakrishnan, *Cell* **1999**, *97*, 491–502.
288. N. Kisseleva, S. Kraut, A. Jäschke, O. Schiemann, *HFSP J.* **2007**, *1*, 127–136.
289. B. Knobloch, M. C. Erat, R. K. O. Sigel, *to be submitted for publication*.
290. J. Loebus, E. A. Peroza, N. Blüthgen, T. Fox, W. Meyer-Klaucke, O. Zerbe, E. Freisinger, *J. Biol. Inorg. Chem.* **2011**, *16*, 683–694.
291. E. A. Peroza, A. Al Kaabi, W. Meyer-Klaucke, G. Wellenreuther, E. Freisinger, *J. Inorg. Biochem.* **2009**, *103*, 342–353.
292. D. Donghi, M. Pechlaner, B. Knobloch, C. Finazzo, R. K. O. Sigel, *Nucleic Acids Res.* **2012**, in press; DOI:10.1093/nar/gks1179.

Chapter 9
Cadmium(II) Complexes of Amino Acids and Peptides

Imre Sóvágó and Katalin Várnagy

Contents

ABSTRACT 276
1 INTRODUCTION 276
2 COMPLEXES OF AMINO ACIDS AND DERIVATIVES 278
2.1 General Characteristics of Cadmium(II) Complexes of Amino Acids 278
2.2 Complexes of Amino Acids with Non-coordinating Side Chains 279
2.3 Complexes of Amino Acids with Coordinating Side Chains 280
2.3.1 Complexes of Amino Acids with O-Donor Side Chains 281
2.3.2 Complexes of Amino Acids with N-Donor Side Chains 281
2.3.3 Complexes of Amino Acids Containing Sulfur Donor Atoms 282
2.3.4 Complexes of Thioether Ligands 282
2.3.5 Complexes of Cysteine and Derivatives 284
3 COMPLEXES OF PEPTIDES AND RELATED LIGANDS 286
3.1 Complexes of Peptides with Non-coordinating Side Chains 286
3.2 Complexes of Peptides with Coordinating Side Chains 287
3.3 Complexes of Peptides Containing Histidine 289
3.4 Complexes of Peptides with Thiol Donor Functions 291
3.4.1 Cadmium(II) Complexes of Small Peptides Containing L-Cysteinyl Residues 291
3.4.2 Complexes of Glutathione 293
3.4.3 Complexes of Peptides with Multiple Cysteinyl Sites 294
3.4.4 Cadmium(II) Binding to Phytochelatins and Related Ligands 294
4 COMPARISON OF CADMIUM(II) COMPLEXES WITH OTHER TRANSITION ELEMENTS 295
ABBREVIATIONS AND DEFINITIONS 299
ACKNOWLEDGMENTS 299
REFERENCES 299

I. Sóvágó (✉) • K. Várnagy
Department of Inorganic and Analytical Chemistry, University of Debrecen,
P.O. Box 21, H-4010 Debrecen, Hungary
e-mail: sovago@science.unideb.hu; varnagy.katalin@science.unideb.hu

A. Sigel, H. Sigel, and R.K.O. Sigel (eds.), *Cadmium: From Toxicity to Essentiality*,
Metal Ions in Life Sciences 11, DOI 10.1007/978-94-007-5179-8_9,

Abstract Cadmium(II) ions form complexes with all natural amino acids and peptides. The thermodynamic stabilities of the cadmium(II) complexes of the most common amino acids and peptides are generally lower than those of the corresponding zinc(II) complexes, except the complexes of thiolate ligands. The coordination geometry of the cadmium(II) amino acid complexes is generally octahedral with the involvement of the amino and carboxylate groups in metal binding. In the case of simple peptides, both octahedral and tetrahedral complexes can be formed depending on the steric conditions. The terminal amino group and the subsequent carbonyl-O atom are the primary binding sites and there is no example for cadmium(II)-induced peptide amide deprotonation and coordination. The various hydrophobic and polar side chains do not have a significant impact on the structural and thermodynamic parameters of cadmium(II) complexes of amino acids and peptides. β-carboxylate function of aspartic acid and imidazole-N donors of histidyl residues slightly enhance the thermodynamic stability of cadmium(II)-peptide complexes. The most remarkable effects of side chains are, however, connected to the involvement of thiolate residues in cadmium(II) binding. Stability constants of the cadmium(II) complexes of both L-cysteine and its peptides and related ligands are significantly higher than those of the zinc(II) complexes. Thiolate donor functions can be bridging ligands too, resulting in the formation of polynuclear cadmium(II) complexes.

Keywords amino acids • cadmium(II) • peptides • histidine • cysteine • thiolate ligands • stability constants • octahedral complexes • polynuclear complexes

1 Introduction

Cadmium is a d-block element with the electronic configuration $4d^{10}5s^2$. The closed d-shell results in the stabilization of the divalent (+2) oxidation state and up to now stable cadmium compounds have not been prepared in any other form. Cadmium is often referred to as the last member of the 4d (or second row) transition elements, while other textbooks describe cadmium as a member of the zinc group (Zn, Cd, and Hg) and do not consider it as a transition element. This dichotomy is reflected in the chemical properties of the element showing similarities to both transition and p-block metals. The basic chemical properties of cadmium and its major compounds including its complexes have been thoroughly described in the major inorganic and coordination chemistry textbooks. It is not the aim of this compilation to give an overview on the chemistry of cadmium(II) compounds. We will focus only on the major characteristics of cadmium(II) complexes affecting the interactions with amino acids and peptides.

The cadmium(II) ion with its d^{10} configuration shows no preferences for any coordination geometry arising from the crystal field stabilization. Therefore, it displays a variety of coordination geometries based upon the interplay of electrostatic effects, the covalency, and the size factor. Similarly to zinc(II) ion, 4 and 6 are the most common coordination numbers existing in tetrahedral and octahedral complexes, respectively. The ionic radius of cadmium(II) is, however, significantly larger than that of zinc(II) resulting in a high preference for the formation of six-coordinated octahedral species with cadmium(II). The donor atom preferences are also slightly different for the two metal ions. The classification of zinc(II) into the hard-soft categories is rather contradictory because it forms stable complexes with both oxygen and sulfur donor ligands; e.g., see the easy formation of $[Zn(OH)_4]^{2-}$ hydroxo complexes and of the ZnS precipitate. The increased size of cadmium(II) ions enhances its affinity towards sulfur containing ligands which is reflected in the binding mode of cadmium(II) under biological conditions, too. Similar differences can be observed in the hydrolytic reactions of the two metal ions. It is well-known that simple zinc(II) compounds are hydrolyzed even in slightly acidic samples (around pH 6.0) but the hydroxide precipitates are easily dissolved under alkaline conditions. On the contrary, cadmium(II) does not show any amphoteric character. The precipitation of cadmium(II)-hydroxide occurs in slightly basic solution (pH ~ 8.0) but this precipitate does not dissolve even at high pH values.

There is a significant difference in the affinity of the two metal ions towards the complexation with halide ions, too. In a diluted aqueous solution of zinc(II) chloride the octahedral aqua ions $[Zn(H_2O)_6]^{2+}$ are the predominating species, while a significant ratio of chloro complexes are formed with cadmium(II) under the same conditions. The stability constants of the complexes formed with bromide or iodide ions are even higher. The consideration of these differences is especially important during the selection of the appropriate counter ions to adjust the ionic strength for thermodynamic or electrochemical studies or even in the synthesis of cadmium(II) compounds.

Finally, it is also important to compare the properties of cadmium(II) and mercury(II) ions. For most of the transition elements the chemical properties of the 4d series are rather similar to those of the 5d elements. This is not true for the zinc(II) group elements and the properties of cadmium(II) significantly differ from those of mercury(II). Coordination numbers 2 (linear) and 4 (tetrahedral) are the most preferred arrangements for mercury(II) complexes, while the octahedron is the major stereochemistry of cadmium(II). Moreover, mercury(II) is a typical soft metal ion with an outstanding affinity for the interaction of sulfur or other heavy donor ligands. It has already been mentioned that cadmium(II) ions also prefer the binding of thiolate sulfur atoms but the various nitrogen and oxygen donor ligands are also promising candidates for a stable interaction with this metal ion. As a consequence, all amino acids and peptides are effective ligands for the complexation with cadmium(II) and the differences in the side chain donor functions result in a great variety of the complex formations with these ligands as it will be shown in the next sections.

2 Complexes of Amino Acids and Derivatives

2.1 General Characteristics of Cadmium(II) Complexes of Amino Acids

Cadmium(II) complexes of almost all natural amino acids and numerous amino acid derivatives were studied in the last few decades. The complex formation processes are generally very simple, so in this review the comparison of their stability and structure with those of other metal ions is emphasized. The enhanced stability and high structural variety of the complexes were observed with sulfur-containing amino acids and their derivatives, the characterization of this type of complexes is described in Section 2.3.5.

The stoichiometry and stability constants of the complexes were determined most frequently by means of potentiometric techniques, but these data were very often completed with results of polarography. The structures of complexes were proposed on the basis of the stoichiometry and stability of various species and *via* the analogy to other metal ion complexes. In some cases, the suggested structures of complexes were supported by the use of IR-spectroscopy, ^{113}Cd NMR, and X-ray studies.

The solution studies were performed in the usual concentration range and metal ion to ligand ratios: metal ion concentrations of $5{\cdot}10^{-4}$ to $5{\cdot}10^{-3}$ M give metal ion to ligand ratios of 1:5 to 1:1. The complex formation processes take place in the pH range 5 to 9. The presence of cadmium(II)-amino acid complexes usually cannot be detected in acidic solutions (below pH 5) with the exception of systems containing thiol derivatives. The hydrolysis of cadmium(II) ions takes place in slightly basic solution and the complex formation processes are often not able to prevent the formation of cadmium(II) hydroxide precipitates. The presence of mixed hydroxo complexes is generally not detected.

Cadmium(II) has a high affinity towards halide anions as ligands: the stability of chloro complexes is around one order of magnitude higher than that of the common 3d transition metal ions (e.g., $\log \beta_1 = 1.59$, $\log \beta_2 = 2.25$, $\log \beta_3 = 2.40$ for Cd(II) [1], $\log \beta_1 = 0.73$, $\log \beta_2 = 1.17$, $\log \beta_3 = 1.20$ for Zn(II) [2], and $\log \beta_1 = 0.69$ for Ni(II) [3]). The presence of chloro complexes could not be neglected in diluted solutions, if chloride is the counter anion to adjust the ionic strength. As a consequence, the potentiometric and electrochemical data were generally determined at NO_3^- or ClO_4^- ionic strength. The preparation of $CdCl_2{\cdot}Gly$ and $CdCl_2{\cdot}2Gly$ complexes in the solid state [4] also proves the high affinity of cadmium(II) for chloride.

The stoichiometry and stability constants of cadmium(II)-amino acid complexes are collected in Tables 1 and 2 together with data of the corresponding zinc(II) complexes for comparison.

These data show that, with the exception of thiol derivatives, exlusively CdL and CdL_2 (and CdL_3 or CdHL in some cases) complexes are formed in all cadmium(II)-amino acid systems. The stoichiometries of the zinc(II) and cadmium(II)

Table 1 Stability constants (log β) of complexes formed between Cd(II) or Zn(II) and amino acid systems (I = 0.1–1 M KNO_3/$NaNO_3$, *I = 3 M $NaClO_4$, T = 293–298 K).

	CdL	CdL_2	CdL_3	Ref.	ZnL	ZnL_2	ZnL_3	Ref.
Glycine	4.26	7.83	10.51	[6]	5.03	9.23	11.65	[22]
Amino acids with hydrophobic side chains								
α-Alanine	3.96	7.37	9.98	[6]	4.63	8.66		[23]
Valine	3.70	6.90		[8]	4.46	8.24		[23]
Leucine	4.04	7.53		[10]	4.89	9.19		[10]
Isoleucine	3.60	6.79	9.32	[12]	4.49	8.49	10.90	[12]
2-Amino-pentanoic acid	3.73	7.03		[13]	4.42	8.52		[13]
2-Amino-hexanoic acid	3.86	7.33		[13]	4.59	8.93		[13]
β-Alanine	3.60	5.80		[16]	4.14			[23]
Amino acids with polar side chains								
Phenylalanine	3.60	6.79	9.32	[6]	4.43	8.50		[24]
Tryptophan	4.51	8.19		[17]	5.14	9.86		[17]
Arginine	3.27	6.45		[18]	4.19	8.12		[18]
Asparagine*	4.07	7.58	9.61	[19]	5.07	9.43	12.30	[19]
Glutamine*	4.10	7.66		[19]	4.83	9.17	11.84	[25]
Amino acids with O-donor side chains								
Serine[a]	3.77	7.03	9.33	[6]	4.45	8.16		[40]
Threonine	3.90	7.10		[8]	4.74	8.51		[41]
Tyrosine	3.56	6.08		[17]	4.20	8.24		[17]
Aspartic acid[a]	4.68	8.27		[6]	5.69	9.77		[42]
Amino acids with N-donor side chains								
Lysine[b]		7.80		[31]	4.06	7.53		[43]
Ornithine (2,5-diaminopentanoic acid)	3.41	5.82		[32]	3.77	6.44		[44]
Histidine[c]	5.58	9.92		[6]	6.45	12.01		[48]
Histamine[c]	4.78	8.05	10.05	[38]	5.21	10.13		[38]

[a] ZnH_{-1} L: –3.73 (serine), –3.20 (aspartic acid).
[b] ZnHL: 14.72, $ZnHL_2$: 19.67, ZnH_2L_2: 28.85.
[c] CdHL: 11.16 (histidine), 11.53 (histamine).

complexes are very similar, though the formation of mixed hydroxo species was also observed in some cases. The presence of a thiol group in the side chain results in the formation of di- or trinuclear cadmium(II) complexes and the preference for formation of polynuclear species is much higher in cadmium(II)-containing systems than in the presence of zinc(II).

2.2 *Complexes of Amino Acids with Non-coordinating Side Chains*

The stoichiometry and thermodynamic stability constants of cadmium(II) complexes of glycine [5–7] and numerous amino acids containing hydrophobic [6,8–16] and polar [6,17–21] side chains were published. The stability constants of CdL and CdL_2 complexes are usually similar to each other (log β(CdL) ~ 3.6 – 4.1,

log $\beta(CdL_2) \sim 6.8 - 8.2$) and these complexes are around one order of magnitude less stable than the analogous zinc(II) complexes [22–25] (log $\beta(ZnL) \sim 4.4 - 5.2$, log $\beta(ZnL_2) \sim 8.2 - 9.9$). In these complexes metal ions bind to the amino and carboxylate groups forming five-membered chelate rings. This coordination mode was also established for the $CdCl_2 \cdot Gly$ complex in the solid state on the basis of infrared spectra [4]. Although these infrared experiments have shown a monodentate coordination of glycine *via* a carboxylate group in the $CdCl_2 \cdot 2Gly$ complex, the single carboxylate group does not offer an effective binding site for cadmium(II) in solution. This fact is proven by the low stability constant of the cadmium(II)-N-acetyl-glycine complex (log $\beta(CdL) = 1.13$) [26]. Comparison of the stability of Cd(II)-glycinamide [27,28] complexes (log $\beta(CdL) = 2.65$, log $\beta(CdL_2) = 4.88$) with those of the cadmium(II)-glycine systems proves the bidentate coordination of amino acids through the NH_2, COO^- donor set as well, while glycinamide is able to bind the metal ion *via* (NH_2, CO) donor groups resulting in a slightly reduced stability.

The stepwise stability constants characterizing the formation of ML_2 complexes and the log (K_1/K_2) values describing the preference for binding of the second ligand to the metal ion correspond to the statistical values, similarly to those of the zinc(II) complexes. For all cadmium(II)- and zinc(II)-phenylalanine and -arginine systems the log (K_1/K_2) values are lower than statistically expected (0.6) suggesting that the binding of the second ligand is favored. This can be explained by the stacking of aromatic rings of phenylalanine in the ML_2 complexes. Similar trends can be observed in the case of the cadmium(II)- and zinc(II)-arginine systems due to a secondary interaction between the polar side chains. The distance between the amino and carboxylate groups is larger in the β-alanine molecule and the simultaneous coordination of the two terminal groups to the metal ion results in six-membered chelate rings decreasing the stability of mono- and bis(ligand) cadmium(II) complexes and increasing the log (K_1/K_2) value.

The octahedral geometry of cadmium(II) complexes also allows the formation of tris(ligand) complexes. Because of steric requirements the presence of ML_3 complexes was suggested only in the case of glycine and for some other amino acids containing small side chain residues. Indeed, the formation of all three cadmium(II)-glycine species was detected by means of ^{113}Cd NMR measurements [29]. These observations strongly support the existence of an octahedral coordination geometry of cadmium(II) in its common amino acid complexes.

2.3 *Complexes of Amino Acids with Coordinating Side Chains*

The O- and/or N-atoms in the side chains of amino acids can be potential binding sites for metal ions depending on the position of the donor atoms and the hard-soft character of the metal ion. Taking into account the soft character of cadmium(II) a negligible effect of O donor side chains can be expected, while the N donor atoms may have an enhanced ability to take part in the complex formation processes.

The characterization of complexes of various amino acids containing –OH (serine, threonine, tyrosine) [6,8,17,30] or –COOH groups (aspartic and glutamic acids) [6] and $–NH_2$ (lysine, ornithine) [31,32] or imidazole N (histidine, histamine) [3,6,33–38] has been published.

2.3.1 Complexes of Amino Acids with O-Donor Side Chains

The stoichiometry and stability constants of the complexes in Table 1 reflect that the presence of an –OH group in the side chain does not affect the metal binding ability of amino acids, not even the –OH group in a chelatable position (serine, threonine) takes part in metal ion binding. A slight enhancement of stability can be detected, however, for aspartic acid, where the tridentate coordination of the ligand is suggested. The coordination of side chain carboxylate groups was found in the solid complex of $Cd(AspH)NO_3$ and Cd(Asp) [39]. The coordination of the (NH_2,α-COO^-) set was detected in the Cd(Asp) species, nevertheless, the crystal structure of the $Cd(AspH)NO_3$ complex shows a two-dimensional polymer in which each cadmium is coordinated to oxygen donor atoms of carboxylate groups and a nitrate anion, the amino group is protonated and the aspartic acid molecules act as bridging ligands. The metal center is seven-coordinated with distorted octahedral geometry. It is worth to compare these data with those of lead(II), which has a similar soft character, and both types of analogous solid complexes were prepared. The metal ion is bound to the same donor atoms in these species, but the metal center in the $Pb(AspH)NO_3$ complex is six-coordinated with regular octahedral geometry.

A similar trend of stability constants can be observed for the corresponding zinc(II) complexes [17,40–42]. The binding of the extra carboxylate group of aspartic acid results in an increased stability. At the same time, similarly to the amino acids containing non-coordinating side chains, these amino acids also form more stable complexes with zinc(II) compared to cadmium(II). The steric effects of bulky side chains or the tridentate binding of the ligands prevent the formation of tris complexes in all cadmium(II)- and zinc(II)-containing systems with the exception of the cadmium(II)-serine system.

2.3.2 Complexes of Amino Acids with N-Donor Side Chains

Lysine and ornithine contain an additional terminal amino group in the side chain. The simultaneous binding of these amino groups with the (NH_2,COO^-) donor set to the metal ion would result in the formation of eight- or seven-membered chelate rings, respectively, which are not favored by transition metal ions. Similarly to other metal ions, the presence of the side chain amino group does not have a significant impact on the thermodynamic stability of these cadmium(II) complexes [31,32,43,44]. There are, however, significant differences in the preferred stoichiometry of the complexes because the non-coordinated amino groups remain protonated below pH 9.0.

The imidazole-nitrogen donor of histidine is one of the most important binding sites for transition metal ions in biological systems. The N(3) atom itself can be a metal binding site which is reflected in the significant complex formation processes in the lead(II) or copper(II) 4-methylimidazole and N-acetyl-histidine-amide systems [45,46]; yet, a much lower affinity of these ligands is observed towards cadmium(II) [45,47]. The presence of the terminal amino group in histidine or histamine, however, enhances the coordination ability of the ligands forming stable six-membered chelate rings. As a consequence, a higher thermodynamic stability of the cadmium(II)-histamine and -histidine complexes was observed compared to other amino acids, or similarly, compared to other metal ions like Cu(II), Ni(II) or Zn(II) [48]. Nevertheless, the stability order follows the same trend as was mentioned for other amino acids: log β(Cd(II) complexes) < log β(Zn(II) complexes). On the other hand, similarly to other metal ions, a tridentate coordination of histidine was suggested, which is reflected in the stability order: log β(Cd(II)(histamine)$_{1,2}$) < log β(Cd(II)(histidine)$_{1,2}$) [6]. The stoichiometry and stability of the complexes were determined using potentiometry [3,6,33–36] or polarography [37]; the tridentate coordination of the ligand and the regular octahedral geometry of the complexes were further supported by means of cyclic voltammetry [49] and IR multiple photon dissociation spectroscopy [50]. In the latter experiments, the structures of Cd(Cl)(HHis), CdL and Cd(HHis)$_2$ species have been determined in the gas phase and the data were completed by quantum mechanical calculations. The results indicated that histidine coordinates to the metal in a charge-solvated tridentate form in the Cd(Cl)(HHis) complex and has a similar tridentate configuration with a deprotonated carboxylic acid terminus in the CdL complex.

2.3.3 Complexes of Amino Acids Containing Sulfur Donor Atoms

The sulfur atom with its soft character can be an important binding site for cadmium(II). Methionine and cysteine (or cystine) are proteinogenic amino acids containing sulfur donor atoms in the side chain in different chemical environments, namely as thioether and thiol (or disulfide) groups, respectively. In addition to their cadmium(II) and zinc(II) complexes [6,51–53] those of numerous amino acid derivatives containing thioether (S-methyl-cysteine) [6] and thiol groups (D-penicillamine, N-acetyl-cysteine, cysteine-methylester, N-acetyl-D-penicillamine, N-2-mercaptopropanoyl-glycine, 2-mercaptosuccinic acid) [27,54–59] were studied. The thermodynamic stability constants of cadmium(II) and zinc(II) complexes of sulfur-containing ligands are collected in Table 2.

2.3.4 Complexes of Thioether Ligands

In both, the cadmium(II) S-methyl-cysteine and methionine systems, mono-, bis-, and tris(ligand) complexes are formed corresponding to the six-coordinated octahedral geometry of cadmium(II). Although the corresponding zinc(II) complexes

Table 2 Stability constants (log β) of complexes formed by Cd(II) or Zn(II) and sulfur-containing ligand systems (I = 0.1–1 M KNO_3/$NaNO_3$, T = 293–298 K).

	CdL	CdL_2	CdL_3	Cd_2L_3	Cd_3L_4	Ref.	ZnL	ZnL_2	ZnHL	Zn_2L_3	Zn_3L_4	Ref.
Amino acids with a sulfur-containing side chain												
S-Methyl-cysteine	3.79	7.04	9.63			[6]	4.46	8.52				[54]
Methionine	3.65	6.76	9.08			[6]	4.38	8.35				[53]
Cysteine[a,b]	12.82	21.71	27.52	40.41		[52]	8.20	12.05	14.76	29.20	42.11	[51]
D-Penicillamine[a,b]	11.53	19.64			50.22	[27]	9.66	19.39	14.80			[51]
N-Acetyl-cysteine[b,c]	7.05	13.49	17.41		35.53	[27]	4.90	11.48				[55]
Cysteine-methylester[b,c]	8.51	16.41	19.28	29.52		[27]	8.21	15.91	11.90			[56]
N-Acetyl-D-penicillamine	7.53	14.11	17.44		35.99	[27]	6.85	14.03				[57]
N-2-Mercaptopropanoyl-glycine	6.83	12.78	16.71		33.01	[27]	5.72	10.45				[58]
2-Mercaptosuccinic acid	10.05	13.51			41.59	[27]	8.24	14.56				[59]

[a] Zn_3HL_4: 49.01 (cysteine), ZnH_2L_2: 29.93 (cysteine), 30.65 (D-penicillamine).
[b] $ZnHL_2$: 24.43 (cysteine), 25.23 (D-penicillamine), 18.39 (N-acetyl-cysteine), 20.76 (cysteine-methylester).
[c] ZnH_{-1} L: 2,71 (N-acetyl-cysteine), 0.41 (cysteine-methylester).

are more stable, the formation of ZnL_3 complexes was not detected. Taking into account the different pK values of the terminal amino groups of amino acids, the relative stability of the complexes can be evaluated by the comparison of the the log β_1 – pK(NH_3^+) values: glycine: –5.30 ~ methionine: –5.41 < S-methyl-cysteine: –4.93. The higher value for S-methyl-cysteine reflects the enhancement of the stability of the cadmium(II) complex of this ligand, which could be explained by the participation of the thioether sulfur atom in metal binding. The tridentate coordination of the ligand results in the formation of two five-membered chelate rings. The contribution of the thioether moiety to metal binding is, however, rather weak and cannot prevent formation of the tris(ligand) complex. Moreover, the same effect cannot be observed for methionine due to the larger distance between thioether and amino/carboxylate groups.

2.3.5 Complexes of Cysteine and Derivatives

The investigation of the complexes of cysteine and a series of amino acid derivatives containing thiol groups gave the possibility to compare the coordination ability of these ligands and assess the trend of stability of the complexes which coordinate to different donor groups. In L-cysteine and D-penicillamine three potential donor groups (NH_2, S^-, COO^-) are present, while in the N-acetyl-cysteine, N-acetyl-D-penicillamine, N-2-mercapto-propanoyl-glycine and 2-mercapto-succinic acid the (S^-,COO^-/CO) and in cysteine-methylester the (NH_2,S^-) donor sets serve as the metal binding sites. All data reveal the significantly enhanced stability of cadmium(II) complexes with these thiolate ligands. The stability of complexes follows the trend: N-2-mercapto-propanoyl-glycine ~ N-acetyl-cysteine ~ N-acetyl-D-penicillamine < cysteine-methylester < 2-mercapto-succinic acid < D-penicillamine ~ L-cysteine. The highest stability constants for D-penicillamine and L-cysteine prove the tridentate coordination of these ligands with (N,S,O) binding mode and this coordination mode is preferred compared to the tridentate (N,O,O) coordination of 2-mercapto-succinic acid. Thiol sulfur donor atoms of cysteine and penicillamine are in chelating position with both amino (five-membered) and carboxylate groups (six-membered) and this tridentate coordination mode is much more favored for binding to cadmium(II) than that of bidentate coordination of the common amino acids. Moreover, the coordination of thiol sulfur atoms together with the carboxylate or/and amino groups results in the enhanced stability of cadmium(II) complexes as compared to those of zinc(II) or nickel(II) [51]. It can be concluded that the thiol group is a more effective binding site for cadmium(II) than for the other two metal ions.

The other characteristic feature of the thiol donor group in cadmium complexes is the formation of oligomeric structures. The existence of Cd_2L_3 was detected in the cadmium(II)-cysteine and -cysteine-methylester system,

while trinuclear Cd_3L_4 species are present for the other thiol derivatives. Similar structures were determined for nickel(II) and zinc(II) [51]. The suggested structure of these complexes contains two or three metal ions connected *via* sulfur bridges. The formation of oligomeric species is the most common in the case of cadmium(II)-containing systems, and these complexes are usually present in the slightly acidic or neutral pH range in equimolar solutions. Increasing the excess of ligand and/or pH makes the formation of CdL_2 and CdL_3 species preferable. The use of polarographic techniques established the formation of polynuclear species as well [27].

Most of the earlier studies on the cadmium(II) complexes of L-cysteine and derivatives have been performed in rather diluted solutions and the tridentate chelating form of the ligand predominated under these conditions. In the last few years the structures of the complexes formed in more concentrated samples or in the solid state were determined by means of X-ray diffraction, ^{113}Cd NMR, Raman, IR, EXAFS, and XANES spectroscopic methods [60–62]. The complexes $[Cd(HCys)_2 \cdot H_2O]$ and $[Cd(HCys)_2 \cdot H_2O] \cdot H_3O^+ClO_4^-$ were prepared from acidic solution and the combined application of various spectroscopic techniques revealed that the cysteine amino group is protonated and not involved in bonding. The existence of CdS_4 and CdS_3O structural units with single thiolate (Cd-S-Cd) bridges were identified, although a minor amount of central Cd(II) with $CdS_3O_{2/3}$ and CdS_4O coordination environments cannot be ruled out. ^{113}Cd NMR measurements were carried out in cadmium(II)-cysteine, -penicillamine, and -N-acetyl-cysteine solutions at two orders of magnitude higher concentration (0.2–2.0 M) than the one used for the potentiometric measurements. Around physiological pH and in the presence of high excess of ligand the complexes are almost exclusively sulfur-coordinated as [Cd(S-cysteinate)$_4$], while the deprotonation of the ammonium groups promotes chelate formation, and the presence of complexes with CdS_3N coordination was also supposed. Similarly to the cadmium(II)-cysteine system the tetrathiolate complex is the major species in the cadmium(II)-N-acetyl-cysteine solution under similar circumstances ([ligand] = 1.0 M, high excess of ligand). Oligomeric complexes with CdS_3O_3, CdS_3O, and CdS_4 coordination sites and a single thiolate bridge between cadmium(II) ions were also detected at a 1:2 metal to ligand ratio.

For the corresponding penicillamine systems, however, the Cd(penicillamine)$_3$ complexes were found to be the dominating species with a CdS_3(N/O) coordination mode around pH 7.5. The increase of pH resulted in the formation of complexes with mixed coordinated CdS_2(N)(N/O) metal centers. These findings are in good agreement with previous conclusions that D-penicillamine has a reduced affinity to form polynuclear complexes. On the basis of these studies it was concluded [61] that the differences between cysteine and penicillamine as metal binding ligands can explain why cysteine-rich metallothioneines are capable of capturing cadmium(II) ions, while penicillamine can be a useful molecule for the treatment of the toxic effects of mercury(II) and lead(II) exposure and is not efficient against cadmium(II) poisoning.

3 Complexes of Peptides and Related Ligands

All major reviews [63–66] published on the metal complexes of peptides came to the conclusion that cadmium(II) complexes of peptides are much less studied than those of the essential 3d transition elements, i.e., copper(II), nickel(II), and zinc(II). The explanation of this is rather simple and evident: Several hundreds of structural and equilibrium studies support the result that the outstanding metal binding affinity of peptide ligands is connected to the involvement of amide groups in metal ion coordination. Up to now, there is no reliable publication in the literature for a cadmium(II)-promoted deprotonation and coordination of the peptide amide bond. As a consequence, the most common peptides without any coordinating side chain residue are relatively weak cadmium(II) binders. The coordination geometry of cadmium(II) peptide complexes is also rather simple, because the characteristic octahedral or tetrahedral species are formed in almost all cases. Unfortunately, the closed d-shell of cadmium(II) and the resulting diamagnetic and colorless complexes rule out the widespead applications of various spectroscopic techniques.

The typical soft character of cadmium(II), however, results in a high selectivity for the complexation with thiol containing ligands including L-cysteine and its peptide derivatives. A great majority of the papers published on cadmium(II)-peptide complexes focus on the various cysteinyl peptides with a special emphasis on the interactions with glutathione, phytochelatins, and various forms of thioneins. The high versatility in the complex formation of these peptides and their outstanding biological significance are thoroughly discussed in other chapters of this book. At this point, we will focus only on: (i) the cadmium(II) complexes of the most common small and oligopeptides revealing the similarities and differences in their structures and thermodynamic stabilities and (ii) the cadmium(II) complexes of the peptides of L-cysteine and related ligands including glutathione and structural models of phytochelatins.

3.1 Complexes of Peptides with Non-coordinating Side Chains

N-terminally protected amino acids and peptides are generally weak complexing agents for most of the divalent transition metal ions. Accordingly, in the cadmium(II)-N-acetylglycine system the monodentate carboxylate coordination of the ligand has been suggested on the basis of both potentiometric and IR spectroscopic measurements [26,67]. The comparison of the stability constants reported for the [ML] type complexes of cadmium(II) and zinc(II) with N-acetylglycine, however, revealed the enhanced tendency of cadmium(II) for carboxylate binding. The values log $K_1 = 1.13$ and 0.71 were published for cadmium(II) and zinc(II), respectively [26]. Similar conclusions were drawn from the NMR studies on the same systems [68].

The di- and tri-peptides with free amino termini are much more effective ligands for complexation with cadmium(II). The cadmium(II) complexes of diglycine and triglycine and some other peptides consisting of Ala, Leu, Pro or Val residues have been studied by potentiometric and NMR spectroscopic measurements [6,69–74]. Exclusive carboxylate binding of the peptides was suggested in acidic solution (pH <5.0), while the formation of the common (NH_2,CO) 5-membered chelate was suggested at increasing pH. NMR spectroscopy proved to be a very useful technique to study the cadmium(II) complexes of amino acids and peptides. The major advantage of the studies on cadmium(II) species is that in addition to the widely applied ^{1}H and ^{13}C NMR techniques [71], also ^{113}Cd NMR [73] can be efficiently applied. In most cases only the existence of [CdL] and [CdL_2] stoichiometries were suggested. As a consequence, there is a contradiction for the proposed structures of cadmium(II)-peptide complexes. Some authors suggest a tetrahedral environment [69], but the formation of octahedral complexes is also possible. This dichotomy probably comes from the experimental conditions used in the cited works. Relatively low ligand to metal ratios ($L/M < 2$) were generally used in these studies, while the formation of tris(ligand) complexes in measurable concentration requires a high ligand excess. The existence of octahedral tris(ligand) complexes is, however, definitely proven for the cadmium(II) complexes of simple amino acids suggesting the same coordination geometry for the small peptides. Unfortunately, exact structural determination studies have not been published for the cadmium(II) complexes of the most common peptide molecules.

Comparison of the stability constants published for the zinc(II) and cadmium(II) complexes of dipeptides leads to the same conclusions as reported for the amino acids. The values $\log \beta_1 = 3.75$ and 2.86 and $\log \beta_2 = 6.61$ and 5.35 were reported for the diglycine complexes of zinc(II) [75] and cadmium(II) [70], respectively. It is evident from these data that the thermodynamic stability of zinc(II) complexes is higher than that of cadmium(II). This trend is just the opposite of what was published for the monodentate carboxylate coordination but shows a good agreement with the data reported for corresponding amino acids. Moreover, these data show that simple dipeptides without any coordinating side chains are less effective ligands to bind cadmium(II) compared with the essential transition elements including zinc(II), cobalt(II), and especially nickel(II) or copper(II).

3.2 Complexes of Peptides with Coordinating Side Chains

The presence of side chain donor atoms generally influences the thermodynamic stability and coordination geometry of peptide complexes significantly. The most important findings in this field have already been reviewed by several authors [63–66]. It is evident from these compilations that the effects of various donor atoms largely depend on the number and location of the extra donor atoms and also on the nature of the metal ions. Most of the data were published for the copper(II) complexes, but nickel(II) and palladium(II) are also widely studied.

In the case of cadmium(II), systematic studies on the role of specific amino acid residues are not available. On the basis of the analogies to other transition elements and from selected data for several systems, some general conclusions on the role of side chain residues can be predicted.

The alcoholic-OH groups of serine and threonine are generally weakly coordinating donors and they do not affect significantly even the stability of copper(II) and zinc(II) peptide complexes. Similar effects can be expected for the interaction of these peptides with cadmium(II) and probably a similar conclusion can be drawn on the role of phenolate-O donor atoms of the tyrosyl residues. The carboxylate functions of aspartyl and glutamyl residues are much more effective metal binding sites and this is reflected in the thermodynamic stability of their cadmium(II) complexes. Stability constants for the GlyGlu complexes of cadmium(II) were determined by potentiometric measurements [76]. The formation of the species [CdHL] and [CdL] was detected with the stability constants log $K = 1.62$ and 3.43 for the reactions Cd + HL and Cd + L, respectively (charges are omitted for simplicity). The protonated complex corresponds to the exclusive carboxylate coordination, while the common (amino, carbonyl) (NH_2,CO) coordination mode is expected for the other species. Comparison of these data with those of GlyGly shows the enhanced stability of the complex formation in the presence of extra carboxylate residues. In another study, the cadmium(II)-induced helical structure of poly-glutamic acid was observed *via* the interaction of the carboxylate residues [77]. The stabilizing effect of the β-carboxylate groups of aspartic acid is generally more enhanced due to the formation of the (NH_2,COO^-) six-membered chelates. This type of interaction was identified in the cadmium(II)-AspAspAsnLysIle system [78] and a slight stability enhancement due to the aspartyl residue was observed in the cadmium(II) complexes of GlyAsp, too [73].

Taking into account the mildly soft character of cadmium(II), the thioether donor functions of peptides containing methionine or S-methyl-cysteine are promising candidates for an extra stabilization of complex formation. It is well known from many literature studies that thioether donor functions of peptides are the primary ligating sites in the silver(I), mercury(II), palladium(II), and platinum(II) complexes [79]. These effects, however, cannot be observed in the stability of the cadmium(II) complexes of either methionine or its simple peptides [6]. Similar conclusions were obtained from the studies on the cadmium(II) complexes of methionine enkephalin and the peptide fragments of prion protein containing also methionine residues [45,80]. In contrast to these results reported for the peptides, the existence of a Cd–S(thioether) bond was suggested in solid phase complexes of several ligands containing aromatic-N and thioether-S donor atoms [81,82]. The disulfide moiety which is a potential binding site of cystine and oxidized glutathione is also not considered as a binding site for the common transition elements. The double dipeptide $(GlyCys)_2$ contains the disulfide moiety in a promising location for metal binding but even in this case a direct M–S(disulfide) bond was not observed in the copper(II), nickel(II), zinc(II), cobalt(II), and cadmium(II) complexes [83]. On the contrary, studies on the cadmium(II) complexes of various thioamides revealed a stability enhancement resulting from a Cd–S(thiocarbonyl) interaction [27].

3.3 Complexes of Peptides Containing Histidine

The imidazole-N donor of the histidyl residue is generally considered as one of the most effective metal ion binding sites of peptides and proteins. A huge number of metalloproteins contain this residue in the active site and the peptide fragments of such proteins are among the most studied ligands. All general reviews on metal complexes of peptides also contain an overview on the complex formation of the peptides containing histidine [1–4], while some others are specifically devoted to these peptides and related ligands [84–86]. Most of the studies in this field are dealing with the interaction of these peptides with copper(II) but complex formation with nickel(II), palladium(II), and zinc(II) is also widely studied. The number of publications on the corresponding cadmium(II) complexes is not large but allows to draw some general conclusions.

One set of the studies includes solution and structural investigations on cadmium(II) complexes of terminally protected peptides containing one to four histidyl residues. It is widely accepted that the imidazole side chains are the primary metal binding sites in these peptides for almost any metal ion. It is also well documented that binding of several metal ions, like copper(II) and nickel(II) (and zinc(II) for some specific sequences [65,66,85]) can induce the parallel deprotonation and coordination of subsequent amide residues. It is important to emphasize that up to now there is no reliable publication for the cadmium(II)-promoted amide binding of peptides. Therefore, the peptide backbone cannot be considered as a potential binding site for complex formation with cadmium(II) and only the N-and/or C-termini and various side chains can be involved in binding. Small (tetra- and penta-) peptide fragments of prion protein provide simple examples for the coordination of imidazole-N donors in cadmium(II) complexes. The stability constants for the Cd-N_{im} bonded species fall into the range 2.2 to 2.7 [45,47]. The comparison of these values to those reported for other transition elements gives the stability order: Pd(II) > Cu(II) > Ni(II) ~ Zn(II) > Cd(II). It is evident from these data that even the presence of a histidyl residue does not significantly enhance the cadmium(II) binding ability of peptide molecules. Because of the relatively low thermodynamic stability of these complexes, the formation of 1:1 CdL species was suggested in most cases. The equilibrium data reported for the prion fragments were also compared to the stability constants of small model ligands, like N-acetyl-histamine [45] and 4-methylimidazole [47]. A slight stability enhancement of the peptide complexes was observed and this was explained by the effect of the other side chain residues of the peptides. The application of high ligand excess made it possible to detect the formation of CdL_2 and CdL_3 complexes with the latter ligand while in a former study even the existence of 1:4 stoichiometries was suggested [46].

The synthesis and studies of multihistidine peptides is a rapidly increasing field in metallopeptide chemistry because these ligands are the most promising models for biological conditions. The exclusive coordination of the imidazole-N side chain donor atoms of these ligands results in the formation of various macrochelates built

up from $2N_{im}$, $3N_{im}$ or $4N_{im}$ donors. The stability constants of these macrochelates are significantly enhanced with increasing number of coordinated imidazoles, but the size of the molecules and the other amino acids in the sequence also affect the overall stability. A huge number of data has been reported for the corresponding copper(II), nickel(II), and zinc(II) complexes [87] and more recently some data for corresponding cadmium(II) complexes also became available [88]. The involvement of sarcosine (N-methylglycine) in the peptide sequence, prevents metal ion coordination of amide residues, thus the peptides containing sarcosyl and histidyl residues in alternating positions (terminally protected HisSarHis, HisSarHisSarHis, and HisSarHisSarHisSarHis) are the best models to study macrochelation. The stability constants of these macrochelates are collected in Table 3. The stability order follows the trend: Cu(II) > Ni(II) > Zn(II) > Cd(II) in all cases. This stability order clearly demonstrates the relatively low affinity of peptides and/or imidazole-containing ligands for complex formation with cadmium(II).

Table 3 Stability constants (log *K*) of the macrochelate complexes of multihistidine peptides.

Binding	copper(II) [87]	nickel(II) [88]	zinc(II) [87]	cadmium(II) [88]
$M–2N_{im}$	6.48	3.89	3.66	3.24
$M–3N_{im}$	8.14	5.28	4.79	3.67
$M–4N_{im}$	9.29	6.04	5.58	4.14

The log *K* values refer to the [CdL] species of peptides with $2N_{im}$, $3N_{im}$ and $4N_{im}$ coordination of Ac-HisSarHis-NH_2, Ac-HisSarHisSarHis-NH_2, and Ac-HisSarHisSarHisSarHis-NH_2, respectively.

The N-terminally free histidine-containing peptides are more effective ligands than their protected counterparts. The cadmium(II) complex of GlyHis was studied by potentiometry and the stability constants log $\beta_1 = 3.69$ and log $\beta_2 = 5.44$ were obtained [6]. The value reported for the 1:1 complex is significantly higher than those of glycylglycine supporting the tridentate coordination mode of GlyHis in this species. On the other hand, this peptide is known as the simplest example for the zinc(II)-induced amide deprotonation and coordination but this reaction was not observed in the corresponding cadmium(II) complexes.

L-Carnosine (β-alanyl-L-histidine) represents one of the most important biologically relevant dipeptides. This peptide forms a very stable imidazole-bridged dinuclear complex with copper(II), but the formation of only simple mono and bis (ligand) complexes was suggested for cadmium(II). The corresponding stability constants are log $\beta_1 = 3.03$ and log $\beta_2 = 5.13$ for the species [CdL] and [CdL_2], respectively [89]. These values are rather similar to those reported for glycylglycine (see Section 3.1) indicating that the stabilizing role of imidazolyl side chains is quite weak in the cadmium(II) complexes. Comparison with the corresponding zinc(II) complexes leads to similar conclusions. The value log $\beta_1 = 4.11$ was reported for the [ZnL] complex of L-carnosine, which is definitely higher than that of cadmium(II). In another study, the cadmium(II)-L-carnosine system was investigated by ^{13}C NMR spectroscopy and the peptide was described as a quadridentate ligand which undergoes a tautomeric change during complex formation [90].

The N-terminus of albumin (AspAlaHis. . .) is known as the most effective metal binding site for the binding of copper(II) and nickel(II) (ATCUN motif) [65,66]. The zinc(II) and cadmium(II) complexes of the corresponding tripeptide (AspAlaHis-NHMe) were studied by potentiometric measurements [91]. It was found that neither zinc(II) nor cadmium(II) are able to induce amide deprotonation and coordination in these peptides. The complex [ML] was suggested as the major species with the stability constants log $K = 4.17$ and 3.66 for zinc(II) and cadmium(II), respectively. These values provide further support for the small stabilization effects of histidyl side chains in cadmium(II) complexes. The interaction of cadmium(II) with various forms of native serum albumins (HSA, BSA, PSA) was also studied by several groups [92,93]. It was found that cadmium(II) and zinc(II) cannot compete with copper(II) and nickel(II) for binding at the amino termini, but the second metal binding site of the protein can be an effective Cd/Zn binding site.

3.4 Complexes of Peptides with Thiol Donor Functions

A huge number of literature data prove that cadmium(II) has a high preference for thiolate-S^- donors. The high covalency of this bond is reflected in the low solubility and characteristic color of the CdS precipitate and also in the great structural variety of cadmium-thiolate complexes. Moreover, the occurrence and effects of cadmium(II) in biological systems are connected to its high affinity for binding in thioneins and phytochelatins. The biological role of these substances and the binding modes of cadmium(II) in metallothioneins and phytochelatins are discussed in other chapters in this book. Here we want to focus on the structural and equilibrium conditions of simple oligopeptides containing cysteinyl residues in different numbers and locations. Among them, the tripeptide glutathione is the best known and its sequence is in a close relation with those of phytochelatins. The peptides with multiple cysteinyl sites are frequently used models for the understanding of the chemistry of phytochelatins and also the effect of cadmium(II) binding to zinc finger proteins.

3.4.1 Cadmium(II) Complexes of Small Peptides Containing L-Cysteinyl Residues

N-acetyl-L-cysteine and N-acetyl-D-penicillamine are the simplest ligands containing the thiolate and amide donor functions in the same molecule. For understanding the coordination chemistry of L-cysteine and its peptide derivatives, it is important to take into account that the thiol group can form a five-membered chelate with the amide-N and a six-membered one with the carboxylate-O donor atoms. All studies rule out a cadmium(II)-induced amide coordination in these complexes, therefore the formation of the (S,O) chelate is the governing factor during complex formation with N-acetyl-L-cysteine. The equilibrium data have

been determined by potentiometric measurements for a series of derivatives of L-cysteine and related ligands [27]. The stability order of the various coordination modes was suggested as follows: (S,N,O) > (S,N) > (S,O,O) > (S,O) [27]. It is obvious from this stability sequence that the parallel coordination of the thiolate and amino donors are the most preferred ones, but the thermodynamic stability of the various (S,O) chelates is also significant. In accordance with the bidentate character of N-acetyl-L-cysteine and N-acetyl-D-penicillamine, the formation of mono, bis, and tris complexes was suggested supporting the octahedral geometry of the metal ion in these complexes. In a more recent study using X-ray absorption and ^{113}Cd NMR spectroscopies the formation of tetrathiolate and sulfur-bridged oligomeric species was also suggested in more concentrated samples [62].

The ability of cadmium(II) to form stable complexes both with (S,N) and (S,O) coordinations results in a significant difference in the coordination modes of dipeptides containing the cystenyl residues in the N- and C-termini. Very stable mono and bis(ligand) complexes ([CdL] and [CdL_2]) were formed in the cadmium(II)-CysGly system with the involvement of the (S^-,NH_2) coordination sites. This binding mode is favored for the high majority of transition metal ions and able to prevent the deprotonation and coordination of the amide goups even in the corresponding nickel(II) complexes [94]. However, in the case of AlaCys and PheCys containing C-terminal Cys residues, the (S^-,COO^-) coordination mode predominates and the uncoordinated amino groups are protonated around the physiological pH range. In the case of these dipeptides, there are significant differences in complex formation of different metal ions. In the case of nickel(II) and palladium(II), the coordination of the amino and thiolate functions promotes the ionization and binding of the internal amide function and very stable species are formed with (NH_2,N^-,S^-) binding sites [95]. The corresponding zinc(II) and cobalt(II) complexes are, however, very similar to those of cadmium(II), because the (S^-,COO^-) chelate is stable enough to prevent amide binding [57]. It is also important to note that the formation of thiolate-bridged polynuclear complexes was negligible in the diluted samples of these cadmium(II)-dipeptide systems. It has already been discussed in Section 2 that oligomerization is very significant with L-cysteine but it is suppressed for D-penicillamine because of the steric effects of the methyl substituents. The formation of oligomers was observed for other small ligands with (S,N) coordination sites, e.g., for 2-mercaptoethylamine [96]. The existence of these thiol-coordinated cadmium(II) centers can be easily followed by the application of ^{113}Cd NMR spectroscopy [97]. In all probability, the lack of oligomerization in diluted samples of peptide complexes can also be interpreted by the steric factors caused by the non-coordinated residues of the peptides.

Apart from glutathione, AlaAlaCys is the only tripeptide the cadmium(II) complexes of which have been studied [94]. Interestingly, its complex formation processes are very similar to those of AlaCys, the (S^-,COO^-)-coordinated C-terminus being the exclusive cadmium(II) binding site. This is a significant difference to the complex formation of any other peptide because in the absence of cysteinyl residues the N-terminal amino acids are the primary metal binding sites.

3.4.2 Complexes of Glutathione

Glutathione (γ-L-glutamyl-L-cysteinylglycine) is the most abundant naturally occurring tripeptide which participates in a series of biochemical processes especially in the defense mechanism against reactive oxygen species (ROS). It has a specific sequence because the γ-carboxylate group of the N-terminal glutamic acid is part of the peptide bond formed with cysteine. This results in the separation of the amino terminus from the amide and thiolate functions and in the high versatility of the complex forming processes of glutathione with any metal ion. The most important findings on the metal complexes of glutathione are discussed in the general reviews [63,64], while another compilation is devoted specifically to this ligand [98].

The complexity of the reactions of glutathione with metal ions comes from the fact that it can behave as an amino acid (*via* the N-terminus), a thiolate ligand (*via* the internal Cys residue), and as a peptide because the thiolate and the amide group from the Gly residue can form a chelate. A series of different experimental techniques has been used to study the interaction of cadmium(II) with glutathione. It is evident from the early potentiometric studies that the speciation of the cadmium(II)-glutathione system is very complicated and the stoichiometry of the major species depends on the metal to ligand ratios [99,100]. The existence of mono and bis(ligand) complexes, as well as various protonated and dinuclear species has been suggested. The published equilibrium data are contradictory but it is evident that the cadmium(II) complexes have a higher thermodynamic stability than the corresponding zinc(II) complexes. Almost any possible coordination mode was suggested to exist in these species with a preference for the involvement of thiolate and amino groups in cadmium(II) binding. Even ionization of the peptide linkage was suggested [99] but it was not supported by further studies.

The application of ^{13}C NMR spectroscopy provided additional insight into the binding sites of glutathione in its cadmium(II) complexes [101]. It was found that the actual sites involved in metal binding are dependent on the cadmium(II)/glutathione ratio and the pH of the solution. The thiolate, amino and glycyl carboxylate functions were suggested as the major cadmium(II) binding sites but the coordination of the amide function was reported to occur only in the zinc(II)-containing systems and not for cadmium(II). More recently, various NMR and ESI-MS experimental techniques and even DFT calculations were used to understand the cadmium(II)-glutathione interaction [102–104]. The preference for binding of the same sites as listed above was suggested in these studies as well, with a specific importance for the thiolate coordination in cadmium(II) binding. The structural similarity of glutathione and phytochelatins and the role of these substances in cadmium(II) detoxification gave a big impetus to the studies on the cadmium(II) complexes of other thiol-containing ligands related to glutathione. The results of these studies will be discussed together with those of phytochelatins in Section 3.4.4.

3.4.3 Complexes of Peptides with Multiple Cysteinyl Sites

There are at least three major types of natural proteins and peptides which are rich in cysteinyl residues: metallothioneins, zinc finger proteins, and phytochelatins. The biological role and structural characteristics of metallothioneins are dealt with in Chapter 11 of this book. Zinc finger peptides are possible targets for cadmium(II) toxicity, while phytochelatins play an important role in the defense mechanisms of plants (Chapter 13). The multicysteine peptides are frequently used to mimic the cadmium(II) binding ability of all these natural substances.

The hexapeptide LysCysThrCysCysAla contains three cysteinyl residues and corresponds to the C-terminal fragment (56–61) of mouse liver metallothionein. Its complexation with cadmium(II) was studied by CD and ^{113}Cd NMR spectroscopies and various electrochemical techniques [105–107]. The low solubility of the polynuclear complexes limited the applicability of the ^{113}Cd NMR spectroscopy. CD spectroscopy, however, provided a definite proof for the formation of a dinuclear cluster and subsequent conformational changes of the peptide [105]. The peptide fragment (49–61) of rabbit liver metallothionein contains four Cys residues and it was found that it can bind a single cadmium(II) ion in a monomeric complex with thiolate coordination [108]. The existence of similar mononuclear thiolate binding sites was also found in other cadmium(II) peptide complexes [109]. The coordination properties of the peptides with a -CXXC- sequence motif were studied with different metal ions. The stability of the complexes is closely related to the number of thiolate residues suggesting the involvement of all sulfur atoms in metal binding. The stability order of the complexes was reported as: Bi(III) >> Cd(II) > Zn(II) > Ni(II) [110]. The metal binding abilities of the -CAAC-, -CACA- and -CCAA- sequences were compared in another study [111].

The cadmium(II) binding ability of peptides containing both cysteinyl and histidyl (and/or aspartyl) residues was also studied. These peptides are promising models for the understanding of the structure of various zinc finger proteins [112] and newly identified types of metallothioneins [113]. It was found that the Cys(4) and Cys(2)His(2) sites have different affinites for zinc(II) and cadmium(II) binding which can contribute to the metal ion selectivity under biological conditions [113,114]. Affinity constants for the tetrahedral metal binding of the Cys(2)His(2) peptides have been determined *via* competition measurements. The relative affinities of the metals followed the order: Cd(II) ~ Zn(II) > Co(II), but the replacement of His by Asp resulted in a completely different coordination geometry [115].

3.4.4 Cadmium(II) Binding to Phytochelatins and Related Ligands

Phytochelatins with the general sequence $(\gamma\text{-Glu-Cys})_n$Gly (n = 2–11) are cysteine rich peptides synthesized by plants and are involved in metal ion bioregulation and phytoremediation. Chapters 12 and 13 of this volume are devoted to the biological

significance and the agricultural/industrial applications of these molecules. It is evident that the amino acid sequence of phytochelatins is closely related to that of glutathione reported in Section 3.4.2. It has already been discussed that the coordination chemistry of glutathione is rather complicated and the speciation for most of the metal ions is still contradictory. Phytochelatins have the same possible binding sites but with multiple cysteinyl residues. This results in an enhanced complexity in the interaction of cadmium(II) with phytochelatins. In the last few years a huge number of papers were published on various aspects of the interactions of cadmium(II) with phytochelatins and related ligands. Most of these studies focus on the biological aspects of this interaction and they are discussed in the above mentioned chapters. Several reviews are also available including the most important findings from a chemical point of view [116,117]. Taking into account these references, we focus here only on the basic coordination chemistry of phytochelatins and related substances.

The cadmium(II) binding ability of a short phytochelatin (γ-GluCys)$_2$Gly (PC2) has been studied by potentiometric, NMR, and UV-vis spectroscopies. It was found that the stoichiometry of the complexes depends very strongly on the molar ratio of the reactants and the pH of the solutions. The formation of mono and bis(ligand) complexes and various protonated species was suggested. The coordination of 4 S atoms was proposed in the bis complexes. In addition, cadmium binding of the terminal amino and both carboxylate residues was suggested for the monomeric complexes. The comparison of the stability constants with those of glutathione revealed the enhanced tendency of phytochelatin for cadmium(II) binding [118]. The application of various voltammetric experiments and parallel mass spectrometric measurements provided further insight in the interaction of cadmium(II) ions with phytochelatins [119–122]. It was found that the phytochelatins containing four or more (γ-GluCys) moieties can form dinuclear species and even mixed metal complexes can be formed with other soft elements including lead(II). In another set of experiments model peptides have been synthesized in which the glutamic acid was replaced by other amino acids, like Asp, Lys, Gly, Ser, and Gln. The cadmium(II) binding affinity of the various peptides was evaluated as: (γ-GluCys)$_7$Gly = (GluCys)$_7$Gly = (AspCys)$_7$Gly > (β-AspCys)$_7$Gly $\gg$ (LysCys)$_7$Gly [123].

4 Comparison of Cadmium(II) Complexes with Other Transition Elements

The results reported in the literature and summarized in the previous sections reveal that cadmium(II) can form complexes with all natural amino acids and peptides. The thermodynamic stabilities of the cadmium(II) complexes are, however, relatively low as compared to those of the corresponding copper(II) and nickel(II) complexes. On the other hand, these data are comparable to those of the essential zinc(II) and the small differences are dependent on the effects of various side chain residues. These effects together with the structural characteristics of the cadmium(II) complexes can be evaluated separately for amino acids and peptides.

The investigations of cadmium(II) complexes of amino acids and related ligands revealed that the amino acids do not have a high binding ability towards cadmium(II) with the exception of ligands containing thiol groups. The monodentate coordination of amino acids through their terminal amino, carboxylate or various side chain O or N donor functions results in a very week or even no interaction in solution but these donors can be binding sites in solid crystals. More significant complex formation processes occur *via* the bidentate (NH_2,COO^-) coordination but even in this case the stability constants of cadmium(II) complexes are more than one order of magnitude smaller than those of other metal ions (log β (Cu(II) complexes) > log β (Ni(II) complexes) > log β (Zn(II) complexes) > log β (Cd(II) complexes). The various hydrophobic and polar side chains do not have a significant impact on this interaction as it is well reflected by the thermodynamic stability constants of complexes given in Table 1. Only for aspartic acid and histidine the presence of the β-carboxylate group and imidazole-N donor site in the side chains, respectively, influences slightly the coordination ability of the ligands. The enhanced stability of these complexes comes from the participation of side chain donor atoms in metal binding resulting in tridentate coordination of the molecules.

Due to the soft character of cadmium(II) a stronger interaction with sulfur donor atoms could be expected. The influence of thioether groups is almost negligible and can be observed only in case the thioether group is bound simultaneously to the (NH_2,COO^-) donor set forming five-membered chelate rings. It is worth to mention that similar enhancement of the stability can be observed in the thioamide analogues of amino acids (methionine-N-methylamide), where the metal ion binds to the (NH_2,CS) set forming a five-membered chelate ring [27].

The most significant effect of the side chain donor atoms is detected for amino acids and related ligands containing thiol groups. Although the exclusive coordination of the thiolate donor atom was also found in solid state complexes and in more concentrated solutions around the physiological pH, but depending on the potential donor atoms the thiol sulfur and amino or/and carboxylate groups offer the main binding sites leading to chelates for most metal ions. Systematic studies on cadmium(II) complexes of thiol ligands have shown that the (NH_2,S^-) coordination is preferred over the (COO^-,S^-) one, and the tridentate binding of the ligand is the most favored situation.

The other general characteristic feature of cadmium(II) complexes with thiol derivatives is the formation of di- or trinuclear species, in which thiol sulfur atoms behave as bridging ligands. The existence of polynuclear species was observed in nickel(II)- and zinc(II)-cysteine systems with similar stoichiometry, but cadmium(II) complexes have usually an octahedral geometry, while in the nickel(II) complexes this coordination mode results in four-coordinated square planar complexes.

Comparison of the stability of cadmium(II) complexes of cysteine and related ligands with those of the corresponding nickel(II) and zinc(II) clearly shows that the stability order follows just opposite trends with respect to that of other amino acids: log β (Cd(II)-complexes) > log β (Ni(II)-complexes) > log β (Zn(II)-complexes).

Figure 1 illustrates the change of the stability order, where the log β values of monoligand cadmium(II) complexes are depicted together with those of the corresponding zinc(II) complexes. It is obvious from this figure that all amino acids form more stable complexes with zinc(II) than with cadmium(II) but the presence of the thiolate function results in an enhanced stability and the opposite trend of complex stability.

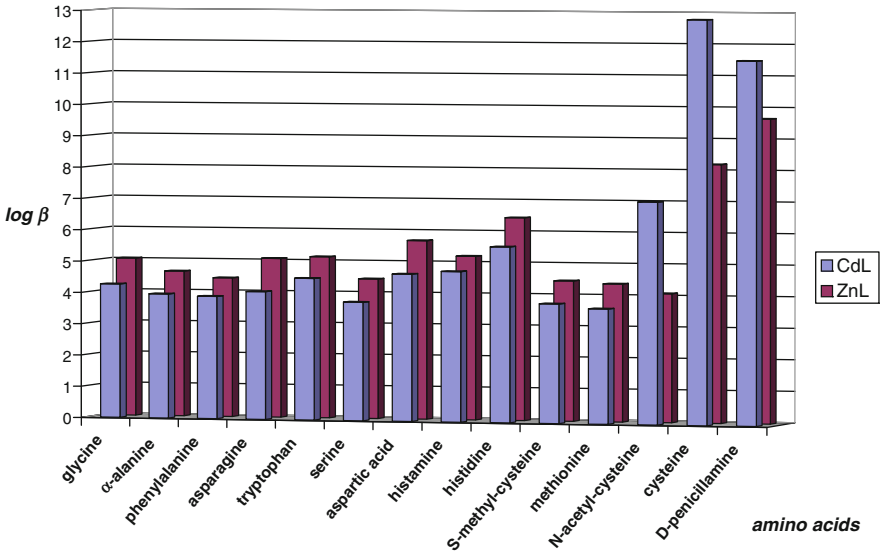

Figure 1 Logarithmic values of the thermodynamic stability of CdL and ZnL complexes for different amino acids or related ligands.

A computer simulation was performed to describe the distribution of cadmium(II) and nickel(II) within low-molecular-weight ligands in human blood plasma [124]. The determination of stability constants of several complexes was performed under "biological conditions", and the conclusions coming from these results are in agreement with the above-mentioned findings: The predominant complexes formed by cadmium(II) are binary cysteinate species, whereas nickel(II) exists mainly as a ternary complex involving both cysteinate and histidinate ligands. As a conclusion, the preference for cadmium(II) binding donor sets can be given as follows: (S^-, NH_2,COO^-) > (S^-,NH_2) > (S^-,COO^-,CO) > (S^-,COO^-) > (NH_2,N(Im),COO^-) > (NH_2,COO^-,S(thioether)) ~ (NH_2,CS(thioamide)) ~ (NH_2,COO^-,COO^-) > (NH_2,COO^-) > (NH_2,CO).

In the case of the common peptides the comparison of the stability constants of zinc(II) and cadmium(II) complexes reveals the same trends as reported for the amino acids: Favored complexation with zinc(II) in almost all cases, except for the thiolate ligands. The binding of several side chain residues may enhance the stability of cadmium(II) complexes but the extent of this stabilization is relatively low. This is true even for the aspartyl or histidyl residues which are generally considered as the most strongly coordinating side chains in the corresponding

copper(II), nickel(II), and zinc(II) complexes. The terminal amino and the neighboring carbonyl groups are the major cadmium(II) binding sites of peptides and there is no example for the cadmium(II)-induced amide deprotonation and coordination in peptide complexes. The coordination geometry of the cadmium(II) complexes of simple peptides is a matter of debate. The formation of octahedral tris(ligand) complexes is reported only in a few cases, but in all probability it depends on the experimental conditions. Namely, the low thermodynamic stability would require the application of high ligand to metal ratios for a reliable detection of tris(ligand) complexes, but such conditions were not considered in the earlier studies. At the same time, bulky side chains of peptide molecules can hinder coordination of three ligating sites and may shift the preference to a tetrahedral coordination geometry in the common peptide complexes.

The presence of one or more cysteinyl residues significantly enhances the thermodynamic stability of cadmium(II)-peptide complexes. The data included in Table 4 provide a definite proof for this statement. The percentages of the peptides GlyGly and CysGly coordinated to nickel(II), zinc(II), and cadmium(II) at pH 7.5 are summarized in this table. The data were calculated for the model systems when one of the three different metal ions and one of the peptides are present in the sample in equimolar concentrations. It can be seen from Table 4 that in the case of GlyGly the complexation is most favored with nickel(II) and only a low, but well measurable percentage of the peptide is bonded to cadmium(II). For CysGly the distribution of the peptide among the three metal ions is completely different. The ratio of bonded zinc(II) ions is relatively low, while the nickel(II) and especially cadmium(II) complexes predominate in this model system.

Table 4 Percentages of the peptides GlyGly and CysGly coordinated to nickel(II), zinc(II) or cadmium(II) at pH 7.5. The metal ions and the peptides are present in 5 mM concentration.

Metal ion	GlyGly (%)	CysGly (%)
free ligand	19.8	$3.5 \cdot 10^{-3}$
Ni(II)	45.2 [125]	19.7 [95]
Zn(II)	30.1 [75]	5.6 [57]
Cd(II)	4.9 [70]	74.7 [94]

The coordination geometry of the CdS_4 tetrathiolate centers which are the most common species formed with multicysteine peptides is always tetrahedral. This stereochemistry is also common for the cadmium(II) complexes of simple peptides containing cysteine or for the amino acid itself. Some small ligands (like N-acetyl-L-cysteine), however, can form stable tris(ligand) complexes with the bidentate (S^-, COO^-) coordination mode suggesting the existence of an octahedral coordination geometry. The complexity and structural variety of cadmium(II) peptide complexes is further enhanced by the propensity of the formation of sulfur-bridged species. The existence of thiolate-bridged oligonuclear or polynuclear complexes is also a common feature of cadmium(II)-peptide complexes containing cysteinyl residues and their biological significance is discussed elsewhere in this book.

Abbreviations and Definitions

Ac	acetyl
Ala	alanine
Asn	asparagine
Asp	aspartic acid
BSA	bovine serum albumin
CD	circular dichroism
Cys	cysteine
DFT	density functional theory
ESI-MS	electrospray ionization mass spectrometry
EXAFS	extended X-ray absorption fine structure
Gln	glutamine
Glu	glutamic acid
Gly	glycine
His	histidine
HSA	human serum albumin
Ile	isoleucine
IR	infrared
L	general ligand
L-carnosine	β-alanyl-L-histidine
Leu	leucine
Lys	lysine
NMR	nuclear magnetic resonance
PC	phytochelatin
Phe	phenylalanine
Pro	proline
PSA	porcine serum albumin
ROS	reactive oxygen species
Sar	sarcosine = N-methylglycine
Thr	threonine
Val	valine
XANES	X-ray absorption near-edge structure

Acknowledgments The authors thank the projects OTKA 77586, OTKA 72956 and TAMOP 4.2.1/B-09/1/KONV-2010-0007, 4.2.2.B-10/1-2010-0024 (Hungary) for financial support.

References

1. I. Eliezer, A. Moreno, *J. Chem. Eng. Data* **1974**, *19*, 226–228.
2. T. Sato, T. Kato, *J. Inorg. Nucl. Chem.* **1977**, *39*, 1205–1208.
3. R. Graham, D. Williams, *J. Chem. Soc., Dalton Trans.* **1974**, 1123–1125.
4. R. F. de Farias, C. Airoldi, *J. Inorg. Biochem.* **1999**, *76*, 273–276.
5. H. A. McKenzie, D. P. Mellor, *Aust. J. Chem.* **1961**, *14*, 562–76.

6. I. Sóvágó, K. Várnagy, A. Bényei, *Magy. Kém. Foly.* **1986**, *92*, 114–116.
7. R. Abdelhamid, M. K. M. Rabia, *Monatshefte Chem.* **1994**, *125*, 1041–1048.
8. M. L. S. S. Goncalves, M. M. D. D. Santos, *J. Electroanal. Chem.* **1985**, *187*, 333–348.
9. G. J. M. Heijne, W. E. Van der Linden, *Talanta* **1975**, *22*, 923–925.
10. J. D. Joshi, P. K. Bhattacharya, *Indian J. Chem.* **1975**, *13*, 88–90.
11. S.P. Datta, R. Leberman, B. R. Rabin, *Trans. Farad. Soc.* **1959**, *55*, 1982–1987.
12. D. L. Leussing, E. M. Hanna, *J. Amer. Chem. Soc.* **1966**, *88*, 693–696.
13. M. Izraeli, L. D. Pettit, *J. Inorg. Nucl. Chem.* **1975**, 999–1003.
14. M. Kodama, Y. Tominga, *Bull. Chem. Soc. Jpn.* **1969**, *42*, 2267–2272.
15. F. Gaizer, G. Gondos, L. Gera, *Polyhedron,* **1986**, *5*, 1149–1156.
16. H. Killa, E. Mabrouk, M. Ghoneim, *Bull. Soc. Chim. Fr.* **1991**, *127*, 44–47.
17. O. A. Weber, V. L. Simeon, *Biochem. Biophys. Acta* **1971**, *244*, 94–102.
18. S. Pelletier, *J. Chim. Phys.* **1960**, *57*, 318–322.
19. M. D. Walker, D. R. Williams, *J. Chem. Soc., Dalton Trans.* **1974**, 1186–1189.
20. F. Khan, K. Nema, *J. Indian Chem. Soc.* **1989**, *66*, 17–20.
21. E. Bottari, M. R. Festa, *Chem. Spec. Bioavailab.* **1996**, *8*, 75–83.
22. T. Kiss, I. Sóvágó, A. Gergely, *Pure Appl. Chem.* **1991**, *63*, 597–638.
23. I. Sóvágó, T. Kiss, A. Gergely, *Pure Appl. Chem.* **1993**, *65*, 1029–1080.
24. V. L. Simeon, O. A. Weber, *Croatica Chemica Acta* **1966**, *38*, 161–167.
25. D. R. Williams, *J. Chem. Soc., Dalton Trans.* **1973**, 1064–1066.
26. J. W. Bunting, K. M. Thong, *Can. J. Chem.* **1970**, *48*, 1654–1656.
27. H. Kozlowski, J. Urbanska, I. Sóvágó, K. Várnagy, A. Kiss, J. Spychala, K. Cherifi, *Polyhedron,* **1990**, *9*, 831–837.
28. J. M. Zhang, Z. W. Wang, Q. Z. Shi, *Chinese J. Inorg. Chem.* **2004**, *20*, 324–330.
29. J. J. Jakobsen, P. D. Ellis, *J. Phys. Chem.* **1981**, *85*, 3367–3369.
30. M. Monajjemi, M. T. Baie, F. Mollaamin, *Russ. Chem. Bull.* **2010**, *59*, 886–889.
31. U. Sharma, *Thermochim. Acta* **1983**, *66*, 369–372.
32. R. L. Rebertus, *Dissertation, Univ. of Illinois,* **1954**.
33. R. Leberman, B. Rabin, *Trans. Faraday Soc.* **1959**, *55*, 1660–1670.
34. P. Morris, R. Martin, *J. Inorg. Nucl. Chem.* **1970**, *32*, 2891–2897.
35. P. Daniele, P. Amico, G. Ostalcoli, *Ann. Chim. (Rome)* **1980**, *70*, 87–97.
36. J. Urbanska, H. Kozlowski, B. Kurzak, *J. Coord. Chem.* **1992**, *25*, 149–154.
37. E. Bottari, M. Festa, *Ann. Chim. (Rome)* **1993**, *83*, 315–329.
38. S. Sjöberg, *Pure Appl. Chem.* **1987**, *68*, 1549–1570.
39. L. Gasque, S. Bernes, R. Ferrari, G. Mendoza-Diaz, *Polyhedron* **2002**, *21*, 935–941.
40. A. Gergely, *Inorg. Chim. Acta* **1981**, *56*, L75–L76.
41. E. V. Raju, H. B. Mathur, *J. Inorg. Nucl. Chem.* **1968**, *30*, 2181–2188.
42. G. Mukherjee, H. Sahu, *J. Ind. Chem. Soc.* **2000**, *77*, 209–212.
43. E. Farkas, A. Gergely, E. Kas, *J. Inorg. Nucl. Chem.* **1981**, *43*, 1591–1597.
44. E. R. Clarke, A. E. Martell, *J. Inorg. Nucl. Chem.* **1970**, *32*, 911–926.
45. V. Jószai, Z. Nagy, K. Ősz, D. Sanna, G. Di Natale, D. La Mendola, G. Pappalardo, E. Rizzarelli, I. Sóvágó, *J. Inorg. Biochem.* **2006**, *100*, 1399–1409.
46. B. Lenarcik, K. Kurdziel, *Pol. J. Chem.* **1981**, *55*, 737–745.
47. V. Guantieri, A. Venzo, V. Di Marco, M. Acampora, B. Biondi, *Inorg. Chim. Acta* **2007**, *360*, 4051–4057.
48. G. Brookes, L. D. Pettit, *J. Chem. Soc., Dalton Trans.* **1976**, 588–594.
49. R. Abdelhamid, M. K. M. Rabia, A. M. El-Nady, *Talanta* **1994**, *41*, 1453–1458.
50. T. E. Hofstetter, C. Howder, G. Berden, J. Oomens, P. B. Armentrout, *J. Phys. Chem. (B)* **2011**, *115*, 12648–12661.
51. I. Sóvágó, A. Gergely, B. Harman, T. Kiss, *J. Inorg. Nucl. Chem.* **1979**, *41*, 1629–1633.
52. J. Benzakour, G. Antonetti, G Ferroni, *Bull. Soc. Chim. Belg.* **1988**, *97*, 541–542.
53. G. Berthon, *Pure Appl. Chem.* **1995**, *67*, 1117–1240.
54. G. Lenz, A. Martell, *Biochemistry* **1964**, *3*, 745–750.

55. P. Gockel, H. Vahrenkamp, A. D. Zuberbuehler, *Helv. Chim. Acta* **1993**, *76*, 511–520.
56. L. Porter, D. Perrin, R. Hay, *J. Chem. Soc.(A),* **1969**, 118–126.
57. I. Sóvágó, T. Kiss, K. Várnagy, B. Decock-Le Révérend, *Polyhedron* **1988**, *7*, 1089–1093.
58. Y. Sugiura, Y. Hirayama, H. Tanaka, H. Sakurai, *J. Inorg. Nucl. Chem.* **1975**, *37*, 2367–70.
59. G. Lenz, A. Martell, *Inorg. Chem.* **1965**, *4*, 378–384.
60. F. Jalilehvand, V. Mah, B. O. Leung, J. Mink, G. M. Bernard, L. Hajba, *Inorg. Chem.* **2009**, *48*, 4219–4230.
61. F. Jalilehvand, B. O. Leung, V. Mah, *Inorg. Chem.* **2009**, *48*, 5758–5771.
62. F. Jalilehvand, Z. Amini, K. Parmar, E. Y. Kang, *Dalton Trans.* **2011**, 12771–12778.
63. H. Sigel, R. B. Martin, *Chem. Rev*. **1982**, *82*, 385–426.
64. I. Sóvágó, in *Biocoordination Chemistry*, Ed K. Burger, Ellis Horwood, New York, 1990, pp. 135–184.
65. H. Kozlowski, W. Bal, M. Dyba, T. Kowalik-Jankowska, *Coord. Chem. Rev.* **1999**, *184*, 319–346.
66. I. Sóvágó, K. Ősz, *Dalton Trans*. **2006**, 3841–3854.
67. G. Marcotrigiano, L. Menabue, G. C. Pellacani, *J. Inorg. Nucl. Chem*. **1975**, *37*, 2344–2346.
68. D. L. Rabenstein, *Can. J. Chem.* **1972**, *50*, 1036–1043.
69. J. Vaissermann, M. Quintin, *J. Chim. Phys*. **1966**, 731–741.
70. A. P. Brunetti, E. J. Burke, M. C. Lim, G. H. Nancollas, *J. Sol. Chem*. **1972**, *1*, 153–164.
71. B. Jezowska-Trzebiatowska, L. Latos-Grazynski, H. Kozlowski, *J. Inorg. Nucl. Chem*. **1977**, *39*, 1269–1273.
72. M. J. A. Rainer, B. M. Rode, *Inorg. Chim. Acta* **1982**, *58*, 59–64.
73. S. M. Wang, R. K. Gilpin, *Talanta* **1985**, *32*, 329–333.
74. S. Sharifi, D. Nori-Shargh, A. Bahadory, *J. Braz, Chem. Soc*. **2007**, *18*, 1011–1016.
75. A. Vaidyan, P. Bhattacharya, *Ind. J. Chem.* **1994**, *33A*, 1003–1007.
76. R. Ferrari, S. Bernes, C. R. de Barbarin, G. Mendoza-Diaz, L. Gasque, *Inorg. Chim. Acta* **2002**, *339*, 193–201.
77. A. Asano, C. M. Sullivan, A. Yanagisawa, H. Kimoto, T. Kurotsu, *Anal. Bioanal. Chem.* **2002**, *374*, 1250–1255.
78. G. Malandrinos, M. Louloudi, N. Hadjiliadis, *Inorg. Chim. Acta* **2003**, *349*, 279–283.
79. B. Decock-Le Reverend, H. Kozlowski, *J. Chim. Phys., Chim. Biol*. **1985**, *82*, 883–890.
80. T. J. Manning, P. Tonui, A. Miller, S. Toporek, D. Powell, *Biochem. Biophys. Res. Comm.* **1996**, *226*, 796–800.
81. P. Ghosh, M. Wood, J. B. Bonanno, T. Hascall, G. Parkin, *Polyhedron* **1999**, *18*, 1107–1113.
82. L. M. Berreau, M. M. Makowska-Grzyska, A. M. Arif, *Inorg. Chem.* **2000**, *39*, 4390–4391.
83. C. G. Ágoston, K. Várnagy, A. Bényei, D. Sanna, G. Micera, I. Sóvágó, *Polyhedron* **2000**, *19*, 1849–1857.
84. P. Tsiveriotis, N. Hadjiliadis, *Coord. Chem. Rev*. **1999**, *190–192*, 171–184.
85. H. Kozlowski, A. Janicka-Klos, P. Stanczak, D. Valensin, G. Valensin, K. Kulon, *Coord. Chem. Rev*. **2008**, *252*, 1069–1078.
86. G. Arena, G. Pappalardo, I. Sóvágó, E. Rizzarelli, *Coord. Chem. Rev*. **2012**, *256*, 3–12.
87. C. Kállay, K. Várnagy, G. Malandrinos, N. Hadjiliadis, D. Sanna, I. Sóvágó, *Inorg. Chim. Acta*, **2009**, *362*, 935–945.
88. S. Timári, C. Kállay, K. Ősz, I. Sóvágó, K. Várnagy, *Dalton Trans*. **2009**, 1962–1971.
89. P. G. Daniele, P. Amico, G. Ostacoli, *Inorg. Chim. Acta* **1982**, *66*, 65–70.
90. A. R. Sarkar, M. Sarkar, *J. Chem. Res. S*. **1997**, 304–305.
91. P. G. Daniele, P. Amico, G. Ostacoli, M. Marzona, *Annali di Chimica* **1983**, *73*, 299–313.
92. W. Bal, J. Christodoulou, P. J. Sadler, A. Tucker, *J. Inorg. Biochem.* **1998**, *70*, 33–39.
93. P. J. Sadler, J. H. Viles, *Inorg. Chem.* **1996**, *35*, 4490–4496.
94. K. Cherifi, B. Decock Le-Reverend, K. Várnagy, T. Kiss, I. Sóvágó, C. Loucheux, H. Kozlowski, *J. Inorg. Biochem.* **1990**, *38*, 69–80.
95. H. Kozlowski, B. Decock-Le Reverend, D. Ficheux, C. Loucheux, I. Sóvágó, *J. Inorg. Biochem.* **1987**, *29*, 187–197.

96. A. Avdeef, J. A. Brown, *Inorg. Chim. Acta* **1984**, *91*, 67–73.
97. B. J. Goodfellow, M. J. Lima, C. Ascenso, M. Kennedy, R. Sikkink, F. Rusnak, I. Moura, J. J. G. Moura, *Inorg. Chim. Acta* **1998**, *273*, 279–287.
98. A. Krezel, W. Bal, *Acta Biochim. Pol. 46*, **1999**, 567–580.
99. D. D. Perrin, A. E. Watt, *Biochim. Biophys. Acta* **1971**, *230*, 96–104.
100. A. M. Corrie, M. D. Walker, D. R. Williams, *J. Chem. Soc., Dalton Trans.* **1976**, 1012–1015.
101. B. J. Fuhr, D. L. Rabenstein, *J. Am. Chem. Soc.* **1973**, *95*, 6944–6950.
102. K. Polec-Pawlak, R. Ruzik, E. Lipiec, *Talanta* **2007**, *72*, 1564–1572.
103. O. Delalande, H. Desvaux, E. Godat, A. Valleix, C. Junot, J. Labarre, Y. Boulard, *FEBS J.* **2010**, *277*, 5086–5096.
104. M. Belcastro, T. Marino, N. Russo, M. Toscano, *J. Inorg. Biochem.* **2009**, *103*, 50–57.
105. J. Mendieta, M. S. Diaz-Cruz, A. Monjonell, R. Tauler, M. Esteban, *Anal. Chim. Acta* **1999**, *390*, 15–25.
106. M. S. Diaz-Cruz, J. M. Diaz-Cruz, M. Esteban, *Electroanlysis* **2002**, *14*, 899–905.
107. M. Erk, B. Raspor, *J. Electroanal. Chem.* **2001**, *502*, 174–179.
108. A. Munoz, F. Laib, D. H. Petering, C.F. Shaw, *J. Biol Inorg. Chem.* **1999**, *4*, 495–507.
109. M. Matzapetakis, D. Ghosh, T-C. Weng, J. E. Penner-Hahn, V. L. Pecoraro, *J. Biol. Inorg. Chem.* **2006**, *11*, 876–890.
110. K. Krzywoszynska, M. Rowinska-Zyrek, D. Witkowska, S. Potocki, M. Luczkowski, H. Kozlowski, *Dalton Trans.* **2011**, *40*, 10434–10439.
111. T. M. DeSilva, G. Veglia, F. Porcelli, A. M. Prantner, S. J. Opella, *Biopolymers* **2002**, *64*, 189–197.
112. X. Chen, M. Chu, D. P. Giedroc, *J. Biol. Inorg. Chem.* **2000**, *5*, 93–101.
113. O. I. Leszczyszyn, C. R. J. White, C. A. Blindauer, *Mol. Biosyst.* **2010**, *6*, 1592–1603.
114. C. A. Blindauer, *J. Inorg. Biochem.* **2008**, *102*, 507–521.
115. N. Romero-Isart, N. Duran, M. Capdevila, P. Gonzalez-Duarte, S. Maspoch, J. L. Torres, *Inorg. Chim. Acta* **1998**, *278*, 10–14.
116. P. Kotrba, T. Macek, T. Rumi, *Coll. Czech. Chem. Comm.* **1999**, *64*, 1057–1068.
117. R. Pal, J. P. N. Rai, *Appl. Biochem. Biotechn.* **2010**, *160*, 945–963.
118. V. Dorcak, A. Krezel, *Dalton Trans.* **2003**, 2253–2259.
119. B. H. Cruz, J. M. Cruz-Diaz, I. Sestakova, J. Velek, C. Arino, M. Esteban, *J. Electroanal. Chem.* **2002**, *520*, 111–118.
120. E. Chekmeneva, J. M. Diaz-Cruz, C. Arino, M. Esteban, *Electroanal.* **2007**, *19*, 310–317.
121. R. Gusmao, S. Cavanillas, C. Arino, J. M. Diaz-Cruz, M. Esteban, *Anal. Chem.* **2010**, *82*, 9006–9013.
122. R. Gusmao, C. Arino, J. M. Diaz-Cruz, M. Esteban, *Analyst* **2010**, *135*, 86–95.
123. H. Satofuka, T. Fukui, M. Takagi, H. Atomi, T. Imanaka, *J. Inorg. Biochem.* **2001**, *86*, 595–602.
124. C. G. Ágoston, Z. Miskolczy, Z. Nagy, I. Sóvágó, *Polyhedron* **2002**, *22*, 2607–2615.
125. A. Cole, C. Furnival, Z.-X. Huang, D. C. Jones, P. M. May, G. L. Smith, J. Whittaker, D. R. Williams, *Inorg. Chim. Acta* **1985**, *108*, 165–171.

Chapter 10
Natural and Artificial Proteins Containing Cadmium

Anna F.A. Peacock and Vincent L. Pecoraro

Contents

ABSTRACT 304
1 INTRODUCTION 304
2 FUNCTION AND COORDINATION CHEMISTRY OF Cd(II) IN METALLOREGULATORY PROTEINS 305
2.1 General Overview of Metalloregulatory Proteins for Heavy Metals 305
2.2 Coordination Chemistry of Cd(II) in CadC 306
2.3 Coordination Chemistry of Cd(II) in CmtR 308
3 STRATEGIES FOR DESIGNING PEPTIDES FOR COMPLEXATION OF Cd(II) 309
3.1 Preparation of Mixed CdS_3/CdS_3O Systems in Coiled Coils 311
3.2 Preparation of Pure CdS_3O Structures in Coiled Coils 315
3.3 Preparation of Pure CdS_3 Structures in Coiled Coils Using Non-coded Amino Acids 317
3.4 Preparation of CdS_4 Systems in Coiled Coils 319
3.5 Design of Coiled Coils Containing Multiple Cd(II) Sites 320
3.6 Complexation of Cd(II) within Helical Bundles 324
4 PHYSICAL PROPERTIES OF Cd(II) IN THIOLATE PROTEINS 325
4.1 Relationship between ^{113}Cd NMR Chemical Shift and ^{111m}Cd PAC 325
4.2 Relationship between Cd(II) Coordination Geometry and pH-Dependent Binding 326
4.3 Influence of Peptide Self-Association Affinity on Cd(II) Binding 330
4.4 Metal Ion Exchange Rates into Helical Systems 331
5 GENERAL CONCLUSIONS: LESSONS FOR UNDERSTANDING THE BIOLOGICAL CHEMISTRY OF Cd(II) 333
ABBREVIATIONS AND DEFINITIONS 334
ACKNOWLEDGMENTS 335
REFERENCES 335

A.F.A. Peacock (✉)
Department of Chemistry, University of Michigan, Ann Arbor, Michigan 48109, USA
e-mail: a.f.a.peacock@bham.ac.uk

V.L. Pecoraro (✉)
School of Chemistry, University of Birmingham, Edgbaston B15 2TT, UK
e-mail: vlpec@umich.edu

A. Sigel, H. Sigel, and R.K.O. Sigel (eds.), *Cadmium: From Toxicity to Essentiality*, Metal Ions in Life Sciences 11, DOI 10.1007/978-94-007-5179-8_10,

Abstract This chapter describes an approach using designed proteins to understand the structure, spectroscopy, and dynamics of proteins that bind Cd(II). We will show that three-stranded coiled coils (3SCCs) based on the parent peptides TRI (Ac-G(LKALEEK)$_4$G-NH$_2$) or GRAND (Ac-G(LKALEEK)$_5$G-NH$_2$) have been essential for understanding how Cd(II) binds to thiolate-rich environments in proteins. Examples are given correlating physical properties such as the binding constants or deprotonation constants relating to structure. We present a scale that relates ^{113}Cd NMR chemical shifts to structures extracted from ^{111m}Cd PAC experiments. In addition, we describe motional processes that help transport from the helical interface of proteins into the hydrophobic interior of helical bundles. These studies help clarify the chemistry of Cd(II) in relation to metal-regulated gene expression and detoxification.

Keywords coiled coil • *de novo* design • peptide • protein • thiol

1 Introduction

As a general rule, when one thinks of the biochemistry of Cd(II), one is confronted with the toxicity of this element with the only known true Cd(II) enzyme being a marine-based carbonic anhydrase [1]. However, there is a rich natural biological chemistry that deals with this metal's sequestration and detoxification by organisms ranging from microbes to humans. In addition, scientists have exploited the similarity of the chemistry between Zn(II) and Cd(II) to understand a broad range of enzymes and proteins. Unlike Zn(II) which is spectroscopically silent, one may utilize the nuclear properties of ^{111}Cd or ^{113}Cd as an NMR nucleus, ^{111m}Cd using perturbed angular correlation or electronic spectroscopy examining the ultraviolet region of the electromagnetic spectrum. These spectroscopic tools provide deep insight into the coordination environment and mechanism of proteins ranging from metallothioneins to metal-substituted phosphatases.

For nearly half a century, bioinorganic chemists have been preparing small molecule models to provide insight into the inner workings of the far more complex natural systems of interest. While this approach has been wildly successful across the gamut of this discipline, as our understanding of metallobiochemistry has increased, the need for more realistic models has become essential.

One approach to model more accurately metal sites in proteins is to apply *de novo* protein design strategies to the problem. Studies with small molecules often are limited by a variety of factors. Sometimes, it is synthetically too difficult to incorporate the exact metal binding functional group into the model. The best example of this is histidine, which is often replaced by pyridine or even alkyl amines as a metal ligand, but has also been problematic for the sulfur-containing ligand cysteine. Another significant limitation is that it is very difficult to engineer second coordination environments (steric bulk, H-bonding residues, local charges) that may be essential for recognition or catalysis. Beyond this, one has great

difficulty with small molecules controlling the dielectric properties, which is then dominated by the choice of solvent. In fact, often one is limited to solvents such as acetonitrile or dichloromethane because of complex stability (hydrolysis or dimerization) or solubility. This limitation is particularly problematic if one is interested in examining enzymes such as phosphatases that use water as a substrate. It also leads to uninterpretable binding or hydrolysis constants as the protic environment doesn't match water.

At the same time, one often needs simpler constructs than the natural systems. This can be because of complex allosteric events that obscure the process of interest. Sometimes, a protein will bind more than one metal in more than one type of site (e.g., the simultaneous presence of a Type 1 and Type 2 copper center), which complicates the interpretation of the center of interest. Metal transporters or electron transfer systems are membrane-associated which presents an entirely new level of complexity. While methodology to clone and express proteins has matured significantly over the past 20 years, one still often will be limited by too little protein to investigate. Site specific incorporation of isotopes (^{13}C or ^{15}N) as a probe of metal site environment is far more easily achieved using synthesized peptides. In addition to these significant limitations, one may be interested in asking more fundamental questions such as whether the secondary structure (α-helix *versus* β-sheet) is required for proper metal function. Even if one uses sophisticated expression approaches, it is far easier to incorporate non-coded amino acids into designed proteins. Thus, one can see that *de novo* protein design provides opportunities heretofore unavailable for the metallobiochemical researcher.

In this chapter, we summarize some of the key Cd(II) binding proteins. Then, we demonstrate how designed peptides can be exploited to understand the structure, spectroscopy or activity of Cd(II) proteins.

2 Function and Coordination Chemistry of Cd(II) in Metalloregulatory Proteins

2.1 General Overview of Metalloregulatory Proteins for Heavy Metals

With metal ions found in approximately a third of all biomolecules [2] there has been significant interest in understanding the mechanisms and coordination chemistry, associated with the transport and regulation of these metal ions. In addition to the essential roles these metal ions play, an excess as a result of misregulation, frequently is associated with various disease states. Furthermore, some metal ions and particularly heavy metal ions, can be exclusively associated with toxicity. Nature has therefore evolved metalloregulatory proteins for heavy metal ion detoxification, which due to the soft nature of the heavy metal ions, is often dominated by Cys coordination chemistry.

These metalloregulatory proteins generally function by changing gene or protein expression in response to the presence of these metal ions. They tend to display high metal ion specificity, which can be achieved as a result of the ligand donor sets and coordination geometries associated with the metal ion binding site. SmtB/ArsR and MerR represent two different families of transcriptional regulatory metalloproteins important in dealing with heavy metal toxicity.

SmtB and ArsR have evolved from a common evolutionary origin. They function as a repressor binding to, in the case of SmtB, the *smt* operator-promoter in the absence of metal ions. On binding Zn(II), the SmtB repressor changes conformation, dissociates from the DNA and induces expression of a metallothionein, a class of cysteine-rich low-molecular-weight proteins.

The first metallothionein to be isolated was in 1957 from horse kidney tissue and found to contain Cd(II) [3]. They are believed to play a role in metal ion regulation and detoxification, and display fascinating coordination chemistry with a range of d^{10} metal ions. The binding of Cd(II) to metallothioneins is discussed in much detail in Chapter 11, and involves the coordination of Cd(II) to multiple thiols from Cys amino acid side chains in the form of Cd(II) thiolate clusters with both bridging and terminal thiolates.

MerR is a Hg(II) sensor metalloregulatory protein which induces transcription of the *mer* operon, responsible for Hg(II) detoxification, on binding Hg(II). MerR is a dimeric protein which is bound to DNA both in the absence and presence of Hg(II), which is one way in which it differs from the SmtB/ArsR family. Despite two potential binding sites, one equivalent of Hg(II) binds at the dimeric interface to three Cys residues, Cys82 from one monomer and Cys117 and Cys126 from the second monomer, in a trigonal fashion as HgS_3 [4]. This results in a conformational change which translates into a 33 degree unwinding of the bound DNA, triggering synthesis of MerA, MerB, MerP, and MerT. Other metal ions, including Cd(II), are capable of triggering a similar response, but require significantly higher concentrations [5].

Cd(II)-substituted proteins, in which the native metal ion has been replaced with the spectroscopically richer Cd(II), are discussed in detail in Chapter 6. In the following two sections of this chapter, the Cd(II) coordination chemistry of two Cd(II) metalloregulatory proteins, CadC and CmtR, are described.

2.2 Coordination Chemistry of Cd(II) in CadC

The *Staphylococcus aureus* pI258 CadC protein is a member of the SmtB/ArsR family of metal-responsive transcriptional repressors and was first isolated in 1968 [6]. Exposure of CadC, a homodimeric repressor, to Cd(II), Pb(II) or Zn(II) results in dissociation from the DNA and exposure of the *cad* operon, as demonstrated by *in vitro* restriction enzyme assays [7–9]. CadC consists of two different metal ion sites, site 1 and site 2 (4 sites in total per homodimer). Site 1 is a thiol-rich mononuclear metal ion binding site, whereas site 2 consists of two metal ion sites

at the homodimer interface [10,11]. Site 1 is responsible for the regulatory role of CadC whereas site 2 has been shown by mutagenesis studies to not be necessary for the correct biological function [10]. In contrast, ArsR contains a site 1 but lacks a site 2 and SmtB contains both a site 1 and 2, where both play an important regulatory role. These observations could suggest that CadC represents an evolutionary midway between ArsR and SmtB [12].

Site 1 consists of a thiol-rich mononuclear metal ion binding site, whereas site 2 consists of two metal ion sites at the homodimer interface with His_{103}, His_{114}, Asp_{101}, and Glu_{117} amino acid side chains as ligands [10,11]. The structure of site 2, based on PDB 1U2W[10], is shown in Figure 1. No crystal structure has to date been reported with a metallated site 1, however, mutagenesis studies have established that the metal ligands are provided by Cys_{58} and Cys_{60} from one monomer and Cys_7 and Cys_{11} from the second [7]. The fourth Cys_{11} residue has been shown to be non-essential by mutagenesis studies [7]. Site 1 displays a preference for Cd(II) over Zn(II), whereas the non-essential site 2 displays the opposite preference for Zn(II) over Cd(II) [10].

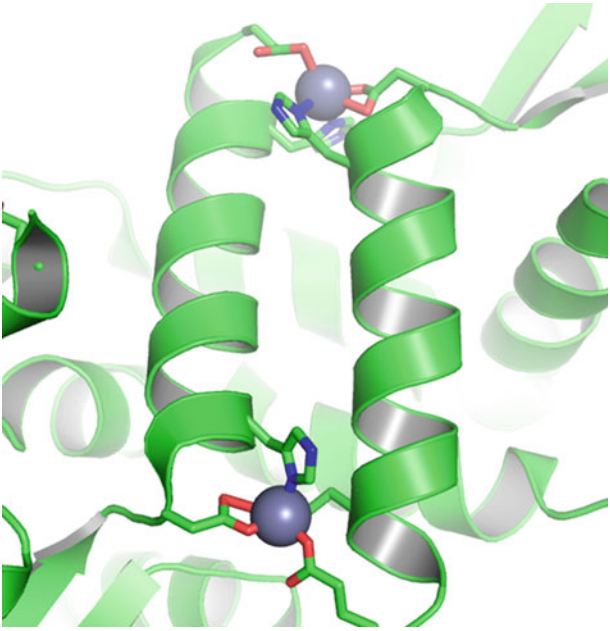

Figure 1 PYMOL ribbon diagram based on PDB 1U2W showing two Zn(II) bound to site 2 of CadC. Both Zn(II) are bound to His_{103} and Asp_{101} from one monomer, and His_{114} and Glu_{117} from the second monomer [10]. Shown are the main chain atoms represented as helical ribbons (green) and His/Asp/Glu side chains in stick form with the nitrogen (blue) and oxygen (red) donor atoms, and the Zn(II) as grey spheres.

A spectroscopic study using chelator competition experiments by Giedroc and coworkers, reported that Cd(II) binds to CadC with a 1:1 stoichiometry and a K_{Cd} of 4.3 ($\pm$1.8) $\times$ 10^{12} M^{-1} was reported for Cd(II) binding [13]. The Cd-CadC

difference (minus apo-CadC) UV-visible spectrum displays a maximum at 238 nm, with an extinction coefficient of ca. 25000 M^{-1} cm^{-1} [13,14]. ^{113}Cd NMR spectroscopy of ^{113}Cd-CadC resulted in a single resonance at 622 ppm [13,15]. These results were unable to distinguish between a CdS_3, CdS_3X (where X = N or O), and CdS_4 site. Mutation of Cys_{60} to a Gly residue resulted in a ^{113}Cd NMR chemical shift of 534 ppm compared to 622 ppm, consistent with loss of a bound thiol [14]. However, a less shifted ^{113}Cd NMR resonance of 592 ppm was obtained on mutating Cys_{11} to Gly [14]. This could suggest that the Cys_{11} residue is more weakly bound to the Cd(II). On replacing Cd(II) with Pb(II), the Cys_{11} residue does not contribute to the coordination sphere [14].

A Cd-S bond length of 2.53 Å was reported from EXAFS experiments [13]. This provides some evidence for a CdS_3Y type structure where Y is a Cys thiol, or an exogenous ligand like water, as one would expect a Cd–S bond length of 2.44 Å for a fully CdS_3 site [16,17], and 2.54 Å for a fully CdS_4 site [18]. Despite the good match in bond length, a reduction in the goodness-of-fit for the EXAFS data was observed for CdS_4 compared to either CdS_3 or CdS_5. A Cd(II) coordination environment of CdS_3N is unlikely as there are no conserved His residues in close proximity to the Cd(II) site. However, an exogenous water molecule or a Glu/Asp amino acid side chain, bound to the Cd(II) to yield CdS_3O, cannot be ruled out. The lack of conserved Met residues and the longer Cd-thioether bond length, rule out a Met residue contributing to the coordination sphere as Cd(Cys-*S*)$_3$(Met-*S*). Finally, though Cys_{11} is not required for activity [7], it may contribute to the Cd(II) coordination sphere as the fourth thiol ligand to generate a distorted CdS_4 site. The latter, with a weakly associated Cys_{11}, is thought to be most likely.

2.3 Coordination Chemistry of Cd(II) in CmtR

Mycobacterium tuberculosis H37Rv CmtR is a recently discovered transcriptional repressor protein [19]. CmtR promotes gene expression on exposure to Cd(II) and Pb(II), but unlike CadC, does not respond in the presence of Zn(II) [19].

Mutating Cys_{57}, Cys_{61}, and Cys_{102} with Ser demonstrated that all three amino acids contribute to the Cd(II) coordination sphere. For example, Cd(II) bound to wild-type CmtR results in a UV-visible spectrum with a maximum absorbance at ca. 240 nm, with an extinction coefficient of ca. 16000 M^{-1} cm^{-1} [20]. This, however, drops to ca. 12000 M^{-1} cm^{-1} for the Cys102Ser mutant, consistent with the loss of a S^- to Cd(II) ligand-to-metal charge-transfer (LMCT) [20]. The importance of Cys_{102} for Cd(II) binding is further supported by a drop in K_{Cd} from 9.9 ($\pm$2.3) $\times$ 10^6 M^{-1} for wild-type CmtR, to 3.2 ($\pm$0.4) $\times$ 10^6 M^{-1} for the Cys102Ser mutant [20].

A single broad ^{113}Cd NMR chemical shift of 480 ppm has been reported for ^{113}Cd(II) bound to CmtR [20]. This was proposed to consist of Cd(II) bound to the two thiols, Cys_{57} and Cys_{61}, and additional undefined ligands. ^{111m}Cd PAC data (*vide infra*) was recorded and could be fit to one species, which was best described

as ^{111m}Cd(II) bound to Cys_{57} and Cys_{61}, with a weakly associated Cys_{102}, and a fourth ligand which is most likely an exogenous water molecule [20].

Recently, the structure of Cd(II) bound to CmtR was solved by 2D NMR, to yield a three coordinate CdS_3 site, see Figure 2 [21]. This structure shows Cd(II) bound to Cys_{102} from the flexible tail of one monomer, and the Cys_{57} and Cys_{61} from an α-helix from the second monomer. Under these conditions the three Cys residues appear to be bound to the Cd(II) in a similar fashion [21], but from different monomers and as part of protein domains with different inherent flexibility.

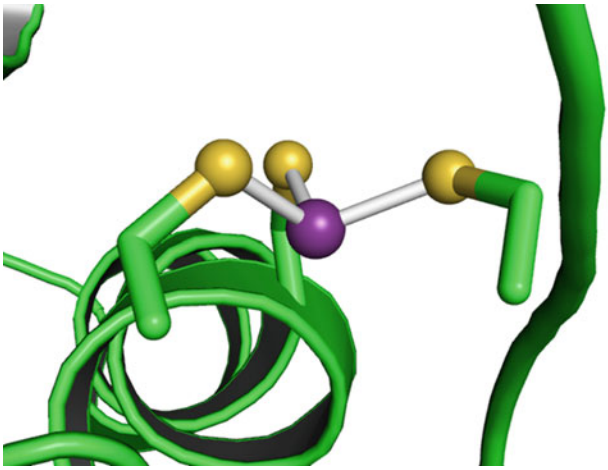

Figure 2 PYMOL ribbon diagram based on the NMR solution structure of CmtR (PDB 2JSC) showing Cd(II) bound to three Cys amino acid side chains in an *endo* geometry [21]. Shown are the main chain atoms represented as helical ribbons (green), the Cys side chains (stick form) with the thiol group (orange) and the Cd(II) (violet), as spheres.

Apo CmtR is thought to be conformationally flexible, with one of these accessible conformations being responsible for DNA binding. However, on binding Cd(II) this flexibility is dramatically reduced, locking the CmtR homodimer in a conformation that is unable to bind to DNA resulting in dissociation from the DNA in a similar fashion to CadC [21].

3 Strategies for Designing Peptides for Complexation of Cd(II)

The natural proteins previously discussed possess large complex structures making it challenging to correlate chemical observation with structure and Cd(II) coordination chemistry. The field of *de novo* peptide design involves the design of artificial minimalist peptide sequences which by virtue of their primary structure predictably fold into well defined secondary, tertiary, and quaternary structures. These systems offer significant opportunities for gaining further understanding

about fundamental processes such as protein folding, protein-protein interactions, and structure-function relationships for biological molecules. Furthermore, they offer the opportunity to investigate the coordination chemistry of metal ions to proteins in a significantly smaller and simple structure, thereby allowing structure-function relationships to readily be established.

Attractive structures extensively investigated by *de novo* peptide design include coiled coils that are based on the common α-helical motif. These can range from low to high numbers of α-helixes [22–25], consist of parallel or antiparallel orientiation of α-helixes [26], and be homo or hetero aggregates [27,28]. However, a number of different protein folds based on different secondary structures, have also been investigated by *de novo* design, including β-sheet structures [29–31], β-hairpin peptides [32,33], $\beta_2\alpha$ motifs based on zinc-finger domains [34–36], and γ-turns [37].

This section will discuss our efforts to elucidate the coordination chemistry of Cd(II) to thiol sites in the interior of α-helical coiled coils, a common motif routinely used in peptide design. Our work has focused primarily on the TRI peptide family (Table 1), which is a 30 amino acid peptide sequence based on the heptad repeat approach, *abcdefg* [38,39]. In water the TRI peptide folds into an α-helix with one face containing hydrophobic Leu residues (*a* and *d* sites). These α-helixes aggregate together, generating a hydrophobic core, to yield two-stranded coiled coils at low pH and three-stranded coiled coils at higher pH (> pH 5) [38,39]. The three-stranded coiled coil is further stabilized by salt bridges between glutamate and lysine residues in the *e* and *g* positions of adjacent α-helixes (Figure 3).

Table 1 Peptide sequences discussed in this chapter.

Peptide	Sequence[a]
TRI	Ac-G LKALEEK LKALEEK LKALEEK LKALEEK G-NH_2
TRIL12C	Ac-G LKALEEK LKA**C**EEK LKALEEK LKALEEK G-NH_2
TRIL16C	Ac-G LKALEEK LKALEEK **C**KALEEK LKALEEK G-NH_2
CoilSer	Ac-E WEALEKK LAALESK LQALEKK LEALEHG-NH_2
TRIL12AL16C	Ac-G LKALEEK LKA**A**EEK **C**KALEEK LKALEEK G-NH_2
TRIL16Pen[a]	Ac-G LKALEEK LKALEEK **X**KALEEK LKALEEK G-NH_2
TRIL12L_DL16C[a]	Ac-G LKALEEK LKA**L_D**EEK **C**KALEEK LKALEEK G-NH_2
TRIL9CL19C	Ac-G LKALEEK **C**KALEEK LKA**C**EEK LKALEEK G-NH_2
GRAND	Ac-G LKALEEK LKALEEK LKALEEK LKALEEK LKALEEK G-NH_2
GRANDL16PenL26AL30C	Ac-G LKALEEK LKALEEK **X**KALEEK LKA**A**EEK **C**KALEEK G-NH_2
GRANDL12L_DL16CL26AL30C[a]	Ac-G LKALEEK LKA**L_D**EEK **C**KALEEK LKA**A**EEK **C**KALEEK G-NH_2
α_3DIV	MGS WAEF K QR LAAIKTR **C**QALGG SEAE**C**AAF EKE IAAFESE LQAY KGKGNPE VEAL R KE AAAIRDE **C**QAY RHN
BABY	Ac-G LKALEEK LKALEEK LKALEEK G-NH_2

[a] X = Pen, L_D = D-leucine. Bold and underlined residues indicate substitutions.

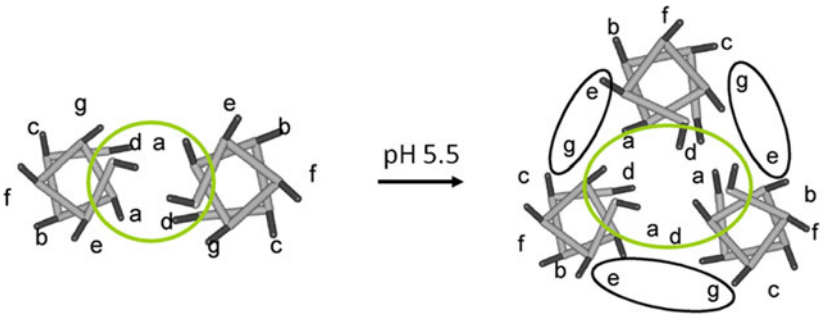

Figure 3 Top down view of the pH dependent conversion of the TRI peptides from a parallel dimer (two-stranded coiled coil) to a trimer (three-stranded coiled coil). Shown are the *abcdefg* heptad positioning of amino acids, demonstrating the hydrophobic core generated by the *a* and *d* sites, and the favorable electrostatics interactions formed between the *e* and *g* sites.

Two general strategies have been exploited in *de novo* peptide design for the introduction of metal ion binding sites. The first strategy involves the use of cofactors, the most common of which are units of heme [40] though examples also exist with $[4Fe\text{-}S_4]^{2+}$ [41]. In this Chapter we take advantage of the second strategy which engineers metal binding sites into the hydrophobic interior of a coiled coil by replacing Leu residues with amino acids capable of coordinating metal ions.

3.1 Preparation of Mixed CdS_3/CdS_3O Systems in Coiled Coils

A soft thiol site is generated on introducing a Cys residue into the hydrophobic core of a three stranded coiled coil based on TRI. Cys containing analogues of TRI have previously been shown to be capable of binding to various heavy metal ions including Hg(II), Bi(III), As(III), and Pb(II) [38–48]. However, two options exist for introducing a Cys residue into the coiled coil interior as Leu side chains in both the *a* and *d* sites are directed towards the hydrophobic core. Initial solution studies involved two peptides, TRIL12C and TRIL16C, in which the Leu (L) in position 12 (*d* site) or 16 (*a* site) has been replaced with a Cys (C) residue. These systems offer an opportunity to investigate the differences afforded by the subtly different orientation of the Cys side chains in these two sites.

The binding of Cd(II) to these two peptides was investigated by UV-visible spectroscopy. The addition of increasing amounts of Cd(II) to an aqueous solution of TRIL16C at pH 8.5, resulted in a steady increase in the characteristic Cd-S LMCT at 232 nm, with an extinction coefficient of 22600 M^{-1} cm^{-1}. This reached a plateau at 1 equivalent of Cd(II) per three strands of TRIL16C (Figure 4) consistent with the formation of $Cd(TRIL16C)_3^-$ [49]. Analogous experiments performed with TRIL12C produced similar results with a λ_{max} of 231 nm, an extinction coefficient of 20600 M^{-1} cm^{-1}, and a binding ratio consistent with formation of $Cd(TRIL12C)_3^-$ [49]. Both peptides required these basic experimental conditions in order to achieve

complete complexation of Cd(II) by the three Cys residues. A pH titration of Cd(II) in the presence of three equivalents of peptide monomer allowed the pK_{a2}, for the simultaneous release of two protons (*vide infra*), to be determined and was found to be lower for *a* sites (TRIL16C) compared to *d* sites (TRIL12C) (Table 2). The properties of the two trigonal Cys sites (*a versus d*) differed further. Cd(II) binding to the three thiols in the interior of the coiled coil results in an induced LMCT in the circular dichroism (CD) spectra. Intriguingly, the induced signals were found to be similar but of opposite polarity for the *a* and *d* sites, respectively [49]. More significantly, the affinity of Cd(II) was found to be higher for *a* sites compared to *d* sites [49,50].

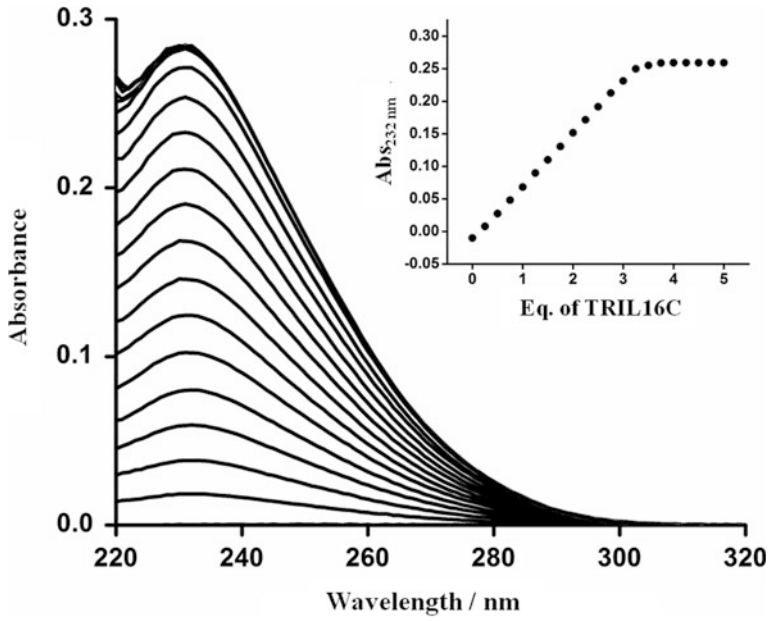

Figure 4 Representative UV-visible difference spectra for the titration of increasing concentrations of TRIL16C into a solution of Cd(II) at pH 8.5. Inset shows the plot of absorbance at 232 nm as a function of peptide equivalence, which plateaus at 1 Cd(II):3 TRIL16C, consistent with Cd(II) binding to three Cys side chains in the hydrophobic interior of a three-stranded coiled coil.

Table 2 Spectroscopic values for some Cd(II) thiol complexes [82][a].

	UV nm (Δε)	^{113}Cd NMR chemical shift	EXAFS Cd–S bond
$Cd(TRIL12C)_3^{-b}$	231 (20600)	619 ppm	2.49 Å
$Cd(TRIL16C)_3^{-b}$	232 (22600)	625 ppm	2.49 Å
CdS_3^{-b}	190–260 (15000–25000)	570–660 ppm	2.42–2.48 Å
CdS_4^{2-}	227–250 (8000–40000)[c]	610–750 ppm[d]	2.47–2.61 Å[b]

[a] Reproduced by permission of the Royal Society of Chemistry; copyright 2009.
[b] Data from Ref. [49] and references therein.
[c] Data from Refs [66,67,70].
[d] Data from Refs [15,55,66].

The differences associated with Cd(II) coordination to three Cys side chains in an *a versus* a *d* site (e.g., pK_{a2} of binding, induced CD signal, affinity) are thought to be related to the orientation of the Cys side chains. Models were prepared, based on the crystal structure of the related CoilV_aL_d [51], of three Cys side chains in an *a* and a *d* site, respectively, and subjected to energy minimizations [38]. The thiol site generated in an *a* site is highly preorganized with the three Cys side chains directed towards the interior of the coiled coil. In contrast, the thiol goups in a *d* site were directed towards the helical interface, suggesting that reorganization was required in order to coordinate to a metal ion [38]. More recently crystal structures have been obtained of related three-stranded coiled coils based on CoilSer [52] with Cys in an *a* site (9 position) or a *d* site (19 position) which are in reasonable agreement with the original findings [53]. The major rotamer of Cys side chains in an *a* site are directed towards the interior of the coiled coil with sulfur-sulfur distances of 3.3–3.4 Å, forming a pre-organized metal binding site (Figure 5, left). In contrast, the Cys side chains in a *d* position are slightly further rotated down the α-helix and as such these do not appear particularly pre-organised for metal binding (Figure 5, right). In this structure, two of the Cys side chains are pointed towards the coiled coil interior, and the third is directed away from the interior towards the helical interface. That latter is likely to require reorganization to position itself for metal binding [53].

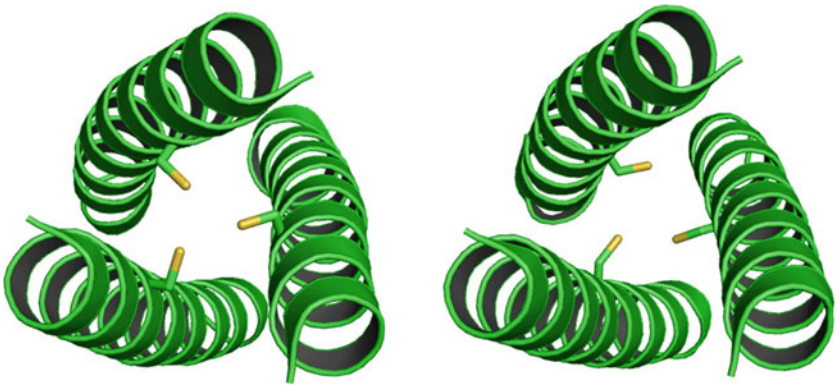

Figure 5 Ribbon diagrams of parallel three-stranded coiled coils showing the orientation of the Cys side chain (major rotamer) in an *a* and *d* site, PDB codes 3LJM and 2X6P. Shown are the main chain atoms represented as helical ribbons (green) and Cys side chains in stick form with the thiol group (orange) in the interior [53].

The Cd(II) binding sites were further characterized by ^{113}Cd NMR and extended X-ray absorption fine structure spectroscopy (EXAFS). ^{113}Cd NMR spectra of solutions containing 3 equivalents of TRIL16C or TRIL12C in the presence of 1 equivalent enriched $^{113}CdCl_2$ at pH 8.5 resulted in single resonances with chemical shifts of 625 and 619 ppm, respectively [49]. The EXAFS data for Cd(II) bound to TRIL16C and TRIL12C are extremely similar and in both cases the best fits were for three sulfurs bound to the Cd(II) at 2.49 Å [49]. The data obtained so far could be consistent with either CdS_3, CdS_4 or CdS_3X (where X = O or N).

^{111m}Cd perturbed angular correlation (PAC) spectroscopy [54,55] was subsequently employed to determine the Cd(II) coordination geometry of Cd(TRIL16C)$_3^-$ as PAC is capable of assessing both the electronic environment of the ^{111m}Cd(II) as well as the symmetry of the site, on an extremely fast timescale (ns compared to the ms timescale of NMR). Unexpectedly it was discovered that the Cd(II) is in fact bound to TRIL16C as a mixture of two species, 40% trigonal planar CdS_3 ($\omega_o = 0.44$ rad/ns) and 60% tetrahedral CdS_3O ($\omega_o = 0.34$ rad/ns), where O corresponds to an exogenous water molecule (Figure 6a and Table 3) [49].

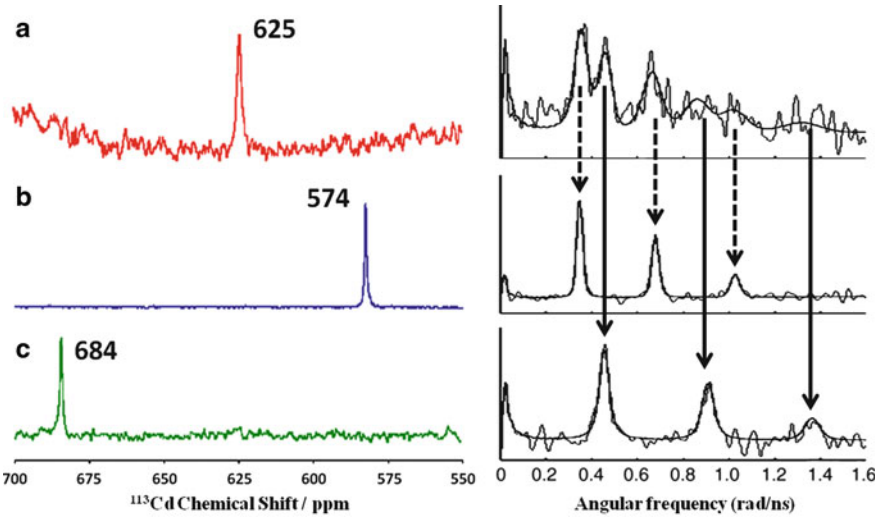

Figure 6 ^{113}Cd NMR and corresponding ^{111m}Cd perturbed angular correlation (PAC) spectra showing (**a**) a mixture of CdS_3 and CdS_3O for Cd(TRIL16C)$_3^-$, (**b**) 100% CdS_3O for Cd(TRIL12AL16C)$_3^-$, and (**c**) 100% CdS_3 for Cd(TRIL16Pen)$_3^-$, respectively.

Table 3 Physical properties of Cd/TRILXC complexes [82][a].

Peptide	Apparent pK_{a2}[b]	^{113}Cd NMR[c]	^{111m}Cd PAC[d]
TRIL9C	13.4	615	–
TRIL19C	14.3	627	–
TRIL9CL19C	–	615 & 623	–
TRIL16C	13.4	625	60% CdS_3O/40% CdS_3
TRIL12AL16C	12.2	574	100% CdS_3O
TRIL16Pen	15.8	684	100% CdS_3
TRIL12L$_D$L16C[e]	15.1	697	100% CdS_3

[a] Reproduced by permission of the Royal Society of Chemistry; copyright 2009.
[b] Fit to a model for the simultaneous release of two protons. Data from Refs [63,65,71] and references therein.
[c] Given in ppm *versus* $Cd(ClO_4)_2$ in D_2O. Data from Refs [49,63,65,71] and references therein.
[d] Percentage of CdS_3 and CdS_3O based on best fit to PAC. Data from Refs [49,60,63,65] and references therein.
[e] L_D = D-leucine.

It was not possible to detect these two distinct species by ^{113}Cd NMR as the interchange between the two occurs rapidly on the NMR timescale and instead a single signal for the average species is observed. The faster timescale of PAC has allowed the species to be observed directly and for us to distinguish between the three structures, CdS_3, CdS_4 or CdS_3X.

3.2 *Preparation of Pure CdS_3O Structures in Coiled Coils*

Though Cd(II) was successfully coordinated to three thiol Cys side chains in the hydrophobic interior of a designed three-stranded coiled coil, the fact that it was bound as a mixture of CdS_3 and CdS_3O was frustrating and lacked the control and specificity of Biology that we had been striving to achieve. We therefore directed our attention towards design strategies that would allow us to coordinate Cd(II) as exclusively tetrahedral CdS_3O. Not only would such a structure demonstrate the potential behind *de novo* peptide design, but it would also allow us to investigate the chemistry associated with coordinated water molecules. These are extremely important in biological sites for enzymatic activity, notably in hydrolytic metalloenzymes, and ultimately would allow us to investigate binding of small substrate molecules to the metal center [56,57].

It was reasoned that a cavity could be generated adjacent to the metal binding site by removing some steric bulk, and that this cavity could be hydrated, encouraging the formation of CdS_3O (see Figure 7) [58–60]. This required replacement of the Leu in position 12 (directly above the Cys at position 16) with a sterically less demanding amino acid. Both Gly, a helix destabilizing, and Ala, a helix stabilizing, amino acid were subsequently incorporated, to generate TRIL12GL16C and TRIL12AL16C, respectively [61]. The Cd(II) coordination environment was probed by ^{113}Cd NMR and resulted in single resonances at 572 and 574 ppm, respectively [59]. As we had previously shown that ^{113}Cd NMR will not distinguish between the two dynamic species, CdS_3 and CdS_3O, ^{111m}Cd PAC data was recorded for ^{111m}Cd(TRIL12AL16C)$_3^-$. This confirmed that Cd(II) was bound to TRIL12AL16C as exclusively tetrahedral CdS_3O as indicated by a signal due to a single species with $\omega_o = 0.34$ rad/ns (Figure 6b and Table 3) [59,60].

Introduction of a cavity directly below the Cys plane, e.g., TRIL16CL19A, binds Cd(II) fully as a CdS_3O species as confirmed by ^{111m}Cd PAC. However the PAC data reported is $\omega_o = 0.27$ rad/ns, which is significantly different to that of 0.34 rad/ns reported for CdS_3O generated on binding Cd(II) to a peptide with the cavity above the Cys plane, Cd(TRIL12AL16C)$_3^-$. Though both species are consistent with a CdS_3O species, they must clearly differ in some way. Pb(II) binds to the three Cys in aminolevulinic acid dehydratase (ALAD) by positioning itself slightly above the Cys plane (Figure 8a) (termed *exo*) [62]. In contrast, we recently showed that As(III) binds to three Cys in the interior of a three-stranded coiled coil, by binding

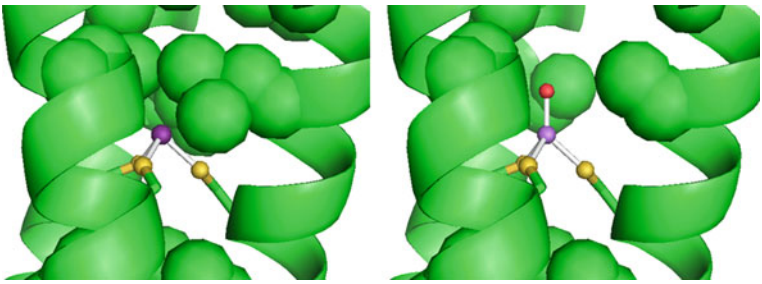

Figure 7 Proposed PYMOL model illustrating that the cavity generated on replacing the Leu layer directly above the metal binding site with a sterically less demanding amino acid (e.g., Ala) could more easily accommodate a coordinated water molecule. Shown are the main chain atoms represented as helical ribbons (green), the Leu/Ala side chains in the hydrophobic core as space filling spheres, the Cys side chains (stick form) with the thiol group (orange) coordinated to the Cd(II) (violet) with a bound water (red).

below the Cys plane (Figure 8b) (termed *endo*) [48]. Cd(II) is an intermediate size and, therefore, may be able to bind in either form. A 2D NMR structure of Cd(II) bound to CmtR as CdS_3 in the *endo* form has been reported, see Figure 2 [21]. Based on these observations, it was proposed that the CdS_3O species with $\omega_o = 0.34$ rad/ns, corresponds to the *exo* form, and that with $\omega_o = 0.27$ rad/ns, corresponds to the *endo* form (Figure 8) [63]. Due to the smaller number of studies on Cd(II)-peptide complexes which contain a contribution from the latter form of CdS_3O ($\omega_o = 0.27$ rad/ns), the remainder of this chapter will focus on the former CdS_3O with $\omega_o = 0.34$ rad/ns, observed for $Cd(TRIL12AL16C)_3^-$.

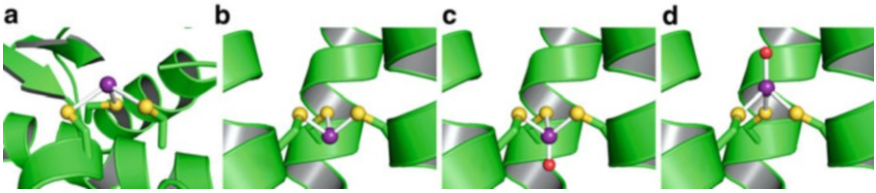

Figure 8 Crystal structure showing coordination to three Cys of (**a**) Pb(II) in an *exo* geometry (PDB 1QNV) [62] and (**b**) As(III) in an *endo* geometry (PDB 2JGO) [48]. Models of CdS_3O bound as (**c**) *endo* and (**d**) *exo*. Shown are the main chain atoms represented as helical ribbons (green), the Cys side chains (stick form) with the thiol group (orange), the metal (violet) and bound water (red), as spheres.

We have just seen how a cavity adjacent to the metal binding site results in the formation of CdS_3O. Intriguingly, introducing cavities at different positions in the coiled coil also altered the extent of CdS_3O formation. A cavity two layers above the Cys, TRIL9AL16C, resulted in the formation of a pure CdS_3O species as confirmed by both ^{113}Cd NMR (583 ppm) [59] and ^{111m}Cd PAC ($\omega_o = 0.33$ rad/ns) [62]. In contrast, introduction of a cavity two layers below the Cys plane,

TRIL16CL23A, resulted in the formation of a more CdS_3 species as determined by ^{113}Cd NMR (643 ppm) [59] and ^{111m}Cd PAC (55% $\omega_o = 0.34$ rad/ns and 45% $\omega_o = 0.45$ rad/ns) [63]. Without crystallographic data it is challenging to elucidate the causes of these subtle differences, however, they are most likely the result of modifications to the packing of Leu side chains in the hydrophobic core and more specifically adjacent to the metal binding site. These changes could also be the result of the subtle interplay between protein-fold stability and coordination chemistry (*vide infra*).

TRIL16C binds Cd(II) as a mixture of CdS_3 and CdS_3O, however, due to the timescales of ^{113}Cd NMR (0.01–10 ms) we observe a single resonance at 625 ppm. In contrast the timescale of ^{111m}Cd PAC (0.1–100 ns) allows us to distinguish between these two species. Therefore we are able to conclude that the water (O in CdS_3O) exchange rate must be between 0.01–10 μs [63].

3.3 Preparation of Pure CdS_3 Structures in Coiled Coils Using Non-coded Amino Acids

We next directed our attention to the more challenging task of preparing a pure trigonal CdS_3 site within our coiled coils. We reasoned that if removing steric bulk above the Cys plane increased the coordination number of the Cd(II) that the introduction of steric bulk may reduce the coordination number. Unfortunately Leu is one of the most sterically demanding of the coded amino acids, however, an advantage of *de novo* peptide design, is that we are not limited to these 20 amino acids. Initial studies involved introducing the sterically demanding synthetic amino acid, hexafluoroleucine (Hfl), in which the hydrogen atoms on the side chain are replaced with fluorine atoms. The observation of a chemical shift at 574 ppm for pure CdS_3O and at 625 ppm for a 60:40 mixture of CdS_3O:CdS_3, suggests that we would expect to observe a resonance downfield of 625 ppm for pure CdS_3. Extrapolating these two values, predicts a resonance at 698 ppm for pure CdS_3 with no contribution from CdS_3O [60]. Surprisingly ^{113}Cd NMR of ^{113}Cd $(TRIL12HflL16C)_3^-$ resulted in a shift towards CdS_3O as indicated by a shift from 625 ppm (TRIL16C) to 607 ppm in the ^{113}Cd NMR spectra [60].

The next approach involved introducing steric bulk directly into the metal binding site. With this in mind, Cys was replaced with the non-coded amino acid penicillamine (Pen), which can be considered as being the analogue of Cys in which the β-methylene protons have been replaced with bulky methyl groups. Alternatively, one could consider Pen as being the thiol-containing analogue of Val. Crystal structures of Pen within the interior of a three-stranded coiled coil (Figure 9) confirm that both these interpretations are correct [64]. The Cd(II) coordination environment of the resulting complex, $^{113}Cd(TRIL16Pen)_3^-$, was probed by ^{113}Cd NMR and resulted in single resonances at 684 ppm, which is extremely close to the earlier predicted value of 698 ppm for pure CdS_3 (Figure 6c) [60]. ^{111m}Cd PAC of $^{111m}Cd(TRIL16Pen)_3^-$, confirmed that Cd(II) was bound as exclusively trigonal planar CdS_3 (100% $\omega_o = 0.45$ rad/ns) (Figure 6c and Table 3) [59,60]. Based on the

crystallographic evidence for Pen [64], it is thought that the exclusion of water from the CdS_3 site, is not as a result of the restricted water access due to the bulky methyl groups. Instead it is thought that these restrict the rotation of the Pen ligand such that the thiol groups are more rigidly pre-organized for metal binding, and that the methyl groups enhance the packing of the Leu layers above and below the Cd(II) plane, preventing water access [64].

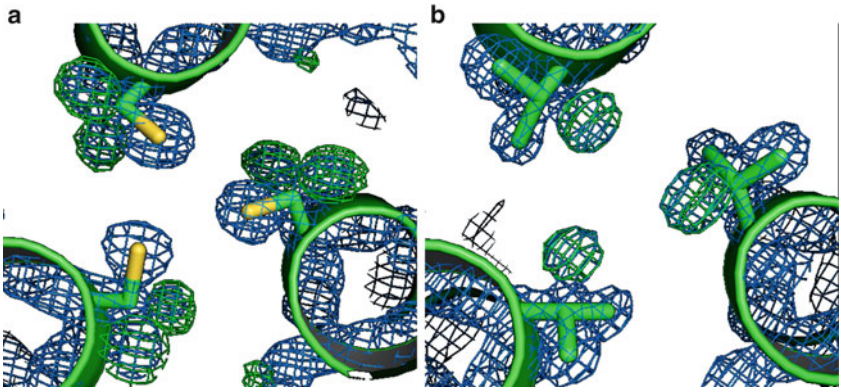

Figure 9 Model for the difference electron density of CoilSerL16Pen using either (**a**) Cys or (**b**) Val as a model for the non-coded for amino acid penicillamine (Pen) in the interior of a three stranded coiled coil. Shown is a top down view from the N-terminus of the three-stranded coiled coil (PDB 3H5F) during the building of the Pen side chain [64]. The $2F_o$-F_c map (blue, contoured at 1.5σ) and F_o-F_c map (green, contoured at 3σ) after one round of refinement, show that the density for the methyl groups (at the position of the β-methylene protons) is missing for the Cys model, as is the thiol group when Val is used. The other amino acid side chains have been omitted for clarity.

In order to evaluate if CdS_3 coordination was a result of using Pen as the coordinating ligand, we set out to prepare a CdS_3O site using Pen. Using the same strategy as described earlier, by generating a cavity directly above the Pen plane (TRIL12AL16Pen), coordination of Cd(II) as exclusively CdS_3O could be achieved using Pen. Both ^{113}Cd NMR (chemical shift of 583 ppm) and ^{111m}Cd PAC (100% $\omega_o = 0.34$ rad/ns) confirmed a fully CdS_3O site for $Cd(TRIL12AL16Pen)_3^-$ [63].

Though we had successfully achieved a fully three-coordinate CdS_3 site, our goal had been to prepare this with Cys. We reconsidered our approach to introducing steric bulk above the Cys plane, and reasoned that by redirecting the Leu side chain towards the Cys site (Figure 10), by use of the D-amino acid, we should exclude water binding [65]. The peptide $TRIL12L_DL16C$ (L_D = D-Leucine) was prepared and the D-Leu was found to be tolerated and resulted in a well folded coiled coil. This itself was an interesting observation as little to nothing had been reported on the influence on protein structure and stability of D-amino acid substitution into a coiled coil form with L-amino acids. This mixed chirality construct was found to bind ^{113}Cd(II) with a single ^{113}Cd NMR chemical shift of 697 ppm [65], which is almost identical to that predicted earlier for 100% CdS_3 (698 ppm) [60]. ^{111m}Cd PAC confirmed the binding site as pure CdS_3 ($\omega_o = 0.46$ rad/ns) [60]. We

have called these peptides, which contain all L-amino acids as well as a D-amino acid in the primary sequence, "diastereopeptides". Though the D-Leu is a non-coded amino acid, the alignment of the Leu side chain towards the C-terminus rather than the N-terminus, would be reproduced in an antiparallel coiled coil or peptide fold.

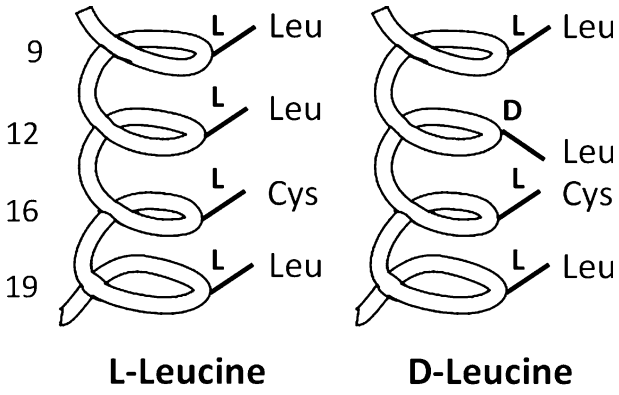

Figure 10 Cartoon representations illustrating the effect of altering the chirality of the Leu amino acid in the layer directly above the metal binding Cys plane. Reorientation of the Leu side chain serves to increase the steric bulk directly above the Cys ligands, preventing water access and resulting in Cd(II) binding as CdS_3.

3.4 Preparation of CdS_4 Systems in Coiled Coils

Many Cd(II) sites in biological systems are thought to involve the coordination of four thiol ligands (metallothioneins and CadC, *vide supra*) and we therefore set out to design α-helical scaffolds capable of coordinating Cd(II) as tetrahedral 4-coordinate CdS_4. Our current designs based on TRI offer a maximum of three Cys side chains for metal ion coordination. We decided to incorporate a double Cys site, with no intervening Leu layers, using an α-helix as the scaffold. This can be achieved by replacing two Leu residues in adjacent *a* and *d* sites on the same face of the α-helix, with Cys. For example, one could replace an *a* site followed by a *d* site, to generate a C_a-X-X-C_d type sequence (where X = any amino acid). Alternatively, one could replace a *d* site followed by an *a* site, to generate a C_d-X-X-X-C_a type motif. Intriguingly, only the C_a-X-X-C_d sequence is commonly found in proteins, while the C_d-X-X-X-C_a sequence is only rarely observed. Two peptides based on TRI were subsequently prepared to allow us to compare Cd(II) chelation by the C_a-X-X-C_d (TRIL9CL12C) and C_d-X-X-X-C_a (TRIL12CL16C) motif, respectively, and to try to establish why the latter sequence is so uncommon [66].

The incorporation of two adjacent Cys sites with no intervening Leu layers is a relatively destabilizing modification. The substitution of two adjacent Leu residues in Ogawa's C16C19-GGY (C_a-X-X-C_d) two-stranded coiled coil, generated a

disordered random coil in solution [67,68]; however, a related peptide was found to be more tolerant of this substitution [69]. Similarly, the C_a-X-X-C_d and C_d-X-X-X-C_a modifications to TRI, TRIL9CL12C, and TRIL12CL16C, are also destabilizing and result in a mixture of two- (major species) and three-stranded (minor species) coiled coils in solution [66].

A UV-visible spectroscopy titration of Cd(II) into buffered solutions of either C16C19-GGY (pH 5.3) or TRIL12CL16C (pH 8.5), results in the linear increase in the LMCT at 238 nm, which both plateau at 1 equivalence of Cd(II) per two strands of peptide monomer [66,67]. However, the extinction coefficients of 14920 M^{-1} cm^{-1}, for Cd(II) bound to TRIL12CL16C, is more consistent with three rather than four thiolates bound to Cd(II) [49,66,70]. While the analogous experiment performed with TRIL9CL12C resulted in similar spectra, the linear increase in absorbance at 241 nm plateaus initially at 0.3 equivalence Cd(II), more consistent with a three- rather than a two-stranded coiled coil, but then increases again until 0.6 equivalence.

^{113}Cd NMR showed the formation of a single resonance at 560 ppm, on addition of ^{113}Cd(II) to TRL12CL16C which contained the C_d-X-X-X-C_a motif. However, the value of 560 ppm is not consistent with either CdS_4 or CdS_3, but is in the range expected for a CdS_3O type coordination environment. ^{111m}Cd PAC for Cd(II) bound to TRIL12CL16C results in one clear signal with $\omega_o = 0.38$ rad/ns [66], which is most similar to the $\omega_o = 0.34$ rad/ns previously assigned to CdS_3O [60], however, this site appears to be more distorted. The current working model is of CdS_3O coordination within a two-stranded coiled coil.

An analogous experiment performed with TRIL9CL12C, results in the formation of two resonances at 650 and 630 ppm, which could be consistent with CdS_4, CdS_3, CdS_3X or a dynamic mixture of these. Though Cd(II) coordination is clearly different to C_a-X-X-C_d (TRIL9CL12C) and C_d-X-X-X-C_a (TRIL12CL16C), the amplitude of the NMR resonances are highest at 1 equivalence of ^{113}Cd(II) per two strands of peptide monomer, which would be consistent with a predominantly two-stranded coiled coil. A large frequency spread was detected by ^{111m}Cd PAC, which is consistent with a flexible metal binding site, with $\omega_o = 0.14$ rad/ns [66]. This is clearly different to the values of ω_o obtained for CdS_3O or CdS_3, and was best fitted to a CdS_4 type species [66]. Here the working model is of CdS_4 as part of both a two-stranded coiled coil (both Cys from each α-helix) and a three-stranded coiled coil (both Cys from one α-helix, and a single Cys from the two remaining α-helixes). These studies illustrate that this *de novo* approach can achieve a desired CdS_4 structure, but also illustrate a design flaw in that the resultant peptides are highly symmetrical because they are homotrimers. Future work is necessary to develop heterotrimeric coiled coils with different amino acid sequences in order to achieve more closely environments found in native proteins.

3.5 Design of Coiled Coils Containing Multiple Cd(II) Sites

We are ideally placed to take advantage of the various Cd(II) sites we have been able to design into the interior of a coiled coil, to answer important questions

concerning metalloprotein coordination chemistry. Do *a* and *d* type sites differ significantly when in close proximity to one another? Can a metal ion discriminate between two extremely similar sites in close proximity to one another? Would two adjacent metal ion sites communicate with one another? Is binding of two metal ions cooperative? Are coordinatively unsaturated CdS_3 or tetrahedral CdS_3O sites preferred?

The peptide TRIL9CL19C was prepared in order to answer questions concerning preferences for two extremely similar Cd(II) sites, with the *a* (9) and the *d* (19) sites differing only in a very subtle shift in the positions of the Cys side chains. In the designed peptide, TRIL9CL19C, the two sites are in very close proximity (15–16 Å), being separated by only two hydrophobic Leu layers. Cd(II) was found to bind selectively to the *a* site, as confirmed by ^{113}Cd NMR (615 ppm), 2D NOESY and CD [50]. Only once this site is fully occupied does the second equivalent of Cd(II) bind to the *d* site, as again confirmed by ^{113}Cd NMR (623 ppm) (Figure 11), 2D NOESY, and CD [50]. These observations are consistent with the higher affinity of Cd(II) for TRIL16C (*a* site) compared to TRIL12C (*d* site) [49], and are thought to be the result of the more pre-organized metal binding site generated by the Cys side chains in an *a* site. However, what was not necessarily predicted, was the observation of two distinct resonances at 615 and 623 ppm for the ^{113}Cd NMR of the fully loaded $Cd_2(TRIL9CL19C)_3^{2-}$ [50]. These are extremely similar to their analogous monosubstituted peptides $Cd(TRIL9C)_3^-$ (615 ppm) [28] and $Cd(TRIL19C)_3^-$ (627 ppm) [71], indicating that these two sites are capable of

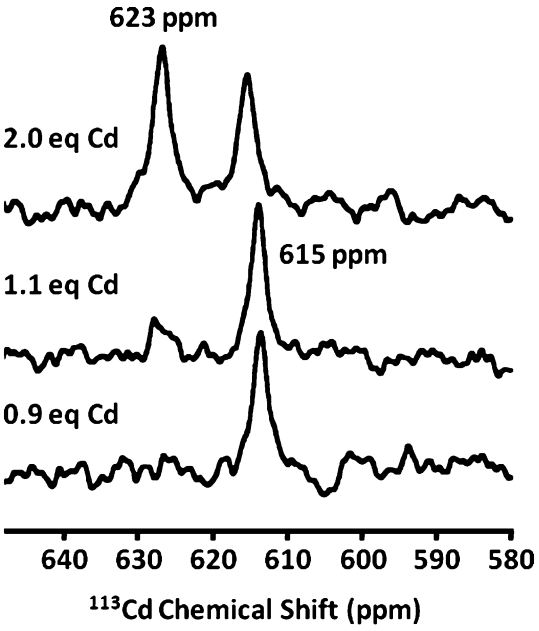

Figure 11 ^{113}Cd NMR spectra for the titration of ^{113}Cd(II) into a solution of TRIL9CL19C, at pH 8.5. ^{113}Cd(II) binds initially to the *a* site (615 ppm) and only when this is fully loaded does ^{113}Cd(II) bind to the *d* site (623 ppm). Reprinted with permission from [50]; copyright 2012 American Chemical Society.

behaving independently. The observation of two distinct resonances, as opposed to an average resonance, provides evidence that there is no significant metal exchange between the two sites on the NMR timescale. Importantly, site-specific metal binding has been achieved between two extremely similar metal ion sites in a relatively short peptide sequence (30 amino acids).

Cd(II) bound to either the *a* or *d* site in the previous example, are bound as a mixture of CdS_3 and CdS_3O. A more challenging design would be to prepare a coiled coil capable of binding two equivalents of Cd(II) to two distinct sites, one as exclusively CdS_3 and the other as exclusively CdS_3O. Initial efforts to prepare two such sites within TRI were unsuccessful due to peptide instability and it was necessary to revert to GRAND which contains one additional heptad compared to TRI (Table 1) [72]. The additional heptad not only provides a longer peptide sequence so that the two sites could be designed further removed from one another, but also provides a ca. 5 kcal mol^{-1} enhancement in stability due to the additional stabilizing hydrophobic layers and salt bridges provided by the fifth heptad [72,73]. This is important when one considers the number of hydrophobic Leu layers which need to be interrupted in order to achieve our design. The non-coded amino acid Pen was used to generate a 3-coordinate site towards the N-terminus end of the peptide (position 16). A Cys with an adjacent cavity (generated by replacement of Leu with Ala), was introduced towards the C-terminus (position 30) in order to generate the 4-coordinate site. The resulting peptide, GRANDL16PenL26AL30C, was found to successfully sequester Cd(II) to the two sites as exclusively CdS_3 (16 site) and CdS_3O (30 site). The first equivalent of ^{113}Cd(II) occupied the 4-coordinate CdS_3O site (588 ppm) and only once this site was fully loaded did the second equivalent of ^{113}Cd(II) bind to the 3-coordinate CdS_3 site (687 ppm) [74].

A second design strategy retained the same 4-coordinate site in position 30, but utilized the repositioning of the Leu side chain (D-Leu) directly above the Cys site, to generate the 3-coordinate CdS_3 site. The resulting peptide, GRANDL12L_D-L16CL26AL30C, provides an opportunity to establish Cd(II) preferences for binding to the Cys residue as exclusively CdS_3 or CdS_3O. These two sites offer identical first coordination sphere ligands, Cys residues in an *a* site, and differ only in the nature of the second coordination sphere (non-coordinating) residue in the layer directly above the Cys plane. ^{113}Cd NMR again supported the selective binding of the first equivalent of ^{113}Cd(II) to the 4-coordinate site with the appearance of a single resonance at 589 ppm. The second equivalent resulted in the appearance of a second distinct resonance at 690 ppm [65]. These results together with those for GRANDL16PenL26AL30C confirm the higher preference for the formation of CdS_3O rather than CdS_3. Furthermore, water exchange between these two sites, if any, must occur slower than the NMR timescale. Peptides that can coordinate two equivalences of the same metal ion, to two distinct sites, but with different coordination geometries and consequently different physical properties (*vide infra*), are called "heterochromic" peptides. We liken this scenario to that of a face (coiled coil) with two eyes (metal ions) but with different colors (coordination geometries and physical properties).

We then turned our attention to the design of coiled coils capable of binding two equivalents of Cd(II) both as exclusively CdS_3, or CdS_3O, in an effort to determine whether, as opposed to the coordination number, the position of these sites within a coiled coil played an important role. Two CdS_3O sites were prepared at either end of GRAND by replacement of the Leu directly above the metal binding Cys site with Ala. The designed peptide, GRANDL12AL16CL26AL30C, bound two equivalents of ^{113}Cd(II) with ^{113}Cd NMR chemical shifts at 589 and 572 ppm. Both these chemical shifts and ^{111m}Cd PAC data are consisted with fully bound CdS_3O indicating that a single peptide capable of binding two 4-coordinate Cd(II) has been successfully designed [75]. The two sites, which are three layers apart and separated by two layers of hydrophobic Leu, behave independently from one another as the chemical shifts of the sites are not sensitive to the metallation state of the other site. Intriguingly, one CdS_3O site, confirmed by 2D NOESY as the 16 position, is populated at a much lower pH (pK_{a2} 11.8) than the second site at position 30 (pK_{a2} 13.9) [75]. However, at pH values where both sites are capable of fully binding Cd(II) as CdS_3O, selectivity is not observed for one site over the other [75].

Our next goal was to design a peptide capable of coordinating two equivalents of Cd(II) exclusively as CdS_3 in GRAND using Pen. It was necessary to position both Pen far from either the N- or C-terminus, as fraying of the coiled coil would result in water access to the Pen sites and a contribution of CdS_3O to the final species. Pen residues were subsequently introduced at positions 16 and 23; however, it was necessary to incorporate an Ile at position 26 to enhance packing and prevent fraying of the coiled coil towards the C-terminus. GRANDL16PenL23PenL26I was capable of coordinating two equivalents of ^{113}Cd(II) resulting in two distinct resonances with chemical shifts of 666 and 678 ppm [75]. Though these are clearly predominantly CdS_3, they do in fact represent a mixture with a significant CdS_3O contribution (20–30%). These sites are separated by a single Leu layer which is less effective at packing than Ile, therefore the Leu in position 19 was replaced with Ile in order to enhance the packing in the single separating layer. The resulting peptide, GRANDL16PenL19IL23PenL26I, was now found to be capable of coordinating two ^{113}Cd(II) with more CdS_3 character, as indicated by two distinct resonances with chemical shifts at 686 and 681 ppm [75]. These two sites, however, do not behave independently of one another. ^{113}Cd(II) bound to the 681 ppm site appears to be sensitive to whether ^{113}Cd(II) is bound to the second site (686 ppm) or not. When the latter site is not fully bound, a resonance is instead detected for the first site 10 ppm downfield at 691 ppm [75]. In contrast, the chemical shift of the second site (686 ppm) appears to be unchanged irrespective of whether ^{113}Cd(II) is bound to the first site (681 ppm) [75].

These systems have allowed us to study Cd(II) coordination to two "identical" first coordination environments within the hydrophobic interior of a coiled coil. Though the physical properties of the two sites are extremely similar in the two examples above, they are not identical or fully independent of one another. Factors contributing to these differences may lie in alternative packing of amino acid side chains and the location of the site along the coiled coil.

3.6 Complexation of Cd(II) within Helical Bundles

The previous examples have all focused on structures generated by the aggregation of three independent peptide strands into a three-stranded coiled coil. Unfortunately, it is challenging to introduce asymmetry into these designed sites as they rely on parallel homoaggregation. An attractive target is therefore to prepare a single peptide chain that spontaneously folds into a three-helix bundle. The peptide α_3D developed by DeGrado and coworkers has been structurally characterized by NMR spectroscopy (PDB code 2A3D) and found to fold into a counterclockwise topology with the second α-helix antiparallel to the first and third α-helices of the bundle [76]. A trigonal Cys site was prepared by introducing one Cys into each α-helix toward the C-terminal end of the bundle in a relatively hydrophobic environment (Table 1 and Figure 12).

Figure 12 Model of α_3DIV generated from the NMR structure of α_3D (PDB code 2A3D) [76]. Shown are the main chain atoms represented as helical ribbons (green), the side chains (stick form) of His at the C-terminus (nitrogen in blue) and Cys (grey) with the thiol group (orange) directed towards the interior of the three-helix bundle [77].

Cd(II) binding to this peptide, α_3DIV, was monitored by the formation of the characteristic LMCT transition at 232 nm with a molar absorption coefficient of 18200 M^{-1} cm^{-1} at pH 8, consistent with three Cys bound to Cd(II) [77]. Titration data confirmed a binding ratio of one Cd(II) per single strand of α_3DIV as well as a binding constant of 2.0×10^7 M^{-1} [77]. ^{113}Cd NMR of ^{113}Cd(α_3DIV)$^-$ has two resonances at 595 (major) and 583 (shoulder) ppm, both of which would be consistent with predominantly CdS_3O sites [77]. ^{111m}Cd PAC confirmed that one signal is the result of 4-coordinate CdS_3O [77] but showed that the second species is best described by a four coordinate CdS_3N ($\omega_o = 0.17$ rad/ns), where N corresponds to the His side chain towards the flexible C-terminus, which is in close proximity to the metal binding site (Figure 12) [77]. Definitive correlation of the ^{113}Cd NMR signals to these two different structures awaits further experimentation.

A trigonal thiol Cd(II) binding site has been successfully engineered into a three helix bundle and it displays very similar spectroscopic properties to the analogous sites engineered in to the three stranded coiled coils based on TRI and GRAND, described previously. These helical bundles now offer significant advantages to

explore asymmetric metal binding sites, which are more common in biology and are crucial in order to introduce important second coordination sphere residues for catalysis.

4 Physical Properties of Cd(II) in Thiolate Proteins

In the previous sections it has become apparent that Cd(II) thiolate complexes can be readily studied by a number of techniques. The S^- to Cd(II) LMCT transitions observed by UV-visible and circular dichroism spectroscopy, provide a readily accessible technique for studying these systems. It has become apparent that both ^{113}Cd NMR and ^{111m}Cd PAC spectroscopy are powerful tools with which to study these sites. Metal ion affinity, solvent exchange rates and pK_a for Cd(II) binding are related to the nature of the coordination site as well as its location within the protein fold. This section will focus on the relationships that have been established between the physical properties of the Cd(II) thiolate site and the nature of these sites, using the three-stranded coiled coil family of *de novo* designed proteins.

4.1 Relationship between ^{113}Cd NMR Chemical Shift and ^{111m}Cd PAC

The coiled coils based on TRI offer a unique opportunity to investigate the different coordination geometries of a given metal (e.g., Cd(II)) within a structure that remains for the most part unchanged. By now the relationship between ^{113}Cd NMR and coordination geometry for fully CdS_3 (700–675 ppm) or CdS_3O (570–600 ppm) sites, will be apparent [63]. Equally we have observed resonances intermediate between these two extremes which correspond to a mixture of these two species, e.g. a resonance at 625 ppm for ^{113}Cd(II) bound to TRIL16C was consistent with a mixed species consisting of 40% CdS_3 and 60% CdS_3O [49]. Assessing a large range of peptides based on TRI by both ^{113}Cd NMR and the complementary ^{111m}Cd PAC, which was able to distinguish between the two species due to the nanosecond timescale of the technique, demonstrated that a linear relationship exists between ^{113}Cd NMR chemical shift and the % of CdS_3 and % CdS_3O which have contributed to that signal (Figure 13) [63]. This linear correlation can be extrapolated to predict a theoretical ^{113}Cd NMR chemical shift of 579 ppm for tetrahedral CdS_3O and 702 ppm for trigonal planar CdS_3 [63]. The linear correlation reported is extremely significant as it allows the scientific community to readily establish the % of CdS_3 and % CdS_3O by the routinely available technique of ^{113}Cd NMR. Though ^{111m}Cd PAC is increasingly gaining recognition, it remains a more elusive technique for general users to take advantage of.

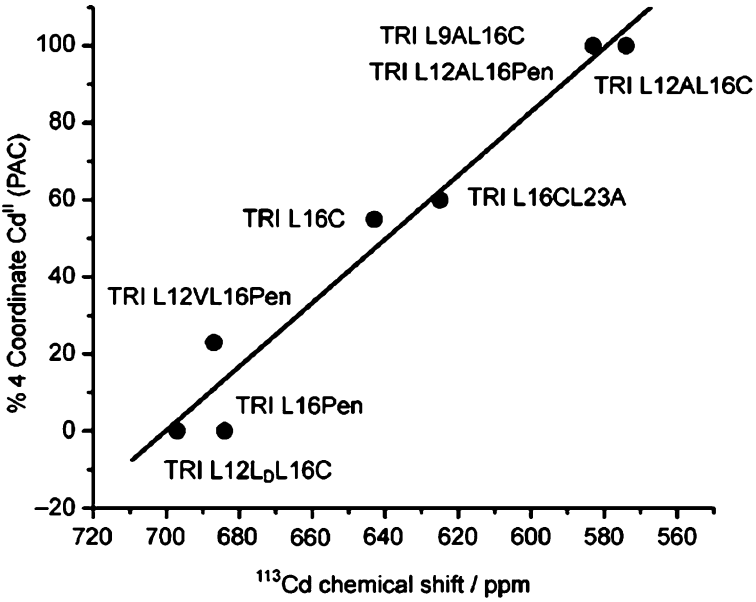

Figure 13 Plot illustrating the linear relationship between ^{113}Cd NMR chemical shift and the percentage of 4-coordinate CdS_3O as determined by ^{111m}Cd PAC spectroscopy. Reprinted from [63] with permission from Wiley-VCH Verlag GmbH & Co. KGaA; copyright 2007.

Commonly in the literature ^{113}Cd NMR chemical shifts are assigned to very specific coordination structures. These are often justified by the fact that the reported chemical shift falls within the wide range of values one would expect for this particular structure. However, the new linear correlation established (Figure 13) suggests that the range of chemical shifts for a specific structure may not be as wide as previously believed. Furthermore, it may be much more appropriate to refer to a coordination structure which is a dynamic model consisting of multiple contributing species, rather than one static well defined structure. For example the reported ^{113}Cd NMR chemical shift of 622 ppm for ^{113}Cd-CadC along with the EXAFS determined Cd–S bond length of 2.53 Å, resulted in that system being assigned as CdS_4 [13]. However, based on our findings, it may be more appropriate to describe this as a rapidly (on the NMR time scale) interconverting mixture of CdS_3 and CdS_3X, where X is a weakly associated thiol from Cys_{11} or an exogenous water molecule. Ultimately ^{111m}Cd PAC data might provide further insight into the structure of this metalloregulatory protein.

4.2 Relationship between Cd(II) Coordination Geometry and pH-Dependent Binding

The physical properties of bound Cd(II) are highly dependent on the coordination environment and geometry. As previously mentioned, monitoring the characteristic

Cd-S LMCT by UV-visible spectroscopy has allowed the binding properties of various peptides to be determined in aqueous solution. Intriguingly, the CdS_3O complex, $Cd(TRIL12AL16C)_3^-$, is fully formed at a significantly lower pH (ca. pH 7.5) compared to the CdS_3 complex, $Cd(TRIL16Pen)_3^-$, which requires a significantly higher pH (ca. pH 9) in order to form fully [74]. The pH profiles were recorded and the data were subsequently fit to a model for the simultaneous release of two protons on binding Cd(II) to the three thiolates provided by the peptide (equation 1) [28,45].

$$Cd\left[(\text{peptide}-H)_2(\text{peptide})\right]^+ \rightleftharpoons Cd(\text{peptide})_3^- + 2H^+ \quad (1)$$

A pK_{a2} value (release of two protons) of 12.2 was determined for Cd(II) binding to TRIL12AL16C as CdS_3O, whereas the higher value of 15.8 was obtained for the binding of Cd(II) to TRIL16Pen as CdS_3 [74]. This same behavior was observed for the binding of Cd(II) to the heterochromic peptide, GRANDL16PenL26AL30C, containing a distinct CdS_3 and CdS_3O site. The first equivalent of Cd(II) binds to the peptide as CdS_3O (as determined by the ^{113}Cd NMR chemical shift at 588 ppm) with a pK_{a2} value of 9.6 [74]. Once this site is fully occupied the second equivalent of Cd(II) binds to the vacant CdS_3 site (indicated by the appearance of a ^{113}Cd NMR chemical shift at 687 ppm) with a pK_{a2} value of 16.1 [74]. These values are in good agreement with those determined for Cd(II) binding to the analogous sites in GRANDL26AL30C and GRANDL16Pen (Figure 14) [74].

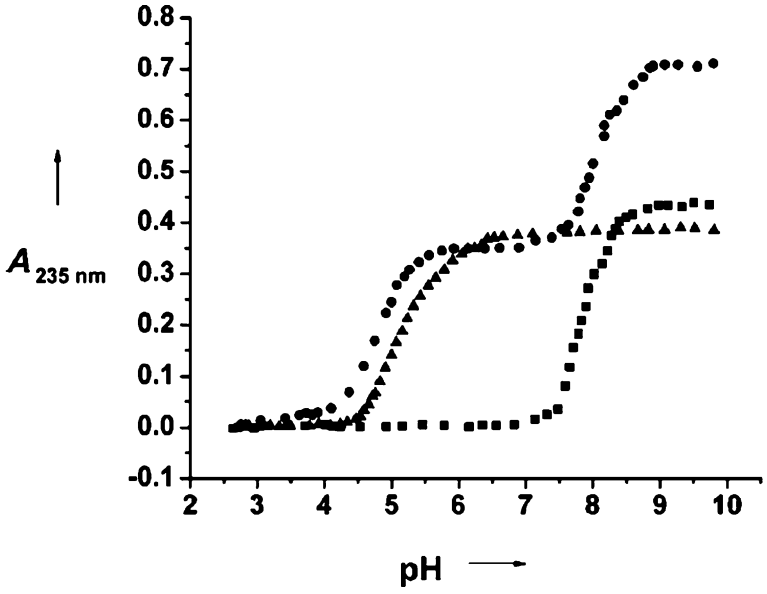

Figure 14 UV spectral changes associated with the pH titration for 2 equivalents of Cd(II) binding to GRANDL16PenL26AL30C (circle), 1 equivalents of Cd(II) binding to GRANDL16Pen (square) and GRANDL26AL30C (triangle). The pH-dependent binding to a 4-coordinate CdS_3O site occurs at a lower pH than for a 3-coordinate CdS_3 site. Reprinted from [74] with permission from Wiley-VCH Verlag GmbH & Co. KGaA; copyright 2007.

Though Pen and Cys both provide a thiol ligand to the Cd(II) ion, they do differ slightly in their basicity [78,79]. Pen contains methyl groups in place of the β-methylene protons from Cys, which could alter the pH at which the thiols bind to Cd(II). Questions concerning whether the pK_{a2} is intrinsically the result of the metal coordination geometry or the nature of the coordinating ligand, can be answered by preparing a 4-coordinate CdS_3O site with Pen and a 3-coordinate CdS_3 site with Cys. Both of these have previously been prepared using peptide design. TRIL12AL16Pen was confirmed by both ^{113}Cd NMR and ^{111m}Cd PAC to bind Cd(II) as fully CdS_3O. The pK_{a2} associated with Cd(II) binding to the three thiols of Pen as CdS_3O was determined to be 12.7, which is extremely similar to the value of 12.2 determined for CdS_3O coordination to Cys. TRIL12L_DL16C was designed and experimentally shown to bind Cd(II) to Cys as fully bound CdS_3. The pK_{a2} associated with Cd(II) binding to the three thiols of Cys as CdS_3 was determined to be 15.1 [65], which is also extremely similar to the value of 15.7 determined for CdS_3 coordination to Pen. These comparisons suggest that the shifts in the pK_{a2} of binding is due primarily to the resulting Cd(II) coordination geometry, although the alkyl substitution for the penicillamine ligand appears to push up the observed pK_{a2} by 0.5 to 0.6 units in either coordination geometry.

TRIL16C, which binds Cd(II) as a mixture of 40% CdS_3 and 60% CdS_3O [49], sequesters Cd(II) with a pK_{a2} of 13.4. This value is consistent with ca. 40% contribution of a pK_{a2} of 15.8 for CdS_3 and a 60% contribution of a pK_{a2} of 12.2 for CdS_3O. This intermediate pK_{a2} suggests that it is also an indication of the speciation of the Cd(II) site. Therefore, one should be able to establish a correlation with data obtained from ^{111m}Cd PAC. Alternatively, as the relationship between ^{111m}Cd PAC and ^{113}Cd NMR has already been established, a linear correlation of pK_{a2} *versus* ^{113}Cd chemical shift, as an indication of % CdS_3O (or % CdS_3), can be plotted (Figure 15) [63]. Once again this correlation could prove very useful in interpreting Cd(II) thiolate sites in metalloproteins. Both of the correlations established (Figures 13 and 15), suggest that a Cd(II) site within a protein type environment, which displays rapid ligand exchange (e.g., coordinated water), can display an average of the physical properties displayed by the two exchanging species (e.g., ^{113}Cd NMR chemical shift and pK_{a2} of binding). Again this is important to consider when assigning a particular structure based on experimentally obtained physical properties, as these could be the result of multiple contributing dynamic structures.

The pK_{a2} *versus* ^{113}Cd chemical shift correlation is independent of the position of the Cd(II) binding site within the coiled coil (for Cys in an *a* site), as the pK_{a2} assigned to the binding of Cd(II) to peptides such as TRIL9C and TRIL23C, all fall on the linear correlation (Figure 15). Furthermore, the correlation is not limited to TRI. Peptides which are both shorter (BABY), more weakly self-associated, and longer (GRAND), more highly self-associated, all agree reasonably well with the trend. Finally, Cys-containing analogues of CoilSer, a related three-stranded coiled coil with a slightly different primary amino acid sequence, also behave in a similar way. This linear correlation is, therefore, more widely applicable and could find

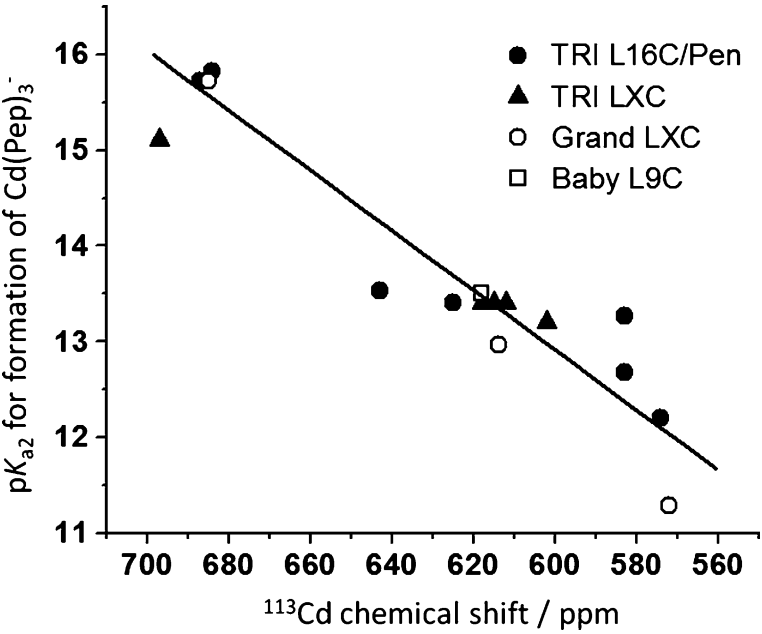

Figure 15 Plot illustrating the linear relationship between ^{113}Cd NMR chemical shift and the pK_{a2} for the formation of $Cd(peptide)_3^-$ [63].

significant use in interpreting coordination geometries in metalloproteins and enzymes, as well as the resulting chemistry associated with the fourth coordinating ligand, at the active metal ion site. However, before this analysis can be fully utilized, a similar study examining the behavior of thiolate deprotonation from cysteines in *d* sites must be completed.

The large spread of pK_{a2} values for the formation of CdS_3O, which ranges from 9.6–13.3, is thought to be the result of varying self-association affinities of the peptides that sequester Cd(II) as CdS_3O [63,74]. As discussed earlier, the introduction of an additional heptad results in a higher self-association energy by ca. 5 kcal mol^{-1} per coiled coil (i.e., GRAND *versus* TRI *versus* BABY) [72,73]. The substitution of hydrophobic Leu layers within the interior of the coiled coil leads to additional destabilization, ca. 6–7 kcal mol^{-1} [72,73]. The data suggests that the pK_{a2} is dependent on formation of the binding site, i.e., a lower pK_{a2} is determined for peptides which are fully folded into coiled coils at a low pH. The lowest pK_{a2} values are determined for peptides based on GRAND and with a minimum number of Leu substitutions, such as GRANDL12AL16C. In contrast, higher pK_{a2} values are determined for peptides with a low self-association affinity. These conclusions are consistent with there being less variability concerning the pK_{a2} of a CdS_3 site, as at the higher pH values required for CdS_3 formation, the majority of peptides are fully folded.

4.3 *Influence of Peptide Self-Association Affinity on Cd(II) Binding*

Efforts have been directed to use *de novo* peptide design of various peptide folds of varying stability and to investigate metal ion binding to these. These systems should allow questions concerning the origin of the resulting metal coordination geometry and affinity, to be answered. Is this the result of the metal ions intrinsic coordination geometry preference or a result of the peptide scaffold enforcing an otherwise less favorable and often distorted geometry on the metal ion? How does the association affinity of the protein or designed peptide in the absence of a metal ion relate to the metal ion binding affinity? How does it relate to its ability to enforce an otherwise less favorable coordination geometry on the metal ion?

In order to answer questions like these, a number of peptides were designed with varying self-association affinities. As previously described, the introduction of an additional heptad results in the formation of additional hydrophobic and salt-bridge stabilizing interactions, thereby stabilizing the coiled coil by ca. 5 kcal mol^{-1} [72,73]. Various derivatives of GRAND (*vide supra*) have already been described. Likewise, the reduction in the number of heptads in the peptide sequence, such as BABY (Table 1), which contains one heptad less than TRI, significantly destabilizes the peptide fold. Furthermore, the reduction of an additional heptad, MINI contains only two heptad repeats in the sequence, destabilizes the coiled coil even further [72]. Similarly, the replacement of hydrophobic Leu residues with smaller and less hydrophobic amino acids (e.g., Cys, Pen, Gly, Ala, D-Leu) destabilizes the peptide fold further. Using these negative design principles it was possible to prepare a range of peptides with varying degrees of self-association affinity in the absence of metal ions. The binding constants of these peptides to Cd(II) were then determined and found to be linearly related to the peptide self-association affinity (Figure 16) [72]. These studies demonstrate that one can use peptide self-association affinity, in *de novo* peptide design, to increase the effective concentration of thiol ligands at the metal binding site, and that the peptide structure in the absence of metal ions dictates the final coordination geometry.

A large spread of pK_{a2} values, ranging from 9.6–13.3, is obtained for the formation of CdS_3O (Figure 15) [63]. This large range is thought to be the result of varying self-association affinities of the different peptides that have been designed to sequester Cd(II) as CdS_3O. The experimental data suggests that the pK_{a2} is dependent on formation of the binding site, i.e., a lower pK_{a2} is obtained for peptides that are fully folded into coiled coils at a low pH. The lowest pK_{a2} values have been determined for peptides based on GRAND and with a minimum number of Leu substitutions, such as GRANDL12AL16C. In contrast, higher pK_{a2} values are measured for peptides with lower self-association affinities. These conclusions are consistent with there being less variability concerning the pK_{a2} of a CdS_3 site. This is due to the fact that the majority of the peptides investigated will be fully folded at the higher pH values required for CdS_3 formation.

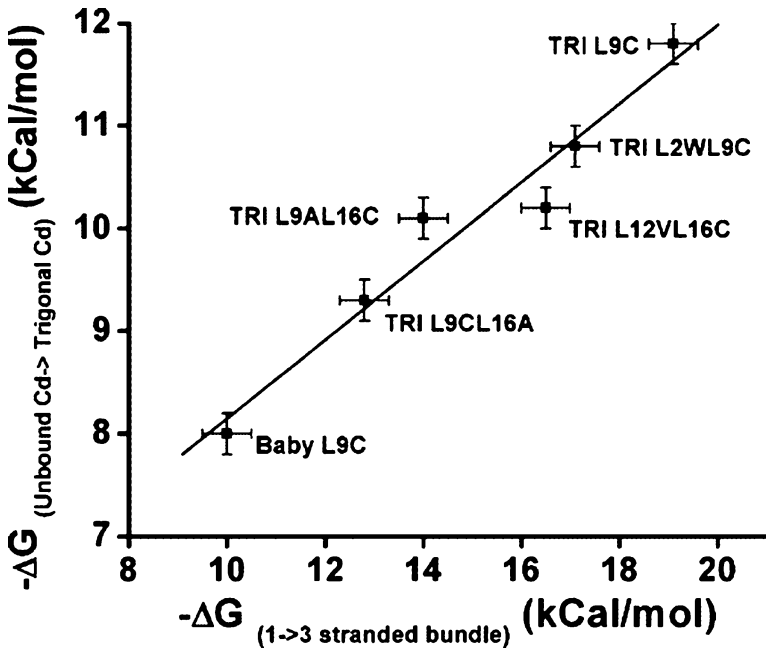

Figure 16 Linear free-energy correlation between folding preferences of the peptides in the absence of Cd(II) to the binding of the peptides to Cd(II) as $Cd(peptide)_3^-$. Reprinted from [72] with permission from the American Chemical Society; copyright 2012.

4.4 Metal Ion Exchange Rates into Helical Systems

Surprisingly, little is known about the pathways involved in metal binding and release in metalloproteins. In particular, there is a lack of information concerning the exchange rates of metal ion insertion in metalloregulatory proteins. Unfortunately, the natural proteins are extremely complex, and individual factors that contribute to the process of metal ion insertion, can be too challenging to identify. It was, therefore, proposed that the helical bundles described here, for which the Cd(II) coordination chemistry is well understood, could be used as models that help clarify some of these questions, and in particular could represent models for Cd(II) insertion into the repressor proteins CadC/CmtR.

Studies were initiated with GRANDL12AL16C and GRANDL26AL30C, which have both been found to bind Cd(II) as exclusively tetrahedral CdS_3O, differing only in the location of the site within the helical coiled coil. The Cd(II) binding site in GRANDL12AL16C is located in the center of the coiled coil, yet that in GRANDL26AL30C is located towards the C-terminus with only one hydrophobic Leu layer between the Cys site and the bulk solvent. These two sites behave extremely similar to one another, differing only in that Cd(II) populates the site at the 30 position at a much lower pH (pK_{a2} 9.9) than that at the 16 position (pK_{a2} 11.3) [75].

Titrations of Cd(II) into a solution of GRANDL12AL16C at pH 8.5 was monitored by ^{113}Cd NMR spectroscopy. In the presence of 1.0 equivalent $^{113}Cd(NO_3)_2$ a single resonance was observed at 572 ppm. On addition of a further 0.5 equivalents ^{113}Cd (1.5 equivalents total), a slight broadening of the peak was observed, however, there was no change to the chemical shift or the presence of additional resonances [80]. The gradual stepwise addition of $^{113}Cd(NO_3)_2$ to GRANDL26AL30C from 0.2 to 0.8 equivalents, resulted in the gradual increase in intensity of a single resonance at 587 ppm [80]. On addition of 1.0 equivalent ^{113}Cd a slight decrease in intensity was detected, however, this was not accompanied by any line broadening. On further addition of ^{113}Cd(II) the peak broadened significantly, so that by 1.7 equivalents it had broadened beyond detection. These results are consistent with metal binding which is dependent upon the position within the coiled coil. Notably a kinetically more labile site is generated towards the C-terminus of the peptide, which due to the single Leu layer in position 34 and peptide fraying, is more exposed to the bulk solvent. The different kinetic behavior of ^{113}Cd(II) binding to the two sites is maintained for the dual site peptide GRANDL12AL16CL26AL30C, with the L26AL30C site being more dynamic than the L12AL16C site.

Mathematical modeling of the exchange process was not consistent with a two-site slow exchange mechanism, but was found to be consistent with a multi-site exchange mechanism. This involves several ^{113}Cd(II) binding sites on the surface of the peptide which destabilize the peptide fold and alter the chemical shift of the ^{113}Cd(II) bound to the three thiol chains in the hydrophobic interior. The proposed model (Figure 17) was further confirmed by studying ^{113}Cd(II) binding to a mutant GRANDL26AE28QL30C. The Glu (E) in position 28 is normally involved in forming stabilizing salt bridge interactions with the Lys (K) of an adjacent α-helix, but has been replaced with a Gln (Q) residue. The ^{113}Cd(II) is thought to bind to the Glu adjacent to the metal binding site, thereby destabilizing the coiled coil. The destabilized structure is able to operate by a "breathing" mechanism whereby the ^{113}Cd(II) is subsequently coordinated by a single Cys residue which adopts a rotamer which is directed towards the α-helical interface. The ^{113}Cd(II) is then internalized into the hydrophobic interior and finally coordinated by the two remaining Cys side chains. The new mutant GRANDL26AE28QL30C lacks the necessary Glu for internalization of ^{113}Cd(II) in this manner, and it was found that a significantly larger equivalent of ^{113}Cd(II) (>2.1) was needed for complete broadening of the NMR signal compared to GRANDL26AL30C which contained the necessary Glu residue.

These studies have investigated the insertion of ^{113}Cd(II) as tetrahedral CdS_3O to Cys. Similar experiments were performed for ^{113}Cd(II) binding to GRANDL16-PenL19IL23PenL26I, which sequesters 2.0 equivalents of ^{113}Cd(II) both as trigonal CdS_3, as indicated by two ^{113}Cd NMR resonances at 681 and 686 ppm [75]. Intriguingly, the addition of excess ^{113}Cd(II) does not cause broadening of either resonance [80]. The two Pen sites are located at position 16 and 23 of the coiled coil, as opposed to position 30 for the dynamic four-coordinate CdS_3O site, and further removed from the fraying termini and bulk solvent. The coiled coil is more stable due to the improved packing of the hydrophobic core due to both the Pen methyl groups and the inclusion of Ile residues in place of Leu at positions 19 and 26. Therefore,

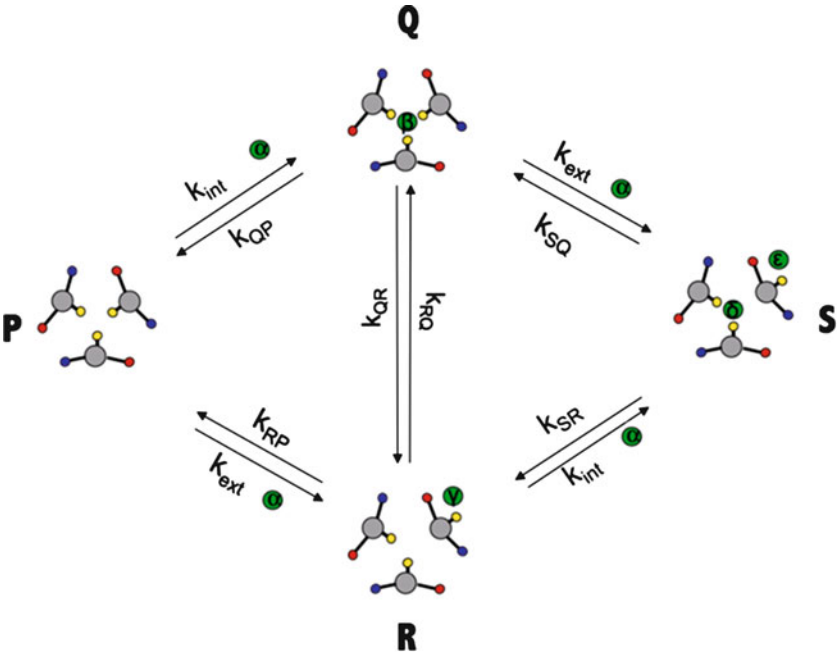

Figure 17 A cartoon representation of a model for five species (*P, Q, R, S*, and free *Cd*) which contribute to the binding of Cd(II) to the internal Cys_3 site within the hydrophobic interior of a three-stranded coiled coil. Initial binding to external Glu residues occurs directly prior to internalization. Shown are Cd(II) (green), Cys thiol (yellow), Glu oxygen (red), and Lys amine groups (blue) represented as circles. Reprinted from [80] with permission from the American Chemical Society; copyright 2012.

the binding of ^{113}Cd(II) to the Glu side chain is much less destabilizing that for the peptides studied capable of coordinating ^{113}Cd(II) as CdS_3O. Furthermore, the nature of the Pen ligand with the bulky methyl groups, is likely to restrict rotation of the thiol group towards the α-helical interface, which is required for the insertion mechanism described here. Investigation of the binding of ^{113}Cd(II) to a Cys ligand as trigonal CdS_3, e.g., GRANDL12L_DL16C, could allow for confirmation as to whether these differences are due to the packing of the hydrophobic core, i.e., the overall stability of the coiled coil, and the restricted rotation of the Pen ligand, or if it is due to the more unlikely scenario of an intrinsic CdS_3 property.

5 General Conclusions: Lessons for Understanding the Biological Chemistry of Cd(II)

The success of the relatively simple coiled coil systems described in this chapter, demonstrates that the large and complex biological architectures found in natural systems may not be entirely necessary in order to display a high degree of

specificity and control of coordinated metal ions. The selectivity and coordination geometry (often distorted or coordinatively unsaturated) of metal ion sites in natural systems is often crucial in order to display the correct function (e.g., structural) or activity (e.g., catalytic). Furthermore, important structure-function relationships can be established with these systems, which subsequently can be used to evaluate natural systems, through systematically correlating chemical observations with modifications to the designed structure.

We hope that this chapter has illustrated the opportunities afforded by *de novo* design of metallopeptide architectures, and how our efforts to date have been directed towards gaining further understanding about the roles of metal ions in biology. From this we believe that it will be possible to understand how this chemistry might relate to their biological functions, to understand the mechanisms behind heavy metal toxicity and ultimately we expect to harness this knowledge to design synthetic metalloenzymes [81], for novel industrial or biomedical applications.

Abbreviations and Definitions

For the definition of the peptides see Table 1.

Ala	alanine
ALAD	aminolevulinic acid dehydratase
Asp	aspartic acid
CD	circular dichroism
Cys	cysteine
EXAFS	extended X-ray absorption fine structure
Glu	glutamic acid
Gly	glycine
His	histidine
Hfl	hexafluoroleucine
Ile	isoleucine
Leu	leucine
LMCT	ligand-to-metal charge-transfer
Met	methionine
NOESY	nuclear Overhauser effect specroscpy
PAC	perturbed angular correlation
PDB	Protein Data Bank
Pen	penicillamine
NMR	nuclear magnetic resonance
3SCC	three-stranded coiled coil
Ser	serine
Val	valine

Acknowledgments A.F.A.P. thanks the University of Birmingham and V.L.P. thanks the University of Michigan and the National Institute of Health for support of this research (R01 ES0 12236).

References

1. T. Lane, M. A. Saito, G. N. George, I. J. Pickering, R. C. Prince, F. F. M. Morel, *Nature* **2005**, *435*, 42.
2. R. H. Holm, P. Kennepohl, E. I. Solomon, *Chem. Rev.* **1996**, *96*, 2239–2314.
3. M. Margoshes, B. L. Vallee, *J. Am. Chem. Soc.* **1957**, *79*, 4813–4814.
4. L. M. Utschig, J. W. Bryson, T. V. O'Halloran, *Science* **1995**, *268*, 380–385.
5. D. M. Ralston, T. V. O'Halloran, *Proc. Natl. Acad. Sci. USA* **1990**, *87*, 3846–3850.
6. R. P. Novick, C. Roth, *J. Bacteriol.* **1968**, *95*, 1335–1342.
7. Y. Sun, M. Wong, B. P. Rosen, *J. Biol. Chem.* **2001**, *276*, 14955–14960.
8. C. Rensing, Y. Sun, B. Mitra, B. P. Rosen, *J. Biol. Chem.* **1998**, *273*, 32614–32617.
9. G. Endo, S. Silver, *J. Bacteriol.* **1995**, *177*, 4437–4441.
10. J. Ye, A. Kandegedara, P. Martin, B. P. Rosen, *J. Bacteriol.* **2005**, *187*, 4214–4221.
11. A. Kandegedara, S. Thiyagarajann, K. C. Kondapalli, T. L. Stemmler, B. P. Rosen, *J. Biol. Chem.* **2009**, *284*, 14958–14965.
12. C. Rensing, *J. Bacteriol.* **2005**, *187*, 3909–3912.
13. L. S. Busenlehner, N. J. Cosper, R. A. Scott, B. P. Rosen, M. D. Wong, D. P. Giedroc, *Biochemistry* **2001**, *40*, 4426–4436.
14. L. S. Busenlehner, T.-C. Weng, J. E. Penner-Hahn, D. P. Giedroc, *J. Mol. Biol.* **2002**, *319*, 685–701.
15. M. F. Summers, *Coord. Chem. Rev.* **1988**, *86*, 43–134.
16. A. K. Duhme, H. Z. Strasdeit, *Z. Anorg. Allg. Chem.* **1999**, *625*, 6–8.
17. R. A. Santos, E. S. Gruff, S. A. Koch, *J. Am. Chem. Soc.* **1991**, *113*, 469–475.
18. N. Govindaswamy, J. Moy, M. Millar, S. A. Koch, *Inorg. Chem.* **1992**, *31*, 5343–5344.
19. J. S. Cavet, A. I. Graham, W. Meng, N. J. Robinson, *J. Biol. Chem.* **2003**, *278*, 44560–44566.
20. Y. Wang, L. Hemmingsen, D. P. Giedroc, *Biochemistry* **2005**, *44*, 8976–8988.
21. L. Banci, I. Bertini, F. Cantini, S. Ciofi-Baffoni, J. S. Cavet, C. Dennison, A. I. Graham, D. R. Harvie, N. J. Robinson, *J. Biol. Chem.* **2007**, *282*, 30181-30188.
22. B. Tripet, K. Wagschal, P. Lavigne, C. T. Mant, R. S. Hodges, *J. Mol. Biol.* **2000**, *300*, 377–402.
23. P. B. Harbury, T. Zhang, P. S. Kim, T. Albert, *Science* **1993**, *262*, 1401–1407.
24. B. Lovejoy, S. Choe, D. Cascio, D. K. McRorie, W. F. DeGrado, D. Eisenberg, *Science* **1993**, *259*, 1288–1293.
25. D. N. Woolfson, *The Design of Coiled-Coil Structures and Assemblies*, in *Advances in Protein Chemistry*, Vol. 70, Eds D. A. D. Parry, J. M. Squire, Academic Press, 2005, pp. 79–112.
26. O. D. Monera, C. M. Kay, R. S. Hodges, *Biochemistry* **1994**, *33*, 3862–3871.
27. E. K. O'Shea, K. J. Lumb, P. S. Kim, *Curr. Biol.* **1993**, *3*, 658–667.
28. O. Iranzo, D. Ghosh, V. L. Pecoraro, *Inorg. Chem.* **2006**, *45*, 9959–9973.
29. J. P. Schneide, J. W. Kelly, *J. Am. Chem. Soc.* **1995**, *117*, 2533–2546.
30. G. Platt, C. Chung, M. Searle, *Chem. Commun.* **2001**, 1162–1163.
31. J. Venkatraman, G. A. Naganagowda, R. Sudha, P. Balaram, *Chem. Commun.* **2001**, 2660–2661.
32. R. P. Cheng, S. L. Fisher, B. J. Imperiali, *J. Chem. Soc., Dalton Trans.* **1996**, *118*, 11349–11356.
33. M. M. Rosenblatt, J. Y. Wang, K. S. Suslick, *Proc. Natl. Acad. Sci. USA* **2002**, *100*, 13140–13145.
34. B. A. Krizek, D. L. Merkle, J. M. Berg, *Inorg. Chem.* **1993**, *32*, 937–940.

35. M. D. Struthers, R. P. Cheng, B. J. Imperiali, *J. Am. Chem. Soc.* **1996**, *118*, 3073–3081.
36. M. D. Struthers, R. P. Cheng, B. J. Imperiali, *Science* **1996**, *271*, 342–345.
37. R. P. Bonomo, L. Casella, L. D. Gioia, H. Molinari, G. Impellizzeri, T. Jordan, G. Pappalardo, E. Rizzarelli, *J. Chem. Soc., Dalton Trans.* **1997**, 2387–2389.
38. G. R. Dieckmann, D. K. McRorie, J. D. Lear, K. A. Sharp, W. F. DeGrado, V. L. Pecoraro, *J. Mol. Biol.* **1998**, *280*, 897–912.
39. G. R. Dieckmann, D. K. McRorie, D. L. Tierney, L. M. Utschig, C. P. Singer, T. V. O'Halloran, J. E. Penner-Hahn, W. F. DeGrado, V. L. Pecoraro, *J. Am. Chem. Soc.* **1997**, *119*, 6195–6196.
40. C. J. Reedy, B. R. Gibney, *Chem. Rev.* **2004**, *104*, 617–649.
41. B. R. Gibney, S. E. Mulholland, F. Rabanal, P. L. Dutton, *Proc. Natl. Acad. Sci. USA* **1996**, *93*, 15041–15046.
42. V. L. Pecoraro, A. F. A. Peacock, O. Iranzo, M. Luczkowski, *Understanding the biological chemistry of mercury using a de novo protein design strategy*, in *Bioinorg. Chem. ACS Sympos. Ser.* 1012, , pp. 183–197.
43. B. T. Farrer, N. P. Harris, K. E. Balchus, V. L. Pecoraro, *Biochem.* **2001**, *40*, 14696–14705.
44. B. T. Farrer, C. P. McClure, J. E. Penner-Hahn, V. L. Pecoraro, *Inorg. Chem.* **2000**, *39*, 5422–5423.
45. M. Matzapetakis, D. Ghosh, T.-C. Weng, J. E. Penner-Hahn, V. L. Pecoraro, *J. Biol. Inorg. Chem.* **2006**, *11*, 876–890.
46. B. T. Farrer, V. L. Pecoraro, *Proc. Natl. Acad. Sci. USA* **2003**, *100*, 3760–3765.
47. O. Iranzo, P. W. Thulstrup, S. Ryu, L. Hemmingsen, V. L. Pecoraro, *Chem. Eur. J.* **2007**, *13*, 9178–9190.
48. D. S. Touw, C. E. Nordman, J. E. Stuckey, V. L. Pecoraro, *Proc. Natl. Acad. Sci. USA* **2007**, *104*, 11969–11974.
49. M. Matzapetakis, B. T. Farrer, T.-C. Weng, L. Hemmingsen, J. E. Penner-Hahn, V. L. Pecoraro, *J. Am. Chem. Soc.* **2002**, *124*, 8042–8054.
50. M. Matzapetakis, V. L. Pecoraro, *J. Am. Chem. Soc.* **2005**, *127*, 18229–18233.
51. N. Ogihara, M. S. Weiss, W. F. DeGrado, D. Eisenberg, *Protein Sci.* **1997**, *6*, 78–86.
52. K. T. O'Neil, W. F. DeGrado, *Science* **1990**, *250*, 646–651.
53. S. Chakraborty, D. S. Touw, A. F. A. Peacock, J. Stuckey, V. L. Pecoraro, *J. Am. Chem. Soc.* **2010**,*132*, 13240–13250.
54. L. Hemmingsen, K. Nárcisz, E. Danielsen, *Chem. Rev.* **2004**, *104*, 4027–4061.
55. L. Hemmingsen, L. Olsen, J. Antony, S. P. A. Sauer, *J. Biol. Inorg. Chem.* **2004**, *9*, 591–599.
56. J. C. L. Reynolds, K. F. Cooke, S. H. Northrup, *J. Phys. Chem.* **1990**, *94*, 985–991.
57. T. L. Poulos, B. C. Finzel, A. J. Howard, *Biochemistry* **1986**, *25*, 5314–5322.
58. O. D. Monera, F. D. Sönnichsen, L. Hicks, C. M. Kay, R. S. Hodges, *Protein Eng.* **1996**, *9*, 353–363.
59. K.-H. Lee, M. Matzapetakis, S. Mitra, E. N. G. Marsh, V. L. Pecoraro, *J. Am. Chem. Soc.* **2004**, *126*, 9178–9179.
60. K.-H. Lee, C. Cabello, L. Hemmingsen, E. N. G. Marsh, V. L. Pecoraro, *Angew. Chem. Int. Ed.* **2006**, *45*, 2864–2868.
61. C. N. Pace, J. M. Scholtz, *Biophys. J.* **1998**, *75*, 422–427.
62. P. T. Erskine, E. M. H. Duke, I. J. Tickle, N. M. Senior, M. J. Warren, J. B. Cooper, *Acta Crystallogr. Sect. D* **2000**, *56*, 421–430.
63. O. Iranzo, T. Jakusch, K.H. Lee, L. Hemmingsen, V. L. Pecoraro, *Chem. Eur. J.* **2009**, *15*, 3761–3772.
64. A. F. A. Peacock. J. A. Stuckey, V. L. Pecoraro, *Angew. Chem. Int. Ed.* **2009**, *48*, 7371–7374.
65. A. F. A. Peacock, L. Hemmingsen, V. L. Pecoraro, *Proc. Natl. Acad. Sci. USA* **2008**, *105*, 16566–16571.
66. M. Łuczkowski, M. Stachura, V. Schirf, B. Demeler, L. Hemmingsen, V. L. Pecoraro, *Inorg. Chem.* **2008**, *47*, 10875–10888.
67. O. A. Kharenko, M. Y. Ogawa, *J. Inorg. Biochem.* **2004**, *98*, 1971–1974.

68. O. A. Kharenko, D. C. Kennedy, B. Demeler, M. J. Maroney, M. Y. Ogawa, *J. Am. Chem. Soc.* **2005**, *127*, 7678–7679.
69. M. Mukherjee, X. Zhu, M. Y. Ogawa, *Inorg. Chem.* **2008**, *47*, 4430–4432.
70. C. J. Henehan, D. L. Pountney, O. Zerbe, M. Vašák, *Protein Sci.* **1993**, *2*, 1756–1764.
71. D. S. Touw, Ph.D. Thesis, University of Michigan, **2007**.
72. D. Ghosh, K.-H. Lee, B. Demeler, V. L. Pecoraro, *Biochemistry* **2005**, *44*, 10732–10740.
73. J. Y. Su, R. S. Hodges, C. M. Kay, *Biochemistry* **1994**, *33*, 15501–15510.
74. O. Iranzo, C. Cabello, V. L. Pecoraro, V. L., *Angew. Chem. Int. Ed.* **2007**, *46*, 6688–6691.
75. O. Iranzo, S. Chakraborty, L. Hemmingsen, V. L. Pecoraro, *J. Am. Chem. Soc.* **2011**, *133*, 239–251.
76. S. T. R. Walsh, H. Cheng, J. W. Bryson, H. Roder, W. F. DeGrado, *Proc. Natl. Acad. Sci. USA* **1999**, *96*, 5486–5491.
77. S. Chakraborty, J. Yudenfreund Kravitz, P. W. Thulstrup, L. Hemmingsen, W. F. DeGrado, V. L. Pecoraro, *Angew. Chem. Int. Ed.* **2011**, *50*, 2049–2053.
78. R. K. Bogess, J. R. Absher, S. Morelen, L. T. Taylor, J. W. Hughes, *Inorg. Chem.* **1983**, *22*, 1273–1279.
79. B. V. Cheesman, A. P. Arnold, D. L. Rabenstein, *J. Am. Chem. Soc.* **1988**, *110*, 6359–6364.
80. S. Chakraborty, O. Iranzo, E. R. P. Zuiderweg, V. L. Pecoraro, *J. Am.Chem. Soc.* **2012**, *134*, 6191–6203.
81. M. Zastrow, A. F. A. Peacock, J. Stuckey, V. L. Pecoraro, *Nature Chem.*, **2012**, *4*, 118–123.
82. A. F. A. Peacock, O. Iranzo, V. L. Pecoraro, *Dalton Trans.* **2009**, *13*, 2271–2280.

Chapter 11
Cadmium in Metallothioneins

Eva Freisinger and Milan Vašák

Contents

ABSTRACT 339
1 INTRODUCTION 340
2 SPECTROSCOPIC CHARACTERIZATION 342
2.1 Divalent Metal-Binding Sites and Their Organization 342
2.2 UV/VIS and Circular Dichroism Spectroscopy 345
2.3 Magnetic Circular Dichroism Spectroscopy 349
2.4 X-Ray Absorption Spectroscopy 351
2.5 Perturbed Angular Correlation of γ-Rays Spectroscopy 352
2.6 Mass Spectrometry 354
3 BINDING AFFINITY AND REACTIVITY 358
3.1 Metal Binding Affinities 358
3.2 Structure Dynamics and Metal Exchange Processes 359
3.3 Cluster Reactivity 361
4 THREE-DIMENSIONAL STRUCTURES 361
5 CONCLUDING REMARKS 365
ABBREVIATIONS 366
ACKNOWLEDGMENT 367
REFERENCES 367

Abstract Metallothioneins (MTs) are low-molecular-mass cysteine-rich proteins with the ability to bind mono- and divalent metal ions with the electron configuration d^{10} in form of metal-thiolate clusters. MTs are thought, among others, to play a role in the homeostasis of essential Zn(II) and Cu(I) ions. Besides these metal ions also Cd(II) can be bound to certain MTs *in vivo*, giving rise to the perception that another physiological role of MTs is in the detoxification of heavy metal ions. Substitution of the spectroscopically silent Zn(II) ions in

E. Freisinger (✉) • M. Vašák (✉)
Institute of Inorganic Chemistry, University of Zürich, Winterthurerstrasse 190,
CH-8057 Zürich, Switzerland
e-mail: freisinger@aci.uzh.ch; mvasak@bioc.uzh.ch

A. Sigel, H. Sigel, and R.K.O. Sigel (eds.), *Cadmium: From Toxicity to Essentiality*,
Metal Ions in Life Sciences 11, DOI 10.1007/978-94-007-5179-8_11,

metalloproteins by Cd(II) proved to be an indispensable tool to probe the Zn(II) sites *in vitro*. In this review, methods applied in the studies of structural and chemical properties of Cd-MTs are presented. The first section focuses on the physical basis of spectroscopic techniques such as electronic absorption, circular dichroism (CD), magnetic CD, X-ray absorption, and perturbed angular correlation of γ-rays spectroscopy, as well as mass spectrometry, and their applications to Cd-MTs from different organisms. The following is devoted to the discussion of metal binding affinities of Cd-MTs, cluster dynamics, the reactivity of bound Cd(II) ions with metal ion chelators and of thiolate ligands with alkylating and oxidizing agents. Finally, a brief summary of the known three-dimensional structures of Cd-MTs, determined almost exclusively by multinuclear NMR techniques, is presented. Besides Cd-MTs, the described methods can also be applied to the study of metal binding sites in other metalloproteins.

Keywords circular dichroism • electronic absorption • electrospray ionization mass spectrometry • magnetic circular dichroism • metal-thiolate cluster structures • metallothionein • perturbed angular correlation of γ-rays spectroscopy • X-ray absorption spectroscopy

1 Introduction

Metallothioneins (MTs) is a collective name for ubiquitous low-molecular-mass metal binding proteins (usually <10 kDa). The designation MT reflects a high cysteine sulfur and metal content ranging between about 10–30% (w/w). These proteins have been isolated from vertebrates, invertebrates, plants, eukaryotic microorganisms, and prokaryotes [1]. MTs are intracellular proteins, but in higher organisms they can also occur in extracellular space such as blood plasma and cerebrospinal fluid, suggesting that they may play different biological roles depending on their localization. The first MT was discovered by Margoshes and Vallee in 1957 as the cadmium binding protein from equine kidney cortex [1]. Thus far, besides carbonic anhydrase in diatoms [2], MTs are the only biological compounds in which cadmium accumulates naturally. However, MTs can bind a variety of metal ions *in vivo,* the most important being Zn(II), Cu(I), and Cd(II). In fact, Zn(II) and/or Cu(I) are the principal metal constituents under normal physiological conditions. The binding of these metal ions is achieved through the formation of cysteine (Cys) sulfur-based metal-thiolate clusters. The majority of the MT literature has focused on vertebrate MTs in terms of their structure, function, and regulation. Mammalian MTs are composed of 61−68 amino acids out of which 20 are conserved cysteine residues. With rare exceptions, the aromatic amino acids and histidine (His) are absent in these MTs. The striking feature of mammalian MTs is their inducibility by various agents such as heavy metals, reactive oxygen species, hormones, and xenobiotics.

Several biological roles have been ascribed to these MTs, including their involvement in zinc and copper homeostasis, the protection against environmental

heavy metals and oxidative stress, the control of redox status of the cell, the antiapoptotic role and recently also in the protection and regeneration of the mammalian brain following neurological injury and disease [3–14]. Whereas a large number of studies have been conducted regarding the biological roles of mammalian MTs, less biological data are available for MTs from other organisms. Here, the most intriguing MTs are those found in plants [12]. The biological studies revealed that four subclasses of plant MTs display differential responses to copper and zinc. Interestingly, the zinc-binding type 4 plant MTs were found to be regulated by hormones rather than zinc. It may be noted that apart from MTs, phytochelatins, an enzymatically synthesized family of short glutathione-related peptides, protect some plants and fungi from the cytotoxic effect of heavy metal ions. The primary structures of plant MTs do not share discernible sequence similarity with the vertebrate forms and often contain a few histidine residues. In addition, these sequences show extended stretches of amino acids devoid of Cys residues, referred to as 'linkers', connecting Cys-rich domains of the protein [15].

The structural studies on MTs are highly challenging because of the dynamic nature of these proteins. Consequently, only a limited number of MT structures are currently available mostly determined in solution by NMR. From the entries made to the Protein Data Bank (PDB), the majority of the determined MT structures are those of vertebrates followed by the echinoderm and crustacean proteins [16]. These structures contain either solely Cd(II) or both, Cd(II) and Zn(II) ions. Two other MT structures containing divalent metal ions are those of cyanobacterial M_4SmtA (PDB code 1JJD, [17]) and the two domains of the wheat M_6E_c–I/II protein (PDB codes 2L61/2L62/2KAK [18,19]). Several structures of the yeast *Saccharomyces cerevisiae* Cup1 protein (PDB codes 1RJU/1AQS [20,21]) and a small MT from *Neurospora crassa* (PDB code 1T2Y [22]), both showing a clear preference for the binding of monovalent Cu(I) ions, have also been reported.

The structural studies till about 1990 have been carried out on MTs isolated from natural sources. Both the yield and sample heterogeneity, due to the presence of several MT isoforms, were the limiting factors in these studies. The advent of a recombinant expression allowed studying the structure and function of a desired MT, in many instances not easily available otherwise. This technique offers a number of advantages including the production of ^{15}N- and ^{13}C-labelled proteins for NMR studies and the preparation of mutants. However, the recombinant heterologous expression brings about also problems as it is often difficult to unambiguously demonstrate the identity of the recombinant protein with the native form. After all, MTs are not enzymes whose activity can be checked. As the native protein was not isolated from natural sources, the presence of the naturally occurring metal ion in the structure of recombinant MTs, i.e., zinc *versus* copper, and consequently the correct protein fold is not known. To address the question of the bound metal ion *in vivo*, a set of criteria based on recombinant expression in *E. coli* was proposed recently to differentiate between intrinsically zinc and copper thioneins [23]. Here, the expression of thionein with a zinc character in zinc- and cadmium-supplemented media leads to the formation of homometallic species, whereas its expression in copper-supplemented media results in mixed-metal

species (Cu,Zn) and partially oxidized forms. The reverse is true for thionein with a copper character expressed in zinc- and copper-supplemented media.

As Zn(II) and Cu(I) are spectroscopically silent, knowledge of the native metal occupancy is crucial for the introduction of a suitable metal ion as a spectroscopic probe required in the elucidation of the MT structure in solution. The NMR-active ^{109}Ag(I) isotope ($I = ½$) has been used to probe for Cu(I) sites in MTs. However, differences in the cluster organization in the yeast Cup1 protein in complex with Cu(I) or ^{109}Ag(I) ions have been seen [20,21]. These results have been ascribed to different coordination properties of both metal ions, putting the use of Ag(I) as a probe for Cu(I) sites in MTs in question. In the study of zinc-containing MTs, the spectral properties of Co(II) or Cd(II) ions have been successfully applied. At this point it should be noted that in the studies of zinc enzymes, zinc substitution by Co(II) or Cd(II) usually preserved their enzymatic activity. Co(II) as a d^7 ion is always paramagnetic and when substituted for Zn(II) in proteins it has always a lower symmetry and is almost invariably in the high-spin state ($S = 3/2$). Here, the electronic *d-d* transitions together with magnetic susceptibility and/or electron spin resonance (EPR) measurements of Co(II)-MTs provided information regarding the geometry of metal binding site(s) and their organization, respectively [24–26].

As discussed above, upon exposure or administration of cadmium to various species this metal often accumulates in MTs. This makes cadmium a biologically relevant probe for divalent metal sites in native or recombinant MTs. In this context, it may be noted that the metal-thiolate clusters of recombinant, mainly cadmium-containing MTs from various species including mammals expressed as glutathione-S-transferase (GST) fusion proteins in *E. coli*, contained inorganic sulfide (S^{2-}) [27]. At this time, the physiological relevance of this finding is not clear. However, pure homometallic MT forms can be obtained by a method of metal reconstitution [28]. Cd(II), owing to its ^{113}Cd and ^{111}Cd NMR active isotopes ($I = ½$), proved to be indispensable in the structure determination of Cd-MTs from various species. In addition to NMR, a number of other spectroscopic techniques including electronic absorption, circular dichroism (CD), magnetic CD, X-ray absorption, and perturbed angular correlation of γ-rays spectroscopy as well as mass spectrometry provided a wealth of structural information about the divalent metal sites in MTs and their organization. In this chapter the application of these spectroscopic techniques in the study of Cd-MTs are discussed.

2 Spectroscopic Characterization

2.1 Divalent Metal-Binding Sites and Their Organization

MTs consist of single polypeptide chains all sharing a high Cys content. These residues are present in Cys-Xaa-Cys and Cys-Xaa-Yaa-Cys motifs, where Xaa and Yaa stand for amino acids other than Cys. Besides these motifs also Cys-Cys and even Cys-Cys-Cys stretches can be found in many MT sequences (Table 1).

Table 1 Amino acid sequences of Cd-MT forms with known three-dimensional structures. Coordinates of the two structures marked with # are only available for the Zn(II)-forms. Grey boxes enclose the amino acid stretches that contain the residues involved in cluster formation. The cysteine and histidine residues are highlighted in black and grey, respectively.

MT	organism	sequence	PDB code	Lit.
Family 1: vertebrate MTs				
MT1	(*Mus musculus*)	MDP-NCSCST-GGSCTGTSSCACKNCKCTSCKKSCCSCCPVGCSKCAQGCVCKG------AADKCTCCA	1DFT / 1DFS	[39]
MT2	(*Homo sapiens*)	MDP-NCSCAA-GDSCTCAGSCKCKECKCTSCKKSCCSCCPVGCAKCAQGCICKG------ASDKCSCCA	2MHU / 1MHU	[34]
MT2	(*Oryctolagus cuniculus*)	MDP-NCSCAAAGDSCTCANSCTCKACKCTSCKKSCCSCCPPGCAKCAQGCICKG------ASDKCSCCA	2MRB / 1MRB	[32]
MT2	(*Rattus norvegicus*)	MDP-NCSCAT-DGSCSCAGSCKCKQCKCTSCKKSCCSCCPVGCAKCSQGCICK-E-----ASDKCSCCA	2MRT / 1MRT	[37]
MT3	(*Homo sapiens*)	MDPETCPCPS-GGSCTCADSCKCEGCKCTSCKKSCCSCCPAECEKCAKDCVCKGGEAAEAEAEKCSCCQ	--- / 2F5H	[38]
MT3	(*Mus musculus*)	MDPETCPCPT-GGSCTCSDKCKCKGCKCTNCKKSCCSCCPAGCEKCAKDCVCKGEEGAKAEAEKCSCCQ	--- / 1JI9	[35]
MTB	(*Notothenia coriiceps*)	MDP--CPCSK-SGTCNCGGSCTCTNCPCKSCKKSCCPCCPSGCTKCASGCVCKG------KTCDTSCCQ	1M0J / 1M0G	[33]
Family 3: crustacean MTs				
MT1	(*Callinectes sapidus*)	MPGHCCNDKCVCQEGCKAGCQCTSCHCSHCQKCTSGCKCATKEECGKTCTKPCSCCPK	1DME / 1DMC	[41]
MT1	(*Homarus americanus*)	MPGHCCKDKCPCAEGGCKTGCKCTSCHCAPCEKCTSGCKCPSKDECAKTCSKPCSCCPT	1J5M / 1J5L	[40]
Family 4: echinodermata MTs				
MTA	(*Strongylocentrotus purpuratus*)	MPDVHCVCCTEGKECACFGQDCCVTGECCKDGTCCGICTNAACKCANGCKCGSGCSCTEGNCAC	1QJK / 1QJL	[36]
Family 14: prokaryota MTs				
MT	(*Synechococcus PCC 7942*)	TSTTLVKCACEECLCNVDPSKAIDRNGLYYCSEACADGHTGGSKGCGHTCGNCHG	1JJD#	[17]
Family 15: plant MTs				
E_c-1	(*Triticum aestivum*)	MGCDDKCGCAVPCPGGTGCRCTSARSGAAAGEHTTCGCGEHCGCNPCACGREGTPSGRANRRANCSCGAACNCASCGSATA	2L61 / 2KAK#	[18,19]

The intrinsic pK_a value of cysteine residues in a protein environment is reported to be around 9.1 [29]. Accordingly, at physiological pH roughly 98% of the Cys residues will be present in the protonated thiol form. However, the pK_a value can be influenced by the surrounding residues. For example, in cysteine proteases such as papain hydrogen bonding between the active site Cys and a charged His residue causes a decrease of the apparent pK_a value by up to 6 log units [29]. In creatine kinase similar hydrogen bonding to both, a serine residue and a backbone amide proton lowers the pK_a of the enzymatically important Cys by 3 log units [29,30]. In MTs it is the competition of thiophilic metal ions with the protons of the thiol groups that leads to a pronounced decrease of the pK_a values by roughly 4.5 to 5.5 log units in the presence of Zn(II) and Cd(II) ions, respectively. This effect results in enhancement of the nucleophilicity of the bound sulfur ligand [31]. A peculiarity of MTs is the formation of metal-thiolate cluster structures. In these clusters, next to terminal thiolate ligands also thiolates that bridge two metal ions are observed. In this way the metal ion binding capacity of a given MT is significantly increased compared to exclusive metal ion coordination in mononuclear MS_4 sites. Lacking direct metal-metal bonds, the metal-thiolate clusters in MTs can be seen as multinuclear coordination compounds of the Werner-type. In recent years, biophysical studies on MTs from lower organisms and plants established that also His residues present in some of the amino acid sequences can act as ligands for Zn(II) or Cd(II) (Figure 1).

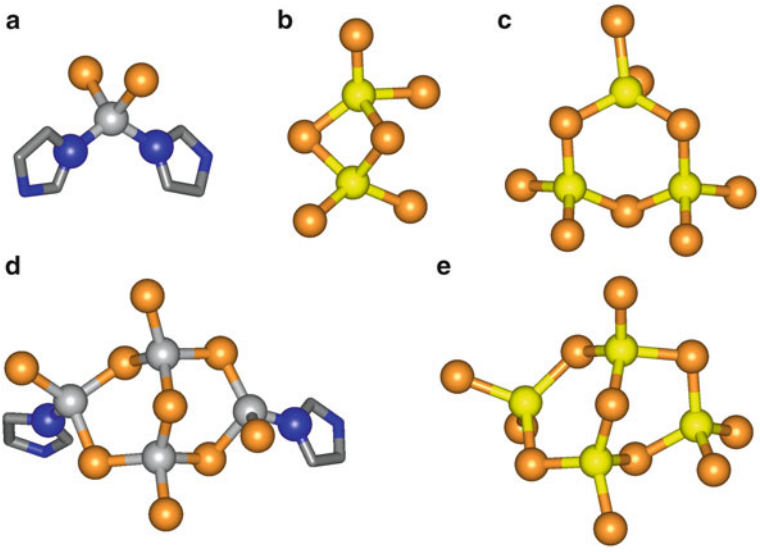

Figure 1 Representative structures of metal binding sites with divalent metal ions and their organization in metallothioneins: (**a**) mononuclear MS_2N_2 site observed in the C-terminal β_E-domain of wheat Zn_6E_c-1 [19], (**b**) M_2S_6 cluster in the N-terminal γ-domain of wheat Cd_6E_c-1 [18], (**c**) M_3S_9 cluster commonly known as β-cluster as found, e.g., in mouse Cd_7MT-1 [39], (**d**) $M_4S_9N_2$ cluster of a cyanobacterial MT [17], (**e**) M_4S_{11} cluster commonly known as α-cluster observed, e.g., in mouse Cd_7MT-1 [39]. Zn(II) and Cd(II) ions are depicted as grey and yellow spheres, respectively, the coordinating atoms of the Cys and His residues as orange and blue spheres and the remaining atoms of the His imidazole ring are additionally shown as sticks.

In a broad sense, four types of binding site motifs with Zn(II) or Cd(II) ions have been reported to occur in MTs, with both metals tetrahedrally coordinated. These include the mononuclear site and the di-, tri-, and tetranuclear metal clusters (Figure 1). The widely present cluster types are the tri- and tetranuclear Zn(II) and/or Cd(II) clusters first observed in vertebrates. The basic units for these clusters are M_3S_9 and M_4S_{11}. In these clusters metals are coordinated by both terminal and μ_2-bridging thiolate ligands, forming a distorted boat cyclohexane-like ring and an adamantane-type geometry with the metals and donor atoms arranged in two fused six-membered rings of distorted boat conformations, respectively (Figure 1). The concomitant presence of both types of clusters has been reported in vertebrate (structures of rat, rabbit, mouse, human, and fish) and sea urchin MTs [32–39]. Two M_3S_9 clusters are present in crustacean MTs [40,41]. The cluster structure present in M_4SmtA from the cyanobacterium *Synechococcus PCC 7942* is unusual in that it contains a single tetranuclear cluster in which besides nine cysteine ligands also two histidines participate in metal binding ($M_4S_9N_2$). Note that the histidines solely act as terminal ligands (Figure 1). The most striking metal binding motifs are present in the seed-specific metallothionein Zn_6E_c-1 from wheat in which three types of metal site organizations occur with the basic units denoted as M_3S_9, M_2S_6, and MS_2N_2. Hence, in this MT apart from a trinuclear thiolate cluster also a dinuclear thiolate cluster, resembling that reported for the GAL4 transcription factor [42], and a mononuclear MS_2N_2 site similar to that found in zinc-finger proteins exist.

2.2 *UV/VIS and Circular Dichroism Spectroscopy*

Our understanding of the electronic absorption and CD spectra of Cd-MTs came from the studies of mammalian forms. In the absence of aromatic amino acids and histidine the absorption spectrum of metal-free MT (apoMT) is characterized by a gradual absorption increase below 230 nm, originating from the peptide backbone amide transitions. However, in the fully metal-loaded Cd_7MT a pronounced shoulder at about 250 nm is discerned (Figure 2). The Gaussian analysis of the metal-induced absorption profile revealed the presence of a minimum of three transitions occurring at 250, 231, and 201 nm [43]. Based on the concept of optical electronegativity differences by Jørgensen [44] the lowest energy Gaussian band at 250 nm has been assigned to the first CysS–Cd(II) LMCT transition in the complex. In a molecular orbital (MO) scheme derived from Jørgensen's theory the electron transfer originates from the highest occupied p_π MO to an unoccupied MO localized on the metal, containing contributions from the 5*s* orbital of the metal and empty 4*s* orbitals of the ligand [45]. Additional contributions to this metal-induced absorption profile including a higher energy LMCT, ligand-to-ligand charge-transfer (LLCT) or intraligand charge-transfer-to-solvent (CTTS) transitions have also been described [45–47].

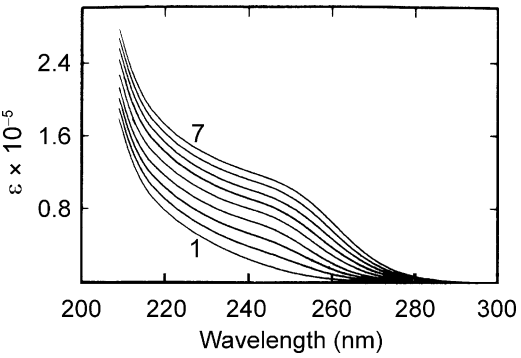

Figure 2 Effect of increasing Cd(II) binding on the electronic absorption spectrum of apoMT from rabbit liver at pH 8.4. The units are based on the protein concentration. Adapted from [43] with permission from the American Chemical Society; copyright 1987.

However, in the titration studies of apoMT with increasing mole equiv of Cd(II) an about 5 nm red shift to 250 nm was observed in the Cd-thiolate absorption envelope when more than 4 Cd(II) were bound (Figure 2). In analogous titration studies of apoMT using Co(II) ions even a larger, about 30 nm, red shift of the CysS–Co(II) LMCT bands (between 300 and 400 nm) occurred at a similar titration point. This red shift in the absorption spectrum has been paralleled by the occurrence of antiferromagnetic coupling in the corresponding EPR spectra of Co(II)-MT, signifying that a cluster structure, i.e., the formation of thiolate bridges, sets in. By analogy with these studies the red shift in the Cd-thiolate absorption profile was attributed to the transformation of certain singly coordinated terminal thiolate ligands in $CdCys_4$ units into two-fold coordinated bridging μ_2-S-Cys ligands in the cluster structure of Cd_7MT [43]. Although the electronic basis of the red shift in this and other metal MT derivatives remains to be established, it most likely reflects a reduction of the actual electronegativity of the thiolate sulfur when μ_2-S-Cys bridges are formed.

The molar absorptivity of the 250 nm shoulder in Cd-MTs has also been used to estimate the number of cysteine ligands involved in metal binding, considering a molar extinction coefficient per cysteine ligand of about 5–6'000 M^{-1} cm^{-1}. This value has been derived from the changes in molar absorptivity at about 250 nm in a number of cadmium-substituted metalloproteins containing a varying number of cysteine ligands [48]. However, since in many newly discovered MTs aromatic amino acids and histidine are present, a difference absorption spectrum Cd-MT *versus* apoMT should be utilized. Note also that while protonated cysteines only contribute to the tailing of amide and carboxylate transitions of apoMT starting at about 230 nm, a fully deprotonated free cysteine amino acid (pK_a 8.3) shows a pronounced π–σ^* absorption band at 235 nm with a molar absorptivity of 3′200 M^{-1} cm^{-1} [49].

The CD spectrum of mammalian Cd_7MT to the red of the peptide CD bands at 215 nm (CD bands are also denoted as Cotton effects) has been proposed to arise from the peptide-induced asymmetry of the binding sites and from chirality brought about by interactions of asymmetrically oriented transition dipole moments of similar chromophores (bridging thiolate ligands) within the cluster structure.

The latter effect, known as the exciton splitting, is giving rise to a biphasic CD profile of fully metal-loaded Cd_7MT [50]. In Cd_7MT both chirooptical effects are best illustrated by changes in the CD profile observed in the cluster formation process (Figure 3).

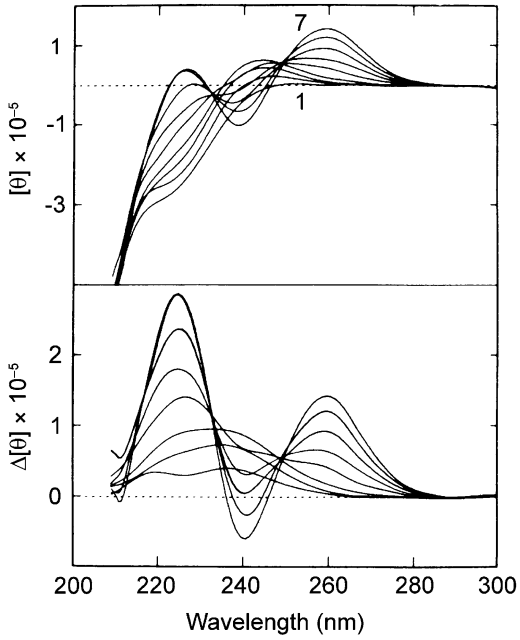

Figure 3 Top: Effect of increasing Cd(II) binding, i.e., addition of 1–7 equivalents, on the circular dichroism (CD) spectrum of apoMT from rabbit liver at pH 8.4. Bottom: Difference CD spectrum of Cd_7MT *versus* apoMT. The units are based on the protein concentration. Adapted from [43] with permission from the American Chemical Society; copyright 1987.

In contrast to the absorption studies, where the transformation of terminal to bridging thiolates resulted in a red shift of the absorption envelope, in the corresponding CD studies this structural transition is accompanied by a striking change of the originally monophasic to a biphasic CD profile with a cross-over point coinciding with the position of the first CysS–Cd(II) LMCT band within the absorption envelope (at 249 nm). Specifically, a broad positive CD band with a maximum centered at about 243 nm, originating from the asymmetry of the binding sites, changes to a CD profile characterized by two oppositely signed CD bands at about (–)240 and (+)260 nm. The biphasic profile has been assigned to an exciton coupling of the manifold of linearly polarized transition dipole moments located at bridging thiolate ligands in the clusters (Figure 3, bottom) [51]. In general, when two or more chromophores are brought to close proximity, where orbital overlap and electron exchange are negligible, they may interact through dipole-dipole coupling of their locally excited states to produce delocalized excitation (exciton) and a splitting (exciton splitting) of the locally excited states (Figure 4) [52].

In the CD spectra such an interaction shows exciton splitting characterized by two oppositely-signed CD bands flanking the relevant absorption band. It may be

noted that the exciton splitting is responsible for the typical biphasic CD profile centered at 260 nm of oligomeric nucleic bases and DNA [53]. The presence of exciton splitting in the CD spectra of mammalian Cd_7MTs and other Cd-MTs has been taken as evidence for the presence of a cluster structure. However, its absence in a Cd-MT cannot exclude a cluster structure, as the exciton splitting depends on interchromophoric distances and their mutual orientation. In theory, the rotational strength should have maximum intensity when the dihedral angle between the chromophores is approximately 45° but zero intensity when they are parallel or perpendicular [53].

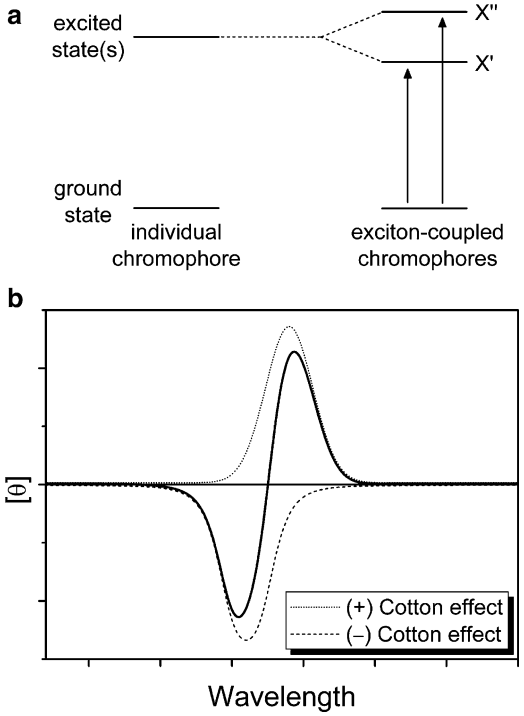

Figure 4 Exciton coupling: (**a**) Two non-degenerate excited states X' and X", termed excitonic states, result from the interaction of two chromophores. Transitions to these excitonic states are excited to different extents by right- and left-circularly polarized light [52]. (**b**) The resulting positive (dotted curve) and negative (dashed curve) peaks or Cotton effects result in a biphasic CD spectrum (solid curve).

As discussed above, a number of recombinant Zn- and Cd-MTs from various species expressed as fusion proteins contained varying amounts of inorganic sulfide (S^{2-}) (up to 14 mole equiv) [27]. Compared to the absorption and CD spectra of Cd-MTs lacking S^{2-}, those with S^{2-} present in the cluster structure are characterized by a red shift of the absorption envelope with a shoulder at about 280 nm and a new CD band at the same wavelength [27]. Similar spectral features have also been reported for S^{2-} containing Zn(II)- or Cd(II)-phytochelatins [54,55]. The computer analysis of CD spectra of proteins between 240–180 nm is often used to determine their secondary structure elements such as the α-helix, β-sheet, and random coil. However, this method cannot be applied to M^{II}-MTs (M^{II} = Zn, Cd), due to the presence of strong optically active metal-induced transitions in this spectral

range [48]. However, the bands of metal-thiolate complexes do not overlap with the secondary amide bands of the polypeptide when similar analyses by FT-IR or Raman spectroscopy are carried out [56–60].

2.3 Magnetic Circular Dichroism Spectroscopy

In recent years, magnetic circular dichroism (MCD) added significantly to our knowledge of the electronic structure of a wide variety of biological molecules mainly heme proteins, non-heme iron proteins, and cobalt-substituted zinc proteins [61,62]. MCD arises if the external magnetic field influences the electronic states of a chromophore in such a way that right- and left-circularly polarized beams are differently absorbed. There are three types of MCD effects designated as the *A*-, *B*-, and *C*-terms (Figure 5).

The *A*-term arises in situations when there is a non-degenerate ground state and a degenerate excited state in the absence of an applied field. In the presence of a magnetic field the excited state undergoes Zeeman splitting into two optically active states that absorb left and right polarized light with equal intensity but of opposite sign. As a result, a symmetrical derivative signal with the crossover point at the maximum of the corresponding absorption band occurs. The *C*-term arises when the ground state is initially degenerate and is split by the applied magnetic field. However, as the electronic differential population of the ground state depends on the Boltzmann distribution, the *C*-term MCD spectra are temperature-dependent

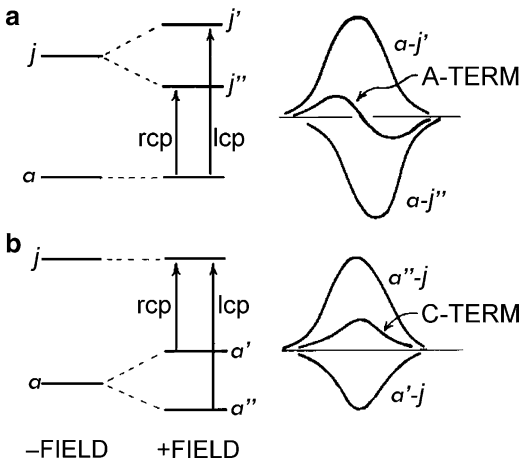

Figure 5 Origin of MCD *A*- and *C*-terms. In (**a**), Zeeman splitting of the excited state *j* by the magnetic field into *j'* and *j''* results in the two absorption curves for left and right circularly-polarized light *a*-*j* and *a*-*j'*. The resultant MCD curve is the biphasic *A*-term. In (**b**), the magnetic field splits the degenerate ground state into *a'* and *a''* resulting in the corresponding absorption bands. The net difference in this case is an MCD *C*-term of symmetrical line shape. Reprinted from [62] with permission from Elsevier; copyright 1986.

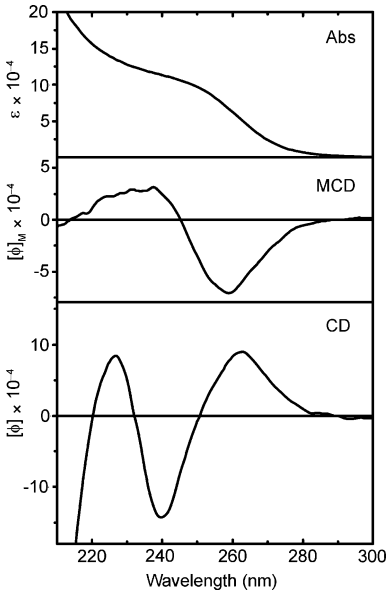

Figure 6 Electronic absorption (Abs), magnetic circular dichroism (MCD), and circular dichroism (CD) spectra of mouse Cd_7MT-1 at pH 8.0. Adapted from [72] with permission from the American Society for Biochemistry & Molecular Biology; copyright 2002.

and the spectral intensity will increase linearly as a function of 1/T. At high temperatures, the *C*-term MCD spectra show two oppositely signed bands of different intensity. When the temperature is low enough that the higher-energy sublevels are completely depopulated, the intensity of the MCD band originating from a degenerate ground state will be maximized and will show absorption band-shape. The *B*-term arises from induced-field mixing of neighboring states. It is temperature-independent and has absorption band shape.

The MCD spectra of proteins are rather insensitive to polypeptide conformation since the MCD signal for the peptide backbone amide transition at 225 nm is weak [63]. Since in Cd-MTs the ground state will be non-degenerate, only the *A*- and *B*-terms can be observed in the MCD spectrum. The MCD spectra of mammalian Cd_7MTs are dominated by a derivative MCD profile with a crossover point at 250 nm assigned to positive *A*-terms, i.e., a positive lobe to high energy of the crossover point, due to the presence of tetrahedral Cd(II)-thiolate units possessing degenerate excited LMCT states (Figure 6, middle) [64].

Figure 6 exemplifies the information content provided by each method. Thus, while the MCD spectra of Cd-MTs afford the information about the geometry of the binding sites (*A*-terms if tetrahedral CdS_4 units are present), the conformational changes accompanying the cluster formation and the presence of a cluster (exciton splitting) is provided by the CD studies. Combination of CD and MCD techniques has been used in a number of structural studies of Zn,Cd or Cd-MTs from different species [65–73].

2.4 X-Ray Absorption Spectroscopy

X-ray absorption spectroscopy (XAS) provides information about the chemical nature and environment of atoms in molecules. Since this technique is selective for a short-range order, the local structural information around the element of interest can be obtained even from disordered samples, such as powders and solution. X-ray absorption spectra are characterized by sharp increases in absorption at specific X-ray photon energies, which are characteristic of the absorbing element (Figure 7a). These sudden increases in absorption are called absorption edges (named for shells of the Bohr atom, i.e., K edges for $n = 1$; L edges for $n = 2$, etc.), and correspond to the energy required to eject a core electron

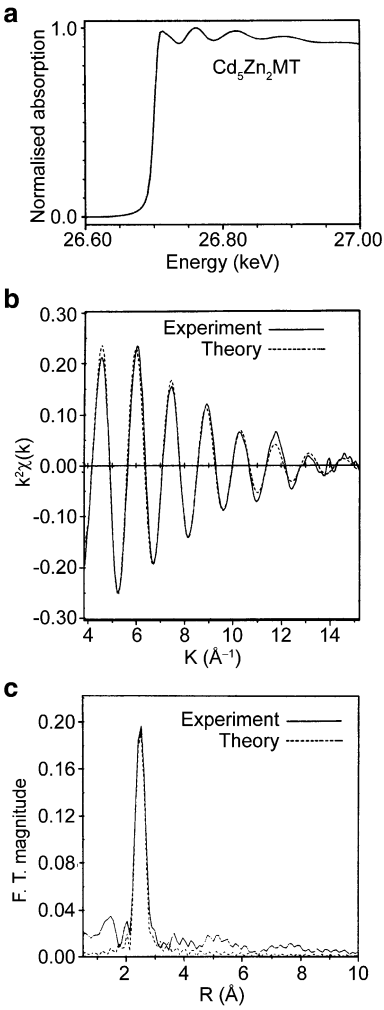

Figure 7 (**a**) Cd K-edge X-ray absorption spectrum of rat liver Cd_5Zn_2MT-1. (**b**) Cd K-edge EXAFS (solid line) and a theoretical simulation (dashed line) with 4 Cd–S distances at 2.53 Å and a Debye-Waller term, σ^2, of 0.006 Å^2 and (**c**) its Fourier transform. Adapted from [76] with permission from Birkhäuser Verlag/Springer; copyright 1987.

of the metal into the excited electronic state (LUMO) or to the continuum thus producing a photoelectron. The former is known as X-ray absorption near-edge structure (XANES), and the latter as extended X-ray absorption fine structure (EXAFS) which studies the fine structure in the absorption at energies greater than the threshold for electron release. These two methods give complementary structural information, the XANES spectra reporting electronic structure and symmetry of the metal site, and EXAFS reporting numbers, types, and distances to ligands and neighboring atoms confined to a radius of up to 8 Å from the absorbing metal ion [74,75].

The majority of XAS investigations of MTs has been conducted on metalloforms containing the physiologically relevant Zn(II) and Cu(I) ions. Early XAS studies on the Cd(II)-containing vertebrate MTs have been carried out prior to knowledge of their 3D structures. The Cd *K*-edge EXAFS studies of rat liver Cd_5Zn_2MT-1 and reconstituted Cd_7MT-1 represented the first biological molecules to be studied by this technique [76].

The EXAFS spectrum shown in Figure 7 established the exclusive Cd coordination to four sulfur atoms at the distance of 2.53 Å. A similar spectrum was also obtained for reconstituted Cd_7MT-1. It may be noted that in contrast to the EXAFS studies on Zn_7MT-1 no clear indication for a second-shell or metal-metal back scattering, diagnostic of a cluster structure, was seen for the Cd(II) metalloform. The reasons given for the absence of second shell Cd-Cd back scattering in Cd_7MT include (i) difficulties in obtaining high quality EXAFS data with wave vectors >15 Å^{-1} which are required to unambiguously establish second shell backscattering, (ii) photoelectron lifetime broadening which smears out the scattering information, and (iii) well established fluxionality of the metal-thiolate bonds in the clusters of MTs and in corresponding inorganic adamantane-like models which is expected to result in dynamic disorder sufficiently large to preclude the observation of mean Cd-Cd distances [76].

Rather recently the XANES and EXAFS data obtained on the structurally well-characterized mammalian Cd_7MTs and their protein domains in combination with the classical molecular mechanics/molecular dynamics (MM/MD) modeling have been used to determine the high resolution metal binding site geometry in these proteins [77].

2.5 *Perturbed Angular Correlation of γ-Rays Spectroscopy*

Information concerning the coordination geometry and dynamics of metal-binding sites in proteins can be obtained from perturbed angular correlation of γ-rays (PAC) spectroscopy. The underlying theory of this nuclear spectroscopic method is described in detail in [78] and with special emphasis on biological applications in [79,80]. PAC provides means to determine the nuclear quadrupole interaction at the site of an appropriate nucleus used as a spectroscopic probe. The nuclear quadrupole interaction (NQI) describes the interaction between the electric quadrupole moment

of the nucleus and the electric field gradient tensor of its coordination environment. PAC requires an isotope that decays emitting two γ-rays in succession. One of the best suited excited nuclei for such purposes is the 49-min isomer of the isotope ^{111}Cd, i.e., metastable ^{111m}Cd, which is generated by bombardment of ^{108}Pd with alpha particles. This metastable ^{111m}Cd isomer decays to the ^{111}Cd ground state via an intermediate 85-ns state (Figure 8a).

The intermediate ^{111m}Cd level has a spin value of 5/2, which is split by the electric field gradient into three levels of different energy giving rise to successive emission of two γ-rays, γ_1 and γ_2, in different directions (Figure 8b). Both γ-rays are related to each other by an angular correlation function $W(\theta, t)$, where θ is the angle between γ_1 and γ_2 and t is the delay time of γ_1 with respect to γ_2. However, if the nucleus is under influence of external forces, e.g., coordinating ligands, during the time between the emissions of two γ-rays, this 'angular correlation' is perturbed giving rise to oscillation in the directionality of emission of the two γ-rays of the cascade (Figure 8c). The PAC spectrum of ^{111m}Cd-labeled Cd_7MT from rabbit liver is shown in Figure 9 (top).

The Cd_7MT sample was prepared using trace amounts (10^{-13} mole) of freshly prepared carrier-free ^{111m}Cd(II) which was mixed at low pH with seven mole equiv of 'cold' Cd(II) and apoMT prior to adjustment to neutral pH. From least-squares fits of the coincident counting $W(180°, t)/W(90°, t)$ ratios of the PAC spectrum, the NQI parameters related to the coordinating ligands as well as their position were determined. As shown in Figure 9 (bottom), two frequency components $\omega_1 = 120$ MHz and $\omega_2 = 580$ MHz with amplitudes of 80% and 20%, respectively, have been resolved in the spectrum of ^{111m}Cd-labeled Cd_7MT. Since pure T_d or O_h symmetries produce a PAC spectrum lacking NQI, the observed vastly different frequencies indicated a distortion from either symmetry. The predominant component ($\omega_1 = 120$ MHz) has been attributed to the distorted tetrahedral CdS_4

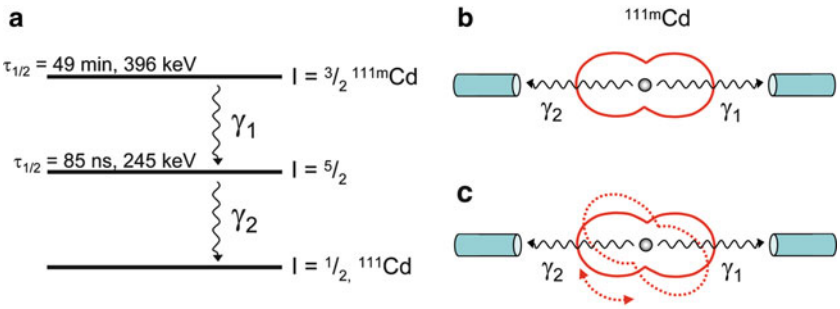

Figure 8 (**a**) The radioactive nucleus ^{111m}Cd is used in PAC spectroscopy as it emits two γ-rays in succession decaying to the stable isotope ^{111}Cd. Spin values and half-life of states as well as the energy of the emitted γ-rays are given. (**b**) The emission of the second γ-ray is anisotropic, i.e., there is an angular correlation between the two γ-rays. The coincidence count rate is illustrated by a red line. (**c**) Upon interaction of the nucleus with its coordination environment this angular correlation is perturbed (red dotted line) providing information about the local structure and its dynamics.

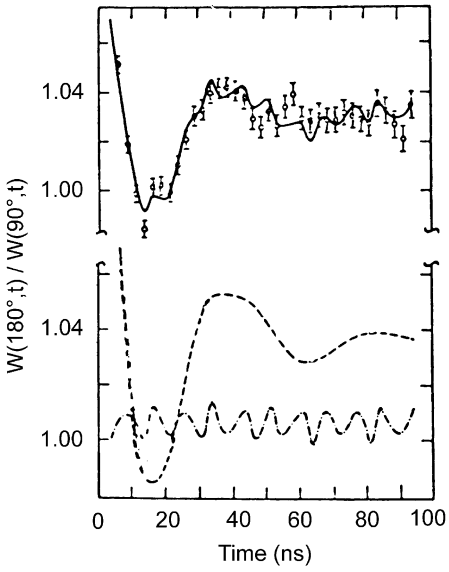

Figure 9 **Top**: Perturbed angular correlation of γ-rays (PAC) spectrum of ^{111m}Cd-labeled Cd_7MT from rabbit liver in 65% sucrose solution at 0 °C, pH 8.0. W(180°)/W (90°) is plotted *versus* delay time. The fully drawn curve represents least-squares fit to the spectrum. The bars indicate ±1 standard deviation. The viscosity of the sucrose solution immobilized the protein within the time scale of the experiment. **Bottom**: Resolution of the least-square fit of the spectrum into a low frequency, $\omega_1 = 116$ MHz (dashed line) and a high frequency component; $\omega_2 = 579$ MHz (stippled line). Adapted from [81] with permission from the American Chemical Society, copyright 1982.

unit in the metal-thiolate clusters and its damping to dynamic processes brought about by charge fluctuations in the immediate vicinity of ^{111m}Cd. As a square-planar CdS_4^{2-} complex would exhibit a frequency of about 880 MHz, the 580-MHz frequency has been attributed to site(s) with a highly distorted tetrahedral geometry [81]. Thus, both structural and dynamic features can be derived from the PAC spectra [82].

Since nanomole quantities are sufficient in data sampling, the PAC technique using ^{111m}Cd has also been applied to living cadmium-resistant cells. The results revealed that > 66% of Cd in the resistant strains was bound to MT, and that MT is apparently freely suspended in the cell cytoplasm [83].

2.6 Mass Spectrometry

Electrospray ionization (ESI) mass spectrometry (MS) and matrix assisted laser desorption ionization (MALDI) have emerged recently as a powerful and sensitive methods for the detection and structural analysis of a wide variety of analytes, including large biomolecules such as nucleic acids and proteins. ESI-MS is a gentle method of ionization based on protonation of the sample at atmospheric pressure. The protonation of multiple basic sites in protein molecules results in multiply

charged ions in the mass spectrum. The mass of the protein can then be calculated, by a process known as deconvolution, according to the formula $m/z = (M + nH^+)/n$, where M is the molecular mass of the protein and n is the number of protons associated with it. The soft nature of ion generation in ESI-MS not only avoids protein fragmentation upon transition to the gas phase, but it often preserves weak non-covalent complexes thus allowing the compositions and binding stoichiometries of metal-protein complexes to be established directly. In comparison, MALDI-MS has been shown to be highly suitable for the mass measurements of protein samples but it has been less successful in the analysis of non-covalent complexes because of the sample preparation method commonly used prior to measurements [84,85].

The capabilities of ESI-MS in studying metal-protein complexes were first recognized in the early 1990s when this technique was successfully applied to investigate the metal binding properties of Zn_7- and Cd_7MT-2a species from rabbit liver [86]. Since then ESI-MS has been widely used in the studies of various metalloforms of other MTs and metalloproteins *per se*. The successful analysis of metal-protein complexes requires preservation of the native state of the protein in solution that is typically accomplished by use of a buffered solution at neutral pH. Since common buffers used in protein isolation as well as high salt concentrations can complicate the ESI mass spectra, the volatile buffers at pH 6–8 ammonium acetate and ammonium hydrogen carbonate are most commonly used. Furthermore, non-native conditions that ensure partial or full unfolding of proteins and their extensive protonation usually involve typically the solvents acetonitrile or methanol acidified with 1% acetic acid or 0.1% formic acid. Under these acidic conditions ESI-MS spectra of metal-free proteins, e.g., apoMT, are obtained.

With the introduction of recombinant technology in MT research, the comparison between calculated and experimentally obtained masses of the desired protein has been routinely used in confirming the correctness of MT expression. ESI-MS has also been used to determine the stoichiometry of the metal-MT complexes obtained upon their expression in metal supplemented media and/or upon apoMT reconstitution with a desired metal ion. The cadmium binding capacity of MTs from widely different species including human, rabbit, rat, crustacean, earthworm, mollusc, algal, plants, and bacteria has been studied [17,86–95]. This method has also been used to demonstrate the presence of inorganic sulfide in the cluster structure of various recombinant Cd-containing MTs [27].

As mentioned above in the commonly used positive ion mode the protein protonation gives rise to protein ion charge state distributions. Charge state distributions of protein ions in ESI mass spectra can be used to evaluate protein compactness in solution [84,85]. Under near-native conditions folded proteins give rise to ions carrying a relatively small number of charges, as their compact shape in solution does not allow a significant number of protons to be accommodated on the surface upon transition from solution to the gas phase. Under non-native conditions the presence of partially or fully unfolded protein conformers gives rise to ions carrying a significantly larger number of charges, as many more protons can be accommodated on the surface of a protein once its compactness is lost. In case of MTs, a comparison between charge state distributions of the zinc and cadmium

metalloforms was used to learn more about the conformational states and thus the compactness of these structures. While for human Cd_7MT-3 nearly exclusively the higher +6 charge state was observed, the spectrum of Zn_7MT-3 shows both, the +6 and +5 charge state, with a slightly higher amount of the latter. From this finding it has been concluded that the protein filled with Cd(II) has a more open conformation than that filled with Zn(II).

Similar analysis of spectra taken during the stepwise addition of metal ions to the apo-forms additionally showed that the β-domain rather than the α-domain has the more open conformation. This is in marked contrast to the analogous experiments performed with rabbit MT-1 where no differences in charge state distribution between the two metalloforms were found [96]. Similar studies on wheat metallothionein $Zn_4\beta_E$-E_c-1 and $Cd_4\beta_E$-E_c-1 revealed that while both spectra were dominated by species with charge states of +4, the spectrum of $Zn_4\beta_E$-E_c-1 showed in addition the +5 charge state and that of $Cd_4\beta_E$-E_c-1 also a considerable population of the +3 charge state (Figure 10). These differences in charge distributions have been interpreted in terms of conformational differences between these species, with the $Cd_4\beta_E$-E_c-1 structure being more compact than that of $Zn_4\beta_E$-E_c-1. The observed conformational differences between the cadmium and zinc metalloforms are opposite of what would be expected considering the larger ionic radius of Cd(II) and contrast the findings for human MT-3 discussed above, providing that both types of metal ions form similar cluster structures in β_E-E_c-1 [95].

Apart from the characterization of isolated or metal-reconstituted MTs, ESI-MS also allows the direct observation of partially metalated MT species during metal uptake, metal release or metal exchange. Early optical and chirooptical (CD) studies of mammalian Cd_7MTs revealed that the formation of metal-thiolate clusters is non-cooperative when carried out at pH 8.4 [43] (see Section 2.2 and Figure 3). At neutral pH or upon partial Cd_7MT demetalation at pH 3.5, however, early ESI-MS studies indicated a largely cooperative cluster formation [86,87]. In the ESI-MS studies virtually no complexes with 1–3 bound Cd(II) ions were detected; however, with six Cd(II) added besides the Cd_7MT form mass peaks corresponding to Cd_5MT and Cd_6MT did also appear in the spectra. In a non-cooperative mechanism metal binding intermediates prior to the cluster formation are seen. In a positive fully cooperative mechanism of metal binding both apoMT and a clustered form coexist, i.e., there is an increasing binding affinity for each additional binding site. The cooperative mechanism for the formation of both clusters in rat liver MT was for the first time established using an experiment where the stepwise titration of rat apoMT with Cd(II) ions was followed by proteolytic digestion with subtilisin [97]. While apoMT or MT with only partially filled clusters is digested, filled clusters and the completely metal-loaded full-length protein are protected against proteolytic cleavage of the backbone. After addition of two Cd(II) mole equiv to rat apoMT at neutral pH and subtilisin treatment the fully metal-loaded 4-metal cluster domain was isolated in 50% yield with respect to the amount of initially used apo-protein. Likewise, when five Cd(II) mole equiv were used then 30% of the molecules were identified as Cd_7MT with the remainder being the 4-metal cluster domain, suggesting the subsequent cooperative formation of the 3-metal cluster.

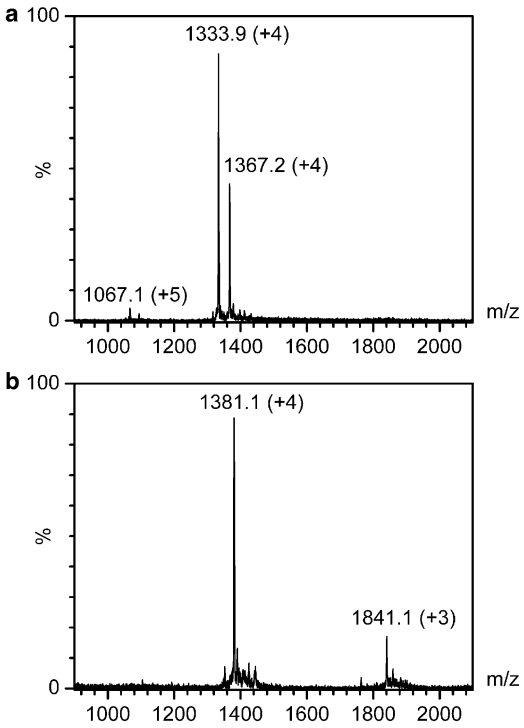

Figure 10 Non-deconvoluted ESI-MS spectra of (**a**) $Zn_4\beta_E$-E_c-1 and (**b**) $Cd_4\beta_E$-E_c-1 showing the different charge states. The signal at 1367.2 m/z in (a) originates from a species with unprocessed N-terminal methionine residue. Adapted from [95].

Insights into the process of MT metallation have been obtained from metal titration studies of rabbit apoMT followed by ^{113}Cd NMR, indicating that the pathway of the cluster formation in $^{113}Cd_7$MT-2 is a pH-dependent process [98]. Whereas at pH 7.2 the formation of both clusters is cooperative with the 4-metal cluster being formed first, at pH 8.6 the cluster structure was formed in a non-cooperative manner. This effect has been interpreted in terms of a different degree of deprotonation of the cysteine residues at both pH values with individual metal binding to the protein through four terminal cysteine ligands being energetically preferred at higher pH. At lower pH, where all Cys ligands are protonated, the formation of metal clusters by cooperative metal-binding over single metal-binding is preferred. As mentioned above, early ESI-MS studies revealed largely cooperative Cd(II) binding to human and rabbit MT-2 at neutral pH, or upon a partial Cd_7MT-2 demetalation, at pH 3.5 [86,87].

After about 20 years from the initial ESI-MS studies, a series of new ESI-MS investigations aiming at the mechanism of cadmium binding to human MT-1a and its α- and β-domains has been initiated. The results obtained at the pH values 9.4, 8.0 and 8.4, respectively, corroborate the non-cooperative mechanism observed in the CD studies (see above) with all individual metal-binding stoichiometries detected in course of the filling up process. In addition, the binding of eight metals has been observed [99,100]. Even though the number of literature reports regarding metalation of mammalian MTs is steadily increasing, detailed ESI-MS studies on

Cd(II) binding to apoMT as a function of pH are lacking. In other ESI-MS studies, contradictory metal-binding properties of human MT-3, also known as the neuronal growth inhibitory factor (GIF), have been reported. On the one hand, the direct metalation of apoMT-3 in 5 mM ammonium acetate buffer (pH 7.5) revealed that the reconstituted M_7MT-3 form (M = Zn(II), Cd(II)) is present in a dynamic equilibrium of different metalloforms. Besides the prevalent metalloform M_7MT-3 additional metalloforms with five to nine M(II) coexist [96]. On the other hand, the same M_7MT-3 metalloforms reconstituted using the standard procedure [28] showed only a single mass peak of monomeric M_7MT-3 [68,101].

The technique behind ESI-MS leads to the promotion of initially electrostatic interactions in the gas phase, whereas hydrophobic interactions are weakened. In this context it may be noted that compared to the overall –1 charge of recombinant mammalian M_7MT-1 that of M_7MT-3 is –9. *In vivo* protein folding and metal binding occur in the presence of 0.1 M intracellular salt concentrations to allow for charge compensation. Accordingly, a substantial ionic strength is also provided during the standard reconstitution method of MTs [28]. It is therefore likely that in the case of the M_7MT-3 structure generated under conditions of mass spectrometry, i.e., the ionic strength of solely 5 mM ammonium acetate buffer, no thermodynamic minimum was reached and hence a multitude of differently metalated species was observed.

At present, the assumption that the species observed in the gas phase are related to the speciation in solution is still the subject of hot debate. Although in some cases non-covalent bonding can be maintained sufficiently for ESI-MS characterization of the solution structure of non-covalent protein complexes, the new gaseous environment can ultimately cause dramatic structural alterations. Based on a variety of ESI-MS studies, in part in combination with molecular dynamics simulations, the temporal evolution, i.e., from 10^{-12} to 10^{2} s, of native protein structures during and after transfer into the gas phase can involve side-chain collapse, unfolding, and refolding into new, non-native structures [102]. As discussed above, the formation of a well-defined MT structure from the largely disordered structure of the apoprotein is dictated by protein-metal interactions. This signifies that protein electrostatics play an important role in the folding process. Consequently, careful control of individual experimental factors appears to be critical in obtaining reliable data on non-covalent metal-MT complexes in the gas phase.

3 Binding Affinity and Reactivity

3.1 Metal Binding Affinities

A variety of metal ions has been reported to bind to MT *in vivo* and *in vitro*. The cadmium metalloform has not only been found naturally but its generation *in vitro* has been proved indispensable in structural studies. In all Cd-MTs studied so far Cd(II) is tetrahedrally coordinated by solely Cys or both Cys and His ligands.

At neutral pH closely similar average apparent stability constants in the order of 10^{14} M^{-1} have been determined for various Cd-MTs with sole cysteine thiolate coordination by different methods.

Most widely used methods are based on (i) the competition of protons with the bound metal ions for thiolate ligands, i.e., the pH stability of the metal-thiolate clusters or (ii) the competition with a metal chelator. In the former case the pH stability of the Cd-thiolate clusters is followed by absorption spectroscopy of the CysS–Cd(II) LMCT band at 250 nm. From the apparent pK_a values the apparent stability constants of the clusters can be derived [103]. The apparent pK_a values are determined either by taking the pH values of half-maximum absorbance or using a non-linear curve fit of the pH plot [104]. The other method is based on the competition for a single metal ion between the chelator 5F-BAPTA (1,2-bis-(2-amino-5-fluorophenoxy)ethane-*N*,*N*,*N*',*N*'-tetraacetic acid) and the protein followed by ^{19}F NMR spectroscopy [71]. Although this method was established for the zinc metalloforms of MTs, its applicability to cadmium metalloforms has also been demonstrated [105]. In this case, by analogy with zinc finger proteins a lower affinity for mixed Cys/His coordination of Cd(II) in MTs compared to sole Cys coordination has been shown.

3.2 Structure Dynamics and Metal Exchange Processes

The mobility of the protein backbone structure enfolding the metal core in vertebrate MTs is well documented. Both the calculated RMSD values from NMR data [37] and the crystallographic B-factors [106] of Cd-containing rat liver Zn_2Cd_5MT-2 indicate that a considerable degree of dynamic structural disorder exists. More direct evidence for the non-rigid nature of the MT structure comes from the ^{1}H NMR ^{1}H-^{2}H amide exchange studies of Cd_7MT-1/-2 [39,107]. In these studies, the enhanced flexibility of the less structurally constrained β-domain compared to the α-domain in both isoforms has been demonstrated. A similar conclusion has also been drawn from the ^{15}N relaxation measurements of mouse Cd_7MT-3 and sea urchin Cd_7MTA [35,36]. Molecular dynamics simulations of the β-domain of rat liver Cd_7MT-2 in aqueous solution also show that the polypeptide loops between cysteine ligands exhibit an extraordinary flexibility without disrupting the geometry of the 3-metal cluster [108]. In the structural NMR studies of the C-terminal β_E-domain of the wheat MT E_c-1, encompassing a mononuclear Cys_2His_2 site and a $M_3^{II}Cys_9$ cluster, similar backbone dynamics of the Zn(II) and Cd(II) metalloforms were seen by ^{15}N relaxation experiments [19].

Apart from the conformational flexibility of the polypeptide chain, dynamic processes within the metal-thiolate clusters have also been recognized. The best evidence for metal fluxionality in Cd_7MT was provided by ^{113}Cd NMR saturation transfer experiments, which established the presence of inter- and/or intramolecular metal exchange within the 3-metal cluster of the β-domain with a half-life of the order of 0.5 s ([109], and refs cited therein). The confirmation of similar processes taking place within the 4-metal cluster, but with a half-life of about 16 minutes,

was afforded by metal exchange studies using the radioactive ^{109}Cd isotope. In this context it should be noted that the intersite cadmium exchange measured in the 3-metal cluster of Cd_7MT-1 was found to be much faster than that in Cd_7MT-2. This finding was in line with the enhanced backbone flexibility recognized in the NMR studies of the former isoform [39]. Thus, despite the high thermodynamic stability of the metal-thiolate MT complexes, the metal sites in non-rigid MT structures are kinetically very labile, i.e., the thiolate ligands undergo both metalation and demetalation rapidly. Although the mechanism underlying this process is not yet understood, a rapid metalation and demetalation of the thiolate ligands must be accompanied by substantial changes in the tertiary structure of the protein. For inorganic complexes the correlation between the ligand properties and complex lability revealed that decreasing ligand rigidity, or ligand preorganization, results in an increasing complex lability [110]. Accordingly, MTs with their large number of cysteine thiolates can be regarded as multidentate ligands resembling chelating inorganic ligands with long bridges, for which a low level of ligand preorganization and hence a high kinetic lability has been shown.

Mammalian Zn_7MT-3 represents the only isoform for which biological activity has been found [13]. In contrast to the Cd_7MT-1/MT-2 isoforms, evidence for unprecedented dynamic processes within the metal-thiolate clusters of the Cd-reconstituted human $^{113}Cd_7$MT-3 was obtained from ^{113}Cd NMR studies [38]. From significant broadening of all ^{113}Cd signals and the very low and temperature-independent intensity of the 3-metal cluster resonances the presence of two dynamic events acting on two different ^{113}Cd NMR time-scales has been suggested: (i) Fast-exchange processes among conformational cluster substates and (ii) very slow exchange processes between configurational cluster substates in the β-domain encompassing the 3-metal cluster [111]. The changes in conformational substates may be visualized as minor dynamic fluctuations of the metal coordination environment and those of the configurational substates as major structural alterations brought about by temporarily breaking and reforming of the metal-thiolate bonds. The existence of interchanging configurational cluster substates of comparable stability have already been demonstrated for inorganic adamantane-like metal-thiolate clusters with the general formula $[M_4(SC_6H_5)_{10}]^{2-}$ (M is Cd(II), Zn(II), Co(II), and Fe(II)) [112].

A comparison of the primary structure of the different mammalian MTs (Table 1) reveals that only the biologically active MT-3 contains the C_6PCP_9 motif in the β-domain, a feature essential for the neuroinhibitory activity of this isoform [13]. To account for slow dynamic events centered at the 3-metal cluster of MT-3, a partial unfolding of the β-domain, whose kinetics could be determined by the *cis*/*trans* interconversion of Cys-Pro amide bonds in the C_6PCP_9 motif, has been suggested [71]. Support for the proposed *cis*/*trans* interconversion of Cys-Pro amide bonds came from the simulation of the partial unfolding of the β-domain of Cd_7MT-3 [113] and from the absence of slow 3-metal cluster dynamics in ^{113}Cd NMR studies of $^{113}Cd_7$MT-3, in which the unique C_6PCP_9 motif was mutated to the C_6SCA_9 sequence found in human MT-2 (Table 1) [71]. As revealed by independent neuronal cell culture studies, the MT-3 mutation abolished its biological activity. It has been concluded, therefore, that both the specific structural

features and the structure dynamics are necessary prerequisites for the extracellular biological activity of Zn_7MT-3.

3.3 Cluster Reactivity

Studies on ligand substitution reactivity conducted on vertebrate Cd_7MT and lobster Cd_6MT have revealed biphasic kinetics and differential reactivity of the two metal clusters. With ethylenediamine-*N*,*N*,*N*',*N*'-tetraacetate (EDTA) the ligand interacts preferentially and cooperatively with Cd(II) ions in the β-domain cluster of mammalian Cd_7MT-2, $\beta > \alpha$ [114], and, in opposite order $\alpha > \beta$ with nitrilotriacetate (NTA) [115]. Since observed rate constants for the reaction with EDTA were sensitive to protein concentration, it has been suggested that the monomer-dimer equilibrium of the protein controls its kinetic reactivity with EDTA. In addition, since bi- and tetradentate ligands such as ethylenediamine and triethylenetetramine were found to be ineffective even at thermodynamically competent concentrations, it has been suggested that a tripod configuration of ligands is required in ligand substitution and that only specific regions of the protein domains may provide easy access to the metal clusters [116].

The reactivity of the thiol groups in MT has also been investigated. In metal-thiolate clusters these groups retain a substantial degree of the nucleophilicity seen with the metal-free protein. This property is reflected by the extremely high reactivity of the coordinated Cys side chains with alkylating and oxidizing agents such as iodoacetamide or 5,5'-dithiobis-(2-nitrobenzoic acid) (DTNB), respectively [117,118]. Another interesting aspect of MT reactivity is its ability to react with radical species. Thus, it has been shown that mammalian M_7MT (M = Zn(II) and/or Cd(II)) are efficient scavengers of free radicals such as hydroxyl ($OH^{\cdot}$), superoxide ($O_2^{\cdot -}$) [119,120] or nitric oxide (NO) [121,122]. In all cases, the free radicals attack occurs at the metal-bound thiolates, leading to protein oxidation and/or modification and subsequent metal release. While $OH^{\cdot}$ radicals show no selectivity, NO reacts preferentially with thiolate ligands of the β-domain of Cd_7MT-1. Interestingly, in many instances these effects could be reversed under reductive conditions and the presence of the appropriate metal ion.

4 Three-Dimensional Structures

Owing to their small size, mammalian MTs were among the first proteins structurally characterized by NMR spectroscopy and actually the first metalloproteins studied with this method. A major challenge in the determination of MT structures is the assignment of the correct metal-thiolate connectivities. Here, the use of the NMR-active ^{111}Cd or ^{113}Cd nuclei bound to the protein instead of the spectroscopically silent Zn(II) ions proved to be an invaluable tool (for details

regarding the application of ^{111}Cd or ^{113}Cd NMR to the structural studies of metalloproteins see Chapter 6 in this volume).

The first MT analyzed was rabbit liver MT-2. Natively bound Zn(II) ions were replaced *in vitro* with ^{113}Cd(II) [123]. Proton decoupled one-dimensional ^{113}Cd NMR spectra showed signals with chemical shifts >600 ppm, which are characteristic for Cd(II) ions in tetrahedral tetrathiolate environments. The signals were split into multiplets due to ^{113}Cd-^{113}Cd spin coupling and hence already provided indications for the presence of metal clustering. Homonuclear decoupling experiments were used to identify sets of spin-coupled ^{113}Cd(II) ions and helped to reveal the presence of two separate polynuclear clusters in mammalian MTs, one containing three (cluster B or β-cluster) and the other one four metal ions (cluster A or α-cluster). With the help of proteolytic digestion the α-cluster was located in the C-terminal half of the protein [124]. In addition, one-dimensional ^{113}Cd NMR spectra of the C-terminal fragment showed four signals. The chemical shifts of these signals coincide with four ^{113}Cd signals in the full-length protein and hence suggest that the α-cluster structures formed in the C-terminal fragment and in the full-length protein are identical [125]. Subsequent to assignment of the signals in the ^{1}H NMR spectrum [126], the polypeptide-metal cluster connectivities in rabbit liver MT-2 could be deciphered with at that time novel heteronuclear two-dimensional NMR experiments [127].

The advent of this method marked a major breakthrough in the determination of MT structures. In [^{113}Cd,^{1}H] correlation spectra the couplings between the Cys-H$^{\beta}$ protons and the bound ^{113}Cd ions were directly monitored and in this way allowed to identify the terminal and the bridging thiolate ligands, i.e., coupling of one H$^{\beta}$ proton with one or two ^{113}Cd nuclei, respectively. In the same publication, application of [^{113}Cd,^{113}Cd] COSY spectra clearly show the presence of a Cd_3 next to a Cd_4 cluster in the structure as proposed in the earlier work. Determination of the complete three-dimensional structure of the protein finally brought the common endeavor to an end roughly eight years after its start [32]. The comparison of the three-dimensional structure of rabbit liver MT-2 with the structure of rat liver MT-2 revealed closely similar folds of the polypeptide chains including identical metal-thiolate connectivities and hence suggested a common structure for all mammalian MTs [128]. Inconsistent with this finding, the sequence-specific metal-cysteine connectivities were distinctively different from those reported in the solid state structure of rat liver Zn_2Cd_5MT-2 also determined at that time [129]. However later, reevaluation of the solid state structure finally led to the same result as obtained with NMR spectroscopy in solution, finalizing a long debate [130].

In a similar way, ^{113}Cd NMR spectroscopy helped to determine the cluster structures present in crustaceans, i.e., two M_3S_9 clusters of the β-type [40,41,131], and echinodermata MTs [36,132]. In the latter MT family a M_3S_9 as well as a M_4S_{11} cluster are observed in analogy to the vertebrate MTs, however, their occurrence within the amino acid sequence is reversed, i.e., the trinuclear β-cluster is hosted by the C-terminal part of the protein while the tetranuclear α-cluster resides in the N-terminal part.

Albeit these success stories, the use of ^{113}Cd NMR to probe the geometry and metal-thiolate connectivities of the clusters found in MTs is not always straightforward. Generally, the β-domains of vertebrate MTs are less well defined and more flexible than the α-domains, but this effect is even more pronounced in the mammalian MT-3 forms. The ^{113}Cd resonances of the 3-metal cluster in the β-domain of mouse $^{113}Cd_7$MT-3 are broad and show low intensity, probably because of partial unfolding of the β-domain, and hence are of no avail [35]. As also the [^{113}Cd,^{1}H] HSQC spectra, determining the Cys-H$^{\beta}$-proton-to-metal connectivities, contained only very few cross-peaks, homology modeling based on published β-domain structures of mammalian Cd_7MTs was used to calculate a structural model of this domain in mouse Cd_7MT-3. Furthermore, the observation of chemical shift degeneracy in a few signals in the [^{113}Cd,^{1}H] HSQC spectra of the α-domain prevented the complete and unambiguous assignment of the coordinating Cys residues to all Cd(II) ions [35]. Hence also in this case additional theoretical calculations for the different possible connectivities were required. In the end, the lowest energy structure revealed the same metal-Cys connectivities already observed for the mammalian MT-1 and MT-2 isoforms. The subsequent structure determination of the α-domain of human $^{113}Cd_7$MT-3 by NMR revealed a closely similar structure to that of the mouse protein [38].

More recent structural studies on bacterial and plant MTs have shown that beside Cys also His residues can act as a ligand**.** The influence of His *versus* Cys ligands on the binding affinities towards Zn(II) and Cd(II) has been previously evaluated using a zinc finger peptide with a Cys_2His_2 metal binding site [133]. While the replacement of only one or both His ligands by Cys has a relatively small effect on the zinc affinity, each substitution increases the affinity of cadmium to this site by 2–3 log units. In a Cys_3His environment, the zinc and cadmium forms of the zinc finger peptide showed nearly equal association constants, but for Cys_2His_2 coordination the zinc form was more stable by 3 log units. Hence, it can be expected that the higher the number of His ligands at a given site, the more difficult it is to replace coordinated Zn(II) ions by Cd(II). The 55 amino acid residues long MT SmtA from the cyanobacteria *Synechococcus* PCC 7942 contains nine Cys and three His residues, but only two of the His residues serve as metal ligands. SmtA binds four Zn(II) ions in form of a $M_4S_9N_2$ cluster closely similar to the α-cluster of mammalian MTs (Figure 1d) [17]. This cluster contains two Cys_4 and two Cys_3His sites, whereby the His residues are exclusively present as terminal ligands.

The overall protein structures obtained for the Zn_4- and Cd_4-forms are closely similar with an RMSD value of 1.24 Å for the backbone atoms [134]. In contrast to mammalian MTs where hardly any secondary structure is present, the secondary structure elements in M_4SmtA include two short antiparallel β-sheets and an α-helix. These structural features around one metal ion constitute the zinc-finger portion of the protein. An inspection of the two-dimensional ^{1}H NMR data for both metalloforms, including the entire structure of Cd_4SmtA, lead to the conclusion that Cd(II) can be used as an isostructural replacement for Zn(II), although a slight expansion of the Cd_4SmtA structure due to the larger size of Cd(II) was seen.

The homometallic Cd_4SmtA species was prepared by the standard reconstitution procedure [28]. In mammalian MTs, the homometallic Cd_7MT can also be generated from the zinc- and cadmium/zinc-containing forms by exposure to an excess of Cd(II) at neutral pH. However, for Zn_4SmtA this is only partly successful. Metal exchange studies of Zn(II) in Zn_4SmtA with ^{113}Cd(II) revealed that the Zn(II) ion present in the zinc finger site is inert to exchange even under Cd(II) excess. Interestingly, the Zn(II) ion in this site is coordinated by four Cys residues and hence the inertness of this cation towards exchange contradicts expectation considering that the affinity of Cd(II) is higher to an isolated Cys_4 site than to a Cys_3His site. However, it has been shown in addition that this Zn(II) ion is also inert to exchange with the heavier ^{67}Zn(II) isotope based on studies with high resolution MS [135]. Accordingly, additional factors such as the local protein structure and the metal site accessibility have to play a role in the pronounced inertness of this site to metal exchange.

In the E_c-1 protein from wheat two highly conserved His residues are present in the 51 amino acids long C-terminal β_E-domain, with both residues being involved in the Zn(II) coordination [19]. Structure calculations revealed that the four metal ions in $Zn_4\beta_E$-E_c-1 are partitioned into a mononuclear $ZnCys_2His_2$ binding site (Figure 1a and Figure 11a) and a Zn_3Cys_9 cluster. Replacement of Zn(II) ions by Cd(II) to probe for the metal-Cys connectivities within the cluster structure gave NMR spectra that showed only minor differences in amide proton and nitrogen chemical shifts between the two metalloforms, indicating a very similar overall architecture of both forms. Nevertheless, the one-dimensional ^{113}Cd NMR spectrum of $Cd_4\beta_E$-E_c-1 revealed only three broad signals between 700–650 ppm, the specific chemical shift range for $CdCys_4$ sites. No ^{113}Cd signal at higher field indicative for a mixed His/Cys site was observed [95]. The observed broadening of the ^{113}Cd signals most likely originates from kinetic instability of the Cd_3Cys_9 cluster, i.e., the presence of dynamic exchange processes among multiple cluster conformations similar to those reported for the β-clusters of mammalian MT-3 forms [38,71]. In addition, also the [^{113}Cd,^{1}H] correlation spectra lacked interpretable signals and thus no information about the sequence specific metal-cysteine connectivities required for the determination of the Cd_3Cys_9 cluster structure was obtained. Consequently, the most likely M_3Cys_9 cluster structure in $M_4\beta_E$-E_c-1 was calculated using automated ^{1}H NOE assignments [19].

Generally, the poorly resolved NMR spectra obtained for the $Cd_4\beta_E$-E_c-1 form suggest that the β_E-domain of wheat E_c-1 with Cd(II) is not properly folded and hence that Cd(II) cannot be used as a spectroscopic probe for Zn(II) in $Zn_4\beta_E$-E_c-1 (Figure 11b) [19,136]. For the N-terminal γ-domain of wheat E_c-1, however, the suitability of Cd(II) to probe the coordination sphere of Zn(II) ions was again underlined. In this case [^{113}Cd,^{1}H] HSQC spectra clearly revealed the sequence specific Cd(II)-Cys connectivities in the Cd_2S_6 cluster, and both the Zn(II) and Cd(II) forms yielded well resolved spectra enabling successful structure calculations [18]. Overall, the structures of the Zn_2- and $Cd_2\gamma$-E_c-1 forms show only minor differences within the error limits (Figure 11c).

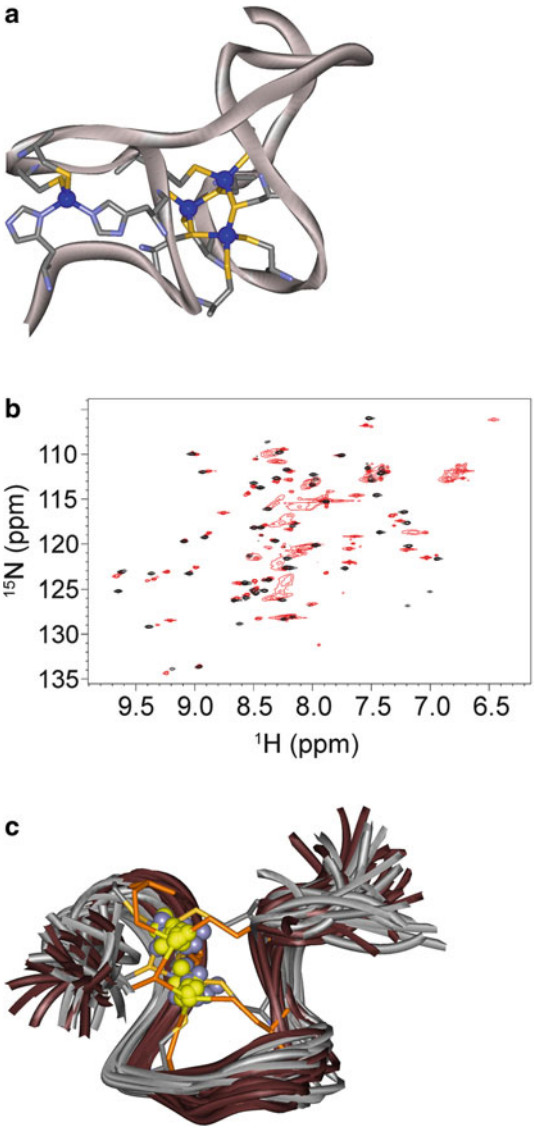

Figure 11 Example of the use of ^{113}Cd isotope in probing the metal binding sites in Zn-MTs by multinuclear NMR spectroscopy: (**a**) β_E-domain of wheat E_c-1 coordinating four Zn(II) ions. (**b**) Overlay of [^{15}N,^{1}H] HSQC spectra of $Zn_4\beta_E$-E_c-1 (black) and $Cd_4\beta_E$-E_c-1 (red) showing the severe peak broadening that hinders the structure determination of the Cd(II) substituted form. (**c**) Overlay of the 20 lowest energy structures of $Zn_2\gamma$-E_c-1 (grey, protein backbone; Cys residues as orange sticks; Zn(II) ions as light blue spheres) and $Cd_2\gamma$-E_c-1 (brown, protein backbone; Cys residues as dark orange sticks; Cd(II) ions as yellow spheres) revealing the close similarity of both structures (for details see text).

5 Concluding Remarks

Zinc, at levels of 2–3 g in adult humans, is next to iron the most prevalent and important "trace" element. In the human genome, about 10% of the genes encode zinc proteins exercising a wide range of function [137]. Zn-MTs represent the major intracellular zinc pool in many organisms. Besides Zn(II) ions, the presence of Cd(II) ions in this class of proteins is of biological relevance as various

MTs play a role in heavy metal detoxification *in vivo*. Because of the NMR-active ^{111}Cd and ^{113}Cd isotopes and, in a specific instance of the metastable ^{111m}Cd isotope, Cd(II) was and is still used extensively as a spectroscopic probe for the spectroscopically silent Zn(II) ions in metalloproteins.

In MTs, the studies of cadmium metalloforms by these and other spectroscopic techniques described in this review allowed to decipher the structural and chemical properties of Cd-MTs from various organisms. In light of the very low abundance of secondary structural elements in MTs such as α-helices and β-sheets, the structure determinations relied heavily on the study of the metal clusters, the core units of MT structures around which the peptide backbone is folded. Especially with the advent of new MT families, including cyanobacterial, nematode, and plant MTs, the use of Cd(II) in the spectroscopic/structural studies of these proteins continues to be of great importance.

The majority of methods making use of Cd(II) as a spectroscopic probe in proteins was pioneered for the study of MTs, but since then they have made their way very successfully into the general area of bioinorganic chemistry. For example, the knowledge gathered from Cd(II) spectroscopy helped to design, analyze, and understand metal binding sites within the hydrophobic core of artificial three-stranded coiled coils [138]. This approach was further advanced to the differentiation of rarely observed threefold coordinated Cd(II) ions from the more common fourfold-coordination geometries. It has become clear, and should be strengthened again, that the appropriate combination of different methods rather than sole application of a specific technique is invaluable for the critical examination of a given structural aspect.

Abbreviations

5F-BAPTA	1,2 -bis-(2-amino-5-fluorophenoxy)ethane-*N,N,N',N'*-tetraacetic acid
CD	circular dichroism
COSY	correlation spectroscopy
CTTS	charge-transfer-to-solvent
Cys	cysteine
DTNB	5,5'-dithiobis-(2-nitrobenzoic acid)
EDTA	ethylenediamine-*N,N,N',N'*-tetraacetate
EPR	electron spin resonance
ESI	electrospray ionization
EXAFS	extended X-ray absorption fine structure
FT-IR	Fourier transform infrared (spectroscopy)
GIF	growth inhibitory factor
GST	glutathione-S-transferase
His	histidine

HSQC	heteronuclear single quantum coherence
LLCT	ligand-to-ligand charge-transfer
LMCT	ligand-to-metal charge-transfer
LUMO	lowest unoccupied molecular orbital
MALDI	matrix assisted laser desorption ionisation
MCD	magnetic circular dichroism
MD	molecular dynamics
MM	molecular mechanics
MO	molecular orbital
MS	mass spectrometry
MT	metallothionein
NMR	nuclear magnetic resonance
NOE	nuclear Overhauser effect
NQI	nuclear quadrupole interaction
NTA	nitrilotriacetate
PAC	perturbed angular correlation
PDB	Protein Data Bank
RMSD	root-mean-square deviation
XANES	X-ray absorption near-edge structure
XAS	X-ray absorption spectroscopy

Acknowledgment Financial support by the Swiss National Science Foundation (SNSF Professorship PP002-119106/1 to E.F.) is gratefully acknowledged.

References

1. M. Margoshes, B. L. Vallee, *J. Am. Chem. Soc.* **1957**, *79*, 4813–4814.
2. T. W. Lane, M. A. Saito, G. N. George, I. J. Pickering, R. C. Prince, F. M. M. Morel, *Nature* **2005**, *435*, 42–42.
3. J. H. R. Kägi, A. Schäffer, *Biochemistry* **1988**, *27*, 8509–8515.
4. M. J. Stillman, *Coord. Chem. Rev.* **1995**, *144*, 461–511.
5. J. Hidalgo, M. Aschner, P. Zatta, M. Vašák, *Brain Res. Bull.* **2001**, *55*, 133–145.
6. A. K. West, J. Hidalgo, D. Eddins, E. D. Levin, M. Aschner, *Neurotoxicology* **2008**, *29*, 489–503.
7. M. Vašák, D. W. Hasler, *Curr. Opin. Chem. Biol.* **2000**, *4*, 177–183.
8. M. Vašák, N. Romero-Isart, in *Encyclopedia of Inorganic Chemistry,* 2nd ed, Ed. R. B. King, John Wiley & Sons Ltd, New York, 2005, pp. 3208–3221.
9. A. Krezel, Q. Hao, W. Maret, *Arch. Biochem. Biophys.* **2007**, *463*, 188–200.
10. G. Henkel, B. Krebs, *Chem. Rev.* **2004**, *104*, 801–824.
11. C. A. Blindauer, O. I. Leszczyszyn, *Nat. Prod. Rep.* **2010**, *27*, 720–741.
12. E. Freisinger, *Dalton Trans.* **2008**, 6663–6675.
13. M. Vašák, G. Meloni, *Met. Ions Life Sci.* **2009**, *5*, 319–351.
14. M. Vašák, G. Meloni, *J. Biol. Inorg. Chem.* **2011**, *16*, 1067–1078.
15. E. Freisinger, *J. Biol. Inorg. Chem.* **2011**, *16*, 1035–1045.
16. http://www.rcsb.org.

17. C. A. Blindauer, M. D. Harrison, J. A. Parkinson, A. K. Robinson, J. S. Cavet, N. J. Robinson, P. J. Sadler, *Proc. Natl. Acad. Sci. USA* **2001**, *98*, 9593–9598.
18. J. Loebus, E. A. Peroza, N. Blüthgen, T. Fox, W. Meyer-Klaucke, O. Zerbe, E. Freisinger, *J. Biol. Inorg. Chem.* **2011**, *16*, 683–694.
19. E. A. Peroza, R. Schmucki, P. Güntert, E. Freisinger, O. Zerbe, *J. Mol. Biol.* **2009**, *387*, 207–218.
20. V. Calderone, B. Dolderer, H. J. Hartmann, H. Echner, C. Luchinat, C. Del Bianco, S. Mangani, U. Weser, *Proc. Natl. Acad. Sci. USA* **2005**, *102*, 51–56.
21. C. W. Peterson, S. S. Narula, I. M. Armitage, *FEBS Lett.* **1996**, *379*, 85–93.
22. P. A. Cobine, R. T. McKay, K. Zangger, C. T. Dameron, I. M. Armitage, *Eur. J. Biochem.* **2004**, *271*, 4213–4221.
23. Ò. Palacios, S. Atrian, M. Capdevila, *J. Biol. Inorg. Chem.* **2011**, *16*, 991–1009.
24. M. Good, M. Vašák, *Biochemistry* **1986**, *25*, 3328–3334.
25. M. Vašák, J. H. R. Kägi, B. Holmquist, B. L. Vallee, *Biochemistry* **1981**, *20*, 6659–6664.
26. M. Vašák, J. H. R. Kägi, *Proc. Natl. Acad. Sci. USA* **1981**, *78*, 6709–6713.
27. M. Capdevila, J. Domenech, A. Pagani, L. Tio, L. Villarreal, S. Atrian, *Angew. Chem. Int. Ed.* **2005**, *44*, 4618–4622.
28. M. Vašák, *Methods Enzymol.* **1991**, *205*, 452–458.
29. T. K. Harris, G. J. Turner, *IUBMB Life* **2002**, *53*, 85–98.
30. M. M. Naor, J. H. Jensen, *Proteins* **2004**, *57*, 799–803.
31. W. Maret, Y. Li, *Chem. Rev.* **2009**, *109*, 4682–4707.
32. A. Arseniev, P. Schultze, E. Wörgötter, W. Braun, G. Wagner, M. Vašák, J. H. R. Kägi, K. Wüthrich, *J. Mol. Biol.* **1988**, *201*, 637–657.
33. C. Capasso, V. Carginale, O. Crescenzi, D. Di Maro, E. Parisi, R. Spadaccini, P. A. Temussi, *Structure* **2003**, *11*, 435–443.
34. B. A. Messerle, A. Schäffer, M. Vašák, J. H. R. Kägi, K. Wüthrich, *J. Mol. Biol.* **1990**, *214*, 765–779.
35. G. Öz, K. Zangger, I. M. Armitage, *Biochemistry* **2001**, *40*, 11433–11441.
36. R. Riek, B. Prêcheur, Y. Wang, E. A. Mackay, G. Wider, P. Güntert, A. Liu, J. H. R. Kägi, K. Wüthrich, *J. Mol. Biol.* **1999**, *291*, 417–428.
37. P. Schultze, E. Wörgötter, W. Braun, G. Wagner, M. Vašák, J. H. R. Kägi, K. Wüthrich, *J. Mol. Biol.* **1988**, *203*, 251–268.
38. H. Wang, Q. Zhang, B. Cai, H. Y. Li, K. H. Sze, Z. X. Huang, H. M. Wu, H. Z. Sun, *FEBS Lett.* **2006**, *580*, 795–800.
39. K. Zangger, G. Öz, J. D. Otvos, I. M. Armitage, *Protein Sci.* **1999**, *8*, 2630–2638.
40. A. Muñoz, F. H. Försterling, C. F. Shaw III, D. H. Petering, *J. Biol. Inorg. Chem.* **2002**, *7*, 713–724.
41. S. S. Narula, M. Brouwer, Y. Hua, I. M. Armitage, *Biochemistry* **1995**, *34*, 620–631.
42. J. D. Baleja, V. Thanabal, G. Wagner, *J. Biomol. NMR* **1997**, *10*, 397–401.
43. H. Willner, M. Vašák, J. H. R. Kägi, *Biochemistry* **1987**, *26*, 6287–6292.
44. C. K. Jørgensen, in *Progress in Inorganic Chemistry*, Ed S. J. Lippard, John Wiley & Sons, Inc., 1970, Vol. 12, pp. 101–158.
45. H. Willner, PhD Thesis, University of Zurich, 1987.
46. H.-J. Liu, J. T. Hupp, M. A. Ratner, *J. Phys. Chem.* **1996**, *100*, 12204–12213.
47. E. I. Solomon, S. I. Gorelsky, A. Dey, *J. Comp. Chem.* **2006**, *27*, 1415–1428.
48. C. J. Henehan, D. L. Pountney, O. Zerbe, M. Vašák, *Protein Sci.* **1993**, *2*, 1756–1764.
49. R. E. Benesch, R. Benesch, *J. Am. Chem. Soc.* **1955**, *77*, 5877–5881.
50. M. J. Stillman, in *Metallothioneins: Synthesis, Structure and Properties of Metallothioneins, Phytochelatins, and Metal-Thiolate Complexes*, Eds M. J. Stillman, C. F. Shaw III, K. T. Suzuki, VCH, New York, 1992, pp. 55–127.
51. H. Willner, W. R. Bernhard, J. H. R. Kägi, in *Metallothioneins: Synthesis, Structure and Properties of Metallothioneins, Phytochelatins, and Metal-Thiolate Complexes*, Eds M. J. Stillman, C. F. Shaw III, K. T. Suzuki, VCH, New York, 1992, pp. 128–143.

52. S. G. Telfer, T. M. McLean, M. R. Waterland, *Dalton Trans.* **2011**, *40*, 3097–3108.
53. N. Berova, K. Nakanishi, in *Circular Dichroism - Principles and Applications*, Eds N. Berova, K. Nakanishi, R. W. Woody, VCH Publishers Inc., New York, 1994, pp. 361–398.
54. C. T. Dameron, B. R. Smith, D. R. Winge, *J. Biol. Chem.* **1989**, *264*, 17355–17360.
55. A. Murasugi, C. Wada, Y. Hayashi, *J. Biochem.* **1981**, *90*, 1561–1564.
56. J. Pande, C. Pande, D. Gilg, M. Vašák, R. Callender, J. H. R. Kägi, *Biochemistry* **1986**, *25*, 5526–5532.
57. Y. B. Shi, J. L. Fang, X. Y. Liu, L. Du, W. X. Tang, *Biopolymers* **2002**, *65*, 81–88.
58. C. Capasso, O. Abugo, F. Tanfani, A. Scire, V. Carginale, R. Scudiero, E. Parisi, S. D'Auria, *Proteins* **2002**, *46*, 259–267.
59. J. Domènech, A. Tinti, M. Capdevila, S. Atrian, A. Torreggiani, *Biopolymers* **2007**, *86*, 240–248.
60. E. Smyth, C. D. Syme, E. W. Blanch, L. Hecht, M. Vašák, L. D. Barron, *Biopolymers* **2001**, *58*, 138–151.
61. P. N. Schatz, A. J. McCaffery, *Q. Rev. Chem. Soc.* **1969**, *23*, 552–584.
62. B. Holmquist, *Methods Enzymol.* **1986**, *130*, 270–290.
63. G. Barth, W. Voelter, Bunnenberg.E, C. Djerassi, *J. Am. Chem. Soc.* **1972**, *94*, 1293–1298.
64. A. Y. C. Law, M. J. Stillman, *Biochem. Bioph. Res. Co.* **1980**, *94*, 138–143.
65. A. Y. C. Law, M. G. Cherian, M. J. Stillman, *Biochim. Biophys. Acta* **1984**, *784*, 53–61.
66. M. J. Stillman, A. J. Zelazowski, *J. Biol. Chem.* **1988**, *263*, 6128–6133.
67. A. J. Zelazowski, J. A. Szymanska, A. Y. C. Law, M. J. Stillman, *J. Biol. Chem.* **1984**, *259*, 2960–2963.
68. G. Meloni, P. Faller, M. Vašák, *J. Biol. Chem.* **2007**, *282*, 16068–16078.
69. P. Faller, M. Vašák, *Biochemistry* **1997**, *36*, 13341–13348.
70. D. W. Hasler, P. Faller, M. Vašák, *Biochemistry* **1998**, *37*, 14966–14973.
71. D. W. Hasler, L. T. Jensen, O. Zerbe, D. R. Winge, M. Vašák, *Biochemistry* **2000**, *39*, 14567–14575.
72. N. Romero-Isart, L. T. Jensen, O. Zerbe, D. R. Winge, M. Vašák, *J. Biol. Chem.* **2002**, *277*, 37023–37028.
73. E. A. Peroza, E. Freisinger, *J. Biol. Inorg. Chem.* **2007**, *12*, 377–391.
74. D. Koningsberger, R. Prins, *EXAFS, SEXAFS, XANES: X-Ray Absorption - Principles, Applications, Techniques of EXAFS, SEXAFS and XANES*, John Wiley & Sons Ltd., Chichester, 1988.
75. R. A. Scott, *Methods Enzymol.* **1985**, *117*, 414–459.
76. S. S. Hasnain, G. P. Diakun, I. Abrahams, I. Ross, C. D. Garner, I. Bremner, M. Vašák, in *Metallothionein II*, Eds J. H. R. Kägi, Y. Kojima, Birkhäuser Verlag, Basel, 1987, pp. 227–236.
77. J. Chan, M. E. Merrifield, A. V. Soldatov, M. J. Stillman, *Inorg. Chem.* **2005**, *44*, 4923–4933.
78. H. Frauenfelder, R. M. Steffen, in *Alpha- beta- and gamma-ray spectroscopy*, Ed K. Siegbahn, North-Holland Pub. Co., Amsterdam, 1965, Vol. 2, pp. 997–1198.
79. R. Bauer, *Q. Rev. Biophy.* **1985**, *18*, 1–64.
80. L. Hemmingsen, K. N. Sas, E. Danielsen, *Chem. Rev.* **2004**, *104*, 4027–4061.
81. M. Vašák, R. Bauer, *J. Am. Chem. Soc.* **1982**, *104*, 3236–3238.
82. E. Danielsen, R. Bauer, *Hyperfine Interact.* **1991**, *62*, 311–324.
83. A. Glennås, H. E. Rugstad, *Environ. Health Persp.* **1984**, *54*, 45–50.
84. A. E. Ashcroft, *Nat. Prod. Rep.* **2005**, *22*, 452–464.
85. I. A. Kaltashov, M. X. Zhang, S. J. Eyles, R. R. Abzalimov, *Anal. Bioanal. Chem.* **2006**, *386*, 472–481.
86. X. L. Yu, M. Wojciechowski, C. Fenselau, *Anal. Chem.* **1993**, *65*, 1355–1359.
87. P. M. Gehrig, C. H. You, R. Dallinger, C. Gruber, M. Brouwer, J. H. R. Kägi, P. E. Hunziker, *Protein Sci.* **2000**, *9*, 395–402.
88. G. Meloni, K. Zovo, J. Kazantseva, P. Palumaa, M. Vašák, *J. Biol. Chem.* **2006**, *281*, 14588–14595.
89. K. Polec, M. Perez-Calvo, O. Garcia-Arribas, J. Szpunar, B. Ribas-Ozonas, R. Lobinski, *J. Inorg. Biochem.* **2002**, *88*, 197–206.

90. M. Serra-Batiste, N. Cols, L. A. Alcaraz, A. Donaire, P. Gonzalez-Duarte, M. Vašák, *J. Biol. Inorg. Chem.* **2010**, *15*, 759–776.
91. T. T. Ngu, S. R. Sturzenbaum, M. J. Stillman, *Biochem. Biophys. Res. Commun.* **2006**, *351*, 229–233.
92. O. Palacios, A. Pagani, S. Perez-Rafael, M. Egg, M. Hockner, A. Brandstatter, M. Capdevila, S. Atrian, R. Dallinger, *BMC Biol.* **2011**, *9:4*.
93. R. Orihuela, J. Domenech, R. Bofill, C. You, E. A. Mackay, J. H. R. Kägi, M. Capdevila, S. Atrian, *J. Biol. Inorg. Chem.* **2008**, *13*, 801–812.
94. M. E. Merrifield, J. Chaseley, P. Kille, M. J. Stillman, *Chem. Res. Toxicol.* **2006**, *19*, 365–375.
95. E. A. Peroza, A. Al Kaabi, W. Meyer-Klaucke, G. Wellenreuther, E. Freisinger, *J. Inorg. Biochem.* **2009**, *103*, 342–353.
96. P. Palumaa, E. Eriste, O. Njunkova, L. Pokras, H. Jornvall, R. Sillard, *Biochemistry* **2002**, *41*, 6158–6163.
97. K. B. Nielson, D. R. Winge, *J. Biol. Chem.* **1983**, *258*, 13063–13069.
98. M. Good, R. Hollenstein, P. J. Sadler, M. Vašák, *Biochemistry* **1988**, *27*, 7163–7166.
99. K. E. R. Duncan, M. J. Stillman, *FEBS J.* **2007**, *274*, 2253–2261.
100. D. E. K. Sutherland, M. J. Stillman, *Biochem. Biophys. Res. Commun.* **2008**, *372*, 840–844.
101. G. Meloni, T. Polanski, O. Braun, M. Vašák, *Biochemistry* **2009**, *48*, 5700–5707.
102. K. Breuker, F. W. McLafferty, *Proc. Natl. Acad. Sci. USA* **2008**, *105*, 18145–18152.
103. Y. J. Wang, E. A. Mackay, M. Kurasaki, J. H. R. Kägi, *Eur. J. Biochem.* **1994**, *225*, 449–457.
104. E. Freisinger, *Inorg. Chim. Acta* **2007**, *360*, 369–380.
105. O. I. Leszczyszyn, S. Zeitoun-Ghandour, S. R. Sturzenbaum, C. A. Blindauer, *Chem. Commun.* **2011**, *47*, 448–450.
106. A. H. Robbins, D. E. McRee, M. Williamson, S. A. Collett, N. H. Xuong, W. F. Furey, B. C. Wang, C. D. Stout, *J. Mol. Biol.* **1991**, *221*, 1269–1293.
107. B. A. Messerle, M. Bos, A. Schäffer, M. Vašák, J. H. R. Kägi, K. Wüthrich, *J. Mol. Biol.* **1990**, *214*, 781–786.
108. C. D. Berweger, W. Thiel, W. F. van Gunsteren, *Proteins* **2000**, *41*, 299–315.
109. J. D. Otvos, C. W. Peterson, C. F. Shaw III, *Commun. Inorg. Chem.* **1989**, *9*, 1–35.
110. A. E. Martell, R. D. Hancock, R. J. Motekaitis, *Coord. Chem. Rev.* **1994**, *133*, 39–65.
111. P. Faller, D. W. Hasler, O. Zerbe, S. Klauser, D. R. Winge, M. Vašák, *Biochemistry* **1999**, *38*, 10158–10167.
112. K. S. Hagen, D. W. Stephan, R. H. Holm, *Inorg. Chem.* **1982**, *21*, 3928–3936.
113. F. Y. Ni, B. Cai, Z. C. Ding, F. Zheng, M. J. Zhang, H. M. Wu, H. Z. Sun, Z. X. Huang, *Proteins* **2007**, *68*, 255–266.
114. T. Gan, A. Munoz, C. F. Shaw III, D. H. Petering, *J. Biol. Chem.* **1995**, *270*, 5339–5345.
115. H. Li, J. D. Otvos, *J. Inorg. Biochem.* **1998**, *70*, 187–194.
116. D. H. Petering, S. Krezoski, P. Chen, A. Pattanaik, C. F. Shaw III, in *Metallothioneins: Synthesis, Structure and Properties of Metallothioneins, Phytochelatins, and Metal-Thiolate Complexes*, Eds M. J. Stillman, C. F. Shaw III, K. T. Suzuki, VCH, New York, 1992, pp. 164–185.
117. C. F. Shaw, III, M. M. Savas, D. H. Petering, *Methods Enzymol.* **1991**, *205*, 401–414.
118. T. Y. Li, D. T. Minkel, C. F. Shaw, D. H. Petering, *Biochem. J.* **1981**, *193*, 441–446.
119. P. J. Thornalley, M. Vašák, *BBA-Protein Struct. M.* **1985**, *827*, 36–44.
120. M. Sato, I. Bremner, *Free Radical Bio. Med.* **1993**, *14*, 325–337.
121. K. Zangger, G. Oz, E. Haslinger, O. Kunert, I. M. Armitage, *FASEB J.* **2001**, *15*, 1303–1305.
122. J. Y. Zhu, J. Meeusen, S. Krezoski, D. H. Petering, *Chem. Res. Toxicol.* **2010**, *23*, 422–431.
123. J. D. Otvos, I. M. Armitage, *Proc. Natl. Acad. Sci. USA* **1980**, *77*, 7094–7098.
124. D. R. Winge, K.-A. Miklossy, *J. Biol. Chem.* **1982**, *257*, 3471–3476.
125. Y. Boulanger, I. M. Armitage, K. A. Miklossy, D. R. Winge, *J. Biol. Chem.* **1982**, *257*, 3717–3719.

126. G. Wagner, D. Neuhaus, E. Wörgötter, M. Vašák, J. H. R. Kägi, K. Wüthrich, *Eur. J. Biochem.* **1986**, *157*, 275–289.
127. M. H. Frey, G. Wagner, M. Vašák, O. W. Sorensen, D. Neuhaus, E. Wörgötter, J. H. R. Kägi, R. R. Ernst, K. Wüthrich, *J. Am. Chem. Soc.* **1985**, *107*, 6847–6851.
128. M. Vašák, E. Wörgötter, G. Wagner, J. H. R. Kägi, K. Wüthrich, *J. Mol. Biol.* **1987**, *196*, 711–719.
129. W. F. Furey, A. H. Robbins, L. L. Clancy, D. R. Winge, B. C. Wang, C. D. Stout, *Science* **1986**, *231*, 704–710.
130. W. Braun, M. Vašák, A. H. Robbins, C. D. Stout, G. Wagner, J. H. R. Kägi, K. Wüthrich, *Proc. Natl. Acad. Sci. USA* **1992**, *89*, 10124–10128.
131. J. D. Otvos, R. W. Olafson, I. M. Armitage, *J. Biol. Chem.* **1982**, *257*, 2427–2431.
132. Y. J. Wang, E. A. Mackay, O. Zerbe, D. Hess, P. E. Hunziker, M. Vašák, J. H. R. Kägi, *Biochemistry* **1995**, *34*, 7460–7467.
133. B. A. Krizek, D. L. Merkle, J. M. Berg, *Inorg. Chem.* **1993**, *32*, 937–940.
134. C. A. Blindauer, M. D. Harrison, J. A. Parkinson, N. J. Robinson, P. J. Sadler, in *Metal Ions in Biology and Medicine*, Eds P. Collery, I. Maymard, T. Theophanides, L. Khassanova, T. Collery, John Libbey Eurotext, Paris, 2008, Vol. 10, pp. 167–173.
135. C. A. Blindauer, N. C. Polfer, S. E. Keiper, M. D. Harrison, N. J. Robinson, P. R. R. Langridge-Smith, P. J. Sadler, *J. Am. Chem. Soc.* **2003**, *125*, 3226–3227.
136. O. I. Leszczyszyn, C. R. J. White, C. A. Blindauer, *Mol. Biosyst.* **2010**, *6*, 1592–1603.
137. C. Andreini, L. Banci, I. Bertini, A. Rosato, *J. Proteome Res.* **2006**, 5, 3173–3178.
138. A. F. A. Peacock, O. Iranzo, V. L. Pecoraro, *Dalton Trans.* **2009**, 2271–2280.

Chapter 12
Cadmium-Accumulating Plants

Hendrik Küpper and Barbara Leitenmaier

Contents

ABSTRACT 373
1 INTRODUCTION: IMPORTANCE OF CADMIUM ACCUMULATION IN PLANTS 374
1.1 Cadmium Accumulation in Indicator and Excluder Plants 374
1.2 Active Cadmium Hyperaccumulation 376
2 ECOLOGICAL ROLE OF CADMIUM HYPERACCUMULATION 377
3 MECHANISMS OF CADMIUM HYPERACCUMULATION 378
3.1 Compartmentation of Cadmium in Tissues, Cells, and Organelles 379
3.2 Expression and Function of Metal Transport Proteins 380
3.3 Role of Metal Ligands in Cadmium Uptake, Transport, and Storage 382
4 BIOTECHNOLOGICAL USE OF CADMIUM HYPERACCUMULATORS 383
5 OUTLOOK 386
ABBREVIATIONS 387
ACKNOWLEDGMENTS 388
REFERENCES 388

Abstract Plants are categorized in three groups concerning their uptake of heavy metals: indicator, excluder, and hyperaccumulator plants, which we explain in this chapter, the former two groups briefly and the hyperaccumulators in detail. The ecological role of hyperaccumulation, for example, the prevention of herbivore attacks and a possible substitution of Zn by Cd in an essential enzyme, is discussed. As the mechanisms of cadmium hyperaccumulation are a very interesting and challenging topic and many aspects are studied worldwide, we provide a broad overview over compartmentation strategies, expression and function of metal

H. Küpper (✉)
Fachbereich Biologie, Universität Konstanz, D-78457 Konstanz, Germany
e-mail: hendrik.kuepper@uni-konstanz.de

B. Leitenmaier
Institut für Anorganische Chemie, Universität Zürich, Winterthurerstraße 190, CH-8057 Zürich, Switzerland

A. Sigel, H. Sigel, and R.K.O. Sigel (eds.), *Cadmium: From Toxicity to Essentiality*, Metal Ions in Life Sciences 11, DOI 10.1007/978-94-007-5179-8_12,

transporting proteins and the role of ligands for uptake, transport, and storage of cadmium. Hyperaccumulators are not without reason a topic of great interest, they can be used biotechnologically for two main purposes which we discuss here for Cd: phytoremediation, dealing with the cleaning of anthropogenically contaminated soils as well as phytomining, i.e., the use of plants for commercial metal extraction. Finally, the outlook deals with topics for future research in the fields of biochemistry/biophysics, molecular biology, and biotechnology. We discuss which knowledge is still missing to fully understand Cd hyperaccumulation by plants and to use that phenomenon even more successfully for both environmental and economical purposes.

Keywords excluder plants • hyperaccumulator plants • indicator plants • natural overexpression of transport proteins • phytoremediation • phytomining • vacuolar metal sequestration

1 Introduction: Importance of Cadmium Accumulation in Plants

Certain heavy metals are well known to be essential microelements needed for plants to grow and complete their life cycle. Elevated concentrations of these metals, however, can be toxic and induce inhibition of various plant metabolic processes (reviewed, e.g., in [1–3]).

Cadmium can occur in very high concentrations in the soil that are detrimental or even lethal to most plants, as described in more detail in Chapters 2 and 13 of this book. Plants have developed a number of strategies to resist the toxicity of heavy metals (see [2–4] for recent reviews). Such strategies include the functioning of metal efflux pumps, sequestration in cells and intracellular compartments where metals can do the least harm, and binding of heavy metals inside the cells by strong ligands. According to the relation between the metal content in the soil or nutrient solution compared to the metal accumulated inside the plant, called "bioaccumulation coefficient" or "bioconcentration factor", plants are divided into three groups: excluder, indicator and hyperaccumulator plants (Figure 1).

1.1 Cadmium Accumulation in Indicator and Excluder Plants

Most heavy metal resistant plants belong to the so-called "excluders", they prevent the accumulation of heavy metals inside their tissues [5]. Metal exclusion can function in several different ways. The probably most simple way is a reduction of the unselective permeability of cells. This is typically reached by lignification of plant cell walls, and the enhancement of lignifying enzymes is a well-known response to cadmium toxicity [6]. In addition, exclusion can occur by precipitation

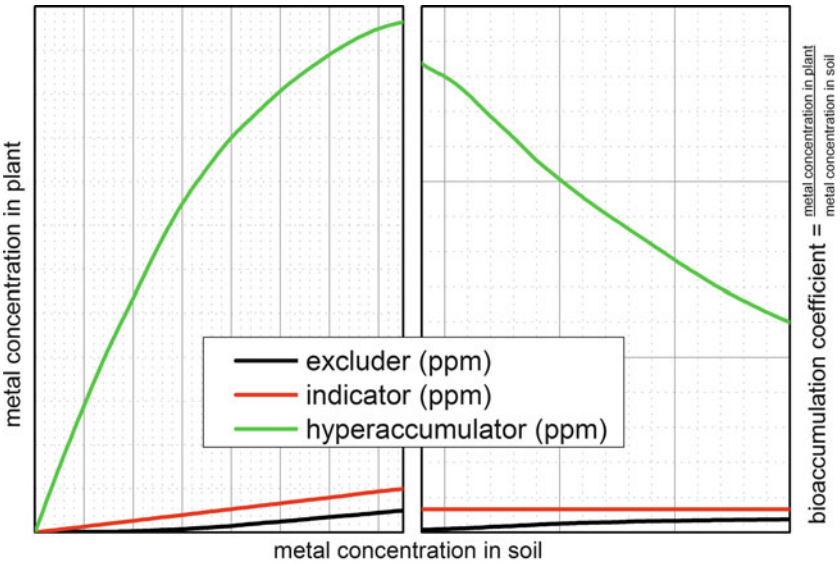

Figure 1 Three main types of heavy metal accumulation in plants: schematic correlations between metal in soil (or nutrient solution) and metal in the plants.

or binding of metals in the apoplast (cell walls) before they pass the plasma membrane. Third, plants can actively reduce concentrations of unwanted metals in their cells by pumping them out. Such ATP-dependent efflux pumps were first found in roots of *Silene vulgaris* [7], but later also in roots of other plants (e.g., [8]). Another efflux carrier is the Cd^{2+}-detoxifying *A. thaliana* Detoxification1 (AtDTX1 [9]).

In addition to efflux pumps in roots, it has also been suggested that active efflux can be achieved by vesicle-mediated excretion of crystals in leaf hairs (trichomes) [10]. Because of the latter two mechanisms, excluder plants typically show only little increase of toxic metals inside their tissues at moderately toxic concentrations, but a steeper slope of the metal in soil/water *versus* metal in plant function at more toxic soil concentrations when the capacity of those efflux transporters is exceeded (Figure 1). Excluder plants cannot be used for phytoremediation in the strict sense of the word (dealt with in Section 4) as they would not remove much metal. But they are used for re-vegetation of toxic sites where extraction of the metal is not possible or not desired. In this case, the particularly low metal content in their above-ground parts is an advantage because grazing animals will not take up much of the toxic metal. In order to identify such plants for re-vegetation of contaminated sites, screening of plant species with such properties has been done since about 15 years with some success [11–13]. Further, exclusion of toxic metals is a desirable feature for crop plants, so that research identifying genes that determine toxic metal uptake, and modification of their expression by breeding or genetic engineering has been a

focus of recent research [12–16]. While screening for suitable low-metal cultivars already had considerable success [14,15], so far there are no genetically modified crop variants achieving this aim.

Indicator plants possess very little defence against uptake of toxic metals, so their internal metal content almost linearly reflects the metal concentration in their environment (Figure 1). Therefore, such plants have been suggested for monitoring environmental pollution already for a long time with research still continuing (e.g., [17–19]). More recent research in this direction deals with the quantitative aspects of the relation between environmental metal concentrations and accumulation in plants, and has shown linear relationships if species are well selected [20,21]. When rather metal-sensitive species are used, not only the element concentrations inside can be measured for quantitative analysis of environmental pollution, but in addition a screening for visual toxicity symptoms can be used as a quick and inexpensive test whether pollution already reached dangerous levels [21]. But even in indicator species, not all metals are taken up with the same efficiency, i.e., the slope of internal *versus* external metal concentration varies considerably, so that for a reliable assessment of environmental pollution with bioindicators an interspecies calibration is necessary [18,22]. Further, seasonal variations in growth of the indicator organisms, as well as abiotic environmental factors such as pH, which strongly influence metal uptake by organisms, lead to variations in this slope and have to be considered in the analysis of bioindicator data [23,24]. Also epiphytic bacteria can modify plant uptake, especially in water plants where they may cover a lot of the surface, compete for metal uptake and thus protect the plants from metal-induced damage [25].

1.2 Active Cadmium Hyperaccumulation

Some plants, called hyperaccumulators, actively take up large amounts of potentially toxic metals and store them in their above-ground tissues (first described by Risse in the article of Sachs in 1865 [26], the term "hyperaccumulator" was introduced by Brooks in 1977 [27]). These plants are the main topic of this chapter, so that important aspects of their ecological role, physiology, and biotechnological use will be described in detail in the following sections. There is no general agreement which level of Cd accumulation under which circumstances is enough for making a Cd-accumulating plant a true hyperaccumulator. But the highest naturally occurring Cd hyperaccumulation is clearly achieved by the southern French (from the Ganges region) ecotype of *Thlaspi caerulescens* = *Noccaea caerulescens* [28]. Shoots of this plant easily reach >2000 ppm Cd on natural soil [29] and >20000 ppm grown until mature state in nutrient solution [28]; the Cd bioaccumulation coefficient of this ecotype in its natural habitat is >70 [29]. This ecotype does not only accumulate most Cd, but is at the same time much more Cd-resistant than most other plants including other *T. caerulescens* ecotypes, maintaining an almost undiminished growth even at 30 μM Cd in nutrient solution [30].

To distinguish these very remarkable capabilities from the multitude of plant species that accumulate only a little Cd while being Cd-sensitive, but still are sometimes called "Cd hyperaccumulators" based on the old definition of Cd hyperaccumulation (">100 ppm in shoot dry weight in the natural habitat" [31]), it might be useful to re-define Cd hyperaccumulation as >500 ppm in shoots under environmentally relevant conditions with less than 20% growth reduction until the stage of maturity and a bioaccumulation coefficient >5 at a Cd concentration leading to >500 ppm in shoots.

2 Ecological Role of Cadmium Hyperaccumulation

In nature, heavy metal hyperaccumulation can serve as a defence against pathogens and herbivores [32–38]. For the best Cd/Zn hyperaccumulator, *T. caerulescens*, unfortunately most studies in this direction were carried out with Zn, but given the even higher toxicity of Cd to animals, fungi, and bacteria, it is almost certain that the results apply at least as much to the ecological role of Cd hyperaccumulation in this species. Herbivores that were given the choice between *T. caerulescens* plants grown on different zinc levels [39] or belonging to ecotypes with different abilities of Zn hyperaccumulation [40] were shown to choose those plants which accumulate the lowest amount of metal. Pathogenic bacteria affected *T. caerulescens* less if it was grown with increasing Zn, and in this study also Cd was tested at least in cell cultures and had the expected effect [41]. A truly Cd-dedicated study on elemental defense in *T. caerulescens* was performed by Jiang et al. [42], who found that Cd accumulation deters thrips (*Frankliniella occidentalis*) from feeding on *T. caerulescens* leaves. These effects of accumulated metals are often additive if more than one metal is accumulated, and a particularly strong effect was found for the Cd+Zn combination where no larvae pupated while the same metal concentrations alone only reduced the likelyhood of pupation [43]. The same study showed that at least sometimes metal effects are further enhanced by organic defence chemicals produced by the plants. Further, already metal concentrations below the hyperaccumulation limit are active in this direction [44].

While it is clear from these studies that hyperaccumulation does protect against a broad range of herbivores and pathogens, like any other defence strategy it has limitations. Zinc accumulation did not protect the Cd/Zn hyperaccumulator *Arabidopsis halleri* from attack by snails [45], the same was found for snails feeding on *T. caerulescens* [46]. It looks like snails are less metal-sensitive than the various herbivores and pathogens that are efficiently deterred from hyperaccumulators, but it remains to be seen whether this applies also to defence by Cd as so far no studies investigating the feeding of snails on Cd-treated *T. caerulescens* have been performed.

Since the amount of heavy metal content accumulated in the plant can easily be controlled by the concentration of the metal in the growth medium [39],

hyperaccumulators may be an ideal model for a systematic study of plant-pathogen/herbivore interactions, as discussed by Pollard [47].

In addition to the protection against herbivores and pathogens, it was proposed that hyperaccumulation may serve as "elemental allelopathy" [48]. This study suggested that hyperaccumulators increase the metal concentration in the surface soil next to them and thereby inhibit the growth of non-accumulators competing for space and nutrients. At the same time, the elevated metal concentrations would encourage growth of hyperaccumulator seedlings [49–52]. Perronnet et al. [52] have shown that the hyperaccumulated metals in leaves of *T. caerulescens* easily become bioavailable again after incorporation of the leaves into the soil. These interesting ideas definitely deserve further investigations.

Another alternative hypothesis about the biological role of hyperaccumulation was the increase of osmotic pressure for increased tolerance to the drought stress that often characterizes the natural habitats of hyperaccumulators. This hypothesis, however, was falsified by a study with the Ni hyperaccumulator *Alyssum murale* and the Cd/Zn hyperaccumulator *T. caerulescens* [53].

Besides all the aforementioned benefits hyperaccumulated metals (may) have for the plants, there is also one recent study that strongly suggests a much more direct role in metabolism – it may be an alternative active center in carboanhydrase of *T. caerulescens*, which is normally a Zn-dependent enzyme [54]. Such a functional replacement of Zn by Cd, leading to growth increase upon addition of Cd, was previously found in the marine alga *Thalassiosira weissflogii* [55], from which Cd-carboanhydrase was even purified and its three-dimensional structure resolved [56]. This case is described in detail in Chapter 16 of this book.

Whatever the main ecological benefit of hyperaccumulation is, plants doing it treat the accumulated metal as something valuable, which becomes obvious during leaf senescence. As it is generally known for metals that are essential plant nutrients (e.g., [57]), also hyperaccumulators recycle beneficial metals, which seem to include the hyperaccumulated heavy metals; Cd concentrations were found to be lower in senescent compared to mature and young leaves of *T. caerulescens* [58,59]. Furthermore, roots of *T. caerulescens* have been found to grow towards rather than away from heavy metals [60].

3 Mechanisms of Cadmium Hyperaccumulation

The mechanisms by which plants hyperaccumulate heavy metals in their shoots and prevent phytotoxicity of these metals have been the subject of many studies. Nonetheless, many of these mechanisms are still under debate.

While the following sections deal with mechanisms of hyperaccumulation on the cellular and molecular level, it should also be noted that hyperaccumulation is modified by interactions between plants and arbuscular mycorrhizal fungi [61]. In this study, the colonisation of the plant roots with these fungi reduced Cd uptake and thus increased metal tolerance of the plants, but in studies on other plants

such a correlation was not observed (e.g., [62]). Another controversial point concerning interactions in metal hyperaccumulation is the interaction between different metals. According to several studies, Cd and Zn compete for uptake due to their well-known chemical similarity in the Zn-hyperaccumulating Prayon ecotype of *T. caerulescens*, but independence of the transport processes of these metals was found in the Cd/Zn-hyperaccumulating Ganges ecotype of *T. caerulescens* [28,63,64]. The Cd-Zn competition in the Prayon ecotype was questioned by a more recent study, where even an enhancement of Cd uptake during growth on high Zn was found [65]. Further, it was reported that Cd uptake in *T. caerulescens* Ganges increased under iron deficiency [66].

A rather comprehensive study of interactions between uptake of different metals in *T. caerulescens* was done by Assunção et al. [67]. Via binary metal combinations they tested interactions between Cd and Zn, Cd and Ni, and Ni and Zn, which confirmed that the Ganges population expresses a highly Cd-specific high-affinity uptake system, which was not found in the other *T. caerulescens* populations. The other populations only had a high-affinity Zn-uptake system (present also in the Ganges population) and a low-affinity Cd/Zn/Ni-uptake system.

3.1 Compartmentation of Cadmium in Tissues, Cells, and Organelles

An enhanced uptake of metals into the root symplasm was found in *T. caerulescens* compared to the related non-accumulator, *T. arvense* [68,69], and a reduced sequestration into the root vacuoles was associated with the higher root to shoot translocation efficiency of *T. caerulescens* [49,69,70]. Xylem loading and xylem transport are key steps in Cd hyperaccumulation, as it will be discussed in detail in the section about transport proteins below, and as it was commented by White et al. already 10 years ago [71]. Also in non-hyperaccumulators, the degree of Cd accumulation in above-ground tissues mainly depends on xylem transport [72].

While metal uptake through the root is the first important step in hyperaccumulation, most of the metal is stored in the above-ground parts. Studies of cellular metal compartmentation have shown that in most hyperaccumulators the metal is sequestered preferentially into compartments where they can not damage metabolic processes, e.g., photosynthesis as a very cadmium-sensitive vital function of plants (see Chapter 13). Therefore, it is important for hyperaccumulators to keep the metal concentration in the cytoplasm of mesophyll cells as low as possible.

Many plants detoxify heavy metals by sequestering them, either as phytochelatin complexes or without specific ligands, in the vacuoles (for reviews see e.g., [73,74]). It makes sense for hyperaccumulating plants to store metal in the vacuoles as well because this organelle only contains enzymes like phosphatases, lipases, and proteinases [75] that were never identified as targets of heavy metal toxicity. Vacuole sequestration is driven to an extreme form in hyperaccumulators, where

the primary metal storage compartment of most species is clearly the leaf vacuoles [50,51,76–79]. This plant-specific (animal and bacterial cells do not possess this organelle) metal detoxification strategy provides an efficient form of protection because the vacuole does not contain any sensitive enzymes.

In most heavy metal-tolerant plants, the vacuolar sequestration mainly occurs in non-photosynthetic cells of the epidermis, reducing toxicity to the heavy metal sensitive photosynthetic apparatus [50,51,76,80–82]. For a general review on mechanisms of such differential ion accumulations in leaves, see Karley et al. [83]. Additionally it has been shown that high amounts of metals are stored specifically in the vacuoles of particularly large epidermal cells [50,51,76]. The approximate volume of this storage site multiplied by the metal concentration in it (data, e.g., for Zn from Küpper et al. [50]) indicates that about 70% of the total accumulated metal in mature leaves is stored in the epidermis of *T. caerulescens*. In the vacuoles of the epidermal metal storage cells, heavy metal concentrations of several hundred mmol.L^{-1} can be reached [50,51], showing that hyperaccumulation must involve active pumping of the metals into specific storage sites. The preferential heavy metal accumulation in epidermal storage cells, previously observed for several metals in intact leaves of various hyperaccumulator species, is due to differences in active metal transport and not differences in passive mechanisms like transpiration stream transport or cell wall adhesion [79]. Combining this with previous studies, it seems likely that the transport steps over the plasma and tonoplast membranes of leaf epidermal storage cells are driving forces behind the hyperaccumulation phenotype.

Like in many other cases, also in this one there is a famous exception from the rule. In the Zn hyperaccumulator *A. halleri*, which also has a limited accumulation capability for Cd, except for a few trichomes epidermal cells are rather small. Therefore, despite their high concentrations of Cd and Zn they contribute only a minor proportion to total storage of Cd and Zn in this species [84]. This may be the reason, however, why in this species Cd accumulation is limited by Cd toxicity as shown in the same study, because Cd accumulation in the mesophyll represents a danger in terms of Cd-induced inhibition of photosynthesis. A seemingly similar situation was recently reported for the Cd/Zn hyperaccumulator *Sedum alfredii* [85], where Cd is accumulated in the mesophyll of leaves beside the pith and cortex of stems [86]. Comparing this to other hyperaccumulators, however, it has to be kept in mind that *S. alfredii* has rather thick, succulent leaves, which means that it has exceptionally large vacuoles in the mesophyll, making Cd storage there safer than it would be in regular sized mesophyll cells.

3.2 Expression and Function of Metal Transport Proteins

In recent years, much progress has been made in identifying genes involved in metal transport. Thus it has been found that metal hyperaccumulation is mediated, at least in part, by an up to 200 times higher expression of metal transporter genes in

hyperaccumulators compared to related non-accumulator plants ([87–95], reviewed by Verbruggen et al. [96]). To achieve a bioaccumulation coefficient greater than one, the metals have to be pumped into their storage sites, i.e., vacuoles, against the concentration gradient. And already before, most likely many steps of the metal transport from root uptake until passage over the plasma membrane of the storage cells are against the concentration gradient or at least there wouldn't be a concentration gradient facilitating passive diffusion. Therefore, all these transport steps require an active, i.e., energy-consuming transport system [97]. Furthermore, specificity of the transport has to be tightly controlled in order to allow for the vast differences in concentrations between hyperaccumulated and non-accumulated metals in the same cell.

The early finding that root uptake and root to shoot translocation are strongly elevated in hyperaccumulators compared to non-accumulators (see Section 3.2. above) obtained a genetic basis in recent years, as it was found that the heavy metal ATPase HMA4 is strongly overexpressed in roots of the Cd/Zn hyperaccumulator plants *A. halleri* and *T. caerulescens* [90,91,98], and that this is linked to HMA4 gene multiplication [93,95,99]. Investigations of the biochemical and biophysical properties of the *T. caerulescens* version of HMA4, TcHMA4, have shown that the ATPase function of this transporter is activated most strongly by Cd and Zn. Gels and western blots (using an antibody specific for TcHMA4) of crude root extract and of the purified protein revealed a size of TcHMA4 of about 50 to 60 kDa, while the mRNA for the TcHMA4 gene predicts a single protein with a size of 128 kDa. This indicates the occurrence of post-translational processing [100]. In recent work by Leitenmaier et al. [101], TcHMA4 showed activity with Cu^{2+}, Zn^{2+}, and Cd^{2+} under various concentrations (0.03–10 μM tested), and all three metal ions activated the ATPase at a concentration of 0.3 μM. Notably, the enzyme worked best at rather high temperatures (optimum at 42°C). Arrhenius plots showed constant activation energy ($E_A = 38$ kJ.mol^{-1}) over the whole concentration range of Zn while it increased from 17 to 42 kJ.mol^{-1} with rising Cu concentration and decreased from 39 to 23 kJ.mol^{-1} with rising Cd concentration. According to EXAFS, TcHMA4 appeared to bind Cd mainly by thiolate sulfur from cysteine, and not by imidazole nitrogen from histidine.

Protein families involved in vacuolar sequestration may be the NRAMP's, CDF's, and CAX's (reviewed by Hall and Williams [102]) as well as CPx-type ATPases. Until now, already several transporters for vacuolar sequestration of zinc (and possibly cadmium) and nickel have been investigated and could be partially characterized [103–107]. Several CDF transporters for vacuolar sequestration of Zn (and possibly Cd and Co) have been characterized, all are homologous, almost identical in sequence. These are MTP1, ZAT, and ZTP (e.g., [88,89,103,108]). The strongly elevated expression of the CPx-type metal ATPase HMA3 was shown to play a decisive role in Cd accumulation not only in *T. caerulescens* [109], but also in rice [110,111], reconfirming also the importance of the sequestration into vacuoles for the hyperaccumulation phenotype. The natural over-expression of NRAMPs was identified both in rice and in *T. caerulescens* to play an important role in Cd tolerance and possibly Cd accumulation [112–114]. When vacuolar

sequestration is coupled to complexation by phytochelatins (i.e., not in hyperaccumulators, but in non-accumulator plants), transport of the Cd-phytochelatin complexes to the vacuoles is mediated by transporters of the ABC family, as recently shown by Mendoza-Cózatl et al. [115].

In contrast to the progress that has been made in finding genes that are expressed at higher levels in hyperaccumulators, the cell-specificity of their expression and regulation in hyperaccumulators has remained largely unknown. Therefore, it remains impossible to judge which of these genes are directly involved in hyperaccumulation by encoding transporters that pump the metal into storage sites, and which may be secondarily up-regulated to prevent Zn deficiency in other compartments. Two recent studies have indicated such secondary up-regulation for members of the IRT micronutrient transporter family: Küpper et al. [116] for ZNT1 in *T. caerulescens* by QISH analysis, and Hanikenne et al. [95] for ZIP4 and IRT3 by expressing HMA4 from the Zn hyperaccumulator *A. halleri* (AhHMA4) under its own promoter in the non-accumulator *A. thaliana*.

Metal storage cells were furthermore found to display a strongly elevated expression of the metal transporters MTP1 and ZNT5 [117]. But for most of these genes the cellular expression pattern and its metal-dependent regulation remains unknown. Quantitative mRNA *in situ* hybridization (QISH) revealed that transporter gene expression changes not only dependent on metal nutrition/toxicity, but even more so during plant and leaf development [117]. Main mRNA abundances found: ZNT1: mature leaves of young plants; ZNT5: young leaves of young plants: MTP1 (= ZTP1 ≈ ZAT): young leaves of both young and mature plants. Surprisingly different cellular expression patterns were found for ZNT1 and ZNT5, both belonging to the ZIP family of transition metal transporters. ZNT1: photosynthetic mesophyll and bundle sheath cells; ZNT5: non-photosynthetic epidermal metal storage cells and bundle sheath cells. Thus, ZNT1 may function in micronutrient nutrition while ZNT5 may be involved in metal storage associated with hyperaccumulation. The latter is in agreement with experiments of knock-outs and heterologous expression of TcZNT5 in *A. thaliana* [118].

3.3 Role of Metal Ligands in Cadmium Uptake, Transport, and Storage

Cadmium is highly toxic to plants (see Chapter 13), so that the extreme Cd accumulation in Cd hyperaccumulators immediately raises the question in which chemical form it is present in these plants, i.e., whether its toxicity is diminished by strong ligands that reduce the likelyhood of binding to proteins. Most reliable information about Cd ligands in plants was gained by X-ray absorption spectroscopy (XAS), especially X-ray absorption near edge structures (XANES) and extended X-ray absorption fine structure (EXAFS), as reviewed, e.g., by Gardea-Torresday et al. [119] and Saraswat and Rai [120]. The big advantage of XAS

compared to chromatographic methods is the possibility to exclude artefactual exchange of Cd ligands during sample preparation and analysis. Crushing cells for tissue/cell fractionation and extraction inevitably destroys membranes that separate the metals accumulated in the vacuole from various proteins in the cytoplasm and from the cell wall in the apoplast. This membrane destruction will immediately result in a change of Cd speciation because very strong Cd ligands are found in the cytoplasm (e.g., active sites of proteins) and cell wall, while vacuoles are well-known to contain weak ligands like organic acids.

For using XAS it is not necessary to extract metal-ligand complexes from their natural compartment (e.g., the vacuole), and using rapid-freeze techniques in combination with measurement of frozen-hydrated samples artefacts of re-distribution can be efficiently prevented. This has been done for Cd by Küpper et al. [59], showing that in mature leaves as the main storage sites of Cd in hyperaccumulators this metal is bound predominantly by weak oxygen ligands such as organic acids. This result was later confirmed via ^{113}Cd NMR [121] and further XAS studies [122,123]. Also by other methods, sulfur-containing metal-binding ligands such as phytochelatins were shown not to be relevant for cadmium or zinc storage or detoxification in *T. caerulescens*. For example, phytochelatin levels were shown to be lower in this plant than in the related non-accumulator *T. arvense* [124], and inhibition of phytochelatin synthesis in hyperaccumulators did not affect their Cd resistance [125]. Nevertheless, metallothionein genes have been found to be highly expressed in *T. caerulescens* [90,126], and differences between *T. caerulescens* and *A. thaliana* metallothioneins have been examined [126,127], but their function remains unclear.

For long-term storage in the vacuoles, hyperaccumulated metals are bound only to weak ligands like organic acids [59,128,129]. So the main detoxification strategy in hyperaccumulators is clearly not binding to strong ligands, but sequestration of the hyperaccumulated heavy metals. Also other genes, e.g., those related to stress responses, are much more highly expressed in hyperaccumulators than in related non-accumulators, but their relevance for hyperaccumulation is not clear.

Only in young, not fully expanded leaves, in stems and petioles as Cd transport organs, as well as in seeds a higher percentage of sulfur ligands was found around Cd [59,123]. In this way, less Cd-accumulating tissues of hyperaccumulators somewhat resemble the situation known from non-accumulator plants, in which most of the Cd is bound to strong ligands, especially phytochelatins (reviewed by Cobbett and Goldsbrough [4]).

4 Biotechnological Use of Cadmium Hyperaccumulators

In all cases of anthropogenic contamination of soils with heavy metals, the highest heavy metal concentrations are found rather close to the surface, although not directly in the uppermost few mm to cm as these are leached by rain like in natural heavy metal sites [130,131]. For this reason, a decontamination of such areas is, in principle,

possible in several ways. The classic way would be the removal of the topsoil and leaching of it in a chemical or microbial way in special facilities. Due to extremely high costs, however, this is only a realistic option for very small (and at the same time economically or socially very important) spots. For larger areas, decontamination by plants seems to be the most attractive option, as on fertile ground (which would be a most attractive kind of site for decontamination as it could be agriculturally valuable) plants should grow well without too much human effort. But it is hotly debated what kind of plants should be used for this task. In principle, three main strategies exist: (i) The use of naturally occurring metal hyperaccumulator plants, probably combined with classical breeding, (ii) the use of high biomass non-accumulator plants, and (iii) the transfer of genes from hyperaccumulator plants to turn originally non-accumulating high biomass plants into high biomass metal hyperaccumulators. We would like to summarize work on these strategies from the perspective of our own work on metal metabolism in plants.

Many natural hyperaccumulators, i.e., plants that actively accumulate several percent of heavy metals in the dry mass of their above-ground parts, have a good potential to be used for phytoremediation, i.e., to extract and remove heavy metals from anthropogenically contaminated soils, which was first proposed by Chaney [132]. Some of them even allow for commercially profitable phytomining, i.e., the extraction of metals from naturally heavy metal rich soils (that are not directly usable as metal ores) with subsequent burning of the plants, the ash of which can be used as a metal ore (first proposed by Baker, Brooks, and Reeves [133]). These applications of metal phytoextraction have been a subject to extensive research (for reviews see [3,31,132,134–141].

For cadmium, the Cd/Zn hyperaccumulator *T. caerulescens* seems to be the best known candidate for phytoremediation. Although it has a rather small biomass of 2–5 $t.ha^{-1}$ [136,142], the extreme bioaccumulation coefficient of its southern French ecotypes [28,29,143] allows it to significantly lower metal concentrations in soil solution [144]. When grown in field conditions, this yields Cd extraction rates high enough for cleaning up moderately Cd-contaminated soils within a few years as tested in the field by Robinson et al. [142], Hammer and Keller [145], and McGrath et al. [146]. Phytoremediation by *T. caerulescens* was furthermore shown to enhance microbial life in soil [147]. The high copper sensitivity of *T. caerulescens*, however, may limit its use; concentrations that occur in multi-contaminated soils were found to strongly inhibit its growth [148]. This might be alleviated by selection of copper-resistant individuals that occur in natural populations of this species [149]. For zinc, the Chinese Cd/Zn hyperaccumulator *Sedum alfredii* may be the most promising candidate for phytoremediation and possibly even commercial phytomining because of its correlation of high zinc accumulation with relatively high biomass [150,151]. In comparison, *T. caerulescens* has a rather low biomass and at high soil zinc concentrations also a low bioaccumulation coefficient [142,143], so that its use in zinc phytoremediation is generally limited to moderate levels of contamination. Indeed, while field trials on moderately contaminated soil were successful [152], those on more heavily Zn-contaminated

soil failed [145]. Metal accumulation by hyperaccumulators may be further enhanced by root-colonising bacteria, as shown for Cd + Zn in *S. alfredii* [153].

In addition to true hyperaccumulator plants, various other plants have been proposed for use in soil phytoremediation. One idea is to use high-biomass plants for absorbing the metals; it is argued that the much higher biomass will yield higher metal extraction per area of land compared to hyperaccumulators, despite the much lower metal content of non-accumulator plants (e.g., [137,138,154]. Those who argue for such an approach, however, mostly ignore that such a strategy would dilute the extracted metal in a much larger amount of toxic biomass compared to hyperaccumulator plants; this biomass would be too toxic for use as compost and would not contain enough metal to make a recycling of the phytoextracted metal feasible (discussed, e.g., by Chaney et al. [155] and Williams [156]). In addition, the bioaccumulation coefficient of metals in non-accumulator plants is usually so low that hundreds of crops would be required for phytoremediation of even a moderately contaminated soil [136,151,155]. Those who argue for this approach because of the low biomass of many hyperaccumulators should also keep in mind the following facts.

(i) The biomass yield of nonaccumulator plants on contaminated soils is reduced by phytotoxicity of the contaminating metal [155,157]; this applies also to the slightly Cd accumulating poplar (*Populus sp.*) that is a popular suggestion for phytoremediation because of its high biomass [158].
(ii) The biomass of hyperaccumulators can be rather easily improved by selecting suitable ecotypes and individuals within the natural population [159,160], breeding [161], and fertilization (2–3 times increase: [159,160,162–164]).
(iii) The metal accumulation of hyperaccumulators can further be optimized by selection. Many recent studies pointed out the more than twentyfold variation of bioaccumulation coefficient for the same metal between ecotypes/populations [28,30,143,165–169]. Furthermore, the accumulation efficiency is not directly correlated to the metal content of the habitat [167], and strong variation of metal bioaccumulation coefficients as well as metal resistance exists even within one population [149,169]. Finally, accumulation is higher on the average moist agricultural land compared to their dry natural habitats [160,170].

In summary, presently it is not the phytoremediation by hyperaccumulators that is a ‘hype’, but the use of non-accumulating plants for this task. The only way that non-hyperaccumulating plant species may become a better alternative would be creating (by genetic engineering or better traditional breeding) metal-accumulating cultivars, or to search for new naturally Cd-accumulating plants with improved properties. Search for high biomass Cd accumulators led to the finding of rather good Cd accumulation by the tropical tree *Averrhoa carambola* and some ecotypes of willow (*Salix alba*) with Cd bioaccumulation coefficients above 10 [158,171], although this is still little compared to the Ganges population of *T. caerulescens* (see Section 3.2).

It is often argued that instead of using natural hyperaccumulators for phytoremediation and phytomining, genetically engineered plants should be used. Looking at the results of classical selection breeding of hyperaccumulators *versus* attempts to create transgenic hyperaccumulators, the former approach appears much more promising, for the following reasons. Research on the mechanisms of hyperaccumulation has revealed that this process involves many different steps in diverse parts of the plant, starting from enhanced uptake into the roots [68] and continuing via enhanced xylem loading [90], translocation to the shoots possibly by transport ligands (e.g., [172]), unloading from the veins and finally sequestration into vacuoles of usually epidermal storage cells [50,51,76,79] as reviewed, e.g., by Küpper and Kroneck [3,141]. Furthermore, individual members of metal transport protein families display vastly different tissue-, age-, and metal nutrition-dependent regulation in the same plant [117]. Therefore, to re-create a hyperaccumulator by genetic engineering, one would have to modify the expression of many genes, in a tissue-specific way and probably at particular stages of plant and leaf ontogenesis. This has not been achieved, not even in an approximation, in any study so far (reviewed, e.g., by Chaney et al. [140]). Therefore, it is not surprising that in all attempts of creating hyperaccumulators by genetic engineering at best a few times enhancement of metal accumulation compared to the original non-accumulator wild-type was achieved, while true (natural) hyperaccumulators usually have hundreds of times higher metal bioaccumulation coefficients than those non-accumulators (see Section 3.2. and for reviews, e.g., [3,140,141]). And such transgenics are not useful to apply, for the same reasons as explained for wild-type non-accumulators. Unless someone finds a general "switch gene" that leads to the changed expression pattern of all the other genes involved in hyperaccumulation, transgenic plants that really extract as much metal per hectare as hyperaccumulators will remain science fiction.

In contrast, field trials have shown that the biomass of natural hyperaccumulators can be dramatically increased by addition of fertilizer, natural selection, and classical breeding to reach levels that are economically attractive (reviewed by Chaney et al. [139]). As a source for selecting species that are suitable for a specific phytoextraction tasks, conservation of metallophyte biodiversity is of prime importance as outlined by Whiting et al. [173].

5 Outlook

This chapter summarized recent advances and earlier important works dealing with the accumulation of cadmium in plants, with a special focus on Cd hyperaccumulators. As described in detail above, a lot of progress has been made in

(i) the analysis of the uptake of Cd from soils into plants, including uptake from contaminated soils into crops and hyperaccumulator plants in terms of phytoremediation.

(ii) the investigation of mechanisms involved in the hyperaccumulation phenotype, including the analysis of tissue- and cell-level metal sequestration patterns and screening of genes that are involved in species- and ecotype-specific difference in Cd accumulation and resistance.

Based on these advances, several attempts have been made to improve plants for phytoremediation, and to modify the metal uptake into crops. The at best partial success of the latter efforts, however, have shown that many questions concerning Cd (and other metals as well) accumulation still remain open and have to be answered before the aims of making better crop plants, improving phytoremediation technology, and understanding general principles of metal metabolism, can be fully reached. In our opinion, based on what we described in this chapter, future efforts should put a strong focus on

(i) the biochemical/biophysical mechanism of function of metal transport proteins, as these proteins are clearly the decisive factor in differential metalaccumulation, but knowledge about almost all of them is still restricted to knowing their genes and knowing effects of their knockout and/or over-expression.
(ii) the regulation of metal transport genes dependent on the nature and concentration of the accumulated metal, on the age of the plant, the age and type of the tissue. Like the previous point, this will greatly help in understanding general principles of metal metabolism, and at the same time generate a basis for the next point concerning phytoremediation.
(iii) the breeding of improved variants of species that already have been demonstrated to be practically useful for phytoremediation, i.e., mainly *T. caerulescens* for Cd and *S. alfredii* for zinc.

Abbreviations

ABC transporters	ATB binding casette transporters
ATP	adenosine 5'-triphosphate
CDF	cation diffusion facilitator
CAX	cation exchanger
E_A	energy of activation in kJ.mol^{-1}
EXAFS	extended X-ray absorption fine structure
HMA	heavy metal ATPase
IRT transporters	iron regulated transporters
mRNA	messenger RNA
NMR	nuclear magnetic resonance
NRAMP	natural resistance-associated macrophage proteins
QISH	quantitative *in situ* hybridization
XANES	X-ray absorption near edge structure
XAS	X-ray absorption spectroscopy

Acknowledgments The authors would like to thank the Landesstiftung Baden-Württemberg, the Deutsche Forschungsgemeinschaft (DFG, project KU 1495/11-1), the Alexander von Humboldt Stiftung, the Deutscher Akademischer Austauschdienst (DAAD), the Schweizer Nationalfonds (SNF, Grant No. PP002-119106/1 to Eva Freisinger), and the University of Konstanz for financial support.

References

1. A. Baumann, *Landwirtschaftliche Versuchs-Stationen* **1885**, *31*, 1–53.
2. M. N. V. Prasad, J. Hagemeyer, Eds, *Heavy Metal Stress in Plants: From Molecules to Ecosystems*, Springer, Berlin, Heidelberg, 1999.
3. H. Küpper, P. M. H. Kroneck, in *Metal Ions in Biological Systems*, Volume 44, Eds A. Sigel, H. Sigel, R. K. O. Sigel, Marcel Dekker, Inc., New York, 2005, pp. 97–142.
4. C. Cobbett, P. Goldsbrough, *Ann. Rev. Plant Biol.* **2002**, *53*, 159–182.
5. A. J. M. Baker, *J. Plant Nutr.* **1981**, *3*, 643–654.
6. A. Schützendübel, P. Schwanz, T. Teichmann, K. Gross, R. Langenfeld-Heyser, D. L. Godbold, A. Polle, *Plant Physiol.* **2001**, *127*, 887–898.
7. N. A. L. M. van Hoof, P. L. M. Koevoets, H. W. J. Hakvoort, W. M. Ten Bookum, H. Schat, J. A. C. Verkleij, W. H. O. Ernst, *Physiol. Plant.* **2001**, *113*, 225–232.
8. M. Migocka, A. Papiernak, E. Kosatka, G. Kłobus, *J. Exper. Bot.* **2011**, *62*, 4903–4916.
9. L. Li, H. Zengyong, G. K. Pandey, T. Tsuchiya, and S. Luan, *J. Biol. Chem.* **2002**, *277*, 5360–5368.
10. Y.E. Choi, E. Harada, M. Wada, H. Tsuboi, Y. Morita, T. Kusano, H. Sano, *Planta* **2001**, *213*, 45–50.
11. X. Yang, V.C. Baligar, D. C. Mertens, R. B. Clark, *J. Environ. Sci. Health* **1995**, *B30*, 569–583.
12. S. Wei, Q Zhou, X. Wang, *Environ. Int.* **2005**, *31*, 829–834.
13. B. G. Lottermoser, H. J. Glass, C. N. Page, *Ecol. Engin.* **2011**, *37*, 1249–1253.
14. H. Yu, J. Wang, W. Fang, J. Yuan, Z. Yang, *Sci. Total Environ.* **2006**, *370*, 302–309.
15. W. Liu, Q. Zhou, J. An, Y. Sun, R. Liu, *J. Hazard. Mat.* **2010**, *173*, 737–743.
16. D. Ci, D. Jiang, S. Li, B. Wollenweber, T. Dai, W. Cao, *Acta Physiol. Plant.* **2012**, *34*, 191–202.
17. D. J. H. Phillips, *Environ. Pollut.* **1977**, *13*, 281–317.
18. A. Melhuus, K.L. Seip, S. Myklestad, *Environ. Pollut.* **1978**, *15*, 101–107.
19. T. Sawidis, M. K. Chettri, G. A. Zachariadis, J. A. Stratis, *Ecotoxicol. Environ. Safety* **1995**, *32*, 73–80.
20. G. Bonanno, R. LoGiudice, *Ecol. Indic.***2010**, *10*, 639–645.
21. M. I. Rucandino, M. D. Petit-Domínguez, C. Fidalgo-Hijano, R. García Giménez, *Environ. Sci. Pollut. Res.* **2011**, *18*, 51–63.
22. L. Folkeson, *Water Air Soil Pollut.* **1979**, *11*, 253–260.
23. P. Guilizzoni, *Aquatic Botany* **1991**, *41*, 87–109.
24. S. Haritonidis, P. Malea, *Environ. Pollut.* **1999**, *104*, 365–372.
25. L. M. Stout, E. N. Dodova, J. F. Tyson, K. Nüsslein, *Water Res.* **2010**, *44*, 4970–4979.
26. J. Sachs, *Handbuch der Experimental-Physiologie der Pflanzen*, Verlag Wilhelm Engelmann, Leipzig, 1865, pp. 153–154, §47.
27. R. R. Brooks, *Plant Soil* **1977**, *48*, 541–544.
28. E. Lombi, F. J. Zhao, S. J. Dunham, S. P. McGrath, *New Phytol.* **2000**, *145*, 11–20.
29. J. Escarré, C. Lefèbvre, S. Raboyeau, A. Dossantos, W. Gruber, J. C. C. Marel, H. Frérot, N. Noret, S. Mahieu, C. Collin, F. van Oort, *Water, Air, Soil Pollut.* **2011**, *216*, 485–504.
30. N. Roosens, N. Verbruggen, P. Meerts, P. Ximénez-Embún, J. A. C. Smith, *Plant Cell Environ.* **2003**, *26*, 1657–1672.

31. A. J. M. Baker, S. P. McGrath, R. D. Reeves, J. A. C. Smith, in *Phytoremediation of Contaminated Soil and Water*, Eds N. Terry, G. Bañuelos, Lewis Publishers, Boca Raton, FL, 2000, pp. 85–107.
32. R. S. Boyd, S. N. Martens, *Oikos* **1994**, *70*, 21–25.
33. S. N. Martens and R. S. Boyd, *Oecologia* **1994**, *98*, 379–84.
34. R. S. Boyd, M. A. Davis, M. A. Wall, K. Balkwill, *Chemoecology* **2002**, *12*, 91–97.
35. B. Hanson, G. F. Garifullina, S. D. Lindblom, A. Wangeline, A. Ackley, K. Kramer, A. P. Norton, C. B. Lawrence, E. A. H. Pilon-Smits, *New Phytol.* **2003**, *159*, 461–469.
36. E. M. Jhee, R. S. Boyd, M. D. Eubanks, *New Phytol.***2005**, *168*, 331–343.
37. M. Palomino, P. G. Kennedy, E. L. Simms, *Plant Soil* **2007**, *293*, 189–195.
38. R. S. Boyd, *Plant Soil* **2007**, *293*, 153–176.
39. J. A. Pollard, A. J. M. Baker, *New Phytol.* **1997**, *135*, 655–658.
40. E. M. Jhee, K. L. Dandridge, A. M. Christy, A. J. Pollard, *Chemoecology*, **1999**, *9*, 93–95.
41. H. Fones, C. A. R. Davis, A. Rico, F. Fang, J. A. Smith, G. M. Preston, *PLoS Pathogens* **2010**, *6*, e1001093, 1–13.
42. R. F. Jiang, D. Y. Ma, F. J. Zhao, S. P. McGrath, *New Phytol.* **2005**, *167*, 805–814.
43. E. M. Jhee, R. S. Boyd, M. D. Eubanks, *J. Chem. Ecol.* **2006**, *32*, 239–259.
44. C. M. Coleman, R. S. Boyd, M. D. Eubanks, *J. Chem. Ecol.* **2005**, *31*, 1669–1681.
45. S. B. Huitson, M. R. Macnair, *New Phytol.* **2003**, *159*, 453–459.
46. N. Noret, P. Meerts, R. Tolra, C. Poschenrieder, J. Barcelo, J. Escarre, *New Phytol.* **2005**, *165*, 763–772.
47. A. J. Pollard, *New Phytol.***2000**, *146*, 179–181.
48. R. S. Boyd, T. Jaffre, *South Afric. J. Sci.* **2001**, *97*, 535–538.
49. Z. G. Shen, F. J. Zhao, S. P. McGrath, *Plant Cell Environ.* **1997**, *20*, 898–906.
50. H. Küpper, F. Zhao, S. P. McGrath, *Plant Physiol.* **1999**, *119*, 305–311.
51. H. Küpper, E. Lombi, F. J. Zhao, G. Wieshammer, S. P. McGrath, *J. Exper. Bot.* **2001**, 52, 2991–2300.
52. K. Perronnet, C. Schwartz, E. Gérard, L. Morel, *Plant Soil* **2000**, *227*, 257–263.
53. S. N. Whiting, P. M. Neumann, A. J. M. Baker, *Plant Cell Environ.* **2003**, *26*, 351–360.
54. M. Q. Liu, J. Yanai, R. F. Jiang, F. Zhang, S. P. McGrath, F. J. Zhao, *Chemosphere* **2008**, *71*, 1276–1283.
55. T. W. Lane, F. M. M. Morel, *Proc. Nat. Acad. Sci. USA* **2000**, *97*, 4627–4631.
56. Y. Xu, L. Feng, P. D. Jeffrey, Y. Shi, F. M. M. Morel, *Nature* **2008**, *452*, 56–61.
57. E. Himelblau, R. M. Amasino, *J. Plant Physiol.* **2001**, *158*, 1317–1323.
58. K. Perronnet, C. Schwartz, J. L. Morel, *Plant Soil* **2003**, *249*, 19–25.
59. H. Küpper, A. Mijovilovich, W. Meyer-Klaucke, P. M. H. Kroneck, *Plant Physiol.* **2004**, *134*, 748–757.
60. S. N. Whiting, J. R. Leake, S. P. McGrath, A. J. M. Baker, *New Phytol.* **2000**, *145*, 199–210.
61. K. Vogel-Mikuš, P. Pongrac, P. Kump, M. Nečemer, M. Regvar, *Environ. Pollut.* **2006***, 139,* 362–371.
62. U. Ahonen-Jonnarth, R. D. Finlay, *Plant Soil* **2001**, *236*, 129–138.
63. E. Lombi, F. J. Zhao, S. P. McGrath, S.D. Young, G. A. Sacchi, *New Phytol.* **2001**, **149**, 53–60.
64. F. J. Zhao, R. E. Hamon, E. Lombi, M. J. McLaughlin, S. P. McGrath, *J. Exper. Bot.* **2002**, *53*, 535–543.
65. A. Papoyan, M. Pineros, L. V. Kochian, *New Phytol.* **2007**, *175*, 51–58.
66. E. Lombi, K. L. Tearall, J. R. Howarth, F. J. Zhao, M. J. Hawkesford, S. P. McGrath, *Plant Physiol.* **2002**, *128*, 1359–1367.
67. A. G. L. Assunção, P. Bleeker, W. M. ten Bookum, R. Vooijs, H. Schat, *Plant Soil* **2008**, *303*, 289–299.
68. M. M. Lasat, A. J. M. Baker, L. V. Kochian, *Plant Physiol.* **1996**, *112*, 1715–1722.
69. M. M. Lasat, A. J. M. Baker, L. V. Kochian, *Plant Physiol.* **1998**, *118*, 875–883.
70. F. J. Zhao, R. F. Jiang, S. J. Dunham, S. P. McGrath, *New Phytol.* **2006**, *172*, 646–654.

71. P. J. White, S. N. Whiting, A. J. M. Baker, M. R. Broadley, *New Phytol.* **2002**, *153*, 201–207.
72. S. Uruguchi, S. Mori, M. Kuramata, A. Kawasaki, T. Aarao, S. Ishikawa, *J. Exper. Bot.* **2009**, *60*, 2677–2688.
73. W. H. O. Ernst, J. A. C. Verkleij, H. Schat, *Act. Bot. Neerland.* **1992**, *41*, 229–248.
74. D. N. De, *Plant Cell Vacuoles,* CSIRO Publishing, Collingwood, Australia, 2000.
75. M. Wink, *J. Exper. Bot.* **1993**, *44*, 231–246.
76. B. Frey, C. Keller, K. Zierold, R. Schulin, *Plant Cell Envi.* **2000**, *23*, 675–687.
77. S. D. Bidwell, S. A. Crawford, I. E. Woodrow, J. Summer-Knudsen, A. T. Marshall, *Plant Cell Environ.* **2004**, *27*, 705–716.
78. C. L. Broadhurst, R. L. Chaney, J. S. Angle, E. F. Erbe, T. K. Maugel, *Plant Soil* **2004**, *265*, 225–242.
79. B. Leitenmaier, H. Küpper, *Plant Cell Environ.* **2011**, *34*, 208–219.
80. A. N. Chardonnens, W. M. ten Bookum, L. D. J. Kuijper, J. A. C. Verkleij, W. H. O. Ernst, *Physiol. Plant.* **1998**, *104*, 75–80.
81. G. K. Psaras, T. H. Constantinidis, B. Cotsopoulos, Y. Manetas, *Ann. Bot.* **2000**, *86*, 73–78.
82. G. K. Psaras, Y. Manetas, *Ann. Bot.* **2001**, *88*, 513–516.
83. A. J. Karley, R. A. Leigh, D. Sanders, *Trends Plant Sci.* **2000**, *5*, 465–470.
84. H. Küpper, E. Lombi, F. J. Zhao, S. P. McGrath, *Planta* **2000**, *212*, 75–84.
85. X. E. Yang, X. X. Long, H. B. He, Z. L. He, D. V. Calvert, P. J. Stofella, *Plant Soil* **2004**, *259*, 181–189.
86. S. Tian, L. Lu, J. Labavitch, X. Yang, Z. He, H. Hu, R. Sarangi, M. Newville, J. Commisso, P. Brown, *Plant Physiol.* **2011**, *157*, 1914–1925.
87. N. S. Pence, P. B. Larsen, S. D. Ebbs, M. M. Lasat, D. L. D. Letham, D. F. Garvin, D. Eide, L. V. Kochian, *Proc. Natl. Acad. Sci. USA* **2000**, *97*, 4956–4960.
88. A. G. L. Assunção, P. D. A. Costa Martins, S. De Folter, R. Vooijs, H. Schat, M. G. M. Aarts, *Plant Cell Environ.* **2001**, *24*, 217–226.
89. M. Becher, I. N. Talke, L. Krall, U. Krämer, *The Plant Journal* **2004**, *37*, 251–268.
90. A. Papoyan, L. V. Kochian, *Plant Physiol.* **2004**, *136*, 3814–3823.
91. M. Weber, E. Harada, C. Vess, E. von Roepenack-Lahaye, S. Clemens, *The Plant Journal* **2004**, *37*, 269–281.
92. J. P. Hammond, H. C. Bowen, P. J. White, V. Mills, K. A. Pyke, A. J. M. Baker, S. N. Whiting, S. T. May, M. R. Broadley, *New Phytol.* **2006**, *170*, 239–260.
93. I. N. Talke, M. Hanikenne, U. Krämer, *Plant Physiol.* **2006**, *142*, 148–167.
94. J. E. van de Mortel, L. A. Villanueva, H. Schat, J. Kwekkeboom, S. Coughlan, P. D. Moerland, E. V. L. van Themaat, M. Koornneef, M. G. M. Aarts, *Plant Physiol.* **2006**, *142*, 1127–1147.
95. M. Hanikenne, I. N. Talke, M. J. Haydon, C. Lanz, A. Nolte, P. Motte, J. Kroymann, D. Weigel, U. Krämer, *Nature* **2008**, *453*, 391–396.
96. N. Verbruggen, C. Hermans, H. Schat, *New Phytol.* **2009**, *181*, 759–776.
97. D. E. Salt, G. J. Wagner, *J. Biol. Chem.* **1993**, *268*, 12297–12302.
98. C. Bernard, N. Roosens, P. Czernic, M. Lebrun, N. Verbruggen, *FEBS Lett.* **2004**, *569*, 140–148.
99. S. O'Lochlainn, H. C. Bowen, R. G. Fray, J. P. Hammond, G. J. King, P. J. White, N. S. Graham, M. R. Broadley, *PLoS One* **2011**, *6*, e17814.
100. A. Parameswaran, B. Leitenmaier, M. Yang, P. M. H. Kroneck, W. Welte, G. Lutz, A. Papoyan, L. V. Kochian, H. Küpper, *Biochem. Biophys. Res. Comm.* **2007**, *363*, 51–56.
101. B. Leitenmaier, A. Witt, A. Witzke, A. Stemke, W. Meyer-Klaucke, P. M. H. Kroneck, H. Küpper, *BBA Biomembranes* **2011,** *1808*, 2591–2599.
102. J. L. Hall, L. E. Williams, *J. Exp. Bot.* **2003**, *54*, 2601–2613.
103. B. J. Van der Zaal, L. W. Neuteboom, J. E. Pinas, A. N. Chardonnens, H. Schat, J. A. C. Verkleij, P. J. J. Hooykaas, *Plant Physiol.***1999**, 119, 1047–1055.
104. B. Elbaz, N. Shoshani-Knaani, O. David-Assael, T. Mizrachy-Dagri, K. Mizrahi, H. Saul, E. Brook, I. Berezin, O. Shaul, *Plant Cell Environ.* **2006**, *29*, 1179–1190.

105. A.G. Desbrosses-Fonrouge, K. Voigt, A. Schroder, S. Arrivault, S. Thomine, U. Krämer, *FEBS Lett.* **2005**, *579*, 4165–4174.
106. M. J. Haydon, C. S. Cobbett, *Plant Physiol.* **2007**, *143*, 1705–1719.
107. M. Morel, J. Crouzet, A. Gravot, P. Auroy, N. Leonhardt, A. Vavasseur, P. Richaud, *Plant Physiol.* **2009**, *149*, 894–904.
108. D. B. Dräger, A. G. Desbrosses-Fonrouge, C. Krach, A. N. Chardonnens, R. C. Meyer, P. Saumitou-Laprade, U. Krämer, *The Plant Journal* **2004**, *39*, 425–439.
109. D. Ueno, M. J. Millner, N. Yamaji, K. Yokosho, E. Koyama, M. C. Zambrono, M. Kaskie, S. Ebbs, L. V. Kochian, J. F. Ma, *The Plant Journal* **2011**, *66*, 852–862.
110. D. Ueno, N. Yamaji, I. Kono, C. F. Huang, T. Ando, M. Yano, J. F. Ma, *PNAS* **2010**, *107*, 16500–16505.
111. D. Ueno, E. Koyama, N. Yamaji, J. F. Ma, *J. Exper. Bot.***2011**, *62*, 2265–2272.
112. R. J. F. J. Oomen, J. Wu, F. Lelièvre, S. Blanchet, P. Richaud, H. Barbier-Brygoo, M. G. M. Aarts, S. Thomine, *New Phytol.* **2008**, *181*, 637–650.
113. W. Wei, T. Chai, Y. Zhang, L. Han, J. Xu, Z. Guan, *Mol. Biotechnol.* **2009**, *41*, 15–21.
114. R. Takahashi, Y. Ishimaru, T. Senoura, H. Shimo, S. Ishikawa, T. Arao, H. Nakanishi, N. K. Nishizawa, *J. Exper. Bot.* **2011**, *62*, 4843–4850.
115. D. G. Mendoza-Cózatl, Z. Zhai, T. O. Jobe, G. Z. Akmakjian, W. Y. Song, O. Limbo, M. R. Russell, V. I. Kozlovskyy, E. Martinoia, O. K. Vatamaniuk, P. Russell, J. I. Schroeder, *J. Biol. Chem.* **2010**, *285*, 40416–40426.
116. H. Küpper, L. O. Seib, M. Sivaguru, O. A. Hoekenga, L. V. Kochian, *The Plant Journal* **2007**, *50*, 159–187.
117. H. Küpper, L. V. Kochian, *New Phytol.* **2010**, *185*, 114–129.
118. J. Wu, F. J. Zhao, A. Ghandilyan, B. Logoteta, M. O. Guzman, H. Schat, X. Wang, M. G. M. Aarts, *Plant Soil* **2009**, *325*, 79–95.
119. J. L. Gardea-Torresday, J. R. Peralta-Videa, G. de la Rosa, J. G. Parsons, *Coord. Chem. Rev.* **2005**, *249*, 1797–1810.
120. S. Saraswat, J. P. N. Rai, *Rev. Environ. Biotechnol.* **2011**, *10*, 327–339.
121. D. Ueno, J. F. Ma, T. Iwashita, F. J. Zhao, S. P. McGrath, *Planta* **2005**, *221*, 928–936.
122. N. Fukuda, A. Hokura, N. Kitajima, Y. Terada, H. Saito, T. Abe, I. Nakai, *J. Anal. At. Spectrom.* **2008**, *23*, 1068–1075.
123. K. Vogel-Mikuš, I. Arčon, A. Kodre, *Plant Soil*, **2010**, *331*, 439–451.
124. S. Ebbs, I. Lau, B. Ahner, L. V. Kochian, *Planta* **2002**, *214*, 635–640.
125. H. Schat, M. Llugany, R. Vooijs, J. Hartley-Whitaker, P. M. Bleeker, *J. Exper. Bot.* **2002**, *53*, 2381–2392.
126. N. H. Roosens, C. Bernard, R. Leplae, N. Verbruggen, *FEBS Lett.* **2004**, *577*, 9–16.
127. N. H. Roosens, R. Leplae, C. Bernard, N. Verbruggen, *Planta* **2005**, *222*, 716–729.
128. D. E. Salt, R. C. Prince, A. J. M. Baker, I. Raskin, I. J. Pickering, *Environ. Sci. Technol.* **1999**, *33*, 712–717.
129. H. Küpper, A. Mijovilovich, B. Götz, F. C. Küpper, W. Meyer-Klaucke, *Plant Physiol.*, **2009**, *151*, 702–714.
130. M. B. McBride, K. A. Barrett, C. E. Martinez, *Water Air Soil Pollut.* **2005**, *171*, 67–80.
131. T. Mitani, M. Ogawa, *J. Environ. Sci. Health* **1998**, *A33*: 1569–1581.
132. R. L. Chaney, in *Land Treatment of Hazardous Wastes*, Eds J. E. Parr, P. B. Marsh, J. M. Kla, Noyes Data Corp., Park Ridge, 1983, pp. 50–76.
133. A. J. M. Baker, R. R. Brooks, R. Reeves, *New Scientist* **1988**, *117*, 44–48.
134. A. J. M. Baker, R. R. Brooks, *Biorecovery* **1989**, *1*, 81–126.
135. S. P. McGrath, C. M. D. Sidoli, A. J. M. Baker, R. D. Reeves, in *Integrated Soil and Sediment Research: A Basis for Proper Protection*, Eds H. J. P. Eijsackers, T. Hamers, Kluwer Academic Publishers, Dordrecht, 1993, pp. 673–677.
136. S. P. McGrath, F. J. Zhao, *Curr. Opin. Biotechnol.* **2003**, *14*, 277–282.
137. D. E. Salt, M. Blaylock, P. B. A. Nanda Kumar, V. Dushenkov, B. D. Ensley, I. Chet, I. Raskin, *Biotechnology* **1995**, *13*, 468–474.

138. D. E. Salt, R. D. Smith, I. Raskin, *Annu. Rev. Plant Physiol. Plant Mol. Biol.* **1998**, *49*, 643–668.
139. R. L. Chaney, J. S. Angle, M. S. McIntosh, R. D. Reeves, Y. M. Li, E. P. Brewer, K. Y. Chen, R.J. Roseberg, H. Perner, E. C. Synkowski, C. L. Broadhurst, S. Wang, A. J. M. Baker, *Z. Naturforsch.* **2005**, *60c*, 190–198.
140. R. L. Chaney, J. S. Angle, C. L. Broadhurst, C. A. Peters, R. V. Tappero, D. L. Sparks, *J. Environ. Qual.* **2007**, *36*, 1429–1443.
141. H. Küpper, P. M. H. Kroneck, in *Metal Ions in Life Sciences*, Volume 2, Eds A. Sigel, H. Sigel, R. K. O. Sigel, Wiley, Chichester, 2007, pp. 31–62.
142. B. H. Robinson, M. Leblanc, D. Petit, R. R. Brooks, J. H. Kirkman, P. E. H. Gregg, *Plant Soil* **1998**, *203*, 47–56.
143. F.J. Zhao, E. Lombi, S. P. McGrath, *Plant Soil* **2003**, *249*, 37–43.
144. B. Knight, F. J. Zhao, S. P. McGrath, Z. G. Shen, *Plant Soil*, **1997**, *197*, 71–78.
145. D. Hammer, C. Keller, *Soil Use Management* **2003**, *19*, 144–149.
146. S. P. McGrath, E. Lombi, C. W. Gray, N. Caille, S. J. Dunham, F. J. Zhao, *Env. Pollut.* **2006**, *141*, 115–125.
147. L. Epelde, J. M. Becerril, J. Hernández-Allica, O. Barrutia, C. Garbisu, *Appl. Soil Ecol.* **2008**, *39*, 299–310.
148. D. J. Walker, M. P. Bernal, *Water, Air, Soil Pollut.* **2004**, *151*, 361–372.
149. A. Mijovilovich, B. Leitenmaier, W. Meyer-Klauck, P. M. H. Kroneck, B. Götz, H. Küpper, *Plant Physiol.***2009**, *151*, 715–731.
150. X. X. Long, X. E. Yang, Z. Q. Ye, W. Z. Ni, W. Y. Shi, *Acta Botan. Sin.* **2002**, *44*, 152–157.
151. H. B. Ye, X. E. Yang, B. He, X. X. Long, W. Y. Shi, *Acta Botan. Sin.* **2003**, *45*, 1030–1036.
152. A. J. M. Baker, S. P. McGrath, C. M. D. Sidoli, R. D. Reeves, *Resources, Conservation, Recycling* **1994**, *11*, 41–49.
153. W. C. Li, Z. H. Ye, M. H. Wong, *J. Exper. Bot.* **2007**, *58*, 4173–4182.
154. I. D. Pulford, C. Watson, *Environ.t Int.* **2003**, *29*, 529–540.
155. R. L. Chaney, M. Malik, Y. M. Li, S. L. Brown, E. P. Brewer, J. S. Angle, A. J. M. Baker, *Curr. Opin. Biotechnol.* **1997**, *8*, 279–284.
156. J. B. Williams, *Crit. Rev. Plant Sci.* **2002**, *21*, 607–635.
157. S. Ebbs, L. V. Kochian, *J. Environ. Qual.***1997**, *26*, 776–781.
158. M. Zacchini, F. Pietrini, G. S. Mugnozza, V. Iori, L. Pietrosanti, A. Massaci, *Water Air Soil Pollut.* **2009**, *197*, 23–34.
159. Y.M. Li, R. Chaney, E. Brewer, R. Roseberg, J. S. Angle, A. Baker, R. Reeves, J. Nelkin, *Plant Soil* **2003**, *249*, 107–115.
160. C. Schwartz, G. Echevarria, J. L. Morel, *Plant Soil* **2003**, *249*, 27–35.
161. E. P. Brewer, J. A. Saunders, J. S. Angle, R. L. Chaney, M. S. McIntosh, *Theor. Appl. Genet.* **1999**, *99*, 761–771.
162. F. A. Bennett, E. K. Tyler, R. R. Brooks, P. E. H. Gregg, R. B. Stewart, in *Plants that Hyperaccumulate Heavy Metals*, Ed R. R. Brooks, CAB International, Wallingford, 1998, pp. 249–259.
163. S. P. McGrath, S. J. Dunham, R. L. Correll, in *Phytoremediation of Contaminated Soil and Water*, Eds N. Terry, G. Bañuelos, Lewis Publishers, Boca Raton, 2000, pp. 109–128.
164. R. R. Brooks, B. H. Robinson, A. W. Howes, A. Chiarucci, *South Afr. J. Sci.* **2001**, *97*, 558–560.
165. P. Meerts, N. Van Isacker, *Plant Ecol.* **1997**, *133*, 221–231.
166. V. Bert, M. R. Macnair, P. de Laguérie, P. Saumitou-Laprade, D. Petit, *New Phytol.* **2000**, *146*, 225–233.
167. V. Bert, I. Bonnin, P. Saumitou-Laprade, P. de Laguérie, D. Petit, *New Phytol.* **2002**, *155*, 47–57.
168. J. Escarré, C. Lefèbvre, W. Gruber, M. Leblanc, J. Lepart, Y. Rivière, B. Delay, *New Phytol.* **2000**, *145*, 429–437.
169. M. R. Macnair, *New Phytol.* **2002**, *155*, 59–66.

170. J. S. Angle, A. J. M. Baker, S. N. Whiting, R. L. Chaney, *Plant Soil* **2003**, *256*, 325–332.
171. J. T. Li, B. Liao, C. Y. Lan, Z. H. E. Ye, A. J. M. Baker, W. S. Shu, *J. Environ. Qual.* **2010**, *39*, 1262–1268.
172. A. Trampczynska, H. Küpper, W. Meyer-Klaucke, H. Schmidt, S. Clemens, *Metallomics* **2010**, *2*, 57–66.
173. S. N. Whiting, R. D. Reeves, D. Richards, M. S. Johnson, J. A. Cooke, F. Malaisse, A. Paton, J. A. C. Smith, J. S. Angle, R. L. Chaney, R. Ginocchio, T. Jaffre, R. Johns, T. McIntyre, O. W. Purvis, D. E. Salt, H. Schat, F. J. Zhao, A. J. M. Baker, *Restoration Ecology* **2004**, *12*, 106–116.

Chapter 13
Cadmium Toxicity in Plants

Elisa Andresen and Hendrik Küpper

Contents

ABSTRACT 395
1 INTRODUCTION: ENVIRONMENTAL RELEVANCE OF CADMIUM TOXICITY IN PLANTS 396
1.1 Naturally Cadmium-Rich Habitats 396
1.2 Anthropogenic Cadmium Pollution of Soil and Water 396
2 CADMIUM TOXICITY TO ROOTS 397
3 CADMIUM-INDUCED INHIBITION OF THE PHOTOSYNTHETIC APPARATUS 399
4 CADMIUM-INDUCED OXIDATIVE STRESS 402
5 GENOTOXICITY OF CADMIUM IN PLANTS 405
6 OUTLOOK 407
ABBREVIATIONS 408
ACKNOWLEDGMENTS 409
REFERENCES 409

Abstract Cadmium is an important pollutant in the environment, toxic to most organisms and a potential threat to human health: Crops and other plants take up Cd from the soil or water and may enrich it in their roots and shoots. In this review, we summarize natural and anthropogenic reasons for the occurrence of Cd toxicity, and evaluate the observed phytotoxic effects of plants growing in Cd-supplemented soil or nutrient solution. Cd-induced effects include oxidative stress, genotoxicity, inhibition of the photosynthetic apparatus, and inhibition of root metabolism. We explain proposed and possible interactions between these modes of toxicity. While discussing recent and older studies, we further emphasize the environmental relevance of the experiments and the physiological response of the plant.

E. Andresen • H. Küpper (✉)
Fachbereich Biologie, Universität Konstanz, D-78457 Konstanz, Germany
e-mail: hendrik.kuepper@uni-konstanz.de

A. Sigel, H. Sigel, and R.K.O. Sigel (eds.), *Cadmium: From Toxicity to Essentiality*, Metal Ions in Life Sciences 11, DOI 10.1007/978-94-007-5179-8_13,

Keywords cadmium • cytotoxicity • genotoxocity • oxidative stress • photosynthesis inhibition • substitution of essential metals

1 Introduction: Environmental Relevance of Cadmium Toxicity in Plants

Cadmium has been found to be a micronutrient for an ecotype of *Thalassiosira weissflogii*, a marine alga [1] and many other heavy metals such as copper, nickel and zinc are well-known for a long time already as essential trace elements for plants. While general aspects of the entry of Cd into the environment are dealt with in detail in Chapter 2 of this book [2], we will summarize here in Sections 1.1 and 1.2 a few plant-specific aspects before discussing mechanisms of Cd toxicity in plants.

1.1 Naturally Cadmium-Rich Habitats

Toxic heavy metal concentrations can have natural reasons; naturally heavy metal-rich soils are found in various locations around the world where metal ores come to the surface and decay due to weathering. A few examples of such locations are the Katangan copper belt in Kongo and Zaire [3,4], nickel-rich serpentine soils in Cuba [5], North America [6] as well as Sulawesi and New Caledonia [7] and some zinc and cadmium sites in Europe [8]. While these locations are usually not regarded as agriculturally relevant, and usually no attempts are made to detoxify them (as it would be futile), the plants growing on them still have to detoxify the stream of nutrients they take up from such soils.

1.2 Anthropogenic Cadmium Pollution of Soil and Water

Cadmium can occur in high concentrations that are detrimental, in many cases even lethal to most plant species, as a result of various human activities. Anthropogenic contaminations can have various reasons, and can be found in many countries of the world although a common misconception is that this is mainly a problem for poor countries. The most obvious reason for anthropogenic heavy metal contamination of soils is the presence of ore mining or refining industry nearby, where emissions of dust particles as well as leakage of contaminated water (e.g., from dumps and storages) are the main causes of environmental pollution (e.g., [9–11]). Another reason for heavy metal pollution is the application of mineral fertilizers, as these often contain cadmium as contaminant [12]. Also sewage sludge is usually not a good fertilizer for the same reason [13]. Another source of metal pollution in heavily industrialized countries like Germany is car traffic. The best known case

is lead that was banned from fuel many years ago and that was more toxic to animals than to plants (plants hardly take it up). Less known, but more toxic, is the release of cadmium from car tires, which leads to significantly enhanced cadmium levels along busy roads [14,15]).

While all these are examples of severe environmental pollution, comparing the Cd concentrations occurring under such conditions with those used in published articles about Cd toxicity reveals that in most laboratory studies far too high, environmentally irrelevant, Cd levels were used. Unfortunately, this is common practice for several technical reasons:

(i) Many authors want to observe effects within a short time period (hours or at most a few days), and therefore they increase Cd concentrations to a level where effects can be seen already within such short periods.
(ii) Many studies on aqueous plants and hydroponics use nutrient solutions with EDTA as a complexing agent for iron. Cd may displace Fe from EDTA, leading to diminished Cd bioavailability (seemingly increased resistance of the plants) but also artefactual iron deficiency as Fe(III) without a ligand is hardly soluble.
(iii) Often the long-term toxicity of Cd is not limited by the Cd concentration, but by the total amount of Cd because too small (compared to environmental conditions) volumes of nutrient solution or soil per plant are used, so that Cd concentration decreases due to uptake into the plant.

For these reasons, it often remains questionable whether the reported effects would really occur in plants growing in a Cd-polluted environment. In the following, we try to point out such problems when discussing the various suggested effects of Cd toxicity. Further, when interpreting the results one has to keep in mind that the threshold for toxic effects will be different depending not only on the organism (higher plants, different phyla of algae) and its lifestyle (terrestrial, aquatic) as everyone would expect, but sometimes even on the sex of the organism. The latter surprising finding was recently reported for poplar, where females were much more sensitive to Cd toxicity than males [16].

2 Cadmium Toxicity to Roots

In terrestrial plants, roots are by far the most important organ for the uptake of metals including cadmium but also for various non-metal nutrients. After a non-specific binding to the cell wall, metal ions are taken up energy-dependend across the plasma membrane. Therefore, roots are the first organs to be affected by Cd present in soil and in terrestrial plants cadmium damage to roots can, in principle, strongly affect the metabolism of the whole plant. For this reason, effects of Cd on shoots of terrestrial plants could be a consequence of damage to the roots, so that such interactions always have to be kept in mind. For studying Cd effects on shoots without root interference, it is possible to analyze Cd stress in algae or submerged macrophytic plants. The basic principles of heavy metal uptake via roots are known

for a long time, as reviewed, e.g., by Cataldo and Wildung in 1978 [17], but many questions how heavy metals are taken up by roots, how they affect roots, and how roots alter the uptake of heavy metals, are still in the focus of intense research.

Though specific transporters solely for Cd have not been found yet and are rather unlikely to exist, many transporters with similar affinities for Zn and Cd have been characterized (reviewed by Clemens [18,19]). Cd may enter the plant also via calcium channels [20]. Addition of Ca to the nutrient solution reduces Cd translocation into the shoots while increasing Cd accumulation in the roots [21], indicating a Ca-Cd competition for transport channels at the xylem loading step of nutrient uptake in the roots. While Cd hyperaccumulators actively enrich Cd in their tissues (see Chapter 12 [22]), most other plants suffer from Cd phytotoxicity.

Inhibition of the uptake of essential micronutrients could contribute to Cd toxicity, as reported, e.g., by Yoshihara et al. [23], Mendoza-Cozatl et al. [24], and Küpper and Kochian [25]. It could be caused not only by inhibited uptake, but also by Cd-stimulated heavy metal efflux as a Cd resistance strategy that could lead to the efflux of other ions as well [26]. Cd inhibited the uptake of Zn, Fe, and Mn, probably by competing for transporters or by interfering with the regulation of transporter gene expression. Siedlicka and Krupa [27] proposed that Cd inhibits iron uptake, and various later studies suggested this as well, but a more recent study by Pietrini et al. [28] found no inhibition of iron uptake by cadmium toxicity.

More effects of Cd to the roots of terrestrial plants, including the role of mycorrhiza, have very recently been reviewed by Lux et al. [29]. Responses like formation of reactive oxygen species, activation of the antioxidative system, genotoxicity and the up- or downregulation of specific genes occur in roots as well as in leaves (see Sections 4 and 5). As a result of direct inhibition of root metabolism, but also of malfunctioning shoot metabolism (especially photosynthesis as the energy-delivering process, see Section 3), Cd-treated plants nearly always showed reduced root elongation and/or deformation and e.g., brownishing compared to control [30–32]. Cd-induced inhibition of root growth was found to involve signalling via nitric oxide, resembling the pathway activated upon iron deprivation, which again points at the Cd-Fe interaction discussed above [33]. Finally, damage to roots certainly also disturbs plant water status as water enters terrestrial plants mainly via the roots [20].

But roots are also the first barrier against Cd. Roots may defend themselves against metal-induced damage by diminishing unwanted metal uptake. This can be achieved by expressing peroxidases, which can be used in lignification and thus reducing the uptake of further heavy metals as proposed by Cuypers et al. [34]. Ederli et al. [35] observed enhanced lignifications in young root tissue (10–20 mm from apex) of *Phragmitis australis* when treated with 100 μM Cd^{2+} for 3 weeks. The signal transduction of this Cd defence mechanism has very recently been investigated in more detail by Elobeid et al. [36]. In roots of *Merwilla plumbea* Cd^{2+} treatment (5 mg/kg soil) led to the formation of hypodermal periderm, a protecting layer with impermeable cell walls and impregnated by suberin [30], reducing the unspecific permeability of the root and protecting the shoot from excessive Cd. Another strategy for reducing damage to the roots, as well as preventing damage to other parts of the plant by reducing metal load, is actively

pumping the excess metal out of the plant. Such ATP-dependent efflux-pumps have been found by van Hoof et al. [37]) for the detoxification of copper in roots of *Silene vulgaris*. This mechanism may be even more important in aquatic microorganisms (in which case physical barriers may be less efficient), as discussed by Wood and Wang [38]. Cd^{2+} treatment changes expression patterns in roots of the low Cd hyperaccumulator *Solanum torvum* [39] and *Arabidopsis* [40]. Genes involved in the antioxidative system and uptake and translocation of heavy metals as well as more general ones for stress response were induced. Defence against Cd toxicity involved enhanced uptake of Mg, Ca, and S. Cd-induced changes in cellular expression for ZNT1, ZNT5, and MTP1 could also be part of plant acclimation to Cd toxicity [25].

3 Cadmium-Induced Inhibition of the Photosynthetic Apparatus

For a detailed general review of mechanisms of photosynthesis inhibition also by other metals than Cd, see reviews by Küpper and Kroneck [41] and Küpper et al. [42]. In the current chapter we will explain those mechanisms where studies dealt with cadmium. The photosynthetic apparatus, both its primary photochemical side and its biochemical carbon-fixing part, is one of the most important sites of inhibition by many heavy metals including cadmium. This was suggested already by very early studies like the highly cited one by Bazzaz et al. in 1974 [43], but these authors used extremely high, unphysiological concentrations of Cd^{2+} (4.5 to 18 mM) that unspecifically inhibit all parts of metabolism but would never occur even in the most polluted environments. Therefore, several studies re-investigated various aspects of Cd-induced inhibition of photosynthesis with lower Cd concentrations.

A recent study using environmentally realistic Cd concentrations (10 ppm in soil) showed an increase of transpiration whereas photosynthesis on the whole plant level was not yet affected [44]. An earlier study with 25 μM Cd^{2+} also reported a change in transpiration at toxic Cd concentrations, but in this case a reduction of transpiration was observed [45]. In both studies, the mechanism by which Cd decreased or increased transpiration remained unclear, but the seemingly contradictory results may be a consequence of photosynthesis inhibition at a particularly sensitive site, the stomata. If these do not close properly, regulation of transpiration is impaired. A study using phase-resolved photoacoustic spectroscopy revealed indeed that Cd-induced decrease in chlorophyll (Chl) (discussed below) was most pronounced in the uppermost layer of the leaf, the epidermis, where only the stomatal guard cells contain chlorophyll, while it was less pronounced in the main photosynthetic tissue, the mesophyll [46]. This was correlated with a diminished stomatal conductance, strongly suggesting that the changes in transpiration observed by Haag-Kerwer et al. [45] and Walley and Huerta [44] are a consequence of photosynthesis inhibition in stomatal guard cells.

In other studies using environmentally relevant concentrations, Cd-induced inhibition of photosynthesis was observed as well [47–50]. The lowest Cd^{2+} concentrations used in a study about the mechanism of Cd^{2+}-induced inhibition of photosynthesis were recently applied to the green alga *Chlamydomonas reinhardtii* by Perreault et al. [50]. These authors used environmentally realistic 0.15 to 4.62 μM Cd^{2+} and investigated biophysical properties of the reaction center (RC) of photosystem II (PS II) in the intact algae by kinetic measurements of *in vivo* UV/VIS fluorescence and absorption [50]. This type of measurements does not allow a final conclusion about the exact inhibition site, but the data clearly showed that such low concentrations are already inhibitory, confirming the results of Larsson et al. [49] on *Brassica napus*, and furthermore showed that activation energies inside PS II RC are modified by Cd^{2+}. The authors suggested multiple inhibition sites, but further evidence will be needed to decide about this. In all studies investigating photosynthesis inhibition by heavy metals including Cd, a much stronger inhibition was found for PS II compared to photosystem I (early works: [51,52]). The relative importance of specific inhibition sites, however, strongly depends on the type and concentration of the heavy metal, the irradiance conditions, and the organism under investigation.

Mechanisms of Cd-induced damage to photosynthesis that were observed under environmentally relevant conditions include the substitution of the central Mg^{2+} in chlorophylls by Cd^{2+} (Küpper et al. [47]), although this is much harder to detect for Cd than for other metals because of the similarity of the UV/VIS absorption spectra of [Cd]-Chl and [Mg]-Chl [42,47]. [Cd]-Chl is unsuitable for photosynthesis for several reasons. First of all, it has an unstable singlet excited state, which leads to thermal relaxation instead of fluorescence [53] or electron transfer [54], or exciton transfer *in vivo*. *In vivo*, such thermal exciton quenching by [Cd]-Chl will inhibit photosynthesis by dissipating all absorbed energy as heat either in the antenna or in the reaction center. Data supporting this mode of action of Cd were published, e.g., by Küpper et al. [47,48], Larsson et al. [49], and Pietrini et al. [28]. In all three studies, Cd led to reduced electron flow through PS II and enhancement of non-photochemical exciton quenching.

In a study on isolated thylakoids, the authors came to the conclusion that several sites can be inhibited by Cd^{2+}, and one of them was primary charge separation [55], but they used extremely high (mM) Cd^{2+} concentrations. The latter inhibition could be due to Cd^{2+} insertion in pheophytin of the PS II RC. In a study about Cd-acclimation of the Cd/Zn hyperaccumulator *Thlaspi (=Noccaea) caerulescens* using Cd^{2+} concentrations naturally encountered by such Cd-resistant plants (10 μM), chlorophyll fluorescence parameters related to photochemistry were more strongly affected by Cd-stress than non-photochemical parameters [48]. This indicated that sublethal Cd inhibits the photosynthetic light reactions more than the Calvin-Benson cycle. In the studies by Krupa et al. [56] and Pietrini et al. [28], the Cd-induced inhibition of RuBisCO activity was stronger than the Cd effects on photosynthetic light reactions. But in these studies Cd toxicity was stronger because less resistant plants were incubated with the same, [56] or higher (50 μM [28]) Cd^{2+} concentrations as used by Küpper et al. [48]. Hence, at the moment it is not clear which of these effects is more important in the environment,

and studies comparing time and concentration thresholds of these effects are needed to resolve this question.

Cd-stress reduced F_v/F_m and Φ_{PSII} stronger at 670–740 nm compared to >740 nm and <670 nm, but it enhanced non-photochemical quenching mainly at <690 nm [48]. This differential spectral distribution of Cd-effects on photochemical *versus* non-photochemical quenching showed that Cd inhibits at least two different targets in/around PS II. Further, [Cd]-Chl has a lower tendency to bind axial ligands than [Mg]-Chl [57]. As these axial ligands are required for Chl binding in proteins [58], which is required for proper folding of LHC II [59] that is the prime target for *in vivo* substitution of Mg^{2+} in Chl [60], formation of [Cd]-Chl will lead to LHC II denaturation. Indeed, Cd-induced changes in LHC II fluorescence indicative of incorrect binding of Chl in the LHC II protein have recently been found at 50 μM Cd in *Secale cereale* [61]. This may contribute to the Cd-induced enhancement of non-photochemical exciton quenching at <690 nm [48]. Finally, [Cd]-Chl is very unstable [47], so that it bleaches out easily. Already in early studies [62] bleaching of leaves ("chlorosis") was observed in Cd-inhibited plants, later studies confirmed this also for the sublethal low micromolar range [48,49]. Bleaching of [Cd]-Chl could explain this at least in part, and at least in the study of Pietrini et al. [28] it could clearly be shown that this chlorosis was not due to iron deficiency as believed earlier, but might be due to [Cd]-Chl.

Another proposed mechanism of Cd-induced inhibition of the PS II reaction center is the substitution of Ca^{2+} by Cd^{2+} in the water splitting complex [55,63], which is understandable in terms of the chemical similarity of Cd^{2+} and Ca^{2+} (Chapter 6 of this book). This idea originated from structural investigations on PS II RC where Cd^{2+} binding was used as a tool [64], and early observations of a partial reversal of Cd toxicity by Mn that was interpreted as Cd^{2+} binding in the Mn cluster of PS II [65]. A further recent study suggested Cd-induced damage to the water splitting complex based on EPR spectroscopy as well as artificial electron donors and acceptors in isolated thylakoids [66]. In addition to the substitution of Ca^{2+}, the study by Sigfridsson et al. [55] suggests several further binding sites of Cd^{2+}. While the data presented by all these studies are convincing per se, they suffer from the same problem as most other studies so far: They used rather high Cd^{2+} concentrations, in the studies of Sigfridsson et al. [55] and Faller et al. [63] most data were obtained in the range of hundreds of μM or even mM Cd^{2+} added to isolated thylakoids. While even in soil solution such concentrations might only be experienced by especially metal-resistant plants (e.g., hyperaccumulators), it is very unlikely that such concentrations of free (or labile complexed) Cd^{2+} ions could ever occur in the chloroplasts of living cells. Cells try to keep concentrations in metabolically active compartments as low as possible as discussed in Chapter 12 about Cd-accumulating plants [22]. Therefore, it is questionable whether the substitution of Ca^{2+} by Cd^{2+} in the water splitting complex is relevant *in vivo*; there is no study showing its occurrence in intact plants or algae under environmentally realistic conditions.

An indirect inhibition of photosynthesis was suggested by Aravind and Prasad [67], who observed a substitution of Zn^{2+} by Cd^{2+} in the active center of carbonic anhydrase of the submerged water plant *Ceratophyllum demersum*. While this

enzyme of the carbon-concentrating mechanism can function with Cd^{2+} in some marine algae (see Chapter 16 [68]), obviously it cannot function with Cd^{2+} in other photosynthetic organisms.

Inhibition of photosynthesis causes marked changes in protein and metabolite abundance as revealed by proteomics and metabolomics studies (see Villiers et al. [69] for a recent review), but although most of these studies have been performed in very recent years the authors often used too high Cd concentrations so that the effects were not very specific. At such Cd concentrations, the abundance of photosynthesis-related proteins and enzymes for processes needing photosynthetic products decreased [70] as part of a comprehensive re-organization of carbon and carbohydrate metabolisms [71]. Proteins involved in defence against oxidative stress (see below), in contrast, increased at 150 μM Cd^{2+} [70]. An increase of enzymes involved in leaf nitrogen remobilization and root nitrogen storage was observed already at relevant (low μM) Cd^{2+} concentrations [72].

During stress, a few mesophyll cells in *T. caerulescens* became more inhibited and accumulated more Cd than the majority. This heterogeneity disappeared during acclimation, indicating that during severe stress a few mesophyll cells were sacrificed for Cd storage to safe the remaining tissue [48]. Hyperaccumulator plants seem to defend themselves against substitution of Mg^{2+} in Chl by Cd^{2+} via enhanced accumulation of Mg in mesophyll cells [43].

4 Cadmium-Induced Oxidative Stress

Many authors reported an increase in oxidative stress under conditions of heavy metal toxicity, early reports about this are reviewed by Prasad and Hagemeyer [74], Clijsters et al. [75], and Pinto et al. [76].

Reactive oxygen species (ROS) are formed from O_2 by its excitation to singlet oxygen ($^1O_2$), or by transfer of electrons to O_2 to form superoxide radical ($O_2^{\bullet -}$), hydrogen peroxide (H_2O_2) or the hydroxyl radical ($HO^{\bullet}$) (see Shaw et al. [77] for detailed description of the single reactions). ROS are potentially dangerous to cells. Especially the molecules with free radicals ($O_2^{\bullet -}$ and $HO^{\bullet}$) are extremely reactive, they react directly after generation and unspecifically. They can react with proteins, lipids, and nucleic acids, causing alteration or loss of structure and function which leads to lipid peroxidation and membrane leakage, enzyme inactivity, and DNA breakage and mutation [78].

ROS are produced not only under stress, but also by normal metabolic processes in plant cells (respiration and photosynthesis) [79] and also in specialized organelles like peroxisomes [80,81]. Low concentrations of, e.g., H_2O_2 and NO, serve as signaling molecules (reviewed by Mittler et al. [82] and Van Breusegem et al. [83]), and plants also use the rapid accumulation of ROS (the oxidative burst) to defend themselves against pathogens [84]. Plants and photoautotrophic organisms therefore contain several antioxidant enzymes to cope with the internally produced oxygen species and the excessive ROS due to stress reactions. The enzymes superoxide dismutase (SOD, dismutating $O_2^{\bullet -}$), catalase (CAT, dismutating H_2O_2),

NADPH dehydrogenases, ascorbate peroxidase (APX), glutathione reductase (GR), the ascorbate-glutathione cycle, and several small molecules can scavenge or neutralize oxygen radicals. Under normal conditions, the formation and neutralization of ROS is balanced. Under stress, however, an imbalance leads to accumulation of ROS, to oxidative stress.

Unlike other heavy metals like, e.g., Cu, Cd is a redox-inert metal and does not produce ROS directly via Fenton and/or Haber Weiss reaction [85], but indirectly by impairment of either oxidative or photosynthetic processes where electrons can be mis-transferred to oxygen instead of their target molecule, or by inhibiting antioxidant enzymes leading to reduced removal of ROS. Although a large percentage of these studies was carried out under very high heavy metal concentrations that would not be environmentally relevant (up to the millimolar range), some studies with lower (but still several micromolar) metal concentrations have shown the induction of oxidative stress as well. The effect of ROS can be measured either by their impact on enzymes, leading to up- or downregulation of gene expression or enzyme activity, staining of ROS directly, or by measuring follow reactions like lipid peroxidation or the oxidative production of carbonyl groups in proteins [78].

ROS accumulation was observed in a time- and dose-dependent manner in *Arabidopsis thaliana* protoplasts. ROS accumulation started in the mitochondria, and was later observed both in the mitochondria and the chloroplasts [86]. In leaf discs of tobacco wild-type (WT) and catalase-deficient plants exposed to 100 or 500 μM Cd^{2+}, DAB staining of H_2O_2 revealed its production at certain spots on the leaf disc, but only little differences between the two cultivars. However, the Cd-treated plants (WT and transgenic genotype) showed inhibition of $O_2^{\bullet -}$ formation when treated with high Cd^{2+} concentrations (500 μM) [87]. Treatment with extremely high Cd^{2+} (1–5 mM) led to cell death of tobacco cell cultures within a few hours [88]. As a cell line unable to accumulate H_2O_2 also was poisoned by Cd, this suggests that H_2O_2 per se is not the main death-inducing substance. However, it should be clearly underlined that the study was carried out using millimolar concentrations of Cd^{2+}, concentrations which plants will never face in their environment. Whether the described reaction is a physiological response of tobacco cannot be answered.

The direct effect of Cd on either expression or activity of antioxidant enzymes was shown in several studies. Sandalio et al. [89] found an increased lipid peroxidation coupled with a reduction in Zn/Cu-superoxide dismutase activity in the shoots, starting at 10 μM Cd^{2+}. In this case, the decrease in SOD activity was most likely the primary effect, which then led to oxidative stress. The decrease of the Zn-dependent SOD was most likely caused by Cd-induced Zn-deficiency, since Cd significantly reduced Zn translocation from roots to shoots [89]. The expression of Cu/Zn-SOD in Cd-treated pea plants (50 μM) decreased but could be reversed by Ca^{2+} supply, suggesting a competition for uptake [90]. This imbalance of other metals or micronutrients due to Cd application has been verified in various studies (e.g., [91–93]). While Mn-SOD expression was also down-regulated, plastidic Fe-SOD expression went up as measured by semiquantitative reverse transcription

PCR [90]. The authors suggest transcriptional regulation for the Mn-SOD and transcriptional and posttranscriptional one for the Fe-SOD and Cu/Zn-SOD, especially as the Fe-SOD previously showed decreased activity under Cd-treatment (10–50 μM Cd^{2+} [89], 50 μM Cd^{2+} [94]).

Comparable results were found for isozymes of antioxidative enzymes in *Solanum nigrum* subjected to 0 and 15 μM Cd^{2+} [95]. In tobacco, Cd-treatment led to six-fold increase of SOD activity in transgenic genotype (catalase-deficient), to a reduction of catalse activity by 60% in the wild-type and a significant decrease of NADPH-oxidase dependent $O_2^{\bullet -}$ formation [87], though in this study very high Cd concentrations of 100 μM and 500 μM were used. Significant higher activities of SOD after lower Cd treatment (1–10 μM) compared to untreated control were also found in tomato plants [96] and the freshwater macrophyte *Ceratophyllum demersum* [97]. Activity of antioxidant enzymes and proline content increase in *Solanum nigrum* occurred with increasing Cd levels (0–30 μM [95]). The involvement of proline and brassinosteroids in protection from Cd stress (3–12 mg/kg soil) in tomato was shown by Hasan et al. [98].

Activity of catalase was reduced in different plant species and organs when treated with Cd^{2+} (*Arabidopsis* leaves [99], sunflower leaves [100], pine roots [101], pea roots [102]). Ascorbate peroxidase activity increased in beans treated with 5 μM Cd^{2+} [103], in *Vicia faba* [104], and in *Arabidopsis thaliana* treated with 50 μM Cd^{2+} [105]. In chamomile APX activity increased only in the roots at 120 μM Cd^{2+} treatment, while 60 μM Cd^{2+} did not alter the activity in a control [106]. In different genotypes of *Pisum sativum*, APX activity increased, decreased, or did not change after Cd treatment, depending on their sensitivity (5 μM; 5 mg/kg soil [107]). The expression of the heme oxygenase 1 gene in alfalfa and tomato increased after Cd exposure and several other stresses, and also in response to depletion of glutathione (GSH) and ascorbic acid. Heme-oxygenase 1 may therefore supply the cells with antioxidants when GSH is limited ([108] and citations within). The different responses of antioxidant enzymes to Cd stress (up- or downregulated, more or less active) may be due to the different experimental setups, involving Cd concentration and treatment duration, application in hydroponic solution or soil and the studied plant organs. However, lower Cd concentrations and shorter treatment duration generally rather increased the antioxidant system [109], while longer exposure and higher Cd concentrations led to decreased activity or content of the antioxidants [89].

Cd tolerance most likely involves the antioxidant system. The Cd hyperaccumulator *Solanum nigrum* possessed a significantly higher amount of antioxidant enzymes compared to related non-hyperaccumulator [110]. Upregulation of small antioxidant molecules like GSH and Cd-binding phytochelatins was observed also for non-accumulators [111,112]. They also were found to be higher in Cd-tolerant plants than sensitive ones, e.g., for rice [113] and *Arabidopsis* [99].

The specific detection of ROS revealed insights in the sub-cellular location of their production during Cd stress. Pea plants treated with 50 μM Cd^{2+} showed reduced NO and enhanced ROS production detected with DAB staining and

electron microscopy [114] and also with specific dyes using confocal laser scanning microscopy [90]. ROS production was mainly observed in the epidermis, mesophyll cells, and the vascular tissue.

If reactive oxygen species are not immediately detoxified, they may lead to oxidation of membranes. A Cd-induced accumulation of lipid peroxides was found for different Cd^{2+} concentrations in bean (10 μM [115]; 5 μM [103]), different genotypes of pea (10 μM [89]), barley (1.5 μM [116]), soybean (200 μM [117]). High Cd^{2+} concentrations (100 μM) led to alterations in the plastidal membrane in tomato [118]. One reason why later studies found little oxidation-related leakage of the plasma membrane may be that plants quickly suppress this type of damage. First, they reduce the oxidative stress by increasing the expression of enzymes that scavenge reactive oxygen species, as reviewed in detail by Clijsters et al. [75]. This mechanism does not seem to work, however, under cadmium stress, which decreases zinc concentrations in the shoot and thereby inhibits the synthesis of superoxide dismutase (see above). Another mechanism counteracting heavy-metal induced oxidative stress is the induction of changes in the membrane composition such as a decrease of the ratios phosphatidylcholine/phosphatidylethanolamine, unsaturated/saturated fatty acids and lipid/protein. Such effects were consistently reported by many authors working with diverse heavy metals and plants (e.g., [119–125]), with variations mainly in the importance of individual changes. These changes make the membranes less vulnerable to reactive oxygen species.

5 Genotoxicity of Cadmium in Plants

Heavy metals, including cadmium, can induce DNA damage by direct interaction with the nucleotides, by inhibiting DNA-repairing enzymes [126], and by inducing ROS that can lead to lipid peroxidation, causing membrane damage and production of mutagenic aldehydes [127]. DNA modifications include base and sugar lesions, strand breaks, DNA-protein crosslinks, and base-free sites [128,129]. The environmental relevance of these reactions, however, remains rather unclear because the concentrations of Cd that were used in the experiments were often higher than those occurring in polluted habitats.

Suspension cell cultures of *Nicotiana tabacum* treated with Cd^{2+} showed strictly dose-dependent changes in viability and DNA integrity. Low, environmentally relevant concentrations (up to 10 μM) did not change DNA integrity. Higher ones (50–100 μM) led to oligonucleosomal DNA fragmentation, triggering apoptosis and the highest (1 mM) led to rapid cell death without chromatin fragmentation [130]. As described previously, this very high Cd^{2+} concentration will never occur in nature and the plant's response can therefore not be accounted as physiological. The same authors [131] showed in 2002 that cell death could be prevented when Cd^{2+} (50 μM) was removed from the growth medium within a certain lag

phase, proving the apoptotic trigger nature of high Cd^{2+} concentrations. DNA repair and telomerase activity were observed during the recovery phase. Kuthanova and colleagues showed a cell cycle phase-specific death for the same tobacco cell line [132].

In the duckweed *Lemna minor*, Cvjetko et al. [133] found a significantly increased amount of destroyed DNA measured as tail DNA of single cells via single cell gel electrophoresis (introduced as Comet Assay by Singh et al. in 1988 [134] and successfully tested for genotoxicity assessment in plant roots by Koppen and Verschaeve in 1996 [135]), when treated for 4 days with Cd^{2+} (5 μM) and Cd^{2+} + Cu^{2+} (5 μM + 2.5 μM or 5 μM + 5 μM). After 7 days of treatment, however, the combination of Cd^{2+} + Cu^{2+} led to contents of DNA tail comparable to control. The authors concluded that DNA damage resulted from lipid peroxidation. Lipid peroxidation as well as DNA damage decreased after 7 days, the decrease of DNA damage was likely also caused by an onset of DNA repair mechanisms. Comparable results were found for *Allium cepa* [136]. Increased Cd^{2+} concentrations, starting from the sub-micromolar range (0.44 μM and 1.78 μM), led to an increase in all measured parameters for DNA damage (tail length, tail DNA in %, tail moment, and olive tail moment), while in combination with the pesticide atrazine the DNA damage was significantly lower. Cd^{2+}-induced DNA damage observed via Comet Assay was also shown in the marine diatom *Chaetoceros tenuissimus* (21–89 μM [137]) as well as in pea roots and leaves [138].

The Cd^{2+}-induced DNA damage was shown by random amplification of polymorphism DNA analyses (RAPD) in maize seedlings [139], barley roots [140,141], *Arabidopsis thaliana* [142], and bean roots [143]. The presence of new or disappearance of DNA fragments (visualized by gel electrophoresis) in Cd^{2+}-treated samples compared to untreated control may be due to mutations or deletions which create new primer binding sites. Cd^{2+} treatment changed the gene expression patterns in *Brassica juncea* [144,145], including many transcription factors and stress responding genes, and also more general ones involved in cell metabolism, which are also upregulated during abiotic stress. In *Arabidopsis thaliana*, genes involved in DNA mismatch repair were induced at low Cd^{2+} treatment (6.7 μM), but repressed at higher concentrations (up to 54 μM) [142]. A biphasic upregulation of the expression of the dNTP providing enzymes were observed in *A. thaliana* treated with 25 μM Cd^{2+} [146], suggesting enhanced DNA repair pathways to cope with Cd stress.

In *Vicia* species, the root tip micronucleus assay is well established [147,148]. Micronuclei (MN) originate from chromatin fragments or by exclusion of whole chromosomes during cell division [149,150]. Cd^{2+}-treated root tips generated significant more MN than untreated controls at different experimental conditions in bean and *Allium sativum* (1, 10, 100, and 200 μM Cd^{2+} [151]), *Allium cepa* (10, 20, and 40 μM [152]) and also at much lower concentrations in bean (75, 100, and 250 nM [153]), although in a study by Rosa et al. a significant induction of MN occurred only above 2 μM Cd [154]. A dose-dependent increase in sister

chromatin exchanges at 100 μM and 200 μM was observed for *V. faba* as well as decreased mitotic index (MI; number of cells in metaphase stage) [104]. Souguir et al. [32] found also a time dependency in MN generation in *V. faba* roots: MN frequency increased proportionally with incubation time. A decline in MN generation of the longest incubation with the highest concentration (200 μM for 48 h) may be due to drastic reduction of mitotic activity (compared to control) [32]. In the same study, different chromosomal aberrations like sticky chromosomes, breaks, and bridges were observed in the root meristematic cells at all incubation durations (12, 24, and 48 h) and concentrations (50, 100, and 200 μM [32]). In *Allium cepa*, chromosomal aberrations occurred already at 10 μM Cd^{2+} [152].

In a study of Villatoro-Pulido et al. [155], radish was grown on metal-contaminated or control soil, harvested, and fed to larvae of *Drosophila melanogaster* for which the somatic mutation and recombination test (SMART) in wings is well established. Radish roots of untreated soils were not genotoxic, the ones of metal-treated soils only at highest concentrations and all shoots of metals-treated soils caused genotoxicity in the fruitfly. To learn more about the genotoxic potential of cadmium, like threshold values, in plants and their consumers is therefore important.

6 Outlook

Cadmium toxicity in plants has been a focus of intense research for several decades. Many mechanisms of Cd-induced damage to plants have been described, and those which seem most important according to our present state of knowledge have been reviewed in this chapter. As discussed in detail in the previous sections of this review, however, the environmental relevance of many of these proposed mechanisms of Cd-induced damage remains unclear, because they were investigated under conditions (especially high Cd concentrations) that never or only very rarely occur in the environment. Therefore, future studies should establish time and Cd concentration thresholds of these mechanisms under environmentally relevant growth conditions.

Furthermore, for almost all described mechanisms it remained unclear how they interact with each other. For example, malfunctioning photosynthesis may generate oxidative damage, but reactive oxygen species could also damage the photosynthetic apparatus. Similarly, malfunctioning photosynthesis means less energy for root growth, but damaged roots may also lead to inhibition of photosynthesis if required nutrients become limiting. Many more such interactions are conceivable as illustrated in Figure 1, but so far it is unclear how much each of them contributes how much to Cd-induced damage in plants in Cd-polluted habitats.

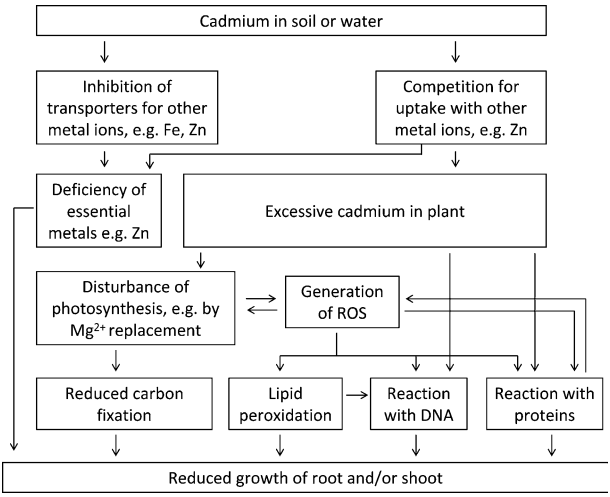

Figure 1 Scheme of damage pathways and interactions that were proposed in the literature (see text).

Abbreviations

APX	ascorbate peroxidase
ATP	adenosine 5'-triphosphate
CAT	catalase
Chl	chlorophyll
DAB	diaminobenzidine
dNTP	deoxyribonucleotide
ETDA	ethylenediamine-N,N,N',N'-tetraacetic acid
EPR	electron paramagnetic resonance
F_0	minimal fluorescence quantum yield of *in vivo* chlorophyll fluorescence of a photosynthetic organism in dark adapted state, when the plastoquinone pool is completely oxidized
F_m	maximal fluorescence quantum yield of *in vivo* chlorophyll fluorescence of a photosynthetic organism in dark adapted state during an oversaturating light flash, leading to complete reduction of the plastoquinone pool
F_v	F_m–F_0 = variable fluorescence
GR	glutathione reductase
GSH	glutathione
LHC II	light harvesting complex II
MI	mitotic index, number of cells in metaphase stage
MN	micronucleus
NADPH	nicotinamide adenine dinucleotide phosphate
PS I	photosystem I

PS II	photosystem II
RAPD	rapid amplification of polymorphism DNA analyses
RC	reaction center
ROS	reactive oxygen species
RuBisCO	ribulose-1,5-bisphosphat-carboxylase/-oxygenase
SOD	superoxide dismutase
SMART	somatic mutation and recombination test
WT	wild-type

Acknowledgments The authors would like to thank the Deutsche Forschungsgemeinschaft (DFG, projects KU 1495/7-1 and KU 1495/8-1), the Deutscher Akademischer Austauschdienst (DAAD), the Fonds der Chemischen Industrie (FCI), and the University of Konstanz for financial support.

References

1. T. W. Lane, F. M. M. Morel, *Proc. Natl. Acad. Sci. USA* **2000**, *97*, 4627–4631.
2. J. T. Cullen, M. T. Maldonado, Chapter 2 of this book.
3. P. Duvigneaud, *Bull. Soc. Roy. Bot. Belg.* **1958**, *90*, 127–286.
4. F. Malaisse, A. J. M. Baker, S. Ruelle, *Biotechnol. Agron. Soc. Environ.* **1999**, *3*, 104–114.
5. R. D. Reeves, A. J. M. Baker, A. Borhidi, R. Berazaín, *New Phytol.* **1996**, *133*, 217–224.
6. N. Rajakaruna, T. B. Harris, E. B. Alexander, *Rhodora* **2009**, *111*, 21–108.
7. J. Proctor, *Persp. Plant Ecol. Evol. Syst.* **2003**, *6*, 105–1024.
8. R. D. Reeves. R. R. Brooks, *J. Geochem. Explor.* **1983**, *18*, 275–283.
9. M. Buchauer, *Environ. Sci. Technol.* **1973**, *7*, 131–135.
10. A. van Geen, J. F. Adkins, E. A. Boyle, C. H. Nelson, A. Palanques, *Geology* **1997**, *25*, 291–294.
11. E. Lombi, F. J. Zhao, S. J. Dunham, S. P. McGrath, *New Phytol.* **2000**, *145*, 11–20.
12. Z. L. He, X. E. Yang, P. J. Stofella, *J. Trace Elem. Med. Biol.* **2005**, *19*, 125–140.
13. M. B. McBride, B. K. Richards, T. Steenhuis, J. J. Russo, S. Sauve, *Soil Sci.* **1997**, *162*, 487–500.
14. J. V. Lagerwerff, A.W. Specht, *Environ. Sci. Technol.***1970**, *4*, 583–586.
15. J. E. Fergusson, R. W. Hayes, T. S. Yong, S. H. Thiew, *New Zealand J. Sci.* **1980**, *23*, 293–310.
16. L. Chen, Y. Han, H. Jiang, H. Korpelainen, C. Li, *J. Exper. Botany* **2011**, *62*, 5037–5050.
17. D. A. Cataldo, R. E. Wildung, *Environ. Health Persp.* **1978**, *27*, 149–159.
18. S. Clemens, *Planta* **2001**, *212*, 475–486.
19. S. Clemens, *Biochimie* **2006**, *88*, 1707–1719.
20. L. Perfus-Barbeoch, N. Leonhart, A. Vavasseur, C. Forestier, *The Plant Journal* **2002**, *32*, 539–548.
21. N. Hayakawa, R. Tomioka, C. Takenaka, *Soil Sci. Plant Nutrition* **2011**, *57*, 691–695.
22. H. Küpper, B. Leitenmaier, Chapter 12 of this book.
23. T. Yoshihara, H. Hodoshima, Y. Miyano, K. Shoji, H. Shimada, F. Goto, *Plant Cell Rep.* **2006**, *25*, 365–373.
24. D. G. Mendoza-Cózatl, E. Butko, F. Springer, J. W. Torpey, E. A. Komives, J. Kehr, J. I. Schroeder, *The Plant Journal* **2008**, *54*, 249–259.
25. H. Küpper, L.V. Kochian, *New Phytol.* **2010**, *185*, 114–129.
26. M. Migocka, G. Klobus, *Physiol. Plant.* **2007**, *129*, 578–587.
27. A. Siedlecka, Z. Krupa, *Photosynthetica* **1999**, *36*, 321–331.

28. F. Pietrini, M. A. Iannelli, S. Pasqualini, A. Massacci, *Plant Physiol.* **2003**, *133*, 829–837.
29. A. Lux, M. Martinka, M. Vaculik, P. J. White, *J. Exper. Bot.* **2011**, *62*, 21–37.
30. A. Lux, M. Vaculik, M. Martinka, D. Liskova, M. G. Kulkarni, W. A. Stirk, J. Van Staden, *Ann. Bot.* **2011**, *107*, 285–292.
31. L. B. Zoghlami, W. Djebali, Z. Abbes, H. Hediji, M. Maucourt, A. Moing, R. Brouquisse, W. Chaibi, *African J. Biotechnol.* **2011**, *10*, 567–579.
32. D. Souguir, E. Ferjani, G. Ledoigt, P. Goupil, *Ecotoxicology* **2010**, *20*, 329–336.
33. A. Besson-Bard, A. Gravot, P. Richaud, P. Auroy, C. Duc, F. Gaymard, L. Taconnat, J. P. Renou, A. Pugin, D. Wendehenne, *Plant Physiol.* **2009**, *149*, 1302–1315.
34. A. Cuypers, J. Vangronsveld, H. Clijsters, *J. Plant Physiol.* **2002**, *159*, 869–876.
35. L. Ederli, L. Reale, F. Ferranti, S. Pasqualini, *Physiol. Plant.* **2004**, *121*, 66–74.
36. M. Elobeid, C. Göbel, I. Feussner, A. Polle, *J. Exper. Bot.* **2012**, *63*, 1413–1421.
37. N. A. L. M. van Hoof, P. L. M. Koevoets, H. W. J. Hakvoort, W. M. Ten Bookum, H. Schat, J. A. C. Verkleij, W. H. O. Ernst, *Physiol. Plant.* **2001**, *113*, 225–232.
38. J. M. Wood, H. Wang, *Envir. Sci. Technol.* **1983**, *17*, 582A–590A.
39. H. Yamaguchi, H. Fukuoka, T. Arao, A. Ohyama, T. Nunome, K. Miyatake, S. Negoro, *J. Exper. Bot.* **2010**, *61*, 423–437.
40. U. Roth, E. von Roepenack-Lahaye, S. Clemens, *J. Exper. Bot.* **2006**, *57*, 4003–4013.
41. H. Küpper, P. M. H. Kroneck, in *Metal Ions in Biological Systems*, Volume 44, Eds A. Sigel, H. Sigel, R. K. O. Sigel, Marcel Dekker, Inc., New York, 2005, pp. 97–142.
42. H. Küpper, F. C. Küpper, M. Spiller, in *Chlorophylls and Bacteriochlorophylls: Biochemistry, Biophysics, Functions and Applications*, Eds B. Grimm, R. Porra, W. Rüdiger, H. Scheer, Vol. 25 of *Advances in Photosynthesis and Respiration* (Series Ed Govindjee), Kluwer Academic Publishers, Dordrecht, 2006, pp. 66–77.
43. F. A. Bazzaz, G. L. Rolfe, R. W. Carlson, *Physiol. Plant.* **1974**, *32*, 373–376.
44. J. W. Walley, A. J. Huerta, *J. Plant Nutr.* **201**0, *33*, 1519–1530.
45. A. Haag-Kerwer, H. J. Schäfer, S. Heiss, C. Walter, T. Rausch, *J. Exper. Bot.* **1999**, *50*, 1827–1835.
46. A. Baryla, P. Carrier, F. Franck, C. Coulomb, C. Sahut, M. Havaux, *Planta* **2001**, *212*, 696–709.
47. H. Küpper, F. Küpper, M. Spiller, *J. Exper. Bot.* **1996**, *47*, 259–266.
48. H. Küpper, P. Aravind, B. Leitenmaier, M. Trtílek, I. Šetlík, *New Phytol.* **2007**, *175*, 655–674.
49. E. H. Larsson, J. F. Bornmann, H. Asp, *J. Exper. Bot.* **1998**, *49*, 1031–1039.
50. F. Perreault, J. Dionne, O. Didur, P. Juneau, R. Popovic, *Photosynth. Res.* **2011**, *107*, 151–157.
51. H. Clijsters, F. Van Assche, *Photosynth. Res.* **1985**, *7*, 31–40.
52. N. Atal, P. P. Saradhi, P. Mohanty, *Plant Cell Physiol.* **1991**, *32*, 943–951.
53. T. Watanabe, M. Kobayashi, *Special Articles on Coordination Chemistry of Biologically Important Substances* **1988**, *4*, 383–395.
54. T. Watanabe, K. Machida, H. Suzuki, M. Kobayashi, K. Honda, *Coord. Chem. Rev.* **1985**, *64*, 207–224.
55. K. G. V. Sigfridsson, G. Bernat, F. Mamedov, S. Styring, *Biochim. Biophys. Acta* **2004**, *1659*, 19–31.
56. Z. Krupa, G. Öquist, N. P. A. Huner, *Physiol. Plant.* **1993**, *88*, 626–630.
57. L. J. Boucher, J. J. Katz, *J. Am. Chem. Soc.* **1967**, *89*, 4703–4708.
58. C. A. Rebeiz, F. C. Belanger, *Spectrochim. Acta* **1984**, *40A*, 793–806.
59. H. Paulsen, B. Finkenzeller, N. Kühlein, *Eur. J. Biochem.* **1993**, *215*, 809–816.
60. H. Küpper, I. Šetlík, M. Spiller, F. C. Küpper, O. Prášil, *J. Phycol.* **2002**, *38*, 429–441.
61. E. Janik, W. Maksymiec, R. Mazur, M. Garstka, W. I. Gruszecki, *Plant Cell Physiol.* **2010**, *51*, 1330–1340.
62. I. S. Sheoran, H. R. Singal, R. Singh, *Photosynth. Res.* **1990**, *23*, 345–351.
63. P. Faller, K. Kienzler, A. Krieger-Liszkay, *Biochim. Biophys. Acta* **2005**, *1706*, 158–164.

64. J. Matysik, A. Alia, G. Nachtegaal, H. J. van Gorkom, A. J. Hoff, H. J. M. de Groot, *Biochemistry* **2000**, *39*, 6751– 6755.
65. T. Baszynski, L. Wajda, M. Król, D. Wolinska, Z. Krupa, A. Tukendorf, *Physiol. Plant*. **1980**, *48*, 365–370.
66. C. Pagliano, M. Raviolo, F. Dalla Vecchia, R. Gabbrielli, C. Gonnelli, N. Rascio, R. Barbato, N. La Rocca, *J. Photochem. Photobiol. B: Biology* **2006**, *84*, 70–78.
67. P. Aravind, M. N. V. Prasad, *J. Anal. Atomic Spectrometry* **2004**, *19*, 52–57.
68. Y. Xu, F. M. M. Morel, Chapter 16 of this book.
69. F. Villiers, C. Ducruix, V. Hugouvieux, N. Jarno, E. Ezan, J. Garin, C. Junot, J. Bourguignon, *Proteomics* **2011**, *11*, 1650–1663.
70. S. Gillet, P. Decottignies, S. Chardonnet, P. Le Maréchal, *Photosynth. Res.***2006**, *89*, 201–211.
71. T. C. Durand, K. Sergeant, S. Planchon, S. Carpin, P. Label, D. Morabito, J.-F. Hausman, J. Renaut, *Proteomics* **2010**, *10*, 349–368.
72. C. Chaffei, K. Pageau, A. Suzuki, H. Gouia, M. H. Ghorbel, C. Masclaux-Daubresse, *Plant Cell Physiol.* **2004**, *45*, 1681–1693.
73. H. Küpper, E. Lombi, F. J. Zhao, and S. P. McGrath, *Planta* **2000**, *212*, 75–84.
74. M. N. V. Prasad, J. Hagemeyer (Eds), *Heavy Metal Stress in Plants: From Molecules to Ecosystems*, Springer, Berlin, Heidelberg, 1999.
75. H. Clijsters, A. Cuypers, J. Vangronsveld, *Z. Naturforsch. C* **1999**, *54*, 730–734.
76. E. Pinto, T. C. S. Sigaud-Kutner, M. A. S. Leitao, O. K. Okamoto, D. Morse, P. Colepicolo, *J. Phycol.* **2003**, *39*, 1008–1018.
77. B. F. Shaw, S. K. Sahu, R. K. Mishra, in *Heavy Metal Stress in Plants: From Biomolecules to Ecosystems*, 2nd ed, Ed M. N. V. Prasad, Springer Verlag, Berlin, 2004, pp. 84–126.
78. B. Halliwell, J. M. C. Gutteridge, *Free Radicals in Biology and Medicine*, 4th ed, Oxford University Press Inc., New York, 2007, pp.1–851.
79. K. Asada, M. Takahashi, in *Photoinhibition*, Eds D. J. Kyle, C. Osmond, C. J. Arntzen, Elsevier, New York, 1987, pp.227–297.
80. L. A. del Rio, F. J. Corpas, L. M. Sandalio, J. M. Palma, M. Gomez, J. B. Barroso, *J. Exper. Bot.* **2002**, *53*, 1255–1272.
81. F. J. Corpas, J. B. Barroso, L. A. del Rio, *Trends Plant Sci.* **2001**, *6*, 145–150.
82. R. Mittler, S. Vanderauwera, N. Suzuki, G. Miller, V. B. Tognetti, K. Vandepoele, M. Gollery, V. Shulaev, F. Van Breusegem, *Trends Plant Sci.* **2011**, *16*, 300–309.
83. F. Van Breusegem, J. Bailey-Serres, R. Mittler, *Plant Physiol.* **2008**, *147*, 978–984.
84. P. Wojtaszek, *Biochem. J.* **1997**, *322*, 681–692.
85. P. Wardman, L. P. Candeias, *Radiat. Res.* **1996**, *145*, 523–531.
86. Y. Bi, W. Chen, W. Zhang, Q. Zhou, L. Yun, D. Xing, *Biol. Cell* **2009**, *101*, 629–643.
87. M. F. Iannone, E. P. Rosales, M. D. Groppa, M. P. Benavides, *Protoplasma*, **2010**, *245*, 15–27.
88. L. Garnier, F. Simon-Plas, P. Thuleau, J.-P. Agnel, J.-P. Blein, R. Ranjeva, J.-L. Montillet, *Plant Cell Environ.* **2006**, *29*, 1956–1969.
89. L. M. Sandalio, H. C. Dalurzo, M. Gomez, M. C. Romero-Puertas, L. A. del Rio, *J. Exper. Bot.* **2001**, *52*, 2115–2126.
90. M. Rodriguez-Serrano, M. C. Romero-Puertas, D. M. Pazmino, P. S. Testillano, M. C. Risueno, L. A. del Rio, L. M. Sandalio, *Plant Physiol.* **2009**, *150*, 229–243.
91. H. Obata, M. Umebayashi, *J. Plant Nutr.* **1997**, *20*, 97–105.
92. J. F. Goncalves, F. G. Antes, J. Maldaner, L. B. Pereira, L. A. Tabaldi, R. Rauber, L. V. Rossato, D. A. Bisognin, V. L. Dressler, E. M. de Moraes Flores, F. T. Nicoloso, *Plant Physiol. Biochem.* **2009**, *47*, 814–821.
93. R. A. Street, M. G. Kulkarni, W. A. Stirk, C. Southway, J. Van Staden, *South African J. Bot.* **2010**, *76*, 332–336.
94. M. C. Romero-Puertas, F. J. Corpas, M. Rodriguez-Serrano, M. Gomez, L. A. del Rio, L. M. Sandalio, *J. Plant Physiol.* **2007**, *164*, 1346–1357.

95. F. Fidalgo, R. Freitas, R. Ferreira, A. M. Pessoa, J. Teixeira, *Environ. Exper. Bot.* **2011**, *72*, 312–319.
96. J. Dong, F. Wu, G. Zhang, *Chemosphere* **2006**, *64*, 1659–1666.
97. S. Mishra, S. Srivastava, R. D. Tripathi, S. Dwivedi, M. K. Shukla, *Environ. Toxicol.* **2008**, *23*, 294–301.
98. S. A. Hasan, S. Hayat, A. Ahmad, *Chemosphere* **2011**, *84*, 1446–1451.
99. U.-H. Cho, N.-H. Seo, *Plant Sci.* **2005**, *168*, 113–120.
100. N. V. Laspina, M. D. Groppa, M. L. Tomaro, M. P. Benavides, *Plant Sci.* **2005**, *169*, 323–330.
101. A. Schützendübel, P. Schwanz, T. Teichmann, K. Gross, R. Langenfeld-Heyser, D. L. Godbold, A. Polle, *Plant Physiol.* **2001**, *127*, 887–898.
102. V. Dixit, V. Pandey, R. Shyam, *J. Exper. Bot.* **2001**, *52*, 1101–1109.
103. A. Chaoui, S. Mazhoudi, M. H. Ghorbal, E. ElFerjani, *Plant Sci.* **1997**, *127*, 139–147.
104. S. Ünyayar, A. Güzel Deger, A. Celik, F. Ö. Cekic, S. Cevik, *Turkish J. Biol.* **2010**, *34*, 413–422.
105. E. Skorzynska-Polit, M. Drazkiewicz, Z. Krupa, *Biol. Plant.* **2003**, *47*, 71–78.
106. J. Kovacik, B. Klejdus, J. Hedbavny, F. Stork, M. Backor, *Plant Soil* **2009**, *320*, 231–242.
107. A. Metwally, V. I. Safronova, A. A. Belimov, K.-J. Dietz, *J. Exper. Bot.* **2005**, *56*, 167–178.
108. W. Cui, G. Fu, H. Wu, W. Shen, *Biometals* **2011**, *24*, 93–103.
109. K. Smeets, A. Cuypers, A. Lambrechts, B. Semane, P. Hoet, A. Van Laere, J. Vangronsveld, *Plant Physiol. Biochem.* **2005**, *43*, 437–444.
110. T. Bao, T. Sun, L. Sun, *African J. Biotechnol.* **2011**, *10*, 7198–7206.
111. S. M. Gallego, M. J. Kogan, C. E. Azpilicueta, C. Pena, M. L. Tomaro, *Plant Growth Regulation* **2005**, *46*, 267–276.
112. M. Smiri, A. Chaoui, N. Rouhier, E. Gelhaye, J.-P. Jacquot, E. El Ferjani, *Biol. Trace Element Res.* **2011**, *142*, 93–105
113. Y. Cai, F. Cao, W. Cheng, G. Zhang, F. Wu, *Biol. Trace Element Res.* **2011**, *143*, 1159–1173.
114. M. C. Romero-Puertas, M. Rodriguez-Serrano, F. J. Corpas, M. Gomez, L. A. Del Rio, L. M. Sandalio, *Plant Cell Environ.* **2004**, *27*, 1122–1134.
115. B.V. Somashekaraiah, K. Padmaja, A. R. K. Prasad, *Physiol. Plant.* **1992**, *85*, 85–89.
116. F. B. Wu, G. P. Zhang, P. Dominy, *Environ. Exper. Bot.* **2003**, *50*, 67–78.
117. K. B. Balestrasse, S. M. Gallego, M. L. Tomaro, *Plant Soil* **2004**, *262*, 373–381.
118. W. Djebali, M. Zarrouk, R. Brouquisse, S. El Kahoui, F. Limam, M. H. Ghorbel, W. Chaibi, *Plant Biol.* **2005**, *7*, 358–368.
119. Z. Krupa, T. Baszynski, *Acta Physiol. Plant.* **1989**, *11*, 111–116.
120. W. Maksymiec, R. Russa, T. Urbaniksypniewska, T. Baszynski, *J. Plant Physiol.* **1992**, *140*, 52–55.
121. O. Ouariti, N. Boussama, M. Zarrouk, A. Cherif, M. H. Ghorbal, *Phytochemistry* **1997**, *45*, 1343–1350.
122. A. H. Berglund, M. F. Quartacci, C. Liljenberg, *Biochem. Soc. Trans.* **2000**, *28*, 905–907.
123. M. F. Quartacci, C. Pinzino, C. L. M. Sgherri, F. Dalla Vecchia, and F. Navari-Izzo, *Physiol. Plant.* **2000**, *108*, 87–93.
124. F. Jemal, M. Zarrouk, M. H. Ghorbal, *Biochem. Soc. Trans.* **2000**, *28*, 907–910.
125. I. A. Guschina, J. L. Harwood, *Biochem. Soc. Trans.* **2000**, *28*, 910–912.
126. Y. H. Jin, A. B. Clark, R. J. C. Slebos, H. Al-Refai, J. A. Taylor, T. A. Kunkel, M. A. Resnick, D. A. Gordenin, *Nature Genetics* **2003**, *34*, 326–329.
127. A. J. Lin, X.-h. Zhang, M.-m. Chen, Q. Cao, *J. Environ. Sci.-China* **2007**, *19*, 596–602.
128. S. Gebicki, J. M. Gebicki, *Biochem. J.* **1999**, *338*, 629–636.
129. T. Roldan-Arjona, R. R. Ariza, *Mutation Res.-Rev. Mutation Res.* **2009**, *681*, 169–179.
130. M. Fojtova, A. Kovarik, *Plant Cell Environ.* **2000**, *23*, 531–537.
131. M. Fojtova, J. Fulneckova, J. Fajkus, A. Kovarik, *J. Exper. Bot.* **2002**, *53*, 2151–2158.
132. A. Kuthanova, L. Fischer, P. Nick, Z. Opatrny, *Plant Cell Environment* **2008**, *31*, 1634–1643.
133. P. Cvjetko, S. Tolic, S. Sikic, B. Balen, M. Tkalec, Z. Vidakovic-Cifrek, M. Pavlica, *Arhiv Za Higijenu Rada I Toksikologiju* **2010**, *61*, 287–296.

134. N. P. Singh, M. T. McCoy, R. R. Tice, E. L. Schneider, *Exper. Cell Res.* **1988**, *175*, 184–191.
135. G. Koppen, L. Verschaeve, *Mutation Res.-Environ. Mutagen. Rel. Subj.* **1996**, *360*, 193–200.
136. A. J. Lin, Y. G. Zhu, Y. P. Tong, C. N. Geng, *Bull. Environ. Contam. Toxicol.* **2005**, *74*, 589–596.
137. S. R. Desai, X. N. Verlecar, Nagarajappa, U. Goswami, *Ecotoxicology* **2006**, *15*, 359–363.
138. S. Hattab, L. Chouba, M. Ben Kheder, T. Mahouachi, H. Boussetta, *Plant Biosyst.* **2009**, *143*, S6–S11.
139. M. Shahrtash, S. Mohsenzadeh, H. Mohabatkar, *J. Cell Mol. Res.* **2010**, *2*, 42–48.
140. W. Liu, P. J. Li, X. M. Qi, Q. Zhou, L. Zheng, T. H. Sun, Y. S. Yang, *Chemosphere* **2005**, *61*, 158–167.
141. W. Liu, Y. S. Yang, P. J. Li, Q. X. Zhou, L. J. Xie, Y. P. Han, *J. Hazard. Mat.* **2009**, *161*, 878–883.
142. W. Liu, Y. S. Yang, D. Francis, H. J. Rogers, P. Li, Q. Zhang, *Chemosphere* **2008**, *73*, 1138–1144.
143. M. S. Taspinar, G. Agar, N. Yildirim, S. Sunar, O. Aksakal, S. Bozari, *J. Food Agricult. Environ.* **2009**, *7*, 857–860.
144. N. Fusco, L. Micheletto, G. Dal Corso, L. Borgato, A. Furini, *J. Exper. Bot.* **2005**, *56*, 3017–3027.
145. L. Minglin, Y. X. Zhang, T. Y. Chai, *Gene* **2005**, *363*, 151–158.
146. C. Mediouni, G. Houlne, M.-E. Chaboute, M. H. Ghorbel, F. Jemal, in *Biosaline Agriculture and High Salinity Tolerance*, Eds C. Abdelly, M. Ozturk, M. Ashraf, C. Grignon, Birkhäuser Verlag AG, Basel, 2008, pp. 325–333.
147. T.-H. Ma, Z. Xu, C. Xu, H. McConnell, E. V. Rabago, G. A. Arreola, H. Zhang, *Mutat. Res.-Environ. Mutagen. Rel. Subj.* **1995**, *334*, 185–195.
148. H. M. Abdel Migid, Y. A. Azab, W. M. Ibrahim, *Ecotoxicol. Environ. Safety* **2007**, *66*, 57–64.
149. G. Krishna, M. Hayashi, *Mutat. Res.-Fundament. Mol. Mech. Mutagen.* **2000**, *455*, 155–166.
150. T. Cavas, S. Ergene-Gozukara, *Mutat. Res.-Genetic Toxicol. Environ. Mutagen.* **2003**, *534*, 93–99.
151. S. Ünyayar, A. Celik, F. Ö. Cekic, A. Gozel, *Mutagenesis* **2006**, *21*, 77–81.
152. C. S. Seth, V. Misra, L. K. S. Chauhan, R. R. Singh, *Ecotoxicol. Environ. Safety* **2008**, *71*, 711–716.
153. N. Manier, A. Deram, F. Le Curieux, D. Marzin, *Water, Air, Soil Pollut.* **2009**, *202*, 343–352.
154. E. V. C. Rosa, C. Valgas, M. M. Souza-Sierra, A. X. R. Correa, C. M. Radetski, *Environ. Toxicol. Chem.* **2003**, *22*, 645–649.
155. M. Villatoro-Pulido, R. Font, M. I. De Haro-Bravo, M. Romero-Jimenez, J. Anter, A. De Haro Bailon, A. Alonso-Moraga, M. Del Rio-Celestino, *Mutagenesis* **2009**, *24*, 51–57.

Chapter 14
Toxicology of Cadmium and Its Damage to Mammalian Organs

Frank Thévenod and Wing-Kee Lee

Contents

ABSTRACT 416
1 INTRODUCTION 417
2 SOURCES AND EXPOSURES 418
2.1 Occupational Sources and Exposures 418
2.2 Non-Occupational Sources and Exposures 419
3 ENTRY PATHWAYS, TRANSPORT, AND TRAFFICKING 421
3.1 Entry Pathways 421
3.1.1 Lungs 421
3.1.2 Gastrointestinal Tract 422
3.1.3 Skin 424
3.1.4 Placenta 424
3.2 Transport and Trafficking 424
3.3 Excretion 425
4 HEALTH EFFECTS 426
4.1 Acute Toxicity 426
4.1.1 Inhalation 426
4.1.2 Ingestion 427
4.1.3 Animal Studies 427
4.2 Chronic Toxicity 428
4.2.1 Teratogenicity 429
4.2.2 Cancer 429
4.3 Target Organs 430
4.3.1 Kidney 430
4.3.2 Liver 433
4.3.3 Respiratory System 434
4.3.4 Bone 436
4.3.5 Cardiovascular System 438
4.3.6 Nervous System 440

F. Thévenod (✉) • W.-K. Lee
Centre for Biomedical Training and Research (ZBAF), Institute of Physiology & Pathophysiology, Faculty of Health, Private University of Witten/Herdecke, D-58453 Witten, Germany
e-mail: frank.thevenod@uni-wh.de; wing-kee.lee@uni-wh.de

A. Sigel, H. Sigel, and R.K.O. Sigel (eds.), *Cadmium: From Toxicity to Essentiality*, Metal Ions in Life Sciences 11, DOI 10.1007/978-94-007-5179-8_14,

4.3.7 Reproductive System 440
4.3.8 Endocrine Glands 441
4.3.9 Hematopoiesis and Hemostasis 442
4.4 Early Biomarkers 443
4.5 Prevention and Therapy of Toxicity 445
4.5.1 Prevention 445
4.5.2 Therapy of Acute Poisoning 446
4.5.3 Therapy of Chronic Poisoning 446
5 CELLULAR AND MOLECULAR MECHANISMS OF TOXICITY 446
5.1 Entry Pathways 446
5.2 Interference with Transport and Homeostasis of Essential Metals and Biological Molecules 447
5.3 Disruption of Physiological Signaling Cascades 450
5.3.1 Cadmium and Calcium Signaling 450
5.3.2 Cadmium and cAMP Signaling 451
5.3.3 Cadmium and Nitric Oxide Signaling 451
5.4 Oxidative Stress and Recruitment of Stress Signaling Pathways 451
5.4.1 Oxidative Stress 452
5.4.2 Endoplasmic Reticulum Stress Signaling 452
5.4.3 Cadmium and Mitogen Activated Protein Kinases 453
5.4.4 Cadmium and Nuclear Factor Kappa B 454
5.5 Activation of Cell Death Pathways 454
5.5.1 Cadmium and Apoptosis 455
5.5.2 Cadmium and Mitochondria 455
5.5.3 Cadmium and Bcl-2 Proteins 457
5.5.4 Other Apoptotic Signaling Pathways Involved in Cadmium Toxicity 457
5.5.5 Cadmium and Necrosis 458
5.5.6 The Apoptosis-Necrosis Switch 458
5.6 Reprogramming of Developmental Signaling Pathways 459
5.6.1 Cadmium and Wnt/β-Catenin 459
5.6.2 Cadmium and Hedgehog 460
5.7 Genetic and Epigenetic Effects 461
5.7.1 Cadmium, DNA Damage, and Inhibition of DNA Repair 461
5.7.2 Cadmium and Epigenetics 461
5.7.3 Cadmium and MicroRNA 462
5.8 Mechanisms of Adaptation, Survival, and Carcinogenesis 462
5.8.1 Adaptation and Survival Mechanisms Induced by Cadmium 462
5.8.2 Cadmium and Carcinogenesis 464
5.9 Metallohormone Effects 465
5.9.1 Cadmium as a Metalloestrogen 465
5.9.2 Cadmium and Androgenic Effects 466
6 ENDOGENOUS DETOXIFICATION 466
7 CONCLUDING REMARKS AND FUTURE DIRECTIONS 468
ABBREVIATIONS AND DEFINITIONS 469
ACKNOWLEDGMENTS 472
REFERENCES 472

Abstract The detrimental health effects of cadmium (Cd) were first described in the mid 19th century. As part of industrial developments, increasing usage of Cd has led to widespread contamination of the environment that threatens human health, particularly today. Rather than acute, lethal exposures, the real challenge in the 21st century in a global setting seems to be chronic low Cd exposure (CLCE),

mainly from dietary sources. Ubiquity of Cd makes it a serious environmental health problem that needs to be thoroughly assessed because it already affects or will affect large proportions of the world's population. CLCE is a health problem that affects increasingly organ toxicity, especially nephrotoxicity, without a known threshold, implying that there is currently no safe limit for CLCE. In this chapter, we summarize current knowledge on the sources of Cd in the environment, describe the entry pathways for Cd into mammalian organisms, sum up the major organs targeted by acute or chronic Cd exposure and review the impact of Cd on organ function and human health. We also aim to put early pioneering studies on Cd poisoning into perspective in the context of recent ground-breaking prospective long-term population studies, which link CLCE to leading causes of diseases in modern societies – cancer, diabetes, and cardiovascular diseases, and of state-of-the-art studies detailing cellular and molecular mechanisms of acute and chronic Cd toxicity.

Keywords biomarkers • cancer • signaling • toxicity • transition metal • transport

1 Introduction

Cadmium (Cd) is a relatively rare metal, which is mainly found in the earth's crust at concentrations between 0.1–0.5 μg/g, mostly in combination with zinc. It was discovered in 1817 by Stromeyer as an impurity in zinc carbonate (latin = "cadmia"). In the environment, Cd exists preferentially in the oxidation state +2 and usually does not undergo oxidation-reduction reactions. Cd occurs naturally in the environment in its inorganic form as a result of volcanic emissions, forest fires, and weathering of rocks. In addition, anthropogenic sources have increased the background levels of Cd in the atmosphere, soil, water, and living organisms (see also Chapters 2 and 3 of this book). But Cd as a chemical element cannot be degraded, therefore its concentration in the environment increases steadily and globally. Since the first systematic studies on chronic Cd poisoning were performed in the 50s (reviewed in [1]), strict safety regulations and controls have been implemented by companies and state authorities, which efficiently prevent recurrence of health hazards in exposed populations. After the health effects of Cd were first described in 1858, where respiratory and gastrointestinal symptoms were observed in persons using Cd-containing polishing agent [1], more than 10,000 studies and reviews have been published on the topic and knowledge on Cd associated health hazards and preventive measures are well established.

Why is Cd^{2+} the species of the metal that is noxious to organisms, toxic? Cellular concentrations of essential metal ions are tightly regulated and both deficiency and overload have adverse effects. Non-essential metal ions, such as Cd^{2+}, compete with essential metal ions for entry into cells. Their interference with the function of essential metal ions disrupts cellular functions and leads to disease. Moreover, iron and zinc deficiencies, which are both most common in humans, enhance Cd^{2+} uptake.

Why should we care about Cd as a toxic compound? Not because of the rare cases of acute Cd intoxication, nor because of its health threat in an occupational context

(Cd is ranked eighth in the Top 20 Hazardous Substances Priority List! [2]). Recently a shift of paradigm has occurred in our understanding of the health problems due to Cd exposure. The real challenge in the 21st century in a global setting seems to be chronic (i.e., over decades or even throughout life) low (i.e., in concentrations barely exceeding the "natural" environmental Cd concentrations) Cd exposure (CLCE), which already affects or will affect large proportions of the world populations. Nowadays CLCE results from dietary sources and cigarette smoking. Modern agriculture globally uses Cd-containing phosphate fertilizers to increase its efficiency of harvests. Plants, including tobacco, accumulate Cd, which is passed on to animals and man in the food chain. Smoking is now established as a major cause of chronic health issues, i.e., cardiovascular diseases and cancer. Still, large parts of the population do not abstain from smoking and though other components of tobacco smoke have been identified as being responsible for the development of smoking-associated diseases, evidence accumulates that Cd in tobacco smoke is one of the factors in its own right that causes smoking-associated chronic diseases.

CLCE causes chronic diseases and increases overall mortality because Cd has a very long biological half-life that may exceed 20–30 years and accumulates in organs, which can result in fibrosis, failure or, as a Class 1 human carcinogen, cancer. Hence, Cd exposure in the childhood may affect health in old age. Only recently has CLCE gained public attention with possible impact on EU legislation. Maximal exposure values for the general population to limit chronic Cd toxicity need to be re-defined as a consequence of the globally much debated CONTAM report from the European Food Safety Authority [3,4], which concluded that current Cd threshold values in food can cause kidney damage and should be reduced.

Ubiquity of Cd make it a serious environmental health problem that needs to be assessed because, besides being a well-known occupational hazard, CLCE is a health problem for ~10% of the general population that increases organ toxicity, especially nephrotoxicity, without a known threshold, implying that there is currently no safe limit for CLCE.

Hence, we found it timely and necessary to summarize and integrate past and current knowledge by reviewing pioneering studies on the mechanisms of Cd toxicity in organisms, tissues, cells, and molecules in addition to recent state-of-the art publications that take novel developments on causes and consequences of CLCE into consideration.

2 Sources and Exposures

2.1 Occupational Sources and Exposures

Areas in the vicinity of zinc mines and smelters often show pronounced Cd contamination [2,5]. Until the 1920s the industrial use of Cd was limited, but the world Cd production has increased steadily to ~20,000 tons/year in the 1980s,

which has remained constant at this level until present. In 2009, China, The Republic of Korea, and Japan were responsible for more than 50% of the world production of Cd (World Bureau of Metal Statistics, Hertfordshire, United Kingdom; http://www.world-bureau.com/). About 80% of Cd produced is still used in batteries, especially nickel-Cd batteries, which have been banned by the European Union since 2004. About 10% of the yearly Cd production is used for color pigments in paints and plastics, and because of its non corrosive properties 5% is consumed for electroplating or galvanizing alloys, particularly in the aircraft industry. Further applications of Cd are solders, its use as a barrier to control nuclear fission, or as a plastic stabilizer (http://www.cadmium.org/; The International Cadmium Association (ICdA)).

Cd waste enters the air, water, and soil through industrial and household wastewater and waste incineration, burning of fossil fuels, and biomass. The primary form of Cd in occupational exposures is Cd oxide (CdO), which is predominantly inhaled from industrial dust and fumes. Improved technologies and regulations mean little Cd now enters air and water in Western Europe or Northern America. But it is still a major source of contamination in developing and newly industrializing countries.

Up to the l960s, very elevated Cd exposure levels in air were measured in some workplaces (exceeding 1 mg/m^3). To decrease this level, the Agency for Toxic Substance and Disease Registry (ATSDR) has set minimal risk levels (MRL) for acute (<14 days) or chronic (>1 year) Cd inhalation exposure of 0.03 respective 0.01 μg/m^3 [2] (http://www.atsdr.cdc.gov/toxprofiles/tp5.pdf), which is well below the value set by the Occupational Safety & Health Administration from the US Department of Labor (OSHA) (legal limit of 2.5–5 μg/m^3 Cd averaged over an 8-hour work day). Ambient air Cd concentrations have been estimated to <10 ng/m^3 (0.1–0.5 ng/m^3 in rural and 2–15 ng/m^3 in urban areas) but concentrations several fold higher, up to 1.2 μg/m^3, can be found near lead or zinc smelters [5,6]. Road traffic and the use of wood-burning fires or stoves increase indoor Cd pollution [7].

2.2 *Non-Occupational Sources and Exposures*

Besides smoking, the major route of Cd intake for non-occupationally exposed humans is through food or water. Cd in drinking water contributes only to less than a few percent of the total Cd intake [8] with the exception of heavily contaminated areas. Food is the major source of Cd for the general population, which is particularly caused by the use of phosphate rock (as opposed to processed phosphoric acid and phosphate fertilizers) for agricultural purposes because most natural and agricultural soils are phosphate-deficient and plants require phosphate for growth.

Compared to those of igneous origin, phosphate rock deposits of sedimentary origin contain higher levels of Cd and are the raw material used in the manufacture of most commercial phosphate fertilizers. In 2009, the world's largest producers of

rock phosphate were China (~40%), Morocco (~17%), and the USA (~16%). Its Cd content varies between <20 to >200 mg Cd/kg rock phosphate (http://ec.europa.eu/environment/enveco/taxation/pdf/cadium.pdf). Whereas China and USA consume their own production, Morocco exports most of its phosphate production, e.g., to other African countries, the USA, and India. During the last 10 years the phosphate rock consumption of Western and Central Europe and Northern America has steadily decreased by 30–70% (http://www.fertilizer.org/). In these areas, decreased Cd contamination is due to replacement of sedimentary phosphate rock by igneous rock phosphate (from South Africa or Russia), by applying lower amounts of fertilizers, or by "decadmiation" technologies (http://ec.europa.eu/environment/enveco/taxation/pdf/cadium.pdf).

Increased Cd uptake by plants depends on plant species, pH, and other soil characteristics [9]; (http://www.environment-agency.gov.uk/static/documents/Research/SCHO0709BQRM-e-e.pdf). Soluble and insoluble complexes with organic matter are also important. Generally, Cd binds strongly to organic matter, which immobilizes it. But soil pH is the most important factor controlling Cd uptake by plants, with its mobility decreasing with increasing alkalinity [9–11]; (http://www.environment-agency.gov.uk/static/documents/Research/SCHO0709BQRM-e-e.pdf). Liming soil to increase its pH has been shown to reduce the mobility and plant availability of Cd in different soils [2,9]. Processes that acidify soil (e.g., acid rain) on the other hand may increase Cd concentrations in food.

Plant food generally contains higher concentrations of Cd than meat, egg, milk, dairy products, and fish [12]. Cereals, such as rice and wheat grains, green leafy vegetables and root vegetables, such as carrot and celeriac, accumulate Cd [9]. High levels of Cd are also found in oil seeds, cocoa beans, peanuts, and in wild mushrooms as well as in shellfish and offal products (liver and kidney), especially from older animals, such as pigs and sheep. Animal liver and kidney can have levels higher than 50 μg/kg; cereal grains concentrate Cd up to 10–150 μg/kg and shellfish accumulate 1–2 mg/kg.

The average Cd intake from food generally varies between 8 and 25 μg per day, depending on the Cd concentration of the food [8,13–16]. Up to 10% of food Cd is absorbed by the body [17]. Based on estimation of Cd intake, more than 80% of the food-Cd comes from cereals and vegetables [8]. Population with specific dietary habits, for example, vegetarians and high consumers of shellfish, can have a higher intake of Cd. Moreover, specific populations may be more susceptible to Cd due to genetic variation. Because of ionic competition, deficiencies of other metal ions, such as Zn, Ca or Fe may increase the accumulation of Cd. Populations in developing countries, where such deficiencies are prevalent, are at risk, and more particularly women of child-bearing age who are Fe-depleted and anemic.

The CONTAM report from the European Food Safety Authority recently concluded that across Europe the average dietary intake of Cd in adults is between 1.9 and 3.0 μg/kg b.w. per week, and can even reach 2.5–3.9 μg/kg b.w. per week in highly exposed adults [3] (http://www.efsa.europa.eu/en/efsajournal/doc/980.pdf). This intake is close to or slightly exceeding the threshold value of 2.5 μg/kg b.w. per

week at which signs of tubular damage are noticeable in 95% of the population by age 50. This report has been criticized by the Joint Food and Agriculture Organisation/World Health Organization (FAO/WHO), which came up with a threshold value of 5.8 μg/kg b.w. per week (http://www.who.int/foodsafety/chem/jecfa/summaries/summary73.pdf). Both assessments used the same epidemiological dataset and had two primary components: a concentration-effect model that relates the concentration of Cd in urine to that of β2-microglobulin, a biomarker of renal tubular effects, and a toxicokinetic model that relates urinary Cd concentration to dietary Cd intake. The CONTAM Panel reevaluated the two assessments and maintained its previous conclusion [4]; http://www.efsa.europa.eu/de/efsajournal/doc/1975.pdf. Hence it can be concluded that the average dietary intake of Cd in adults in Europe ("CLCE") may affect human health in the long run.

Cigarette smoking is a major non-occupational source of Cd exposure, which is inhaled mainly as CdO. Accumulation of Cd in tobacco plants can vary widely: average concentrations are 1–2 μg/g of dry weight or 0.5–1 μg per cigarette [18]. Roughly 10% of the CdO produced during cigarette smoking is inhaled with an approximate 50% absorption in the lung (see Section 3.1.1). The concentration of Cd in smokers is 4–5 times higher in blood, and 2–3 times higher in the kidneys, when compared with non-smokers [17]. Smoking is thought to roughly double the life time body burden of Cd [19]. There is also some evidence of Cd exposure from "second-hand" or "passive" smoking in children [20] and adults [21].

3 Entry Pathways, Transport, and Trafficking

3.1 Entry Pathways

Cd enters the body mainly through the lungs and the gastrointestinal (GI) tract. The absorption of Cd from the lungs is much more effective than that from the gut. However, Cd absorption from the GI tract is the main route of Cd exposure in humans.

3.1.1 Lungs

After inhalation exposure, the absorption of Cd compounds varies greatly depending on the physico-chemical properties of the Cd compounds involved, site of deposition in the lungs and particle size [22]. In the lungs, deposition, mucociliary clearance, and alveolar clearance determine the absorption of inhaled particles. Large particles, dusts (>10 μm in diameter) tend to be deposited in the upper airways, while small particles, fumes, cigarette smoke (approximately 0.1 μm in diameter) penetrate into the alveoli, which are the major site of absorption. Between 50–100% of Cd in the alveoli are transferred to the blood. In the average

human population, the amount of Cd absorbed by the lungs is not greater than ~0.2 μg per day based on the assumption that up to 50% of the retained Cd is absorbed [23]. On the basis of data on organ burdens of Cd and smoking history, Elinder et al. [24] calculated that about 50% of the Cd inhaled via cigarette smoke are absorbed by the lungs.

Inhaled Cd partly dissolves in the respiratory tract lining fluid and may be found as Cd particle, as a free ion or complexed to secreted proteins or glutathione (L-γ-glutamyl-L-cysteinyl-glycine) [25], an important cellular antioxidative metabolite involved in defense against Cd-induced oxidative stress and a Cd chelator. In principle Cd may be absorbed transcellularly (via ion channels, transporters, and endocytosis) or paracellularly. Experimental studies on rat lungs have demonstrated that more Cd is accumulated by alveolar macrophages than by type II alveolar epithelial cells [26] and has been confirmed in human studies [27]. It is likely that Cd complexes are endocytosed by alveolar macrophages, resulting in either detoxification of the metal [27], toxicity [28], or inflammatory processes [29] rather than in systemic absorption of Cd. Net transport of Cd into the body is more likely to occur via alveolar epithelia. Both, para- and transcellular free Cd transport has been demonstrated through epithelial monolayers of rat and human alveolar cell lines [30]. Paracellular Cd fluxes may, however, be the consequence of direct toxic effects of Cd, which disrupts adherens junctions [31].

Recently, several solute carriers have been cloned, which transport divalent metals (including Fe and Cd) with high affinity (K_m 0.1–1 μM), such as SLC39A8 or Zrt-, Irt-like protein 8 (ZIP8) [32] and SLC11A2 or divalent metal-ion transporter-1 (DMT1, also abbreviated to DCT1 for divalent cation transporter-1; or NRAMP2 for natural resistance-associated macrophage protein-2) [33,34] (see below). ZIP8 is strongly [35] and DMT1 weakly expressed [34] in rodent lung tissues. Both transporters are also expressed in human lung cell lines and may contribute to apical Cd uptake into lung cells [36,37]. *In vivo* studies in homozygous Belgrade rats, which are functionally deficient in DMT1 have shown that DMT1 is involved in toxic metal clearance from lungs [38]. However, overall evidence for DMT1-mediated Cd uptake by lung cells is weak. Basolateral efflux pathways for free Cd in lung epithelia are unknown.

3.1.2 Gastrointestinal Tract

The other major route of entry of Cd into the body is via the GI tract after oral exposure. Factors affecting the absorption of ingested Cd include mammalian species, type of Cd compound, dose, frequency of administration, etc.. The absorption of Cd after a single exposure ranges from 0.5–8% [39]. After chronic exposure (12 months) to Cd in drinking water rats retain less than 1% of the total amount ingested [40]. Observations in humans given radioactive Cd indicate that the average GI absorption during chronic background exposure is about 2–8% [5,41]. For a given individual, the absorption following oral exposure to Cd depends on the individual (age, body stores of Fe, Ca, and Zn; pregnancy

history; lactation; etc.) and also on the levels of ions (Zn, Ca) and other dietary components ingested with Cd. Animal experiments have shown that diets with low levels of Ca and protein may increase the intestinal absorption of Cd up to 3 times [39,42] and neonatal animals absorb Cd to a much greater extent than adult animals [43]. However, data from human studies showing a relationship between GI absorption of Cd and age are missing.

In people with low body stores of Fe the absorption of Cd is higher than in subjects with normal Fe stores [44], which has been also observed in experimental animals [45]. Interestingly, dietary Cd absorption tends to be higher in females than in males [46] because of increased incidence of low Fe stores or overt Fe deficiency in women at fertile age [47,48]. Women with low body Fe stores, as reflected by low serum ferritin levels, have on average twice (about 10% but up to 20%) the normal rate of oral Cd absorption [49]. This may be explained by the close correlation between Cd absorption and the expression of DMT1, whose expression is induced by Fe deficiency and transports Fe and Cd into the mucosa cell equally well [34,50]. This situation is exacerbated during pregnancy when enterocytes have an increased DMT-1 density at the apical surface to optimize micronutrients absorption [46,48].

Other candidates for free Cd uptake in the duodenum are ZIP14, which is encoded by the SLC39A14 gene and transports Cd with high affinity [35], and the Ca^{2+}-selective channel TRPV6, which belongs to the vanilloid family of the transient receptor potential channel (TRP) superfamily (also known as CaT1) that transports Cd^{2+} at concentrations $\geq$10 μM [51]. Cd efflux from intestinal cells by the Fe export transporter ferroportin 1 (FPN1, IREG1, MTP1), a Fe-regulated transporter implicated in the basolateral transfer of Fe from the duodenum to the circulation [52,53], has not been demonstrated so far although increased Cd uptake in Fe-deficient mice was correlated with increased expression of DMT1 and FPN1 in duodenum [54]. Interestingly, Cd absorption appears to occur independently of the enterocyte expression level of metallothioneins (MTs), small metal-binding proteins which form high-affinity complexes with divalent metals, such as Zn, Cu or Cd, and store and detoxify these metals in organs and cells (see Section 6) (reviewed in [55]).

Other nutritional forms of Cd apart from Cd^{2+} are Cd complexes with cysteine-rich peptides and proteins, such as Cd-metallothioneins (CdMT) (see also Chapter 11), Cd-phytochelatins (CdPC), and Cd-glutathione (CdGSH). In plants, Cd accumulates as a complex with MT or PC. PCs are glutathione (GSH)-derived peptides. A significant part of CdMT and CdPC from animal and plant food reaches the intestinal lumen in intact form [56,57] and is mainly broken down in the colon by GI bacterial fermentation [58]. Experimental evidence in rodents suggests that CdMT and CdPC may be absorbed intact by enterocytes, possibly via transcytosis [56,59]. Recently, a novel high-affinity multiligand receptor, the lipocalin-2 (24p3/Neutrophil Gelatinase-associated Lipocalin (NGAL)) receptor, has been identified, which mediates endocytosis of protein-metal complexes [60]. Current studies in the laboratory indicate that the lipocalin-2 receptor is expressed in rodent colon as well as in colon-like Caco-2 cells where it mediates transcytosis of CdMT and CdPC (F. Thévenod and C. Langelueddecke, unpublished).

3.1.3 Skin

A dermal route of entry through contamination of the skin has been described *in vitro* but is extremely low [61]. Percutaneous absorption of Cd chloride from water and soil into and through human skin was performed using samples of cadaver skin and did not exceed 0.6%. This route of entry may therefore be of concern only in situations where concentrated solutions would be in contact with the skin for several hours or longer.

3.1.4 Placenta

The Cd concentration of the human placenta is usually about 5–20 μg/kg wet weight [62]. The placentas of women who smoke during pregnancy have higher Cd levels than those of non-smokers [63]. But placental transfer of Cd is limited. Cd concentration in newborn blood (umbilical cord) is on average 40–50% lower than in maternal blood [64]. Transplacental transport of Cd is minimized in the normal healthy placenta presumably by the binding of Cd to MT. Placental Cd accumulation in humans [65] and experimental animals [66] may be mediated by Cd transport via placental DMT1 [67] and TRPV6 [68], which could indirectly affect the fetus.

3.2 Transport and Trafficking

Human data on the transport of Cd in the circulation from the site of absorption to the various organs are scarce. Following absorption in the lungs and/or intestine, Cd in the blood initially primarily binds to albumin and other thiol-containing high- (HMW) and low-molecular-weight (LMW) proteins in the plasma, including MT, as well as to blood cells [23]. Studies in experimental animals show that immediately after parenteral administration, most of the Cd is present in the plasma [69]. Plasma concentrations decrease rapidly during the first hours after injection of 1 mg/kg body weight, reaching a level that is less than 1% of the initial value at 24 h, and this level then decreases much more slowly. The proportion of plasma Cd bound to MT and larger proteins, respectively, varies with the length and type of exposure. During the early, fast-elimination phase, Cd in mouse plasma is mainly bound to plasma proteins with a molecular weight of 40–60 kDa (mainly albumin) [70] with low affinity (apparent stability constant ~10^{-5} M^{-1}; [71]) whereas in the slower phase (more than 24 h after injection), it is partly bound to LMW proteins, mainly MT [72] and glutathione [73] with high affinity (apparent stability constants for MT and GSH ~10^{-25}–10^{-14} M^{-1} and ~10^{-9} M^{-1}, respectively [74,75]. Similar observations were made in chronically (up to 14 weeks) Cd-treated rats [76,77]. In healthy humans, the concentrations of plasma MT (to which Cd is mostly

bound during CLCE) significantly differ in non-smokers and smokers (3.42 ± 2.30 ng/mL *versus* 4.40 ± 2.76 ng/mL) [78], whereas in occupationally exposed Cd workers plasma MT levels vary between 2–11 ng/g [79].

It is important to note that Cd also tends to concentrate in blood cells (mainly erythrocytes, but also leukocytes); only a small percentage (<10%) remains in the plasma [80]. For this reason, the monitoring of blood samples for levels of Cd exposure typically involves the analysis of whole blood. The total Cd in the leukocyte portion of the blood is negligible compared to that in the red blood cells [81]. In rodents acutely or chronically exposed to Cd, Cd in erythrocytes is partly bound to hemoglobin [82], but mostly to MT (reviewed in [5]). Red blood cells [83], lymphocytes [84], and platelets [85] contain MT, which is inducible by Cd, and contributes to the trafficking of Cd as CdMT via the systemic circulation. MT-I/II mRNA in blood and peripheral lymphocytes has recently been used as a sensitive biomarker for Cd exposure in humans [86,87]. Since MT-bound Cd is quickly cleared from the plasma by the kidneys [88,89], this protein fraction is of great importance for the transport of Cd from liver to kidney during long-term exposure [77,90–92] (see below).

The blood level of Cd largely reflects recent Cd exposure with a half life of 75–128 days (fast component); however, it also has a slow component with a half life of 7–16 years, which correlates well with total body Cd load [93] (however, as a caveat, see [94]). Non-smoking adults living in non-polluted areas have blood Cd concentrations that vary between 0.1 and 1.0 μg Cd/L in whole blood (1–10 nM) [95], and values just under 5 μg/L in smokers; values above this concentration are an indication for medical surveillance in industrial workers who do not yet have signs of renal damage.

3.3 Excretion

Once absorbed, Cd is very poorly excreted, mainly in urine and feces. In humans the amount excreted daily in urine represents only about 0.005–0.015% of the total body burden [39,96]. The mean concentration of urinary Cd in people not exposed to high Cd levels is ~0.5–2.0 μg/L [23] and increases with age [97–99] and body burden [2,100,101]. Smokers have higher urinary excretion than non-smokers [97,99]. Increased urinary Cd excretion occurs when tubular proteinuria develops [100,102]. Most of the Cd in urine is transported bound to MT. Tohyama et al. [103] found good correlation between urinary MT and Cd in the general population as well as in smokers [104]. Roels et al. [105] confirmed this correlation in Cd workers. Over a range of doses, an increase in urinary excretion of Cd is associated with an increase of Cd in the renal cortex [106–108]. Chronic studies on several mammalian species have shown that urinary excretion of Cd increases slowly for a considerable time but, as kidney dysfunction develops, a sharp increase in excretion occurs [5,106,107,109]. This leads to a decrease in renal and liver Cd concentrations [5,106].

Fecal Cd concentrations range between 0.1–0.4 μg/g wet weight [96], whilst Japanese populations display 2.5–3.5-fold higher Cd concentrations than other populations. In contrast to urinary Cd excretion there is no age dependence of fecal excretion. The average daily fecal Cd varies between 18 μg in Sweden and 40 μg in Japan. A large proportion of the GI Cd excretion is directly related to the daily intake. Hence the average daily fecal Cd is slightly higher among smokers than among non-smokers (by 1.8–3.8 μg Cd/day) [96].

It is difficult to study experimentally GI excretion after oral exposure, since it is not possible to distinguish net GI excretion from unabsorbed Cd in feces. Animal studies of GI excretion following injections of Cd (summarized in [39]) show that a few percent of the dose is excreted in the feces within the first few days after injection. After chronic exposure of rats, fecal excretion amounts to about 0.03% of the body burden, which is considerably more than the urinary excretion [107,110]. The mechanism of fecal excretion may involve a transfer of Cd via the intestinal mucosa, but biliary excretion may also be involved. The biliary excretion in the first 24 h after intravenous injection of Cd is dependent on the dose [111,112]. Biliary Cd has been partially characterized as a GSH complex [113]. Indeed, mutant rats (EHB and GY rats) that lack mrp2 activity, which exports GSH [114], exhibit impaired ability to transport Cd into bile [115–117]. Multidrug resistance-associated protein 2 (MRP2) also called canalicular multispecific organic anion transporter 1 (CMOAT) or ATP-binding cassette sub-family C member 2 (ABCC2) is a protein that in humans is encoded by the ABCC2 gene and represents a conjugate export pump expressed in the apical membrane of hepatocytes [118].

Cd is also eliminated through hair [119,120] and breast milk [121,122], but these routes are of limited importance for total excretion and do not significantly alter the biological half-time.

4 Health Effects

4.1 Acute Toxicity

Acute high-dose Cd toxicity in humans is now a rarity in Western countries. Its symptoms depend on the route of ingestion [123]. Toxicity also depends on the solubility of Cd compounds [2].

4.1.1 Inhalation

Acute intoxication mostly occurs by inhalation of fumes in an industrial setting [5]. There is usually a latent period of 4–12 hours between the exposure and the onset of symptoms [5]. In severe intoxication, patients develop a respiratory distress syndrome due to acute pneumonitis and pulmonary edema with respiratory failure, which can progress to death in 3–7 days [5,124,125]. Symptoms develop when CdO

fumes reach concentrations of 200–500 μg Cd/m^3 [23]. Concentrations above 1 mg/m^3 in air for 8 hours lead to acute chemical pneumonitis [5] and death occurs at about 5 mg Cd/m^3 for an 8-hour exposure [39]. Histology has shown congestion with intra-alveolar hemorrhage, metaplasia of the alveoli lining cells and fibrinous intra-alveolar exudates [5]. Inhalation exposure to Cd at concentrations of 5–20 mg/m^3 for 50–120 min gives rise to pulmonary edema in rats and rabbits (reviewed in [5,126]).

4.1.2 Ingestion

Cd ingestion, on the other hand is mostly accidental or even intentional [127], but can also occur from heavily contaminated dust exposure, food or beverages. Liver is the major target organ of toxicity following acute Cd ingestion, and Cd hepatotoxicity is the major cause of acute Cd lethality. Symptoms begin almost immediately and include salivation, nausea, vomiting, diarrhea, and abdominal pain [5,23,128]. In cases of fatal intoxication the initial symptoms have been followed by either shock due to fluid loss and death within 24 hours, or by acute renal failure with cardiopulmonary depression, liver damage and death in 7–14 days [5,23,125,128]. Necropsy has shown pulmonary edema, pleural effusions, and ascites, and hemorrhagic necrosis of organs in the GI tract [5,128]. Damage to the pancreas also resulted in glucose intolerance [5,128]. Oral administration of Cd compounds induces epithelial desquamation and necrosis of the gastric and intestinal mucosa, together with dystrophic changes of the liver, heart, and kidneys [5]. In non-fatal cases, recovery from acute poisoning is rapid and complete. The amount of Cd absorbed is probably very limited due to vomiting and the consequential short presence of Cd in the GI tract.

4.1.3 Animal Studies

In experimental animals, the readily soluble compounds have lower LD_{50} values than the insoluble ones after acute oral ingestion or inhalation of Cd compounds [5,129]. In experimental animals, LD_{50} inhalation values are in the range of 500 to 15 000 mg/m^3min for different species [5,130]. The LD_{50} after the injection of soluble Cd compounds is in the range of 2.5–25 mg/kg b.w. [5,131]. For most Cd compounds, the LD_{50} after oral administration is about 10-20 times higher than after parenteral administration. Liver damage is probably the cause of death after high parenteral Cd application [132,133].

Numerous studies on the effects of Cd on the testes and other reproductive organs have been reviewed by Gunn and Gould [134] and Barlow and Sullivan [135]. Testicular necrosis occurs in experimental animals given a single subcutaneous injection of 2–4 mg Cd/kg b.w. [136,137]. Shortly after dose levels similar to the LD_{50} are injected, severe endothelial damage is seen in the small vessels of the testis [136]. This damage gives rise to increased capillary permeability, which results in edema, decreased capillary blood flow, ischemia, and testicular cell necrosis [138]. A single injection of Cd salts at a dose that induces testicular hemorrhagic necrosis has been shown to induce hemorrhages and necroses in the

ovaries of prepubertal rats [139], and in the ovaries of adult rats in persistent oestrus [140]. Cd-induced testicular necrosis generally results in permanent infertility. Recent findings have shed light on the underlying mechanisms that cause acute Cd-induced damage to the testis (reviewed in [141]). They involve disruption of the blood-testis-barrier by damaging effects of Cd on E-cadherins [142] as well as p38 MAPK pathway-mediated disruption of adherens junctions [143]. ZIP8, which is expressed in Sertoli cells and in vascular endothelial cells, was found in the interstitium of the testis in mouse strains sensitive to Cd toxicity in the testis [32]. Cell damage and death may then occur via formation of reactive oxygen species (ROS) [144] (see Section 5.4).

At the molecular level, oxidative stress may play a major role to account for the cellular damage observed in organs affected by acute Cd intoxication, such as lung, liver or testes. Using electron spin resonance (ESR) for ROS detection following acute Cd overload in rats and mice, Liu et al. [145,146] have provided direct evidence for Cd-generated radical formation. In Cd-treated rats, radical adducts were formed in the liver, excreted into the bile, and were probably derived from endogenous lipids [146]. Whereas the presence or absence of MT did not affect ROS formation induced by Cd [145], depletion of hepatic glutathione significantly increased ROS production and inactivation of Kupffer cells or chelation of Fe inhibited it [146]. This suggests that disruption of the cellular GSH system, inflammatory processes in the liver, and the Fenton reaction driven by Fe, mainly contribute to ROS formation in acute hepatotoxicity by Cd. No data are available for lungs.

4.2 Chronic Toxicity

Autopsy studies in humans with CLCE have demonstrated that the Cd burden differs between organs [24,96,147]. About 50% of the retained Cd was found in the kidneys and liver with one third in the kidneys alone. More recent estimates showed that the kidneys and liver together contain ~85% of the Cd body burden, and more than 60% was found in the kidneys in the age range of 30-60 years [148]. Based on calculations of organ Cd burden according to age of 160 deceased Tokyo inhabitants, Tsuchiya et al. [98,149] estimated a biological half-life of Cd in the body of 13.4 years, in the liver of 6.2 years, and in the kidney of 17.6 years, but with large individual variations. Using a similar approach with 292 persons autopsied in Stockholm a biological half-life of kidney cortex of ~30 years was estimated in non-smokers [24]. The differential distribution of Cd in different organs and the very long biological half-life of Cd in kidney cortex may explain the increased sensitivity of the kidney cortex to Cd [150] and may also account for an increased incidence of chronic kidney disease in populations with CLCE (e.g., due to smoking [151]) or of end-stage renal failure [152].

Apart from the kidneys, other organs are also affected by Cd, which may lead to damage and dysfunction as well (see Section 4.3). In fact, Cd exposure increases the risk of mortality in affected populations. This was recently demonstrated in

two prospective population-based cohort studies [153,154], which showed higher risk for death in association with Cd exposure. Of note, in both studies, there was no indication of renal disease, indicating that Cd-induced damage to other organs contributed to increased mortality.

4.2.1 Teratogenicity

There have been few studies on the fetal toxicity of Cd transported across the placenta, which acts as a barrier to Cd. Nevertheless, a small amount may reach the fetus. Cd is also transferred to neonates through lactation. Maternal hypertension and decrease in birth weight have been associated with elevated levels of Cd in the neonate [155]. A depletion of zinc with increasing number of births and a progressive increase in Cd in smokers negatively affect infant birth weight [156]. Moreover, Marlowe et al. [157] found an association between mental retardation and raised concentrations of Cd in hair in school age children. But overall, there is no substantial evidence that Cd has caused teratogenic effects in humans.

Embryotoxicity and teratogenicity have been demonstrated in experimental animals treated with Cd compounds. Large doses of Cd salts induce severe placental damage and fetal deaths when given at a late stage of pregnancy, and teratogenic effects, such as exencephaly, hydrocephaly, cleft lips and palate, microphthalmia, micrognathia, clubfoot, and dysplastic tail, when given at early stages of gestation [158–161] (reviewed in [162]). Recent studies have attempted to identify the genes [163,164] and signaling pathways [165,166] that are affected by Cd and contribute to embryotoxicity and teratogenicity in experimental animals. However, in all these studies the observed effects were induced by very high concentrations of Cd and may therefore not address relevant issues of CLCE.

4.2.2 Cancer

A causal relationship has been observed between Cd exposure and the occurrence of cancer in various organs in humans and the administration of Cd have resulted in tumors of multiple organs/tissues in experimental animals (reviewed in [167], see also Chapter 15). This has led the International Agency for Research on Cancer (IARC) to classify Cd as a human carcinogen based on increased incidences of lung tumors [168]. Moreover, human Cd exposure has been associated with increased incidences of renal cancers [169,170]. Nevertheless, results of studies involving Cd carcinogenesis have been contested because of confounding factors such as co-exposure to other toxic chemicals and life style factors, for example, cigarette smoking.

Recent epidemiological studies have accounted for all these factors and endorse the role of exposure to Cd in the development of cancer of various organs in humans, such as female breast and endometrial [171,172], lung [173], pancreatic [174,175], and bladder cancer [176]. Though of 11 cohort studies, only 3 implied Cd as a cause

of prostate cancer [177], a recent case-control study [178] showed an excess cancer risk in subjects with increased Cd exposure. Multiple rodent studies have confirmed that Cd exposure leads to lung cancer (reviewed in [179]). Cd cancers in the prostate of rats occur at doses below the threshold for significant testicular toxicity because of a requirement for androgen production; in contrast, the rat testis will only develop tumors if Cd is given parenterally at high doses [180]. Cd exposure can also induce tumors of the pancreas, adrenals, liver, kidney, pituitary, and hematopoietic system in mice, rats, or hamsters (reviewed in [181]).

This raises the question about the underlying mechanisms for carcinogenesis, especially those relevant at comparatively low exposure conditions. Current evidence suggests that no direct genotoxicity but rather multiple indirect mechanisms are operative to induce cancer (reviewed in [182–184]).The most important among them are alterations in gene expression patterns, interactions with the cellular DNA damage response systems, and induction of oxidative stress. For further details, the reader is referred to Chaper 15 of this book by Andrea Hartwig.

The available evidence indicates that, perhaps, oxidative stress plays a central role in Cd carcinogenesis because of its involvement in Cd-induced aberrant gene expression, inhibition of DNA damage repair, and apoptosis (reviewed in [182,185,186]). In contrast, Liu et al. [187] emphasize that CLCE-induced carcinogenesis may develop independently of formation of ROS. Exposure of liver cells to a low dose (1.0 μM) of Cd that does not produce ROS induces malignant transformation after 28 weeks of continuous exposure, as evidenced by forming highly aggressive tumors upon inoculation of cells into nude mice [188]. To examine the role of ROS in Cd carcinogenesis, cellular ROS levels in control and Cd-transformed cells were determined using fluorescence probes. In Cd-transformed cells, the intracellular levels of ROS were significantly lower at basal conditions as compared to passage-matched control cells, and these transformed cells were also highly tolerant to high dose of Cd (50 μM) induced ROS production. These data indicated the minimal role of ROS in Cd-induced malignant transformation in rat liver cells, a target for Cd carcinogenesis [187,188]. These Cd transformed cells also showed acquired apoptotic tolerance, with marked reduction of redox-sensitive JNK signal transduction pathways [189]. Hence the role of ROS in malignant transformation induced by Cd needs to be clarified further.

4.3 Target Organs

4.3.1 Kidney

As a result of Cd's tendency to accumulate in epithelial cells of the proximal tubule (PT), the kidney is usually the primary critical target organ of chronic Cd toxicity in the body [17]. The kidney is, in effect, a "sentinel of Cd exposure" [190]. Cd is not only toxic to PT cells, but also to glomeruli and distal tubules [191]. For several decades the following scenario has prevailed to account for chronic nephrotoxicity mediated by Cd [88]: After uptake into the systemic circulation, Cd is initially

found in the blood plasma either loosely associated with molecules, such as albumin, amino acids or the sulfhydryl compounds, glutathione or cysteine, or tightly bound to specific metal binding proteins such as the low-molecular-weight protein MT (MW ~7 kDa) [192]. Cd which binds with low affinity to plasma components can dissociate and bind to other target molecules on cell surfaces and also enter the cells [193]. CdMT is not available for uptake by most tissues, but can be taken up by the epithelium of the PT [89]. Cd in plasma is initially transported to the liver, taken up, and in the cell Cd induces the synthesis of MT which efficiently binds and sequesters Cd, thereby buffering its toxic effects in the cell. A small proportion of liver MT is slowly released into blood plasma as the hepatocytes in which Cd is sequestered die off, either through normal turnover or as a result of Cd injury [90,194,195]. Gunn and Gould [196] and later Nordberg and Nishiyama [197] showed that in long-term exposure and even at long time intervals after a single exposure, the level of Cd initially is highest in the liver and then gradually increases in the kidneys. The strongest evidence for the concept that the major source of renal Cd in chronic Cd exposure is derived from hepatic Cd which is transported in the form of CdMT in blood plasma was provided by Chan et al. [198], who transplanted livers of Cd-exposed rats to normal rats. The levels of Cd and MT in the liver of recipient rats were decreased (106 and 1503 micrograms/g, respectively) with time after surgery. On the other hand, renal Cd and MT levels were markedly increased (195 and 1468 micrograms/g, respectively) and most of the Cd in the kidney was bound to MT [198].

Circulating Cd is filtered by the glomerulus because of the small molecular mass of the various circulating Cd forms, and mainly internalized by the S1-segment of the PT because this segment of the PT cells possess apical transporters, metabolizing brush-border enzymes, and receptors for free Cd^{2+} as well as for the complexed forms of Cd^{2+} (for a review see [193,199]). Like other low-molecular-weight proteins [200], MT is reabsorbed from primary urine into PT cells of the kidneys by megalin/cubilin receptor-mediated endocytosis (RME) [201,202]. There is also evidence that Cd and Cd-thiol conjugates can be taken up at the basolateral surface of PT cells [203–206] although the *in vivo* relevance of the contributing transporters is questionable considering their low affinity to Cd. With low, or even moderate, levels of exposure, little or no Cd is excreted in the urine. Only when the body burden of Cd is large and/or kidney injury begins to appear, urinary excretion of Cd increases significantly.

Even though the CdMT complex is non-toxic, its accumulation in the PT cells may eventually cause kidney damage. A continuous catabolism of endocytosed CdMT takes place in cultured PT cells where CdMT is trafficked to lysosomes [207,208]. Cd is split from MT in lysosomes and released into the cytosol via lysosomal DMT1-mediated transport [209,210] and bound to newly formed MT in the tubular cells. It is supposed that kidney damage is prevented until a stage is reached at which the kidneys can no longer produce enough MT (see below) though evidence for this process is lacking.

The scenario that CdMT filtered by the glomerulus is responsible for chronic Cd toxicity was recently questioned [55], mainly based on the following experimental data: (i) MT-null mice, which are unable to form the CdMT complex, are

hypersensitive to chronic Cd nephropathy [211], even though the accumulation of Cd in the kidneys was only 7% of that in wild-type mice; (ii) In cultured renal cells, cytotoxicity of CdMT is much less than $CdCl_2$, corresponding to less Cd uptake and accumulation from CdMT than from $CdCl_2$ [212,213]. Thus, it has been proposed that Cd nephrotoxicity is due to accumulation of inorganic Cd, rather than CdMT [55]. However, the studies with MT-null mice only prove that MT synthesis in renal tubular tissue protects the kidney against Cd toxicity and that in MT-null mice where no CdMT complex is formed Cd can also mediate nephrotoxicity. The studies using MT-knockout mice [211] also showed that MT-null mice accumulate much lower Cd levels in their kidneys (10 μg/g wet weight) than control mice (140 μg/g), thus showing the importance of MT for transport of Cd to the kidney and accumulation in this tissue. The *in vitro* studies by Prozialeck et al. [212] and Liu et al. [213] tested Cd for short periods of time or used high CdMT concentrations on LLCPK1 cells. Cells did not survive long enough after Cd or CdMT exposure. In contrast, using 10 μM free or 10 μM CdMT (1.4 μM MT and 10 μM Cd) Erfurt et al. [214] have demonstrated that in PT cells Cd and CdMT can reach similar levels of toxicity though at different time points (12 h for Cd and 72 h for CdMT), most likely because intracellular trafficking of CdMT to lysosomes delays the onset of toxicity (see above). Experiments with chronic subcutaneous injections of Cd in mice deficient in DMT1-mediated transport [215] or renal megalin/cubilin [216] should be able to elucidate the exact role of RME of CdMT in toxicity of the renal PT.

There appears to be a critical concentration of Cd in the renal cortex that, once exceeded, is associated with tubular dysfunction. This concentration depends on the individual, and chronic Cd nephropathy is seen in about 10% of the population at renal concentrations of ~200 μg/g and in about 50% of the population at about 300 μg/g [17,217]. In fact, more than 7% of general populations may have significant Cd-induced kidney alterations due to chronic exposure with kidney Cd levels as low as 50 μg/g renal cortex [17]. The current dogma is that as this threshold concentration is approached, the Cd chelating capacities (e.g., MT, GSH) of cells and adaptive antioxidant defense mechanisms to offset Cd-induced ROS and oxidative stress (GSH, ROS metabolizing enzymes) are overwhelmed, lipid peroxidation and oxidative damage ensue that lead to injury and cell death (reviewed in [187]). Reabsorptive dysfunction is then associated with a general transport defect of the PT that mimics the de Toni-Debré-Fanconi-Syndrome and is characterized by polyuria, phosphaturia, aminoaciduria, glucosuria, and low-molecular-weight proteinuria [218,219]. This transport defect may be a possible result of ROS-induced damage of the Na/K-ATPase [220,221]. Tubular apoptosis due to generation of ROS has also been described *in vivo* and *in vitro* that could also contribute to the Fanconi-like syndrome [211,220].

Pathologically, the PT lesions consist of initial tubular cell apoptosis or necrosis, depending on the degree of cellular damage and degeneration. With chronic exposure, damage progresses to interstitial inflammation, renal fibrosis, and failure [152]. The earliest manifestations of tubular toxicity are increased excretion of low-molecular-weight proteins, such as β2-microglobulin, retinol-binding protein, MT, etc. [222].

The urinary excretion of markers of cytolysis such as the lysosomal enzyme N-acetyl glucosaminidase (NAG) also increases. Tubular proteinuria may progress to glomerular damage with a decreased glomerular filtration rate (GFR), as demonstrated in studies of occupationally exposed workers [223]. Recent studies in environmentally exposed populations suggest that decreased GFR and creatinine clearance as well as increased serum creatinine may occur at similar Cd dose levels as the tubular damage [224,225]. The presence of larger proteins in urine, like albumin or transferrin, has been attributed to glomerular damage. But these proteins are also filtered by the intact glomerulus and reabsorbed via RME [200,226]. Overall, the pathogenesis of the glomerular lesion in Cd nephropathy is not well understood. *In vitro* studies in cultured rat glomerular mesangial cells indicate that Cd induces *c-fos* protooncogene via ERK- and stress-activated protein kinase-dependent MAPK pathways and inhibits both extrinsic and intrinsic apoptosis signaling, which may contribute to cell survival and mesangial cell hyperproliferation, as observed in certain forms of glomerulonephritis [227,228].

Sporadic evidence for chronic toxicity of the distal portions of the nephron (reduced urinary kallikrein excretion) induced by Cd exposure has also been obtained, both in experimental animals following CLCE [229] and in Cd-exposed workers [230], but the mechanisms of distal tubular damage are unclear.

Kidney damage may further progress to chronic kidney diseases with albuminuria in populations with low levels of exposure, e.g., in smokers [151] or even to end-stage renal disease (ESRD). An increased risk of ESRD has been observed at environmental exposure levels based on records of all persons residing in Cd-polluted areas near battery plants [152]. Cd may also potentiate diabetes-induced effects on the kidney [224,231,232].

4.3.2 Liver

The liver is a major metabolic organ for the *in vivo* handling of Cd (see the previous paragraph), but little is known about the metal transporters and molecular mechanisms involved in hepatic uptake of Cd. Work with isolated hepatocytes and human liver cell lines have demonstrated two possible routes of uptake: One is for the free (ionic) form of Cd (Cd^{2+}) and the other is for the complexed form of Cd^{2+} [233]. Cd^{2+} is most likely taken up by the same metal transporters that liver cells use to acquire physiologically essential metals, notably Fe^{2+}, Zn^{2+}, Mn^{2+}, and Cu^{2+}. Among those transporters is DMT-1, which is weakly expressed in liver [34,234]. Metal transporters of the Zrt-/Irt-like protein family, such as ZIP8 and ZIP14 [35,234] are also expressed in liver. However, the localization and cellular orientation of these transporters in liver cells, has not been established. Many reports have postulated Cd^{2+} uptake by voltage-dependent calcium channels in hepatic cells, however, whereas whole liver expresses transcripts for L-type Ca^{2+} channels, hepatocytes do not [235].

In vitro studies have shown that CdMT enters liver cells by receptor-mediated endocytosis [236]. However, Sabolic et al. recently demonstrated that CdMT is not

taken up by rat hepatocytes *in vivo* [237]. Rather, Kupffer cells endocytose CdMT, which could lead to the release of various pro-inflammatory cytokines, including interleukin 6 (IL-6) and tumor necrosis factor-α (TNF-α). However, no specific molecular mechanism for this process has been identified so far. Hence, not much is known about Cd uptake by the liver. Nevertheless, liver tissues store Cd. Of note, liver Cd in humans varies between 1.5–8 μg/g dry weight depending on age, sex, environmental exposure, etc., which is 10–20 times lower than in the kidney [24,238,239]. This difference is striking considering that the liver is the first organ targeted following oral Cd uptake.

In rodents, but not in humans, Cd is hepatotoxic after chronic exposure. However, hepatotoxicity is much less prominent than renal damage [131,240–242]. The mild morphological and functional alterations associated with chronic hepatotoxicity by Cd may be due to a pronounced induction of MT and GSH in the liver, which chelate (and thereby inactivate) Cd respective prevent oxidative stress [243–245]. Moreover, both Cd-bound MT and GSH may be released into the circulation and bile, respectively, via ABCC2-mediated efflux of Cd-GSH [115–117] and exocytotic or necrotic release of CdMT into the circulation [90,194]. Based on recent studies [246,247], Liu et al. [187] have questioned a role of ROS formation in chronic hepatotoxicity (and carcinogenesis) during long-term exposure to Cd at low doses. Adaptive mechanisms including induction of MT, GSH, and cellular antioxidants could diminish Cd-induced oxidative stress. This view is, however, in contrast to other reports from the literature [243,248].

In summary, the liver has a large reserve capacity and ability to induce antioxidant systems and to excrete Cd complexes luminally into the bile and basolaterally into the circulation. This may account for the lower Cd content of the liver compared to the kidney and explain why Cd toxicity has not been reported in humans. However, it cannot be excluded that subtle alterations of liver function also occur during chronic Cd exposure, which cannot be detected by liver-related biomarkers. Lee and coworkers [249] examined statistical relationships between Cd in urine and circulating antioxidants in blood of humans from the NHANES III database. Circulating levels of a number of these antioxidant markers are primarily controlled by the liver. They found inverse relationships between Cd levels in urine and the levels of circulating antioxidant markers in blood. Thus, these effects may be indirectly linked to the oxidative effects of Cd in the liver and some of these parameters could be useful as Cd biomarkers for liver toxicity in the future.

4.3.3 Respiratory System

Cd concentrations in the lungs have been determined in humans and vary between 0.4–3.0 μg/g dry weight depending on age, sex, environmental exposure, smoking status, etc. [238,250,251]. Chronic obstructive lung disease frequently occurs as a result of long-term occupational exposure to Cd dusts and fumes (reviewed in [2,5]). The severity of the disease depends on exposure time and Cd dosage. Its manifestation may be slow and become apparent only after several years of exposure. In the upper respiratory system, chronic inflammation of the nose,

pharynx, and larynx have been reported [5]. In the lower respiratory tract, the changes normally involve chronic bronchitis which may lead to a mild form of obstructive lung disease with functional impairment, while following more heavy exposure this condition may progress to diffuse interstitial fibrosis of the lower airways with alveolar damage and, in severe cases, emphysema [5,100,131,252,253]. The effects on the lung increase the mortality of Cd workers with high exposure [96,252,254]. However, if working conditions are improved the pulmonary changes are mild and occur less frequently and at a later stage than renal damage [255,256]. It is not clear whether lung impairment results from long-term exposure above a critical airborne Cd concentration or from several episodes of exposure leading to permanent changes. To prevent deleterious effects on the respiratory system, exposure to CdO fumes or dust should not exceed a Cd concentration of 20 $\mu g/m^3$ during a 40 hour working week for working life [5].

In animal studies, Snider et al. [257] observed signs of emphysema in rats 10 days after 5–15 daily 1 h periods of exposure to $CdCl_2$ aerosol (10 mg/m^3). CdO fumes (10–90 $\mu g\ Cd/m^3$), Cd salts (30–100 $\mu g/m^3$) or dust (10–270 $\mu g/m^3$) had similar effects [258–260]. Systemic chronic Cd appears to induce lung inflammation and cell proliferation *in vivo* in mice with up-regulation of proinflammatory cytokines (Cox-2, IL-6) and cell cycle regulatory molecules (STAT3, Akt, cyclin D1) and subsequent cell proliferation [261]. Pulmonary inflammation and emphysema induced by Cd inhalation appears to be associated with pulmonary oxidative stress. Rats undergoing chronic inhalation with $CdCl_2$ aerosols show significant increase of bronchoalveolar lavage fluid macrophages, neutrophils and oxidant markers (8-iso-PGF(2α), uric acid) [262]. Moreover, reduced ascorbic acid and GSH were significantly lower in Cd-exposed rats, indicating antioxidant depletion, and pulmonary emphysema developed.

In vitro studies with cultured human airway epithelial cells and *in vivo* experiments in mice demonstrated that Cd (2–50 μM for 24 h or instillation of 10 nM Cd and tissue processing after 72 h) activates the proinflammatory cytokine IL-8 in an NF-κB-independent but ERK1/2-dependent manner to elicit lung inflammation [263]. Short-duration exposure to lower doses of Cd increased the growth of human lung adenocarcinoma epithelial A549 cells, whereas higher doses were toxic and caused cell death [264]. Cd induced elevated expression of epidermal growth factor receptor (EGFR) along with different proinflammatory cytokines like interleukin-1 beta (IL-1β), TNF-α, and IL-6 [264]. ZIP8 expression has been recently shown to be under the control of TNF-α in a NF-κB-dependent manner in primary human lung epithelia [37,265], and is associated with increased Cd uptake and toxicity. Consistent with these findings, a significant increase in ZIP8 mRNA and protein expression was observed in the lung of chronic smokers compared to non-smokers [37]. Moreover, when small-cell lung cancer-derived cell lines, SR3A, were stably transfected with glutamate cysteine ligase catalytic subunit to produce higher levels of GSH, cells became Cd-resistant, possibly because of down-regulation of ZIP8 through GSH-dependent suppression of the ZIP8 transcription factor Sp1 [266]. Interestingly, Cd exposure of human airway epithelial cells is also accompanied by decreased expression of the epithelial ion channel

cystic fibrosis transmembrane conductance regulator (CFTR) [267], which plays a central role in maintaining fluid homeostasis and lung function, and also affects transcellular GSH levels and the cellular redox state in lung epithelia [268,269]. This may additionally contribute to oxidative stress and inflammation of Cd-affected pulmonary epithelia.

Chronic exposure to Cd may also be associated with lung cancer. In a population-based prospective cohort study with a median follow-up of 17.2 years in an area close to three zinc smelters, the association between incident lung cancer and urinary Cd was assessed [173]. The risk of lung cancer was 3.58 higher in a high exposure area compared to an area with low exposure. The risk for lung cancer was increased by 70% for a doubling of 24 h urinary Cd excretion, and confounding by co-exposure to arsenic was excluded. In a recent study, prospective data from a NHANES III cohort were examined to investigate the relationship between Cd exposure and cancer mortality, and the specific cancers associated with Cd exposure, in the general population [270]. In men and women urinary Cd was associated with mortality from lung cancer though this study was limited by the possibility of uncontrolled confounding by cigarette smoking or other factors, and the limited number of deaths due to some cancers. A population-based lung cancer case-control study in Central/Eastern Europe and UK was conducted in 1998–2003, including 2853 cases and 3104 controls with adjustment for confounding factors and concluded that occupational exposure to Cd (and other metals) is an important risk factor for lung cancer [271].

In experimental studies, lung cancers were induced in rats by exposure to $CdCl_2$ aerosols for 13 months as a function of the Cd concentration (12.5–50 $\mu g/m^3$) [272]. Whereas there seems to be sufficient evidence for pulmonary carcinogenicity of inhaled Cd compounds in rats no such evidence was found in mice and hamsters, indicating significant species differences in the pulmonary response to inhaled Cd. It has been demonstrated that expression of MT in the lung after inhalation of Cd differs between species due to genetic variability in pulmonary MT, which may influence the susceptibility of rats or mice to lung carcinogenesis induced by inhalation of Cd compounds [273,274].

4.3.4 Bone

The relationship between Cd toxicity and bone disease was first described in Japan in the 1950s, when people living in the Jinzu river basin area began developing multiple bone fractures, severe bone pain, and malformations of their long bones. Fractures occurred mainly in elderly multiparous women, with a form of osteomalacia, osteoporosis, renal dysfunction and renal stone formation, a syndrome that became known as Itai-Itai disease [275,276] (reviewed in [1]). Intoxication due to relatively high Cd concentrations was eventually found to be due to industrial waste discharged into the river from an upstream zinc mine. At the concentrations encountered in Itai-Itai disease Cd disrupts renal calcium and phosphate transport as well as the actions of parathyroid hormone and vitamin D metabolism, at least

partially through renal dysfunction with cellular damage and death (mainly of proximal tubules), but also inhibition and/or reduced expression of epithelial calcium channels (TRPV5) and Na-phosphate co-transporters (SLC34A1) (reviewed in [277]), and excess excretion of calcium often occurs in the urine. Hence the skeletal changes are probably related to renal Fanconi syndrome (see Section 4.3.1).

But issues with loss of bone density, height loss, and increased bone fractures have now been reported in populations exposed to far lower levels of environmental Cd than Itai-Itai victims [278]. Recent epidemiological evidence accumulates suggesting that besides kidney the bone is also a primary target organ of Cd toxicity in humans [279–283]. Sughis et al. [284] found that even in young children, low-level environmental exposure to Cd is associated with evidence of bone resorption, suggesting a direct osteotoxic effect with increased calciuria. These findings might have clinical relevance when these populations reach an older age.

Experimental studies have also addressed the question whether very low concentrations of dietary Cd that do not damage the kidney can negatively impact the skeleton by directly affecting bone tissues. Ogoshi et al. [285] reported a decrease in mechanical strength of bones in weanling rats after only 4 weeks of exposure to 5 or 10 μg Cd/mL in the drinking water – exposure levels that give urine Cd concentrations in the range of smokers. Other studies in rats designed to model human CLCE [286,287] showed that Cd affects the mineral status leading to weakening in its mechanical properties and that these processes occur prior to skeletal maturity [285,288]. Acute or chronic Cd administration resulting in low blood Cd levels increased calcium excretion in rodents well before the onset of kidney damage leading to aminoaciduria and proteinuria [289–291].

In vitro experiments with cultured cells support these *in vivo* studies. In a mouse osteoblast-like cell line, MC3T3-E1, 0.1 to 1 μM Cd decreased cellular alkaline phosphatase activity, a marker of osteoblast differentiation [292]. Moreover, >1 μM Cd increased prostaglandin E2 secretion by MC3T3-E1 cells, which could stimulate formation and activation of osteoclasts and lead to osteoclast-mediated bone resorption [293,294]. These effects, taken together, could clearly cause an uncoupling of the normal balance between bone formation and bone resorption. Moreover, Cd at 10 to 100 nM has been also shown to stimulate the formation and bone degrading activity of osteoclast-like multinuclear cells from progenitors in bone marrow cultures [295,296]. Some of the damaging effects of Cd on bone tissues may be caused by increased oxidative stress [297]. Further, gene expression microarray and gene knock-out mouse models have shown that Cd induces MT1 and MT2 to protect the cells but also stimulates bone demineralization via a fos-independent, but src- and p38 MAPK-dependent pathway involving osteoclast activation and resulting in the breakdown of bone matrix (reviewed in [298]).

Uptake of low micromolar Cd concentrations into human osteoblast-like MG-63 cells [299] and mouse MC3T3-E1 cells [300] has been recently demonstrated. The studies suggested that uptake of Cd and cytotoxicity are mediated by transient receptor potential melastatin-related 7 (TRPM7) channels though the permeability of TRPM7 to Cd is weak [301]. The authors also proposed that deficiency of Ca^{2+} or Mg^{2+}, which are preferentially transported by TRPM7 [301], may enhance Cd uptake into osteoblast cells.

4.3.5 Cardiovascular System

Most early studies on chronic occupational or environmental Cd exposure did not find any evidence for cardiovascular disease or increased mortality due to cardiovascular disease (reviewed in [5]). Cross-sectional and prospective studies by Staessen et al. [302] showed that blood pressure, or the risk of hypertension or cardiovascular diseases risk in environmentally exposed populations were not associated with 24-h urinary Cd. Subjects with Itai-Itai disease also failed to develop hypertension [303]. Similar conclusions were obtained from other epidemiological studies [304], and from studies in Belgian populations, which did not show any correlations between measures of arterial function and blood Cd and failed to confirm that increased Cd body burden was associated with decreased arterial function [305].

In contrast to these negative findings, Thun et al. [306] found that mean systolic and diastolic blood pressures were higher in 45 Cd workers (134 and 80 mmHg, respectively) than in 32 male controls (120 and 73 mmHg respectively). Systolic but not diastolic blood pressure was significantly associated with Cd dose in multivariate analyses. Recently, Navas-Acien et al. [307,308] reported that peripheral arterial disease might be associated with increased blood and urinary Cd. Satarug et al. [309] showed a positive association between blood pressure and urinary Cd in a population sample of 200 subjects that also showed tubular dysfunction. The Atherosclerosis Risk Factors in Female Youngsters (ARFY) study showed that increased blood Cd level are associated with early atherosclerotic vessel wall thickening [310]. The population-based U.S. NHANES study found that Cd exposure is associated with an increased risk of cardiovascular disease [311–314]. Cd concentrations in cardiovascular tissues (heart, aorta) have been determined in human populations and vary between 0.05 and 1 μg/g dry wet and depend on age, environmental exposure, and other aspects [238].

Animal studies support effects of Cd on blood pressure and the cardiovascular system and suggest that Cd may cause atherosclerosis and/or be toxic to the myocardium (reviewed in [315], see also [316]). Maternal exposure during pregnancy may even reprogram cardiovascular development without detectable Cd in fetal and adult tissues of the offspring [317]. The cellular and molecular foundations and pathophysiology of vascular diseases associated with chronic Cd toxicity are beginning to emerge [318,319]. Kaji et al. [320] have demonstrated that Cd inhibits proliferation and destroys the monolayer of vascular endothelial cells in a culture system. Abu-Hayyeh et al. [321] found a positive correlation between the smoking status of humans and Cd concentrations in the aortic wall, with selective accumulation in the medial layer. Their finding that the aortic wall accumulates ~7 μmol/L Cd, in contrast to nanomolar blood concentrations, indicates that the arterial wall takes up Cd and may be a target of Cd toxicity. Uptake mechanisms are unclear. SLC39A8 (ZIP9) is expressed in endothelial cells of the testis vasculature [32] and may account for testicular hemorrhage associated with acute Cd toxicity (see acute toxicity). Other endothelial localizations of SLC39A8, however, have not been described. DMT1

is also expressed in vasculature [322] and human umbilical vascular endothelial cells [323]. In the latter study, DMT1 was increased by the inflammatory mediator TNF-α. This was associated with increased iron uptake and oxidative stress [323], and could also occur in Cd-induced vascular disease. Whether Cd protein complexes are taken up by endothelia via endocytosis is unknown. Megalin is expressed in cerebral vascular endothelia where it contributes to protein transfer [324]. However, Kaji et al. [325] showed that CdMT and CdGSH are less likely to be taken up by bovine aortic endothelial cells than Cd and also cause less cytotoxicity. Free Cd may also disrupt VE cadherin-dependent cell adherens junctions of endothelial monolayers, as evidenced by *in vitro* and *in vivo* studies (reviewed in [318]), which could account for an increased permeability of the endothelial lining and development of atherosclerosis. Cd may also inhibit endothelial proliferation [325] and induce cell death by apoptosis [326] or necrosis [320,325]. ROS formation may be the mechanism underlying vascular dysfunction *in vivo* [327,328] and endothelial damage and death *in vitro* [329,330]. An additional effect of Cd contributing to atherosclerosis may be induction of smooth muscle cell proliferation, which could induce arterial wall thickening [331] and interference with fibrinolysis [332]. Cd may also reduce vasodilatatory NO [333] by inhibiting endothelial NO synthase [334,335]. As a consequence of the release of pro-inflammatory mediators, such as TNF-α [323,336] and increased leukocyte adhesion [337,338] Cd may induce vascular inflammation and thereby promote atherosclerosis [339].

Cd has also been shown to induce cardiac damage in experimental settings by two possible mechanisms: (i) disruption of tissue structure and integrity; (ii) effects on cardiac conduction (reviewed in [5]). These effects were thought to be related to (i) decreased high-energy phosphate storage in the myocardium, (ii) reduced myocardial contractility, (iii) diminished excitability of the cardiac conduction system, and (iv) a reduction in coronary blood flow by Cd in isolated heart studies due to direct actions on the coronary vasculature [340].

Morphological alterations, including necrosis, cellular degeneration, and damage to intercalated discs, have been described in rats chronically exposed to CdO fumes or Cd gavage [341,342]. Damage of cardiac cells by Cd may involve oxidative stress to the heart by an alteration of antioxidant defense and an increased generation of ROS [343], inhibition of cardiomyocyte electron transfer chain [344], as well as a direct interactions of Cd with troponin C [345] or myoglobin [346]. Cardiac cell Cd uptake could be mediated by DMT1 [34,347], megalin [348], or the lipocalin-2 receptor [349]. Nevertheless, their exact cardiac localization remains to be determined.

Effects on cardiac excitability may be based on blocking effects of Cd on ion channels, e.g. voltage-dependent calcium channels (see [199] for a review) or Na channels of Purkinje fibres [350]. Cd may also increase outward potassium currents of ventricular myocytes and shift their voltage dependency of activation to more positive voltages [351], or interfere with Ca-dependent processes in the heart [352].

4.3.6 Nervous System

Initial reports described nervous system symptoms, including headache, vertigo, and sleep disturbance [353]. Physical examination revealed increases in knee-joint reflexes, tremor, dermographia, and sweating. In human studies, anosmia has been described among Cd workers exposed to CdO dust for long periods of time in some studies [131], but not in others [354]. At the cellular level, Cd may damage neuronal function by disrupting synaptic transmission [355], by affecting intracellular sulfhydryl homeostasis as a consequence of oxidative stress [356,357], and resulting in apoptosis or necrosis [358,359].

The blood-brain barrier (BBB) severely limits Cd access to the central nervous system. A direct toxic effect of Cd on the brain occurs only prior to BBB formation and is hence age-dependent in experimental animals [360]. The brain of newborn animals is permeable to Cd which decreases with age, probably due to increased MT expression (MT-3 in brain [361]; see below) and blood brain barrier maturation [362,363]. BBB dysfunction under certain pathological conditions increases the permeability to Cd, as described in a case report following acute Cd intoxication [364]. Additionally, the choroids plexus may accumulate high levels of Cd (reviewed in [365]). Nishimura et al. [366] observed strong MT immunostaining in ependymal cells and choroid plexus epithelium in younger rats (1–3 weeks old) poisoned with Cd. Thus, the sequestration of Cd by MT may partly contribute to the high accumulation of Cd in the choroid plexus.

Because of the functional resemblance between renal proximal tubular and inner ear epithelial cells it has been hypothesized that Cd might also impair the function of inner ear cells. In rats exposed to drinking water containing 15 ppm $CdCl_2$ for 30 days, high Cd accumulation in ear ossicles and labyrinth was associated with signs of defective hearing and nephrotoxicity, but 5 ppm $CdCl_2$ caused hearing loss without affecting kidney function [367]. These results suggested that hair cells are more sensitive to Cd than kidney tubule cells.

4.3.7 Reproductive System

Animal studies on chronic Cd toxicity of the reproductive system are mostly limited to male reproductive organs. They are also inconsistent due to the variability of the Cd dosage and period of exposure. To summarize the data, chronic exposure leads to smaller testis weight and reduced endocrine function, reduced spermatogenesis, reduced spermatozoa motility, decreased fertility, sterility, DNA damage in primary spermatocytes [368] and damage to testicular cells and structures, such as Sertoli cells and seminiferous tubules (early data reviewed in [5]). Recently, chronic exposition to low doses of Cd (0.015 g/L of $CdCl_2$ in drinking water) for 3, 6, 12, and 18 months) was investigated in male mice [369]. Vascular lesions were evident from 6 months of Cd exposure and the severity of Leydig cells morphological changes increased with exposure time. Cellular degeneration was frequent

after 12 months of Cd exposure. Also two Leydig cell tumors were observed after ≥12 months Cd exposure. In contrast, in a study by Zenick et al. [370] there were no significant effects on any of the parameters of reproductive toxicity or mating in male rats exposed to ≤70 ppm Cd for 70 days. Recent studies on Sertoli cells *in vitro* [371,372] have demonstrated a number of early molecular responses to Cd exposure. Yu et al. [371] reported dose- and time-dependent morphological changes associated with apoptosis signaling in rat Sertoli cells. They also observed disruption of the ubiquitin-proteasome system, up-regulation of cellular stress response proteins and the tumor suppressor protein p53.

In a recent review, Thompson and Bannigan [373] noted that Cd accumulates in the ovary with age and is associated with decrements in oocyte development. Whereas several animal studies noticed decreased ovarial steroid hormone synthesis and release in rats following CLCE [374,375], *in vitro* studies have demonstrated increased progesterone production (reviewed in [376]). The reasons for these differences are unclear.

Human studies are also variable in their outcome. No difference was found in fertility between men occupationally exposed to Cd and an appropriately matched control group (n = 118) by assessing birth experiences of their wives [377]. In contrast, a hospital sample of the general population with infertility problems showed that blood and seminal Cd were significantly higher among infertility patients than controls [378]. The percentage of motile sperm and sperm concentration inversely correlated with seminal plasma Cd among the infertility patients. In a recent study [379], human fetal male and female gonads were recovered during the first trimester and cultured with or without Cd. Cd, at concentrations as low as 1 μM, significantly decreased germ cell density and increased apoptosis, but did not affect proliferation in human fetal ovaries. Similarly, in the human fetal testis, Cd (1 μM) reduced germ cell number without affecting testosterone secretion [379]. Further experimental as well epidemiological studies are necessary to clarify the role of chronic Cd exposure on gonadotoxicity and fertility. Nevertheless, there is an increasing awareness of the possible impact of CLCE on fertility (reviewed in [380,381]).

4.3.8 Endocrine Glands

Experimental data *in vitro* and in animals suggest that Cd may disrupt the regulatory mechanisms of the hypothalamic-pituitary axis and change the secretory pattern of pituitary hormones like prolactin, ACTH, GH or TSH, resulting in disorders of the endocrine and/or immune system [382] (reviewed in [383]), which could account for the dysfunction of adrenal and thyroid glands observed in experimental animals during chronic exposure to Cd [384–387]. But direct effects of Cd on metabolism and secretion of peripheral glands have also been suggested [388–391]. No data are available from human studies.

Cd exposure has recently been considered to be a risk factor linked to diabetes mellitus type-2. Edwards and Prozialeck [392] and Chen et al. [393] reviewed the

literature supporting a relationship between Cd exposure, elevated blood glucose levels, and the development of type-2 diabetes. In the Third National Health and Nutrition Examination Survey, a significant and dose-dependent association was found between elevations in urinary Cd levels and both impaired fasting blood glucose levels (110–126 mg/dL) and type-2 diabetes in persons >40y without renal damage [394]. A recent evaluation of Cd concentrations in biological samples of diabetes mellitus patients type-2 (age range 31–60y) has shown that the mean concentrations of blood Cd of male non-smoker and smoker diabetic patients were significantly higher than in their respective controls [395]. A prospective study, in which Cd levels are determined before the development of disease, is necessary to confirm a causal link between Cd exposure and development of diabetes. Edwards and Prozialeck [392] also provided experimental evidence indicating that Cd elevates fasting blood glucose levels in an animal model of subchronic Cd exposure before overt signs of renal dysfunction become evident. This study also showed that Cd reduces insulin levels and has direct cytotoxic effects on the pancreas. The pathogenesis of Cd-associated islet dysfunction remains to be explored. These findings also raise the possibility that Cd and diabetes-related hyperglycemia may act synergistically to damage the kidney.

4.3.9 Hematopoiesis and Hemostasis

After Cd exposure, decreased hemoglobin concentration and hematocrit are among the early signs of Cd toxicity (reviewed in [5]). Fe administration is beneficial suggesting decreased gastrointestinal absorption of Fe due to Cd [5]. Subsequent experimental studies in rats [396–399], cultured erythropoietin (EPO) producing cells [400] and populations with Itai-Itai disease [401,402] indicated that three main factors are involved in the development of Cd-induced anemia: hemolysis, Fe deficiency, and renal damage. Hemolysis can occur at the early stage of Cd exposure. Fe deficiency occurs because of competition of Cd with Fe for absorption in the intestine. However, an increase in body Fe content along with anemia is often observed in cases of parenteral Cd exposure or Itai-Itai disease, which may be caused by Fe from hemolysis, insufficient erythropoiesis, and hepatic ferritin overproduction induced by Cd-dependent interleukin-6 production [398]. Renal anemia is observed during the last phase of chronic, severe Cd intoxication, such as Itai-Itai disease. Cd suppresses renal EPO production through a direct effect, accumulation of toxic concentrations of Fe in kidney tissues, and destruction of EPO-producing cells [398,400].

Only a few studies have investigated the impact of chronic Cd exposure on immunity and hemostasis. Chronic exposure of mice to Cd by ingestion or inhalation inhibited cell-mediated immunity [403] and induced lymphopenia [404], but not in humans [405] or monkeys [406]. In contrast, *in vitro* studies with human peripheral blood mononuclear cells demonstrated Cd-induced interleukin-8 production with a concomitant generation of superoxide radicals [407]. Exposure of rats to Cd also increased platelet aggregation [408]. Moreover, chronic oral Cd

exposure shortened prothrombin time and activated partial thromboplastin time [409]. Protein C and antithrombin also decreased in rat plasma after Cd exposure, but thrombocyte counts were not affected [409]. Hence, animal studies suggest that chronic Cd toxicity induces a hypercoagulable state and thereby increases the risk of thrombosis.

4.4 Early Biomarkers

One of the major challenges of public health and Cd toxicology is monitoring of affected populations for early signs of exposure and toxicity. Due to the kinetics of Cd in the body, which redistributes to organs such as liver and kidney and is stored there for years, blood Cd levels provide only information on acute exposure to Cd, but not on total body burden of Cd or organ damage. Nevertheless, the blood levels of Cd in non-exposed populations are normally less than 0.5 μg/L and blood levels higher than 1.0 μg/L are indicative of Cd exposure; levels higher than 5 μg/L are considered hazardous. Excellent reviews on the topic have been recently published by experts in the field [12,190,410,411]. This section summarizes the most important features of these reviews and also focuses on novel and promising early biomarkers of damage.

Many classical biomarkers detect Cd toxicity at a stage when functional damage is already advanced and perhaps irreversible. Moreover, results of recent studies have shown that even low ("normal") levels of Cd exposure over a long period of time (CLCE) have subtle but insidious adverse effects on the kidney (see [3,4]), where traditional biomarkers may have their limitations [94]. Therefore, there is an increasing need for sensitive biomarkers of early exposure to low Cd concentrations where no overt pathology is apparent.

A Cd biomarker is "any substance or molecule that can serve as an indicator of the functional state or level of toxic injury in an organism, organ, tissue or cell" [190]. Practically, sampling of Cd biomarkers should be easy and without expensive, invasive or damaging procedures because it should be applied to large populations. Measurements should be limited to urine (and/or blood) samples because the kidney is the "sentinel of Cd toxicity" [190] (see Section 4.3.1). For the above reasons a recent suggestion to measure renal autophagy as an early biomarker of subtoxic Cd exposure is not practical [412].

Functionally, urinary markers of Cd nephrotoxicity can be classified into 3 groups: (1) Cd and Cd-binding proteins such as MT, (2) low-molecular-weight proteins, and (3) proteins and enzymes derived from the brush border, intracellular organelles or the cytosol of proximal tubule epithelial cells.

Ad (1) Urinary excretion of Cd and MT have been used both as markers of Cd exposure and of Cd-induced proximal tubule injury (reviewed in [222,413]). At early stages of Cd exposure, urinary Cd or MT most likely results from normal turnover and shedding of epithelial cells and is a reflection of the level of Cd exposure and the body burden of Cd (but see as a caveat the animal study by

Thijssen et al. [94] when the body Cd burden is low). When the concentration of Cd in the epithelial cells reaches a threshold value of ~150–200 μg/g wet weight [17,217,219] Cd disrupts tubular reabsorptive processes and the excretion of Cd and MT begin to increase in a linear manner, which is associated with the onset of polyuria and proteinuria (see section on kidney). The early, linear phases of Cd and MT excretion mirror the level of Cd exposure whereas the later increases in excretion reflect Cd-induced tubular injury. Urinary levels of Cd in non-exposed populations are usually below 0.5 μg/g creatinine. The critical urinary Cd concentration that is associated with the onset of renal injury is about 2–10 μg/g creatinine, which corresponds to the critical renal cortical Cd concentration of ~150–200 μg/g tissue [17,217,219]. But there is significant evidence that even lower urinary levels of Cd may be associated with adverse renal effects [150,414,415]. The critical urinary level of MT that is associated with the onset of overt kidney injury is ~300 μg/g creatinine, which is based on a value of 2–3 μg urinary Cd/g creatinine [416,417] or even less [418].

Ad (2) Low molecular weight proteins such as β2-microglobulin, Clara-cell protein (CC-16), α1-microglobulin, and retinol binding protein are plasma proteins, which are small enough to be filtered at the glomerulus. Intact PT cells almost completely reabsorb these proteins via megalin and cubilin [419]; they are therefore not detected in the urine [420] (reviewed in [222]). As Cd accumulates and damages the PT, reabsorption of these proteins becomes impaired and they appear in the urine. β2-microglobin has been most widely employed as a standard marker for monitoring early stages of Cd exposure and toxicity. Urinary levels of β2-microglobulin greater than (300–1,000 μg/g creatinine) are indicative of PT dysfunction [421] (http://www.osha.gov/pls/oshaweb/owadisp.show_document?p_table=standards&p_id=10035) but lower critical levels have also been suggested [415].

Ad (3) Enzymes, such as N-acetyl-β-D-glucosamidase (NAG), lactate dehydrogenase (LDH), alkaline phosphatase, and α-glutathione-S-transferase (α-GST) are released from dead PT cells that are washed out into the urine. The lysosomal enzyme NAG has been very useful in the monitoring of human populations [414,422]. Recent studies suggest that α-GST may be a more sensitive early marker of Cd-induced kidney injury than NAG in human populations and animal experiments [423–425]. It is up-regulated by both Cd and oxidative stress, which could explain why it appears in urine before other cytosolic enzymes.

Another promising novel early biomarker is kidney injury molecule-1 (Kim-1). Kim-1 is a transmembrane protein that is not detectable in normal kidney but is expressed at high levels in the proximal tubule after ischemic or toxic injury (reviewed in [426]). Kim-1 regulates cell adhesion and endocytosis in regenerating cells of the injured tubule as they reform a functional epithelial barrier [427]. This process is associated with the proteolytic cleavage of the ectodomain of Kim-1 into the urine [427]. It is now used as a sensitive marker for the monitoring and diagnosis of kidney disease in humans ([428]; http://www.fda.gov/bbs/topics/NEWS/2008/NEW01850.html). Studies of chronic Cd toxicity in rats showed that Kim-1 is detected in the urine 4–5 weeks before the onset of proteinuria, i.e., when there was little PT cell death, and 2–5 weeks before the appearance of MT and

CC-16 [428,429]. Recently, Pennemans et al. [430] have demonstrated that urinary Kim-1 levels positively correlated with urinary Cd concentration in an elderly population living in an area with long-term low-dose exposure to Cd, while other classical markers did not show any association. Therefore, urinary Kim-1 might be considered as a biomarker for early-stage metal-induced kidney injury by Cd.

Another very promising early biomarker of kidney damage may be neutrophil gelatinase-associated lipocalin or lipocalin-2, an acute phase 25 kDa glycoprotein which is part of the lipocalin family. NGAL is highly induced in inflammatory conditions and ischemia, and is a critical component of innate immunity to bacterial infection because it sequesters bacterial iron chelating siderophores and consequently blocks bacterial growth [431]. NGAL is also involved in growth and differentiation, especially in response to renal tissue damage and during nephrogenesis [432]. Studies in humans and experimental animals have shown that serum and urine NGAL are diagnostic and prognostic markers of acute kidney injury (reviewed in [433]) and a relevant biomarker of chronic renal failure [434]. A recent experimental study in mice demonstrated that increases in urinary NGAL (uNGAL) excretion were much more rapid (after 3–6 h) and sensitive than urinary Kim-1 (which significantly increased after 24 h) in assessing early acute kidney injury [435]. Hence, with earlier detection via Kim-1 or NGAL, it may be possible to reverse, or at least more effectively treat, Cd-induced kidney injury.

4.5 Prevention and Therapy of Toxicity

4.5.1 Prevention

In the household, practical preventive measures seek to remove Cd contaminated dusts (reviewed in [167]). In a work environment with occupational exposure to Cd fumes or dust, engineering control and ventilation should ensure that concentration levels are kept low. If constant safe air levels are not feasible, respiratory protection must be used. General rules for handling of toxic compounds should apply as well, i.e., smoking, eating, and drinking in work areas should be prohibited. Medical examination of Cd-exposed workers should be carried out at least once every year with a focus on the respiratory system and the kidneys. Cd and other early biomarker levels in blood and in urine should be checked regularly. WHO and OSHA (USA) recommend that the Cd concentration should not exceed 5–10 μg Cd/g urinary creatinine. This value is in contrast to the Cadmibel study in Belgium, which was the first to link urinary Cd with tubular proteinuria in a population study and showed that there was a 10% chance of developing tubular dysfunction at urinary Cd levels of 2–3 μg/g creatinine [436,437].

4.5.2 Therapy of Acute Poisoning

Apart from symptomatic treatment, there is currently no effective clinical treatment for Cd intoxication. One approach consists of trying to eliminate Cd using metal chelators such as ethylenediamine-N,N,N',N'-tetraacetate (EDTA) given by intravenous infusion to increase its urinary excretion [438], or if toxicity is so severe that renal function is impaired, EDTA is added to the dialysate during hemodialysis [439]. However, the role of EDTA remains unclear because of the limited number of reports in the literature and because chelation therapy for Cd may increase the uptake of Cd by the kidneys and increase the risk of nephrotoxicity. Friberg and Elinder [437] therefore recommended that EDTA is contra-indicated because of its nephrotoxicity when administered in combination with Cd. In experimental systems some chelators can reduce acute Cd-induced mortality [440]. Oral dimercaptosuccinic acid (DMSA) [441,442] or calcium disodium diethylene-triaminepentaacetate (DTPA) given parenterally [443] are the most effective antidotes, provided that treatment is started very soon after Cd ingestion.

4.5.3 Therapy of Chronic Poisoning

There is no recommended chelation treatment for chronic Cd exposure in humans [444]. However, in their review Jones and Cherian [444] highlighted a reduction of whole body, renal and hepatic levels of Cd in mice treated with compounds, such as sodium N-(4-methoxylbenzyl)-D-glucamine dithiocarbamate, or in rats using DTPA with or without 2,3-dimercaptopropanol [445]. One recent report described a combined intravenous administration of EDTA and GSH in a patient with chronic Cd intoxication [446]. Renal damage did not develop over the observation period of 6 months.

5 Cellular and Molecular Mechanisms of Toxicity

5.1 Entry Pathways

To enter the intracellular space, Cd^{2+} in extracellular fluids that is present as a free ion or complexed to proteins or peptides must permeate lipophilic cellular membranes. This occurs through intrinsic proteinous pathways. Free Cd^{2+} may be transported via ion channels and solute carriers and Cd^{2+} complexes may be taken up through receptor-mediated endocytosis. Cd^{2+} has similar chemical properties as essential metals ("ionic mimicry") and Cd^{2+} complexes are analogous to endogenous biological molecules ("molecular mimicry") [447,448]. Hence, transport (and toxicity) of Cd^{2+} can only occur if cells possess transport pathways for essential

metals or biological molecules. After entering the intracellular compartment, higher affinity complex formation of free Cd^{2+} to other proteins may take place by ligand exchange, thereby also preventing back diffusion and forming a sink for Cd^{2+}.

A variety of pathways have been suggested to allow Cd^{2+} entry in excitable and non-excitable cells [193]. The most likely candidates, whose molecular structures have been identified, are listed in Table 1. Proof of their Cd^{2+} transporting abilities has been obtained using stringent experimental approaches, such as radiotracer, fluorescent dye and/or electrophysiological transport assays combined with molecular biology techniques. Further information is available in a recent detailed review [199].

5.2 *Interference with Transport and Homeostasis of Essential Metals and Biological Molecules*

Several exhaustive reviews have summarized the literature on the effect of Cd on biomolecules involved in signal transduction [460], ion transport [277] and metalloproteins [461]. Cd binds to and/or interferes with a large number of transporters (e.g., pumps, channels, or carriers), signaling molecules (receptors, enzymes, transcription factors, etc.) and metalloproteins (e.g., Zn-, Ca-, Fe-, Mn-, Cu-binding proteins). Apart from metalloproteins and transporters for essential metals, most binding sites are "non-specific" low-affinity domains of biological molecules, but interaction with Cd may induce conformational changes and thereby affect their function. Binding occurs only when high concentrations of Cd are used, which will never be achieved *in vivo*. In fact, blood Cd concentrations in the general population are in the range of 1–10 nM [95] and may not exceed 100–300 nM in occupationally exposed workers [462]. The free Cd concentrations in the extracellular fluid that cause tissue damage are unknown but are likely to be in the submicromolar range: Acute poisoning with oral intake of a high dose of Cd resulted in a Cd concentration in the blood of ~0.2 μM [127]. Moreover, experimental studies in rats have shown that keeping artificially the free plasma Cd concentration to ~5 μM for only 30 min causes PT damage with a Fanconi-like syndrome [463] suggesting that (sub-) micromolar concentrations of Cd directly affect transport functions.

Hence, most of the studies describing direct effects of Cd on the function of transporters (reviewed in [277]) may have only *in vitro* or mechanistic relevance and are not likely to significantly contribute to *in vivo* toxicity of Cd in tissues. Indeed, few mammalian transporters are directly affected by submicromolar Cd concentrations: Ca-ATPase of rat intestinal and renal basolateral plasma membrane is blocked with an IC_{50} of 1.6 nM [464] and apical Na-dependent glucose and amino transporters of isolated rabbit PT (S2-segment) by nanomolar concentrations of CdMT [221]. However, it cannot be excluded that the effects observed were due to CdMT-induced endocytosis of apical membranes containing Na-dependent

Table 1 Putative uptake pathways for Cd^{2+} and Cd^{2+}-protein complexes in mammalian cells. For further details, refer to the text. M^{2+} = divalent metal.

Name	Endogenous substrates	Localization	Transport mechanism	Function	Cd^{2+}affinity (K_m/K_D/EC_{50})	References
SLC39A8 (ZIP8)	Zn^{2+}, Mn^{2+}	Lung, testis, kidney	M^{2+}/HCO_3^- symport	Zn^{2+}/Mn^{2+} homeostasis	~0.5 μM	[32,449,450]
SLC39A14A/B (ZIP14A/B)	Zn^{2+}, Mn^{2+}	Liver, dodenum, kidney (14A), brain (14B), testis	M^{2+}/HCO_3^- symport	Zn^{2+}/Mn^{2+} homeostasis	1.1 μM (14A) 0.14 μM (14B)	[35,451,452]
SLC11A2 (DMT1, DCT1, NRAMP2)	Fe^{2+}, Zn^{2+}, Mn^{2+}, Cu^{2+}, Co^{2+}	Duodenum, Red blood cell precursors, macrophages, kidney	M^{2+}/H^+ symport	Iron homeostasis	1.0 μM	[34,453–455]
Megalin/ Cubilin	Albumin, vitamin D binding protein, hemoglobin, myoglobin, receptor-associated protein, transferrin, MT	Polarized epithelia (kidney, intestine, inner ear, yolk sac), neurons	Receptor-mediated endocytosis	Protein endocytosis	100 μM (CdMT)	[200–202]
Lipocalin-2 (NGAL, 24p3) receptor	Lipocalin-2, transferrin, albumin, MT	Kidney, intestine, liver, lung, heart, testis	Receptor-mediated endocytosis	Protein endocytosis	0.1 μM (CdMT)	[60,349]
TRPM7	Ca^{2+}, Mg^{2+}, Zn^{2+}, Mn^{2+}, Co^{2+}	Ubiquitous, including osteoblasts	Ion channel	Ca^{2+} and Mg^{2+} homeostasis, cell adhesion, cell growth and proliferation, cell death	Not determined (low affinity)	[299,301]
TRPV6 (CaT1)	Ca^{2+}	Duodenum, placenta	Ion channel	Vitamin D-dependent Ca^{2+} homeostasis	> 10 μM	[51]
MCU	Ca^{2+}	Inner membrane of mitochondria	Ion channel	Control of energy production, Ca^{2+} signaling, cell death	9 μM	[456–459]

transporters [465]. As shown in Table 1, ZIP8 and ZIP14 (SLC39A8 and SLC39A14) as well as SLC11A2 (DMT1, DCT1, NRAMP2) transport Cd at submicromolar Cd concentrations, which indicates that Cd may disrupt Fe, Zn, and Mn homeostasis by competing for transport with these essential metals. This in turn will affect metalloproteins whose function depends on these metals (e.g., MAP kinases, PKC, NF-κB, Nrf2, Sp1, CREB, MnSOD, Cu-ZnSOD, MT, GSH, etc.; reviewed in [461]) with their resulting impact on cellular redox status, signaling, and gene transcription.

Effects of nanomolar Cd concentrations on various signaling pathways have also been described (summarized in [460]). Several observations suggest that submicromolar Cd affects Ca signaling: (i) Cd inhibits plasma membrane Ca-ATPase [464]; (ii) Cd activates protein kinase C directly [466]; (iii) long-term (14 days) Cd exposure studies in rat liver epithelial cells at doses of 0.03–2.5 μM $CdCl_2$ showed disruption of gap junctional intercellular communication [467]; (iv) a Ca-sensing G-protein coupled receptor expressed in fibroblasts and renal MDCK cells similar to the Ca-receptor expressed in parathyroid, kidney, and gut cells is activated by submicromolar Cd with subsequent Ca mobilization [468,469]. Cd (0.01–1 μM) also interferes with NO signaling directly by blocking phosphorylation of NO synthase 3 [334] or suppressing NO synthase 2 activity indirectly by displacing MT-bound Zn [470,471]. Not being a Fenton metal, Cd cannot generate redox reactions in biological systems by itself. But because Cd interferes with SH groups, it may deplete endogenous intracellular radical scavengers, such as GSH or protein sulfhydryls (e.g., thioredoxins), inhibit the function of redox metabolizing enzymes (reviewed in [182]) but also the redox status of the cell and hence the cellular levels of redox active species. Cd has been shown to produce hydroxyl radicals in the presence of MT containing Fenton metals [472]. But Cd may also induce ROS formation by inhibiting the mitochondrial electron transfer chain [344]. Immediate early genes (*c-myc* and *c-jun*) are also up-regulated by low Cd concentrations (reviewed in [473]). However, up-regulation could be indirect and mediated by increases in cytosolic calcium or ROS signaling.

A large diversity of proteins require essential metals for their function by binding to functional groups with sulfur, nitrogen or oxygen atoms with high affinity. These metalloproteins have important cellular functions, such as metabolic, signaling or transcriptional regulation (e.g., Zn-finger and EF-hand proteins). They also play a role in the control of the cellular redox status, such as ROS metabolizing enzymes (e.g., SODs, catalases), mitochondrial electron-transport chain proteins, oxidoreductases, to name a few [474]. Cd has been shown to bind to metalloproteins with high affinity (apparent stability constants for MT and GSH $\sim 10^{-25}$–10^{-14} M^{-1} and $\sim 10^{-9}$ M^{-1}, respectively [74,75]) and displace essential metals from these proteins by ligand exchange [475–477], which may result in inhibition of their function. However, Moulis [461] emphasizes that replacement of essential metals by Cd may not necessarily impact folding suggesting that inhibition of function may also be unrelated to metal replacement. This may be the case for Cd-induced inactivation of the Zn-finger tumor-suppressor protein p53 [478] where phosphorylation of p53 could be the mechanism responsible for inactivation [479].

Cd binding may shield reactive cysteine thiolates and thereby prevent formation of disulfide bridges in nascent proteins and disrupt folding, resulting in inhibition of function and/or increased degradation by cellular protein quality control systems [220,480].

Hence Cd, at free ion concentrations, which have been measured in mammalian organisms during acute or chronic exposition *in vivo* may not disrupt transport and homeostasis of essential metals and biological molecules directly, but rather indirectly by interfering with signal transduction pathways, by inducing ROS formation, by protein damage, and regulation of gene transcription. Nevertheless, experiments with higher Cd concentrations and shorter time periods *in vitro* may also be useful in their own place as a model of cumulative effects of CLCE *in vivo*.

5.3 Disruption of Physiological Signaling Cascades

Signaling cascades are present in all mammalian cells and are vital to physiological functions to maintain cellular and systemic homeostasis. Second messenger systems are required for the communication between different tissues and organs that are remitted via specific receptors for first messenger hormones and neurotransmitters, culminating in a cellular response, which normally entails changes in protein function and/or gene expression.

5.3.1 Cadmium and Calcium Signaling

To prevent calcium overload in the cell, which would result in cell death, Ca^{2+} pumps in the endoplasmic reticulum (ER) membrane (named SERCA pumps) as well as in the plasma membrane ensure that cytosolic Ca^{2+} is maintained at a low level (10–100 nM). Hormones, neurotransmitters and Ca^{2+} sensors act through G-protein coupled receptors to activate phospholipase C, which cleaves PIP_2 into diacylglycerol and inositol trisphosphate (IP_3) to elicit a short lived increase in the cytosolic Ca^{2+} concentration. Many of Ca^{2+}'s effects are mediated through binding of Ca^{2+} to calmodulin and activating Ca^{2+}-calmodulin dependent kinases (CaMKII) that are important for downstream signaling cascades. The Ca^{2+} ion is also important for other cellular processes, such as exocytosis, muscle contraction, and maintaining depolarization, depending on the cell type and stimulus.

The influence of Cd^{2+} on physiological Ca^{2+} signaling has been reviewed elsewhere [460] and the role of Ca^{2+} in Cd^{2+}-induced cell death is detailed in Section 5.5.4.2. Many groups have reported the release of Ca^{2+} following Cd^{2+} treatment but these data have to be taken with care as Cd^{2+}-binding fluorescent dyes, or inhibitors, such as Fura-2 or BAPTA-AM, were employed. Cd^{2+} can increase cytosolic Ca^{2+} by inactivating the SERCA pump and calmodulin-dependent Ca^{2+} ATPases. In addition, Cd^{2+} is well known to interact with calmodulin to activate CaMKII [481] as well as affect calreticulin-mediated signaling [482].

A direct interaction of Cd^{2+} with calmodulin is doubtful as measurements using electrospray ionization mass spectrometry demonstrated that Cd^{2+} had lower affinity than Ca^{2+}, Mg^{2+} and Sr^{2+} for apo-calmodulin. However, in the presence of Ca^{2+} the affinities change to $Ca^{2+} > Cd^{2+} > Sr^{2+} > Mg^{2+}$ [483]. More likely, CaMKII are activated by Cd^{2+}-induced Ca^{2+} release as was demonstrated by Chen et al. in neuronal cell apoptosis [481].

5.3.2 Cadmium and cAMP Signaling

Amplification of cAMP begins with ligand binding to a G-protein coupled receptor that activates adenylyl cyclase, which in turn produces cAMP from ATP. cAMP stimulates protein kinase A (PKA), which goes on to phosphorylate target proteins, such as ion channels, or activates gene transcription. Alternatively, cAMP-dependent protein kinases are activated directly by cAMP and downstream effects depend on cell type. A review of the literature on perturbed cAMP signaling by Cd^{2+} was recently published [460]. Cd^{2+} can increase or decrease cAMP levels; the variance of effects seems to depend on the cell type. On a more unified note, Cd^{2+} inhibits PKA activity in both *in vitro* and *in vivo* studies.

5.3.3 Cadmium and Nitric Oxide Signaling

Nitric oxide (or nitrogen oxide) (NO) is synthesized by nitric oxide synthases (NOS) from L-arginine, oxygen and NADPH and works by activating guanylyl cyclase to amplify cGMP, which in turn activates cGMP-dependent kinases, resulting in protein phosphorylation and alteration in cellular functions. In all studies that were recently reviewed regarding Cd^{2+} and NO [460], NO production and NOS expression were decreased by Cd^{2+}. More recent data support these observations [484] but also observe increases in NO or NOS expression or activity [485].

5.4 Oxidative Stress and Recruitment of Stress Signaling Pathways

The multitude of cellular signaling pathways involved in stress responses is entangled with other signaling pathways, such as those in cell death and cell survival, and cannot be separated in their entirety. The stress response protein, metallothionein, which is integral in Cd^{2+} detoxification has been covered in Sections 2–4 and 6 as well as in Chapters 1 and 11 of this book.

5.4.1 Oxidative Stress

Because reactive oxygen species are continuously produced from mitochondria and are highly reactive and damaging to a multitude of cellular structures, i.e., proteins and lipids, they must be quickly metabolized to non-damaging forms. Defense mechanisms include the superoxide dismutases, catalase (CAT), thioredoxins, peroxidases as well as enzymes responsible for the synthesis and reduction of the peptide glutathione [474,486]. Augmented ROS levels can lead to DNA damage (see Chapter 15) and cell death but they can also be employed as signaling molecules, which depends on the amount of ROS generated: high levels of ROS initiate cell death whereas low levels of ROS can induce cellular adaptation responses (Section 5.8).

5.4.1.1 Cadmium and Oxidative Stress

The increased formation of ROS by Cd^{2+} is essential to its multifaceted cellular effects and has been summarized in a number of excellent recent reviews [187,460, 487–489]. Furthermore, urine excretion of an oxidative DNA damage marker in breast-fed infants was found to positively correlate with Cd^{2+} concentrations in breast milk [490]. The commonly used antioxidans N-acetylcysteine binds to Cd^{2+}, therefore, studies employing N-acetylcysteine should be taken with caution.

There are a number of mechanisms that can be affected by Cd^{2+} to increase ROS levels: displacement of Fenton metals [472], inhibition of the mitochondrial electron transport chain [344], decrease of antioxidant enzyme activities [182], reduction of GSH levels [491], and activation of NADPH oxidases [492]. The formation of ROS is integral to downstream signaling pathways, which are implicated in all types of stress and cell death, and could very well be one of the first responses in the cell following Cd^{2+} entry.

5.4.2 Endoplasmic Reticulum Stress Signaling

Endoplasmic reticulum stress develops when ER function is perturbed by accumulation of misfolded proteins, depletion of Ca^{2+} stores or oxidative stress in the ER lumen [493] and is sensed by three upstream signaling proteins: PERK, IRE1 and ATF6, collectively known as the unfolded protein response (UPR). They are found in the luminal ER membrane where, under ER stress, GRP78 chaperone binds to unfolded proteins allowing the ER sensors to homodimerize and activate their downstream signaling cascades. Initially, the cells try to prevent accumulation of unfolded proteins by halting transcription through the phosphorylation of PERK and eIF2α and to reduce the amount of unfolded proteins by initiating ER-associated degradation (ERAD) or autophagy to promote cell survival. But chronic or excessive ER stress can lead to activation of apoptosis mediated by the induction of CHOP, phosphorylation of JNK or activation of caspase-12 [494].

The importance of ER stress in mediating cellular life and death decisions is demonstrated by its involvement in a number of major modern diseases, including cancer, neurodegenerative and heart diseases. Some cancers have increased expression of GRP78 and GRP94, which could contribute to the ability of a cancer cell to resist proapoptotic challenges [495].

5.4.2.1 Cadmium and Endoplasmic Reticulum Stress

ER stress response genes are highly upregulated by Cd^{2+} treatment [496] and the pattern of genes affected appears to be distinct from other divalent heavy metals [497]. Proapoptotic CHOP is strongly upregulated by Cd^{2+} and this has been shown to be mediated by both the PERK and IRE1 arms of the UPR because of increases in their targets, eIF2α phosphorylation and XBP1 mRNA splicing, respectively [498–500]. Our laboratory detected phosphorylated PERK [501]. Furthermore, Cd^{2+} increases GRP78 indicating augmented unfolded proteins, but GRP94 has not been as reproducible. Cd^{2+}-induced ER stress can cause phosphorylation of JNK [498], caspase activation [499] and crosstalk with mitochondria to release cytochrome c [502] to induce apoptosis.

How does Cd^{2+} induce ER stress? Several laboratories could attenuate ER stress and apoptosis by applying a pharmacological antioxidant or by overexpressing ROS metabolizing enzymes [487,500]. Yokouchi et al. went one step further and defined superoxide anion ($O_2^{\cdot -}$) as the responsible ROS for inducing ER stress. Interestingly, peroxynitrite anion ($ONOO^-$) and hydrogen peroxide did not increase ER stress though H_2O_2 induced apoptosis [500]. In our recently published work, we could extend our observations to upregulation of a novel ER stress-counteracting factor, namely Bestrophin-3. Bestrophin-3 is upregulated by ER stress and appears to act by preventing CHOP upregulation as PERK and eIF2α were unaffected [501].

In summary, the UPR induced by Cd^{2+} can be perceived as an initial mechanism to alleviate ER stress but more often than not, CHOP is upregulated and causes apoptosis even though counteracting survival mechanisms are intact.

5.4.3 Cadmium and Mitogen Activated Protein Kinases

Mitogen activated protein kinases (MAPK) are serine/threonine-specific kinases and are activated by various stimuli to regulate a number of cellular activities. The kinases can be broadly divided into three groups: ERK, p38 MAPK and JNK. Initially it was thought that ERK mediates cell survival and p38 MAPK and JNK cause cell death, but recent data indicate otherwise.

Oxidative stress is a strong inducer of MAPK and they are therefore modulated by Cd^{2+}, which has been summarized in the review by Thévenod [460], and JNK can be inhibited by glutathione [503]. Generally, Cd^{2+}-activated JNK leads to apoptotic cell death, although JNK has been shown to have an antiapoptotic role too [504]. In agreement, p38 MAPK is also phosphorylated by Cd^{2+} in the stress response. The role of ERK in Cd^{2+} effects is still somewhat unclear. The literature

summarized in the review by Thévenod either showed no effect or a negative effect on ERK signaling. Only two studies reported an increase in ERK [505,506]. Some recent data support a role for ERK in protection against Cd^{2+} toxicity and increased cell proliferation [492,507], but ERK activation by Cd^{2+} can also lead to cell death [506].

5.4.4 Cadmium and Nuclear Factor Kappa B

The redox sensitive transcription factor NF-κB is responsible for mediating a number of stress responses, most notably inflammation and cell survival [508]. Extracellular and intracellular stimuli transmit their signals to the NF-κB/IκB complex via IκB kinases (IKKs), which phosphorylate IκB to mark it for degradation. NF-κB can then translocate to the nucleus and activate or repress genes involved in cell stress, survival, death, and differentiation.

The effect of Cd^{2+} on NF-κB activity was recently reviewed [460]. In general, Cd^{2+} increases NF-κB transcriptional activity to upregulate multidrug resistance P-glycoprotein ABCB1 as well as genes involved in cell survival (BcL-xL), inflammation (interleukin-8), oxidative stress (metallothionein, heme oxygenase 1), and injury (ICAM-1, heat shock factor 1). With respect to cell death, opposing observations have been made in NF-κB activity. Whilst Hart et al. [509] reported increased NF-κB activity in response to oxidative stress by Cd^{2+}, Xie and Shaikh [510] saw decreased NF-κB DNA binding and IKK activity. Furthermore, NF-κB activity is inhibited during necrotic cell death [511,512]. It is plausible that necrotic cell death was also induced in the study by Xie and Shaikh and therefore NF-κB activity was reduced. Unfortunately, necrosis was not measured. Taken together, Cd^{2+} increases NF-κB transcriptional activity to upregulate stress, survival and injury response genes.

5.5 Activation of Cell Death Pathways

Programmed cell death is a tightly regulated physiological process which is integral for the removal of damaged, unwanted, aged, and superfluous cells in the body and comes in various forms: apoptosis, necrosis, and autophagic cell death [513]. During apoptosis, the cell shrinks in size and volume, whilst maintaining their plasma membrane integrity whereas necrotic cell death involves swelling and rupture of the plasma membrane. Autophagy describes the breakdown of a cell's own components, such as mitochondria or unused proteins, and has been associated with cell death. However, decisive evidence is currently lacking on whether cell death is a direct consequence of autophagy or whether these two events occur in parallel [514]. The role of autophagy in Cd^{2+} toxicity will be discussed in further detail in Section 5.8.

Perturbance of apoptosis execution results in a wide array of diseases such as cancer, neurodegenerative diseases, and abnormal development. The end point of the intracellular biochemical cell death process in apoptotic cells is the condensation and fragmentation of chromatin within the nucleus. The receptor-mediated pathway involves the binding of a death ligand, such as Fas, to its receptor, which activates caspase-8 and caspase-3/6 leading to cleavage of intracellular substrates and DNA condensation and/or fragmentation. The mitochondrial pathway is normally activated by other injurious compounds, such as ROS and Ca^{2+}. The mitochondria release proapoptotic factors, which normally reside in the intracellular space, and once in the cytosol, they can either activate caspase-9 and caspase-3 to induce apoptosis, such as cytochrome c, or they can cause apoptosis in a caspase-independent manner, such as apoptosis inducing factor (AIF) and endonuclease G [515]. Cross-talk has been shown to exist between the extrinsic and intrinsic pathways [516].

5.5.1 Cadmium and Apoptosis

In early studies, apoptosis was identified as an important feature of Cd^{2+} toxicity in a number of organs, including the kidneys, liver, testis, and lung, using *in vitro* and *in vivo* methods [517,518]. Once taken up into the cell, Cd^{2+} elicits a general cellular stress response (as described in Section 5.4) that culminates in activation of apoptosis pathways beginning with mitochondria (Section 5.5.2) [460]. There is evidence for the involvement of the extrinsic pathway [519]. It is uncertain how Cd^{2+} might activate the receptor-mediated apoptosis pathway. Eichler and colleagues found accumulation of Fas ligand in Cd^{2+} exposed podocytes [519], but it must be secreted to activate the death receptor. A more plausible reason is that caspase-8 can be activated by genotoxic stress [520] which could be a result of Cd^{2+}-induced ROS, or even by activation of the Ripoptosome complex [521] (see also Section 5.5.6).

As well as activating the classical intrinsic pathway involving activation of caspases-9 and -3, Cd^{2+} can also utilize caspase-independent pathways, in a context dependent manner. Our laboratory demonstrated calpain activation at early time points (3–6 hours) whereas mitochondrial damage, cytochrome c and AIF release and subsequent caspase activation was seen only after 24 hours with 10 μM Cd^{2+} [522]. Other studies have reported similar observations: multiple apoptosis signaling pathways can be affected by Cd^{2+} to induce apoptotic cell death [523,524].

5.5.2 Cadmium and Mitochondria

Generally, Cd^{2+} damages mitochondria. Mitochondria are the ‘powerhouses’ of a cell; they represent the metabolic and bioenergetic centers involved in a variety of functions to maintain cell sustenance including respiration, ATP production and

Ca^{2+} homeostasis. Under normal physiological conditions, mitochondria maintain an electrochemical gradient across the inner membrane, known as the mitochondrial membrane potential ($\Delta\psi_m$). The outer mitochondrial membrane (OMM) is generally non-selective with the voltage-dependent anion channel (VDAC) being the most abundant protein present. In contrast, permeability to ions dramatically decreases at the inner mitochondrial membrane (IMM) and is freely permeable to just a few molecules, such as O_2, CO_2, and NH_3. It is generally accepted that mitochondrial function is altered by Cd^{2+}; loss of $\Delta\psi_m$, release of proapoptotic factors, swelling and inhibition of the electron transport chain have been observed in various cell lines and isolated mitochondria [344,458,525,526].

5.5.2.1 Mitochondrial Permeability Transition

The mitochondrial permeability transition describes a dramatic increase in the permeability of the IMM, which can be mediated by two mechanisms. The first involves opening of a pore, the so-called permeability transition pore (PTP), which is cyclosporin A (CsA) sensitive, to molecules <1.5 kDa, such as cytosolic solutes, which causes progressive osmotic swelling of the matrix, dissipation of $\Delta\psi_m$, and ultimately leading to the disruption of the OMM, spilling the intermembrane contents into the cytosol [527]. The second mechanism is the formation of cytochrome c conducting "megapores" through the insertion of proapoptotic Bax into the OMM in the absence of mitochondrial swelling, which has been demonstrated in Cd^{2+} exposed lung fibroblasts [528].

5.5.2.2 Cadmium and the Permeability Transition Pore

The effect of Cd^{2+} on the PTP has been investigated in only a handful of studies. Using isolated mitochondria from liver or kidney, Cd^{2+} induces swelling of mitochondria, as determined by light scattering [458,525,529–531]. The role of PTP in mitochondrial swelling could be demonstrated through inhibition by CsA. Cd^{2+} could open the PTP by entering the mitochondrial matrix via the mitochondrial Ca^{2+} uniporter where it can directly bind to ANT [532] or interfere with the electron transport chain to induce ROS formation [344,530].

However, in two studies, CsA had no significant effect in blocking mitochondrial changes associated with Cd^{2+} [458,529], indicating that PTP opening is not always essential for MMP breakdown and apoptosis induction. So how does Cd^{2+} cause mitochondrial swelling in the absence of PTP opening? Though Li and colleagues still insisted that the PTP was functioning even when CsA was ineffective [529], our laboratory found that aquaporin-8 present in the IMM were activated by Cd^{2+} and were responsible for mediating water influx into the matrix and increasing swelling [458,533].

5.5.3 Cadmium and Bcl-2 Proteins

Whether a cell undergoes apoptosis appears to be determined by the balance of Bcl-2 family proapoptotic (e.g., Bax, Bak) and anti-apoptotic (e.g., Bcl-2, Bcl-x_L) proteins [534]. Bax itself induces cytochrome c release from isolated mitochondria [535] and proapoptotic members bind to VDAC to form a large cytochrome c conducting channel [536]. In Cd^{2+}-exposed cell lines, generally antiapoptotic Bcl-2 is decreased and/or proapoptotic Bax translocates to the mitochondria where it can release propapoptotic proteins [528,537,538] but a lack of effect of Cd^{2+} on Bcl-2 family proteins has also been reported [523,539]. Addition of Bcl-2 can protect cells from undergoing Cd^{2+}-induced apoptosis [539]. Furthermore, Cd^{2+} exposure can increase Bcl-2 as part of a survival mechanism.

5.5.4 Other Apoptotic Signaling Pathways Involved in Cadmium Toxicity

5.5.4.1 Ceramides and Calpains

Ceramides have long been known to be intimately involved in apoptotic signaling pathways [540]. Ceramides induce cytochrome c release via ceramide channel formation [541] or activate Ca^{2+}-dependent proteases, calpains [542]. Our laboratory were the first to show that Cd^{2+} increases ceramide formation, possibly via *de novo* synthesis, which activates calpain activity by increasing cytosolic Ca^{2+}. Apoptosis was then executed in a caspase-independent manner [542]. Interestingly, ceramide and its metabolites are also implicated in multidrug resistance and evasion of apoptosis in tumor cells (see Section 5.8). Active calpains cleave a wide array of substrates that can lead to apoptosis as well as survival and autophagy [543]. Apoptotic substrates include caspases, Bcl-2, Bax, and AIF. In Cd^{2+}-treated cells, calpains are activated at early time points (3–6 hours) and provide a point for crosstalk with caspases, which are activated later (24 hours) [522] and can also cleave Bax to release cytochrome c [528].

5.5.4.2 Calcium

Ca^{2+} release from the ER triggers the UPR (Section 5.4.2), and ultimately leads to cell death. Conclusive evidence for Ca^{2+} release induced by Cd^{2+} has been hampered by the lack of adequate tools since Cd^{2+} can also bind to EGTA-based fluorescent indicators and chelators, such as Fura-2 and BAPTA, due to the very similar ionic radii and often elicits stronger fluorescent intensity than Ca^{2+} itself [544]. Recently, aequorin, a photoprotein from luminescent jellyfish, has been tested as an appropriate Ca^{2+} indicator with little interference from Cd^{2+}. Similar to an initial cell-free study by Izutsu and colleagues [545], Biagioli et al. found that

aequorin did not respond to 5 μM Cd^{2+} but increased slightly with 15 μM Cd^{2+} in digitonin-permeabilized cells [546]. However, whilst Ca^{2+} is normally present in the cytosol in the nanomolar range, aequorin can only detect increases in Ca^{2+} at 0.5–10 μM. To circumvent this problem, the effect of Cd^{2+} on bradykinin-induced Ca^{2+}-release was investigated. Cd^{2+} treatment resulted in reduced Ca^{2+} release by bradykinin indicating that Ca^{2+} homeostasis had been disturbed, which was attributed to inhibition of the SERCA in the ER by Cd^{2+}, and lead to activation of apoptosis [499].

More recently, no interference of up to 2 mM Cd^{2+} with a protein-based Ca^{2+} sensor yellow chameleon, YC3.60 was observed. The authors concluded from their study that Ca^{2+} is not necessary for Cd^{2+} (1–30 μM)-induced transcription and that as cells succumb to metal toxicity, Ca^{2+} is released [547]. Further studies would be required to confirm these observations and to finally resolve the role of Ca^{2+} in Cd^{2+}-induced stress and cell death signaling pathways.

5.5.5 Cadmium and Necrosis

Recent studies indicate that necrosis is indeed a form of programmed cell death, rather than a passive process of cell swelling and rupture, termed "necroptosis", which uses many of the tools available for apoptosis induction [548].

Cd^{2+} is a well known necrosis inducer, especially at higher concentrations and/or in sensitive cell lines. *In vivo* necrosis by Cd^{2+} has been documented in the kidney, heart, liver, and testis. A wider variety of cell types have been employed for *in vitro* testing and have similarly shown both apoptosis and necrosis simultaneously or necrosis alone [359]. Using pharmacological inhibitors, Yang et al. could demonstrate a role for Ca^{2+}, calpains, mitochondrial membrane potential, ROS formation and NF-κB in Cd^{2+} necrosis of CHO cells. The authors suggested that cytosolic Ca^{2+} overload might be important in the execution phase of necrotic cell death while sustained depletion of Ca^{2+} stores in ER leads to apoptosis [511].

In a follow up study, necrostatin-1 is shown to be active in blocking Cd^{2+}-induced necrosis by inhibiting $\Delta\psi_m$ loss. Interestingly, necrostatin-1 + Cd^{2+} increased Ca^{2+} overload further over Cd^{2+} alone cells without a concurrent increase in calpain activity. In fact, necrostatin-1 could attenuate Cd^{2+} induced calpain activity [512]. In line with their previous observations, necrostatin-1 restored Cd^{2+}-induced decrease of NF-κB activity, indicating that this transcription factor is integral to the necrotic response.

5.5.6 The Apoptosis-Necrosis Switch

Inhibition of cell death signaling pathways can initiate a cell to "re-wire" its cell death program from apoptosis to necrosis [549] through a molecular switch. Earlier studies put forward ATP [550] or caspases [551] as the mediator. Depletion of ATP would favor necrosis, which can be explained by energy demands during

apoptosis execution whereas general caspase inhibitors may affect mitochondrial functions that constitute a deciding event in both cell death types. The type of ROS and redox status has been suggested as an apoptosis-necrosis mediator. H_2O_2 induces necrosis due to reduction of GSH levels but other ROS forms, such as superoxide anion, induce apoptosis [552]. However, this has been contested by another study where inhibiton of superoxide anion producing NADPH oxidases suppresses the switch from apoptosis to necrosis [553]. The latest data report the Ripoptosome as a signaling platform that governs the form of cell death that will be executed [521].

Necrosis occurrence is dependent on the concentration of Cd^{2+} applied and the levels of ATP appear to be very important. The scenario for cell death switch in Cd^{2+}-treated cells is somewhat more complicated but ATP, GSH status and peroxide accumulation are all involved [552]. In addition, metallothionein-3 (MT-3) seems to have an important role in controlling the form of cell death. In kidney cells with low MT-3 expression, Cd^{2+} causes apoptosis but MT-3 overexpressing cells show necrosis by Cd^{2+} [554]. The mechanism by which MT-3 predisposes cells to necrotic cell death was not investigated but previous studies report a non-canonical neuronal cell growth inhibitory activity of MT-3, which may be related to its necrosis inducing abilities.

5.6 Reprogramming of Developmental Signaling Pathways

Aberrant signaling during the gestation period can lead to a multitude of developmental defects, such as stunted or absence of limbs and loss of organ function. A number of signaling pathways are crucial for development, namely, Wnt/β-catenin, Hedgehog, Notch, Hippo, and the transforming growth factor beta family (partly reviewed in [555,556]). The activity of these signaling pathways goes beyond development, remaining active in adults, where they have been implicated in a number of diseases, in particular, cancer. At the time of writing, a literature search on Notch or Hippo signaling and Cd^{2+} retrieved no articles.

5.6.1 Cadmium and Wnt/β-Catenin

Wnt is the mammalian form of the Drosophila gene wingless, which is mutated in flies without wings, and is secreted. An intracellular response is triggered through binding of Wnt to its receptor, Frizzled, and can be signaled through canonical and non-canonical Wnt pathways [557]. The canonical pathway involves the multifunctional protein β-catenin and is responsible for cell transformation. Cytosolic levels of β-catenin are kept low by targeting it to the proteasome for degradation through a destruction complex. Upon activation, the destruction complex is disassembled and β-catenin translocates to the nucleus where it serves as a transcriptional co-factor for the TCF/LEF transcription factor family. Target

genes of TCF transcription include cyclin D1, c-myc and ABCB1, which are genes responsible for cell proliferation and survival. In another role distinct from Wnt signaling, β-catenin is found in cell borders where it forms part of the adherens junctions along with E-cadherin and α-catenin. The disruption of the adherens junctions has been associated with epithelial-to-mesenchymal transition (EMT), a phenomenon linked to malignant cell transformation and metastasis, as cells detach themselves from the extracellular matrix through loss of cell adhesion and increase their motility.

In development, Cd^{2+} exposure and interference with the Wnt signaling pathway can lead to birth defects (reviewed in [460]). The group of Thompson has demonstrated that the non-canonical Wnt pathway is engaged by Cd^{2+} leading to ventral body wall defects in a chick embryonic model [482]. In further studies, the adherens junctions was disrupted either through redistribution of β-catenin to cytosol and nucleus and actin disorganisation [558] or decreased calreticulin, E-cadherin and β-catenin mRNAs [482] in the same model. Elsewhere aberrant thymus development in embryos of Cd^{2+} treated pregnant mice was a result of decreased signaling activity of Sonic Hedgehog and β-catenin [559].

In addition to developmental defects, Cd^{2+} has been shown to target the Wnt signaling pathway as a means of exerting its carcinogenic effects. From our laboratory, we have reported translocation of β-catenin from the periphery to the nucleus and upregulation of c-myc, cyclin D1, and ABCB1 via TCF4 activation in subconfluent cells [560]. Moreover, chronically Cd^{2+}-exposed mice exhibited significant increases in mRNA in a number of Wnts, Frizzled receptors and Lrp co-receptors [561]. Increased EMT markers (collagen I, Twist, and fibronectin, but not α-smooth muscle actin, mRNAs) were also observed [561]. Both Twist and fibronectin are under the control of β-catenin mediated transcription, thus providing the crucial link that Cd^{2+} supports EMT and therefore tumor progression [562].

5.6.2 Cadmium and Hedgehog

The Hedgehog family of proteins function as intercellular messengers and are secreted to regulate morphogenesis of organs and tissues and control stem cell proliferation in adults [563]. The effect of Cd^{2+} on developmental defects as a result of aberrant Hedgehog signaling has been reviewed elsewhere [460]. Collectively, downregulation of the Sonic Hedgehog (Shh) isoform was observed in Cd^{2+}-treated pregnant mice that correlated with disrupted embryonic development in mice and in zebrafish. A recent study also reported decreased Shh in the thymus of Cd^{2+}-treated pregnant mice that could be responsible for the change in thymocyte phenocyte [559]. Interestingly, the offspring demonstrated increased expression of Hedgehog signaling components indicating a mechanism of adaptation in response to depleted Shh in the embryonic environment. This may have implications in developmental malfunctions as well as tumor progression potential.

5.7 Genetic and Epigenetic Effects

A mutagen is defined as an agent that alters genetic material, usually DNA, increasing the frequency and likelihood of mutations. As a weak mutagen, Cd^{2+} does not directly affect the DNA structure, which is in contrast to other toxic and carcinogenic metals, such as chromium which forms DNA adducts. However, Cd^{2+} exposure results in changes in gene expression that ultimately influence cell characteristics and behavior.

5.7.1 Cadmium, DNA Damage, and Inhibition of DNA Repair

DNA damage by Cd^{2+} is linked to DNA damage by ROS and inhibition of DNA repair mechanisms. ROS, in particular hydroxyl radicals, react with the DNA bases giving rise to altered function or DNA damage [564]. Cd^{2+} can block repair mechanisms for DNA, such as mismatch and base excision repair [565,566], which could be attributed to Zn^{2+} displacement in zinc finger DNA repair proteins [567].

It has been shown that ROS induced DNA damage occurs at low levels under physiological conditions; probably as a result of mitochondrial ATP production where ROS are produced. In combination with the inhibition of DNA repair, ROS-induced DNA damage changes the genetic makeup and could contribute to promotion of carcinogenic cells, which acquire a number of mutations to achieve the hallmarks of cancer. For further details, please refer to Chapter 15.

5.7.2 Cadmium and Epigenetics

Epigenetics is the study of inheritable changes in gene expression without any modifications in the DNA sequence and is strongly elicited by environmental factors [568]. Failure to maintain epigenetic information leads to incorrect gene expression, which can be passed onto daughter cells or offspring, and apoptosis. The most studied epigenetic changes are a result of either aberrant DNA methylation or histone modifications. Cytosine nucleotides can be methylated by DNA methyltransferases (DNMT) to 5-methylcytosine. Excessive methylation, e.g. from methyl groups found in the diet, can switch off a gene through blockade of transcription factor access. Following synthesis, the DNA is wound around histone proteins to aid compaction and can influence the accessibility and thus expression of a gene. A gene is only active if it is accessible. Modification of the histone proteins may affect how the DNA is wound and therefore the accessibility of a gene.

Heavy metals, including Cd^{2+}, may elicit their toxic and carcinogenic effects by epigenetic mechanisms. It seems that DNA hypermethylation and concomitant increase in DNMT expression is associated with malignant transformation of cells exposed to Cd^{2+} [569,570] or cells that develop Cd^{2+} resistance [571].

In contrast, cells with increased proliferation exhibited both hypermethylation [570] and hypomethylation [572], which may be dependent on the concentration and exposure time of Cd^{2+}. Histone modification by Cd^{2+} has only been demonstrated in one report by Somji et al., where it affects MT-3 expression [573].

5.7.3 Cadmium and MicroRNA

MicroRNAs are short RNA sequences (21–25 nucleotides) that control gene expression at the post-transcriptional level. MicroRNAs bind to complementary messenger RNA sequences to prevent their translation and are part of a RNA-induced silencing complex. Binding to a complementary sequence causes degradation of the mRNA or inhibition of translation, resulting in gene silencing [574]. Cd^{2+} has been associated with modification of microRNA expression [575] but an in-depth study in a mammalian system is currently not available.

5.8 Mechanisms of Adaptation, Survival, and Carcinogenesis

5.8.1 Adaptation and Survival Mechanisms Induced by Cadmium

Cellular stress signals induced by Cd^{2+} forces the cell to engage counteracting adaptation and survival mechanisms in an attempt to prevent itself from dying. These mechanisms can tackle the cellular stress response in a variety of ways: removal of damaged or death-inducing proteins through degradation by autophagy or the proteasome, upregulation of pro-survival genes, activation of survival signaling pathways, and inhibition of stress and cell death signaling cascades.

5.8.1.1 Cadmium and Autophagy

Autophagy is a process of self-eating. By degrading intracellular components, damaged proteins and organelles, the cell can increase its chances of survival during stress or nutrient starvation conditions [576]. Membrane-bound vesicles called autophagosomes form to “engulf” cytosolic contents, which subsequently fuse with lysosomes to form autophagolysosomes that degrade the engulfed contents. Autophagy can be detected by (i) the conversion of LC3 from LC3-I to LC3-II or the redistribution of LC3 from cytosol to puncta; (ii) uptake of monodansylcadaverine (MDC) or acridine orange into autophagolysosomes: (iii) changes in autophagy-specific proteins, e.g., increase in Beclin-1. Persistence of autophagy can lead to cell death although cell death is not always a direct consequence of autophagy. In fact, the existence of autophagic cell death has been contested [514].

Cd^{2+}-induced autophagy is mediated via ROS formation [577,578], GSK3β [578], AMPK [577], p38 [579] or ERK [580] activation, decreases in mTOR, PARP, and ATP [577] and Ca^{2+} signaling [580], though Cd^{2+}-binding BAPTA was employed (see Section 5.5.4.2). Autophagy by Cd^{2+} appears to suppress apoptosis execution because changes in autophagy markers were observed in the absence of apoptosis in low Cd^{2+} (< 10 μM) treated rat kidneys *in vivo* after 3–5 days [412], endothelial cells [581], hematopoietic stem cells after 48 hours [582] and kidney proximal tubule cells after 1 h (Lee and Thévenod, unpublished data). This has led to the proposal of autophagy as an early biomarker of Cd^{2+} toxicity [412] (see Section 4.4). Though Cd^{2+} exposure eventually leads to apoptotic cell death, there is not enough evidence to conclude that it is a direct consequence of autophagy induction.

5.8.1.2 Cadmium and Nrf2-Keap1 Signaling

Nrf2-Keap1 is brought into play by oxidative stress leading to long term adaptation of the cell and enhanced survival. Upon oxidative or electrophilic stress, Nrf2 escapes its suppressor Keap1, which is inactivated by direct modification of its cysteine thiol residues, and translocates to the nucleus to bind to the antioxidant response element. Target genes of Nrf2 include antioxidant defense proteins and detoxifying enzymes [583].

Environmental insults are potent inducers of the Nrf2-Keap1 signaling pathway. In agreement, Cd^{2+} activates Nrf2 nuclear translocation to prevent apoptosis [584]. Though Cd^{2+} may activate Nrf2 through the induction of ROS, it has been demonstrated that Cd^{2+} can increase the stability of Nrf2 [585], possibly through direct binding of Cd^{2+} to the cysteine residues on Keap1.

5.8.1.3 Cadmium and Akt-PI3K Signaling

The Akt-PI3K signaling pathway is downstream of oncogenic Ras. Phosphoinositide-3-kinase (PI3K) phosphorylates PIP_2 to PIP_3, which binds Akt. Once correctly positioned at the membrane via binding of PIP_3, Akt is activated by kinases. Active Akt then promotes cell survival primarily by counteracting proapoptotic processes, for example, antagonizing proapoptotic Bad.

Akt can also stimulate cell growth and proliferation by activating mTOR to increase protein synthesis and inhibiting GSK3β to increase β-catenin-induced transcription of proliferation genes. Cd^{2+} generally activates Akt signaling in various cell types, concentrations and exposure times [460,586,587], not only as a stress response, but as an adaptive reaction to prevent cell death.

5.8.2 Cadmium and Carcinogenesis

As a class I carcinogen, Cd^{2+} causes cancer of the lung, kidney, and the prostate in humans [168]. Chronic exposure to Cd^{2+} gives rise to apoptosis-resistant cells that are potentially carcinogenic [214,588] and low Cd^{2+} exposures induce transcription of proto-oncogenes [589]. This is partly due to oxidative DNA damage [185]. Through the induction of adaptation and survival mechanisms, cells acquire tumor cell characteristics that are known collectively as the hallmarks of cancer; they include sustaining proliferative signaling, evading growth suppressors, resisting cell death, enabling replicative immortality, inducing angiogenesis, and activating invasion and metastasis [590] that are all part of the multistep process in tumor development.

Important signaling pathways in cancer include, but are not limited to p53, cell cycle regulation, Wnt/β-catenin (see Section 5.6.1), EMT, proto-oncogenic immediate early genes, Akt-PI3K as well as the stress response pathways discussed in Section 5.4. For an in-depth review of cellular and molecular mechanisms leading to carcinogenesis by Cd^{2+}, the reader is referred to Chapter 15 of this book as well as to recent reviews available [184,591].

5.8.2.1 Cadmium, p53, and Cell Cycle Regulation

The tumor suppressor gene, p53, is the master regulator of cell death and acts as a cell cycle guardian [592]. p53 is normally marked for degradation by the proteasome through the ubiquitylating action of Mdm2. Phosphorylation of p53 disrupts the binding of Mdm2 and p53 can elicit its effects. The tumor suppressing functions of p53 are: to initiate apoptosis of irreparable cells, arrest damaged cells at cell cycle check points, activate DNA repair proteins, and inhibit angiogenesis. If the damage cannot be repaired, the cells are removed by apoptotic cell death. Furthermore, p53 has a DNA binding domain and acts as a transcription factor to increase the expressions of proteins that are integral to its functions, such as growth arresting p21 and apoptosis-inducing Bax. In circa 50% of cancers, p53 is mutated allowing cancer cells to grow limitlessly harboring their mutations.

The double edged sword effect of Cd^{2+}, namely apoptosis and cancer progression, is reflected in its opposing effects on p53. Cd^{2+} inhibits DNA base excision repair in p53-dependent and -independent manners [593], increases p53 phosphorylation as a prelude to apoptosis [594,595], and arrests cells in G1 and G2/M checkpoints via p53-dependent [510] and -independent [596] mechanisms. Cd^{2+} can affect p53 in two ways: p53 is activated by phosphorylation via phosphatidylinositol-3-kinase related kinases [479] or Cd^{2+} replaces zinc to maintain its mutated non-DNA binding form preventing apoptosis induction [597].

5.8.2.2 Cadmium and Multidrug Resistance P-Glycoprotein (MDR1/ABCB1)

ABCB1 confers cellular resistance to apoptosis inducers and is upregulated in many cancers [598]. Cd^{2+} increases ABCB1 expression and long-term Cd^{2+} exposure results in lowered apoptosis occurrence [588,599]. Initial studies supported the hypothesis that Cd^{2+} is transported out of the cell by ABCB1 to reduce apoptosis [600]. In contrast, our laboratory found that Cd^{2+} augmented ceramides, which were in turn effluxed by ABCB1 to prevent cell death [601]. This discrepancy can only be explained by different experimental conditions.

5.9 Metallohormone Effects

A metallohormone is defined as an inorganic metal ion which can mimic hormone-like activities and effects. Generally, the receptors are localized in the cytosol and upon hormone binding, they translocate to the nucleus where they exert their effects as transcription factors and modulate gene expression through DNA binding to the promoter region of target genes. The DNA binding is accomplished by zinc fingers forming a Zn^{2+}-$[Cys]_4$ metal-protein complex with cysteine residues.

The primary and most important androgen is testosterone. In the adult male, its active metabolite dihydrotestosterone supports spermatogenesis for reproduction as well as maintaining muscle mass and fat distribution. Estrogens are associated with development of female secondary sex characteristics and comprise of estrone, estradiol, and estriol. Steroid hormones are not exclusively gender specific and have important roles in both males and females.

5.9.1 Cadmium as a Metalloestrogen

Endocrine status is acknowledged as a prominent risk factor for breast cancer, more so than family history, and led to the focus on environmental estrogens as potential sources that contribute to a higher risk of breast cancer development. Cd^{2+} has been widely studied as a metalloestrogen, summarized in recent excellent reviews [602,603].

Several studies have proven that Cd^{2+} increases MCF-7 proliferation [604], a human breast cancer cell line that is dependent on estrogens for growth, potentially through direct binding to the ligand binding domain of the estrogen receptor [605], and can be abolished by the anti-estrogen ICI-164,384. Metalloestrogenic effects are not restricted to Cd^{2+} and increased cell proliferation has been observed with a number of other inorganic metal ions [606], but they do not seem to work in the same way. Only Zn^{2+}, Cd^{2+}, Hg^{2+}, and Co^{2+} could preserve DNA binding of the estrogen receptor-α [607]. In other studies, Cd^{2+} did not bind to or activate the estrogen receptor or did not induce cell proliferation when measured by a recombinant yeast estrogen screen or protein labelling with sulforhodamine-B [608].

The groundbreaking report of Johnson et al. was the first study of Cd^{2+}-induced estrogenic effects in whole animals [609]. The authors reported classical changes associated with increased estrogenic activity: increased uterine wet weight, increased height of the uterine epithelium, early onset of puberty, increased cell proliferation in the endometrium, increased mammary gland density and augmented expression of estrogen receptor driven genes in ovariectomized rats. Subsequent studies showed a partial estrogenic response [610,611]. The authors concluded that other intracellular signaling pathways are involved, namely ERK1/2.

In summary, the case of Cd^{2+} as a metalloestrogen is a yet unclear one. Whilst the *in vitro* data in mammalian cell lines are comprehensive and convincing, the *in vivo* data are somewhat inconsistent. Fechner and colleagues hypothesize that different cellular pools of estrogen receptor-α exist and may respond to Cd^{2+} differently based on the state of the cysteine residues in the ligand binding domain [612].

5.9.2 Cadmium and Androgenic Effects

Endocrine status is also a risk factor for the progression of prostate cancer and several epidemiological studies, though not all, indicate a connection to Cd^{2+} [613]. Alongside estrogenic effects, Cd^{2+} also activates the androgen receptor and increases cell proliferation, gene expression [614] as well as testosterone production. Employing a reporter gene assay, Cd^{2+} activated the androgen response element in human prostate epithelial and liver cells [614] but, contrary to other studies, there was no increase in proliferation. Furthermore, malignant transformation of normal prostate cells through repeated exposure to Cd^{2+} has been documented [615], increasing the prominence of Cd^{2+} as a risk factor in prostate cancer.

6 Endogenous Detoxification

The body has several means to detoxify Cd and also alleviate its toxic effects. For instance, Cd can be complexed by MTs and thereby detoxified. Several excellent reviews on MTs have been recently published [55,237,616]. MTs are low-molecular weight (MW ranging from 3.5-14 kDa), cysteine-rich metal-binding proteins. MTs have the capacity to bind both, physiological Zn^{2+} and toxic Cd^{2+}, through the thiol group of its cysteine residues, which represents nearly 30% of its amino acidic residues. All cysteines are known to participate in the coordination of 7 mol of Cd or Zn per mol of MT [617]. Of the four common MTs, MT-1 and MT-2 are expressed in most tissues, MT-3 is predominantly present in brain, whereas MT-4 is restricted to certain epithelia (see also Chapter 11). MT genes are readily induced by various physiologic and toxicologic stimuli because the promoter region of MTs contains several response elements, including glucocorticoid, antioxidant, and – most importantly – metal responsive elements.

The candidate metal responsive element-binding protein (MTF-1 for metal transcription factor-I) is a Zn-finger (Cys_2His_2) transcription factor [618].

Because the cysteines in MTs are absolutely conserved across species, it is assumed that these cysteines are necessary for function and MTs are essential for life. Their major physiological function appears to be homeostasis of essential metals, mainly Zn and Cu, and redox metabolism, which are coupled processes [616,619]. The experimentally determined apparent stability constants for MT binding to Zn are in the range of ~10^{-25}–10^{-14} M^{-1} [74]. Their thiolate coordination environments make MTs redox-active Zn proteins that exist in different molecular states depending on the availability of cellular zinc and the redox status [616,619]: Oxidative conditions make more Zn available, while reductive conditions make less Zn available. MTs move from the cytosol to cellular compartments, are secreted or internalized by cells. MTs have been localized largely in the cell cytoplasm, but also in lysosomes, mitochondria and nuclei (reviewed in [237]).

MTs protect against Cd toxicity because the affinity of Cd to MT is about 10^4 = 10,000 times higher than that of Zn [74]. But, as the toxicity of Cd is also partly due to binding to charged sites of target proteins or the displacement of Zn bound to Zn metalloproteins, ZnMTs may restore structures and functions of such proteins through removal of bound Cd or through a reciprocal Cd/Zn transfer reaction [461,620]. This would confer on MT an active role in the protective response to Cd toxicity, rather than a passive one that is solely dependent on the high affinity for binding free metal ions. Mice which lack MT genes were more susceptible to renal [621], bone [622], and liver injury [245] mediated by CLCE than mice expressing MT. Therefore, MT appears to be crucial to detoxify Cd in the body. Moreover, induction of MT respective MT-transgenic mice show increased resistance against chronic Cd toxicity and lethality [623] (reviewed in [624]). Hence, MT-null mice are hypersensitive and MT-transgenic mice resistant to Cd toxicity. The other side of the coin is that MT mainly contributes to the long biological half-life of Cd in the body [625] and thereby increases the likelihood of long-term organ damage associated with chronic Cd accumulation. In humans, there are large individual variations in MT expression, possibly due to polymorphisms [626]. Indeed, polymorphisms in the human MT-2A gene can limit MT expression [627] and increase the susceptibility to organ Cd toxicity [628,629]. These differences in MT expression may be responsible for inter-individual differential predispositions to Cd toxicity [630].

Cd may also be detoxified by chelation with intracellular GSH (apparent stability constant for GSH ~10^{-9} M^{-1}, [75]) and excretion through the bile, urine or pulmonary fluids. Hepatic secretion of Cd-GSH complexes has been shown to be mediated by ABCC2/MRP2 (see Sections 3.3 and 4.3.2). Moreover, L'Hoste et al. [491] have provided evidence in cultured mouse PT cells that Cd-GSH complexes are secreted via ABCC7/CFTR. A similar mechanism could be operative in pulmonary epithelia [269], where CFTR, but not MRP2 or BCRP/ABCG2, has been shown to play a crucial role for maintaining basal epithelial lining fluid GSH and increasing epithelial lining fluid GSH in response to cigarette smoke *in vitro* and *in vivo* [631].

Finally, metabolism and inactivation of Cd-induced ROS by cells and tissues can also be perceived as indirect processes that contribute to Cd detoxification. The cellular antioxidative defense mechanisms responsible for ROS scavenging have been thoroughly reviewed [474,489]. They include antioxidative enzymes (e.g., superoxide dismutases, catalases, glutathione peroxidases, antioxidative metabolites (GSH, ascorbic acid, vitamin E) and the enzymes involved in their regeneration (thioredioxins, glutaredoxins, glutathione reductases).

7 Concluding Remarks and Future Directions

Apart from summarizing current knowledge of the field, this review aimed to deliver an appraisal of missing long-term epidemiological studies that will allow narrowing down and identifying health hazards caused by CLCE in order to design landmark studies that will clarify the molecular mechanisms by which organs and cells accumulate low Cd concentrations and how CLCE causes disease. Due to space limitations, many relevant studies on the subject could not be included in this review.

Current understanding of the biological effects of Cd and the existing knowledge of Cd-induced diseases are mainly based on results obtained by exposure to high doses of the toxic metal. But there is accumulating evidence for adverse health effects even under low exposure conditions. CLCE appears to be associated with an increasing spectrum of health hazards. In addition, susceptibilities of specific populations (e.g., children, elderly), genetic variation, and cumulative risks that result from deficiencies of nutrients, such as Fe and Zn, have not been considered.

Hence, the aims for the future will be to characterize further the impact of CLCE on major health issues by prospective long-term population studies to evaluate and strengthen the evidence for the links of CLCE with widespread diseases and leading causes of death in modern societies, e.g., osteoporosis, diabetes, cardiovascular diseases, and cancer. Implementation of preventive measures will also call for further follow-up studies to demonstrate their efficacy. Cellular and molecular research will need to establish experimental models and valid hypotheses to test causal relationships between CLCE and the aforementioned disease entities. Another challenge will be to identify likely candidates for Cd uptake into cells at the low extracellular free Cd concentrations measured in a setting of CLCE in order to design strategies for prevention or therapy of Cd toxicity. Finally, the initial processes underlying Cd-induced cell death, survival and cancer signaling need to be delineated in more detail. Identifying the signals at the top of the chain of command will help to eradicate the noxious effects of Cd at their roots and ultimately contribute to the development of preventive and novel therapeutic strategies for acute and chronic Cd toxicity.

Abbreviations and Definitions

ABCB1	multidrug resistance protein 1
ABCC2	multidrug resistance-associated protein 2
ABCC7	cystic fibrosis transmembrane conductance regulator
ABCG2	ATP-binding cassette sub-family G member 2; breast cancer resistance protein
AIF	apoptosis-inducing factor
Akt	protein kinase B
AMPK	AMP-activated protein kinase
ANT	adenine nucleotide translocase
ARFY	Atherosclerosis Risk Factors in Female Youngsters
ATF6	activating transcription factor 6
ATP	adenosine 5'-triphosphate
ATSDR	Agency for Toxic Substance and Disease Registry
b.w.	body weight
Bak	Bcl-2 homologous antagonist/killer
BAPTA	1,2-bis(o-aminophenoxy)ethane-N,N,N',N'-tetraacetic acid
BAPTA-AM	BAPTA acetoxymethyl ester
Bax	Bcl-2–associated X protein
BBB	blood-brain barrier
Bcl-2	B-cell lymphoma 2
BCRP	breast cancer resistance protein
CaMKII	Ca^{2+}/calmodulin-dependent protein kinase II
cAMP	cyclic 3'-5'-adenosine monophosphate
CAT	catalase
CC-16	Clara-cell protein
CFTR	cystic fibrosis transmembrane conductance regulator
cGMP	cyclic 3'-5'-guanosine monophosphate
CHO	Chinese hamster ovary
CHOP	CCAAT/-enhancer-binding protein homologous protein
CLCE	chronic low cadmium exposure
cMOAT	canalicular multispecific organic anion transporter; multidrug resistance-associated protein 2
Cox-2	cyclooxygenase-2
CREB	cAMP response element-binding
CsA	cyclosporin A
CTH	adrenocorticotropic hormone
Cu-ZnSOD	copper-zinc superoxide dismutase
Cys	cysteine
DCT1	divalent cation transporter 1
DMSA	dimercaptosuccinic acid
DMT1	divalent metal transporter 1
DNMT	DNA methyltransferase

DTPA	diethylenetriaminepentaacetate
EDTA	ethylenediamine-N,N,N',N'-tetraacetate
EF-hand	helix-loop-helix structural domain in calcium-binding proteins
EGFR	epidermal growth factor receptor
EGTA	ethyleneglycoltetraacetic acid
eIF2α	eukaryotic translation initiation factor 2A
EMT	epithelial-to-mesenchymal transition
EPO	erythropoietin
ER	endoplasmic reticulum
ERAD	ER-associated degradation
ERK	extracellular signal-regulated kinases
ESR	electron spin resonance
ESRD	end-stage renal disease
EU	European Union
FAO	Food and Agriculture Organization
Fas	pro-apoptotic type-II transmembrane protein; CD95L
FPN1	ferroportin 1
G1	post-mitotic Gap 1 cell cycle phase
G2/M	post-mitotic Gap 2 / mitosis cell cycle phases
GCLC	glutamate cysteine ligase catalytic subunit
GFR	glomerular filtration rate
GH	growth hormone
GI	gastrointestinal
G-protein	guanosine 5'-triphosphate-binding protein
GPx	glutathione peroxidase
GRP78	glucose-regulated protein, 78kDa
GRP94	glucose-regulated protein, 94kDa
GSH	glutathione
GSK3β	glycogen synthase kinase 3 beta
α-GST	α-glutathione-S-transferase
His	histidine
HMW	high molecular weight
i.v.	intravenous
IARC	International Agency for Research on Cancer
IC_{50}	half maximal inhibitory concentration
ICAM-1	intercellular adhesion molecule 1
ICdA	International Cadmium Association
IKK	IκB kinase
IL	interleukin
IMM	inner mitochondrial membrane
IP_3	inositol 1,4,5-trisphosphate
IRE1	inositol-requiring enzyme 1
IREG1	iron-regulated transporter 1; ferroportin 1
IκB	inhibitor of NF-κB

JNK	c-Jun N-terminal kinases
Keap1	Kelch-like ECH-associated protein 1
Kim-1	kidney injury molecule-1
K_m	Michaelis constant
LC3	microtubule-associated protein 1 light chain 3
LD_{50}	median (50%) lethal dose
LDH	lactate dehydrogenase
LEF	lymphoid enhancer factor-1 transcription factor
LMW	low molecular weight
Lrp	low-density-lipoprotein-related protein
MAPK	mitogen activated protein kinase
MCU	mitochondrial calcium uniporter
MDC	monodansylcadaverine
MDCK	Madin-Darby canine kidney (cells)
Mdm2	murine double minute 2
MDR1	multidrug resistance protein 1
MMP	mitochondrial membrane potential
MnSOD	manganese superoxide dismutase
MRL	minimal risk level
MRP2	multidrug resistance-associated protein 2
MT	metallothionein
mTOR	mammalian target of rapamycin
MTP1	metal-transporter protein 1; ferroportin 1
MW	molecular weight
NADPH	nicotinamide adenine dinucleotide phosphate (reduced)
NAG	N-acetyl-β-D-glucosamidase
NF-κB	nuclear factor-κB
NGAL	neutrophil gelatinase-associated lipocalin
NHANES III	Third National Health and Nutrition Examination Survey
NO	nitric oxide
NOS	nitric oxide synthase
NRAMP2	natural resistance-associated macrophage protein-2
Nrf2	NF-E2-related factor 2
$O_2^{\bullet -}$	superoxide anion
OMM	outer mitochondrial membrane
$ONOO^-$	peroxinitrite anion
OSHA	Occupational Safety & Health Administration from the US Dept. of Labor
p38	p38 mitogen activated protein kinase
p53	tumor suppressor protein 53
PARP	poly (ADP-ribose) polymerase
PC	phytochelatin
PERK	protein kinase RNA-like endoplasmic reticulum kinase
PGF	placental growth factor

PI3K	phosphoinositide 3 kinase
PIP_2	phosphatidylinositol 4,5-bisphosphate
PIP_3	phosphatidylinositol (3,4,5)-triphosphate
PKA	protein kinase A
PKC	protein kinase C
PT	proximal tubule
PTP	permeability transition pore
Px	peroxidase
Ras	rat sarcoma proto-oncogene
RME	receptor-mediated endocytosis
ROS	reactive oxygen species
SERCA	sarco/endoplasmic reticulum Ca^{2+}-ATPase
SH	sulfhydryl
Shh	sonic Hedgehog
SOD	superoxide dismutase
Sp1	specificity protein 1 transcription factor
STAT3	signal transducer and activator of transcription 3 transcription factor
TCF	T-cell specific transcription factor 1
TNF-α	tumor necrosis factor α
TRP	transient receptor potential (channel)
TRPM7	transient receptor potential malastatin 7 (channel)
TRPV5,6	transient receptor potential vanilloid 5,6 (channel)
TSH	thyroid-stimulating hormone
uNGAL	urinary NGAL
UPR	unfolded protein response
VDAC	voltage-dependent anion channel
VE	vascular endothelial
WHO	World Health Organization
Wnt	wingless/Int-1 signaling protein
XBP1	X-box binding protein 1
ZIP	Zrt-/Irt-like protein
$\Delta\Psi m$	mitochondrial membrane potential

Acknowledgments The authors acknowledge the scientific contributions of past and present coworkers, in particular Drs. M. Abouhamed, P. K. Chakraborty, J. M. Friedmann, C. Langelüddecke, and N. A. Wolff. Research in the laboratory is funded by The German Research Foundation (DFG) (grants FT345/8-1 to FT345/11-1) and the Centre for Biomedical Research and Training (ZBAF) at the University of Witten/Herdecke.

References

1. G. F. Nordberg, *Toxicol. Appl. Pharmacol.* **2009**, *238*, 192–200.
2. ATSDR, *Toxicological Profile for Cadmium*, Ed U. S. Agency for Toxic Substance and Disease Registry, Department of Health and Humans Services, Public Health Service, Centers for Disease Control, Atlanta, GA, USA, 2008.

3. CONTAM, *The EFSA Journal* **2009**, *980*, 1–139.
4. CONTAM, *The EFSA Journal* **2011**, *9*, 1975.
5. WHO, *Cadmium*, World Health Organization, 1992.
6. OECD, *Cadmium*, Organisation for Economic Co-operation and Development, Environment Directorate, Paris, France, 1994.
7. I. Meyer, J. Heinrich, U. Lippold, *Sci. Total Environ.* **1999**, *234*, 25–36.
8. I. M. Olsson, I. Bensryd, T. Lundh, H. Ottosson, S. Skerfving, A. Oskarsson, *Environ. Health Perspect.* **2002**, *110*, 1185–1190.
9. B. J. Alloway, in *Heavy Metals in Soils*, Ed B. J. Alloway, Blackie Academic & Professional, London, 1995, pp. 122–151.
10. P. E. Holm, H. Rootzen, O. K. Borggaard, J. P. Moberg, T. H. Christensen, *J. Environ. Qual.* **2003**, *32*, 138–145.
11. A. Kabata-Pendias, H. Pendias, *Trace Elements in Soils and Plants*, CRC Press, Boca Raton, Florida, 2001.
12. L. Jarup, A. Akesson, *Toxicol. Appl. Pharmacol.* **2009**, *238*, 201–208.
13. E. H. Larsen, N. L. Andersen, A. Moller, A. Petersen, G. K. Mortensen, J. Petersen, *Food Addit. Contam.* **2002**, *19*, 33–46.
14. S. K. Egan, P. M. Bolger, C. D. Carrington, *J. Expo. Sci. Environ. Epidemiol.* **2007**, *17*, 573–582.
15. D. L. MacIntosh, J. D. Spengler, H. Ozkaynak, L. Tsai, P. B. Ryan, *Environ. Health Perspect.* **1996**, *104*, 202–209.
16. K. W. Thomas, E. D. Pellizzari, M. R. Berry, *J. Expo. Anal. Environ. Epidemiol.* **1999**, *9*, 402–413.
17. L. Jarup, M. Berglund, C. G. Elinder, G. Nordberg, M. Vahter, *Scand. J. Work Environ. Health* **1998**, *24 Suppl 1*, 1–51.
18. C. G. Elinder, T. Kjellstrom, B. Lind, L. Linnman, M. Piscator, K. Sundstedt, *Environ. Res.* **1983**, *32*, 220–227.
19. S. Satarug, M. R. Moore, *Environ. Health Perspect.* **2004**, *112*, 1099–1103.
20. S. Willers, L. Gerhardsson, T. Lundh, *Respir. Med.* **2005**, *99*, 1521–1527.
21. G. Bolte, D. Heitmann, M. Kiranoglu, R. Schierl, J. Diemer, W. Koerner, H. Fromme, *J. Expo. Sci. Environ. Epidemiol.* **2008**, *18*, 262–271.
22. G. Oberdorster, *IARC Sci. Publ.* **1992**, 189–204.
23. A. Bernard, R. Lauwerys, in *Handbook of Experimental Pharmacology*, Ed E. C. Foulkes, Springer, Berlin, Heidelberg, 1986, Vol. 80, pp. 135–177.
24. C. G. Elinder, B. Lind, T. Kjellstrom, L. Linnman, L. Friberg, *Arch. Environ. Health* **1976**, *31*, 292–302.
25. C. E. Cross, A. van der Vliet, C. A. O'Neill, S. Louie, B. Halliwell, *Environ. Health Perspect.* **1994**, *102, Suppl. 10*, 185–191.
26. B. A. Hart, Q. Gong, J. D. Eneman, C. C. Durieux-Lu, *Toxicol. Appl. Pharmacol.* **1995**, *133*, 82–90.
27. R. M. Grasseschi, R. B. Ramaswamy, D. J. Levine, C. D. Klaassen, L. J. Wesselius, *Chest* **2003**, *124*, 1924–1928.
28. M. Niitsuya, M. Watanabe, M. Okada, H. Shinji, T. Satoh, Y. Aizawa, Y. C. Cho, M. Kotani, *J. Toxicol. Environ. Health A* **2003**, *66*, 365–378.
29. M. Lag, D. Rodionov, J. Ovrevik, O. Bakke, P. E. Schwarze, M. Refsnes, *Toxicol. Lett.* **2010**, *193*, 252–260.
30. C. Jumarie, *Biochim. Biophys. Acta* **2002**, *1564*, 487–499.
31. C. A. Pearson, P. C. Lamar, W. C. Prozialeck, *Life Sci.* **2003**, *72*, 1303–1320.
32. T. P. Dalton, L. He, B. Wang, M. L. Miller, L. Jin, K. F. Stringer, X. Chang, C. S. Baxter, D. W. Nebert, *Proc. Natl. Acad. Sci. USA* **2005**, *102*, 3401–3406.
33. M. D. Fleming, C. C. Trenor, 3rd, M. A. Su, D. Foernzler, D. R. Beier, W. F. Dietrich, N. C. Andrews, *Nat. Genet.* **1997**, *16*, 383–386.

34. H. Gunshin, B. Mackenzie, U. V. Berger, Y. Gunshin, M. F. Romero, W. F. Boron, S. Nussberger, J. L. Gollan, M. A. Hediger, *Nature* **1997**, *388*, 482–488.
35. K. Girijashanker, L. He, M. Soleimani, J. M. Reed, H. Li, Z. Liu, B. Wang, T. P. Dalton, D. W. Nebert, *Mol. Pharmacol.* **2008**, *73*, 1413–1423.
36. M. Mantha, L. El Idrissi, T. Leclerc-Beaulieu, C. Jumarie, *Toxicol. In Vitro* **2011**, *25*, 1701–1711.
37. J. R. Napolitano, M. J. Liu, S. Bao, M. Crawford, P. Nana-Sinkam, E. Cormet-Boyaka, D. L. Knoell, *Am. J. Physiol. Lung Cell Mol. Physiol.* **2012**, *302,* L909–L918.
38. A. J. Ghio, C. A. Piantadosi, X. Wang, L. A. Dailey, J. D. Stonehuerner, M. C. Madden, F. Yang, K. G. Dolan, M. D. Garrick, L. M. Garrick, *Am. J. Physiol. Lung Cell Mol. Physio.l* **2005**, *289*, L460–L467.
39. L. Friberg, M. Piscator, G. Nordberg, T. Kjellström, *Cadmium in the Environment*, CRC Press, Cleveland, Ohio, 1974.
40. L. E. Decker, R. U. Byerrum, C. F. Decker, C. A. Hoppert, R. F. Langham, *AMA Arch. Ind. Health* **1958**, *18*, 228–231.
41. J. S. McLellan, P. R. Flanagan, M. J. Chamberlain, L. S. Valberg, *J. Toxicol. Environ. Health* **1978**, *4*, 131–138.
42. S. Suzuki, T. Taguchi, G. Yokohashi, *Ind. Health* **1969**, *7*, 155–162.
43. D. Kello, K. Kostial, *Environ. Res.* **1977**, *14*, 92–98.
44. P. R. Flanagan, J. S. McLellan, J. Haist, G. Cherian, M. J. Chamberlain, L. S. Valberg, *Gastroenterology* **1978**, *74*, 841–846.
45. H. A. Ragan, *J. Lab. Clin. Med.* **1977**, *90*, 700–706.
46. M. Vahter, A. Akesson, C. Liden, S. Ceccatelli, M. Berglund, *Environ. Res.* **2007**, *104*, 85–95.
47. M. Kippler, E. C. Ekstrom, B. Lonnerdal, W. Goessler, A. Akesson, S. El Arifeen, L. A. Persson, M. Vahter, *Toxicol. Appl. Pharmacol.* **2007**, *222*, 221–226.
48. A. Akesson, M. Berglund, A. Schutz, P. Bjellerup, K. Bremme, M. Vahter, *Am. J. Public Health* **2002**, *92*, 284–287.
49. M. Berglund, A. Akesson, B. Nermell, M. Vahter, *Environ. Health Perspect.* **1994**, *102*, 1058–1066.
50. H. Zoller, R. O. Koch, I. Theurl, P. Obrist, A. Pietrangelo, G. Montosi, D. J. Haile, W. Vogel, G. Weiss, *Gastroenterology* **2001**, *120*, 1412–1419.
51. G. Kovacs, T. Danko, M. J. Bergeron, B. Balazs, Y. Suzuki, A. Zsembery, M. A. Hediger, *Cell Calcium* **2011**, *49*, 43–55.
52. S. Abboud, D. J. Haile, *J. Biol. Chem.* **2000**, *275*, 19906–19912.
53. A. T. McKie, P. Marciani, A. Rolfs, K. Brennan, K. Wehr, D. Barrow, S. Miret, A. Bomford, T. J. Peters, F. Farzaneh, M. A. Hediger, M. W. Hentze, R. J. Simpson, *Mol. Cell* **2000**, *5*, 299–309.
54. D. W. Kim, K. Y. Kim, B. S. Choi, P. Youn, D. Y. Ryu, C. D. Klaassen, J. D. Park, *Arch. Toxicol.* **2007**, *81*, 327–334.
55. C. D. Klaassen, J. Liu, B. A. Diwan, *Toxicol. Appl. Pharmacol.* **2009**, *238*, 215–220.
56. Y. Fujita, H. I. el Belbasi, K. S. Min, S. Onosaka, Y. Okada, Y. Matsumoto, N. Mutoh, K. Tanaka, *Res. Commun. Chem. Pathol. Pharmacol.* **1993**, *82*, 357–365.
57. H. M. Crews, J. R. Dean, L. Ebdon, R. C. Massey, *Analyst* **1989**, *114*, 895–899.
58. N. I. McNeil, *Am. J. Clin. Nutr.* **1984**, *39*, 338–342.
59. M. G. Cherian, *Environ. Health Perspect.* **1979**, *28*, 127–130.
60. C. Langelueddecke, E. Roussa, R. A. Fenton, N. A. Wolff, W. K. Lee, F. Thévenod, *J. Biol. Chem.* **2012**, *287*, 159–169.
61. R. C. Wester, H. I. Maibach, L. Sedik, J. Melendres, S. DiZio, M. Wade, *Fundam. Appl. Toxicol.* **1992**, *19*, 1–5.
62. R. Thieme, P. Schramel, E. Kurz, *Geburtshilfe Frauenheilkd.* **1977**, *37*, 756–761.
63. P. G. Bush, T. M. Mayhew, D. R. Abramovich, P. J. Aggett, M. D. Burke, K. R. Page, *Placenta* **2000**, *21*, 247–256.

64. R. Lauwerys, J. P. Buchet, H. Roels, G. Hubermont, *Environ. Res.* **1978**, *15*, 278–289.
65. M. Kippler, A. M. Hoque, R. Raqib, H. Ohrvik, E. C. Ekstrom, M. Vahter, *Toxicol. Lett.* **2010**, *192*, 162–168.
66. T. M. Leazer, Y. Liu, C. D. Klaassen, *Toxicol. Appl. Pharmaco.l* **2002**, *185*, 18–24.
67. M. K. Georgieff, J. K. Wobken, J. Welle, J. R. Burdo, J. R. Connor, *Placenta* **2000**, *21*, 799–804.
68. J. B. Peng, X. Z. Chen, U. V. Berger, S. Weremowicz, C. C. Morton, P. M. Vassilev, E. M. Brown, M. A. Hediger, *Biochem. Biophys. Res. Commun.* **2000**, *278*, 326–332.
69. J. J. Walsh, G. E. Burch, *J. Lab. Clin. Med.* **1959**, *54*, 59–65.
70. S. T. Trisak, P. Doumgdee, B. M. Rode, *Int. J. Biochem.* **1990**, *22*, 977–981.
71. W. Goumakos, J. P. Laussac, B. Sarkar, *Biochem. Cell Biol.* **1991**, *69*, 809–820.
72. M. Nordberg, *Environ. Res.* **1978**, *15*, 381–404.
73. B. J. Fuhr, D. L. Rabenstein, *J. Am. Chem. Soc.* **1973**, *95*, 6944–6950.
74. J. H. Kägi, B. L. Vallee, *J. Biol. Chem.* **1961**, *236*, 2435–2442.
75. D. D. Perrin, A. E. Watt, *Biochim. Biophys. Acta* **1971**, *230*, 96–104.
76. M. G. Cherian, Z. A. Shaikh, *Biochem. Biophys. Res. Commun.* **1975**, *65*, 863–869.
77. Z. A. Shaikh, K. Hirayama, *Environ. Health Perspect.* **1979**, *28*, 267–271.
78. H. Milnerowicz, A. Bizon, *Acta. Biochim. Pol.* **2010**, *57*, 99–104.
79. G. F. Nordberg, J. S. Garvey, C. C. Chang, *Environ. Res.* **1982**, *28*, 179–182.
80. G. F. Nordberg, T. Kjellstrom, G. Nordberg, in *Cadmium and Health: A Toxicological and Epidemiological Appraisal*, Ed L. Friberg, C. G. Elinder, T. Kjellstrom, TG. F. Nordberg, CRC Press, Boca Raton, 1986, pp. 103–178.
81. M. Garty, K. L. Wong, C. D. Klaassen, *Toxicol. Appl. Pharmacol.* **1981**, *59*, 548–554.
82. L. A. Carlson, L. Friberg, *Scand. J. Clin. Lab. Invest.* **1957**, *9*, 67–70.
83. M. T. Rahman, A. Vandingenen, M. De Ley, *Cell Physiol. Biochem.* **2000**, *10*, 237–242.
84. J. Lu, T. Jin, G. Nordberg, M. Nordberg, *Toxicol. App.l Pharmacol.* **2005**, *206*, 150–156.
85. T. Sugiura, H. Nakamura, *Int. Arch. Allergy Immunol.* **1994**, *103*, 341–348.
86. J. Lu, T. Jin, G. F. Nordberg, M. Nordberg, *Biometals* **2004**, *17*, 569–570.
87. X. Chang, T. Jin, L. Chen, M. Nordberg, L. Lei, *Exp. Biol. Med.* **2009**, *234*, 666–672.
88. M. Nordberg, G. F. Nordberg, *Environ. Health Perspect.* **1975**, *12*, 103–108.
89. K. S. Squibb, B. A. Fowler, *Environ. Health Perspect.* **1984**, *54*, 31–35.
90. R. E. Dudley, L. M. Gammal, C. D. Klaassen, *Toxicol. Appl. Pharmacol.* **1985**, *77*, 414–426.
91. C. Tohyama, Z. A. Shaikh, K. J. Ellis, S. H. Cohn, *Toxicology* **1981**, *22*, 181–191.
92. K. Nomiyama, H. Nomiyama, N. Kameda, *Toxicology* **1998**, *129*, 157–168.
93. L. Jarup, A. Rogenfelt, C. G. Elinder, K. Nogawa, T. Kjellstrom, *Scand. J. Work Environ. Health* **1983**, *9*, 327–331.
94. S. Thijssen, J. Maringwa, C. Faes, I. Lambrichts, E. Van Kerkhove, *Toxicology* **2007**, *229*, 145–156.
95. C. G. Elinder, L. Friberg, B. Lind, M. Jawaid, *Environ. Res.* **1983**, *30*, 233–253.
96. T. Kjellstrom, *Environ. Health Perspect.* **1979**, *28*, 169–197.
97. C. G. Elinder, T. Kjellstrom, L. Linnman, G. Pershagen, *Environ. Res.* **1978**, *15*, 473–484.
98. K. Tsuchiya, M. Sugita, Y. Seki, *Keio J. Med.* **1976**, *25*, 73–82.
99. N. E. Kowal, D. E. Johnson, D. F. Kraemer, H. R. Pahren, *J. Toxicol. Environ. Health* **1979**, *5*, 995–1014.
100. R. R. Lauwerys, J. P. Buchet, H. A. Roels, J. Brouwers, D. Stanescu, *Arch. Environ. Health* **1974**, *28*, 145–148.
101. H. A. Roels, R. R. Lauwerys, J. P. Buchet, A. Bernard, *Environ. Res.* **1981**, *24*, 117–130.
102. S. Kojima, Y. Haga, T. Kurihara, T. Yamawaki, *Environ. Res.* **1977**, *14*, 436–451.
103. C. Tohyama, Z. A. Shaikh, K. Nogawa, E. Kobayashi, R. Honda, *Toxicology* **1981**, *20*, 289–297.
104. H. Koyama, H. Satoh, S. Suzuki, C. Tohyama, *Arch. Toxicol.* **1992**, *66*, 598–601.
105. H. Roels, R. Lauwerys, J. P. Buchet, A. Bernard, J. S. Garvey, H. J. Linton, *Int. Arch. Occup. Environ. Health* **1983**, *52*, 159–166.

106. Y. Suzuki, *J. Toxicol. Environ. Health* **1980**, *6*, 469–482.
107. Y. Suzuki, H. Yoshikawa, *Ind. Health* **1983**, *21*, 43–50.
108. A. Bernard, R. Lauwerys, P. Gengoux, *Toxicology* **1981**, *20*, 345–357.
109. G. F. Nordberg, M. Piscator, *Environ. Physiol. Biochem.* **1972**, *2*, 37–49.
110. C. G. Elinder, M. Pannone, *Environ. Health Perspect.* **1979**, *28*, 123–126.
111. M. Cikrt, M. Tichy, *Br. J. Ind. Med.* **1974**, *31*, 134–139.
112. C. D. Klaassen, F. N. Kotsonis, *Toxicol. Appl. Pharmacol.* **1977**, *41*, 101–112.
113. M. G. Cherian, J. J. Vostal, *J. Toxicol. Environ. Health* **1977**, *2*, 945–954.
114. G. Jedlitschky, I. Leier, U. Buchholz, K. Barnouin, G. Kurz, D. Keppler, *Cancer Res.* **1996**, *56*, 988–994.
115. N. Sugawara, Y. R. Lai, K. Arizono, T. Ariyoshi, *Toxicology* **1996**, *112*, 87–94.
116. N. Sugawara, Y. R. Lai, K. Arizono, T. Kitajima, H. Inoue, *Arch. Toxicol.* **1997**, *71*, 336–339.
117. M. Dijkstra, R. Havinga, R. J. Vonk, F. Kuipers, *Life Sci.* **1996**, *59*, 1237–1246.
118. M. Buchler, J. Konig, M. Brom, J. Kartenbeck, H. Spring, T. Horie, D. Keppler, *J. Biol. Chem.* **1996**, *271*, 15091–15098.
119. S. B. Gross, D. W. Yeager, M. S. Middendorf, *J. Toxicol. Environ. Health* **1976**, *2*, 153–167.
120. Z. A. Shaikh, L. M. Smith, *Experientia Suppl.* **1986**, *50*, 124–130.
121. M. Kippler, B. Lonnerdal, W. Goessler, E. C. Ekstrom, S. E. Arifeen, M. Vahter, *Toxicology* **2009**, *257*, 64–69.
122. M. Kippler, B. Nermell, J. Hamadani, F. Tofail, S. Moore, M. Vahter, *Toxicol. Lett.* **2010**, *198*, 20–25.
123. N. Johri, G. Jacquillet, R. Unwin, *Biometals* **2010**, *23*, 783–792.
124. D. H. Yates, K. P. Goldman, *Br. J. Ind. Med* .**1990**, *47*, 429–431.
125. M. J. Ellenhorn, D. G. Barceloux, *Medical Toxicology – Diagnosis and Treatment of Human Poisoning*, Elsevier, New York, 1996.
126. R. H. Strauss, K. C. Palmer, J. A. Hayes, *Am. J. Pathol.* **1976**, *84*, 561–578.
127. Y. M. Hung, H. M. Chung, *Nephrol. Dial. Transplant* **2004**, *19*, 1308–1309.
128. H. M. Buckler, W. D. Smith, W. D. Rees, *Br. Med. J. (Clin. Res. Ed.)* **1986**, *292*, 1559–1560.
129. H. J. Klimisch, *Toxicology* **1993**, *84*, 103–124.
130. J. G. Hadley, A. W. Conklin, C. L. Sanders, *Toxicol. Lett.* **1979**, *4*, 107–111.
131. L. Friberg, *Acta Med. Scand. Suppl.* **1950**, *240*, 1–124.
132. R. E. Dudley, D. J. Svoboda, C. Klaassen, *Toxicol. Appl. Pharmacol.* **1982**, *65*, 302–313.
133. E. O. Hoffmann, J. A. Cook, N. R. di Luzio, J. A. Coover, *Lab. Invest.* **1975**, *32*, 655–664.
134. S. A. Gunn, T. C. Gould, in *The Testis*, Eds A. Johnson, W. Gomes, N. VanDeMark, Academic Press, New York, London, 1970, Vol. 3, pp. 377–481.
135. S. M. Barlow, F. M. Sullivan, in *Reproductive Hazards of Industrial Chemicals. An Evaluation of Animal and Human Data*, Ed S. Barlow, Academic Press, New York, London, 1982, pp. 137–173.
136. J. Parizek, *J. Endocrinol.* **1957**, *15*, 56–63.
137. J. Parizek, Z. Zahor, *Nature* **1956**, *177*, 1036.
138. A. Aoki, A. P. Hoffer, *Biol. Reprod.* **1978**, *18*, 579–591.
139. A. B. Kar, R. P. Das, J. N. Karkun, *Acta Biol. Med. Ger.* **1959**, *3*, 372–399.
140. J. Parizek, I. Ostadalova, I. Benes, J. Pitha, *J. Reprod. Fertil.* **1968**, *17*, 559–562.
141. E. R. Siu, D. D. Mruk, C. S. Porto, C. Y. Cheng, *Toxicol. Appl. Pharmacol.* **2009**, *238*, 240–249.
142. A. Janecki, A. Jakubowiak, A. Steinberger, *Toxicol. Appl. Pharmacol.* **1992**, *112*, 51–57.
143. C. H. Wong, D. D. Mruk, W. Y. Lui, C. Y. Cheng, *J. Cell Sci.* **2004**, *117*, 783–798.
144. R. Sen Gupta, E. Sen Gupta, B. K. Dhakal, A. R. Thakur, J. Ahnn, *Mol. Cells* **2004**, *17*, 132–139.
145. J. Liu, M. B. Kadiiska, J. C. Corton, W. Qu, M. P. Waalkes, R. P. Mason, Y. Liu, C. D. Klaassen, *Free Radic. Biol. Med.* **2002**, *32*, 525–535.
146. J. Liu, S. Y. Qian, Q. Guo, J. Jiang, M. P. Waalkes, R. P. Mason, M. B. Kadiiska, *Free Radic. Biol. Med.* **2008**, *45*, 475–481.

147. K. Tsuchiya, Y. Seki, M. Sugita, *Keio J. Med.* **1976**, *25*, 83–90.
148. S. S. Salmela, E. Vuori, A. Huunan-Seppala, J. O. Kilpio, H. Sumuvuori, *Sci. Total Environ.* **1983**, *27*, 89-95.
149. M. Sugita, K. Tsuchiya, *Environ. Res.* **1995**, *68*, 31-37.
150. L. Jarup, L. Hellstrom, T. Alfven, M. D. Carlsson, A. Grubb, B. Persson, C. Pettersson, G. Spang, A. Schutz, C. G. Elinder, *Occup. Environ. Med.* **2000**, *57*, 668–672.
151. P. M. Ferraro, S. Costanzi, A. Naticchia, A. Sturniolo, G. Gambaro, *BMC Public Health* **2010**, *10*, 304.
152. L. Hellstrom, C. G. Elinder, B. Dahlberg, M. Lundberg, L. Jarup, B. Persson, O. Axelson, *Am. J. Kidney Dis.* **2001**, *38*, 1001–1008.
153. A. Menke, P. Muntner, E. K. Silbergeld, E. A. Platz, E. Guallar, *Environ. Health Perspect.* **2009**, *117*, 190–196.
154. T. S. Nawrot, E. Van Hecke, L. Thijs, T. Richart, T. Kuznetsova, Y. Jin, J. Vangronsveld, H. A. Roels, J. A. Staessen, *Environ. Health Perspect.* **2008**, *116*, 1620–1628.
155. G. Huel, C. Boudene, M. A. Ibrahim, *Arch. Environ. Health* **1981**, *36*, 221–227.
156. B. R. Kuhnert, P. M. Kuhnert, T. J. Zarlingo, *Obstet. Gynecol.* **1988**, *71*, 67–70.
157. M. Marlowe, J. Errera, J. Jacobs, *Am. J. Ment. Defic.* **1983**, *87*, 477–483.
158. V. H. Ferm, S. J. Carpenter, *Nature* **1967**, *216*, 1123.
159. N. Chernoff, *Teratology* **1973**, *8*, 29–32.
160. B. P. Schmid, J. Kao, E. Goulding, *Experientia* **1985**, *41*, 271–272.
161. M. Webb, D. Holt, N. Brown, G. C. Hard, *Arch. Toxicol.* **1988**, *61*, 457–467.
162. N. G. Carmichael, B. L. Backhouse, C. Winder, P. D. Lewis, *Hum. Toxicol.* **1982**, *1*, 159–186.
163. J. F. Robinson, X. Yu, E. G. Moreira, S. Hong, E. M. Faustman, *Toxicol. Appl. Pharmacol.* **2011**, *250*, 117–129.
164. C. M. Schreiner, S. M. Bell, W. J. Scott, Jr., *Birth Defects Res. A Clin. Mol. Teratol.* **2009**, *85*, 588–598.
165. A. F. Elsaid, E. C. Delot, M. D. Collins, *Mol. Genet. Metab.* **2007**, *92*, 258–270.
166. W. J. Scott, Jr., C. M. Schreiner, J. A. Goetz, D. Robbins, S. M. Bell, *Reprod. Toxicol.* **2005**, *19*, 479–485.
167. T. S. Nawrot, J. A. Staessen, H. A. Roels, E. Munters, A. Cuypers, T. Richart, A. Ruttens, K. Smeets, H. Clijsters, J. Vangronsveld, *Biometals* **2010**, *23*, 769–782.
168. IARC, "Beryllium, cadmium, mercury, and exposures in the glass manufacturing industry. Working Group views and expert opinions, Lyon, 9–16 February 1993", Lyon, 1993.
169. D. Il'yasova, G. G. Schwartz, *Toxicol. Appl. Pharmacol.* **2005**, *207*, 179–186.
170. DFG, *Cadmium and Its compounds (in the form of inhalable dusts/aerosols)*, Ed Deutsche Forschungsgemeinschaft, Wiley-VCH, Weinheim, Germany, 2006.
171. A. Akesson, B. Julin, A. Wolk, *Cancer Res.* **2008**, *68*, 6435–6441.
172. J. A. McElroy, M. M. Shafer, A. Trentham-Dietz, J. M. Hampton, P. A. Newcomb, *J. Natl. Cancer Inst.* **2006**, *98*, 869–873.
173. T. Nawrot, M. Plusquin, J. Hogervorst, H. A. Roels, H. Celis, L. Thijs, J. Vangronsveld, E. Van Hecke, J. A. Staessen, *Lancet Oncol.* **2006**, *7*, 119–126.
174. A. M. Kriegel, A. S. Soliman, Q. Zhang, N. El-Ghawalby, F. Ezzat, A. Soultan, M. Abdel-Wahab, O. Fathy, G. Ebidi, N. Bassiouni, S. R. Hamilton, J. L. Abbruzzese, M. R. Lacey, D. A. Blake, *Environ. Health Perspect.* **2006**, *114*, 113–119.
175. G. G. Schwartz, I. M. Reis, *Cancer Epidemiol. Biomarkers Prev.* **2000**, *9*, 139–145.
176. E. Kellen, M. P. Zeegers, E. D. Hond, F. Buntinx, *Cancer Detect. Prev.* **2007**, *31*, 77–82.
177. V. Verougstraete, D. Lison, P. Hotz, *J. Toxicol. Environ. Health B Crit. Rev.* **2003**, *6*, 227–255.
178. M. Vinceti, M. Venturelli, C. Sighinolfi, P. Trerotoli, F. Bonvicini, A. Ferrari, G. Bianchi, G. Serio, M. Bergomi, G. Vivoli, *Sci. Total Environ.* **2007**, *373*, 77–81.
179. M. P. Waalkes, *Mutat. Res.* **2003**, *533*, 107–120.
180. R. A. Goyer, J. Liu, M. P. Waalkes, *Biometals* **2004**, *17*, 555–558.

181. J. Huff, R. M. Lunn, M. P. Waalkes, L. Tomatis, P. F. Infante, *Int. J. Occup. Environ. Health* **2007**, *13*, 202–212.
182. M. Waisberg, P. Joseph, B. Hale, D. Beyersmann, *Toxicology* **2003**, *192*, 95–117.
183. D. Beyersmann, A. Hartwig, *Arch. Toxicol.* **2008**, *82*, 493–512.
184. P. Joseph, *Toxicol. Appl. Pharmacol.* **2009**, *238*, 272–279.
185. M. Filipic, T. K. Hei, *Mutat. Res.* **2004**, *546*, 81–91.
186. M. Valko, C. J. Rhodes, J. Moncol, M. Izakovic, M. Mazur, *Chem. Biol. Interact.* **2006**, *160*, 1–40.
187. J. Liu, W. Qu, M. B. Kadiiska, *Toxicol. Appl. Pharmacol.* **2009**, *238*, 209–214.
188. W. Qu, B. A. Diwan, J. M. Reece, C. D. Bortner, J. Pi, J. Liu, M. P. Waalkes, *Int. J. Cancer* **2005**, *114*, 346–355.
189. W. Qu, R. Fuquay, T. Sakurai, M. P. Waalkes, *Mol. Carcinog.* **2006**, *45*, 561–571.
190. W. C. Prozialeck, J. R. Edwards, *Biometals* **2010**, *23*, 793–809.
191. J. Liu, R. A. Goyer, M. P. Waalkes, in *Casarett and Doull's Toxicology*, Ed C. D. Klaassen, McGraw-Hill, New York, NY, 2008, pp. 931–979.
192. C. D. Klaassen, J. Liu, S. Choudhuri, *Annu. Rev. Pharmacol. Toxicol.* **1999**, *39*, 267–294.
193. R. K. Zalups, S. Ahmad, *Toxicol. Appl. Pharmacol.* **2003**, *186*, 163–188.
194. H. M. Chan, Y. Tamura, M. G. Cherian, R. A. Goyer, *Proc. Soc. Exp. Biol. Med.* **1993**, *202*, 420–427.
195. K. Tanaka, *Dev. Toxicol. Environ. Sci.* **1982**, *9*, 237–249.
196. S. A. Gunn, T. C. Gould, *Proc. Soc. Exp. Biol. Med.* **1957**, *96*, 820–823.
197. G. F. Nordberg, K. Nishiyama, *Arch. Environ. Health* **1972**, *24*, 209–214.
198. H. M. Chan, L. F. Zhu, R. Zhong, D. Grant, R. A. Goyer, M. G. Cherian, *Toxicol. Appl. Pharmacol.* **1993**, *123*, 89–96.
199. F. Thévenod, *Biometals* **2010**, *23*, 857–875.
200. H. Birn, E. I. Christensen, *Kidney Int.* **2006**, *69*, 440–449.
201. R. B. Klassen, K. Crenshaw, R. Kozyraki, P. J. Verroust, L. Tio, S. Atrian, P. L. Allen, T. G. Hammond, *Am. J. Physiol. Renal Physiol.* **2004**, *287*, F393–F403.
202. N. A. Wolff, M. Abouhamed, P. J. Verroust, F. Thévenod, *J. Pharmacol. Exp. Ther.* **2006**, *318*, 782–791.
203. W. C. Prozialeck, P. C. Lamar, *Arch. Toxicol.* **1993**, *67*, 113–119.
204. F. Thévenod, G. Ciarimboli, N. A. Wolff, E. Schlatter, H. Koepsell, *FASEB J.* **2008**, *22*, 1202.1206.
205. S. Soodvilai, J. Nantavishit, C. Muanprasat, V. Chatsudthipong, *Toxicol. Lett.* **2011**, *204*, 38–42.
206. R. K. Zalups, *Toxicol. Appl. Pharmacol.* **2000**, *164*, 15–23.
207. N. A. Wolff, W. K. Lee, M. Abouhamed, F. Thévenod, *Toxicol. Appl. Pharmacol.* **2008**, *230*, 78–85.
208. N. A. Wolff, W. K. Lee, F. Thévenod, *Toxicol. Lett.* **2011**, *203*, 210–218.
209. M. Abouhamed, J. Gburek, W. Liu, B. Torchalski, A. Wilhelm, N. A. Wolff, E. I. Christensen, F. Thévenod, C. P. Smith, *Am. J. Physiol. Renal Physiol.* **2006**, *290*, F1525–F1533.
210. M. Abouhamed, N. A. Wolff, W. K. Lee, C. P. Smith, F. Thévenod, *Am. J. Physiol. Renal Physiol.* **2007**, *293*, F705–F712.
211. J. Liu, Y. Liu, S. S. Habeebu, C. D. Klaassen, *Toxicol. Sci.* **1998**, *46*, 197–203.
212. W. C. Prozialeck, D. R. Wellington, P. C. Lamar, *Life Sci.* **1993**, *53*, PL337–342.
213. J. Liu, Y. Liu, C. D. Klaassen, *Toxicol. Appl. Pharmacol.* **1994**, *128*, 264–270.
214. C. Erfurt, E. Roussa, F. Thévenod, *Am. J. Physiol. Cell Physiol.* **2003**, *285*, C1367–C1376.
215. J. E. Levy, L. K. Montross, N. C. Andrews, *J. Clin. Invest.* **2000**, *105*, 1209–1216.
216. K. Weyer, T. Storm, J. Shan, S. Vainio, R. Kozyraki, P. J. Verroust, E. I. Christensen, R. Nielsen, *Nephrol. Dial. Transplant* **2011**, *26*, 3446–3451.
217. H. Roels, A. Bernard, J. P. Buchet, A. Goret, R. Lauwerys, D. R. Chettle, T. C. Harvey, I. A. Haddad, *Lancet* **1979**, *1*, 221.

218. H. C. Gonick, *Indian J. Med. Res.* **2008**, *128*, 335–352.
219. L. Jarup, *Nephrol. Dial. Transplant* **2002**, *17 Suppl 2*, 35–39.
220. F. Thévenod, J. M. Friedmann, *FASEB J.* **1999**, *13*, 1751–1761.
221. S. Tsuruoka, K. Sugimoto, S. Muto, K. Nomiyama, A. Fujimura, M. Imai, *J. Pharmacol. Exp. Ther.* **2000**, *292*, 769–777.
222. A. Bernard, *Biometals* **2004**, *17*, 519–523.
223. L. Jarup, B. Persson, C. G. Elinder, *Occup. Environ. Med.* **1995**, *52*, 818–822.
224. A. Akesson, T. Lundh, M. Vahter, P. Bjellerup, J. Lidfeldt, C. Nerbrand, G. Samsioe, U. Stromberg, S. Skerfving, *Environ. Health Perspect.* **2005**, *113*, 1627–1631.
225. Y. Suwazono, S. Sand, M. Vahter, A. F. Filipsson, S. Skerfving, J. Lidfeldt, A. Akesson, *Environ. Health Perspect.* **2006**, *114*, 1072–1076.
226. A. G. Norden, M. Lapsley, P. J. Lee, C. D. Pusey, S. J. Scheinman, F. W. Tam, R. V. Thakker, R. J. Unwin, O. Wrong, *Kidney Int.* **2001**, *60*, 1885–1892.
227. C. G. Gunawardana, R. E. Martinez, W. Xiao, D. M. Templeton, *Am. J. Physiol. Renal Physiol.* **2006**, *290*, F1074–1082.
228. Z. Wang, D. M. Templeton, *J. Biol. Chem.* **1998**, *273*, 73–79.
229. J. P. Girolami, J. L. Bascands, C. Pecher, G. Cabos, J. P. Moatti, J. F. Mercier, J. M. Haguenoer, Y. Manuel, *Toxicology* **1989**, *55*, 117–129.
230. R. Lauwerys, A. Bernard, *Toxicol. Lett.* **1989**, *46*, 13–29.
231. T. H. Yen, J. L. Lin, D. T. Lin-Tan, C. W. Hsu, K. H. Chen, H. H. Hsu, *Nephrol. Dial. Transplant* **2011**, *26*, 998–1005.
232. J. P. Buchet, R. Lauwerys, H. Roels, A. Bernard, P. Bruaux, F. Claeys, G. Ducoffre, P. de Plaen, J. Staessen, A. Amery, P. Lijnen, L. Thijs, D. Rondia, F. Sartor, A. Saint Remy, L. Nick, *Lancet* **1990**, *336*, 699–702.
233. T. N. Pham, J. A. Segui, C. Fortin, P. G. Campbell, F. Denizeau, C. Jumarie, *J. Cell Physiol.* **2004**, *201*, 320–330.
234. H. Fujishiro, S. Okugaki, K. Kubota, T. Fujiyama, H. Miyataka, S. Himeno, *J. Appl. Toxicol.* **2009**, *29*, 367–373.
235. B. P. Hughes, K. Both, L. Harland, J. Hunt, K. M. Hurst, M. Lewis, G. J. Barritt, *Biochem. Mol. Biol. Int.* **1993**, *31*, 193–200.
236. Q. Hao, S. H. Hong, W. Maret, *J. Cell Physiol.* **2007**, *210*, 428–435.
237. I. Sabolic, D. Breljak, M. Skarica, C. M. Herak-Kramberger, *Biometals* **2010**, *23*, 897–926.
238. E. Vuori, A. Huunan-Seppala, J. O. Kilpio, S. S. Salmela, *Scand. J. Work Environ. Health* **1979**, *5*, 16–22.
239. S. Satarug, J. R. Baker, P. E. Reilly, M. R. Moore, D. J. Williams, *Arch. Environ. Health* **2002**, *57*, 69–77.
240. H. D. Stowe, M. Wilson, R. A. Goyer, *Arch. Pathol.* **1972**, *94*, 389–405.
241. K. Nomiyama, H. Nomiyama, Y. Nomura, T. Taguchi, K. Matsui, M. Yotoriyama, F. Akahori, S. Iwao, N. Koizumi, T. Masaoka, S. Kitamura, K. Tsuchiya, T. Suzuki, K. Kobayashi, *Environ. Health Perspect.* **1979**, *28*, 223–243.
242. N. Y. Tarasenko, R. S. Vorobeva, V. S. Spiridinova, L. P. Shabalina, *J. Hyg. Epidemiol. Microbiol. Immunol.* **1974**, *18*, 144–153.
243. Z. A. Shaikh, T. T. Vu, K. Zaman, *Toxicol. Appl. Pharmacol.* **1999**, *154*, 256–263.
244. T. Kamiyama, H. Miyakawa, J. P. Li, T. Akiba, J. H. Liu, J. Liu, F. Marumo, C. Sato, *Res. Commun. Mol. Pathol. Pharmacol.* **1995**, *88*, 177–186.
245. S. S. Habeebu, J. Liu, Y. Liu, C. D. Klaassen, *Toxicol. Sci.* **2000**, *55*, 223–232.
246. S. Thijssen, A. Cuypers, J. Maringwa, K. Smeets, N. Horemans, I. Lambrichts, E. Van Kerkhove, *Toxicology* **2007**, *236*, 29–41.
247. D. Djukic-Cosic, M. Curcic Jovanovic, Z. Plamenac Bulat, M. Ninkovic, Z. Malicevic, V. Matovic, *J. Trace Elem. Med. Biol.* **2008**, *22*, 66–72.
248. D. Bagchi, P. J. Vuchetich, M. Bagchi, E. A. Hassoun, M. X. Tran, L. Tang, S. J. Stohs, *Free Radic. Biol. Med.* **1997**, *22*, 471–478.

249. D. H. Lee, J. S. Lim, K. Song, Y. Boo, D. R. Jacobs, Jr., *Environ. Health Perspect.* **2006**, *114*, 350–354.
250. H. Kollmeier, J. Seemann, P. Wittig, G. Rothe, K. M. Muller, *Int. Arch. Occup. Environ. Health* **1990**, *62*, 373–377.
251. P. Paakko, P. Kokkonen, S. Anttila, P. L. Kalliomaki, *Environ Res* **1989**, *49*, 197–207.
252. B. G. Armstrong, G. Kazantzis, *Lancet* **1983**, *1*, 1425–1427.
253. D. J. Hendrick, *Thorax* **1996**, *51*, 947–955.
254. G. Kazantzis, T. H. Lam, K. R. Sullivan, *Scand. J. Work Environ. Health* **1988**, *14*, 220–223.
255. C. Edling, C. G. Elinder, E. Randma, *Br. J. Ind. Med.* **1986**, *43*, 657–662.
256. D. Stanescu, C. Veriter, A. Frans, L. Goncette, H. Roels, R. Lauwerys, L. Brasseur, *Scand. J. Respir. Dis.* **1977**, *58*, 289–303.
257. G. L. Snider, J. A. Hayes, A. L. Korthy, G. P. Lewis, *Am. Rev. Respir. Dis.* **1973**, *108*, 40–48.
258. U. Heinrich, L. Peters, H. Ernst, S. Rittinghausen, C. Dasenbrock, H. Konig, *Exp. Pathol.* **1989**, *37*, 253–258.
259. K. U. Thiedemann, N. Luthe, I. Paulini, A. Kreft, U. Heinrich, U. Glaser, *Exp. Pathol.* **1989**, *37*, 264–268.
260. E. Prigge, *Arch. Toxicol.* **1978**, *40*, 231–247.
261. S. Kundu, S. Sengupta, S. Chatterjee, S. Mitra, A. Bhattacharyya, *J. Inflamm. (Lond)* **2009**, *6*, 19.
262. N. Kirschvink, N. Martin, L. Fievez, N. Smith, D. Marlin, P. Gustin, *Free Radic. Res.* **2006**, *40*, 241–250.
263. E. Cormet-Boyaka, K. Jolivette, A. Bonnegarde-Bernard, J. Rennolds, F. Hassan, P. Mehta, S. Tridandapani, J. Webster-Marketon, P. N. Boyaka, *Toxicol. Sci.* **2012**, *125*, 418–429.
264. S. Kundu, S. Sengupta, A. Bhattacharyya, *Inhal. Toxicol.* **2011**, *23*, 339–348.
265. B. Besecker, S. Bao, B. Bohacova, A. Papp, W. Sadee, D. L. Knoell, *Am. J. Physiol. Lung Cell Mol. Physiol.* **2008**, *294*, L1127–1136.
266. I. Aiba, A. Hossain, M. T. Kuo, *Mol. Pharmacol.* **2008**, *74*, 823–833.
267. J. Rennolds, S. Butler, K. Maloney, P. N. Boyaka, I. C. Davis, D. L. Knoell, N. L. Parinandi, E. Cormet-Boyaka, *Toxicol. Sci.* **2010**, *116*, 349–358.
268. M. Childers, G. Eckel, A. Himmel, J. Caldwell, *Med. Hypotheses* **2007**, *68*, 101–112.
269. I. Kogan, M. Ramjeesingh, C. Li, J. F. Kidd, Y. Wang, E. M. Leslie, S. P. Cole, C. E. Bear, *EMBO J.* **2003**, *22*, 1981–1989.
270. S. V. Adams, M. N. Passarelli, P. A. Newcomb, *Occup. Environ. Med.* **2012**, *69*, 153–156.
271. A. t Mannetje, V. Bencko, P. Brennan, D. Zaridze, N. Szeszenia-Dabrowska, P. Rudnai, J. Lissowska, E. Fabianova, A. Cassidy, D. Mates, L. Foretova, V. Janout, J. Fevotte, T. Fletcher, P. Boffetta, *Cancer Causes Control* **2011**, *22*, 1669–1680.
272. S. Takenaka, H. Oldiges, H. Konig, D. Hochrainer, G. Oberdorster, *J. Natl. Cancer Inst.* **1983**, *70*, 367–373.
273. G. Oberdorster, M. G. Cherian, R. B. Baggs, *Toxicol. Lett.* **1994**, *72*, 339–343.
274. I. M. McKenna, T. Gordon, L. C. Chen, M. R. Anver, M. P. Waalkes, *Toxicol. Appl. Pharmacol.* **1998**, *153*, 169–178.
275. K. Nogawa, A. Ishizaki, M. Fukushima, I. Shibata, N. Hagino, *Environ. Res.* **1975**, *10*, 280–307.
276. T. Inaba, E. Kobayashi, Y. Suwazono, M. Uetani, M. Oishi, H. Nakagawa, K. Nogawa, *Toxicol. Lett.* **2005**, *159*, 192–201.
277. E. Van Kerkhove, V. Pennemans, Q. Swennen, *Biometals* **2010**, *23*, 823–855.
278. G. Kazantzis, *Biometals* **2004**, *17*, 493–498.
279. T. Alfven, C. G. Elinder, L. Hellstrom, F. Lagarde, L. Jarup, *J. Bone Miner. Res.* **2004**, *19*, 900–905.
280. R. Schutte, T. S. Nawrot, T. Richart, L. Thijs, D. Vanderschueren, T. Kuznetsova, E. Van Hecke, H. A. Roels, J. A. Staessen, *Environ. Health Perspect.* **2008**, *116*, 777–783.
281. L. Jarup, T. Alfven, *Biometals* **2004**, *17*, 505–509.

282. C. M. Gallagher, J. S. Kovach, J. R. Meliker, *Environ. Health Perspect.* **2008**, *116*, 1338–1343.
283. T. Nawrot, P. Geusens, T. S. Nulens, B. Nemery, *J. Bone Miner. Res.* **2010**, *25*, 1441–1445.
284. M. Sughis, J. Penders, V. Haufroid, B. Nemery, T. S. Nawrot, *Environ. Health* **2011**, *10*, 104.
285. K. Ogoshi, T. Moriyama, Y. Nanzai, *Arch. Toxicol.* **1989**, *63*, 320–324.
286. M. M. Brzoska, *J. Appl. Toxicol.* **2012**, *32*, 34–44.
287. M. M. Brzoska, J. Moniuszko-Jakoniuk, *Toxicol. Appl. Pharmacol.* **2005**, *207*, 195-211.
288. K. Ogoshi, Y. Nanzai, T. Moriyama, *Arch. Toxicol.* **1992**, *66*, 315–320.
289. A. K. Wilson, M. H. Bhattacharyya, *Toxicol. Appl. Pharmacol.* **1997**, *145*, 68–73.
290. M. Ando, Y. Sayato, T. Osawa, *Toxicol. Appl. Pharmacol.* **1978**, *46*, 625–632.
291. M. H. Bhattacharyya, B. D. Whelton, D. P. Peterson, B. A. Carnes, M. S. Guram, E. S. Moretti, *Toxicology* **1988**, *50*, 205–215.
292. K. Iwami, T. Moriyama, *Arch. Toxicol.* **1993**, *67*, 352–357.
293. T. Miyahara, T. Katoh, M. Watanabe, Y. Mikami, S. Uchida, M. Hosoe, T. Sakuma, N. Nemoto, K. Takayama, T. Komurasaki, *Toxicology* **2004**, *200*, 159–167.
294. T. Miyahara, H. Tonoyama, M. Watanabe, A. Okajima, S. Miyajima, T. Sakuma, N. Nemoto, K. Takayama, *Calcif. Tissue Int.* **2001**, *68*, 185–191.
295. A. K. Wilson, E. A. Cerny, B. D. Smith, A. Wagh, M. H. Bhattacharyya, *Toxicol. Appl. Pharmacol.* **1996**, *140*, 451–460.
296. T. Miyahara, M. Takata, M. Miyata, M. Nagai, A. Sugure, H. Kozuka, S. Kuze, *Bull. Environ. Contam. Toxicol.* **1991**, *47*, 283–287.
297. M. M. Brzoska, J. Rogalska, E. Kupraszewicz, *Toxicol. Appl. Pharmacol.* **2010**, *250*, 327–335.
298. M. H. Bhattacharyya, *Toxicol. Appl. Pharmacol.* **2009**, *238*, 258–265.
299. M. Levesque, C. Martineau, C. Jumarie, R. Moreau, *Toxicol. Appl. Pharmacol.* **2008**, *231*, 308–317.
300. C. Martineau, E. Abed, G. Medina, L. A. Jomphe, M. Mantha, C. Jumarie, R. Moreau, *Toxicol. Lett.* **2010**, *199*, 357–363.
301. M. K. Monteilh-Zoller, M. C. Hermosura, M. J. Nadler, A. M. Scharenberg, R. Penner, A. Fleig, *J. Gen. Physiol.* **2003**, *121*, 49–60.
302. J. A. Staessen, T. Kuznetsova, H. A. Roels, D. Emelianov, R. Fagard, *Am. J. Hypertens.* **2000**, *13*, 146–156.
303. H. Nakagawa, M. Nishijo, *J. Cardiovasc. Risk* **1996**, *3*, 11–17.
304. I. Kurihara, E. Kobayashi, Y. Suwazono, M. Uetani, T. Inaba, M. Oishiz, T. Kido, H. Nakagawa, K. Nogawa, *Arch. Environ. Health* **2004**, *59*, 711–716.
305. R. Schutte, T. Nawrot, T. Richart, L. Thijs, H. A. Roels, L. M. Van Bortel, H. Struijker-Boudier, J. A. Staessen, *Occup. Environ. Med.* **2008**, *65*, 412–419.
306. M. J. Thun, A. M. Osorio, S. Schober, W. H. Hannon, B. Lewis, W. Halperin, *Br. J. Ind. Med.* **1989**, *46*, 689–697.
307. A. Navas-Acien, E. Selvin, A. R. Sharrett, E. Calderon-Aranda, E. Silbergeld, E. Guallar, *Circulation* **2004**, *109*, 3196–3201.
308. A. Navas-Acien, E. K. Silbergeld, R. Sharrett, E. Calderon-Aranda, E. Selvin, E. Guallar, *Environ. Health Perspect.* **2005**, *113*, 164–169.
309. S. Satarug, M. Nishijo, P. Ujjin, Y. Vanavanitkun, M. R. Moore, *Toxicol. Lett.* **2005**, *157*, 57–68.
310. B. Messner, M. Knoflach, A. Seubert, A. Ritsch, K. Pfaller, B. Henderson, Y. H. Shen, I. Zeller, J. Willeit, G. Laufer, G. Wick, S. Kiechl, D. Bernhard, *Arterioscler. Thromb. Vasc. Biol.* **2009**, *29*, 1392–1398.
311. S. Agarwal, T. Zaman, E. M. Tuzcu, S. R. Kapadia, *Angiology* **2011**, *62*, 422–429.
312. C. J. Everett, I. L. Frithsen, *Environ. Res.* **2008**, *106*, 284–286.
313. J. L. Peters, T. S. Perlstein, M. J. Perry, E. McNeely, J. Weuve, *Environ. Res.* **2010**, *110*, 199–206.

314. M. Tellez-Plaza, A. Navas-Acien, C. M. Crainiceanu, A. R. Sharrett, E. Guallar, *Am. J. Epidemiol.* **2010**, *172*, 671–681.
315. H. M. Perry, Jr., S. J. Kopp, *Sci. Total Environ.* **1983**, *26*, 223–232.
316. G. Oner, U. K. Senturk, V. N. Izgut-Uysal, *Nephron* **1996**, *72*, 257–262.
317. A. M. Ronco, M. Montenegro, P. Castillo, M. Urrutia, D. Saez, S. Hirsch, R. Zepeda, M. N. Llanos, *Toxicol. Appl. Pharmacol.* **2011**, *251*, 137–145.
318. W. C. Prozialeck, J. R. Edwards, D. W. Nebert, J. M. Woods, A. Barchowsky, W. D. Atchison, *Toxicol. Sci.* **2008**, *102*, 207–218.
319. B. Messner, D. Bernhard, *Biometals* **2010**, *23*, 811–822.
320. T. Kaji, A. Mishima, C. Yamamoto, M. Sakamoto, F. Koizumi, *Toxicology* **1992**, *71*, 267–276.
321. S. Abu-Hayyeh, M. Sian, K. G. Jones, A. Manuel, J. T. Powell, *Arterioscler. Thromb. Vasc. Biol.* **2001**, *21*, 863–867.
322. J. R. Burdo, S. L. Menzies, I. A. Simpson, L. M. Garrick, M. D. Garrick, K. G. Dolan, D. J. Haile, J. L. Beard, J. R. Connor, *J. Neurosci. Res.* **2001**, *66*, 1198–1207.
323. M. Nanami, T. Ookawara, Y. Otaki, K. Ito, R. Moriguchi, K. Miyagawa, Y. Hasuike, M. Izumi, H. Eguchi, K. Suzuki, T. Nakanishi, *Arterioscler. Thromb. Vasc. Biol.* **2005**, *25*, 2495–2501.
324. B. V. Zlokovic, C. L. Martel, E. Matsubara, J. G. McComb, G. Zheng, R. T. McCluskey, B. Frangione, J. Ghiso, *Proc. Natl. Acad. Sci. USA* **1996**, *93*, 4229–4234.
325. T. Kaji, A. Mishima, M. Machida, K. Yabusaki, M. Suzuki, C. Yamamoto, Y. Fujiwara, M. Sakamoto, H. Kozuka, *Bull. Environ. Contam. Toxicol.* **1995**, *54*, 501–506.
326. Y. S. Jung, E. M. Jeong, E. K. Park, Y. M. Kim, S. Sohn, S. H. Lee, E. J. Baik, C. H. Moon, *Eur. J. Pharmacol.* **2008**, *578*, 11–18.
327. H. Martynowicz, A. Skoczynska, A. Wojakowska, B. Turczyn, *Int. J. Occup. Med. Environ. Health* **2004**, *17*, 479–485.
328. K. Sompamit, U. Kukongviriyapan, W. Donpunha, S. Nakmareong, V. Kukongviriyapan, *Toxicol. Lett.* **2010**, *198*, 77–82.
329. M. B. Wolf, J. W. Baynes, *Biometals* **2007**, *20*, 73–81.
330. F. Liu, K. Y. Jan, *Free Radic. Biol. Med.* **2000**, *28*, 55–63.
331. Y. Fujiwara, S. Watanabe, T. Kaji, *Toxicol. Lett.* **1998**, *94*, 175–180.
332. C. Yamamoto, T. Kaji, M. Sakamoto, H. Kozuka, *Toxicology* **1996**, *106*, 179–185.
333. A. Skoczynska, H. Martynowicz, *Hum. Exp. Toxicol.* **2005**, *24*, 353–361.
334. S. Majumder, A. Muley, G. K. Kolluru, S. Saurabh, K. P. Tamilarasan, S. Chandrasekhar, H. B. Reddy, S. Purohit, S. Chatterjee, *Biochem. Cell Biol.* **2008**, *86*, 1–10.
335. N. Yoopan, P. Watcharasit, O. Wongsawatkul, P. Piyachaturawat, J. Satayavivad, *Toxicol. Lett.* **2008**, *176*, 157–161.
336. A. Szuster-Ciesielska, I. Lokaj, M. Kandefer-Szerszen, *Toxicology* **2000**, *145*, 135–145.
337. M. Hernandez, M. Macia, *Arch. Environ. Contam. Toxicol.* **1996**, *30*, 437–443.
338. S. L. Park, Y. M. Kim, J. H. Ahn, S. H. Lee, E. J. Baik, C. H. Moon, Y. S. Jung, *J. Pharmacol. Sci.* **2009**, *110*, 405–409.
339. M. Knoflach, B. Messner, Y. H. Shen, S. Frotschnig, G. Liu, K. Pfaller, X. Wang, B. Matosevic, J. Willeit, S. Kiechl, G. Laufer, D. Bernhard, *Circ. J.* **2011**, *75*, 2491–2495.
340. G. M. Kisling, S. J. Kopp, D. J. Paulson, J. P. Tow, *Toxicol. Appl. Pharmacol.* **1993**, *118*, 58–64.
341. J. Kolakowski, B. Baranski, B. Opalska, *Toxicol. Lett.* **1983**, *19*, 273–278.
342. I. M. Ozturk, B. Buyukakilli, E. Balli, B. Cimen, S. Gunes, S. Erdogan, *Toxicol. Mech. Methods* **2009**, *19*, 308–317.
343. R. V. Zikic, A. S. Stajn, B. I. Ognjanovic, Z. S. Saicic, M. M. Kostic, S. Z. Pavlovic, V. M. Petrovic, *J. Environ. Pathol. Toxicol. Oncol.* **1998**, *17*, 259–264.
344. Y. Wang, J. Fang, S. S. Leonard, K. M. Rao, *Free Radic. Biol. Med.* **2004**, *36*, 1434–1443.
345. O. Teleman, T. Drakenberg, S. Forsen, E. Thulin, *Eur. J. Biochem.* **1983**, *134*, 453–457.
346. S. V. Lepeshkevich, B. M. Dzhagarov, *Biochim. Biophys. Acta* **2009**, *1794*, 103–109.

347. Y. Ke, Y. Y. Chen, Y. Z. Chang, X. L. Duan, K. P. Ho, D. H. Jiang, K. Wang, Z. M. Qian, *J. Cell Physiol.* **2003**, *196*, 124–130.
348. A. Van Dijk, R. A. Vermond, P. A. Krijnen, L. J. Juffermans, N. E. Hahn, S. P. Makker, L. A. Aarden, E. Hack, M. Spreeuwenberg, B. C. van Rossum, C. Meischl, W. J. Paulus, F. J. Van Milligen, H. W. Niessen, *Eur. J. Clin. Invest.* **2010**, *40*, 893–902.
349. L. R. Devireddy, C. Gazin, X. Zhu, M. R. Green, *Cell* **2005**, *123*, 1293–1305.
350. D. DiFrancesco, A. Ferroni, S. Visentin, A. Zaza, *Proc. Royal Soc. Lond. B Biol. Sci.* **1985**, *223*, 475–484.
351. C. H. Follmer, N. J. Lodge, C. A. Cullinan, T. J. Colatsky, *Am. J. Physiol.* **1992**, *262*, C75–83.
352. R. C. Prentice, P. L. Hawley, T. Glonek, S. J. Kopp, *Toxicol. Appl. Pharmacol.* **1984**, *75*, 198–210.
353. R. S. Vorob'eva, *Neuropatol. Psikkiatr.* **1957**, *57*, 385–388.
354. K. Tsuchiya, *Arch. Environ. Health* **1967**, *14*, 876–880.
355. A. Minami, A. Takeda, D. Nishibaba, S. Takefuta, N. Oku, *Brain Res.* **2001**, *894*, 336–339.
356. M. E. Figueiredo-Pereira, S. Yakushin, G. Cohen, *J. Biol. Chem.* **1998**, *273*, 12703–12709.
357. J. Y. Im, S. G. Paik, P. L. Han, *J. Neurosci. Res.* **2006**, *83*, 301–308.
358. S. Hossain, H. N. Liu, M. Nguyen, G. Shore, G. Almazan, *Neurotoxicology* **2009**, *30*, 544–554.
359. E. Lopez, S. Figueroa, M. J. Oset-Gasque, M. P. Gonzalez, *Br. J. Pharmacol.* **2003**, *138*, 901–911.
360. H. Andersson, K. Petersson-Grawe, E. Lindqvist, J. Luthman, A. Oskarsson, L. Olson, *Neurotoxicol. Teratol.* **1997**, *19*, 105–115.
361. M. Ebadi, P. L. Iversen, R. Hao, D. R. Cerutis, P. Rojas, H. K. Happe, L. C. Murrin, R. F. Pfeiffer, *Neurochem. Int.* **1995**, *27*, 1–22.
362. K. L. Wong, R. Cachia, C. D. Klaassen, *Toxicol. Appl. Pharmacol.* **1980**, *56*, 317–325.
363. S. Choudhuri, W. L. Liu, N. E. Berman, C. D. Klaassen, *Toxicol. Lett.* **1996**, *84*, 127–133.
364. J. P. Provias, C. A. Ackerley, C. Smith, L. E. Becker, *Acta Neuropathol.* **1994**, *88*, 583–586.
365. W. Zheng, *Microsc Res Tech* **2001**, *52*, 89–103.
366. N. Nishimura, H. Nishimura, A. Ghaffar, C. Tohyama, *J. Histochem. Cytochem.* **1992**, *40*, 309–315.
367. H. U. Ozcaglar, B. Agirdir, O. Dinc, M. Turhan, S. Kilincarslan, G. Oner, *Acta Otolaryngol.* **2001**, *121*, 393–397.
368. M. P. Nava-Hernandez, L. A. Hauad-Marroquin, S. Bassol-Mayagoitia, G. Garcia-Arenas, R. Mercado-Hernandez, M. A. Echavarri-Guzman, R. M. Cerda-Flores, *DNA Cell Biol.* **2009**, *28*, 241–248.
369. A. Blanco, R. Moyano, A. M. Molina Lopez, C. Blanco, R. Flores-Acuna, J. R. Garcia-Flores, M. Espada, J. G. Monterde, *Toxicol. Ind. Health* **2010**, *26*, 451–457.
370. H. Zenick, L. Hastings, M. Goldsmith, R. J. Niewenhuis, *J. Toxicol. Environ. Health* **1982**, *9*, 377–387.
371. X. Yu, S. Hong, E. M. Faustman, *Toxicol. Sci.* **2008**, *104*, 385–396.
372. T. Kusakabe, K. Nakajima, K. Nakazato, K. Suzuki, H. Takada, T. Satoh, M. Oikawa, K. Arakawa, T. Nagamine, *Toxicol. In Vitro* **2008**, *22*, 1469–1475.
373. J. Thompson, J. Bannigan, *Reprod. Toxicol.* **2008**, *25*, 304–315.
374. P. Pillai, C. Pandya, S. Gupta, *J. Biochem. Mol. Toxicol.* **2010**, *24*, 384–394.
375. W. Zhang, F. Pang, Y. Huang, P. Yan, W. Lin, *Toxicol. Lett.* **2008**, *182*, 18–23.
376. M. C. Henson, P. J. Chedrese, *Exp. Biol. Med. (Maywood)* **2004**, *229*, 383–392.
377. J. P. Gennart, J. P. Buchet, H. Roels, P. Ghyselen, E. Ceulemans, R. Lauwerys, *Am. J. Epidemiol.* **1992**, *135*, 1208–1219.
378. S. Benoff, R. Hauser, J. L. Marmar, I. R. Hurley, B. Napolitano, G. M. Centola, *Mol. Med.* **2009**, *15*, 248–262.
379. G. Angenard, V. Muczynski, H. Coffigny, C. Pairault, C. Duquenne, R. Frydman, R. Habert, V. Rouiller-Fabre, G. Livera, *Environ. Health Perspect.* **2010**, *118*, 331–337.
380. E. W. Wong, C. Y. Cheng, *Trends Pharmacol. Sci.* **2011**, *32*, 290–299.

381. C. Y. Cheng, D. D. Mruk, *Pharmacol. Rev.* **2011**, *64*, 16–64.
382. A. Caride, B. Fernandez-Perez, T. Cabaleiro, G. Bernardez, A. Lafuente, *J. Appl. Toxicol.* **2010**, *30*, 84–90.
383. A. Lafuente, A. I. Esquifino, *Toxicol. Lett.* **1999**, *110*, 209–218.
384. R. B. Rastogi, R. L. Singhal, *Endocr. Res. Commun.* **1975**, *2*, 87–94.
385. Z. Anca, S. Gabor, V. V. Papilian, *Endocrinologie* **1982**, *20*, 95–100.
386. R. Der, M. Yousef, Z. Fahim, M. Fahim, *Res. Commun. Chem. Pathol. Pharmacol.* **1977**, *17*, 237–253.
387. G. A. Jackl, W. E. Kollmer, *Sci. Total Environ.* **1982**, *25*, 53–59.
388. S. A. Mathias, O. P. Mgbonyebi, E. Motley, J. R. Owens, J. J. Mrotek, *Cell Biol. Toxicol.* **1998**, *14*, 225–236.
389. O. P. Mgbonyebi, C. T. Smothers, J. J. Mrotek, *Cell Biol. Toxicol.* **1993**, *9*, 223–234.
390. B. Pilat-Marcinkiewicz, B. Sawicki, M. M. Brzoska, J. Moniuszko-Jakoniuk, *Folia Histochem. Cytobiol.* **2002**, *40*, 189–190.
391. M. Yoshizuka, N. Mori, K. Hamasaki, I. Tanaka, M. Yokoyama, K. Hara, Y. Doi, Y. Umezu, H. Araki, Y. Sakamoto, M. Miyazaki, S. Fujimoto, *Exp. Mol. Pathol.* **1991**, *55*, 97–104.
392. J. R. Edwards, W. C. Prozialeck, *Toxicol. Appl. Pharmacol.* **2009**, *238*, 289–293.
393. Y. W. Chen, C. Y. Yang, C. F. Huang, D. Z. Hung, Y. M. Leung, S. H. Liu, *Islets* **2009**, *1*, 169–176.
394. G. G. Schwartz, D. Il'yasova, A. Ivanova, *Diabetes Care* **2003**, *26*, 468–470.
395. H. I. Afridi, T. G. Kazi, N. Kazi, M. K. Jamali, M. B. Arain, N. Jalbani, J. A. Baig, R. A. Sarfraz, *Diabetes Res. Clin. Pract.* **2008**, *80*, 280–288.
396. H. Hiratsuka, O. Katsuta, N. Toyota, M. Tsuchitani, T. Umemura, F. Marumo, *Toxicol. Appl. Pharmacol.* **1996**, *137*, 228–236.
397. H. Horiguchi, E. Oguma, F. Kayama, *Arch. Toxicol.* **2006**, *80*, 680–686.
398. H. Horiguchi, E. Oguma, F. Kayama, *Toxicol. Sci.* **2011**, *122*, 198–210.
399. H. Horiguchi, M. Sato, N. Konno, M. Fukushima, *Arch. Toxicol.* **1996**, *71*, 11–19.
400. H. Horiguchi, F. Kayama, E. Oguma, W. G. Willmore, P. Hradecky, H. F. Bunn, *Blood* **2000**, *96*, 3743–3747.
401. H. Horiguchi, K. Aoshima, E. Oguma, S. Sasaki, K. Miyamoto, Y. Hosoi, T. Katoh, F. Kayama, *Int. Arch. Occup. Environ. Health* **2010**, *83*, 953–970.
402. H. Horiguchi, H. Teranishi, K. Niiya, K. Aoshima, T. Katoh, N. Sakuragawa, M. Kasuya, *Arch. Toxicol.* **1994**, *68*, 632–636.
403. S. Muller, K. E. Gillert, C. Krause, G. Jautzke, U. Gross, T. Diamantstein, *Experientia* **1979**, *35*, 909–910.
404. R. F. Borgman, B. Au, R. K. Chandra, *Int. J. Immunopharmacol.* **1986**, *8*, 813–817.
405. W. R. Williams, S. Kagamimori, M. Watanabe, T. Shinmura, N. Hagino, *Clin. Exp. Immunol.* **1983**, *53*, 651–658.
406. R. K. Chopra, K. K. Kohli, R. Nath, *Toxicol. Lett.* **1984**, *23*, 99–107.
407. H. Horiguchi, N. Mukaida, S. Okamoto, H. Teranishi, M. Kasuya, K. Matsushima, *Lymphokine Cytokine Res.* **1993**, *12*, 421–428.
408. S. V. Kumar, S. Bhattacharya, *In Vitro Mol. Toxicol.* **2000**, *13*, 137–144.
409. M. Kocak, E. Akcil, *Pathophysiol. Haemost. Thromb.* **2006**, *35*, 411–416.
410. G. F. Nordberg, *Biometals* **2004**, *17*, 485–489.
411. B. A. Fowler, *Toxicol. Appl. Pharmacol.* **2009**, *238*, 294–300.
412. A. Chargui, S. Zekri, G. Jacquillet, I. Rubera, M. Ilie, A. Belaid, C. Duranton, M. Tauc, P. Hofman, P. Poujeol, M. V. El May, B. Mograbi, *Toxicol. Sci.* **2011**, *121*, 31–42.
413. P. W. Mueller, R. G. Price, W. F. Finn, *Environ. Health Perspect.* **1998**, *106*, 227–230.
414. C. W. Noonan, S. M. Sarasua, D. Campagna, S. J. Kathman, J. A. Lybarger, P. W. Mueller, *Environ. Health Perspect.* **2002**, *110*, 151–155.
415. T. Uno, E. Kobayashi, Y. Suwazono, Y. Okubo, K. Miura, K. Sakata, A. Okayama, H. Ueshima, H. Nakagawa, K. Nogawa, *Scand. J. Work Environ. Health* **2005**, *31*, 307–315.
416. Z. A. Shaikh, C. Tohyama, *Environ. Health Perspect.* **1984**, *54*, 171–174.

417. Z. A. Shaikh, K. J. Ellis, K. S. Subramanian, A. Greenberg, *Toxicology* **1990**, *63*, 53–62.
418. L. Chen, T. Jin, B. Huang, G. Nordberg, M. Nordberg, *Toxicol. Appl. Pharmacol.* **2006**, *215*, 93–99.
419. E. I. Christensen, J. Gburek, *Pediatr. Nephrol.* **2004**, *19*, 714–721.
420. A. Bernard, R. Lauwerys, *Toxicol. Lett.* **1995**, *77*, 145–151.
421. J. Huang, *Biometals* **2004**, *17*, 511.
422. T. Jin, G. Nordberg, X. Wu, T. Ye, Q. Kong, Z. Wang, F. Zhuang, S. Cai, *Environ. Res.* **1999**, *81*, 167–173.
423. G. Garcon, B. Leleu, T. Marez, F. Zerimech, J. M. Haguenoer, D. Furon, P. Shirali, *Sci. Total Environ.* **2007**, *377*, 165–172.
424. W. C. Prozialeck, J. R. Edwards, V. S. Vaidya, J. V. Bonventre, *Toxicol. Appl. Pharmacol.* **2009**, *238*, 301–305.
425. A. Sundberg, E. L. Appelkvist, G. Dallner, R. Nilsson, *Environ. Health Perspect.* **1994**, *102 Suppl 3*, 293–296.
426. V. S. Vaidya, M. A. Ferguson, J. V. Bonventre, *Annu. Rev. Pharmacol. Toxicol.* **2008**, *48*, 463–493.
427. V. Bailly, Z. Zhang, W. Meier, R. Cate, M. Sanicola, J. V. Bonventre, *J. Biol. Chem.* **2002**, *277*, 39739–39748.
428. V. S. Vaidya, G. M. Ford, S. S. Waikar, Y. Wang, M. B. Clement, V. Ramirez, W. E. Glaab, S. P. Troth, F. D. Sistare, W. C. Prozialeck, J. R. Edwards, N. A. Bobadilla, S. C. Mefferd, J. V. Bonventre, *Kidney Int.* **2009**, *76*, 108–114.
429. W. C. Prozialeck, V. S. Vaidya, J. Liu, M. P. Waalkes, J. R. Edwards, P. C. Lamar, A. M. Bernard, X. Dumont, J. V. Bonventre, *Kidney Int.* **2007**, *72*, 985–993.
430. V. Pennemans, J. M. Rigo, J. Penders, Q. Swennen, *Clin. Chem. Lab. Med.* **2012**, *50*, 539–543.
431. N. Borregaard, J. B. Cowland, *Biometals* **2006**, *19*, 211–215.
432. K. M. Schmidt-Ott, K. Mori, J. Y. Li, A. Kalandadze, D. J. Cohen, P. Devarajan, J. Barasch, *J. Am. Soc. Nephrol* .**2007**, *18*, 407–413.
433. P. Devarajan, *Nephrology (Carlton)* **2010**, *15*, 419–428.
434. D. Bolignano, A. Lacquaniti, G. Coppolino, V. Donato, S. Campo, M. R. Fazio, G. Nicocia, M. Buemi, *Clin. J. Am. Soc. Nephrol.* **2009**, *4*, 337–344.
435. N. Paragas, A. Qiu, Q. Zhang, B. Samstein, S. X. Deng, K. M. Schmidt-Ott, M. Viltard, W. Yu, C. S. Forster, G. Gong, Y. Liu, R. Kulkarni, K. Mori, A. Kalandadze, A. J. Ratner, P. Devarajan, D. W. Landry, V. D'Agati, C. S. Lin, J. Barasch, *Nat. Med.* **2011**, *17*, 216–222.
436. R. Lauwerys, A. Bernard, J. P. Buchet, H. Roels, P. Bruaux, F. Claeys, G. Ducoffre, P. De Plaen, J. Staessen, A. Amery, R. Fagard, P. Lijnen, L. Thijs, D. Rondia, F. Sartor, A. Saint-Remy, L. Nick, *Acta Clin. Belg.* **1991**, *46*, 219-225.
437. L. Friberg, C. G. Elinder, in *Encyclopedia of Occupational Health and Safety*, Ed L. Parmeggiani, International Labour Organization Publications, Geneva, 1983, pp. 356–357.
438. R. H. Dreisbach, Lange Medical Publications, Los Altos, California, 1983, pp. 247–250.
439. F. Z. Sheabar, S. Yannai, U. Taitelman, *Pharmacol. Toxicol.* **1989**, *65*, 13–16.
440. C. D. Klaassen, M. P. Waalkes, L. R. Cantilena, Jr., *Environ. Health Perspect.* **1984**, *54*, 233–242.
441. M. A. Basinger, M. M. Jones, M. A. Holscher, W. K. Vaughn, *J. Toxicol. Environ. Health* **1988**, *23*, 77–89.
442. O. Andersen, J. B. Nielsen, *Pharmacol. Toxicol.* **1988**, *63*, 386–389.
443. O. Andersen, *Crit. Rev. Toxicol.* **1989**, *20*, 83–112.
444. M. M. Jones, M. G. Cherian, *Toxicology* **1990**, *62*, 1–25.
445. M. G. Cherian, *Nature* **1980**, *287*, 871–872.
446. H. W. Gil, E. J. Kang, K. H. Lee, J. O. Yang, E. Y. Lee, S. Y. Hong, *Hum. Exp. Toxicol.* **2011**, *30*, 79–83.
447. T. W. Clarkson, *Annu. Rev. Pharmacol. Toxicol.* **1993**, *33*, 545–571.
448. C. C. Bridges, R. K. Zalups, *Toxicol. Appl. Pharmacol.* **2005**, *204*, 274–308.

449. L. He, K. Girijashanker, T. P. Dalton, J. Reed, H. Li, M. Soleimani, D. W. Nebert, *Mol. Pharmacol.* **2006**, *70*, 171–180.
450. Z. Liu, H. Li, M. Soleimani, K. Girijashanker, J. M. Reed, L. He, T. P. Dalton, D. W. Nebert, *Biochem. Biophys. Res. Commun.* **2008**, *365*, 814–820.
451. D. J. Eide, *Pflugers Arch.* **2004**, *447*, 796–800.
452. L. He, B. Wang, E. B. Hay, D. W. Nebert, *Toxicol. Appl. Pharmacol.* **2009**, *238*, 250–257.
453. D. I. Bannon, R. Abounader, P. S. Lees, J. P. Bressler, *Am. J. Physiol. Cell Physiol.* **2003**, *284*, C44–C50.
454. M. D. Garrick, S. T. Singleton, F. Vargas, H. C. Kuo, L. Zhao, M. Knopfel, T. Davidson, M. Costa, P. Paradkar, J. A. Roth, L. M. Garrick, *Biol. Res.* **2006**, *39*, 79–85.
455. M. Okubo, K. Yamada, M. Hosoyamada, T. Shibasaki, H. Endou, *Toxicol. Appl. Pharmacol.* **2003**, *187*, 162–167.
456. D. De Stefani, A. Raffaello, E. Teardo, I. Szabo, R. Rizzuto, *Nature* **2011**, *476*, 336–340.
457. Y. Kirichok, G. Krapivinsky, D. E. Clapham, *Nature* **2004**, *427*, 360–364.
458. W. K. Lee, U. Bork, F. Gholamrezaei, F. Thévenod, *Am. J. Physiol. Renal Physiol.* **2005**, *288*, F27–F39.
459. S. Y. Ryu, G. Beutner, R. T. Dirksen, K. W. Kinnally, S. S. Sheu, *FEBS Lett.* **2010**, *584*, 1948–1955.
460. F. Thévenod, *Toxicol. Appl. Pharmacol.* **2009**, *238*, 221–239.
461. J. M. Moulis, *Biometals* **2010**, *23*, 877–896.
462. E. Hassler, B. Lind, M. Piscator, *Br. J. Ind. Med.* **1983**, *40*, 420–425.
463. O. Barbier, G. Jacquillet, M. Tauc, P. Poujeol, M. Cougnon, *Am. J. Physiol. Renal Physiol.* **2004**, *287*, F1067–1075.
464. P. M. Verbost, M. H. Senden, C. H. van Os, *Biochim. Biophys. Acta* **1987**, *902*, 247–252.
465. I. Sabolic, M. Ljubojevic, C. M. Herak-Kramberger, D. Brown, *Am. J. Physiol. Renal Physiol.* **2002**, *283*, F1389–1402.
466. G. J. Long, *Toxicol. Appl. Pharmacol.* **1997**, *143*, 189–195.
467. S. H. Jeon, M. H. Cho, J. H. Cho, *Hum. Exp. Toxicol.* **2001**, *20*, 577–583.
468. J. B. Smith, S. D. Dwyer, L. Smith, *J. Biol. Chem.* **1989**, *264*, 7115–7118.
469. K. Yamagami, S. Nishimura, M. Sorimachi, *Brain Res.* **1998**, *798*, 316–319.
470. G. Abou-Mohamed, A. Papapetropoulos, J. D. Catravas, R. W. Caldwell, *Eur. J. Pharmacol.* **1998**, *341*, 265–272.
471. A. Persechini, K. McMillan, B. S. Masters, *Biochemistry* **1995**, *34*, 15091–15095.
472. P. O'Brien, H. J. Salacinski, *Arch. Toxicol.* **1998**, *72*, 690–700.
473. D. Beyersmann, S. Hechtenberg, *Toxicol. Appl. Pharmacol.* **1997**, *144*, 247–261.
474. B. Halliwell, J. M. C. Gutteridge, *Free Radicals in Biology and Medicine*, Oxford University Press Inc., Oxford, New York, 2007.
475. M. Margoshes, B. L. Vallee, *J. Am. Chem. Soc.* **1957**, *79*, 4813–4814.
476. E. Carvalho, P. O. Gothe, R. Bauer, E. Danielsen, L. Hemmingsen, *Eur. J. Biochem.* **1995**, *234*, 780–785.
477. T. W. Lane, F. M. Morel, *Proc. Natl. Acad. Sci. USA* **2000**, *97*, 4627–4631.
478. C. Meplan, K. Mann, P. Hainaut, *J. Biol. Chem.* **1999**, *274*, 31663–31670.
479. M. Matsuoka, H. Igisu, *Biochem. Biophys. Res. Commun.* **2001**, *282*, 1120–1125.
480. B. Medicherla, A. L. Goldberg, *J. Cell Biol.* **2008**, *182*, 663–673.
481. S. Chen, Y. Xu, B. Xu, M. Guo, Z. Zhang, L. Liu, H. Ma, Z. Chen, Y. Luo, S. Huang, L. Chen, *J. Neurochem.* **2011**, *119*, 1108–1118.
482. T. Doi, P. Puri, J. Bannigan, J. Thompson, *Pediatr. Surg. Int.* **2010**, *26*, 91–95.
483. S. L. Shirran, P. E. Barran, *J. Am. Soc. Mass Spectrom.* **2009**, *20*, 1159–1171.
484. S. Majumder, R. Gupta, H. Reddy, S. Sinha, A. Muley, G. K. Kolluru, S. Chatterjee, *Biochem. Cell Biol.* **2009**, *87*, 605–620.
485. S. Soyupek, T. Oksay, R. Sutcu, A. Armagan, O. Gokalp, H. Perk, N. Delibas, *Toxicol. Ind. Health* **2012**, *28*, 624–628.
486. N. Haugaard, *Physiol. Rev.* **1968**, *48*, 311–373.

487. M. Kitamura, N. Hiramatsu, *Biometals* **2010**, *23*, 941–950.
488. G. Gobe, D. Crane, *Toxicol. Lett.* **2010**, *198*, 49–55.
489. A. Cuypers, M. Plusquin, T. Remans, M. Jozefczak, E. Keunen, H. Gielen, K. Opdenakker, A. R. Nair, E. Munters, T. J. Artois, T. Nawrot, J. Vangronsveld, K. Smeets, *Biometals* **2010**, *23*, 927–940.
490. M. Kippler, M. B. Hossain, C. Lindh, S. E. Moore, I. Kabir, M. Vahter, K. Broberg, *Environ. Res.* **2012**, *112*, 164–170.
491. S. L'Hoste, A. Chargui, R. Belfodil, C. Duranton, I. Rubera, B. Mograbi, C. Poujeol, M. Tauc, P. Poujeol, *Free Radic. Biol. Med.* **2009**, *46*, 1017–1031.
492. V. Souza, C. Escobar Mdel, L. Bucio, E. Hernandez, L. E. Gomez–Quiroz, M. C. Gutierrez Ruiz, *Toxicol. Lett.* **2009**, *187*, 180–186.
493. D. Ron, P. Walter, *Nat. Rev. Mol. Cell Biol.* **2007**, *8*, 519–529.
494. I. Tabas, D. Ron, *Nat. Cell Biol.* **2011**, *13*, 184–190.
495. M. Moenner, O. Pluquet, M. Bouchecareilh, E. Chevet, *Cancer Res.* **2007**, *67*, 10631–10634.
496. N. Hiramatsu, A. Kasai, S. Du, M. Takeda, K. Hayakawa, M. Okamura, J. Yao, M. Kitamura, *FEBS Lett.* **2007**, *581*, 2055–2059.
497. M. G. Permenter, J. A. Lewis, D. A. Jackson, *PLoS One* **2011**, *6*, e27730.
498. M. Yokouchi, N. Hiramatsu, K. Hayakawa, A. Kasai, Y. Takano, J. Yao, M. Kitamura, *Cell Death Differ.* **2007**, *14*, 1467–1474.
499. M. Biagioli, S. Pifferi, M. Ragghianti, S. Bucci, R. Rizzuto, P. Pinton, *Cell Calcium* **2008**, *43*, 184–195.
500. M. Yokouchi, N. Hiramatsu, K. Hayakawa, M. Okamura, S. Du, A. Kasai, Y. Takano, A. Shitamura, T. Shimada, J. Yao, M. Kitamura, *J. Biol. Chem.* **2008**, *283*, 4252–4260.
501. W. K. Lee, P. K. Chakraborty, E. Roussa, N. A. Wolff, F. Thévenod, *Biochim. Biophys. Acta* **2012**, *1823*, 1864–1876.
502. Y. L. Ji, H. Wang, X. F. Zhao, Q. Wang, C. Zhang, Y. Zhang, M. Zhao, Y. H. Chen, X. H. Meng, D. X. Xu, *Toxicol. Sci.* **2011**, *124*, 446–459.
503. Y. MacKinnon, C. M. Kapron, *Birth Defects Res. A Clin. Mol. Teratol.* **2010**, *88*, 707–714.
504. J. Liu, A. Lin, *Cell Res.* **2005**, *15*, 36–42.
505. Y. Iryo, M. Matsuoka, B. Wispriyono, T. Sugiura, H. Igisu, *Biochem. Pharmacol.* **2000**, *60*, 1875–1882.
506. P. Martin, M. C. Poggi, J. C. Chambard, K. E. Boulukos, P. Pognonec, *Biochem. Biophys. Res. Commun.* **2006**, *350*, 803–807.
507. G. Jiang, W. Duan, L. Xu, S. Song, C. Zhu, L. Wu, *Toxicol. In Vitro* **2009**, *23*, 973–978.
508. N. D. Perkins, *Nat. Rev. Cancer* **2012**, *12*, 121–132.
509. B. A. Hart, C. H. Lee, G. S. Shukla, A. Shukla, M. Osier, J. D. Eneman, J. F. Chiu, *Toxicology* **1999**, *133*, 43–58.
510. J. Xie, Z. A. Shaikh, *Toxicology* **2006**, *224*, 56–65.
511. P. M. Yang, H. C. Chen, J. S. Tsai, L. Y. Lin, *Chem. Res. Toxicol.* **2007**, *20*, 406–415.
512. T. S. Hsu, P. M. Yang, J. S. Tsai, L. Y. Lin, *Toxicol. Appl. Pharmacol.* **2009**, *235*, 153–162.
513. A. L. Edinger, C. B. Thompson, *Curr. Opin. Cell Biol.* **2004**, *16*, 663–669.
514. D. Denton, S. Nicolson, S. Kumar, *Cell Death Differ.* **2012**, *19*, 87–95.
515. D. R. Green, *Cell* **2005**, *121*, 671–674.
516. X. M. Yin, *Cell Res.* **2000**, *10*, 161–167.
517. S. S. Habeebu, J. Liu, C. D. Klaassen, *Toxicol. Appl. Pharmacol.* **1998**, *149*, 203–209.
518. M. Ishido, S. Homma-Takeda, C. Tohyama, T. Suzuki, *J. Toxicol. Environ. Health A* **1998**, *55*, 1–12.
519. T. Eichler, Q. Ma, C. Kelly, J. Mishra, S. Parikh, R. F. Ransom, P. Devarajan, W. E. Smoyer, *Toxicol. Sci.* **2006**, *90*, 392–399.
520. J. P. Vit, C. Guillouf, F. Rosselli, *Exp. Cell Res.* **2001**, *269*, 2–12.
521. T. Tenev, K. Bianchi, M. Darding, M. Broemer, C. Langlais, F. Wallberg, A. Zachariou, J. Lopez, M. MacFarlane, K. Cain, P. Meier, *Mol. Cell* **2011**, *43*, 432–448.
522. W. K. Lee, M. Abouhamed, F. Thévenod, *Am. J. Physiol. Renal Physiol.* **2006**, *291*, F823–832.

523. M. Li, T. Kondo, Q. L. Zhao, F. J. Li, K. Tanabe, Y. Arai, Z. C. Zhou, M. Kasuya, *J. Biol. Chem.* **2000**, *275*, 39702–39709.
524. W. P. Mao, J. L. Ye, Z. B. Guan, J. M. Zhao, C. Zhang, N. N. Zhang, P. Jiang, T. Tian, *Toxicol. In Vitro* **2007**, *21*, 343–354.
525. W. K. Lee, M. Spielmann, U. Bork, F. Thévenod, *Am. J. Physiol. Cell Physiol.* **2005**, *289*, C656–664.
526. A. Lemarie, D. Lagadic-Gossmann, C. Morzadec, N. Allain, O. Fardel, L. Vernhet, *Free Radic. Biol. Med.* **2004**, *36*, 1517–1531.
527. M. Crompton, *Biochem. J.* **1999**, *341*, 233–249.
528. S. H. Oh, B. H. Lee, S. C. Lim, *Biochem. Pharmacol.* **2004**, *68*, 1845–1855.
529. M. Li, T. Xia, C. S. Jiang, L. J. Li, J. L. Fu, Z. C. Zhou, *Toxicology* **2003**, *194*, 19–33.
530. E. A. Belyaeva, V. V. Glazunov, S. M. Korotkov, *Arch. Biochem. Biophys.* **2002**, *405*, 252–264.
531. W. K. Lee, U. Bork, F. Thévenod, *Toxicol. Mech. Methods* **2004**, *14*, 67–71.
532. C. Zazueta, C. Sanchez, N. Garcia, F. Correa, *Int. J. Biochem. Cell Biol.* **2000**, *32*, 1093–1101.
533. W. K. Lee, F. Thévenod, *Am. J. Physiol. Cell Physiol.* **2006**, *291*, C195–202.
534. A. Schinzel, T. Kaufmann, C. Borner, *Biochim. Biophys. Acta* **2004**, *1644*, 95–105.
535. J. M. Jurgensmeier, Z. Xie, Q. Deveraux, L. Ellerby, D. Bredesen, J. C. Reed, *Proc. Natl. Acad. Sci. USA* **1998**, *95*, 4997–5002.
536. S. Shimizu, M. Narita, Y. Tsujimoto, *Nature* **1999**, *399*, 483–487.
537. Y. Li, S. C. Lim, *Environ. Toxicol. Pharmacol.* **2007**, *24*, 231–238.
538. E. S. Papadakis, K. G. Finegan, X. Wang, A. C. Robinson, C. Guo, M. Kayahara, C. Tournier, *FEBS Lett.* **2006**, *580*, 1320–1326.
539. M. Ishido, R. Ohtsubo, T. Adachi, M. Kunimoto, *Environ. Health Perspect.* **2002**, *110*, 37–42.
540. R. N. Kolesnick, M. Kronke, *Annu. Rev. Physiol.* **1998**, *60*, 643–665.
541. L. J. Siskind, R. N. Kolesnick, M. Colombini, *J. Biol. Chem.* **2002**, *277*, 26796–26803.
542. W. K. Lee, B. Torchalski, F. Thévenod, *Am. J. Physiol. Cell Physiol.* **2007**, *293*, C839–847.
543. S. J. Storr, N. O. Carragher, M. C. Frame, T. Parr, S. G. Martin, *Nat. Rev. Cancer* **2011**, *11*, 364–374.
544. I. Johnson, M. T. Z. Spence, *The Molecular Probes Handbook, A Guide to Fluorescent Probes and Labeling Technologies*, Life Technologies Corporation, Paisley, UK, 2010, pp. 1076.
545. K. T. Izutsu, S. P. Felton, I. A. Siegel, W. T. Yoda, A. C. Chen, *Biochem. Biophys. Res. Commun* **1972**, *49*, 1034–1039.
546. M. Biagioli, P. Pinton, R. Scudiero, M. Ragghianti, S. Bucci, R. Rizzuto, *Toxicology* **2005**, *208*, 389–398.
547. B. E. Tvermoes, G. S. Bird, J. H. Freedman, *PLoS One* **2011**, *6*, e20542.
548. P. Golstein, G. Kroemer, *Trends Biochem. Sci.* **2007**, *32*, 37–43.
549. P. Nicotera, G. Melino, *Oncogene* **2004**, *23*, 2757–2765.
550. P. Nicotera, M. Leist, E. Ferrando-May, *Toxicol. Lett.* **1998**, *102–103*, 139–142.
551. T. Hirsch, P. Marchetti, S. A. Susin, B. Dallaporta, N. Zamzami, I. Marzo, M. Geuskens, G. Kroemer, *Oncogene* **1997**, *15*, 1573–1581.
552. P. Sancho, C. Fernandez, V. J. Yuste, D. Amran, A. M. Ramos, E. de Blas, S. A. Susin, P. Aller, *Apoptosis* **2006**, *11*, 673–686.
553. E. Niemczyk, A. Majczak, A. Hallmann, J. Kedzior, M. Wozniak, T. Wakabayashi, *Acta Biochim. Pol.* **2004**, *51*, 1015–1022.
554. S. Somji, S. H. Garrett, M. A. Sens, V. Gurel, D. A. Sens, *Toxicol. Sci.* **2004**, *80*, 358–366.
555. H. McNeill, J. R. Woodgett, *Nat. Rev. Mol. Cell Biol.* **2010**, *11*, 404–413.
556. J. M. Bailey, P. K. Singh, M. A. Hollingsworth, *J. Cell Biochem.* **2007**, *102*, 829–839.
557. R. van Amerongen, R. Nusse, *Development* **2009**, *136*, 3205–3214.
558. J. Thompson, L. Wong, P. S. Lau, J. Bannigan, *Reprod. Toxicol.* **2008**, *25*, 39–46.
559. M. L. Hanson, K. M. Brundage, R. Schafer, J. C. Tou, J. B. Barnett, *Toxicol. Appl. Pharmacol.* **2010**, *242*, 136–145.

560. P. K. Chakraborty, W. K. Lee, M. Molitor, N. A. Wolff, F. Thévenod, *Mol. Cancer* **2010**, *9*, 102.
561. P. K. Chakraborty, B. Scharner, J. Jurasovic, B. Messner, D. Bernhard, F. Thévenod, *Toxicol. Lett.* **2010**, *198*, 69–76.
562. F. Thévenod, P. K. Chakraborty, *Curr. Mol. Med.* **2010**, *10*, 387–404.
563. M. Varjosalo, J. Taipale, *Genes Dev.* **2008**, *22*, 2454–2472.
564. M. S. Cooke, M. D. Evans, M. Dizdaroglu, J. Lunec, *FASEB J.* **2003**, *17*, 1195–1214.
565. A. Hartwig, D. Beyersmann, *Biol. Trace Elem. Res.* **1989**, *21*, 359–365.
566. Y. H. Jin, A. B. Clark, R. J. Slebos, H. Al-Refai, J. A. Taylor, T. A. Kunkel, M. A. Resnick, D. A. Gordenin, *Nat. Genet.* **2003**, *34*, 326–329.
567. M. Asmuss, L. H. Mullenders, A. Hartwig, *Toxicol. Lett.* **2000**, *112–113*, 227–231.
568. J. C. Mathers, G. Strathdee, C. L. Relton, *Adv. Genet.* **2010**, *71*, 3–39.
569. M. Takiguchi, W. E. Achanzar, W. Qu, G. Li, M. P. Waalkes, *Exp. Cell Res.* **2003**, *286*, 355–365.
570. G. Jiang, L. Xu, S. Song, C. Zhu, Q. Wu, L. Zhang, L. Wu, *Toxicology* **2008**, *244*, 49–55.
571. H. Fujishiro, S. Okugaki, S. Yasumitsu, S. Enomoto, S. Himeno, *Toxicol. Appl. Pharmacol.* **2009**, *241*, 195–201.
572. K. P. Singh, R. Kumari, C. Pevey, D. Jackson, J. W. DuMond, *Cancer Lett.* **2009**, *279*, 84–92.
573. S. Somji, S. H. Garrett, C. Toni, X. D. Zhou, Y. Zheng, A. Ajjimaporn, M. A. Sens, D. A. Sens, *Cancer Cell Int.* **2011**, *11*, 2.
574. S. L. Ameres, J. Martinez, R. Schroeder, *Cell* **2007**, *130*, 101–112.
575. S. Li, Y. Wang, H. Wang, Y. Bai, G. Liang, N. Huang, Z. Xiao, *Biomaterials* **2011**, *32*, 3807–3814.
576. N. Mizushima, M. Komatsu, *Cell* **2011**, *147*, 728–741.
577. Y. O. Son, X. Wang, J. A. Hitron, Z. Zhang, S. Cheng, A. Budhraja, S. Ding, J. C. Lee, X. Shi, *Toxicol. Appl. Pharmacol.* **2011**, *255*, 287–296.
578. S. H. Wang, Y. L. Shih, T. C. Kuo, W. C. Ko, C. M. Shih, *Toxicol. Sci.* **2009**, *108*, 124–131.
579. S. C. Lim, K. S. Hahm, S. H. Lee, S. H. Oh, *Toxicology* **2010**, *276*, 18–26.
580. S. H. Wang, Y. L. Shih, W. C. Ko, Y. H. Wei, C. M. Shih, *Cell Mol. Life Sci.* **2008**, *65*, 3640–3652.
581. Z. Dong, L. Wang, J. Xu, Y. Li, Y. Zhang, S. Zhang, J. Miao, *Toxicol. In Vitro* **2009**, *23*, 105–110.
582. M. Di Gioacchino, C. Petrarca, A. Perrone, S. Martino, D. L. Esposito, L. V. Lotti, R. Mariani-Costantini, *Autophagy* **2008**, *4*, 537–539.
583. K. Taguchi, H. Motohashi, M. Yamamoto, *Genes Cells* **2011**, *16*, 123–140.
584. X. He, M. G. Chen, Q. Ma, *Chem. Res. Toxicol.* **2008**, *21*, 1375–1383.
585. D. Stewart, E. Killeen, R. Naquin, S. Alam, J. Alam, *J. Biol. Chem.* **2003**, *278*, 2396–2402.
586. Y. Jing, L. Z. Liu, Y. Jiang, Y. Zhu, N. L. Guo, J. Barnett, Y. Rojanasakul, F. Agani, B. H. Jiang, *Toxicol. Sci.* **2012**, *125*, 10–19.
587. S. H. Oh, S. Y. Lee, C. H. Choi, S. H. Lee, S. C. Lim, *Arch. Pharm. Res.* **2009**, *32*, 883–891.
588. F. Thévenod, J. M. Friedmann, A. D. Katsen, I. A. Hauser, *J. Biol. Chem.* **2000**, *275*, 1887–1896.
589. W. Ding, D. M. Templeton, *Toxicol. Appl. Pharmacol.* **2000**, *162*, 93–99.
590. D. Hanahan, R. A. Weinberg, *Cell* **2011**, *144*, 646–674.
591. A. Hartwig, *Biometals* **2010**, *23*, 951–960.
592. A. J. Levine, *Cell* **1997**, *88*, 323–331.
593. I. Hamann, C. Konig, C. Richter, G. Jahnke, A. Hartwig, *Mutat. Res.* **2011**.
594. M. Tokumoto, Y. Fujiwara, A. Shimada, T. Hasegawa, Y. Seko, H. Nagase, M. Satoh, *J. Toxicol. Sci.* **2011**, *36*, 191–200.
595. W. E. Achanzar, K. B. Achanzar, J. G. Lewis, M. M. Webber, M. P. Waalkes, *Toxicol. Appl. Pharmacol.* **2000**, *164*, 291–300.
596. U. Bork, W. K. Lee, A. Kuchler, T. Dittmar, F. Thévenod, *Am. J. Physiol. Renal Physiol.* **2010**, *298*, F255–265.

597. C. Meplan, M. J. Richard, P. Hainaut, *Oncogene* **2000**, *19*, 5227–5236.
598. M. M. Gottesman, T. Fojo, S. E. Bates, *Nat. Rev. Cancer* **2002**, *2*, 48–58.
599. C. Huynh-Delerme, H. Huet, L. Noel, A. Frigieri, M. Kolf-Clauw, *Toxicol. In Vitro* **2005**, *19*, 439–447.
600. O. Kimura, T. Endo, Y. Hotta, M. Sakata, *Toxicology* **2005**, *208*, 123–132.
601. W. K. Lee, B. Torchalski, N. Kohistani, F. Thévenod, *Toxicol. Sci.* **2011**, *121*, 343–356.
602. C. Byrne, S. D. Divekar, G. B. Storchan, D. A. Parodi, M. B. Martin, *Toxicol. Appl. Pharmacol.* **2009**, *238*, 266–271.
603. N. Silva, R. Peiris-John, R. Wickremasinghe, H. Senanayake, N. Sathiakumar, *J. Appl. Toxicol* **2011**.
604. C. L. Siewit, B. Gengler, E. Vegas, R. Puckett, M. C. Louie, *Mol. Endocrinol.* **2010**, *24*, 981–992.
605. A. Stoica, B. S. Katzenellenbogen, M. B. Martin, *Mol. Endocrinol.* **2000**, *14*, 545–553.
606. M. B. Martin, R. Reiter, T. Pham, Y. R. Avellanet, J. Camara, M. Lahm, E. Pentecost, K. Pratap, B. A. Gilmore, S. Divekar, R. S. Dagata, J. L. Bull, A. Stoica, *Endocrinology* **2003**, *144*, 2425–2436.
607. B. J. Deegan, A. M. Bona, V. Bhat, D. C. Mikles, C. B. McDonald, K. L. Seldeen, A. Farooq, *J. Mol. Recognit.* **2011**, *24*, 1007–1017.
608. E. Silva, M. J. Lopez-Espinosa, J. M. Molina-Molina, M. Fernandez, N. Olea, A. Kortenkamp, *Toxicol. Appl. Pharmacol.* **2006**, *216*, 20–28.
609. M. D. Johnson, N. Kenney, A. Stoica, L. Hilakivi-Clarke, B. Singh, G. Chepko, R. Clarke, P. F. Sholler, A. A. Lirio, C. Foss, R. Reiter, B. Trock, S. Paik, M. B. Martin, *Nat. Med.* **2003**, *9*, 1081–1084.
610. W. Zhang, J. Yang, J. Wang, P. Xia, Y. Xu, H. Jia, Y. Chen, *Toxicology* **2007**, *241*, 84–91.
611. I. Ali, P. E. Penttinen-Damdimopoulou, S. I. Makela, M. Berglund, U. Stenius, A. Akesson, H. Hakansson, K. Halldin, *Environ. Health Perspect.* **2010**, *118*, 1389–1394.
612. P. Fechner, P. Damdimopoulou, G. Gauglitz, *PLoS One* **2011**, *6*, e23048.
613. G. S. Prins, *Endocr. Relat. Cancer* **2008**, *15*, 649–656.
614. J. Ye, S. Wang, M. Barger, V. Castranova, X. Shi, *J. Environ. Pathol. Toxicol. Oncol.* **2000**, *19*, 275–280.
615. W. E. Achanzar, B. A. Diwan, J. Liu, S. T. Quader, M. M. Webber, M. P. Waalkes, *Cancer Res.* **2001**, *61*, 455–458.
616. W. Maret, *J. Biol. Inorg. Chem.* **2011**, *16*, 1079–1086.
617. J. H. Kagi, B. L. Vallee, *J. Biol. Chem.* **1960**, *235*, 3188–3192.
618. R. D. Palmiter, *Proc. Natl. Acad. Sci. USA* **1994**, *91*, 1219–1223.
619. W. Maret, *Antioxid. Redox Signal* **2006**, *8*, 1419–1441.
620. G. Roesijadi, *Cell Mol. Biol. (Noisy-le-grand)* **2000**, *46*, 393–405.
621. Y. Liu, J. Liu, S. M. Habeebu, M. P. Waalkes, C. D. Klaassen, *Toxicol. Sci.* **2000**, *57*, 167–176.
622. S. S. Habeebu, J. Liu, Y. Liu, C. D. Klaassen, *Toxicol. Sci.* **2000**, *56*, 211–219.
623. Y. Liu, J. Liu, M. B. Iszard, G. K. Andrews, R. D. Palmiter, C. D. Klaassen, *Toxicol. Appl. Pharmacol.* **1995**, *135*, 222–228.
624. C. D. Klaassen, J. Liu, *Environ. Health Perspect.* **1998**, *106 Suppl 1*, 297–300.
625. J. Liu, Y. Liu, A. E. Michalska, K. H. Choo, C. D. Klaassen, *Toxicol. Appl. Pharmacol.* **1996**, *136*, 260–268.
626. M. T. Wu, B. Demple, R. A. Bennett, D. C. Christiani, R. Fan, H. Hu, *J. Toxicol. Environ. Health A* **2000**, *61*, 553–567.
627. K. Kita, N. Miura, M. Yoshida, K. Yamazaki, T. Ohkubo, Y. Imai, A. Naganuma, *Hum. Genet.* **2006**, *120*, 553–560.
628. Z. Kayaalti, V. Aliyev, T. Soylemezoglu, *Toxicol. Appl. Pharmacol.* **2011**, *256*, 1–7.
629. Z. Kayaalti, G. Mergen, T. Soylemezoglu, *Toxicol. Appl. Pharmacol.* **2010**, *245*, 252–255.
630. N. Miura, *Ind. Health* **2009**, *47*, 487–494.
631. N. S. Gould, E. Min, R. J. Martin, B. J. Day, *Free Radic. Biol. Med.* **2012**, *52*, 1201–1206.

Chapter 15
Cadmium and Cancer

Andrea Hartwig

Contents

ABSTRACT 491
1 INTRODUCTION 492
2 EPIDEMIOLOGY AND ANIMAL CARCINOGENICITY 493
2.1 Carcinogenicity in Humans 493
2.2 Carcinogenicity in Experimental Animals 494
3 DIRECT AND INDIRECT GENOTOXICITY 494
3.1 DNA Damage, Mutagenicity, and Clastogenicity 494
3.2 Oxidative Stress 495
4 INTERACTIONS WITH THE DNA DAMAGE RESPONSE SYSTEM 496
4.1 Nucleotide Excision Repair 497
4.2 Base Excision Repair 498
4.3 Mismatch Repair 499
4.4 P53 Tumor Suppressor Functions 499
5 IMPACT ON GENE EXPRESSION AND DEREGULATION OF CELL PROLIFERATION 500
6 INTERACTIONS ON THE MOLECULAR LEVEL: MECHANISTIC CONSIDERATIONS AND THE ROLE OF ADAPTATION 500
7 CONCLUDING REMARKS 502
ABBREVIATIONS AND DEFINITIONS 503
ACKNOWLEDGMENTS 504
REFERENCES 504

Abstract Cadmium is an established human and animal carcinogen. Most evidence is available for elevated risk for lung cancer after occupational exposure; however, associations between cadmium exposure and tumors at other locations including kidney, breast, and prostate may be relevant as well. Furthermore, enhanced cancer risk may not be restricted to comparatively high occupational exposure, but may also

A. Hartwig (✉)
Food Chemistry and Toxicology, Karlsruhe Institute of Technology (KIT),
D-76131 Karlsruhe, Germany
e-mail: andrea.hartwig@kit.edu

A. Sigel, H. Sigel, and R.K.O. Sigel (eds.), *Cadmium: From Toxicity to Essentiality*,
Metal Ions in Life Sciences 11, DOI 10.1007/978-94-007-5179-8_15,

occur via environmental exposure, for example in areas in close proximity to zinc smelters. The underlying mechanisms are still a matter of manifold research activities. While direct interactions with DNA appear to be of minor importance, elevated levels of reactive oxygen species (ROS) have been detected in diverse experimental systems, presumably due to an inactivation of detoxifying enzymes. Also, the interference with proteins involved in the cellular response to DNA damage, the deregulation of cell growth as well as resistance to apoptosis appears to be involved in cadmium-induced carcinogenicity. Within this context, cadmium has been shown to disturb nucleotide excision repair, base excision repair, and mismatch repair. Particularly sensitive targets appear to be proteins with zinc-binding structures, present in DNA repair proteins such as XPA, PARP-1 as well as in the tumor suppressor protein p53. Whether or not these interactions are due to displacement of zinc or due to reactions with thiol groups involved in zinc complexation or in other critical positions under realistic exposure conditions remains to be elucidated. Further potential mechanisms relate to the interference with cellular redox regulation, either by enhanced generation of ROS or by reaction with thiol groups involved in the regulation of signaling pathways. Particularly the combination of these multiple mechanisms may give rise to a high degree of genomic instability evident in cadmium-adapted cells, relevant not only for tumor initiation, but also for later steps in tumor development.

Keywords cadmium • carcinogenicity • DNA damage response • genomic instability • genotoxicity • redox regulation • signal transduction • zinc

1 Introduction

Cadmium is a rare naturally occurring element. Nevertheless, due to its specific chemical properties, including corrosion resistance, low melting temperature, and high thermal and electrical conductivity, there are manifold industrial applications, encompassing nickel-cadmium batteries, pigments, coatings, paints, and stabilizers for plastics. With respect to the general population, relevant exposure occurs via food and – less important – via inhalation of ambient air. Also, due to an accumulation of cadmium in tobacco plants, smoking contributes considerably to cadmium exposure. Occupational exposure occurs predominantly via inhalation, and additionally, there may also be incidental ingestion of dust from contaminated hands and food.

The toxicity of cadmium has been known for more than 150 years, as summarized recently by Nordberg [1]; nevertheless, there is still an ongoing discussion on cadmium-induced toxicity at comparatively low exposure conditions. With respect to non-cancer endpoints, the European Food Safety Authority (EFSA) has lowered the Provisional Tolerable Weekly Intake (PTWI) of 7 μg/kg bw established previously by the Joint FAO/WHO Expert Committee on Food Additives to a TWI of 2.5 μg/kg bw based on cadmium-induced nephrotoxicity [2]. One other endpoint of toxicological concern on low exposure conditions of the general population

towards cadmium is bone demineralization [3]. In addition, since many years, also cadmium-induced carcinogenicity is a matter of debate; thus, current evidence and underlying mechanisms will be summarized. Most promising hypotheses are the increased formation of reactive oxygen species, interactions with the cellular DNA damage response system, such as DNA repair processes, cell cycle control and apoptosis as well as disturbance of cellular signaling processes and epigenetic changes in DNA methylation patterns, which may act together, leading to a high degree of genomic instability.

2 Epidemiology and Animal Carcinogenicity

2.1 Carcinogenicity in Humans

Early observations of an increased incidence of prostate carcinomas among British workers exposed to nickel and cadmium led to the assumption that this may be due to cadmium exposure; however, this was not confirmed in other cohort studies. Nevertheless, mainly based on sufficient evidence for an increased relative risk of lung cancer in workers occupationally exposed to cadmium, in 1993 and 2009, cadmium and its inorganic compounds were classified by the International Agency for Research on Cancer (IARC) as carcinogenic to humans (IARC Group 1) [4–6] and 2004 as carcinogens group 1 (carcinogenic to humans) by the German MAK Commission [7]. Until today extended follow-up studies of the original cohorts in United Kingdom, Sweden, and the United States have been conducted [8–11], confirming elevated risks of lung cancer in most studies. Some major constraints are, however, the small number of long-term, highly exposed workers and the lack of historical data on exposure to cadmium in some studies. Furthermore, confounding factors are cigarette smoke and simultaneous exposure to nickel and arsenic (summarized in [6,7]).

Supportive evidence from environmental exposure provided a recent study in Belgium with subjects living near three smelters when compared to subjects not exposed to elevated levels of cadmium, investigated from 1985 until 2004. Based on urinary cadmium excretion and cadmium in garden soil as exposure indicators, elevated lung cancer risks were observed in the high-exposure group [12]. With respect to other cancer sites, especially the kidney may be of elevated risk due to high and persistent body burden in this organ and the known nephrotoxicity in this organ. No elevated risks for renal cancer due to cadmium exposure were observed in a Swedish or in a British cohort study [9,11]. However, case-control studies estimating the relative risk of kidney cancer due to occupational cadmium exposure, which have been conducted in the United States, in Finland, Germany, and Canada and which estimated cadmium exposure via job-exposure-matrices (JEM), observed higher incidences of renal cancer upon cadmium exposure at the workplace [13–16].

Altogether, the German MAK Commission concluded that an increased relative risk of renal cancer has to be assumed (summarized in [7]) and also IARC stated a positive association with respect to renal and prostate cancer [6]. Finally, new data indicate that human cadmium exposure may also be associated with female breast and endometrial cancer, even though the causalities are not definitively established [17,18].

2.2 Carcinogenicity in Experimental Animals

With respect to long term inhalation studies, several cadmium compounds ($CdCl_2$, $CdSO_4$, CdS and CdO) caused lung cancer (mainly adenocarcinomas) in the rat [19,20], but not in the hamster [21]. Remarkably, in the rat, lung tumors were induced at very low Cd concentrations. Thus, the lowest concentration inducing primary lung carcinoma in rats (15 versus 0 % in controls) was 12.5 μg Cd/m^3, even though under an unusual exposure regimen (23 h/day, 7 days per week for 18 months exposure to $CdCl_2$ aerosols) [19]. In a later study, no lung tumors were induced when the rats were exposed continuously for 18 months to CdO fumes at a concentration of 10 μg Cd/m^3, whereas 21 % of the animals developed tumors when exposed to 30 μg Cd/m^3 [20]. Considering oral exposure, most older studies are of limited use due to too low dose, too short duration or insufficient histopathological investigation. Adequately conducted studies revealed increased incidences of large granular lymphocytes, leukemia, prostate and testis tumors in Wistar rats (summarized in [4,7,22]).

3 Direct and Indirect Genotoxicity

Cadmium salts do not cause DNA damage in cell extracts or with isolated DNA [14] but rather interact with proteins; therefore, the genotoxicity of cadmium is likely due to indirect mechanisms. Predominantly the induction of oxidative stress and interactions with the DNA damage response systems may be relevant in cadmium-induced genotoxicity.

3.1 DNA Damage, Mutagenicity, and Clastogenicity

Cadmium compounds are not mutagenic in classical short term test systems, but rather exert clastogenic activity in mammalian cells. Thus, in most bacterial assays water soluble cadmium compounds were not mutagenic, and in standard mammalian mutagenicity tests effects of cadmium salts with respect to point mutations were usually weak and/or restricted to comparatively high concentrations. In contrast,

pronounced co-mutagenic effects in combination with DNA alkylating agents and with UVC radiation were observed both in bacteria and in mammalian cells, pointing towards an interaction with the cellular response to DNA damage (see below). In contrast to the missing mutagenicity, in mammalian cells cadmium compounds provoked clastogenic effects such as chromosomal aberrations and micronuclei [4,7,23–25]. This was also demonstrated by the pronounced positive effects of cadmium chloride in a modified mammalian test system capable of detecting large multilocus deletions [26]. The clastogenicity is moreover evident *in vivo* in exposed rodents, while evidence for chromosomal damage in cadmium-exposed humans via environmental or workplace exposure is equivocal, partly due to simultaneous exposure to other metal compounds [4,7,27].

3.2 Oxidative Stress

Reactive oxygen species (ROS) such as superoxide anion ($O_2^{\cdot -}$), hydrogen peroxide (H_2O_2), and hydroxyl radical ($HO^{\cdot}$) are byproducts of cellular respiration, generated by incomplete reduction of oxygen to H_2O. To enable the use of oxygen for energy production and yet to minimize oxygen-derived toxicity, a complex antioxidant network has evolved including the scavenging of reactive species by glutathione and vitamins, the enzymatic conversion of highly reactive oxygen species to less harmful ones by superoxide dismutase, catalase, and glutathione peroxidase, and finally the repair or elimination of damaged macromolecules.

However, even under normal cellular conditions, protection is not complete and for example a measurable amount of oxidative cellular damage exists in mammalian cells. Oxidative stress occurs if the equilibrium between the generation of ROS and the efficiency of their detoxification is disrupted [28]. Especially the generation of elevated levels of DNA damage has been implicated in carcinogenicity. Oxidative DNA damage induced by ROS includes a range of lesions like DNA base modifications, sugar lesions, DNA single- and double-strand breaks, DNA–protein crosslinks, and abasic sites (for recent review see [29]). Among these, several oxidative DNA base modifications such as 8-oxoguanine (8-oxoG) have miscoding and thus premutagenic properties and therefore may act as initiators in carcinogenesis [30].

Especially transition metal ions play an important role in the induction of oxidative DNA damage. While neither superoxide anions nor hydrogen peroxide are able to react with DNA directly, in the presence of transition metals like iron, copper, cobalt, or nickel they are converted into highly reactive hydroxyl radicals by Fenton-type reactions. In contrast, cadmium ions are not able to participate in redox reactions under physiological conditions, yet, oxidative stress and the interference with cellular redox regulation may be of high relevance in cadmium-induced carcinogenicity. Increased levels of ROS due to cadmium exposure have been observed both *in vitro* and *in vivo* [31]. Different cadmium compounds have been shown to induce DNA strand breaks and oxidative DNA base modifications in

mammalian cells, but effects were usually small and/or restricted to comparatively high concentrations (e.g., [32,33]).

The induction of DNA strand breaks and chromosomal aberrations by cadmium in mammalian cells was suppressed by antioxidants and antioxidant enzymes, indicating the involvement of ROS [34–36]. Since the extent of ROS and damage to cellular macromolecules depends on the equilibrium between their generation and detoxification or repair, respectively, the occurrence of oxidative DNA damage is assumed to be due to an inhibition of the antioxidant defense by cadmium, such as the antioxidant enzymes catalase, superoxide dismutase, glutathione reductase, and glutathione peroxidase. One other mechanism proposed consists in the displacements of redox active metal ions, e.g., Fe^{2+}, for example in metallothionein, giving rise to Fenton reactions [35–37].

Finally, enhanced frequencies of oxidative DNA lesions in cells and *in vivo* may also be due to impaired removal of the respective lesions (see below). Thus, ROS may be involved in cadmium-induced genotoxicity, but – perhaps more important – also in later steps of cadmium-induced carcinogenicity, by interaction with redox-controlled signaling pathways. With respect to the latter, moderately elevated levels of ROS have been implicated in later steps of tumor formation, such as cell proliferation due to mitotic stimuli and the activation of redox-sensitive transcription factors [36,38] (see below).

4 Interactions with the DNA Damage Response System

Maintenance of genetic information is essential for basically all cellular processes and for the prevention of tumor development. However, many environmental agents as well as food mutagens have been identified which compromise genetic stability by inducing different types of DNA lesions. They include ionizing radiation, UV radiation, alkylating agents, polycyclic aromatic hydrocarbons as well as heterocyclic aromatic amines. Furthermore, DNA is also damaged by endogenous processes, such as ROS generation due to leakage of the electron transport chain in cellular respiration [36,39]. DNA damage interferes with DNA transcription and replication; potential consequences are cell cycle arrest, programmed cell death, mutagenesis, genomic instability, and cancer. To maintain the integrity of the genome, a complex DNA damage response network has evolved [40–42].

Cadmium has been shown to impair almost all major DNA repair pathways. Convincing evidence is available for its interference with nucleotide excision repair (NER), base excision repair (BER), and mismatch repair (MMR); frequently, effects were observed at comparatively low, non-cytotoxic concentrations (reviewed in [43–46]). Since DNA repair systems are not only required for the repair of DNA damage induced by environmental, workplace and food mutagens, but also for the elimination of DNA lesions due to endogenous processes and to keep replication errors low, the disturbance of DNA repair processes may explain co-mutagenic

effects in combination of UVC-radiation, benzo[*a*]pyrene, and alkylating agents on the one side but may also lead to genomic instability and thus contribute to cadmium-induced carcinogenicity on the other side (for recent reviews see [23,45,47]).

4.1 Nucleotide Excision Repair

NER is the most versatile repair system involved in the removal of structurally unrelated bulky base adducts which cause significant helical distortions. It can be subdivided into global genome repair (GG-NER) and, as a sub-pathway, transcription-coupled nucleotide excision repair (TC-NER), which removes preferentially transcription-blocking bulky DNA lesions. At least 30 different proteins and enzymes are required in mammalian cells, including those which are defective in patients suffering from the DNA repair disorder xeroderma pigmentosum (XP) complementation groups A through G. The most crucial step is the damage recognition, followed by the incision at both sides of the lesion and the repair polymerisation leading to the displacement of the damaged oligonucleotide; repair is completed by the ligation of the repair patch (for recent reviews see [40–42,48]).

Cadmium has been shown to inhibit GG-NER in several studies and with respect to different DNA-damaging agents. Thus, it interfered with the removal of benzo[*a*]pyrene- and UVC-induced DNA lesions in cultured mammalian cells [33,49,50]. As one underlying mechanism, an interaction with zinc-binding proteins has been identified. They comprise a family of proteins where zinc is complexed to four cysteine and/or histidine residues, folding a protein domain mostly involved in DNA-protein or protein-protein interactions [51]. First discovered in transcription factors, similar structures have been identified in DNA repair proteins and tumor suppressor proteins like p53. Examples for DNA repair proteins with zinc-binding structures include the bacterial formamidopyrimidine-DNA glycosylase (Fpg) involved in the removal of oxidative DNA base modifications and the mammalian xeroderma pigmentosum group A protein (XPA) essential for the formation of the DNA damage recognition complex during NER (reviewed in [52,53]). In subcellular test systems, cadmium disturbed the activity of the isolated Fpg and diminished DNA binding of XPA to an UVC-irradiated oligonucleotide [54,55]. One molecular mechanism related to the inactivation of zinc-binding proteins appears to involve the displacement of zinc by cadmium, as evident from the reversal of cadmium-induced protein inactivation by excess of zinc as well as from structural investigations of XPA or a peptide resembling the zinc-binding domain of XPA [54–57]. Detailed studies in cadmium treated A549 cells revealed an impaired assembly/disassembly of the DNA damage recognition proteins XPC and XPA at the repair complex after UVC irradiation [33].

4.2 Base Excision Repair

In contrast to NER which detects a rather broad spectrum of DNA lesions, BER is initiated by a specific class of DNA repair enzymes called glycosylases, which act specifically on one or few substrates. BER is mainly responsible for the removal of different types of endogenous DNA damage, including oxidative DNA base modifications like 8-oxoG. This process generates abasic (AP) sites, which are further processed in a multistep process with slight differences depending on the type of damage [39–41,48]. Regarding the impact of cadmium on this repair pathway, low concentrations of cadmium disturbed the repair of oxidative DNA base damage induced by visible light as well as DNA alkylation damage in mammalian cells [32,58].

When compared with the induction of oxidative DNA base modifications such as 8-oxoG, inhibitory effects on the repair of this lesion were observed at much lower cadmium concentrations. This has been observed by direct comparison in HeLa cells: While the induction of DNA strand breaks by cadmium was restricted to 10 μM and higher, the removal of oxidative DNA base modifications induced by visible light and recognized by the bacterial Fpg was inhibited starting at 0.5 μM cadmium, yielding complete inhibition at 5 μM, a non-cytotoxic concentration in this test system [32]. With respect to isolated DNA repair enzymes, an inhibition of the murine 8-oxoguanine DNA glycosylase 1 (mOgg1), an enzyme responsible for recognition and excision of the premutagenic 8-oxoG during BER, as well as of 8-oxo-dG 5'-triphosphate pyrophosphohydrolase (8-oxo-dGTPase), required for the removal of 8-oxo-dG from the deoxynucleotide pool, by cadmium have been described [59,60]. Also, cadmium has been shown to inhibit the activity of the human 8-oxoguanine glycosylase (hOGG1) in mammalian cells [61–63]. Different mechanisms may be responsible, based on different experimental results, including the inactivation of the enzyme as such [62] or the diminished DNA binding of the zinc finger-containing transcription factor SP1 to the OGG1 promotor [64], presumably due to displacement of zinc by cadmium [65].

Inhibition of the repair of oxidative DNA damage is also evident *in vivo*: When investigating, for example, the impact of cadmium on rat testis, a target organ for cadmium carcinogenesis, a gradual decrease in testicular 8-oxo-dGTPase activity was observed, accompanied with progressive increase of 8-oxo-dG levels in testicular DNA [66]. Therefore, increases in oxidative DNA damage *in vivo* may at least in part be due to the repair inhibition of endogenously induced oxidative DNA lesions. One other enzyme involved in DNA damage signaling, apoptosis, and BER is poly(ADP-ribose) polymerase 1 (PARP-1). It contains three zinc fingers in its DNA binding domain involved in the recognition of DNA breaks and the subsequent synthesis of poly(ADP-ribose) [67,68]. In HeLa cells, H_2O_2-induced PARP activity was decreased by cadmium chloride [69]; detailed molecular interactions are currently investigated in our laboratory.

4.3 Mismatch Repair

One other DNA repair system of particular relevance for maintaining genomic stability is MMR. This evolutionary conserved pathway is responsible for the repair of mismatched normal bases after DNA replication, contributing significantly to the extraordinary fidelity of DNA replication. Cells deficient in MMR exert a "mutator phenotype", in which the rate of spontaneous mutations is greatly elevated, and defects in MMR are associated with an increased risk of different types of cancer.

The MMR system also plays a key role in cell killing in response to alkylating agents, and MMR-deficient cells are about 100 times more resistant to the cytotoxicity of alkylating agents [70,71]. With respect to cadmium, exposure towards low concentrations resulted in pronounced hypermutability in yeast. Furthermore, in extracts of human cells, cadmium inhibited at least one step leading to mismatch repair [72]. Since then, different studies demonstrated the interference by cadmium with proteins involved in the initial step of MMR, i.e., damage recognition by MSH2-MSH6 and MSH2-MSH3. As underlying mechanisms, cadmium affected ATP binding and hydrolysis of MMR enzymes, reducing their DNA binding activity and their ability to discriminate between mismatched and matched DNA base pairing in isolated systems and in mammalian cells in culture [44,73,74].

4.4 P53 Tumor Suppressor Functions

Besides DNA repair systems, further DNA damage responses are activated upon genotoxic stress in mammalian cells. They include cell cycle control mechanisms, increasing the time for DNA repair, as well as apoptosis eliminating heavily damaged cells. The DNA damage response is strictly coordinated, for example by the tumor suppressor protein p53. P53 regulates cell cycle control and apoptosis by several coordinated pathways and thus exerts pronounced impact on the processing of DNA damage and on genomic stability [75].

Cadmium has been shown to interfere with structure and function of p53, but opposite effects have been reported. In some studies, a stabilization of p53 through phosphorylation followed by the induction of the p53-mediated stress response was observed [76–78]; others demonstrated an inactivation of p53 via structural changes. P53 contains a zinc-binding structure in its DNA-binding domain, essential for its tumor suppressor functions and rendering the protein redox-sensitive. Exposure of either the isolated p53 protein or human breast cancer MCF7 cells to cadmium resulted in the disruption of the zinc-binding structure, yielding a so-called "mutant" conformation; consequences were the inhibition of DNA binding and the inhibition of the activation of p53 target genes including p21. Furthermore, suppression of the p53-mediated cell cycle arrest in response to DNA damage induced by γ-irradiation was observed [79]. Similar effects were demonstrated in A549 human lung tumor cells, where CdO and $CdCl_2$ induced structural alterations of the zinc binding domain of p53, followed by diminished induction of the

p53-regulated nucleotide excision repair gene XPC and diminished removal of UVC and benzo[*a*]pyrene induced DNA damage [33]. Thus, it appears that cadmium destroys the zinc-binding structure of p53; whether or not this is due to the displacement of zinc is currently not clear.

5 Impact on Gene Expression and Deregulation of Cell Proliferation

Cadmium has been shown to interfere with several signaling pathways in a complex manner. This includes Ca^{2+}-signaling, cAMP-signaling, NO-signaling, as well as Ca^{2+}- and cAMP-independent protein kinase signaling. Furthermore, cadmium interacts with the oxidative stress response, such as the activation of nuclear factor κB (NF-κB) and NF-E2-related factor (Nrf2). Immediate early response genes induced by cadmium include protooncogenes like *c-fos*, *c-jun*, and *c-myc* activated in response to mitotic stimuli and frequently found to be overexpressed in tumors. C-fos and c-jun constitute the AP-1 transcription factor, activating several genes involved in cell growth and division. Also, cadmium interacts with developmental signaling pathways, such as those activated by secreted *Hedgehog* and *Wnt* proteins. Apart from potential teratogenic effects during development, by mimicking Wnt/β-catenin signaling, cadmium may induce cell survival and proliferation and thus promote carcinogenicity. Cadmium may induce second messenger signaling by activating extracellular G-protein-coupled receptors, but also by affecting intracellular signaling cascades. During physiological signaling, short-lived second messengers are generated which act specifically in space and time as a consequence of mostly non-covalent binding to receptors, resulting in their transient activation. In contrast, cadmium appears to disrupt the physiological control of signaling pathways via permanent alterations of second messenger levels, leading to a disturbance of control of cell growth and survival (for excellent reviews see [25,37,80,81]). In addition to directly stimulating mitogenic signals, cadmium also inhibits negative controls of cell proliferation, for example by inactivation of p53 (see above) [79]. Furthermore, long-term treatment of prostate epithelial cells resulted in cadmium-induced malignant transformation; transformed cells exerted an acquired resistance to apoptosis, which appeared to be linked to an increase in the anti-apoptotic action of Bcl-2 that perturbs the JNK signal transduction pathway [82].

6 Interactions on the Molecular Level: Mechanistic Considerations and the Role of Adaptation

Current evidence suggests that Cd^{2+} is the ultimate damaging species, since water-soluble and particulate, water-insoluble cadmium compounds exert similar effects in experimental cell culture systems and in experimental animals. In a recent study,

both cadmium chloride and largely water insoluble cadmium oxide induced oxidative DNA lesions and inhibited the removal of benzo[*a*]pyrene-induced DNA lesions. Furthermore, cadmium-induced conformational changes of p53 were comparable when applying cadmium chloride or cadmium oxide. Repair inhibitory effects were strongly correlated with cadmium levels in the nuclei, indicating the bioavailability of both compounds [33]. While water-soluble cadmium compounds are taken up via ion channels [83], particulate cadmium compounds may be taken up by phagocytosis and, due to the low pH, may dissolve gradually in lysosomes, yielding high concentrations of cadmium ions in the cytoplasm and in the nucleus, as described in detail for nickel compounds [84,85]. This assumption is also supported by inhalation studies where water-soluble cadmium sulfate, poorly water-soluble cadmium oxide and cadmium sulfide pigment with intermediate water solubility induced lung tumors in rats [86].

While direct interactions of cadmium ions with DNA appear to be of little importance, interactions with proteins are of high significance. Especially the DNA repair inhibitions but also altered cell proliferation and/or diminished cell cycle control have frequently been observed at low, non-cytotoxic concentrations of cadmium, raising the question of particularly sensitive targets of cadmium ions. Relevant mechanisms include elevated levels of ROS, interactions with homeostasis and cellular functions of essential metal ions like zinc, calcium, and iron and the interference with cellular redox regulation.

Since cadmium ions exert high affinity towards SH groups, potential targets are zinc-binding structures frequently found in transcription factors, DNA repair and tumor suppressor proteins [52,53]. As indicated above, one molecular mechanism related to the inactivation of zinc-binding proteins appears to involve the competition between zinc and cadmium. Compared to Zn^{2+}, the radius of Cd^{2+} ion is larger, but still cadmium ions can substitute for zinc ions in many enzymes and transcription factors [25,87]. Considering the example of the nucleotide excision repair protein XPA or a peptide resembling the zinc binding domain of XPA, binding constants for cadmium were about 1000-fold higher as compared to zinc. Replacement of zinc by cadmium yielded only minor structural alterations [56,57], but provoked a pronounced disturbance of XPA within the assembly and disassembly of the nucleotide excision repair complex [33]. In addition to direct interactions with DNA repair proteins, cadmium may disturb DNA repair processes via interaction with zinc-containing transcription factors. Thus, human OGG1 (hOGG1), a glycosylase responsible for recognition and excision of the premutagenic 8-oxoG during BER in mammalian cells, was inhibited by cadmium [88]. Even though hOGG1 contains no zinc-binding motif itself, its inhibition was shown to be due to diminished DNA binding of the zinc finger-containing transcription factor SP1 to the *OGG1* promotor [64], presumably due to displacement of zinc by cadmium [65]. Also, a downregulation of DNA repair genes like XPC has been observed recently in cultured cells [33] and *in vivo* in mouse testes [89], which may be due to a disturbed transcriptional activity of p53. However, whether or not the inactivations of the respective zinc-binding repair proteins are mediated via displacement of zinc by cadmium or whether interactions with other protein structures, such as critical thiols outside the

zinc-binding structure, are relevant for the observed inhibitions has to be further elucidated. Furthermore, systematic investigations on the relevance of these mechanisms for *in vivo* situations are still missing.

Multiple mechanisms appear to be involved in cadmium-induced alterations of gene expression. With respect to the induction of metallothionein, cadmium ions bind directly to the transcription factor MTF1 [90]. In some other cases, specific interactions have been identified. With respect to epigenetic effects cadmium inhibited DNA-(cytosine-5) methyltransferase and led to diminished DNA methylation during cadmium-induced cellular transformation, provoking augmented expression of cellular proto-oncogenes [91]. One example for a direct competition with calcium concerns the cadherin-mediated cell-cell adhesion system; here, cadmium specifically displaced calcium from the protein E-cadherin and impaired the cell-cell adhesion in kidney epithelial cells [92,93]. A fast transient increase in levels of second messengers like Ca^{2+} and inositol-1,4,5-trisphosphate by low concentrations of cadmium may be due to its binding to G-protein coupled receptors in the plasma membrane; however, cadmium affects also intracellular signaling mediated by mitogen activated protein kinases (MAPK) as well as cAMP-dependent and calmodulin-dependent pathways. Even though zinc binding structures are involved in many of these pathways, at present it is unclear whether a direct replacement of zinc is the underlying mechanism [25,37,94]. One interesting hypothesis consists in the interference by cadmium with the cellular redox regulation. Thus, diverse signaling pathways have been identified to be redox regulated via reversible oxidation and reduction of thiol groups [95–97]. Cadmium has been shown to induce several redox-regulated signal transduction pathways, such as NF-κB and Nrf2, but also mitotic signaling, which may be due to the increased formation of ROS or to direct interaction with redox-sensitive cysteines in signal transduction proteins. In most cases the molecular interactions have not been fully explored experimentally, but are subject of current research activities [97,98].

7 Concluding Remarks

In summary, cadmium-induced carcinogenicity is likely based on multiple distinct mechanisms. As opposed to direct DNA damage, interactions with proteins appear to be more relevant for carcinogenicity and several targets have been identified such as antioxidative defense systems, DNA repair processes as well as tumor suppressor and signal transduction proteins. All these features taken alone could contribute to carcinogenicity, but most likely their combination seems to be of particular importance. Thus, long-term exposure to low concentrations of cadmium leads to adapted cells exerting increased cadmium accumulation, increased proliferation, diminished DNA repair and cell cycle control as well as resistance to apoptosis. The outcome is a severe decrease in genomic stability, which may play an important role in cadmium-induced tumor initiation and progression (summarized in Figure 1).

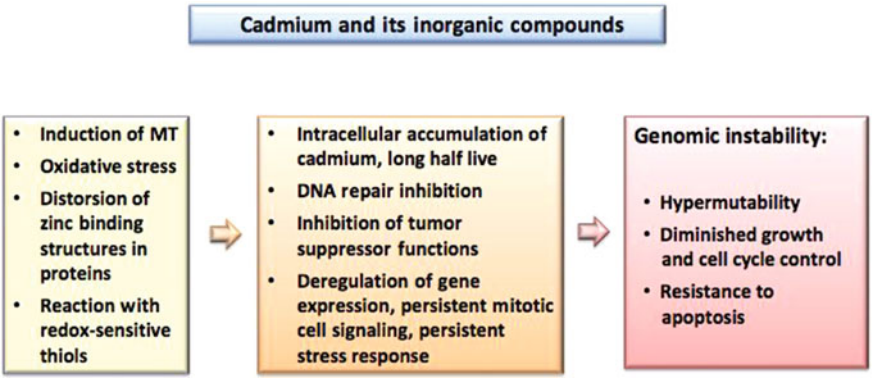

Figure 1 Proposed series of events leading to genomic instability and tumor formation by cadmium and its inorganic compounds.

One important question concerns specific mechanisms explaining the organ-specificity of cadmium-induced carcinogenicity. After inhalative exposure, the lung is a plausible target organ, but other organs like kidney, prostate, breast, and endometrium may be affected as well. Since tumors in prostate, breast, and endometrium are frequently hormone-dependent, one aspect addressed by several groups concerns a potential impact of cadmium on steroid hormone-dependent signaling [99]. Nevertheless, respective experimental evidence is contradictory and needs to be further explored [45]. One other key issue in cadmium-induced carcinogenicity appears to be adaptation and the role of MT. Cadmium induces several genes for cadmium and ROS tolerance such as those coding for MT, GSH synthesis and function, catalase and superoxide dismutase. Hence, a condition for prolonged cell survival in the presence of cadmium is established, which may be beneficial in terms of protection from acute cadmium toxicity, also evident from comparative studies with MT-transgenic and MT-null mice [100]. However, adaptation may be a double-edged sword, since increased MT contents leads not only to cadmium accumulation und long half lives, but also to reduced DNA repair activities as well as suppressed apoptosis [80,101].

Considering recent reports on cadmium-related carcinogenicity in different target organs under low exposure conditions, future research will have to focus on the relevance of the respective mechanisms in experimental animals and in exposed humans.

Abbreviations and Definitions

BER	base excision repair
Bw	body weight
cAMP	cyclic adenosine 3',5'-monophosphate

EFSA	European Food Safety Authority
FAO	Food and Agriculture Organization of the United Nations
Fpg	formamidopyrimidine DNA glycosylase
GG-NER	global genome nucleotide excision repair
GSH	glutathione
IARC	International Agency for Research on Cancer
JEM	job-exposure-matrix
JNK	c-jun-N-terminal kinase
MAK Commission	(= maximale Arbeitsplatzkonzentration) German Commission for the Investigation of Health Hazards of Chemical Compounds in the Work Area
MAPK	mitogen activated protein kinases
MMR	mismatch repair
MT	metallothionein
NER	nucleotide excision repair
NF-κB	nuclear factor κB
Nrf2	NF-E2-related factor
Ogg1	8-oxoguanine DNA glycosylase 1
PARP	poly(ADP-ribose) polymerase
PTWI	provisional tolerable weekly intake
ROS	reactive oxygen species
TC-NER	transcription-coupled nucleotide excision repair
TWI	tolerable weekly intake
UVC	ultraviolet C light (the full range is 100–280 nm; but usually in biological experiments 254 nm is applied)
WHO	World Health Organization
XP	xeroderma pigmentosum
XPA	xeroderma pigmentosum group A protein
8-oxoG	8-oxoguanine
8-oxo-dGTPase	8-oxo-dG 5'-triphosphate pyrophosphohydrolase

Acknowledgments The author would like to thank Dr. Gunnar Jahnke for critical reading of the manuscript. Research conducted in the author's laboratory was supported by the Deutsche Forschungsgemeinschaft and by BWPLUS.

References

1. G. F. Nordberg, *Toxicol. Appl. Pharmacol.* **2009**, *238*, 192–200.
2. EFSA, *The EFSA Journal* **2009**, *980*, 1–139.
3. M. Sughis, J. Penders, V. Haufroid, B. Nemery, T. S. Nawrot, *Environmental Health: A Global Access Science Source* **2011**, *10*, 104.
4. IARC, *Beryllium, Cadmium, Mercury and Exposures in the Glass Manufacturing Industry*, 1993.
5. IARC, *Supplement: Cadmium and Cadmium compounds*, 1997.

6. IARC, *A Review of Human Carcinogens; Part C: Arsenic, Metals, Fibres, and Dusts*, 2012, pp. 121–145.
7. *Cadmium and Its Compounds (in the form of inhable dusts/aerosols)*, Vol. 22, *The MAK Collection for Occupational Health and Safety*, Ed H. Greim, Wiley-VCH, Weinheim, Germany, 2006.
8. L. Stayner, R. Smith, T. Schnorr, R. Lemen, M. Thun, *Ann. Epidemiol.* **1993**, *3*, 114–116.
9. T. Sorahan, N. A. Esmen, *Occupat. Environ. Med.* **2004**, *61*, 108–116.
10. T. Sorahan, *Occupat. Med.* **2009**, *59*, 264–266.
11. L. Jarup, T. Bellander, C. Hogstedt, G. Spang, *Occupat. Environ.M.* **1998**, *55*, 755–759.
12. T. Nawrot, M. Plusquin, J. Hogervorst, H. A. Roels, H. Celis, L. Thijs, J. Vangronsveld, E. Van Hecke, J. A. Staessen, *The Lancet Oncology* **2006**, *7*, 119–126.
13. B. Pesch, J. Haerting, U. Ranft, A. Klimpel, B. Oelschlägel, W. Schill, *Int. J. Epidemiol.* **2000**, *29*, 1014–1024.
14. J. Hu, Y. Mao, K. White, *Occupat. Med.* **2002**, *52*, 157–164.
15. J. Siemiatycki, *Risk Factors for Cancer in the Workplace*, CRC Press, Boca Raton, Florida, 1991.
16. E. Kellen, M. P. Zeegers, E. D. Hond, F. Buntinx, *Cancer Detec. Prev.* **2007**, *31*, 77–82.
17. J. A. McElroy, M. M. Shafer, A. Trentham-Dietz, J. M. Hampton, P. A. Newcomb, *J. Natl. Cancer Inst.* **2006**, *98*, 869–873.
18. A. Akesson, B. Julin, A. Wolk, *Cancer Res.* **2008**, *68*, 6435–6441.
19. S. Takenaka, H. Oldiges, H. Konig, D. Hochrainer, G. Oberdörster, *J. Natl. Cancer Inst.* **1983**, *70*, 367–373.
20. U. Glaser, D. Hochrainer, F. J. Otto, H. Oldiges, *Toxicol. Environ. Chem.* **1990**, *27*, 153–162.
21. U. Heinrich, L. Peters, H. Ernst, S. Rittinghausen, C. Dasenbrock, H. König, *Exp. Pathol.* **1989**, *37*, 253–258.
22. J. Huff, R. M. Lunn, M. P. Waalkes, L. Tomatis, P. F. Infante, *Int. J. Occupat. Environ. Health* **2007**, *13*, 202–212.
23. D. Beyersmann, A. Hartwig, *Arch. Toxicol.* **2008**, *82*, 493–512.
24. M. Filipic, T. Fatur, M. Vudrag, *Hum. Exp. Toxicol.* **2006**, *25*, 67–77.
25. M. Waisberg, P. Joseph, B. Hale, D. Beyersmann, *Toxicology* **2003**, *192*, 95–117.
26. M. Filipic, T. K. Hei, *Mutat. Res.* **2004**, *546*, 81–91.
27. J. T. Tapisso, C. C. Marques, L. Mathias Mda, G. Ramalhinho Mda, *Mutat. Res.* **2009**, *678*, 59–64.
28. M. Valko, C. J. Rhodes, J. Moncol, M. Izakovic, M. Mazur, *Chem. Biol. Interact.* **2006**, *160*, 1–40.
29. J. Cadet, T. Douki, J. L. Ravanat, *Free Radical Biol. Med.* **2010**, *49*, 9–21.
30. T. B. Kryston, A. B. Georgiev, P. Pissis, A. G. Georgakilas, *Mutat. Res.* **2011**, *711*, 193–201.
31. J. Liu, W. Qu, M. B. Kadiiska, *Toxicol. Appl. Pharmacol.* **2009**, *238*, 209–214.
32. H. Dally, A. Hartwig, *Carcinogenesis* **1997**, *18*, 1021–1026.
33. T. Schwerdtle, F. Ebert, C. Thuy, C. Richter, L. H. Mullenders, A. Hartwig, *Chem. Res. Toxicol.* **2010**, *23*, 432–442.
34. T. Ochi, M. Ohsawa, *Mutat. Res.* **1985**, *143*, 137–142.
35. S. J. Stohs, D. Bagchi, E. Hassoun, M. Bagchi, *J. Environ. Pathol. Toxicol. Oncol.* **2001**, *20*, 77–88.
36. M. Valko, C. J. Rhodes, J. Moncol, M. Izakovic, M. Mazur, *Chem. Biol. Interact.* **2006**, *160*, 1–40.
37. F. Thevenod, *Toxicol. Appl. Pharmacol.* **2009**, *238*, 221–239.
38. M. Genestra, *Cell Signal.* **2007**, *19*, 1807–1819.
39. R. Hakem, *EMBO J.* **2008**, *27*, 589–605.
40. U. Camenisch, H. Naegeli, *EXS* **2009**, *99*, 111–150.
41. M. Christmann, M. T. Tomicic, W. P. Roos, B. Kaina, *Toxicology* **2003**, *193*, 3–34.
42. M. Fousteri, L. H. Mullenders, *Cell Res.* **2008**, *18*, 73–84.
43. A. Hartwig, *Environ. Health Perspect.* **1994**, *102 Suppl 3*, 45–50.

44. C. Giaginis, E. Gatzidou, S. Theocharis, *Toxicol. Appl. Pharmacol.* **2006**, *213*, 282–290.
45. A. Hartwig, *Biometals* **2010**, *23*, 951–960.
46. P. Koedrith, Y. R. Seo, *Int. J. Mol. Sci.* **2011**, *12*, 9576–9595.
47. M. Filipic, *Mutat. Res.* **2012**, *733*, 69–77.
48. J. de Boer, J. H. Hoeijmakers, *Carcinogenesis* **2000**, *21*, 453–460.
49. A. Hartmann, G. Speit, *Environ. Mol. Mutagen.* **1996**, *27*, 98–104.
50. R. D. Snyder, G. F. Davis, P. J. Lachmann, *Biol. Trace El. Res.* **1989**, *21*, 389–398.
51. J. P. Mackay, M. Crossley, *Trends Biochem. Sci.* **1998**, *23*, 1–4.
52. A. Hartwig, *Antioxid. Redox Signal.* **2001**, *3*, 625–634.
53. A. Witkiewicz-Kucharczyk, W. Bal, *Toxicol. Lett.* **2006**, *162*, 29–42.
54. M. Asmuss, L. H. Mullenders, A. Hartwig, *Toxicol. Lett.* **2000**, *112–113*, 227–231.
55. M. Hartmann, A. Hartwig, *Carcinogenesis* **1998**, *19*, 617–621.
56. G. W. Buchko, N. J. Hess, M. A. Kennedy, *Carcinogenesis* **2000**, *21*, 1051–1057.
57. E. Kopera, T. Schwerdtle, A. Hartwig, W. Bal, *Chem. Res. Toxicol.* **2004**, *17*, 1452–1458.
58. T. Fatur, T. T. Lah, M. Filipic, *Mutat. Res.* **2003**, *529*, 109–116.
59. K. Bialkowski, K. S. Kasprzak, *Nucleic Acids Res.* **1998**, *26*, 3194–3201.
60. D. O. Zharkov, T. A. Rosenquist, *DNA Repair (Amst)* **2002**, *1*, 661–670.
61. R. J. Potts, R. D. Watkin, B. A. Hart, *Toxicology* **2003**, *184*, 189–202.
62. I. Hamann, C. König, C. Richter, G. Jahnke, A. Hartwig, *Mutat. Res.* **2011**, *May 13 Epub ahead of print*; Mutat. Res. **2012**, *736*, 56–63.
63. A. Bravard, A. Campalans, M. Vacher, B. Gouget, C. Levalois, S. Chevillard, J. P. Radicella, *Mutat. Res.* **2010**, *685*, 61–69.
64. C. K. Youn, S. H. Kim, D. Y. Lee, S. H. Song, I. Y. Chang, J. W. Hyun, M. H. Chung, H. J. You, *J. Biol. Chem.* **2005**, *280*, 25185–25195.
65. R. K. Kothinti, A. B. Blodgett, D. H. Petering, N. M. Tabatabai, *Toxicol. Appl. Pharmacol.* **2010**, *244*, 254–262.
66. K. Bialkowski, A. Bialkowska, K. S. Kasprzak, *Carcinogenesis* **1999**, *20*, 1621–1624.
67. S. Beneke, A. Bürkle, *Nucleic Acids Res.* **2007**, *35*, 7456–7465.
68. S. Petrucco, *Nucleic Acids Res.* **2003**, *31*, 6689–6699.
69. A. Hartwig, M. Asmuss, I. Ehleben, U. Herzer, D. Kostelac, A. Pelzer, T. Schwerdtle, A. Bürkle, *Environ. Health Perspect.* **2002**, *110 Suppl 5*, 797–799.
70. V. O'Brien, R. Brown, *Carcinogenesis* **2006**, *27*, 682–692.
71. P. Hsieh, K. Yamane, *Mech. Ageing Dev.* **2008**, *129*, 391–407.
72. Y. H. Jin, A. B. Clark, R. J. Slebos, H. Al-Refai, J. A. Taylor, T. A. Kunkel, M. A. Resnick, D. A. Gordenin, *Nat. Genet.* **2003**, *34*, 326–329.
73. A. Lutzen, S. E. Liberti, L. J. Rasmussen, *Biochem. Biophys. Res. Commun.* **2004**, *321*, 21–25.
74. M. Wieland, M. K. Levin, K. S. Hingorani, F. N. Biro, M. M. Hingorani, *Biochemistry* **2009**, *48*, 9492–9502.
75. P. Hainaut, M. Hollstein, *Adv. Cancer Res.* **2000**, *77*, 81–137.
76. F. Cao, T. Zhou, D. Simpson, Y. Zhou, J. Boyer, B. Chen, T. Jin, M. Cordeiro-Stone, W. Kaufmann, *Toxicol. Appl. Pharmacol.* **2007**, *218*, 174–185.
77. S. Chatterjee, S. Kundu, S. Sengupta, A. Bhattacharyya, *Mutat. Res.* **2009**, *663*, 22–31.
78. X. Yu, J. S. Sidhu, S. Hong, J. F. Robinson, R. A. Ponce, E. M. Faustman, *Toxicol. Sci.* **2011**, *120*, 403–412.
79. C. Meplan, K. Mann, P. Hainaut, *J. Biol. Chem.* **1999**, *274*, 31663–31670.
80. B. A. Hart, R. J. Potts, R. D. Watkin, *Toxicology* **2001**, *160*, 65–70.
81. P. Joseph, *Toxicol. Appl. Pharmacol.* **2009**, *238*, 272–279.
82. W. Qu, H. Ke, J. Pi, D. Broderick, J. E. French, M. M. Webber, M. P. Waalkes, *Environ. Health Perspect.* **2007**, *115*, 1094–1100.
83. F. Thevenod, *Biometals* **2010**, *23*, 857–875.
84. M. Costa, J. D. Heck, S. H. Robison, *Cancer Res.* **1982**, *42*, 2757–2763.
85. R. M. Evans, P. J. Davies, M. Costa, *Cancer Res.* **1982**, *42*, 2729–2735.

86. U. Heinrich, *IARC Sci. Publ.* **1992**, 405–413.
87. A. Martelli, E. Rousselet, C. Dycke, A. Bouron, J. M. Moulis, *Biochimie* **2006**, *88*, 1807–1814.
88. R. J. Potts, I. A. Bespalov, S. S. Wallace, R. J. Melamede, B. A. Hart, *Toxicology* **2001**, *161*, 25–38.
89. T. Zhou, X. Jia, R. E. Chapin, R. R. Maronpot, M. W. Harris, J. Liu, M. P. Waalkes, E. M. Eddy, *Toxicol. Lett.* **2004**, *154*, 191–200.
90. P. Lichtlen, W. Schaffner, *BioEssays* **2001**, *23*, 1010–1017.
91. M. Takiguchi, W. E. Achanzar, W. Qu, G. Li, M. P. Waalkes, *Exp. Cell Res.* **2003**, *286*, 355–365.
92. W. C. Prozialeck, P. C. Lamar, *Biochim. Biophys. Acta* **1999**, *1451*, 93–100.
93. W. C. Prozialeck, P. C. Lamar, S. M. Lynch, *Toxicol. Appl. Pharmacol.* **2003**, *189*, 180–195.
94. J. M. Moulis, *Biometals* **2010**, *23*, 877–896.
95. R. Brigelius-Flohe, L. Flohe, *Antioxidants & Redox Signaling* **2011**, *15*, 2335–2381.
96. G. I. Giles, *Curr. Pharm. Design* **2006**, *12*, 4427–4443.
97. P. D. Ray, B. W. Huang, Y. Tsuji, *Cell. Signalling* **2012**, *24*, 981–990.
98. M. Valko, H. Morris, M. T. Cronin, *Curr. Med. Chem.* **2005**, *12*, 1161–1208.
99. C. Byrne, S. D. Divekar, G. B. Storchan, D. A. Parodi, M. B. Martin, *Toxicol. Appl. Pharmacol.* **2009**, *238*, 266–271.
100. C. D. Klaassen, J. Liu, B. A. Diwan, *Toxicol. Appl. Pharmacol.* **2009**, *238*, 215–220.
101. K. P. Singh, R. Kumari, C. Pevey, D. Jackson, J. W. DuMond, *Cancer Lett.* **2009**, *279*, 84–92.

Chapter 16
Cadmium in Marine Phytoplankton

Yan Xu and François M.M. Morel

Contents

ABSTRACT 510
1 INTRODUCTION 510
2 CADMIUM DISTRIBUTION IN THE OCEAN 511
2.1 Vertical Profiles 511
2.2 Isotope Composition 513
3 EFFECTS OF CADMIUM ON PHYTOPLANKTON GROWTH 513
3.1 Beneficial Effect 513
3.2 Toxic Effect 514
4 CADMIUM UPTAKE BY PHYTOPLANKTON 515
4.1 Transport System and Effect of Manganese and Zinc 515
4.2 Effect of Other Metals and Macronutrients 516
4.3 Effect of pH/pCO_2 on and Role of Weak Ligands in Cadmium Uptake 516
4.4 Phytoplankton Species 517
5 CADMIUM AND THIOL PRODUCTION 517
5.1 Phytochelatins 517
5.2 Other Thiols 519
6 CADMIUM CARBONIC ANHYDRASE 520
6.1 Cadmium Carbonic Anhydrase Expression 520
6.2 Diversity of cdca 521
6.3 Structure and Properties of Cadmium Carbonic Anhydrase 524
7 CONCLUDING REMARKS AND FUTURE DIRECTIONS 525
ABBREVIATIONS 526
REFERENCES 526

Y. Xu
Department of Geosciences, Princeton University, Princeton, NJ 08544, USA

Department of Molecular and Cellular Physiology, School of Medicine, Stanford University, Stanford, CA 94305, USA
e-mail: yanxu12@stanford.edu

F.M.M. Morel (✉)
Department of Geosciences, Princeton University, Princeton, NJ 08544, USA
e-mail: morel@princeton.edu

A. Sigel, H. Sigel, and R.K.O. Sigel (eds.), *Cadmium: From Toxicity to Essentiality*, Metal Ions in Life Sciences 11, DOI 10.1007/978-94-007-5179-8_16,

Abstract The distribution of cadmium in the ocean is very similar to that of major nutrients suggesting that it may be taken up by marine phytoplankton at the surface and remineralized at depth. This interpretation is supported by recent data on Cd isotope distribution showing an increase in the $^{112}Cd/^{110}Cd$ ratio in Cd-depleted surface water. While at high concentrations, Cd is toxic to phytoplankton as it is to many organisms, at relatively low concentrations, Cd can enhance the growth of a number of phytoplankton species under zinc limitation. Kinetic studies suggest that Cd is taken up through either the Mn or the Zn transport system, depending on the ambient concentrations of these metals. In addition to inorganic Cd complexes (including the free Cd^{2+} ion), Cd complexes with relatively weak organic ligands may also be bioavailable. Cd is very effective to induce the production of phytochelatin and other thiols in phytoplankton, probably as a detoxification mechanism as well as a control of Cd homeostasis in cells. The only known biological function of Cd is to serve as a metal cofactor in Cd-carbonic anhydrase (CDCA) in diatoms. The expression of CDCA is regulated by Cd and Zn availabilities and by the pCO_2/pH of the ambient seawater in cultured diatoms and natural assemblages. The conformation of CDCA active site is similar to that of β-CA and both Zn and Cd can be used as its metal cofactor and exchanged for each other. Understanding of the biological role of Cd in marine phytoplankton provides insights into the biogeochemical cycling of this element in the ocean.

Keywords cadmium • carbonic anhydrase • growth • metal replacement • phytochelatin • phytoplankton • uptake

1 Introduction

Marine phytoplankton are a diverse group of unicellular photosynthetic microorganisms that live in the sunlit surface waters of the ocean. While their standing biomass is miniscule compared to that of land plants, they grow rapidly and account for nearly half of primary production on earth [1]. To grow, phytoplankton take up nutrients from surface seawater; part of the resulting biomass is continuously exported to deep water where the nutrients are remineralized and slowly returned to the surface by ocean mixing. The concentrations of major and trace nutrients in surface seawater thus reflect both the activity of the phytoplankton which export them to the abyss and the geochemical processes that cycles elements in and out of the oceans. The mutual influence of nutrient concentrations and phytoplankton physiology results in a coupling between the geochemistry of biologically essential elements and the evolution of phytoplankton over geological time [2].

Cadmium is a highly toxic element and there have been instances of Cd pollution with some well-documented cases of impact on human health (e.g., Itai-itai disease [3]). Elevated Cd concentrations occur in some polluted coastal regions and are cause for concern, particularly as a result of the ability of some marine bivalves to accumulate the metal, posing health risks to humans and other animals that consume them (e.g., [4,5]). However, the concentration of Cd in the open ocean is extremely low, and like that of Zn and other essential metals, its vertical profile is

closely correlated to that of major nutrients such as phosphate. This "nutrient-like" concentration profile suggests that Cd maybe removed from surface seawater by the same mechanisms as algal nutrients and that it may itself serve as a nutrient to marine phytoplankton [6–8].

After many years of research, the first protein that uses Cd naturally has been discovered in marine diatoms: a carbonic anhydrase with Cd as its catalytic center (CDCA) [9,10]. It appears that CDCA plays a pivotal role in the acquisition of inorganic carbon in diatoms, and thus the use of Cd in CDCA provides a link between the biogeochemical cycles of carbon and Cd. The existence of CDCA is an example of the unique mechanisms phytoplankton have evolved over geological times as an adaptation to life in the metal-poor environment of surface seawater. But CDCA may not be the only biological use of Cd in seawater. While we are beginning to understand how and how much Cd is utilized by phytoplankton cells, there are still many challenging questions that need to be answered.

2 Cadmium Distribution in the Ocean

2.1 Vertical Profiles

As discussed in Chapter 2, the vertical distribution of Cd is very similar to that of major nutrients such as phosphate and nitrate; it is depleted in the surface water as a result of biological uptake by phytoplankton and regenerated in deep water (Figure 1). This nutrient-like profile has been observed across ocean basins and in

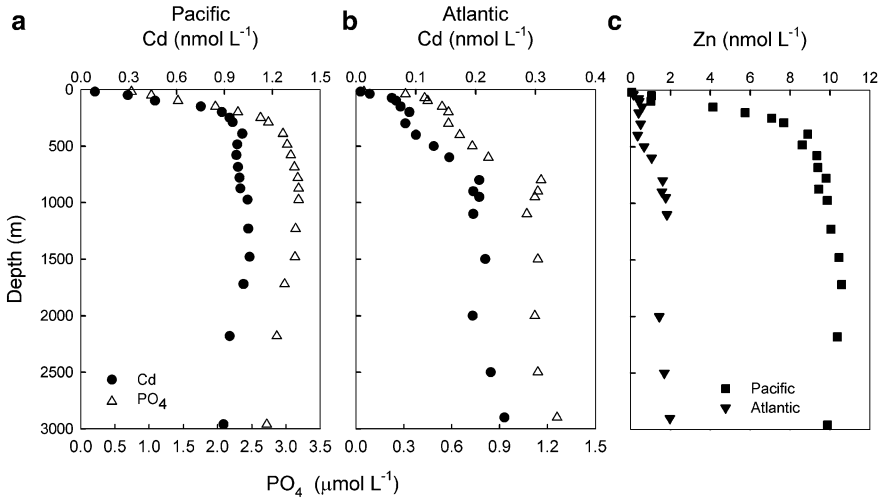

Figure 1 The distribution of phosphate, Cd, and Zn in the Pacific and Atlantic oceans. Pacific data are from station T7 (50.0°N, 145.0°W) [15]; Atlantic data are from a station at 47.0°N, 20.0°W [8].

both open ocean and coastal upwelling regions [6,7,11–14]. The strong correlation between dissolved Cd and P concentrations in seawater is also seen in suspended particles, further confirming that the distribution of Cd is governed by biological activity [11,12]. Vertical mixing of Cd-rich deep water to the surface is the main input of Cd to the surface waters of the open ocean while atmospheric deposition is insignificant [7,12].

The concentration of dissolved Cd in the open ocean is on the order a few pmol L^{-1} at the surface, around 1 nmol L^{-1} in the deep Pacific, and sub-nmol L^{-1} in the deep Atlantic [7,8,14–16] (Figure 1). In surface seawater, the bulk of dissolved Cd is complexed to organic ligands with high conditional stability constants (log $K'_{CdL,Cd'} \approx 9.8–10.9$) [14,16]. As a result, the inorganic Cd concentration, Cd′, which is dominated by chloride complexes (97.2%) [17] is maintained in the sub-pmol L^{-1} range, [14,16,18]. Microorganisms are presumably the source of the strong organic ligands that bind Cd in surface seawater; they likely also release weaker ligands that are not detectable by current electrochemical techniques. For example, in an estuary where the dissolved Cd concentration is elevated by anthropogenic activities, most of the Cd is complexed by organic ligands with a mean conditional stability constant of 8.9 (log $K'_{CdL,Cd'}$) [19]. As discussed below, the formation of weak Cd complexes may enhance the bioavailability of Cd to phytoplankton [20].

The demonstration that Cd might be utilized as a nutrient by phytoplankton – as implied by its nutrient-like profile in the ocean – came from culture studies in which the growth rate of Zn-limited phytoplankton species was markedly increased by addition of Cd to the medium (Figure 2) [21]. The concentration of bioavailable free Zn in the surface waters of the open ocean is indeed quite low [14,22–25] and in the range found to limit phytoplankton growth in cultures [24–26]. Some field studies have in fact found evidence of Zn-limitation of primary production in ocean water [27–29]. It is therefore plausible that phytoplankton may take up Cd to replace Zn for biological functions in the Zn-depleted conditions of the surface ocean.

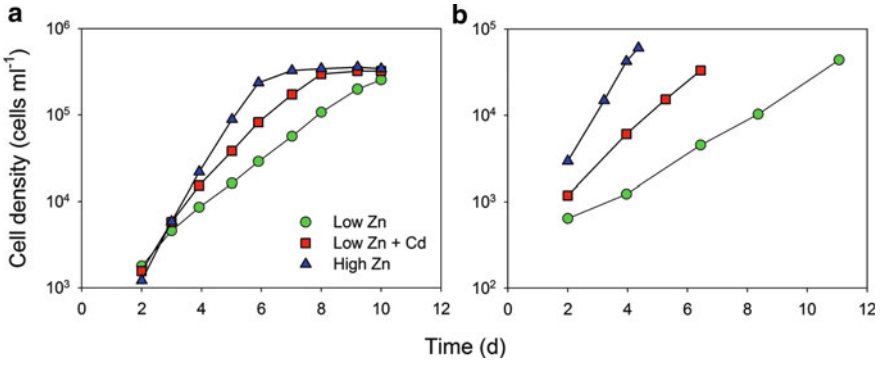

Figure 2 Growth curves of *Emiliania huxleyi* (**a**) and *Thalassiosira weissflogii* (**b**) under various inorganic Zn (Zn′) and Cd (Cd′) concentrations. (**a**): low Zn = 0.7 pmol L^{-1} Zn′; low Zn + Cd = 0.7 pmol L^{-1} Zn′ and 20 pmol L^{-1} Cd′; high Zn = 15 pmol L^{-1} Zn′. Data from [37]. (**b**): low Zn = 4 pmol L^{-1} Zn′; low Zn + Cd = 4 pmol L^{-1} Zn′ and 30 pmol L^{-1} Cd′; high Zn = 20 pmol L^{-1} Zn′. Unpublished data from Y. Xu.

2.2 Isotope Composition

Recent measurements of the isotope composition of Cd in seawater and marine Fe-Mn deposits provide insight into the processes that affect the biogeochemical cycle of Cd [30–34]. An inverse correlation between dissolved Cd concentration and the $^{112}Cd/^{110}Cd$ and $^{114}Cd/^{110}Cd$ ratios in the upper water column suggests that the isotope composition of Cd is controlled by Rayleigh fractionation [30–33]. A systematic trend has also been observed in the isotope signal of Cd in marine Fe-Mn deposits [34]. This isotope fractionation is consistent with a preferential uptake of the light Cd isotope by phytoplankton, as also seen in the only culture study using a freshwater phytoplankton species [31]. In accord with this interpretation, the lack of measurable isotopic fractionation of Cd observed in the northwest Mediterranean Sea simply reflects the small depletion of Cd in these waters [31]. Different negative correlations between the $^{112}Cd/^{110}Cd$ ratio and Cd concentration in different regions of the Southern Ocean indicate that the physiological status and species composition of the phytoplankton may cause variations in the fractionation of Cd isotopes [30].

In contrast to the upper water column, deep water has rather uniform and small Cd isotopic fractionation despite the fact that Cd concentrations increase along the global deep-water pathway from the Atlantic to the Pacific Ocean [31–34]. The Cd in deep water that is remineralized from exported organic matter, must thus have a small Cd isotopic fractionation [32]. To the extent that the bulk of the surface Cd is taken up by phytoplankton, this result is not inconsistent with isotopic fractionation by phytoplankton: the isotopic composition of any nutrient in the biomass must converge to that of the source (upwelled) water when the fraction of nutrient taken up increases, as observed, for example, for nitrogen [35]. More studies on Cd isotopic fractionation by different phytoplankton taxa under various conditions are warranted to help understand the isotopic composition of Cd in the oceans.

3 Effects of Cadmium on Phytoplankton Growth

3.1 Beneficial Effect

As mentioned above, the first demonstration of the biological use of Cd in phytoplankton was obtained with Zn-limited cultures of the diatom *Thalassiosira weissflogii* [21]. Since then the positive effect of Cd on growth rate under conditions of Zn limitation has also been observed in several other phytoplankton species such as *Thalassiosira pseudonana*, *Pleurophrysis carterae*, *Tetraselmis maculata*, and *Emiliania huxleyi* (Figure 2) [36,37]. In *E. huxleyi*, different strains have similar response to Cd addition suggesting that the use of Cd is a general attribute of Zn-limited *E. huxleyi* [37].

Two lines of evidence indicate that Cd is used to substitute for Zn either as a metal center in Zn proteins or in Cd-specific proteins that replace Zn proteins: (i) the beneficial effect of adding Cd in phytoplankton cultures can only be observed when Zn is limiting and is more pronounced when Zn is more limiting [21,37,38]; (ii) the size distribution of Zn and Cd in soluble intracellular proteins of *T. weissflogii* is remarkably similar [21]. However, Zn in phytoplankton cells can only be replaced partially by Cd and there is a minimum requirement for Zn that cannot be replaced by Cd [37,38]. For example, in *E. huxleyi* cells, only up to 50% of cellular Zn can be replaced by Cd [37]. Moreover, the use of Cd by phytoplankton is less efficient than that of Zn such that the growth rates observed upon addition of Cd to Zn-limited cultures are never as high as those of Zn-sufficient cultures (Figure 2) [9,37].

In *T. weissflogii*, carbonic anhydrases (CA) account for a major fraction of soluble Zn proteins especially under low pCO_2/high pH conditions. Addition of Cd to Zn-limited cultures of *T. weissflogii* restores CA activity [9,39]. This had led to the discovery of CDCA, the first and only known native Cd protein (see below). The utilization of Cd in CDCA explains, at least in part, the beneficial effect of Cd in Zn-limited cultures of other organisms that are known to also possess the *cdca* gene, including *T. pseudonana* [40]. But Cd must have other biochemical functions in phytoplankton than as a metal cofactor in CDCA since the beneficial effect of Cd is observed in organisms such as *T. maculata* and *E. huxleyi* that do not have the *cdca* gene. Cd also has a beneficial effect on cultures of *T. weissflogii* at high pCO_2/low pH condition when CDCA expression is down regulated (Xu, unpublished data).

3.2 Toxic Effect

It is well known that elevated Cd concentrations are toxic to phytoplankton and that different species have different sensitivity to Cd toxicity [36,41–46]. For example, in a comparison of phytoplankton taxa, Brand and coworkers showed that cyanobacteria were the most sensitive to Cd toxicity, and diatoms the least sensitive with coccolithophores and dinoflagellates having intermediate sensitivity [41]. Another study found no systematic differences among taxa [44]. Differences in sensitivity can also be found within the same genus; for example, oceanic *Thalassiosira* species are more resistant to Cd toxicity than coastal ones [45]. The free Cd ion concentration that causes 50% reduction in growth rate ranges from a few pmol L^{-1} to several hundred nmol L^{-1} [41,44].

The biochemical mechanisms of Cd toxicity in phytoplankton are in some respects similar to those in higher plants (see Chapter 13). One of the well-known effects is that Cd can compete with essential metals for uptake sites on the cell surface. High concentration of Cd inhibits the uptake of Mn and thus causes Mn deficiency in cells at low Mn concentrations [47–49]. Similarly, Cd also inhibits Fe uptake and assimilation and thus causes Fe deficiency, as evidenced by decreases in cytochrome *f* to chlorophyll *a* ratio and nitrate reductase activity

[50,51]. Interestingly, even at a concentration where it is beneficial to growth, Cd can become toxic if the Zn concentration becomes severely limiting [37,38]. This presumably reflects a loss of activity caused by Cd substitution for Zn in some essential Zn enzymes ([36,37] and references therein). Other mechanisms of Cd toxicity include oxidative stress, as reviewed in [52] and inhibition of photosynthesis via interference with the xanthophyll cycle in the diatom *Phaeodactylum tricornutum* [53].

The differences in sensitivity to Cd toxicity between phytoplankton species may be related to differences in their ability to detoxify the metal [43,44]. Cd-induced phytochelatin production is the most common detoxification mechanism in phytoplankton (see Section 5.1), but other thiol-containing peptides or proteins may also be involved. For example, a Cd-tolerant phytoplankton species, *Isochrysis galbana*, produces a metal-binding protein rich in cysteine [54]; the cyanobacterium *Synechococcus sp.* produces a metallothionein-like protein to complex metals [55]. In addition, some species may induce efflux systems to remove intracellular Cd [47,56,57], or sequester Cd into the vacuole to reduce the cytosolic Cd concentration [58].

4 Cadmium Uptake by Phytoplankton

4.1 Transport System and Effect of Manganese and Zinc

The molecular mechanism of Cd uptake by phytoplankton is not known but kinetic studies in the laboratory using cultured model species show that Cd may be taken up through two separate metal transport systems depending on the concentrations of competing metals [47]. Several studies showed that the rate of Cd uptake depends not only on the concentration of Cd, but also on the concentrations of Zn and Mn (Figure 3) [37,38,47,59,60]. The data can be interpreted quantitatively by considering that Cd is taken up competitively by the high affinity Zn uptake system under Zn-limited conditions and that Cd, Zn, and Mn share the same uptake system under Zn-sufficient conditions. Accordingly, Cd uptake kinetics follow a competitive saturation equation [59]:

$$V_{Cd} = \frac{V_{max1}[Cd^{2+}]_s K_{Cd1}}{[Cd^{2+}]_s K_{Cd1} + [Zn^{2+}]_s K_{Zn1} + 1} + \frac{V_{max2}[Cd^{2+}]_s K_{Cd2}}{[Mn^{2+}]_s K_{Mn2} + [Cd^{2+}]_s K_{Cd2} + [Zn^{2+}]_s K_{Zn2} + 1}$$

K values are the affinity constants for binding of the subscripted metals to the uptake ligands; V_{max1} and V_{max2} are the maximum uptake rates for the two systems; the free metal ion concentrations of Cd, Zn and Mn are those at the cell surface. The first term gives Cd uptake by the system induced at low cellular Zn and the second term uptake by Mn transport system. Interestingly, V_{max2} was found to equal V_{maxMn} in the coastal diatom *T. pseudonana*, indicating that both metals have similar internalization rate constants (k_{in}). This suggests that V_{maxCd} is controlled by a rate-limiting internalization step, e.g., physical movement of Cd across the membrane by transport molecules [47]. Similar effects of Mn and Zn on Cd uptake have been observed in field studies as well: the short-term Cd uptake rate and

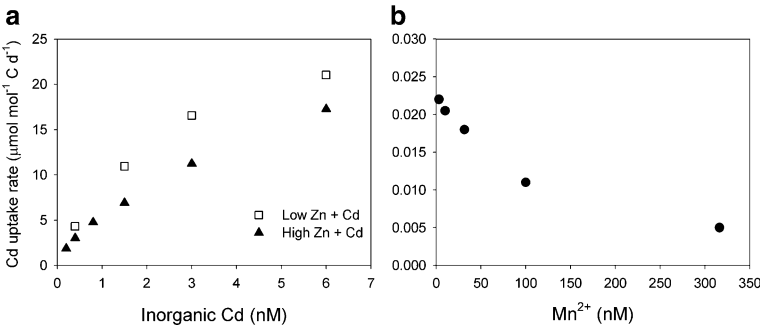

Figure 3 (**a**) Short-term Cd uptake rate by *T. weissflogii* preconditioned at different Zn concentrations in the presence of Cd. Low Zn + Cd: 1.6 pmol L^{-1} Zn′ and 460 pmol L^{-1} Cd′; High Zn + Cd: 16 pmol L^{-1} Zn′ and 460 pmol L^{-1} Cd′. Data are from [38]. (**b**) Short-term Cd uptake by *T. pseudonana* at different Mn concentrations. Data are from [48].

the cellular Cd:P ratio in natural assemblages were lower with addition of Zn or Mn [61,62] (Xu unpublished data).

Unlike Zn and Co, whose uptake rates can reach 60 to 90% of the maximum diffusion rates of unchelated Zn and Co to the cell surface, Cd uptake rate only reaches up to 20% of the maximum diffusion rate of unchelated Cd in *E. huxleyi* [37]. This may be because the dissociation of Cd^{2+} from the strong chloride complexes in seawater slows down the binding to uptake molecules [37].

4.2 *Effect of Other Metals and Macronutrients*

Both laboratory culture studies and shipboard incubation experiments have shown that cellular Cd concentrations are elevated in Fe-limited phytoplankton cells [60,63]. For example, the average estimated particulate Cd:P ratio in samples from Fe-limited waters was 2.3-fold higher than that from other samples [64]. The effect of Fe-limitation can be partly explained by biodilution since cells often grow slower under Fe limitation while the Cd uptake rate remains unchanged [60]. Another possible mechanism is uptake of Cd via a putative divalent metal transporter that is up-regulated under Fe-limitation [65].

Colloid-bound Cd is taken up by phytoplankton either through dissolution of Cd^{2+} or, possibly, through direct internalization of lipophilic colloid-bound Cd [66]. As is the case for other metals, Cd complexes with low molecular weight lipophilic organic ligands enter phytoplankton by passive diffusion across the plasma membrane [67].

4.3 *Effect of pH/pCO_2 on and Role of Weak Ligands in Cadmium Uptake*

Since Cd is used in CDCA in diatoms and CDCA expression is regulated by the pH/pCO_2 of seawater (see Section 6.1), we might expect that Cd uptake should be

affected by pH/pCO_2 as well. Indeed, field studies showed that the Cd:P ratio in natural assemblages dominated by diatoms increased as seawater pCO_2 decreased/pH increased and short-term Cd uptake was inversely related to seawater pCO_2 [20,61,62]. However, at low ambient Zn concentrations, the Cd uptake rate is only controlled by the bioavailable concentration, Cd′, and independent of seawater pH/pCO_2 [20]. In field samples, the Cd uptake rate decreased at lower pH [20]. This effect is likely explained by the role of weak organic complexes that make Cd bioavailable through a ligand exchange reaction with uptake ligands [68]. The decrease in Cd uptake at lower pH is caused by a lower concentration of bioavailable weak complexes, while Cd′ is maintained constant by complexation to a strong ligand. This effect has been demonstrated in the laboratory using simultaneously EDTA and cysteine to complex Cd [20,68]. Therefore, both strong and weak complexing agents in surface seawater may play an important role in controlling the bioavailability of Cd (and other essential metals) to phytoplankton.

4.4 Phytoplankton Species

A survey study that measured the elemental composition of marine eukaryotic phytoplankton species in cultures showed that all 15 species take up Cd under Zn replete condition, and in general, coccolithophores have the highest Cd quota followed by diatoms and then green algae [69]. Another culture study showed that oceanic diatoms have higher Cd quota than prymnesiophytes [64]. It seems that higher Cd quota in oceanic phytoplankton is an intrinsic trait reflecting their potential to substitute Cd for Zn in a Zn-poor environment. Consistently, Cd quotas in oceanic particles are much larger than the reported coastal values ([69] and references therein).

5 Cadmium and Thiol Production

5.1 Phytochelatins

Phytochelatins are small metal-binding polypeptides with the general formula $(\gamma\text{-Glu-Cys})_n\text{-Gly}$ (n = 2–11) produced by organisms in response to metal exposure. Cd is the most effective inducer of phytochelatins in marine phytoplankton, resulting in cellular phytochelatin content more than 10 times that induced by other metals such as Cu or Pb at similar concentrations [70–74]. Although phytoplankton produce phytochelatins even without metal exposure, the production of intracellular phytochelatins is elevated significantly with Cd addition even at picomolar concentrations [71,75] (Figure 4). In general, the production of intracellular phytochelatins is well correlated with the free or inorganic Cd concentrations in phytoplankton culture medium [71,75–79] (Figure 4). The ubiquity of phytochelatin synthesis in response to Cd exposure suggests that phytochelatin production is the primary detoxification mechanism in phytoplankton.

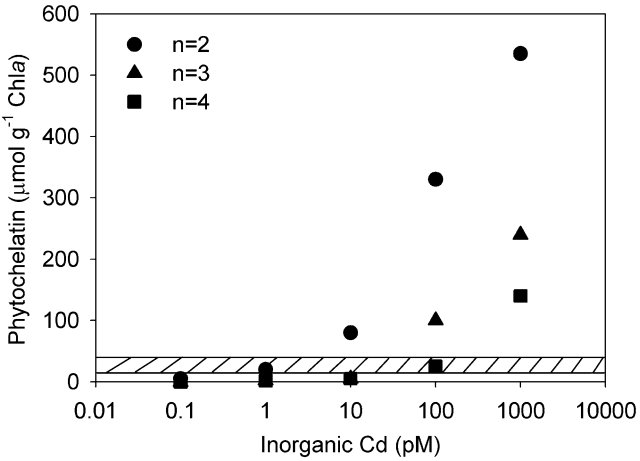

Figure 4 Phytochelatin ($(\gamma$-Glu-Cys$)_n$-Gly, n = 2, 3, and 4) concentrations in *T. weissflogii* induced by Cd exposure (closed symbols, data are from [70]) and the range of phytochelatin (n = 2) concentrations found in the top 50 m in the Equatorial Pacific (shaded area, data are from [74]).

Although the oligomer chain lengths of phytochelatins may vary in different species, the shorter oligomers (n = 2 and 3) are the predominant forms in most species and the stoichiometric ratio of phytochelatin to intracellular Cd is maintained at 2 to 4 γ-Glu-Cys per Cd at high Cd concentrations [75,80,81]. However, other studies also found that the ratio of intracellular Cd to phytochelatin increased with increasing $[Cd^{2+}]$ [82,83]. It seems that the production of phytochelatins is tightly regulated in cells to detoxify Cd and to maintain Cd homeostasis. A kinetic study showed that phytochelatin was rapidly accumulated in *T. weissflogii* and *P. tricornutum* cells shortly after Cd exposure and then the concentration rapidly decreased once Cd stress was removed [70,84]. At high Cd concentrations ($Cd' > 1$ nM), *T. weissflogii* and *T. pseudonana* cells export Cd as well as phytochelatin, suggesting that cells export the Cd-phytochelatin complexes to maintain low internal Cd concentrations as part of the detoxification mechanism [57,85]. Although the dissolved phytochelatin may be removed quickly by microbial degradation, phytochelatins released by phytoplankton may nonetheless be a source of organic metal-complexing agents in seawater [85].

The production of phytochelatins in response to Cd exposure is also modulated by the presence of other metals. For example, the production of phytochelatins induced by Cd exposure decreased with addition of Zn or Co, probably because these metals compete with each other for transporters and cellular binding sites and addition of Zn and Co decreases Cd uptake and thus the cellular Cd concentrations [74,86,87]. A similar antagonistic effect has been observed between Cd and Mn as well [87]. However, synergistic effects were also observed between Cd and Cu with higher production of phytochelatins in the presence of both Cd and Cu than that in the presence of individual metals [87]. Therefore, the interaction of metals may partly explain the lack of correlation between phytochelatin concentrations measured in natural seawater and metal concentrations [74,85].

Major nutrients may also affect the production of phytochelatins in response to Cd exposure but the effect may vary between species. For example, at stationary phase caused by major nutrient limitation, *E. huxleyi* did not increase the production of phytochelatins with time of Cd exposure but *T. pseudonana* did [76].

Besides detoxification, phytochelatins likely play a role as a buffer of intracelllar Cd and perhaps, more generally, in trace metal homeostasis. Such a role is suggested by the fact that phytochelatin synthesis is induced even at metal concentrations much below those that affect the growth of phytoplankton [57,72,75]. This is consistent with the remarkably high affinity of the phytochelatin synthase of *T. pseudonana* for one of its substrates, Cd-GS_2 [88]. Also, contrary to the general trend of decreasing phytochelatins with decreasing metal concentrations, phytochelatin concentrations increase at very low Zn concentration when Cd becomes beneficial to phytoplankton [74]. This is likely the explanation for the relatively high concentrations of phytochelatin observed in the metal-poor surface water of the Equatorial Pacific (Figure 4). I*n vitro* experiments show that Cd complexed to phytochelatin can be incorporated in CDCA [89]. However, there is yet no evidence that phytochelatin delivers Cd to a functional protein *in vivo*.

5.2 Other Thiols

Besides phytochelatins, other thiols are also produced in marine phytoplankton in response to Cd exposure. The cellular glutathione [GSH = (γ-Glu-Cys)-Gly, the precursor of phytochelatin] concentration remains relatively constant upon Cd exposure in various phytoplankton species even as phytochelatin concentration increases many folds [73,76,87,90]. Apparently, cells tightly regulate their GSH concentration, presumably because of its essential role in cellular functions, particularly the detoxification of reactive oxygen species [91]. The production of other low molecular weight thiols varies among species. For example, γ-Glu-Cys increased in response to Cd exposure in *E. huxleyi*, *T. weissflogii*, and *P. tricornutum* but remained constant in *T. pseudonana* and was below detection in *Dunaliella sp*. [76,87]. *E. huxley*i also produces Cys, Arg-Cys, and Gln-Cys and the concentrations of the former two thiols increased at higher [Cd^{2+}]. The presence of other metals like Zn and Cu at high concentrations suppresses thiol production in *E. huxleyi* [90].

The coccolithophore *E. huxleyi* releases a variety of thiols into the external medium upon exposure to elevated Cd concentrations [90]. Cys and GSH were the primary thiols released by cells exposed to Cd only, whereas γ-Glu-Cys was the primary thiol when Cu and Zn were also present at high concentrations. Like phytochelatins, these low molecular weight thiols released by phytoplankton may also serve as organic metal-complexing agents in surface seawater.

6 Cadmium Carbonic Anhydrase

Cadmium carbonic anhydrase (CDCA) is the first member of a new class of carbonic anhydrases, the ζ class. CDCA1, which uses Cd as its metal cofactor when Zn is limiting, was isolated from the marine diatom *T. weissflogii*. The amino acid sequence of CDCA1 contains a triple repeat with ~85% identity between repeats [10]. CDCA1 is a key enzyme in the carbon concentrating mechanism (CCM) through which *T. weissflogii* increases the concentration of CO_2 at the site of fixation by RuBisCO [92].

6.1 Cadmium Carbonic Anhydrase Expression

The regulation of CDCA expression, has been studied in detail in the diatom *T. weissflogii*. The expression of CDCA1 at transcript and protein levels is modulated by both pCO_2 and metal concentrations in the growth medium [61,93]. The *cdca1* transcript level at steady state increases with decreasing pCO_2 [93]. At low pCO_2, the CDCA protein abundance increases with the concentration of available Zn in the absence of Cd and increases with the concentration of available Cd when Zn is limiting (Figures 5a and b). Interestingly, the cellular concentration of another CA, TWCA1 also increases upon Cd addition, although this enzyme can only use Zn or Co as its metal center. The effect of Cd on the concentration of TWCA1 is interpreted as the re-allocation of Zn from CDCA1 upon incorporation of Cd (Figure 5b). Upon addition of Cd in Zn-limited cultures, the *cdca1* transcript level increases by a factor of 2 in 4 hours and then decreases slightly at 24 hours, while CDCA1 protein abundance increases gradually over time [93].

A CDCA homolog, TpCDCA, containing only a single sequence (25.5 kDa) has been identified in the genome of the diatom *T. pseudonana*, [10]. The expression of TpCDCA at both transcript and protein levels is also regulated by metal availability and pCO_2 level, with an increase in expression with decreasing pCO_2 and increasing Zn availability [94]. Similar results have been observed in the field. In water samples from Great Bay, New Jersey, *cdca* transcript level and protein abundance increased as the pCO_2 of the medium decreased, coincident with an increase in CA activity (Figure 5c and d) [93,94]. In samples collected off the Peruvian coast, synthesis of a CDCA-like protein was induced by incubation at low pCO_2 (pH = 8.6) or with addition of Cd [93]. Interestingly, only a 26-kDa protein was revealed by CDCA antiserum in samples from the Great Bay whereas a 70-kDa protein in samples from the Peruvian coast, suggesting that a single sequence of CDCA was the dominant form expressed in the Great Bay and a three-repeat form off the Peruvian coast [93,94].

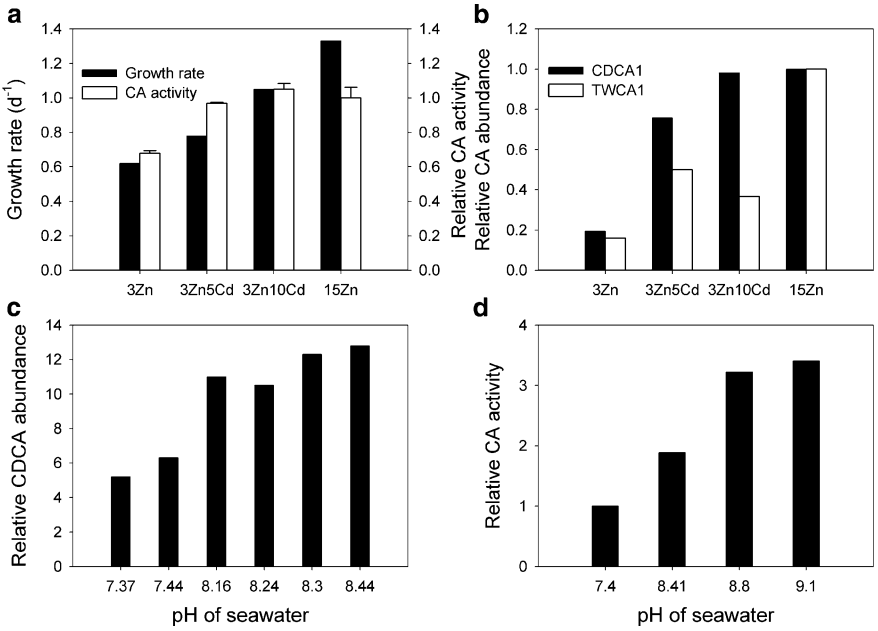

Figure 5 (**a**) and (**b**): CA expression in *T. weissflogii* under various Zn′ and Cd′ (unpublished data from Y. Xu). 3Zn = 3 pmol L^{-1} Zn′; 3Zn5Cd = 3 pmol L^{-1} Zn′ and 5 pmol L^{-1} Cd′; 3Zn10Cd = 3 pmol L^{-1} Zn′ and 10 pmol L^{-1} Cd′; 15Zn = 15 pmol L^{-1} Zn′. (**a**): black bars are growth rate and white bars are relative CA activity; (**b**): black bars are relative CDCA1 abundance and white bars are relative TWCA1 abundance. The pH of the cultures was around 8.8 at the time of measurements for CA activity and CA abundance. (**c**) and (**d**): CA expression in natural assemblages collected from the Great Bay, New Jersey (data are from [93,94]). pH values at the time of measurements for CDCA abundance and total CA activity are indicated on the x-axis.

6.2 *Diversity of cdca*

CDCA, the only known Cd protein, was first identified in the model diatom *T. weissflogii*. Homolog genes have so far been found exclusively in diatom species [40,93]. They have also been found in all environmental samples that have been tested, suggesting that the use of Cd in CDCA likely accounts, at least partially, for the nutrient-like behavior of Cd in the oceans.

cdca-like genes have been amplified from about two thirds of the diatom species that have been tested but not from any other phytoplankton taxa [40]. The translated amino acid sequences from these genes are very similar to each other and over 64% identical to TpCDCA. Phylogenetic analysis showed that these sequences can be clustered into three groups: the Tw group, the Np group, and the Tp group (Figure 6). Interestingly, unlike the 18 S rRNA gene, the CDCA sequences show no clear difference between pennate and centric diatoms.

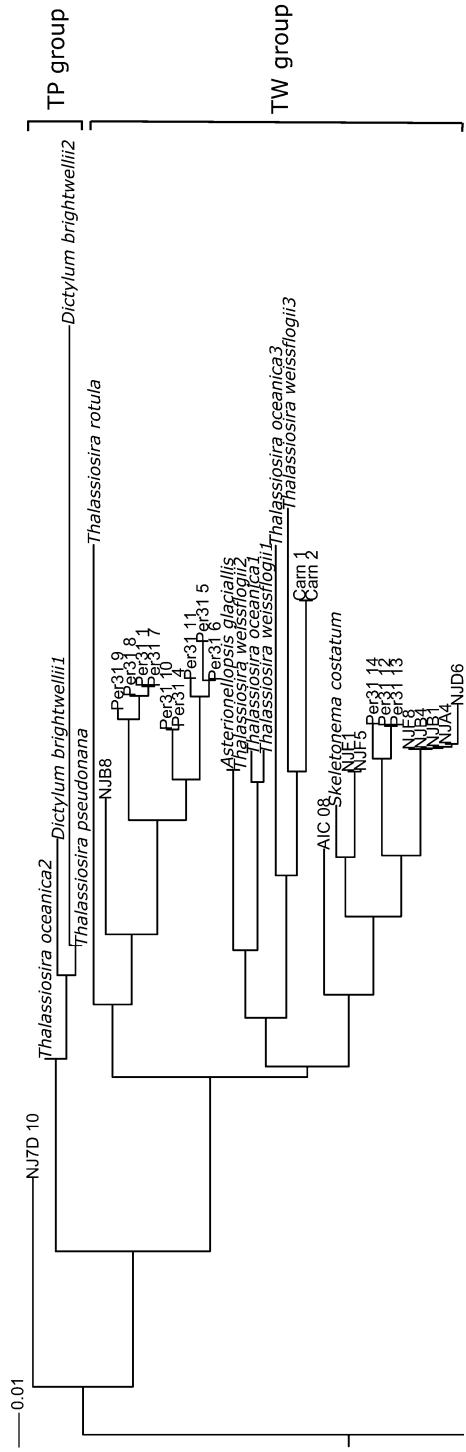
TP group
TW group
Dictylum brightwellii2
Thalassiosira rotula
Per31 9
Per31 8
Per31 7
Per31 10
Per31 4
Per31 11
Per31 5
Per31 6
Asterionellopsis glaciallis
Thalassiosira weissflogii2
Thalassiosira oceanica1
Thalassiosira weissflogii1
Thalassiosira oceanica3
Thalassiosira weissflogii3
Carn 1
Carn 2
Thalassiosira oceanica2
Dictylum brightwellii1
Thalassiosira pseudonana
NJB8
AIC 08
Skeletonema costatum
NJE1
NJF5
Per31 14
Per31 12
Per31 13
NJE8
NJB4
NJB1
NJA4
NJD6
NJ7D 10
0.01

Figure 6 Phylogenetic tree of translated amino acid sequences of CDCA-like genes from cultured diatoms and environmental samples [40].

cdca-like sequences have also ben found in four geographically distinct environments: the New Jersey coast, Lake Carnegie in New Jersey, the Arabian Sea, and the Peruvian coast [40,93]. These environmental sequences are over 80% identical to TpCDCA at the amino acid level. The variation in these sequences is substantial between environments but very small within the same environment and even smaller within the same water sample. Most of the environmental sequences fall within the Np group and can be clustered into four subgroups. The rest of the sequences fall within the Tw group and are clustered into one subgroup that is similar to *Skeletonema costatum* but separated from other centric diatoms (Figure 6). Interestingly, two sequences closely related to CDCA1 were identified in a freshwater sample (Lake Carnegie); it should be noted that *Thalassiosira* species are widely distributed in both freshwater and marine environments.

6.3 Structure and Properties of Cadmium Carbonic Anhydrase

The 3D structures of all three repeats of CDCA1 have been determined by X-ray [89,95]. The overall structure is a novel protein fold without similarity to any other proteins reported in the Protein Data Bank (Figure 7a). In the active site, Cd is bound to three conserved residues (Cys, His, and Cys) and a water molecule to form a complete tetrahedral coordination (Figure 7b). Interestingly, although CDCA has no sequence homology to any other CAs, it contains five highly conserved residues found in β-CAs [93]. The active site conformation of CDCA1 also closely resembles that of the β-CA, indicating a common catalytic mechanism between these two types of CA. Strikingly, a monomer of a CDCA single repeat is a structural and functional mimic of a β-CA dimer. The fundamental differences between the structures of ζ-CA and β-CA, together with the similarity of their functional units offer a remarkable example of convergent evolution.

Studies showed that CDCA1 repeats are sensitive to sulfonamide and sulfamate derivatives and other anion inhibitors and the inhibition constants are comparable to that observed in β-CAs [95–97]. Intriguingly, *in vitro* experiments have demonstrated that Cd in the active site of CDCA1 can be readily substituted by Zn, and *vice versa* (Figure 7d). The facile metal exchange is explained by a stable opening of the active site in the absence of metal (Figure 7c). A 9-amino acid linker sequence with a Gly residue on each end provides flexibility to open and close the active site. Loss of the metal exchange capability in the mutants in which either of the two Gly residues was mutated to Ala has been observed (Figure 7d). CDCA1 is a very fast enzyme with a catalytic efficiency near the diffusion limit. Although the Zn form of the enzyme has higher catalytic activity than the Cd form, both are sufficiently fast to satisfy the needs of fast growing diatoms, a significant competitive advantage in the low metal environment of the oceans [89].

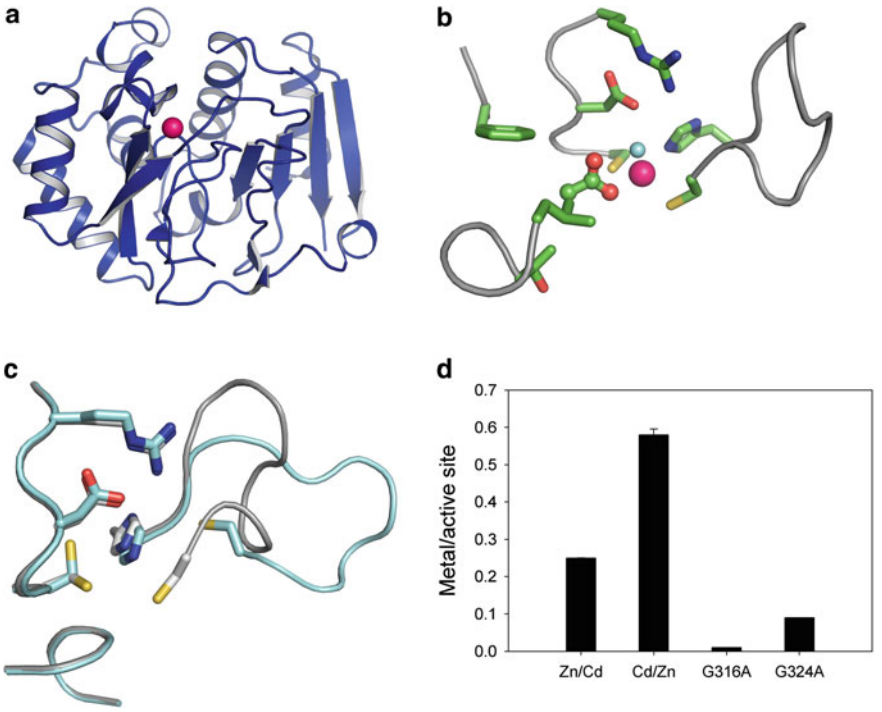

Figure 7 (**a**) Overall structure of CDCA repeat 2 with Cd (purple ball) at the active site. (**b**) The active site of CDCA repeat 2. The substrate analog, acetate, a water molecule (blue ball), and Cd (purple ball) are shown in the active site. (**c**) Comparison of the active site conformation between metal-free CDCA repeat 1 (cyan) and the Cd-bound CDCA repeat 1 (grey). (**d**) Metal exchange in CDCA1 repeat 2. Bars represent the amount of exchanged metal at the active site after 24 hr incubation with Zn- or Cd-phytochelatin complexes. Zn/Cd: Zn in CDCA-R2 was exchanged by Cd; Cd/Zn: Cd in CDCA-R2 was exchanged by Zn; G316A and G324A: Cd in mutants was exchanged by Zn (see text). Data are from [89].

7 Concluding Remarks and Future Directions

It is now clear that, like many other trace metals, Cd can be either beneficial or detrimental to phytoplankton depending on conditions. The bioavailability of Cd is mainly determined by the presence of complexing agents. Although Cd complexed by strong organic ligands is generally not bioavailable, new data show that Cd complexed by relatively weaker organic ligands can be taken up by phytoplankton. Elucidating the chemistry, origins, and function of the strong and weak ligands in seawater remains a great challenge.

Phytochelatins and other thiol-containing compounds produced and released by phytoplankton presumably contribute to the pool of metal binding ligands, but it is unclear how stable these compounds are in seawater and whether they play a significant role in the complexation of metals such as Cd.

According to kinetic studies, Cd is actively taken up by phytoplankton via either the Mn or Zn transport systems depending on ambient concentrations. Other factors such as Fe limitation and ambient pH may also contribute to the variation in Cd uptake rates observed in cultures or natural assemblages. Cd has toxic effects on growth at elevated concentrations and various species have different sensitivities and detoxification mechanisms. Cd also enhances the growth of a number of phytoplankton species under Zn-limitation. Fundamental studies are required to characterize molecules involved in transporting Cd in and out of cells, shuttling Cd into different cellular compartments for storage/detoxification or biochemical use and maintaining Cd homeostasis. At present, the only known biochemical use of Cd is to serve as a metal cofactor in CDCA in marine diatoms. However, Cd is beneficial to the growth of Zn-limited phytoplankton even in situations where CDCA is clearly not involved. There are likely other biochemical functions of Cd in marine phytoplankton that await to be discovered.

Abbreviations

CA	carbonic anhydrase
Cd′	inorganic Cd, including Cd complexes with the major inorganic ligands of seawater and Cd^{2+}
CDCA	cadmium carbonic anhydrase
Cd-GS_2	(gluathionato)-Cd complex
EDTA	ethylenediamine-N,N,N',N'-tetraacetic acid
GSH	glutathione
RuBisCO	ribulose-1,5-bisphosphate carboxylase/oxygenase
Zn′	inorganic Zn, including Zn complexes with the major inorganic ligands of seawater and Zn^{2+}

References

1. C. B. Field, M. J. Behrenfeld, J. T. Randerson, P. Falkowski, *Science* **1998**, *281*, 237–240.
2. F. M. M. Morel, *Geobiology* **2008**, *6*, 318–324.
3. M. Kasuya, *Water Sci. Technol.* **2000**, *42*, 147–154.
4. T. Y. T. Ng, W. X. Wang, *Environ. Toxicol. Chem.* **2005**, *24*, 2299–2305.
5. K. Chong, W. X. Wang, *Environ. Toxicol. Chem.* **2000**, *19*, 1660–1667.
6. E. A. Boyle, F. Sclater, J. M. Edmond, *Nature* **1976**, *263*, 42–44.
7. K. W. Bruland, *Earth Planet. Sci. Lett.* **1980**, *47*, 176–198.
8. J. H. Martin, S. E. Fitzwater, R. M. Gordon, C. N. Hunter, S. J. Tanner, *Deep-Sea Res. Part II* **1993**, *40*, 115–134.
9. T. W. Lane, F. M. M. Morel, *Proc. Natl. Acad. Sci. USA* **2000**, *97*, 4627–4631.
10. T. W. Lane, M. A. Saito, G. N. George, I. J. Pickering, R. C. Prince, F. M. M. Morel, *Nature* **2005**, *435*, 42–42.
11. K. W. Bruland, G. A. Knauer, J. H. Martin, *Limnol. Oceanogr.* **1978**, *23*, 618–625.
12. K. W. Bruland, K. J. Orians, J. P. Cowen, *Geochim. Cosmochim. Acta* **1994**, *58*, 3171–3182.
13. L. G. Danielsson, *Mar. Chem.* **1980**, *8*, 199–215.

14. M. J. Ellwood, *Mar. Chem.* **2004**, *87*, 37–58.
15. J. H. Martin, R. M. Gordon, S. Fitzwater, W. W. Broenkow, *Deep-Sea Res., Part A* **1989**, *36*, 649.
16. K. W. Bruland, *Limnol. Oceanogr.* **1992**, *37*, 1008–1017.
17. R. H. Byrne, L. R. Kump, K. J. Cantrell, *Mar. Chem.* **1988**, *25*, 163–181.
18. C. M. Sakamoto-Arnold, A. K. Hanson, D. L. Huizenga, D. R. Kester, *J. Mar. Res.* **1987**, *45*, 201–230.
19. P. B. Kozelka, K. W. Bruland, *Mar. Chem.* **1998**, *60*, 267–282.
20. Y. Xu, D. Shi, L. Aristilde, F. M. M. Morel, *Limnol. Oceanogr.* **2012**, *57*, 293–304.
21. N. M. Price, F. M. M. Morel, *Nature* **1990**, *344*, 658–660.
22. K. W. Bruland, *Limnol. Oceanogr.* **1989**, *34*, 269–285.
23. M. C. Lohan, P. J. Statham, D. W. Crawford, *Deep-Sea Res. Part II* **2002**, *49*, 5793–5808.
24. L. E. Brand, W. G. Sunda, R. R. L. Guillard, *Limnol. Oceanogr.* **1983**, *28*, 1182–1198.
25. W. G. Sunda, S. A. Huntsman, *Limnol. Oceanogr.* **1992**, *37*, 25–40.
26. M. A. Anderson, F. M. M. Morel, R. R. L. Guillard, *Nature* **1978**, *276*, 70–71.
27. K. H. Coale, *Limnol. Oceanogr.* **1991**, *36*, 1851–1864.
28. D. W. Crawford, M. S. Lipsen, D. A. Purdie, M. C. Lohan, P. J. Statham, F. A. Whitney, J. N. Putland, W. K. Johnson, N. Sutherland, T. D. Peterson, P. J. Harrison, C. S. Wong, *Limnol. Oceanogr.* **2003**, *48*, 1583–1600.
29. V. M. Franck, K. W. Bruland, D. A. Hutchins, M. A. Brzezinski, *Mar. Ecol.: Prog. Ser.* **2003**, *252*, 15–33.
30. W. Abouchami, S. J. G. Galer, H. J. W. de Baar, A. C. Alderkamp, R. Middag, P. Laan, H. Feldmann, M. O. Andreae, *Earth Planet. Sci. Lett.* **2011**, *305*, 83–91.
31. F. Lacan, R. Francois, Y. C. Ji, R. M. Sherrell, *Geochim. Cosmochim. Acta* **2006**, *70*, 5104–5118.
32. S. Ripperger, M. Rehkamper, D. Porcelli, A. N. Halliday, *Earth Planet. Sci. Lett.* **2007**, *261*, 670–684.
33. Z. C. Xue, M. Rehkamper, M. Schonbachler, P. J. Statham, B. J. Coles, *Anal. Bioanal. Chem.* **2012**, *402*, 883–893.
34. A. D. Schmitt, S. J. G. Galer, W. Abouchami, *Earth Planet. Sci. Lett.* **2009**, *277*, 262–272.
35. D. M. Sigman, M. A. Altabet, D. C. McCorkle, R. Francois, G. Fischer, *J. Geophys. Res., [Oceans]* **2000**, *105*, 19599–19614.
36. J. G. Lee, F. M. M. Morel, *Mar. Ecol. Prog. Ser.* **1995**, *127*, 305–309.
37. Y. Xu, D. Tang, Y. Shaked, F. M. M. Morel, *Limnol. Oceanogr.* **2007**, *52*, 2294–2305.
38. J. G. Lee, S. B. Roberts, F. M. M. Morel, *Limnol. Oceanogr.* **1995**, *40*, 1056–1063.
39. F. M. M. Morel, J. R. Reinfelder, S. B. Roberts, C. P. Chamberlain, J. G. Lee, D. Yee, *Nature* **1994**, *369*, 740–742.
40. H. Park, B. Song, F. M. M. Morel, *Environ. Microbiol.* **2007**, *9*, 403–413.
41. L. E. Brand, W. G. Sunda, R. R. L. Guillard, *J. Exp. Mar. Biol. Ecol.* **1986**, *96*, 225–250.
42. G. S. Braek, D. Malnes, A. Jensen, *J. Exp. Mar. Biol. Ecol.* **1980**, *42*, 39–54.
43. M.-J. Wang, W.-X. Wang, *Aquat. Toxicol.* **2009**, *95*, 99–107.
44. C. D. Payne, N. M. Price, *J. Phycol.* **1999**, *35*, 293–302.
45. P. D. Tortell, N. M. Price, *Mar. Ecol. Prog. Ser.* **1996**, *138*, 245–254.
46. A. J. Miao, W. X. Wang, P. Juneau, *Environ. Toxicol. Chem.* **2005**, *24*, 2603–2611.
47. W. G. Sunda, S. A. Huntsman, *Sci. Total Environ.* **1998**, *219*, 165–181.
48. W. G. Sunda, S. A. Huntsman, *Limnol. Oceanogr.* **1996**, *41*, 373–387.
49. J. R. Reinfelder, R. E. Jablonka, M. Cheney, *Environ. Toxicol. Chem.* **2000**, *19*, 448–453.
50. G. I. Harrison, F. M. M. Morel, *J. Phycol.* **1983**, *19*, 495–507.
51. P. L. Foster, F. M. M. Morel, *Limnol. Oceanogr.* **1982**, *27*, 745–752.
52. E. Pinto, T. C. S. Sigaud-Kutner, M. A. S. Leitao, O. K. Okamoto, D. Morse, P. Colepicolo, *J. Phycol.* **2003**, *39*, 1008–1018.
53. M. Bertrand, B. Schoefs, P. Siffel, K. Rohacek, I. Molnar, *FEBS Letters* **2001**, *508*, 153–156.
54. G. H. Wikfors, A. Neeman, P. J. Jackson, *Mar. Ecol. Prog. Ser.* **1991**, *79*, 163–170.
55. R. W. Olafson, W. D. McCubbin, C. M. Kay, *Biochem. J.* **1988**, *251*, 691–699.

56. T. Brembu, M. Jorstad, P. Winge, K. C. Valle, A. M. Bones, *Environ. Sci. Technol.* **2011**, *45*, 7640–7647.
57. J. G. Lee, B. A. Ahner, F. M. M. Morel, *Environ. Sci. Technol.* **1996**, *30*, 1814–1821.
58. Y. Nassiri, J. L. Mansot, J. Wery, T. Ginsburger-Vogel, J. C. Amiard, *Arch. Environ. Contam. Toxicol.* **1997**, *33*, 147–155.
59. W. G. Sunda, S. A. Huntsman, *Environ. Sci. Technol.* **1998**, *32*, 2961–2968.
60. W. G. Sunda, S. A. Huntsman, *Limnol. Oceanogr.* **2000**, *45*, 1501–1516.
61. J. T. Cullen, T. W. Lane, F. M. M. Morel, R. M. Sherrell, *Nature* **1999**, *402*, 165–167.
62. J. T. Cullen, R. M. Sherrell, *Limnol. Oceanogr.* **2005**, *50*, 1193–1204.
63. J. T. Cullen, Z. Chase, K. H. Coale, S. E. Fitzwater, R. M. Sherrell, *Limnol. Oceanogr.* **2003**, *48*, 1079–1087.
64. E. S. Lane, D. M. Semeniuk, R. F. Strzepek, J. T. Cullen, M. T. Maldonado, *Mar. Chem.* **2009**, *115*, 155–162.
65. E. S. Lane, K. Jang, J. T. Cullen, M. T. Maldonado, *Limnol. Oceanogr.* **2008**, *53*, 1784–1789.
66. W. X. Wang, L. D. Guo, *Mar. Ecol. Prog. Ser.* **2000**, *202*, 41–49.
67. J. T. Phinney, K. W. Bruland, *Environ. Sci. Technol.* **1994**, *28*, 1781–1790.
68. L. Aristilde, Y. Xu, F. M. M. Morel, *Environ. Sci. Technol.* **2012**, *46*, 5438–5445.
69. T. Y. Ho, A. Quigg, Z. V. Finkel, A. J. Milligan, K. Wyman, P. G. Falkowski, F. M. M. Morel, *J. Phycol.* **2003**, *39*, 1145–1159.
70. B. A. Ahner, F. M. M. Morel, *Limnol. Oceanogr.* **1995**, *40*, 658–665.
71. B. A. Ahner, N. M. Price, F. M. M. Morel, *Proc. Natl. Acad. Sci. USA* **1994**, *91*, 8433–8436.
72. B. A. Ahner, F. M. M. Morel, in *Prog. Phycol. Res.*, Eds F. E. Round, D. J. Chapman, Biopress Ltd., Bristol, UK, 1999, Vol. 13, pp. 1–31.
73. S. K. Kawakami, M. Gledhill, E. P. Achterberg, *J. Phycol.* **2006**, *42*, 975–989.
74. B. A. Ahner, J. G. Lee, N. M. Price, F. M. M. Morel, *Deep-Sea Res. Part II* **1998**, *45*, 1779–1796.
75. B. A. Ahner, S. Kong, F. M. M. Morel, *Limnol. Oceanogr.* **1995**, *40*, 649–657.
76. B. A. Ahner, L. P. Wei, J. R. Oleson, N. Ogura, *Mar. Ecol. Progr. Ser.* **2002**, *232*, 93–103.
77. M. J. Wang, W. X. Wang, *Environ. Sci. Technol.* **2008**, *42*, 8603–8608.
78. E. Morelli, G. Scarano, *Chem. Speciat. Bioavail.* **1995**, *7*, 43–47.
79. E. Morelli, L. Fantozzi, *Bull. Environ. Contam. Toxicol.* **2008**, *81*, 236–241.
80. E. Torres, A. Cid, P. Fidalgo, C. Herrero, J. Abalde, *Aquat. Toxicol.* **1997**, *39*, 231–246.
81. J. W. Rijstenbil, J. A. Wijnholds, *Mar. Bio.* **1996**, *127*, 45–54.
82. M. J. Wang, W. X. Wang, *Aquat. Toxicol.* **2009**, *95*, 99–107.
83. M. J. Wang, W. X. Wang, *Aquat. Toxicol.* **2011**, *101*, 377–386.
84. E. Morelli, G. Scarano, *Mar. Environ. Res.* **2001**, *52*, 383–395.
85. L. P. Wei, B. A. Ahner, *Limnol. Oceanogr.* **2005**, *50*, 13–22.
86. S. Kawakami, M. Gledhill, E. Achterberg, *Biometals* **2006**, *19*, 51–60.
87. L. P. Wei, J. R. Donat, G. Fones, B. A. Ahner, *Environ. Sci. Technol.* **2003**, *37*, 3609–3618.
88. T. Gupton-Campolongo, L. M. Damasceno, A. G. Hay, B. A. Ahner, *J. Phycol.*, in press.
89. Y. Xu, L. Feng, P. D. Jeffrey, Y. G. Shi, F. M. M. Morel, *Nature* **2008**, *452*, 56–U53.
90. C. L. Dupont, B. A. Ahner, *Limnol. Oceanogr.* **2005**, *50*, 508–515.
91. C. L. Dupont, T. J. Goepfert, P. Lo, L. P. Wei, B. A. Ahnerz, *Limnol. Oceanogr.* **2004**, *49*, 991–996.
92. F. M. M. Morel, E. H. Cox, A. M. L. Kraepiel, T. W. Lane, A. J. Milligan, I. Schaperdoth, J. R. Reinfelder, P. D. Tortell, *Funct. Plant Biol.* **2002**, *29*, 301–308.
93. H. Park, P. J. McGinn, F. M. M. Morel, *Aquat. Microb. Ecol.* **2008**, *51*, 183–193.
94. P. J. McGinn, F. M. M. Morel, *Physiol. Plant.* **2008**, *133*, 78–91.
95. V. Alterio, E. Langella, F. Viparelli, D. Vullo, G. Ascione, N. A. Dathan, F. M. M. Morel, C. T. Supuran, G. De Simone, S. Maria Monti, *Biochimie,* in press.
96. F. Viparelli, S. M. Monti, G. De Simone, A. Innocenti, A. Scozzafava, Y. Xu, F. M. M. Morel, C. T. Supuran, *Bioorg. Med. Chem. Lett.* **2010**, *20*, 4745–4748.
97. Y. Xu, C. T. Supuran, F. M. M. Morel, in *Handbook of Metalloproteins*, Ed A. Messerschmidt, John Wiley & Sons Ltd., Chichester, UK, 2010, Vol. 4 & 5, pp. 717–721.

ERRATUM

Chapter 10
Natural and Artificial Proteins Containing Cadmium

Anna F.A. Peacock and Vincent L. Pecoraro

DOI 10.1007/978-94-007-5179-8_17

The correct authors' affiliations for Chapter 10 should be:

A.F.A. Peacock (✉)
School of Chemistry, University of Birmingham, Edgbaston B15 2TT, UK
e-mail: a.f.a.peacock@bham.ac.uk

V.L. Pecoraro
Department of Chemistry, University of Michigan, Ann Arbor,
Michigan 48109, USA
e-mail: vlpec@umich.edu

A. Sigel, H. Sigel, and R.K.O. Sigel (eds.), *Cadmium: From Toxicity to Essentiality*,
Metal Ions in Life Sciences 11, DOI 10.1007/978-94-007-5179-8_10,

Index

A
AAS. *See* Atomic absorption spectrometry
ABC proteins, 13, 382, 426
Acetic acid or acetate, 89, 121, 197, 248, 355
  hydroxy-, 202–204
  iminodi-, 180–182
  nitrilotri-, 73, 180, 361
Acetonylphosphonate (AnP^{2-}), 200, 201, 263
Acetoxymethyl ester, 104
N-Acetylcysteine, 282–284, 297, 452
N-Acetyl-β-D-glucosaminidase, 93, 94, 433, 444
N-Acetylglycine, 280, 286
Acetyl phosphate (AcP^{2-}), 200, 201, 263
Acidity constants (of), 5, 196–199, 224, 344
  buffers, 250
  dinucleotides, 254, 255
  imidazole derivatives, 205, 206
  nucleosides, 198, 204, 208, 211, 213
  nucleotides, 225, 228–233, 235–239, 242, 246
  orotidine, 215
  phosphate monoesters, 219, 220
  pyridine derivatives, 205, 206, 211, 213
  thiouridines, 216, 217
  xanthosine, 215, 216
Acid rain, 420
Acridine orange, 462
Actin
  α-smooth muscle, 460
Activating transcription factor 6 (ATF6), 452, 469
Acute Cd toxicity (*see also* Toxicity of Cd), 417, 426–428
  animal studies, 427, 428
  biomarkers, 436, 437
  high dose, 18, 426
  ingestion, 427
  inhalation, 426, 427
  prevention, 445
  therapy, 424, 446
Acyclic nucleotide analogues, 243–245
Acyclovir, 150
Adamantane
  -like cage, 173, 174
  -like metal-thiolate clusters, 352, 360
Adefovir. *See* 9-[2-(Phosphonomethoxy)ethyl]-adenine
Adenine and derivatives (*see also* individual names)
  complexes, 147–151, 154, 183, 200, 204, 205, 223, 231, 234, 235, 240, 241, 244, 251, 253, 260, 261, 263
  9-methyl-, 150, 206
  N3 protonation, 151
  nucleotide translocase, 456
  9-[2-(phosphonoethoxy)ethyl]- ($PEEA^{2-}$), 245, 265
  9-[2-(phosphonomethoxy)ethyl]- ($PMEA^{2-}$), 227, 241, 243–246
Adeninium(1+) cation, 148, 150
Adenosine, 194, 198
  Cd complexes, 206
  7-deaza-. *See* Tubercidin
  2'-deoxy-. *See* 2'-Deoxyadenosine
  ε-, 240, 241, 264
Adenosine 5'-diphosphate (ADP^{3-}), 199, 200, 204, 230, 232–234
Adenosine 2'-monophosphate ($2'AMP^{2-}$), 199, 200, 204, 233, 234
Adenosine 3'-monophosphate ($3'AMP^{2-}$), 199, 200, 233, 234
Adenosine 5'-monophosphate (AMP^{2-}), 223, 224

A. Sigel, H. Sigel, and R.K.O. Sigel (eds.), *Cadmium: From Toxicity to Essentiality*, Metal Ions in Life Sciences 11, DOI 10.1007/978-94-007-5179-8,

Adenosine 5'-monophosphate (AMP^{2-}) (*cont.*)
ε- (ε-AMP^{2-}). *See* 1,N^6-Ethenoadenosine phosphates
(N1)oxide, 240
cyclic. *See* Cyclic adenosine 3',5'-monophosphate
metal complexes, 226–229, 231
ternary complexes, 251–253
Adenosine 5'-*O*-thiomonophosphate, 242, 243
Adenosine 5'-triphosphate (ATP^{4-}), 147, 223, 230–233, 258–260, 263, 387, 408, 451, 469
-binding cassette sub-family C member 2 (ABCC2), 426
Cd complexes, 231, 233, 240
2'-deoxy, 231
depletion, 458, 459, 463
dependent efflux-pumps, 375, 399
ε- (ε-ATP^{4-}). *See* 1,N^6-Ethenoadenosine phosphates
hydrolysis, 232, 241, 499
production, 455, 461
ternary complexes, 247–253
ADP^{3-}. *See* Adenosine 5'-diphosphate
Adrenal
cancer, 430
glands, 441
Adrenocorticotropin (ACTH), 441
Aequorin, 457, 458
Aerosols, 65, 435, 494
Affinity constants. *See* Stability constants
Agency for Toxic Substances and Disease Registry (ATSDR), 24, 100, 113, 419, 469
Alanine or alaninate (Ala) and residues, 316, 322, 334
complexes, 155, 157–160, 183, 279, 280, 297, 299
β-Alanine
complexes, 279, 280
β-alanyl-L-histidine. *See* Carnosine
Albumin, 10, 20, 93, 94, 124, 291, 299, 424, 431, 448
α-lact-, 119, 123, 124
ATCUN motif, 291
parv-, 124
Albuminuria, 433
Aldehydes
mutagenic, 405
Algae (*see also* individual names), 397, 401
Cd uptake, 47
green, 400, 517
marine, 378, 396, 402
nutrients, 511
photosynthetic, 47
Alkali metal ions (*see also* individual elements), 101
Alkaline earth metal ions (*see also* individual elements), 11, 101, 220, 221
Alkaline phosphatase, 119–121, 124, 126–138, 437, 444
Allium
cepa, 406, 407
sativum, 406
Aluminum(III), 39
hydroxide, 41
silicate, 41, 66
Alyssum murale, 378
Alzheimer's disease, 100
America
Cd burden, 42
Cd production, 56, 57
Amide
groups/bond, 286, 289, 291, 293, 298
transitions, 346
Amines
N,N-bis(pyridin-2-ylmethyl)benzen-, 107
Cd complexes, 72, 73, 74, 76, 77, 197, 304
heterocyclic aromatic, 496
Amino acids (*see also* individual names)
aromatic, 340, 345
Cd complexes, 8, 20, 21, 64, 69, 72, 73, 76, 77, 94, 101, 129, 132, 134, 147, 155–160, 182, 198, 252, 260, 261, 275–285, 305–311, 315–320, 322, 328, 330, 340–346, 364, 431, 520, 521, 523, 524
characteristics of Cd complexes, 278, 279
coordinating side chains, 280–285
hydrophobic side chains, 279, 296
N-donor side chains, 279, 281, 282
non-coordinating side chains, 279, 280
O-donor side chains, 279, 281
polar side chains, 279
sulfur donor atoms (*see also* Cysteine), 282, 283
thioether ligands, 282–284
2-Amino-2-hydroxymethyl-propane-1,3-diol (Tris). *See* Tris
Aminolevulinic acid dehydratase (ALAD), 315
2'AMP. *See* Adenosine 2'-monophosphate
3'AMP. *See* Adenosine 3'-monophosphate
2-Aminohexanoic acid complexes, 279
2-Amino-2-hydroxymethyl-propane-1,3-diol. *See* Tris
2-Aminopentanoic acid complexes, 279

Ammonia, 456
complexes, 72, 245, 246, 251
Amyotrophic lateral sclerosis, 100
Analytical methods (*see also* individual methods), 87–90
detection limits, 88–91
quality control, 92
Analyses of Hazardous Substances in Biological Materials, 86, 88
Androgen, 465
effects, 466
receptor, 466
Anemia, 15, 18, 442
Animals (*see also* individual names)
carcinogen, 493, 494
Cd toxicity, 377
Anodic stripping voltammetry (ASV), 46, 47, 57
differential pulse, 79, 90, 91, 95
Antarctic, 38, 40
ice core, 36
Anthracene-based fluorescent sensors, 106
Anthropogenic Cd sources. *See* Cadmium, anthropogenic sources
Antibodies, 381
anti-human β2-M, 93
Anticorrosion agent, 3
Antioxidant(s) (*see also* individual names), 16, 18, 21, 402–404, 432, 435, 439, 452, 453, 463, 466, 468, 495, 496
defense mechanism, 16, 18, 432
enzymes, 402–404, 468, 496
in blood, 434
Antithrombin, 443
Antiviral drugs (*see also* individual names), 150, 243, 244
Apoplast, 375, 383
Apoptosis, 100, 101, 405, 430, 433, 439–441, 451–459, 461, 463–465, 492, 493, 498–500, 502, 503
necrosis switch, 458, 459
Apoptotic signaling pathways
calcium, 457, 458
calpains, 457
ceramides, 457
Aquatic environment. *See* Lakes, Ocean, River, *and* Water
Arabidopsis, 399
halleri, 377, 381, 382
thaliana, 376, 382, 383, 403, 404, 406
Arbuscular mycorrhizal fungi, 378
Arctic, 38
Monitoring and Assessment Program (AMAP), 40, 57
Ocean. *See* Ocean
Arginine and residues, 451, 519
complexes, 279, 280
kinase, 258
Aromatic amino acids (*see also* individual names), 340, 345
Arsenate Cd complexes, 71
Arsenic(III), 311, 315, 316, 436
exposure, 493
Artificial peptides, 309–325
α3D, 310, 324
coiled coils. *See* Coiled coils
EXAFS studies, 308, 312, 313, 326, 334
sequences, 310
Ascorbic acid or ascorbate, 404, 435, 468
glutathione cycle, 403
peroxidase, 403, 404, 408
Asia
Cd burden, 42
Cd production, 56
Asparagine (Asn) and residues
complexes, 155, 156, 183, 279, 297, 299
Aspartic acid or aspartate (Asp) and residues
complexes, 3, 155, 159, 160, 183, 276, 279, 281, 288, 296, 297, 299, 307, 334
ASV. *See* Anodic stripping voltammetry
Atherosclerosis, 15, 438, 439
Risk Factors in Female Youngsters (ARFY) study, 438, 469
Atmosphere
Cd in, 32, 35, 37–41, 45, 56, 78, 417, 419
Cd speciation, 64–66
Atomic absorption spectrometry (AAS), 87–90
graphite furnace (GF-AAS), 71, 88, 90, 95
Atmospheric Deposition and Impact on the Open Mediterranean Sea (ADIOS), 40, 57
ATP^{4-}. *See* Adenosine 5'-triphosphate
ATPases
Ca, 447, 449, 450, 458
Cd activation, 381
Cu activation, 381
Na/K, 432
Zn activation, 381
Atrazine, 406
Autofluorescence, 103, 107
Autophagolysosomes, 462
Autophagy, 21, 443, 452, 454, 457, 462, 463
Averrhoa carambola, 385

B
Bacteria
pathogenic, 377
epiphytic, 376
metallothioneins, 341, 355, 363
plant root colonizing, 385
Cd toxicity, 377
BAL. *See* British Anti-Lewisite
BAPTA (bis(*o*-aminophenoxy)ethane-N,N,N',N'-tetraacetate), 104–106, 113, 457, 463, 469
5-fluorophenoxy-, 359
Barium(II), 209, 239
nucleotide complexes, 212, 237
Base excision repair (BER), 461, 464, 492, 496, 498, 503
Bcl-2 proteins, 16, 456, 457, 464
Beclin-1, 462
Benzimidazole, 205
5-dimethylamino-2-(2-pyridinyl)-, 111, 113
Benzo[*a*]pyrene, 497, 500, 501
Bicine complexes, 249–251, 264
Binding constants (*see also* Stability constants), 501
Bioaccumulation coefficient, 374, 376, 377, 381, 384–386
Bioavailability of Cd, 40, 43, 47, 66, 512, 517, 525
Bioconcentration factor, 374
Biogeochemistry of Cd, 6–14, 31–57
continental crust (*see also* Earth crust), 34, 35
cycling, 47–56, 511
marine, 87
Biological samples
determination of Cd, 85–95
digestion of, 89–91
Biomarkers, 9, 14, 15, 22–25, 86–95
biological material, 86, 87
blood, 87
for Cd exposure and toxicity, 425, 434, 443–445, 463
for kidney diseases, 92
metallothionein, 443
β2-microglobulin, 93, 421, 444
quality control, 92
retinol-binding protein, 94, 444
urinary Cd excretion, 87, 443–445
Biomass, 419
burning, 36, 38
2,2'-Bipyridine (Bpy), 178, 201
in ternary complexes, 251–253
4,4'-Bipyridine, 159, 178, 179
Bis(*o*-aminophenoxy)ethane-N,N,N',N'-tetraacetic acid. *See* BAPTA
2-[Bis(2-hydroxyethyl)amino]-2-(hydroxymethyl)-1,3-propanediol (Bistris), 193, 249–251, 264
N,N-Bis(2-hydroxyethyl)glycine. *See* Bicine
Bismuth(III)
peptide complexes, 294, 311
N,N-Bis(pyridin-2-ylmethyl)benzenamine, 107
Bistris. *See* 2-[Bis(2-hydroxyethyl)amino]-2-(hydroxymethyl)-1,3-propanediol
Bladder
cancer, 429
Cd toxicity, 22
Blood
-brain barrier (BBB), 9, 440, 469
Cd in, 8, 86–95, 100, 421, 424, 425, 438, 447
glucose, 442
-testis barrier, 428
whole, 8, 89, 91, 92, 425
BODIPY (4,4-difluoro-4-bora-3a,4a-diaza-*s*-indacene). *See* Fluorescence probes
Bone
Cd in, 8, 9, 15, 17, 22, 24, 100, 170, 436, 437, 467, 493
mineral density, 9, 15
Boradiazaindacene (BODIPY)-based fluorescence probes, 107, 109, 110
Bovine cardiac Na^+-Ca^{2+} exchanger, 105
Brain, 446
Cd in, 9, 17, 100, 341, 440, 448, 466
damage, 15
Brassica
juncea, 406
napus, 400
Breast
cancer, 429, 465, 494, 499
Cd toxicity, 22, 503
milk, 426, 452
British Anti-Lewisite (2,3-dimercaptopropanol) (BAL), 175, 183, 446
Bromide
complexes, 67, 68, 150, 154, 161, 277
Brønsted–Guggenheim–Scatchard Specific Ion Interaction Theory (SIT), 67
BTC-5N. *See* Fluorescence sensors
Buffer(s)
acetate, 248
ammonium acetate, 355, 358

ammonium hydrogen carbonate, 355
Bicine, 249–251
Bistris, 249–251
borate, 248
complexes, 248–251
HEPES, 110–112
imidazole, 248
MOPS, 106
phosphate, 248
Tris, 248–251, 280–282, 284, 287, 292, 298
n-Butyl diphosphate, 230
n-Butyl phosphate, 225, 227

C
CadC proteins, 125, 306–308
Staphylococcus aureus pI258, 306
Cadherin, 20, 428, 439, 460, 502
Cadmian metacinnabar ((Hg,Cd)S), 34
Cadmium
^{109}Cd, 103, 360
^{110}Cd, 513
^{111}Cd NMR. *See* Nuclear magnetic resonance
^{111m}Cd, 5, 304, 308, 314–318, 320, 323–326, 328, 353, 354, 366
^{112}Cd, 127, 128, 513
^{113}Cd, 5, 118, 136, 262, 332, 333, 383
^{113}Cd NMR. *See* ^{113}Cd NMR
^{114}Cd, 513
anthropogenic sources, 3, 32, 33, 36, 37, 41, 65, 417–421, 512
atmosphere, 32, 35, 37–41, 45, 56, 64–66, 78, 417, 419
biochemistry, 6–14
biogeochemical cycling, 47–56
contamination, 383–386, 396, 397, 420
environment, 3, 31–57, 87, 92
history, 2
industrial use, 3, 418, 419
inhalation. *See* Inhalation of Cd
in ocean. *See* Ocean
in organs. *See* individual organs
in particulate matter, 66
mobilization, 3, 17, 35–37, 41
naturally rich habitats, 396
natural sources, 32, 35, 36, 65, 417, 419–421
occupational exposure, 15, 88, 91–93, 417–421, 425, 433, 434, 438, 445, 447, 492
ores, 34, 35
production, 36, 37
provisional tolerable weekly intake (PTWI), 23, 492
radioisotopes, 34, 103
reference dose and recommendations, 23, 24
release, amounts, 32, 33
technology and use, 3, 36–38, 66, 100, 396, 397, 419, 492
threshhold values, 420, 421
volcanic emission, 35
Cadmium(II) (in), 245–246, 253–262, 286, 289, 291–295, 297, 298
accidental intake, 14, 15
accumulation in plants (*see also* Excluder plants, Indicator plants, *and* Hyperaccumulator plants), 3, 374
acute high dose, 18, 426
acute toxicity. *See* Acute Cd toxicity
affected organs, 22, 23, 430–443, 503
and cancer. *See* Cancer
beneficial effect, 513, 514
binding to nucleic acids, 258–262
bioaccumulation. *See* Hyperaccumulator plants
bioavailability, 40, 43, 47, 66, 512, 517, 525
biological half-life, 3–6, 8, 418, 426, 428, 467
biological relevance, 3–6
biomarkers. *See* Biomarkers
blood. *See* Blood
body burden, 7, 8, 11, 13, 14, 87, 92, 95
carcinogenicity, 15, 17, 464, 465, 493, 494
class I carcinogen, 464, 493
complexes. *See* Cadmium(II) complexes
coordination chemistry, 3–6, 305–309, 326–329
coordination sphere. *See* Coordination spheres of Cd(II)
crystal structures of DNA/Cd/protein complexes, 259–261
determination in biological samples, 85–95
detoxification, 8, 170, 175, 293, 515, 517–519, 526
dichloride, 20, 47, 66, 68, 162, 278, 280, 432, 435, 436, 440, 449, 494, 499, 501
dinucleoside monophosphates binding, 257
DNA damage/mutagenicity and clastogenicity, 494, 495
entry pathways, 421–424
excretion, 425, 427, 467
homeostasis. *See* Homeostasis
hydrolysis (constant), 196, 278

Cadmium(II) (in) (*cont.*)
hydroxide, 67, 68, 71, 278
hyperaccumulation. *See* Hyperaccumulator plants
imaging and sensing, 99–113
in diet. *See* Diet
in phytoplankton. *See* Marine phytoplankton
interaction with metalloproteins. *See* Metalloproteins/Metalloenzymes
interdependency with other metals. *See* Interdependencies
intracellular (free), 6, 13, 103–107, 110–112
in waters. *See* Waters
isotope composition in seawater, 513
lithosphere, 34, 56, 65, 87, 91, 111, 378, 379, 417, 447
mechanism of toxicity. *See* Mechanisms of Cd toxicity
metalloestrogen, 465, 466
metallothioneins. *See* Metallothioneins *and* Mammalian metallothioneins
molecular level interactions, 500–502
nephrotoxicity. *See* Nephrotoxicity of Cd
organ toxicity. *See* Target organs for Cd toxicity
oxidative stress, 495,496
oxide, 34, 150, 419, 421, 426, 435, 439, 440, 494, 499, 501
phosphate ratio, 48–50, 55, 56, 516, 517
physical properties, 3, 4, 33, 34, 119, 195–198
pollution, 510
pro-apoptotic action, 16
proteome, 4
rescue experiments, 258, 259
resistant cells, 354
selenide, 34, 100
sequestration, 381, 383
signaling, 451, 450
speciation, 25, 42–44, 46, 47, 63–79
storage, 383
streams, rivers, and lakes, 42
sublethal exposure, 7
substituted metalloproteins, 346
substituted zinc proteins, 19, 349
sugar interactions, 198–204
sulfate. *See* Sulfate
sulfide. *See* Sulfide
telluride, 100
threshold values, 420, 421
toxicity. *See* Cadmium(II) toxicity
toxicology in mammalian organs. *See* Toxicology of Cd in mammalian organs
trafficking, 9–14, 18, 424, 425
transport, 9–14, 18, 44, 381, 382, 398, 424, 425, 515
uptake, 101, 104, 427, 446
uptake by phytoplankton, 515
uptake pathways, list, 448
urine. *See* Urine
Cadmium carbonic anhydrase (CDCA), 7, 340, 378, 401, 511, 514, 516, 519–525
diversity of, 521–524
expression, 520, 521
genes, 521
in diatoms, 340, 511, 516, 521
in phytoplankton. *See* Marine phytoplankton
phylogenetic analysis, 521–524
properties, 524, 525
sequences, 524
structure, 525
Cadmium(II) complexes (of), 63–79
amino acids and derivatives (*see also* Amino acids *and* individual names), 72, 278–285, 295–297
buffers, 249–253
carbohydrates, 198, 199
carbonyl interactions, 210, 212
characteristics, 278, 279
chloride. *See* Chloride
complexones, 73, 76, 77, 79
coordination spheres. *See* Coordination spheres of Cd(II)
detoxification, 422, 423, 468, 515
dichloride. *See* Cadmium(II), dichloride
dinucleotides, 254–257
histidine (*see also* Histidine), 289–291
hydroxyacetate, 202–204
metallothioneins. *See* Metallothioneins *and* Mammalian metallothioneins
mixed ligand, 249–253
(N3) purine bound, 148–150, 154, 234, 235
(N7) purine bound, 148–150, 154, 201, 226, 227, 237, 255–257, 260
NH_2(C6), steric inhibition, 210–212, 228, 231
nucleic acids (*see also* DNA *and* RNA), 258–263
nucleosides, 206, 208–214
nucleotides, 74, 212, 222–239, 248
O(C6) exocyclic purine bound, 151, 231, 237, 257, 260
peptides (*see also* individual names), 286–298

monoesters, 218–222
pyrimidines, 210–214
selective, 101, 107, 110, 111, 113
stability constants. *See* Stability constants
sugars, 198–204
thiolates. *See* Thiolate complexes
thiophosphates, 241–243
thiouridines, 216, 217
tubercidin, 214, 215
xanthosinate, 216
Cadmium(II) toxicity (for) or toxicology, 1–25, 64, 101, 103, 147, 304, 374, 395–409, 457, 458, 503
acute. *See* Acute Cd toxicity
bacteria, 377
chronic. *See* Chronic toxicity of Cd
fungi, 377
geno-. *See* Genotoxicity
in mammalian organs. *See* Toxicology of Cd in mammalian organs
mechanisms. *See* Mechanisms of Cd toxicity
nephro-. *See* Nephrotoxicity
plants. *See* Toxicity of Cd in plants
target organs. *See* Target organs for Cd toxicity *and* individual organs
Cadmiumuria, 9
Cadmoselite (CdSe), 34, 100, 176
Calbindin D_{9k}, 18, 124
mutants, 129–132
Calcite, 41
Calcitriol, 9
Calcium(II), 11, 101, 111, 239
apoptotic signaling pathways, 457, 458
binding proteins, 126–134, 449, 470
calmodulin. *See* Calmodulin
carbohydrate interaction, 199
carbonyl interactions, 210–214
channel. *See* Calcium channel
chemical properties, 195–198
complexes. *See* Calcium(II) complexes
deficiency, 420, 437
fluorescent probes, 104–106
flux, 10
homeostasis. *See* Homeostasis
hydrolysis constant, 196
interdependency with other metals. *See* Interdependencies
intracellular, 113
overload, 458
physical properties, 195–198
signaling, 17, 20, 21, 448–452, 455, 463, 500
transporter, 101, 456
uptake, 9
Calcium channel, 398, 433, 439
blocker, 105
L-type, 11
TRPV6, 423, 437
T-type, 11
vanilloid family, 11, 423
Calcium(II) complexes of
buffers, 249, 250
cytidine, 210, 212
hydroxyacetate, 202
nucleosides, 210–214
nucleotides, 226–228, 230–233, 237
phosphate monoesters, 220–222
pyridines, 210, 211, 213
Calciuria, 15
Callinectes sapidus, 136, 343
Calmodulin (CaM), 20, 118, 124, 129, 132–134, 138, 450, 502
crystal structure, 132, 134
fragments, 133
metal ion affinities, 451
Calpains, 457, 458
cAMP signaling, 451, 500, 502
Canalicular multispecific organic anion transporter 1, 426
Cancer or carcinoma (*see also* Carcinogenesis or carcinogenicity *and* Tumors), 15, 418, 429, 430, 435, 436, 453, 455, 459, 461, 464–466, 468, 491–503
adrenals, 430
bladder, 429
breast, 429, 465, 494, 499
endometrium, 429, 494
hematopoietic, 430
kidney, 430, 464, 493, 494
liver, 430
lung, 15, 430, 435, 436, 464, 493, 494, 499
pancreas, 429, 430
pituitary, 430
prostate, 430, 464, 466, 493, 494
Carbamate
diseleno-, 176
dithio-. *See* Dithiocarbamate
Carbohydrates (*see also* Sugars)
Cd complexes, 69, 72
hydroxyl coordination, 198, 199
metabolism, 402
Carbon
^{13}C-labeled proteins, 305, 341
^{13}C NMR. *See* Nuclear magnetic resonance

Carbon (*cont.*)
biogeochemical cycle, 511
Carbonate
Cd, 34, 67, 68, 71, 78
hydrogen, 355, 448
Zn, 2, 34, 417
Carbon dioxide, 456
in seawater, 514, 516, 517, 519
Carbonic anhydrase, 7, 47, 48, 193, 304, 511
Cd in. *See* Cadmium carbonic anhydrase
Co in, 520
human, 121
in diatoms, 340, 511, 516
Zn in, 378, 401, 514
Carbonyl groups, 130, 201
metal ion binding, 209–214, 231, 260, 298
oxidative production in proteins, 403
Carboxylic acids or carboxylates and groups, 64, 69, 70, 72–74, 76, 77, 130, 156–158, 164, 167, 168, 198, 235, 280, 281, 296, 346
poly-, 180–182
polyaminopoly-, 73
Carboxypeptidase A, 124
Carcinogenesis or carcinogenicity (in), 15, 17, 23, 100, 429, 430, 461, 464
animals, 493, 494
Cd, 15, 17, 464, 465, 493, 494
DNA damage response system, 496–500
epidemiological studies, 463
humans, 418, 493, 494
mechanisms, 464, 465, 500–502
Cardiovascular system
Cd toxicity, 438
Cd uptake, 439
damage, 439
disease, 418
Carnosine, 290
Caspases, 16, 452, 453, 455, 458, 459
Catalases, 16, 402, 408, 449, 452, 468, 469, 495, 496, 503
-deficient plants, 403, 404
Catenin, 459, 460
Cation diffusion facilitator, 381, 387
Cation exchanger, 381, 387
CD. *See* Circular dichroism
CD4/CD8 T-cell receptor, 19
^{113}Cd NMR (studies of) (*see also* Nuclear magnetic resonance), 71, 117–137, 262, 278, 280, 285, 287, 292, 294, 304, 332, 362, 383
^{113}Cd,^{1}H heteronuclear single quantum correlation (HSQC), 363, 364
^{113}Cd-^{13}C J coupling, 127–129
^{113}Cd-^{113}Cd spin coupling, 362
^{1}H-^{113}Cd dipolar relaxation, 121, 122
^{1}H-^{113}Cd heteronuclear multiple quantum correlation (HMQC), 118, 135, 136
alkaline phosphatase, 126–129
basic principles, 119–122
biological applications, 120
Ca-binding proteins, 125, 126, 129–134
CadC, 308, 326
calbindin D_{9k} mutants, 129–132
calmodulin, 132–134
chemical exchange broadening, 119, 120
chemical shifts for ^{113}Cd substitution, 120, 121, 123–126
chemical shifts, 117, 118, 120, 123, 125, 126, 130, 133, 134, 136,137, 328
coiled coils, 313–318, 320–329
coupling constants, 120, 135
exchange rate, 121
metallothioneins, 134–137, 342, 357, 359–365
nuclear Overhauser effect, 121, 122
relaxation properties, 121, 122
CDP^{3-}. *See* Cytidine 5'-diphosphate
Cells
Caco-2, 423
Cd-resistant, 354
CHO, 102, 104, 458
cos-7, 107
cycle regulation, 464, 493, 496, 499–501
dendritic, 110, 113
Hela, 102, 109, 111, 112, 498
imaging and sensing, 99–113
Kupffer, 434
LLCPK1, 432
macrophage, 112
NIH 3T3, 102, 112
organelles, 379, 380
PC12, 105, 108
respiration, 496
Saos-2, 107
Sertoli, 428, 440, 441
vascular endothelial, 428, 438, 439
vacuoles. *See* Vacuoles
Cell death, 12, 13, 16, 21, 101, 403, 405, 432, 435, 439, 444, 448, 450–459, 462, 464, 465, 468, 496
apoptosis. *See* Apoptosis
Bcl-2 proteins, 457
mitochondria, 455–456
necrotic, 101, 454, 458, 459
Cement production, 38
Center of Toxicology in the National Institute of Public Health of Québec, 92

Central nervous system, 15, 106, 440
Ceramides, 457, 465
Ceratophyllum demersum, 401, 404
Cerebrospinal fluid, 340
Ceruloplasmin, 20
Chaetoceros tenuissimus, 406
Chalcogenides (CdS, CdSe, CdTe), 100
Chalcopyrite, 35
Channels
  calcium. *See* Calcium channel
  ion. *See* Ion channels
  potassium, 20
  voltage-dependent anion, 456, 457
Charge-transfer
  ligand-to-ligand, 345
  ligand-to-metal, 308, 311, 312, 320, 324, 325, 327, 345–347, 350, 359
  photoinduced, 104
  to-solvent, 345, 366
Chelation therapy, 175, 176, 180, 446
Chemical exchange broadening, 119, 126
Chemical shift anisotropy (CSA), 121, 138
Chirooptical effects, 347
Chlamydomonas reinhardtii, 400
Chloride, 46, 161, 176, 277, 278, 512, 516
  complexes, 43, 47, 66–68, 78, 121, 150, 151, 153–155, 158, 159, 161–164, 168, 169, 173, 277, 278, 424
  di-. *See* Cadmium(II), dichloride
Chlorophyll, 48, 49, 399, 408, 514
  metal exchange, 400–402
Chlorosis, 401
CHO cells, 102, 104, 458
Chromate
  Cd complexes, 71
Chromatin fragments, 406
Chromatographic methods, 70, 383
  high performance liquid chromatography (HPLC), 70
  ion exchange, 70, 71
Chromosomes, 406, 407
  aberration, 496
Chronic
  Cd nephropathy, 430–432
  inflammation of the nose, 434
  low Cd exposure, 417, 418, 421, 425, 428–430, 433, 437, 441, 443, 450, 467, 468
  poisoning therapy, 446
Chronic toxicity of Cd (exposure), 417, 428–430, 441–443
  cancer, 429, 430
  prevention, 445
  teratogenicity, 429
  therapy, 446
Cigarette smoking (*see also* Smoking), 14, 418, 421, 429, 436
Circular dichroism (CD) (studies of), 299, 312, 321, 325, 334
  magnetic. *See* Magnetic circular dichroism spectroscopy
  metallothioneins, 342, 345–350, 366
Citrate, 3, 75, 91
Clara-cell protein, 444, 469
Class I carcinogen, 464
Clastogenicity, 494, 495
Cleft lips and palate, 429
Clubfoot, 429
Clusters (*see also* Coordination spheres of Cd(II) *and* Mammalian metallothioneins), 5, 311, 344, 352
  Cd_2S_6, 364
  Cd_3, 362
  Cd_3S_4, 173
  Cd_4, 362
  Cd_4S_6, 173, 174
  Cd_6, 136
  Cd_7, 344, 345
  Cu_6, 137
  dynamics, 340, 360
  $M(II)_3S_9$, 7, 344, 345, 362
  $M(II)_4S_{11}$, 7, 344, 345, 362
  M_2S_6, 344
  M_3Cys_9, 364
  $M_4S_9N_2$, 344, 363
  reactivity, 362
  Zn_6, 344
CmtR protein, 308, 309, 331
  Mycobacterium tuberculosis H37Rv, 308
CMP^{2-}. *See* Cytidine 5'-monophosphate
Cobalt(II), 239, 287, 288, 292, 349, 448, 465, 495
  carbohydrate interaction, 199
  carbonyl interaction, 201
  complexes. *See* Cobalt(II) complexes
  coordination numbers, 196
  hydrolysis constant, 196
  interdependency with other metals. *See* Interdependencies
  sequestration, 381
  uptake by phytoplankton, 516
Cobalt(II) complexes
  buffer complexes, 250
  dinucleoside monophosphate complexes, 257
  metallothioneins, 342, 346, 360

Cobalt(II) complexes (*cont.*)
nucleotide complexes, 213, 228–232
peptides, 287, 288, 292, 294
phosphate monoesters, 220, 221
pyrimidine complexes, 210–214
ternary complexes, 250, 252
xanthosinate, 216
Coccolithophores, 514, 517, 519
Coiled coils
^{111m}Cd PAC spectroscopy, 314–317
^{113}Cd NMR, 313–318, 320–329
BABY, 310, 328, 329, 331
CdS_3, 312, 313, 317–319, 322, 323, 325, 327, 329, 330, 332, 333
CdS_3/CdS_3O, 311–315
CdS_3O, 315–317, 320, 322, 323–327, 329, 330, 332, 333
CdS_4, 312, 319, 320, 326
CoilSer, 310, 328
GRAND, 310, 322–324, 327–333
MINI, 330
non-coded amino acids, 317–319
physical properties, 312, 314
structures, 315–317
thiol complexes, 312–317
three-stranded, 304, 310–313, 315, 317, 318, 320, 324, 325, 328, 333, 366
TRI, 310–322, 324–331
two-stranded, 319, 320
UV–vis spectroscopy, 311, 312, 320
Collagen I, 460
Commission for the Investigation of Health Hazards of Chemical Compounds in the Work Area, 86, 88
Community Bureau of Reference, 69, 79
Complexones (*see also* individual names), 64
Cd complexes, 73, 76, 77, 79
CONTAM report, 418, 420, 421
Continental runoff, 36
Coomassie Brilliant Blue reaction, 94
Co-operative Programme for Monitoring and Evaluation of the Long-Range Transmission for Pollutants in Europe (EMEP), 40, 57
Coordination spheres of Cd(II) (*see also* Clusters), 3, 5, 123, 157, 148–183, 193, 196, 221, 247, 248, 250, 251, 262, 296, 308, 322, 325, 344, 358, 359, 364
CdS, 34, 66, 100, 176, 243, 291, 494
CdS_3, 170, 308, 309, 311–323, 325–330, 332, 353
CdS_3N, 308
CdS_3O, 285, 308, 311–318, 320–333
CdS_4, 285, 298, 308, 312, 313, 315, 319, 320, 326, 350, 353
CdS_5, 308
Cu(I) complexes, 495
Ag(I) as probe, 342
metallotioneins, 134, 340–342, 352
Copper(II), 7, 8, 10, 17, 18, 20, 77, 101, 103, 137, 239, 305, 340–342, 384, 396, 399, 448, 495
^{64}Cu, 103
(N3) purine bound, 204
carbohydrate interaction, 199, 204
carbonyl interaction, 201, 204, 209
complexes. *See* Copper(II) complexes
coordination numbers, 196
detoxification, 324, 399
homeostasis. *See* Homeostasis
hydrolysis constant, 196
interdependency with other metals. *See* Interdependencies
nucleoside complexes, 208, 209, 212
phytochelatin induction, 517
sequestration, 383
Copper(II) complexes of
amino acids, 282, 297, 298
2'AMP, 204
buffers, 250, 251
nucleotides, 226, 229, 234, 235, 237
orotidine, 215
peptides, 286–291
phosphate monoesters, 220, 221
thiouridines, 216, 217
Copper-containing ferrooxidase, 20
Correlation spectroscopy (COSY)
^{113}Cd,^{113}Cd, 362
^{113}Cd,^{1}H, 362, 364
Cortical neurons, 11
Cotton effects, 346, 348
Coumarin (7-amino-4-methyl-coumarin), 110
5-nitrobenzothiazole-, 105
Creatine, 9
kinase, 344
Creatinine, 89, 92, 94, 433, 444, 445
Crustal enrichment factors, 39
Crystal structures (*see also* X-ray structures)
Ca_4CaM, 132
cadmium-thiolate complexes, 173
coiled coils, 316
determination methods, 147
pyrimidine complexes, 154, 155, 209
rat metallothionein-2, 176
trichomes, 375
vitamin B_3, 163
vitamin B_6, 163

CTP^{4-}. *See* Cytidine 5'-triphosphate
Cubilin, 444
Cyanate
  thio-, 162, 166–168
Cyanide Cd complex, 71
Cyanobacteria, 514, 515
  metallothioneins, 341
  Synechococcus PCC 7942, 345
Cyclic adenosine 3',5'-monophosphate ($cAMP^{2-}$) signaling, 451, 500, 502
Cyclic nucleotides, 241, 243–246
Cyclic voltammetry, 282
Cyclin D1, 460
Cyclosporin A, 456
Cysteine or cysteinate (Cys) and residues and complexes (*see also* Thiols or thiolates), 3, 7, 13, 20, 101, 113, 123–125, 136, 155, 157, 170, 184, 282–286, 291–293, 294, 296, 298, 299, 303–334, 339–366, 381, 423, 431, 435, 450, 463, 465, 466, 469, 497, 515, 517, 519
  N-acetyl-, 282–284, 297, 452
  S-methyl-, 282–284, 297
  methylester, 282–284
Cystic fibrosis trans-membrane conductance regulator, 13, 467
Cystine, 288
Cytidine (Cyd), 194, 198
  complexes, 209–214
  2-thio-, 214, 217, 218
Cytidine 5'-diphosphate (CDP^{3-}), 223, 229, 230
Cytidine 5'-monophosphate (CMP^{2-}), 223, 224
  complexes, 212, 213, 225, 226
  2'-deoxy. *See* 2'-Deoxycytidine
Cytidine 5'-triphosphate (CTP^{4-}), 223, 224
Cytochrome
  c, 453, 455–457
  f, 514
Cytokines
  pro-inflammatory, 434, 435
Cytosine (Cyt), 154, 155, 184, 194, 209, 217, 223, 226
  iso-, 155
  5-methyl-, 461
Cytosolic Ca^{2+} concentration, 450

D
DAB staining, 403, 404
Dead Sea, 68
7-Deazaadenosine. *See* Tubercidin
Debye-Hückel term, 67
Decadmiation technologies, 420
Deficiency of
  Ca, 420, 437
  Fe, 9, 379, 417, 420, 423, 442, 514
  Mg, 437
  Mn, 514
  Zn, 9, 382, 403, 408, 417, 420, 468
Dehydrogenases
  lactate, 444
  NADPH, 403
Dendritic cells, 110, 113
de novo peptide design (*see also* Peptides), 309–311
Density functional theory (DFT) calculations, 293
2'-Deoxyadenosine, 199
2'-Deoxyadenosine 5'-monophosphate ($dAMP^{2-}$), 229
2'-Deoxycytidine 5'-monophosphate ($dCMP^{2-}$)
  complexes, 212, 245
2'-Deoxyguanosine
  complexes, 206–208
2'-Deoxyguanosine 5'-monophosphate ($dGMP^{2-}$), 229, 255, 256
2'-Deoxy-3'-guanosine monophosphate, 235
1-(2-Deoxy-β-D-ribofuranosyl)thymine. *See* Thymidine
Detoxification (of)
  Cd, 422, 423, 468, 515
  Cu, 324
  Cu in roots, 399
  endogenous, 466–468
  Hg, 306
  metals, 379, 380, 383
  Zn, 423
Developmental signaling pathways
  hedgehog, 460
  Wnt/β-catenin, 459, 460
Diabetes type II, 15, 441, 442
Diabetic nephropathies, 9
Diacylglycerol, 450
Dialysis, 70
Diaminobenzidine, 403, 404
2,5-Diaminopentanoic acid. *See* Ornithine
2,6-Diaminopurine, 147, 149, 150
Diastereopeptides, 319
Diatoms (*see also* Phytoplankton *and* individual names), 7, 47–49, 55, 193, 195, 340, 406, 511, 513–517, 520, 521, 523, 524, 526

Diatoms (*cont.*)
blooming, 56
Cd carbonic anhydrase, 340, 511, 516, 521
oceanic (*see also* Marine phytoplankton), 49, 51–53, 406, 511, 513, 514, 526
Dielectric constant and properties (*see also* Permittivity), 305
Diels-Alder ribozyme, 260, 261
Diet
Cd in, 417, 418, 420, 421
iron-manipulated, 11
list of food, 420
vegetarian, 9
Diethylenetriamine (Dien), 208, 246
Diethylenetriamine-N,N,N',N'',N''-pentaacetate (DTPA), 73, 79, 446
Differential pulse anodic stripping voltammetry (DPASV), 79, 90, 91, 95
Dihydroxyacetone phosphate ($DHAP^{2-}$), 200, 201, 204
Diltiazem, 105
2,3-Dimercapropanol. *See* British Anti-Lewisite
2,3-Dimercapto-1-propanesulfonate (DMPS, Unithiol), 175, 183
Dimercaptosuccinic acid (DMSA), 175, 183, 446, 469
5-Dimethylamino-2-(2-pyridinyl)-benzoimidazole (DBI), 111, 113
1,4-Dimethylbenzimidazole (DMBI), 205
Dinoflagellates, 49, 514
Dinucleoside monophosphate complexes, 208, 253, 254, 257
Dinucleotide complexes, 253–257
Dioxygen, 456
Diphosphate(s)
n-butyl-, 230
methyl, 230
monoesters, 218–222
phenyl, 230
Di(2-picolyl)amine (DPA), 111, 112
Diseases (*see also* individual names)
Alzheimer's, 100
cardiovascular, 418
renal, 15, 93, 370, 429, 433, 470
heart, 453
Itai-Itai, 15, 22, 436–438, 442, 510
kidney (*see also* Kidney), 92, 93, 95
liver (*see also* Liver), 15
lung (*see also* Lung), 434, 435
neurodegenerative, 100, 453, 455
Parkinson's, 100
Diselenocarbamate, 176
Disruption of the blood-testis barrier, 428
Dissolved organic carbon or matter (DOC/DOM), 43, 57, 69, 70, 79
Dissociation constants (*see also* Stability constants)
Ca complexes, 104, 105
Cd complexes, 102, 104, 105, 107–110, 112, 259
Zn complexes, 104
Distribution coefficients, 43, 58
5,5'-Dithiobis-(2-nitrobenzoic) acid (DTNB), 361
Dithiocarbamate Cd complexes, 147, 176–180, 446
Dithiolate, 174–176, 183
Divalent metal transporter 1 (DMT1), 8, 11, 12, 48, 422,–424, 431–433, 438, 439, 448, 449, 469
DMSA. *See* Dimercaptosuccinic acid
DNA, 101, 194, 246
alkylation, 495–499
damage, 258, 405, 406, 430, 440, 452, 461, 464, 493–500, 502
damage response system, 494, 496–500
integrity, 405
methylation, 461, 493, 502
methyltransferases, 461
mutation (*see also* Mutation studies), 402
oxidative base modifications, 495–498
polymerase β, 260, 261
repair, 17, 19, 100, 125, 258, 405, 406, 430, 464, 492, 493, 496–499, 501–503
repair inhibition, 17, 461, 498, 501, 503
strand breaks, 402, 405, 495, 496, 498
transcription, 496
unwinding, 306
Donnan equilibrium, 71
DPASV. *See* Differential pulse anodic stripping voltammetry
Drosophila, 459
melanogaster, 407
Drugs (*see also* individual names), antiviral, 150, 243, 244
dThd. *See* Thymidine
$dTMP^{2-}$. *See* Thymidine 5'-monophosphate
DTPA. *See* Diethylenetriamine-N,N,N',N'',N''-pentaacetate
Dust
Cd in, 419, 421, 434, 435, 445, 492
Dunaliella sp., 519

E
Earth crust (*see also* Lithosphere)
Cd, 2, 36, 39, 65, 193, 417
Zn, 2, 417
EF hand motif, 20, 129–132, 134
Electric field gradient tensor, 353
Electric quadrupole moment, 352
Electronic d-d transitions, 342
Electron microscopy, 405
Electron spin resonance (EPR) (studies of), 261, 262, 401, 428
Co(II) metallothioneins, 342, 346
silent, 202
Electron transfer or transport, 452, 496
mitochondria, 101, 449
photoinduced, 103, 104, 106, 109
Electrophoresis
single cell gel, 406
Electroplating, 419
Electrospray ionization mass spectrometry (ESI-MS), 293, 299, 354, 358, 451
Electrothermal atomic absorption spectrometry (ET-AAS), 88
Emiliania huxleyi, 512–516, 519
Endocrine glands
Cd exposure, 441, 442
Endocytosis, 422, 423, 439, 444, 446, 447
receptor-mediated, 8, 14, 431, 432, 433, 446, 448, 472
Endometrium
cancer, 429, 494
Cd toxicity, 22, 503
Endonucleases, 17
apurinic/apyrimidinic, 17
Endoplasmic reticulum, 6, 450, 470
stress signaling, 452, 453, 457
Enterocytes, 10, 11, 423
Environment, 3, 31–57, 87, 92
Cd measurement, 32
cadmium speciation, 64, 65
Enzyme-linked immunosorbent assay (ELISA), 93–95
Enzymes (*see also* individual names)
Cd-substituted, 5
lignifying, 374
metallo. *See* Metalloproteins/Metalloenzymes
restriction, 306
Epidermal growth factor receptor, 435, 470
Epidermis, 380, 399, 405
Epigenetic effects, 15, 461, 462, 502
Epithelial-to-mesenchymal transition, 460, 470
EPR. *See* Electron spin resonance
Equilibrium constants (*see also* Stability constants), 67, 68, 224
Erythrocytes, 425, 448
Erythropoietin (EPO), 442
Escherichia coli, 118, 126, 341, 342
ESR. *See* Electron spin resonance
Estrogen, 465
metallo-, 465
receptor, 20, 25, 465, 466
Ethanedithiolate, 175
Ethanephosphonate, 227
1,N^6-Ethenoadenosine, 264
phosphates, 240, 241
Ethylenediamine (En), 151, 165, 176
Ethylenediamine-N,N'-diacetate (EDDA), 73, 80
Ethylenediamine-N,N,N',N'-tetraacetate (EDTA), 25, 73, 76, 79, 80, 180, 181, 183, 361, 397, 408, 446, 470, 517
Ethylene glycol-bis(2-aminoethylether)-N,N,N',N'-tetraacetate (EGTA), 73, 80, 457
9-Ethylguanine, 150
complexes, 208
Eukaryotes, 9, 49, 340
metallothioneins, 340
phytoplankton, 517
Europe
Cd burden, 9, 39, 40, 42
Cd production, 56
European Community, 23, 65, 418, 419
European Food Safety Authority (EFSA), 23, 418, 420, 492, 504
European Standard, Measurements and Testing (SM&T) program, 69, 80
EXAFS. *See* Extended X-ray absorption fine structure spectroscopy
Excluder plants, 374–376
Extended X-ray absorption fine structure spectroscopy (EXAFS), 66, 80, 285, 299, 381, 382, 387
artificial peptides, 308, 312, 313, 326, 334
metallothioneins, 351, 352, 366
Extinction coefficients, 110, 320, 346

F
FAO/WHO. *See* Joint Food and Agriculture Organization/World Health Organization
Fatty acids, 405
Feces
Cd excretion, 425, 426
Fenton reaction, 403, 428, 449, 452, 495, 496

Ferritin, 18
Ferrochelatase, 19
Ferroportin, 12, 423, 470
Fertilizer, 396, 418, 419
Fetus, 9, 22, 424, 429
  death, 429
Fibrinolysis, 439
Fibroblasts, 11, 12, 449, 456
Fibronectin, 460
Flavin adenine dinucleotide (FAD), 107, 113, 150
Flavin mononucleotide (FMN^{2-}), 236–239
Fluorescence imaging, 101, 103
Fluorescence probes
  BODIPY, 107, 109, 110
  Ca-selective, 104
  Ca/Zn, 104–106
  Cd-selective, 104
Fluorescence sensors, 101, 450
  anthracene-based, 106
  auto-, 103, 107
  BAPTA, 105, 450, 457, 463
  BTC-5N, 102, 105
  CadMQ, 102, 110, 111
  CYP-1, 102, 109
  CYP-2, 102, 109
  DBITA, 102, 111, 112
  DQCd1, 102, 112
  Fluo-3, 102, 104
  fluorescein-based, 109, 110
  Fura-2, 102, 104, 105, 450, 457
  Fura-5F, 102, 105
  Quin-2, 105
  yellow cameleon (YC3.60), 106
Fluoride Cd complexes, 67, 68
Formation constants. *See* Stability constants
Fossil fuels, 419
Fourier transform infrared spectroscopy (FT-IR), 349
Frankliniella occidentalis, 377
Fructose, 199
Fulvic acid
  Cd complexes, 69–71
Fungi
  arbuscular mycorrhizal, 378
  Cd toxicity, 377

G
Galena (PbS), 35
Gastrointestinal tract
  Cd in, 100, 422, 423, 426
  chronic exposure, 422
  Fe in, 423
Gel electrophoresis
  single cell, 406
Gene
  expression, 101, 398, 403, 406, 430, 461, 462, 465, 466, 500, 502
  metal transporter, 8, 11, 48, 305, 380, 382, 433
  transcription, 449–451
Genome
  instability, 496, 497, 503
  repair, 497
Genotoxicity, 398, 405–407, 430, 494–496
  Cd^{2+}-induced DNA damage, 405, 406
GEOTRACES program, 49, 57
German Commission "Human Biomonitoring", 92
German External Quality Assessment Scheme (E-QUAS), 92
German MAK Commission, 493, 494
GF-AAS. *See* Graphite furnace atomic absorption spectrometry
Gibbsite, 41
Global climate change, 57, 66
Globulin
  α1-micro-, 86, 93, 94, 444
  β2-micro-, 92, 93, 421, 431, 444
Glomerular filtration rate, 94, 433, 470
Glucose-, 199
  in blood, 442
  intolerance, 427
  in urine, 442
  transporters, 447
  regulated proteins, 453, 453, 470
Glutamic acid or glutamate (Glu) and residues, 155, 158, 184, 295, 299, 307, 332, 333, 435, 519
  poly-, 288
Glutamine (Gln) and residues, 332, 519
  complexes, 279, 299
γ-Glutamylcysteine synthase, 18
γ-L-Glutamyl-L-cysteinylglycine. *See* Glutathione
Glutathione (GSH), 4, 10, 13, 16, 19, 25, 79, 80, 101, 170, 286, 291–293, 295, 341, 404, 408, 422–424, 428, 435, 436, 446, 449, 452, 459, 467, 468, 470, 496, 519, 526
  Cd complexes, 13, 423, 426, 431, 432, 434, 439
  S-transferase, 342, 444
  peroxidase, 468, 495, 496
  reductase, 403, 408, 468, 496

Glycerol
diacyl-, 450
1-phosphate ($G1P^{2-}$), 200, 201, 204, 236, 239, 264
Glycinamide complexes, 280
Glycine or glycinate (Gly) and residues, 330
N-acetyl-, 280, 286
complexes, 10, 155, 156, 158, 159, 184, 249, 279, 280, 282, 284, 297, 299, 334
N-2-mercaptopropanoyl-, 282–284
Glycogen synthase kinase 3β, 463, 470
Glycosylases, 497, 498
G-protein coupled receptor, 17, 449–451, 500, 502
Goethite, 41
Graphite furnace atomic absorption spectrometry (GF-AAS), 71, 88, 90, 95
Greenockite, 34
Group I introns, 204, 259
Group II introns, 204, 259, 262
Growth hormone, 441, 470
Growth inhibitory factor, 358
Guanine (Gua) and derivatives, 149–151, 184, 194, 208, 211, 231, 235, 246, 255, 256, 259–261, 264
9-ethyl-, 150, 208
9-methyl-, 150
8-oxo-, 495, 498, 501
8-oxoguanine DNA glycosylase, 498, 501
Guanosine, 194, 198
Cd complexes, 206
2'-deoxy-. *See* 2'-Deoxyguanosine
Guanosine 5'-diphosphate (GDP^{3-}), 230–232
Guanosine 2'-monophosphate, 235
Guanosine 3'-monophosphate, 235
Guanosine 5'-monophosphate (GMP^{2-}), 224
cyclic, 451
metal complexes, 226–229, 255, 256
Guanosine 5'-triphosphate (GTP^{4-}), 231, 234
Gut, 449

H

Haber-Weiss reaction, 403
Hair
Cd in, 86, 88, 90, 91, 95, 426, 429
Halides (*see also* individual names)
as ligand, 166, 277, 278
Hammerhead ribozyme, 259–261
Hamster
Cd studies, 430, 436, 494
HDV ribozyme, 204
Heart, 458
disease, 453
Hedgehog proteins, 460
Helix-loop-helix motif, 129–132, 134, 449, 470
Heme oxygenase, 18, 404, 454
Heme proteins, 349
Hematopoiesis, 442–443
cancer, 430
Hemostasis, 442, 443
Hepatitis B, 243
Hepatocytes, 13
rat, 434
HEPES, 110–112
Herbivores, 377, 378
Hexafluoroleucine, 317
High nutrient-low chlorophyll ocean region, 49–55
High performance liquid chromatography (HPLC), 70
Himalaya, 38–40
Hippuric acid, 154
Histamine complexes, 253, 279, 282, 297
Histidine or histidinate (His) and residues
as N donor (*see also* Imidazole), 123, 124, 156, 307, 497
β-alanyl-L-histidine. *See* Carnosine
Cd complexes, 289–291
complexes, 279, 282, 297
in metallothioneins, 340, 344, 345, 358, 359, 363
in peptides, 289–291
Histone modification, 461, 462
Homarus americanus, 343
Homeostasis (of)
Ca, 448, 456, 458, 501
Cd, 518
Cu, 8, 18, 340, 467
essential metal ions, 17–19, 467, 519
Fe, 12, 448, 449, 501
Mg, 448
Mn, 12, 18, 448, 449
redox, 16, 17
Zn, 5, 6, 8, 12, 18, 340, 448, 449, 467, 501
Homo sapiens (*see also* Human), 343
Hormones (*see also* individual names), 20, 340, 341, 450
growth, 441
parathyroid, 436
pituitary, 441
steroid, 465, 503
thyroid stimulating, 441
HPLC. *See* High performance liquid chromatography

Human
metallothioneins, 345, 355–358, 360, 363
Humic acid
complexes, 43, 66, 69, 71
Hydrocarbons
aromatic, 496
Hydrocephaly, 429
Hydrogen peroxide, 48, 89–91, 121, 402, 403, 453, 459, 465, 495, 498
Hydrolysis constants, 196, 197
Hydrophobic sites, regions or interactions, 133, 252, 253, 311, 312, 316, 317, 321–323, 329–332, 358, 366
Hydroxo complexes, 251, 277
Hydroxyacetate, 202–204
1-Hydroxyethane-1,1-diphosphonic acid
complexes, 79
(4-(2-Hydroxyethyl)-1-piperazineethanesulfonic acid. *See* HEPES
Hydroxyl groups, 198, 199, 249–251
Hydroxyl radical ($HO^{\cdot}$), 361, 402, 449, 461, 495
Hydroxymethylphosphonate, 202, 203
o-(Hydroxymethyl)pyridine, 202, 203
8-Hydroxyquinoline, 106
Hyperaccumulator plants, 374, 375–387, 402
biotechnological use, 383–386
Cd, 377–381, 384, 385, 398–400, 404
ecological role, 377, 378
mechanisms in, 379–383
Ni, 378
Zn, 377–381, 384, 385, 400
Hyperglycemia, 442
Hypertension, 15, 23, 429, 438
Hypoxanthine, 153, 154, 194, 231
Hypoxia, 16, 21

I

IARC. *See* International Agency for Research on Cancer
ICP-AES. *See* Inductively coupled plasma atomic emission spectroscopy
ICP-MS. *See* Inductively coupled plasma mass spectrometry
ICP-OES. *See* Inductively coupled plasma optical emission spectroscopy
Imidazole and residues (*see also* Histidine), 127, 128, 156, 178, 179, 281, 282, 289, 290, 296, 344, 381
benz-, 205
buffer, 248
5-dimethylamino-2-(2-pyridinyl)-benzo-, 111, 113
5-dimethylbenz-, 205
1-methylbenz-, 205, 206, 265
ternary complexes, 251–253
Iminodiacetate, 180–182
Immunoassays, 93, 94
latex, 86, 93, 94
radio-, 86
Immunonephelometry, 94
Indicator plants, 374–376
Inductively coupled plasma atomic emission spectrometry (ICP-AES), 66, 88, 89, 95
flow injection, 89
Inductively coupled plasma mass spectrometry (ICP-MS), 87–90, 95
Inductively coupled plasma optical emission spectroscopy (ICP-OES), 88
Infants, 9, 429, 452
Inflammatory response, 14, 422, 439, 445
Infrared (IR)
Fourier transform spectroscopy, 349
radiation, 66, 109, 280
spectroscopy, 175, 278, 282, 285, 286
Inhalation of Cd, 8, 10, 14, 15, 22–24, 65, 100, 419, 421, 422, 426, 427, 435, 436, 492–494, 501
Inhibition of
root metabolism, 398
photosynthesis, 380, 399–402, 515
Inosine (Ino), 194, 215, 240, 254, 257
complexes, 206–208
Inosine 5'-diphosphate (IDP^{3-}), 230–232
Inosine 5'-monophosphate (IMP^{2-}), 224
metal complexes, 226–229, 257
(N1) oxide, 240
Inosine 5'-triphosphate (ITP^{4-}), 230–233
Inositol
phosphatidyl-, 450, 463
triphosphate, 450, 502
Insulin, 123, 124
Integration host factor, 260
Interdependencies between metal ions
Ca-Mg, 195, 448
Ca-Na, 105
Ca-Sr, 195
Ca-Zn, 195
Cd-Ca, 4, 9, 16, 20, 94, 101, 103, 105, 106, 119, 170, 195, 398, 401, 403, 423, 450, 502
Cd-Co, 47, 110, 195, 518
Cd-Cu, 110, 195, 518
Cd-Fe, 9, 18, 110, 398, 423, 442, 514

Cd-Hg, 110
Cd-Mg, 400
Cd-Mn, 47, 514, 515, 518
Cd-Ni, 110, 379
Cd-phosphate correlation, 45, 46, 48–55
Cd-Se, 195
Cd-Zn, 3, 7, 9, 17–19, 47, 101, 103, 105, 110, 119, 170, 193, 195, 204, 280, 307, 362, 377, 379, 423, 498, 501, 514, 515, 517, 518, 525
Co-Zn, 516, 518
Cu-Fe, 195
Cu-Pb, 195
Cu-Zn, 195
Fe-Zn, 48, 195
Mn-Zn, 48, 448
Ni-Zn, 379
Si-Zn, 48
Interleukins, 434, 435, 442
International Agency for Research on Cancer (IARC), 429, 493, 494
International Cadmium Association (ICdA), 419
Intestine, 9, 11, 17, 424, 442, 448
calcium binding protein, 129
Intracellular cadmium, 6, 13, 101, 103–107, 110–112
Intramolecular charge transfer (ICT), 104, 107, 110–112
Invertebrates, 340, 345
Intramolecular equilibria. *See* Isomeric complexes *and* Isomeric equilibria
Iodide
as ligand, 179, 277
propidium, 107
Iodoacetamide, 361
Ion channels (*see also* individual elements), 10, 11, 422, 448, 456, 501
Ion exchange chromatography, 70, 71
IR. *See* Infrared
Iron, 101, 495
^{59}Fe, 103
bioavailability, 48, 55
inibition by Cd, 514
deficiency, 9, 417, 420, 423, 442, 514
deficiency in plants, 379, 397, 401, 468
homeostasis. *See* Homeostasis
interdependency with other metals. *See* Interdependencies
limitation, 48, 49, 56, 516, 526
marine deposit, 513
oxide, 69
regulatory protein 1, 18
sulfur clusters, 19
transporter, 101, 382
Iron(II), 448, 496
adamantane-like cluster, 360
coordination numbers, 196
hydrolysis constant, 196
phosphate monoester complexes, 220
uptake, 398, 433, 439
Iron(III), 397
hydroxide, 41
Irving-Williams series, 4, 221
Isochrysis galbana, 515
Isoleucine or isoleucinate (Ile) and residues, 323, 332
complexes, 279
Isomeric complexes (of)
cytidine, 211, 212
ternary, 251–253
uridine, 213, 214
Isomeric equilibria, 209, 216, 222, 226, 228, 229, 232, 233, 238, 244
Isotopes (*see also* individual elements)
NMR-active (*see also* Nuclear magnetic resonance), 5, 262, 342, 366
radio-, 34
Itai-Itai disease, 15, 22, 436–438, 442, 510
International Union of Pure and Applied Chemistry (IUPAC), 64

J

Japan
Cd burden, 9
Cd excretion, 426
Cd production, 419
Itai-Itai disease. *See* Itai-Itai disease
Jellyfish
luminescent, 457
Joint Food and Agriculture Organization/World Health Organization (FAO/WHO), 421, 445, 492
Expert Committee on Food Additives, 23, 492

K

Kaolinite, 43, 70
Katangan copper belt, 396
Kidney (*see also* Renal)
cancer, 430, 464, 493, 494
Cd in, 86–89, 91, 92, 94, 95, 100, 113, 134, 193, 194, 258, 306, 340, 420, 421, 425, 427, 428, 434, 437, 440, 442–446, 449, 464, 502, 503
Cd metallothioneins, 5, 7, 10, 431, 432, 459

Kidney (*cont.*)
Cd nephropathy, 432, 433
Cd toxicity, 5–10, 12–15, 22–24, 430–433, 455, 456, 458, 463
cortex, 7, 86, 88, 89, 134, 194, 258, 340, 428
damage, 418, 431, 444, 445, 467
disease, 92, 93, 95
failure, 9
glomerular filtration rate, 431, 433
malfunction, 15
proximal tubules, 8, 9, 22, 86, 430, 431, 436, 444
Kinases, 450, 453, 463, 500
creatine, 344
cGMP-dependent, 451
glycogen synthase, 463, 479
IκB, 454
lck, 19
mitogen activated protein. *See* Mitogen activated protein kinases
phosphoinositide-3, 463, 464
protein, 435, 449, 451, 463, 464, 469
serine-specific, 453
threonine-specific, 453
Kinetically inert processes, 6, 208, 245, 257

L
α-Lactalbumin, 119, 123, 124
Lactate dehydrogenase, 444
Lakes
Cd in, 42–44
Larynx, 435
Lead(II), 306, 311, 316
phytochelatin induction, 517
interdependency with other metals. *See* Interdependencies
Lead(II) complexes of
amino acids, 281, 282, 285
dinucleotides, 255
peptides, 295
sulfide, 35
Lemna minor, 406
Lethal dose of Cd, 11, 374, 396
Leucine or leucinate (Leu) and residues, 315–319, 321–323, 329–332
complexes, 252, 253, 279, 287, 310
hexafluoro-, 317
Leukemia, 494
Leukocytes, 425
Lewis acids, 3, 5, 146
Ligand-to-ligand charge transfer, 345
Ligand-to-metal charge transfer, 308, 311, 312, 320, 324, 325, 327, 345–347, 350, 359
Lipases, 379
phospho-, 124, 450
Lipid peroxidation, 101, 402, 403, 405, 406, 408, 432
Lipocalin, 14, 423, 439, 445, 448
Lipoic acid, 16
Liposomes, 106
Lithosphere
Cd concentration, 34, 56, 65, 87, 91, 111, 378, 379, 417, 447
Liver, 448
cancer, 430
Cd in, 5, 8, 88, 89, 91, 100, 113, 134, 135, 193, 294, 346, 347, 351–356, 359, 362, 420, 425, 427, 428, 443, 448, 449, 466
Cd toxicity, 5, 8, 15, 22, 24, 431, 433, 434, 455, 456, 458, 467
disease, 15
hepatocytes, 433, 434
metal transporters, 433
Lung, 448
cancer or tumor, 15, 430, 435, 436, 464, 493, 494, 499
Cd in, 88, 89
Cd inhalation, 15, 421, 422, 424, 428, 434, 503
Cd toxicity, 8, 22, 24, 434–436, 455
disease, 434, 435
Lymphocytes, 425
granular, 494
Lysine or lysinate (Lys) and residues, 310, 332, 333
complexes, 176, 279, 281, 310
Lysosomes, 501
compartments, 8, 431
enzymes, 433, 444
Lysozyme, 123, 124

M
Macrochelates, 200, 222, 228, 231–233, 237, 239, 242, 257, 289, 290
Macrocycles, 73
chelate effect, 76, 77
Magnesium(II), 10, 101, 111, 239, 451
2'AMP, 204
carbohydrate interactions, 199
carbonyl interactions, 210, 212
chemical properties, 195–198
complexes. *See* Magnesium(II) complexes
deficiency, 437

homeostasis. *See* Homeostasis
hydrolysis constant, 196
in chlorophyll, 400–402
interdependency with other metals. *See* Interdependencies
physical properties, 195198
Magnesium(II) complexes
dinucleoside monophosphates, 257
dinucleotides, 254
9-ethylguanine, 208
nucleosides, 212
nucleotides, 228–233, 237
orotidine, 215
phosphate monoesters, 220, 221
thiophosphates, 242, 243
Magnetic circular dichroism (MCD) spectroscopy studies of
metallothioneins, 340, 342, 343, 349, 350
Magnetic resonance imaging (MRI), 101
Magnetic susceptibility, 342
MALDI. *See* Matrix assisted laser desorption ionization mass spectrometry
Malonate complexes, 253
Mammals (or mammalian)
metallothioneins. *See* Mammalian methallothioneins
Mammalian metallothioneins (*see also* Metallothioneins), 134, 341
Cd, 3, 5, 7, 8, 10, 12, 18
Cd_7, 346–348, 350, 353–356, 359, 360, 361, 363
CdZn, 8, 350
Cd_5Zn_2, 350, 352, 359, 362
cluster reactivity, 361
crystal structure, 134
Cu(I), 340–342
function, 8
HMQC experimental methods, 135, 136
human, 345, 355–358, 360, 363
M_7, 361
rabbit (liver), 134, 135, 345–347, 353–355, 357, 362
mouse (liver), 294, 344, 345, 350, 359, 363
rat (liver), 7, 8, 345, 355, 356, 359
spectroscopic characterization, 342–358
structure dynamics and metal exchange processes, 359, 360
three-dimensional structures, 361–365
vertebrates, 340, 341
Zn, 340–34
Zn_7, 355, 356, 360
Mammalian organs
Cd in. *See* individual organs
damage to, 415–468
Manganese(II), 239
Cd inhibition, 514
bioavailability, 47
complexes. *See* Manganese(II) complexes
deficiency, 514
effect on Cd uptake, 515
homeostasis. *See* Homeostasis
interdependency between elements. *See* Interdependencies
marine deposit, 513
oxide, 69
transport, 515, 526
uptake, 333, 398
Manganese(II) complexes, 401
dinucleotides, 254
nucleotides, 237
ribozymes, 261, 262
ternary, 251
Mannose, 199
Marine phytoplankton (*see also* Diatoms), 47, 193, 500–526
beneficial effects of Cd, 513, 514
Cd and thiol production, 517–519
Cd carbonic anhydrase, 511, 514, 519–526
Cd in, 509–526
Cd uptake, 515–517
detoxification of Cd, 515, 517–519, 526
effects of Cd on growth, 513–515, 521
eukaryotic, 517
Fe-limited, 516
species, 517
toxic effects of Cd, 514, 515
Zn carbonic anhydrase, 514
Mass spectrometry (MS) (studies of), 89, 293, 295, 451
deconvolution, 355
electrospray ionization (ESI), 293, 299, 354–358, 451
matrix assisted laser desorption ionization (MALDI), 354, 355
metal-protein complexes, 355
metallothioneins, 342, 354–358, 364
non-deconvolution, 356, 357
Matrix assisted laser desorption ionization mass spectrometry (MALDI), 354, 355
MCD. *See* Magnetic circular dichroism
Mechanisms of Cd toxicity, 16–22, 103, 446–466, 500–502
activation of cell death pathways, 454–459
adaptation, 462, 463
genetic and epigenetic effects, 461, 462
in signaling cascades, 450, 451, 462, 500
interference with transport and homeostasis of metals, 447–450
metallohormone effects, 465, 466
oxidative stress, 451, 452

Mechanisms of Cd toxicity (*cont.*)
recruitment of stress signaling pathways, 451–454
reprogramming of signaling pathways, 459, 460
Megalin, 439
cubilin scavenger receptor pathway, 8, 13, 431, 444, 448
Membrane
mitochondrial. *See* Mitochondria
potential, 456
receptor 24p3R, 13, 14
6-Mercaptopurine, 151–153, 182
2-Mercaptosuccinic acid, 284
Mercury, 2, 33, 90, 147
electrodes, 90
Mercury(II), 285, 288, 465
detoxification, 306
interdependency with other metals. *See* Interdependencies
peptide complexes, 288, 311
properties, 277
sulfide, 34, 35, 306
Merwilla plumbea, 398
Mesophyll, 380, 399
cells, 379, 380, 382, 402, 405
Metabolism
carbohydrates, 402
methyl, 15
vitamin D, 436
Metacinnabar (HgS), 34, 35, 306
Metal carriers, 422, 438, 448, 449
Metallohormones
androgenic effects, 466
metalloestrogen, 465, 466
Metalloproteins/Metalloenzymes, 4, 5, 7, 14, 19, 20, 22, 24, 170, 289, 340, 346, 355, 362, 366, 447, 449, 467
Ca, 119
^{113}Cd substituted (list of), 124, 125
Cd toxicology, 447, 449
Cu, 119
Fe, 119
Mg, 119
Mn, 119
probed by ^{113}Cd NMR, 117–137
synthetic, 306, 321, 328, 329, 331, 334
Zn, 5, 7, 119, 126, 193, 342
Metalloregulatory proteins, 305–309
ArsR, 306
CadC. *See* CadC
CmtR, 308, 309
MerR, 306
p53, 19, 441, 449, 464, 492, 497, 499–501
SmtA, 363, 364
SmtB, 306
Metallothioneins (MT) (in), 3, 93, 119, 124, 125, 134, 170, 193, 243, 291, 294, 304, 306, 319, 423, 428, 448, 449, 451, 496, 515
^{113}Cd NMR. *See* ^{113}Cd NMR
Ag(I) as probe, 342
algae, 355
amino acid sequences, 343
bacteria, 341, 355, 363
biosynthesis, 134
blue crab, 136, 137
CD studies, 342, 345–350, 366
Cd, 134, 175, 176, 339–366, 423, 425, 431–434, 439, 444, 447, 466, 502
cluster reactivity, 361
Co(II), 342, 346, 360
crustaceans, 341, 343, 345, 355, 361, 362
Cu(I), 134, 340–342
cyanobacteria, 341, 344, 345, 363
earthworm, 355
E_c-1. *See* Wheat metallothioneins
echinoderms, 341, 343, 362
eukaryotes, 340
EXAFS studies, 351, 352, 366
extracellular, 8
fish, 345
in meat, 10
invertebrates, 340
-like protein, 515
mammalian. *See* Mammalian metallothioneins
metal binding affinity, 358, 359
metal binding sites, 342–345, 363, 364
metal clusters. *See* Clusters *and* Mammalian metallothioneins
metal exchange processes, 359–365
metal load, 7, 18, 345, 356, 398
molluscs, 355
MT1, 136, 137, 343, 344, 356, 357, 360, 437, 466
MT2, 134, 135, 343, 357, 359–362, 437, 466
MT3, 343, 356, 358, 360, 363, 440, 459, 462, 466
MT4, 466
MTA, 343
MTB, 343
MTF-1, 7, 12, 18, 19, 467, 502
MTOR, 463
MTP1, 381, 382, 399, 423

nematodes, 366
plant genes, 383
plant. *See* Plant metallothioneins
prokaryotic, 340, 343
recombinant, 341, 342, 348, 355
sea urchin, 345, 359
spectroscopic characterization, 342–358
three-dimensional structures, 118, 134, 136, 352, 361–365, 524
vertebrate, 340, 341, 343, 345, 352, 359, 361–363
yeast, 341, 342
Zn(II), 5, 134, 135, 339–366, 466, 467
Metal response element, 7, 12
binding transcription factor-1, 7, 11, 18, 19, 467, 502
Metal substitution and exchange processes
metallothioneins, 359–365
chlorophyll, 400–402
Metal-thiolate clusters (*see also* Clusters), 7, 170, 340, 342, 344, 349, 352, 354, 356, 359–361, 363
Metal transport proteins, 381, 382
Methanephosphonate, 225, 227
Methionine or methioninate (Met) and residues complexes,123, 124, 155, 156, 282–284, 288, 296, 297, 308, 357
9-Methyladenine, 150, 206
1-Methylbenzimidazole, 205, 206, 265
S-Methylcysteine complexes, 282–284, 297
Methyl diphosphate, 230
9-Methylguanine, 150
1-Methylimidazole, 205, 206
2-Methylpyridine, 205, 206, 210, 211
Methyl thiophosphate, 242, 243
Mice, 498
Cd studies, 12, 428, 430, 436, 437, 440, 442, 445, 446, 460, 467, 501
metallothioneins. *See* Mammalian metallothioneins
MT-null, 431, 432, 467, 503
MT-1/-2 knock-out, 8
α1-Microglobulin, 86, 93, 94, 444
β2-Microglobulin, 92, 93, 421, 431, 444
MicroRNA, 462
Microscopy
electron, 405
laser scanning, 405
Minimal risk levels, 419
Mitochondria, 448, 453
damage, 455, 456
electron transport chain, 101, 449
inner membrane, 456
in plants, 403
outer membrane, 456
potential, 458
respiratory chain, 16
Mitogen activated protein kinases (MAPK), 16, 428, 433, 437, 449, 453, 454, 502
signaling cascade, 21
Mixed ligand complexes. *See* Ternary complexes
Molar absorptivity. *See* Extinction coefficient
Molecular mechanics/molecular dynamics modeling, 352, 358, 359
Molecular mimicry, 446
Molecular toxicity mechanisms, 17–22
Monkey
Cd studies, 442
Monodansylcadaverine (MDC), 449, 462
Monophosphate monoesters, 218–222
Monteponite, 34
Montmorillonite, 41
MOPS (*see also* Buffers), 106
3-(N-Morpholino)propanesulfonic acid (MOPS) buffer, 106
MRI. *See* Magnetic resonance imaging
mRNA, 381, 382, 435, 460, 462
splicing, 453
MT. *See* Metallothioneins
Mt. Blanc, 40
Mt. Everest, 39, 40
Multidrug resistance associated proteins, 426, 454, 460, 465, 467, 469
Muscle, 8, 439, 450, 460, 465
Mus musculus, 343
Mutagenicity or mutagenesis
Cd, 494–496
Mutation studies, 307, 308, 341, 461, 524, 525
Mycobacterium tuberculosis, 308
Myoglobin, 125, 439, 448

N

NAA. *See* Neutron activation analysis
NADH. *See* Nicotinamide adenine dinucleotide (reduced)
Nail
Cd in, 86, 88, 89
Natural resistance-associated macrophage proteins (NRAMP), 381, 422, 448, 449
Natural waters (*see also* Water), 32, 66–69, 78
Cd concentration, 67, 68, 396, 397
inorganic Cd^{2+} species, 67, 68, 78

Nausea, 14, 427
Necrosis, 12, 22, 427, 428, 432, 434, 439, 440, 454, 458, 459
Necrostatin-1, 458
Nephritis, 15
Nephropathy, 15, 92, 432, 433
Nephrotoxicity (of)
  Cd, 86, 93, 95, 432, 440, 446, 492, 493
  chronic, 430, 431
Nervous system
  Cd exposure, 440
  damage, 15
Neurodegenerative diseases (*see also* individual names), 100, 453, 455
Neurons, 105, 360, 448, 451, 459
  Cd in, 10
Neurospora crassa, 137, 341
Neurotransmitters, 450
Neutron activation analysis (NAA), 86, 87, 91, 95
Newborn, 9, 424, 440
NHANES III database, 434
NiCd batteries, 3, 36, 37, 419, 492
Nickel(II), 77, 381, 396, 493, 495, 501
  amino acid complexes, 284, 285, 297, 298
  carbohydrate interactions, 199, 200
  chloro complexes, 278
  exposure, 493
  hyperaccumulation in plants. *See* Hyperaccumulator plants
  in serpentine soil, 396
  interdependency with other metals. *See* Interdependencies
  nucleoside complexes, 208, 213
  nucleotide complexes, 229, 235
  peptide complexes, 286–292
Nicotiana tabacum, 405
Nicotinamide, 161, 163, 168
Nicotinamide adenine dinucleotide (reduced) (NADH), 107
Nicotinamide adenine dinucleotide phosphate (reduced) (NADPH), 451
  dehydrogenase, 403
  oxidase, 404, 452, 459
Nicotinic acid, 161, 163–168
Nifedipine, 105
Nitrate
  as ligand, 148, 149, 151–153, 159, 160, 166, 167, 173, 174
  as nutrient, 33, 38
  in ocean, 511
  reductase, 514
Nitric acid, 87–91
Nitric oxide (NO), 133, 361, 404
  radical, 361
  signaling, 402, 449–451
  synthase, 439, 449, 451
  vasodilatatory, 439
Nitrilotriacetate (NTA), 73, 180, 361
Nitrogen
  ^{15}N-labeled proteins, 305, 341
  donors, 3, 166, 178, 282
  monoxide (NO). *See* Nitric oxide
NMP^{2-}. *See* Nucleoside 5'-monophosphate
NMR. *See* Nuclear magnetic resonance
Noccaea. *See Thlaspi*
NOESY. *See* Nuclear Overhauser effect spectroscopy
Non-coded amino acids
  diastereopeptides, 319
  Leu side chain, 318, 319
Non-ferrous metal production, 33, 38, 56, 66
Notothenia coriiceps, 343
NRAMP. *See* Natural resistance-associated macrophage proteins
N-substituted purines, 153, 154, 204
  non-coordinating pendant arms, 149, 150
  potential chelating pendant arms, 150, 151
Nuclear factor κB (NF-κB), 21, 435, 449, 454, 458, 463, 500, 502
Nuclear magnetic resonance (NMR)
  ^{109}Ag, 341
  ^{111}Cd, 120, 262, 304, 342, 353, 361, 362, 366
  ^{113}Cd. *See* ^{113}Cd NMR
  ^{13}C, 120, 126, 129, 287, 290, 293
  ^{19}F, 359
  ^{15}N, 120, 136, 259
  ^{15}N,^{1}H heteronuclear single quantum correlation (HSQC), 365
  ^{1}H, 120, 135, 136, 231, 241, 251–253, 287
  ^{1}H-^{1}H dipolar constraints, 136
  ^{1}H-^{1}H nuclear Overhauser effect, 136
  ^{31}P, 120, 126, 129, 259, 262
  correlation spectra, 362
Nuclear Overhauser effect spectroscopy (NOESY), 121, 122, 136, 321, 323, 364
Nuclear quadrupole interaction, 352, 353
Nucleic acids (*see also* DNA and RNA)
  metal binding, 258–263
Nucleobases and residues (*see also* individual names), 74, 147–155, 182
  adenine, 148, 149
  complexes, 204–218, 222–263
  N-substituted purines, 149–151, 153, 154, 204
  pyrimidines, 154–155

Nucleophiles, 5, 16, 197, 259
Nucleoside 5'-diphosphates (*see also* individual names), 229–232
Nucleoside 2'-monophosphates, 234, 235
Nucleoside 3'-monophosphates, 234, 235
Nucleoside 5'-monophosphates, 148
  equilibrium constants, 224
  pyrimidine. *See* Pyrimidine-nucleoside monophosphates
Nucleosides (*see also* individual names), 194
Nucleoside 5'-*O*-thiomonophosphates (*see also* individual names), 241–243
Nucleoside 5'-triphosphates (*see also* individual names), 148, 229–232
  pyrimidine-, 229
Nucleotide analogue interference mapping/suppression(NAIM/NAIS), 258
Nucleotide excision repair (NER), 496–498, 500, 501
Nucleotides (*see also* individual names)
  analogues, 239–246
  complexes, 233–239
Nutricline, 45, 49, 50, 52, 54–56

O

Occupational exposure to Cd, 15, 88, 91–93, 417–421, 425, 433, 434, 438, 445, 447, 492
Occupational Safety & Health Administration from the US Department of Labor (OSHA), 419
Ocean
  Antarctic, 39, 45, 46, 53
  Arctic, 39, 51
  Atlantic, 39, 44–46, 50, 53, 54, 511, 512, 513
  Bering Sea, 51, 56
  cadmium/phosphorus ratio, 48–55
  Cd in, 33, 36, 44–56, 513, 521
  Cd distribution, 44–46, 49–56, 511–513
  high nutrient-low chlorophyll conditions, 49–55
  Indian, 45, 51, 53, 54
  Mediterranean, 513
  Pacific, 39, 44–47, 50, 52, 53, 511–513, 518, 519
  Sargasso Sea, 54
  Southern, 48, 51–53, 513
  Tasman Sea, 51, 52
  vertical profile of Cd, 510–512
  vertical profile of phosphate, 510–512
  vertical profile of Zn, 510–512
  Zn availability, 48, 511
Optical imaging with fluorescence probes, 101, 103
Ores
  Al, 41
  Cu, 35, 36
  Fe, 35, 41
  Hg, 34, 35
  mining, 396
  Pb, 35, 36
  Zn, 34–36, 65
Ornithine complexes, 279, 281
Orotidinate 5'-monophosphate (OMP^{2-}), 215, 235, 236
Orotidine, 214, 215
Oryctolagus cuniculus, 343
Osteoblasts, 437
Osteomalacia, 9, 15, 22, 436
Osteoporosis, 9, 15, 22, 436, 468
Otavite, 34
Oxalate as ligand, 148
Oxidases
  NADPH, 404, 452, 459
Oxidative stress, 16, 341, 451–454, 463, 494–496, 500, 515
  Cd induced, 402–405, 422, 428, 430, 432, 434, 436, 437, 439, 440, 444, 503
Oxides
  hydrous, 70
8-Oxo-dG 5'-triphosphate pyrophosphohydrolase (8-oxo-dGTPase), 498
8-Oxoguanine, 495, 498, 501
  DNA glycosylase, 498, 501
Oxopurines, 182
  hypoxanthine, 153–154
  tripodal tetradentate ligand, 154
Oxygen
  donors, 4, 166, 197, 277, 281
  singlet, 402
Oxygenases
  ribulose-1,5-bisphosphate-carboxylase/-, 400
  heme, 18, 404, 454

P

PAC. *See* Perturbed angular correlation γ-ray spectroscopy
Palladium, 88
  ^{108}Pd, 353
Palladium(II), 287–289, 292
  peptide complexes, 208, 235

Pancreas, 427
cancer, 429, 430
Cd toxicity, 8, 15, 22, 24, 442
Parathyroid hormone, 436
Parkinson's disease, 100
Parvalbumin, 124
Pathogens, 377, 378, 402
Pathophysiology, 100, 438
D-Penicillamine, 79, 317, 318, 322, 323, 327, 328, 330, 333
N-acetyl, 282–284, 297, 452
complexes, 282–285, 291, 292, 297
Peptides
artificial. *See* Artificial peptides
coiled coils. *See* Coiled coils
complexes, 286–298
containing histidine, 289–291
coordinating side chains, 287, 288
de novo design, 309–311
diastereo-, 319
non-coordinating side chains, 286, 287
self-association affinity, 330, 331
with thiol donor functions, 291–295
Permittivity, 200–204, 229, 239, 305
Peroxidase(s), 123, 124, 452
ascorbate, 403, 404, 408
glutathione, 468, 495, 496
horseradish, 93
Peroxide, 459
Peroxiredoxin, 16
Peroxisomes, 402
Perturbed angular correlation γ-ray (PAC) spectroscopy, 340, 352–354
biological applications, 352
metallothioneins, 342, 353, 354
nuclear quadrupole interaction (NQI), 352, 353
^{111m}Cd, 5, 304, 308, 309, 314–318, 320, 323–326, 328, 353, 354
Phaeodactylum tricornutum, 515, 518, 519
Pharynx, 435
1,10-Phenanthroline, 166, 178, 201
in ternary complexes, 251–253
Phenylalanine complexes, 279, 280, 297
Phenyl diphosphate, 230
Phenyl phosphate, 225, 227
4-nitro-, 227
Pheophytin, 400
Phosphatases, 20, 118–121, 124, 126–129, 304, 305, 379, 437, 444
Phosphate rock, 419, 420
Phosphate(s) (*see also* individual names), 3, 32, 64, 88, 100, 126, 147, 418, 498, 510
acetyl- (AcP^{2-}), 200, 201, 263
as nutrient, 33, 45–48, 50–55, 510–512
n-butyl-, 225, 227
Cd ratio, 48–50, 55, 56, 516, 517
complexes, 71, 74, 77, 195–198, 218–222, 225
glycerol 1- (G1P), 200, 201, 204, 236, 239, 264
diammonium hydrogen, 88, 90
dihydroxyacetone ($DHAP^{2-}$), 200, 201, 204
distribution in ocean, 510–512
esters. *See* individual names
methyl di-, 230
phenyl, 225, 227
rock, 419, 420
thio-, 241–243, 262
transport, 436, 437
Phosphatidylcholine, 405
Phosphatidylethanolamine, 405
Phosphatidylinositol
4,5-bisphosphate, 450, 463
3,4,5-triphosphate, 450, 463
Phosphine as ligand, 178
Phosphodiester bridge, 198, 202, 218–221, 254, 255
thio-, 254, 256, 258
Phosphoinositide-3 kinase, 463, 464
Phospholipase C, 124, 450
Phosphonate(s) (*see also* individual names), 225
acetonyl- (AnP^{2-}), 200, 201, 263
Cd complexes, 74, 77, 225, 227, 243, 244, 246
ethane-, 227
hydroxymethyl-, 202, 203
methane-, 225, 227
Phosphonic ligands, 72–74, 77
9-[2-(Phosphonoethoxy)ethyl]adenine ($PEEA^{2-}$), 245, 265
9-[2-Phosphonomethoxy)ethyl]adenine ($PMEA^{2-}$), 227, 241, 243–246
(Phosphonylmethoxy)ethane (PME^{2-}), 244
Phosphorothioate nucleotides, 258
Photoinduced
charge transfer (PCT), 104
electron transfer (PET), 103, 104, 106, 109
proton transfer (PPT) process, 106, 107
Photosynthesis, 193, 379, 399–402, 407
by unicellular microorganisms, 510
Cd-induced damage mechanisms, 400, 401, 408
inhibition of, 380, 399–402, 515
Photosystem II (PS II), 124
metal exchange, 400, 401
reaction center, 400, 401
Phragmitis australis, 398

Phylogenetic analysis of Cd carbonic anhydrase, 521–524
Phytochelatins, 10, 286, 291, 341, 379, 383, 404, 525
  Cd, 348, 382, 383, 404, 423, 515, 519, 525
  in marine phytoplankton, 517–519
  Pb, 517
  synthesis, 383, 517–519
  Zn, 348, 525
Phytomining, 384–386
Phytoplankton, 55, 56, 193
  Cd in, 33, 44, 47–49
  elemental composition of, 517
  growth, 513–516
  marine. *See* Marine phytoplankton
  transport system, 515–516
  Zn-limited, 47, 512, 526
Phytoremediation, 294, 374, 375, 384–387
Pigment, 419, 492
Pisum sativum, 404
Pituitary cancer, 430
Placenta, 9, 448
  Cd concentration, 424
  damage, 429
Plants, 3, 44, 65, 294, 340, 373–388, 418, 492, 510
  Cd compartmentation, 379, 380
  Cd-tolerant, 380, 381, 404
  Cd uptake, 379, 420
  damage pathways, scheme, 408
  excluder, 374–376
  Fe deficiency, 379
  genetically engineered, 386, 387
  hybridization, 105
  hyperaccumulators. *See* Hyperaccumulator plants
  indicators, 374–376
  metal ion availability, 70
  metal transport proteins, 380–382
  metal uptake, 379
  roots. *See* Roots
  toxicity. *See* Toxicity of Cd in plants
  Zn deficiency, 382, 403, 408
Plant metallothioneins, 340, 342, 343, 355, 363, 366
  wheat. *See* Wheat metallothioneins
Plasma
  Cd in, 424, 431
  metallothionein levels, 425
  metals in, 89, 297
Plastic stabilizer, 3, 37, 419, 492
Platelets, 425, 442
Platinum(II), 90, 208, 209, 235, 245, 246, 257
  peptide complexes, 288
Pleurophrysis carterae, 513
Pollution
  Cd, 38, 65, 66, 405
  environmental monitoring, 376
Polarographic techniques, 285
Polyacrylic acid, 72
Polycarboxylate ligands (*see also* individual names)
  EDTA type, 180–182
Poly(ADP-ribose) polymerase 1 (PARP1), 19, 492, 498
Polymerase chain reaction, 403, 404
Polystyrene-latex particles, 9
Populus sp., 385
Positron emission tomography, 101
Post-menopausal women, 15
Potassium, 10, 11, 101
  channel, 20
  current, 439
Potentiometric stripping analysis (PSA), 90, 91, 291
Prasinophytes, 49
Prion protein, 288, 289
Proboscia inermis, 55
Progesteron, 441
Prokaryotes
  metallothioneins, 340
Prolactin, 441
Proline or prolinate (Pro) and residues, 155, 159, 404
Propidium iodide, 107
Prostaglandin, 437
Prostate
  cancer or carcinoma, 430, 464, 466, 493, 494
  Cd toxicity, 15, 22, 503
Proteases, 344
Proteinases, 379
Proteins (*see also* individual names), 303–333
  ^{13}C-labeled, 305, 341
  ^{15}N-labeled, 305, 341
  ABC, 13, 382, 426
  artificial, 303–333
  backbone, 136, 137, 359, 365
  Bcl-2, 16, 456, 457, 464
  Ca-binding, 126–134, 449, 470
  Clara-cell, 444, 469
  de novo design, 310
  G-. *See* G-protein
  glucose-regulated, 453, 453, 470
  Hedghog, 460
  iron-regulatory, 18
  kinases, 435, 449, 463, 464, 469
  metal transport, 380–382

Proteins (*cont.*)
metallo-. *See* Metalloproteins/Metalloenzymes
metalloregulatory. *See* Metalloregulatory proteins
multidrug resistance associated, 426, 454, 460, 465, 467, 469
natural resistance-associated macrophage (NRAMP), 381, 422, 448, 449
oxidatively modified, 101, 403
prion, 288, 289
retinol binding (RBP), 86, 92–95, 432, 444
signaling, 452, 453
two-dimensional NMR structures, 309, 316
wingless/Int-1 signaling (Wnt), 459, 460, 464, 500
Proteinuria, 9, 87, 93–95, 432, 437, 444
tubular, 86, 94, 95, 425, 433, 445
Protoporphyrin IX, 19
Provisional Tolerable Weekly Intake (PTWI), 23, 492
Prymnesiophytes, 49, 517
PSA. *See* Potentiometric stripping analysis
Pulmonary irritation upon Cd inhalation, 14
Purine-nucleoside 5'-monophosphates (*see also* individual names), 226–229
Purines and derivatives (*see also* individual names), 152, 199, 222, 223, 225, 226, 229, 231, 235, 245, 251, 256, 262
complexes, 204–208
2,6-diamino-, 147, 149, 150
6-mercapto-, 151–153, 182
oxo-, 153, 154, 182
N-substituted, 149–151, 153, 154, 204
Pyrimidine-nucleoside 5'-monophosphates (*see also* individual names), 224–226, 233
Pyrimidines and derivatives (*see also* individual names), 161–163, 182, 204
Cd complexes, 209–215, 219, 225, 227–229, 236
(N1)-substituted, 204
solid state structures, 154, 155
Pyridine
as ligand, 178, 205, 206, 210, 211, 234
o-(hydroxymethyl)-, 202, 203
2-methyl-, 205, 206, 210, 211
3-Pyridinecarboxamide. *See* Nicotinamide
3-Pyridinecarboxylic acid. *See* Nicotinic acid
Pyridoxal, 161
Pyridoxamine, 161
Pyridoxine, 161, 168, 169
Pyrocatecholate complexes, 253

Q
Quadrupole mass spectrometry, 89
laser ablation, 89
Quinoline-based ratiometric detection, 112
Quinoline, 112
derivatives, 106
8-hydroxy-, 106

R
Rabbit
Cd studies, 362, 427, 447
Radiation
γ-, 499
ionizing, 496
UV, 495–497, 500
Radicals
hydroxyl ($HO^{\cdot}$), 361, 402, 449, 461, 495
nitric oxide (NO), 361
superoxide ($O_2^{\cdot-}$), 361, 402, 442, 453, 459, 495
Radioisotopes of Cd, 34
Radiotracer technique, 103
Raman spectroscopy, 285, 349
Rat
Belgrade, 422
Cd studies, 15, 427, 428, 430, 434, 436, 437, 440–442, 444, 447, 449, 463, 466, 494, 498
metallothioneins. *See* Mammalian metallothioneins
mutant, 426
Whistar, 494
Ratiometric measurements, 104, 108, 110–112
quinoline-based, 112
Rattus norvegicus (*see also* Rat), 343
RBP. *See* Retinol binding protein (RBP)
Reactive oxygen species (ROS), 16, 101, 113, 258, 293, 340, 428, 430, 432, 434, 439, 449, 450, 452, 453, 455, 456, 458, 459, 461, 463, 468, 492, 493, 495, 496, 501–503, 519
Cd tolerance, 404, 405
in plants, 398, 402–405, 407, 408
Redox
cellular status, 449, 467, 502
potential, 3, 33, 40
switches, 5
Reductases
glutathione, 403, 408, 468, 496
nitrate, 514
Refining industry, 396

Renal
diseases, 15, 93, 370, 429, 433, 470
dysfunction, 87, 436, 437, 442
erythropoietin production, 442
failure, 94, 427, 445
Fanconi syndrome, 9, 432, 437, 447
Reproductive system (*see also* Testes)
Cd exposure, 441
Cd toxicity, 440
Rescue experiments, 192, 193, 197, 243, 256
Cd, 258, 259
Respiratory tract (*see also* Lung), 8, 22, 422, 435
Cd concentrations, 434–436
Retinol binding protein (RBP), 86, 92–95, 432, 444
Ribonuclease P, 259
D-Ribose 5-monophosphate, 221, 225, 227
Ribosome
prokaryotic, 260
Ribozymes, 194, 195, 243, 256, 258–262
Diels-Alder, 260, 261
group I introns, 204, 259
group II introns, 204, 259, 262
hammerhead, 259–61
HDV, 204
Ribulose-1,5-bisphosphate-carboxylase/-oxygenase (RuBisCO), 400
Rice
Cd content, 3, 14, 15, 381, 404, 420
Rivers
Amazon, 43
Cd in, 36, 42–44, 65, 68, 69
Chanjiang, 43
Gironde, 43
Jinzu, 436
Orinoco, 43
Rhône, 43
RNA (*see also* Ribozymes), 194, 201, 246, 258–261, 263
m-. *See* mRNA
micro-, 462
polymerase, 258
t-. *See* tRNA
T7-transcribed, 258
Rodents, 425
Cd studies, 430, 434, 495
colon, 423
lung, 42
Roots, 404, 406, 408
Cd toxicity, 397–399
Cu detoxification, 399
efflux pumps, 375
inhibition of metabolism, 398
N storage, 402
symplasm, 379

S
Saccharomyces cerevisiae (*see also* Yeast), 341
Safety regulations, 417
Saliva
Cd in, 86, 88, 90, 95, 427
Salix alba, 385
Sarco/endoplasmic reticulum Ca^{2+}-ATPase (SERCA) pump, 450, 458
Sarcosine, 290
Seawater (*see also* Ocean)
Cd in, 65, 68
nutrients in, 510, 511
phosphate in, 512
surface, 511, 512, 517, 519
Zn in, 512
Secale cereale, 401
Sector field mass spectrometry, 89
Sediments. *See* Soils and sediments
Sedum alfredii, 385
Selenium interdependency with other metals. *See* Interdependencies
Semi-conductor
Cd-chalcogenide, 100
solar cells, 3
Semi-quantitative reverse transcription polymerase chain reaction, 403
Serine, 288
Cd complexes, 279, 297
specific kinase, 453
Serum
Cd in, 89, 91, 93
β2-microglobulin in, 93
Sewage sludge, 396
Siderophores, 70
Signaling pathways or cascades, 450, 451, 457–460, 462, 466
Signaling proteins, 463
ATF6, 452
IRE1, 452, 453
PERK, 452, 453
Silene vulgaris, 375, 399
Silicon
interdependency with other metals. *See* Interdependencies
transport, 48
Silver(I)
^{109}Ag NMR, 341
in metallothioneins, 342
peptide complexes, 288

Skeletonema costatum, 524
Skin
  Cd exposure, 424
Small angle X-ray scattering
  calmodulin, 132, 134
Smelter, 493
  Pb, 66, 419
  Zn, 418, 419
Smithsonite, 34
Smoking, 3, 8, 11, 12, 14, 15, 92, 100, 418, 421, 422, 424–426, 429, 433, 434, 436, 438, 442, 445, 467, 492, 493
Snails, 377
Sodium, 10, 11, 101
  channel, 439
  interdependency with other metals. *See* Interdependencies
Soils and sediments, 3, 14, 23, 24, 33, 35, 40–43, 56, 64, 65, 78, 100, 378, 396–401, 404, 419, 420, 493
  acid soluble fraction, 69
  anthropogenic contamination, 383–386, 396, 397, 417
  Cd in, 40, 41, 69–71, 374–376, 407, 408, 493
  lime, 420
  oxidizable fraction, 69
  phytoremediation. *See* Phytoremediation
  reducible fraction, 69
  Ni-rich serpentine, 396
  solution, 70, 71, 78
Solanum
  nigrum, 404
  torvum, 399
Solid state structures of Cd complexes with
  α-amino acids, 155–158
  cadmium-thiolate complexes, 170–174
  dithiocarbamates, 176–180
  nucleobases and related ligands, 148–155
  polycarboxylate ligands, 180–182
  vitamins and derivatives, 161–169
Somatic mutation and recombination test (SMART), 407
Speciation of Cd in
  atmosphere, 64–66
  environment, 63–79
  natural waters, 66–69
  soils and sediments, 69–71, 78
Spectroscopic characterization of metallothioneins
  divalent metal-binding sites, 342–345
  γ-rays perturbed angular correlation (PAC), 352–354
  magnetic circular dichroism (MCD), 349–350
  mass spectrometry, 354–358
  nuclear magnetic resonance. *See* Nuclear magnetic resonance
  UV/Vis and circular dichroism, 345–349
  X-ray absorption spectroscopy (XAS), 351–352
Spharelite, 34, 36
Spleen, 8
Spliceosome
  eukaryotic, 259
Stability ruler, 3
Stability constants (of) (*see also* Dissociation constants), 3, 197, 198, 248
  acetate complexes, 196, 197
  amino acid complexes, 196, 197
  ammonia complexes, 196, 197
  apparent/conditional, 43, 46, 196–198, 359, 424, 449, 467, 512
  buffer complexes, 250
  correlations, 72–77, 331
  Cu complexes, 77
  dinucleotide complexes, 254, 255
  dipeptide complexes, 287
  diverse Cd complexes, 67–69, 71, 72, 74, 205, 206, 208, 424, 512
  hydroxyacetate complexes, 203
  imidazole derivative complexes, 206
  Ni complexes, 71, 208
  nucleoside complexes, 211–213, 215–218
  nucleotide complexes, 225, 230–233, 242
  peptide complexes, 290, 291
  phosphate monoester complexes, 218–222
  protein complexes, 307, 324, 359, 424, 448
  pyridine derivative complexes, 206, 211
  ternary complexes, 250, 253
  Zn complexes, 77, 279
Stacking
  π-π, 151–153, 223, 231, 251, 252, 257, 280
Staphylococcus aureus, 306
Steel production, 38
Strontium(II), 195, 237, 239
  interdependency with other metals. *See* Interdependencies
Strongylocentrotus purpuratus, 343
Subtilisin, 356
Sugars (*see also* Carbohydrates and individual names)
  Cd interactions, 198–204
  hydroxyl coordination, 198, 199
  metal ion affinity, 199, 200
  permittivity, 200–204

Sulfamate, 524
Sulfate, 501
as ligand, 148, 151–153
Cd, 66–68, 71, 494
Sulfide (S^{2-})
Cd(II), 34, 66, 100, 173, 243
in metallothioneins, 342, 348, 355
M(II)S_2N_2, 344
Pb(II), 35
Zn(II), 34
Sulfonamide, 524
Sulforhodamine-B, 465
Sulfur ligands. *See* Thio ligands *and* Thioether groups
Superoxide dismutase(s), 16, 124, 254, 402, 405, 449, 452, 468, 495, 496, 503
Cu/Zn, 403, 404, 449
Fe, 403, 404
Mn, 403, 404, 449
Superoxide radical ($O_2^{\cdot-}$), 361, 402, 442, 453, 459, 495
Sweat, 9, 440
Synechococcus sp., 343, 345, 363, 515

T
Target organs for Cd toxicity (*see also* individual organs), 22, 23, 430–443, 503
bone, 436, 437
cardiovascular system, 438, 439
Cd levels, 444
endocrine glands, 441, 442
hematopoiesis and hemostasis, 442–443
kidney, 430–433, 437, 463
liver, 433, 434
nervous system, 440
reproductive system, 440, 441
respiratory system, 434–436
Tautomeric equilibria, 198–204
Teeth
Cd in, 86
Telomerase activity, 406
Teratogenicity, 429
Ternary complexes, 247–253
ATP^{4-}/buffer molecule, 248–251
ATP^{4-}/imidazole, 251–253
ATP^{4-}/OH^-, 251
M(Bpy)$(NTP)^{2-}$, 231
Testes, 427, 428, 430, 438, 440, 441, 448, 494, 498
Cd toxicity, 8, 12, 22, 455, 458, 498, 501
tumors, 494
Testosteron, 465, 466
Tetraselmis maculata, 513, 514
N,N,N',N'-Tetrakis(2-pyridylmethyl) ethylenediamine, 109, 111, 112
Thalassiosira
in freshwater, 524
oceanica, 48
pseudonana, 55, 513, 514, 516, 518–520, 521, 524
weissflogii, 7, 47, 48, 378, 396, 512–514, 516, 518–521, 524
Theophylline, 153 154
Thiamine, 161–164
Thiocyanate, 162, 166–168
2-Thiocytidine, 214, 217, 218
acidity constants, 217
complexes, 217, 218
Thioether groups, 282–284, 288, 296, 308
Thiolate proteins, 306, 307, 325–327, 330–333, 515
Thio ligands (*see also* Thiols or thiolates *and* individual names), 3–5, 13, 217, 277, 340
Thiols or thiolate(s) and derivatives
bridge, 345–347, 362, 450
clusters. *See* Clusters *and* Metal-Thiolate clusters
complexes, 4, 5, 7, 74, 101, 170–176, 182, 197, 218, 277, 284–286, 291–294, 296–298, 311–317, 320, 340, 344, 359–362, 381, 431, 450, 461, 502
di-, 174–176, 183
proteins, physical properties, 325–333
Thioneins, 19, 286, 291, 341
Thiophosphate groups (*see also* individual names), 241–243, 262
Thioredoxin, 16, 449, 452, 468
Thiouracil nucleotides, 237, 238
Thiouridines, 214, 216, 217
Third National Health and Nutrition Examination Survey (NHANESIII), 436, 438, 442
Thlaspi (= Noccaea)
arvense, 379
caerulescens, 376, 377–387, 400, 402
Threonine, 288, 453
complexes, 279, 281
specific kinase, 453
Thrombosis, 443
Thylakoids, 400, 401
Thymidine, 194, 213, 227, 230, 264
Thymidine 5'-diphosphate, 229, 230
Thymidine 5'-monophosphate, 224, 225, 227

Thymidine 5'-triphosphate, 229, 230
Thymine, 194, 213, 227, 230, 264, 266
Thymocytes, 102, 104, 460
Thyroid gland, 24, 441
Thyroid stimulating hormone, 441
Tissues
  Cd in, 86, 89, 91, 95
Tobacco, 3, 12, 403, 404, 406, 418, 421, 492
Toxicity (of)
  Cd. *See* Acute Cd toxicity, Chronic toxicity of Cd, Toxicology of Cd in mammalian organs, Toxicity of Cd in plants, *and* Target organs for Cd toxicity
  gonado-, 441
  Zn, 8
Toxicity of Cd in plants, 374, 376, 378, 380, 395–408
  anthropogenic pollution, 396, 397
  damage pathways and interactions, 407, 408
  naturally rich habitats, 396
  genotoxicity, 405–407
  oxidative stress, 402–405
  mechanisms of photosynthesis inhibition, 399–402
  resistance to, 374
  roots, 397–399
Toxicology of Cd in mammalian organs (*see also* individual organs), 415–468
  chronic low Cd exposure (CLCE), 417, 418, 421, 425, 428–430, 433, 437, 441, 443, 450, 467, 468
  target organs. *See* Target organs for Cd toxicity
Trace metal
  availability, 47
  biogeochemical cycling, 49
Transcription, 18, 243, 258, 306, 449–452, 496
Transcription factors, 3, 20, 124, 433, 447, 448, 449, 464, 465, 496–498, 501, 502
  activating transcription factor 6 (ATF6), 452, 469
  GATA1, 19
  metal response element binding, 7, 11, 18, 19, 467, 502
  signal transducer and activator (STAT3), 435
  TCF/LEF, 459, 460
  transcription-coupled nucleotide excision repair (TC-NER), 497
Transcription repressors
  CmtR, 308, 309
  SmtB/ArsR, 306
Transferases
  glutathione, 342, 444
Transferrin, 10, 20, 124, 433, 448
Transforming growth factor β family, 459
Transient receptor potential channel superfamily, 11, 423, 448
Transmembrane conductance regulator ABCC7/CFTR, 467
Transport (of), 436
  Cd in plants, 398
  Fe, 18, 422
  metal, 380–382
  Mn, 18
Tremor, 440
Tren. *See* Tris-(2-aminoethyl)amine
1,4,7-Triazaheptane (Dien), 208, 246
Triethylenetetramine (Trien), 361
Triethylenetetraamine-N,N,N',N",N"',N"'-hexaacetate, 73
Trifluoperazine, 133
Triphosphate monoester, 218–222
Tris (= 2-amino-2-hydroxymethyl-propane-1,3-diol) complexes, 109, 193, 248–251, 280–282, 284, 287, 292, 298
Tris-(2-aminoethyl)amine (Tren), 148, 159, 160
Triticum aestivum, 343
Triton® X-100, 88
tRNA, 217
  archaeal, 216, 237
  bacterial, 216, 237
Troponin, 20, 124, 439
Trypsin, 123, 132
Tryptophan complexes, 155–157, 252, 253, 279, 297
Tubercidin, 205, 206
  complexes, 211, 214, 215
Tubercidin 5'-monophosphate ($TuMP^{2-}$), 224, 225, 233, 234
Tumors (*see also* Cancer or carcinoma), 494
  overview of formation, 503
Tumor necrosis factor α (TNF-α), 12, 434, 435, 439, 445
Tumor suppressor protein p53, 19, 441, 449, 464, 492, 497, 499–501
$TuMP^{2-}$ (= 7-deaza-AMP^{2-}). *See* Tubercidin 5'-monophosphate
Tyndall effect, 94
Tyrosine, 258
  complexes, 279

U

Unfolded protein response (UPR), 452, 453, 457
Uracil (Ura), 155, 194, 213, 25, 235, 238, 242, 253–255, 260
  thio-, 237, 238

Uric acid, 435
Uridine or uridinate (Urd), 194, 213, 215, 216
  complexes, 213, 214
  thio-, 214, 216, 217, 237, 238
Uridine 5'-diphosphate (UDP^{3-}), 229, 230
Uridine 5'-monophosphate (UMP^{2-}), 225, 227, 235, 252
  Cd complexes, 215, 235, 254
Uridine 5'-*O*-thiomonophosphate, 241–243
Urine
  Cd in, 9, 13, 15, 22, 87–95, 421, 425, 426, 431, 433, 436, 437, 442–445, 452, 467, 493
  glucose, 442
  β2-microglobulin in, 93
  retinol-binding protein in, 94
UV radiation, 495–497, 500
UV/Vis spectroscopy, 251, 295, 342
  CadC, 308
  coiled coils, 311, 312, 320, 327
  extinction coefficient, 110, 320, 346
  metallothioneins, 345–350, 359
  ligand-to-metal charge-transfer (LMCT). *See* Ligand-to-metal charge transfer
  photosystem II, 400, 401

V
Vacuoles, 379–383, 386, 515
  sequestration of Zn, 380–383
Valine or valinate (Val) and residues, 317, 318
  complexes, 279
Vertebrates, 132, 340, 341, 345, 361
Vicia faba, 404, 406, 407
Viruses
  DNA, 243
Vitamins (*see also* individual names), 147, 160–169, 238, 495
  cadmium complexes, 160
  D, 9, 436, 448
  E, 468
  hydrosoluble, 160
  liposoluble, 160
  vitamin B_1. *See* Thiamine
  vitamin B_6, 168, 169
Volcanic Cd emission, 35, 36, 417
Voltage-dependent anion channel, 456, 457
Voltammetry, 295
  anodic stripping, 46, 47, 57
  cyclic, 282
  differential pulse anodic stripping, 79, 90, 91, 95
Vomiting, 14, 22, 427

W
Waste
  Cd in, 419
  disposal, 38, 71, 436
  incineration, 419
  water, 65, 419
Water (*see also* Ocean *and* River)
  Cd in, 14, 15, 43, 67, 396, 397, 408, 417, 419, 422
  drinking, 419, 422, 437, 440
  hypersaline, 68
  natural. *See* Natural waters
  sea-. *See* Seawater
Wheat,
  Cd in, 14, 22, 420
Wheat metallothioneins, 341, 344, 345, 356, 359, 364
  Cd_2E_c-1, 364, 365
  Cd_4E_c-1, 356, 364, 365
  Cd_6E_c-1, 344
  Zn_2E_c-1, 364
  Zn_4E_c-1, 356, 364, 365
  Zn_6E_c-1, 344, 343
Wingless/Int-1 signaling protein (Wnt), 459, 460, 464, 500
World Health Organization (WHO), 441, 445, 492
Wurtzite, 34

X
XANES. *See* X-ray absorption near-edge structure
Xanthine, 153
Xanthophyll cycle, 515
Xanthosine, 214–216
XAS. *See* X-ray absorption spectroscopy
Xenobiotics, 340
Xeroderma pigmentosum (XP), 497, 501
X-ray absorption near-edge structure (XANES), 285, 352
X-ray absorption spectroscopy (XAS) (studies of), 292, 382, 383
  metallothioneins, 342, 351, 352
X-ray crystal structures, 145–183, 209, 212, 217
  adenine derivatives, 235
  alkaline phosphatase, 129
  Ba(CMP), 212
  calmodulin, 132, 134
  DNA-protein complexes, 259–261
  Mg(2'AMP), 200
  PMEA, 241

X-ray crystal structures (*cont.*)
RNA-protein complexes, 259–261
stacked complexes, 251
X-ray diffraction (XRD), 66
X-ray fluorescence spectroscopy (XRF), 87, 91, 95

Y
Yeast, 465, 499
metallothioneins, 341, 342
Yellow cameleon (YC), 106

Z
Zeeman splitting, 349
Zinc
mines, 418, 436
ores, 34
smelters, 418, 419
Zinc(II), 2–10, 12, 16–18, 101, 103–106, 111, 193, 195–198, 239, 306, 377, 381, 383, 384, 387, 396, 405, 417, 429, 465, 497, 498, 500–502, 515, 516
^{65}Zn, 103
^{67}Zn, 364
bioavailability, 47
cancer, 497, 499, 501
carbohydrate interaction, 199, 200
carbonate, 2, 34, 417
carbonyl interaction, 101
chemical properties, 195–198, 277
complexes. *See* Zn(II) complexes
deficiency, 9, 417, 420, 468
detoxification, 423
dimeric metalloenzymes, 118, 126
distribution in ocean, 510–512
effect on Cd uptake, 515, 516
fingers. *See* Zinc fingers
cellular free, 4, 6
homeostasis. *See* Homeostasis
hyperaccumulation in plants. *See* Hyperaccumulator plants
in plants. *See* Plants
interdependency with other metals. *See* Interdependencies
limitation, 47, 512, 513, 519, 520, 526
physical properties, 195–198, 277
proteome, 6
sequestration, 380–383
signaling, 6
storage, 383
substitution, 5, 19, 349, 359–365, 461, 467, 498, 514, 515, 524
sulfide, 34, 348
toxicity, 8
transporters (*see also* ZIP family), 5, 6, 11, 12, 18, 101, 381, 382
uptake, 11, 398, 433, 515, 524
Zn(II) complexes (of), 276–278
amino acids, 279–285, 297, 298
Co(II) as probe, 342, 346, 360
dinucleoside monophosphates, 257
dinucleotides, 255
metallothioneins. *See* Metallothioneins
nucleosides, 208, 212
nucleotides, 228, 229, 231–233, 237
orotidine, 215
peptides, 286–294
phosphate monoesters, 220, 221
ternary, 251–253
thiophosphates, 242, 243
xanthosinate, 216
Zinc fingers, 19, 310, 345, 359, 363, 449, 461, 465, 498
transcription factors, 3, 467
ZIP family proteins, 5, 12, 18, 22, 382, 422, 423, 428, 433, 435, 448, 449